NASA Technical Memorandum 84297

NASA-TM-84297 19830021653

The 1980 Stratospheric-Tropospheric Exchange Experiment

Edited by A. P. Margozzi

June 1983

NASA

National Aeronautics and
Space Administration

NASA Technical Memorandum 84297

The 1980 Stratospheric-Tropospheric Exchange Experiment

Edited by A. P. Margozzi, Ames Research Center, Moffett Field, California

NASA
National Aeronautics and
Space Administration

Ames Research Center
Moffett Field, California 94035

TABLE OF CONTENTS

N83-29924 #

Page

FOREWORD

On April 20, 1979, a group of atmospheric theoreticians and experimenters met at NASA's Ames Research Center to discuss stratospheric-tropospheric exchange and how to study it. This working group — Professor James R. Holton, University of Washington, chairman — recommended and developed guidelines for a field experiment in the Republic of Panama to study scales and mechanisms of exchange as a result of tropical cumulonimbus convection. This volume is a report of the data collected during that experiment.

Because of the work by Edwin F. Danielsen and his co-workers much is known about the downward flow of ozone into the troposphere associated with jet folding events in midlatitudes. However, very little experimental work had been done on the important upward motions in the tropics. It is believed that these upward motions cause most of the transport into the stratosphere of tropospheric constituents — such as water vapor, methane, nitrous oxide, sulfur, and halocarbons — that affect the natural balance of ozone. The need for additional knowledge of the mass exchange between the troposphere and stratosphere has been noted often in conferences, such as the 1976 Middle Atmosphere Program meetings in Urbana, Illinois, the 1977 CFM Workshop in Warrenton, Virginia, and the 1981 Joint WMO, NASA, FAA, and NOAA workshop at Hampton, Virginia, on the State of the Stratosphere.

The Stratospheric-Tropospheric Exchange Experiment working group met again in July 1980 to review the status of preparations for the field experiment. The experiment was conducted successfully in the Republic of Panama in August and September of 1980 and a brief meeting in December 1980 revealed that the experiment had met most of the objectives. The data review meeting at Ames Research Center in December 1980 confirmed that a very rich data source had indeed been collected. Summaries of the data and some interpretations were presented to the scientific community in a special session at the San Francisco meeting of the American Geophysical Union in December 1981. In addition, seven papers were published in a special issue of Geophysical Research Letters, June 1982.

This volume has been compiled and published in order to make all the information collected during this unique field experiment available. It contains 10 chapters describing the objectives and individual experiments and results. Detailed compilations of data are provided in appendixes, as well as the seven GRL papers mentioned above. These papers are reprinted here for completeness and convenience for the reader, with the permission of the American Geophysical Union and the authors.

It is not possible, of course, to compile a complete set of data. Work continues in the experimenters' laboratories on further reduction and refinement of the data. Many of the data, especially the balloon soundings, are available on computer-compatible tapes, and many satellite photographs are on file. Tapes and photographs can be requested from Christopher Riegel and the experimenters can be contacted for further information about their specific sets of measurements.

A field program of this complexity could not have been so successful without the enthusiasm, dedication, and professional commitment of many individuals and organizations. I am pleased to have this opportunity to thank everyone involved; this includes, but is certainly not limited to, the following:

Professor James Holton and the experiment working group listed below, who guided and encouraged all the participants in the program.

Leo Poppoff, who organized the Exchange Experiment, and Bill Page, who managed the overall operations in the field, both of Ames Research Center.

Jim Cherbonneaux and his High Altitude Missions Branch at Ames Research Center, who arranged the complex logistics and support for the U-2.

The U-2 pilots, Jerry Hoyt, Ivor Webster, and Ron Williams, and the Lockheed support group who performed in their usual highly competent and professional manner.

Tom Perry and his associates at the Wallops Flight Center, who made their ozonesondes available for this experiment.

Richard Bradford and his associates from Wallops Flight Center, who launched ozonesondes at Albrook Air Force Base.

Major Leggett and his staff at Howard Air Force Base, who provided hangars, shops, laboratory space, and accommodations for the aircraft and personnel at the site.

The U.S. Air Force Military Airlift Command, which transported personnel and equipment to the field site, and the USAF Aerospace Rescue and Recovery Service, which provided over-water escort for the U-2 aircraft.

Lawrence Greenwood and Shelby Tilford, who, as Managers of the Upper Atmosphere Research Office at NASA Headquarters, encouraged us to conduct the experiment and supported our efforts.

Barbara Garner of the International Affairs Office at NASA Headquarters, who arranged all the necessary diplomatic clearances.

Don Gaby at NESS Satellite Field Services Station in Coral Gables, Florida, who provided special satellite photographic coverage.

And finally, Edwin Danielsen of the Ames Research Center, who studied the development and motion of cloud clusters on satellite imagery early each morning, at the NOAA satellite center in Miami, so as to plan that day's U-2 flights over active convective storms.

Angelo Paul Margozzi
Technical Assistant
Atmospheric Experiments Branch
Ames Research Center, NASA

STRATOSPHERIC-TROPOSPHERIC EXCHANGE EXPERIMENT WORKING GROUP

Name	Institution
James R. Holton, Chairman	University of Washington, Seattle, Washington
Reginald E. Newell	Massachusetts Institute of Technology, Cambridge, Massachusetts
G. D. Robinson	Center for the Environment and Man, Hartford, Connecticut
Christopher A. Riegel	San Jose State University, San Jose, California
David G. Murcray	University of Denver, Denver, Colorado
H. J. Mastenbrook	Naval Research Laboratory, Washington, D.C.
Dieter Kley	NOAA, APCL, Boulder, Colorado
Peter M. Kuhn	NOAA, APCL, Boulder, Colorado
Robert G. Knollenberg	Particle Measuring Systems, Inc., Boulder, Colorado
Max Loewenstein	Ames Research Center, Moffett Field, California
Neil H. Farlow	Ames Research Center, Moffett Field, California
Edward C. Y. Inn	Ames Research Center, Moffett Field, California
Stanley G. Scott	Ames Research Center, Moffett Field, California
Edwin F. Danielsen	Ames Research Center, Moffett Field, California
Robert C. Whitten	Ames Research Center, Moffett Field, California
Richard E. Young	Ames Research Center, Moffett Field, California

Ames Support Staff

I. G. Poppoff	William A. Page
Angelo P. Margozzi	Robert M. Munoz

INTRODUCTION AND SUMMARY

James R. Holton*

Stratospheric-tropospheric exchange is a crucial aspect of the global cycle of chemically active trace species. The global "averaged" view of trace-species exchange (i.e., Hadley-cell mean motions) provides bulk values of the exchange of mass to within perhaps a factor of 2, but is not a realistic model of the actual exchange processes which are primarily a result of eddy motions. In midlatitudes, it is primarily synoptic scale eddies that are responsible for the exchange. Many studies have shown this to be primarily a transfer from the stratosphere to the troposphere associated with cyclogenesis. In the tropics, on the other hand, it is the convective scale that appears to be responsible for the exchange (although convection may itself be organized on the synoptic scale).

In regions of active convection (e.g., the Intertropical Convergence Zone, or ITCZ) cumulonimbus "hot towers" provide chimneys for rapid vertical transfer from the boundary layer to the region of the tropopause. Much evidence suggests that the mean "Hadley" motion in the tropics is just the average of the rapid vertical transport taking place in the convective clouds of the ITCZ. What is the role of the cumulonimbus in the transport of tracers into the stratosphere? An understanding of the stratospheric water-vapor budget is crucial to this issue. The magnitude of stratospheric-tropospheric exchange owing to tropical cumulonimbus convection, as well as the detailed mechanisms of this exchange, is not yet understood, but very important progress has been made as a result of the Panama experiments carried out in 1977 and 1980 by Ames Research Center (Poppoff et al., 1979). Before the 1977 Panama experiment, it had been suggested that overshooting cumulus turrets which penetrated into the stratosphere might actually serve primarily to entrain small amounts of stratospheric air into the troposphere, as they collapsed, because of their negative buoyancy, rather than acting as sources of transfer of tropospheric air into the stratosphere. Although the U-2 used in the 1977 experiment had no in situ water-vapor measuring capability, the water vapor radiometer did provide evidence that in fact cumulonimbus convection serves to hydrate the lower stratosphere, and thus it appears that the overshooting turrets do serve as sources for the flux of tropospheric tracers into the stratosphere. Evidence from the aerosol spectrometer in the 1980 Panama experiment suggests, however, that overshooting turrets entrain about 40% stratospheric air and thus should have their levels of neutral buoyancy raised sufficiently to be very effective mechanisms for injection of tropospheric air into the stratosphere.

An additional critical finding of the 1977 experiment was evidence of very large amplitude, internal gravity wave motions in the tropical stratosphere, apparently excited by dynamical adjustments occurring in convective clouds. High temporal resolution measurements of ozone and temperature on the U-2 established that stable layers with wave-like vertical excursions of nearly 1 km were interspersed with turbulent adiabatic layers. The confirmation of such waves may have important implications for the dynamics of the entire equatorial middle atmosphere. From the point of view of tropospheric-stratospheric exchange, however, their significance remained obscure following the 1977 experiment since no velocity measurements were available on the U-2;

---

*U. of Washington, Seattle, Washington.

as a result, no direct deductions could be made concerning the possible role of gravity-wave-type fluctuations in the vertical transport of tracers in the lower tropical stratosphere.

The suggestions from the 1977 experiment that cumulus convective elements might be the physical entities responsible for most of the vertical transfer of trace species across the tropical tropopause, as well as the realization that an understanding of these processes was essential to resolving the long-standing paradox of the "dry" stratosphere, led to a second Panama experiment in 1980 with emphasis on water-vapor exchange. Because of the apparent importance of wave-like perturbations as found in 1977, a second planned emphasis of the 1980 experiment was on the measurement of air motions with the hope of obtaining correlative motions of velocity and tracer perturbations.

For the 1980 experiment, the U-2 was equipped with two new water-vapor instruments: the Lyman-alpha hygrometer and the frost-point hygrometer. There was also a pair of particle-size spectrometers for measuring the aerosol and ice-crystal budgets. An inertial navigation system was installed to provide air-motion information for direct flux calculations; unfortunately, this device failed very early in the experiment and it proved impossible to get it repaired or replaced during the month of the experiment. The weather was also rather unfavorable during the early portion of the experiment; hurricanes in the Atlantic disturbed the normal tropical circulation, and convection in the Panama region was very much suppressed. Despite these difficulties, the experiment was successful in most regards. Most of the instruments worked well, and information was obtained that certainly confirmed without reasonable doubt that overshooting cumulus clouds have an initial effect of hydrating the lower stratosphere as the ice crystals in the turrets are evaporated into stratospheric air. However, Danielsen's (1982a) analyses of the enhanced infrared satellite cloud images obtained during the 1980 experiment, together with the radiosonde profiles, suggested that the extensive cirrus-anvil clouds produced by overshooting cumulus turrets may provide a mechanism for dehydration of the stratosphere.

Because of entrainment, the equilibrium level for the strongest overshooting turrets may be sufficiently raised so that the cirrus anvils have their upper surfaces in the stratosphere. Danielsen (1982b) has suggested that such extended anvils would become radiatively destabilized by the cooling of their upper surfaces through radiation to space and warming of their lower surfaces by radiative exchange with the ground. The resulting increase in lapse-rate within the anvils would drive convective fluxes which by providing an upward flux of water vapor would promote rapid ice-crystal growth and fallout, hence serving as a net dehydration mechanism for the tropical stratosphere.

The occurrence of a water-vapor mixing ratio minimum in Panama at 19 km (well above the tropopause), in agreement with some previous balloon measurements, indicates that the dryness of the stratosphere cannot be accounted for in a simple and direct way in terms of the Brewer-Dobson freeze-dry hypothesis as applied to the Panama region. In any case, all evidence indicates that mass flux across the tropopause occurs in cumulus clouds, not in association with mean motions. The Brewer-Dobson hypothesis as traditionally stated would seem to imply a rather uniform cirrus cloud shield at the tropical tropopause, since if rising air is "freeze dried" the resulting ice crystals would obviously produce cloudiness. In fact, the cirrus shields that do exist are generated by anvil formation associated with the hot-tower cumulonimbus. Although in a general sense it seems clear that the dryness of the stratosphere must be related to the cold tropical tropopause, it is still unclear what physical mechanism is responsible for the very low mixing ratios observed.

Currently, a number of members of the Water Vapor Exchange working group seem to favor a variant of the Brewer-Dobson freeze-dry mechanism in which the bulk of the transport across the tropical tropopause occurs in the Indonesian "maritime continent" region (Newell and Gould-Stewart, 1981) where tropopause temperatures are observed to be significantly lower than those in Panama (at least in the northern hemisphere winter). Thus, it would appear that very deep and strong convective systems occurring in that region could freeze-dry the stratosphere to the very low mixing ratios observed at 19 km over Panama. In this view, the vertical profiles of mixing ratio observed in Panama cannot be understood in terms of local processes, but result from horizontal transport of air that was forced to enter the stratosphere by the spreading of anvils from convective overshooting of clouds with varying equilibrium buoyancy levels. Possible confirmation of the importance of this "stratospheric fountain" region must await future experiments.

REFERENCES

Danielsen, E. F.: Statistics of Cold Cumulus Anvils Based on Enhanced Infrared Photographs. Geophys. Res. Lett., vol. 9, 1982a, pp. 601-604.

Danielsen, E. F.: A Dehydration Mechanism for the Stratosphere. Geophys. Res. Lett., vol. 9, 1982b, pp. 605-608.

Newell, R. J.; and Gould-Stewart, S.: A Stratospheric Fountain? J. Atmos. Sci., vol. 38, 1981, pp. 2789-2796.

Poppoff, I. G.; Page, W. A.; and Margozzi, A. P.: 1977 Intertropical Convergence Zone Experiment. NASA TM-78577, 1979.

ORIENTATION AND DESCRIPTION OF SATELLITE PHOTOGRAPHS

Edwin F. Danielsen

INTRODUCTION

In preparation for the 1980 Panama Experiment, special arrangements were made with Don Gaby, Manager of the NOAA Satellite Field Service Station, Miami, Florida, to obtain visible and enhanced infrared photographs of clouds in the Panama region. The desire was to obtain enhanced photographs every half hour on a noninterference basis plus visible photographs just after sunrise. The low sun angle in the latter photos would side-light any turrets protruding above the anvil and cast their shadows on the anvil. Therefore, just after sunrise the visible photographs offering some upper-level topographic relief could be compared with the enhanced infrared photographs. The latter are severe abstractions which initially tend to confuse the viewer. However, in this section, eight out of ten flight missions have a visible photograph printed above an enhanced infrared photograph for direct comparison. Both represent the same space and are almost simultaneous in time. After examining a few, with the aid of the subsequent discussion, the enhanced images will be as easily comprehended as the visible.

FORMAT OF FLIGHT SETS

Photographs for each flight mission are arranged in sets in appendix A. On the first page, a visible and an enhanced infrared photograph are reproduced with the corresponding temperature scale between them. These photographs, centered at lat. 8° N and long. 78° W, near Panama, extend from lat. 3° to 12° N and from long. 71.5° to 84.5° W. They include eastern Nicaragua, Costa Rica, Panama, Columbia, and the western parts of the Gulf of Venezuela and Lake Maricaibo. With these paired photographs one can determine the large-scale distribution of clouds.

Continental outlines and national boundaries are delineated by white dots on a dark background or by black dots on a light background. Sometimes, as in the first set for August 30, these boundaries are difficult to discern. We recommend scanning the complete sets to establish an orientation.

The second page of each set is a pair of enlargements restricted to the area of the flight itself. Both include the continental outlines as dots from the satellite image and as a continuous line from a relatively detailed map. They include also the flightpath and several designated times along the path. These times are in universal, not local, time. Note that in the visible photographs, the enlarging reveals the topography of the anvil: bumps correspond to individual turrets and lumps correspond to their nacent anvils. Some of this structure appears in the enlarged infrared photographs but the resolution of the latter is limited to 8 km, whereas the visible has a 1-km resolution limit. The steps in the infrared gives their enlarged images the appearance of a Navajo rug.

All subsequent pictures are enlarged, infrared photographs taken at one-half-hour intervals — if and when they are available. There were times, of course, when the sectorizer was not available to us because of other higher priority needs. With these

sequential photographs one can determine the temporal evolution of cells and anvils in the flight region.

DESCRIPTION AND INTERPRETATION OF TEMPERATURE SCALE

The temperature scale reproduced on the first page of each flight set is black for temperatures above 28°C and black for temperatures between -64°C and -70°C. One determines which of these two ranges applies by pattern recognition. At the warm range the values change linearly from black through all grays to white as the temperatures decrease from +28°C to +8°C. In the cold range, where black changes abruptly to white, the temperature is -70°C; where it changes abruptly to light gray it is -64°C. In the infrared photograph for 1235 UT, August 30, for example, only a few small black areas are bounded by light gray, T ≤ -64°C, and a subset of these includes a boundary with white, T ≤ -70°C.

A comparison with the visible photographs above indicates that these black (cold) areas correspond to anvil clouds, that is, to portions of each anvil cloud. The visible cloud extends well beyond the black through light, medium, and dark gray as distinct value steps and even into the very light to medium gray transition region. At the step from light to medium gray, the temperature is -53°C. The step from medium to dark gray occurs at -42°C and from dark to very light gray denotes a temperature of -300°C.

If one interpreted these temperatures as representative cloud-top temperatures, the cloud tops would have a convex shape and would be called umbrellas rather than anvils. To be consistent with their anvil shape, we must consider the emissivity of the cirrus cloud as decreasing as the thickness of the anvil decreases with increasing distance from the center.

In the following discussion, the infrared temperatures will be called equivalent black-body temperatures (EBBTs) because they are based on the assumption that the emissivity is 1. When the emissivity is less than 1, the radiation received at the satellite is a mixture of radiation emitted at the cloud and radiation emitted from the warmer atmosphere below the cloud. Therefore, in general, the EBBTs are higher than the cloud-top temperatures and approach the cloud-top temperatures as the emissivity approaches 1.

As shown in table 1 of Danielsen[1] (1982), an anvil whose upper surface temperature is 190 K, as observed when the U-2 penetrated, could yield EBBTs from -30°C to ≤-80°C, that is, corresponding to the entire right side of the temperature scale reproduced between each visible and infrared photograph. The corresponding range in emissivities is from 1 to 0.36, which probably is related to an anvil depth of >2 km decreasing to <0.3 km.

The cloud statistics reported in the above publication were computed from EBBTs in the white range, ≤-70°C. Percentage area covered by this range varied dramatically from day to day, providing a reliable indicator of the intensity of cumulus convection. Figure 2 of Danielsen (1982) indicates an unusually inactive period from

[1]Danielsen, E. F.: Statistics of Cold Cumulonimbus Anvils Based on Enhanced Infrared Photographs. Geophys. Res. Lett., vol. 9, 1982, pp. 601-604.

August 30 to September 7 which was caused by a decrease in the strength of the intertropical convergence zone (ITCZ). During this period, a series of three tropical storms developed in the eastern Atlantic — two attained hurricane intensity — which deflected the flow from the ITCZ toward the storm centers.

For examples of larger, colder anvils, the reader is advised to study the visible and infrared photographs for September 9 and 15. On September 9 the visible photograph shows a large, almost circular anvil along the southern coast of Columbia (lower center of the photograph). In the infrared, this anvil includes a light gray outline, a narrow dark gray band, a variable width medium gray band, a light gray band, a black band, and a large white central area. This corresponds to EBBTs ranging from -25°C to ≤-70°C. Inside the white area are two small areas of light gray, EBBTs ≤ -76°C and small dots with EBBTs ≤ -82°C. One of these corresponds to the location of the sunlit turret in the visible photograph.

Larger light and medium gray areas are evident also in the anvil cluster located over the gulf of Darien, just north of the border between Panama and Columbia. These colder portions of the anvil are the active portions where new turrets are reinforcing the anvil. These active portions have the largest ice loading, the greater optical depths, and emissivities close to 1.

BALLOON-BORNE OZONESONDE AND WIND DATA

Christopher A. Riegel*

The Stratospheric-Tropospheric Exchange Experiment conducted from August 30 to September 18, 1980, included a series of balloon-borne ozone soundings. Approximately two soundings per day were scheduled. The agency responsible for making the soundings was the Wallops Flight Center, NASA, Wallops Island, Virginia. The soundings were made at Albrook Air Force Base, Panama (lat. 8°59' N, long. 79°33' W). There was a total of 38 soundings, 27 of which were successful in the sense that they reached the ozone peak (maximum O_3 pressure).

The ozonesonde instrument is described in an earlier report by Schmidlin and Kloos.[1]

Table 1 provides a quick summary of the ozonesonde flight history during the experiment. Altitudes are given in geopotential meters (gpm); but these may be treated as actual (geometric) meters for all practical applications of the exhibited data. A complete set of tabular data and figures is provided in appendix B.

---

*Department of Meteorology, San Jose State University, San Jose, California.

[1]Schmidlin, Francis, J.; and Kloos, Greg: Balloon-Borne Ozonesonde and Rocket Temperatures and Wind Data Gathered during the July 1977 Intertropical Convergence Zone Experiment. 1977 Intertropical Convergence Zone Experiment, I. G. Poppoff, W. A. Page, and A. P. Margozzi, eds., 1979, pp. 28-31.

TABLE 1.- BALLOON OZONESONDE FLIGHT HISTORY

Ascent No.	Date	Release time, GMT	Approximate tropopause			Ozone (pressure) peak					Final altitude, gpm	Final pressure, mbars	Integrated total ozone, m-atm-cm	Remarks
			Altitude, gpm	Pressure, mbars	Temperature, °K	Altitude, gpm	Pressure, mbars	Mixing ratio, μg/g	Partial pressure, μmbars	Number density, 10^{18} m^{-3}				
August 1980														
1	30	0358	16617	101.0	198.83	26618	20.3	11.95	146.4	4.75	33342	7.4	290	
2	30	1608	16668	98.7	197.52	26894	19.2	13.14	152.3	4.88	34593	6.2	307	
3	31	0358	--	--	--	--	--	--	--	--	16139	107.0	--	Balloon burst near tropopause
4	31	1611	16510	102.0	195.34	26515	20.4	12.90	158.8	5.06	36019	5.0	289	
September 1980														
5	1	0412	16297	104.0	193.16	--	--	--	--	--	17054	91.0	--	Balloon burst near tropopause
6	1	1553	17059	92.5	193.07	25799	22.7	11.32	155.1	4.96	35493	5.4	288	
7	2	0342	--	--	--	--	--	--	--	--	--	--	--	Data not processed
8	2	1712	--	--	--	--	--	--	--	--	4920	563.0	--	Data unusable
9	3	0347	16346	103.0	193.96	26933	18.7	13.16	148.5	4.76	32826	7.7	263	
10	3	1609	--	--	--	--	--	--	--	--	--	--	--	Unrealistic ozone data
11	4	0340	16018	110.0	197.16	25680	23.0	11.06	153.6	4.98	34265	6.4	273	
12	4	1609	16036	110.0	198.97	25296	24.6	10.71	158.9	5.09	36259	4.8	300	
13	5	0346	--	--	--	--	--	--	--	--	15225	127.0	--	Early balloon burst
14	5	1542	17274	89.4	197.55	25490	20.4	11.79	145.2	4.72	34805	5.9	296	
15	6	0323	16595	100.0	195.73	--	--	--	--	--	17012	93.0	--	Balloon burst near tropopause
16	6	1703	17231	90.1	193.73	24838	26.3	9.4	149.1	4.85	35277	5.5	308	
17	7	1613	17182	89.8	192.65	25460	34.7	10.77	154.1	5.01	32576	8.1	327	
18	8	1254	--	--	--	--	--	--	--	--	--	--	--	Unusable data
19	8	2025	16150	108.0	194.84	25914	22.3	11.84	159.4	5.19	36562	4.6	322	
20	9	1311	15631	117.0	193.93	26932	18.8	15.86	179.9	5.77	32883	7.7	359	
21	9	2019	16624	99.0	195.91	26450	20.2	12.58	153.4	4.94	37658	3.8	288	
22	10	1242	16867	95.8	195.66	26465	20.5	13.05	161.5	5.25	38145	3.6	333	
23	10	2008	16135	108.0	195.59	25094	25.0	10.50	158.4	5.18	28435	15.0	324	
24	11	1318	15184	126.0	197.53	25770	22.3	11.50	154.8	4.99	33640	6.8	321	
25	11	1929	--	--	--	--	--	--	--	--	--	--	--	Early balloon burst (thunderstorm)
26	12	1330	17141	91.0	197.81	24749	26.8	10.25	165.7	5.42	32565	8.2	349	
27	12	2004	16805	96.2	193.94	25487	23.8	11.05	158.7	5.13	33369	7.3	297	
28	13	1302	16710	98.3	196.06	26002	22.0	11.40	151.4	4.95	34960	5.8	307	
29	13	1958	15881	109.0	193.08	24857	25.0	9.65	145.6	4.83	31579	9.0	291	Thunderstorm
30	14	1307	15471	121.0	192.73	25937	21.9	12.62	166.8	5.49	27910	16.2	306	
31	14	1934	15906	112.0	195.47	25362	24.0	10.08	146.0	4.81	31348	9.6	325	
32	14	2159	16100	107.0	191.44	26174	20.8	12.43	156.0	5.07	30123	11.4	298	
33	15	1256	15436	121.0	196.13	25611	23.2	11.27	157.8	5.07	30536	11.0	300	
34	15	1950	16834	95.7	196.86	26490	20.1	13.66	165.7	5.36	38043	3.6	323	
35	15	2211	17014	91.0	195.30	--	--	--	--	--	24324	28.0	--	Early balloon burst
36	16	1353	16852	94.8	196.91	26645	19.7	12.67	150.6	4.82	35350	5.4	291	
37	17	1312	16851	95.0	197.15	26588	19.9	14.62	175.6	5.54	36036	4.9	335	
38	18	1345	17278	88.8	195.09	--	--	--	--	--	19684	59.4	--	Early balloon burst

ATMOSPHERIC OZONE AND TEMPERATURE MEASUREMENTS FROM THE 1980 PANAMA WATER-VAPOR EXCHANGE EXPERIMENT

Max Loewenstein and Michael E. McGhan*

INTRODUCTION

As a part of a multiexperiment, water-vapor exchange study carried out by NASA in Panama during August and September, 1980, ozone and total air temperature measurements were made on a series of nine U-2 aircraft flights at altitudes ranging from well below the tropopause up to 21 km. These measurements were made primarily to satisfy the need for a stratospheric tracer that could be determined simultaneously with water-vapor and aerosol measurements described in the accompanying research reports.

In addition to providing data useful in the interpretation of the water-vapor and aerosol data sets, several types of analyses of the ozone-temperature data are envisioned: (1) comparison of tropopause heights determined from the ozone data with those determined from radiosondes; (2) the relationship of ozone mixing-ratio variations to growing cumulus cells; and (3) cross-correlation of variations in ozone mixing ratio and variations in potential temperature, which will provide information on the nature of observed stratospheric waves in the ozone and temperature data.

Reduction of the ozone and temperature data has been completed and some general features of the data are discussed in this report.

EXPERIMENT

A block diagram of the ozone instrument, a Dasibi model 1003 AH photometer suitably modified for aircraft measurements, is shown in figure 1. A measurement is carried out by comparing the transmission of the Hg 253.7-nm line through an atmospheric sample containing ozone with its transmission through a similar sample after passage of the sample through a gas filter that completely removes ozone. The difference in the transmitted 253.7-nm intensities is proportional to ozone concentration for low ozone concentrations (linear region of Beer's Law). This difference, along with the measured, unattenuated 253.7-nm line intensity, the known absorption coefficient of ozone at 253.7 nm, and the absorption chamber length, allows the direct computation of ozone concentration in the absorption chamber.

The instrument operates in two modes, measure and null. The high effective stability of the lamp, which is required for measuring the very small O_3 absorption, is achieved by monitoring the Hg lamp output reflected from the X-window (see fig. 1). With the gas valve in the null mode (gas filter in-line), signals are accumulated in the reversible integrator until a preset count is reached in the reference integrator of counting chain No. 1. At this point, a cease-integrate signal turns off the reversible integrator.

---

*Gas Tech, Mountain View, California.

The gas valve is switched to "measure" and, after an absorption chamber flush interval, a measure signal is subtracted from the previously accumulated null signal in the reversible integrator. The measure period is controlled by the same preset count in the reference chain; thus, the same total lamp energy at 253.7 nm passes through the absorption chamber in both the measure and null modes. The stored count in the reversible integrator, up-count minus down-count, is proportional to the O_3 concentration in the absorption chamber during the measure mode.

The ozone instrument sensitivity, as determined from our laboratory studies, is ~3 ppbv O_3 at a sample pressure of 1 atm. The instrument actually measures O_3 concentration, so its mixing-ratio sensitivity varies inversely with the sample or atmospheric pressure; for example, its sensitivity is ~30 ppbv at 0.1 atm.

Since the atmospheric ozone mixing ratio is typically 40-80 ppbv in the troposphere and increases rapidly above the tropopause, the sensitivities available with this instrument are entirely adequate for the present tracer studies.

The accuracy of the ozone measurement is determined primarily by heterogeneous loss of O_3 in the inlet system preceding the absorption chamber. Inlet heterogeneous losses are variable, but are found to be generally less than 15% of the input ozone under realistic sampling conditions that we have simulated in the laboratory. We estimate a residual error in stratospheric ozone measurements of 10% or less after corrections have been made for heterogeneous losses.

Even though the ozone photometer is an absolute instrument requiring only knowledge of the ozone absorption coefficient at 253.7 nm, we carry out frequent laboratory calibrations of the instrument to demonstrate its linearity of response and to derive data for the correction of heterogeneous losses in the inlet lines to the system. A specially built and calibrated laboratory ozone generator is used for these tests.

The sampling time, one complete measurement cycle, of the ozone instrument is 5 sec, giving a spatial resolution of 1 km on the U-2.

Total-air-temperature measurements are made with a Rosemount-type 102 probe. (The deice heater is not powered during temperature measurements.) Static air temperatures are computed using the measured total air temperatures and the measured aircraft Mach numbers taken from the aircraft air data computer. The time-constant of the Rosemount total-temperature probe is 5 sec at 21 km, decreasing to 3 sec at 16 km.

DISCUSSION OF O_3 AND T_{static} RESULTS

Over the manifold of nine flights carried out during the Panama 1980 experiment several general features can be discerned. Ozone mixing ratios of about 50 ppbv are generally found below the tropopause. On passing through the tropopause a rapid increase of the ozone mixing ratio is observed. On flight No. 8 (13 Sept. 1980) the transition from troposphere-like ozone values to high values characteristic of the stratospheric occurs at 16.2 ±0.2 km. This value agrees well with the tropopause altitude determined from radiosonde data for that day. Within the lower stratosphere over the altitude range of 16 to 21 km covered by the 1980 Panama sampling flights, ozone increases of 0.3 to 0.4 ppm/km are consistently observed.

Superimposed on the smooth increase of O_3 and temperature in the lower stratosphere are fluctuations that are observed both in their horizontal and vertical structures. Figure 2 shows an abrupt increase of O_3 and temperature occurring at 17.5 km on the flight of August 31. A temperature increase of 10°C and an ozone increase of 0.3 ppmV occur over a vertical distance of a few hundred meters. Such dramatic layering in ozone and temperature occurs rarely in these data sets.

A much more commonly observed phenomenon is strongly correlated fluctuation in ozone and temperature occurring over a horizontal scale of tens of kilometers. This type of fluctuation is illustrated in figure 3. We also observed wave-like structures of this type during horizontal profile measurements over Panama in 1977 (Poppoff et al.[1]). They appear in the data of all the 1980 Panama flights and occur most frequently in the first 1-2 km above the tropopause. The nature of the waves producing this type of fluctuation is the subject of further analysis of the data.

Also commonly observed are fluctuations in ozone on a horizontal scale of several kilometers. These finer scale fluctuations are generally not correlated with temperature fluctuations. They occur predominantly at altitudes above 17 km and are extremely variable in amplitude from day to day.

Complete O_3 and temperature data sets (figs. 4-11) for the nine Panama flights are presented in graphical form at the end of this chapter.

CONCLUSION

Tracer measurements of ozone and temperature were carried out during a series of flights in Panama in 1980 in conjunction with the NASA water-vapor exchange study. In addition to the expected rapid increase of ozone above the mean tropopause, ozone fluctuations at various horizontal and vertical scales were also observed. The detailed analysis of these fluctuations, as well as examination of correlations between ozone and temperature and between ozone and water vapor, is the subject of further study.

---

[1]Poppoff, I. G.; Page, W. A.; and Margozzi, A. P.: 1977 Intertropical Convergence Zone Experiment. NASA TM-78577, 1979, pp. 35-50.

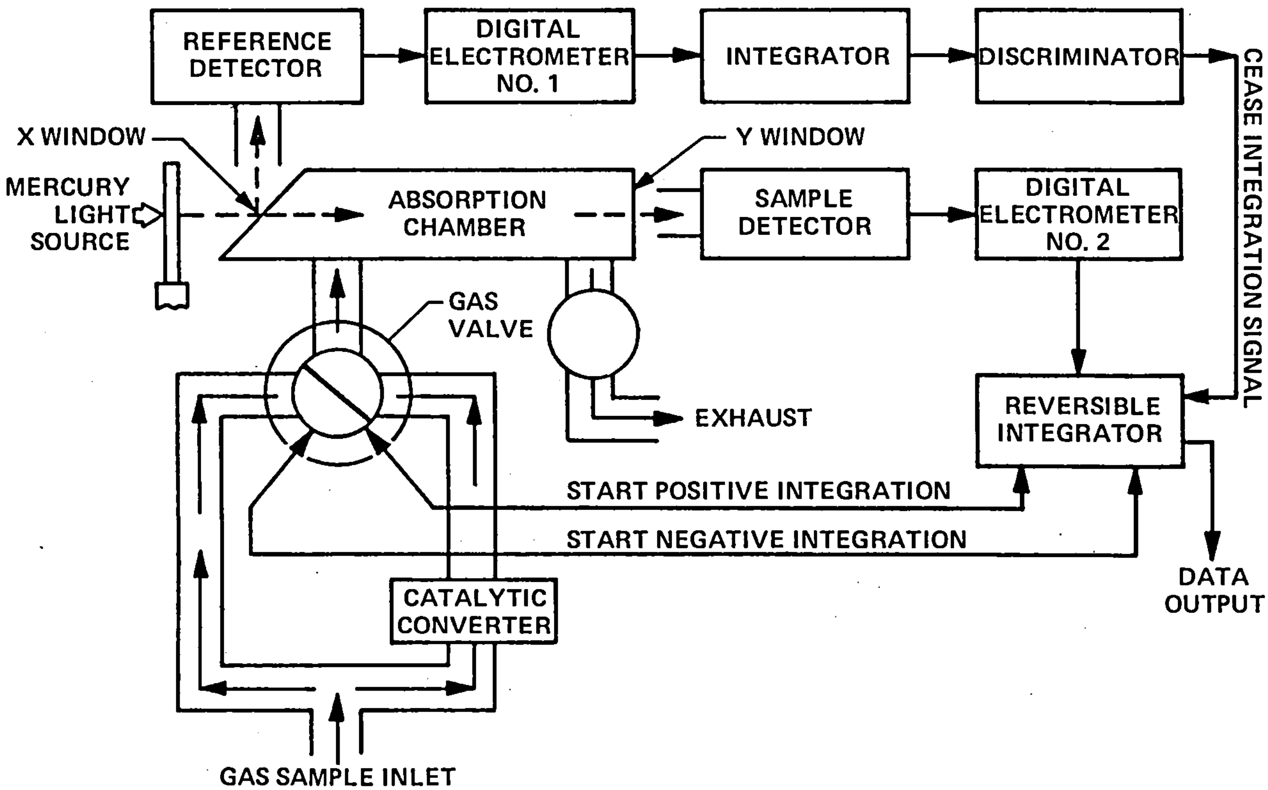

Figure 1.- Schematic of the ozone photometer used in these studies; it is a commercial Dasibi model 1003AH suitably modified for aircraft application.

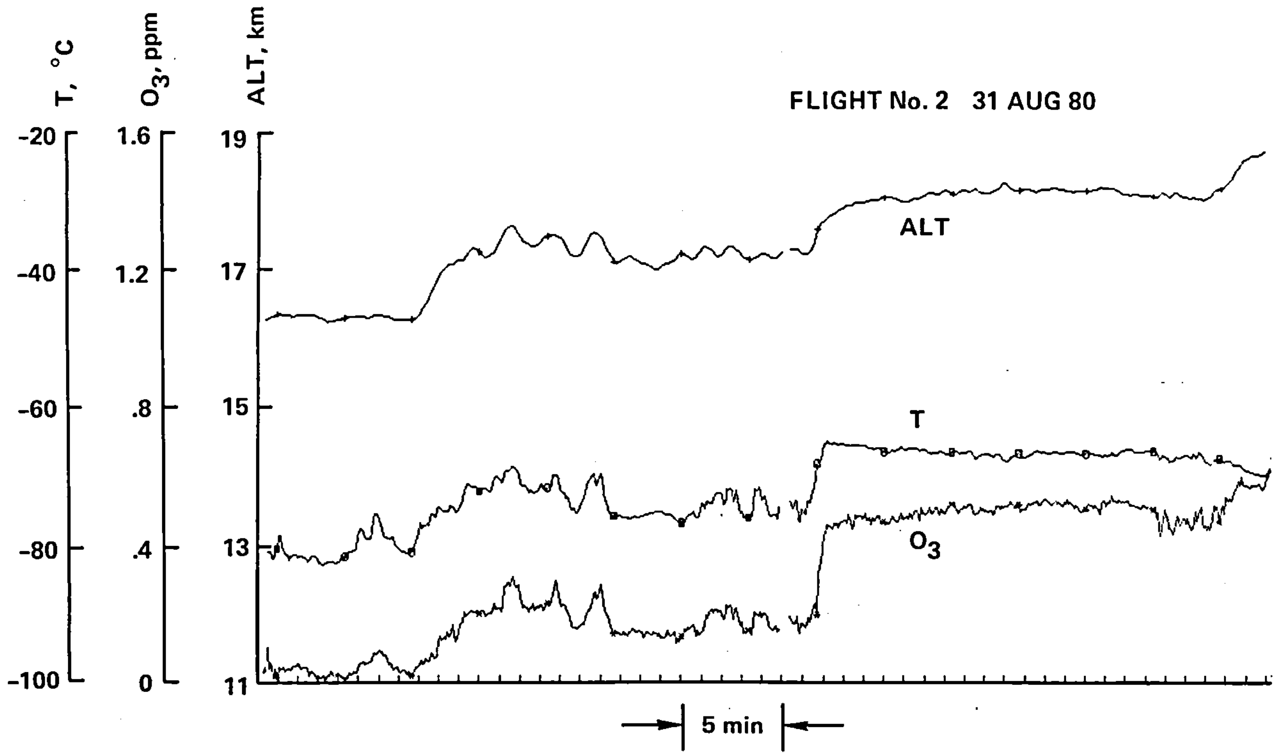

Figure 2.- Ozone and temperature "layer" observed on the flight of 31 August 1980.

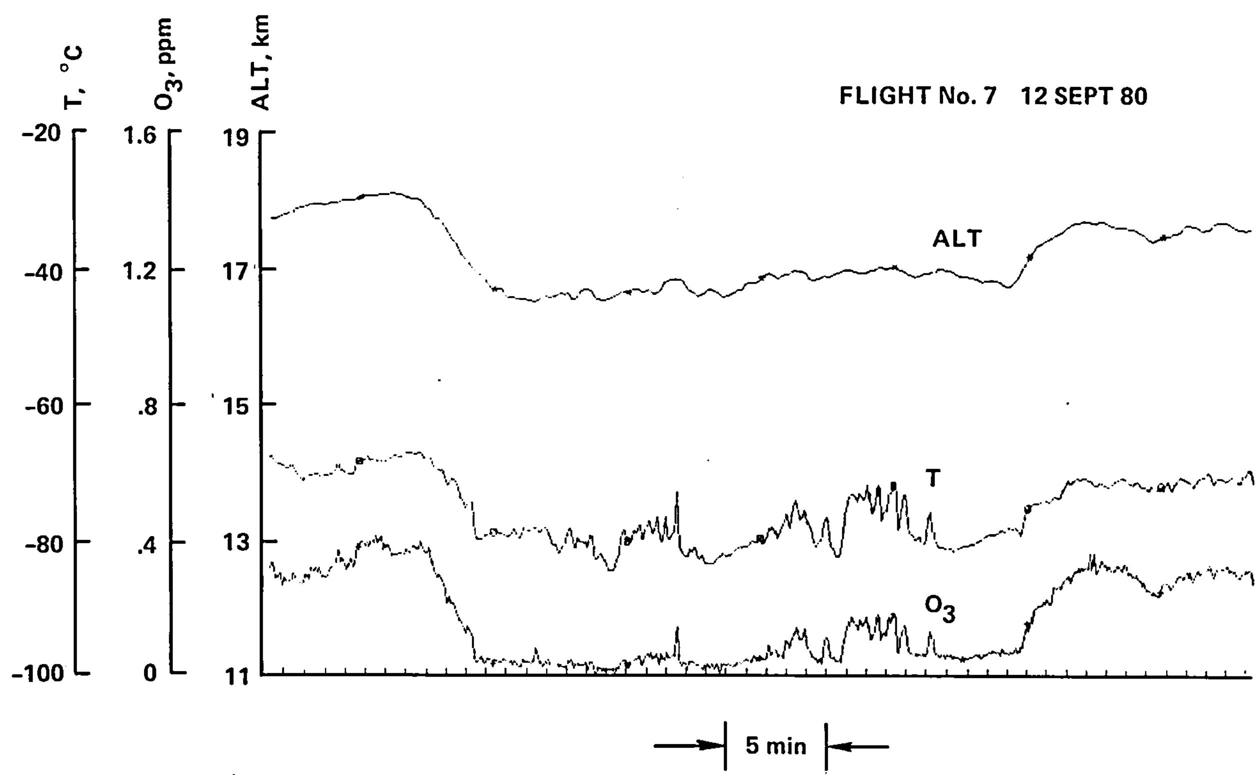

Figure 3.- Correlated ozone and temperature fluctuations observed on the flight of 12 September 1980.

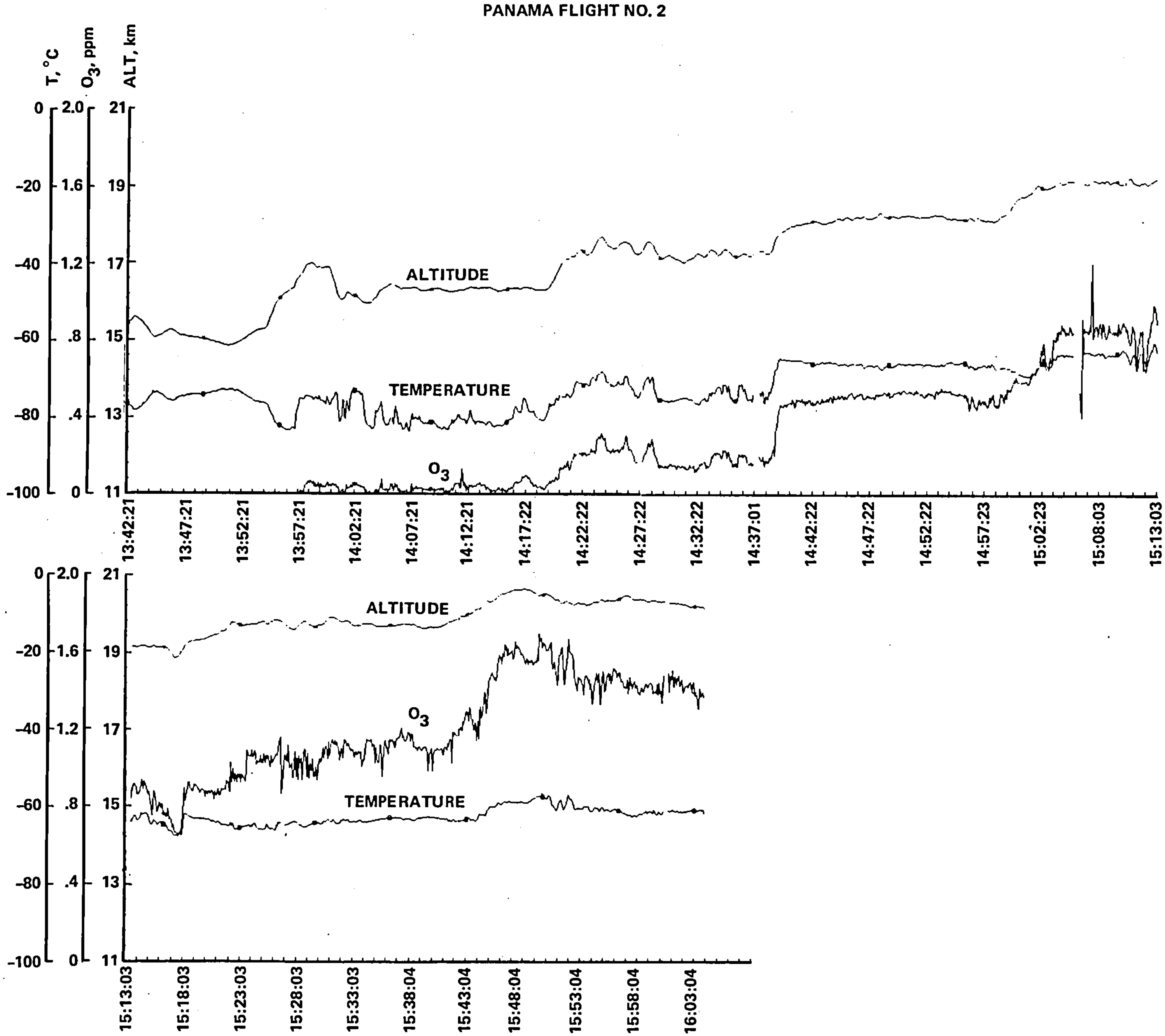

Figure 4.- Altitude, ozone, and temperature versus time for flight No. 2, 31 August 1980.

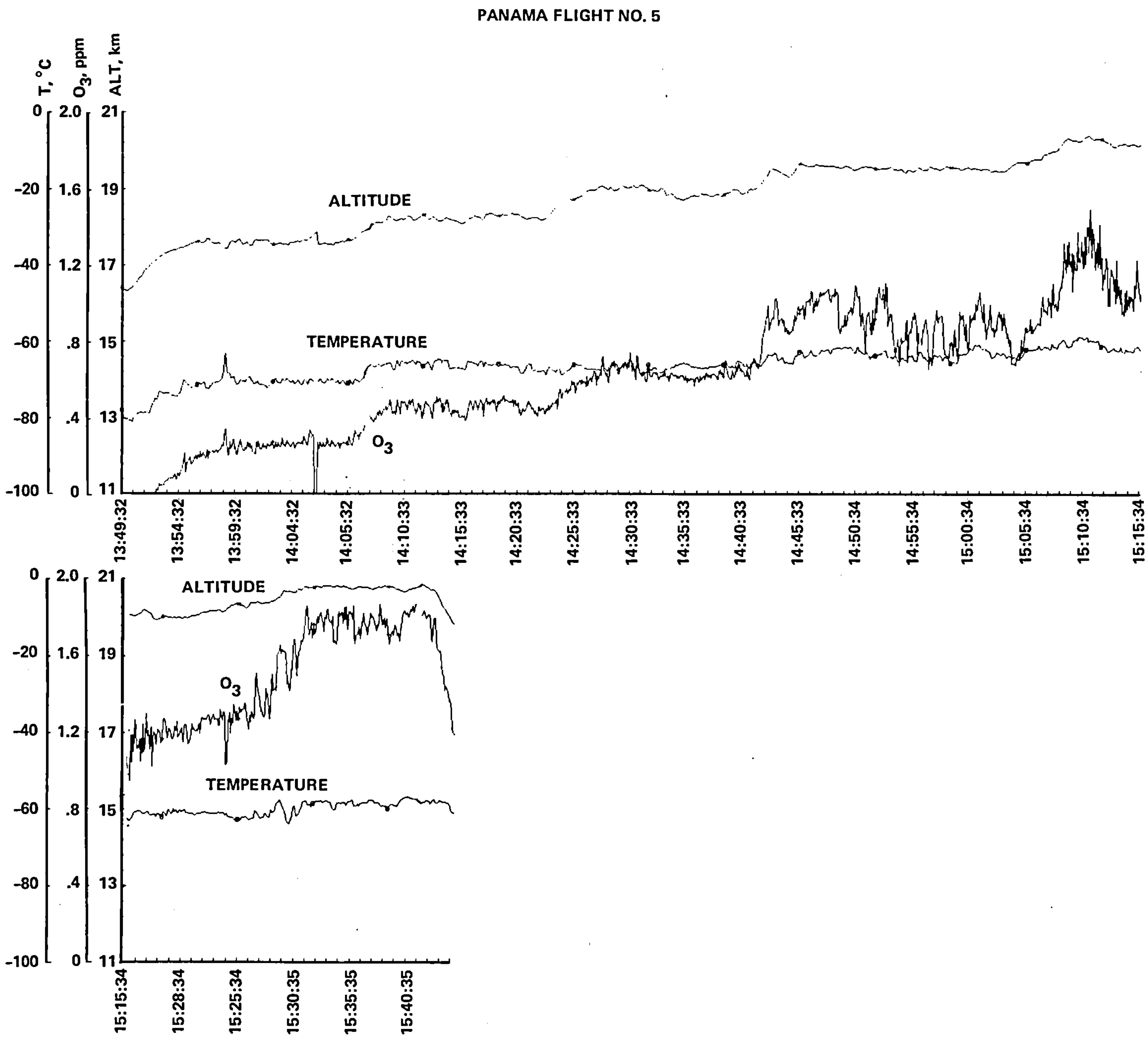

Figure 5.- Altitude, ozone, and temperature versus time for flight No. 5, 9 September 1980.

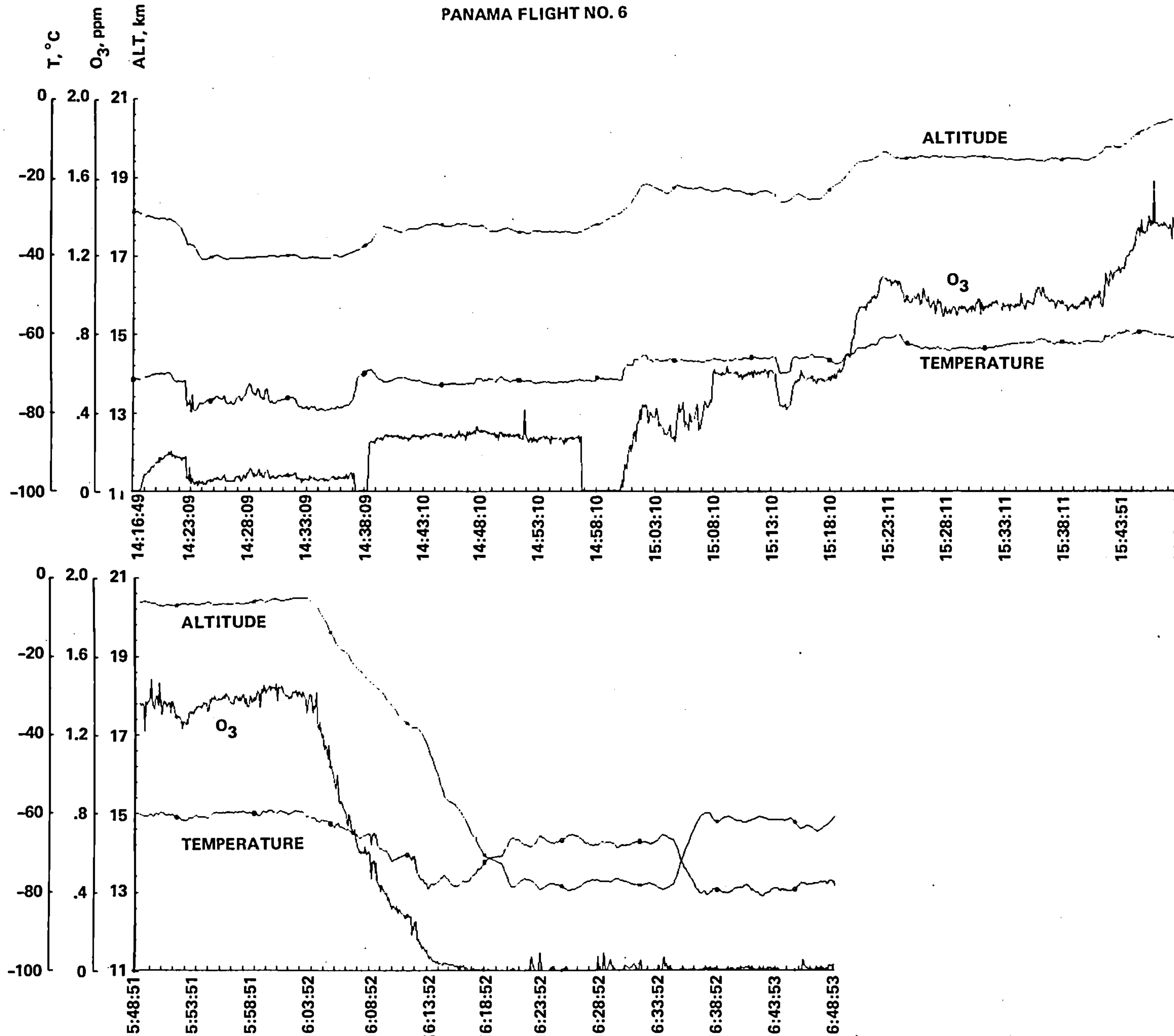

Figure 6.- Altitude, ozone, and temperature versus time for flight No. 6, 11 September 1980.

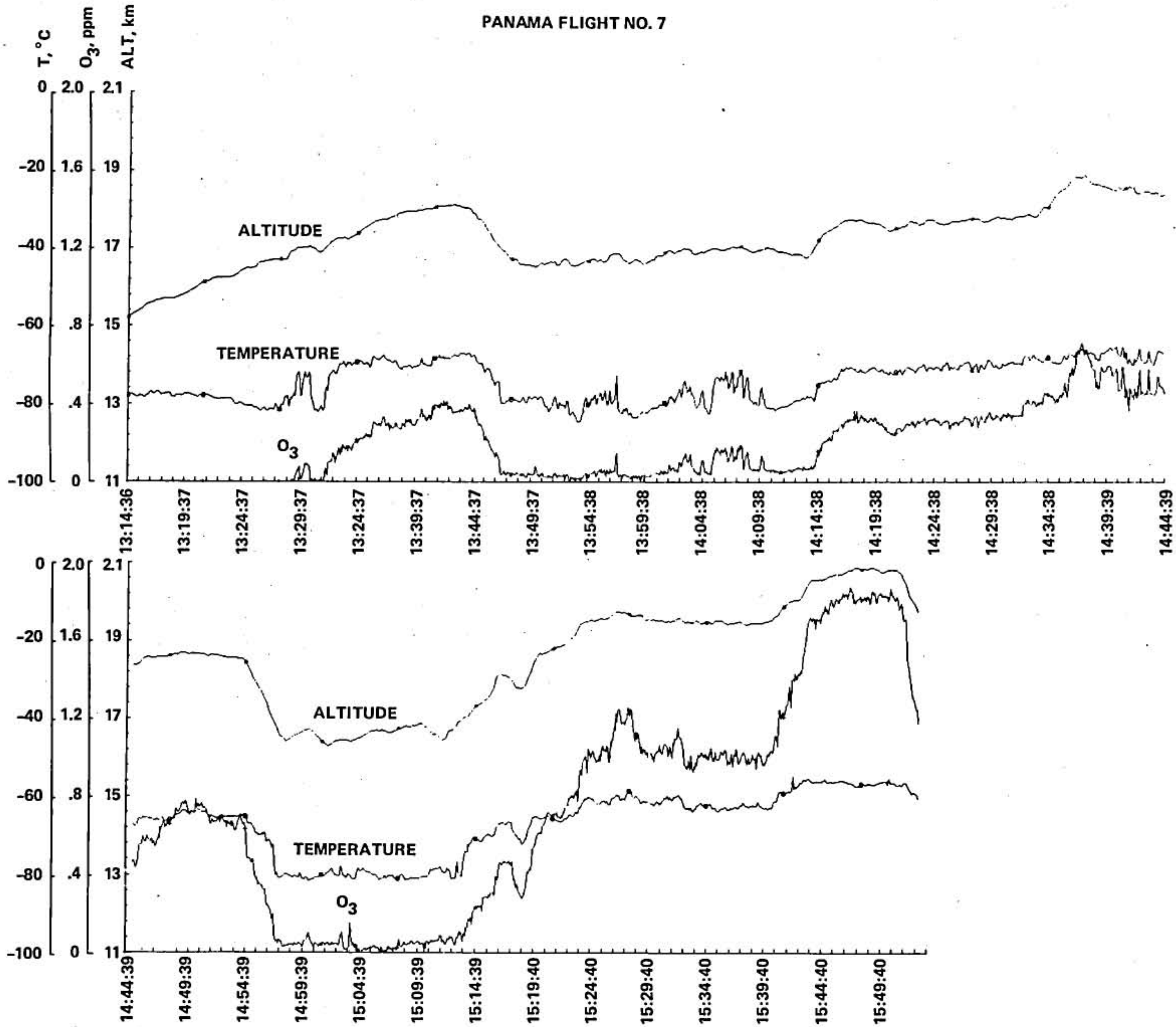

Figure 7.- Altitude, ozone, and temperature versus time for flight No. 7, 12 September 1980.

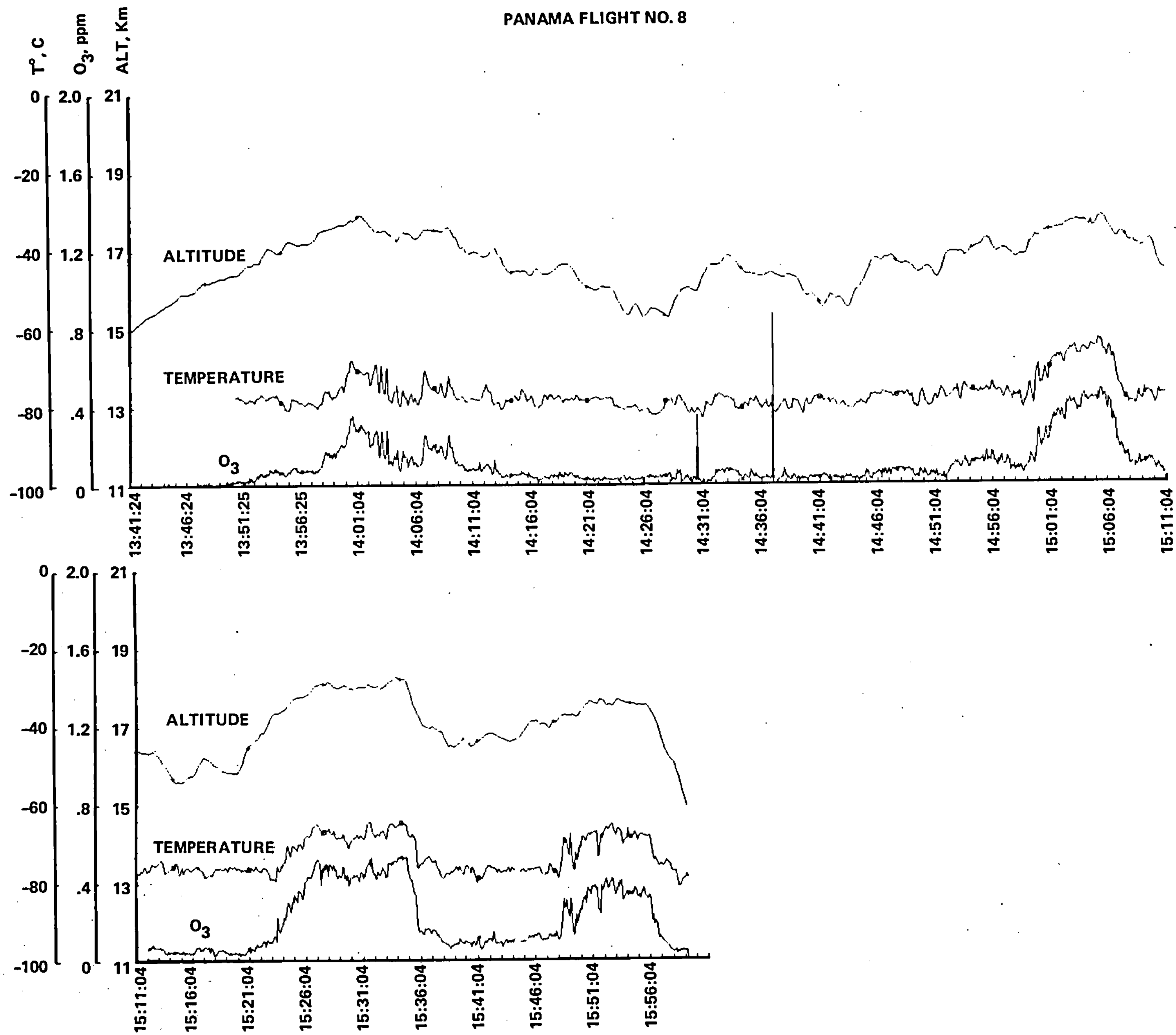

Figure 8.- Altitude, ozone, and temperature versus time for flight No. 8, 13 September 1980.

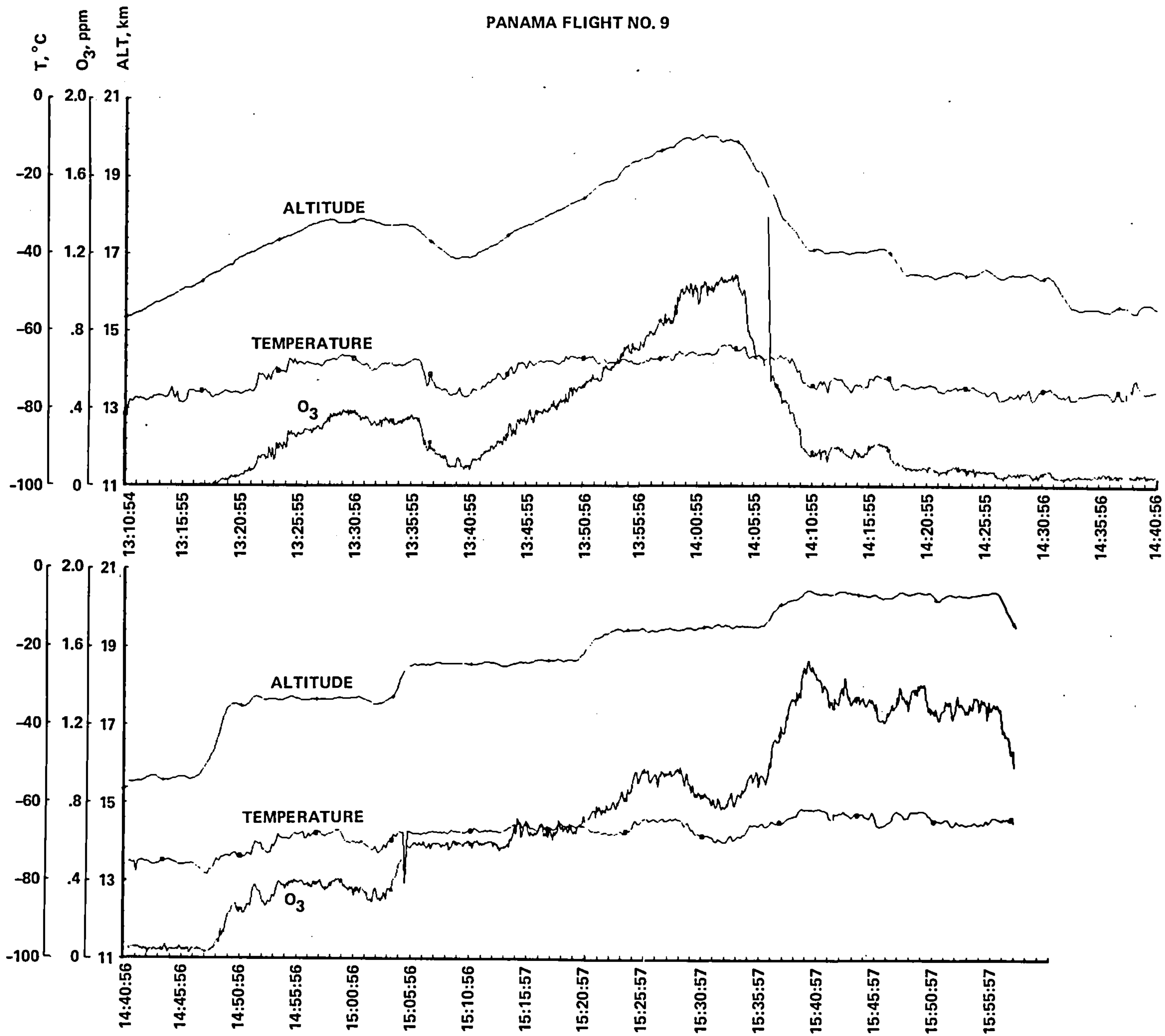

Figure 9.- Altitude, ozone, and temperature versus time for flight No. 9, 15 September 1980.

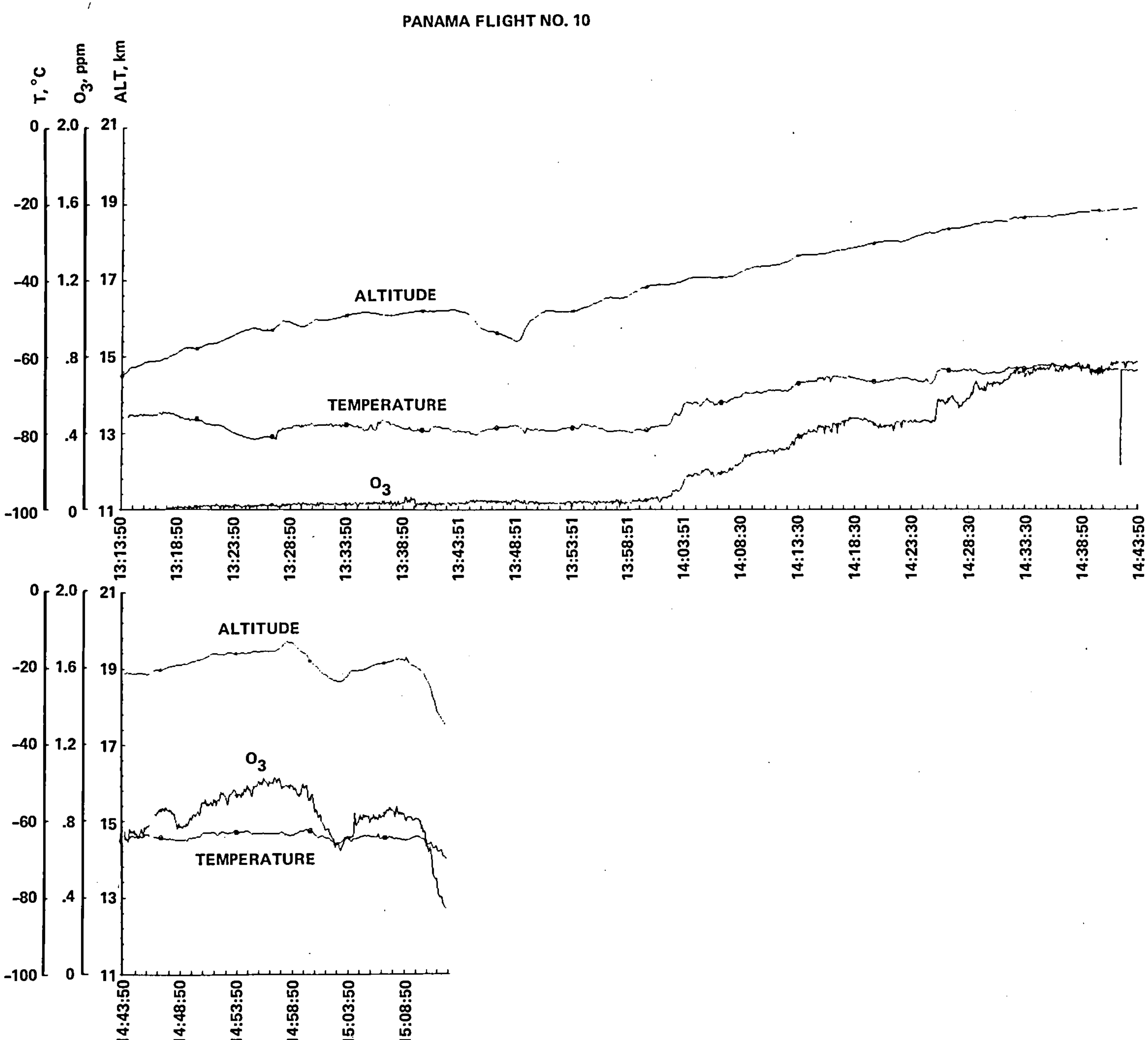

Figure 10.- Altitude, ozone, and temperature versus time for flight No. 10, 16 September 1980.

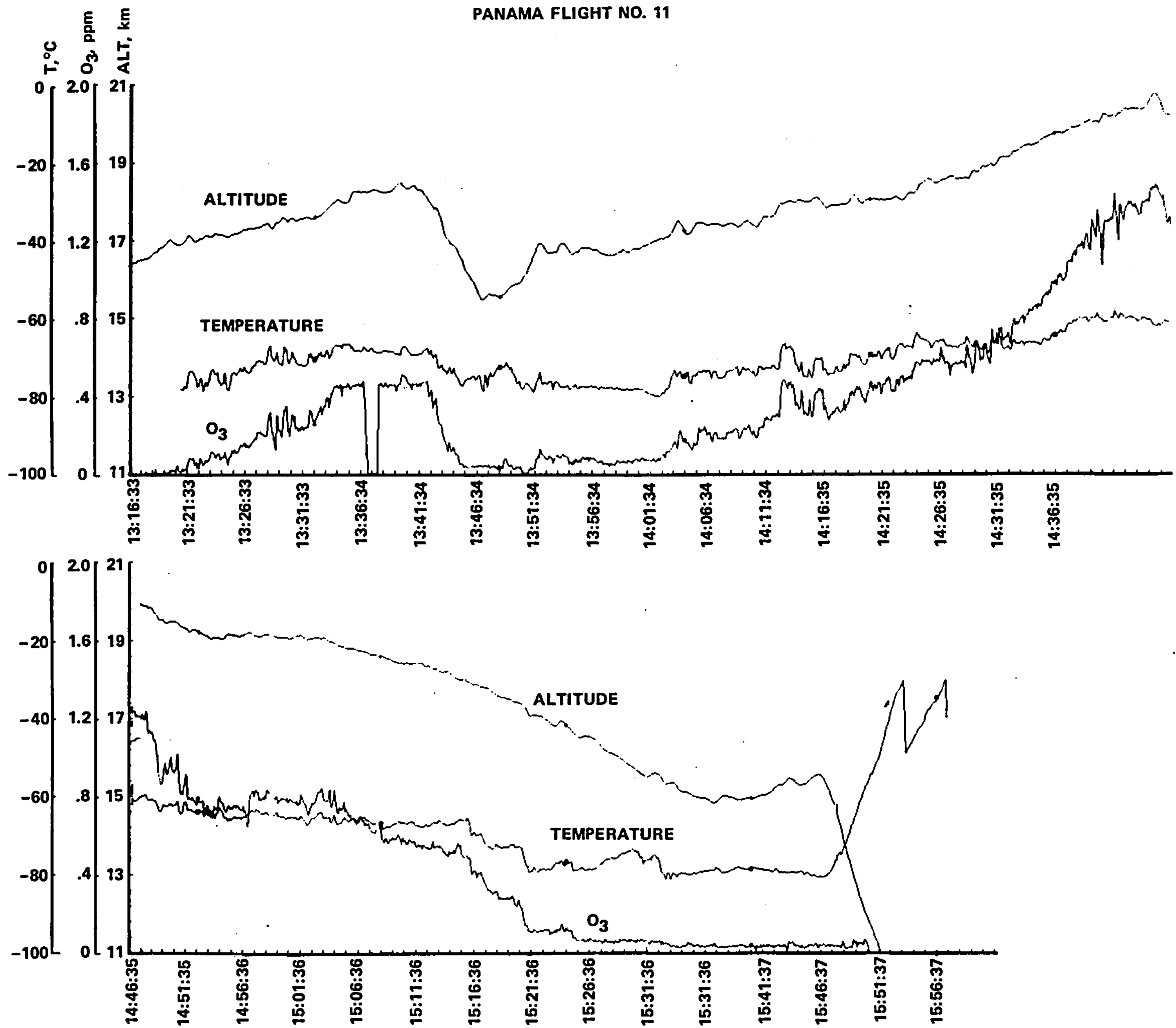

Figure 11.- Altitude, ozone, and temperature versus time for flight No. 11, 18 September 1980.

TRACE GAS MEASUREMENTS DURING THE NASA WATER-VAPOR EXCHANGE EXPERIMENT

J. F. Vedder, E. C. Y. Inn, D. O'Hara, E. P. Condon, and R. F. Miranda

In meteorologically active areas, variations of mixing ratios of photochemically reactive trace gases in the stratosphere near the tropopause generally occur (Cronn et al., 1977; Schmeltekopf et al., 1977). Anthropogenic CF_2Cl_2 and $CFCl_3$ and naturally occurring N_2O are uniformly distributed in a stable troposphere, but their mixing ratios decrease with increasing altitude in the stratosphere because of photochemical activity and transport. In the lower stratosphere, the distribution of these trace gases is controlled mainly by transport. Measured distributions of these species used as tracers of tropospheric air may contribute to our understanding of exchange processes between these regions of the atmosphere in the intertropical convergence zone (ITCZ).

From August 30 to September 19, 1980, we made a series of measurements of the mixing ratios of CF_2Cl_2, $CFCl_3$, and N_2O in conjunction with the NASA water-vapor exchange experiment. The measurements were made with an automated airborne gas chromatograph (AGC) carried in a NASA U-2 aircraft based at Howard Air Force Base in the Republic of Panama. Distributions of these trace gases were obtained between pressure altitudes of 13 and 21 km in the ITCZ. Results of these flights are presented here.

We are grateful to C. A. Boitnott for the design and initial construction of the AGC and to J. Wedekind and B. Langedyk for attending to the many details in the fabrication and assembly of the flight instrument. We also thank B. Langedyk and L. Robello for their tireless efforts in the field to support these flight experiments; S. Monfort for the computer programming for analysis and display of the data; and the pilots and crew of the U-2 aircraft, the service personnel at Howard Air Force Base, and the many others for their support in the mission.

SAMPLING SYSTEM

Analyses of the air along the flight track were conducted by gas chromatography during flight by the AGC mounted in the instrument bay of the U-2 aircraft. A flow diagram of the device is shown in figure 1. Note that the rack also carried the ozone monitor, results from which are reported elsewhere in this publication (Loewenstein and McGhan, 1983). The airflow through the system is maintained by ram pressure at the inlet scoop in the free airstream. Concentrated samples are obtained with a flow-through, liquid-nitrogen-cooled trap for gases condensable at the temperature of the trap. The mass of air flowing through the trap is measured with a venturi flowmeter and is limited to a maximum of 340 ml (STP) or to a flow period of 4 min if the limit is not reached. To increase further the concentration of the trace gases, the residual air in the trap when the flow stops is evacuated by a sorption pump. The sample is then vaporized and injected into the gas chromatograph for analysis. The removal of air leaves CO_2 as the primary constituent and eliminates from the analysis an air peak whose size would vary with the altitude of sampling and on whose tail the CF_2Cl_2 peak would arise. A sample manifold containing approximately 1 liter (STP) of air at ram pressure at an altitude of 21 km retains a mass of air from which a sample is drawn for analysis. A sample of air from approximately 1 km along the flight track is obtained by this sampling procedure, which is repeated

every 12 min. In the time between samples, a bypass valve opens to purge the manifold at a flow rate exceeding 30 liters/min.

The separation of the gases occurs in two columns in series, each followed by an electron-capture detector. The first column separates the halocarbons and the second separates CO_2 and N_2O. The exhaust pressure of the final detector is maintained at 121 ±3 kPa by an absolute-pressure relief valve. A reference gas, $C_2F_4Cl_2$, may be added to the airstream through a small orifice located upstream of the trap. The mixing ratio of this gas in the stratosphere (Fabian et al., 1981) is negligible relative to the amount added to the airflow. No reference gas was added for analysis by the second column. The $C_2F_4Cl_2$ signal provides a monitor for the performance of the AGC and may be used to normalize the flight data to remove small variations caused by changes in various operating parameters of the AGC. Some features of the AGC are listed in table 1.

The system for calibrating the AGC in the laboratory utilizes vacuum manifolds that are attached to the flexible stainless-steel tubes that in flight are connected to the intake and exhaust parts of the airscoop. Each manifold is equipped with a pressure gage and throttle valve for setting pressures to simulate flight conditions. A liquid-nitrogen-cooled trap and mechanical vacuum pump follow the exhaust manifold. The manifold is supplied with appropriate gases by a flow-dilution system. Secondary standards of CF_2Cl_2, $CFCl_3$, and N_2O were prepared by static dilutions of commercially supplied primary standards. These are then diluted with nitrogen (by factors of about 1000) in the flow-dilution system to obtain a range of amplitudes of signal peaks spanning those occurring in actual flight experiments.

Experimental errors occur primarily in the measurements of the volume of air sampled, the areas of the peaks, and the concentrations of the gas mixtures used for calibration. A spurious peak generated by the injection procedure increased the estimated uncertainty of the CF_2Cl_2 measurement from 7% to 10%. The CF_2Cl_2 and $CFCL_3$ data were normalized by comparison with the data obtained from the reference gas, $C_2F_4Cl_2$. The normalization is based on laboratory measurements obtained under simulated flight conditions. The scatter in the data from day to day is reduced by this normalization. The precision of measurement of the mixing ratios for CF_2Cl_2, $CFCl_3$, and N_2O are 10%, 6%, and 7%, respectively. The estimated accuracies for these same species are 15%, 13%, and 11%, respectively.

In level flight, the precision of measurement is better. This is demonstrated by the results of a flight originating at Moffett Field, California, on August 24, 1981. The U-2 aircraft followed a path similar in shape to that of an elongated race track in an east-west direction and spent about 2 hr at each of two altitudes. Table 2 shows the precision of measurements of the mixing ratios of CF_2Cl_2 and N_2O and the areas of the peaks of the reference gas $C_2F_4Cl_2$. We have assumed that the mixing ratios are constant at a given altitude. Values for $CFCl_3$ do not appear because the amplitude of its peak exceeded the range of the amplifier in most cases. These figures are close to the precision of about 3% found for repetitive cycles during laboratory tests. The flight results are for a single day of operation.

RESULTS AND DISCUSSION

The results of our measurements are listed in table 3. In figure 2, the altitude dependence of the mixing ratios is shown for flights that yielded the best data. These are not true vertical profiles, because the aircraft covered areas as large as

4×10^4 km^2 while the AGC was operating. The data are similar to those found in 1977 (Vedder et al., 1981). Increases are apparent for the halocarbons since 1977. Similar increases with time have been reported for the troposphere (e.g., Fraser and Pearman, 1978; Goldan et al., 1980; Rasmussen et al., 1981) and the stratosphere (Fabian et al., 1981). The altitude gradients for CF_2Cl_2 and $CFCl_3$ are greater than in July 1977, in agreement with findings of Fabian et al. (1981) for lat. 44° N in September 1980.

REFERENCES

Connell, P. S.; Perry, R. A.; and Howard, C. J.: Tunable Diode Laser Measurement of Nitrous Oxide in Air. Geophys. Res. Lett., vol. 7, 1980, pp. 1093-1096.

Cronn, D. R.; Rasmussen, R. A.; Robinson, E.; Harsch, D. E.: Halogenated Compound Identification and Measurement in the Troposphere and Lower Stratosphere. J. Geophys. Res., vol. 82, 1977, pp. 5935-5944.

Fabian, P.; Borchers, R.; Penkett, S. A.; and Prosser, N. J. D.: Halocarbons in the Stratosphere. Nature, vol. 294, 1981, pp. 733-735.

Fraser, P. J. B.; and Pearman, G. I.: Atmospheric Halocarbons in the Southern Hemisphere. Atmos. Environ., vol. 12, 1978, pp. 839-844.

Goldan, P. D.; Kuster, W. C.; Albritton, D. L.; and Schmeltekopf, A. L.: Stratospheric $CFCl_3$, CF_2Cl_2, and N_2O Height Profile Measurements at Several Latitudes. J. Geophys. Res., vol, 85, 1980, pp. 413-423.

Goldan, P. D.; Kuster, W. C.; Schmeltekopf, A. L.; Feshenfeld, F. C.; and Albritton, D. L.: Correction of Atmospheric N_2O Mixing-Ratio Data. J. Geophys. Res., vol. 86, 1981, pp. 5385-5386.

Loewenstein, M.; and McGhan, M. E.: (this publication).

Rasmussen, R. A.; Khalil, M. A. K.; and Dalluge, R. W.: Atmospheric Trace Gases in Antarctica. Science, vol. 211, 1981, pp. 285-287.

Schmeltekopf, A. L.; et al.: J. Atmos. Sci., vol. 34, 1977, pp. 729-736.

Vedder, J. F.; Inn, E. C. Y.; Tyson, B. J.; Boitnott, C. A.; and O'Hara, D.: Measurements of CF_2Cl_2, $CFCl_3$, and N_2O in the Lower Stratosphere between 2° S and 73° N Latitude. J. Geophys. Res., vol. 86, 1981, pp. 7363-7368.

Weiss, R. F.: The Temporal and Spatial Distribution of Tropospheric Nitrous Oxide. J. Geophys. Res., vol. 86, 1981, pp. 7185-7196.

TABLE 1.- AUTOMATED AIRBORNE GAS CHROMATOGRAPH

Sampling method:	Liquid-nitrogen-cooled flow-through trap for condensable gases. Residual air removed by sorption pumping before vaporization and injection
Volume of air sampled:	175 to 340 ml (STP)
Concentration factor:	3×10^3
Reference gas:	$C_2F_4Cl_2$
Columns:	Two in series each followed by a detector: (1) Porasil C in a 274-cm-long 0.18-cm-i.d. SS tube for separation of CF_2Cl_2, $C_2F_4Cl_2$, and $CFCl_3$; (2) Carbosieve B in a 38-cm long, 0.48-cm-i.d. SS tube for separation of CO_2 and N_2O
Detectors:	Ni 63 electron capture, pulsed, variable frequency
Carrier gas:	95% argon, 5% methane
Control:	Microprocessor
Data storage:	Cassette magnetic tapes
Cycle time:	12 min
Origin of sample:	1 km along flight track
Laboratory calibration:	A flow-dilution system for secondary standards supplies vacuum manifolds connected to the AGC for simulation of stratospheric conditions

TABLE 2.- PRECISION OF DATA FOR AN AGC FLIGHT, AUGUST 24, 1981

Altitude, km	Cycles	Mixing ratios, % CF_2Cl_2	N_2O	Peak area, % $C_2F_4Cl_2$
15.2	6	2	4	6
18.3	7	4	6	2

TABLE 3.- MIXING RATIOS OF CF_2Cl_2, $CFCl_3$, AND H_2O

Cycle No.	Altitude,[a] km	Universal time[b]	$C_2F_2Cl_2$		CF_2Cl_2		$CFCl_3$		N_2O		Remarks
			Factor[c]	Quality[d]	pptv	Quality[d]	pptv	Quality[d]	ppbv	Quality[d]	
Flight No. 1, Aug. 30											
No data; data recorder failure											
Flight No. 2, Aug. 31, lat. 6.3° N to 8.3° N; long. 77.2° W to 78.9° W											
1	15.1	13:47:46	--	--	(184)	3	(85)	3	307	2	No reference gas
2	16.9	13:59:46	1.14	--	241	--	108	--	296	--	
3	16.4	14:11:46	1.15	--	238	--	115	--	282	--	
4	17.7	14:23:46	1.10	--	219	--	102	--	297	--	
5	17.3	14:35:46	1.06	--	237	1	110	1	302	1	
6	18.3	14:47:46	--	--	(221)	1	(94)	1	296	--	No reference gas
7	18.7	14:59:46	.97	--	216	--	92	--	286	--	
8	19.2	15:11:46	.97	--	209	--	90	--	293	1	
9	19.8	15:23:46	.94	--	197	1	80	1	280	1	
10	19.8	15:35:46	.95	--	163	--	76	--	295	--	
11	20.8	15:47:46	--	--	(180)	1	(57)	1	--	--	No reference gas
Flight No. 3, Sept. 3, lat. 7.8° N to 9.8° N; long. 79.3° W to 79.7° W											
1	14.1	13:22:36	--	--	(198)	4	(89)	4	279	3	
2	15.1	13:34:36	1.50	--	286	2	124	2	251	1	
3	15.0	13:45:36	1.57	--	302	2	124	2	--	--	Data recorder failure
Flight No. 4											
AGC did not participate											
Flight No. 5, Sept. 9, lat. 9.1° N to 11.2° N; long. 79.3° W to 81.7° W											
1	17.5	13:55:02	--	--	(174)	4	(72)	4	250	3	Trap cooling failure
2	18.0	14:07:02	0.99	--	211	5	94	5	194	5	
3	18.4	14:19:02	1.06	--	199	6	94	6	96	8	
4	19.1	14:31:02	1.13	--	201	6	91	6	44	8	
5	19.6	14:43:02	1.12	--	168	6	70	6	--	9	
6	19.6	14:55:02	--	--	--	7	--	7	19	9	
7	19.9	15:07:02	--	--	--	6	--	6	68	9	
8	20.1	15:19:02	1.22	--	76	7	37	6	172	9	
9	20.8	15:31:02	1.02	--	101	6	39	6	177	9	
10	20.7	15:43:02	1.22	--	153	6	63	7	169	9	
11	16.1	15:55:02	--	--	(136)	7	(102)	8	132	9	
Flight No. 6, Sept. 11, lat. 10.1° N to 11.0° N; long. 77.7° W to 80.2° W											

TABLE 3.- CONTINUED.

Cycle No.	Altitude,[a] km	Universal time[b]	$C_2F_2Cl_2$ Factor[c]	$C_2F_2Cl_2$ Quality[d]	CF_2Cl_2 pptv	CF_2Cl_2 Quality[d]	$CFCl_3$ pptv	$CFCl_3$ Quality[d]	N_2O ppbv	N_2O Quality[d]	Remarks
Flight No. 6, Sept. 11, lat. 10.1° N to 11.0° N; long. 77.7° W to 80.2° W											
1	17.8	14:21:57	--	1	(144)	3	(89)	3	321	2	
2	17.0	14:33:57	1.05	--	244	--	127	--	328	--	
3	17.9	14:45:57	1.01	--	217	--	111	--	335	--	
4	17.9	14:57:57	.99	--	240	--	112	--	313	--	
5	18.7	15:09:57	.99	--	201	--	100	--	300	--	
6	19.6	15:21:57	--	1	(216)	5	--	5	318	--	
7	19.5	15:33:57	.98	--	165	1	82	--	293	--	
8	20.3	15:45:57	.96	--	176	1	56	1	300	2	
9	20.4	15:57:57	1.01	--	156	1	55	1	301	1	
10	18.1	16:09:57	1.00	--	210	2	110	2	295	2	
11	13.4	16:21:57	--	1	(159)	3	(72)	3	233	3	
12	13.1	16:33:57	2.81	--	204	5	119	5	--	--	
Flight No. 7, Sept. 12, lat. 5.6° N to 8.4° N; long. 78.1° W to 79.8° W											
1	16.0	13:20:05	--	1	(196)	3	(89)	3	304	2	
2	17.3	13:32:05	0.99	--	219	--	106	--	316	--	
3	18.1	13:44:05	.93	--	214	--	98	--	295	--	
4	16.8	13:56:05	.97	--	234	--	118	--	284	--	
5	17.1	14:08:05	.96	--	213	1	115	1	291	1	
6	17.7	14:20:05	--	1	(211)	3	(110)	3	277	2	
7	17.9	14:32:05	.91	--	206	3	102	2	253	2	
8	18.4	14:44:05	.91	--	213	3	96	3	243	4	
9	17.6	14:56:05	.91	--	217	3	105	3	233	4	
10	16.8	15:08:05	1.00	--	187	3	96	3	180	4	
11	18.8	15:20:05	--	1	(189)	4	(80)	4	219	4	
12	19.7	15:32:05	.92	--	184	4	67	4	216	4	
13	20.7	15:44:05	.88	--	129	4	41	4	--	--	
Flight No. 8, Sept. 13, lat. 8.4° N to 10.5° N; long. 77.3° W to 79.3° W											
1	16.1	13:47:13	--	1	(178)	3	(80)	3	308	2	
2	17.7	13:59:13	1.03	--	221	--	108	--	328	--	
3	17.1	14:11:13	1.01	--	228	--	116	--	310	--	
4	16.2	14:23:13	1.02	--	231	--	124	--	300	--	
5	16.5	14:35:13	1.62	--	227	3	90	3	258	3	
6	16.9	14:47:13	--	1	(216)	1	(106)	1	276	--	
7	17.0	14:59:13	1.16	--	227	--	108	--	271	--	
8	16.6	15:11:13	1.07	--	227	--	120	--	279	--	
9	17.3	15:23:13	1.14	--	222	--	114	--	270	--	
10	18.1	15:35:13	--	5	(205)	2	(60)	7	272	1	
11	17.1	15:47:13	--	1	--	9	(122)	2	--	--	

TABLE 3.- CONCLUDED.

Cycle No.	Altitude,[a] km	Universal time[b]	$C_2F_2Cl_2$ Factor[c]	$C_2F_2Cl_2$ Quality[d]	CF_2Cl_2 pptv	CF_2Cl_2 Quality[d]	$CFCl_3$ pptv	$CFCl_3$ Quality[d]	N_2O ppbv	N_2O Quality[d]	Remarks
Flight No. 9, Sept. 15, lat. 8.2° N to 10.4° N; long. 76.7° W to 79.3° W											
1	16.3	13:16:45	1.19	1	235	3	118	3	314	2	
2	18.0	13:28:45	1.02	1	200	1	99	1	291	3	
3	17.0	13:40:45	.94	--	220	--	110	--	300	--	
4	18.9	13:52:45	.91	--	188	--	90	--	306	--	
5	19.8	14:04:45	.90	--	187	1	76	1	297	1	
6	17.2	14:16:45	.95	--	233	--	114	--	301	--	
7	16.6	14:28:45	.94	--	219	--	121	--	289	4	
8	15.6	14:40:45	.99	--	233	1	130	1	299	1	
9	17.7	14:52:45	.94	--	206	--	108	--	287	--	
10	18.3	15:04:45	.96	--	198	1	104	1	275	1	
11	18.8	15:16:45	.94	--	201	--	97	--	279	--	
12	19.6	15:28:45	.94	--	183	--	78	--	267	--	
13	20.5	15:40:45	.95	--	142	--	51	--	268	1	
Flight No. 10, Sept. 16, lat. 5.7° N to 8.0° N; long. 78.2° W to 81.2° W											
1	15.3	13:19:37	1.32	--	234	3	114	3	286	2	
2	16.1	13:31:37	1.06	--	227	--	118	--	319	--	
3	16.3	13:43:37	1.03	--	235	--	119	--	300	--	
4	16.5	13:55:37	.98	--	238	--	120	--	296	--	
5	17.2	14:07:37	1.08	--	211	--	100	--	266	--	
6	18.0	14:19:37	.99	--	218	--	97	--	282	--	
7	18.6	14:31:37	.98	--	191	--	95	--	--	9	
8	19.0	14:43:37	.97	--	195	1	87	1	275	1	
9	19.6	14:55:37	.96	1	199	2	77	1	264	2	
Flight No. 11, Sept. 18, lat. 8.2° N to 10.1° N; long. 79.3° W to 81.2° W											
1	17.2		1.53	--	218	3	92	3	270	2	
2	18.2		1.28	--	212	1	86	1	293	2	
3	15.8		1.25	--	247	1	111	1	281	4	
4	16.8		1.26	--	236	1	109	1	265	2	
5	17.5		1.31	--	222	1	106	1	294	2	
6	18.2		1.31	--	217	1	90	1	264	2	
7	19.5		1.32	--	178	1	73	1	247	2	
8	20.2		1.35	--	153	1	50	1	232	2	
9	19.3		1.41	--	183	2	70	2	242	3	
10	18.5		1.28	--	211	1	78	1	252	2	
11	17.2		1.18	--	230	1	107	1	245	5	
12	15.3		1.37	--	260	1	116	2	238	2	
13	15.7		1.26	--	253	1	126	1	--	--	

[a]Pressure altitude of aircraft.
[b]Universal time of closure of bypass value to retain a volume of air for sampling (±1 sec).
[c]Normalization factor derived from the predicted and measured peak amplitudes for $C_2F_4Cl_2$. This factor is applied to the CF_2Cl_2 and $CFCl_3$ data.
[d]A measure of the reliability of the measurement based on various conditions of the data and performance of the AGC. For values greater than 2, the validity of the data is questionable. The best data have no entries in this column.

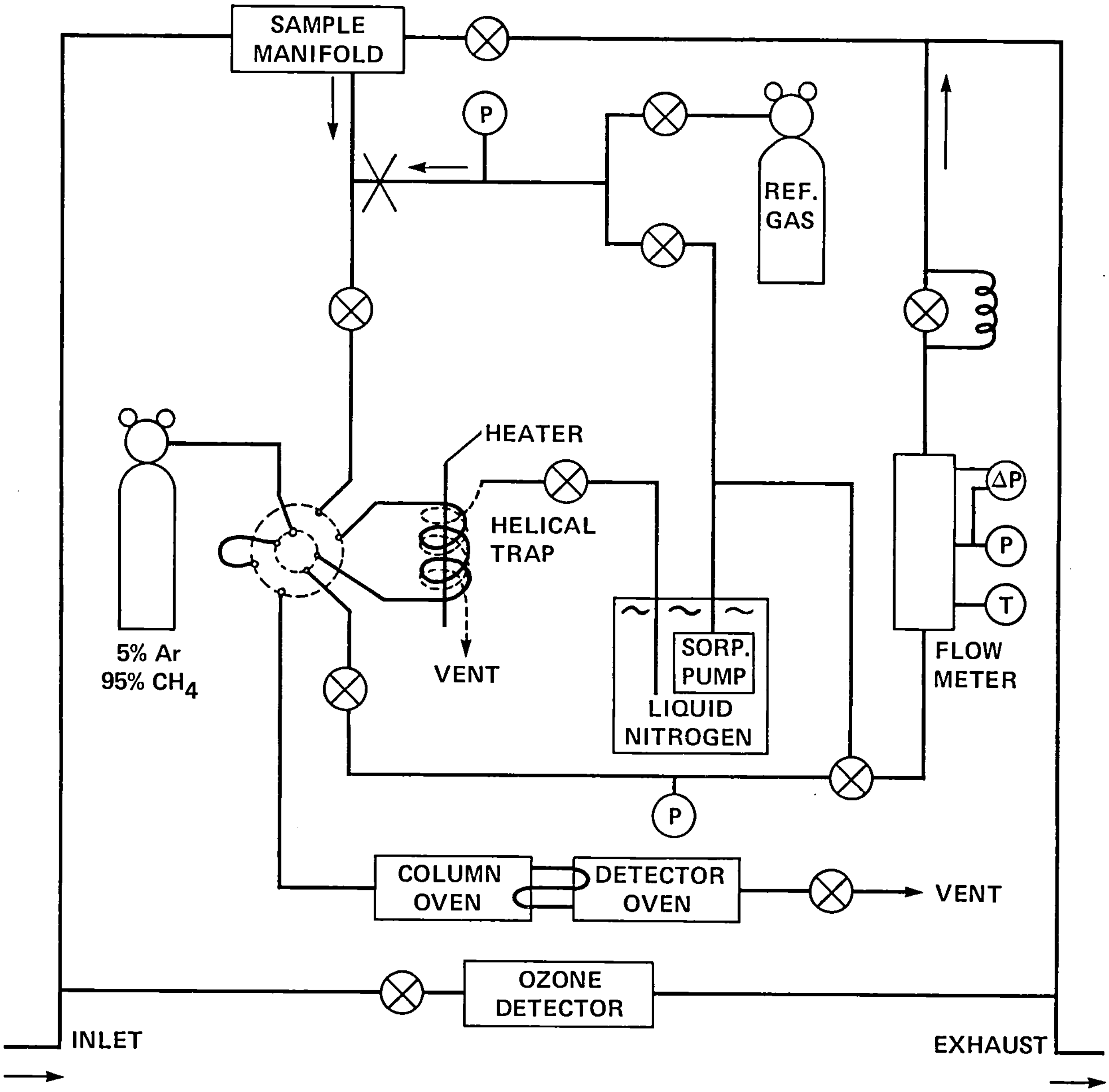

Figure 1.- Flow diagram for the automated airborne gas chromatograph and ozone detector.

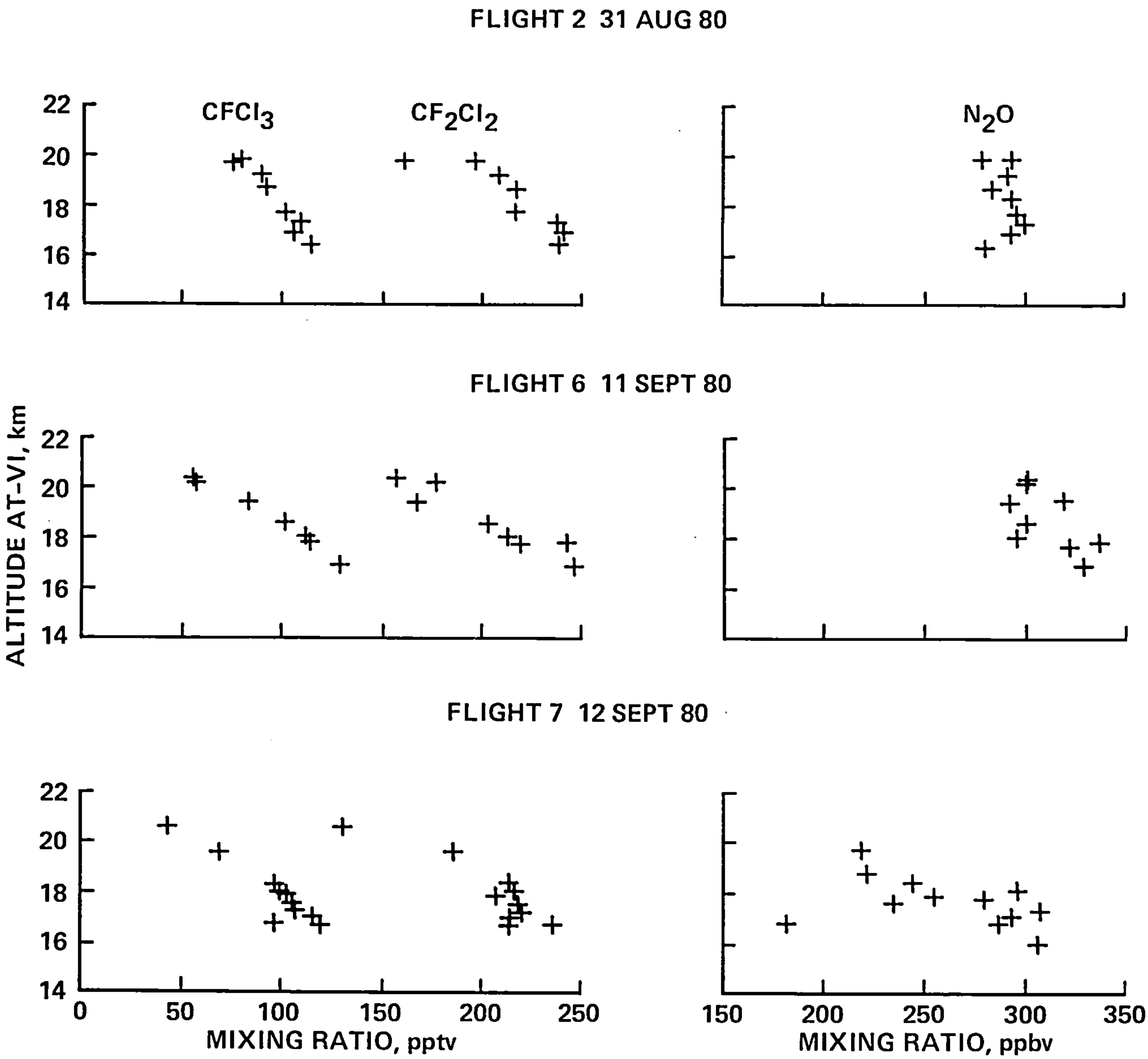

Figure 2.- The mixing ratios are displayed as a function of the pressure altitude of the aircraft. For comparison, in January 1980, at ground level at the South Pole and at a site in the Pacific northwest in January 1980, Rasmussen et al. (1981) give values of 284 pptv and 322 pptv for CF_2Cl_2, and 166 pptv and 188 pptv for $CFCl_2$, respectively. The best estimate for N_2O is probably a value between 298 and 305 ppbv (Connell et al., 1980; Goldan et al., 1981; Weiss, 1981). The mean height of the tropopause was between 15 and 16 km.

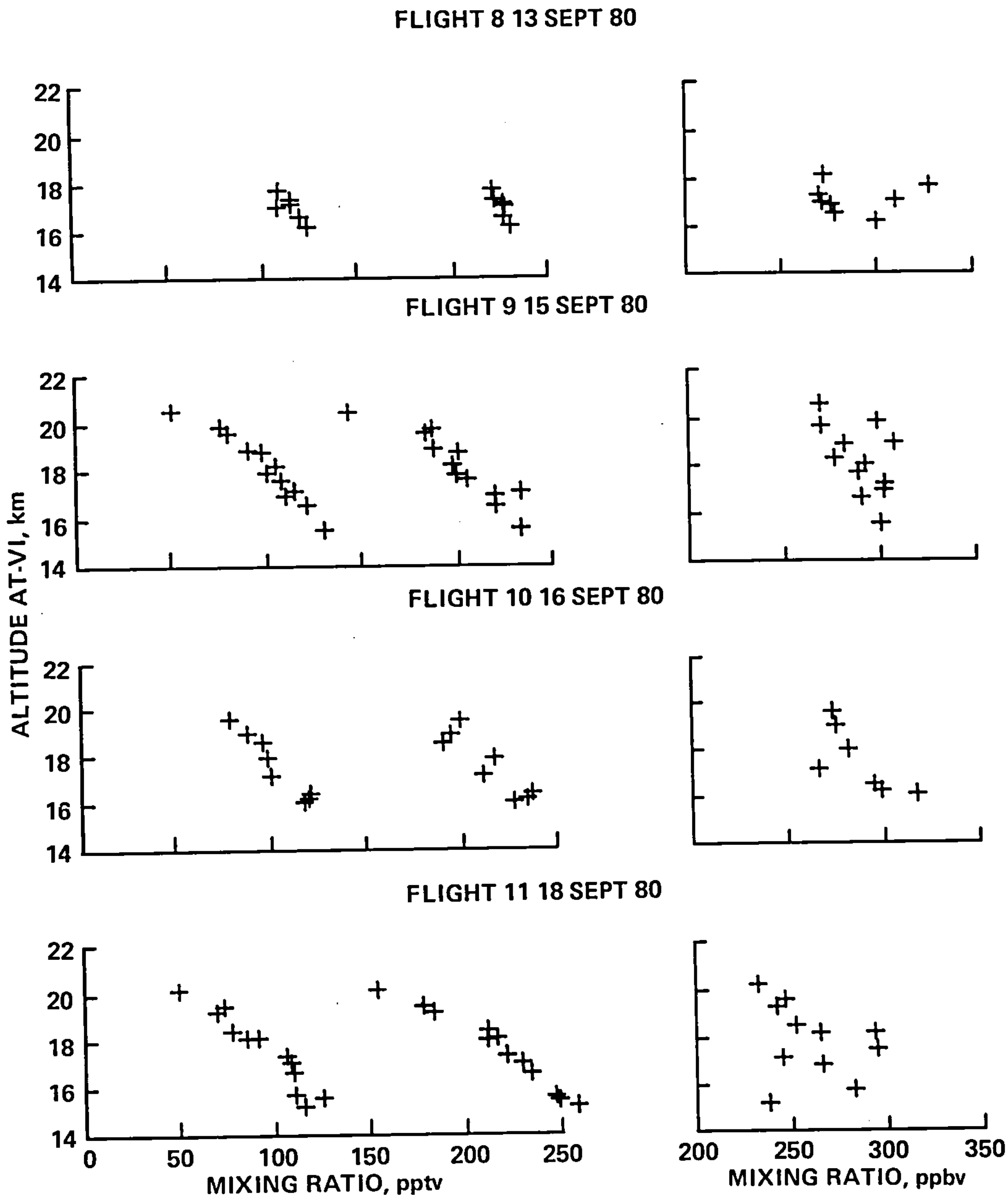

Figure 2.- Concluded.

UNIVERSITY OF DENVER SPECTROMETER AND FROST-POINT MEASUREMENTS DURING THE 1980 PANAMA STRATOSPHERE-TROPOSPHERE EXCHANGE EXPERIMENT

D. B. Barker,* J. Kosters,* D. B. Murcray,* and H. J. Mastenbrook†

EQUIPMENT AND OPERATIONS

The primary University of Denver instruments carried in the U-2 right wing pod during the 1980 Panama program were a liquid-helium-cooled infrared spectrometer to measure the overburden of various minor atmospheric constituents (emphasis on nitric acid) and a specially adapted frost-point unit to measure in situ water vapor. A secondary mission to study thunderhead-top temperatures was attempted with the last-minute addition of a down-looking filter radiometer and a pilot-controlled mirror carriage which permitted the spectrometer to look down rather than at the normal 13° above the horizon. All instrumentation was controlled and monitored by integral electronics and programmer (the pilot manipulated on-off and mirror-control switches) and data were stored on an attached recorder.

The helium-cooled emission spectrometer normally looks at right angles to the flightpath with a field of view of 1° vertical and 4° horizontal. Molecular radiation from the atmosphere enters through a zinc selenide window, is scanned by a grating, and focused onto copper-doped germanium detectors. Primary emphasis for this program was on a long-wavelength channel scanning, from 8.6 to 15 μm, with an average resolution of about 1.5 cm^{-1} and a normal scan time of 125 sec.

The down-looking mirror and carriage were mounted outside the wing pod in a streamlined fairing but rigidly attached to the spectrometer window through the pod opening to preclude relative vibrations. Under pilot control, a motor-driven lead screw would slide the mirror in front of the spectrometer window permitting spectra of cloud-top radiation patterns to be recorded. The down-looking filter spectrometer was a modification of an existing balloon instrument with a 2-μm-wide filter centered at 12 μm. It was mounted on the recorder frame looking down through a hole in the bottom of the wing pod. Output became erratic during the initial California test flights; the integrated pyroelectric detector/preamplifier failed before any useful data were obtained in Panama.

The frost-point instrument was an optical unit of the type developed by Mastenbrook (1968) for use on balloons. Air passes through a small chamber containing a cryogenically cooled metal mirror and the frost buildup from moisture in the air can be monitored by a light source/photocell assembly. A small heater on the mirror, controlled by the photocell, holds the temperature at a level that will maintain a specified frost thickness. A measure of the mirror temperature is then a direct frost-point measurement. The unit was modified for use on the U-2 by increasing the cryogen hold time, converting to liquid nitrogen as the cryogen, and adding interface electronics to record the data on the Denver U. recorder. The frost-point assembly was mounted on the front of the spectrometer in the wing pod. Air was ducted to the optical head through stainless steel tubing from a modified Rosemont probe (enlarged orifice) which was mounted on the nose cone; exhaust was vented into the rear of the pod.

---

*U. of Denver, Denver, Colorado.
†Naval Research Laboratory, Washington, D.C.

A nationwide problem with production and distribution of liquid helium in the summer of 1980 forced us to acquire the cryogen from an untested source. The 500-liter Dewars that were supplied were either filled without adequate prechilling or had an excessive loss rate and arrived in Panama with a significantly reduced volume. This, coupled with a slight vacuum leak which developed in the spectrometer cryostat causing above-normal liquid helium use for each cooldown, restricted our spectral studies to the first three flights. The spectrometer performed well and significant data for HNO_3 profiles or cloud top spectra or both were obtained on the three missions.

Mechanical and electronics problems affected the frost-point unit on the first two flights; pilot-switching errors caused a freeze up on the third and seventh. In general, this first program with the unit in a high-humidity situation caused operational difficulties (in spite of the remarkable effectiveness of the Ames dehumidified tent) which required several modifications of equipment and procedures before reliable operation was achieved. The range of frost points measured, compared with those reported by Mastenbrook (1972) at higher latitudes, seems at first too large; however, the operational procedures (including the programmed, periodic clearing and refrosting of the mirror) and the data have been carefully examined and there is no indication that the instrument was not operating properly. Flights 4, 5, 6, and 11 produced useful humidity profiles along with other interesting observations on the dynamic processes occurring around and above the large cumulus buildups.

DATA AND RESULTS

Water-vapor mixing-ratio profiles calculated from the frost-point data are shown in figure 1. Because this is a relatively new application of this instrument, we do not have enough data under various operating conditions to be sure of the time response to sudden changes in mixing ratio, although the data plotted in figure 2 for selected times during flight 11 begin to give some estimate of time response if we can interpret the pilot's remarks at point D as a step-function entrance into the cirrus layer. However, the points plotted are only those which could be calculated from data taken when the U-2 was in level flight with the resulting stable temperature and pressure. Both the level-to-level and flight-to-flight variations are greater than those measured by Mastenbrook (1972) for extended, stable air masses and seem to reflect localized, dynamic conditions. The points marked with an exclamation point (!) represent flight regions where the pilot remarked (on the in-flight voice recorder) that the U-2 was going through thin cirrus or going through what appeared to be "blowoff" from the top of a collapsing thunderhead cell or in a region of turbulence and uplift related to an unstable, rising air mass. In terms of general atmospheric activity, flight 5 was made on a day when the pilot reported many cells punching up through the cirrus in the general region; at the highest point (near 21 km) he reported an uplift that carried the U-2 about 300 m higher than the previously obtainable maximum. Conversely, on flight 11 the same pilot noted an almost complete lack of active cells above the cirrus except for a few points at the beginning of the flight; the lowest two points on the curve, near 15 and 16 km, were taken at the end of the last descending profile in an unsuccessful search for active cells.

Although the 1980 flights were not controlled, step-ascents as were those flown in 1977, enough altitudes were covered in flights 1 and 2 to allow the calculation of vertical profiles of nitric acid concentration. The data shown in figure 3 are the overburden of HNO_3 molecules at each altitude at which the U-2 was held steady for

several spectral scans. Data from two Panama flights in 1977 and two Alaska flights in 1979 are shown for comparison.

Figure 4 shows the results of one pass over a storm cell with the down-looking mirror inserted in front of the spectrometer window. The U-2 was at 20.5 km; the pilot estimated the cloud top at about 15.5 km. The aircraft traveled about 5 km during the time of each scan, with the spectrometer viewing a cloud area of approximately 1.5×6.0 km. Figure 4(a) is a plot of four sequential records of spectral radiance as the U-2 flew over the top of the cell, with the expected radiance of a black body at four temperatures shown for reference. The semiperiodic variations in radiance are probably a result of small calibration errors; nonhomogeneity in cloud temperature and emissivity are also possible causes of variability. Figure 4(b) shows a satellite infrared scan of the area about one-half hour before the time of the pass, indicating the temperature range associated with each of four different shadings. Figure 4(c) shows the next IR scan in sequence (taken just after the pass), indicating on the flight track the position from which each spectral scan was taken. The good correlation between satellite and spectrometer temperatures suggests that this is a potentially useful technique for thunderhead studies. Narrowing the spectrometer field of view and decreasing the scan time would improve spatial resolution; the addition of a filter radiometer could improve the calibration accuracy.

The authors would like to thank F. J. Murcray for the early modifications on the frost-point unit, T. Dow for operations in Panama, and J. Van Allen for assistance in data processing.

REFERENCES

Mastenbrook, H. J.: Water Vapor Distribution in the Stratosphere and High Troposphere. J. Atmos. Sci., vol. 25, 1968, p. 299.

Mastenbrook, H. J.: Concurrent Measurements of Water Vapor and Ozone over Washington, D.C., during 1969 and 1970. Report 7489, Naval Research Laboratory, Washington, D.C., 1972.

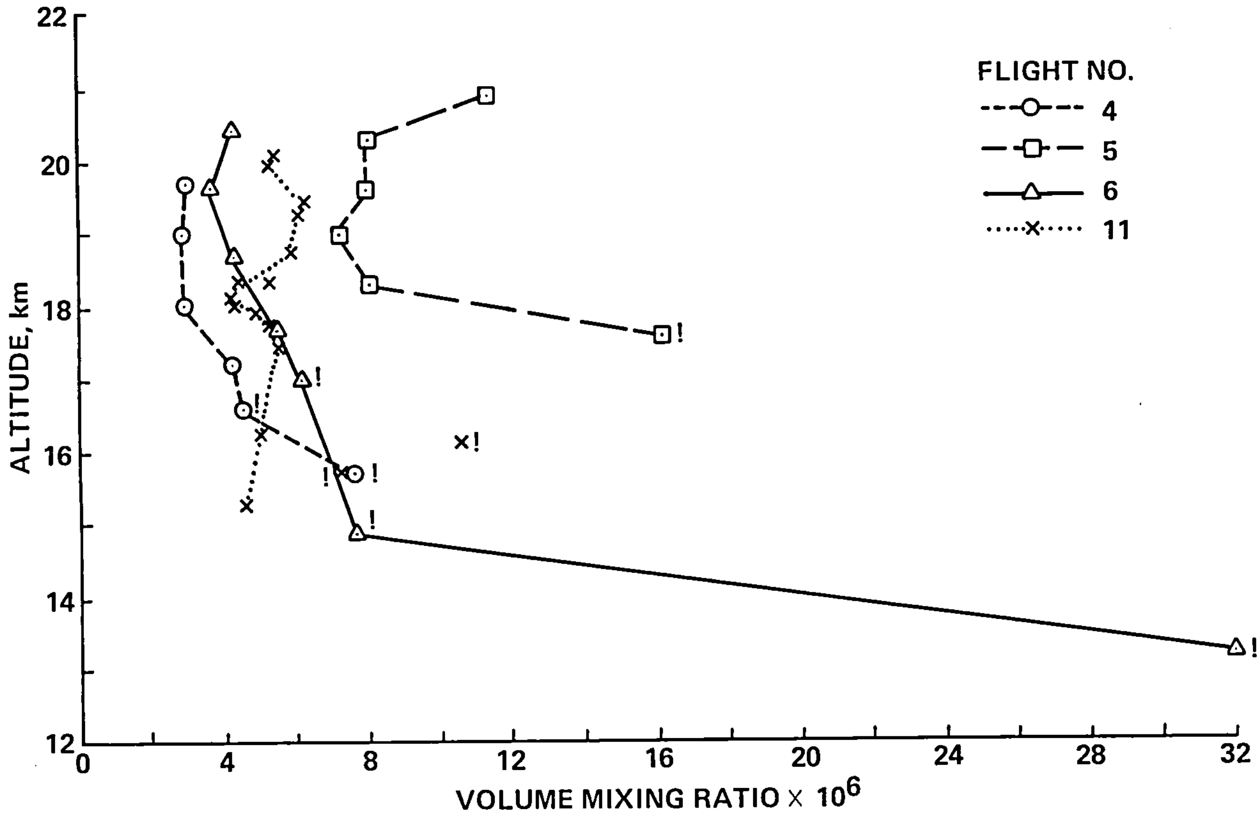

Figure 1.- Water-vapor volume mixing-ratio profiles for flights 4, 5, 6, and 11. Exclamation point indicates that the U-2 pilot recorded being in cirrus clouds.

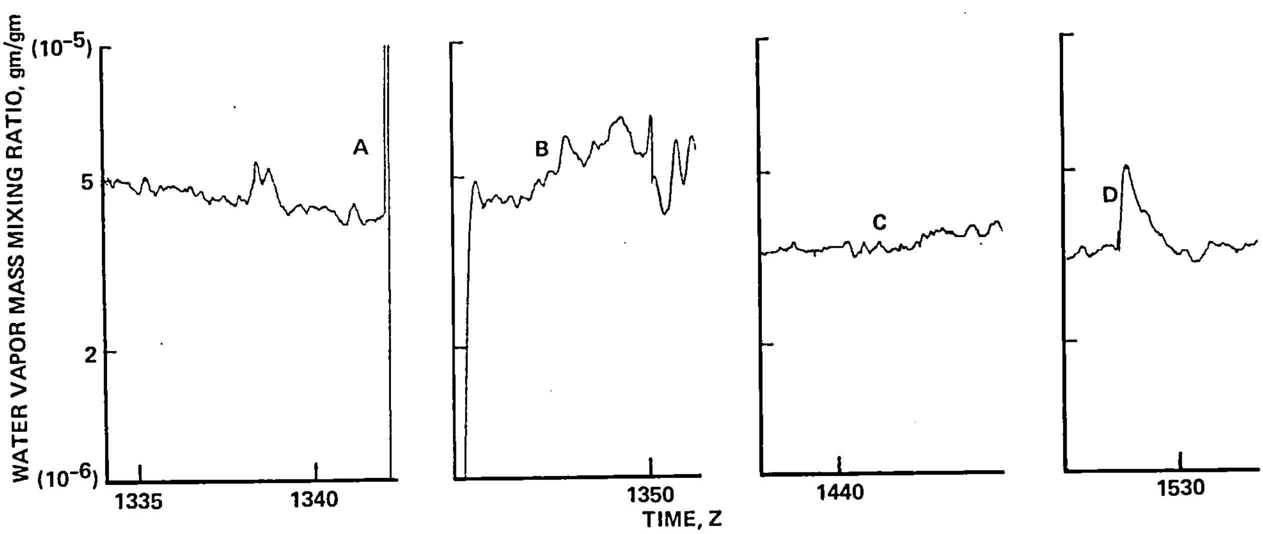

Figure 2.- Mass mixing ratios calculated from recorded frost-point temperatures for selected times during flight 11. A: periodic mirror clear and renucleation; B: (pilot) "I'm just in the top of the cirrus. . ."; C: (pilot) "I'm climbing slowly through 65.7 kft (20 km)"; D: (pilot) "I'm into the top of that cirrus. . . about 52 kft (15.8 km) and a light to moderate turbulence. . ."

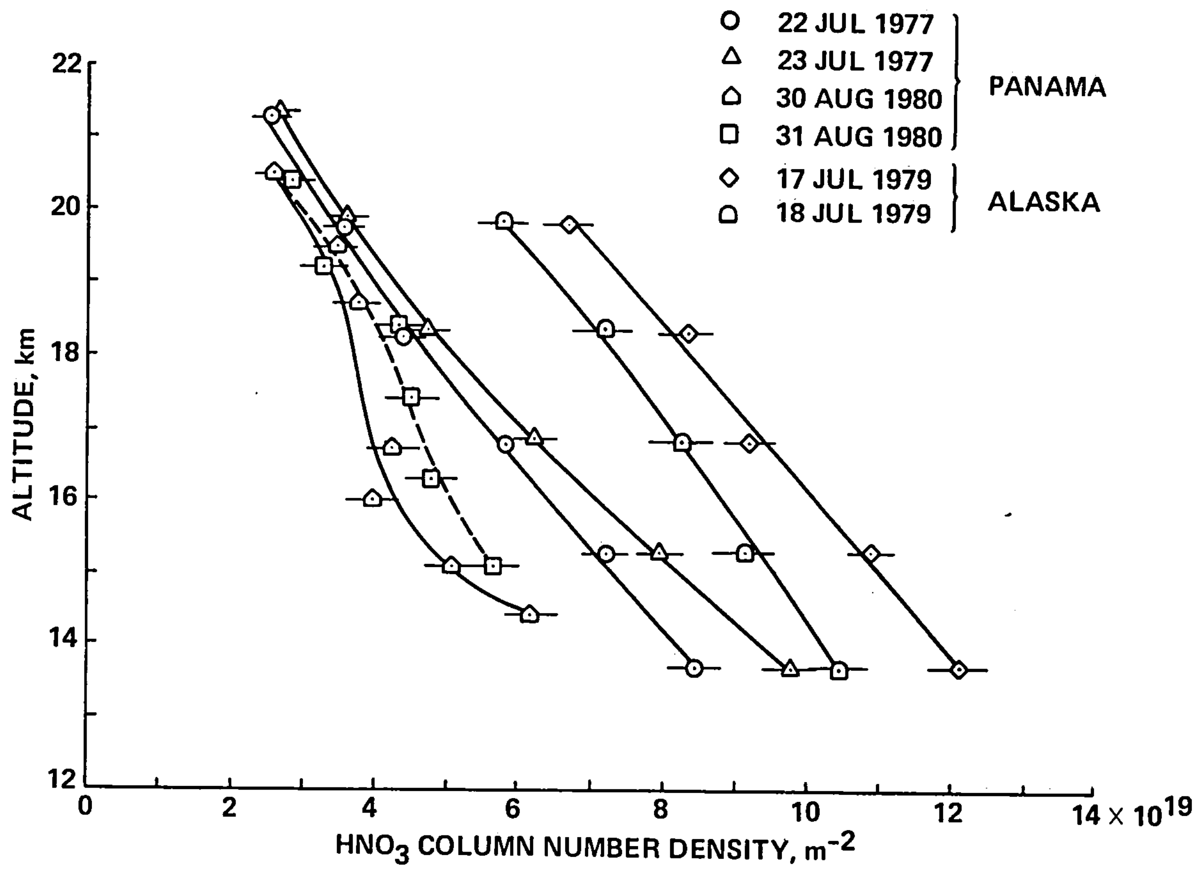

Figure 3.- Nitric acid vertical profiles.

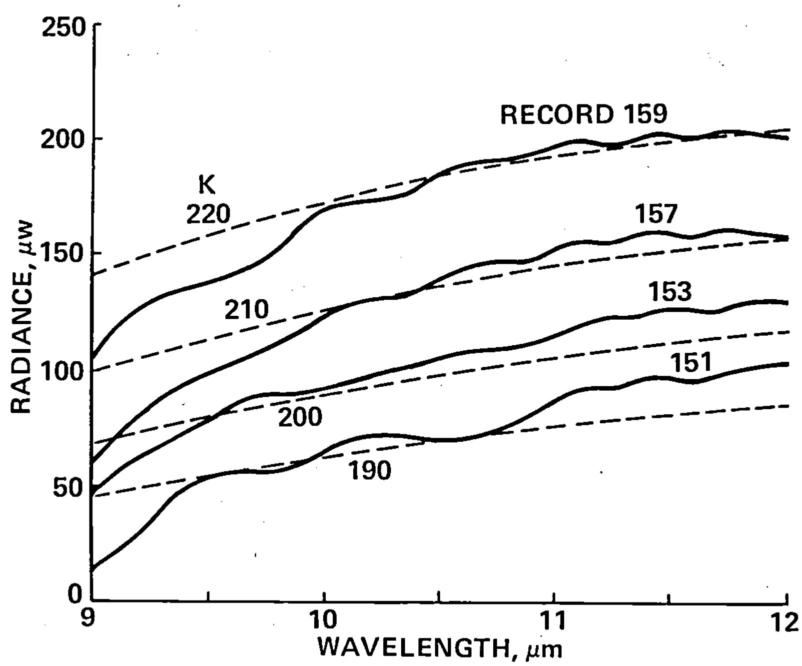

(a) Cloud top radiance scans; dotted curves are calculated black-body radiance at indicated absolute temperatures.

Figure 4.- U-2 aircraft and satellite measurements of storm cell.

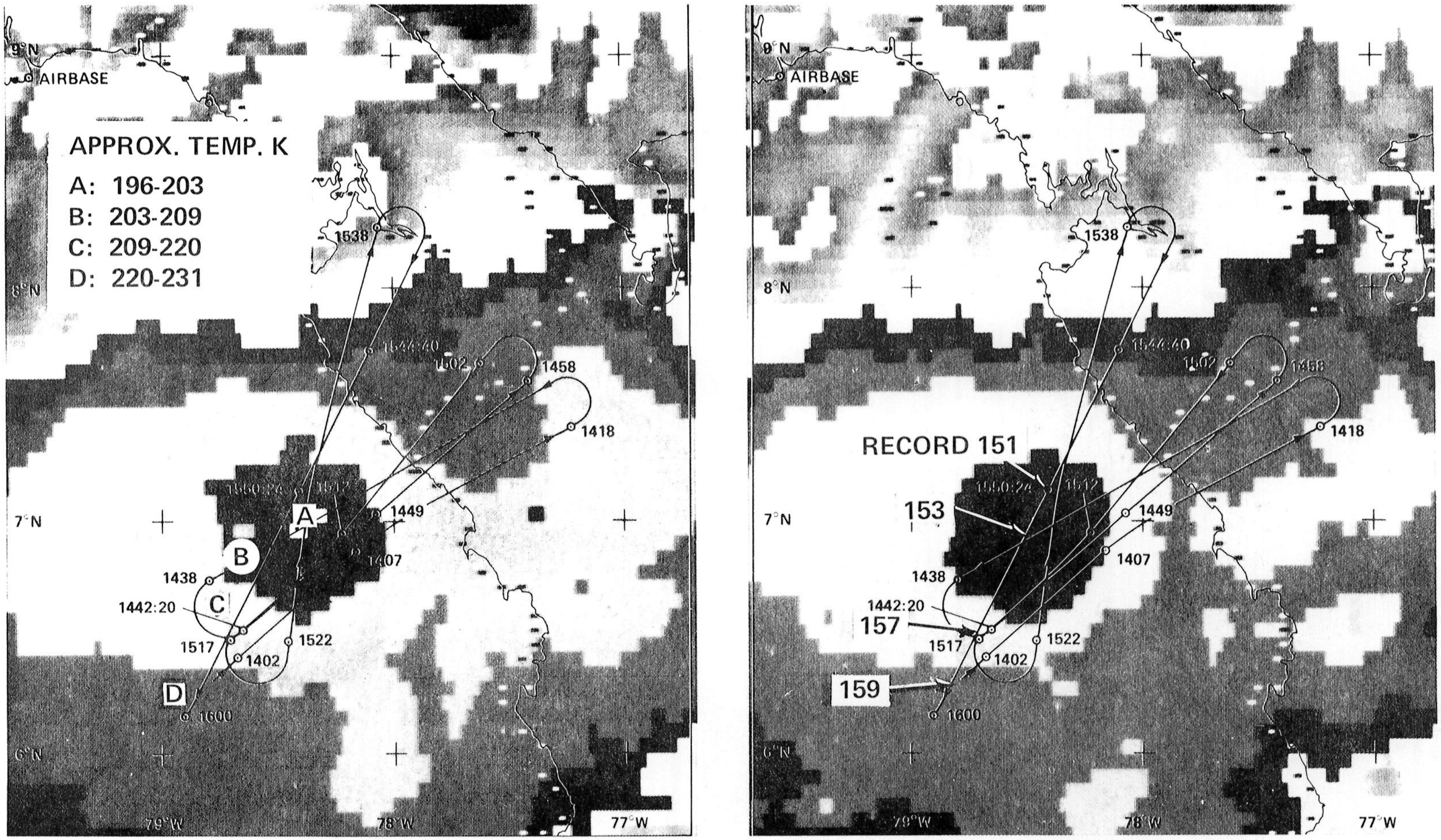

1533 UT, INFRARED

(b) Satellite infrared scan showing indicated temperature ranges.

1605 UT, INFRARED

(c) Satellite infrared scan showing monitored areas along flight track.

Figure 4.- Concluded.

ALTITUDE VARIATIONS IN STRATOSPHERIC AEROSOLS OF A TROPICAL REGION

Jindra Goodman,* K. G. Snetsinger, G. V. Ferry, N. H. Farlow,

H. Y. Lem,† and D. M. Hayes†

SUMMARY

To investigate the possibility that significant amounts of tropical tropospheric air may be convectively introduced into the stratosphere, aerosol samplings over Panama were made at various altitudes, using a highly efficient wire-impactor collector. The percentage of particles with diameters less than the mean mode decreases with height above the tropopause, suggesting depletion of small particles, possibly because of coagulation. Larger aerosols (diameters greater than 0.3 μm) are more abundant farther above the tropopause, indicating growth, mainly by condensation. Total particle concentration decreases with increasing height above the tropopause, and also with increasing temperature. Aerosols containing smaller-size particles are thus found closer to the tropopause, and larger-size, more-evolved aerosols occur at higher altitudes. These data indicate that convective activity at the intertropical convergence zone may be a source mechanism for stratospheric aerosols.

INTRODUCTION

It has been pointed out that the upward-flowing branch of the Hadley cell moves significant amounts of tropical tropospheric air into the stratosphere (Reiter, 1975). As argued by Reihl and Malkus (1958), this upward flux of mass does not occur as a continuous, relatively slow motion. Instead, updrafts that penetrate through the tropopause into the stratosphere are concentrated in narrow "hot towers" of cumulus convection. If this is the case, and if stratospheric aerosols originate as small tropospheric particles, then one should find a relatively high concentration of small particles in the tropical stratosphere. The Panama Water Vapor Exchange Experiment, 1980, provided an excellent opportunity to test this aerosol evolution theory.

METHODS

Aerosol particles were collected in the lower stratosphere by a NASA U-2 aircraft. The sampling device (Farlow et al., 1979) was exposed below the aircraft wing outside the boundary layer, and particles were collected by direct impaction on carbon-coated, 0.075-mm-diam palladium wires. A sampling time of 1 min was sufficient to obtain adequate numbers of particles for size-distribution analysis. After samples were returned to the laboratory, a scanning electron microscope was used to examine the wire surfaces, at 10,000X. Particle sizes and concentrations were manually determined by photographic methods. Details on data reduction methods are given by Farlow et al. (1979) and Oberbeck et al. (1981). Collections were made during the first 2 weeks of September 1980, in a rectangular region bounded by lat. 7.5° N and 11° N and long. 77° W and 81.5° W.

---

*San Jose State University, San Jose, California.
†EAL Corporation, Richmond, California.

SYNOPTIC SITUATION

During the period of sampling, equatorial circulation within the intertropical convergence zone (ITCZ) (as the ITCZ is typically positioned over Panama) was disturbed by several hurricanes in the upstream Atlantic region. The tropopause was typically located between 130 to 110 mbars, and pronounced wave motions in the temperature field were observed in the lower stratosphere (fig. 1). Wave periods averaged 3-3.5 days, with temperature variations of ±5°C. Wind speeds ranged from 3 to 12 m/sec with a predominant easterly component in the lower stratosphere. The U-2 aircraft pilots often reported individual cloud turrets penetrating well into the stratosphere, and minimum temperatures were recorded near cells. Above these areas of penetration, pilots typically experienced turbulence or wave-like motions or both.

DATA ANALYSIS AND RESULTS

The objectives of this study were to analyze stratospheric particles, to study the dynamics of their growth, and to correlate the results with possible microphysical processes. Therefore, the data were compiled and presented in a format that would help reveal the effects of these processes. Specifically, plots of radius versus concentration were generated, these being the principal variables. Processes of interest are nucleation, coagulation, condensation, evaporation, and sedimentation, the most important of which in our sampling range ($r \gtrsim 0.03$ μm) being thermal (Brownian) coagulation and condensation growth. Brownian coagulation, which affects the smallest particles most, causes the concentration of these particles to decrease with time. Condensation growth (or loss by evaporation) is dependent on the water-vapor pressure and hence is temperature-dependent; concentration of sulfuric acid vapor is also important. Thus, particles can grow or evaporate as conditions vary, and the largest particles can be affected by sedimentation. Because all these processes are dependent on environmental conditions and time, we analyzed aerosol samples with respect to temperature and distance from the tropopause. If it is accepted that the tropical troposphere is a source region for stratospheric aerosols, then particles in upper levels should represent more evolved aerosols.

The summer tropical tropopause is the level of the coldest atmospheric temperature. Temperature increases with height in the lower stratosphere, but also frequently fluctuates ±5°C because of wave motions (fig. 1). For this reason we find it more convenient to study size changes of aerosol particles as a function of temperature, instead of using direct distance above the tropopause, as was done by Oberbeck et al. (1981) for polar areas. The samples discussed here were taken in the temperature range from -79.3°C to -61.7°C, and at tropopause distances that varied between 400 m to 5550 m, respectively. Actual sampling altitude and the temperature at the time of collection are identified in figure 1, and other pertinent data regarding the samples are shown in table 1.

Theoretical models (Hamill et al., 1977; Turco et al., 1979; and Toon et al., 1979) assumed that coagulation and condensation are important processes that owing to growth, reduce the number of particles with radii < 0.05 μm. The 0.05-μm-radius size range roughly corresponds to the statistical average mode of our aerosol distributions. Modes of the sampled aerosols ranged from 0.0576 to 0.077 μm but did not shift noticeably with altitude. To simplify statistical analysis and avoid additional errors caused by slight mode variations, the mean mode of 0.0689 μm was used. The

percentage of particles in the size range less than or equal to the mean mode is plotted versus temperature in figure 2. The plot shows a decrease in number of small particles as temperature increases or as distance from the tropopause increases. The correlation coefficient (0.82) is statistically significant at the 1% significance level (analysis of variance test). The data show that there is a significant depletion of small particles. Since the total number of particles decreases (fig. 3), together with the number of small particles below the mode (fig. 2), coagulation is the most likely process responsible for this trend of decreasing particle concentration with increasing altitude and temperature.

We examined concentration variations with temperature of particles with radii >0.15 μm; these are affected mostly by condensation growth. The percentage of these larger particles increases with increasing temperature (see fig. 4), and the correlation coefficient of 0.67 is still statistically significant. Loss of particles owing to sedimentation is not an important process here, because of small sedimentation velocities: at 20 km a particle of $r = 0.64$ μm has a sedimentation velocity of only 3.25×10^{-2} cm/sec. Typical size distributions of the aerosols, one taken close to the tropopause (0.4 km above) and the other far from the tropopause (5.5 km), are presented in figure 5. These graphs also suggest that large particles are more abundant farther above the tropopause.

All the data strongly suggest that particle sizes of stratospheric aerosols increase with increasing temperature (or distance from the tropopause) and are controlled by the microphysical processes of coagulation and condensation.

DATA COMPARISONS

Because of differences in aerosol sampling methods it is difficult to directly compare results obtained by different techniques. Our results regarding concentration per cubic centimeter, concentration per milligram of air, and particle size ratios (table 1) are, however, consistent with the findings of Farlow et al. (1979) over Panama in 1976 and 1977. Further, concentrations of large particles agree quite well with the results obtained by Rosen et al. (1975), who used a two-channel photoelectric particle counter which detects particles having radii greater than 0.15 μm and those greater than 0.25 μm. Analysis of Aitken nuclei (AN) in tropical and subtropical regions by Podzimek et al. (1977) indicated that large fluctuations occurred in the concentration of AN. Sometimes these concentrations exceeded 150/cm^3 in the ITCZ above mountainous thunderheads, which is further evidence that the tropical troposphere is a source region of stratospheric particles. Our measurements suggest that background concentration of AN was relatively low, rarely exceeding 20/cm^3 at an altitude of 18 km. We are, however, unable to measure particles with radii smaller than 0.03 μm.

Compared with other latitudes (Bigg, 1976; Gras and Michael, 1979; Farlow et al., 1979 and 1981; Ivlev and Ogorodnikov, 1975), aerosol size distributions for tropical aerosols show fewer large particles and higher concentrations of smaller particles.

CONCLUSION

The Panama aerosol results strongly indicate that convective activity in the ITCZ is a source region for stratospheric aerosols. Young aerosols with high concentrations of small particles are found close to the tropopause; larger, more mature aerosol particles are located at upper levels.

REFERENCES

Bigg, K. E.: Size Distributions of Stratospheric Aerosols and their Variations with Altitude and Times. J. Atmos. Sci., vol. 33, 1976, pp. 1080-1086.

Farlow, N. H.; Ferry, G.; Lem, H. Y.; and Hayes, D. M.: Latitudinal Variations of Stratospheric Aerosols. J. Geophys. Res., vol. 84, 1979, pp. 33-743.

Farlow, N. H.; et al.: Comparison of Stratospheric Aerosol Measurements over Poker Flat, Alaska, July 1979. Geophys. Res. Lett., vol. 8, 1981, pp. 15-17.

Gras, J. L.; and Michael, C. G.: Measurements of the Stratospheric Aerosol Particles Size Distribution. J. Appl. Meteor., vol. 18, 1979, pp. 855-860.

Hamill, P.; Toon, O. B.; and Kiang, C. S.: Microphysical Processes Affecting Stratospheric Aerosol Particles. J. Atmos. Sci., vol. 34, 1977, pp. 1104-1119.

Ivlev, L. S.; and Ogorodnikov, B. I.: Nature of Aerosol in the Upper Atmospheric Layers. Meteorologicheshiye Issledovaniya, vol. 22, 1975, pp. 26-33 (in Russian).

Oberbeck, V. R., Farlow, N. H.; Ferry, G. V.; Lem, H. Y.; and Hayes, D. M.: A Study of Stratospheric Aerosol Maturity. Geophys. Res. Lett., vol. 8, 1981, pp. 18-20.

Podzimek, J.; Sedlacek, W. A.; and Brookshaberl, J.: Aitken Nuclei Measurements in the Lower Stratosphere. Tellus, vol. 29, 1977, pp. 116-127.

Reiter, E. R.: Stratospheric-Tropospheric Exchange Processes. Rev. Geophys. and Space Phys., vol. 13, 1975, pp. 459-474.

Riehl, H.; and Malkus, J. S.: On the Heat Balance of the Equatorial Trough Zone. Geophysica, vol. 6, 1958, pp. 505-538.

Rosen, J. M.; Hofmann, D. J.; and Laby, J.: Stratospheric Aerosol Measurements. II. The Worldwide Distribution. J. Atmos. Sci., vol. 32, 1975, pp. 1457-1462.

Toon, O. B.; Turco, R. P.; Hamill, P.; Kiang, C. S.; and Whitten, R. C.: A One-Dimensional Model Describing Aerosol Formation and Evolution in the Stratosphere. II. Sensitivity Studies and Comparison with Observations. J. Atmos. Sci., vol. 36, 1979, pp. 718-736.

Turco, R. P.; Hamill, P.; Toon, O. B.; Whitten, R. C.; and Kiang, C. S.: A One-Dimensional Model Describing Aerosol Formation and Evolution in the Stratosphere. I. Physical Processes and Mathematical Analogs. J. Atmos. Sci., vol. 36, 1979, pp. 699-771.

TABLE 1.- 1980 PANAMA AEROSOL DATA

Date, Sept. 1980	Sampling height, km	Distance above tropo-sphere, km	Tempera-ture, °C	Number of particles with r, >0.03 μm/cm^3	Number of particles with r, >0.15 μm/cm^3	Mixing ratio, >0.03 μm/mg air	Mixing ratio, >0.15 μm/mg air	Ratio, >0.15/>0.25	Mass,[a] μg/m^3
7	18.3	3.3	-79	19.9	3.7	172	32	2.9	0.52
7	19.0	4.0	-71	22.3	3.6	214	35	4.4	.39
9	16.0	.4	-77	18.1	.9	108	5.0	--	.10
9	17.6	2.0	-69	14.0	2.7	108	21	2.9	.33
9	20.2	4.6	-62	10.0	2.4	116	28	5.2	.23
11	17.8	3.0	-72	18.1	4.1	144	33	3.2	.63
11	18.8	4.0	-67	13.7	2.1	128	20	4.3	.25
11	19.6	4.8	-63	7.6	2.1	80	22	3.9	.22
12	18.3	3.8	-67	15.8	3.5	136	30	2.6	.52
15	17.9	2.8	-69	15.4	3.2	124	26	3.2	.39
15	20.6	5.6	-62	7.2	1.6	91	21	7.3	.14

[a]Assumes aerosol content of 75% H_2SO_4.

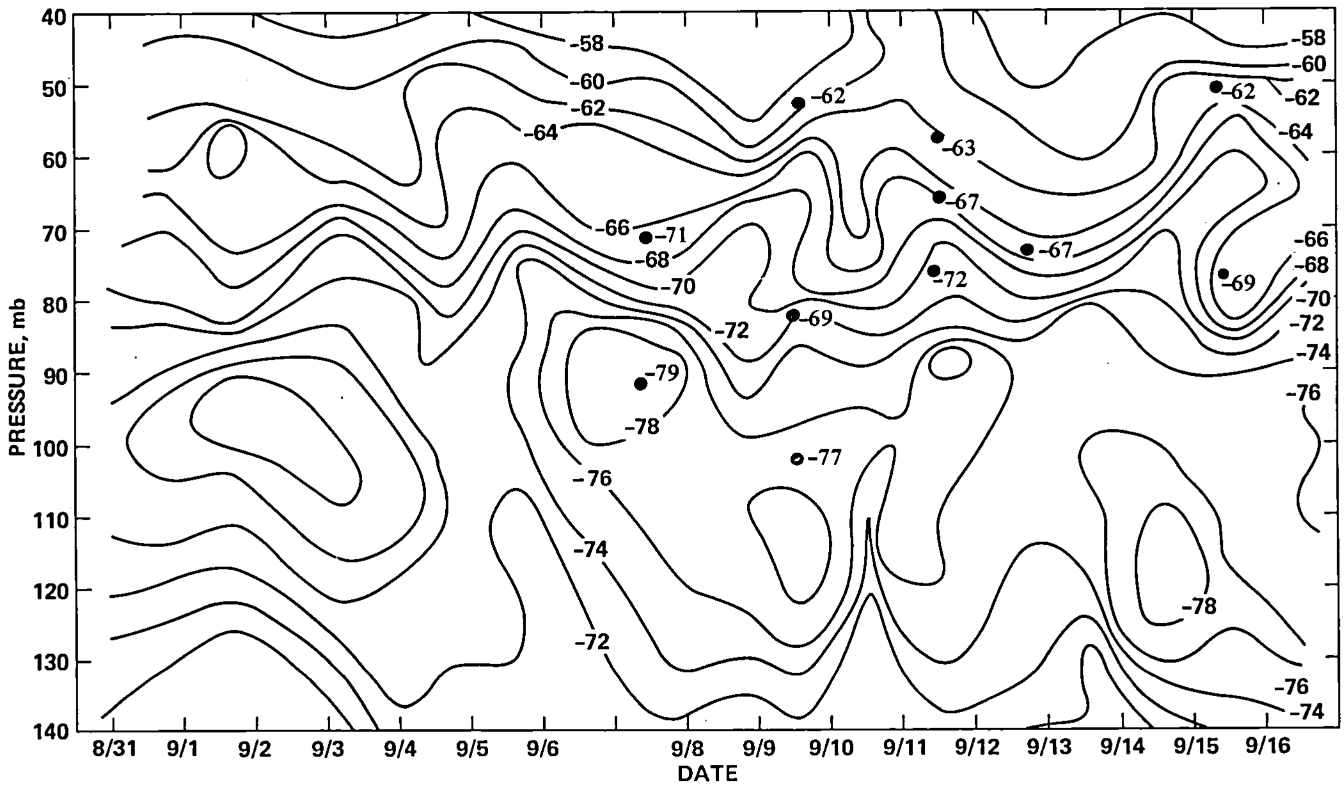

Figure 1.- Vertical cross section of thermal structure of upper troposphere and lower stratosphere at Panama from August 8 to September 16, 1980. Isotherms were constructed from radiosonde data taken two to four times a day. Dots represent the actual location of aerosol samples and temperature during sampling is indicated next to the dot. Note wave structure above about 80 mbars.

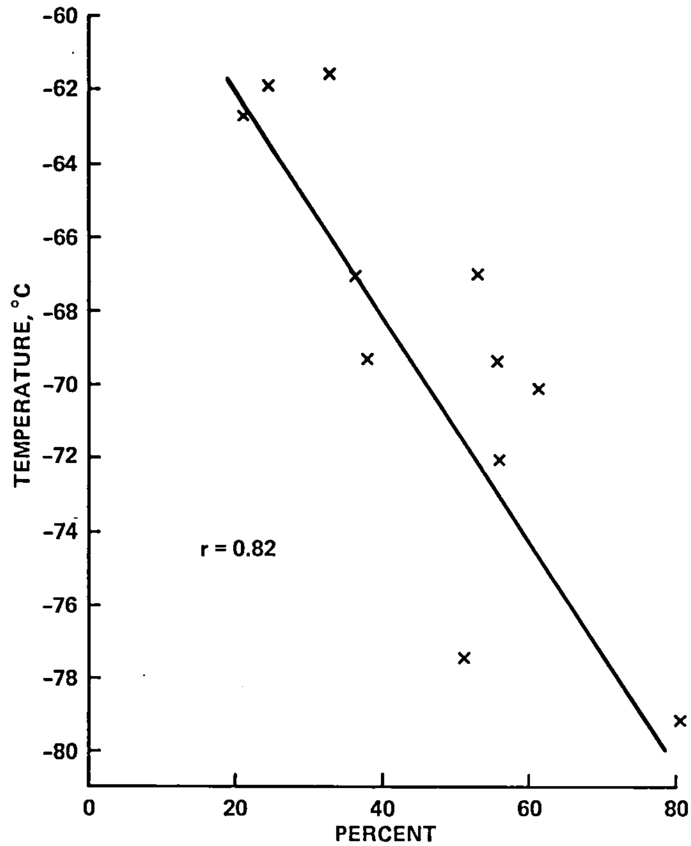

Figure 2.- Normalized distribution of particles with radii less than the mode, plotted against temperature.

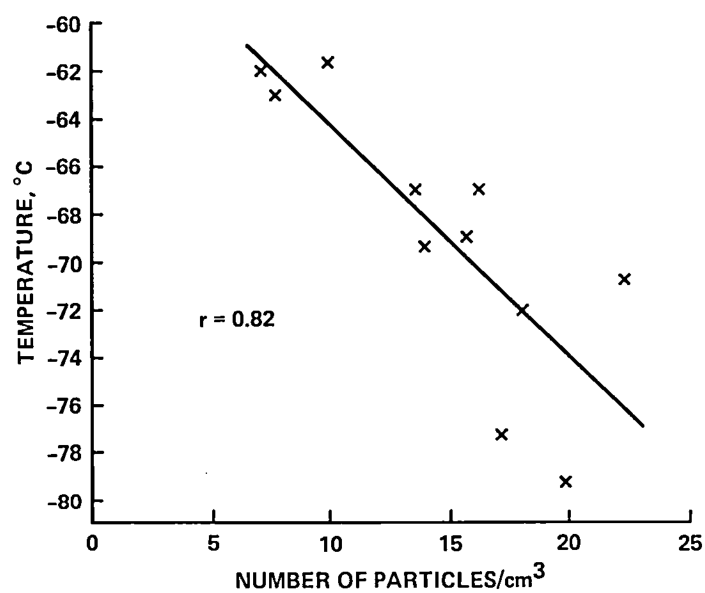

Figure 3.- Variation in total particle concentration plotted against temperature.

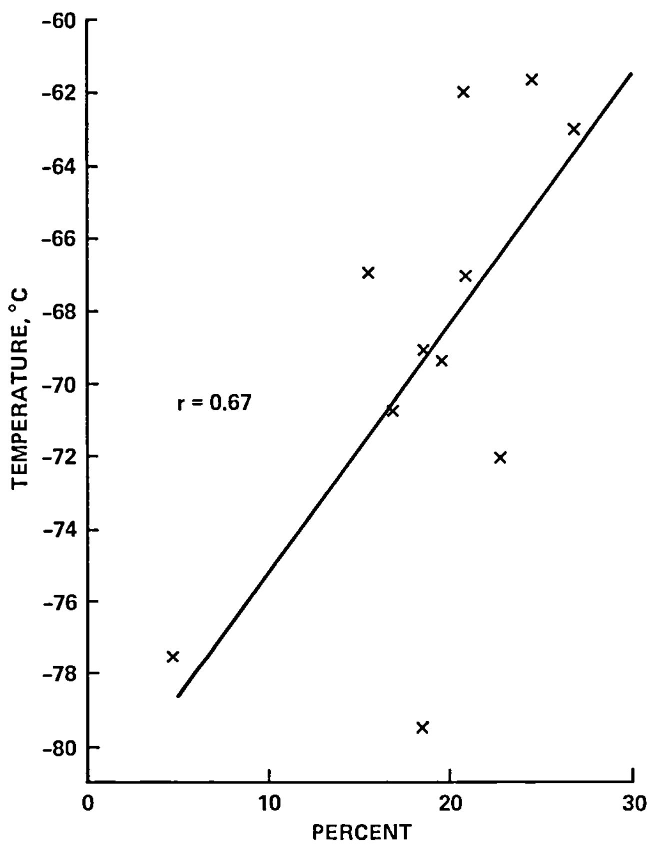

Figure 4.- Normalized distribution of particles with radii larger than 0.15 μm, plotted against temperature.

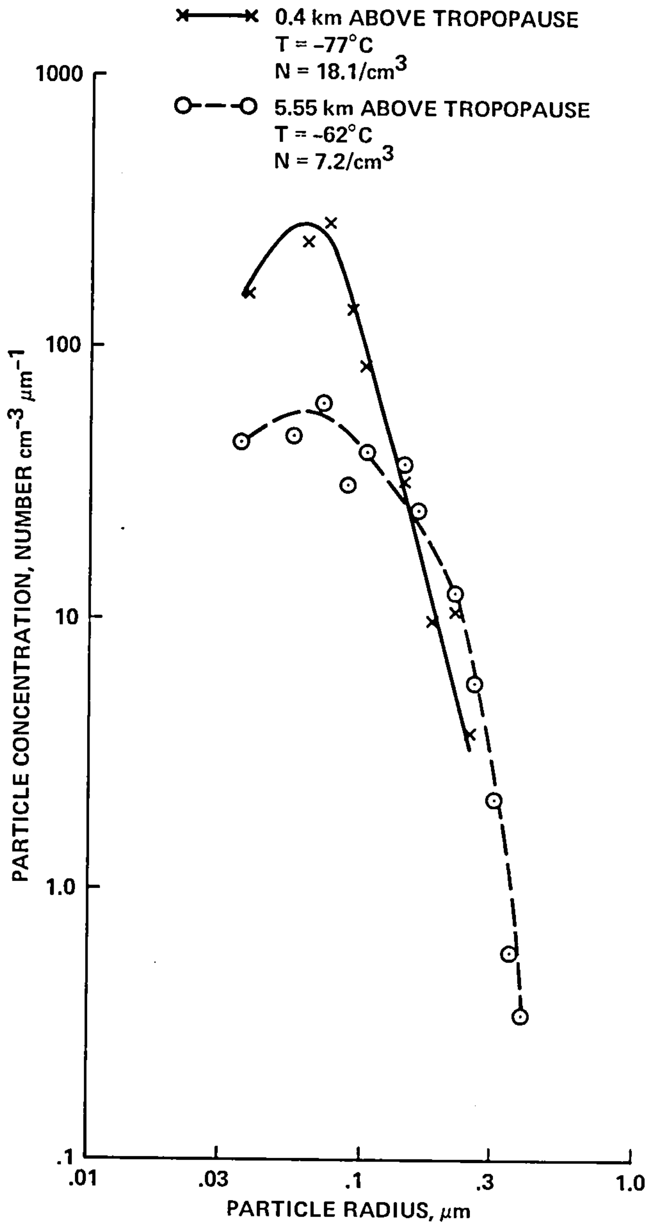

Figure 5.- Stratospheric aerosol size distributions for September 9 and September 15, 1980, over Panama. On September 9, the sampling temperature was -77°C and the distance above the tropopause was 0.4 km; on September 15 sampling temperature was -62°C and the distance from the tropopause was 5.5 km.

MEASUREMENTS OF STRATOSPHERIC AEROSOLS AND TROPOSPHERIC/STRATOSPHERIC ICE-CRYSTAL POPULATIONS DURING THE 1980 PANAMA TROPOSPHERIC/ STRATOSPHERIC WATER-VAPOR EXCHANGE EXPERIMENT

Robert G. Knollenberg,* Albury J. Dascher,* and Dale Huffman*

INTRODUCTION

The observed dryness of the stratosphere is thought to be the result of a tropopause "cold trapping" of vertically transported moisture. Robinson (1978) believes that the stratospheric water vapor, although controlled by the tropical tropopause as suggested by Dobson et al. (1946), is primarily injected by large cumulonimbus towers in regions of the highest/coldest tropopause heights and lowest water-vapor abundances. The effect of such thunderstorms on water-vapor transport and ultimate hydration or dehydration of the stratosphere depends to a great extent on the life cycle of ice crystals transported through the tropopause.

The particle-size spectrometer experiment flown for the tropospheric-stratospheric water-vapor exchange experiment on the NASA U-2 aircraft was primarily designed to provide information on the ice-water mass budget at near tropopause levels. For this purpose an imaging instrument called a 2-D Grey Imaging Probe, manufactured by Particle Measuring Systems, Inc. (PMS), Boulder, Colorado, was used. This device captures two-dimensional shadow images of particles and either stores or processes these images as size-distribution parameters. The 2-D Grey Imaging Probe covered sizes of 40-2500 µm and operated in situ, sampling volumes of ~20 liters/min. A second objective of the particle-size spectrometer experiment was to quantify the aerosol size distribution and to define roles it may directly play in assisting the maintenance of a dry stratosphere or as a tracer of other processes operating. The instrument used for aerosol measurements was an "active cavity" aerosol spectrometer. This aerosol probe employs an active laser cavity and a parabolic collector of large solid angle, operating on an aerodynamically focused aerosol sample stream to size particles in a 0.1-3.0-µm-size range at sample flows of 2 cm^3/sec. Data from these measurements were logged on small magnetic tape cassettes, the recording rates programmed for periods up to 8 hr. The entire instrument package was located in the forward half of a wing-tank pod. The rear of this pod housed the water-vapor hygrometer of Kley et al. (1983). We will first describe the instrument package in detail and discuss the theoretical and empirical calibration procedures. Measurements of the ice-water and aerosol budgets are then presented, followed by interpretations of the results obtained and conclusions drawn.

DESCRIPTION OF PARTICLE-SIZE SPECTROMETER INSTRUMENTATION

The two particle-size spectrometers used on the U-2 are uniquely different devices. One is an imaging instrument whereas the aerosol probe operates through light scattering. About the only common aspect of the two is their laser light source. The imaging probe was mounted in the forwardmost location in the wing tank

---

*Particle Measuring Systems, Inc., Boulder, Colorado.

pod with its optical viewing volume ahead of flow disturbance (see fig. 1). The active scattering aerosol spectrometer draws air samples through a Rosemount air sampling probe which is skin-mounted below the wing tank. A block diagram of the particle spectrometer experiment is shown in figure 2. A central data acquisition system services both probes and records other analog data. We will first describe the 2-D Grey Imaging Probe.

The 2-D Grey Imaging Probe is a recent variant of the standard two-dimensional probe described by Knollenberg (1976a). Both instruments are generically optical array spectrometers (Knollenberg 1970). An optical array spectrometer sizes shadows of particles imaged by a laser-fed optical system, using a linear array of photodetector elements (see fig. 3). The shadow size can be simply determined by knowing optical magnification, array element spacing, and the number of elements occulted during a particle's transit through the laser beam. A maximum projected dimension colinear with the array is measured. Two-dimensional optical array spectrometers yield two-dimensional data. Here, thresholding circuitry determines when the leading edge of a shadow enters the array (typically 32-64 elements) and serial shadow (or no shadow) data are taken from each array element in parallel, in the form of "image slices" containing 1's for shadow data and 0's for no-shadow data. The image slices are taken at rates up to 5 MHz and thus can develop 20-μm resolution at 100-m/sec particle velocities. Examples of two-dimensional image data are shown in figure 4. Typically, 1024 bits of storage are available per each array element. Double buffering precludes data loss during unloading cycles. The 2-D Grey Imaging Probe differs from the above instrument in two primary ways: (1) the array has 64 instead of 32 elements, and (2) four levels of shadow density (gray) information are encoded. Image samples for the 2-D Grey Imaging Probe (hereinafter simply imaging probe) are shown in figure 5.

The active scattering aerosol spectrometer (hereinafter aerosol probe) was integrated with the data acquisition system shown in the photograph in figure 6. This instrument employs aerodynamic focusing of the inlet sample air with a filtered sheath flow which constrains the sample flow to a well-defined jet as it intersects the laser beam. This intersection is located at the focus of a 5-mm parabolic mirror which provides a scattered light collecting angle of 2.2π sr (see fig. 7). The resulting large collection angle, combined with the high-intensity beam of the open-cavity laser arrangement, provides for sizing particles with diameters down to 0.1 μm and a response that is fairly insensitive to particle shape and refractive index (see fig. 8).

The intensity of the laser beam is monitored from leakage through the end mirror of the laser plasma tube with a photodiode detector. The signal from this detector becomes the reference signal to the pulse-height analyzer (PHA) and also is recorded on one of the analog inputs to the data system. The scattered light from each particle collected by the parabolic reflector is focused by an aspheric lens onto another photodiode detector whose signal output becomes the scattered light signal to the PHA.

The PHA is basically a flash converter whose output is latched in 1 of 32 conditions following the occurrence of each scattered light pulse. Each condition corresponds to 1 of 31 size classes plus an oversize class for all particles with diameters larger than 3 μm. The size classes are log-weighted over the range of 0.1 to 3 μm, with 0.012-μm resolution at the small-size end and 0.311-μm resolution at the large-size end.

Since each scattered light pulse is compared with the reference light signal in each case to determine the particle size, accurate sizing can be maintained over a wide range of laser intensity. This makes the spectrometer insensitive to normal laser aging and slight optics contamination which can reduce laser intensity.

The internal aerosol probe draws its air sample from an externally mounted Rosemount air-sampling probe which is mounted on the bottom of the forward portion of the main tank skin (fig. 1). A short section of tubing brings the sample air from the Rosemount to the sample inlet which is located at the bottom of the main package just above the Rosemount when the main package is installed in the wing tank. The aerosol particles are required to make a right-angle bend to enter the sample section. Experience has shown that any such inlet will fractionate at some aerosol particle size. Tests described in the next section indicated fractionation above sizes of 1 μm but good performance at submicron sizes.

The data acquisition system (hereinafter DAS) was designed to provide continuous recording of particle-size spectra as generated by the spectrometers and housekeeping analog information. The spectra data are recorded as 10-sec accumulations in 32 size classes for both probes along with data from eight differential analog inputs. The external probe can actually be any standard PMS, aircraft-mountable instrument. When the imaging probe is used, spectra data are generated as 10-sec accumulations in 63 size classes for the external probe. The spectra data for the imaging probe are derived by counting the total number of elements shadowed for each particle image received and classifying the particle according to an equivalent circle diameter for the area determined in each case. We will refer to all imaging probe sizes as equivalent circle diameters throughout this paper. Spectra data are received directly from the aerosol probe as a size code and as an accompanying strobe signal for each particle encountered. An accumulating memory is provided for both probes to total the number of particles received for all size classes during each 10-sec interval. (Actually, a dual memory is employed such that sampling may continue in an alternative memory area while data are recorded from the memory area most recently completed in each case. This allows for continuous sampling at all times for both probes.)

Recording is accomplished on an internal, ruggedized cartridge magnetic tape recorder using standard Scotch DC300A data cartridges. All data are recorded in standard ASCII code with four decimal characters plus a space for all words, except the first 16 size classes of the spectra data for the aerosol probe, which have six-decimal character length.

Image data from the imaging probe are recorded as 64 characters plus a space for each image slice. Each of the 64 characters represents the shadow level of a corresponding element in the photodiode array of the imaging probe as follows:

Character	Shadow level
.	None
:	Minimum
+	Middle
#	Maximum

Examples of such image data from the Exchange Experiment are shown in figure 9.

The number of slices recorded depends on the length of the particle image in each case. Only complete images are recorded, and the amount of image data recorded is limited to provide at least 5 hr of recording on a single tape cartridge. This

results in an average of 48 image slices per minute, which provides important shape/habit information to supplement the spectra data that are accumulated from all images received from the imaging probe.

A special "maximum images" mode, which can be selected by the pilot, allows an average of 1080 image slices per minute to be recorded. If this mode is sustained, only 30 min of recording time per cartridge is possible in a constant 2-D Grey probe activity situation. In either recording mode, the actual recording time will be lengthened if the imaging probe activity is less than the allowable level. In the complete absence of image data, the tape cartridge will last for over 10 hr. Since the data frame length is shorter with an external nonimaging probe, almost 13 hr of recording is possible on a single tape cartridge with other configurations.

This system automatically initializes itself at power turn-on and begins recording data every 10 sec thereafter. An incrementing frame number is recorded in each data frame to uniquely identify each data set. Access to the magnetic tape cartridge is possible, after the nose cone has been removed, without removing the main DAS package from the wing tank. The pilot must log the time of day that power was turned on to the system in order to relate the frame numbers to real time of day for each flight. Once power is turned off to the system it may not be turned on again until the tape cartridge has been removed. Since the system automatically rewinds the tape and begins recording at power turn-on, any previously recorded data will be written over and lost. On several occasions transients on the U-2 power inadvertently initiated rewind.

CALIBRATION AND PERFORMANCE

The imaging and aerosol probes flown aboard the U-2 cannot be truly optimized because of the flight environment. In the case of the imaging probe, the resolution had to be reduced from the nominal 20 μm to 40 μm because of the U-2's higher airspeed. For large hydrometeors this would still provide adequate resolution; however, many of the limited number of recorded images were of 100-200-μm size in the cirrus anvils, and it was necessary to assume that the crystalline habit was the same as for the larger resolved images. Fortunately area-to-mass conversions (see Knollenberg, 1976b) are less sensitive to crystalline habit, the smaller the size. With reference to the aerosol probe we previously mentioned the right-angle bend taken by the sample. Had the forward wing tank nose location not been required by the higher-priority imaging probe, a standard airborne aerosol spectrometer could have been used that uses nearly ideal straight-through sample introduction. To try to quantify anticipated losses in the inlet, two laboratory test series were conducted. First, the Rosemount probe was mounted in the PMS wind tunnel and the fractionation characterized over a range of tunnel airspeeds. Secondly, tests were conducted at simulated U-2 altitudes, using a modeled flow inlet tube having a right-angle bend.

The tunnel tests involved measuring the aerosol size distribution at the tunnel inlet and comparing it with samples taken through the Rosemount air-sampling probe. There, tests revealed no size-distribution distortion that could be attributed to fractionation at tunnel speeds up to 120 m/sec at pressures of about 850 mbars. These results were subsequently verified when the imaging probe was replaced by an FSSP-100 instrument covering the size range of 2-32 μm and by comparison U-2 flights conducted.

The second series of laboratory tests was conducted using a right-angle section of tubing to simulate the flow inside the Rosemount probe. In one respect, these tests are worst-case tests in that the diameter (0.75 mm) of the plumbing was several times smaller than the smallest dimensions within the Rosemount probe. The results at 70 mbars are shown in figure 10. The submicron performance appears satisfactory but fractionation is indicated above 1 μm. The cutoff is fairly sharp, falling to 50% less at 1.4 μm and >90% at 3 μm.

We initially proposed to perform high-altitude flight calibrations of the Rosemount aerosol sampler inlet, using a standard airborne aerosol instrument mounted, in the nose location, to replace the imaging probe. This instrument has no right-angle bend in its inlet but has identical illuminating and collecting optics. Because of demand for this instrument location for probes covering larger sizes (e.g., the FSSP-100), such an intercomparison has not been completed at the time of this writing. The FSSP itself does provide for a reasonable intercomparison of particles larger than 2 μm and several such intercomparisons exist. These results are shown in figure 11 for lower altitudes, where there are generally sufficient large aerosol particles to make such intercomparisons possible. At higher altitudes, statistics are usually too poor to make meaningful comparisons above 2 μm. This was certainly the case in Panama (1980); however, more recently data were taken at altitudes above the continental United States in a region of enhanced large-particle activity and the agreement between the FSSP and aerosol probe appear quite good. In July 1981 an intercomparison between a balloon-borne instrument of Rosen and Hofmann (1981) and the aerosol probe on the U-2 also gave very comparable number densities above 0.3 μm in the 13-18-km region (Rosen and Hofmann, 1981). Thus, it appears that the laboratory results of figure 10, suggesting fractionation above 1.0 μm with cutoff above 2 μm, are too pessimistic. In any case, the Rosemount air-sampling probe has recently been replaced by a probe with a 10:1 diffuser/decelerator and larger tube plumbing to reduce fractionation potential. Initial results indicate little change in performance.

The entire particle-size spectrometer experiment underwent thorough environmental testing before its test flights aboard the U-2. During both of these test periods, temperatures were measured throughout the instrument package. The data revealed that minimum temperatures were typically reached between 30,000 and 40,000 ft, thereafter stabilizing or increasing with higher altitudes. The maximum temperature at that altitude was typically +35°C (in the imaging probe power supply section) and the minimum temperature was -10°C (in the DAS tape cartridge area). No heaters are used within the instrument package; the favorable temperatures are a result of unpressurized operation and self-heating by the electronics. Operating unpressurized requires desiccant packages to prevent condensation during descent but otherwise results in a lower overall weight and power savings.

During operations at Howard AFB in the Canal Zone, preflight calibrations were performed routinely with a quick-look playback of the flight data immediately after retrieval of the tape cartridge. The only problems encountered were tape-rewinds, with partial loss of data on several flights. Housekeeping data showed satisfactory alignment of both spectrometer probes during all flights and nearly identical temperature histories.

RESULTS AND DISCUSSION

The Panama exchange experiment covered the period of August 28 to September 22. In addition to the 11 flights from Howard AFB, data were taken on the ferry flights

from Ames Research Center to Langley Research Center to Howard AFB, and return. Table 1 lists the flights conducted, flight duration, and types of data gathered by the particle-size spectrometer experiment. The only problem encountered was data loss through inadvertent tape rewinds. The exchange experiment flights had a number of goals and only a few of the flights were specified for cumulonimbus cirrus penetrations. A number of flights were clear-air flights designed to provide background data on air-mass parameters in the upper troposphere and stratosphere. Other flights were survey-type flights during which air was sampled above and around rising cloud turrets and anvils. (The U-2 was not designed for thunderstorm penetrations; it is a delicate aircraft, especially when flown near maximum altitude. Pilots were required to fully familiarize themselves with the cumulonimbus buildups in this region without taking unnecessary risks. The first several flights provided this necessary preparation.) The clear-air flights and those without cirrus-anvil penetrations necessarily focused on other experiments, even though the aerosol probe gathered data on all flights. The primary flights involving cirrus-anvil penetrations were flights 7 and 8. It is noteworthy that nearly all flights provided cirrus deck penetrations (although quick ones), for it is difficult to find days without at least thin cirrus shields. These were, however, typically at altitudes of 30,000-45,000 ft and well below the tropopause. We will discuss these penetrations in more detail later.

Aerosols are ever present in the tropical atmosphere whereas ice crystals are restricted to higher altitudes, and then only when moisture permits. Thus, there are many more aerosol samples than cirrus samples. Considering that the aerosol probe develops statistically stable distributions in ~2 min or less at all altitudes, at least 1400 samples could be extracted. Presentation of these extensive data sets is precluded here; however, these data are available from the authors in 1-min averages on hard copy. The ice-crystal data are largely limited to flights 7 and 8 and, to a lesser extent, flights 5 and 6. The cirrus deck penetrations were often too brief to obtain statistically stable penetrations. Samples and summaries of these data are presented here. Detailed data are available from the authors.

Flights 7 and 8 both involved cirrus-anvil penetrations and provided the bulk of ice-crystal data at the higher altitudes (>50,000 ft). Flight 7 revealed four cirrus-anvil penetrations, with two of them in a satellite-selected primary cloud target. Flight 8 included nine penetrations in cirrus anvils. Both flights lasted about 3.5 hr; however, data were lost for about 50 min during flight 7, which included most of the second pass through the primary cirrus-anvil target. The first pass was completely documented.

Since flight 8 provided continuous data, involved the largest number of cirrus-anvil penetrations, and generally depicts the observed aerosol observations, we have presented a selected data set for its full duration in figure 12. Figure 12 shows the altitude, temperature, and number and mass densities from the aerosol and imaging probes. Several features of these data are worth amplifying. Takeoff is obvious from the rapid rise in altitude and drop in aerosol number-density from $10^3/cm^3$ to $1\text{-}10/cm^3$ at 15 km. Penetration through the cirrus deck is indicated by increases in aerosol and imaging probe mass. However, note that the aerosol number-density is near minimum values in this region. The slight positive correlation in aerosol and imaging probe number-densities is attributed to small ice crystals transmitted by the Rosemount probe. The cirrus-anvil penetrations at altitudes of 15-18 km and temperatures ranging from 195 K-205 K, show lower ice-water contents (imaging probe mass density) than during the lower cirrus deck penetrations by approximately an order of magnitude. The values for cirrus-anvil penetration are a few hundredths of a gram per cubic meter, maximum. Most of the mass within these anvils was concentrated in

particles less than 100 μm in diameter; the largest were about 150 μm in diameter. This contrasts with sizes of 1 mm in the cirrus deck just below. A comparison of the size distribution in the cirrus-anvil and cirrus deck is shown in figure 13. The aerosol populations show only small changes in number-density during cirrus-anvil penetrations but fairly large increases in mass. The latter is attributed to small (near-micron) sized ice crystals. The submicron aerosol population shows interesting spectral features; however, we will defer additional discussion of the aerosol data.

Flight 7 included two penetrations in a cirrus anvil, including the best sample for extensive study of water-vapor exchange. Unlike the penetrations in flight 8, which involved aged anvils, this was a newly formed anvil still growing at penetration time. Only the first of the two penetrations was fully recovered by this experiment. Data for a 25-min period associated with this cloud are shown in figure 14. The ascent and descent profiles were very similar to those of flight 7. The first penetration was at 16.4 km, where the temperature was 194 K. The number-density of both ice crystals and aerosol increase dramatically within this cirrus anvil. Maximum crystal sizes of 1 mm were observed, with ice-water contents of several hundredths of a gram per cubic meter. The mass distribution for this first penetration is presented in figure 15. The distribution is bimodal, with greater mass at sizes above 100 μm than below. This bimodality correlates with the pass structure, showing the small crystals concentrated in the first part of the pass and the larger crystals in the second half of the pass. The median mass size averages 400-500 μm. The crystal images produced by the imaging probe shown in figure 9 are identified as bullet rosettes. Rosettes are the most common cirrus crystal, although active anvils at lower altitudes usually reveal a number of heavily rimed structures and frequent graupel.

Turning now to the aerosol data, we previously mentioned that spectral changes are observed during the anvil penetrations. The increase in the number-density of larger aerosol and associated mass is obvious in figure 15. At submicron sizes, spectral features are observed which cannot be related to crystals. First of all, the number-density of submicron particles actually decreases within the cloud. Compare the size and mass distributions before and after penetration in figure 16 for flight 7. The typical mass mode just before penetration is at 0.4 μm. During the penetration, this single mass mode is essentially replaced by a mode at 0.17 μm (excluding values above 1 μm). The other spectral features are statistically noisy. The behavior at 0.17 μm appears to be characteristic of the aerosol within anvil cirrus but not of that in the lower cirrus deck. For instance, figure 17 shows similar distributions just before and during the fifth penetration during flight 8, along with the aerosol population during ascent through the cirrus deck. The overall aerosol population is slightly reduced in the cirrus deck compared with out-of-cloud values. Otherwise there is little difference between in-cloud and out-of-cloud aerosol characteristics. The number-densities are simply much lower within the cirrus deck as compared with the cirrus anvils.

Turning now to the general aerosol population, it is apparent from figure 8 that starting at lift-off from a maximum of about 1000 cm^3 the number density decreases with altitude to just a few per cubic centimeter at sub-tropopause levels and then increases in the stratosphere to a maximum value of 15-20/cm^3. (The U-2 climbs so fast that resolution is poor; however, the same sub-tropopause minimum is evident during descent.) The stratospheric aerosol particles are of some considerable concern as they represent possible "chemical getters" of water via their high H_2SO_4 content. A number of the Exchange Experiment flights concentrated flight time in the 15-22-km region. Number-densities for several of these survey flights are presented in figure 18. A typical maximum number-density of 15-20/cm^3 is found at 18 ±0.5 km. The

corresponding mass profiles are shown in figure 19, including data from flights 7 and 8 as well. Here we have also indicated how the mass mode gradually decreases from 0.45 μm to 0.35 μm between 16 and 21 km. Comparison of size and mass distributions for altitudes of 16, 18, and 20 km are shown in figure 20 for flight 6. These aerosol particles are likely highly concentrated H_2SO_4. The relative humidity varies from 10%-20% in this region and the particles were positively identified as H_2SO_4 droplets via other experiments (see Goodman et al., 1983). The overall stratospheric aerosol burden is much larger than normal background. However, there is probably no significant influence from the eruption of Mt. St. Helens on 18 May 1981. The enhancement is most likely the result of volcanic activity nearer the equator.

CONCLUSIONS

In summary, the particle-size distributions measured during the Exchange Experiment contain information on the ice-water content and aerosol properties at altitudes near and above the tropopause levels. Determining the mass transport of ice water and the fate of ice crystals requires supporting data on parameters of state and air-motion data. Modeling may also be applied to support and test hypotheses relating to stratospheric hydration or dehydration. Thus far, our efforts have been restricted to examining suggestive operative mechanisms using growth/sublimation rate computations coupled with inferred fall velocities. Comparisons of in-anvil and out-of-anvil aerosol spectra have been used to estimate stratospheric entrainment also.

REFERENCES

Danielson, E.; Bleck, R.; and Morris, D.: Hail Growth by Stochastic Collection in a Cumulus Model. J. Atmos. Sci., vol. 29, 1972, pp. 135-155.

Dobson, G. M. B.; Brewer, A. W.; and Cwilong, B. M.: Meteorology of the Lower Stratosphere. Proc. R. Soc. of London, Ser. A, vol. 185, 1946, pp. 144-175.

Goodman, J.; et al.: This publication, 1983.

Kley, D.; et al.: This publication, 1983.

Knollenberg, R. G.: The Optical Array: An Alternative to Extinction and Scattering for Particle Size Measurements. J. Applied Met., vol. 9, no. 1, 1970, pp. 86-103.

Knollenberg, R. G.: Three New Instruments for Cloud Physics Measurements: The 2-D Spectrometer Probe, and the Active Scattering Aerosol Spectrometer. Am. Met. Soc., International Conf. on Cloud Physics, 1976a, pp. 554-561.

Knollenberg, R. G.: The Response of Optical Array Spectrometers to Ice and Snow: A Study of 2-D Probe Area-to-Mass Relationships. Final Report, Mar. 22-June 30, Air Force Geophysics Laboratory, AFGL-TR-76-9273, 1976b.

Knollenberg, R. G.; and Luehr, R. E.: Open Cavity Laser "Active" Scattering Particle Spectrometry from 0.05 to 5 Microns. Fine Particles, Aerosol, Generation Msmt., Sampling & Analysis, Benjamin Y. H. Lui, ed., Academic Press, May 1975, pp. 669-696.

Robinson, G. D.: Water Vapor in the Lower Stratosphere. EOS, vol. 59, 1978, p. 1085.

Rosen, J. M.; and Hofmann, D. J.: Results of Instrument Comparisons for the July 1981 Ace Mission. Report No. AP-69, U. of Wyoming, Laramie, Wyo., 1981.

TABLE 1.- 1980 PANAMA U-2 FLIGHT SUMMARY

Flight number	1980 date	Total hours	Data hours	Remarks
Ferry	8/26	5.26	5.26	Moffett to Wallops
Ferry	8/28	5.49	4.03	Wallops to Howard
1	8/30	3.45	3.45	Background survey flight
2	8/31	3.09	1.42	Background survey flight
3	9/03	3.43	0.26	Clear-air flight
4	9/07	2.53	2.53	Background survey flight
5	9/09	3.20	3.20	Cloud survey flight
6	9/11	3.53	2.75	Cloud survey flight
7	9/12	3.46	2.58	Cirrus-anvil flight
8	9/13	3.11	3.11	Cirrus-anvil flight
9	9/15	3.68	3.68	Background survey flight
10	9/16	2.50	2.50	Background survey flight
11	9/18	3.33	2.79	Clear-air flight
Ferry	9/21	5.34	5.34	Howard to Wallops
Ferry	9/22	5.97	4.96	Wallops to Moffett

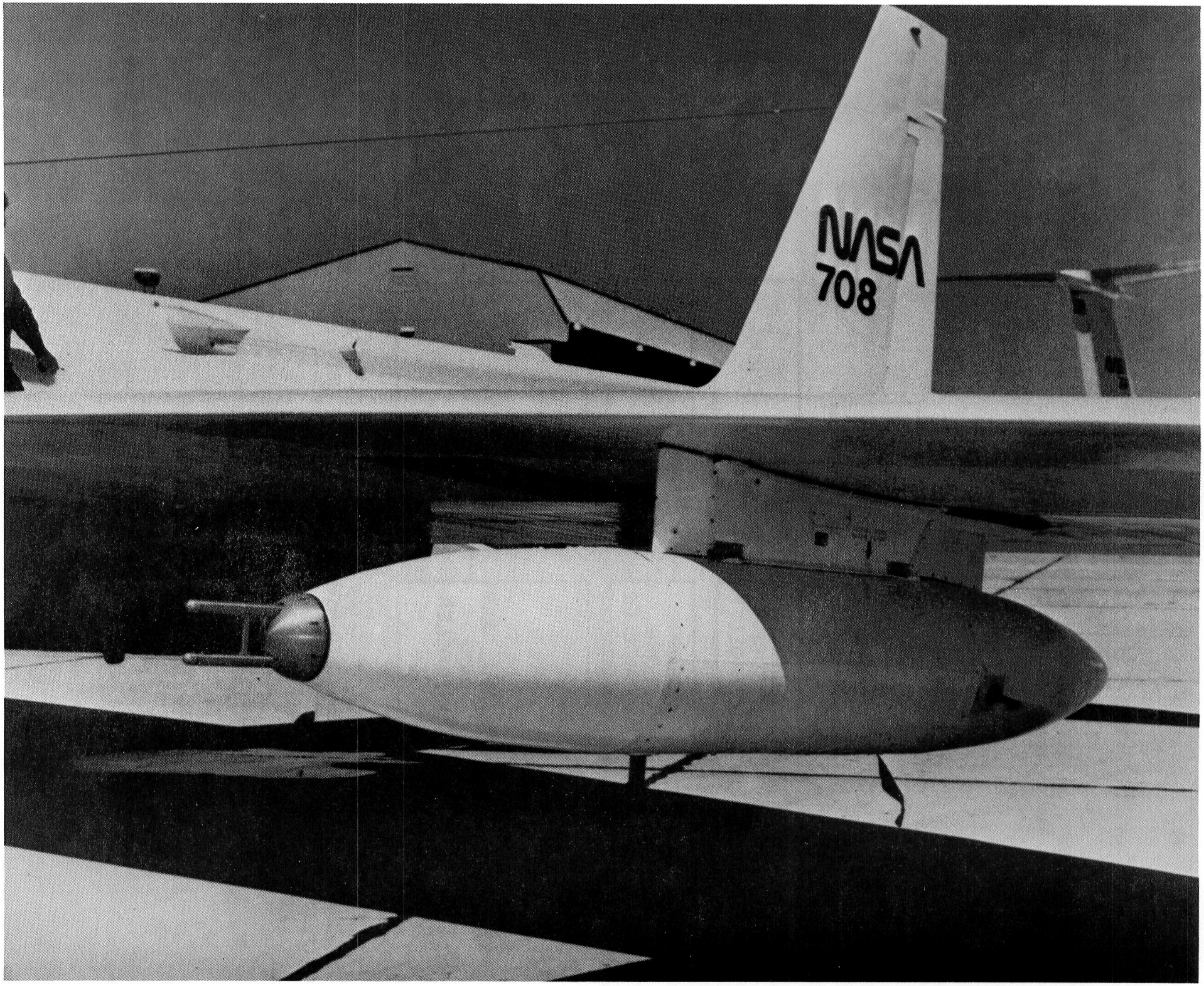

Figure 1.- U-2 particle spectrometer experiment.

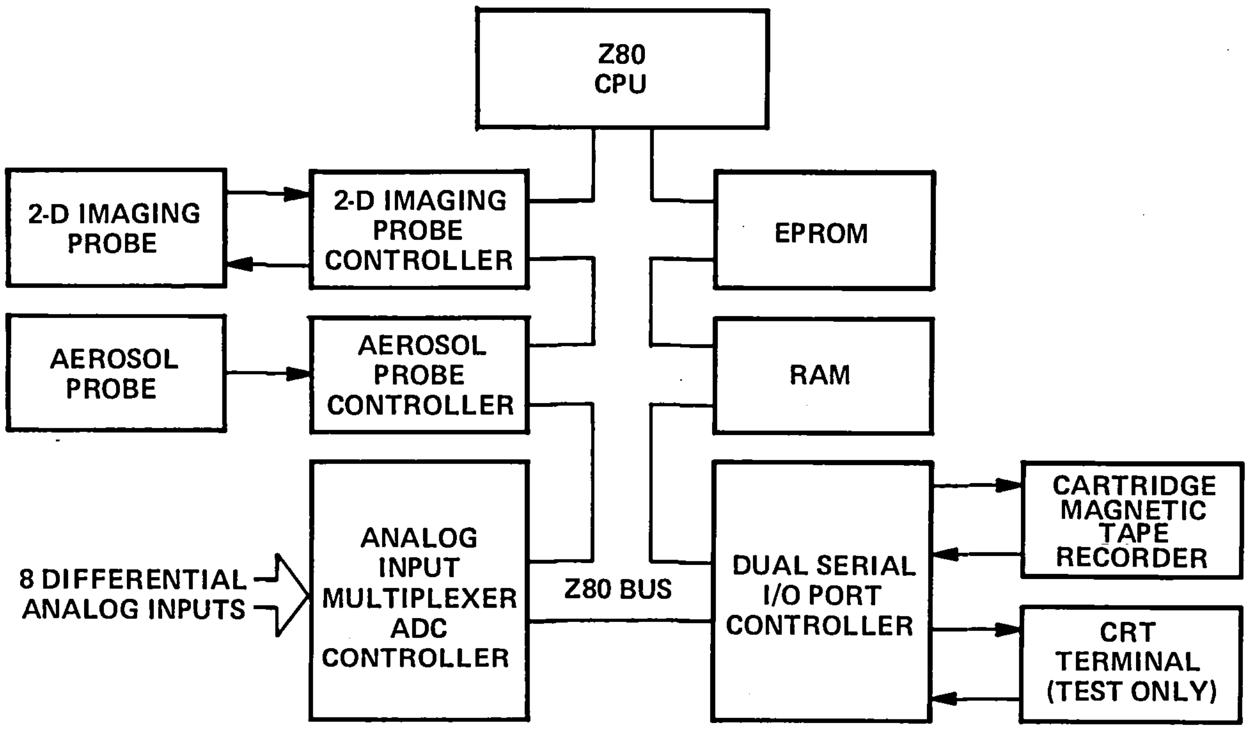

Figure 2.- U-2 particle spectrometer experiment block diagram. The data acquisition system is based around a Z-80 microcomputer; the CRT terminal is used for pre-flight checks and quick looks.

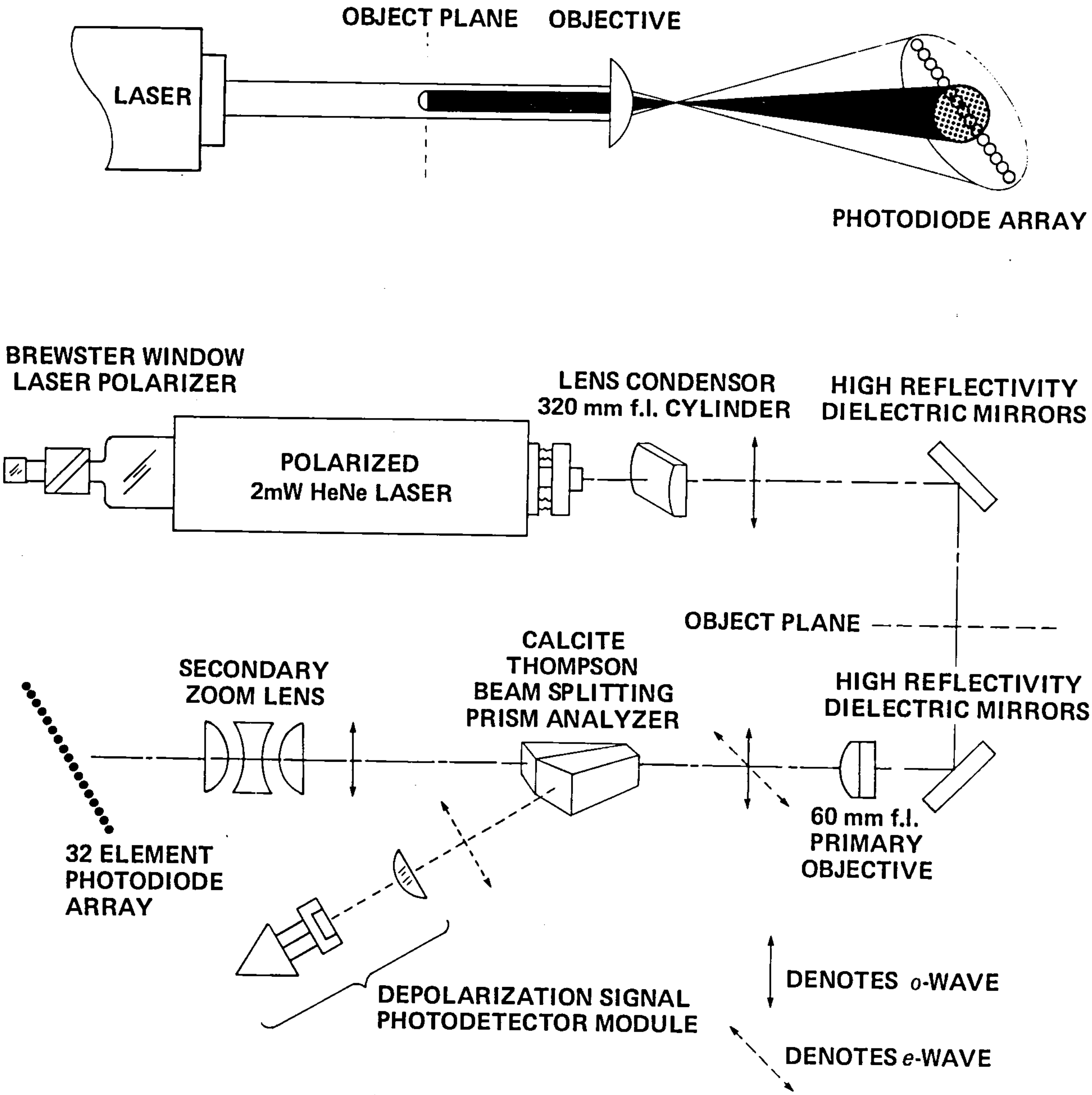

Figure 3.- 2-D imaging probe optical system. The simplified diagram at the top depicts the image-formation process in the imaging probe. The lower figure shows the actual optical system including polarized optics which can be used to distinguish ice from water hydrometeors.

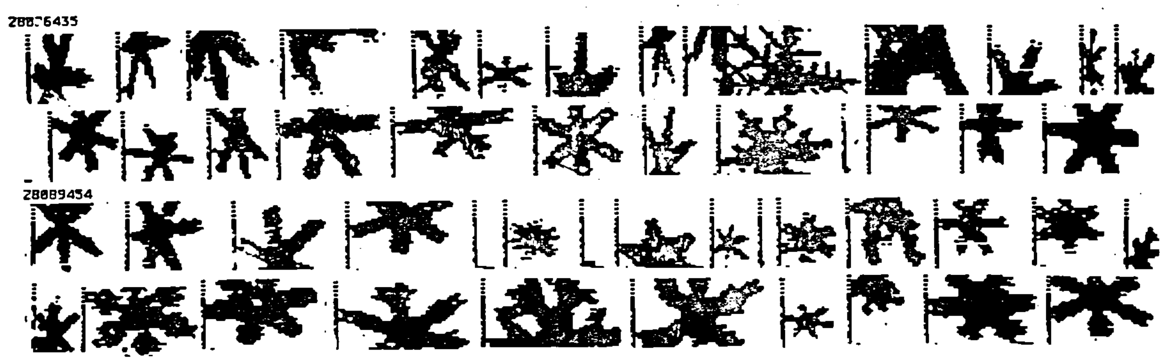

A

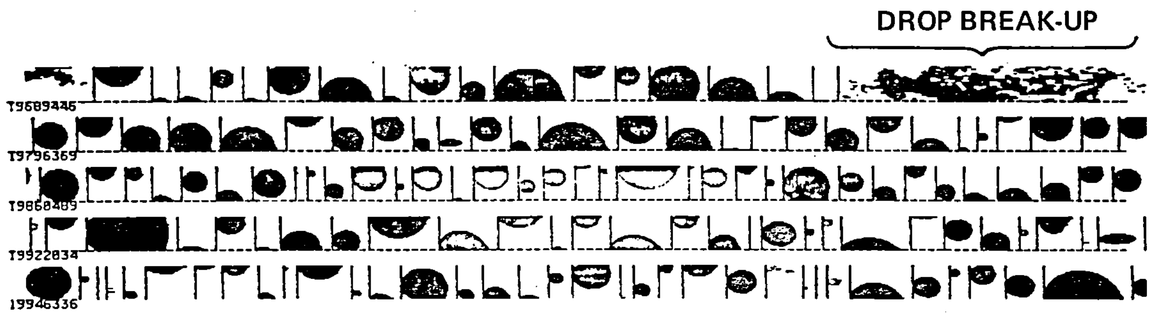

B

FLIGHT DATA SAMPLES OF 2-D IMAGERY IN SNOW AND RAIN. THE SNOW CRYSTALS ABOVE ARE DISPLAYED AT TWICE THE MAGNIFICATION AS THE RAINDROPS. NOTE THE PLUME FROM A FRACTURED DROP IN B

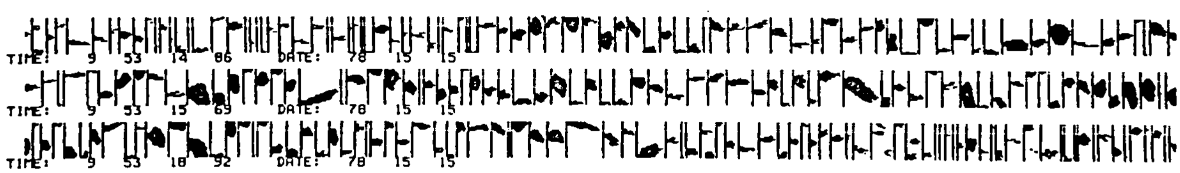

C

Figure 4.- Image samples from nongray, 2-D imaging probe; the vertical line between each image is an image separator.

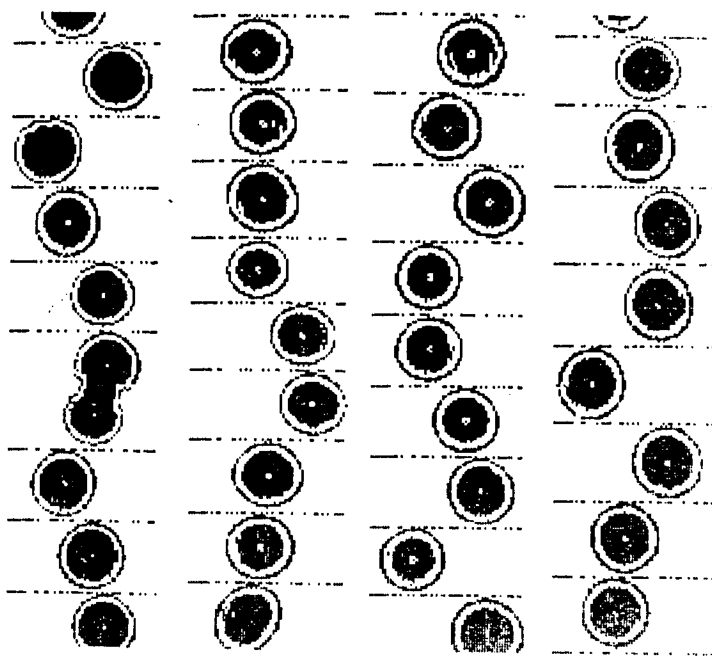

Figure 5.- Image samples from 2-D Gray Imaging Probe; size of droplets is 80 μm.

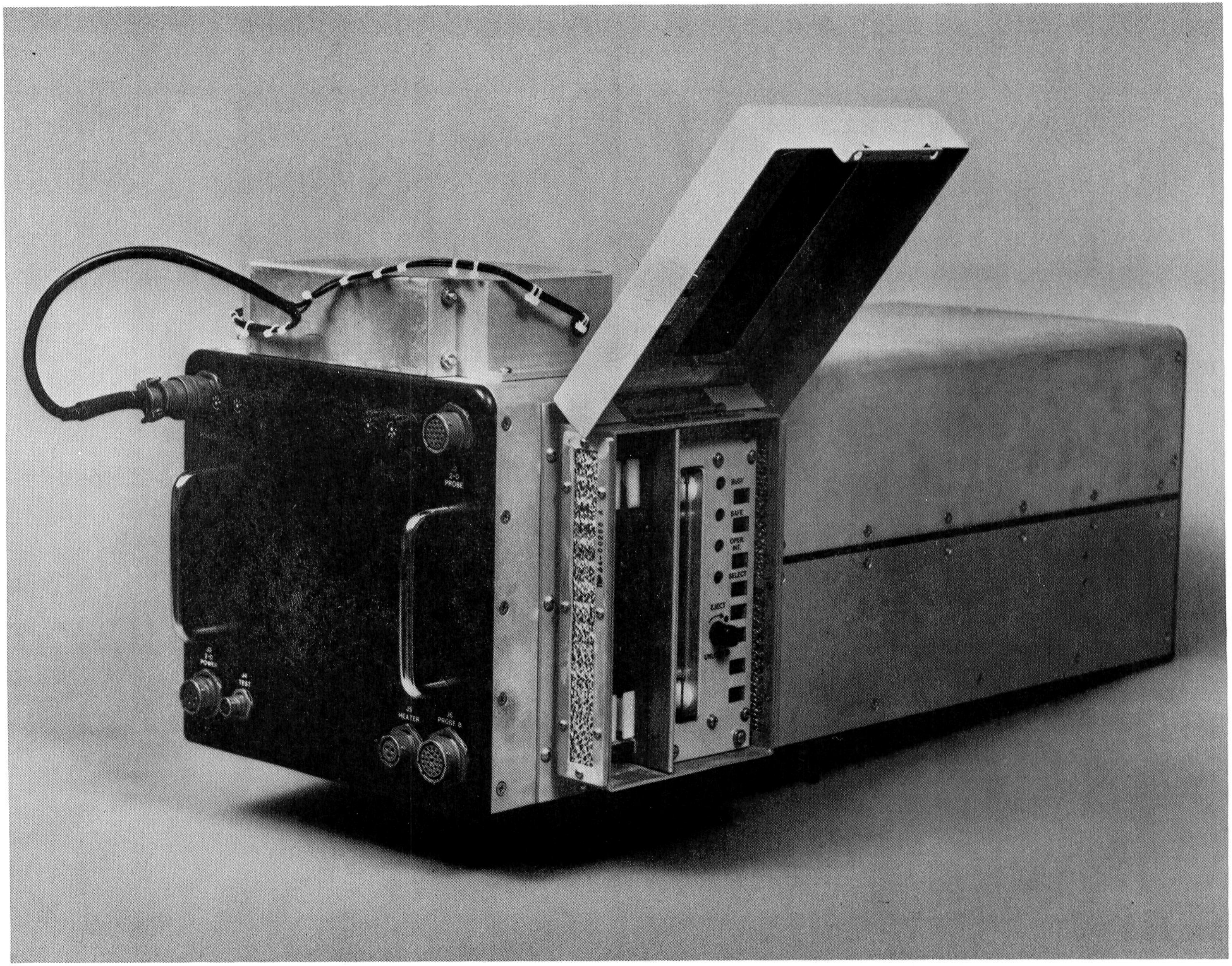

Figure 6.- Data acquisition system; aerosol probe is in the lower half of the package.

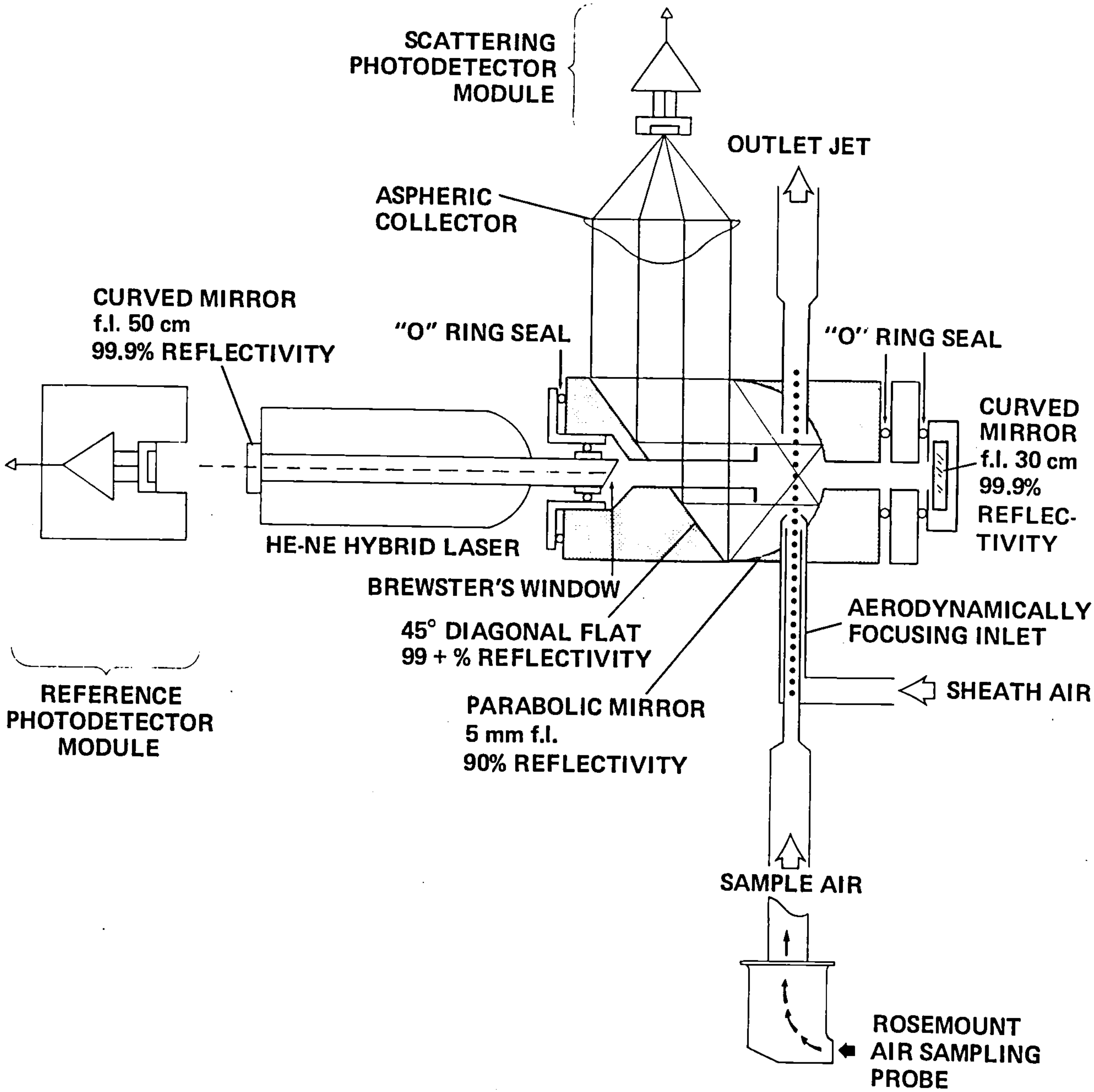

Figure 7.- Aerosol probe optical system diagram.

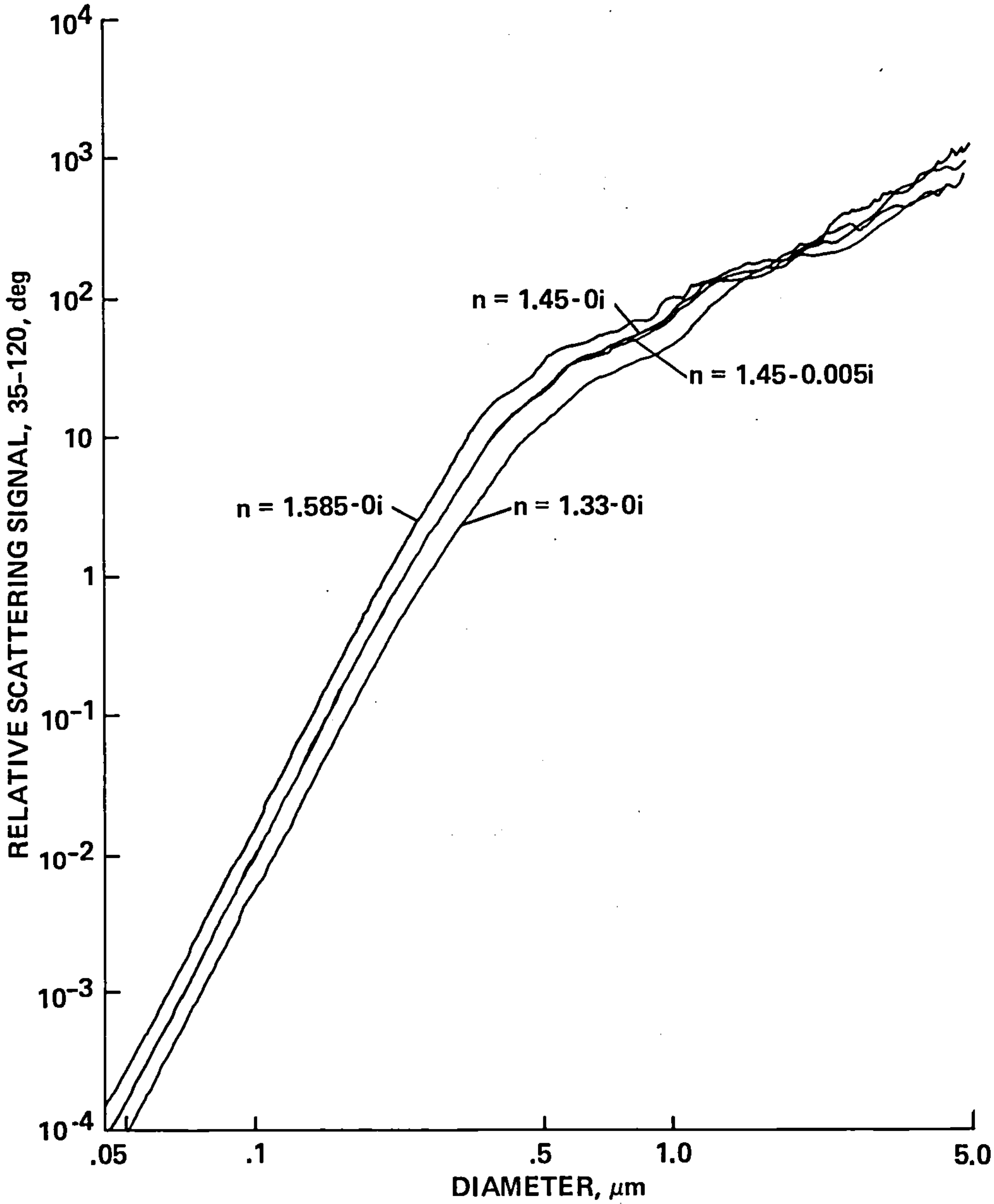

Figure 8.- Mie computed response of aerosol probe. Higher values of imaginary index will begin to cause weakened response at larger sizes. In the submicron range, imaginary values as high as 0.1 cause negligible sizing error.

Figure 9.- Image samples from flights 7 and 8. The top four images are from flight 7, the lower three from flight 8. Maximum crystal length is 1.3 mm.

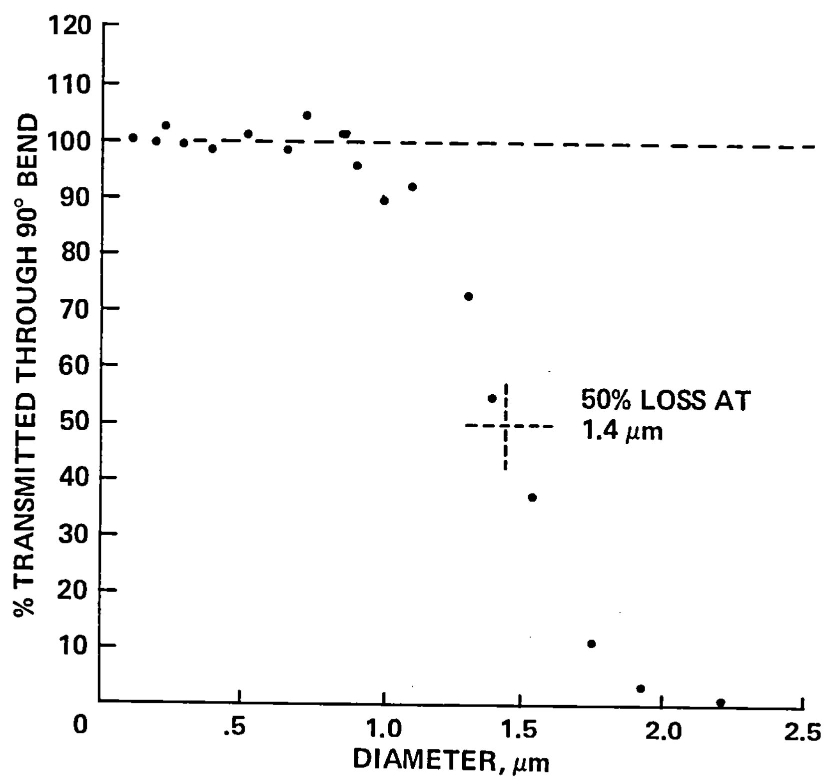

Figure 10.- Effects of 90° bend in aerosol inlet at 70 mbars. The above data were generated by comparing the size distributions as measured by the aerosol probe with and without a 90° bend (1 cm radius) in the aerosol inlet.

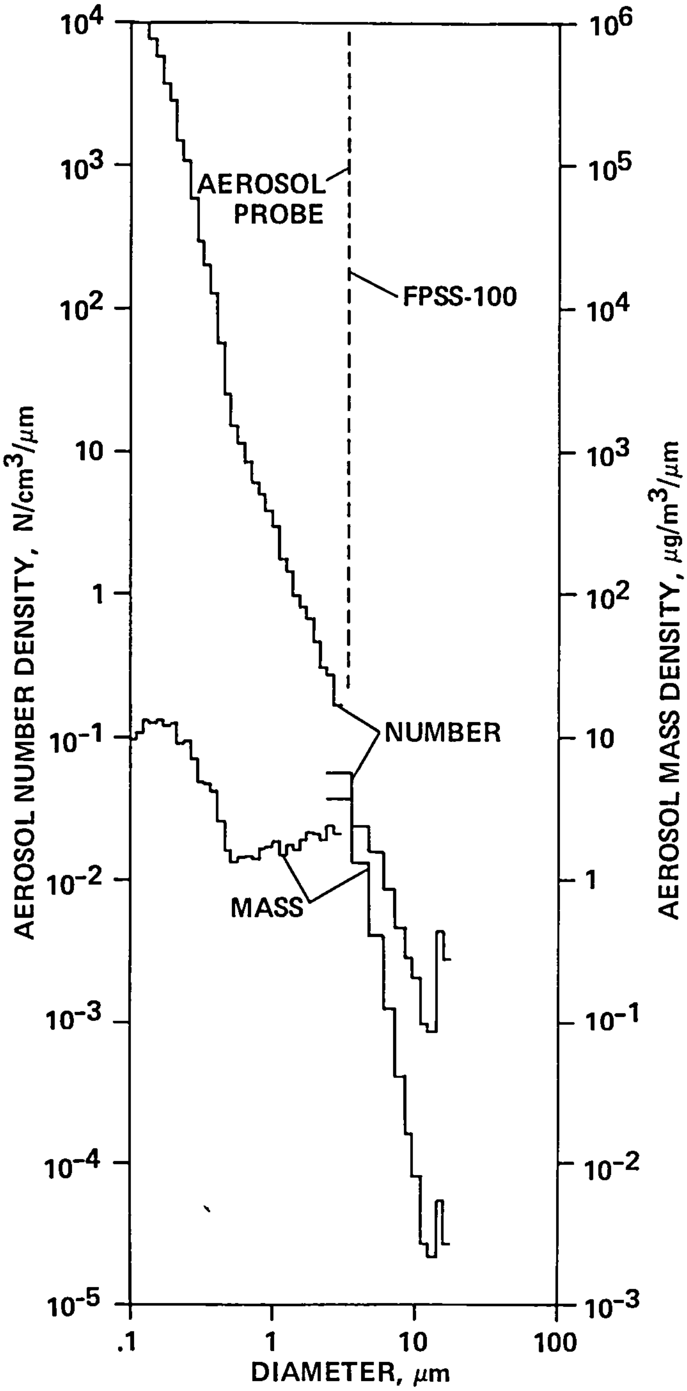

Figure 11.- Aerosol size and mass distribution comparisons from flight on July 14, 1981. This comparison is of data from U-2 aerosol probe covering particle sizes from 0.1-3.0 μm and an FSSP-100 instrument covering sizes from 2-32 μm.

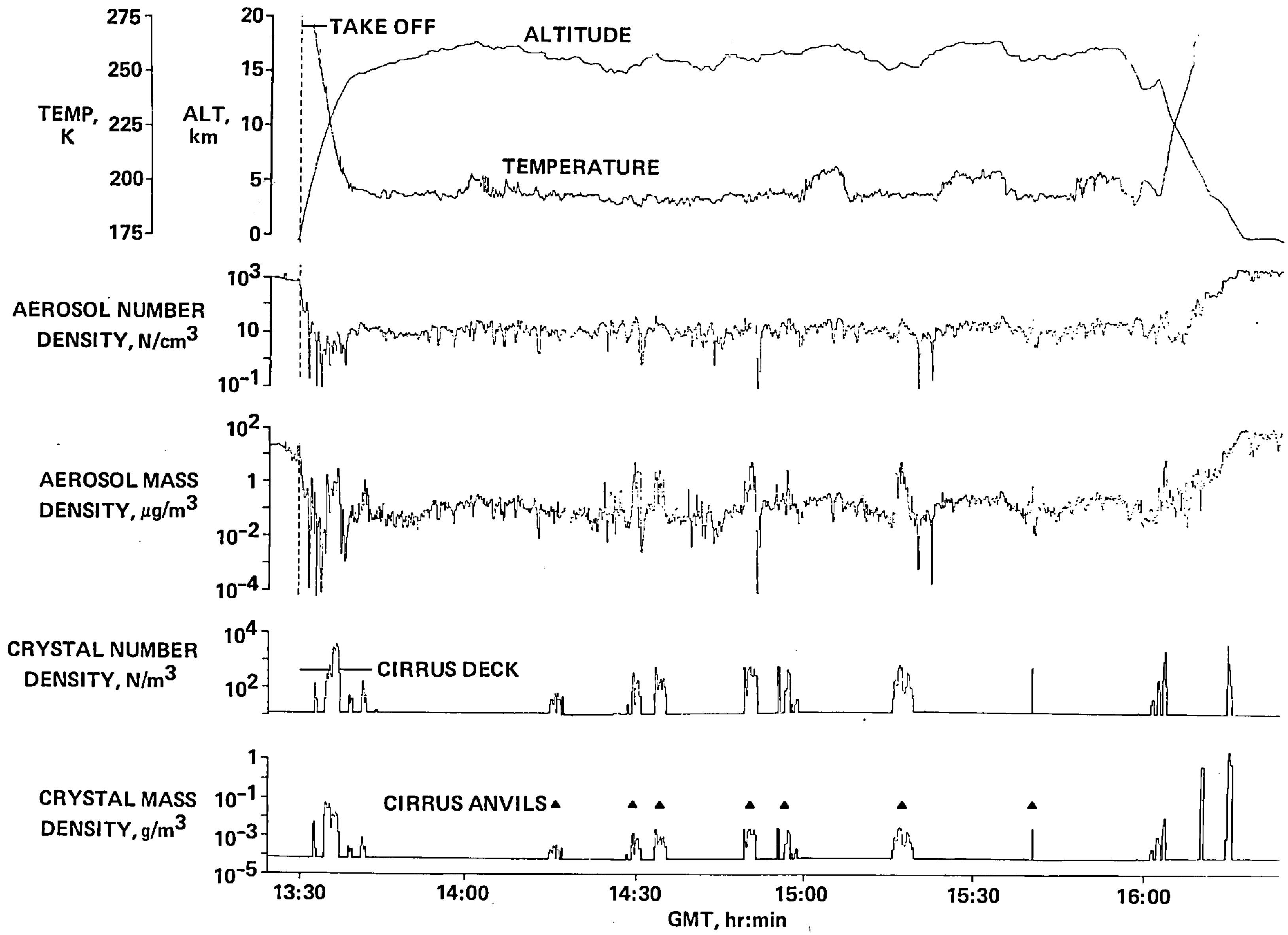

Figure 12.- Complete data set for flight 8. In processing the image data, aera-to-mass conversions were applied according to Knollenberg (1976b). The aerosol mass computations assume spherical particles from $\rho = 2.0$ g/cm^3. The bracketed pass is that selected for aerosol size and mass distribution display in figure 16.

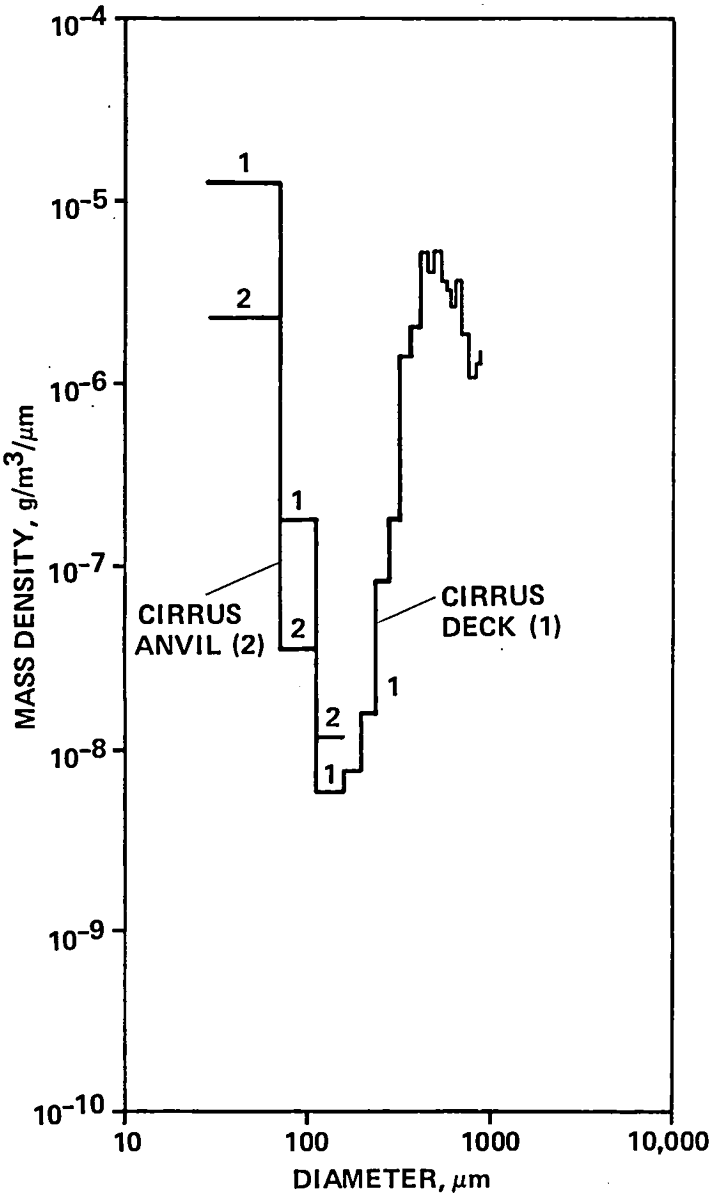

Figure 13.- Comparison of mass distributions of ice crystals in cirrus deck and cirrus anvil (fifth pass) from flight 8. In processing the image data, area-to-mass conversions were applied according to Knollenberg (1976b). The aerosol mass computations assume spherical particles with $\rho = 2.0$ g/cm^3.

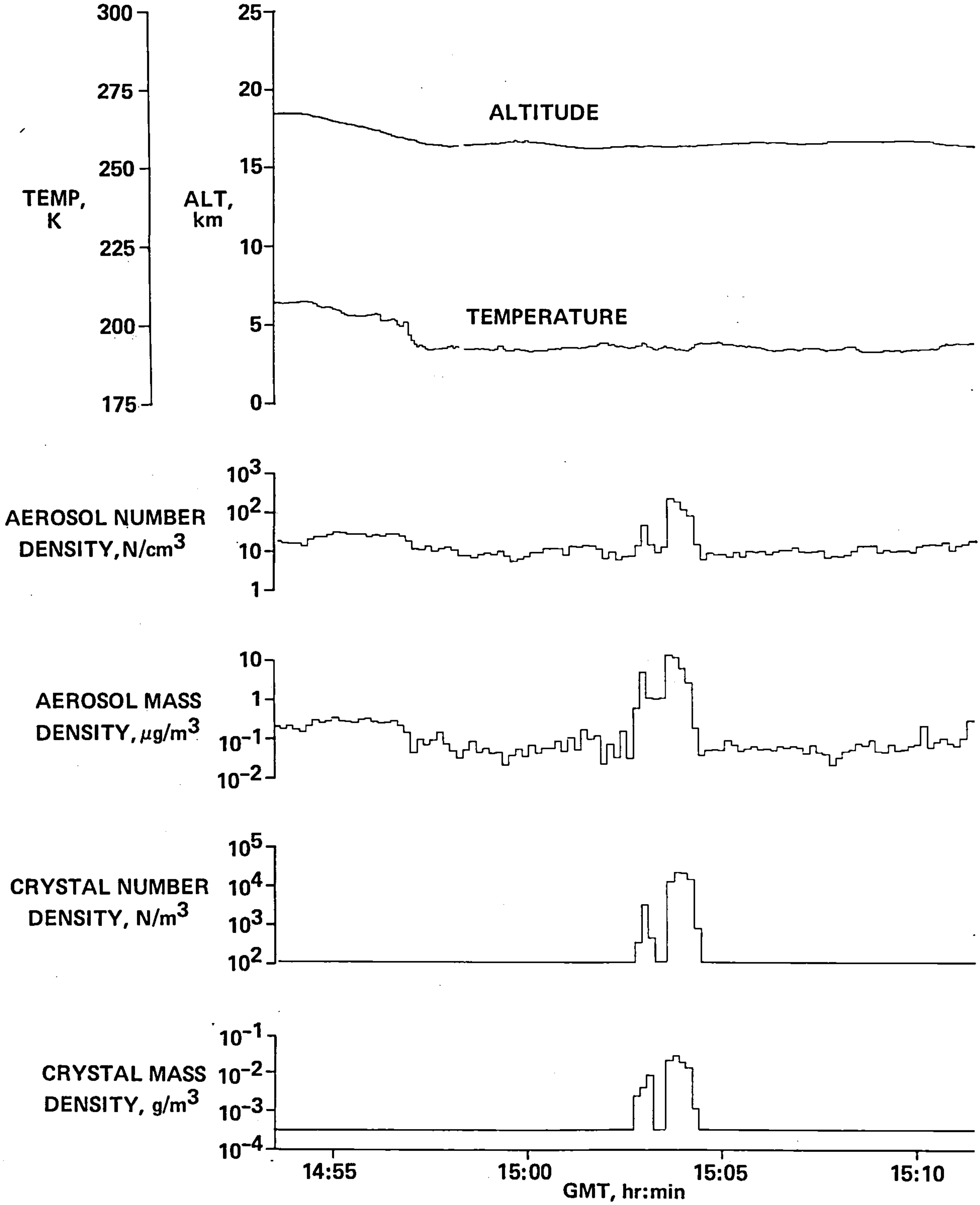

Figure 14.- Partial data set for flight 7. Samples of the ice crystals represented here were shown in figure 9. In processing the image data area-to-mass conversions were applied according to Knollenberg (1976b). The aerosol mass computations assume spherical particles with ρ = 2.0 g/cm^3.

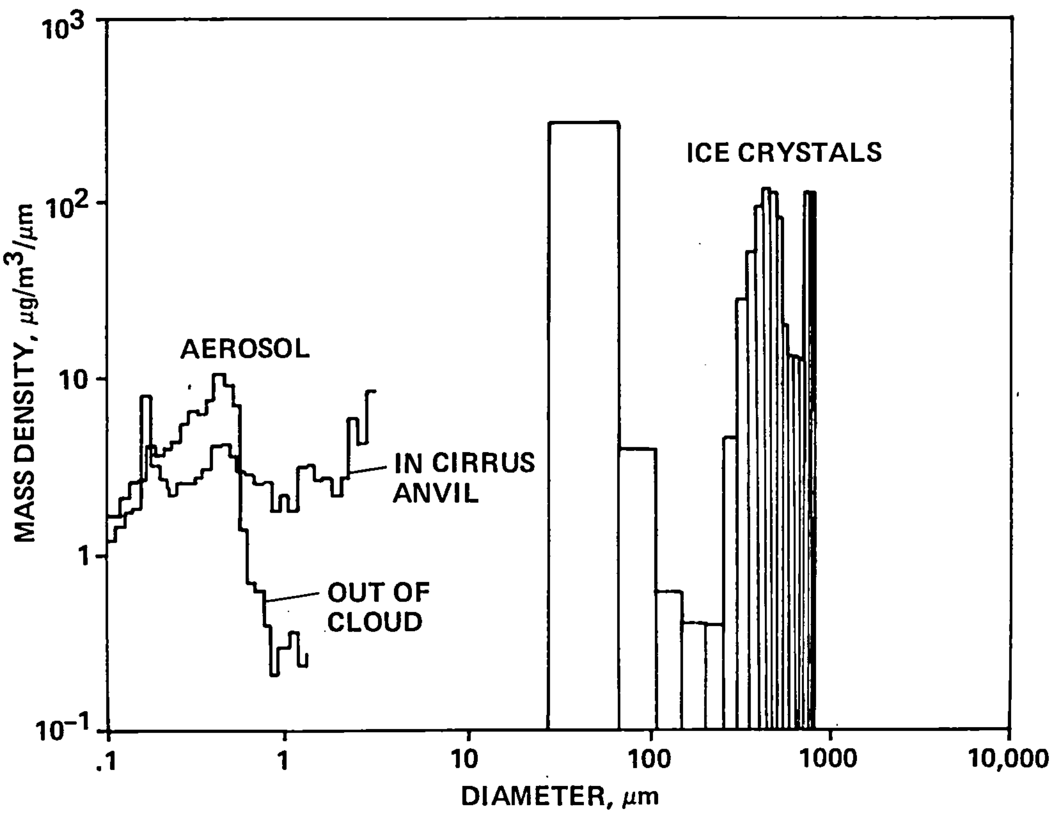

Figure 15.- Ice-crystal and aerosol mass distributions for flight 7. The bimodal crystal mass distribution actually represents two separate regions of the cloud pass. However, the strong aerosol mode at 0.17 μm is characteristic of the entire pass length.

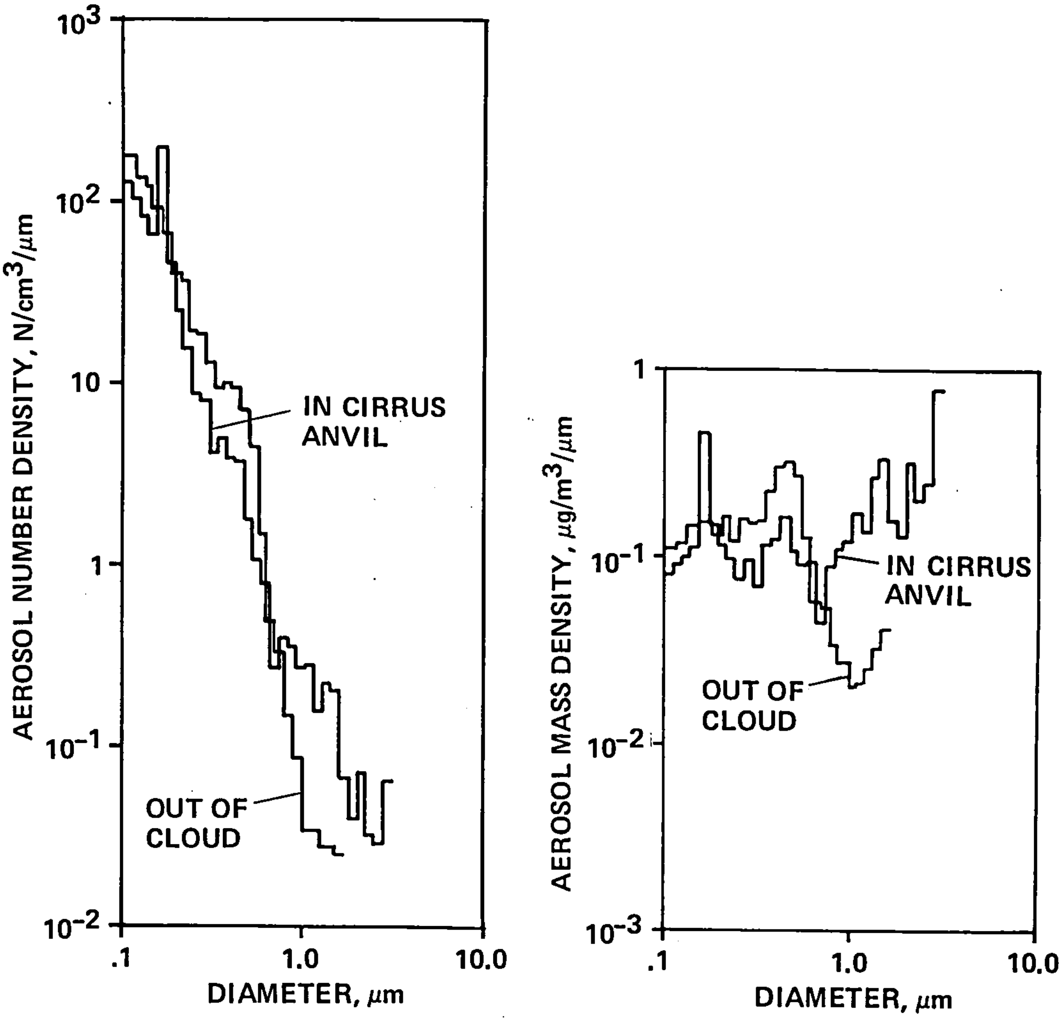

Figure 16.- Comparison of aerosol size and mass distributions in and out of cloud for flight 7.

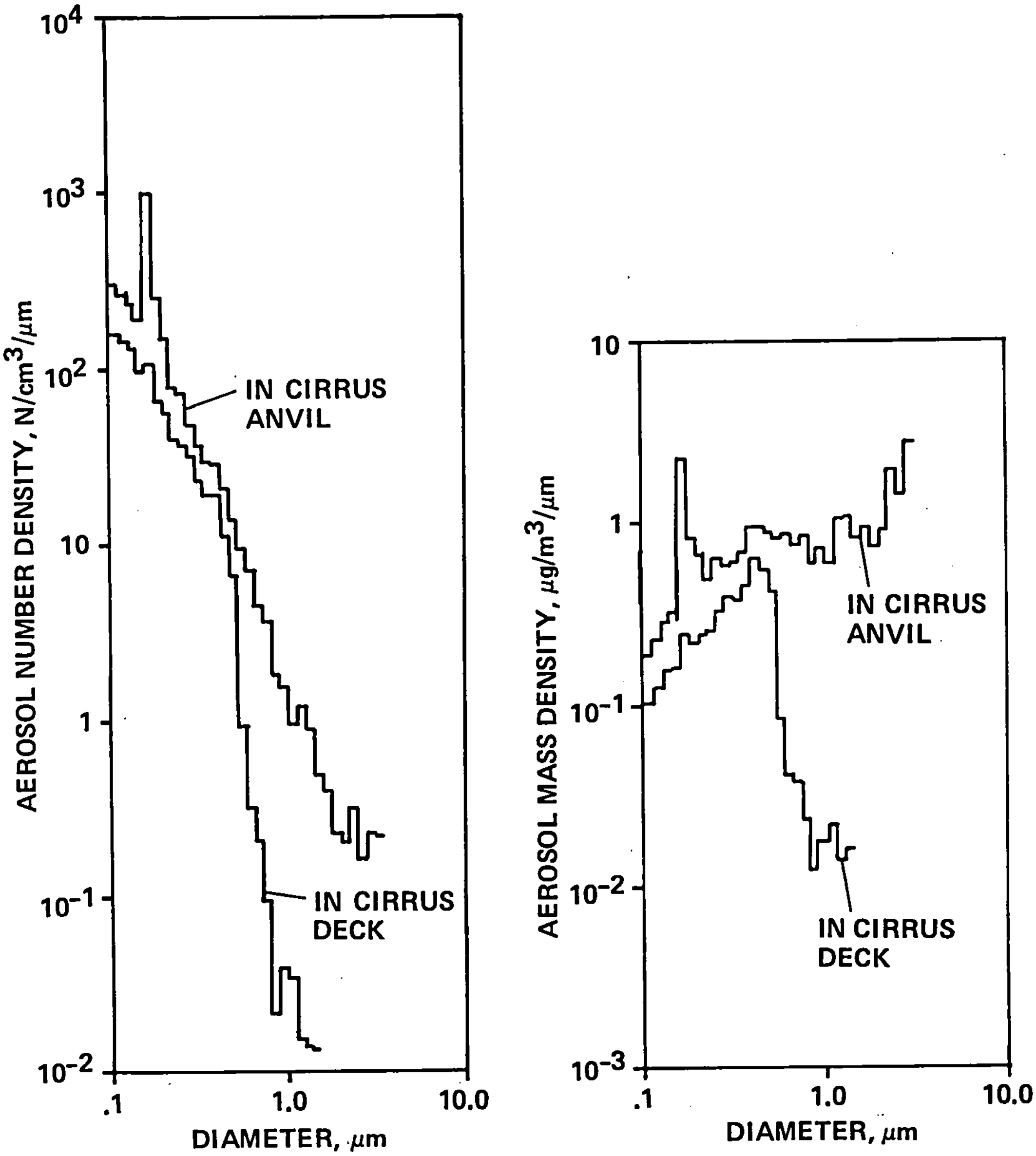

Figure 17.- Comparison of aerosol size and mass distributions in cirrus anvil and in cirrus deck for flight 8.

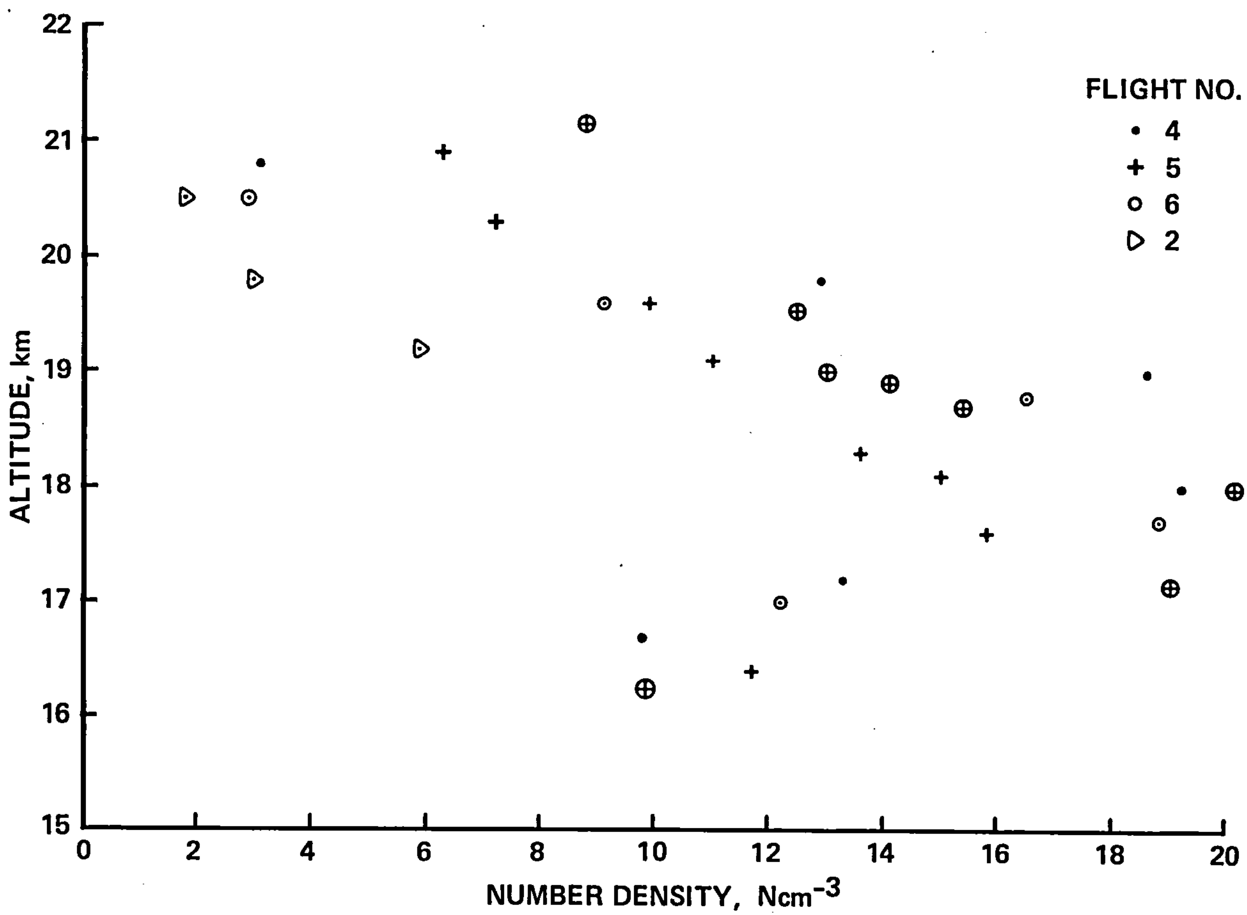

Figure 18.- Vertical profile of stratospheric aerosol number-density. The number-density is seen to read maximum values of $20/cm^3$ at 18 km and appears very stable from day to day.

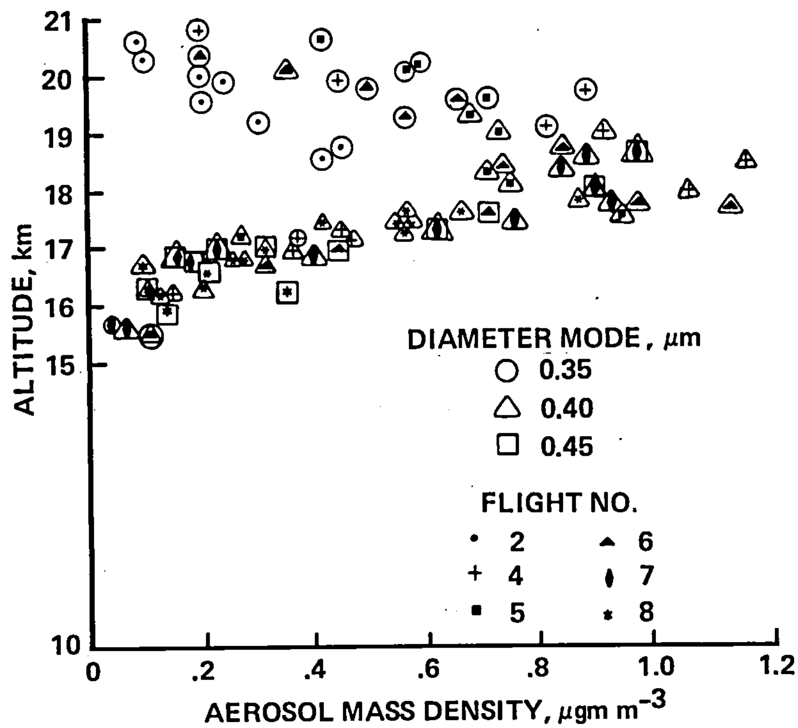

Figure 19.- Vertical profile of stratosphere aerosol mass density. The modal diameter for the mass distributions is seen to decrease with altitude, indicating that the region is not well mixed and is the likely result of sedimentation.

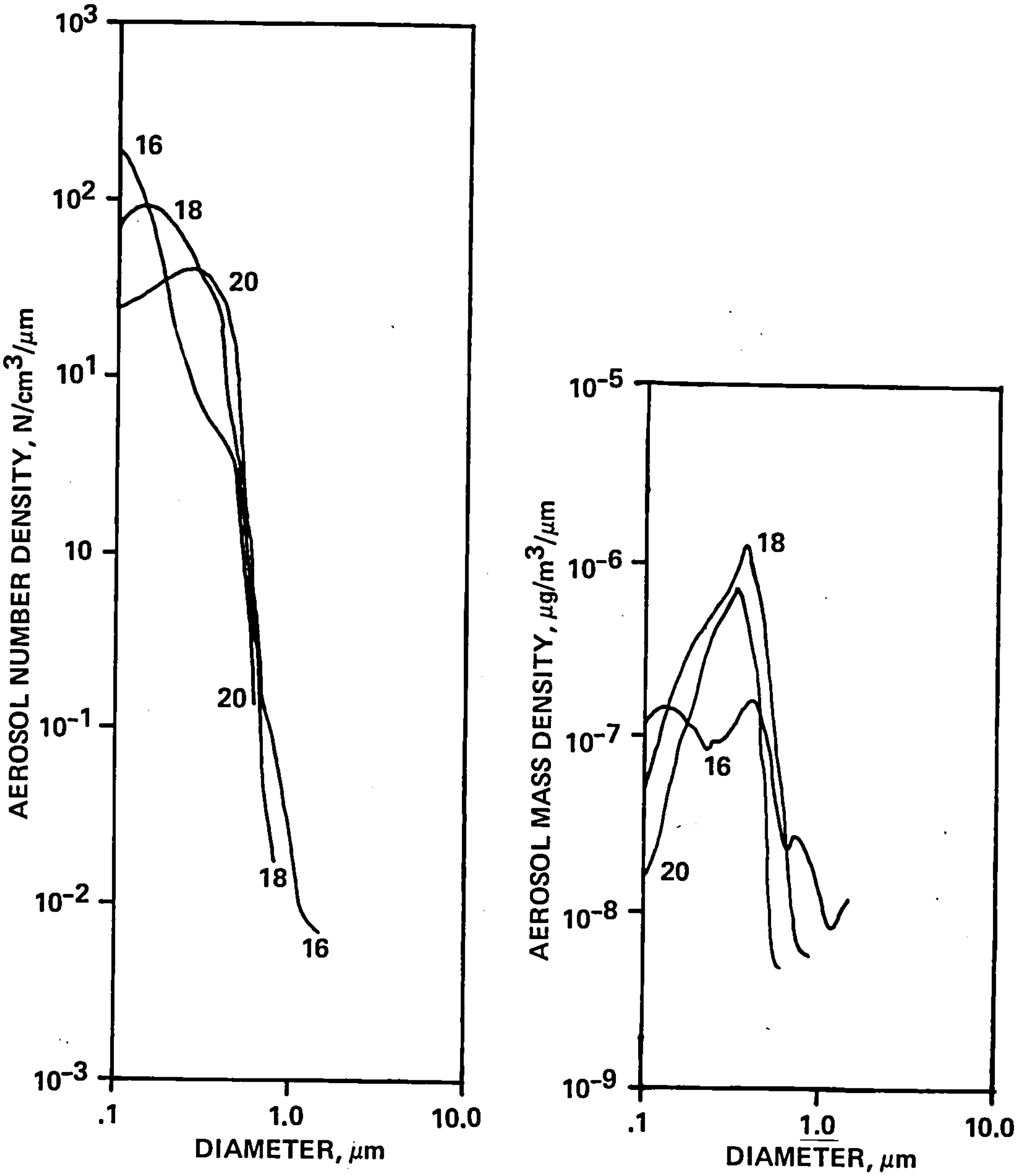

Figure 20.- Size and mass distributions at altitudes of 16, 18, and 20 km from flight 6. Note development of stable mass mode at 16 and 18 km around 0.4 μm.

THE U-2 LYMAN-ALPHA HYGROMETER RESULTS FROM THE 1980 PANAMA EXPERIMENT

D. Kley,* A. L. Schmeltekopf,* K. Kelly,* R. H. Winkler,*

T. L. Thompson,* and M. McFarland*

SUMMARY

The U-2 Lyman-alpha hygrometer is described, its accuracy and precision are assessed in detail, and results obtained with it during the 1980 Tropospheric/ Stratospheric Water Vapor Exchange Experiment are reported.

INSTRUMENTAL

General Considerations

The Lyman-alpha hygrometer (Kley and Stone, 1978) uses vacuum UV light at $\lambda = 1216$ Å to dissociate atmospheric water vapor:

$$H_2O + h\nu_1 \xrightarrow{J_x} OH^* + H \tag{1}$$

A fraction of the product hydroxyl radicals are produced in an electronically excited $OH(A^2\Sigma^+, v' = 0)$ state, denoted by the asterisk. The excited OH will either fluoresce or get quenched by air molecules,

$$OH^* \xrightarrow{A} OH + h\nu_2 \tag{2}$$

$$OH^* + air \xrightarrow{k_q} products \tag{3}$$

The coefficient J_x is defined by

$$J_x = \phi_x \cdot \sigma_H \cdot F^* \tag{3a}$$

where ϕ_x is the Lyman-alpha flux in the interaction region, σ_H is the absorption cross section of H_2O at 1216 Å, and F^* is the quantum yield for production of excited OH. The quantity A is the Einstein coefficient of the $OH(A^2\Sigma^+ \rightarrow X^2\Pi)$ transition and k_q is the quenching rate coefficient. Numerical values of the above quantities and some other parameters are assembled in table 1.

*Aeronomy Laboratory, National Oceanic and Atmospheric Administration, Environmental Research Laboratories, Boulder, Colorado.

The intensity of the fluorescence is

$$I_{F1} = \frac{J_x[H_2O]A}{A + k_q[air]} \tag{4}$$

for pressures higher than a few millibars, $A \ll k_q[air]$. If this approximation is used and if the mixing ratio $R \equiv [H_2O]/[air]$ is introduced, we obtain

$$I_{F1} = \frac{J_x \cdot A \cdot R}{k_q} \tag{5}$$

The photomultiplier measuring the fluorescence has a certain collection efficiency and quantum yield. If the symbol S is used for the photomultiplier count rate and equation (5) is solved for the mixing ratio, equation (6) is obtained. All quantities of constant values have been combined into C':

$$R = C'S/J_x \tag{6}$$

The Lyman-Alpha Hygrometer

Figure 1 shows a schematic view of the Lyman-alpha hygrometer. Light from a Lyman-alpha light source (LA) radiates through a series of circular apertures (CO) into the scattering chamber (SC). A quartz window (not shown) slides into the light path between light source and collimator every 15 min. The purpose of this window is to periodically absorb the Lyman-alpha light while passing near-UV light (see Kley et al., 1979).

Two photomultipliers are attached to the SC. The principal one (PM1, fig. 1) detects the OH-fluorescence. In front of PM1 is a combination of an $NiSO_4 \cdot 7H_2O$ crystal with a Corning 7-54 cutoff filter plus a suprasil lens (L) to limit the spectral response of PM1 to a wavelength region $3000 \lesssim \lambda \lesssim 3250$ Å and to image a region of the optical axis onto the photocathode. The optical arrangement is F/4. The second photomultiplier (PM2) is only sensitive in the vacuum UV. It is directly attached to the SC, and serves as a monitor for backscattered Lyman-alpha radiation. Backscatter consists mainly of Rayleigh scatter at $\lambda = 1216$ Å and, to a small extent, of surface and resonance scatter. A nitric oxide ionization cell (NOA) is located opposite the Lyman-alpha light source and monitors the intensity of the transmitted light. The light source is a sealed off discharge of H_2 in helium. Uranium hydride in a side arm is heated to about 125°C to provide a constant partial pressure of H_2. The light source is operated from a stabilized microwave power supply. The light source has two MgF_2 windows (W), one at each end. Radiation emerging through the window facing away from the SC passes through an O_2 filter cell (ABS) onto an NO ionization cell (NOB). The purpose and mode of operation of the O_2/NO cell combination is discussed in a following subsection (Calibration). The gas inlet (I) is a 1-in.-diam stainless steel tube, heated to about 20°C, connecting the SC to a heated Rosemount (HK102) probe, modified for maximum airflow. The gas exits through the collimator to a 1-in.-diam tube and is vented under an angle of 11° to the outside airstream. The airflow was somewhat variable; it depends on Mach number and altitude. Typical values are 10 liters/sec under ambient conditions. The reaction chamber SC is made from stainless steel and is completely lined with black glass (Schott Optical Glass). Glass panels were cut to size and glued to the stainless steel surface by silicone rubber. The geometrical shape of the SC in conjunction with the black glass

is optimized for minimum scattered light from inside surfaces. Pressure is measured alternatively upstream or downstream from the SC, and the temperatures of the scattering chamber and the NO cells are kept constant. Currents from the NO cells are converted to voltages; the voltages are amplified and voltage-proportional frequencies are generated by voltage-to-frequency converters. Photomultiplier count rates and NO cell frequencies are counted by electronic counters. The instrument is microprocessor controlled. Principal data, as well as a multitude of housekeeping signals and universal time, are recorded on magnetic tape by a cassette recorder. Count rates are measured and recorded every 0.1 sec. The instrument and associated electronics and cassette recorder are all packed into a pressurized container; the container consists of three cylindrical cans, each of which has a different diameter, so that the instrument could be fitted into the rear half of a U-2 wing tank (the front part of the wing tank houses the Particle Measuring Systems, Inc., aerosol spectrometer). The air inlet system, the scattering chamber, and the exhaust line are the only parts of the instrument at ambient pressure.

The Lyman-alpha hygrometer is powered by three-phase, 400-Hz aircraft power at 115 Vac. A photograph of the main part of the hygrometer is shown in figure 2.

Determination of the Water Mixing Ratio

Recall from the earlier discussion that the photodissociation coefficient J_x in equation (3a) consists, apart from constants, of the Lyman-alpha light flux in the interaction region, defined by a volume element comprised by the cross section of the light beam and the conical shape of the photomultiplier viewing geometry. The Lyman-alpha light emanating from the light source window facing the scattering chamber (SC) will be partially absorbed before reaching the interaction region. The two absorbers that need to be considered are H_2O and O_2. As figure 1 shows, a nitric oxide photoionization counter is located at a distance L_A away from the light source window. The Lyman-alpha intensity at distance L_A will be

$$I_A = I_o\{\exp(-\sigma_H[H_2O] - \sigma_o[O_2])L_A\} \tag{7}$$

where I_o is the intensity at the lamp window, and σ_H and σ_o are the cross sections of H_2O and O_2, respectively. Similarly, the intensity at the distance L_x (see fig. 1) will be

$$I_x = I_o\{\exp(-\sigma_H[H_2O] - \sigma_o[O_2])L_x\} \tag{8a}$$

Combining equations (7) and (8a) we get

$$I_x = I_A \exp\{(-\sigma_H[H_2O] - \sigma_o[O_2])(L_x - L_A)\} \tag{8b}$$

If expression (8b) is substituted in equation (6), we obtain

$$R = C \exp(-\sigma_H[H_2O] - \sigma_o[O_2])(L_A - L_X)(S/I_A) \tag{9}$$

where C is yet another constant. Note that the quantity I_o does not occur in equation (9). This means that changes in lamp intensity will not influence the determination of R.

The exponent in equation (9) consists of two terms, the first one accounting for absorption by H_2O and the second one for absorption by O_2, where σ_O is the O_2 absorption cross section. We will investigate how each of them influences the result. Introducing two abbreviations, the water optical depth $\tau_H \equiv \sigma_H[H_2O](L_A - L_X)$ and the oxygen optical depth $\tau_O \equiv \sigma_O[O_2](L_A - L_X)$, we will first consider the magnitude of τ_H. If a stratospheric mixing ratio of 10 ppmv is conservatively assumed to occur at the 200-mbars pressure level, then $\tau_H = 0.009$ and $\exp(-\tau_H) = 0.991$. Therefore, it is justified to set $\exp(-\tau_H) = 1$. However, since we anticipate that "events" with large mixing ratios will be occasionally encountered, that is, when flying through stratospheric cirrus or, if we want to measure tropospheric water mixing ratios, we must go one step further: If τ_H is not too large (i.e., $\tau_H \lesssim 0.3$), the exponent can be expanded into $e^{-\tau_H} \approx 1 - \tau_H$. In doing so, a new equation is obtained from which the mixing ratio can be determined

$$R = \frac{C \exp(-\tau_O)}{1 + C[\text{air}]\sigma_H(L_A - L_X)\exp(-\tau_O)(S/I_A)} \frac{S}{I_A} \tag{10}$$

In order to evaluate equation (10), the optical depth τ_O must be known. There is a substantial amount of literature on the absorption cross section of O_2 at the Lyman-alpha line. The most recent paper, which also gives a survey of earlier work, is by Carver et al. (1977). At room temperature, the cross section is

$$\sigma_O = 0.96\times10^{-20}(1 + 1.6\times10^{-3}P)[\text{cm}^2] \tag{11}$$

where P is the total pressure in units of millibars. It is noted that the oxygen absorption cross section is pressure dependent. The pressure-dependent coefficient in equation (11) is a mean from eight values measured by various authors as listed in the Carver et al. (1977) paper. We have also made a determination of σ_O using the U-2 instrument. We found that the results could be best fitted to a cross section of

$$\sigma_O = 1.42\times10^{-20}(1 + 1.1\times10^{-3}P)[\text{cm}^2] \tag{12}$$

A possible explanation for the discrepancy is that our light source emits some non-Lyman-alpha light in the wavelength range $1150 < \lambda < 1340$ Å. This is the spectral region over which the nitric oxide photoionization detector responds. Since the O_2 absorption cross section at $\lambda = 1215.7$ Å has a deep minimum, any non-Lyman-alpha radiation that the lamp emits yields a somewhat larger effective cross section. We have used σ_O as given by equation (12) in the data reduction rather than the literature values from equation (11). Values of the exponential term $\exp(-\tau_O)$, using equations (11) and (12), are compiled in table 2 for some pressures. Also shown in table 2 are the ratios of cross sections compiled from either equation. For the range of relevant pressures, these ratios are between 0.98 and 0.95.

Calibration

The numerical value of the sensitivity constant C in equation (10) must be determined. This is a straightforward procedure and involves measuring the fluorescence count rate at known mixing ratios of water. If the assumption is made that the OH fluorescence detection sensitivity of the photomultiplier and the sensitivity of the NO photoionization cell, measuring the transmitted Lyman-alpha light, do not change with time, the calibration could be performed in the laboratory. However, we

do not rely on this assumption and prefer to determine C during each flight at various altitudes. As a matter of fact, it has turned out that the calibration constant C does change over a time span of months, most likely because of changes in the photoionization detector efficiency with time.

The method is based on Beer's law,

$$I = I_o \exp(-\sigma_H[H_2O]L) \tag{13}$$

and assumes knowledge of σ_H, the absorption cross section of water vapor at $\lambda = 1215.7$ Å. We have used $\sigma_H = 1.4\times10^{-17}$ cm^2 (Preston, 1940; Watanabe et al., 1953).

Since the absorption measurements are carried out in flight, there is always a variable amount of oxygen present. We have used an experimental method that cancels the effects of O_2 absorption during calibration. Details are given in the following (refer to fig. 1). The Lyman-alpha light source (LA) emits light in two directions. The light flux through the set of apertures (CO) is measured by ionization cell NOA after having undergone absorption by H_2O and O_2 in the main cell (SC). The light flux emanating from the light source through the opposite window is monitored by ionization cell NOB. In between is a small cell of a length $L_B = 0.21L_A$. Pure O_2 is allowed to continuously flow through that cell. The oxygen supply is a stainless steel cylinder (volume = 100 cm^3) which is filled to about 100 atm before each flight. A single-stage pressure regulator reduces the pressure to about 10 atm. A stainless steel capillary provides a flow resistance to the flowing O_2 so that the mass flow is given by $Q = \beta(P_1^2 - P_c^2) \approx \beta P_1^2$, where β is the capillary constant, $P_1 \approx 100$ atm is the upstream pressure, and P_c is the pressure in the cell. The flowing O_2 is mixed into the exhaust of the main cell through a 1/4-in.-o.d. line. The conductance of the capillary is very small relative to that of the line connecting the O_2 cell to the main exhaust line so that virtually identical pressures P inside the O_2 cell and the main cell will exist. Since $L_B = 0.21L_A$, this arrangement will cause identical O_2 column abundances in both cells, independent of atmospheric pressure and altitude of the aircraft. The photoionization currents will be

$$I_A = C_A I_o \exp\{-\sigma_H[H_2O]L_A - \sigma_o 0.21[\text{air}]L_A\} \tag{14}$$

$$I_B = C_B I_o \exp\{-\sigma_o[O_2]L_B\} \tag{15}$$

The quantities C_A and C_B in equations (14) and (15), respectively, are, in theory, constants containing geometry factors, window transmissions, and a factor that we can describe best as NO-cell sensitivity. We have already noted that over long time periods (of the order of months), there seems to be a slight loss of sensitivity of the NO cells. Also, even if the internal window transmission of the Lyman-alpha light source is considered to be constant, there is usually a loss of transmission, owing to some buildup of either discharge products on the inside surface of either window or hydrocarbon polymerization on the outside surface of the window facing the main cell. It was observed that C_A was constant for the duration of the Exchange Experiment and that C_B changed significantly during each of the flights of the Exchange Experiment. However, over time periods of minutes, C_B was also constant. We have identified buildup of discharge products on the inside surface of the lamp window facing the O_2 cell as the cause for this. (The reason this buildup occurs significantly faster on one of the two windows is not clear at present.)

Dividing equation (14) by equation (15) and solving for R, we obtain

$$R = \frac{\ln(C_A/C_B) - \ln(I_A/I_B)}{\sigma_H[\text{air}]L_A} \tag{16}$$

During normal stratospheric flight with background mixing ratios of about 5 ppmv, the absorption by water vapor is too small to be observable. However, the situation is different during so-called "events" and during ascent or descent through the upper troposphere. Events are sudden and temporary excursions of the water mixing ratios to large values, caused by flying through cirrus or cumulonimbus anvils. These events were frequently observed during the Exchange Experiment and were used for calibration. It is important to note that the events were brief occurrences and that before and after normal background mixing ratios prevailed.

If we denote mixing ratio and NOA-cell intensity before and after the event by a prime and the same quantities during an event by double primes, we get, from equation (16) by subtraction,

$$\Delta R(t) \equiv R''(t) - R' = \frac{\ln(I_A/I_B)' - \ln(I_A/I_B)''}{\sigma_H[\text{air}]L_A} \tag{17}$$

All quantities on the right side of equation (17) are either known or being measured.

Similarly, an expression for ΔR is obtained from equation (10)

$$\Delta R(t) = \frac{C[(S/I_A)'' - (S/I_A)']\exp(-\tau_o)}{1 + C\sigma_H[\text{air}](L_A - L_X)\exp(-\tau_o)[(S/I_A)' + (S/I_A)'']} \tag{18}$$

Second-order terms in the denominator were neglected. It is clear that from the combination of equations (17) and (18), a value of the calibration constant C can be obtained.

Calibration Constant

We have determined calibration constants for individual flights of the Exchange Experiment. Events during level flights, as well as those during the aircraft descents, were selected.

The resulting calibration constants C are plotted in figure 3 against flight number. For flight U208, no useful event could be found. The calibration constant for flight U206 was very much lower than those for the rest of the series. We believe that some contamination on the window of photoionization cell NOA had drastically reduced its efficiency. Consequently, the cell was exchanged with a spare after that flight. For the remainder of the Exchange Experiment, the NOA cell was not changed. (We are at present, May 1982, still using the same NO cell.)

The straight line in figure 3 is the result of a linear regression to the individual values. For the final data reduction we have used calibration constants as predicted by the regression line for each flight, except for flight U206, where the value of C, determined for that flight, was used. If it is assumed that the apparent

trend of C to increase with time is accidental, a value of $\bar{C} = 8.1\times10^{-5}$, with a standard deviation of 0.45×10^{-5}, is obtained.

Background and Outgassing

If the mixing ratio of water is zero, there would still be a photomultiplier signal. That signal,

$$S_B = S_D + S_S + \gamma[\text{air}] \tag{19}$$

is composed of the photomultiplier dark count rate, S_D, and a contribution $S_S + \gamma[\text{air}]$ from light, emitted by the Lyman-alpha source at a wavelength falling into the passband of the photomultiplier/filter combination. The Lyman-alpha source is very nearly monochromatic in the vacuum UV around Lyman-alpha. However, there is some emission in the quartz UV and particularly around 3100 Å at the center wavelength of the passband. In fact, this light is composed mostly of the $OH(A^2\Sigma^+ \rightarrow X^2\Pi)$ transition, which is somehow excited in the lamp and is, therefore, indistinguishable from the OH fluorescence produced by the Lyman-alpha radiation in the main cell. This produces a photomultiplier signal (1) from surface scattering at the inside walls of the main cell (S_S) and (2) from Rayleigh scattering in air ($\gamma[\text{air}]$). The photomultiplier dark signal is negligible compared with the two other contributions. Surface scatter plus Rayleigh scattering signal are measured every 15 min by inserting a quartz window into the beam between the light source and reaction cell. This procedure has been described before (Kley et al., 1979).

If zero-mixing-ratio air is passed through the instrument, there is a signal generated from water which desorbs from internal surfaces and voids, and is mixed with the inflowing gas.

Those contributions could come from the inlet probe, the plumbing, and the reaction cell. An extensive laboratory test series was made after the Exchange Experiment. We found that the outgassing was most likely caused by a slow release of water from RTV (silicone rubber), which was used to glue the glass plates to stainless steel surfaces of the reaction cell. In addition to the slow outgassing process, there seems to be one occurring on a shorter time scale. The latter one may be caused by normal surface desorption. The laboratory results showed that outgassing effects on the mixing ratio could be approximated by

$$R_o = [8.5 \exp(-0.00152t) + 0.95 \exp(-0.000127t)] \frac{100}{P} \text{ [ppmv]} \tag{20}$$

Table 3 gives some values calculated from equation (20) for $P = 100$ millibars. The accuracy of these numbers is estimated to be only 50%, since the outgassing rate was variable and seemed to depend on the previous use of the instrument. A look at table 3 shows that the contribution from outgassing is quite significant for the first hour of operation or flight. We have, therefore, decided not to use the first hour of flight data. The data for times >1 hr were corrected during the final data analysis by subtracting R_o values as calculated from equation (20).

Accuracy and Precision

Starting with equation (10) and using the abbreviations $B \equiv \exp(-\tau_o)$, $A \equiv \sigma_H(L_A - L_X)[\text{air}]$, and $S \equiv S/I_A$, we get

$$R = \frac{CBS}{1 + CABS} - R_o \tag{21}$$

where R_o is the outgassing contribution from equation (20). Some sources of error have been identified in the previous paragraphs. An error analysis reveals that

$$\frac{\Delta R}{R} \approx \left[\left(\frac{\Delta C}{C}\right)^2 + (\Delta ACBS)^2 + \left(\frac{\Delta B}{B}\right)^2 + \left(\frac{\Delta S}{S}\right)^2 + \left(\frac{\Delta R_o}{R}\right)^2\right]^{1/2} \tag{22}$$

where ΔC is the error in the determination of calibration constant, ΔA in the optical depth of water, ΔB in the oxygen transmission, ΔS in the normalized fluorescence signal, and ΔR_o the error in the determination of the outgassing contribution. Each of the identified errors will be discussed in the following.

Two kinds of errors contribute to the calibration constant. If equations (17) and (18) are combined and solved for C, and if a standard error analysis of C is made, we see that $\Delta C/C = \Delta\sigma_H/\sigma_H$. This is a systematic error to which we must add the error that is made in the experimental determination of C. The latter can be obtained from the variability of the individual C determinations assembled in figure 3. The 1 σ standard deviation of C is 6%, about a mean of $C = 8.1\times10^{-5}$. As far as the accuracy of σ_H error is concerned, we have searched the literature and found only two independently measured values, of which one (Preston, 1940) is believed not to be "very accurate" by the author. We use $\sigma_H = 1.4\times10^{-17}$ cm^2, measured by Watanabe et al. (1953). These authors give no error estimate. From a consideration of their technique, we assume (maybe too conservatively) that σ_H is known with an accuracy of $\Delta\sigma_H/\sigma_H = 0.2$. Therefore, including both errors, we have $\Delta C/C = 0.21$.

The $\Delta ABCS$ error was estimated to be $\sim 8\times10^{-4}$. For $\Delta B/B = [O_2](L_A - L_X)\Delta\sigma_o$ see the discussion of the oxygen transmission in a preceding subsection (Determination of the Water Mixing Ratio). We conservatively assume that $\Delta\sigma_o \approx 0.5\times10^{-20}$ cm^2, which then yields $\Delta B/B = 0.04$.

The signal $S \equiv S/I_A$ is not free from error. This error comes from the subtraction of background (quartz window in) which is measured every 15 min. The background signal is fitted to equation (19). Its magnitude is usually about 10% of the signal from typical stratospheric water vapor. We estimate that the background signal is known with 20% accuracy. This gives typical values of $\Delta S/S \approx 0.022$.

The total systematic error, from adding the individual ones, is

$$\frac{\Delta R}{R} = 0.21 + \frac{\Delta R_o}{R} \tag{23}$$

For certain applications, we can ignore the $\Delta\sigma_H$ error. This systematic error will not change from flight to flight and it is justified to compare results from different flights without considering this error. Values of $\Delta R/R$ and $\Delta R/R - \Delta\sigma_H/\sigma_H$ for $R = 5$ ppmv are given in table 4 for pressures of 200, 100, and 50 mbars, respectively.

The precision of the results is mainly governed by the statistical signal/noise ratio, and it depends on the light source intensity. For each flight during the Exchange Experiment, a new light source was used. Its intensity dropped by about 30%-50% during a given flight. Typical count rates after 2 hr of flight were about 5000 c/sec at stratospheric background mixing ratios, so that a signal/noise ratio of ~70 for integration times of 1 sec was achieved.

RESULTS

The Exchange Experiment took place over Panama (lat. 9° N, long. 81° W) between August 30 and September 16, 1980. The Lyman-alpha hygrometer was on board during the first 10 flights. Relevant information is listed in table 5. The results discussed in this section are from flight 1 and flights 3 through 10 (the data from flight 2 were not analyzed). There are three principal groups of results: one set of "horizontal" plots and two sets of "vertical" plots.

In the horizontal plots, water mixing ratios, aircraft altitude, and ambient temperatures are plotted against time. The altitude and temperature information was provided by Scott (1981). (The aircraft altitude on all figures is pressure altitude, based on U.S. Standard Atmosphere (1976). Pressure altitude based on pressures for August/September at the equator are given in table 6. The table indicates that actual aircraft altitude was significantly higher than that given in the figures.)

These horizontal plots are further subdivided into two series. The first series, figures 4 through 12, provides panels of 1-hr length on the horizontal scale. The vertical scales are water mixing ratio (R) 0-10 ppmv, altitude (A) 12-22 km, and temperature (T) 180 K-230 K. No altitude and temperature information was obtained during flight 2. Instead, we have plotted pressure as recorded by the Lyman-alpha hygrometer pressure sensor. Note that this pressure may deviate from ambient pressure by a few millibars.

The second series of horizontal plots, figures 13 through 21, shows selected parts from individual flights. Selected were those portions that showed large deviations from "background" mixing ratios. Also, as in the previous series, there is altitude and temperature information. In addition, saturation mixing ratios (S) of water vapor over ice were calculated and plotted. To indicate when the actually observed water mixing ratio exceeded saturation, the area between the water mixing ratio and the saturation mixing ratio is speckled.

Figures 22 through 29 show the vertical plots. The horizontal scales are mixing ratio and temperature and the ordinates are aircraft altitude. These plots were generated from data taken during the aircraft descents. For each of these plots, 2-sec integrated values of mixing ratios were sorted in intervals of 100-m altitude range, averaged, and the standard deviation about the mean calculated. The means and the $\pm 1\ \sigma$ standard deviation about the means are given. It should be noted that points with large standard deviations are the result of flying through areas with large spatial water inhomogeneity. Temperatures were treated similarly. However, only their 100-m averaged values are shown.

Another series of vertical plots, figures 30 through 37, depicts water mixing ratio versus altitude. Different from the previous series, the abscissas in the figures are 3-decade logarithmic scales. In addition, slanted lines represent frost-point coordinates, every 10°C from -90° to -40°C. Descent temperature profiles are

plotted on the altitude/frost-point coordinates. These figures allow the determination of apparent supersaturation with respect to ice. Whenever it occurred, this apparent supersaturation is indicated by speckling.

DISCUSSION

This report is a documentation of results from the Exchange Experiment. A discussion of the science will be published in the literature. (A first paper (Kley et al., 1982) has already been published.) This paragraph contains a discussion of the accuracy and precision of the results and emphasizes certain details.

Linear Vertical Plots

The vertical plots (figs. 22-29) show a minimum of the water mixing ratios ranging from altitudes of about 18 to 19 km. Values of the minimum mixing ratios are plotted in figure 38 against flight number (solid circles in the figure). There seems to be a trend for the mixing ratios to increase with flight number, that is, with time. To investigate whether this trend is significant, we have also plotted error bars. The length of the error bars was obtained from ($\Delta R/R$ - $\Delta\sigma_H/\sigma_H$)-values in table 4.

It is noted that the results were derived by using linear regression (see fig. 38) for the calibration constant. On the other hand, if a constant calibration constant of $\bar{C} = 8.1 \times 10^{-5}$ for flights 4 through 10 and $C = 3.1 \times 10^{-6}$ for flight 1 is used instead, the results indicated by the open circles in figure 38 are obtained. A linear regression line through the open circles yields a somewhat smaller slope than one through the solid circles. It is quite obvious, from looking at the error bars, that a zero slope line fits the result as well. If this is done, the dashed line is obtained, and the result is $R = 3.81$ ppmv with a standard deviation of $\Delta R = 0.37$ ppmv. Here, it is noted that the result $\Delta R/R = 0.37/3.81 = 0.1$ is experimentally equal to what was predicted from the results of the error analysis (table 4). We therefore conclude that the trend is not significant, and that $R = 3.81$ ppmv is the water mixing ratio between 18 and 19 km. The standard deviation of $\Delta R = 0.37$ ppmv does not take into account the estimated $\Delta\sigma_H$ error. If it is included, the result is $R = (3.81 \pm 1.1)$ ppmv. However, for comparison of the Exchange Experiment results with those from other programs using the Lyman-alpha hygrometer (Kley et al., 1979), $\Delta R = 0.37$ ppmv should be used, since the $\Delta\sigma_H$ error was not included in the earlier work. (An effort is now under way in our laboratory to study the Lyman-alpha absorption cross section of water vapor with higher accuracy.

Logarithmic Vertical Plots

The speckled areas of figures 30-37 show apparent supersaturation of water vapor with respect to ice. Whenever supersaturation is indicated, it must be remembered that total H_2O is measured, that is, the sum of the mixing ratio of water vapor and ice or liquid. At low temperatures, the saturation mixing ratio of gas-phase water with respect to liquid water is about twice as large as that of gas-phase water with respect to ice. Therefore, whenever the observed apparent supersaturation is no larger than about two, the possibility exists that the water vapor would have not been supersaturated with respect to liquid water. Very large supersaturations are found on flights 5, 6, 9, and 10 (figs. 32, 33, 36, and 37), certainly the result of

flying through clouds. Interestingly, flights 7 and 8, on which very large supersaturations occurred during horizontal flight, show only moderate or practically no supersaturation during the descents. It will be necessary to compare all of these figures with the set of infrared and visible photographs provided in appendix A.

Horizontal Plots

Figures 4 through 12, with a vertical water mixing ratio of 0-10 ppmv, are provided for the information they contain on the stratospheric "background" mixing ratio. Some periods during which the water mixing ratio is off scale are unavoidable. In order to show those "events" and to give information on apparent supersaturation, figures 13 through 21 were prepared.

Note Added in Proof

As discussed in section 7, "Accuracy and Precision," we used $\sigma_H = 1.4\times10^{-17}$ cm^2 for the Ly(α) cross section of water vapor with an estimated accuracy of 20%. We have recently performed a new determination of σ_H and the result is $\sigma_H = 1.59\times10^{-17}$ cm^2. The accuracy of the new value is better than 5%. As a consequence, all mixing ratios in this report, as well as those in Kley et al. (1982), must be multiplied by 0.88.

REFERENCES

Carver, H. J.; Gies, H. P.; Hobbs, T. I.; Lewis, B. R.; and McCoy, D. G.: J. Geophys. Res., vol. 82, 1977, p. 1955.

Cole, E. Allen; and Kantor, Arthur J.: Air Force Reference Atmospheres, AFGL-TR-78-0051, Air Force Surveys in Geophysics, No. 382, Air Force Geophysics Laboratory, Hanscom AFB, Mass., 1978.

Crosley, D. R.; and Lengel, R. K.: J. Quant. Spectrosc. Radiat. Transfer, vol. 15, 1975, p. 579.

Kley, D.; and Stone, E. J.: Rev. Sci. Instrum., vol. 49, 1978, p. 691.

Kley, D.; et al.: Science, vol. 36, 1979, p. 2514.

Kley, D.; et al.: Transport of Water through the Tropical Tropopause. Geophys. Res. Lett., vol. 9, 1982, pp. 617-620.

Lee, L. C.: J. Chem. Phys., vol. 72, 1980, p. 4334.

Preston, W. M.: Phys. Rev., vol. 52, 1940, p. 887.

U.S. Standard Atmosphere. NOAA-S/T 76-1562, 1976.

Watanabe, K.; Zelikoff, M.; and Inn, E. C. Y.: AFCRC Report 53-23, Air Force Cambridge Research Center, Cambridge, Mass., 1953.

TABLE 1.- INSTRUMENTAL AND OTHER PARAMETERS

Quantity	Value	Reference
ϕ	~2.0(12) photons/cm^2 sec measured at a distance of 20 cm from lamp	Laboratory measurement
σ_H	1.4(-17) cm^2	Watanabe et al. (1953)
A	1.26(6) sec^{-1}	Crosley and Lengel (1975)
k_q	2.3(-11) cm^3 sec^{-1}	Kley and Stone (1978)
σ_o	See text	--
L_A	23 cm	--
L_X	10.9 cm	--
ν_2	$\lambda_2 \approx 3100$ Å	--
F^*	0.09	Lee (1980)

TABLE 2.- OPTICAL DEPTH OWING TO O_2 ABSORPTION

P	$\exp(-\tau_o)^{\#}$	$\exp(-\tau_o)^{\$}$	$\dfrac{\exp(-\tau_o)^{\#}}{\exp(-\tau_o)^{\$}}$
50	0.935	0.954	0.98
100	.867	.904	.96
150	.799	.851	.94
200	.731	.795	.92
300	.600	.680	.88
1000	.068	.105	.65

Notes: P = atmospheric pressure, millibars; $\exp(-\tau_o)^{\#}$ = optical depth owing to O_2 absorption from laboratory determination; $\exp(-\tau_o)^{\$}$ = optical depth owing to O_2 absorption from literature values; $\exp(-\tau_o)^{\#}/\exp(-\tau_o)^{\$}$ = ratio of column 2 to column 3.

TABLE 3.- CONTRIBUTION TO THE MIXING RATIO FROM OUTGASSING AND ESTIMATED ERROR

τ, sec	R_o,[a] ppmv	ΔR_o, ppmv
1800	1.31	0.65
3600	.64	.32
5400	.48	.24
7200	.38	.19
9000	.30	.15
10800	.24	.12
12600	.19	.09
14400	.15	.08

[a]At 100 mbars.

TABLE 4.- ERROR ANALYSIS[a]

t, hr	$\Delta R/R$, mbars			$\Delta R/R - \Delta\sigma_H/\sigma_H$, mbars		
	200	100	50	200	100	50
1.0	0.25	0.28	0.36	0.09	0.12	0.19
1.5	.23	.27	.33	.08	.11	.16
2.0	.23	.26	.31	.08	.10	.14
2.5	.23	.25	.28	.08	.09	.12
3.0	.22	.24	.27	.07	.08	.11
3.5	.22	.24	.26	.07	.08	.10
4.0	.22	.24	.25	.07	.08	.09

[a]Relative mixing-ratio errors at different times and pressures during flight. In columns 2-4, all systematic errors are considered. Columns 5-7 show systematic errors without the uncertainty of σ_H.

TABLE 5.- U2 FLIGHT PARAMETERS

Flight	Synonym	Time[a]	Date
1	U206	12:55:00	8/30
2[b]	U207	13:25:00	8/31
3[c]	U208	12:56:00	9/03
4	U209	13:25:00	9/07
5	U210	12:25:00	9/09
6	U211	13:57:00	9/11
7	U212	12:57:00	9/12
8	U213	13:25:00	9/13
9	U214	12:54:00	9/15
10	U215	12:55:00	9/16
11[d]	--	--	9/18

[a]Universal time at instrument turn-on.
[b]Not analyzed.
[c]No altitude and temperature information available.
[d]Instrument was not flown.

TABLE 6.- AIRCRAFT PRESSURE ALTITUDE

Pressure, mbars	Altitude,[a] km	Altitude,[b] km
264.4	10.0	10.6
226.3	11.0	11.6
193.3	12.0	12.7
165.1	13.0	13.7
141.0	14.0	14.6
120.4	15.0	15.6
102.8	16.0	16.5
87.8	17.0	17.4
75.0	18.0	18.4
64.1	19.0	19.3
54.7	20.0	20.3
46.8	21.0	21.2

[a]Altitude based on U.S. Standard Atmosphere (1976).
[b]Altitude based on Air Force Reference Atmosphere for August/September at equator (Cole and Kantor, 1978).

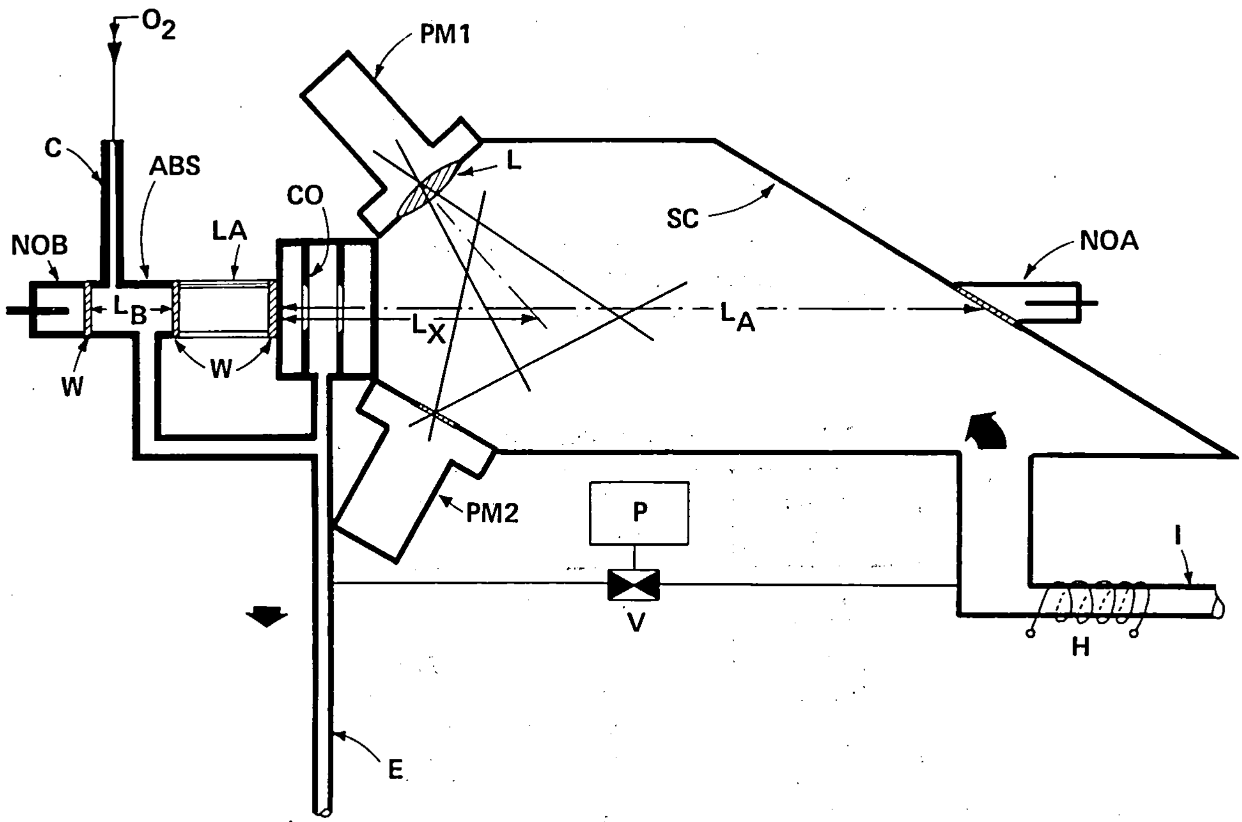

Figure 1.- Lyman-alpha hygrometer. Legend: SC = scattering cell; PM1, PM2 = photomultipliers; L = suprasil lens plus filter combination; LA = Lyman-alpha light source; CO = set of circular apertures; NOA, NOB = nitric oxide ionization cells; I = inlet line; E = exhaust line; V = three-way valve; P = pressure sensor; C = capillary; O_2 = oxygen supply; H = heater; L_A = distance between light-source window and NOA cell; L_X = distance between light-source window and center of viewing angle of PM1; ABS = oxygen cell; L_B = length of oxygen cell.

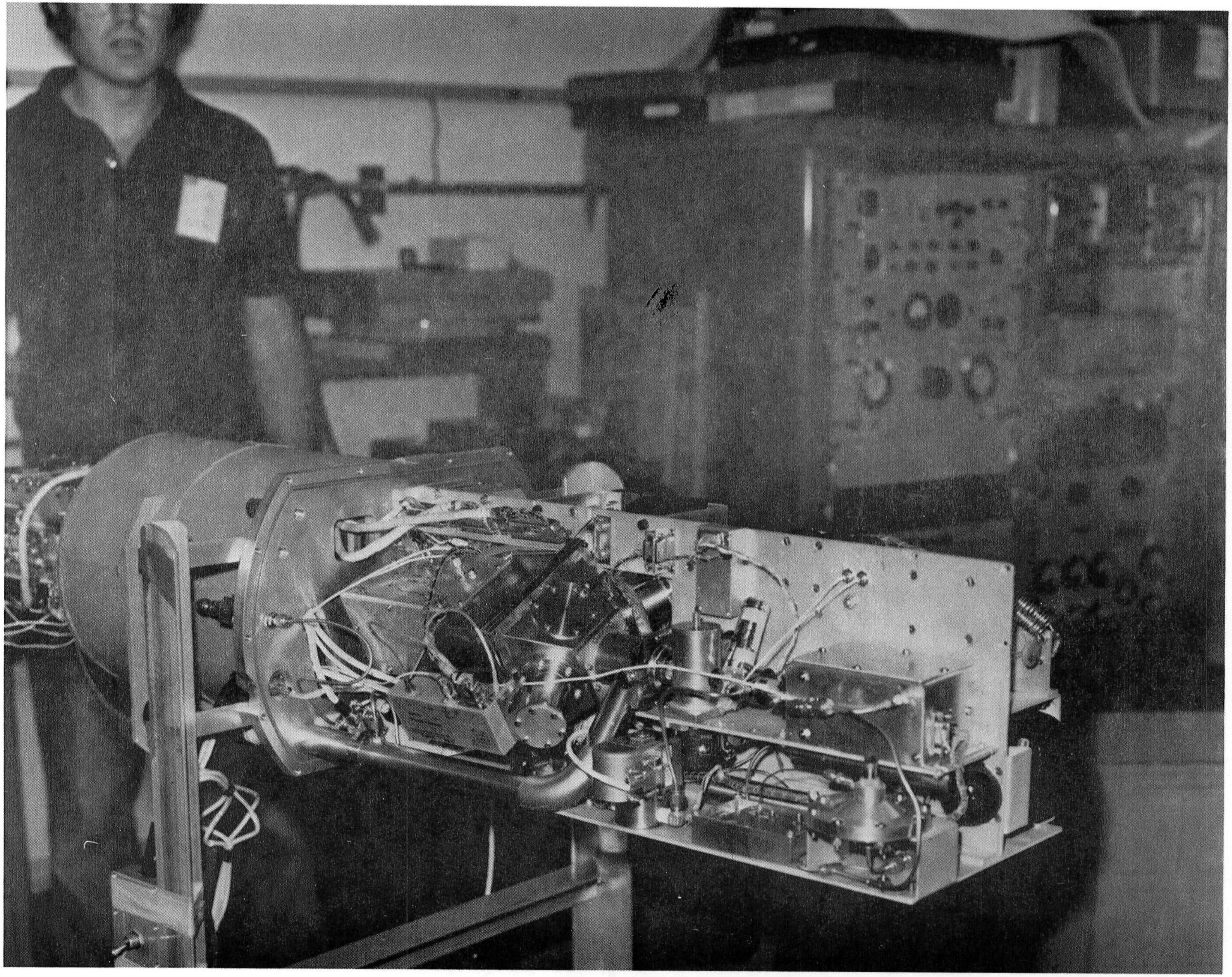

Figure 2.- Main instrumental section of the Lyman-alpha hygrometer, showing scattering chamber, light source, exit line and more.

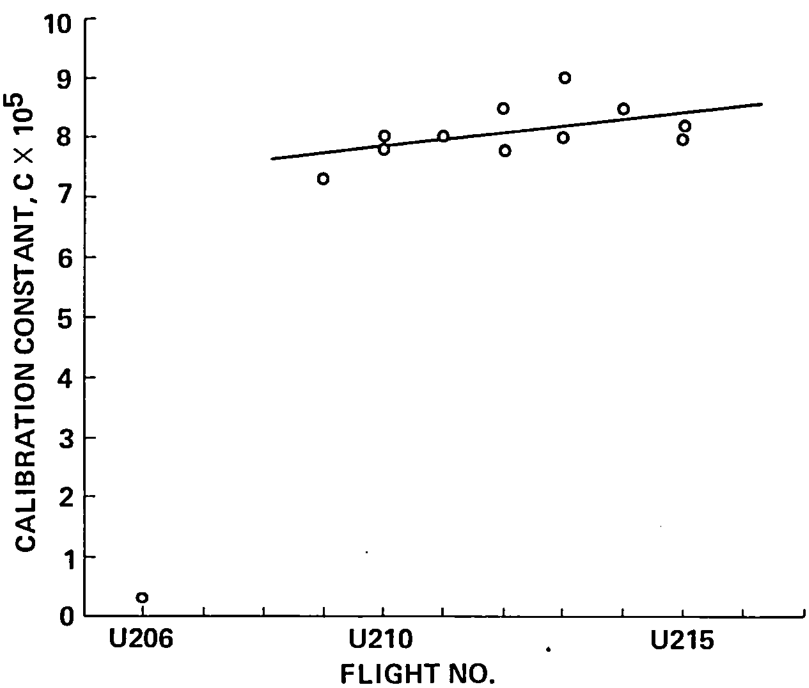

Figure 3.- Calibration constants C for the Panama experiment.

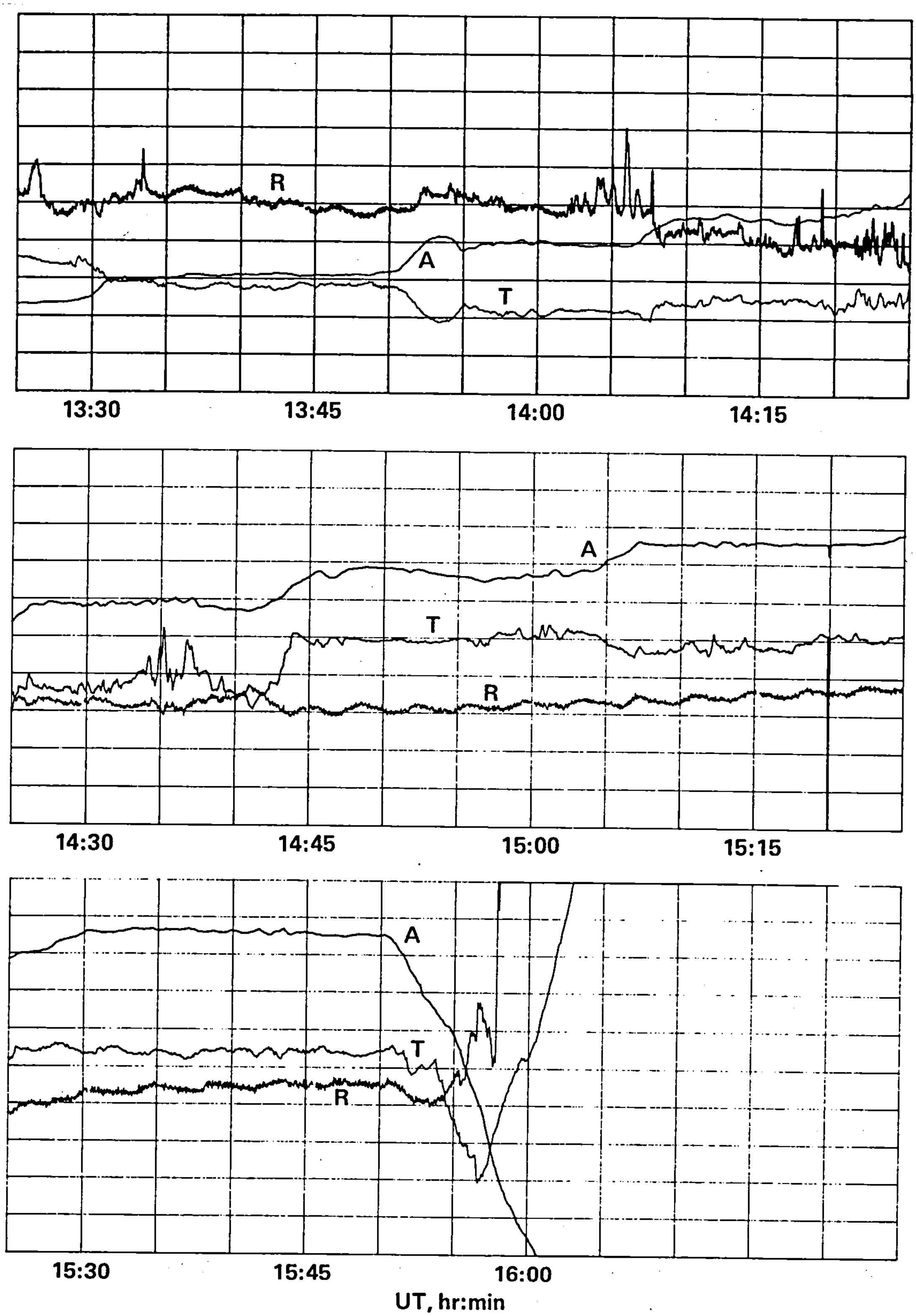

Figure 4.- Flight 1: mixing ratio R, altitude A, and temperature T versus time. Vertical scales: 0-10 ppmv (R); 12-22 km (A); 185 K-235 K (T).

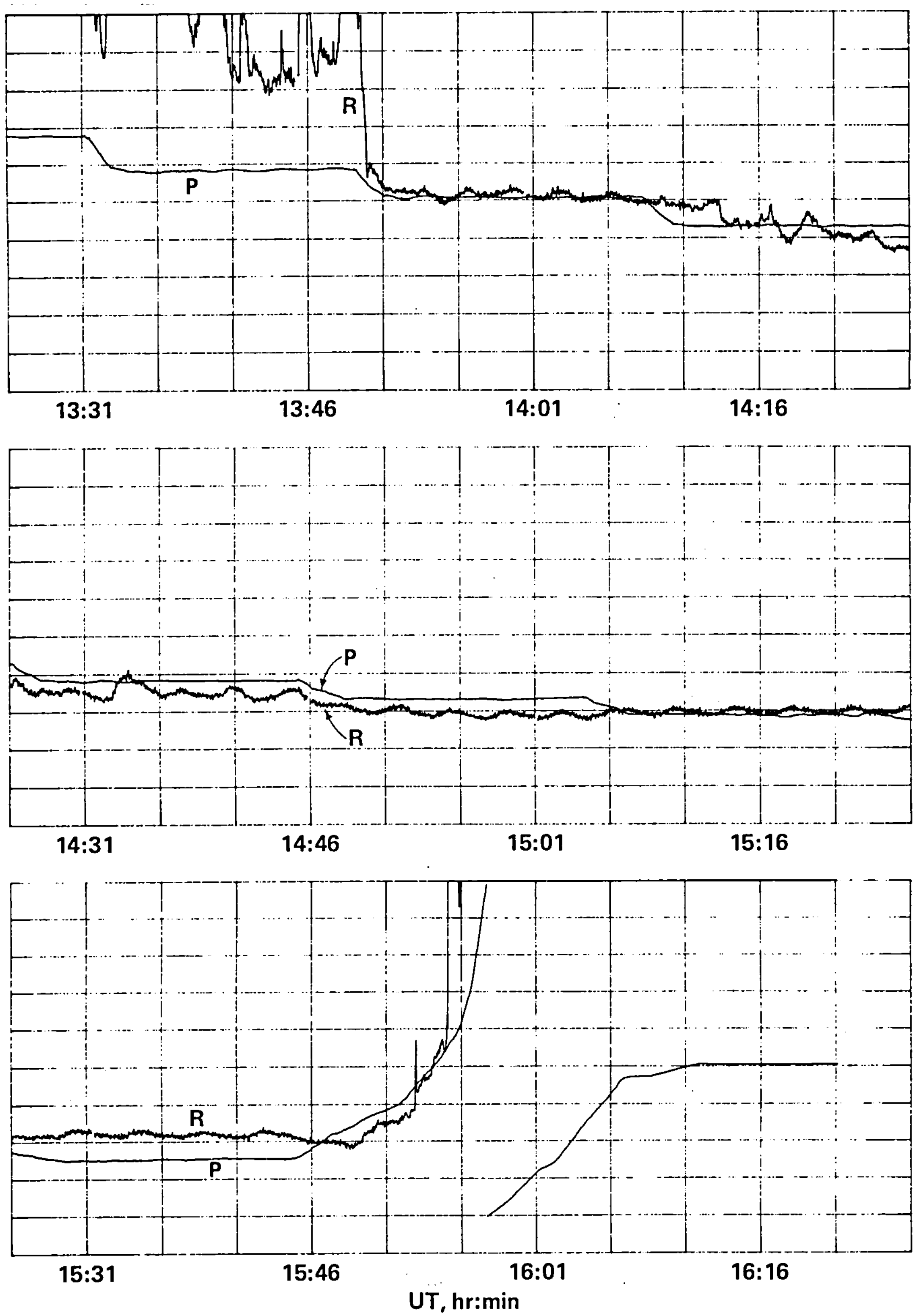

Figure 5.- Flight 3: mixing ratio R and internal pressure P versus time. Vertical scales: 0-10 ppmv (R); 0-200 mbars (P).

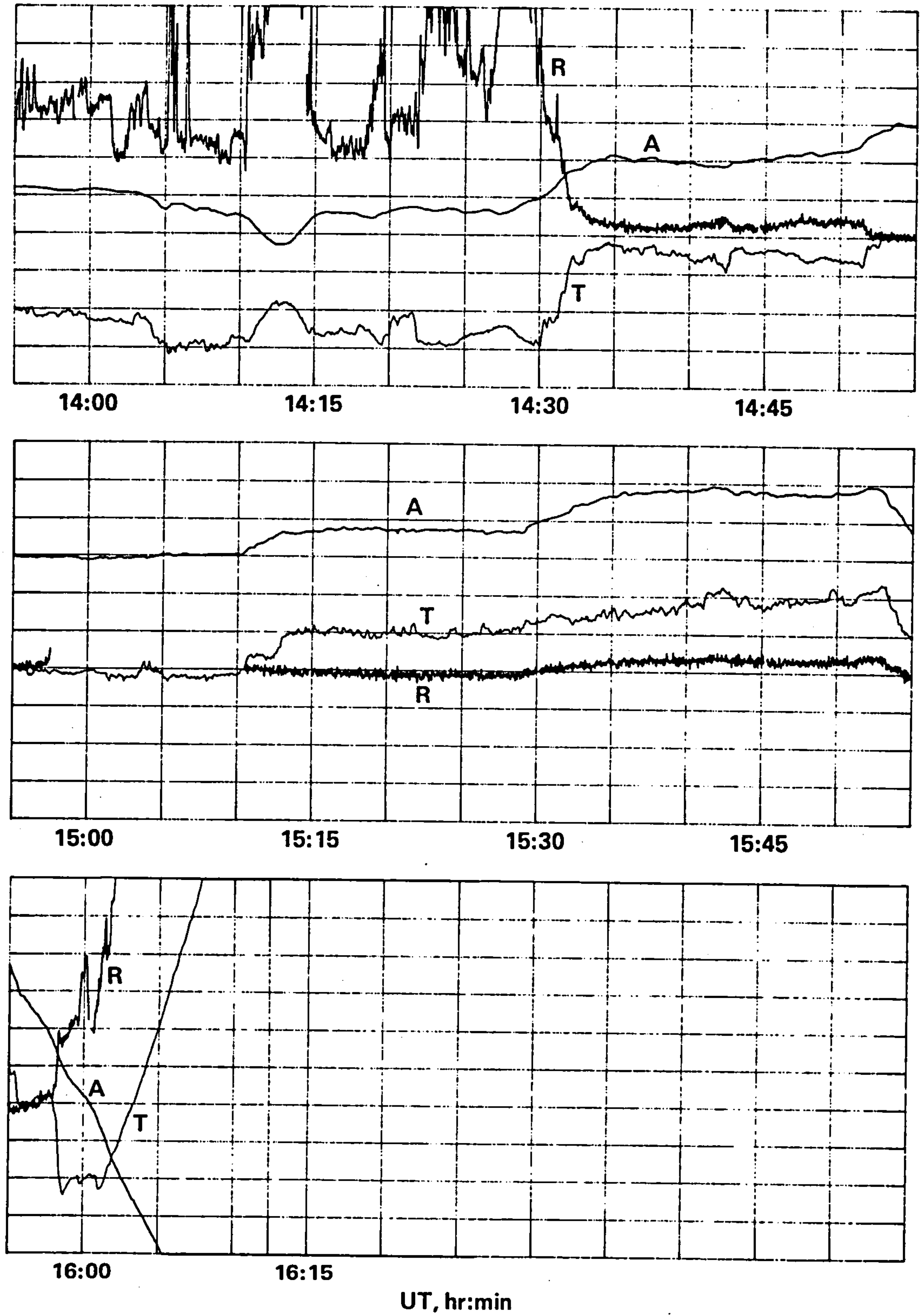

Figure 6.- Flight 4: mixing ratio R, altitude A, and temperature T versus time. Vertical scales: 0-10 ppmv (R); 12-22 km (A); 185 K-235 K (T).

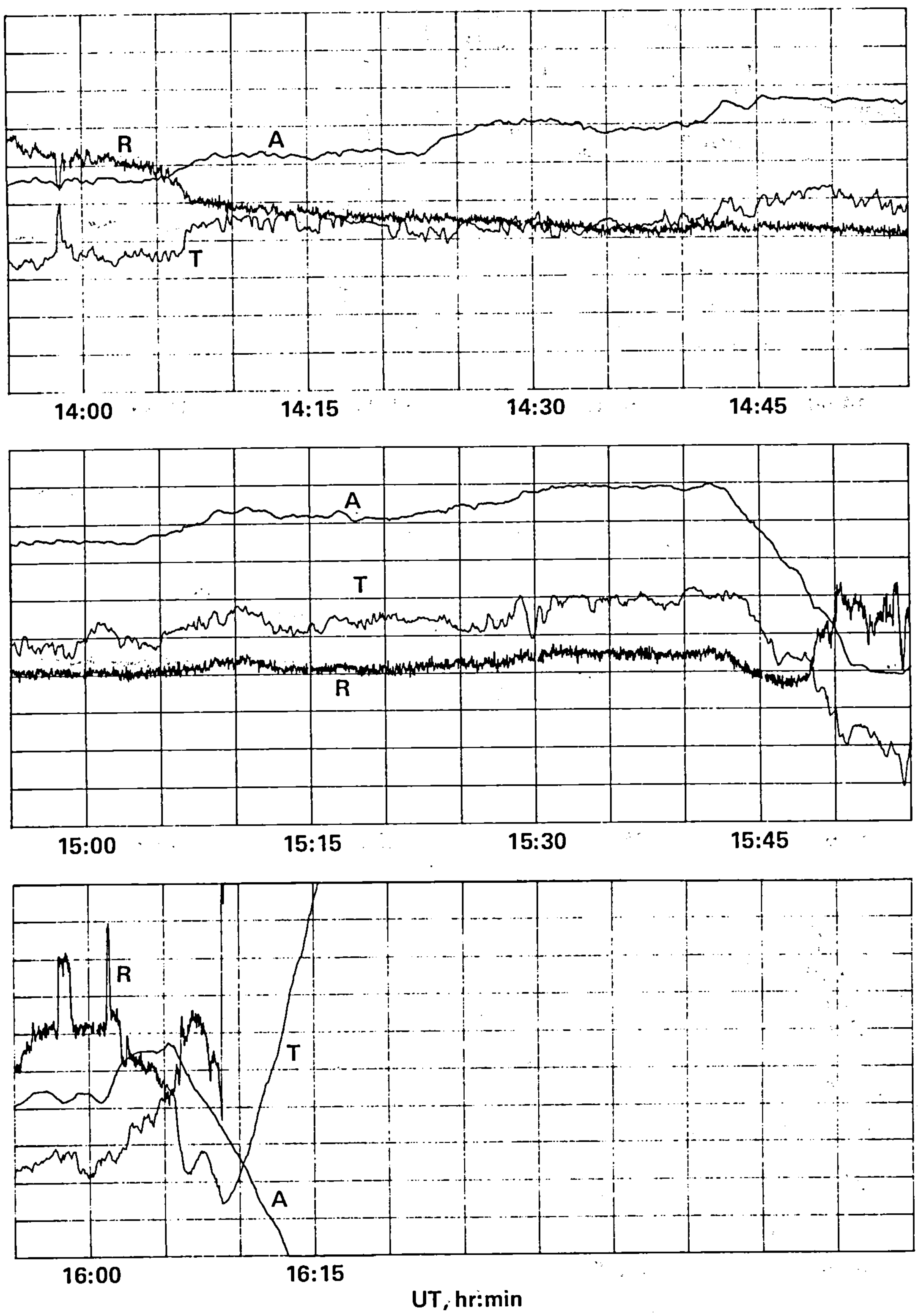

Figure 7.- Flight 5: mixing ratio R, altitude A, and temperature T versus time. Vertical scales: 0-10 ppmv (R); 12-22 km (A); 185 K-235 K (T).

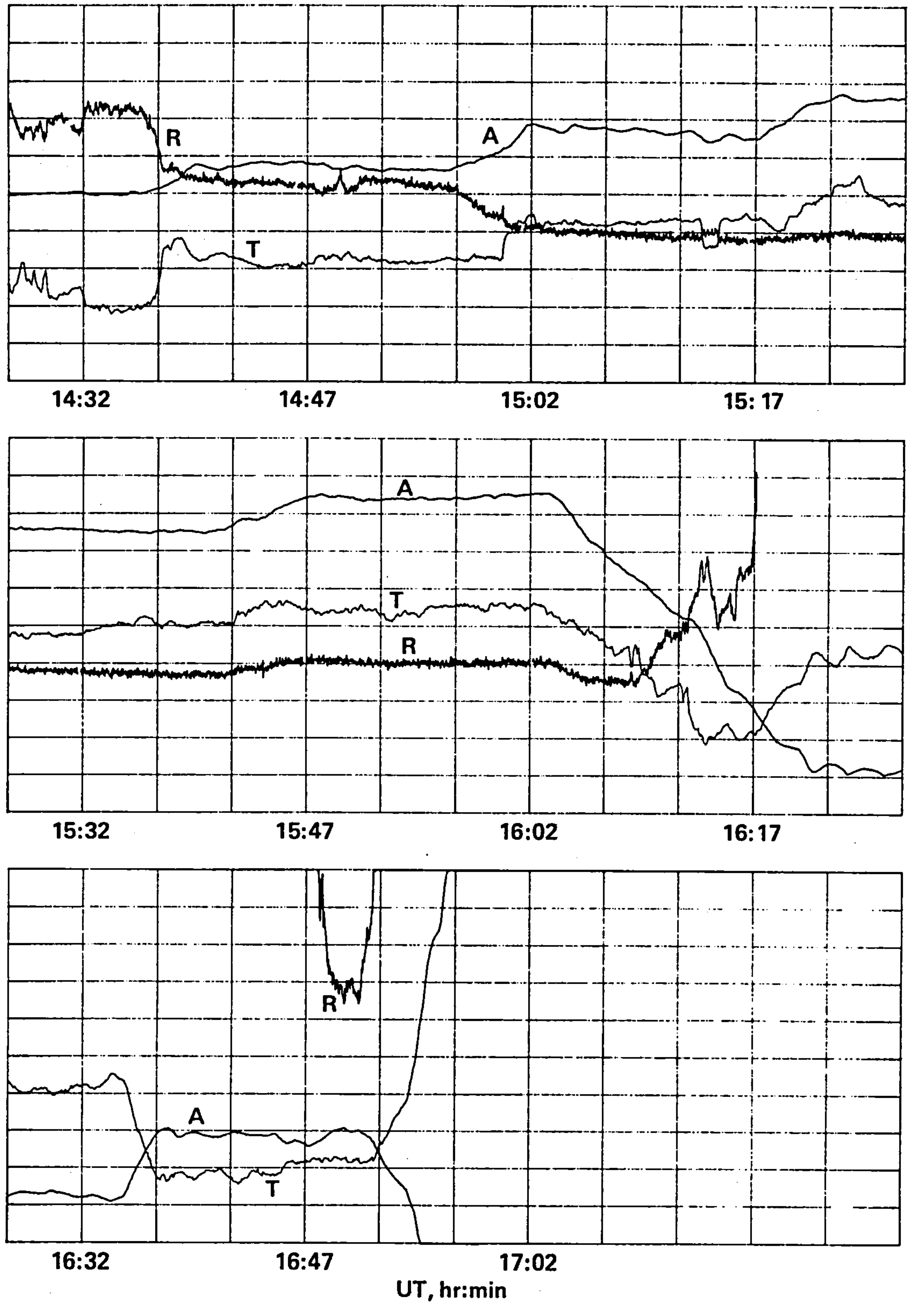

Figure 8.- Flight 6: mixing ratio R, altitude A, and temperature T versus time. Vertical scales: 0-10 ppmv (R); 12-22 km (A); 185 K-235 K (T).

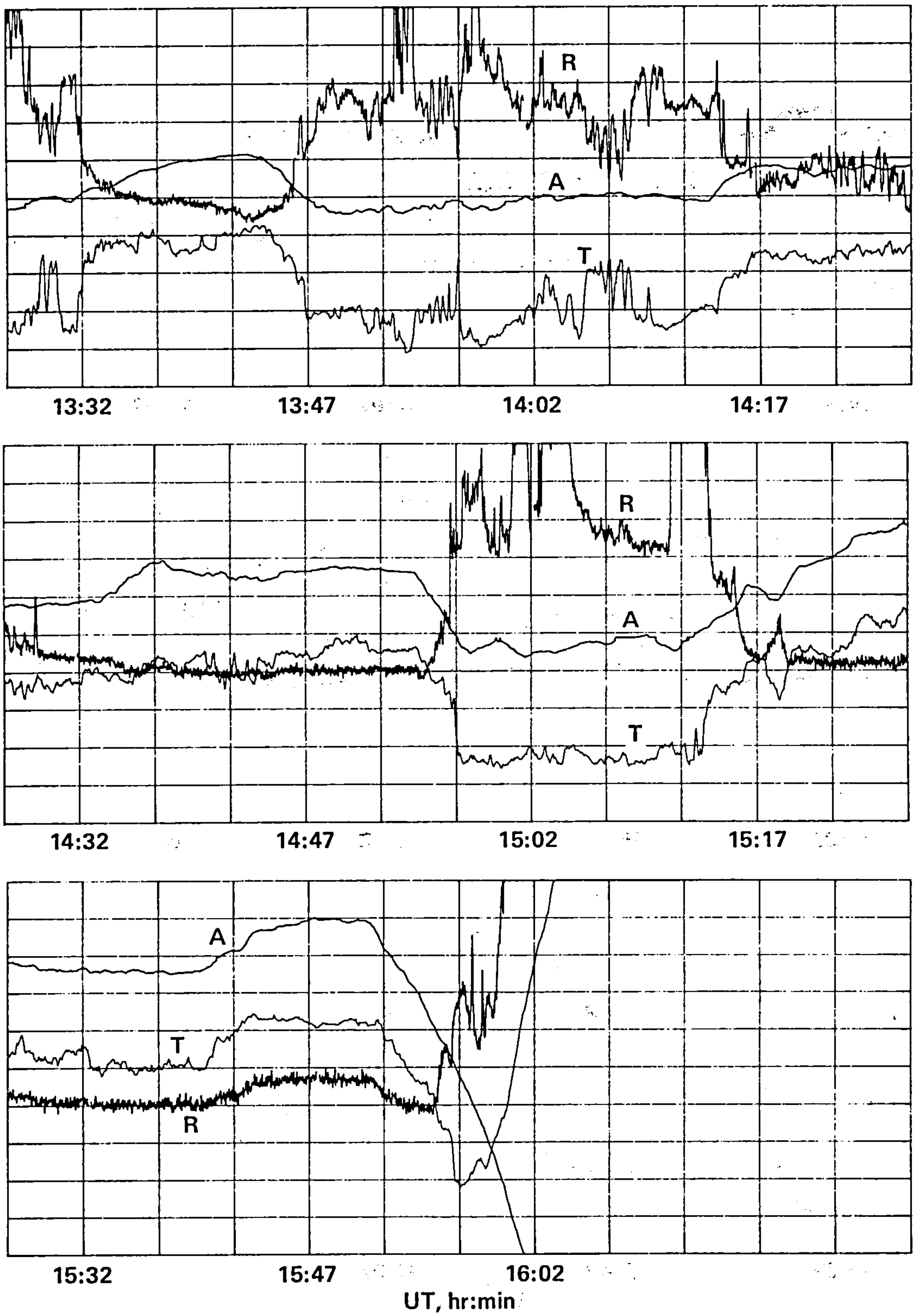

Figure 9.- Flight 7: mixing ratio R, altitude A, and temperature T versus time. Vertical scales: 0-10 ppmv (R); 12-22 km (A); 185 K-235 K (T).

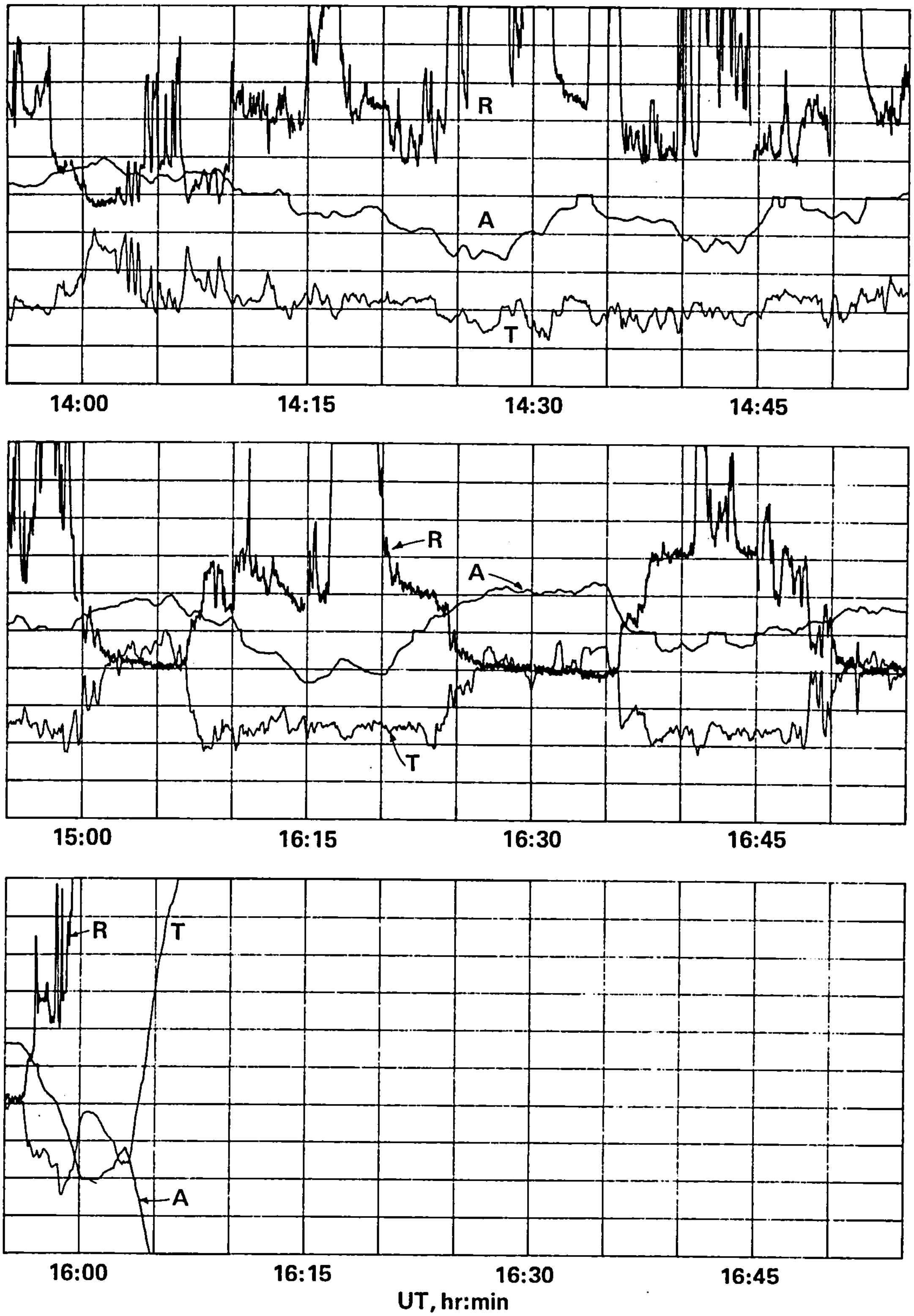

Figure 10.- Flight 8: mixing ratio R, altitude A, and temperature T versus time. Vertical scales: 0-10 ppmv (R); 12-22 km (A); 185 K-235 K (T).

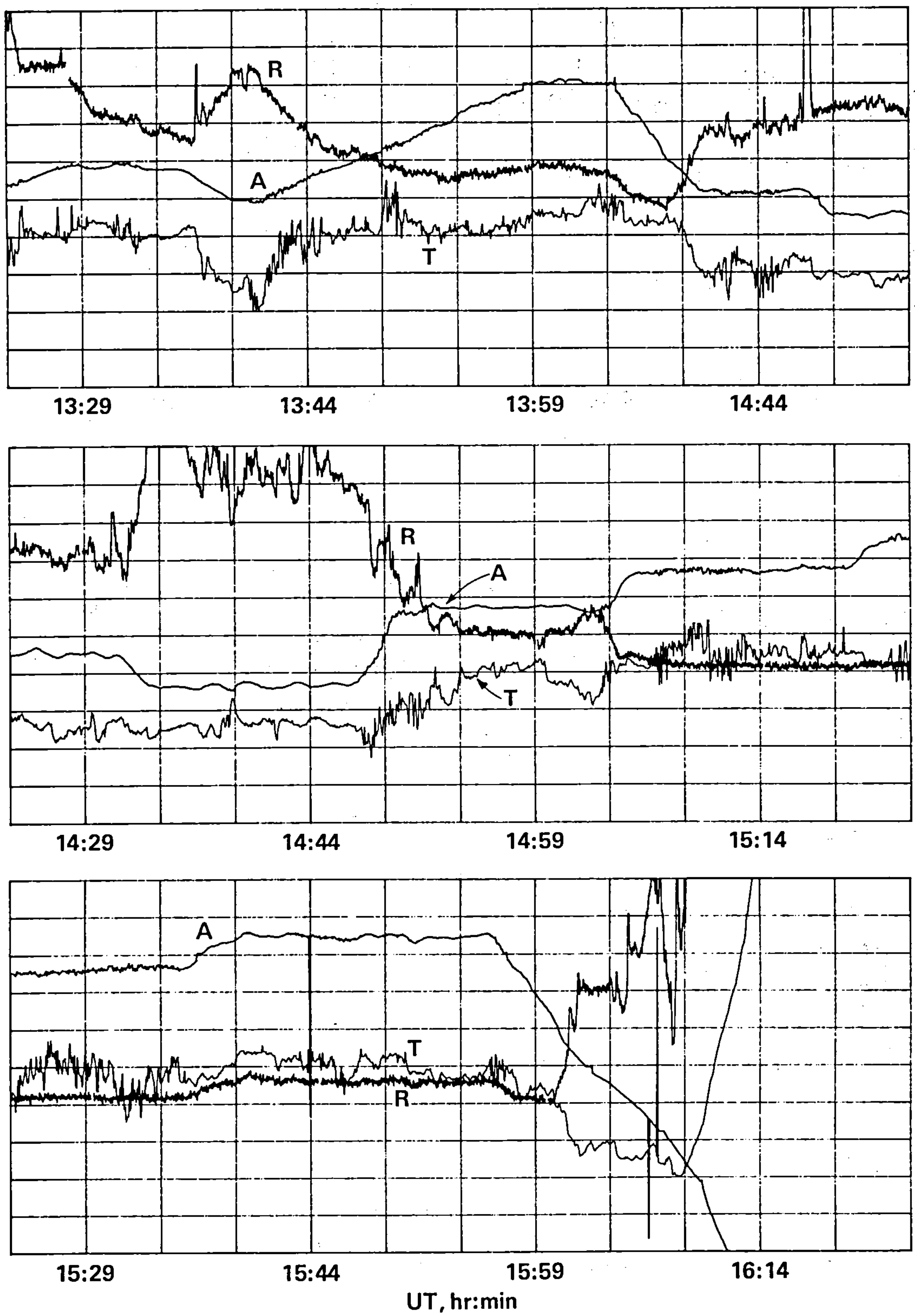

Figure 11.- Flight 9: mixing ratio R, altitude A, and temperature T versus time. Vertical scales: 0-10 ppmv (R); 12-22 km (A); 185 K-235 K (T).

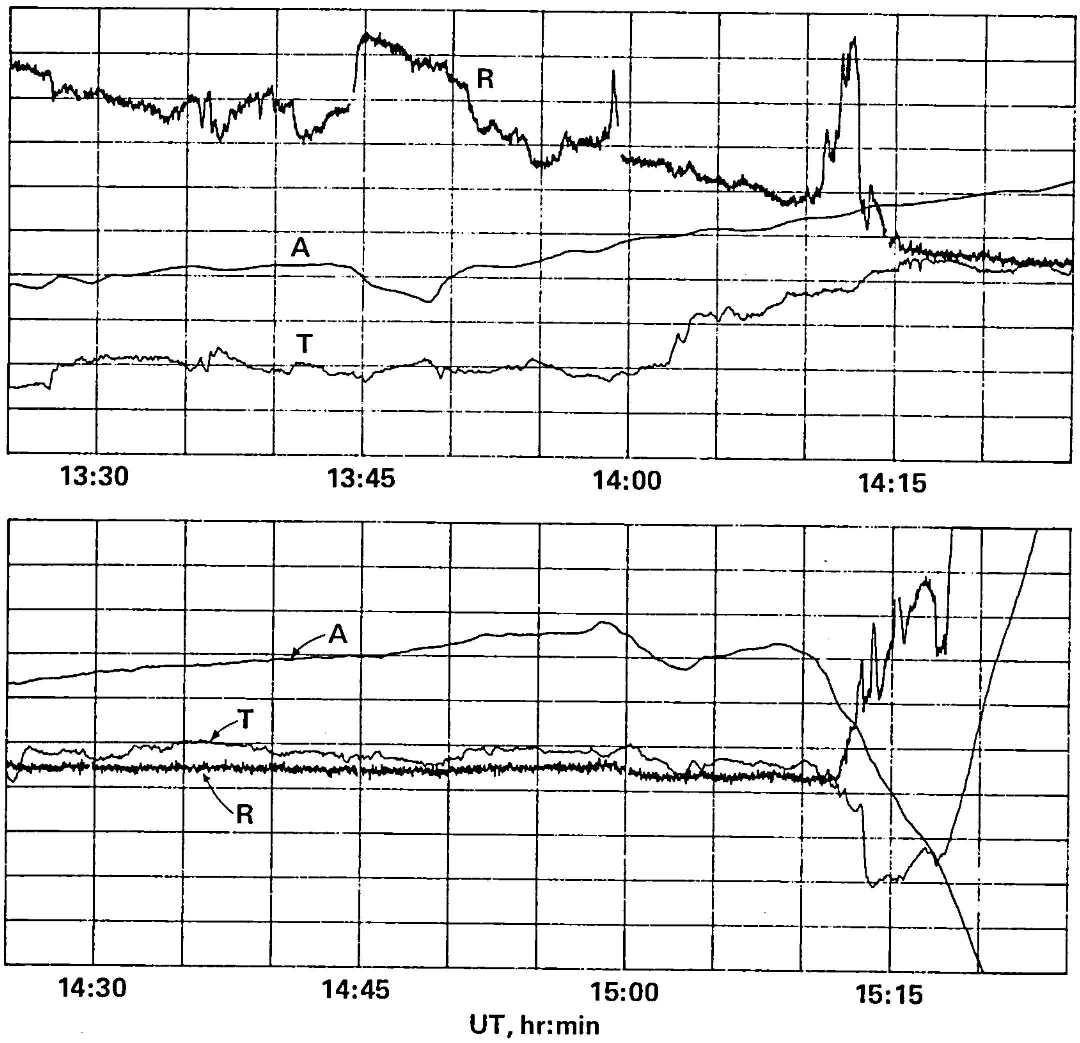

Figure 12.- Flight 10: mixing ratio R, altitude A, and temperature T versus time. Vertical scales: 0-10 ppmv (R); 12-22 km (A); 185 K-235 K (T).

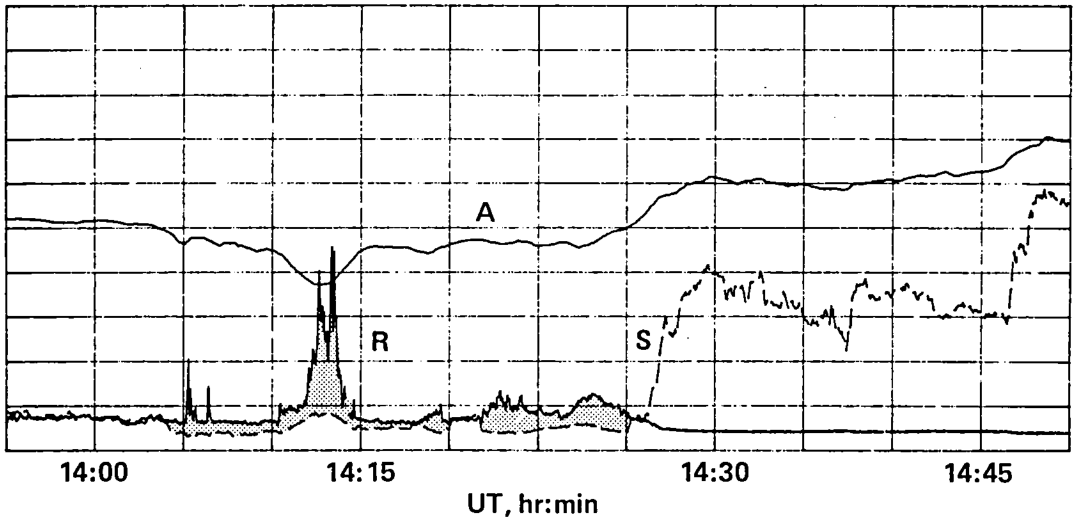

Figure 13.- Flight 4: mixing ratio R, altitude A, and saturation mixing ratio S versus time. Periods of apparent supersaturation indicated by speckling. Vertical scale: 0-100 ppmv (R); 12-22 km (A); 0-100 ppmv (S).

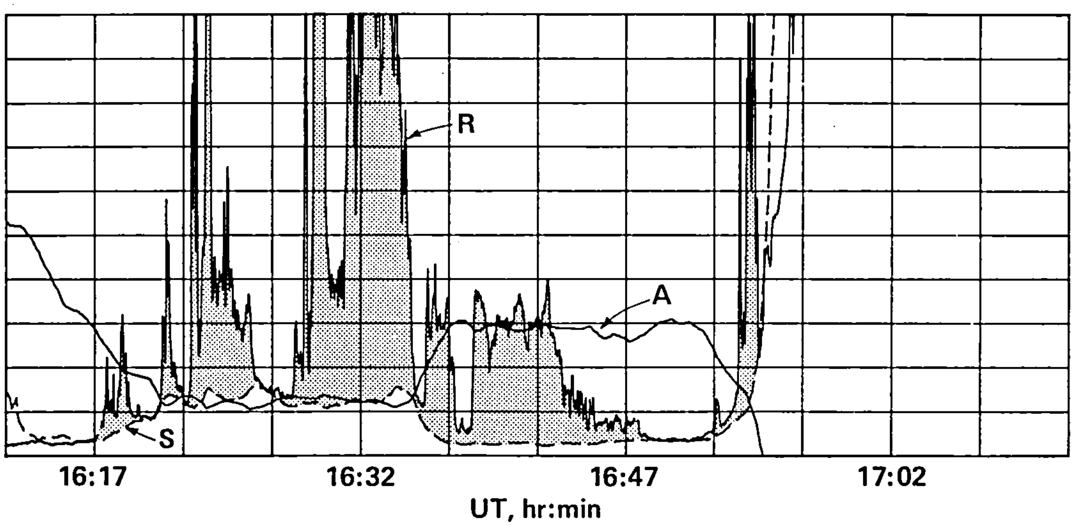

Figure 14.- Flight 6: mixing ratio R, altitude A, and saturation mixing ratio S versus time. Periods of apparent supersaturation indicated by speckling. Vertical scale: 0-200 ppmv (R); 0-22 km (A); 0-200 ppmv (S).

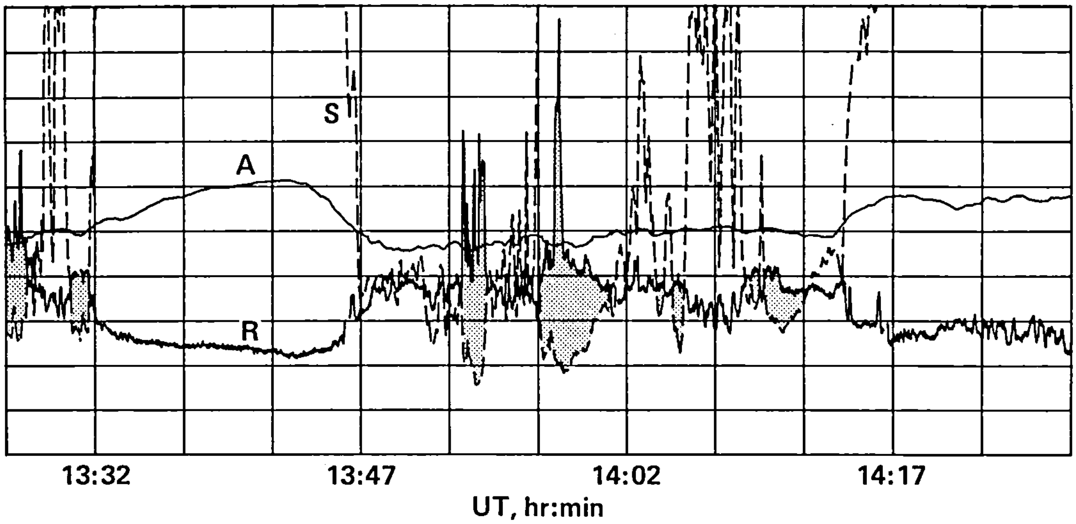

Figure 15.- Flight 7: mixing ratio R, altitude A, and saturation mixing ratio S versus time. Periods of apparent supersaturation indicated by speckling. Vertical scale: 0-20 ppmv (R); 12-22 km (A); 0-20 ppmv (S).

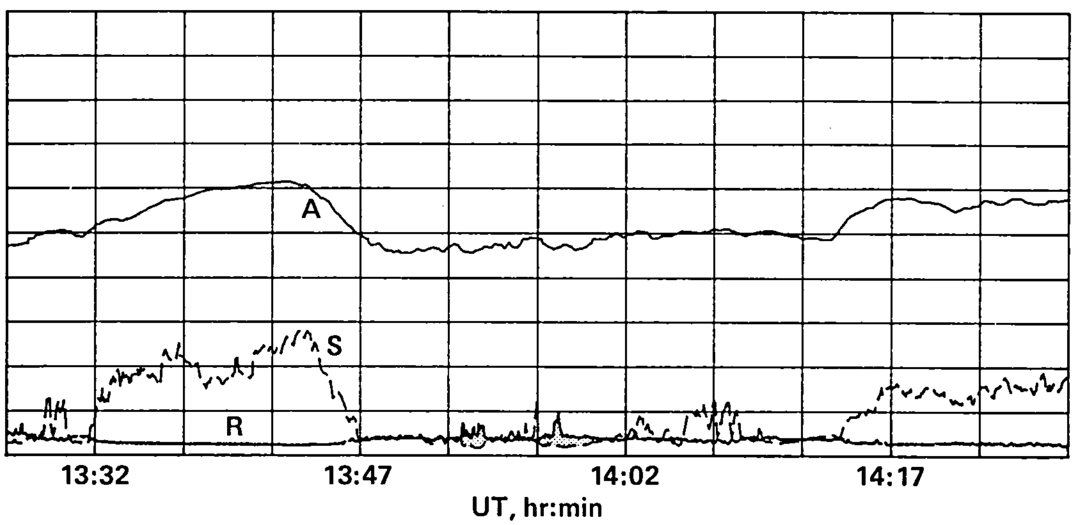

Figure 16.- Flight 7: mixing ratio R, altitude A, and saturation mixing ratio S versus time. Periods of apparent supersaturation indicated by speckling. Vertical scale: 0-200 ppmv (R); 12-22 km (A); 0-200 ppmv (S).

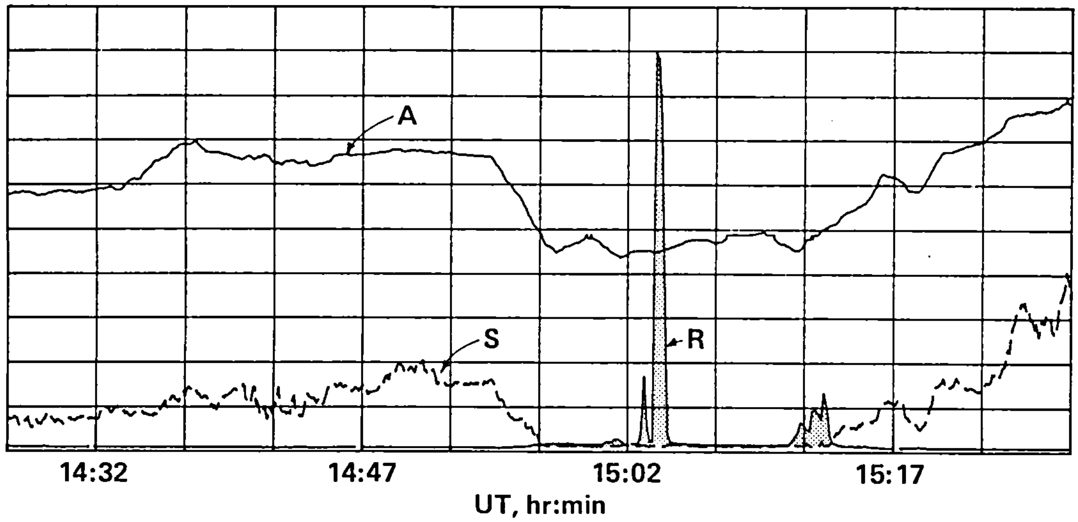

Figure 17.- Flight 7: mixing ratio R, altitude A, and saturation mixing ratio S versus time. Periods of apparent supersaturation indicated by speckling. Vertical scale: 0-500 ppmv (R); 12-22 km (A); 0-500 ppmv (S).

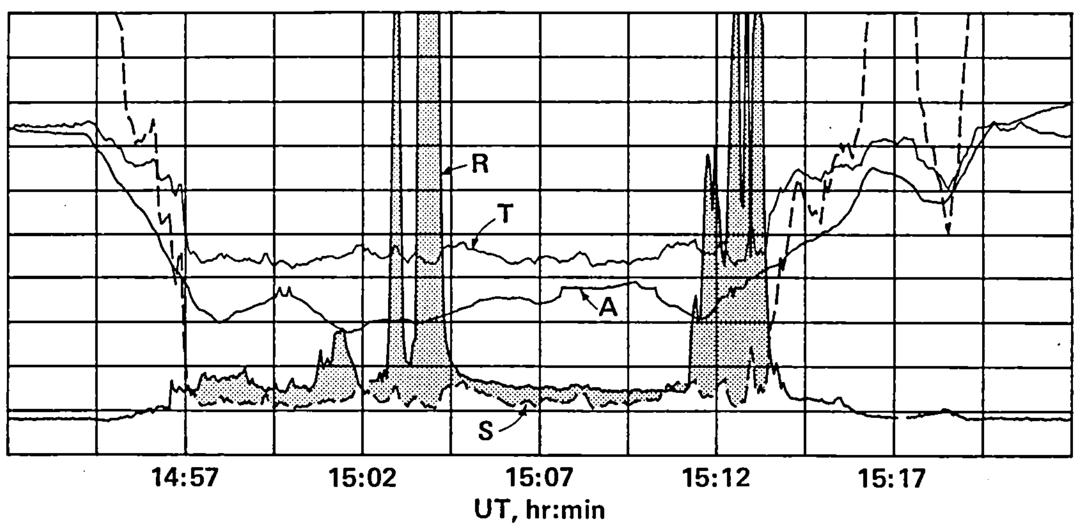

Figure 18.- Flight 7: mixing ratio R, altitude A, temperature T, and saturation mixing ratio S versus time. Periods of apparent supersaturation indicated by speckling. Vertical scale: 0-50 ppmv (R); 15-20 km (A); 172 K-220 K (T); 0-50 ppmv (S).

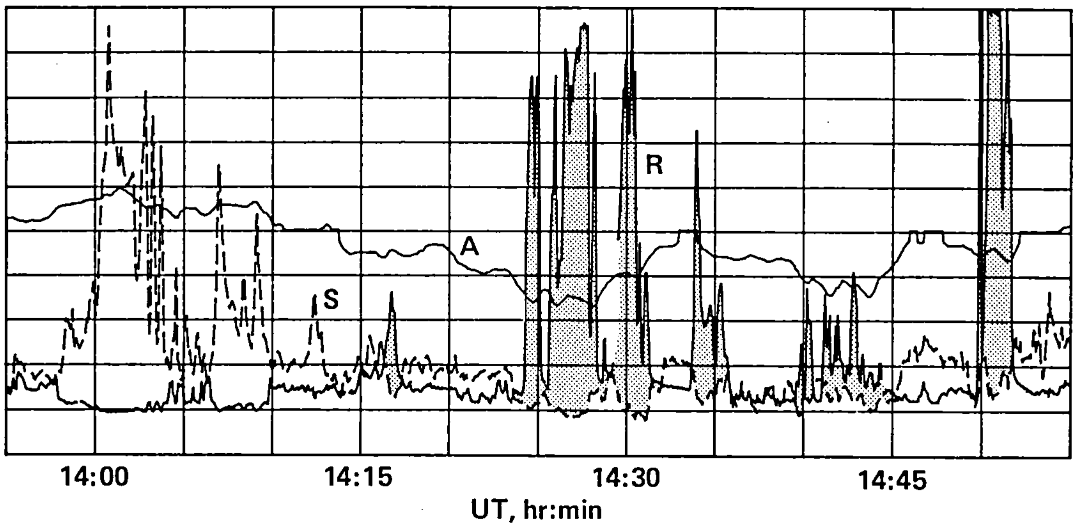

Figure 19.- Flight 8: mixing ratio R, altitude A, and saturation mixing ratio S versus time. Periods of apparent supersaturation indicated by speckling. Vertical scale: 0-50 ppmv (R); 12-22 km (A) 0-50 ppmv (S).

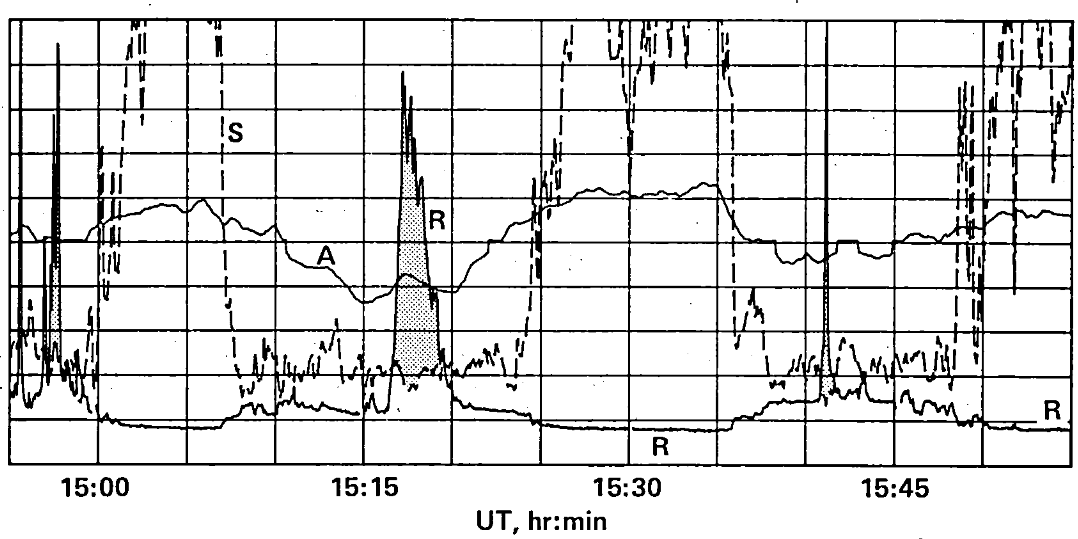

Figure 20.- Flight 8: mixing ratio R, altitude A, and saturation mixing ratio S versus time. Periods of apparent supersaturation indicated by speckling. Vertical scale: 0-50 ppmv (R); 12-22 km (A); 0-50 ppmv (S).

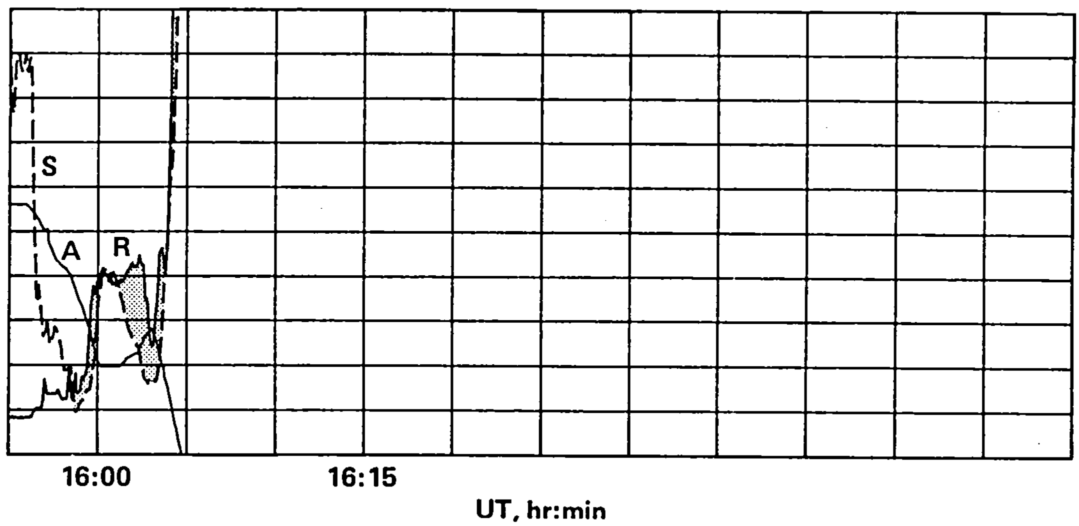

Figure 21.- Flight 8: mixing ratio R, altitude A, and saturation mixing ratio S versus time. Periods of apparent supersaturation indicated by speckling. Vertical scale: 0-50 ppmv (R); 12-22 km (A); 0-50 ppmv (S).

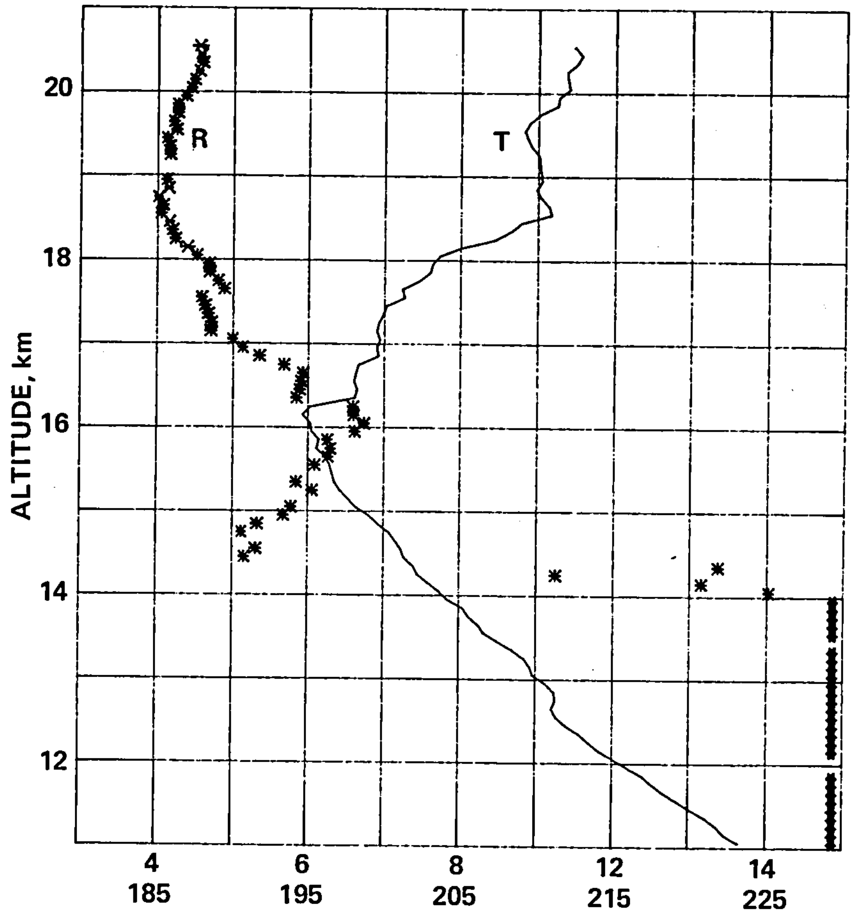

Figure 22.- Flight 1: vertical plot during descent (t ≥ 15:50). Horizontal scales: mixing ratio R and temperature T.

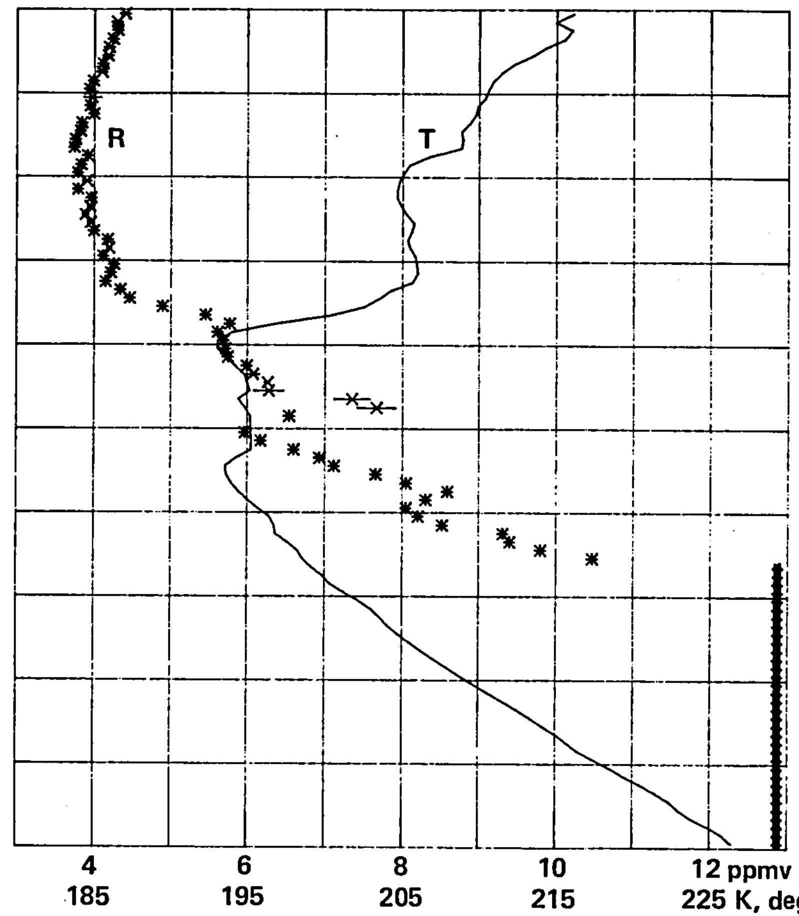

Figure 23.- Flight 4: vertical plot during descent (t ≥ 15:50). Horizontal scales: mixing ratio R and temperature T.

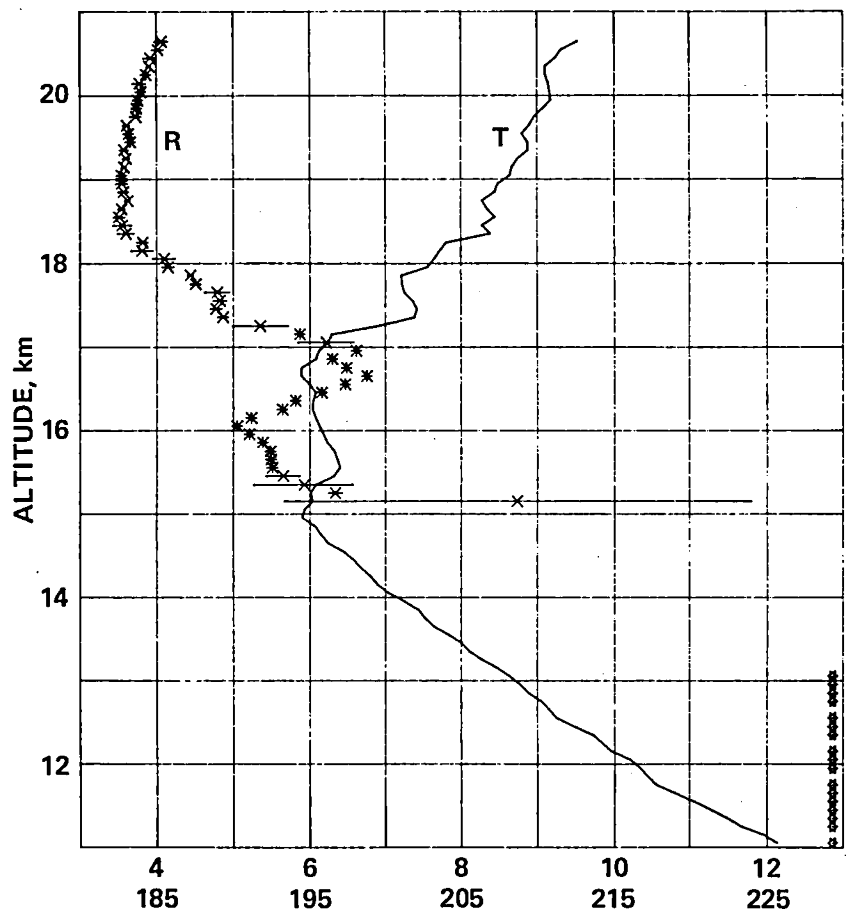

Figure 24.- Flight 5: vertical plot during descent (t ≥ 14:40). Horizontal scales: mixing ratio R and temperature T.

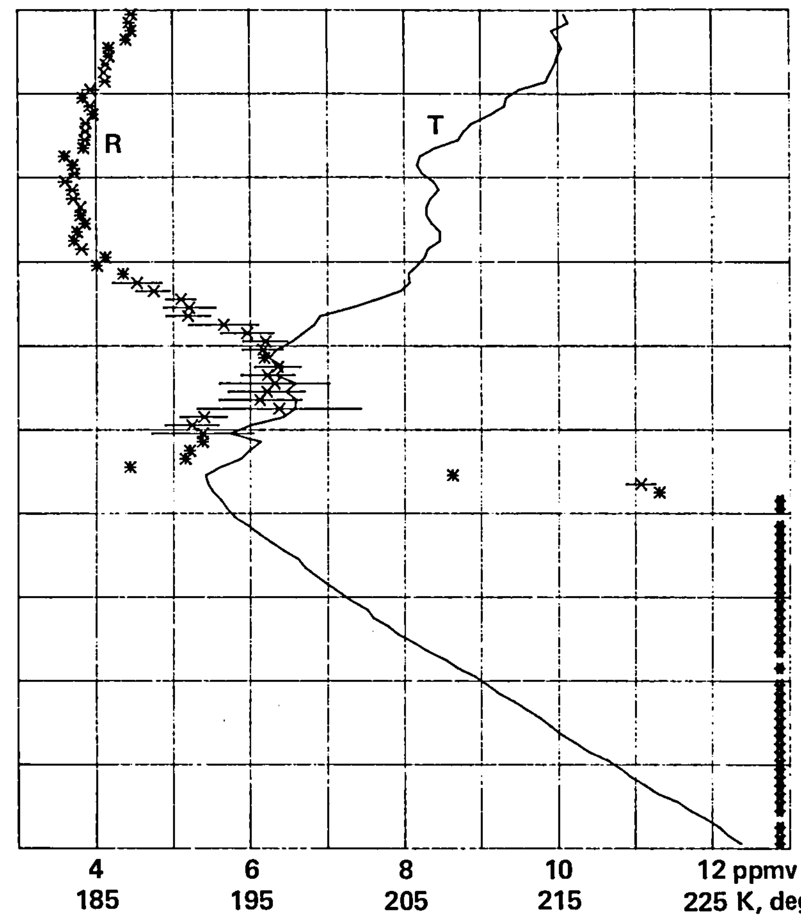

Figure 25.- Flight 6: vertical plot during descent (t ≥ 16:02). Horizontal scales: mixing ratio R and temperature T.

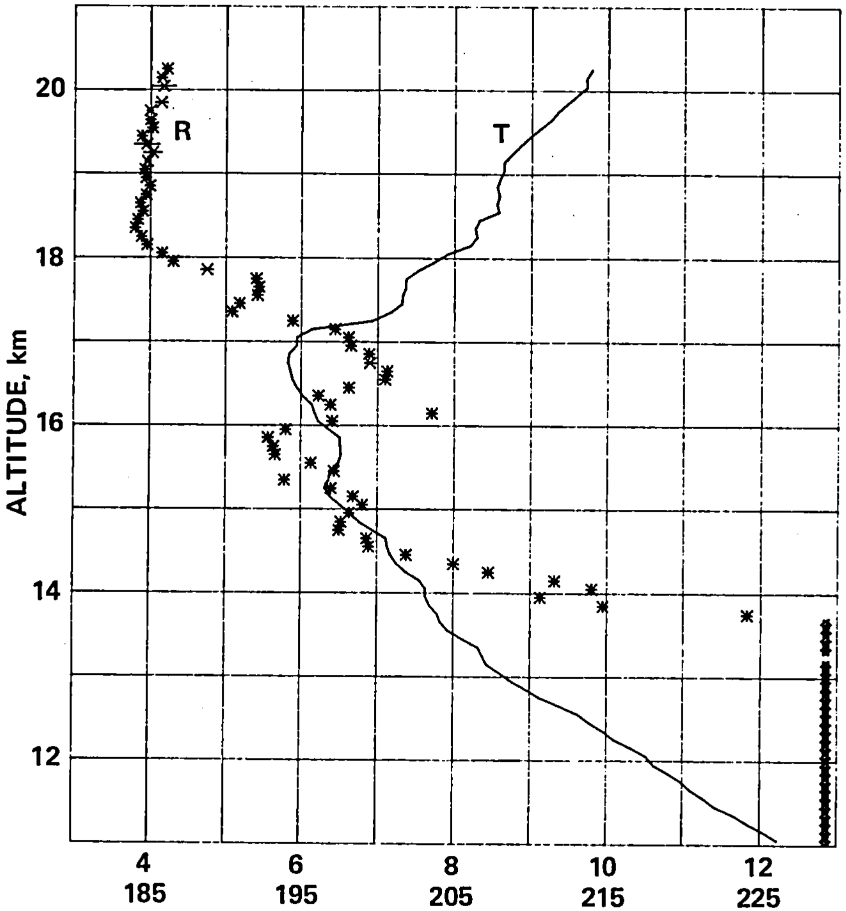

Figure 26.- Flight 7: vertical plot during descent (t ≥ 15:52). Horizontal scales: mixing ratio R and temperature T.

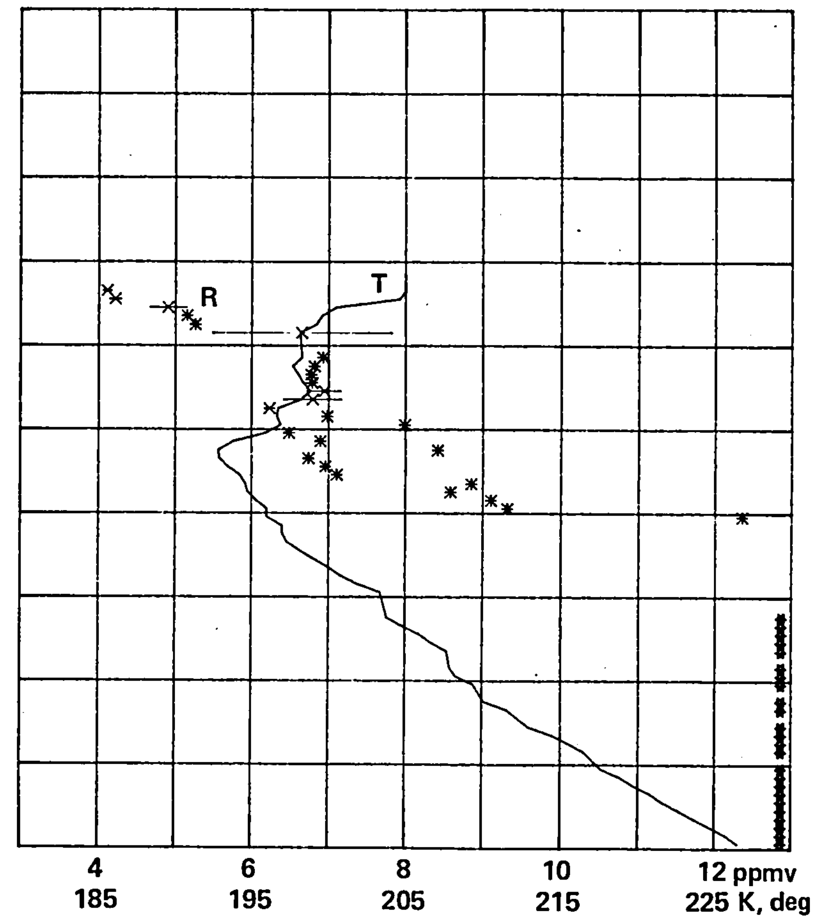

Figure 27.- Flight 8: vertical plot during descent (t ≥ 15:55). Horizontal scales: mixing ratio R and temperature T.

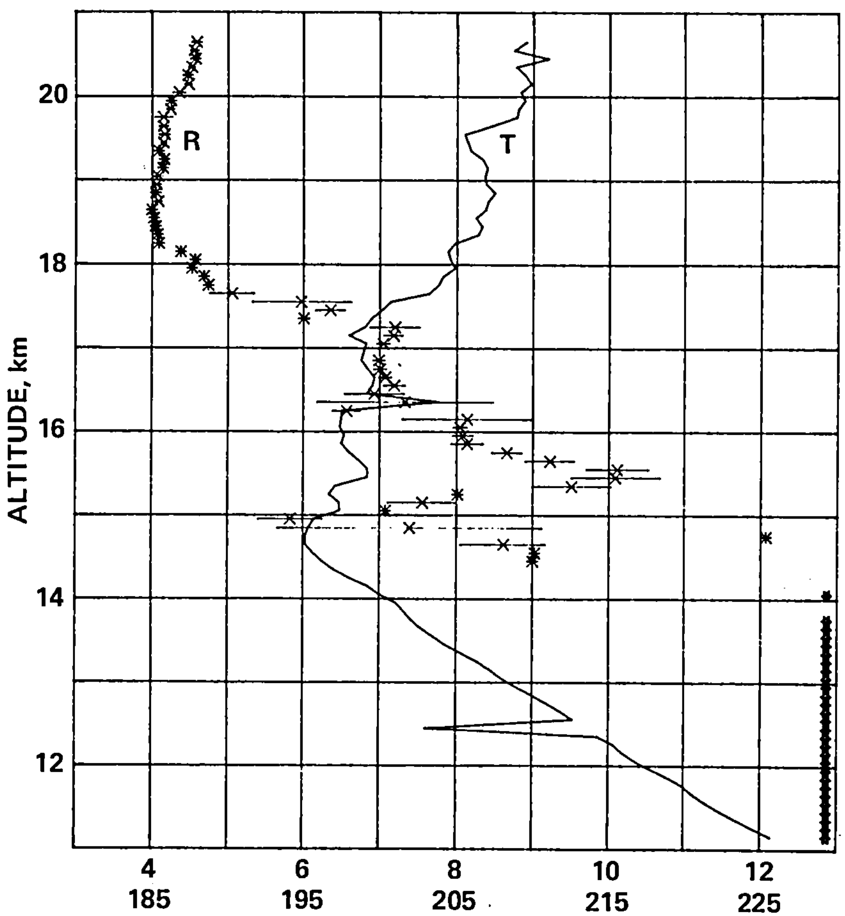

Figure 28.- Flight 9: vertical plot during descent (t ≥ 15:54). Horizontal scales: mixing ratio R and temperature T.

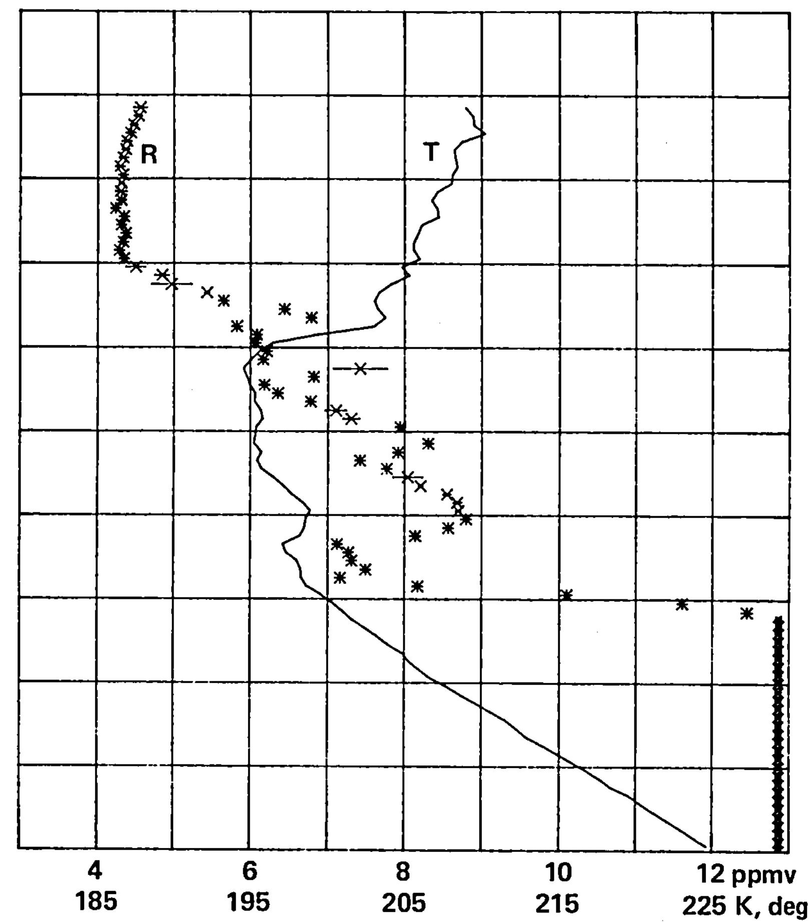

Figure 29.- Flight 10: vertical plot during descent (t ≥ 15:57:30). Horizontal scales: mixing ratio R and temperature T.

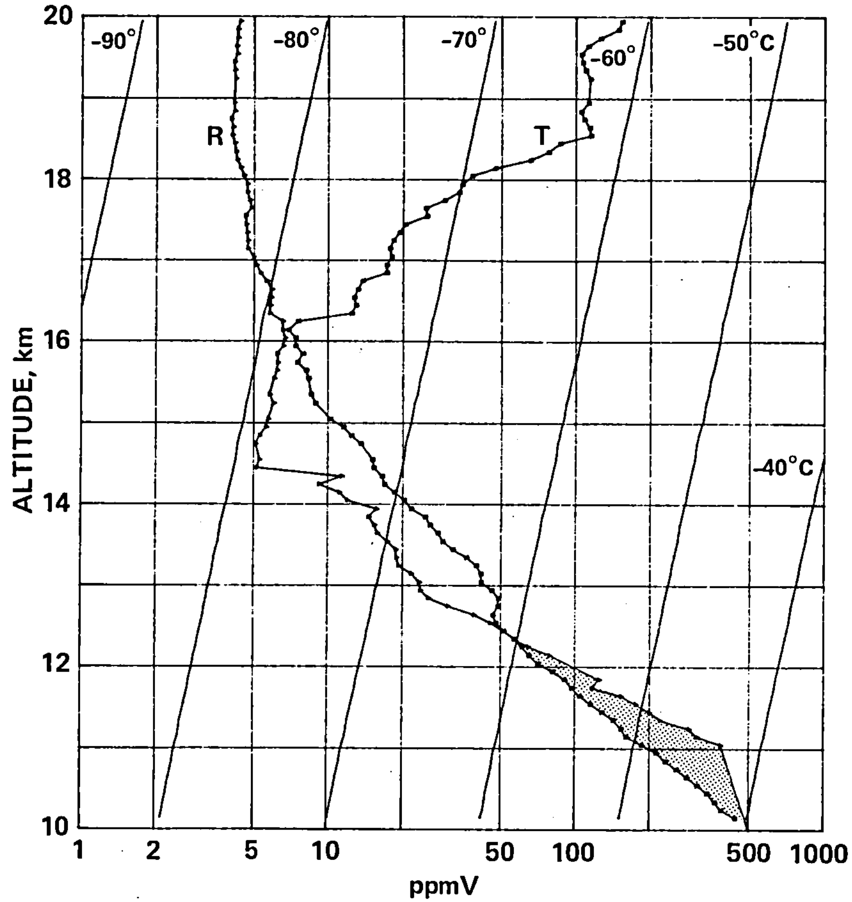

Figure 30.- Flight 1: vertical plot during descent (t ≥ 15:50). Horizontal scale: mixing ratio R between 1 and 1000 ppmv; slanted lines - frost-point coordinates; temperature T in altitude/frost-point coordinates; apparent regions of supersaturation are speckled.

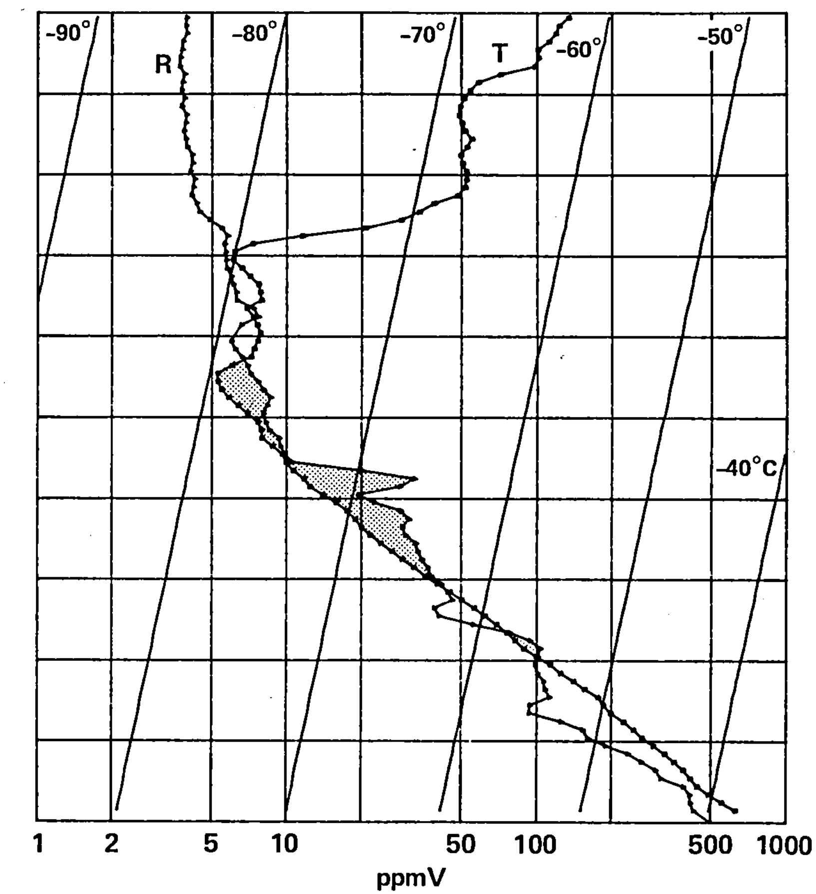

Figure 31.- Flight 4: vertical plot during descent (t ≥ 15:50). Horizontal scale: mixing ratio R between 1 and 1000 ppmv; slanted lines = frost-point coordinates; temperature T in altitude/frost-point coordinates; apparent regions of supersaturation are speckled.

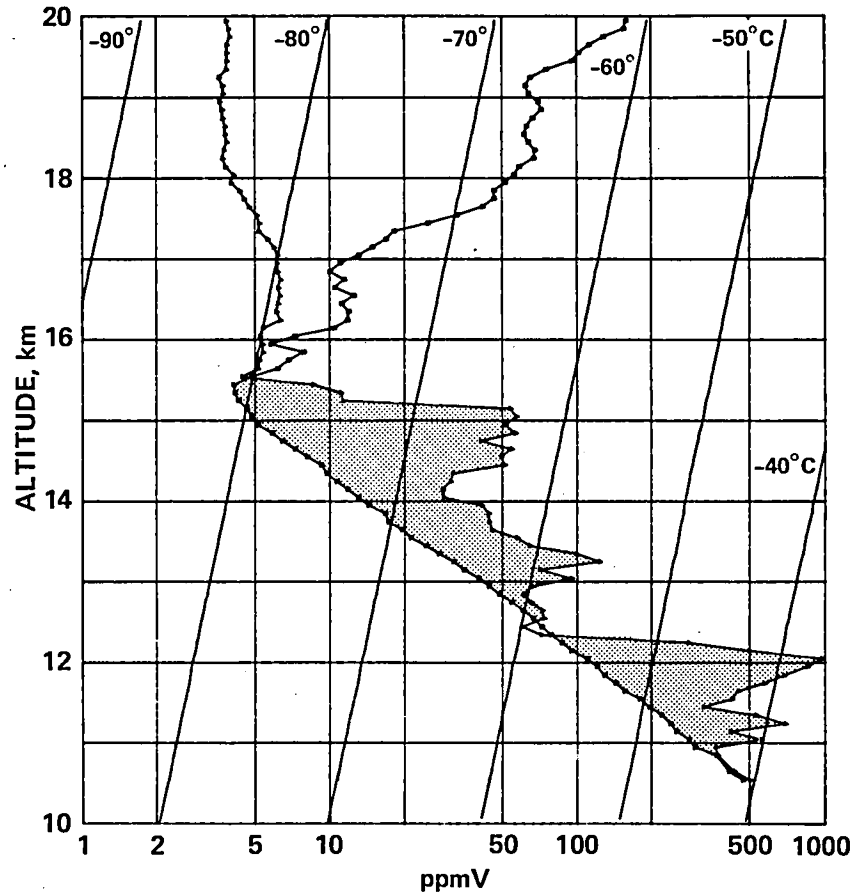

Figure 32.- Flight 5: vertical plot during descent (t ≥ 14:40). Horizontal scale: mixing ratio R between 1 and 1000 ppmv; slanted lines = frost-point coordinates; temperature T in altitude/ frost-point coordinates; apparent regions of supersaturation are speckled.

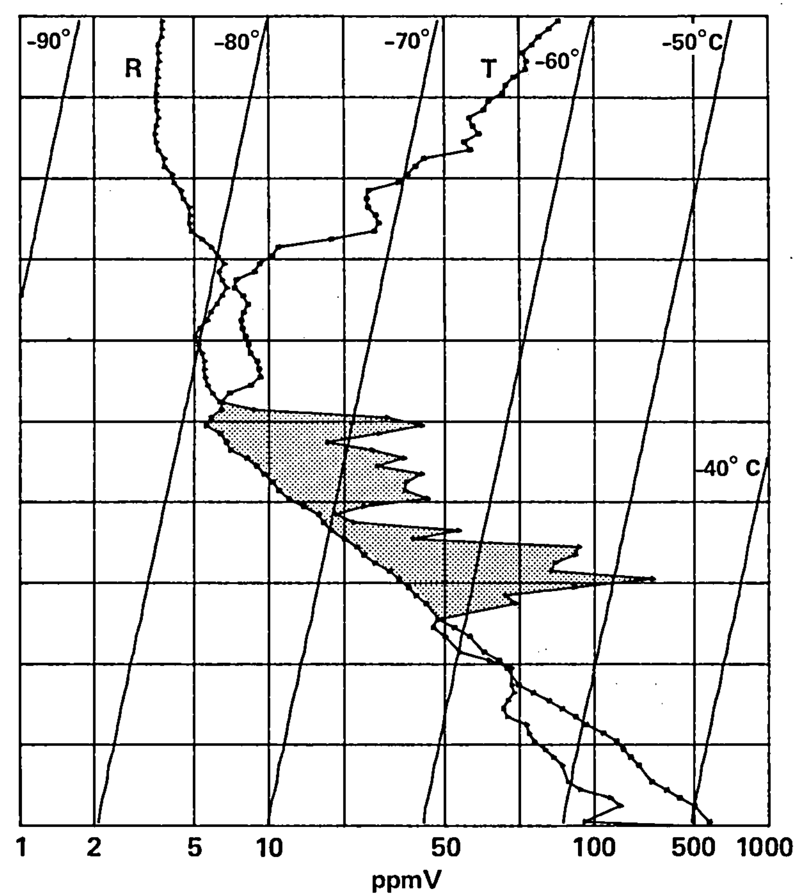

Figure 33.- Flight 6: vertical plot during descent (t ≥ 16:02). Horizontal scale: mixing ratio R between 1 and 1000 ppmv; slanted lines = frost-point coordinates; temperature T in altitude/ frost-point coordinates; apparent regions of supersaturation are speckled.

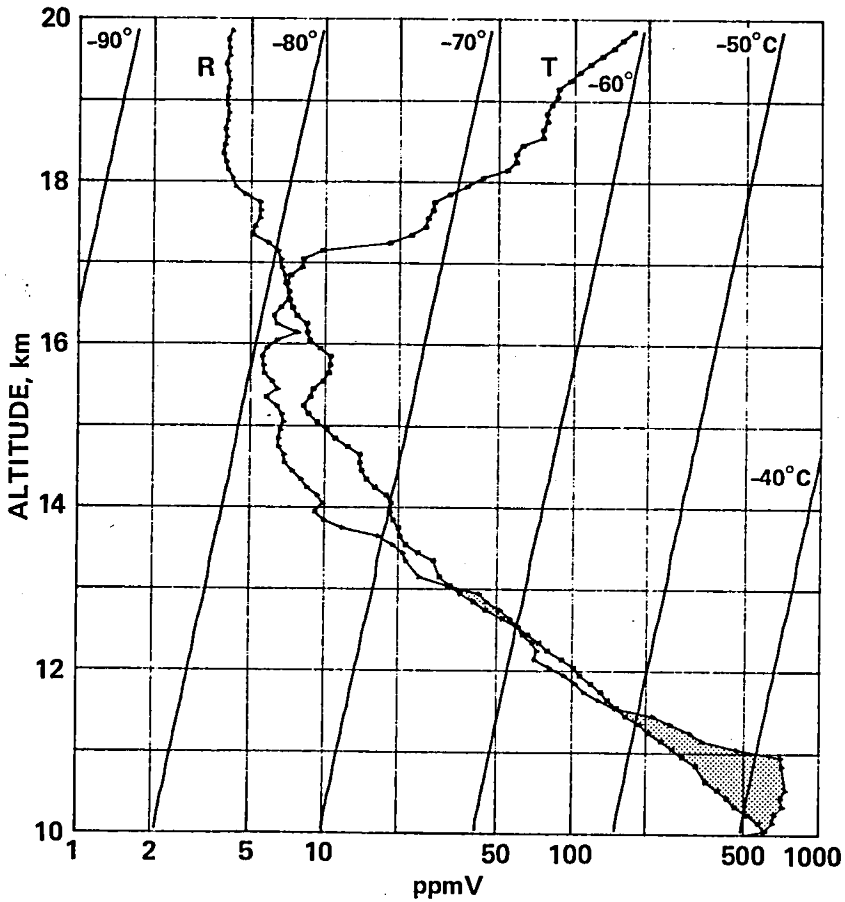

Figure 34.- Flight 7: vertical plot during descent (t ≥ 15:22). Horizontal scale: mixing ratio R between 1 and 1000 ppmv; slanted lines = frost-point coordinates; temperature T in altitude/ frost-point coordinates; apparent regions of supersaturation are speckled.

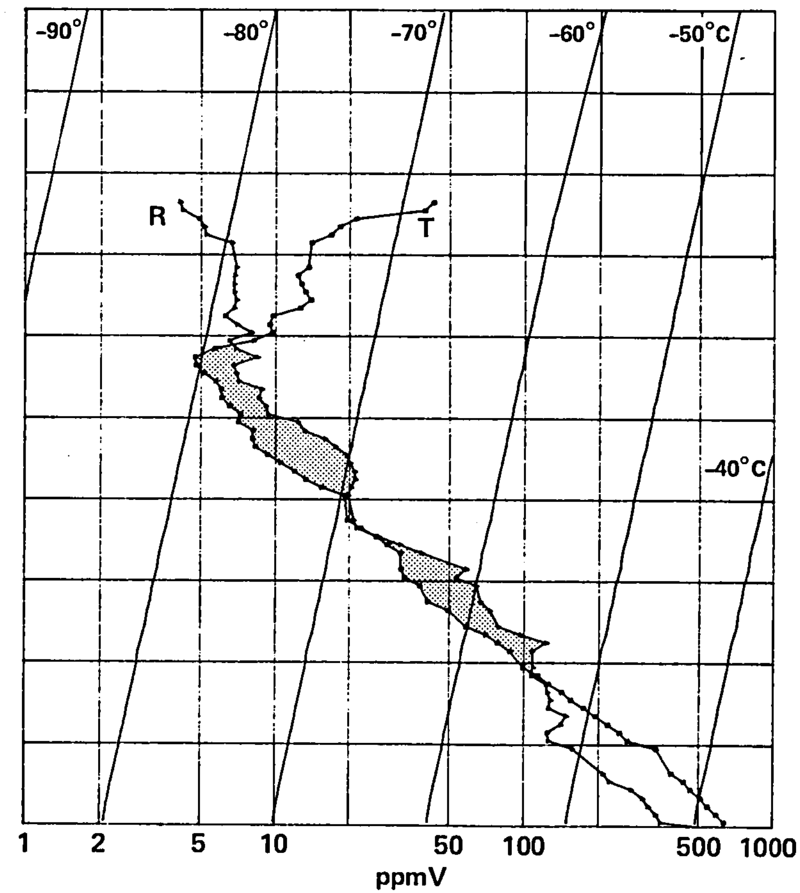

Figure 35.- Flight 8: vertical plot during descent (t ≥ 15:55). Horizontal scale: mixing ratio R between 1 and 1000 ppmv; slanted lines = frost-point coordinates; temperature T in altitude/ frost-point coordinates; apparent regions of supersaturation are speckled.

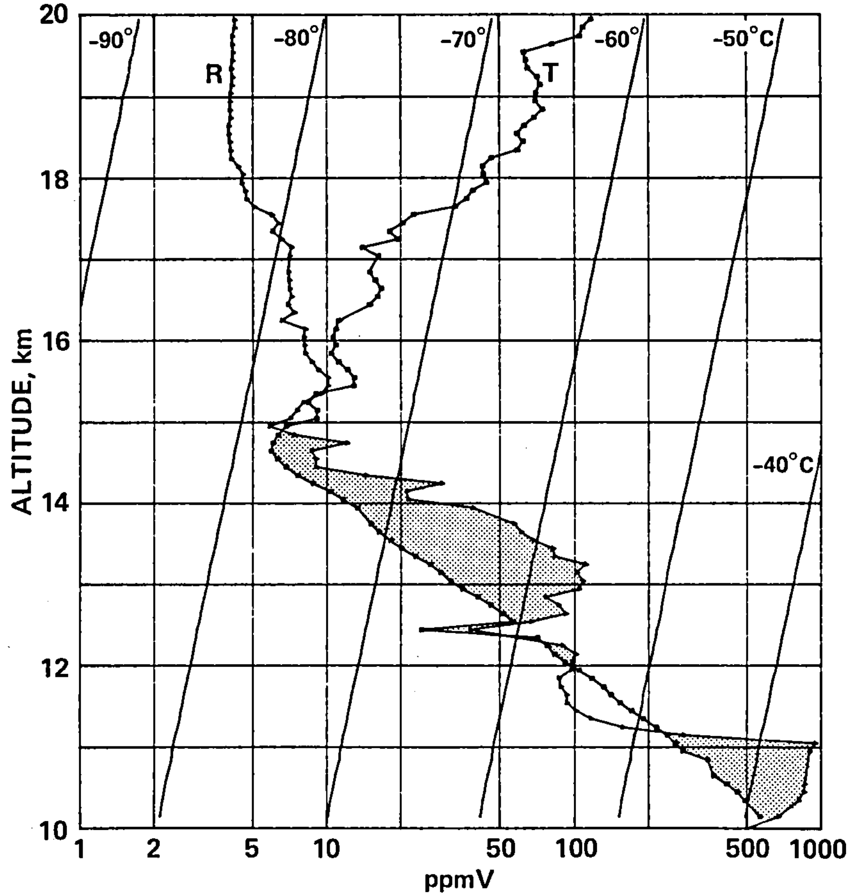

Figure 36.- Flight 9: vertical plot during descent ($t \geq$ 15:54). Horizontal scale: mixing ratio R between 1 and 1000 ppmv; slanted lines = frost-point coordinates; temperature T in altitude/frost-point coordinates; apparent regions of supersaturation are speckled.

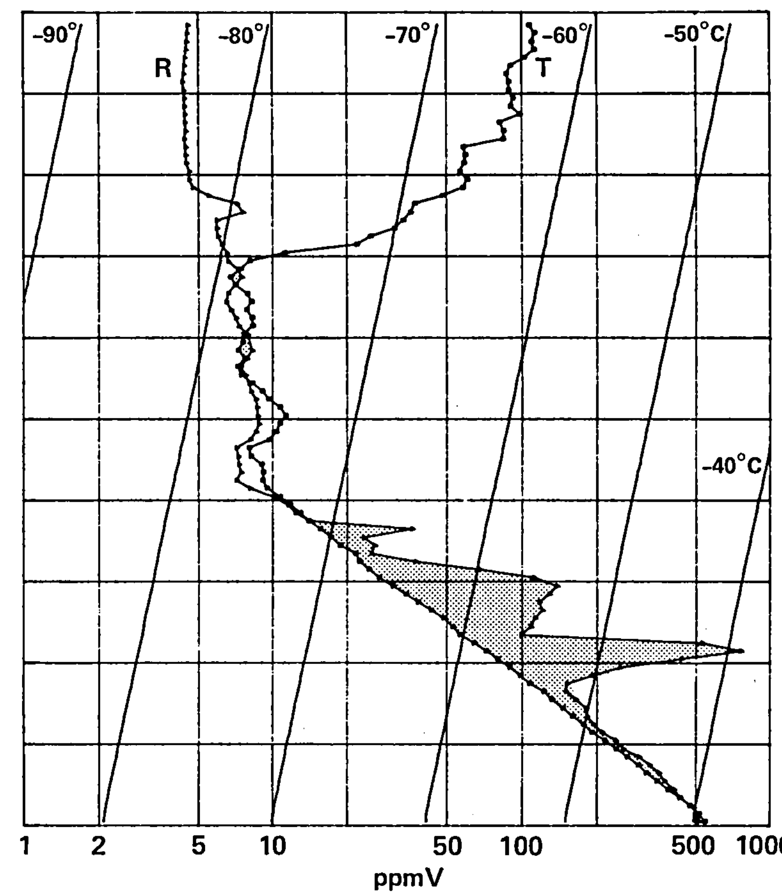

Figure 37.- Flight 10: vertical plot during descent ($t \geq$ 15:57). Horizontal scale: mixing ratio R between 1 and 1000 ppmv; slanted lines = frost-point coordinates; temperature T in altitude/frost-point coordinates; apparent regions of supersaturation are speckled.

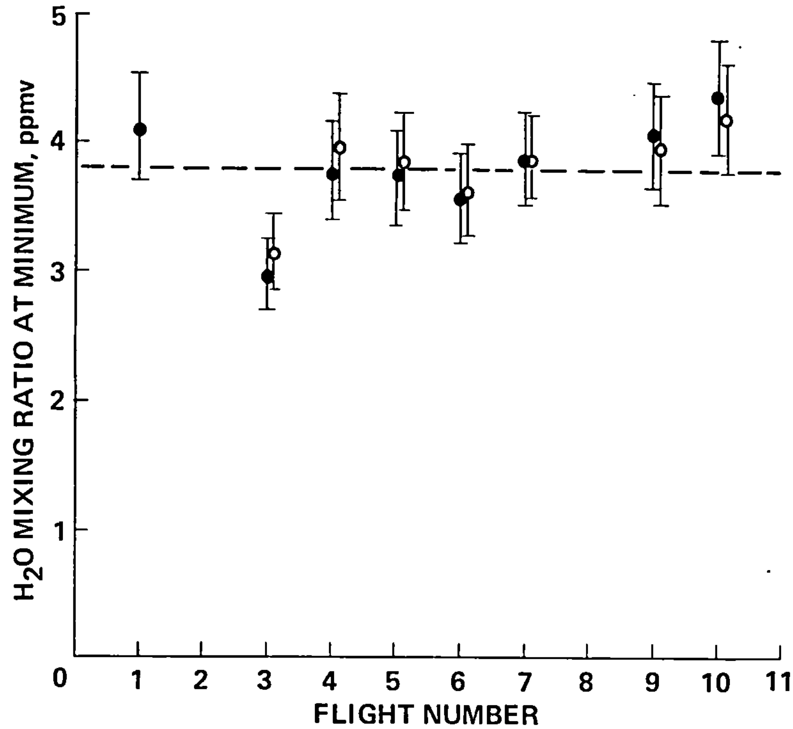

Figure 38.- Water mixing ratios between altitudes of 18 and 19 km versus flight number. Solid circles: calibration constant from linear regression line of figure 3. Open circles: calibration constant $C = 8.1\times10^{-6}$ (flights 4 through 10) and $C = 3.1\times10^{-6}$ (flight 1).

BROAD-BAND AIRBORNE WATER-VAPOR RADIOMETRY

Peter M. Kuhn*

SUMMARY

An infrared radiometer with a passband of 280 to 520 cm^{-1} (35.7 to 19.2 μm) is employed on Ames Research Center U-2 and C-141A aircraft in the measurement of water-vapor burden in the upper troposphere and stratosphere. Coincidentally with altitude changes, the water-vapor mass mixing ratio is also inferred by observing the change in optical depth over a known vertical distance. Data from the December 1980 U-2 Water-Vapor Exchange Experiment over the Panama Canal Zone add credence to the belief that overshooting cumulonimbus towers "moisten" the lower stratosphere. The average mass mixing ratio near or above such towers ranges from 3.5 to 5.0 ppm above 18 km, whereas the average background mass mixing ratio is only 2.9 ppm. Generally, the lowest background mixing ratios, averaging 2.6 ppm, occurred in the 18-to-21-km layer. At the same altitudes (18-21 km), the background mass mixing ratios over Panama averaged from 1.0 to 3.0 ppm higher than in middle latitudes.

INTRODUCTION

The Water-Vapor Exchange Experiment was conducted out of Howard Air Force Base, Panama, from 26 August to 22 September 1980. An Ames Research Center U-2 aircraft carried the broad-band water-vapor radiometer and eight other related experiments on nine high-altitude missions between lat. 5° N and 12° N and between long. 76° W and 82° W. The purpose of the experiment was to determine the mass exchange of water vapor between the upper troposphere and lower stratosphere and to examine the role "overshooting" cumulonimbus towers may play in the process.

Primarily, the water-vapor mass mixing ratio was measured at a series of altitudes from 15 to 22 km and in a variety of changing atmospheric conditions in the direct vicinity of the normal location of the Intertropical Convergence Zone (ITCZ). Unfortunately, during the experiment the normal equatorial circulation was so upset as to render the ITCZ virtually nonexistent. The time of the experiment, then, was one of general inactivity.

Past experiments (Kuhn, 1971) had produced evidence, although somewhat controversial, that overshooting cumulonimbus towers might increase the water-vapor burden of the stratosphere. The overburden of water had been observed to be as high as 6.0×10^{-4} g/cm^2 (6.0 precipitable micrometers) at an altitude of 20 km. As a result of the Water-Vapor Exchange Experiment, it may be possible to determine, by virtue of new data and analyses, the validity of this conjecture. Ellsaesser et al. (1980) discuss the discrepancies between observations and hypotheses and provide the developments preceding this experiment.

This research was supported by the Atmospheric Experiments Branch, Space Sciences Division, NASA Ames Research Center, under Contract NAS2-10592.

---

*Northrop Services, Inc., NASA Ames Research Center, Moffett Field, California.

INFRARED RADIOMETER

The infrared radiometer (Kuhn, 1975) that was used on board the U-2 for the experiment measures the zenith radiance in a spectral band extending from 280 to 520 cm^{-1} (35.7 to 19.2 μm). The system response factor of the radiometer, R, is a calibration constant which is a function of the radiometer's field of view, optical collecting powers, the detector responsivity, and the system electronic gain. The shape of the radiometer response function versus wave number (cm^{-1}) or wavelength (μm) is determined from the response curves of the separate components. The responsivity constant of the radiometer system (V/W) cm^2 sr is calibrated under laboratory conditions using a cooled and purged blackbody source under partial vacuum. It is given by

$$R = GV/(N - N_r) \qquad (1)$$

where G is gain, V is voltage output of radiometer, N is radiance in $W/cm^2/sr^1$, and N_r is the radiometer source radiance.

DATA REDUCTION PROCEDURE

In flight, the radiometer "sees" the sky chopped against a 250 K controlled, blackbody reference. A separate radiometer, operating in the Q-branch of the 15-μm CO_2 band determines the air temperature at flight level. The precipitable water-vapor overburden (g/cm^2) above the aircraft is then determined by adjusting the water-vapor input iteratively in a multilevel, radiative transfer model so that predicted and observed radiance agree within experimental tolerance. Pressure, temperature, and overburden of water vapor, as a set of observations, are inputs to the model to iteratively determine first U and then q. The line strength data compilation of McClatchey et al. (1973), with pressure broadening and temperature corrections to the absorption coefficients, are adapted to the transfer model.

The mass mixing ratio is finally determined by the change in the burden of water vapor observed over a short period of time (about 3-6 min) at two different altitudes (1-2 km apart). This produces the mean mixing ratio for the layer from the expression

$$\bar{q} = \Delta U/\rho \; \Delta z \qquad (2)$$

where $\bar{q}$ is in units of grams of water vapor per gram of dry air; ΔU is the change in water-vapor burden between the two levels; ρ is the mean atmospheric density, and Δz is the change in altitude.

The accuracy of the radiometer system for the inference of water-vapor burden and derived mixing ratio increases as the radiance observations increase. Calculating the mixing ratio from equation (2) for an average layer depth of 1 km and observing for 3 min (96 samples), the standard error of the mean layer mixing ratio inferred is $\pm 0.6\times10^{-6}$ g/g (0.6 ppm). To illustrate the accuracy of the radiometer, figure 1 shows a comparison of water-vapor column density, U in equation (2), obtained simultaneously with Ames Research Center's Michelson interferometer and the broad-band radiometer previously described. Comparisons were made during five NASA C-141A missions flown during the period 1976 through 1978 (Erickson et al., 1979). The correlation for all 36 points is 0.90. These totally independent instrument observations do,

however, show a systematic difference. One explanation may be that a single-level model was used above flight level with the interferometer radiance data that were reduced to water-vapor overburden, whereas the radiometer data were input into a 14-level radiative transfer model.

RESULTS SUMMARY

As stated, the purpose of the experiment was to determine tropospheric-stratospheric water-vapor exchange in the tropics and to include the possible role overshooting cumulus towers may play in the process (Johnston and Solomon, 1979). The tropical freeze-dry hypothesis by Brewer (1949) may also be examined relative to these late summer Panama observations.

In line with the goals of the experiment, four main observation results are discussed: (1) the observed mean mixing ratio sounding related to the freeze-dry hypothesis; (2) the poleward gradient, at constant altitudes, of mass mixing ratio from the Panama maximum; (3) the total water-vapor burden above reference levels; and (4) classification of the atmosphere as "wet" or "dry" throughout the experimental flights.

Figure 2 summarizes the radiometric observations of the mean water-vapor mass mixing ratios as functions of height and corresponding mean temperatures. There are an average of 1207 observations per plotted point. Four seconds were required for each observation; thus, about 90 min of radiometric data are averaged into each point. The period of the observation was 30 August through 16 September 1980. It should be noted that except within clouds, remote radiometric techniques are generally less sensitive to contamination than in situ measurements.

Assuming a temperature-determined tropopause for the Panama vicinity of about 17 km, the mixing ratios observed (fig. 2) are below the saturation mixing ratio at 17 km for the averaged observed temperature of −76 °C. Saturation here would occur at this height and at the observed average temperature when the mixing ratio was 7.9 ppm. However, freeze-out cannot take place for the observed mean 17-km mixing ratio of 3.0 ppm at temperatures above −82°C. There does not appear to be sufficient evidence from this experiment, at least not from the average sounding, that overshooting cumulonimbus towers can adiabatically cool and dry the lower stratosphere sufficiently to provide a satisfactory tropical cold trap.

The mean mass mixing ratios of 2.9 and 2.7 ppm at 18.2 and 20 km, respectively (fig. 2), are higher than similar altitude values from mid-latitudes, even during this relatively quiescent period for the atmosphere over Panama. They do agree favorably with all but one set of experimental results of stratospheric water-vapor observations for lat. 5° N to 15° N, summarized by Ellsaesser et al. (1980).

In a broad, climatic sense, the observations plotted in figure 3, obtained from 1976 through 1980 aboard C-141A, Convair 990, and U2 aircraft (Ames Research Center) and an RB57 (U.S. Air Force) relate to the previous discussion in that they display mean column densities and mean mass mixing ratios for not only an equatorial region but also for mid-latitudes. The data analysis is more general than that of figure 2 in that it embraces data obtained over a period of 5 years and from three different aircraft types. However, the same radiometric remote sensing technique was used on each aircraft. Poleward, as well as upward vertical, gradients from an equatorial maximum are evident in the profiles. Again this is in agreement with comments by

Ellsaesser et al. (1980). Of interest is the mean equatorial mass mixing ratio of 6.7 ppm at 16 km; the mean ratio of lat. 40° N (and at 16 km) being 3.2 ppm. Although this is a comparison of data obtained below the Panama tropopause and generally below the mid-latitude tropopause, it nevertheless displays a pronounced poleward gradient.

Perhaps a better measure of increasing water vapor or changes in the water vapor is the overburden, which is displayed as a function of latitude and altitude in figure 3. This is so because the mixing ratios refer to measurements at a single level, whereas changes in the burden of water vapor assess additions to or subtractions of water vapor in an entire column above a reference level. It appears evident that the Panama region, and in fact most of the equatorial region, was more moist during this experiment than was the mid-latitude region, bounded by long. 95° W and 175° W, which was checked earlier.

During this experiment, the water-vapor radiometer soundings were categorized as one or the other of two classifications defined by Kuhn (1979): "wet" or "dry" day soundings. However, the soundings of 1979 were more sharply divided into one or the other classification. Somewhat analogous profiles did occur in 1980, but the differences are much less pronounced (fig. 4). The "dry" sounding of 7 September reaches a minimum of 2.5 ppm at 20.5 km, and the "wet" sounding of 12 September has a minimum mixing ratio of 3.1 ppm at 21.0 km. This is just barely significant in view of the limits of the instrumentation. However, the atmospheric regime in 1980 was, as stated, not one of normal convective activity. In both cases the mixing ratios are below those corresponding to saturation at 20.5 km and an average temperature of -64°C. In this instance, saturation occurs with 63 ppm of water vapor.

The lowest temperature observed as a 4-min average, -80.1°C, occurred at 16.7 km during the "wet" mission of 12 September. The mixing ratio observed at that time was 3.4 ppm; the saturation mixing ratio for -80.1°C is 3.7 ppm. Freeze-out of water vapor could not quite take place. On the "dry" mission of 7 September, the lowest 7-min average temperature was -81.5°C at 16.7 km. The observed mixing ratio during that period was 2.9 ppm, and the saturation mixing ratio for -81.5°C is about 2.9 ppm. Here freeze-out of water vapor could possibly occur. But it is a singular case in one shallow layer centered on 16.7 km.

Below 16 km, the differences in the mixing ratios between the observed soundings of the two days are more pronounced, reaching 2 ppm at 15 km. The analyses for the radiometer water-vapor profiles on these two days is typical of such comparisons during the full period of the experiment. There were only two days during the 1980 experiment that could be classified as "wet." This is in contrast to 1979 when at least half of the days were designated as "wet." However, on those occasions when convection was noted and when the U-2 flight track passed relatively close to a turret at or slightly above the top, the mixing ratio did reach 5.5 to 6.5 ppm at 18 km. This occurred just above the tropopause and again indicates the inability of the lower Panama stratosphere to freeze-out water vapor as a sink or cold trap. Temperatures averaging -76°C at and just above the mean tropopause were simply not low enough to provide a suitable cold trap. In fact, the sporadic increases in the mixing ratio of the lower stratosphere above a background level of 2.6 to 2.9 ppm suggest that overshooting cumulonimbus turrets may locally increase the water-vapor concentration. However, residence times for the increases may be relatively short. The results are summarized by Kuhn (1982) in a final publication.

REFERENCES

Brewer, A. W.: Evidence for a World Circulation Provided by Measurements of Helium and Water Vapor Distribution in the Stratosphere. Quart. J. R. Met. Soc., vol. 75, 1949, p. 351.

Ellsaesser, E. F.; Harries, J. E.; Kley, D.; and Penndorf, R.: Stratospheric Water Vapor. Space Sci., vol. 28, 1980, pp. 827-835.

Erickson, E. F.; Simpson, U. P.; Kuhn, P. M.; and Stearns, L. P.: Determination of the Telluric Water Absorption Correction for Astronomical Data Obtained from the Kuiper Airborne Observatory. NASA TM-75582, 1979.

Johnston, H. S.; and Solomon, S.: Thunderstorms as Possible Micrometeorological Sinks for Stratospheric Water. J. Geophys. Res., vol. 84, 1979, p. 3155.

Kuhn, P. M.: Water Vapor: Stratospheric Injection by Thunderstorms. Science, vol. 174, 1971, pp. 1319-1321.

Kuhn, P. M.; and Stearns, L. P.: Latitudinal Profiles of Stratospheric Water Vapor. Geophys. Res. Lett., vol. 2, 1975, pp. 227-230.

Kuhn, P. M.: U-2 Water Vapor Burden Observations through the Tropopause. Section XI, 1977 Intertropical Convergence Zone Experiment, NASA TM-78577, 1979.

Kuhn, P. M.: Broad-Band Airborne Water Vapor Radiometry. Geophys. Res. Lett., vol. 9, no. 6, 1982, pp. 621-624.

McClatchey, R. A.; et al.: AFCRL Atmospheric Absorption Line Parameters Compilation. AFCRL-TR-73-0096, Air Force Geophysical Laboratories, L. G. Hanscom Field, Bedford, Mass., 1973.

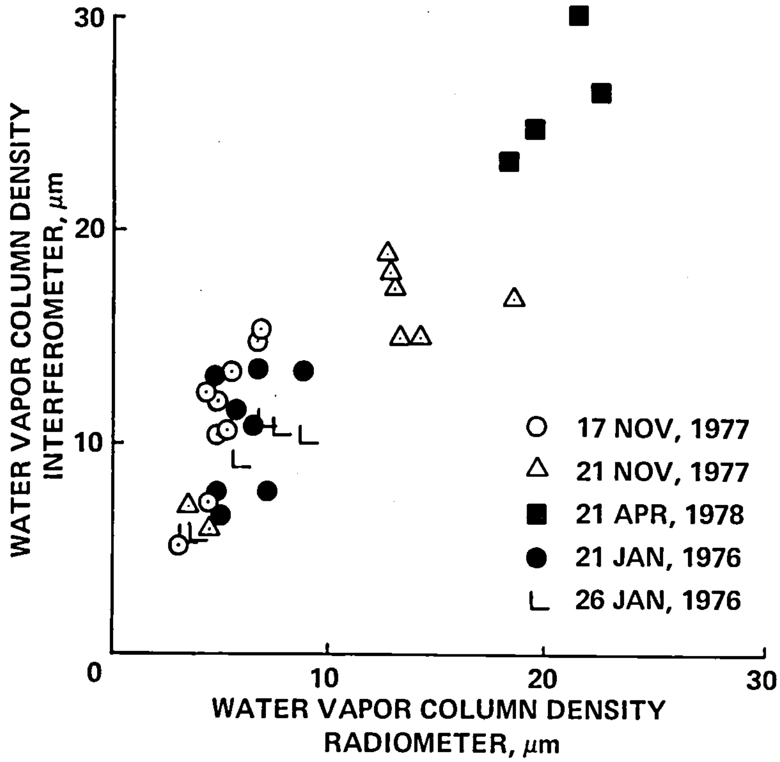

Figure 1.- Comparison of water-vapor column overburden measured with Michelson interferometer and broad-band radiometer (Erickson et al., 1979).

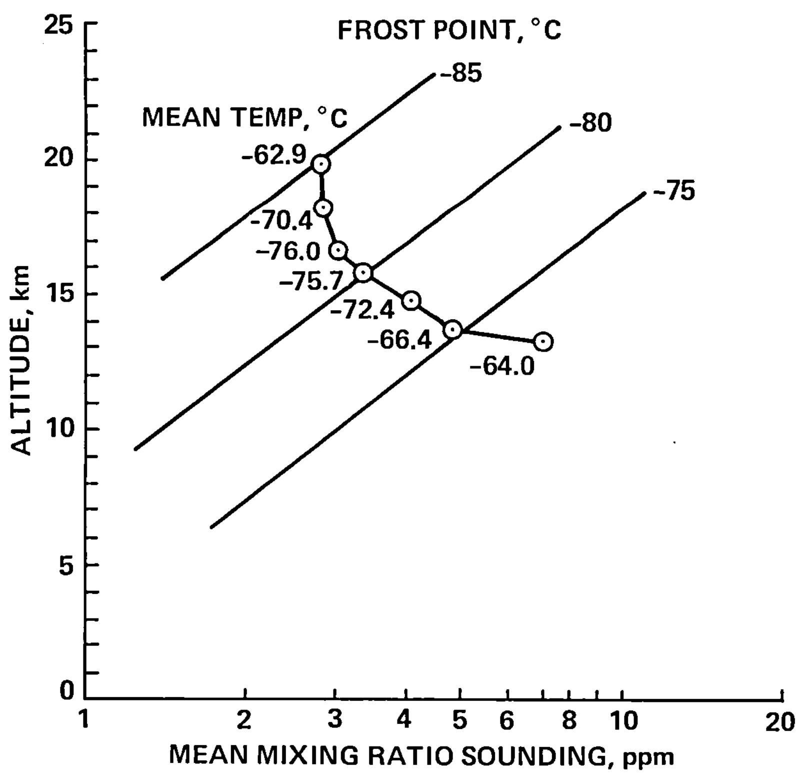

Figure 2.- Radiometer inferred mean water-vapor mixing ratio sounding from data of 30 August to 16 September 1980; average of 1207 observations per point.

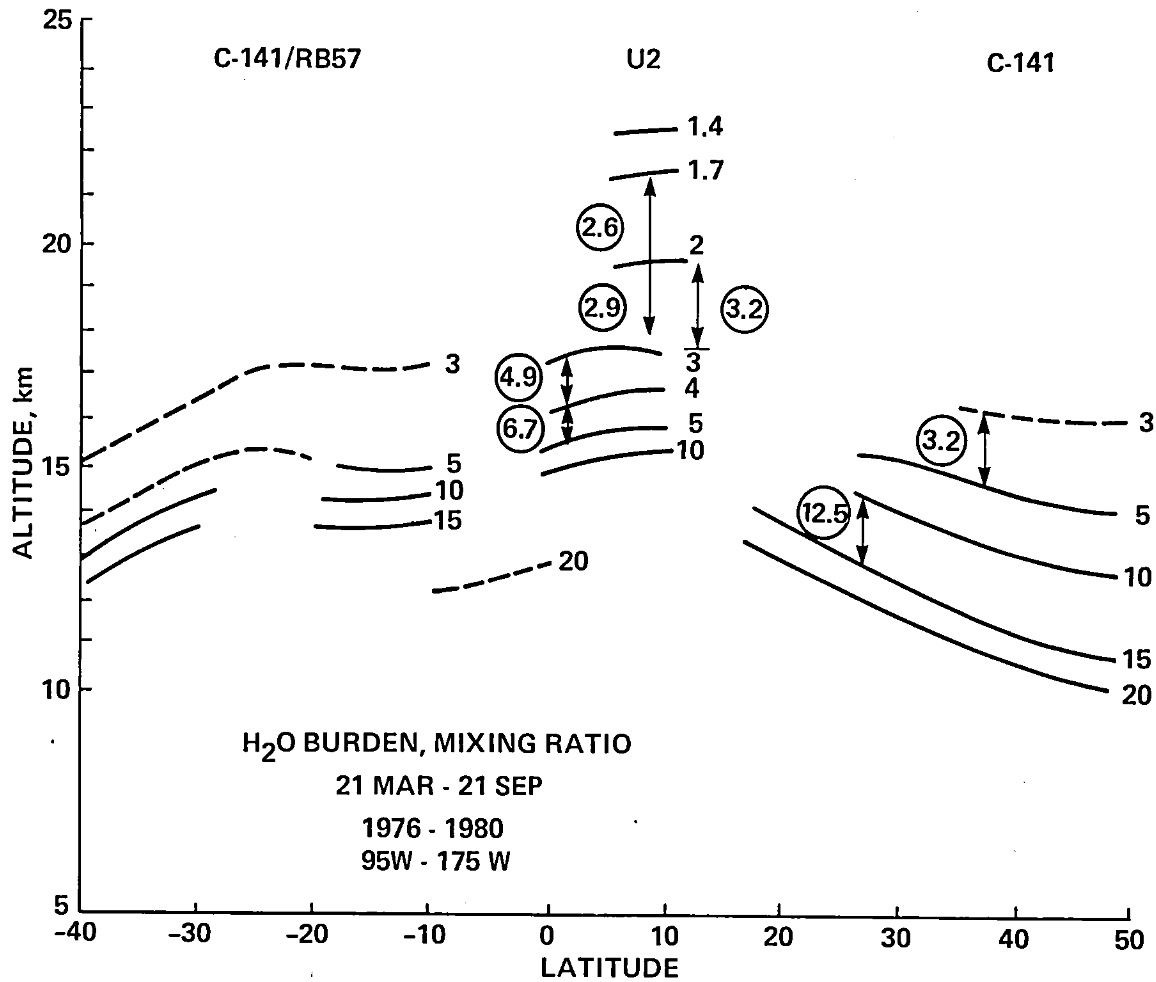

Figure 3.- Mean water-vapor burdens (μm) and mean mixing ratios (ppmm) as a function of latitude, longitude band, and altitude. Mixing ratios are plotted within circles as mean for a layer, and burdens are the plotted curves. Dashed curves indicate limited data availability from RB57 aircraft observations.

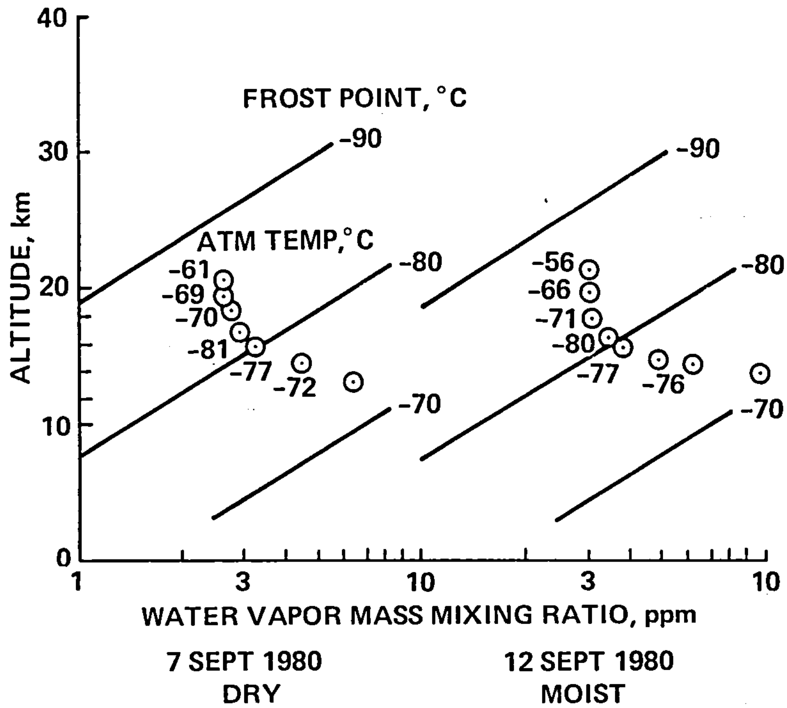

Figure 4.- Comparison of radiometer inferred water-vapor mass mixing ratios for "dry" and "wet" days.

METEOROLOGICAL MEASUREMENTS

Stanley G. Scott and Stuart W. Bowen*

Meteorological data (pressure and temperature) were obtained from calibrated U-2 aircraft instrumentation. Because of a failure of the inertial navigation system, the data for position and data required for the wind calculations were not acquired.

The data system recorded the sensor instrumentation data and GMT at 4.2-sec intervals. Data were obtained on all flights except flight No. 3 on September 2 and flight No. 11 on September 17, 1980. Table 1 summarizes the sensor data recorded.

The air data computer (ADC) in the airplane takes inputs from the static and pitot total pressure taps to produce analog signals of pressure altitude and Mach number. The geopotential pressure altitude is converted in our software to yield pressure (millibars), using the relationships embodied in the 1976 U.S. Standard Atmosphere. An independent Rosemont-type 102 stagnation temperature sensor on the U-2 lower hatch provides data used to compute the total air temperature.

The digitized analog signals from the ADC and the Rosemont have been calibrated under laboratory conditions and the corrections to the nominal values are accurately known. In the calibration procedure for the ADC, the static pressure P and the total pressure Pt = P + dP (dP is the dynamic pressure) appropriate to the operating conditions of the U-2 are generated by setting the altitude and indicated airspeed controls of an air-data generator attached to the ADC. These static and dynamic pressures are monitored by high-precision, differential, quartz, Bourdon tube temperature-controlled manometers whose calibrations are traceable to NBS standards. The precision of the applied static pressure, P, is 0.10 mbars; the dynamic pressure, dP, precision is 0.08 mbars. The static pressure cell is referenced to vacuum and the dynamic pressure cell is connected so as to directly measure between the static and total pressure inputs to the ADC. The ADC synchro outputs are recorded both by direct measurement (accurate to 0.002 V) and on tape, recorded by the Datel digital air-data recorder for subsequent decoding, just as in flight. Relying on the manometer calibration, the true Mach number, Ma, is computed using

$$Ma = \sqrt{\left(\frac{2}{g - 1}\right)\left(1 + \frac{dP}{P}\right)^{g-1/g} - 1}$$

where g = 1.4 is the specific heat ratio. The static air temperature T is related to the total air temperature by

$$T = \frac{T_t}{1 + [(g - 1)/2]Ma^2}$$

The Rosemont total-temperature probe is calibrated in the laboratory by first immersing the entire probe in a series of constant-temperature baths monitored by a quartz thermometer accurate to 0.02°C traceable to NBS and measuring the platinum element resistance to a precision of 0.2 ohm or, equivalently, 0.1°C. The lower-hatch Rosemont amplifier voltage output as a function of input resistance was also measured

*Beam Engineering, Inc., Sunnyvale, California.

to within 0.0023 V or, equivalently, 0.03°C. The overall uncertainty of the Rosemont total air temperature is 0.2°C, including the corrections for nonunity recovery factor, increase in Mach number at the lower hatch location, and possible self-heating errors.

The results of the U-2 ADC corrections are as follows: Mach uncertainty (1 σ), 0.001; altitude uncertainty (1 σ), 5 m; total temperature uncertainty, 0.2°C; and GMT time error, 0.0.

Figures 1-9 are plots of pressure and temperature versus GMT. Complete data sets are available from one of the authors (S.G.S) at Ames Research Center.

TABLE 1.- SENSOR DATA SUMMARY

Pressure altitude (coarse)	A_c	Air data computer
Pressure altitude (fine)	A_f	Air data computer
Mach number (fine)	M_f	Air data computer
Stagnation air temperature	T_t	Rosemont 102 sensor
Time	GMT	Internal clock

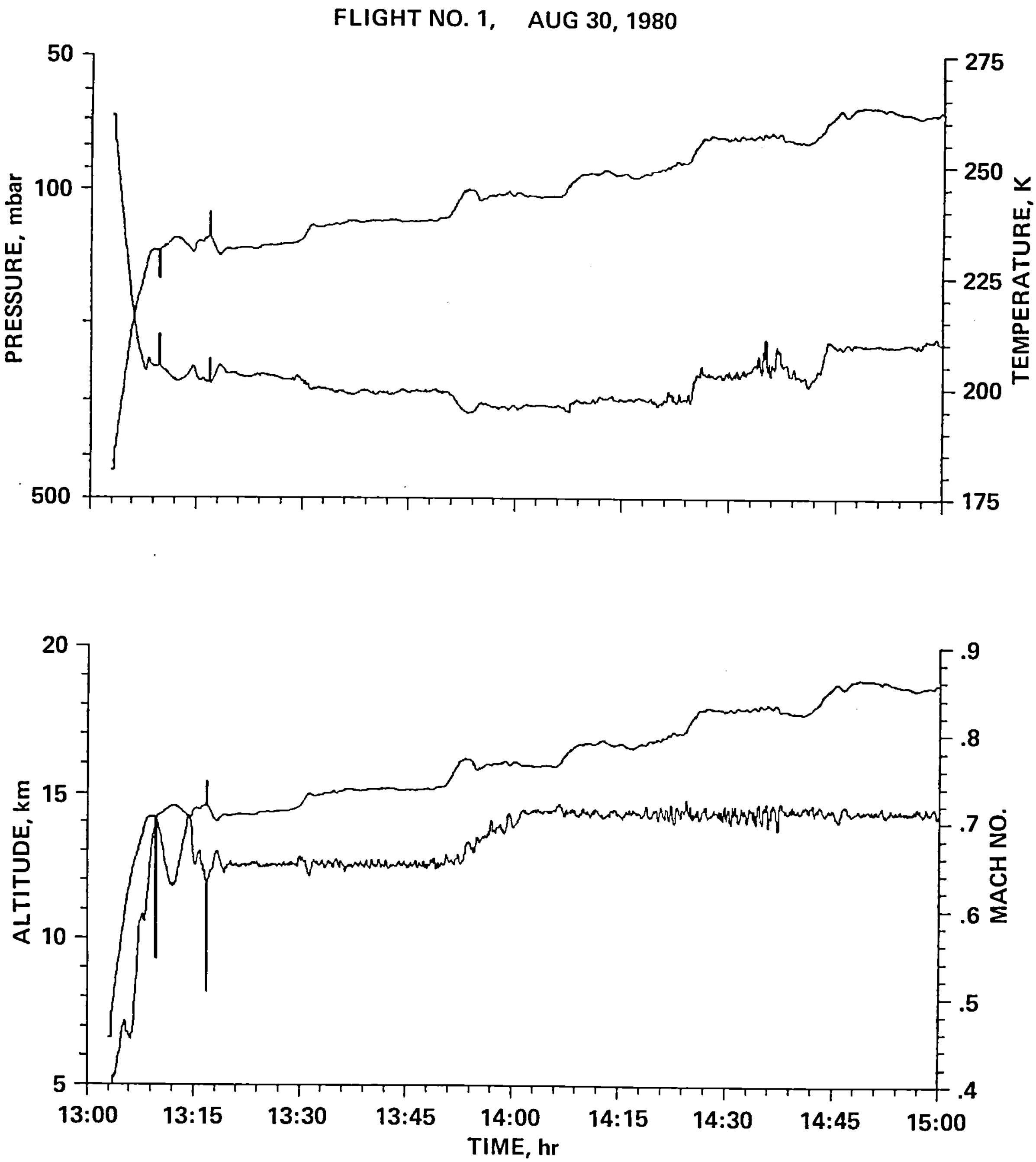

Figure 1.- Pressure, temperature, altitude, and Mach number for flight No. 1, August 30, 1980.

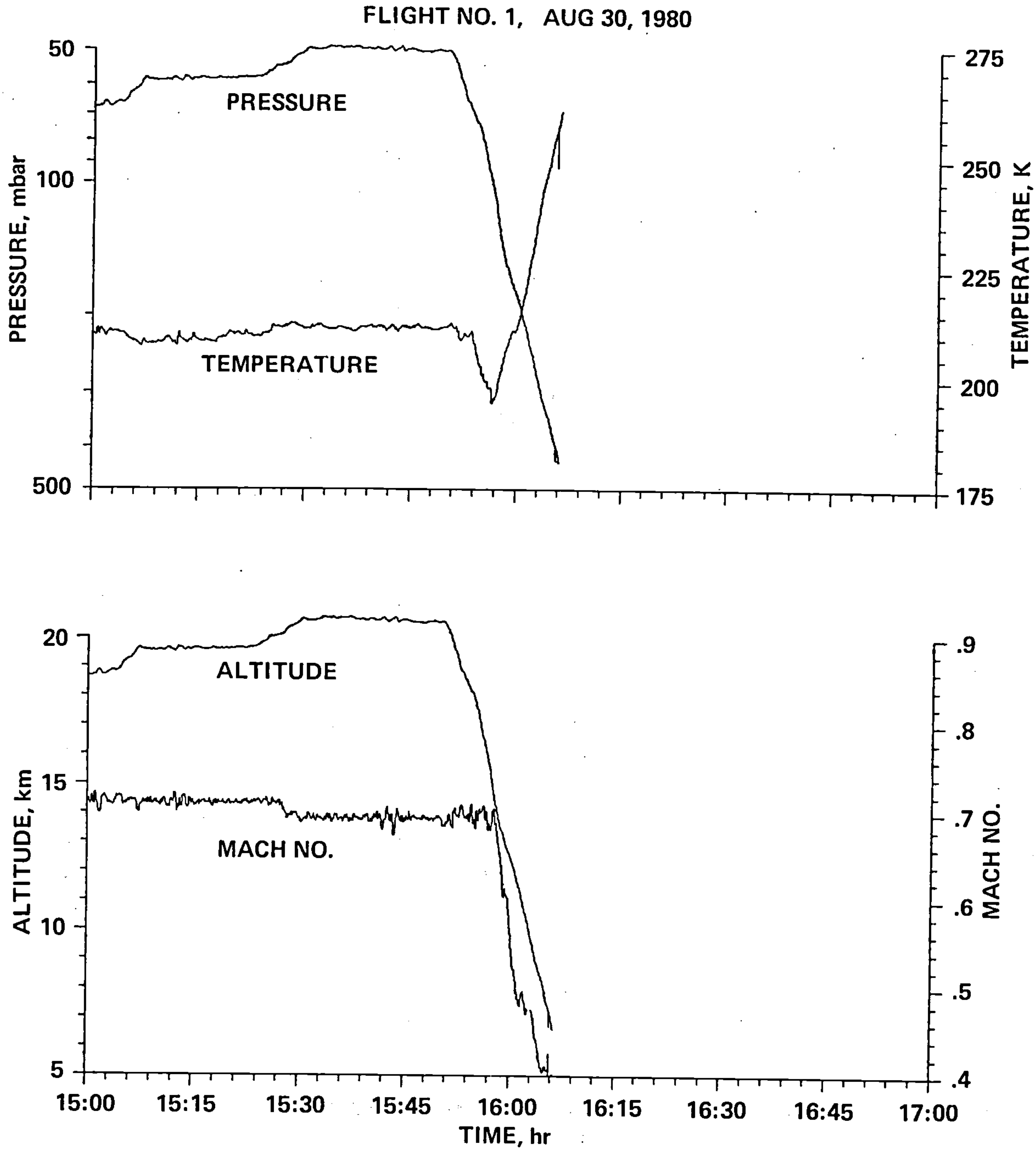

Figure 1.- Concluded.

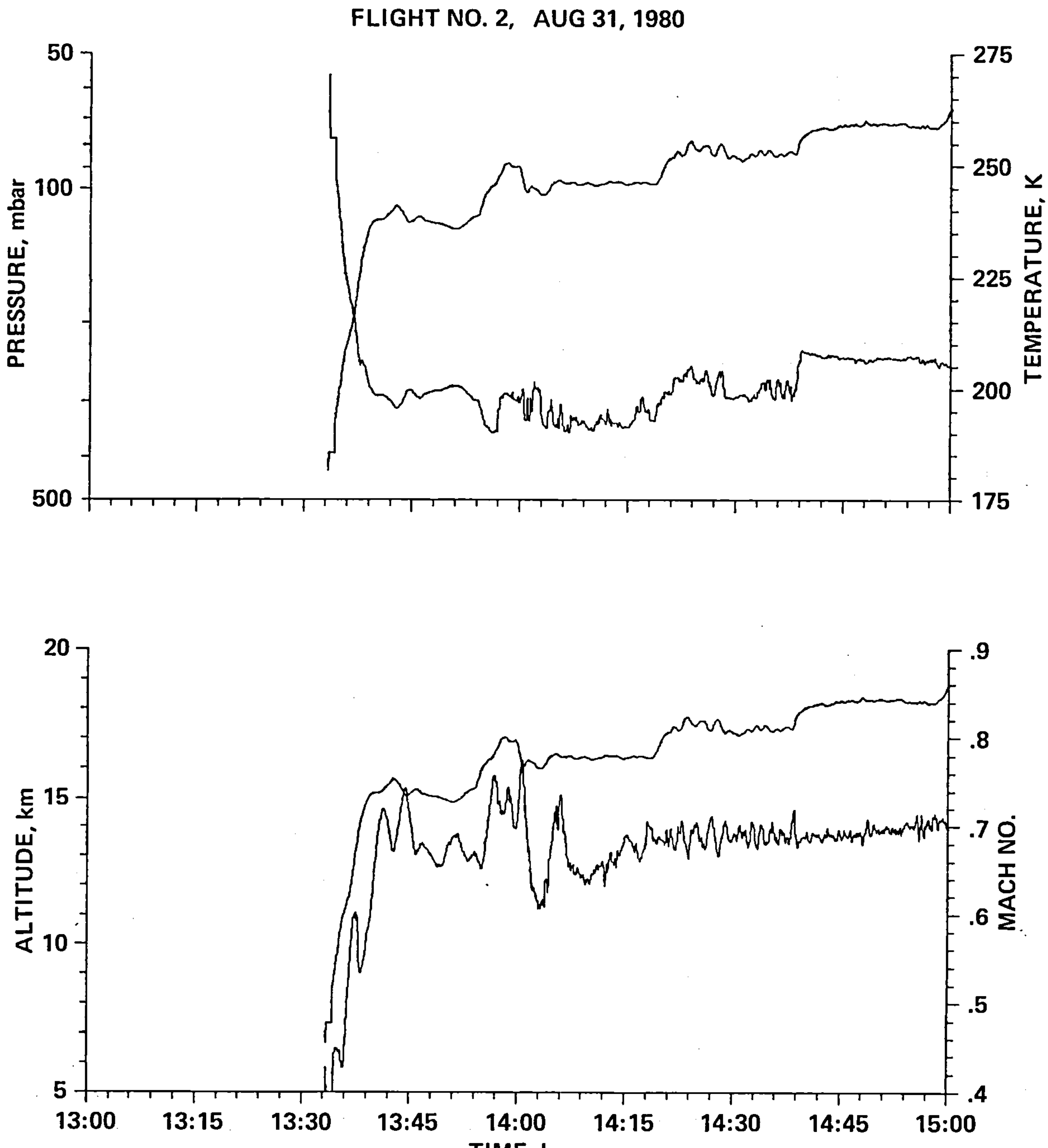

Figure 2.- Pressure, temperature, altitude, and Mach number for flight No. 2, August 31, 1980.

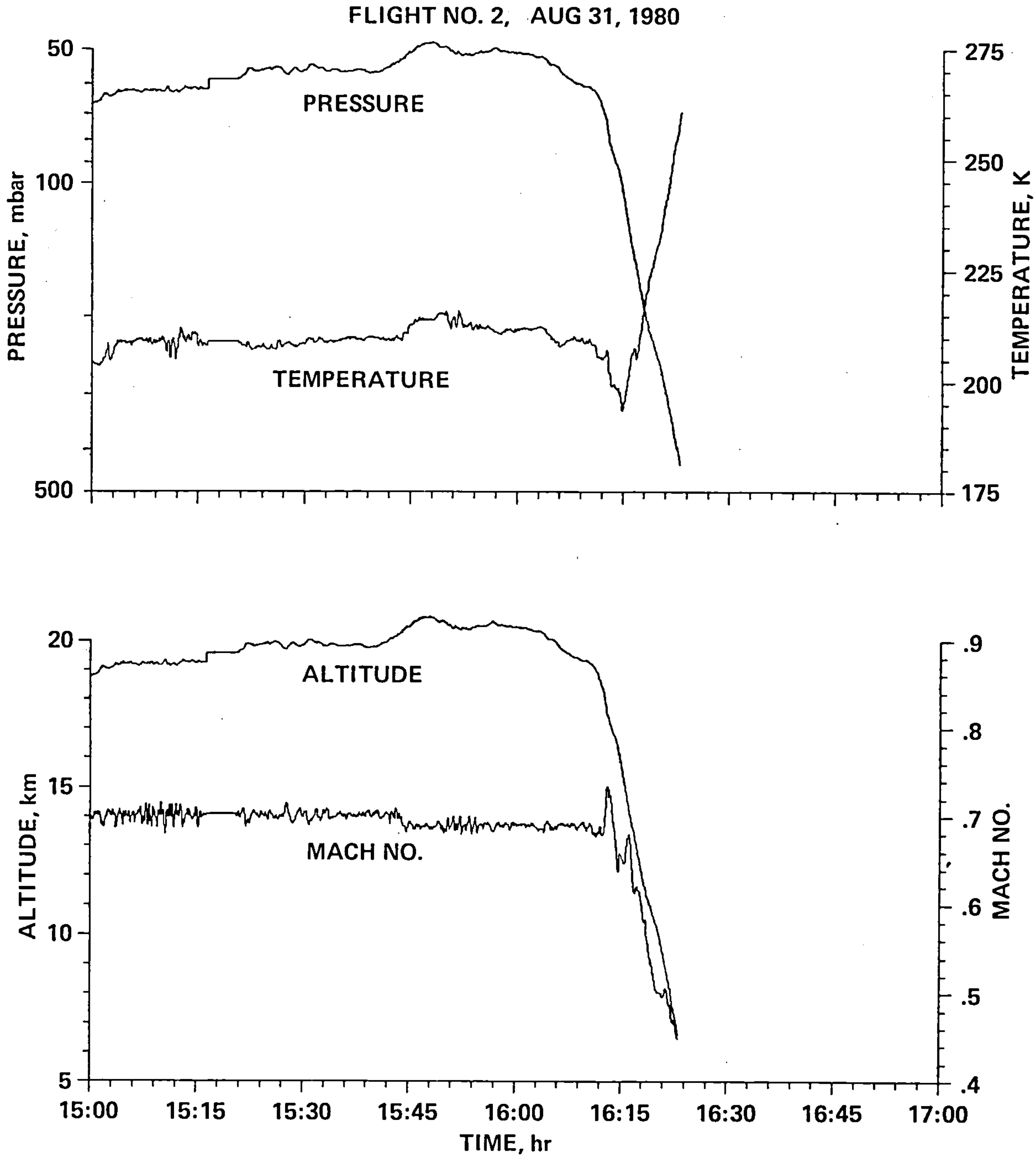

Figure 2.- Concluded.

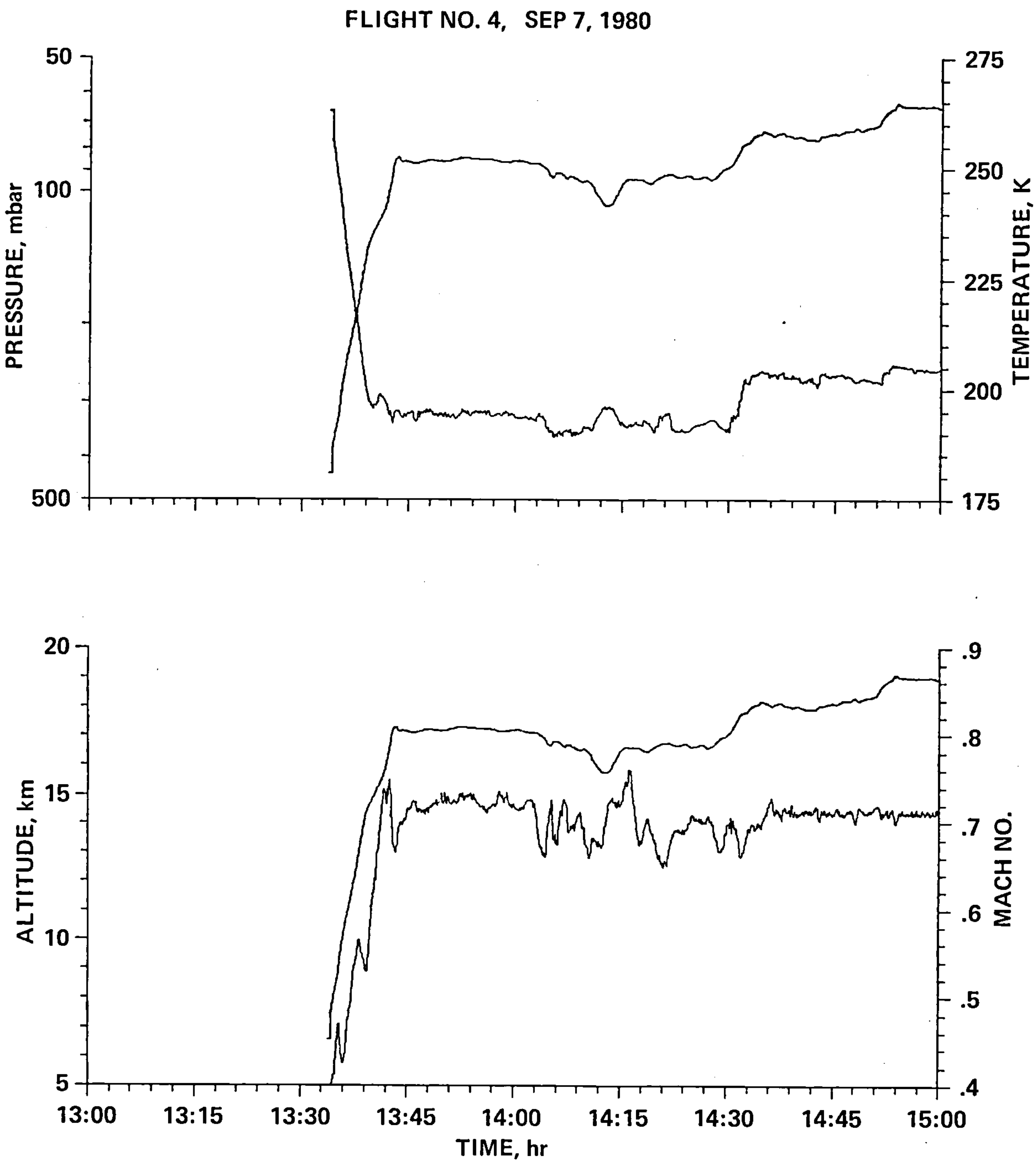

Figure 3.- Pressure, temperature, altitude, and Mach number for flight No. 4, September 7, 1980.

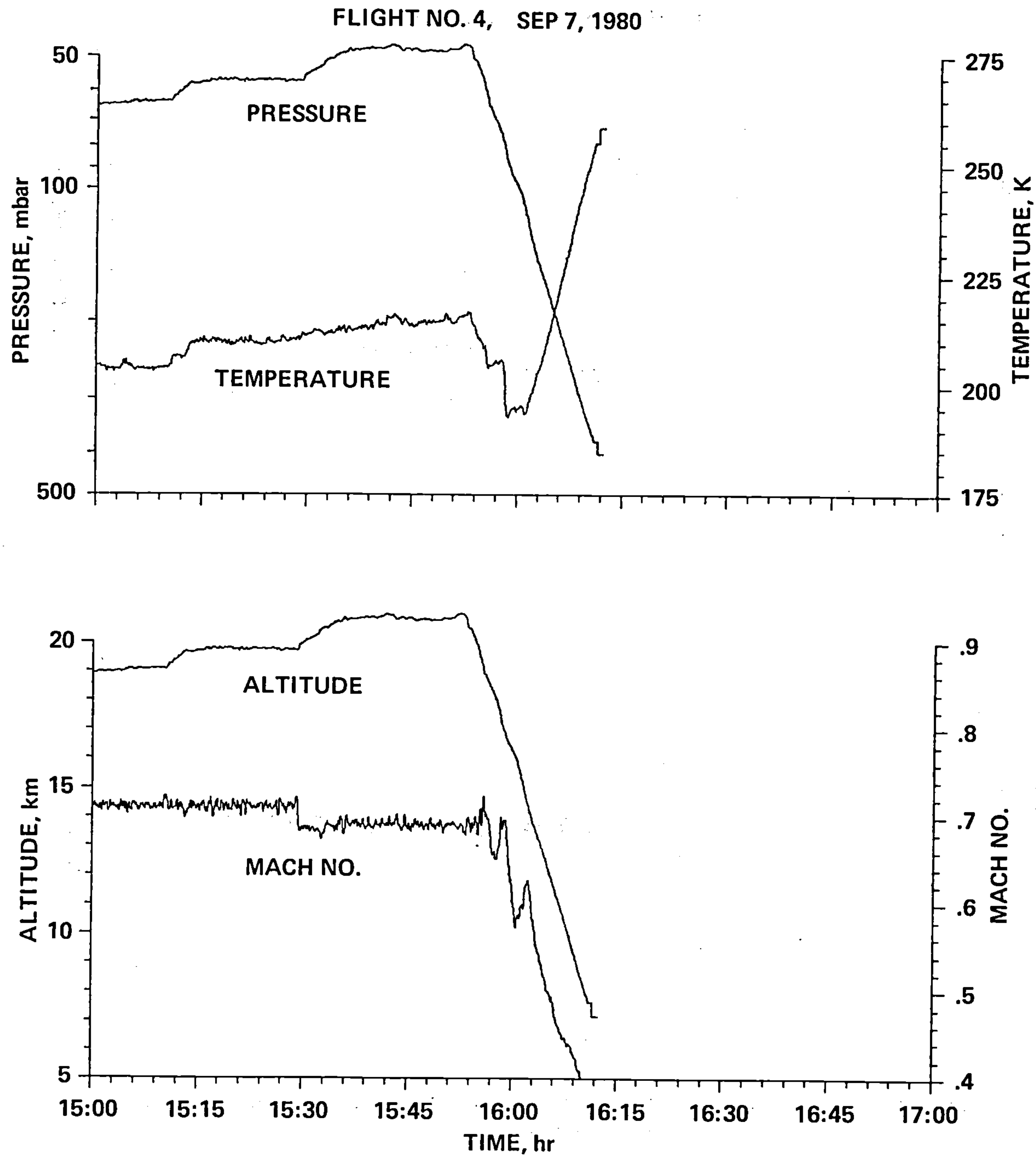

Figure 3.- Concluded.

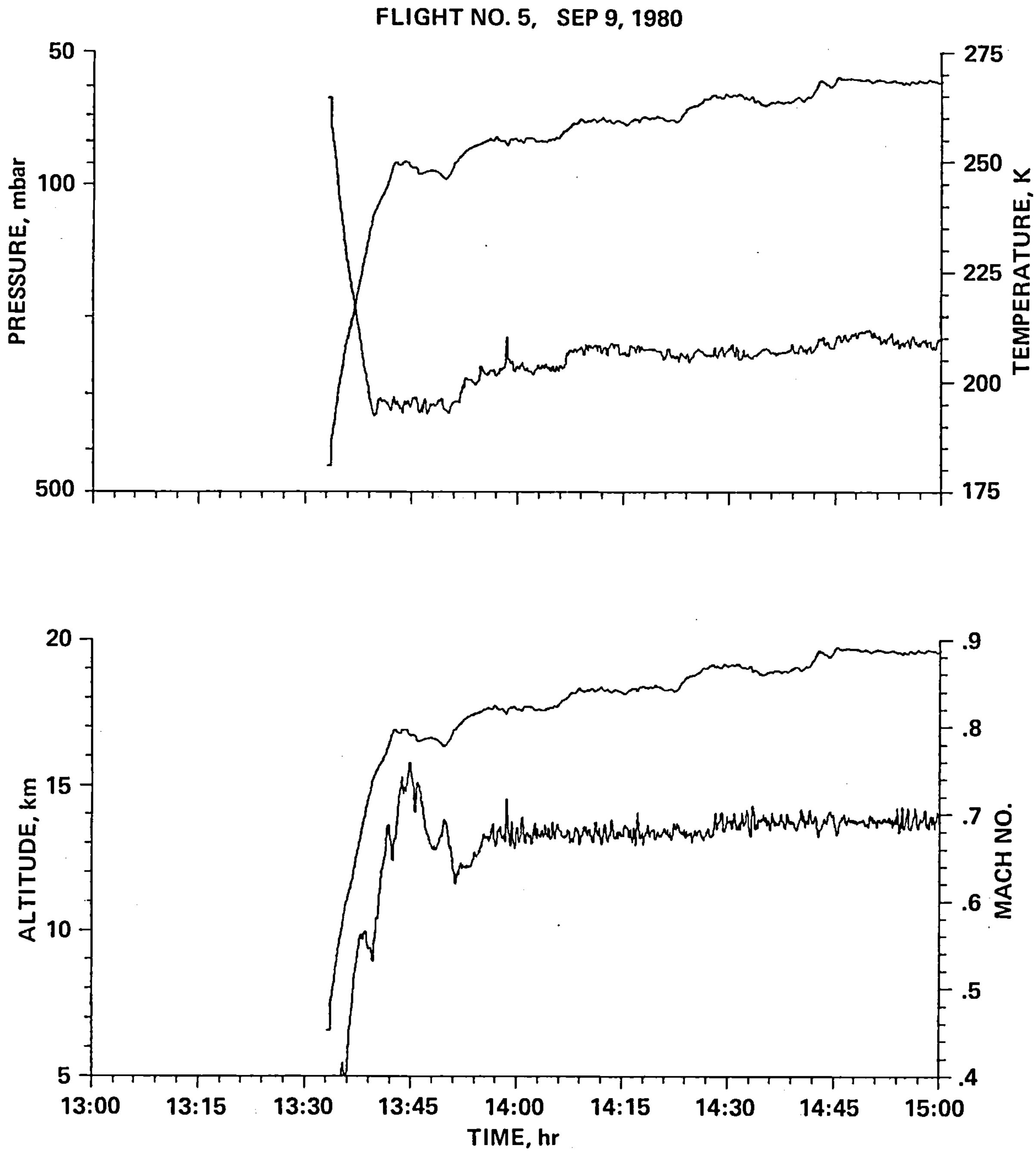

Figure 4.- Pressure, temperature, altitude, and Mach number for flight No. 5, September 9, 1980.

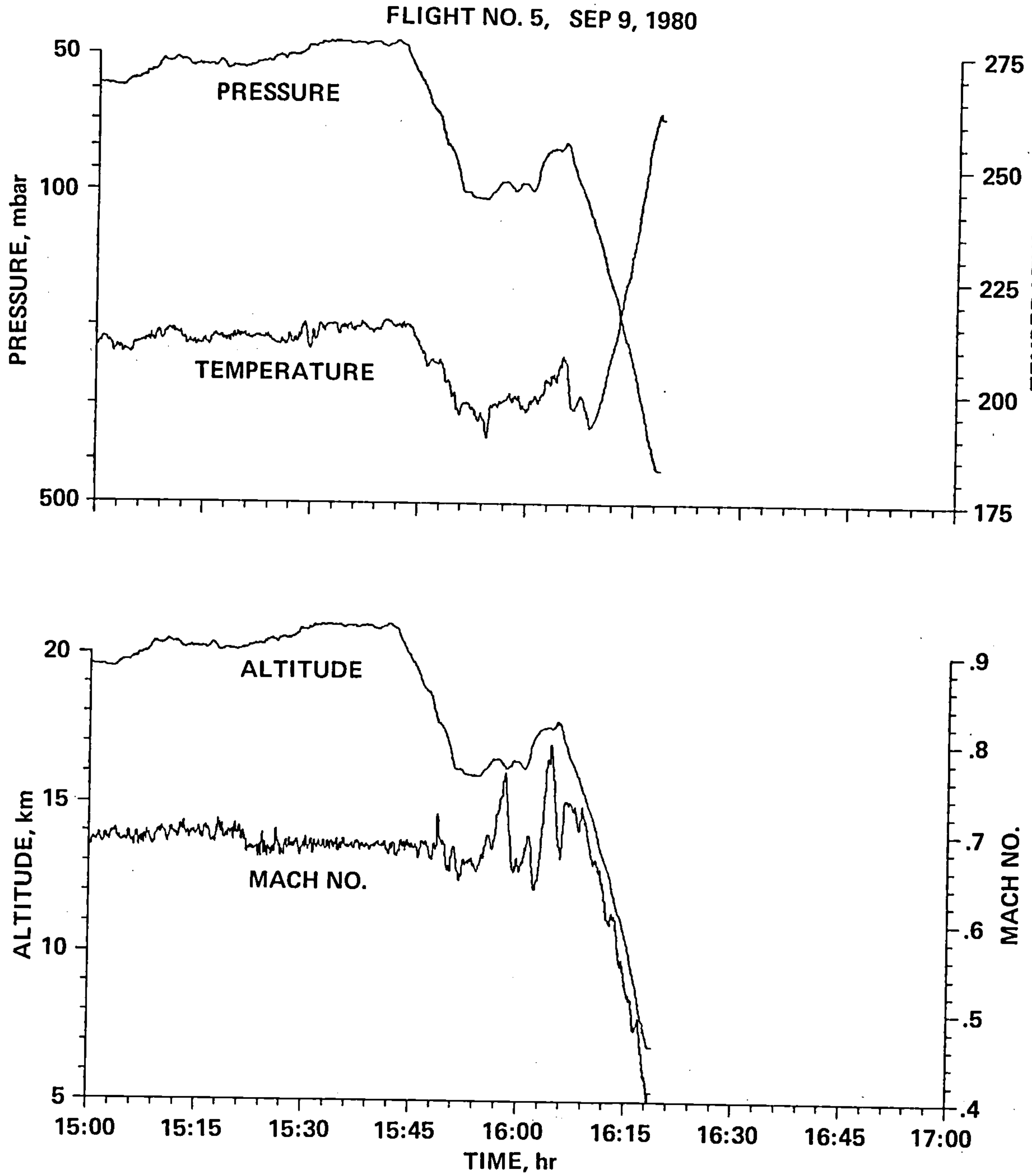

Figure 4.- Concluded.

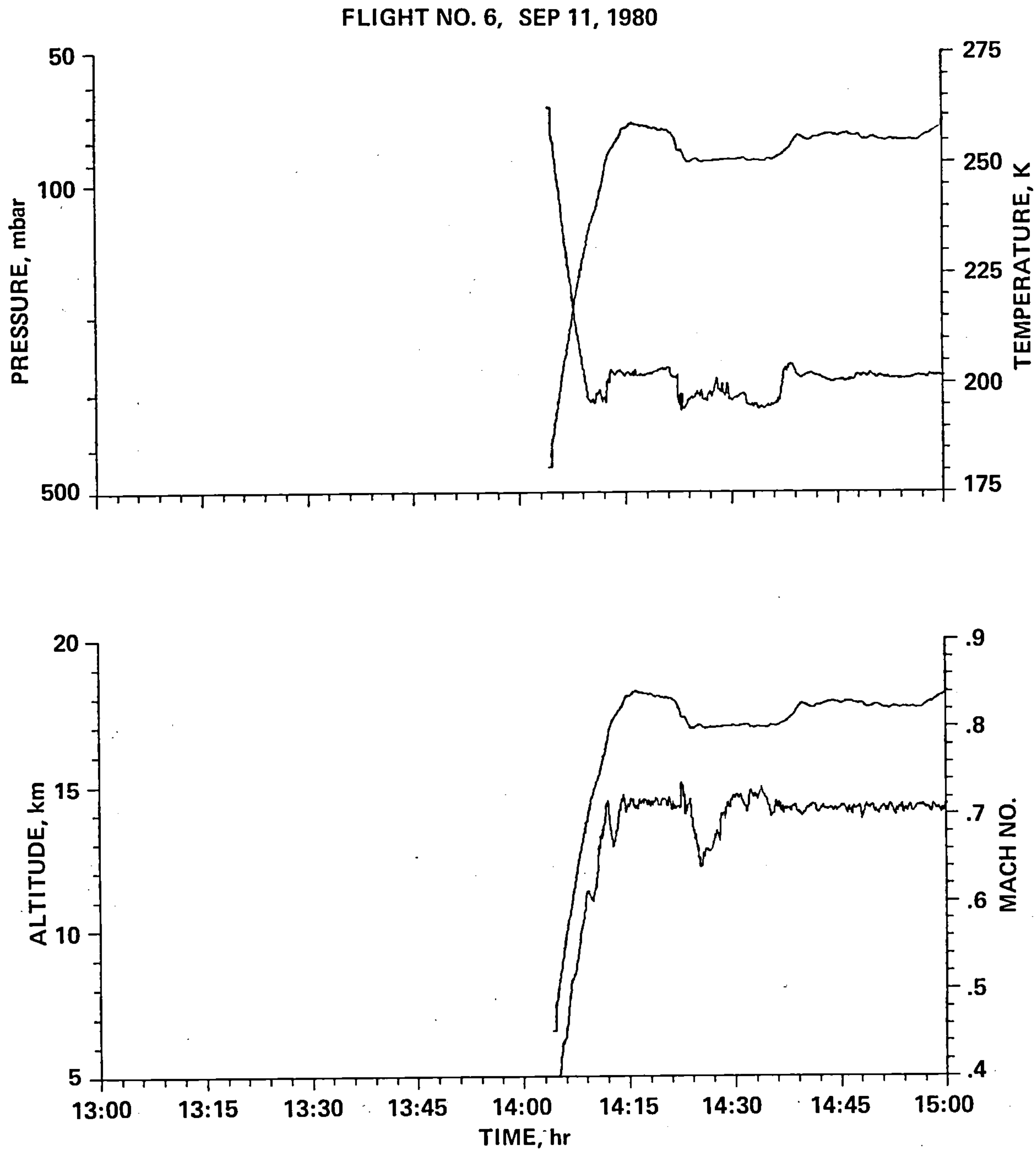

Figure 5.- Pressure, temperature, altitude, and Mach number for flight No. 6, September 11, 1980.

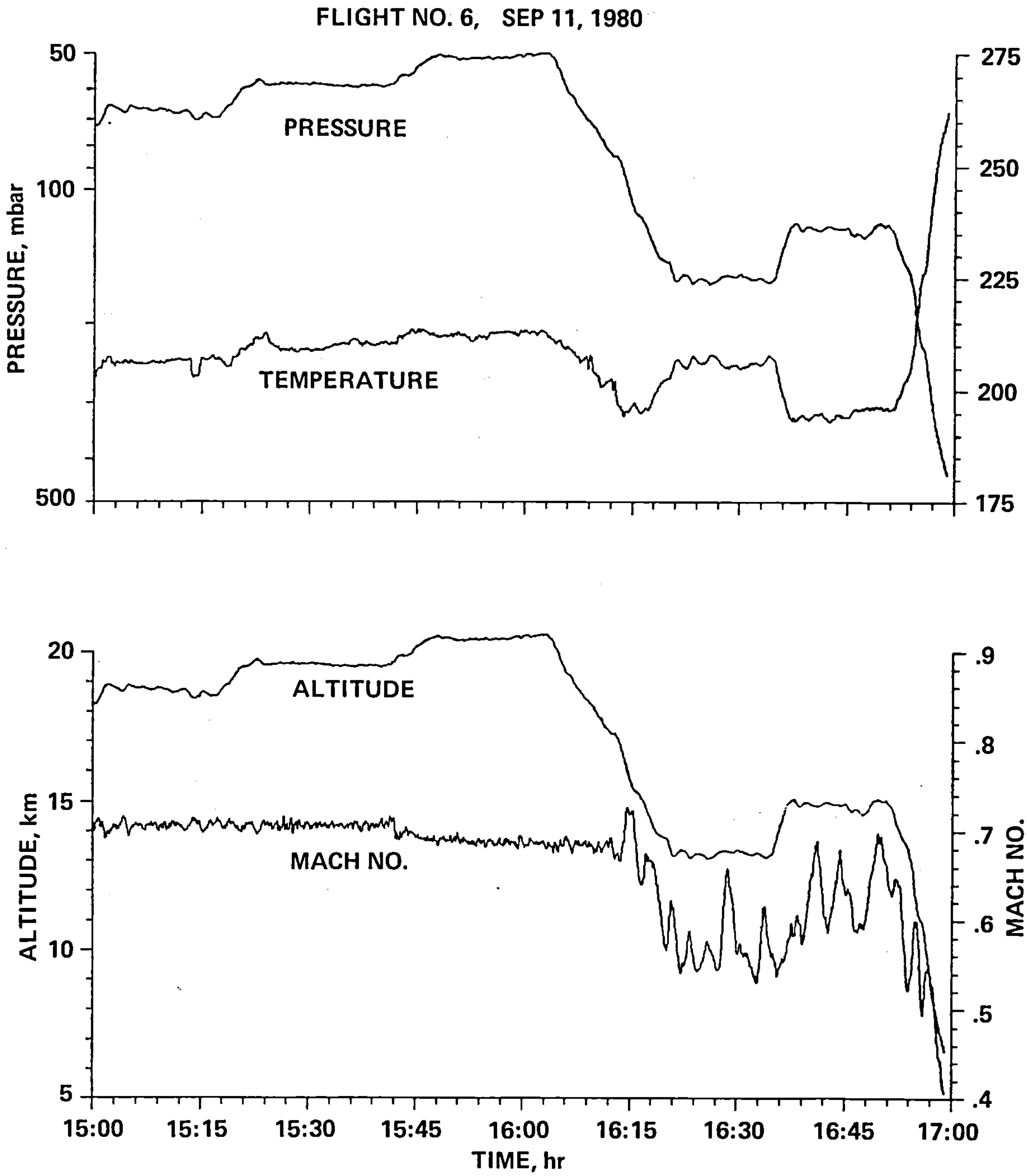

Figure 5.- Concluded.

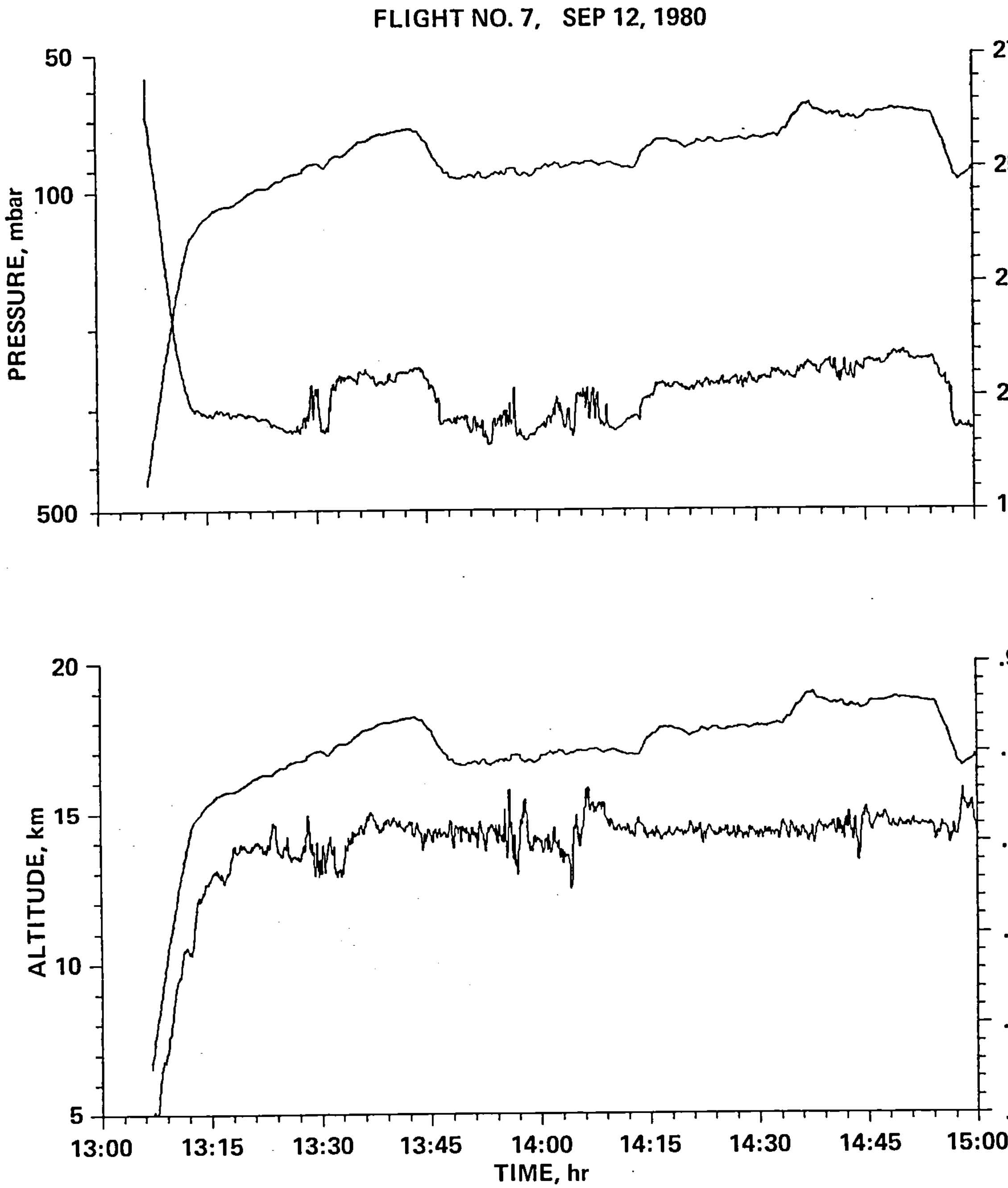

Figure 6.- Pressure, temperature, altitude, and Mach number for flight No. 7, September 12, 1980.

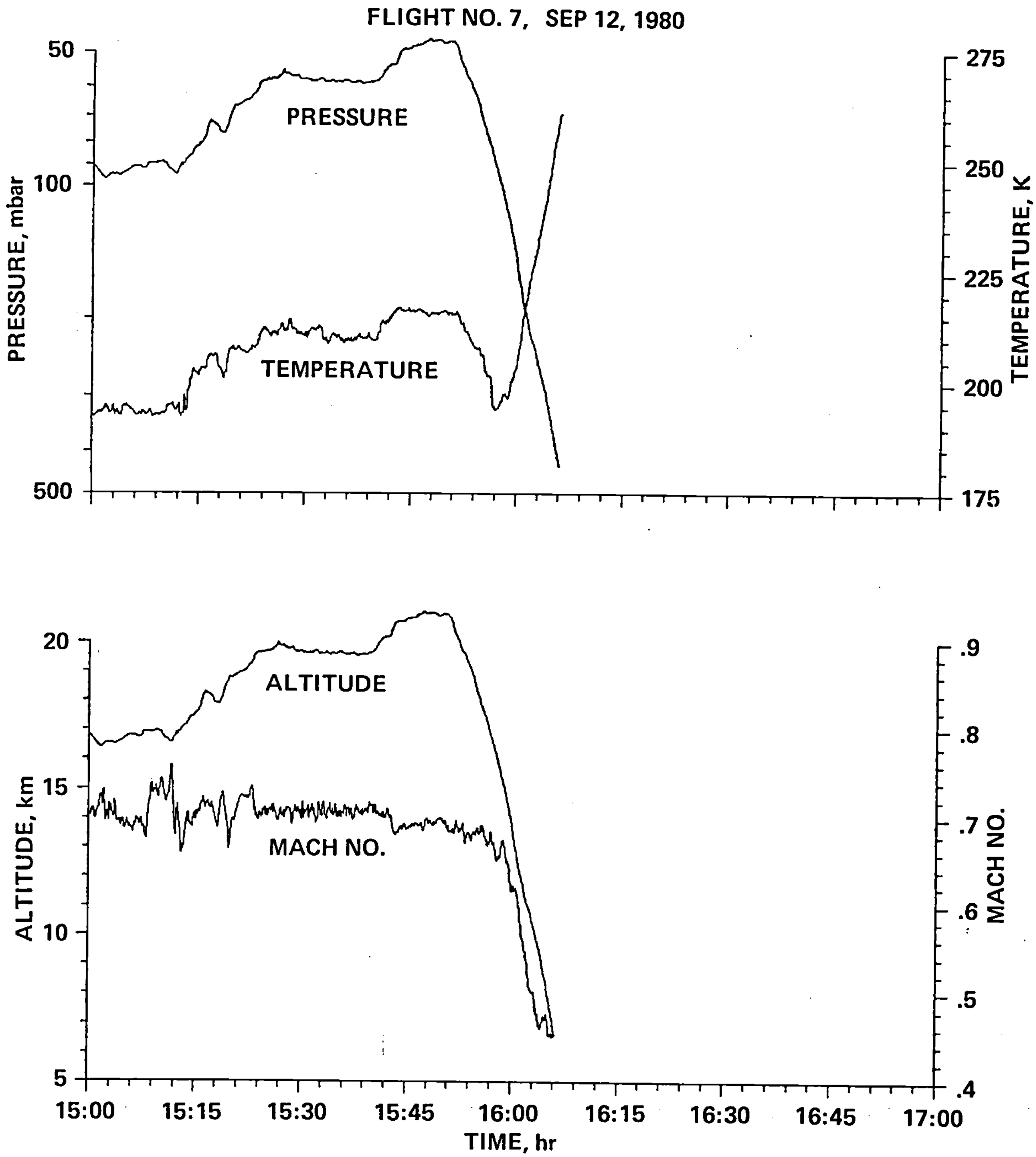

Figure 6.- Concluded.

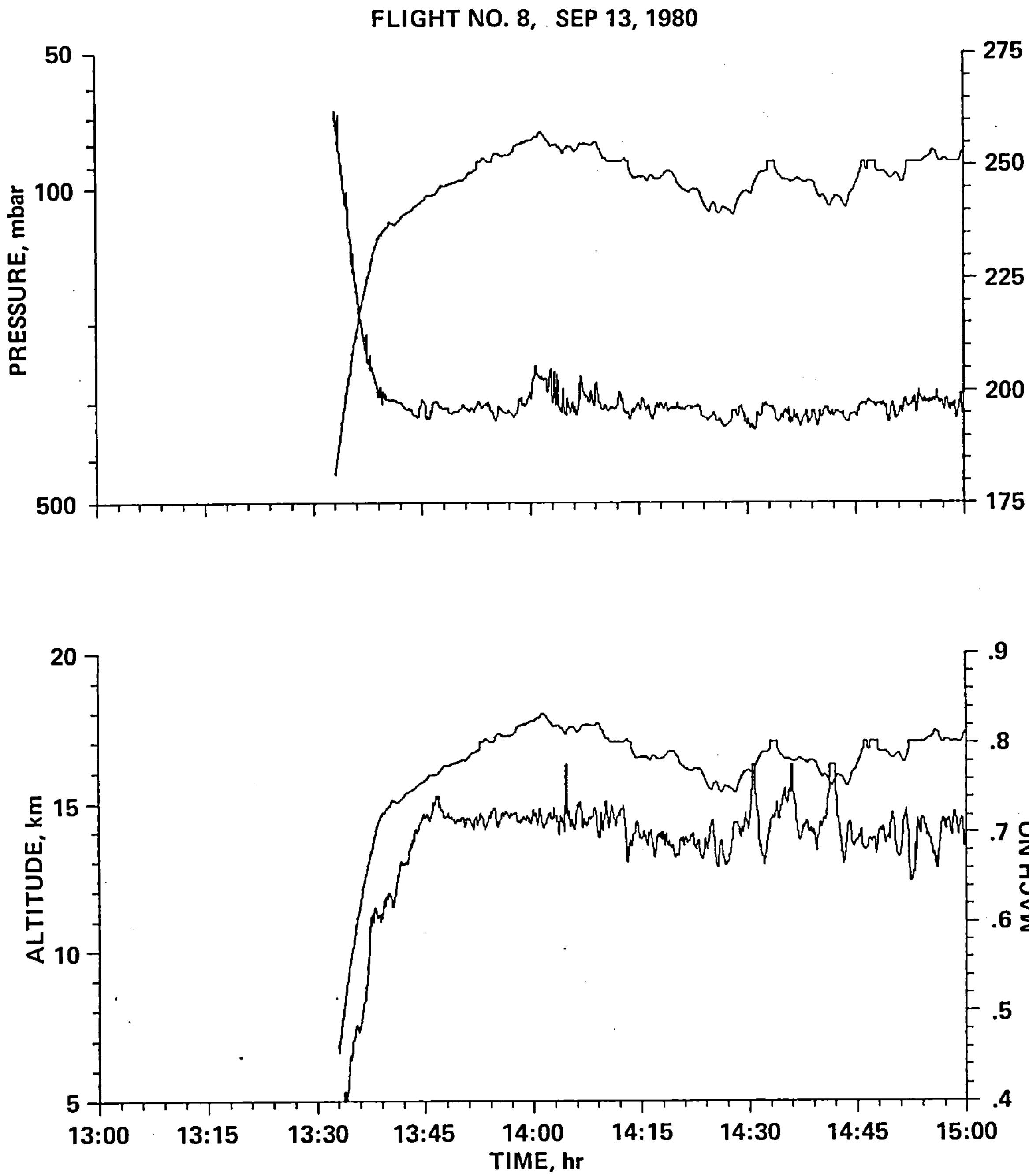

Figure 7.- Pressure, temperature, altitude, and Mach number for flight No. 8, September 13, 1980.

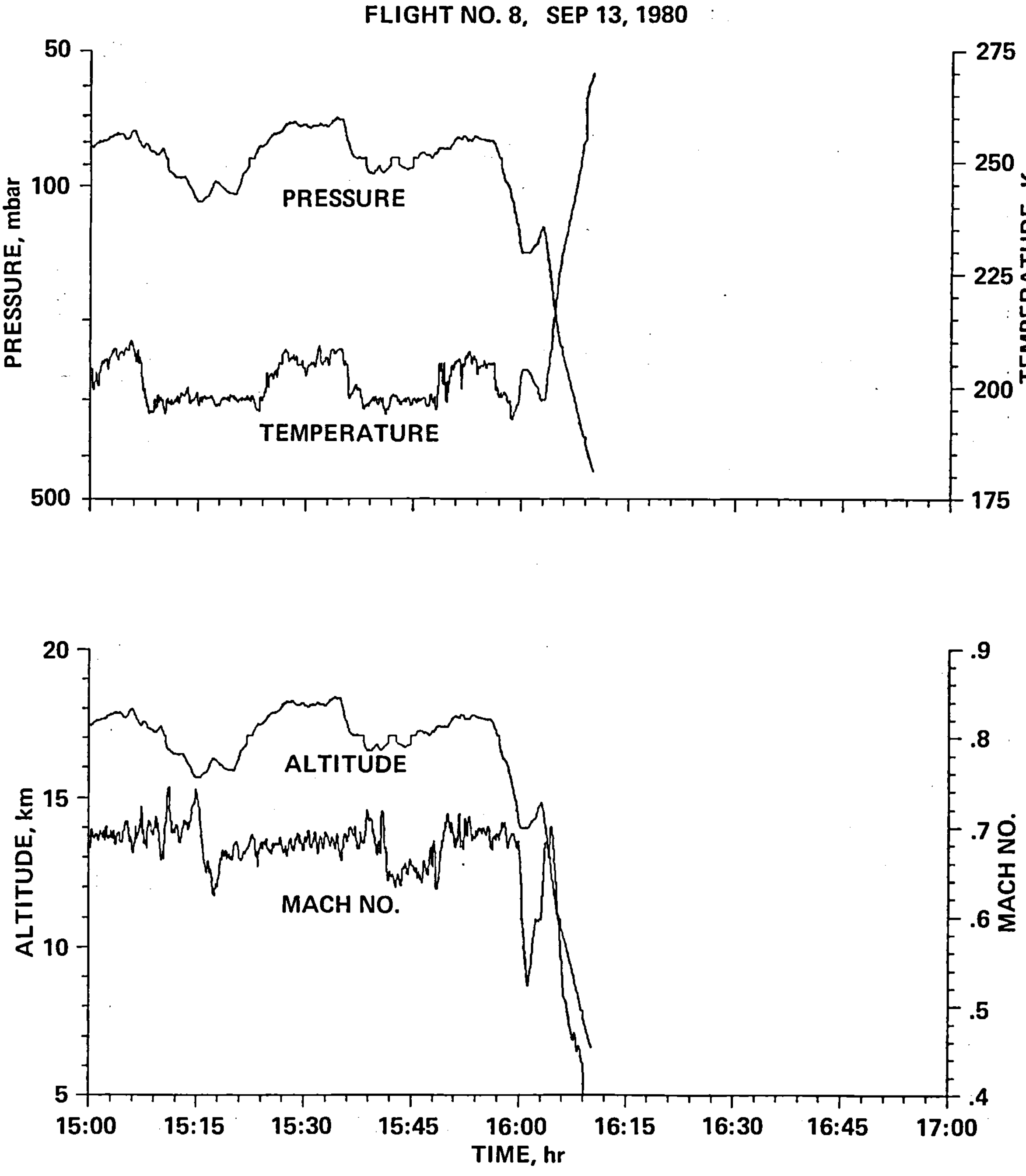

Figure 7.- Concluded.

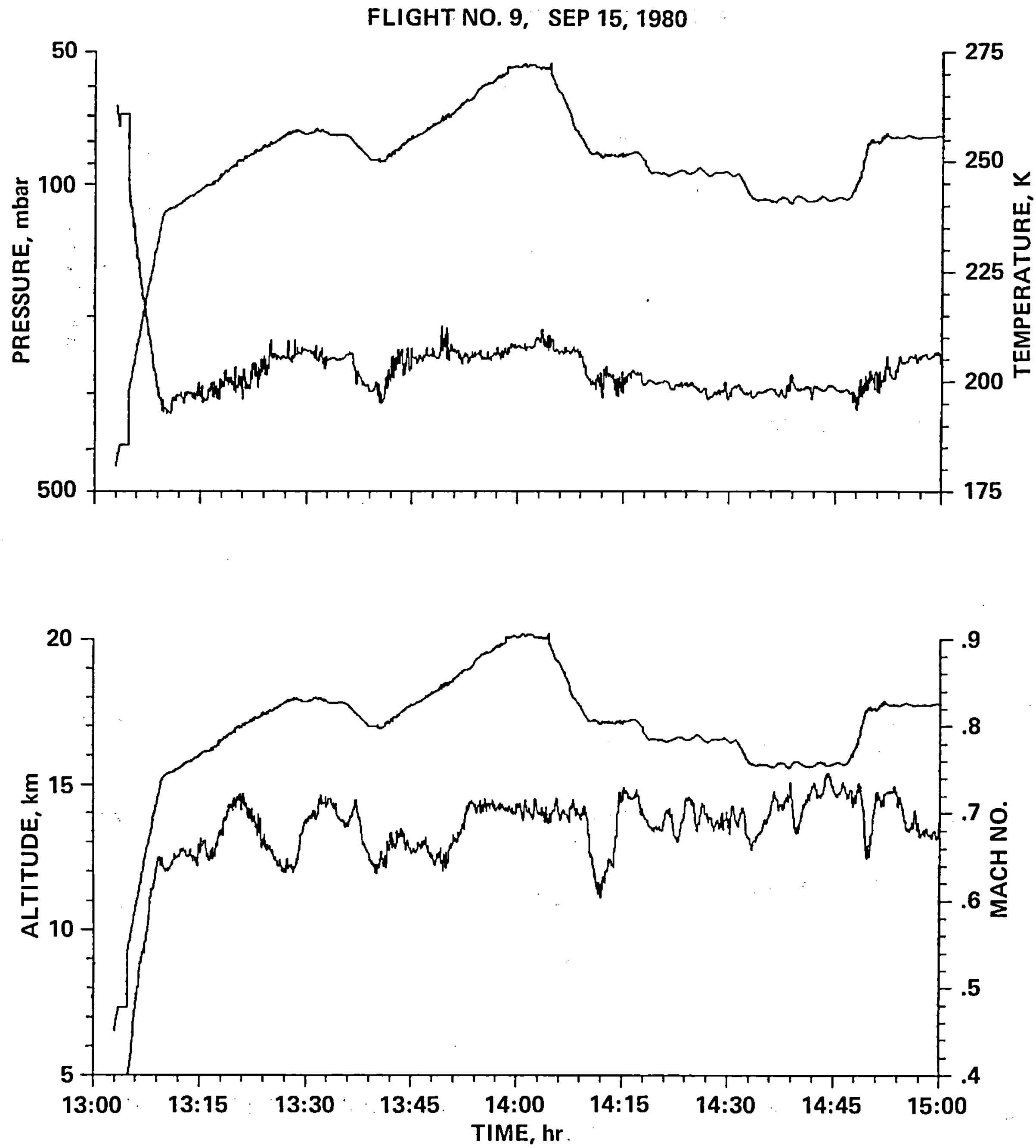

Figure 8.- Pressure, temperature, altitude, and Mach number for flight No. 9, September 15, 1980.

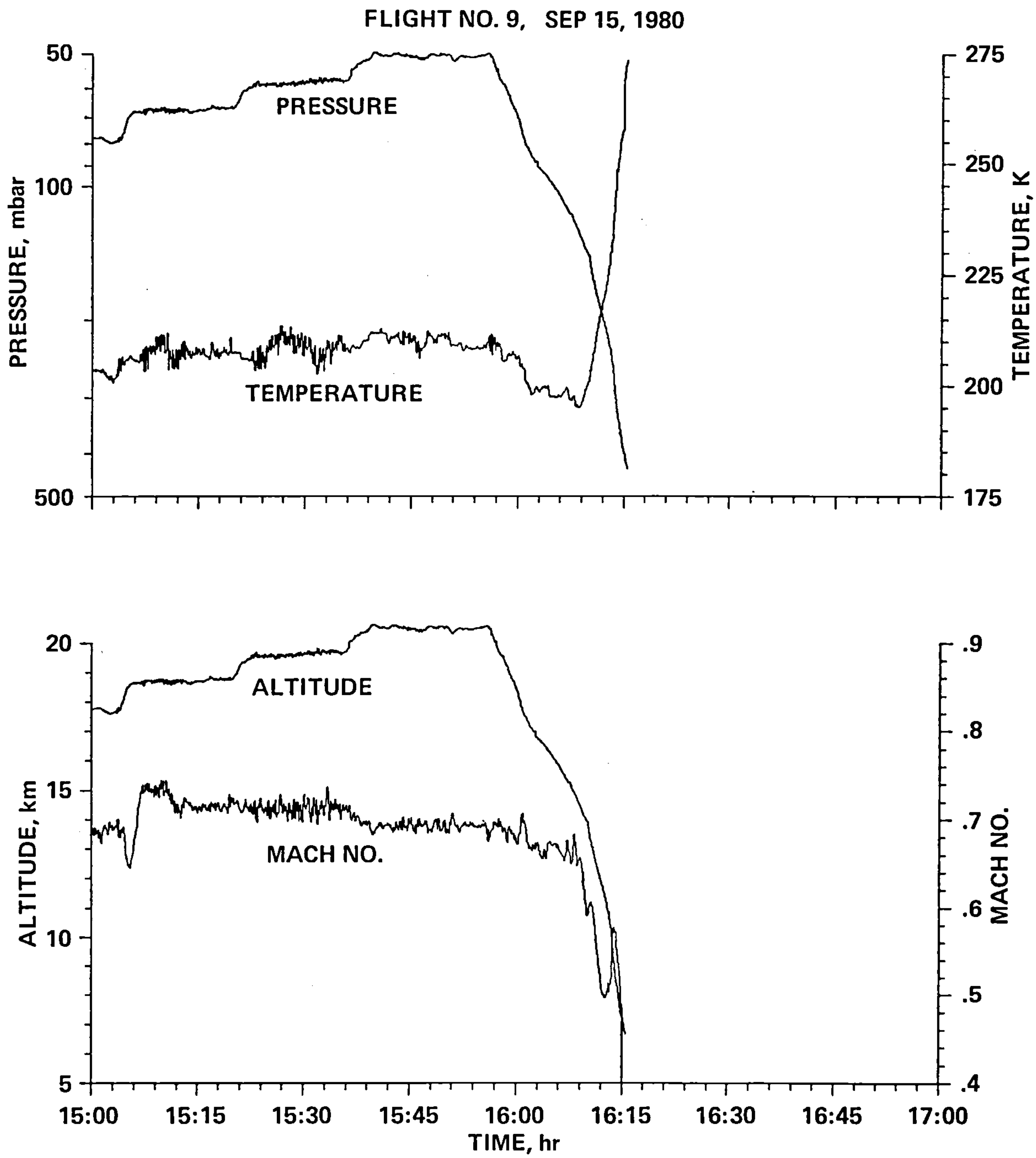

Figure 8.- Concluded.

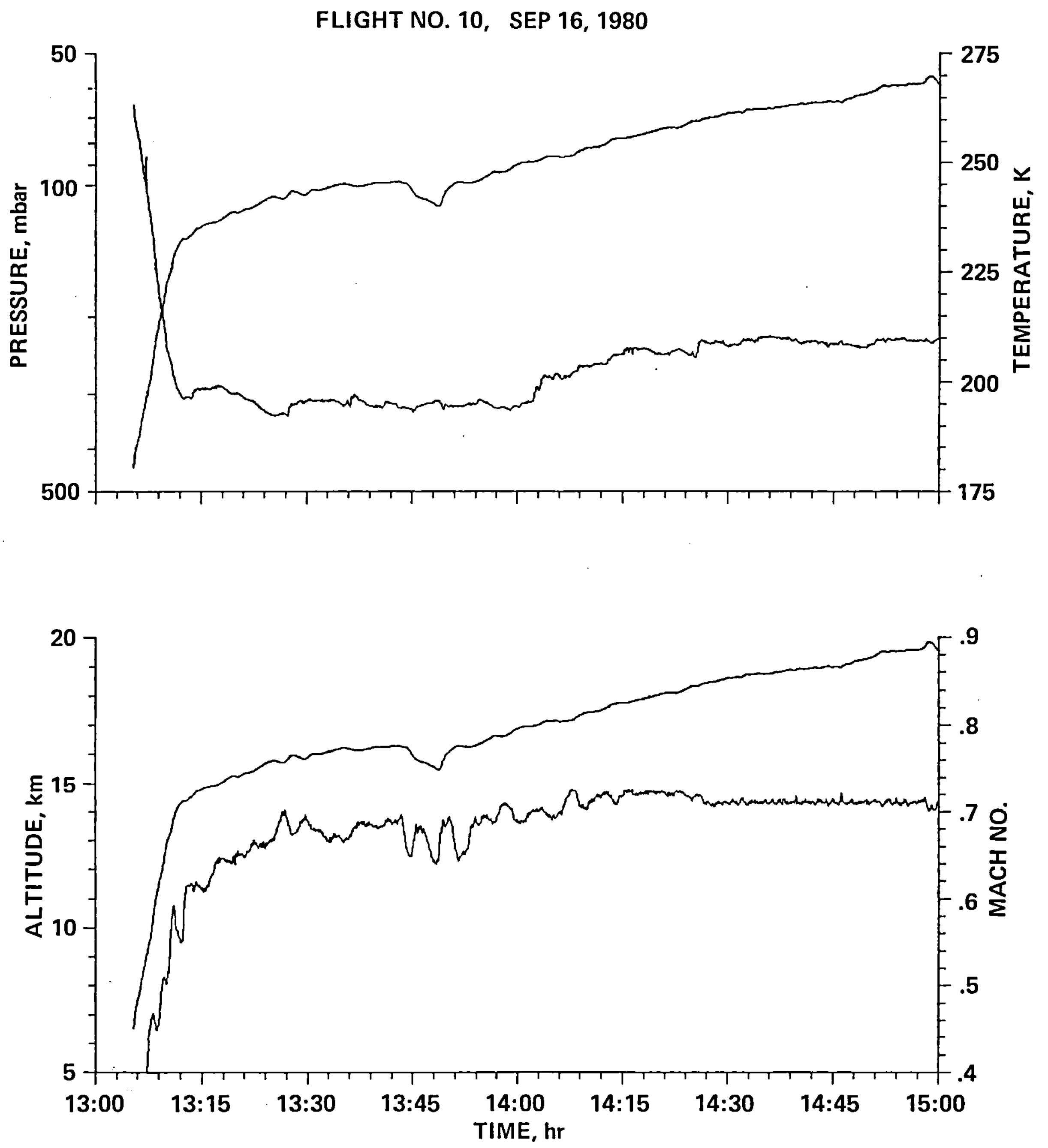

Figure 9.- Pressure, temperature, altitude, and Mach number for flight No. 10, September 16, 1980.

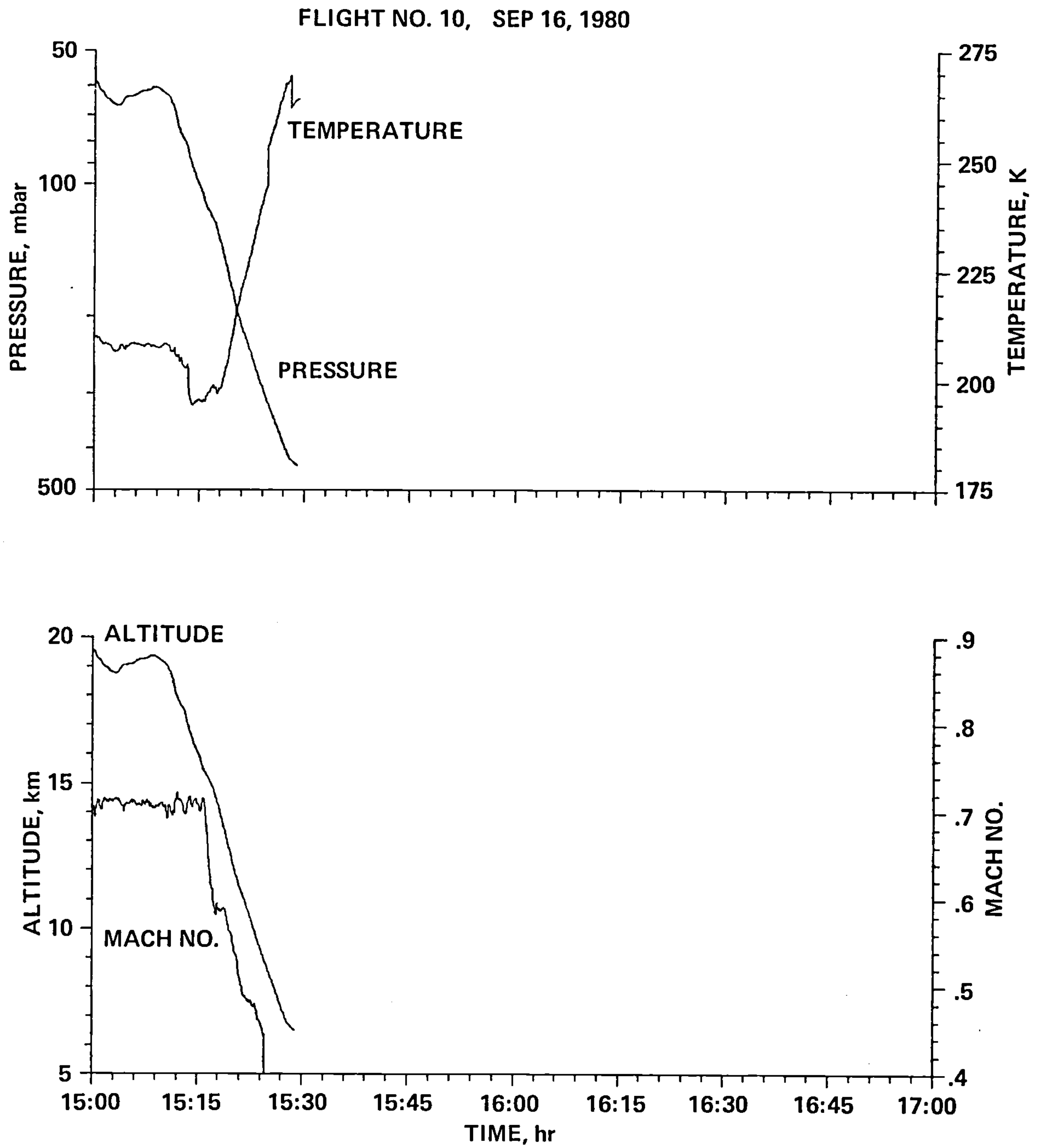

Figure 9.- Concluded.

APPENDIX A

SATELLITE PHOTOGRAPHS

Edwin F. Danielsen

See section 1 for description of photographs.

Flight number	Date
1	August 30, 1980
2	August 31, 1980
3	September 3, 1980
4	September 7, 1980
5	September 9, 1980
6	September 11, 1980
7	September 12, 1980
8	September 13, 1980
9	September 15, 1980
10	September 16, 1980

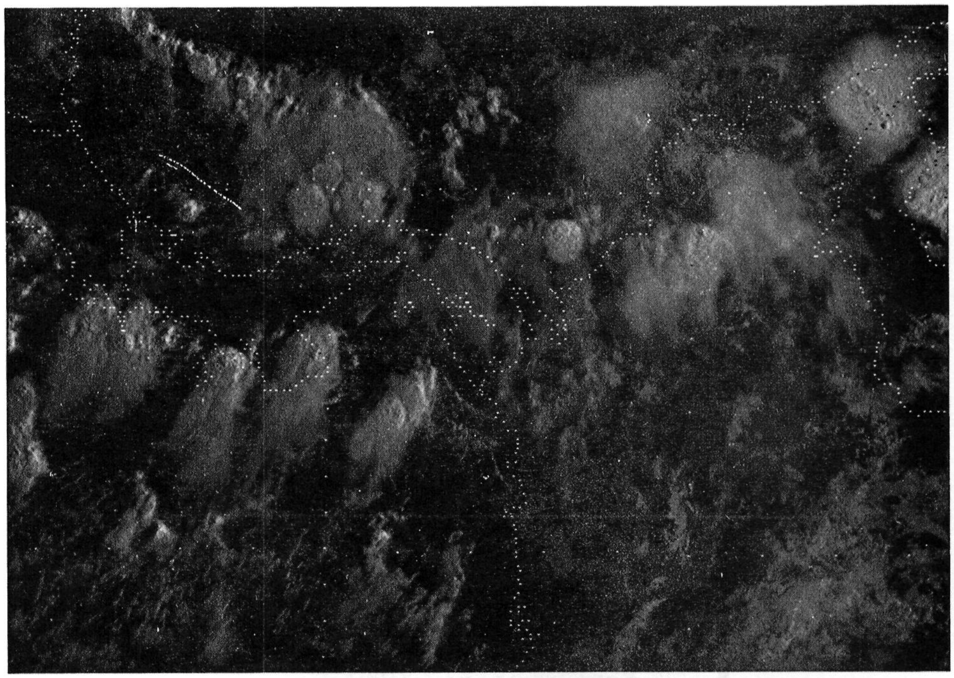

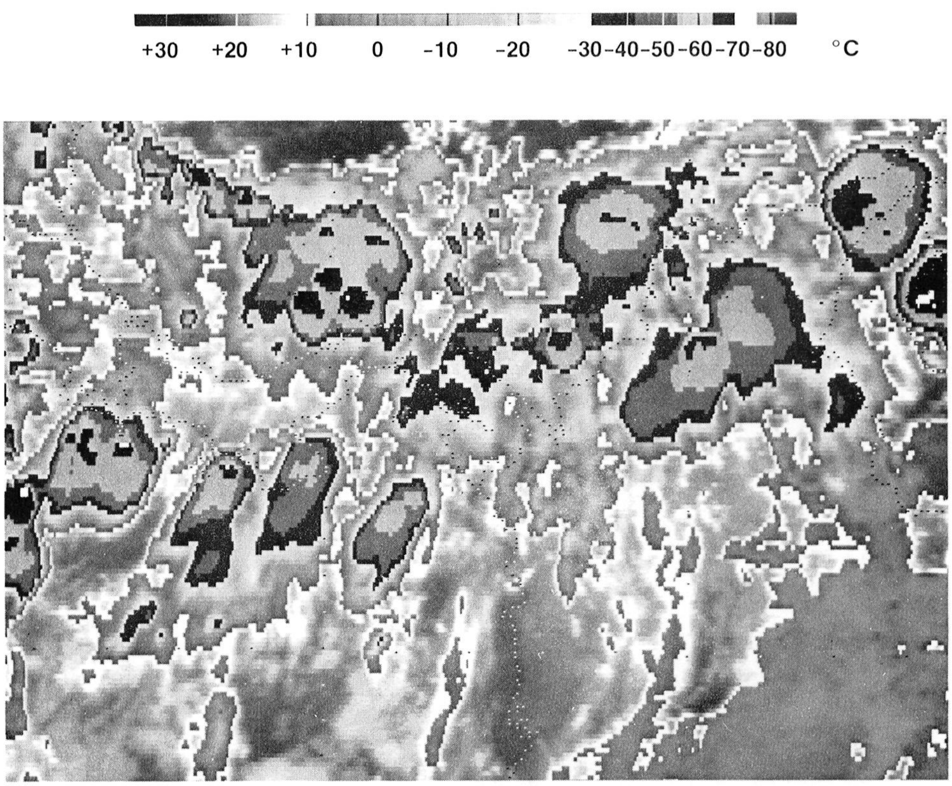

1235 UT, AUG 30 1980

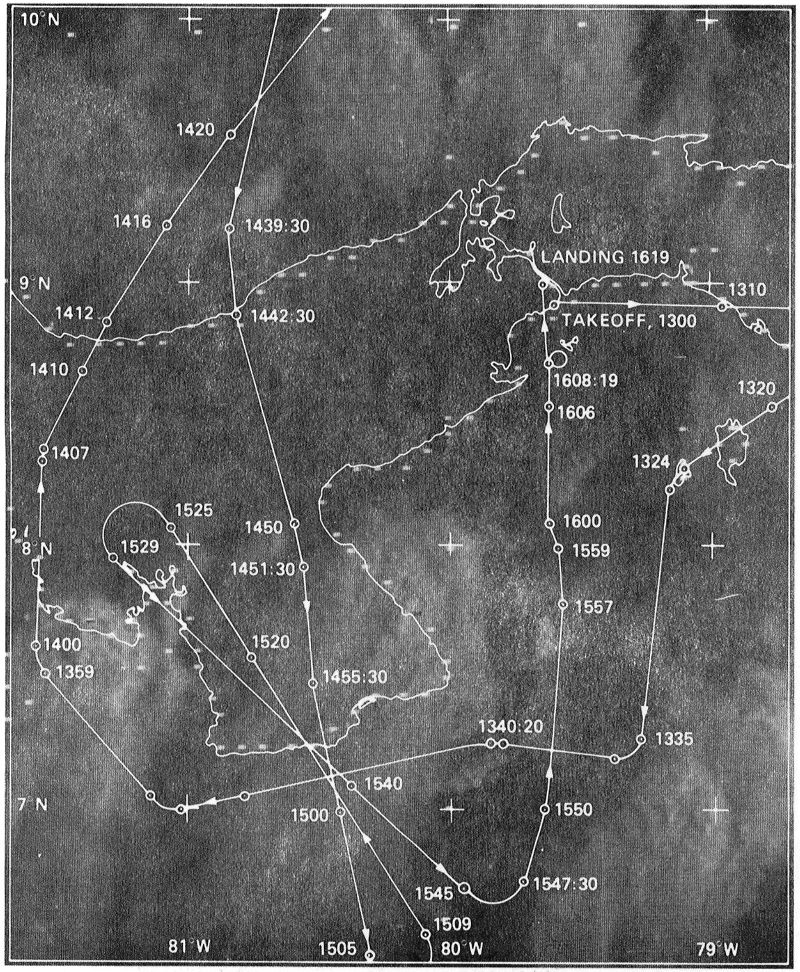

1230 UT, VISIBLE

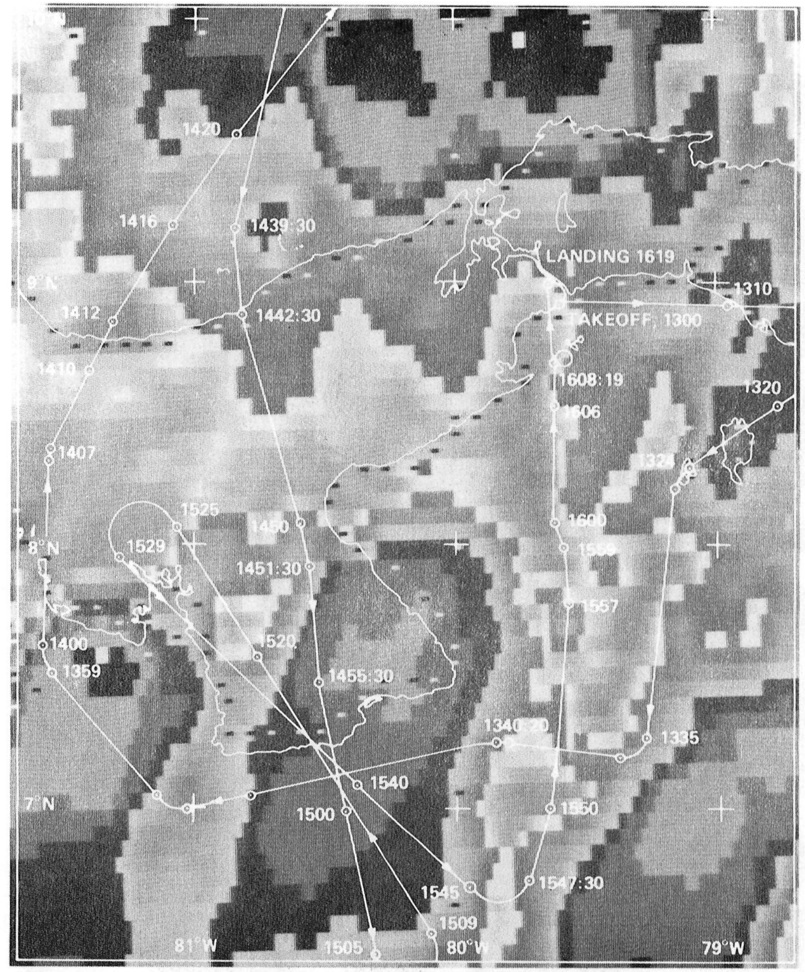

1235 UT, INFRARED

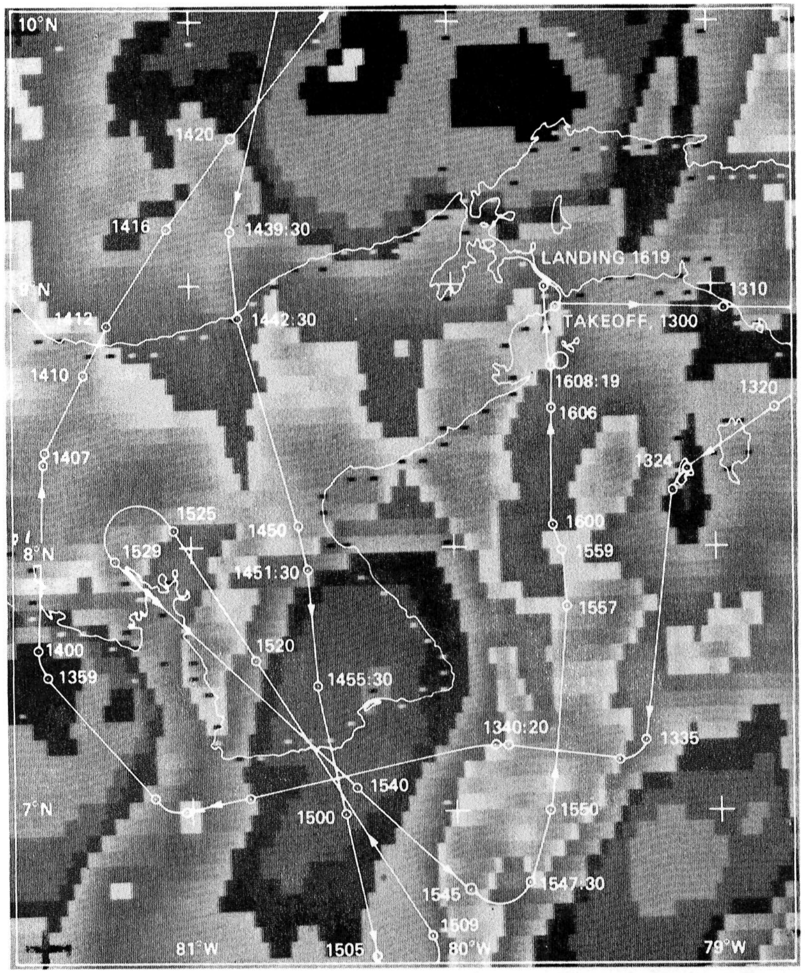

1305 UT, INFRARED

1405 UT, INFRARED

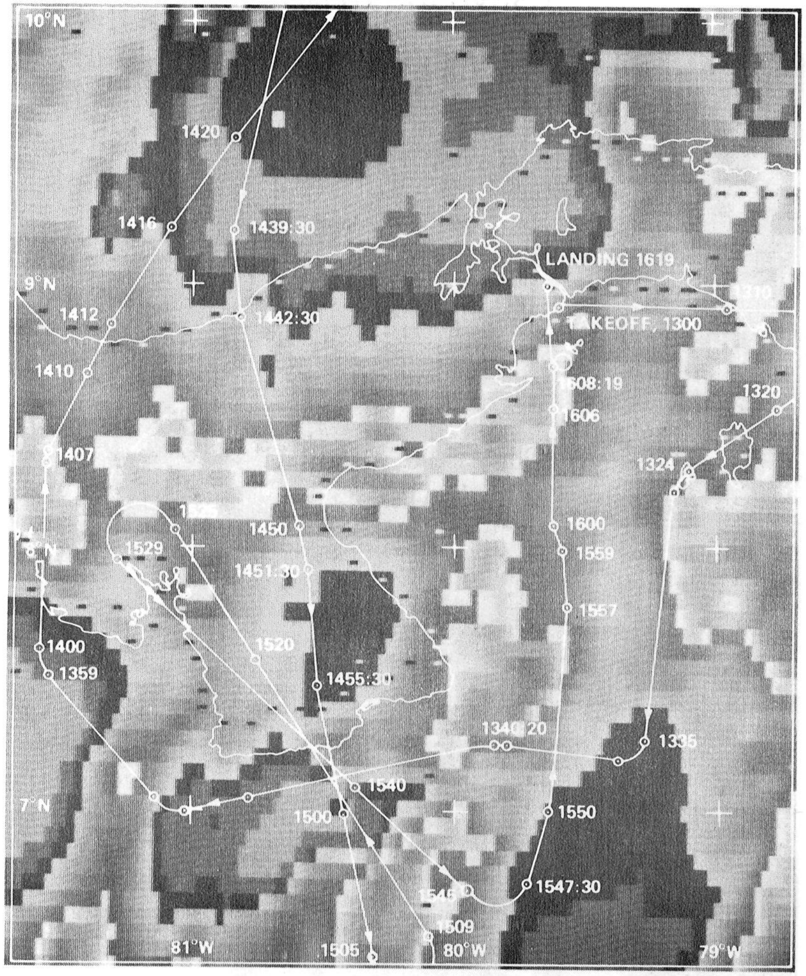

1435 UT, INFRARED

1505 UT, INFRARED

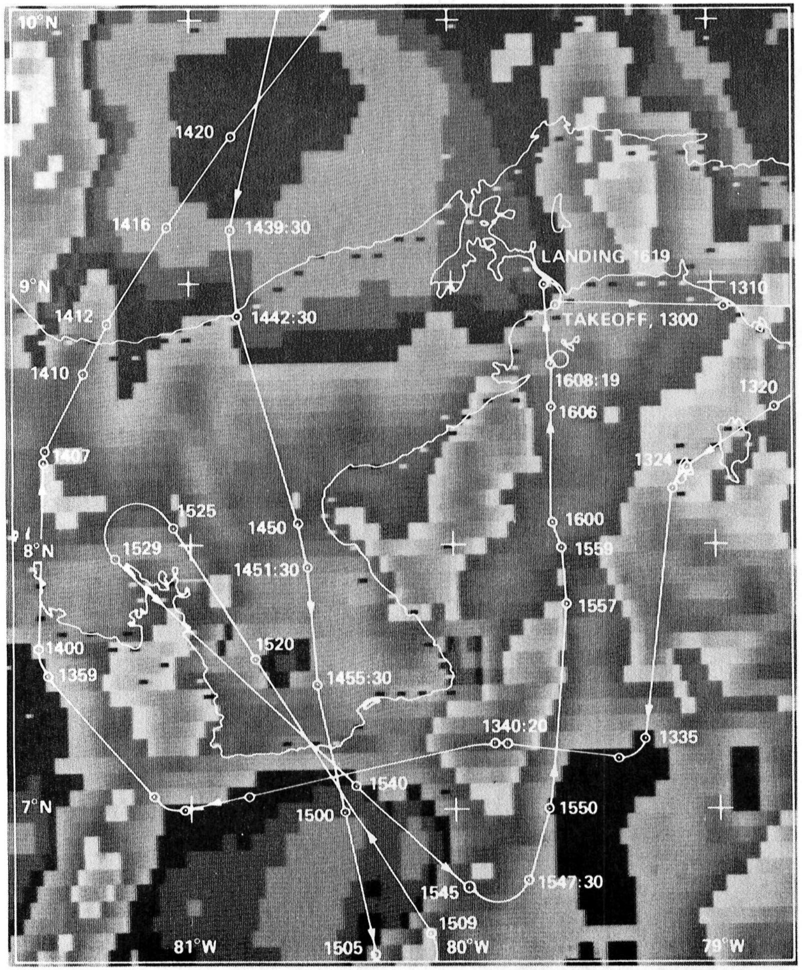

1533 UT, INFRARED

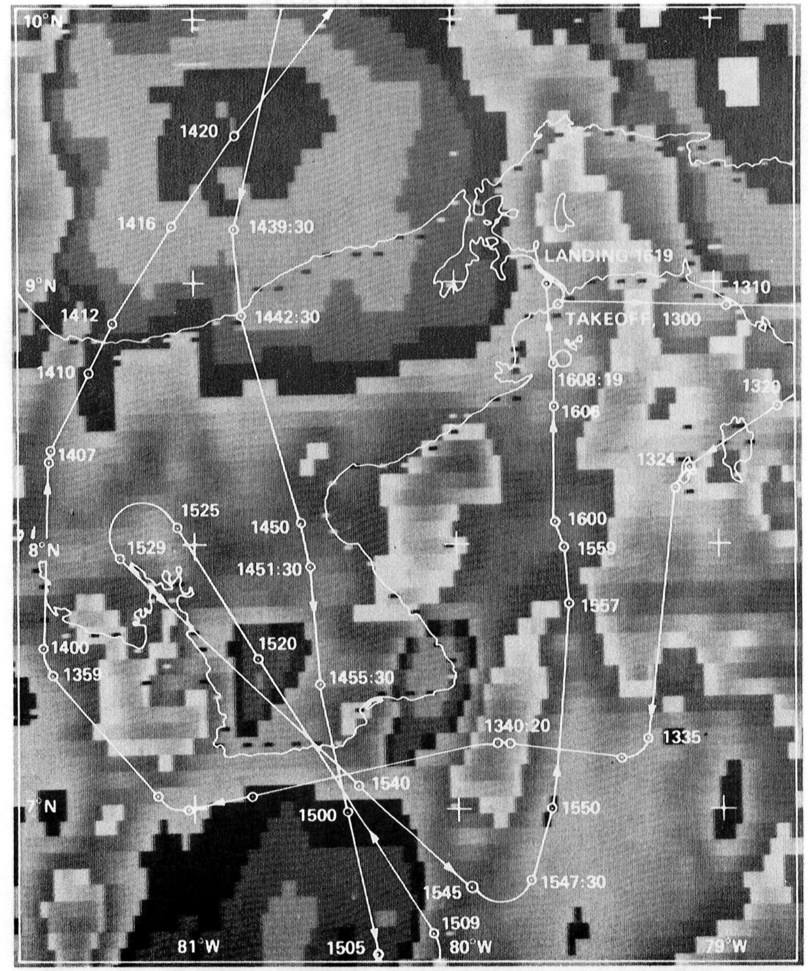

1605 UT, INFRARED

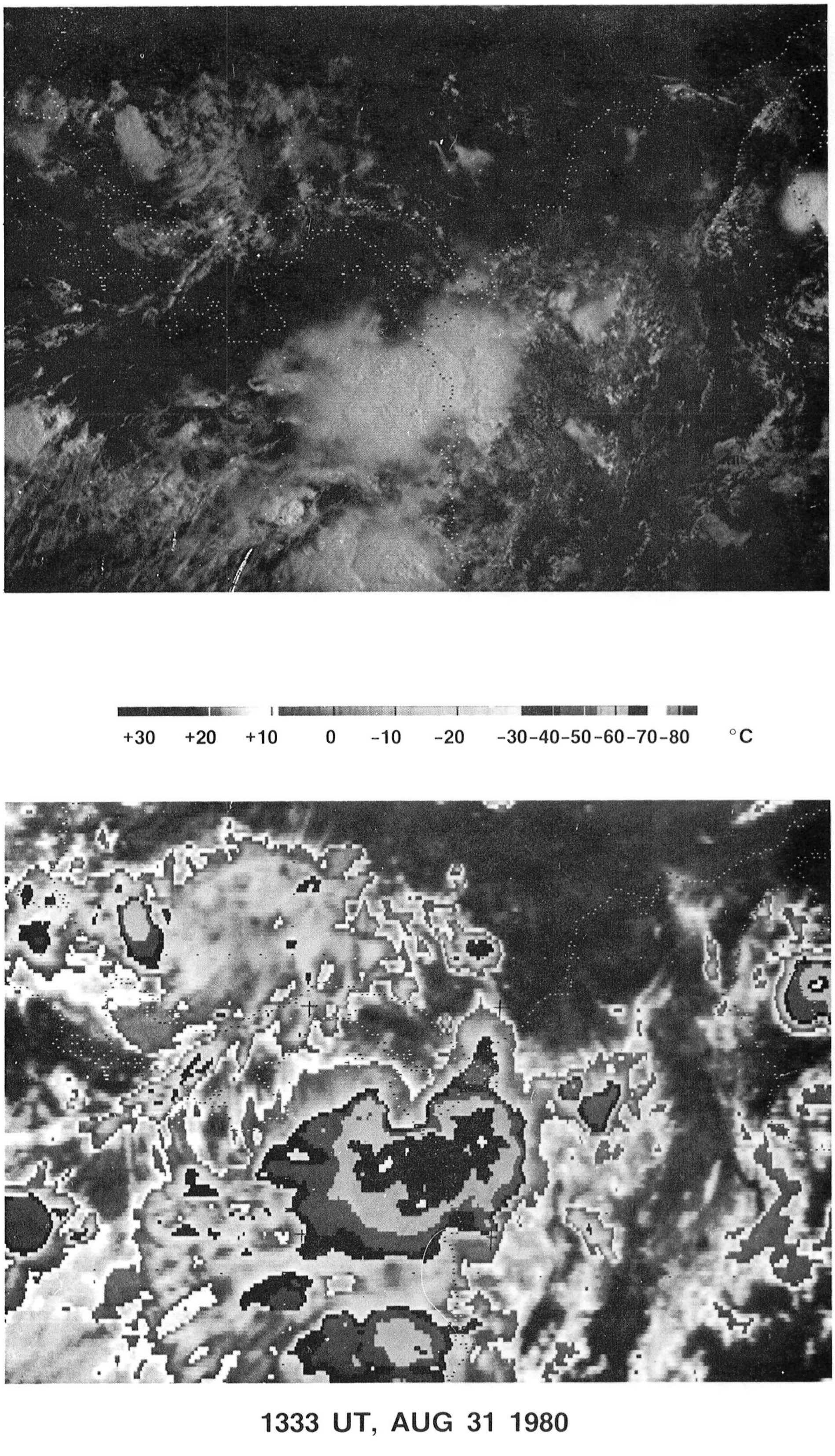

1333 UT, AUG 31 1980

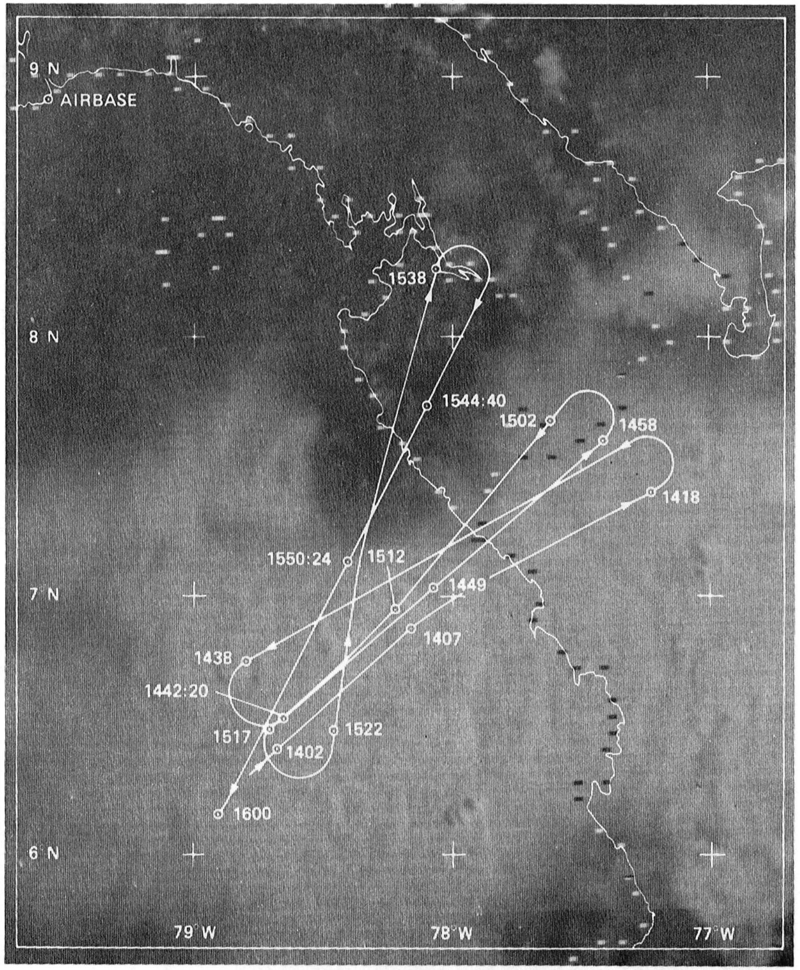

1330 UT, VISIBLE

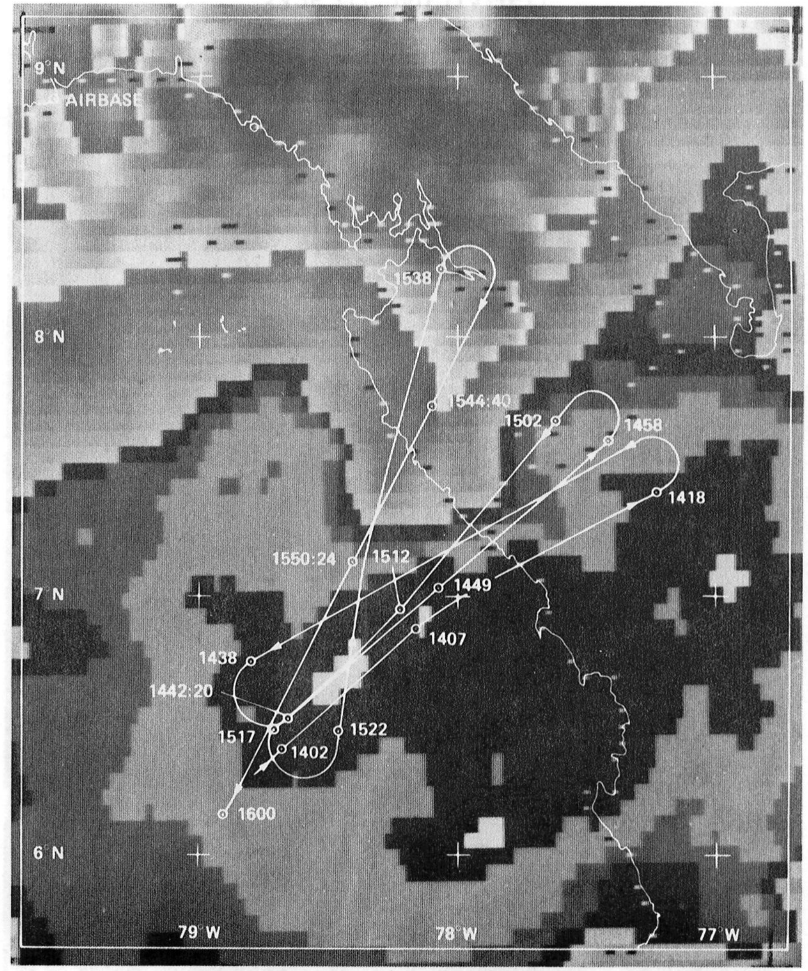

1333 UT, INFRARED

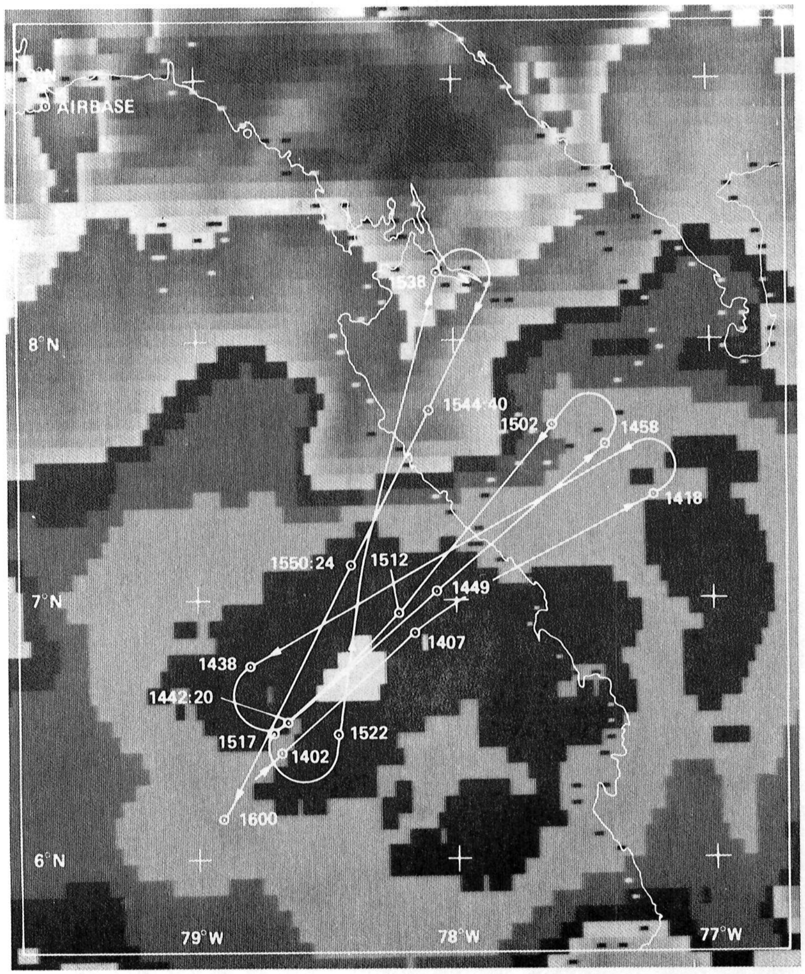

1405 UT, INFRARED

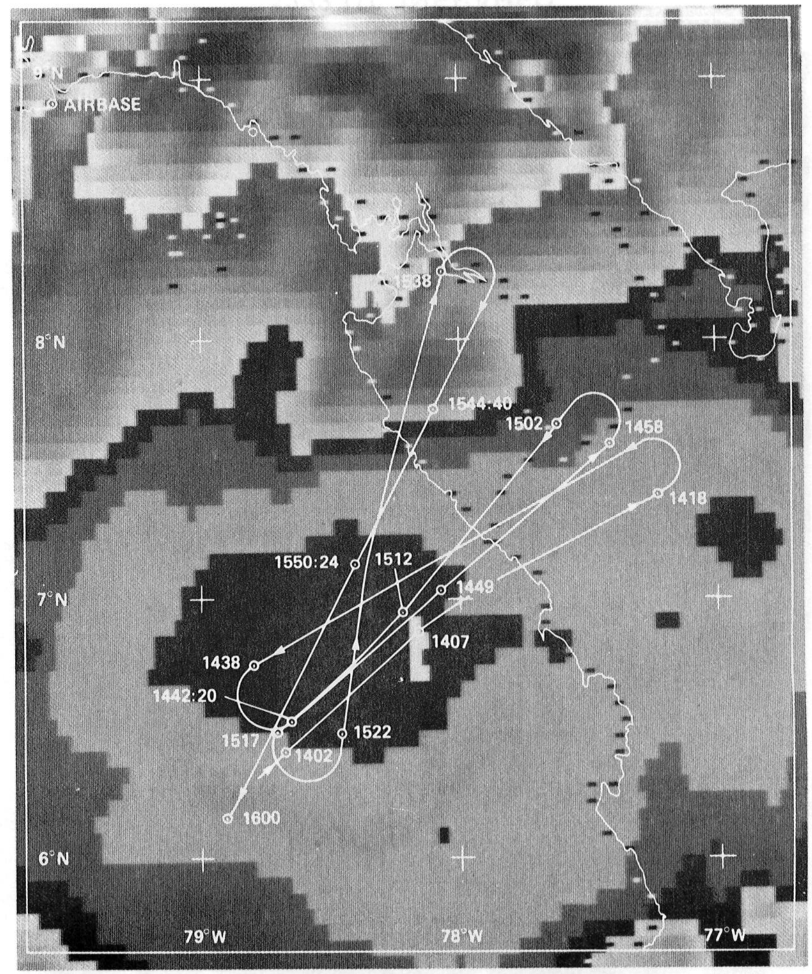

1435 UT, INFRARED

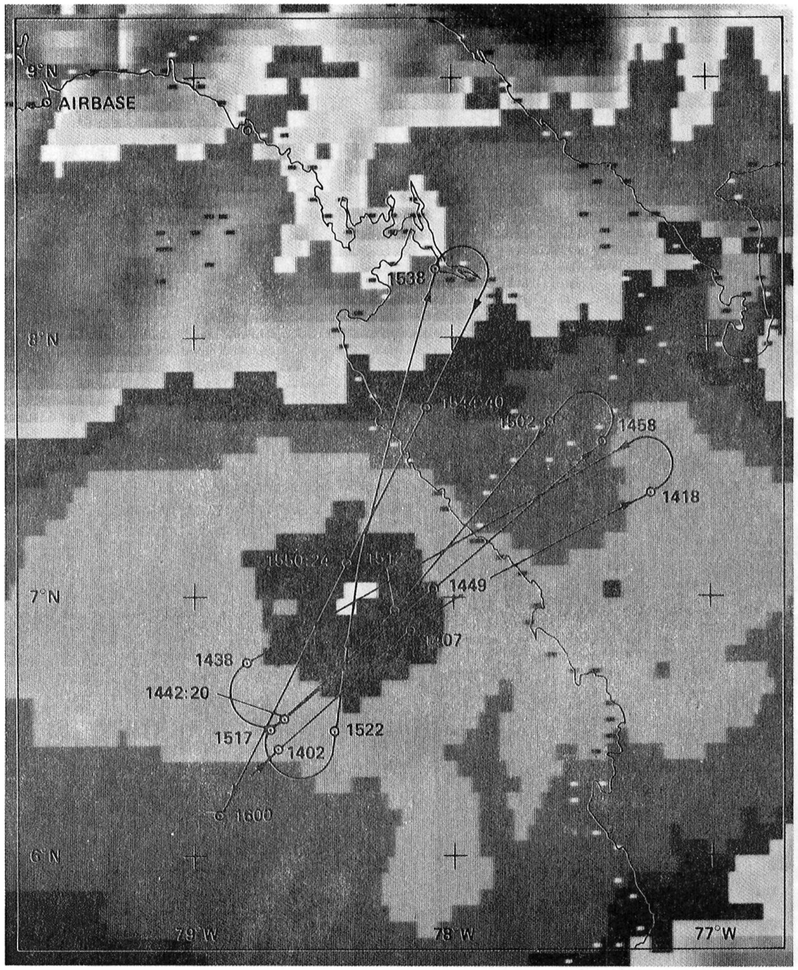

1533 UT, INFRARED

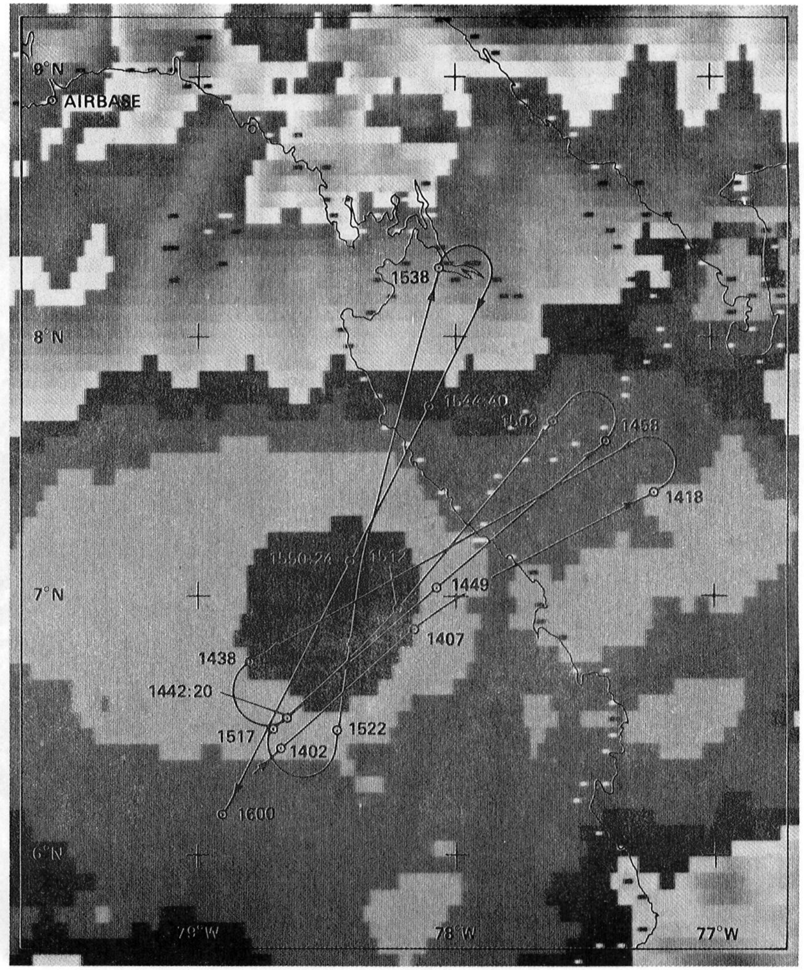

1605 UT, INFRARED

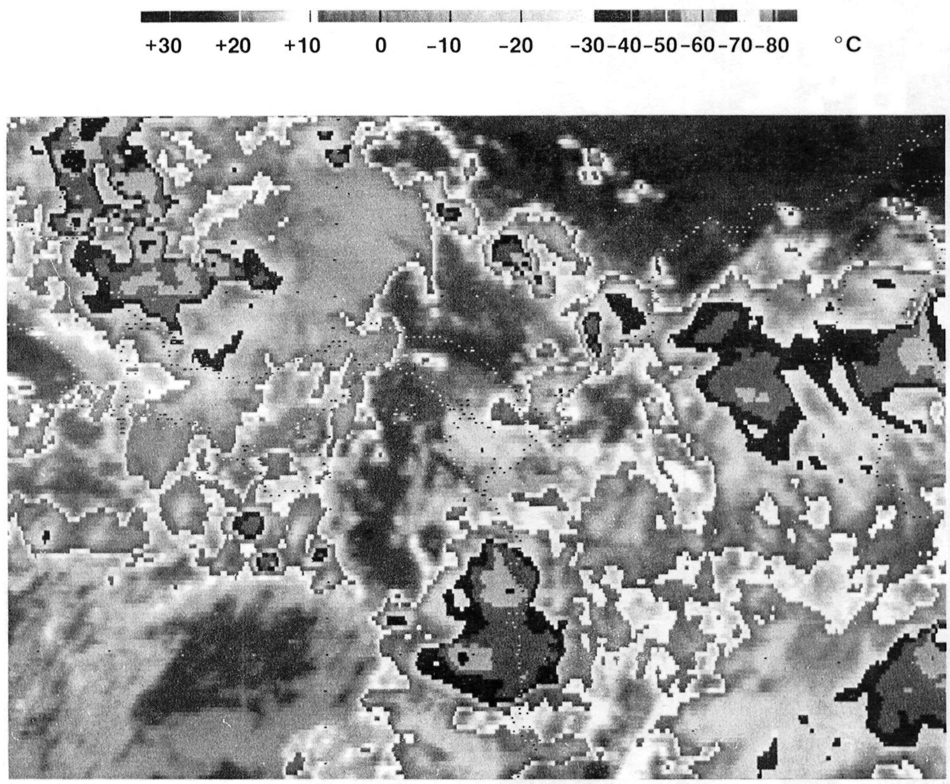

1305 UT, SEPT 3 1980

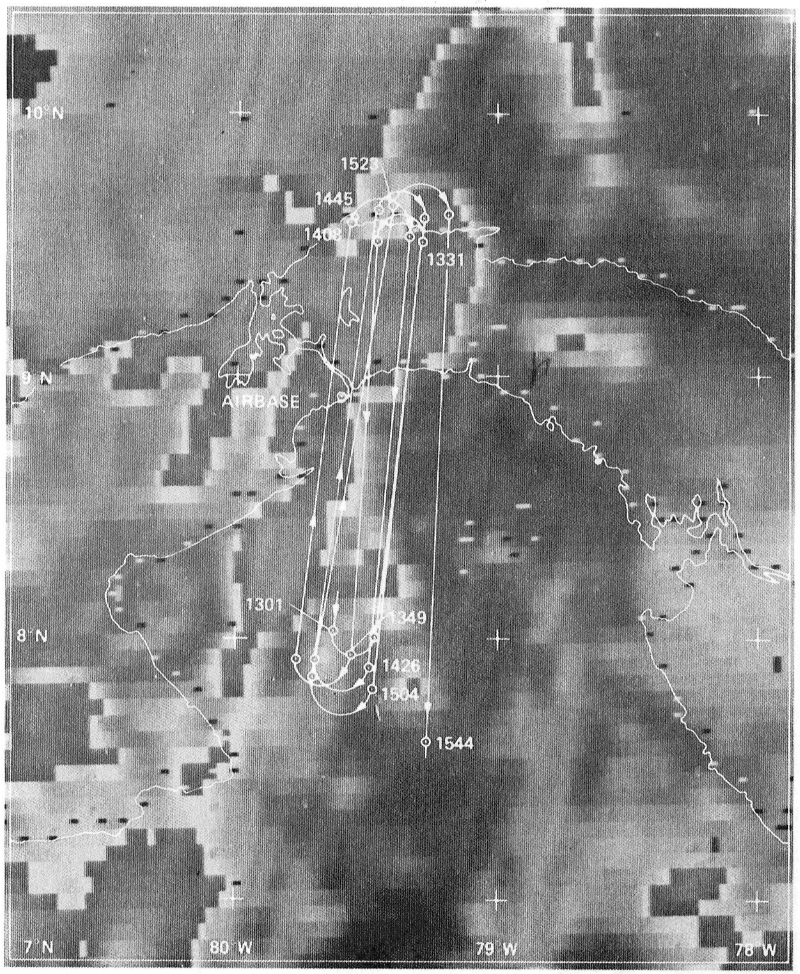

1305 UT, INFRARED

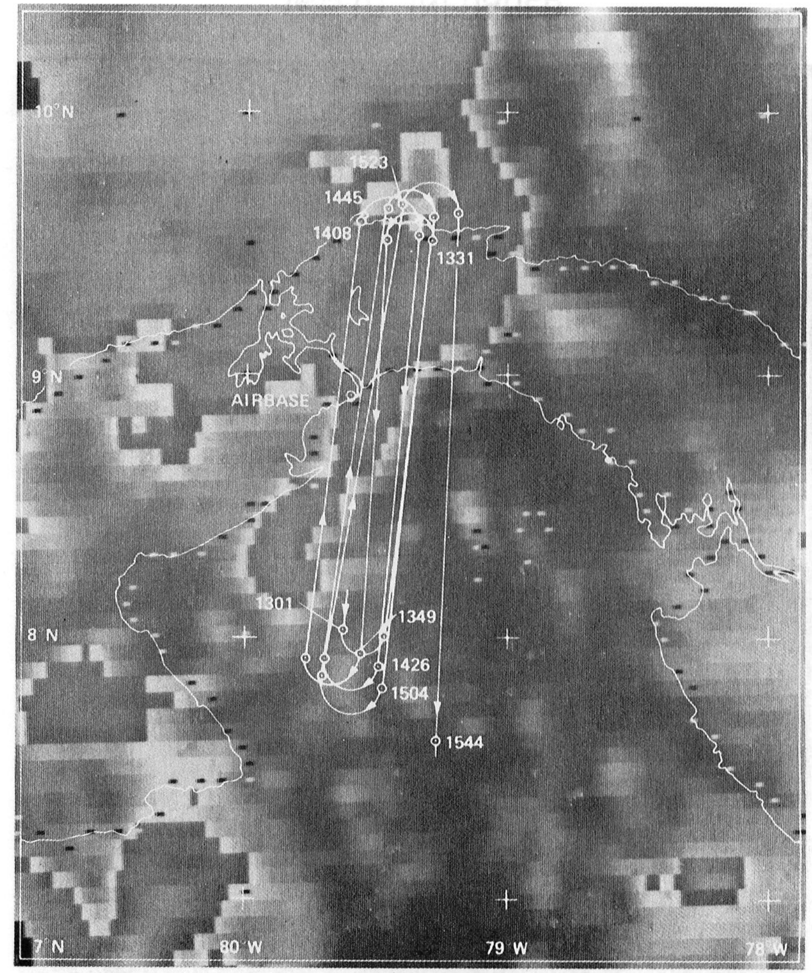

1333 UT, INFRARED

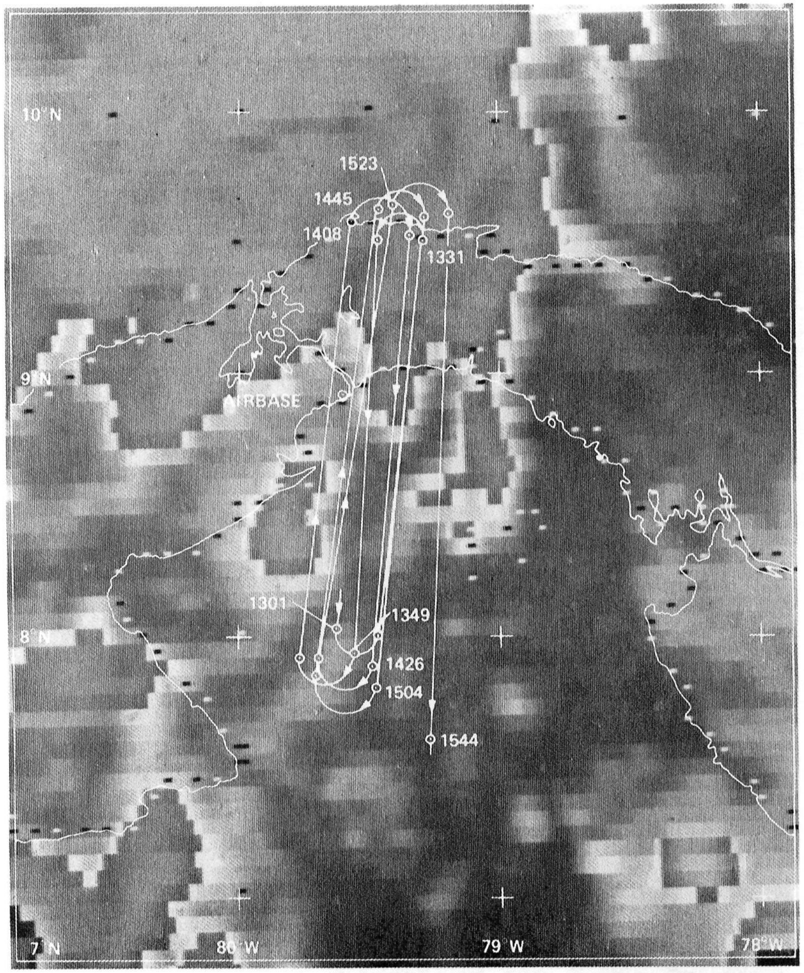

1405 UT, INFRARED

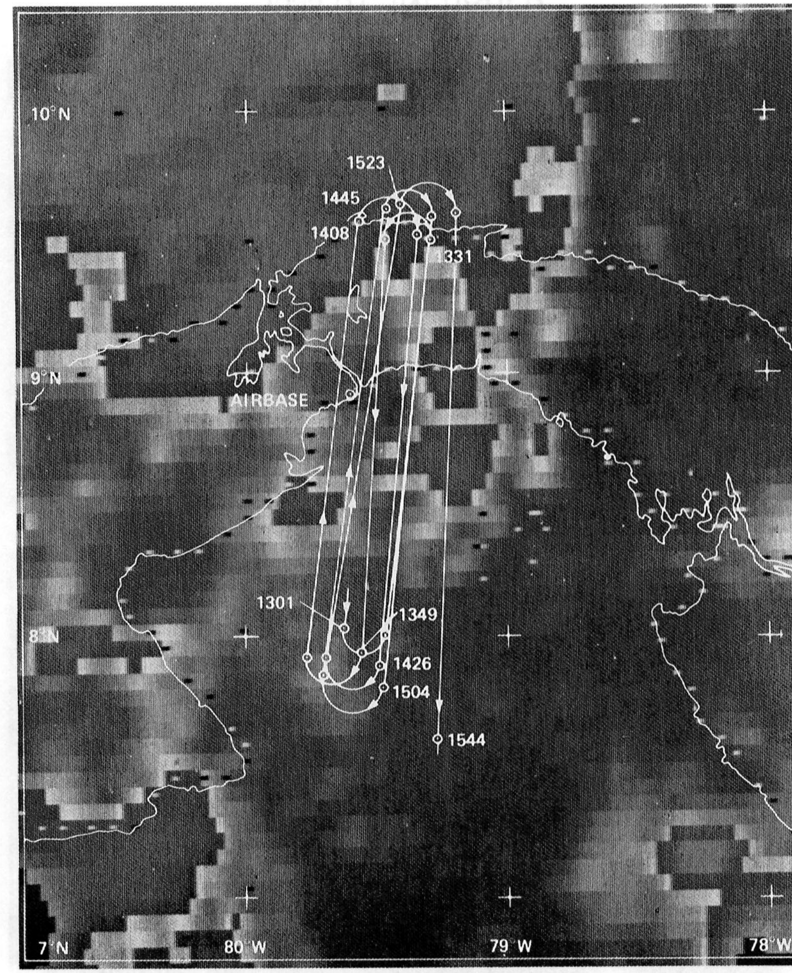

1435 UT, INFRARED

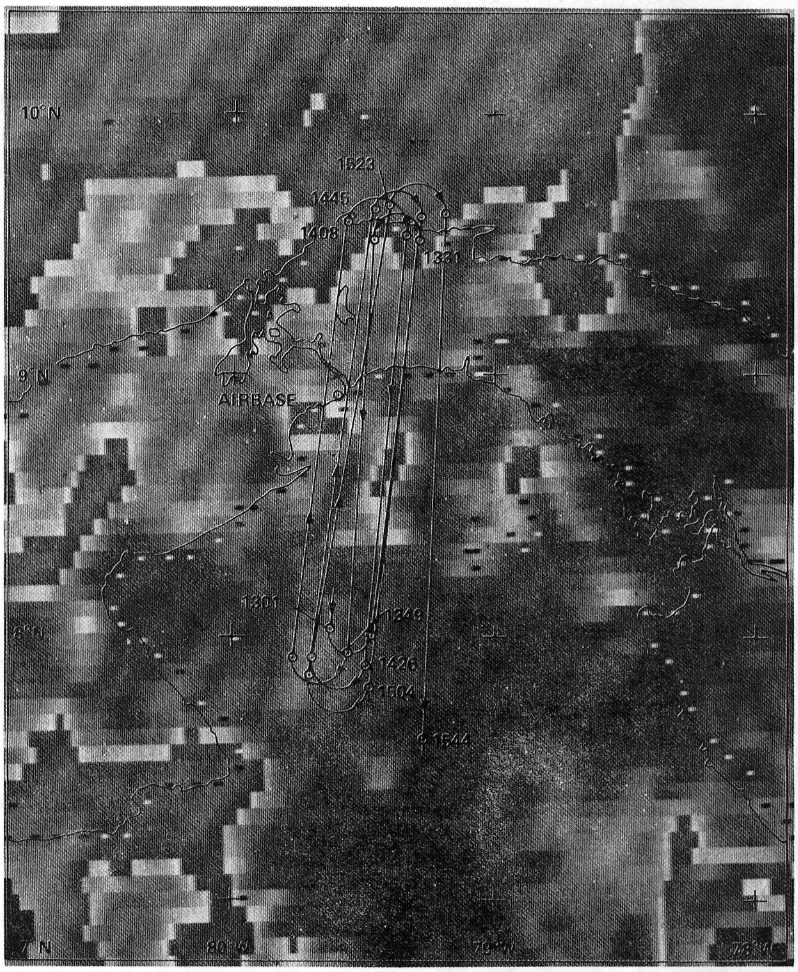

1533 UT, INFRARED

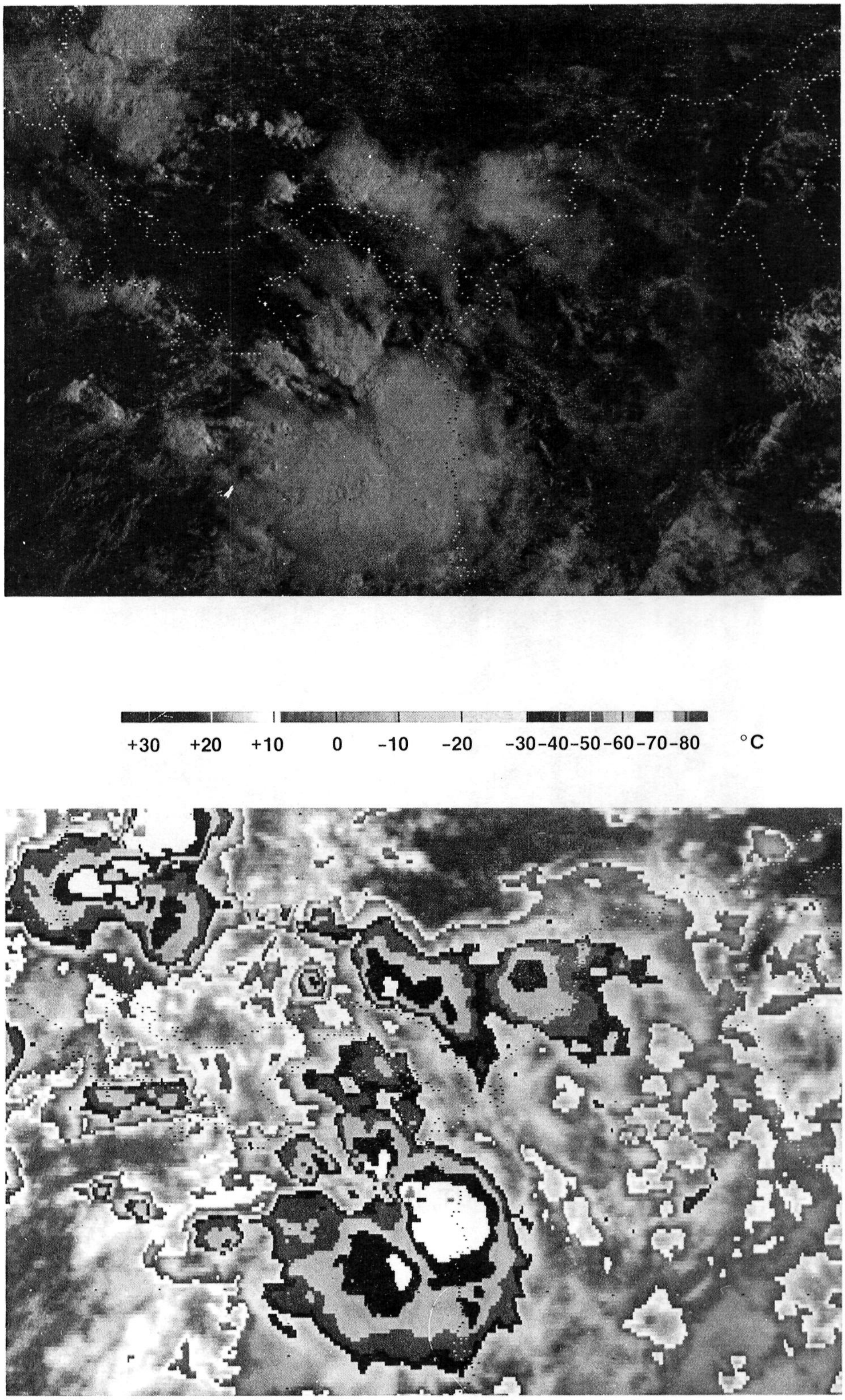

1305 UT, SEPT 7 1980

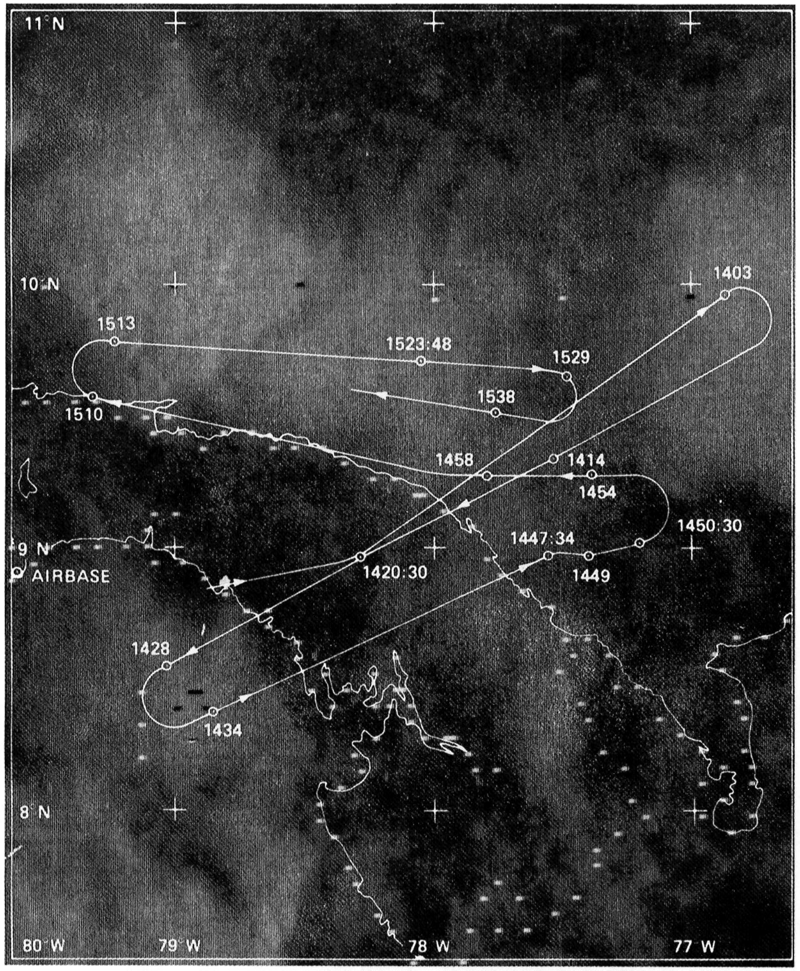

1303 UT, VISIBLE

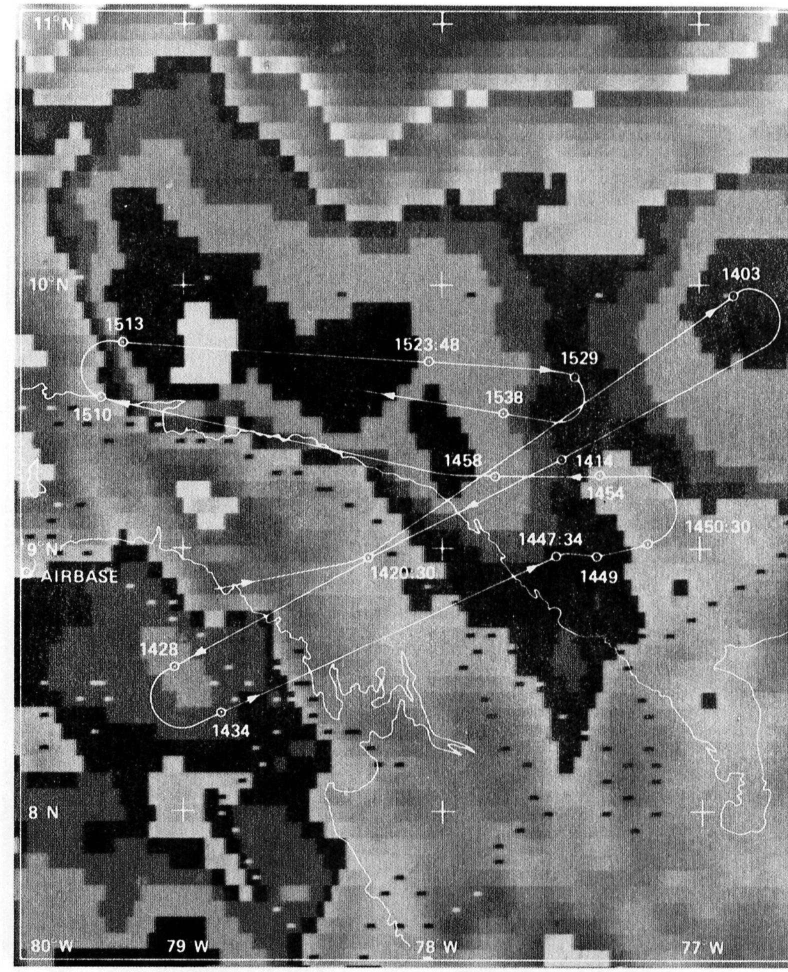

1305 UT, INFRARED

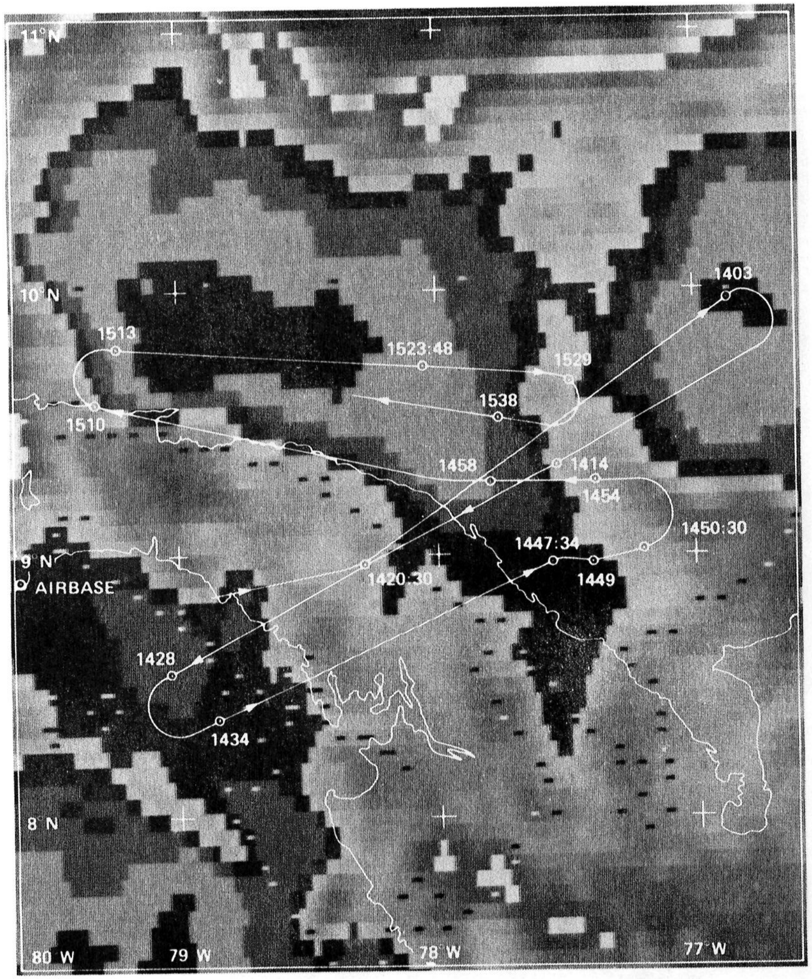

1333 UT, INFRARED

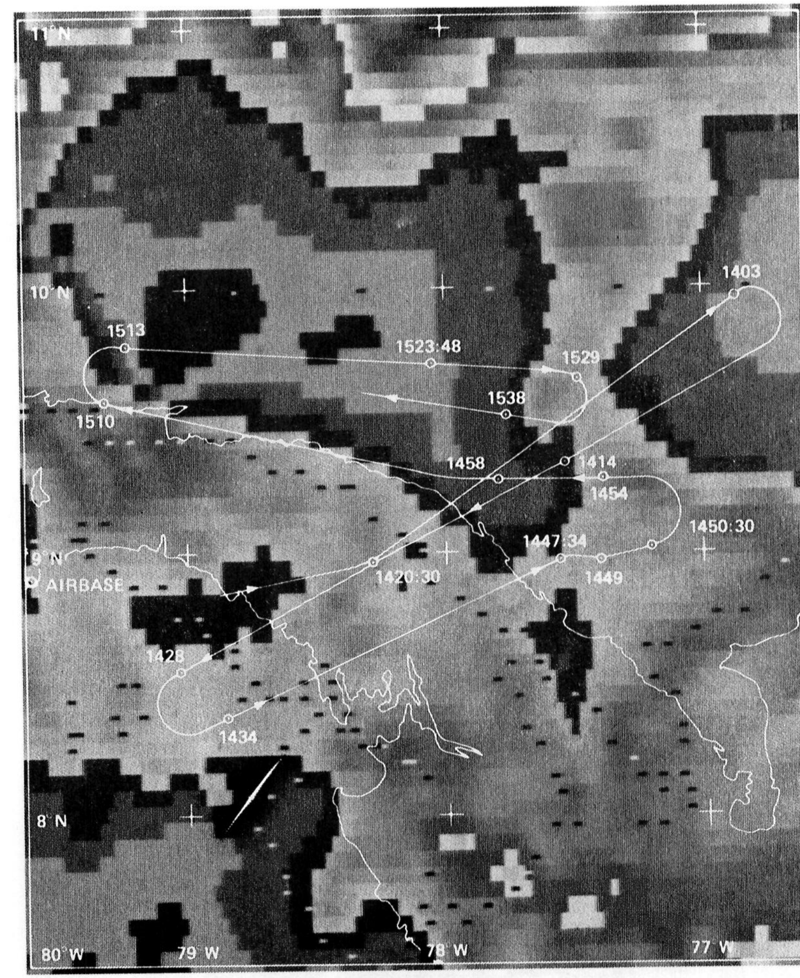

1405 UT, INFRARED

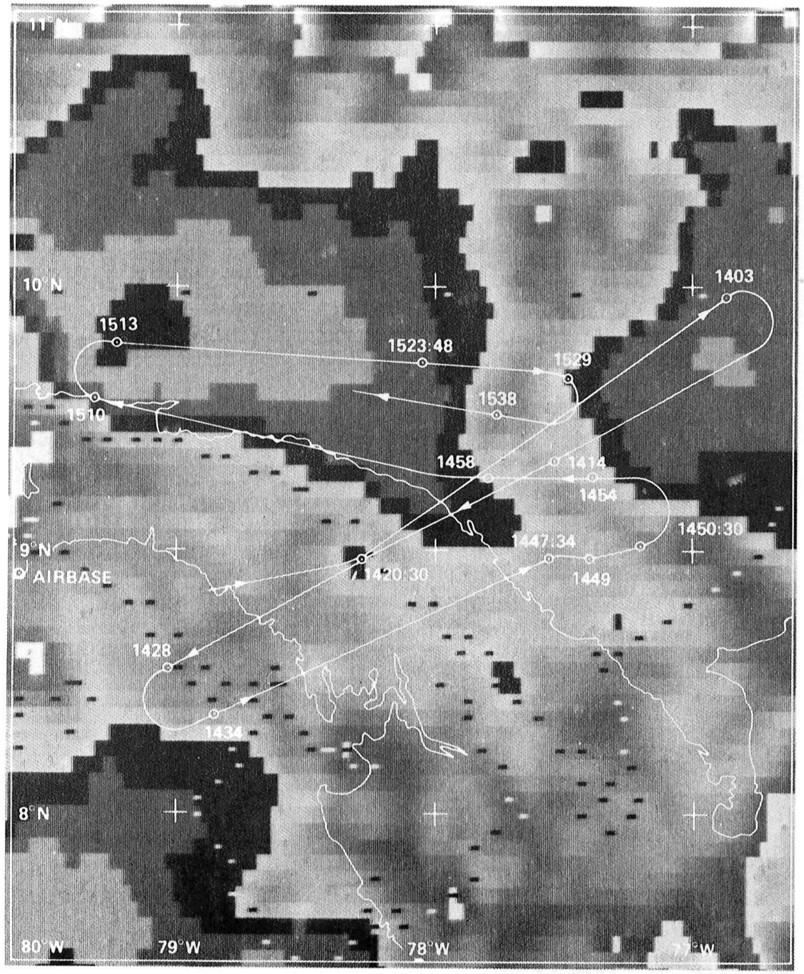

1435 UT, INFRARED

1533 UT, INFRARED

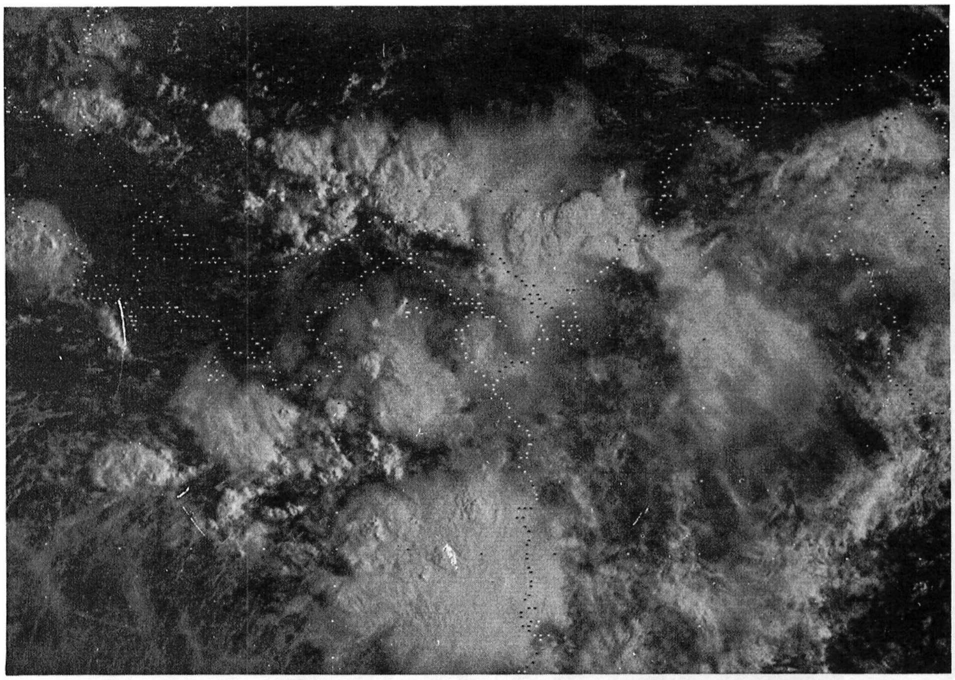

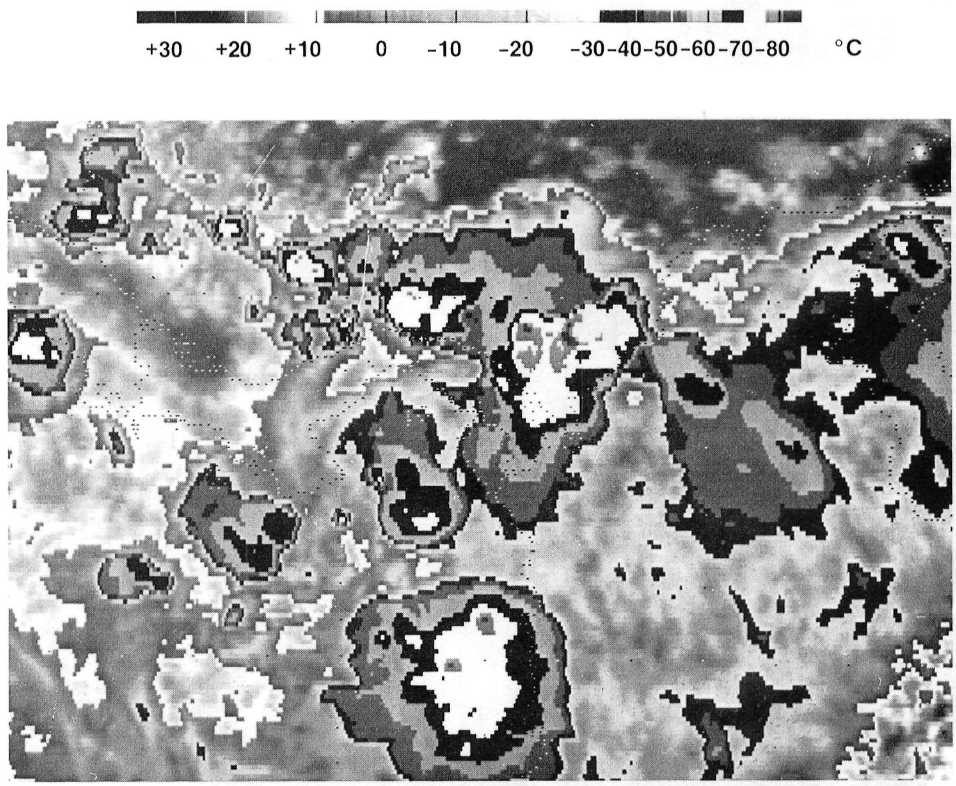

1305 UT, SEPT 9 1980

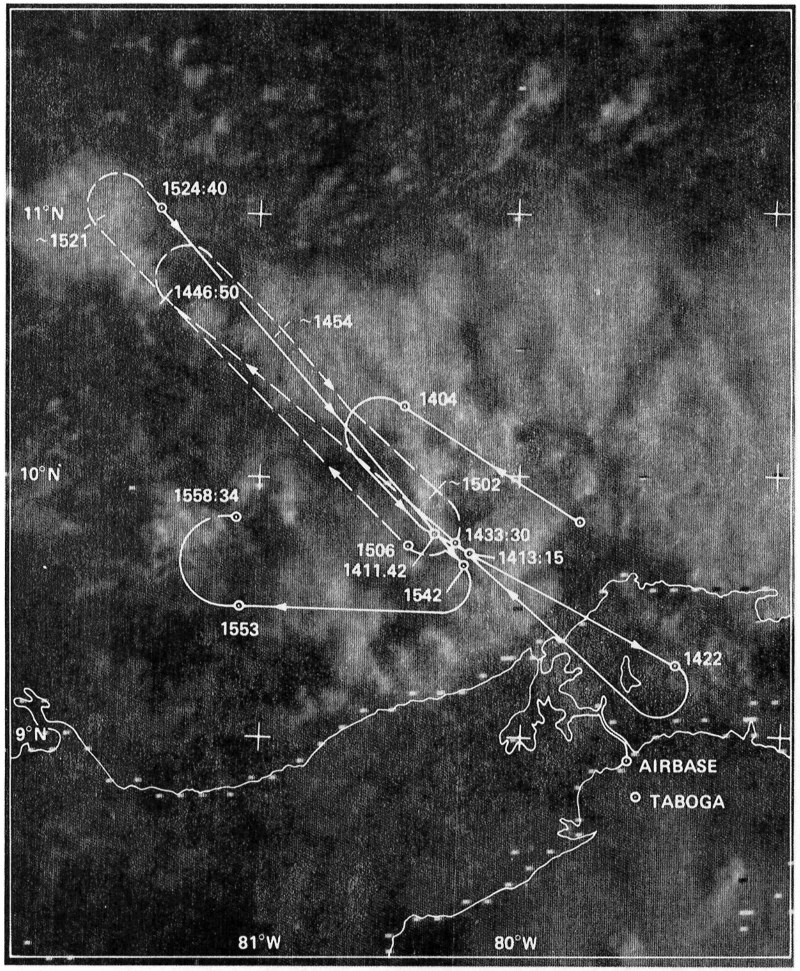

1301 UT, VISIBLE

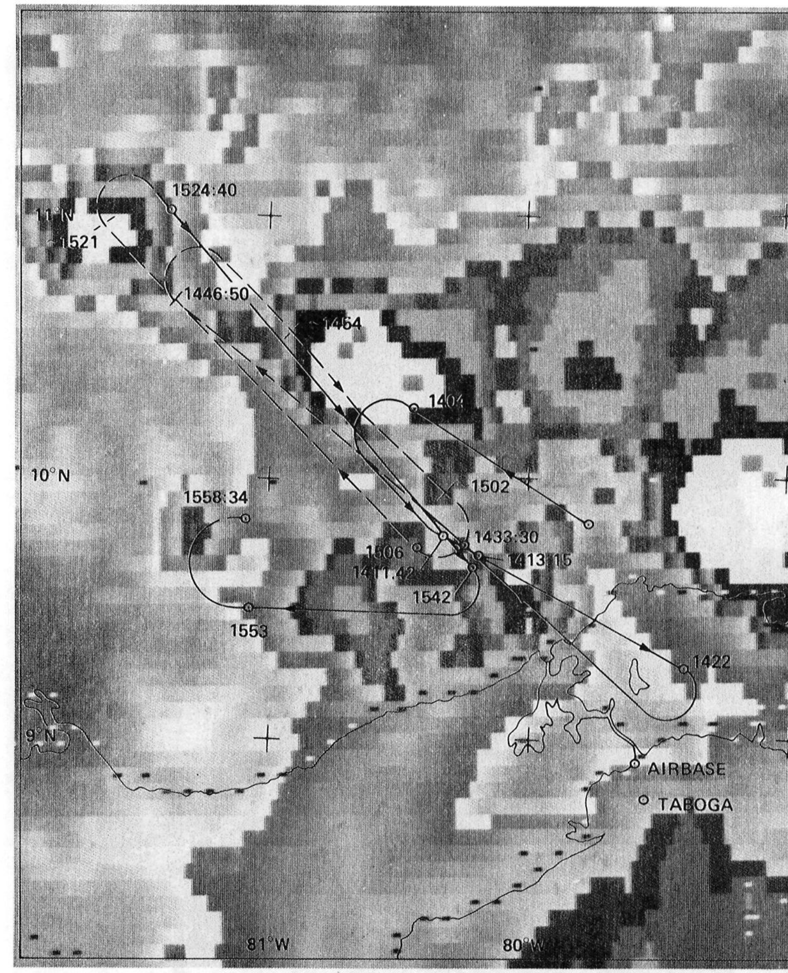

1305 UT, INFRARED

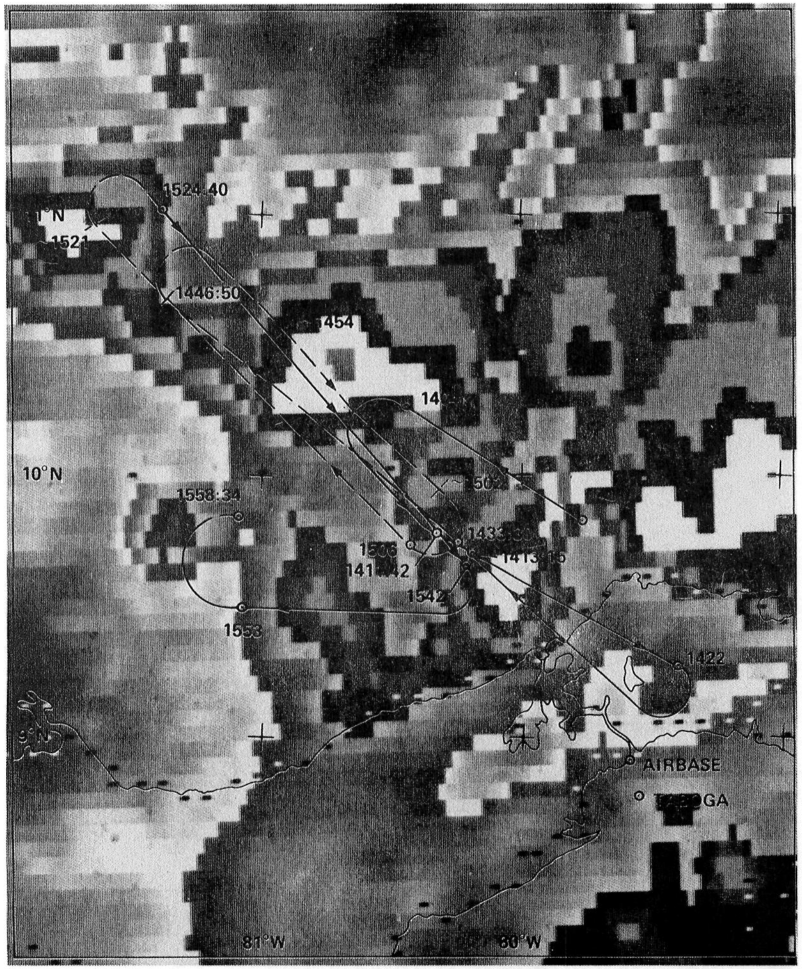

1333 UT, INFRARED

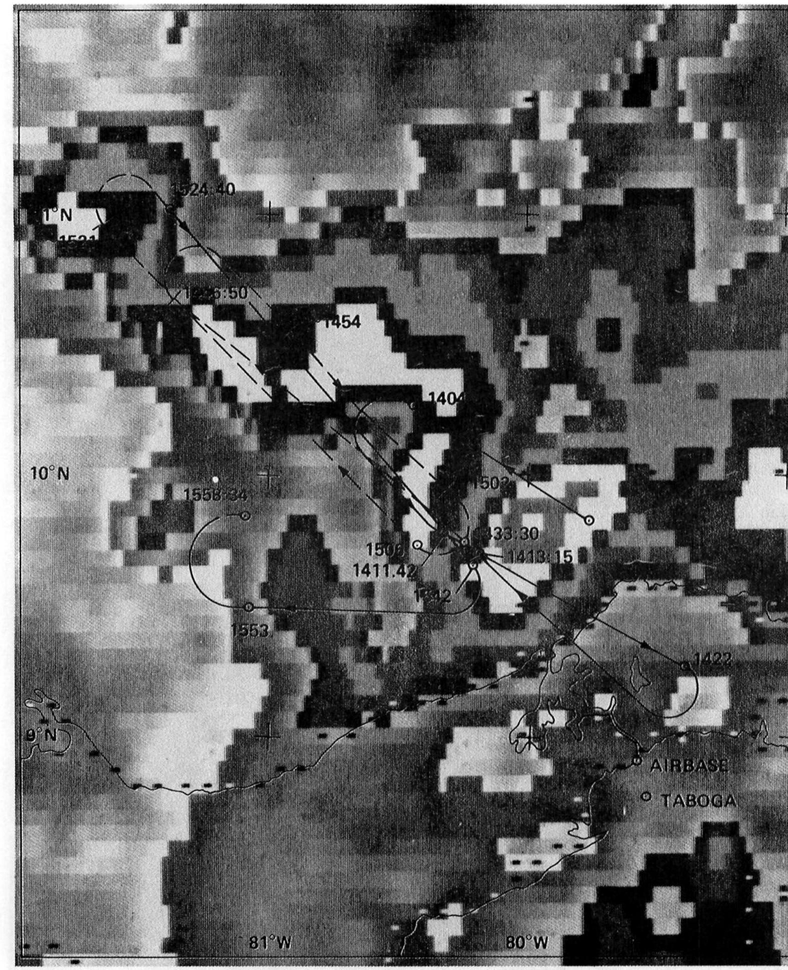

1405 UT, INFRARED

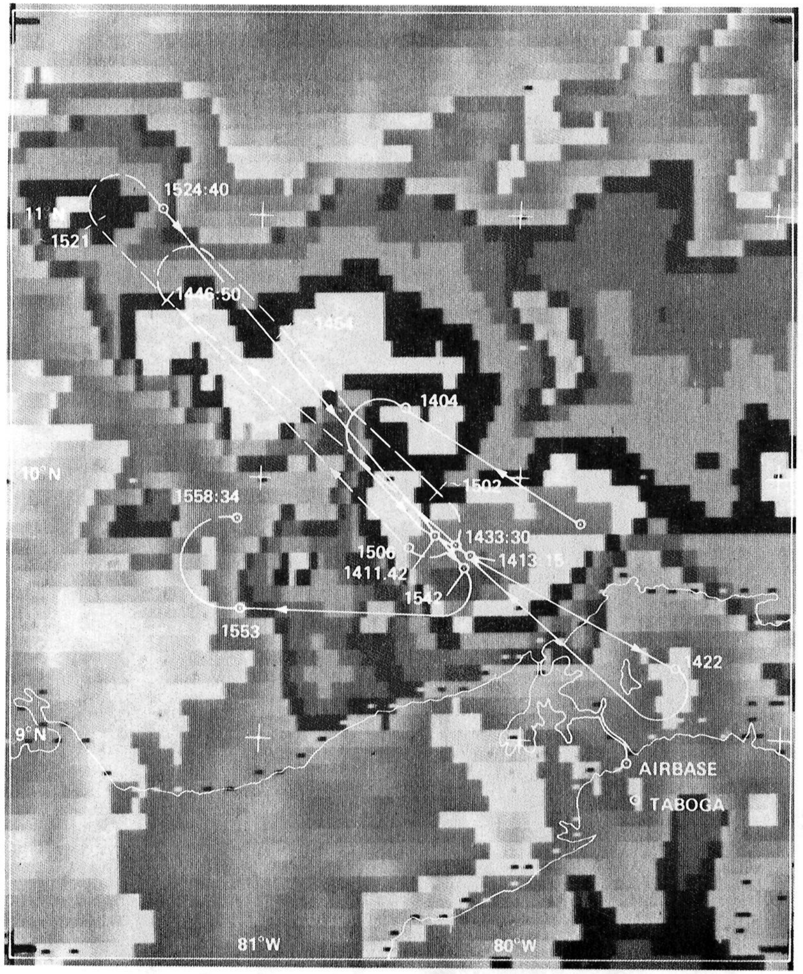

1435 UT, INFRARED

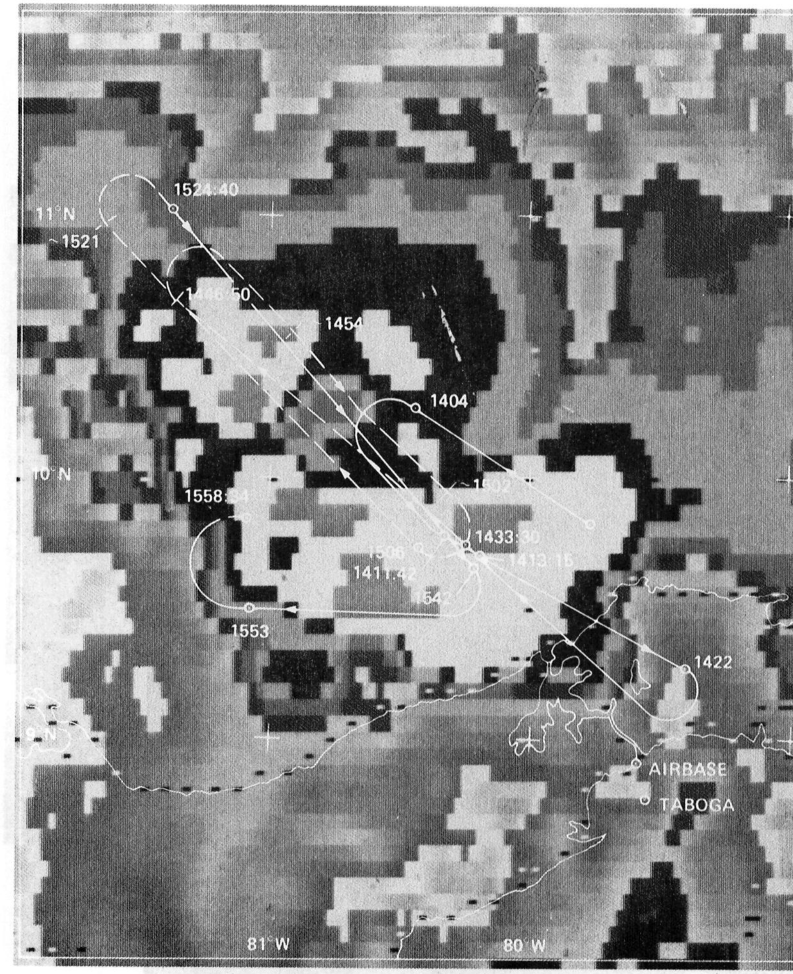

1533 UT, INFRARED

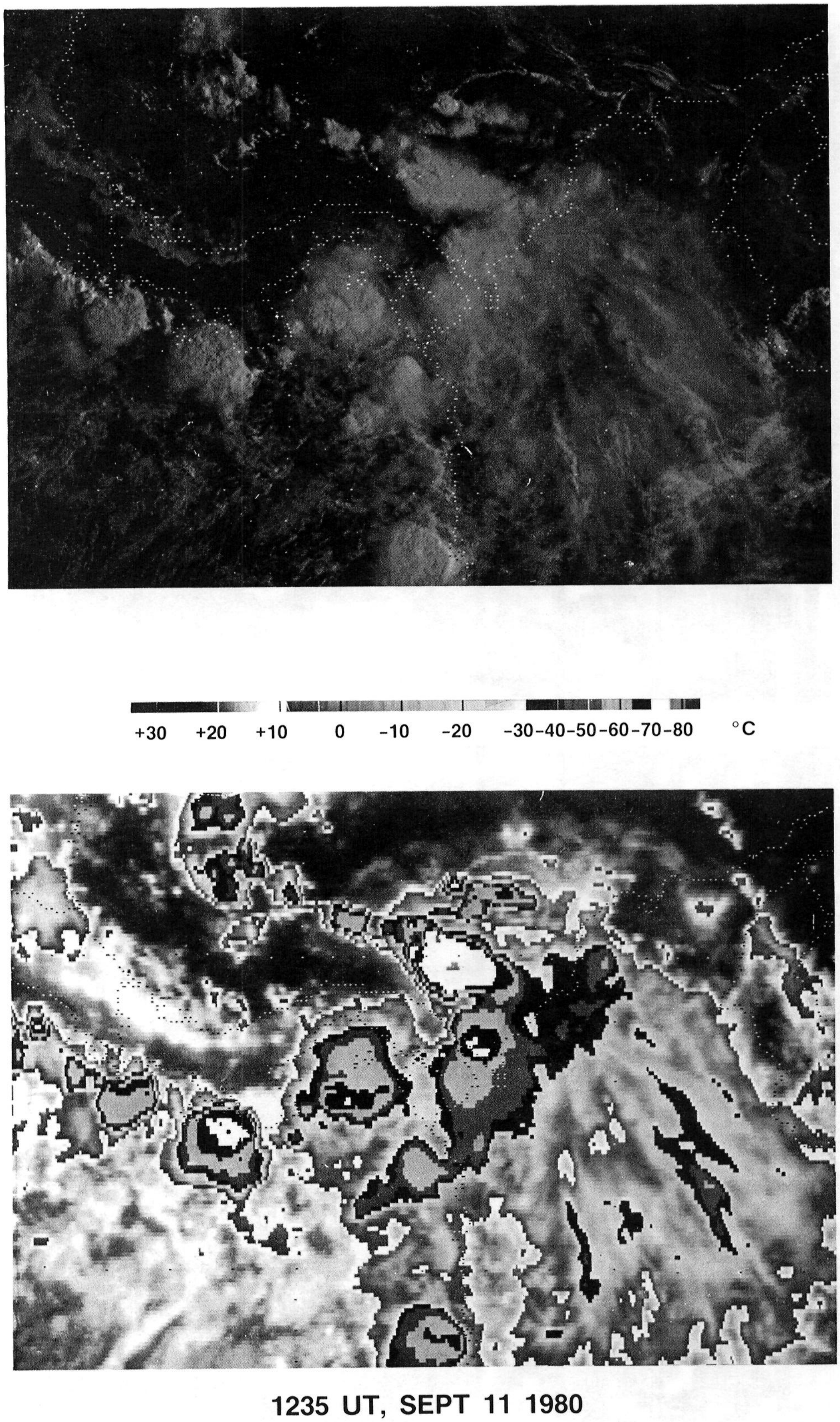

1235 UT, SEPT 11 1980

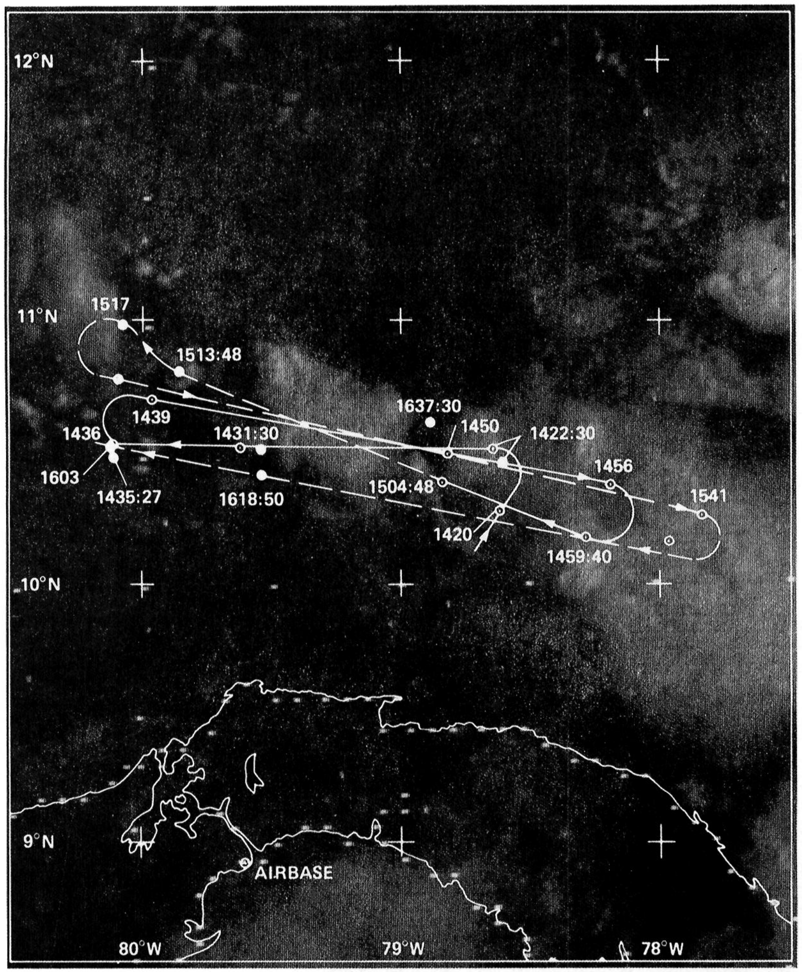

1231 UT, VISIBLE

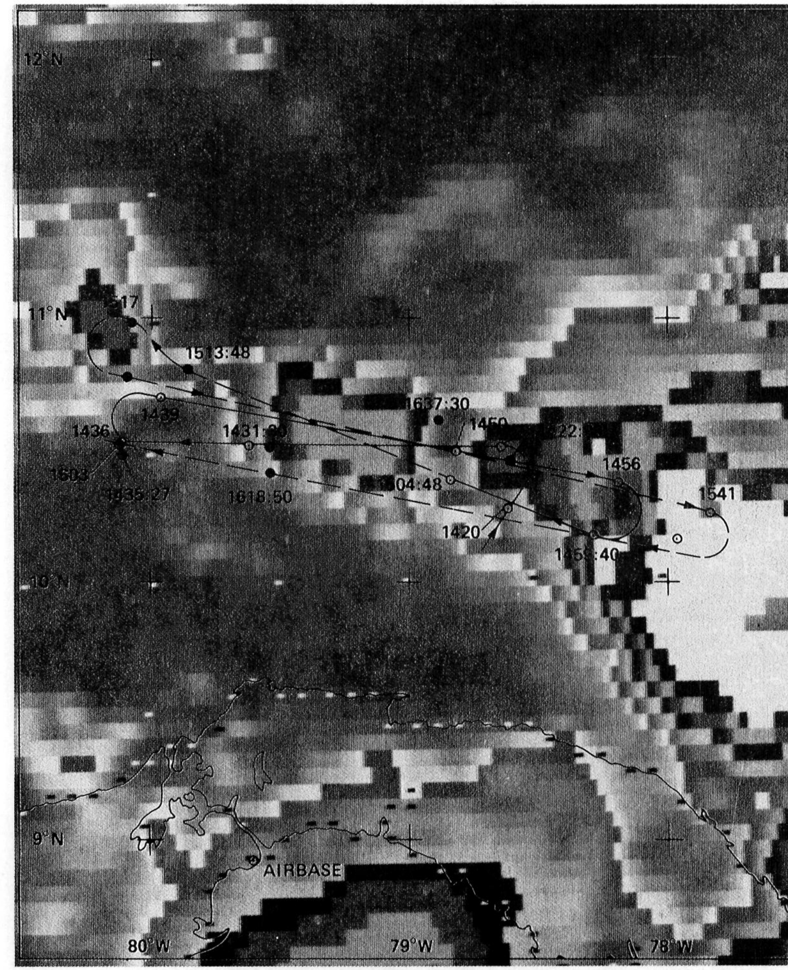

1235 UT, INFRARED

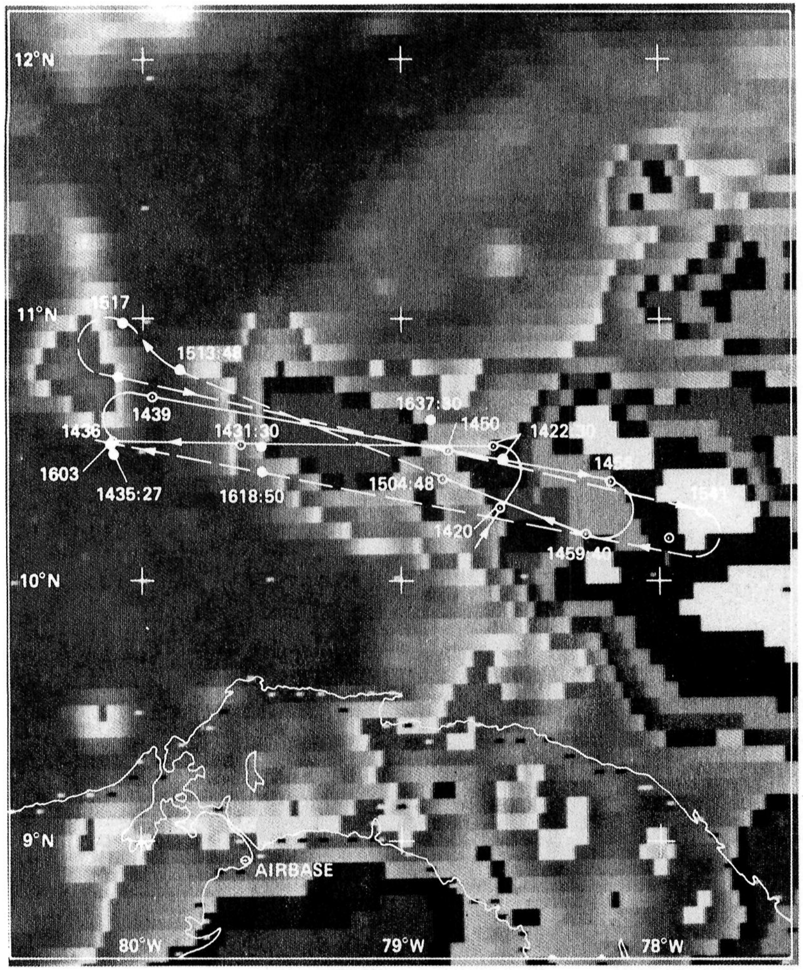

1333 UT, INFRARED

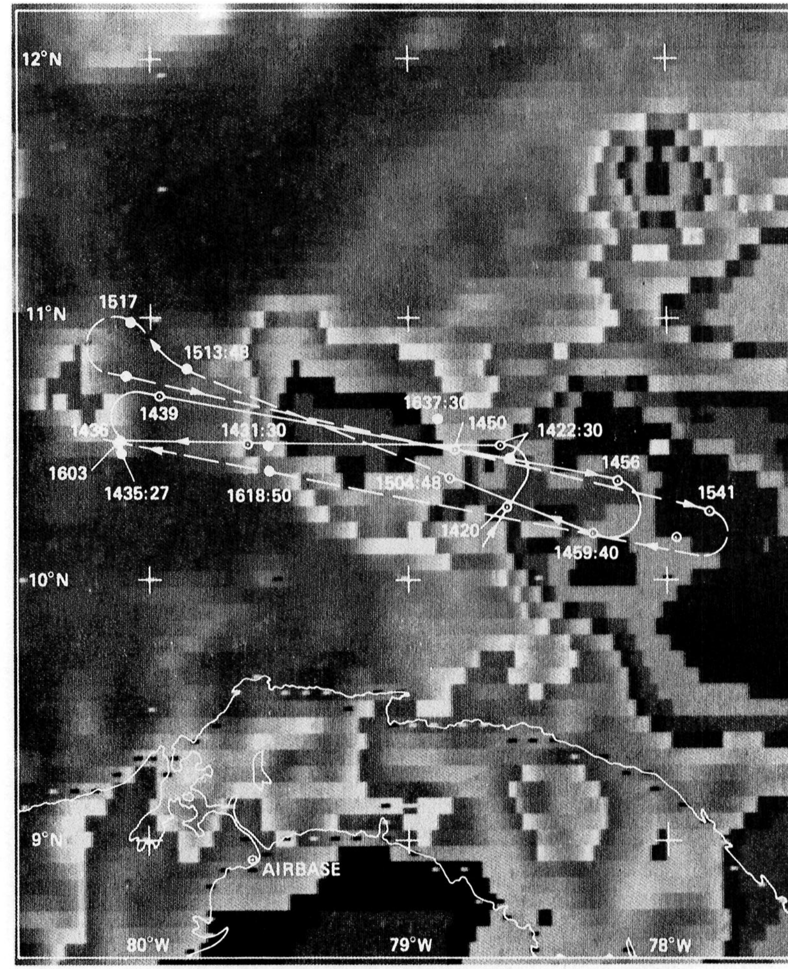

1405 UT, INFRARED

1435 UT, INFRARED

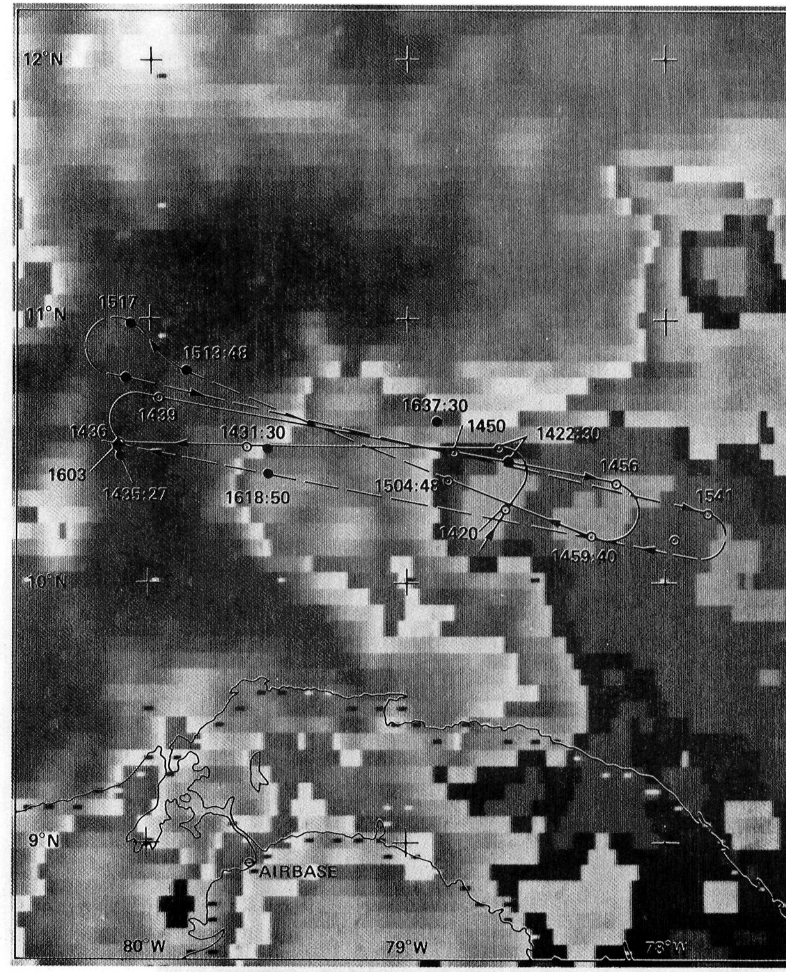

1604 UT, INFRARED

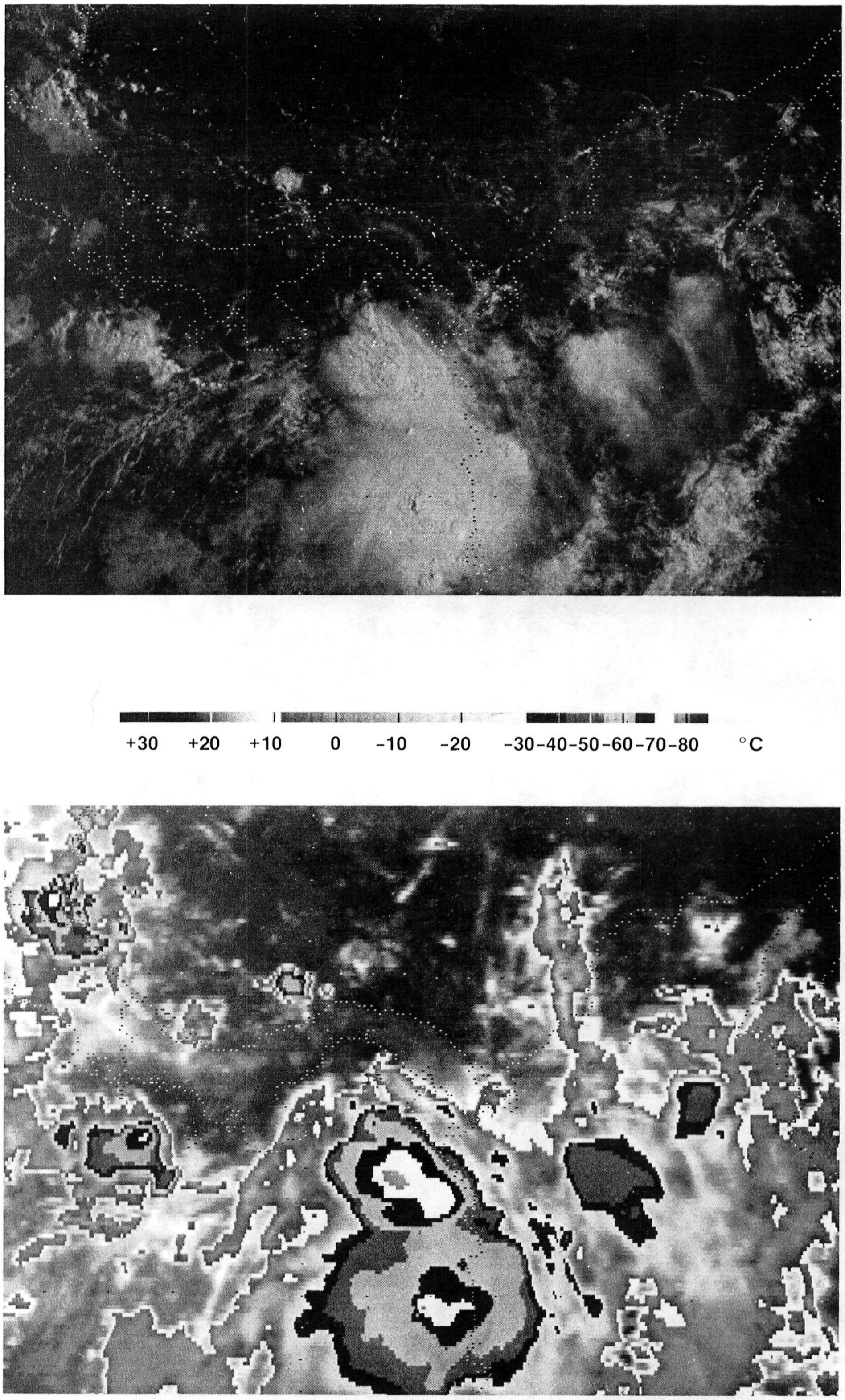

1305 UT, SEPT 12 1980

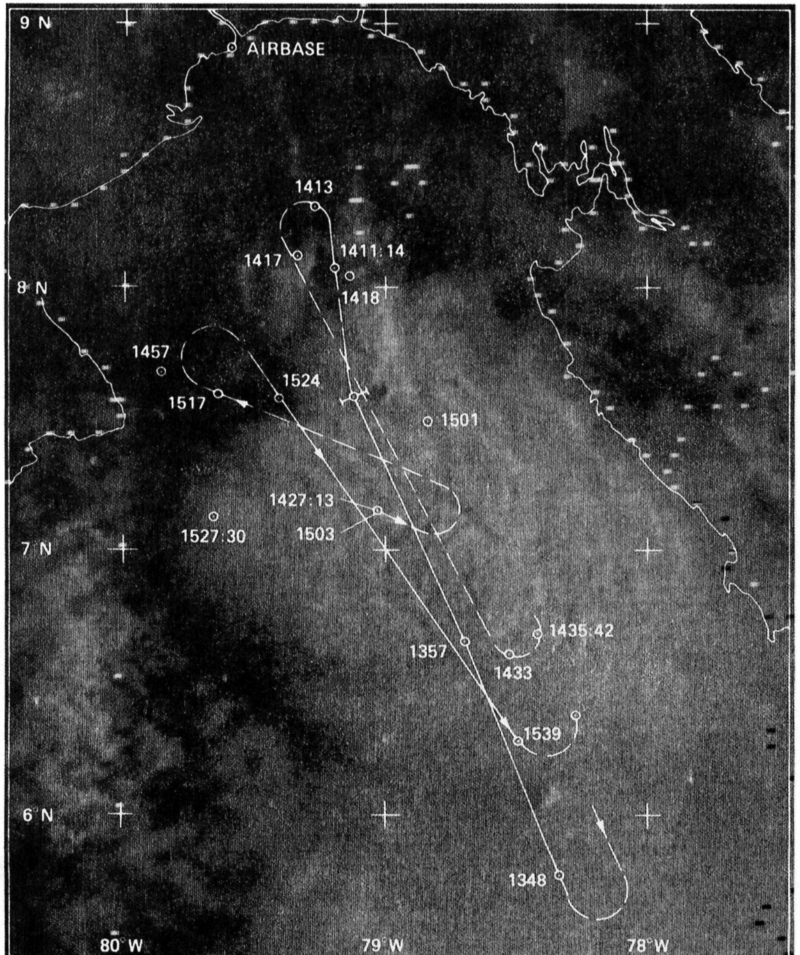

1300 UT, VISIBLE

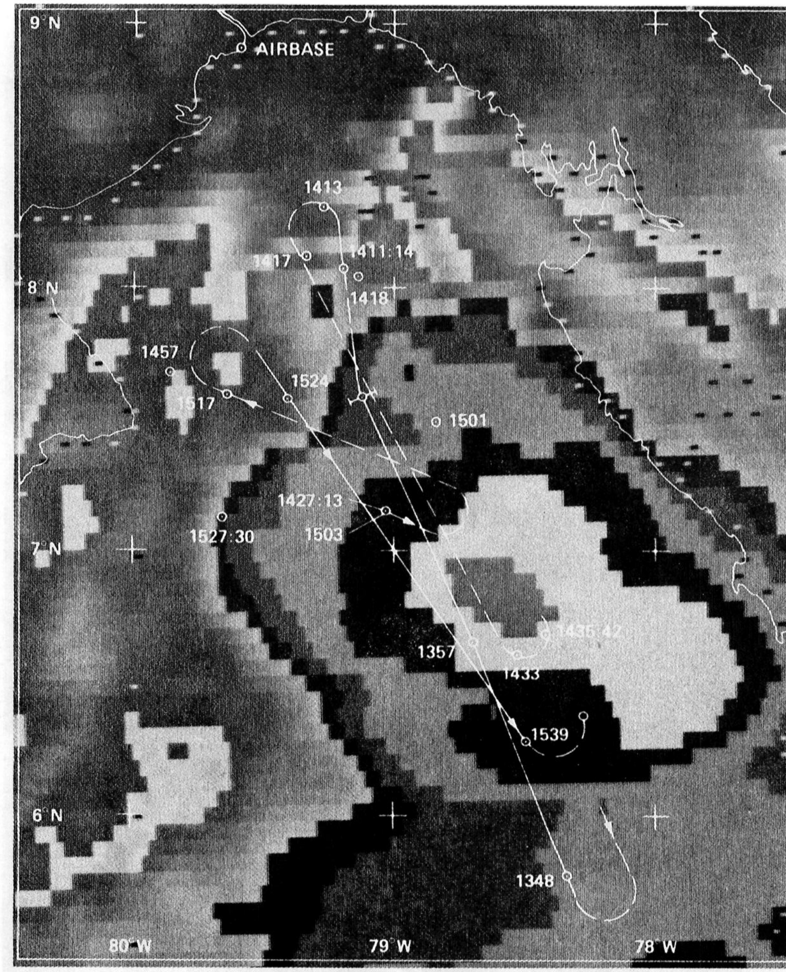

1305 UT, INFRARED

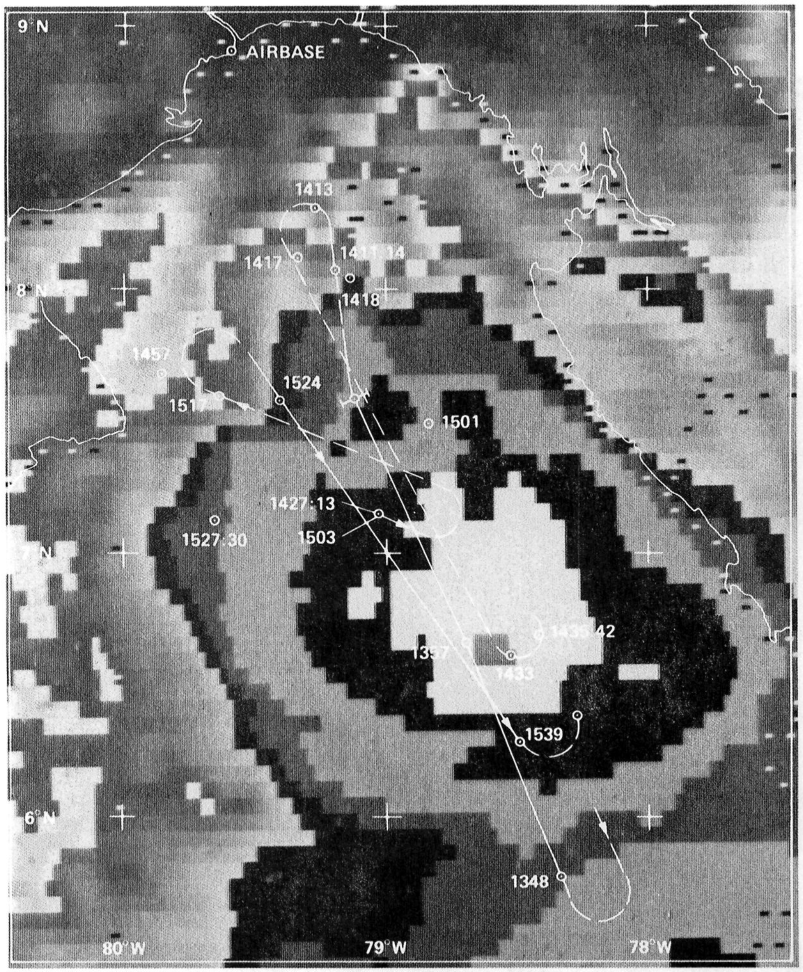

1333 UT, INFRARED

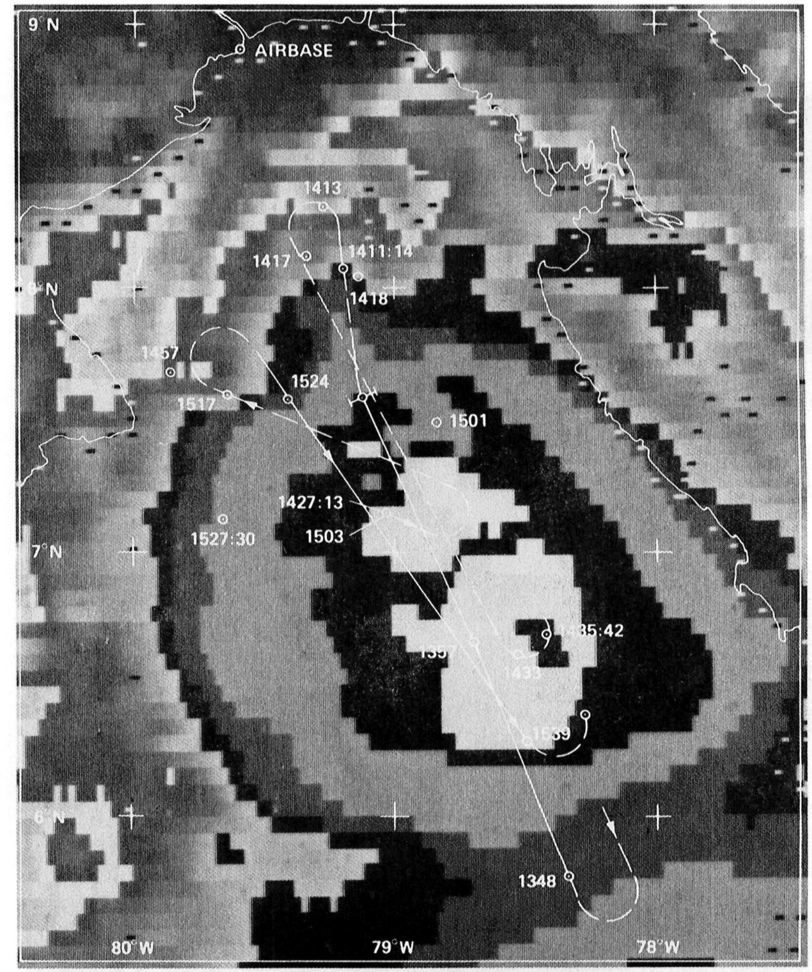

1405 UT, INFRARED

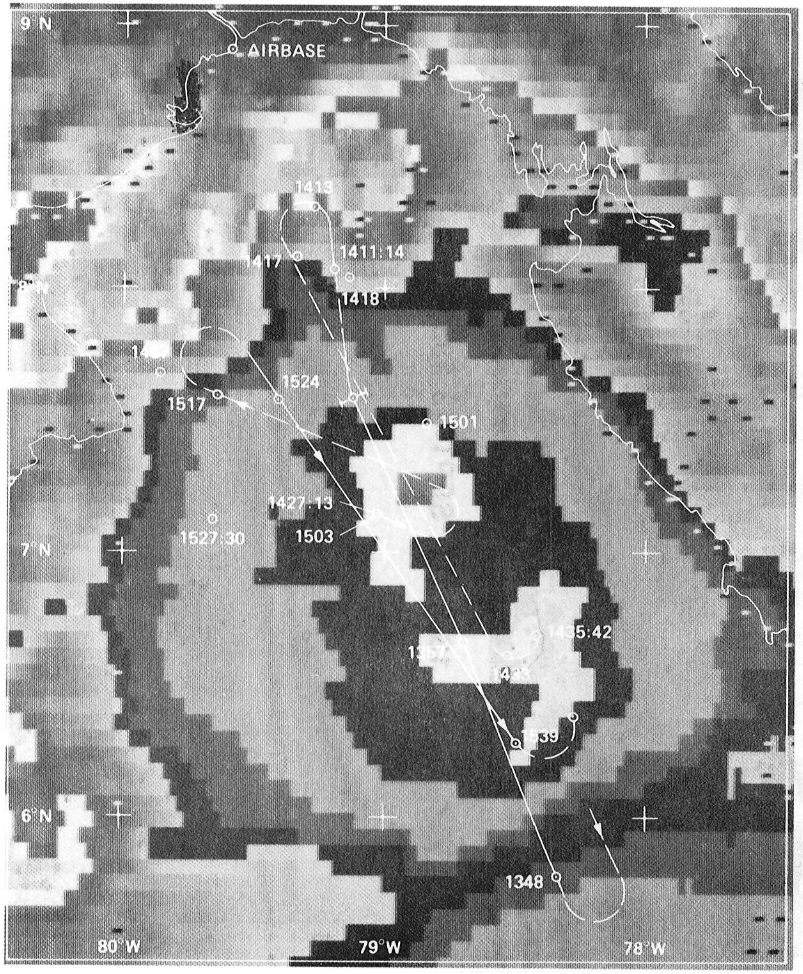

1435 UT, INFRARED

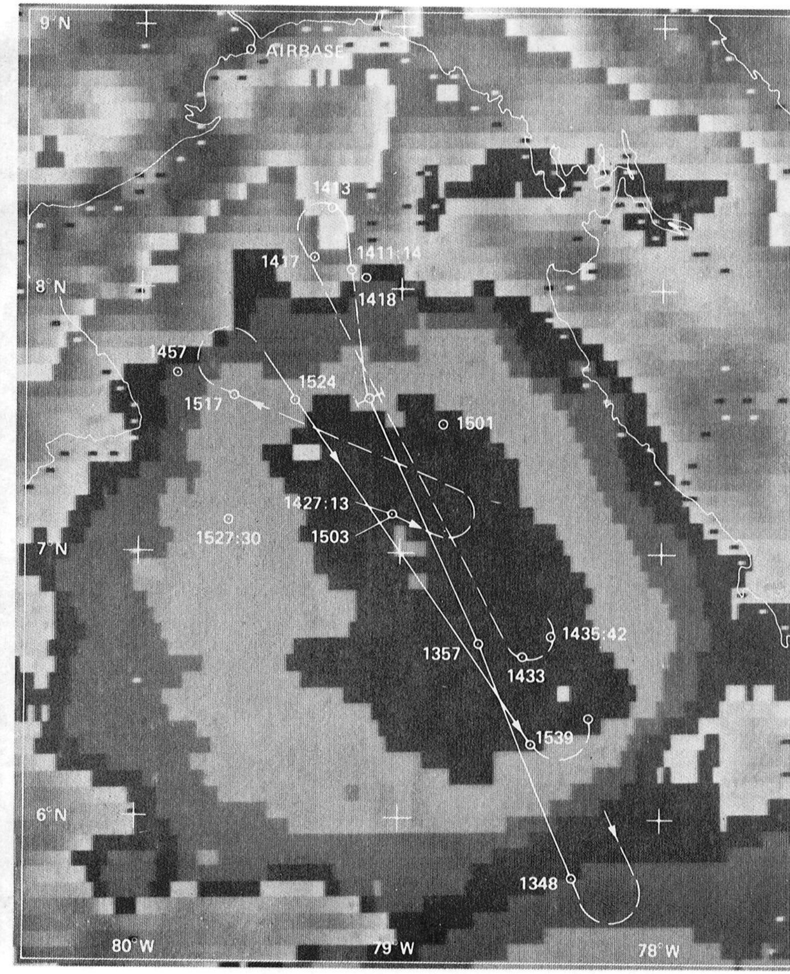

1533 UT, INFRARED

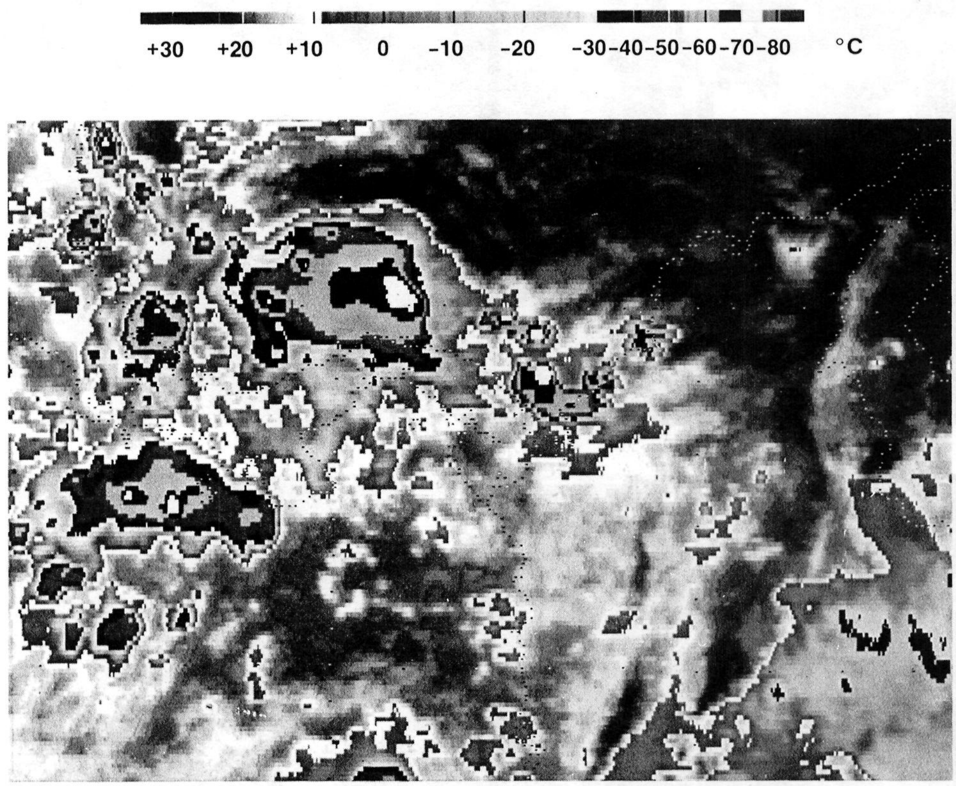

1305 UT, SEPT 13 1980

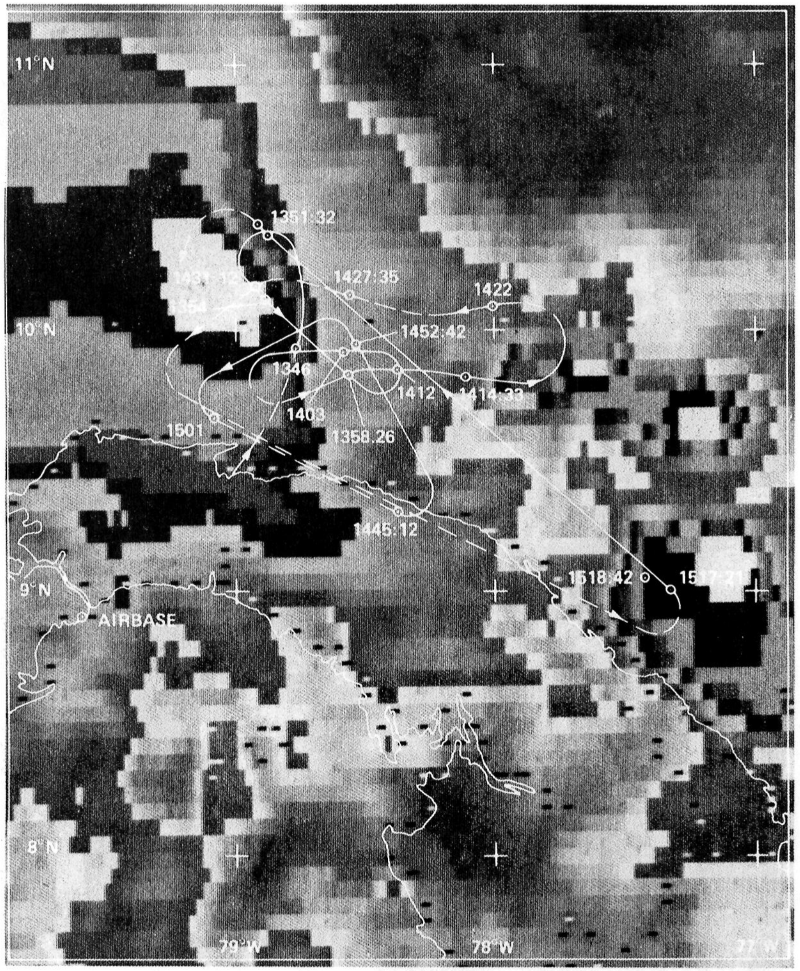

1305 UT, INFRARED

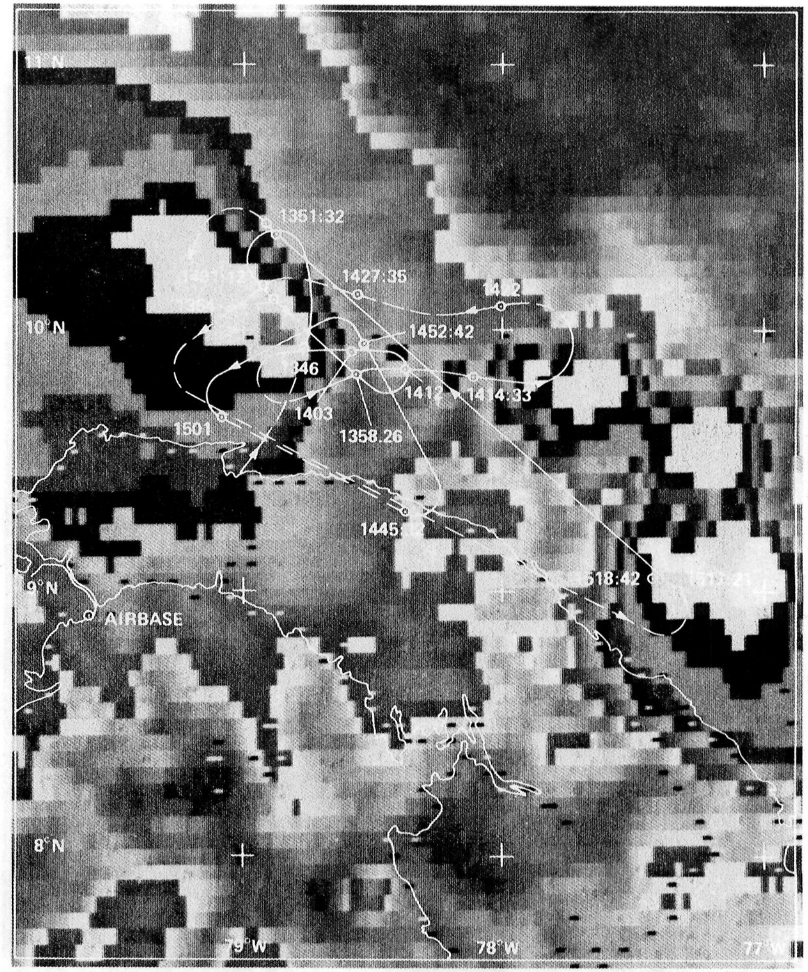

1333 UT, INFRARED

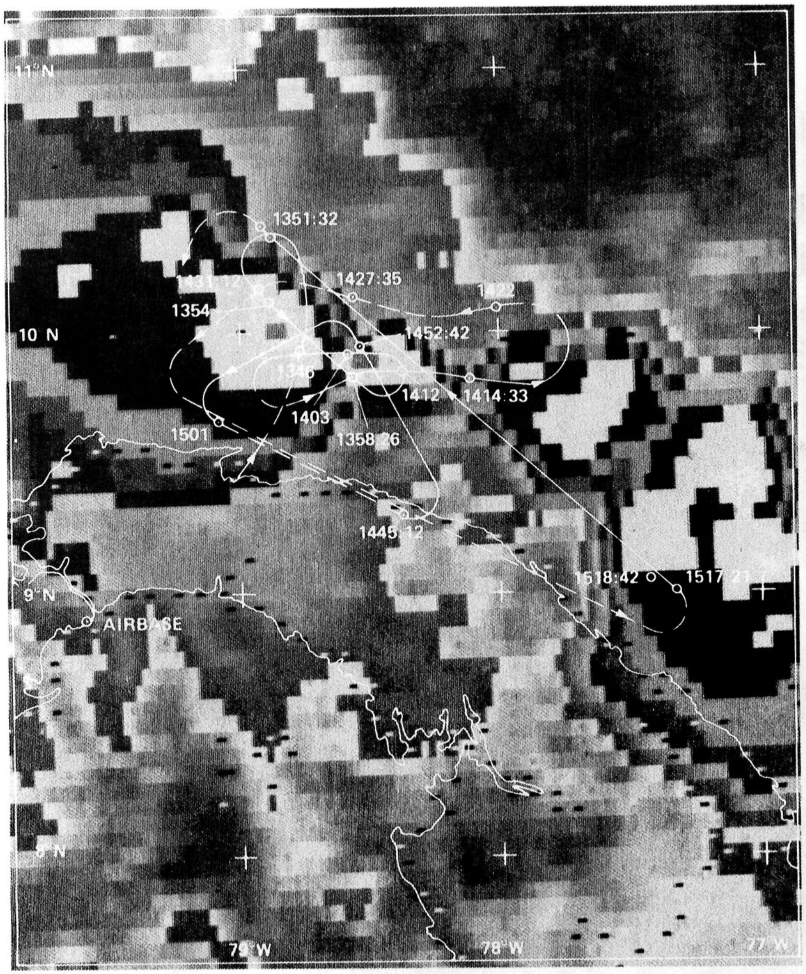

1405 UT, INFRARED

1435 UT, INFRARED

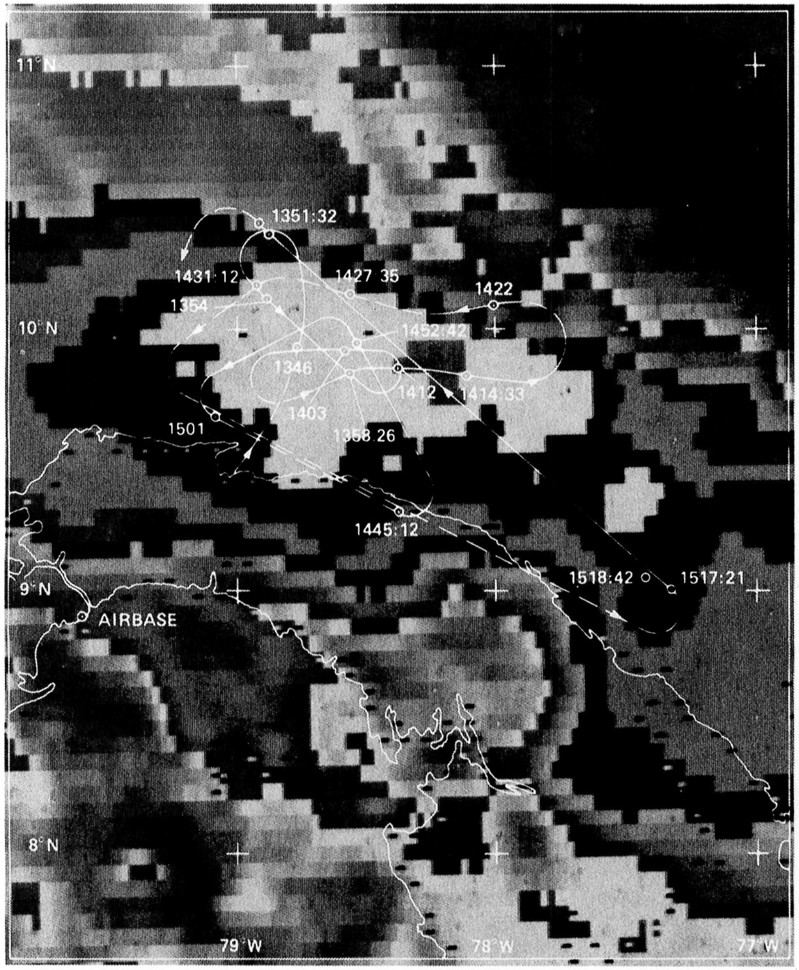

1533 UT, INFRARED

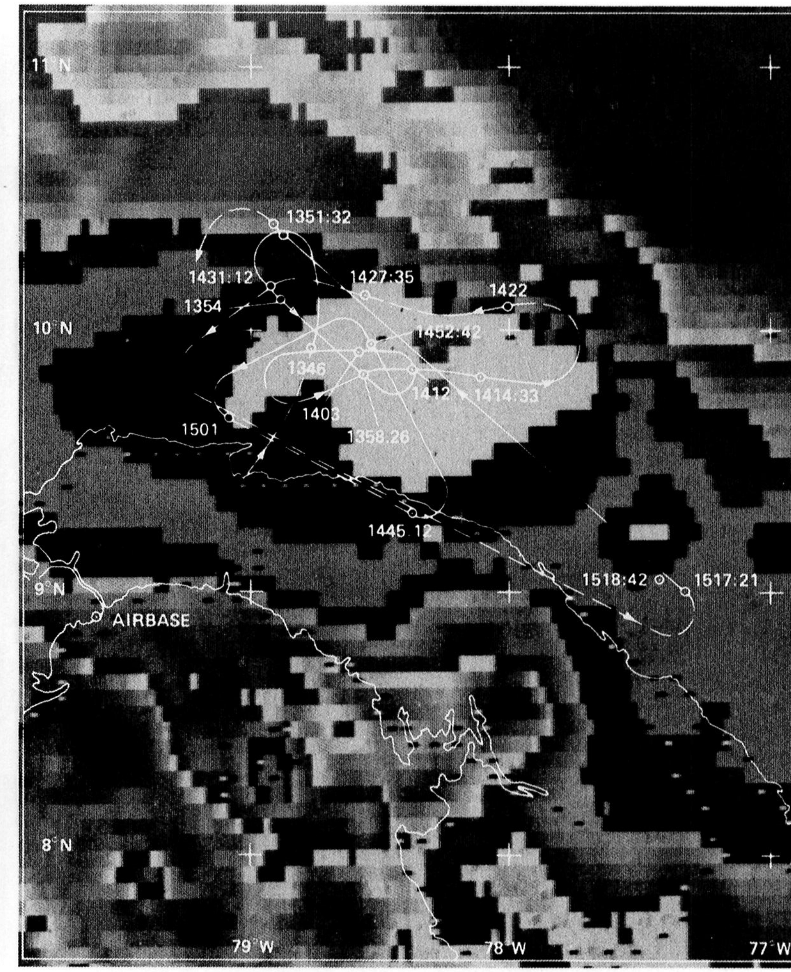

1605 UT, INFRARED

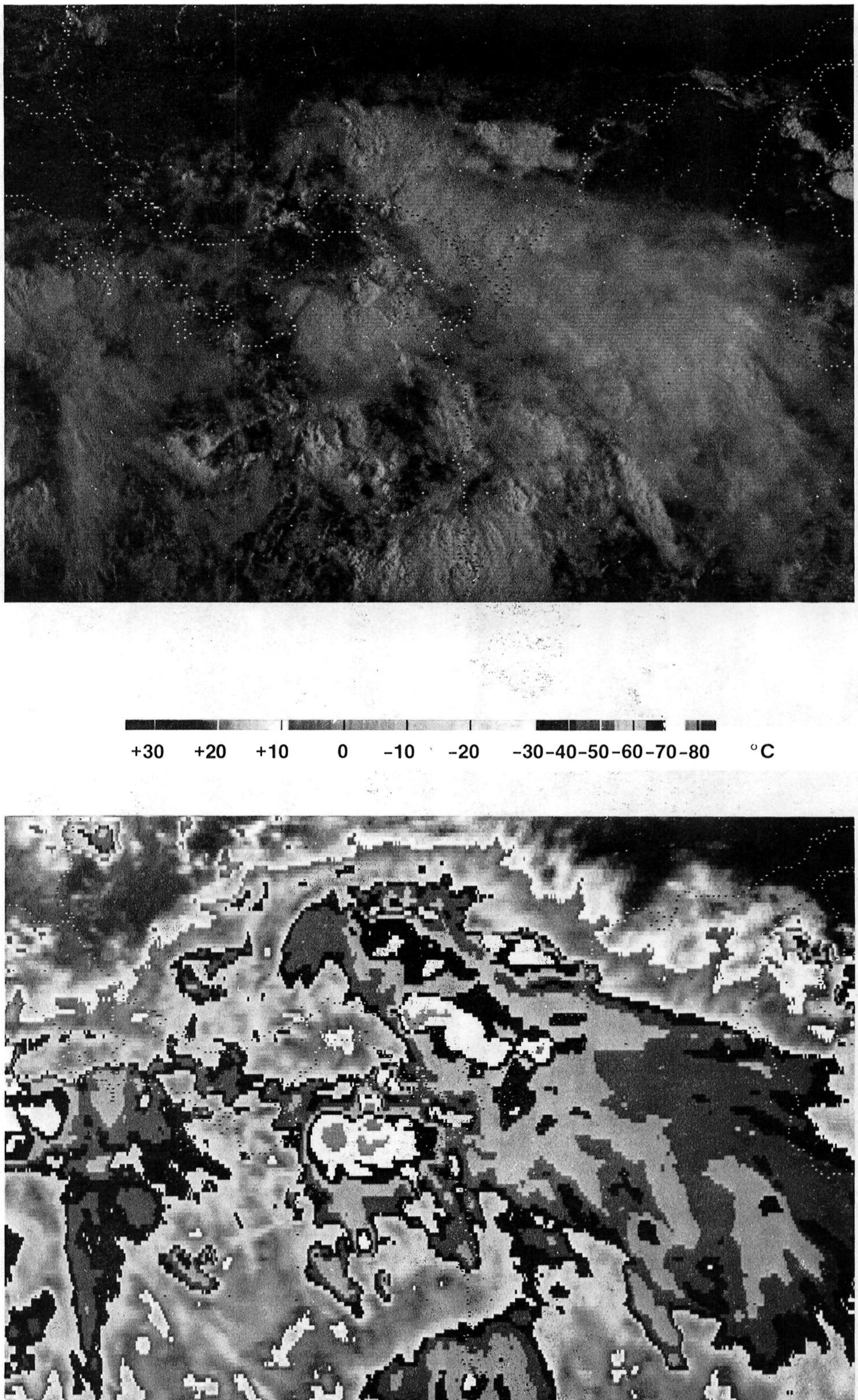

1305 UT, SEPT 15 1980

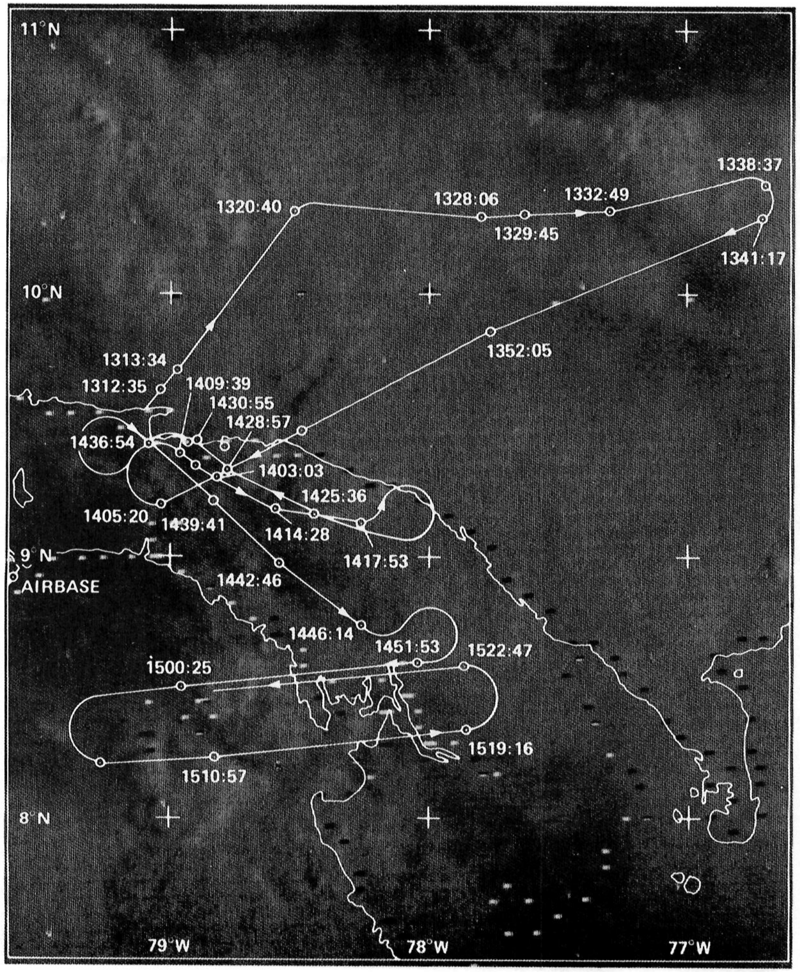

1303 UT, VISIBLE

1305 UT, INFRARED

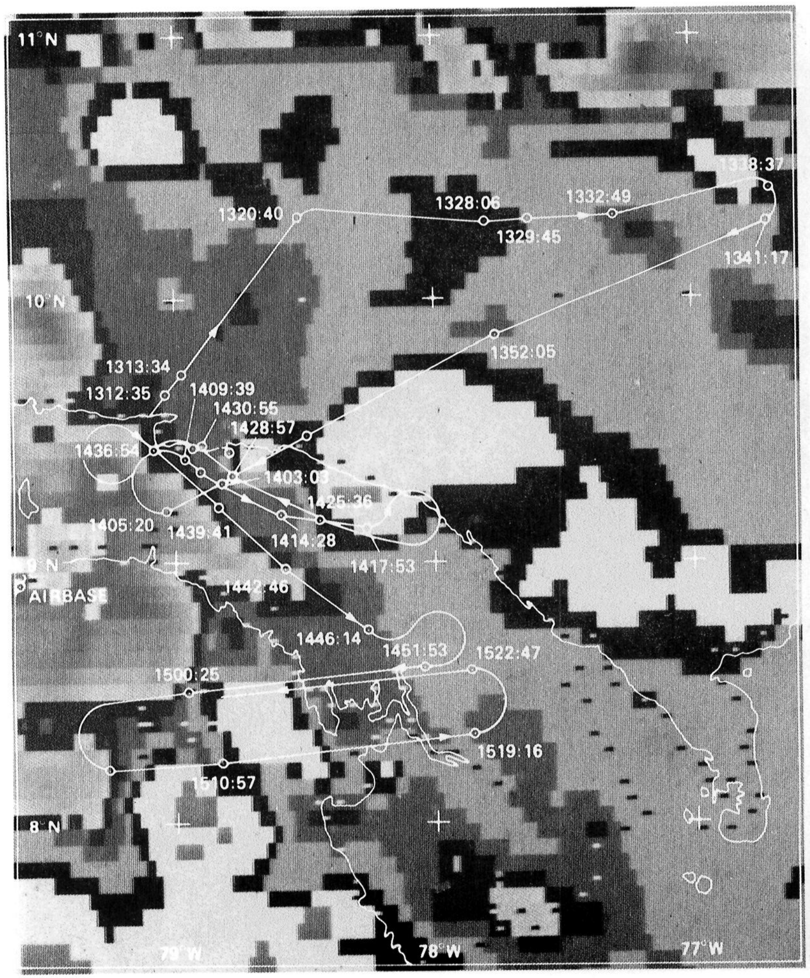

1333 UT, INFRARED

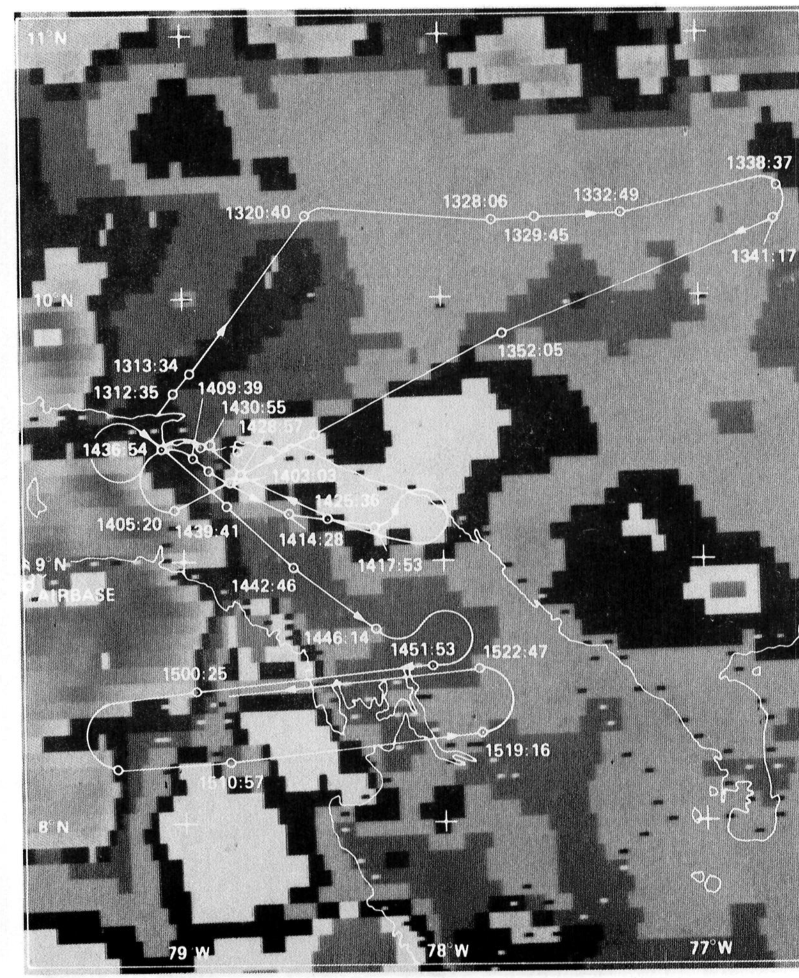

1405 UT, INFRARED

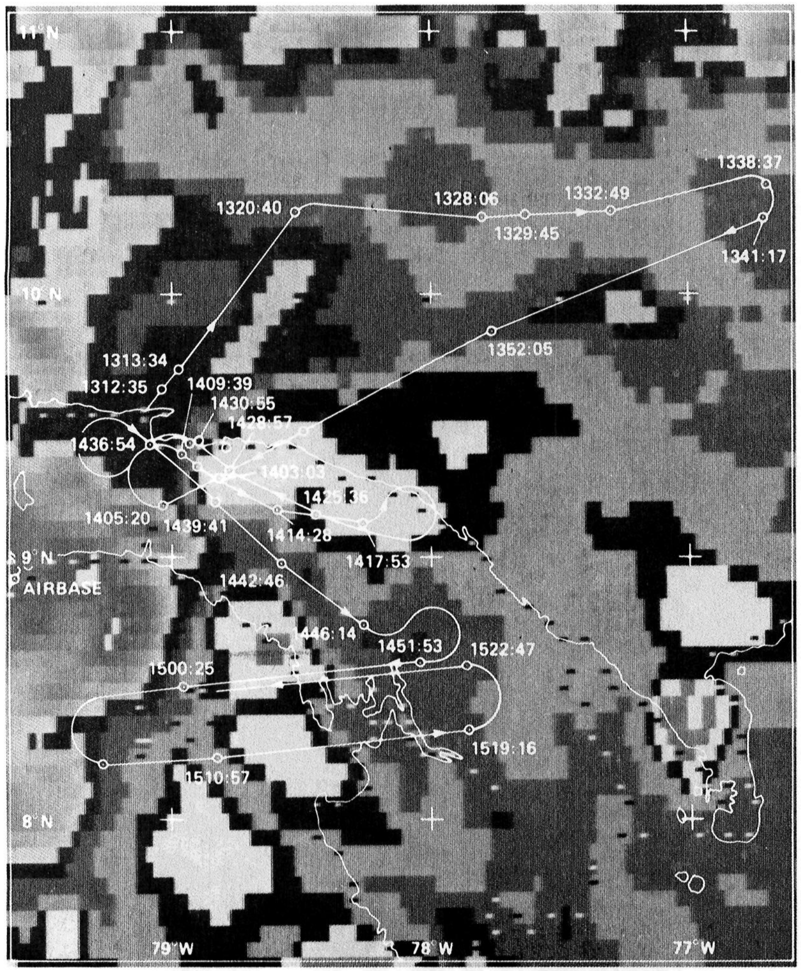

1435 UT, INFRARED

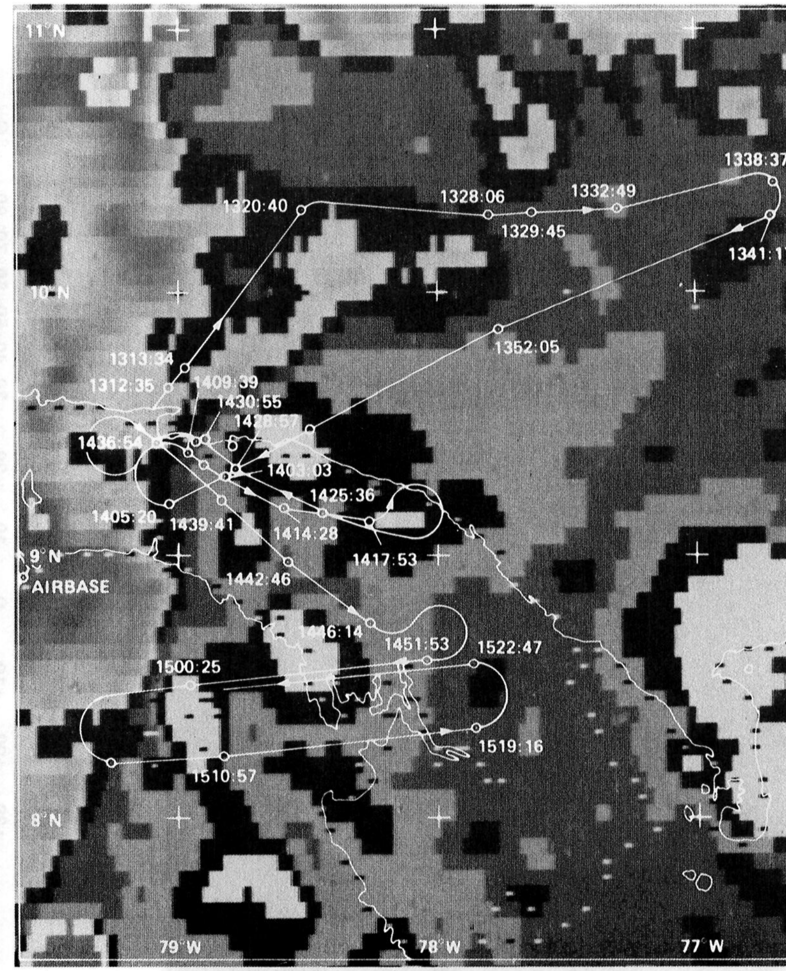

1533 UT, INFRARED

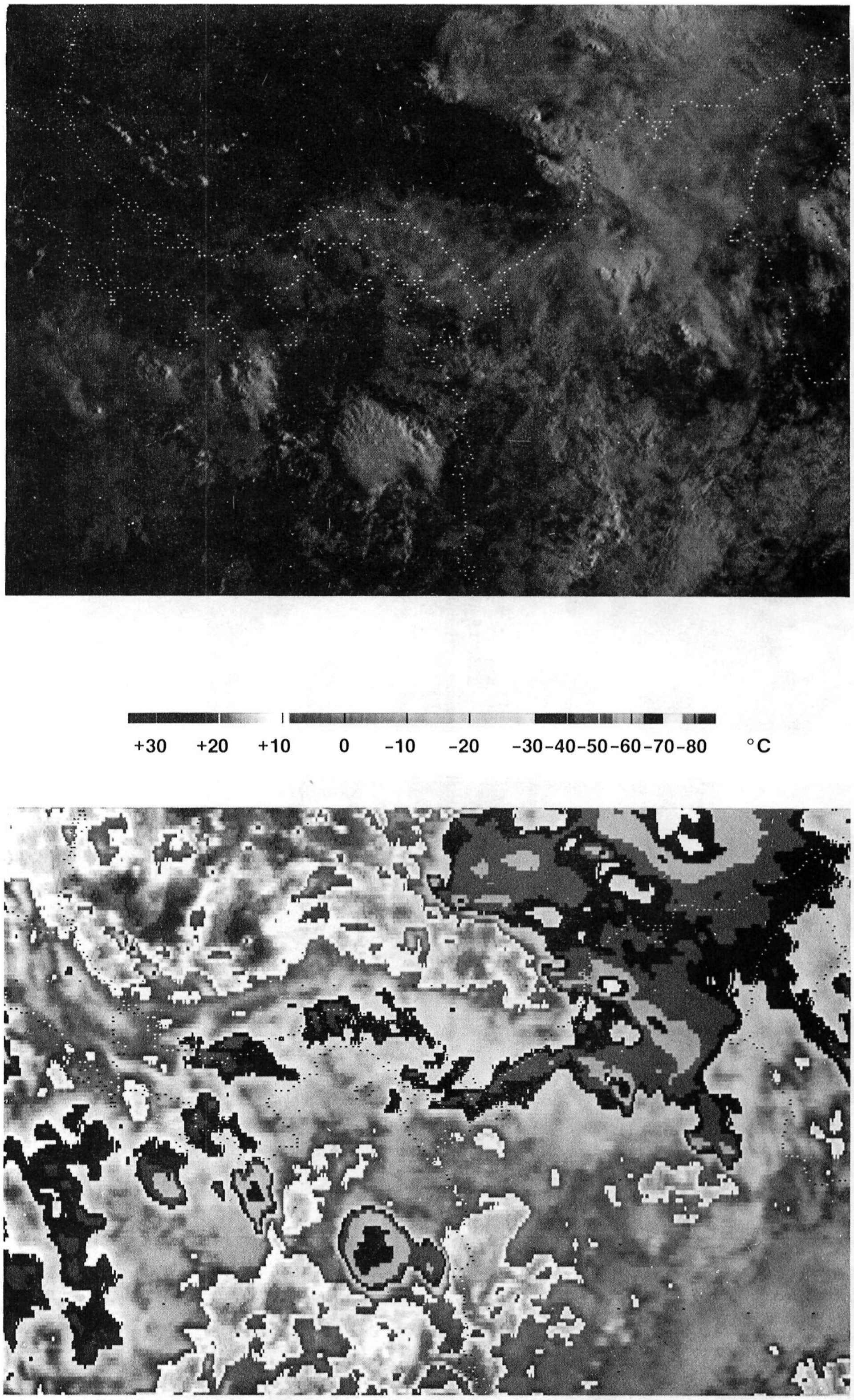

1235 UT, SEPT 16 1980

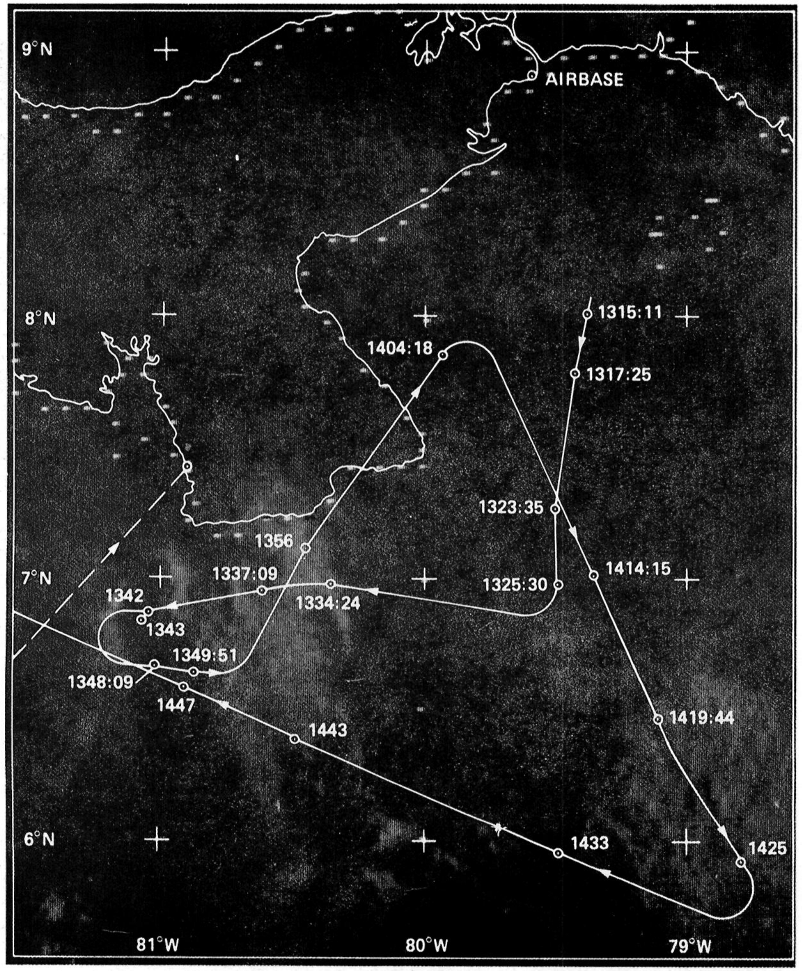

1231 UT, VISIBLE

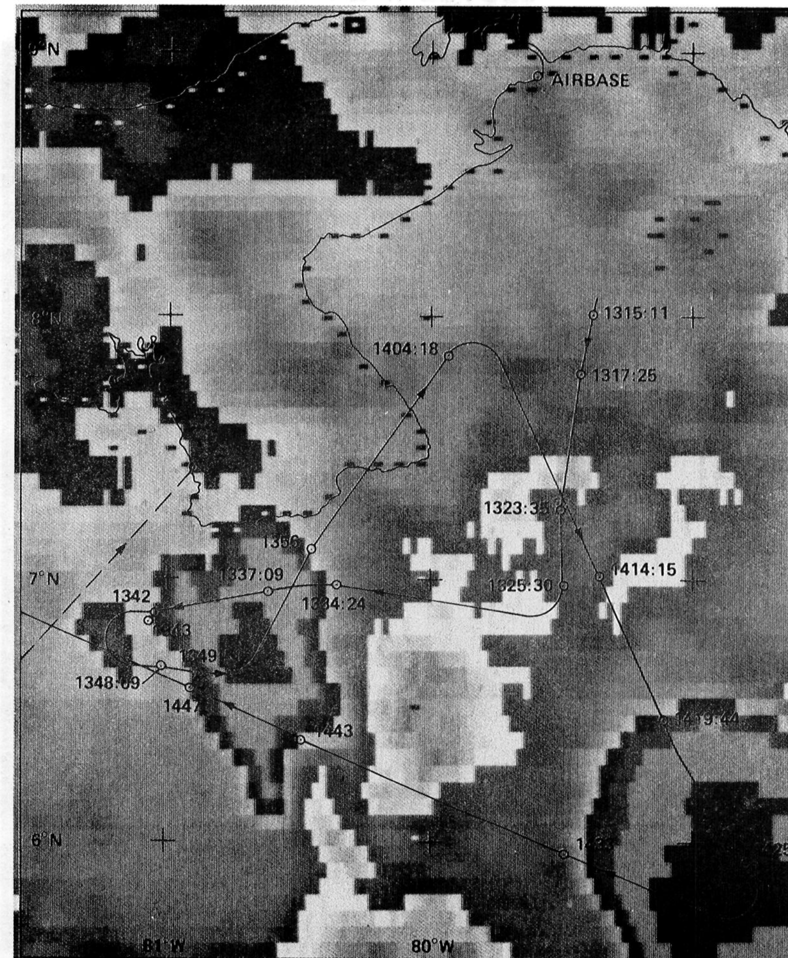

1235 UT, INFRARED

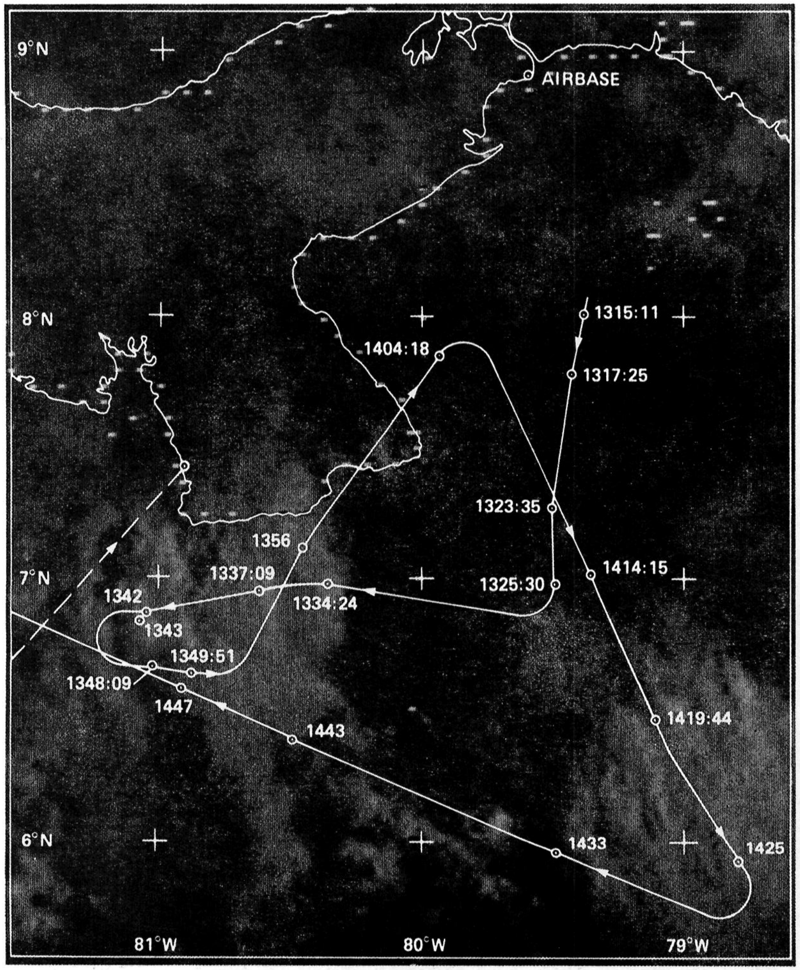

1307 UT, VISIBLE

1533 UT, INFRARED

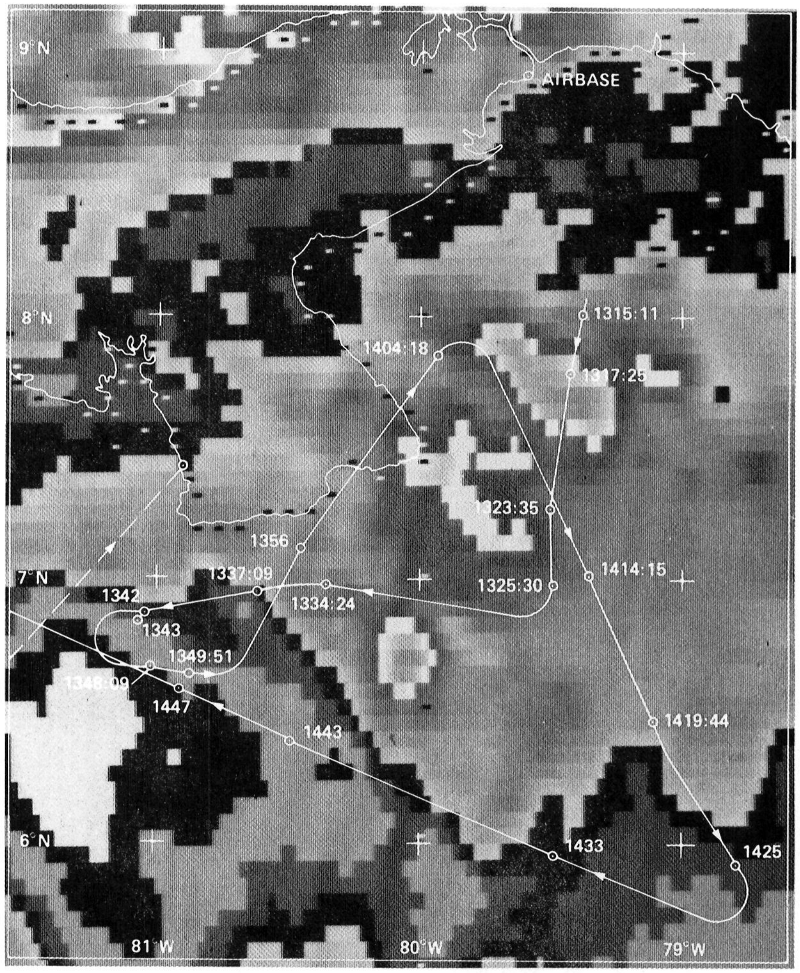

1602 UT, INFRARED

APPENDIX B

BALLOON-BORNE ECC OZONESONDE DATA

Christopher A. Riegel* and David F. Matson*

In the figure on the right in each ozonagram the solid line represents air temperature; the dashed line is the dew-point temperature (with respect to water). Wind speed is in knots, and the wind direction is the direction from which the wind blows. The usual convention has been used for the wind barbs:

o calm

1-2 knots

3-7 knots

8-12 knots

47-52 knots

(A wind from the west at 33 knots appears as).

The data in the tables (from which the figures were drawn) were supplied by the Wallops Flight Center, NASA, Wallops Island, Virginia.

*Department of Meteorology, San Jose State U., San Jose, California.

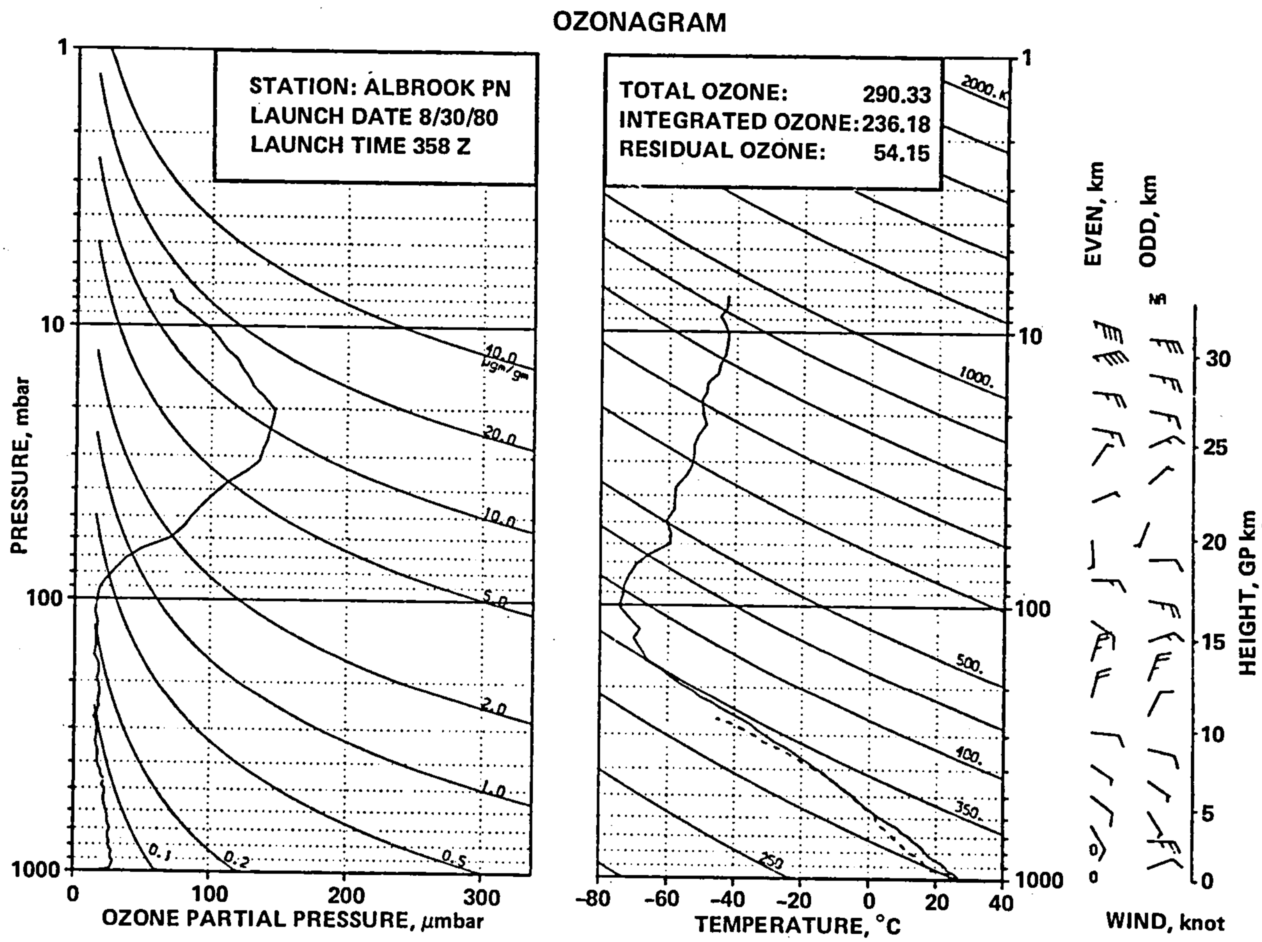

OZONAGRAM
STATION: ALBROOK PN
LAUNCH DATE 8/30/80
LAUNCH TIME 358 Z
TOTAL OZONE: 290.33
INTEGRATED OZONE: 236.18
RESIDUAL OZONE: 54.15
PRESSURE, mbar
OZONE PARTIAL PRESSURE, μmbar
TEMPERATURE, °C
WIND, knot
EVEN, km
ODD, km
HEIGHT, GP km

STATION ALBROOK PN LAUNCH DATE 8/30/80 TIME 358Z ECC SONDE 3A1309

SURFACE CONDITIONS PRESS 1005.8MB TEMP 295.9 DEG K HUMIDITY 100.0 PRCNT

TIME MIN	ALT GPM	OZONE MICMB	TOTOZ ATMCM	OZDEN MG/M3	OZMXR MICGG	PRESS MB	TEMP DEG K	PTEMP DEG K	VTEMP DEG K	HMDTY PRCNT	DEWPT DEG K	SPCFC HMDTY	SPD MPS	DIR DEG	NS MPS	EW MPS
0.0	66	14.6	0.00000	28.5	.02	1005.8	295.6	295.1	298.69	100.0	295.6	.0170	1.0	330.0	-.9	.5
.2	116	17.2	.00010	33.5	.03	1000.0	296.5	296.5	299.67	98.2	296.2	.0182	1.5	334.7	-1.3	.6
1.0	313	27.2	.00046	52.4	.05	978.0	299.7	301.7	303.48	91.2	298.2	.0204	3.3	340.3	-3.1	1.1
2.0	570	28.3	.00110	54.7	.05	950.0	298.6	303.0	302.20	92.8	297.3	.0199	2.7	41.4	-2.1	-1.8
3.0	823	29.2	.00175	56.8	.05	923.0	296.5	303.4	299.13	74.1	291.6	.0144	4.[illegible]	70.0	-1.4	-3.9
4.0	1043	28.1	.00232	54.7	.05	900.0	296.1	305.1	298.63	72.2	290.8	.0140	4.6	69.2	-1.6	-4.3
4.0	1053	28.0	.00235	54.6	.05	899.0	296.1	305.2	298.61	72.1	290.8	.0140	4.6	69.2	-1.6	-4.3
5.0	1319	27.3	.00301	53.6	.05	872.0	294.7	306.5	297.14	72.0	289.5	.0133	5.4	68.6	-2.0	-5.0
5.8	1540	28.4	.00358	55.9	.06	850.0	292.9	306.9	295.30	77.7	288.9	.0132	5.8	69.6	-2.0	-5.5
6.0	1581	28.6	.00368	56.4	.06	846.0	292.6	306.9	294.96	78.8	288.8	.0132	5.9	69.8	-2.1	-5.6
7.0	1839	26.3	.00433	52.1	.05	821.0	291.0	307.8	293.13	79.1	287.3	.0123	12.8	71.6	-4.0	-12.2
7.9	2060	26.4	.00487	52.5	.05	800.0	290.2	309.3	292.16	72.5	285.2	.0109	.3	130.6	.2	-.2
8.0	2082	26.4	.00492	52.5	.05	798.0	290.1	309.5	292.07	71.9	285.0	.0109	1.1	237.3	.6	.9
9.0	2364	26.4	.00561	52.8	.06	772.0	289.1	311.3	290.99	71.3	283.9	.0105	13.1	258.5	2.6	12.9
10.0	2621	25.1	.00623	50.4	.06	749.0	288.0	312.7	289.72	71.5	282.9	.0100	1.2	352.2	-1.2	.2
11.0	2931	25.7	.00696	51.9	.06	722.0	286.2	314.1	287.85	71.6	281.2	.0093	12.8	89.5	-.1	-12.8
11.9	3190	26.7	.00760	54.1	.06	700.0	285.2	315.8	286.76	71.9	280.3	.0090	13.2	93.6	.8	-13.2
12.0	3215	26.8	00766	54.3	.06	698.0	285.1	315.9	286.66	71.9	280.2	.0090	13.3	94.0	.9	-13.3
13.0	3519	25.4	.00841	51.9	.06	673.0	282.7	316.6	284.19	77.3	278.9	.0085	4.9	117.6	2.3	-4.3
14.0	3795	24.8	.00907	50.9	.06	651.0	281.8	318.6	283.20	75.0	277.6	.0081	4.7	139.1	3.5	-3.1
15.0	4065	25.1	.00972	51.8	.07	630.0	279.4	318.8	280.58	75.8	275.4	.0071	5.0	148.5	4.3	-2.6
16.0	4342	24.4	.01038	50.7	.07	609.0	277.5	319.7	278.72	84.8	275.2	.0072	4.1	143.2	3.3	-2.4
16.4	4462	23.9	.01066	50.0	.07	600.0	276.7	320.1	277.89	90.2	275.2	.0074	3.8	138.6	2.8	-2.5
17.0	4627	23.4	.01104	48.9	.07	588.0	275.5	320.6	276.77	97.4	275.1	.0075	3.5	131.1	2.3	-2.6
18.0	4920	22.6	.01170	47.6	.07	567.0	273.9	322.1	275.06	98.6	273.7	.0070	3.7	142.7	2.9	-2.2
19.0	5208	21.9	.01233	46.5	.07	547.0	272.0	323.2	273.02	97.5	271.6	.0062	3.5	150.8	3.0	-1.7
20.0	5535	22.4	.01305	47.8	.07	525.0	270.3	324.9	271.22	97.0	269.9	.0057	3.7	148.4	3.2	-2.0
21.0	5842	23.2	.01375	49.8	.08	505.0	268.8	326.7	269.62	96.9	268.3	.0053	4.5	142.6	3.6	-2.7
21.3	5920	22.5	.01392	48.4	.07	500.0	268.4	327.1	269.21	97.0	267.9	.0051	4.5	137.4	3.3	-3.0
22.0	6143	20.5	.01441	44.2	.07	486.0	267.3	328.4	268.05	97.1	266.9	.0049	4.6	122.7	2.5	-3.9
23.0	6454	22.7	.01509	49.5	.08	467.0	265.0	329.4	265.75	100.0	265.0	.0044	4.3	107.0	1.2	-4.1
24.0	6776	19.9	.01579	43.6	.07	448.0	263.4	331.4	264.10	100.0	263.4	.0041	3.6	119.5	1.8	-3.2
25.0	7091	19.7	.01643	43.6	.08	430.0	261.2	332.4	261.72	100.0	261.2	.0035	3.8	124.9	2.2	-3.1
26.0	7417	17.7	.01706	39.4	.07	412.0	259.8	334.6	260.25	95.5	259.2	.0031	3.2	98.7	.5	-3.2
26.7	7640	17.3	.01746	38.8	.07	400.0	258.0	335.2	258.44	93.7	257.2	.0026	2.9	95.9	.3	-2.9
27.0	7755	17.1	.01767	38.4	.07	394.0	257.1	335.5	257.52	92.8	256.2	.0026	2.8	94.3	.2	-2.8
28.0	8106	17.4	.01831	39.5	.08	376.0	254.9	337.1	255.25	87.5	253.4	.0021	3.0	127.3	1.8	-2.4
29.0	8429	17.4	.01891	39.7	.08	360.0	252.5	338.1	252.76	87.3	250.9	.0018	3.8	123.0	2.1	-3.2
29.7	8636	16.4	.01928	37.8	.08	350.0	251.2	339.0	251.39	84.4	249.2	.0015	4.4	111.9	1.6	-4.1
30.0	8742	16.0	.01947	36.8	.08	345.0	250.5	339.5	250.69	82.9	248.4	.0015	4.8	107.4	1.4	-4.5
31.0	9044	15.9	.01999	37.0	.08	331.0	248.1	340.2	248.24	76.7	245.2	.0011	3.9	102.3	.8	-3.8
32.0	9333	16.6	.02050	39.2	.09	318.0	245.1	340.1	245.27	73.6	241.9	.0009	3.8	108.6	1.2	-3.6
33.0	9725	16.5	.02122	39.4	.09	301.0	242.5	341.7	242.58	73.6	239.3	.0007	4.2	109.3	1.4	-4.0
33.1	9748	16.5	.02126	39.4	.09	300.0	242.3	341.8	242.40	73.2	239.1	.0007	4.2	108.4	1.3	-4.0
34.0	10037	16.5	.02180	39.7	.09	288.0	240.2	342.8	240.28	68.6	236.4	.0006	4.1	96.9	.5	-4.0
35.0	10437	14.2	.02249	34.4	.09	272.0	237.8	344.9	237.83	57.2	232.3	.0004	3.5	75.4	-.9	-3.4
36.0	10722	16.8	.02299	41.3	.11	261.0	235.0	345.0	235.08	45.4	227.7	.0002	3.5	38.2	-2.8	-2.2
37.0	11016	18.1	.02359	45.0	.12	250.0	232.0	344.7	231.99	0.0	0.0	0.0000	5.2	28.6	-4.5	-2.5
38.0	11319	17.4	.02422	43.9	.12	239.0	229.0	344.7	229.00	0.0	0.0	0.0000	6.8	17.3	-6.5	-2.0
39.0	11633	18.1	.02488	46.1	.13	228.0	226.4	345.4	226.38	0.0	0.0	0.0000	8.8	7.3	-8.8	-1.1
40.0	11928	18.6	.02552	48.3	.14	218.0	223.0	344.7	223.05	0.0	0.0	0.0000	10.0	11.4	-9.8	-2.0
41.0	12327	17.9	.02641	46.9	.14	205.0	220.4	346.6	220.37	0.0	0.0	0.0000	9.9	18.0	-9.4	-3.1
41.5	12484	17.3	.02675	45.5	.14	200.0	218.8	346.6	218.83	0.0	0.0	0.0000	10.2	20.3	-9.6	-3.6
42.0	12647	16.6	.02709	44.1	.14	195.0	217.2	346.6	217.24	0.0	0.0	0.0000	10.6	22.5	-9.8	-4.1
43.0	13048	18.2	.02796	49.1	.17	183.0	214.1	347.8	214.11	0.0	0.0	0.0000	13.8	20.6	-12.9	-4.8
44.0	13470	17.6	.02892	48.2	.17	171.0	211.3	350.1	211.35	0.0	0.0	0.0000	16.9	18.6	-16.0	-5.4
45.0	13877	14.5	.02977	40.4	.15	160.0	207.2	349.7	207.18	0.0	0.0	0.0000	14.5	12.3	-14.1	-3.1
45.8	14266	15.5	.03054	43.5	.17	150.0	205.9	354.0	205.88	0.0	0.0	0.0000	11.7	22.1	-10.9	-4.4
46.0	14389	15.8	.03078	44.4	.18	147.0	205.5	355.4	205.47	0.0	0.0	0.0000	11.0	26.1	-9.8	-4.8
47.0	15032	15.8	.03212	44.9	.20	132.0	203.0	362.1	203.01	0.0	0.0	0.0000	7.6	66.5	-3.0	-7.0
47.7	15357	16.6	.03283	47.0	.22	125.0	204.3	370.0	204.26	0.0	0.0	0.0000	5.7	107.4	1.7	-5.4
48.0	15502	17.0	.03314	48.0	.23	122.0	204.8	373.6	204.82	0.0	0.0	0.0000	6.0	129.2	3.8	-4.7
49.0	16064	15.2	.03434	43.6	.23	111.0	201.6	377.8	201.59	0.0	0.0	0.0000	8.0	123.8	4.4	-6.6
50.0	16617	16.4	.03552	47.6	.27	101.0	198.8	382.8	198.83	0.0	0.0	0.0000	11.6	104.4	2.9	-11.2
50.1	16675	16.6	.03566	48.1	.28	100.0	198.9	384.1	198.93	0.0	0.0	0.0000	11.6	103.7	2.8	-11.3
51.0	17225	18.3	.03695	52.8	.33	91.0	199.9	396.4	199.86	0.0	0.0	0.0000	12.1	97.2	1.5	-12.0
52.0	17617	22.5	.03803	65.0	.44	85.1	200.1	404.6	200.11	0.0	0.0	0.0000	8.3	98.7	1.3	-8.2
52.7	17980	27.5	.03930	78.9	.57	80.0	201.1	414.0	201.14	0.0	0.0	0.0000	7.7	92.0	.3	-7.7
53.0	18137	29.6	.03985	84.9	.63	77.9	201.6	418.0	201.59	0.0	0.0	0.0000	7.5	88.7	-.2	-7.5
54.0	18670	37.5	.04223	106.3	.87	71.2	203.7	433.4	203.69	0.0	0.0	0.0000	6.2	79.0	-1.2	-6.0
54.2	18772	39.9	.04281	112.5	.95	70.0	204.4	437.1	204.45	0.0	0.0	0.0000	6.1	81.3	-.9	-6.0
55.0	19172	49.2	.04508	136.8	1.24	65.5	207.4	451.8	207.38	0.0	0.0	0.0000	5.9	90.7	.1	-5.9
56.0	19711	69.6	.04920	188.2	1.92	60.0	213.5	476.9	213.45	0.0	0.0	0.0000	4.5	99.8	.8	-4.5
56.0	19722	70.0	.04928	189.2	1.94	59.9	213.6	477.4	213.57	0.0	0.0	0.0000	4.5	100.1	.8	-4.4
57.0	20290	79.6	.05464	214.7	2.41	54.7	213.9	490.7	213.93	0.0	0.0	0.0000	1.7	225.5	1.2	1.2
57.9	20850	86.1	.06054	233.7	2.86	50.0	212.6	500.5	212.64	0.0	0.0	0.0000	1.0	223.3	.7	.7
58.0	20926	86.9	.06133	236.2	2.92	49.4	212.5	501.8	212.47	0.0	0.0	0.0000	.9	222.8	.7	.6
59.0	21523	95.0	.06819	255.3	3.51	44.9	214.8	521.4	214.82	0.0	0.0	0.0000	2.9	130.9	1.9	-2.2
60.0	22094	103.6	.07531	278.2	4.19	41.0	215.0	535.5	215.00	0.0	0.0	0.0000	3.5	63.8	-1.6	-3.1
60.3	22249	106.0	.07742	284.6	4.40	40.0	215.0	539.5	215.04	0.0	0.0	0.0000	4.0	57.2	-2.2	-3.4
61.0	22672	112.6	.08315	302.1	4.99	37.4	215.2	550.2	215.17	0.0	0.0	0.0000	5.5	45.7	-3.9	-3.9
61.6	23092	121.7	.08941	323.2	5.78	35.0	217.2	566.2	217.24	0.0	0.0	0.0000	2.5	48.0	-1.7	-1.9
62.0	23333	126.8	.09299	335.3	6.24	33.7	218.4	575.4	218.41	0.0	0.0	0.0000	.8	56.6	-.5	-.7

TIME MIN	ALT GPM	OZONE MICMB	TOTOZ ATMCM	OZDEN MG/M3	OZMXR MICGG	PRESS MB	TEMP DEG K	PTEMP DEG K	VTEMP DEG K	HMDTY PRCNT	DEWPT DEG K	SPCFC HMDTY	SPD MPS	DIR DEG	NS MPS	EW MPS
63.0	23869	135.6	.10163	355.8	7.25	31.0	220.0	593.7	220.05	0.0	0.0	0.0000	2.7	344.9	-2.6	.7
63.3	24080	136.4	.10517	357.6	7.55	30.0	220.3	599.9	220.27	0.0	0.0	0.0000	3.2	13.4	-3.1	-.7
64.0	24480	138.0	.11185	361.1	8.11	28.2	220.7	611.7	220.69	0.0	0.0	0.0000	5.4	40.0	-4.1	-3.5
65.0	25005	141.2	.12080	369.3	9.00	26.0	220.7	626.1	220.69	0.0	0.0	0.0000	7.2	62.3	-3.3	-6.3
65.5	25258	141.9	.12519	370.3	9.42	25.0	221.3	634.9	221.28	0.0	0.0	0.0000	8.2	74.3	-2.2	-7.9
66.0	25550	142.8	.13023	371.5	9.90	23.9	222.0	645.0	221.96	0.0	0.0	0.0000	9.6	84.5	-.9	-9.6
67.0	26121	145.2	.14017	373.8	10.99	21.9	224.3	668.2	224.27	0.0	0.0	0.0000	8.5	101.9	1.8	-8.3
68.0	26618	146.4	.14889	378.2	11.95	20.3	223.5	680.6	223.51	0.0	0.0	0.0000	6.5	97.3	.8	-6.5
68.2	26715	145.5	.15059	375.8	12.05	20.0	223.4	683.3	223.44	0.0	0.0	0.0000	7.0	98.2	1.0	-6.9
69.0	27016	142.5	.15584	368.5	12.36	19.1	223.2	691.6	223.20	0.0	0.0	0.0000	8.3	100.3	1.5	-8.2
70.0	27439	137.4	.16300	356.0	12.72	17.9	222.9	703.5	222.89	0.0	0.0	0.0000	8.2	108.4	2.6	-7.8
70.3	27586	135.3	.16540	349.8	12.81	17.5	223.3	709.6	223.34	0.0	0.0	0.0000	9.6	102.6	2.1	-9.4
71.0	27893	130.9	.17035	337.0	12.99	16.7	224.3	722.1	224.27	0.0	0.0	0.0000	12.6	94.9	1.1	-12.6
72.0	28425	127.5	.17861	327.7	13.71	15.4	224.6	740.0	224.58	0.0	0.0	0.0000	11.4	96.1	1.2	-11.3
72.3	28599	125.9	.18121	322.2	13.90	15.0	225.6	749.0	225.59	0.0	0.0	0.0000	11.5	98.3	1.7	-11.4
73.0	28962	122.5	.18661	310.7	14.30	14.2	227.7	767.9	227.70	0.0	0.0	0.0000	11.8	103.0	2.6	-11.5
74.0	29500	118.7	.19428	300.1	15.01	13.1	228.3	787.8	228.28	0.0	0.0	0.0000	20.5	87.4	-.9	-20.5
74.7	29814	113.7	.19854	286.5	15.07	12.5	229.2	801.8	229.23	0.0	0.0	0.0000	22.0	80.4	-3.7	-21.7
75.0	29977	111.2	.20074	279.4	15.10	12.2	229.7	809.0	229.72	0.0	0.0	0.0000	22.8	77.1	-5.1	-22.3
76.0	30553	105.6	.20805	264.6	15.62	11.2	230.3	831.1	230.29	0.0	0.0	0.0000	17.8	79.8	-3.1	-17.5
77.0	31118	99.5	.21483	249.1	16.01	10.3	230.7	852.8	230.72	0.0	0.0	0.0000	19.4	95.6	1.9	-19.3
77.3	31317	96.3	.21703	241.2	15.93	10.0	230.4	858.9	230.40	0.0	0.0	0.0000	20.0	97.6	2.7	-19.9
78.0	31734	89.4	.22165	224.7	15.76	9.4	229.7	871.6	229.72	0.0	0.0	0.0000	21.4	101.6	4.3	-20.9
79.0	32176	82.0	.22611	207.5	15.45	8.8	228.3	882.6	228.28	0.0	0.0	0.0000	23.7	109.7	8.0	-22.3
80.0	32650	73.3	.23043	183.8	14.81	8.2	230.2	908.0	230.15	0.0	0.0	0.0000	20.6	104.3	5.1	-19.9
80.2	32816	72.2	.23182	180.9	14.94	8.0	230.3	914.9	230.25	0.0	0.0	0.0000	999.9	999.9	999.9	999.9
81.0	33342	68.6	.23618	171.7	15.35	7.4	230.6	936.7	230.58	0.0	0.0	0.0000	999.9	999.9	999.9	999.9

INTEGRAL .23618 RESIDUAL .05415 INTEGRATED TOTAL OZONE .29033

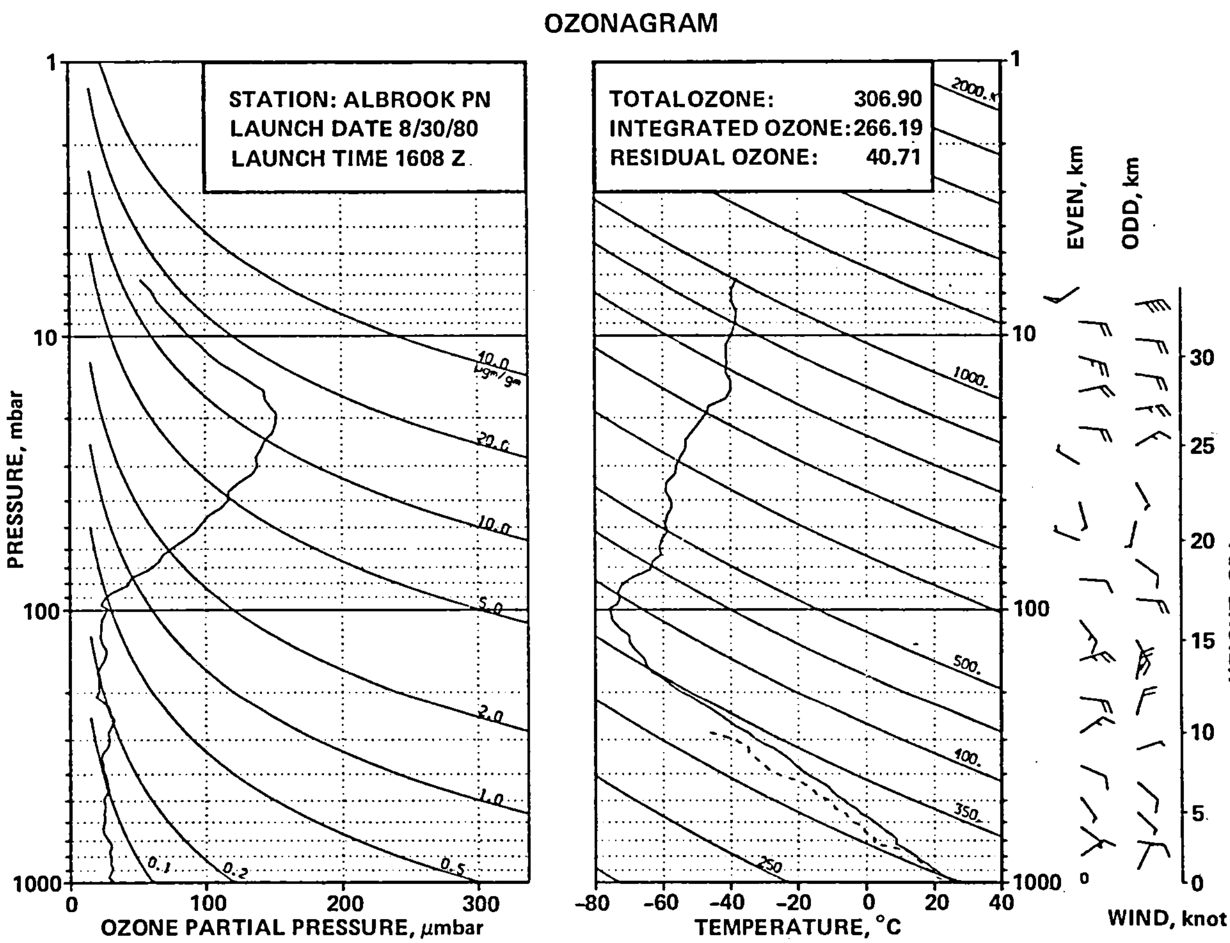
OZONAGRAM
STATION: ALBROOK PN
LAUNCH DATE 8/30/80
LAUNCH TIME 1608 Z
TOTALOZONE: 306.90
INTEGRATED OZONE:266.19
RESIDUAL OZONE: 40.71
PRESSURE, mbar
OZONE PARTIAL PRESSURE, μmbar
TEMPERATURE, °C
EVEN, km
ODD, km
HEIGHT, GP km
WIND, knot

STATION ALBROOK PN   LAUNCH DATE 8/30/80   TIME 1600Z   ECC   SONDE 3A1310

SURFACE CONDITIONS   PRESS 1006.1MB   TEMP 303.4 DEG K   HUMIDITY 84.0 PRCNT

TIME MIN	ALT GPM	OZONE MICMB	TOTOZ ATMCM	OZDEN MG/M3	OZMXR MICGG	PRESS MB	TEMP DEG K	PTEMP DEG K	VTEMP DEG K	HMDTY PRCNT	DEWPT DEG K	SPCFC HMDTY	SPD MPS	DIR DEG	NS MPS	EW MPS
0.0	66	29.0	0.00000	55.3	.05	1006.1	303.2	302.6	307.06	79.5	299.2	.0211	1.0	320.0	-.8	.6
.3	120	29.5	.00014	56.4	.05	1000.0	302.3	302.3	306.06	80.1	298.5	.0198	1.3	334.5	-1.2	.6
1.0	282	31.0	.00057	59.6	.05	982.0	299.7	301.3	303.06	82.1	296.4	.0182	2.6	351.3	-2.5	.4
2.0	500	27.8	.00115	54.1	.05	958.0	296.9	300.6	299.80	82.2	293.7	.0158	2.8	13.7	-2.8	-.7
3.0	740	29.2	.00177	57.1	.05	932.0	295.1	301.1	298.04	90.5	293.5	.0161	4.5	25.5	-4.0	-1.9
4.0	967	30.1	.00238	59.1	.05	908.0	294.0	302.3	296.79	89.5	292.3	.0153	5.5	27.9	-4.9	-2.6
4.3	1043	30.3	.00259	59.6	.06	900.0	293.5	302.5	296.22	89.2	291.7	.0146	5.4	26.9	-4.8	-2.5
5.0	1228	30.8	.00310	60.9	.06	881.0	292.3	303.1	294.84	88.4	290.4	.0140	5.2	24.5	-4.8	-2.2
6.0	1506	29.3	.00387	58.2	.06	853.0	290.9	304.4	293.30	91.2	289.4	.0136	5.3	33.6	-4.5	-3.0
6.1	1536	29.4	.00395	58.3	.06	850.0	290.7	304.5	293.06	91.8	289.3	.0135	5.5	35.4	-4.5	-3.2
7.0	1770	29.7	.00459	59.3	.06	827.0	288.9	305.0	291.17	96.5	288.3	.0130	6.9	46.4	-4.8	-5.0
7.9	2051	29.4	.00536	58.9	.06	800.0	287.8	306.7	289.99	97.0	287.3	.0126	7.3	54.9	-4.2	-6.0
8.0	2073	29.3	.00542	58.9	.06	798.0	287.7	306.8	289.90	97.1	287.2	.0126	7.4	55.5	-4.2	-6.1
9.0	2408	28.7	.00633	58.1	.06	767.0	285.6	308.1	287.62	99.6	285.5	.0117	6.8	72.9	-2.0	-6.5
10.0	2697	30.2	.00713	61.5	.07	741.0	283.7	309.1	285.20	79.7	280.4	.0086	6.5	85.3	-.5	-6.5
11.0	2947	29.6	.00784	60.7	.07	719.0	281.7	309.6	282.79	63.9	275.3	.0062	6.0	95.4	.6	-6.0
11.7	3168	28.3	.00845	57.9	.07	700.0	282.0	312.2	233.11	64.5	275.7	.0066	5.4	99.7	.9	-5.3
12.0	3252	27.7	.00867	56.8	.07	693.0	282.1	313.2	283.23	64.8	275.8	.0066	5.2	101.6	1.0	-5.1
13.0	3531	25.5	.00938	52.4	.06	670.0	280.7	314.7	281.72	64.2	274.3	.0062	4.2	104.9	1.1	-4.1
14.0	3818	24.0	.01006	49.7	.06	647.0	278.8	315.7	279.71	63.9	272.5	.0056	3.6	117.3	1.7	-3.2
15.0	4126	24.0	.01078	50.0	.06	623.0	277.2	317.4	278.22	71.9	272.6	.0059	2.8	128.2	1.8	-2.2
16.0	4404	24.9	.01144	52.1	.07	602.0	275.6	318.6	276.37	63.5	269.4	.0048	2.8	126.1	1.6	-2.2
16.1	4430	24.9	.01151	52.3	.07	600.0	275.4	318.7	276.23	63.4	269.2	.0047	2.8	126.3	1.6	-2.2
17.0	4690	25.3	.01214	53.3	.07	581.0	274.1	320.1	274.85	63.2	267.9	.0044	2.8	128.5	1.8	-2.2
18.0	4999	24.8	.01291	52.6	.07	559.0	271.6	320.7	272.29	72.1	267.2	.0044	3.0	131.5	2.0	-2.2
19.0	5333	25.5	.01374	54.6	.08	536.0	270.2	322.9	270.76	63.0	264.1	.0036	3.0	138.5	2.2	-2.0
20.0	5633	25.4	.01451	54.8	.08	516.0	267.9	323.6	268.47	71.3	263.5	.0035	3.2	143.7	2.6	-1.9
20.8	5879	24.8	.01513	53.8	.08	500.0	266.7	325.1	267.24	71.1	262.3	.0033	3.4	144.9	2.8	-2.0
21.0	5942	24.7	.01529	53.5	.08	496.0	266.4	325.5	266.93	71.0	262.0	.0033	3.5	145.2	2.9	-2.0
22.0	6197	25.6	.01594	55.9	.09	480.0	264.6	326.4	265.06	63.3	258.9	.0026	3.7	142.3	2.9	-2.3
23.0	6492	28.4	.01675	62.4	.10	462.0	263.2	328.2	263.59	65.4	258.0	.0025	4.1	137.4	3.0	-2.8
24.0	6815	27.8	.01768	61.2	.10	443.0	261.9	330.5	262.26	62.7	256.2	.0023	4.4	134.0	3.1	-3.2
25.0	7132	26.9	.01858	59.9	.10	425.0	259.5	331.4	259.80	60.9	253.6	.0019	3.8	129.8	2.4	-2.9
26.0	7478	26.2	.01954	58.9	.11	406.0	256.6	332.0	256.78	46.8	247.9	.0012	3.6	128.8	2.2	-2.8
26.3	7589	25.6	.01983	57.7	.11	400.0	255.8	332.4	256.00	45.4	246.9	.0011	3.8	125.2	2.2	-3.1
27.0	7836	24.2	.02049	55.0	.10	387.0	254.1	333.3	254.28	42.5	244.6	.0009	4.2	118.4	2.0	-3.7
28.0	8189	24.3	.02140	55.7	.11	369.0	252.1	335.2	252.24	42.4	242.7	.0008	4.4	109.1	1.4	-4.1
29.0	8536	22.9	.02228	52.9	.11	352.0	250.4	337.4	250.48	40.2	240.6	.0007	3.9	109.6	1.3	-3.7
29.1	8577	23.0	.02239	53.2	.11	350.0	250.1	337.5	250.18	40.2	240.3	.0007	3.8	108.1	1.2	-3.6
30.0	8854	23.7	.02308	55.1	.12	337.0	248.1	338.5	248.19	40.1	238.5	.0006	3.1	95.1	.3	-3.0
31.0	9183	27.2	.02400	63.8	.14	322.0	245.8	339.8	245.93	49.2	238.5	.0006	3.1	59.4	-1.6	-2.7
32.0	9454	28.6	.02483	68.1	.15	310.0	242.8	339.3	242.86	53.0	236.3	.0005	4.4	55.8	-2.5	-3.7
32.8	9685	28.6	.02557	68.6	.16	300.0	240.9	339.8	240.97	51.2	234.2	.0004	6.2	60.4	-3.1	-5.4
33.0	9733	28.6	.02572	68.7	.16	298.0	240.5	339.9	240.58	50.8	233.8	.0004	6.6	61.1	-3.2	-5.7
34.0	10120	27.8	.02695	67.3	.16	282.0	238.2	342.0	238.27	29.6	226.7	.0002	7.8	55.8	-4.4	-6.5
35.0	10447	30.3	.02803	74.4	.19	269.0	234.8	341.8	234.86	0.0	0.0	0.0000	8.3	51.6	-5.2	-6.5
36.0	10839	32.4	.02945	80.7	.21	254.0	231.9	343.1	231.95	0.0	0.0	0.0000	9.4	33.6	-7.8	-5.2
36.3	10946	31.4	.02984	78.5	.21	250.0	231.2	343.5	231.16	0.0	0.0	0.0000	9.7	24.8	-8.8	-4.1
37.0	11166	29.4	.03063	73.9	.20	242.0	229.5	344.3	229.55	0.0	0.0	0.0000	10.9	9.2	-10.8	-1.8
38.0	11505	28.4	.03179	72.4	.20	230.0	226.8	345.1	226.80	0.0	0.0	0.0000	11.0	355.8	-11.0	.8
39.0	11798	25.0	.03273	64.5	.19	220.0	224.1	345.4	224.12	0.0	0.0	0.0000	11.2	355.7	-11.2	.8
40.0	12163	19.1	.03371	49.9	.15	208.0	221.3	346.7	221.34	0.0	0.0	0.0000	11.4	5.1	-11.4	-1.0
40.8	12414	20.9	.03433	55.2	.17	200.0	218.6	346.3	218.64	0.0	0.0	0.0000	13.0	3.8	-13.0	-.9
41.0	12479	21.3	.03450	56.5	.18	198.0	218.0	346.2	217.95	0.0	0.0	0.0000	13.5	3.5	-13.4	-.8
42.0	12841	20.7	.03544	55.4	.18	187.0	215.1	347.2	215.06	0.0	0.0	0.0000	13.7	.9	-13.7	-.2
43.0	13150	21.4	.03626	57.9	.20	178.0	212.9	348.6	212.92	0.0	0.0	0.0000	12.5	13.7	-12.2	-3.0
44.0	13471	19.9	.03710	54.8	.20	169.0	209.7	348.5	209.72	0.0	0.0	0.0000	15.8	33.7	-13.1	-8.8
45.0	13844	22.8	.03813	63.3	.24	159.0	208.3	352.3	208.34	0.0	0.0	0.0000	14.6	49.4	-9.5	-11.1
46.0	14198	25.6	.03925	71.3	.28	150.0	207.5	356.8	207.53	0.0	0.0	0.0000	12.5	87.1	-.6	-12.5
47.0	14571	26.9	.04053	75.7	.32	141.0	205.2	359.1	205.21	0.0	0.0	0.0000	13.5	113.4	5.3	-12.4
48.0	14965	23.2	.04183	65.9	.29	132.0	203.4	362.8	203.43	0.0	0.0	0.0000	10.1	142.4	8.0	-6.2
48.9	15289	22.3	.04281	63.5	.30	125.0	203.2	368.2	203.23	0.0	0.0	0.0000	9.1	167.6	8.9	-2.0
49.0	15337	22.2	.04295	63.1	.30	124.0	203.2	368.9	203.20	0.0	0.0	0.0000	9.1	171.6	9.0	-1.3
50.0	15680	22.9	.04399	66.0	.32	117.0	200.4	369.9	200.36	0.0	0.0	0.0000	8.9	175.0	8.9	-.8
51.0	16093	23.2	.04527	67.5	.35	109.0	198.3	373.6	198.32	0.0	0.0	0.0000	7.8	139.5	5.9	-5.1
51.9	16592	27.0	.04700	78.7	.45	100.0	197.6	381.6	197.63	0.0	0.0	0.0000	7.7	115.3	3.3	-7.0
52.0	16668	27.5	.04726	80.5	.46	98.7	197.5	382.8	197.52	0.0	0.0	0.0000	7.8	111.8	2.9	-7.3
53.0	16823	22.7	.04779	65.6	.39	96.1	199.6	389.8	199.61	0.0	0.0	0.0000	9.2	101.9	1.9	-9.0
54.0	17078	24.7	.04861	71.3	.45	92.0	200.4	396.2	200.36	0.0	0.0	0.0000	11.5	94.7	.9	-11.5
55.0	17419	30.2	.04987	87.4	.58	86.8	199.9	401.8	199.86	0.0	0.0	0.0000	11.1	96.8	1.3	-11.0
56.0	17803	42.4	.05174	121.9	.87	81.3	201.1	411.9	201.09	0.0	0.0	0.0000	7.2	101.8	1.5	-7.0
56.3	17898	43.1	.05230	123.3	.89	80.0	201.9	415.4	201.86	0.0	0.0	0.0000	6.6	99.5	1.1	-6.5
57.0	18179	45.1	.05394	127.7	.98	76.3	204.1	425.7	204.11	0.0	0.0	0.0000	4.9	89.6	0.0	-4.9
58.0	18581	57.6	.05663	158.8	1.34	71.4	209.5	445.4	209.53	0.0	0.0	0.0000	4.3	83.1	-.5	-4.3
58.3	18702	59.9	.05759	165.0	1.42	70.0	209.7	448.3	209.70	0.0	0.0	0.0000	4.0	95.7	.4	-4.0
59.0	18990	65.4	.05986	179.7	1.62	66.8	210.1	455.2	210.11	0.0	0.0	0.0000	4.2	128.2	2.6	-3.3
60.0	19352	68.7	.06296	186.7	1.81	63.0	212.6	468.3	212.56	0.0	0.0	0.0000	7.8	115.3	3.3	-7.1
60.8	19655	74.4	.06575	202.5	2.06	60.0	212.3	474.3	212.28	0.0	0.0	0.0000	5.2	109.4	1.7	-4.9
61.0	19749	76.2	.06661	207.3	2.14	59.1	212.2	476.1	212.19	0.0	0.0	0.0000	4.5	106.1	1.2	-4.3
62.0	20174	85.6	.07097	232.2	2.57	55.2	212.9	487.2	212.92	0.0	0.0	0.0000	.5	354.2	-.5	.1
63.0	20547	92.7	.07517	249.4	2.95	52.0	214.5	499.3	214.53	0.0	0.0	0.0000	.7	28.1	-.6	-.3
63.6	20792	95.4	.07811	257.4	3.17	50.0	214.1	503.9	214.10	0.0	0.0	0.0000	.6	182.6	.6	0.0
64.0	20945	97.2	.07993	262.4	3.30	48.8	213.8	506.8	213.82	0.0	0.0	0.0000	1.4	190.6	1.4	.3

TIME MIN	ALT GPM	OZONE MICMB	TOTOZ ATMCM	OZDEN MG/M3	OZMXR MICGG	PRESS MB	TEMP DEG K	PTEMP DEG K	VTEMP DEG K	HMDTY PRCNT	DEWPT DEG K	SPCFC HMDTY	SPD MPS	DIR DEG	NS MPS	EW MPS
65.0	21398	102.3	.08561	275.3	3.73	45.4	214.5	519.0	214.53	0.0	0.0	0.0000	2.8	197.7	2.6	.8
66.0	21843	112.4	.09160	300.7	4.40	42.3	215.8	532.6	215.76	0.0	0.0	0.0000	2.5	201.3	2.4	.9
67.0	22195	116.9	.09666	313.1	4.84	40.0	215.6	540.8	215.59	0.0	0.0	0.0000	1.7	142.4	1.4	-1.0
67.0	22211	117.1	.09689	313.6	4.86	39.9	215.6	541.2	215.58	0.0	0.0	0.0000	1.7	139.1	1.3	-1.1
68.0	22651	117.3	.10337	316.6	5.23	37.2	214.0	548.1	214.00	0.0	0.0	0.0000	2.6	109.0	.9	-2.5
68.9	23033	123.5	.10919	333.0	5.85	35.0	214.2	558.1	214.16	0.0	0.0	0.0000	2.3	146.1	1.9	-1.3
69.0	23087	124.4	.11001	335.3	5.94	34.7	214.2	559.5	214.18	0.0	0.0	0.0000	2.4	151.4	2.1	-1.1
70.0	23598	135.0	.11830	359.3	6.99	32.0	216.9	580.0	216.95	0.0	0.0	0.0000	2.4	218.2	1.9	1.5
71.0	24008	138.5	.12526	368.2	7.65	30.0	217.1	591.3	217.12	0.0	0.0	0.0000	3.5	295.5	-1.5	3.1
72.0	24493	137.5	.13355	363.5	8.20	27.8	218.4	608.0	218.45	0.0	0.0	0.0000	3.9	349.2	-3.9	.7
73.0	24947	141.3	.14134	370.9	9.04	25.9	219.9	624.6	219.91	0.0	0.0	0.0000	6.7	49.6	-4.3	-5.1
73.5	25174	142.6	.14532	374.3	9.46	25.0	219.9	631.0	219.91	0.0	0.0	0.0000	7.9	69.2	-2.8	-7.4
74.0	25384	143.8	.14898	377.5	9.84	24.2	219.9	636.8	219.91	0.0	0.0	0.0000	9.5	81.8	-1.4	-9.4
75.0	25797	149.4	.15638	389.1	10.90	22.7	221.7	653.7	221.66	0.0	0.0	0.0000	10.2	99.6	1.7	-10.0
76.0	26304	151.8	.16562	391.5	11.97	21.0	223.8	674.9	223.82	0.0	0.0	0.0000	9.5	92.0	.3	-9.5
76.5	26625	152.1	.17148	390.0	12.61	20.0	225.1	688.5	225.12	0.0	0.0	0.0000	10.5	86.9	-.6	-10.5
77.0	26894	152.3	.17637	388.7	13.14	19.2	226.2	699.8	226.21	0.0	0.0	0.0000	11.4	83.4	-1.3	-11.3
78.0	27285	147.8	.18336	376.3	13.53	18.1	226.8	713.6	226.80	0.0	0.0	0.0000	13.1	79.3	-2.4	-12.9
78.5	27511	145.8	.18724	366.7	13.80	17.5	229.6	729.4	229.57	0.0	0.0	0.0000	12.0	78.3	-2.4	-11.7
79.0	27706	144.0	.19058	358.5	14.04	17.0	231.9	743.0	231.95	0.0	0.0	0.0000	11.0	77.2	-2.4	-10.7
80.0	28161	143.4	.19817	354.9	14.95	15.9	233.3	761.8	233.33	0.0	0.0	0.0000	8.8	78.0	-1.8	-8.6
80.7	28559	135.7	.20452	335.9	14.99	15.0	233.3	774.7	233.33	0.0	0.0	0.0000	8.5	78.2	-1.7	-8.3
81.0	28697	133.1	.20673	329.3	15.00	14.7	233.3	779.1	233.33	0.0	0.0	0.0000	8.4	78.3	-1.7	-8.2
82.0	29226	123.0	.21459	306.4	14.99	13.6	231.8	791.4	231.81	0.0	0.0	0.0000	11.5	107.9	3.5	-10.9
83.0	29691	112.7	.22095	280.4	14.71	12.7	232.1	808.0	232.08	0.0	0.0	0.0000	14.9	115.7	6.5	-13.5
83.2	29798	110.9	.22231	276.0	14.70	12.5	232.1	811.6	232.05	0.0	0.0	0.0000	14.2	113.3	5.6	-13.0
84.0	30190	104.4	.22725	259.8	14.66	11.8	231.9	824.7	231.95	0.0	0.0	0.0000	11.7	102.1	2.5	-11.5
85.0	30791	96.6	.23427	240.5	14.82	10.8	231.9	845.8	231.95	0.0	0.0	0.0000	9.3	95.3	.9	-9.3
85.9	31315	88.7	.23987	219.5	14.69	10.0	233.4	870.1	233.42	0.0	0.0	0.0000	10.2	95.9	1.0	-10.2
86.0	31384	87.7	.24060	216.7	14.68	9.9	233.6	873.3	233.61	0.0	0.0	0.0000	10.3	95.9	1.1	-10.3
87.0	32114	79.1	.24761	194.7	14.74	8.9	234.7	904.5	234.71	0.0	0.0	0.0000	9.3	94.8	.8	-9.2
88.0	32677	71.9	.25249	176.6	14.53	8.2	235.0	927.0	234.99	0.0	0.0	0.0000	13.6	81.7	-2.0	-13.5
88.3	32846	69.9	.25382	172.1	14.47	8.0	234.6	932.1	234.60	0.0	0.0	0.0000	16.2	80.6	-2.6	-16.0
89.0	33289	64.8	.25730	160.2	14.32	7.5	233.6	945.4	233.61	0.0	0.0	0.0000	23.0	78.8	-4.5	-22.6
89.7	33760	61.4	.26070	151.8	14.53	7.0	233.6	964.3	233.61	0.0	0.0	0.0000	24.8	79.7	-4.4	-24.4
90.0	33959	60.0	.26213	148.2	14.61	6.8	233.6	972.2	233.61	0.0	0.0	0.0000	25.6	80.0	-4.4	-25.2
91.0	34593	51.6	.26619	126.6	13.78	6.2	235.1	1004.7	235.12	0.0	0.0	0.0000	999.9	999.9	999.9	999.9

INTEGRAL .26619 RESIDUAL .04071 INTEGRATED TOTAL OZONE .30690

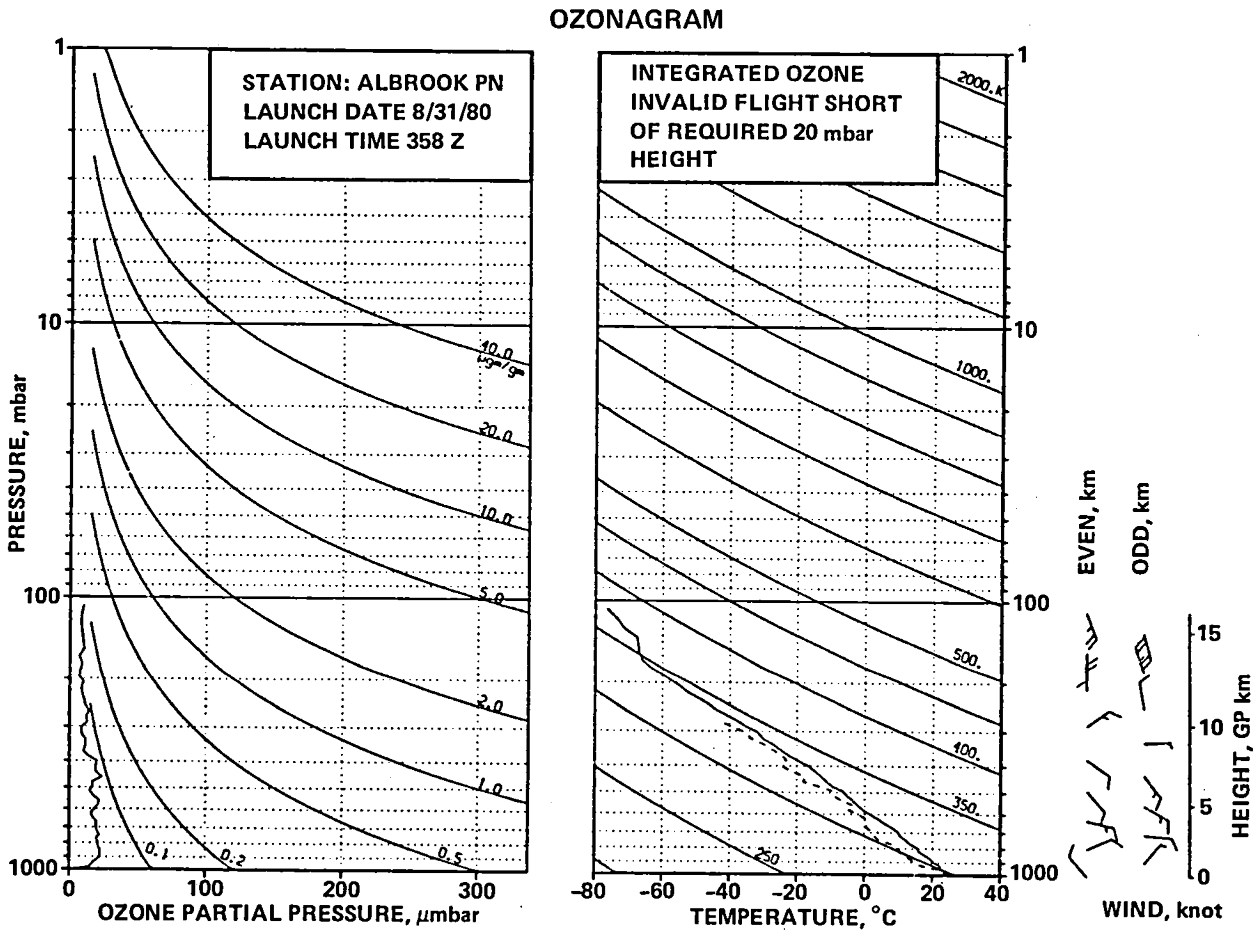

OZONAGRAM
STATION: ALBROOK PN
LAUNCH DATE 8/31/80
LAUNCH TIME 358 Z
INTEGRATED OZONE
INVALID FLIGHT SHORT
OF REQUIRED 20 mbar
HEIGHT
PRESSURE, mbar
OZONE PARTIAL PRESSURE, μmbar
TEMPERATURE, °C
EVEN, km
ODD, km
HEIGHT, GP km
WIND, knot
1
10
100
1000
0
100
200
300
-80
-60
-40
-20
0
20
40
15
10
5
0
2000.K
1000.
500.
400.
350.
250
40.0
20.0
10.0
5.0
2.0
1.0
0.5
0.2
0.1

STATION ALBROOK PN   LAUNCH DATE 8/31/80   TIME 358Z   ECC   SONDE 3A1311

SURFACE CONDITIONS   PRESS 1005.1MB   TEMP 296.0 DEG K   HUMIDITY 100.0 PRCNT

TIME MIN	ALT GPM	OZONE MICMB	TOTOZ ATMCM	OZDEN MG/M3	OZMXR MICGG	PRESS MB	TEMP DEG K	PTEMP DEG K	VTEMP DEG K	HMDTY PRCNT	DEWPT DEG K	SPCFC HMDTY	SPD MPS	DIR DEG	NS MPS	EW MPS
0.0	66	1.1	0.00000	2.2	0.00	1005.1	295.8	295.3	298.80	98.7	295.5	.0169	4.0	320.0	-3.1	2.6
.2	110	3.7	.00003	7.3	.01	1000.0	296.1	296.1	299.24	98.3	295.8	.0176	4.7	316.5	-3.4	3.2
1.0	297	14.6	.00016	28.3	.02	979.0	297.6	299.4	301.09	96.6	297.0	.0190	7.8	309.0	-4.9	6.1
2.0	542	16.7	.00051	32.6	.03	952.0	295.5	299.7	298.58	95.1	294.7	.0169	6.4	329.2	-5.5	3.3
3.0	793	19.3	.00092	37.7	.03	925.0	295.5	302.2	297.88	71.3	290.1	.0130	3.9	10.7	-3.8	-.7
4.0	1030	22.1	.00137	43.4	.04	900.0	293.6	302.5	295.65	69.9	287.9	.0116	3.6	37.4	-2.9	-2.2
4.0	1040	22.2	.00138	43.6	.04	899.0	293.5	302.6	295.56	69.9	287.8	.0116	3.6	38.5	-2.8	-2.2
5.0	1303	22.2	.00192	43.8	.04	872.0	292.6	304.3	294.58	68.3	286.6	.0110	4.1	54.9	-2.4	-3.4
5.8	1522	22.3	.00237	44.2	.04	850.0	291.1	305.0	292.98	67.[illegible]	285.1	.0102	4.8	66.0	-2.0	-4.4
6.0	1563	22.3	.00245	44.2	.04	846.0	290.9	305.1	292.68	67.8	284.9	.0102	5.0	67.7	-1.9	-4.6
7.0	1829	20.9	.00298	41.7	.04	820.0	289.2	306.1	290.89	68.7	283.4	.0095	5.6	69.7	-1.9	-5.2
7.8	2038	20.9	.00339	41.7	.04	800.0	288.7	307.7	290.35	68.1	282.8	.0093	6.1	66.5	-2.4	-5.6
8.0	2081	20.9	.00347	41.7	.04	796.0	288.6	308.0	290.24	68.0	282.7	.0093	6.2	65.9	-2.5	-5.6
9.0	2362	19.5	.00400	39.2	.04	770.0	286.6	308.8	288.09	69.0	281.0	.0086	7.0	69.3	-2.5	-6.6
10.0	2628	21.6	.00451	43.6	.05	746.0	285.4	310.3	286.61	58.0	277.4	.0069	7.8	77.5	-1.7	-7.6
11.0	2924	20.1	.00509	40.9	.05	720.0	283.7	311.6	284.81	59.1	276.0	.0065	6.6	88.7	-.1	-6.6
11.8	3158	19.5	.00553	39.8	.05	700.0	283.1	313.5	284.21	58.9	275.4	.0064	5.4	99.0	.8	-5.3
12.0	3230	19.3	.00566	39.5	.05	694.0	282.9	314.1	284.03	58.8	275.3	.0064	5.1	103.0	1.1	-5.0
13.0	3521	20.0	.00621	41.2	.05	670.0	281.1	315.2	282.10	59.5	273.7	.0059	5.4	104.1	1.3	-5.2
14.0	3821	17.2	.00675	35.5	.04	646.0	278.9	316.0	279.99	68.6	273.6	.0061	6.4	103.5	1.5	-6.2
15.0	4130	15.7	.00724	32.7	.04	622.0	277.0	317.3	278.11	78.1	273.6	.0063	6.9	102.7	1.5	-6.7
16.0	4422	18.5	.00772	38.9	.05	600.0	274.7	317.8	275.60	77.1	271.1	.0055	7.1	104.2	1.7	-6.8
17.0	4708	21.0	.00828	44.4	.06	579.0	272.7	318.8	273.50	73.2	268.5	.0047	7.0	114.7	2.9	-6.4
18.0	5003	21.7	.00890	46.1	.06	558.0	271.1	320.3	272.03	92.5	270.1	.0054	6.7	120.4	3.4	-5.8
19.0	5337	17.5	.00955	37.5	.05	535.0	269.7	322.5	270.42	77.6	266.4	.0043	5.9	118.1	2.8	-5.2
20.0	5653	14.8	.01006	31.9	.05	514.0	268.0	324.2	268.63	74.1	264.1	.0037	5.7	111.2	2.0	-5.3
20.7	5869	16.3	.01041	35.2	.05	500.0	267.1	325.6	267.70	79.1	264.0	.0038	4.4	123.4	2.4	-3.7
21.0	5964	16.9	.01056	36.6	.06	494.0	266.7	326.2	267.29	81.3	264.0	.0038	3.9	131.1	2.6	-3.0
22.0	6252	16.8	.01105	36.8	.06	476.0	263.8	326.2	264.31	73.1	259.9	.0029	4.7	153.3	4.2	-2.1
23.0	6566	23.8	.01170	52.4	.09	457.0	262.0	327.7	262.29	56.9	255.1	.0020	6.5	134.7	4.6	-4.6
24.0	6908	19.0	.01246	42.2	.07	437.0	260.4	329.9	260.75	67.3	255.6	.0022	6.8	137.4	5.0	-4.6
25.0	7246	19.0	.01313	42.5	.08	418.0	258.6	331.8	258.83	54.1	251.4	.0016	7.7	148.7	6.6	-4.0
25.9	7578	19.7	.01380	44.3	.08	400.0	256.5	333.2	256.70	51.4	248.8	.0013	8.1	146.5	6.7	-4.4
26.0	7597	19.7	.01384	44.4	.08	399.0	256.4	333.[illegible]	256.58	51.2	248.7	.0013	8.1	146.4	6.7	-4.5
27.0	7922	13.4	.01441	30.5	.06	382.0	253.3	333.4	253.49	75.8	250.1	.0015	6.0	134.1	4.2	-4.3
28.0	8197	10.3	.01476	23.8	.05	368.0	251.0	334.0	251.20	83.9	249.0	.0015	3.3	116.6	1.5	-3.0
29.0	8564	11.8	.01519	27.4	.06	350.0	248.3	335.2	248.51	81.1	246.0	.0012	2.9	106.0	.8	-2.8
30.0	8902	11.7	.01563	27.6	.06	334.0	246.0	336.5	246.11	76.9	243.2	.0009	3.5	86.1	-.2	-3.5
31.0	9231	8.9	.01600	21.0	.05	319.0	243.1	336.9	243.19	71.7	239.6	.0007	3.8	88.0	-.1	-3.8
32.0	9643	8.9	.01641	21.2	.05	301.0	241.3	340.0	241.35	68.3	237.4	.0006	4.3	71.6	-1.4	-4.1
32.1	9666	9.2	.01644	22.0	.05	300.0	241.0	339.9	241.09	68.0	237.1	.0006	4.5	70.1	-1.5	-4.2
33.0	9928	13.1	.01676	31.7	.08	289.0	238.1	339.5	238.17	64.5	233.8	.0004	6.5	59.0	-3.4	-5.6
34.0	10247	12.2	.01722	29.8	.07	276.0	235.6	340.3	235.64	57.3	230.3	.0003	7.0	48.9	-4.6	-5.3
35.0	10577	14.2	.01772	35.3	.09	263.0	232.5	340.6	232.52	0.0	0.0	0.0000	4.8	30.7	-4.1	-2.4
36.0	10919	11.4	.01823	28.8	.08	250.0	229.0	340.2	228.97	0.0	0.0	0.0000	4.2	353.4	-4.1	.5
37.0	11191	10.7	.01859	27.3	.07	240.0	227.0	341.3	227.01	0.0	0.0	0.0000	7.7	347.5	-7.5	1.7
38.0	11500	9.3	.01896	24.0	.07	229.0	224.2	341.5	224.15	0.0	0.0	0.0000	8.3	353.1	-8.2	1.0
39.0	11820	8.5	.01931	22.3	.06	218.0	221.0	341.6	221.04	0.0	0.0	0.0000	9.6	358.3	-9.6	.3
40.0	12184	9.9	.01972	26.2	.08	206.0	218.4	343.0	218.42	0.0	0.0	0.0000	10.2	358.7	-10.2	.2
40.6	12371	8.2	.01992	21.8	.07	200.0	216.8	343.4	216.79	0.0	0.0	0.0000	10.2	349.9	-10.0	1.8
41.0	12500	7.0	.02005	18.8	.06	196.0	215.7	343.6	215.69	0.0	0.0	0.0000	10.3	343.9	-9.9	2.9
42.0	12828	7.5	.02035	20.4	.07	186.0	213.2	344.7	213.16	0.0	0.0	0.0000	14.2	338.0	-13.1	5.3
43.0	13170	9.0	.02071	24.6	.08	176.0	210.0	344.9	209.97	0.0	0.0	0.0000	12.5	342.5	-11.9	3.[illegible]
44.0	13564	6.8	.02111	19.0	.07	165.0	207.3	346.9	207.32	0.0	0.0	0.0000	4.3	347.5	-4.2	.9
45.0	13942	10.4	.02154	29.0	.11	155.0	206.3	351.5	206.34	0.0	0.0	0.0000	3.5	171.6	3.4	-.5
45.5	14139	10.0	.02180	27.9	.11	150.0	206.2	354.6	206.23	0.0	0.0	0.0000	5.0	182.1	5.0	.2
46.0	14303	9.7	.02201	27.0	.11	146.0	206.1	357.2	206.14	0.0	0.0	0.0000	6.3	186.8	6.[illegible]	.8
47.0	14730	8.9	.02253	25.0	.11	136.0	205.7	363.8	205.73	0.0	0.0	0.0000	5.8	184.3	5.[illegible]	.4
48.0	15185	8.2	.02305	23.4	.11	126.0	201.9	364.9	201.92	0.0	0.0	0.0000	12.1	158.4	11.2	-4.4
48.1	15231	8.2	.02310	23.5	.11	125.0	201.7	365.4	201.70	0.0	0.0	0.0000	12.1	156.6	11.1	-4.8
49.0	15621	8.2	.02352	23.7	.12	117.0	199.9	368.9	199.86	0.0	0.0	0.0000	12.7	142.2	10.0	-7.8
50.0	16139	10.1	.02417	29.6	.16	107.0	196.7	372.4	196.66	0.0	0.0	0.0000	999.9	999.9	999.9	999.9

CALIBRATIONS APPLIED FOR PARTIAL PRESSURE OF OZONE
TOTAL INTEGRATED OZONE INVALID. BALLOON SHORT OF 20 MB HEIGHT

OZONAGRAM

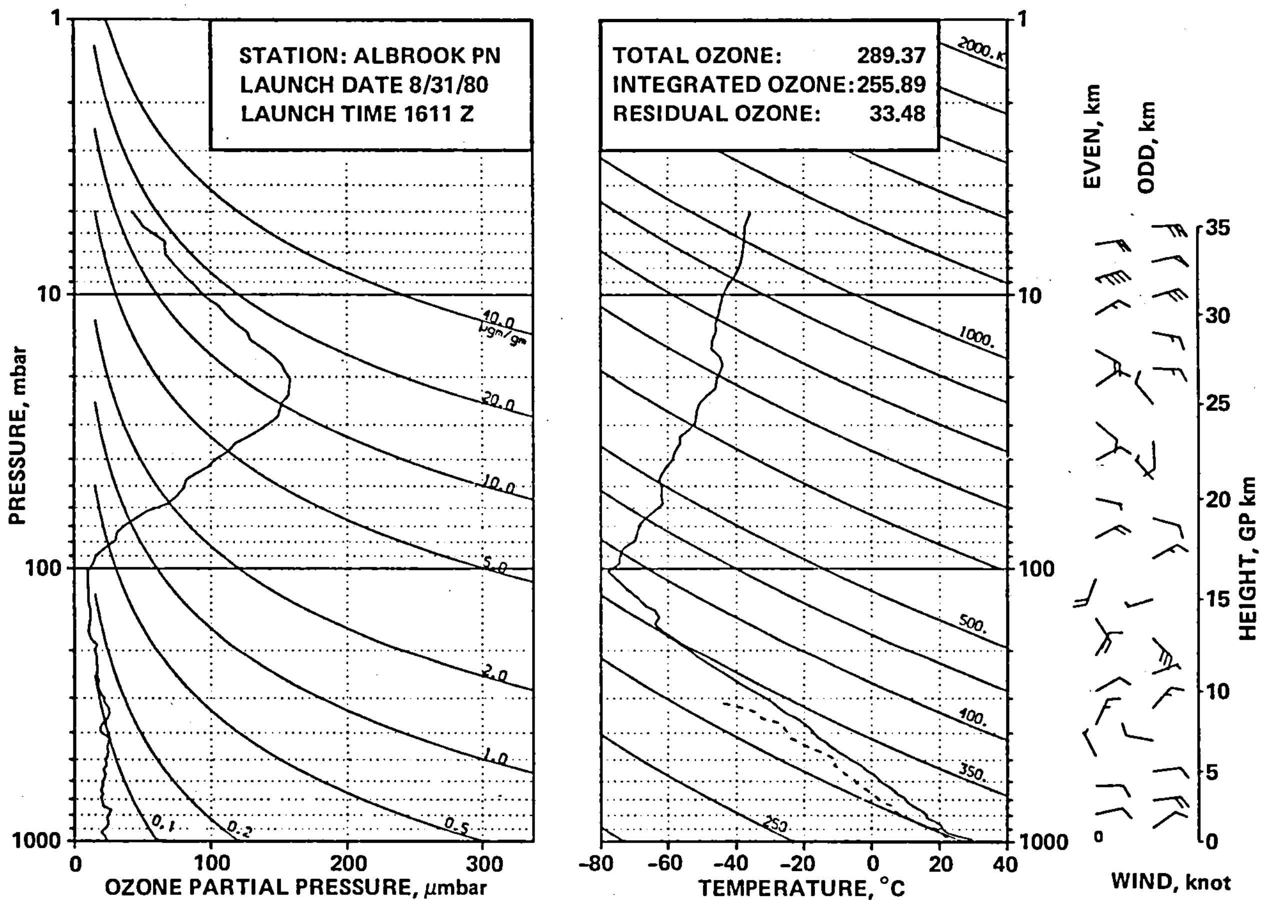
STATION: ALBROOK PN
LAUNCH DATE 8/31/80
LAUNCH TIME 1611 Z
TOTAL OZONE: 289.37
INTEGRATED OZONE: 255.89
RESIDUAL OZONE: 33.48
PRESSURE, mbar
1
10
100
1000
0
100
200
300
OZONE PARTIAL PRESSURE, μmbar
-80
-60
-40
-20
0
20
40
TEMPERATURE, °C
10.0 μgm/gm
20.0
10.0
5.0
2.0
1.0
0.5
0.2
0.1
2000. K
1000.
500.
400.
350.
250.
EVEN, km
ODD, km
HEIGHT, GP km
35
30
25
20
15
10
5
0
WIND, knot

STATION ALBROOK PN   LAUNCH DATE 8/31/80   TIME 1611Z   ECC   SONDE 3A1313

SURFACE CONDITIONS   PRESS 1005.2MB   TEMP 303.0 DEG K   HUMIDITY 65.0 PRCNT

TIME MIN	ALT GPM	OZONE MICMB	TOTOZ ATMCM	OZDEN MG/M3	OZMXR MICGG	PRESS MB	TEMP DEG K	PTEMP DEG K	VTEMP DEG K	HMDTY PRCNT	DEWPT DEG K	SPCFC HMDTY	SPD MPS	DIR DEG	NS MPS	EW MPS
0.0	66	22.9	0.00000	43.6	.04	1005.2	302.9	302.5	305.79	59.9	294.3	.0156	1.0	320.0	-.8	.6
.2	112	22.9	.00009	43.7	.04	1000.0	302.9	302.9	305.86	62.2	294.8	.0168	1.2	334.6	-1.0	.5
1.0	293	23.0	.00046	43.9	.04	980.0	302.7	304.4	306.12	71.0	296.8	.0187	2.2	1.6	-2.2	-.1
2.0	550	21.6	.00097	41.8	.04	952.0	298.3	302.5	301.31	79.2	294.4	.0166	2.8	27.1	-2.5	-1.3
3.0	802	19.2	.00143	37.5	.03	925.0	295.3	302.0	298.34	92.6	294.1	.0168	3.2	41.7	-2.4	-2.1
3.9	1040	21.9	.00188	43.1	.04	900.0	294.1	303.1	296.92	90.9	292.6	.0156	4.3	52.5	-2.6	-3.4
4.0	1060	22.2	.00192	43.5	.04	898.0	294.0	303.2	296.80	90.8	292.4	.0156	4.4	53.2	-2.6	-3.5
5.0	1334	24.4	.00250	48.0	.05	870.0	293.6	305.5	295.76	71.1	288.1	.0122	6.0	68.4	-2.2	-5.5
5.7	1534	24.4	.00295	48.3	.05	850.0	292.2	306.0	294.16	69.3	286.4	.0109	6.6	74.6	-1.8	-6.4
6.0	1606	24.4	.00311	48.4	.05	843.0	291.7	306.2	293.59	68.7	285.8	.0108	6.9	76.4	-1.6	-6.7
7.0	1863	23.5	.00368	47.0	.05	818.0	289.4	306.5	291.12	68.9	283.7	.0097	6.4	77.2	-1.4	-6.2
7.7	2052	24.6	.00410	49.1	.05	800.0	289.3	308.3	290.83	62.1	282.0	.0086	5.9	77.5	-1.3	-5.7
8.0	2138	25.1	.00430	50.0	.05	792.0	289.2	309.1	290.70	59.1	281.2	.0085	5.7	77.6	-1.2	-5.5
9.0	2410	26.7	.00495	53.6	.06	767.0	287.6	310.3	289.00	59.1	279.7	.0079	6.7	85.1	-.6	-6.7
10.0	2700	20.8	.00560	42.1	.05	741.0	285.5	311.0	286.93	67.9	279.7	.0082	8.9	86.5	-.5	-8.9
11.0	3010	20.2	.00620	41.0	.05	714.0	283.6	312.3	284.76	58.9	275.9	.0065	9.4	82.8	-1.2	-9.4
11.6	3174	19.6	.00650	40.0	.05	700.0	283.2	313.6	284.31	58.3	275.4	.0063	8.7	82.0	-1.2	-8.6
12.0	3294	19.2	.00673	39.2	.05	690.0	282.9	314.5	283.99	57.9	275.0	.0063	8.2	81.4	-1.2	-8.1
13.0	3537	20.6	.00719	42.4	.05	670.0	280.9	315.0	281.91	58.6	273.3	.0057	7.4	81.8	-1.0	-7.3
14.0	3799	19.0	.00769	39.2	.05	649.0	279.7	316.5	280.62	58.5	272.1	.0054	6.8	81.3	-1.0	-6.7
15.0	4068	20.4	.00820	42.4	.05	628.0	278.3	317.9	279.15	56.2	270.3	.0049	5.9	89.3	-.1	-5.9
16.0	4345	20.5	.00875	42.8	.06	607.0	276.3	318.7	277.05	57.5	268.7	.0045	4.9	88.8	-.1	-4.9
16.3	4438	20.9	.00894	43.7	.06	600.0	275.9	319.3	276.66	57.7	268.4	.0044	4.9	86.3	-.3	-4.9
17.0	4630	21.7	.00933	45.5	.06	586.0	275.1	320.5	275.87	58.1	267.8	.0043	4.9	81.0	-.8	-4.8
18.0	4924	22.5	.00997	47.4	.07	565.0	273.7	322.2	274.30	53.7	265.4	.0038	6.0	87.5	-.3	-6.0
19.0	5227	21.0	.01062	44.6	.06	544.0	271.5	323.0	272.04	57.3	264.1	.0035	5.3	76.3	-1.3	-5.2
20.0	5524	23.4	.01127	49.9	.07	524.0	270.2	325.0	270.73	53.7	262.2	.0031	3.1	47.1	-2.1	-2.3
21.0	5846	22.5	.01201	48.6	.07	503.0	267.5	325.5	268.04	70.5	263.0	.0035	2.9	343.6	-2.8	.8
21.2	5892	22.8	.01212	49.2	.08	500.0	267.2	325.7	267.72	70.2	262.6	.0033	3.0	340.7	-2.8	1.0
22.0	6114	23.9	.01264	52.0	.08	486.0	265.7	326.5	266.19	68.6	260.9	.0031	3.7	330.0	-3.2	1.9
23.0	6390	24.5	.01332	53.7	.09	469.0	263.5	327.1	263.91	65.4	258.3	.0025	2.3	329.5	-2.0	1.2
24.0	6691	23.7	.01407	52.4	.09	451.0	261.5	328.3	261.81	57.1	254.7	.0020	3.5	285.5	-.9	3.4
25.0	6984	24.6	.01480	54.7	.09	434.0	259.8	329.8	260.07	52.1	252.1	.0016	4.5	271.7	-.1	4.5
26.0	7268	25.5	.01554	57.1	.10	418.0	257.6	330.5	257.79	48.6	249.2	.0013	2.9	302.3	-1.5	2.4
27.0	7599	19.3	.01632	43.5	.08	400.0	256.1	332.7	256.27	51.3	248.4	.0013	3.8	3.0	-3.7	-.2
28.0	7885	18.4	.01689	41.6	.08	385.0	255.1	335.1	255.30	50.6	247.4	.0012	5.4	23.7	-5.0	-2.2
29.0	8181	20.4	.01750	46.4	.09	370.0	253.2	336.4	253.40	56.2	246.8	.0012	7.3	27.0	-6.5	-3.3
30.0	8507	24.1	.01827	55.3	.11	354.0	251.1	337.8	251.17	37.7	240.6	.0007	7.3	37.2	-5.8	-4.4
30.3	8589	24.4	.01849	56.4	.12	350.0	250.2	337.7	250.27	40.5	240.4	.0007	7.3	37.8	-5.8	-4.5
31.0	8801	25.4	.01906	59.2	.12	340.0	247.9	337.4	247.97	47.6	240.0	.0007	7.2	39.3	-5.6	-4.6
32.0	9105	24.7	.01989	57.9	.13	326.0	246.0	339.9	246.08	36.4	235.6	.0005	7.3	41.4	-5.5	-4.8
33.0	9466	21.7	.02081	51.3	.12	310.0	243.8	340.6	243.79	20.1	228.1	.0002	5.6	47.4	-3.8	-4.1
33.8	9698	21.1	.02136	50.3	.12	300.0	241.9	341.3	241.95	0.0	0.0	0.0000	4.7	48.6	-3.1	-3.5
34.0	9770	20.9	.02153	50.0	.12	297.0	241.4	341.5	241.39	0.0	0.0	0.0000	4.4	49.0	-2.9	-3.3
35.0	10084	18.6	.02223	45.1	.11	284.0	238.6	341.8	238.59	0.0	0.0	0.0000	5.3	61.4	-2.5	-4.6
36.0	10409	16.8	.02288	41.2	.10	271.0	235.6	342.1	235.62	24.7	222.9	.0001	5.4	70.1	-1.8	-5.1
37.0	10719	17.6	.02350	43.6	.11	259.0	233.0	342.8	233.01	0.0	0.0	0.0000	4.3	73.4	-1.2	-4.1
37.7	10958	16.6	.02397	41.3	.11	250.0	231.1	343.4	231.09	0.0	0.0	0.0000	3.7	70.3	-1.2	-3.5
38.0	11068	16.1	.02418	40.3	.11	246.0	230.2	343.7	230.22	0.0	0.0	0.0000	3.4	68.5	-1.2	-3.2
39.0	11403	16.8	.02483	42.7	.12	234.0	227.4	344.3	227.36	0.0	0.0	0.0000	3.8	66.6	-1.5	-3.5
40.0	11751	16.0	.02551	41.3	.12	222.0	224.4	345.0	224.41	0.0	0.0	0.0000	5.1	36.9	-4.1	-3.1
41.0	12113	16.0	.02622	41.7	.13	210.0	221.4	345.7	221.35	0.0	0.0	0.0000	5.9	28.9	-5.1	-2.8
41.9	12427	14.6	.02680	38.3	.12	200.0	219.6	347.9	219.63	0.0	0.0	0.0000	6.0	80.0	-1.0	-5.9
42.0	12460	14.4	.02686	37.9	.12	199.0	219.5	348.1	219.45	0.0	0.0	0.0000	6.2	84.4	-.6	-6.2
43.0	12755	16.4	.02742	43.5	.14	190.0	217.0	348.8	216.99	0.0	0.0	0.0000	10.9	118.4	5.2	-9.5
44.0	13096	11.8	.02802	31.6	.11	180.0	214.8	350.6	214.77	0.0	0.0	0.0000	14.5	138.3	10.9	-9.7
45.0	13453	10.2	.02852	27.9	.10	170.0	211.7	351.3	211.72	0.0	0.0	0.0000	16.6	151.7	14.6	-7.9
46.0	13826	10.9	.02902	30.1	.11	160.0	209.3	353.2	209.25	0.0	0.0	0.0000	15.6	150.9	13.7	-7.6
47.0	14181	11.7	.02954	32.0	.13	151.0	210.6	361.4	210.60	0.0	0.0	0.0000	8.2	144.8	6.7	-4.7
47.1	14221	11.7	.02960	32.0	.13	150.0	210.5	361.9	210.45	0.0	0.0	0.0000	7.3	146.6	6.1	-4.0
48.0	14558	11.7	.03011	32.2	.14	142.0	209.3	365.5	209.25	0.0	0.0	0.0000	2.0	230.0	1.3	1.6
49.0	14776	10.8	.03042	30.1	.13	137.0	206.6	364.6	206.64	0.0	0.0	0.0000	3.6	257.2	.8	3.5
50.0	15184	10.1	.03098	28.4	.13	128.0	204.3	367.6	204.29	0.0	0.0	0.0000	3.5	251.4	1.1	3.4
50.3	15324	10.1	.03117	28.6	.13	125.0	203.2	368.1	203.24	0.0	0.0	0.0000	4.4	231.1	2.7	3.4
51.0	15616	10.0	.03156	28.8	.14	119.0	201.1	369.4	201.07	0.0	0.0	0.0000	7.0	209.8	6.1	3.5
52.0	16075	9.7	.03217	28.3	.15	110.0	198.1	372.1	198.07	0.0	0.0	0.0000	11.2	200.6	10.5	3.9
53.0	16510	9.7	.0327[illegible]	28.6	.16	102.0	195.3	375.0	195.34	0.0	0.0	0.0000	5.9	184.3	5.9	.4
53.3	16623	11.0	.032[illegible]3	32.2	.18	100.0	196.4	379.3	196.44	0.0	0.0	0.0000	3.5	153.4	3.1	-1.6
54.0	16847	13.5	.03329	39.2	.23	96.2	198.6	387.7	198.59	0.0	0.0	0.0000	6.0	67.1	-2.3	-5.5
55.0	17234	15.7	.03405	45.6	.29	90.0	198.8	395.6	198.84	0.0	0.0	0.0000	10.6	55.1	-6.0	-8.7
56.0	17622	22.2	.03505	64.3	.44	84.2	199.9	405.3	199.85	0.0	0.0	0.0000	11.9	59.1	-6.1	-10.2
56.8	17923	28.6	.03611	81.4	.59	80.0	202.7	417.1	202.70	0.0	0.0	0.0000	11.7	59.9	-5.9	-10.1
57.0	17998	30.2	.03637	85.6	.63	79.0	203.4	420.1	203.39	0.0	0.0	0.0000	11.7	60.1	-5.8	-10.1
58.0	18388	31.0	.03795	87.6	.69	74.0	204.1	429.4	204.06	0.0	0.0	0.0000	9.4	68.5	-3.4	-8.8
58.8	18720	36.2	.03944	102.3	.86	70.0	204.6	437.4	204.61	0.0	0.0	0.0000	6.9	84.4	-.7	-6.9
59.0	18789	37.3	.03975	105.3	.89	69.2	204.7	439.1	204.72	0.0	0.0	0.0000	6.5	89.0	-.1	-6.5
60.0	19138	45.5	.04165	127.1	1.15	65.3	206.6	450.6	206.64	0.0	0.0	0.0000	4.4	109.8	1.5	-4.1
61.0	19483	53.0	.04385	146.4	1.42	61.7	209.1	463.3	209.06	0.0	0.0	0.0000	3.6	93.3	.2	-3.6
61.5	19655	59.9	.04519	164.3	1.66	60.0	210.3	469.8	210.26	0.0	0.0	0.0000	3.8	93.4	.2	-3.8
62.0	19864	68.2	.04681	186.0	1.95	58.0	211.7	477.6	211.72	0.0	0.0	0.0000	4.1	93.5	.2	-4.1
63.0	20283	75.3	.05065	205.6	2.30	54.2	211.3	486.1	211.35	0.0	0.0	0.0000	3.0	110.9	1.1	-2.8
64.0	20708	80.4	.05487	219.6	2.63	50.6	211.5	496.2	211.54	0.0	0.0	0.0000	1.2	256.6	.3	1.1
64.2	20781	80.7	.05563	220.5	2.68	50.0	211.4	497.5	211.36	0.0	0.0	0.0000	1.3	282.7	-.3	1.3

TIME MIN	ALT GPM	OZONE MICMB	TOTOZ ATMCM	OZDEN MG/M3	OZMXR MICGG	PRESS MB	TEMP DEG K	PTEMP DEG K	VTEMP DEG K	HMDTY PRCNT	DEWPT DEG K	SPCFC HMDTY	SPD MPS	DIR DEG	NS MPS	EW MPS
65.0	21111	82.0	.05905	224.7	2.86	47.4	210.6	503.3	210.60	0.0	0.0	0.0000	3.5	323.1	-2.8	2.1
66.0	21432	89.2	.06256	243.4	3.28	45.0	211.5	513.1	211.54	0.0	0.0	0.0000	4.4	1.0	-4.4	-.1
67.0	21772	98.0	.06661	266.0	3.81	42.6	212.8	524.3	212.82	0.0	0.0	0.0000	3.3	38.4	-2.6	-2.1
68.0	22166	103.6	.07162	278.7	4.29	40.0	214.6	538.3	214.60	0.0	0.0	0.0000	5.1	69.7	-1.8	-4.7
69.0	22572	112.9	.07713	302.8	4.99	37.5	215.3	550.1	215.29	0.0	0.0	0.0000	4.9	105.6	1.3	-4.8
70.0	23008	118.4	.08343	315.3	5.61	35.0	216.8	565.1	216.82	0.0	0.0	0.0000	5.4	174.8	5.4	-.5
71.0	23362	128.0	.08886	340.8	6.41	33.1	216.8	574.1	216.82	0.0	0.0	0.0000	4.9	187.8	4.9	.7
72.0	23760	137.1	.09537	360.7	7.30	31.1	219.5	591.5	219.45	0.0	0.0	0.0000	4.2	140.2	3.2	-2.7
72.6	23991	141.5	.09937	370.4	7.82	30.0	220.5	600.6	220.51	0.0	0.0	0.0000	4.0	132.7	2.7	-2.9
73.0	24144	144.3	.10199	376.7	8.16	29.3	221.2	606.5	221.20	0.0	0.0	0.0000	3.9	127.5	2.4	-3.1
74.0	24438	149.5	.10726	389.9	8.85	28.0	221.4	614.8	221.35	0.0	0.0	0.0000	.9	131.4	.6	-.7
75.0	24819	151.0	.11423	393.2	9.47	26.4	221.7	626.1	221.66	0.0	0.0	0.0000	4.1	311.6	-2.8	3.1
75.9	25172	152.3	.12075	395.2	10.10	25.0	222.5	638.4	222.53	0.0	0.0	0.0000	4.5	324.0	-3.7	2.7
76.0	25199	152.4	.12123	395.3	10.14	24.9	222.[illegible]	639.3	222.59	0.0	0.0	0.0000	4.6	324.8	-3.7	2.6
77.0	25605	157.4	.12883	404.8	11.15	23.4	224.6	656.6	224.56	0.0	0.0	0.0000	3.4	16.4	-3.2	-1.0
78.0	26013	157.7	.13650	401.0	11.88	22.0	227.1	675.7	227.07	0.0	0.0	0.0000	4.3	52.8	-2.6	-3.4
79.0	26515	158.8	.14593	403.0	12.90	20.4	227.5	691.8	227.50	0.0	0.0	0.0000	4.8	80.0	-.8	-4.7
79.3	26647	157.6	.14838	399.5	13.06	20.0	227.8	696.6	227.81	0.0	0.0	0.0000	5.2	83.2	-.6	-5.1
80.0	26954	154.9	.15407	391.3	13.44	19.1	228.5	708.0	228.51	0.0	0.0	0.0000	6.2	89.0	-.1	-6.2
81.0	27351	152.2	.16126	383.3	14.01	18.0	229.2	722.4	229.23	0.0	0.0	0.0000	8.8	101.3	1.7	-8.7
81.4	27539	149.9	.16459	378.1	14.19	17.5	228.8	727.0	228.84	0.0	0.0	0.0000	9.3	105.3	2.5	-9.0
82.0	27773	147.0	.16870	371.6	14.41	16.9	228.4	732.7	228.37	0.0	0.0	0.0000	10.0	109.7	3.4	-9.4
83.0	28220	139.3	.17631	356.1	14.61	15.8	225.9	738.9	225.90	0.0	0.0	0.0000	10.2	123.4	5.6	-8.5
83.7	28563	132.4	.18182	338.1	14.62	15.0	226.1	750.7	226.11	0.0	0.0	0.0000	8.5	122.2	4.5	-7.2
84.0	28697	129.7	.18397	331.1	14.62	14.7	226.2	755.3	226.19	0.0	0.0	0.0000	7.9	121.6	4.1	-6.7
85.0	29164	127.1	.19110	323.0	15.37	13.7	227.2	774.1	227.21	0.0	0.0	0.0000	7.3	94.7	.6	-7.3
86.0	29616	119.1	.19771	302.8	15.42	12.8	227.1	788.8	227.07	0.0	0.0	0.0000	7.7	83.6	-.9	-7.6
86.3	29773	116.8	.19987	296.6	15.47	12.5	227.4	795.2	227.35	0.0	0.0	0.0000	7.2	75.9	-1.8	-7.0
87.0	30101	112.0	.20435	283.6	15.59	11.9	227.9	808.5	227.94	0.0	0.0	0.0000	6.7	57.1	-3.6	-5.6
88.0	30626	106.2	.21112	268.4	16.00	11.0	228.5	828.9	228.51	0.0	0.0	0.0000	13.6	67.5	-5.2	-12.5
89.0	31198	95.3	.21791	239.9	15.63	10.1	229.2	852.0	229.23	0.0	0.0	0.0000	16.7	74.8	-4.4	-16.2
89.1	31264	94.5	.21863	237.8	15.65	10.0	229.4	855.1	229.40	0.0	0.0	0.0000	16.9	74.5	-4.5	-16.3
90.0	31753	88.8	.22390	222.2	15.82	9.3	230.6	877.7	230.64	0.0	0.0	0.0000	18.4	71.8	-5.7	-17.5
91.0	32284	81.3	.22915	201.6	15.66	8.6	232.7	905.7	232.73	0.0	0.0	0.0000	26.1	72.6	-7.8	-24.9
91.7	32778	75.5	.23356	186.3	15.62	8.0	234.0	929.6	233.95	0.0	0.0	0.0000	26.4	76.0	-6.4	-25.6
92.0	32951	73.4	.23511	180.9	15.60	7.8	234.4	937.9	234.38	0.0	0.0	0.0000	26.5	77.2	-5.9	-25.9
93.0	33597	66.4	.24030	163.2	15.50	7.1	235.1	966.3	235.06	0.0	0.0	0.0000	26.8	81.0	-4.2	-26.4
93.1	33694	66.4	.24104	163.1	15.73	7.0	235.1	970.6	235.14	0.0	0.0	0.0000	27.5	81.2	-4.2	-27.2
94.0	34312	66.3	.24573	162.6	17.17	6.4	235.6	997.7	235.60	0.0	0.0	0.0000	32.2	81.7	-4.6	-31.9
94.6	34757	57.6	.24871	141.2	15.82	6.0	235.7	1016.7	235.68	0.0	0.0	0.0000	35.0	84.8	-3.2	-34.8
95.0	35111	50.7	.25108	124.2	14.74	5.7	235.7	1031.8	235.74	0 0	0.0	0.0000	37.2	86.9	-2.0	-37.2
96.0	36019	42.4	.25589	103.1	14.05	5.0	237.5	1079.2	237.50	0.0	0.0	0.0000	999.9	999.9	999.9	999.9

INTEGRAL .25589 RESIDUAL .03348 INTEGRATED TOTAL OZONE .28937

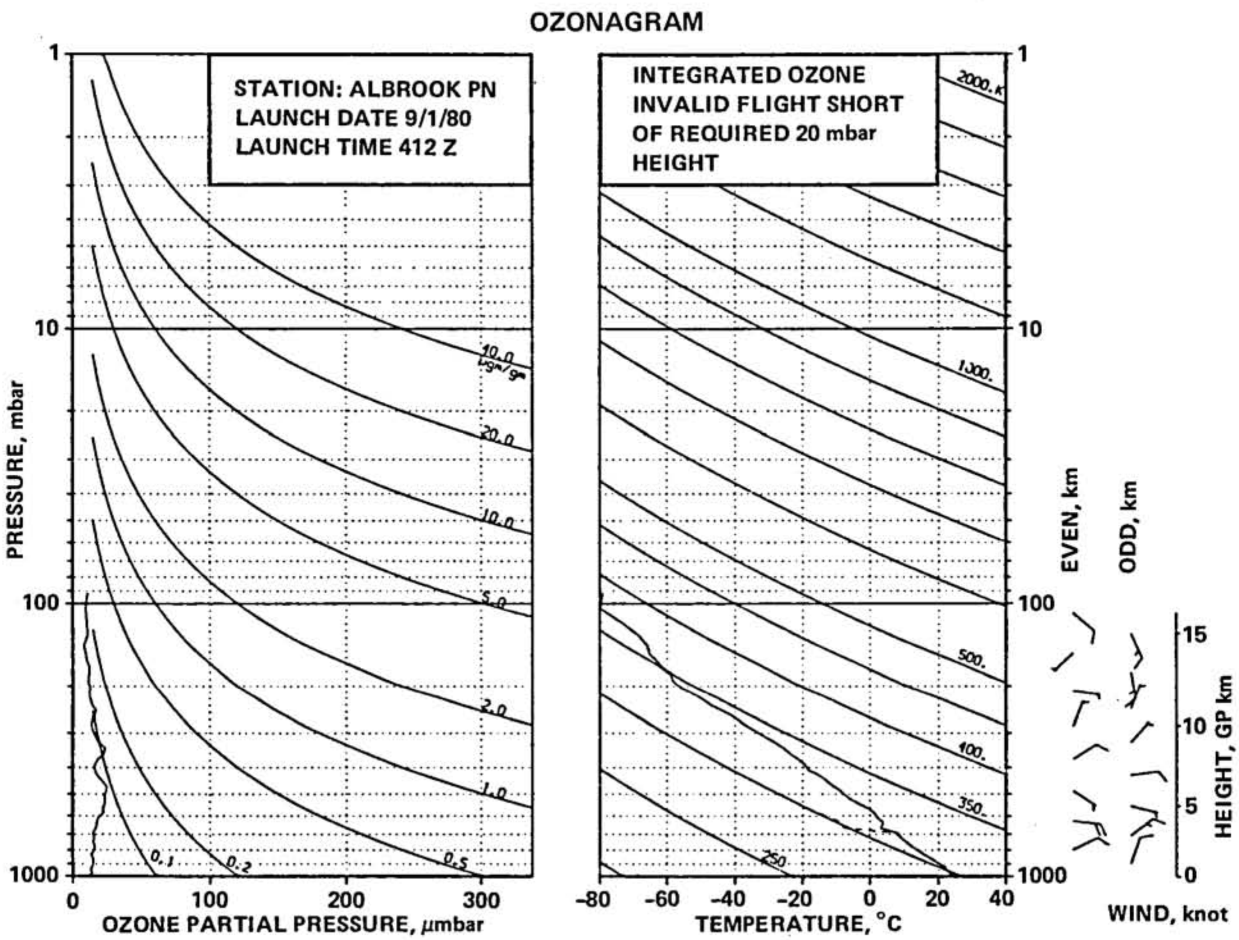
OZONAGRAM
STATION: ALBROOK PN
LAUNCH DATE 9/1/80
LAUNCH TIME 412 Z
INTEGRATED OZONE
INVALID FLIGHT SHORT
OF REQUIRED 20 mbar
HEIGHT
PRESSURE, mbar
OZONE PARTIAL PRESSURE, μmbar
TEMPERATURE, °C
EVEN, km
ODD, km
HEIGHT, GP km
WIND, knot

STATION ALBROOK PN LAUNCH DATE 9/ 1/80 TIME 412Z ECC SONDE 3A1314

SURFACE CONDITIONS PRESS 1004.6MB TEMP 298.6 DEG K HUMIDITY 100.0 PRCNT

TIME MIN	ALT GPM	OZONE MICMB	TOTOZ ATMCM	OZDEN MG/M3	OZMXR MICGG	PRESS MB	TEMP DEG K	PTEMP DEG K	VTEMP DEG K	HMDTY PRCNT	DEWPT DEG K	SPCFC HMDTY	SPD MPS	DIR DEG	NS MPS	EW MPS
0.0	66	10.0	0.00000	19.4	.02	1004.6	298.5	298.1	302.13	98.5	298.2	.0199	2.0	270.0	0.0	2.0
.2	106	10.7	.00004	20.7	.02	1000.0	298.2	298.2	301.81	98.8	298.0	.0196	2.3	289.8	-.8	2.1
1.0	329	14.3	.00029	27.9	.02	975.0	296.6	298.8	300.02	100.0	296.6	.0186	5.8	330.1	-5.0	2.9
2.0	584	12.9	.00060	25.2	.02	947.0	295.5	300.2	298.61	95.6	294.8	.0171	6.7	349.0	-6.6	1.3
3.0	855	14.3	.00093	28.1	.03	918.0	294.9	302.1	297.91	95.8	294.2	.0170	5.9	15.4	-5.7	-1.6
3.6	1026	14.8	.00116	29.1	.03	900.0	293.6	302.6	296.56	98.5	293.3	.0163	5.3	18.1	-5.0	-1.6
4.0	1124	15.1	.00129	29.7	.03	890.0	292.9	302.8	295.79	100.0	292.9	.0162	5.0	19.9	-4.7	-1.7
5.0	1419	15.1	.00170	29.9	.03	860.0	291.0	303.8	293.65	100.0	291.0	.0149	3.9	20.0	-3.7	-1.3
5.4	1518	14.6	.00183	29.0	.03	850.0	290.3	304.1	292.83	100.0	290.3	.0141	3.5	26.7	-3.1	-1.6
6.0	1702	13.6	.00208	27.3	.03	832.0	289.0	304.6	291.35	100.0	289.0	.0135	2.8	44.1	-2.0	-1.9
7.0	2003	15.8	.00249	31.8	.03	803.0	287.2	305.8	289.37	100.0	287.2	.0125	4.2	64.7	-1.8	-3.8
7.1	2034	15.9	.00254	31.9	.03	800.0	287.0	305.9	289.15	100.0	287.0	.0123	4.4	64.4	-1.9	-4.0
8.0	2270	16.5	.00289	33.4	.04	778.0	285.5	306.7	287.46	100.0	285.5	.0115	5.6	62.6	-2.6	-4.9
9.0	2577	15.2	.00335	30.9	.03	750.0	284.0	308.3	285.82	100.0	284.0	.0108	5.8	59.6	-2.9	-5.0
10.0	2894	15.8	.00382	32.4	.04	722.0	282.3	309.8	284.03	100.0	282.3	.0100	7.5	48.8	-4.9	-5.7
10.8	3150	15.2	.00419	31.2	.04	700.0	281.5	311.7	283.17	100.0	281.5	.0097	8.7	54.5	-5.0	-7.1
11.0	3234	15.0	.00431	30.8	.04	693.0	281.2	312.3	282.90	100.0	281.2	.0097	9.1	56.1	-5.1	-7.5
12.0	3584	17.2	.00486	35.9	.04	664.0	276.4	310.7	276.95	44.9	265.6	.0032	9.5	71.6	-3.0	-9.0
13.0	3946	17.9	.00548	37.3	.05	635.0	277.2	315.7	277.78	39.8	264.8	.0032	10.8	95.0	.9	-10.8
14.0	4284	18.6	.00608	39.0	.05	609.0	275.4	317.3	275.83	34.0	261.2	.0025	8.2	99.7	1.4	-8.1
14.3	4403	20.0	.00632	42.0	.06	600.0	275.1	318.3	275.48	31.6	260.0	.0022	6.4	99.1	1.0	-6.3
15.0	4649	22.8	.00682	48.0	.06	582.0	274.4	320.3	274.75	26.8	257.4	.0019	2.7	94.9	.2	-2.7
16.0	4915	22.1	.00741	46.8	.07	563.0	272.8	321.5	272.97	0.0	0.0	0.0000	2.5	86.7	-.1	-2.5
17.0	5188	23.4	.00803	50.1	.07	544.0	270.2	321.5	270.47	34.4	256.7	.0019	.8	117.8	.4	-.7
18.0	5453	23.4	.00865	50.5	.07	526.0	267.9	321.8	268.28	52.1	259.6	.0025	1.3	204.9	1.2	.5
19.0	5771	23.4	.00940	50.9	.08	505.0	265.8	323.1	266.18	57.1	258.8	.0025	1.2	90.9	0.0	-1.2
19.3	5848	23.8	.00959	51.8	.08	500.0	265.4	323.6	265.83	57.1	258.4	.0024	1.4	103.2	.3	-1.3
20.0	6069	24.9	.01013	54.3	.08	486.0	264.5	325.0	264.83	56.9	257.5	.0023	2.1	123.6	1.2	-1.7
21.0	6377	24.9	.01092	54.8	.09	467.0	262.3	326.0	262.60	53.3	254.7	.0019	2.9	134.2	2.0	-2.1
22.0	6729	21.4	.01176	47.4	.08	446.0	260.2	327.7	260.42	50.4	252.1	.0016	4.2	96.7	.5	-4.2
23.0	7113	17.8	.01254	39.8	.07	424.0	257.7	329.2	257.94	65.1	252.6	.0017	5.9	79.9	-1.0	-5.8
24.0	7402	16.3	.01305	36.9	.07	408.0	254.9	329.3	255.17	71.2	251.0	.0016	5.2	84.8	-.5	-5.2
24.5	7549	16.3	.01331	37.0	.07	400.0	254.5	330.6	254.68	67.6	250.0	.0014	4.8	80.8	-.8	-4.8
25.0	7700	16.3	.01357	37.1	.07	392.0	254.0	331.9	254.18	64.0	248.9	.0014	4.5	76.0	-1.1	-4.3
26.0	8028	18.4	.01417	42.1	.08	375.0	252.1	333.6	252.22	45.6	243.5	.0009	5.2	58.3	-2.7	-4.4
27.0	8348	22.7	.01488	52.4	.10	359.0	249.7	334.6	249.78	39.4	239.8	.0006	6.2	58.8	-3.2	-5.3
27.5	8532	23.4	.01535	54.2	.11	350.0	248.6	335.6	248.72	37.3	238.2	.0005	5.7	59.0	-3.0	-4.9
28.0	8722	24.1	.01583	56.1	.12	341.0	247.6	336.6	247.63	35.1	236.7	.0005	5.2	59.3	-2.7	-4.5
29.0	9090	19.1	.01670	45.0	.10	324.0	244.8	337.8	244.85	43.5	236.3	.0005	3.3	39.0	-2.5	-2.1
30.0	9450	16.9	.01742	40.4	.09	308.0	241.7	338.4	241.79	47.3	234.2	.0004	2.2	34.3	-1.8	-1.2
30.5	9634	15.9	.01775	38.2	.09	300.0	240.2	338.9	240.30	46.1	232.6	.0003	1.9	26.9	-1.7	-.8
31.0	9849	14.7	.01813	35.7	.08	291.0	238.5	339.4	238.58	44.7	230.8	.0003	1.6	15.0	-1.5	-.4
32.0	10191	13.9	.01868	33.9	.08	277.0	235.6	340.0	235.59	26.5	223.4	.0001	2.8	25.3	-2.6	-1.2
33.0	10599	15.2	.01937	37.8	.10	261.0	232.8	341.8	232.84	0.0	0.0	0.0000	4.1	31.3	-3.5	-2.1
33.8	10889	17.0	.01992	42.8	.11	250.0	230.0	341.8	230.02	0.0	0.0	0.0000	2.7	22.0	-2.5	-1.0
34.0	10944	17.4	.02002	43.7	.12	248.0	229.5	341.8	229.49	0.0	0.0	0.0000	2.5	19.1	-2.3	-.8
35.0	11246	14.5	.02059	37.0	.10	237.0	226.2	341.3	226.18	0.0	0.0	0.0000	2.5	20.9	-2.3	-.9
36.0	11617	13.0	.02121	33.7	.10	224.0	223.4	342.5	223.35	0.0	0.0	0.0000	2.8	32.9	-2.4	-1.5
37.0	11974	12.3	.02176	32.1	.10	212.0	220.3	343.1	220.26	0.0	0.0	0.0000	2.7	94.3	.2	-2.7
38.0	12283	13.0	.02224	34.5	.11	202.0	217.2	343.0	217.18	0.0	0.0	0.0000	4.4	108.3	1.4	-4.2
38.2	12345	12.7	.02233	33.8	.10	200.0	216.8	343.3	216.78	0.0	0.0	0.0000	4.3	110.1	1.5	-4.0
39.0	12604	11.5	.02273	30.7	.10	192.0	215.1	344.8	215.15	0.0	0.0	0.0000	3.9	118.7	1.9	-3.4
40.0	12940	12.1	.02322	32.5	.11	182.0	214.3	348.6	214.28	0.0	0.0	0.0000	5.8	162.4	5.5	-1.7
41.0	13292	12.7	.02378	34.6	.12	172.0	211.8	350.2	211.76	0.0	0.0	0.0000	8.5	184.2	8.5	.6
42.0	13662	10.5	.02433	28.9	.11	162.0	210.1	353.4	210.08	0.0	0.0	0.0000	7.1	209.9	6.2	3.5
43.0	14052	9.7	.02483	27.1	.11	152.0	207.9	356.2	207.93	0.0	0.0	0.0000	3.3	228.7	2.2	2.5
43.2	14132	9.5	.02493	26.3	.10	150.0	207.8	357.3	207.81	0.0	0.0	0.0000	2.8	215.7	2.3	1.6
44.0	14465	8.3	.02532	23.1	.10	142.0	207.3	362.1	207.32	0.0	0.0	0.0000	3.3	143.1	2.6	-2.0
45.0	14997	11.2	.02600	31.7	.14	130.0	204.6	366.5	204.59	0.0	0.0	0.0000	7.2	153.7	6.4	-3.2
45.4	15229	10.9	.02634	31.1	.14	125.0	202.7	367.2	202.72	0.0	0.0	0.0000	6.9	162.2	6.6	-2.1
46.0	15570	10.5	.02683	30.2	.15	118.0	200.0	368.2	199.97	0.0	0.0	0.0000	6.9	175.2	6.9	-.6
47.0	16297	9.6	.02783	28.7	.15	104.0	193.2	368.8	193.16	0.0	0.0	0.0000	4.2	108.3	1.3	-4.0
47.3	16519	10.0	.02815	29.9	.17	100.0	193.4	373.5	193.43	0.0	0.0	0.0000	999.9	999.9	999.9	999.9
48.0	17054	11.0	.02892	32.8	.20	91.0	194.1	384.9	194.06	0.0	0.0	0.0000	999.9	999.9	999.9	999.9

CALIBRATIONS APPLIED FOR PARTIAL PRESSURE OF OZONE
TOTAL INTEGRATED OZONE INVALID. BALLOON SHORT OF 20 MB HEIGHT

OZONAGRAM

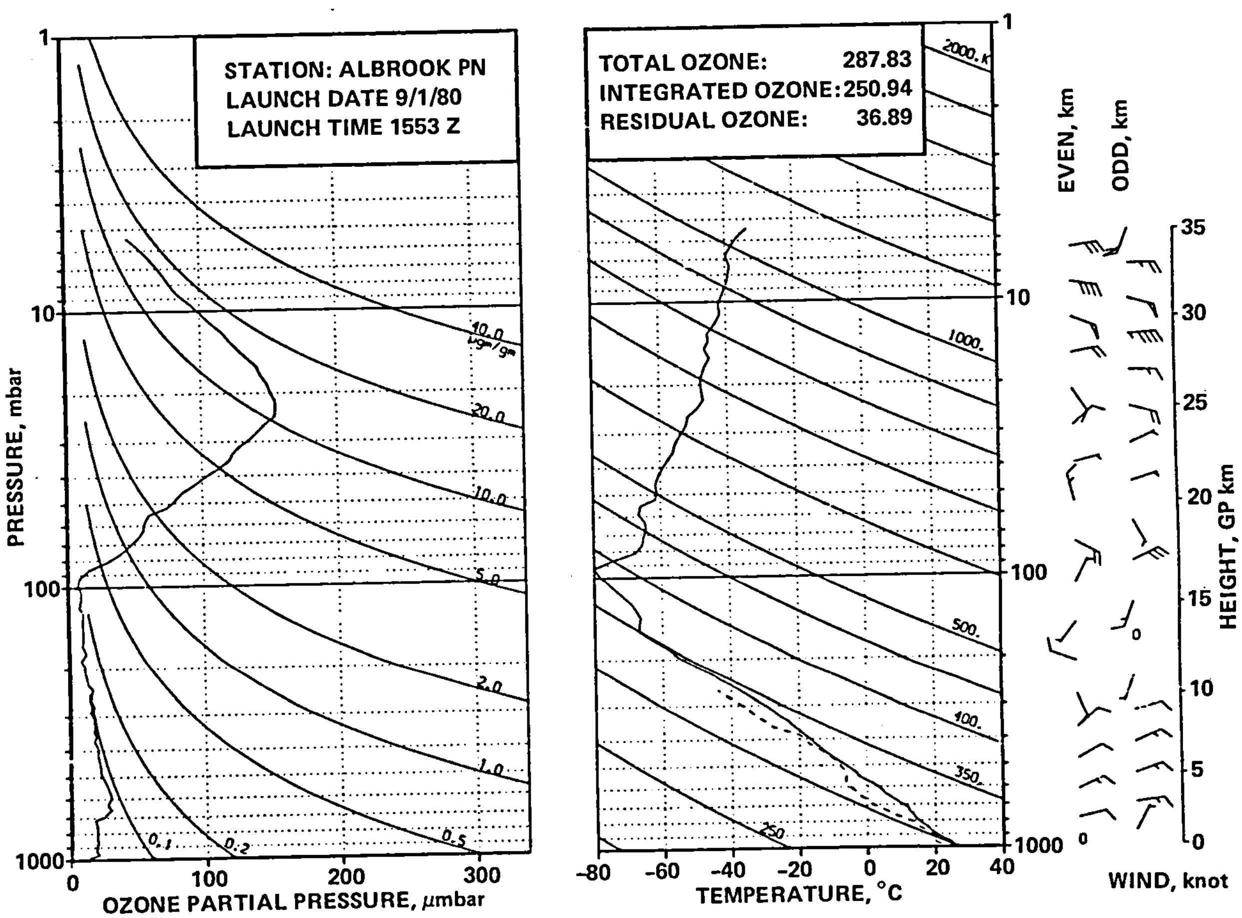
STATION: ALBROOK PN
LAUNCH DATE 9/1/80
LAUNCH TIME 1553 Z
TOTAL OZONE: 287.83
INTEGRATED OZONE: 250.94
RESIDUAL OZONE: 36.89
PRESSURE, mbar
OZONE PARTIAL PRESSURE, μmbar
TEMPERATURE, °C
EVEN, km
ODD, km
HEIGHT, GP km
WIND, knot
10.0 μg/g
20.0
10.0
5.0
2.0
1.0
0.5
0.2
0.1
2000. K
1000.
500.
400.
350.
250
1
10
100
1000
0
100
200
300
-80
-60
-40
-20
0
20
40
35
30
25
20
15
10
5
0

STATION ALBROOK PN   LAUNCH DATE 9/ 1/80   TIME 1553Z   ECC   SONDE 3A1315

SURFACE CONDITIONS   PRESS 1005.2MB   TEMP 300.0 DEG K   HUMIDITY 90.0 PRCNT

TIME MIN	ALT GPM	OZONE MICMB	TOTOZ ATMCM	OZDEN MG/M3	OZMXR MICGG	PRESS MB	TEMP DEG K	PTEMP DEG K	VTEMP DEG K	HMDTY PRCNT	DEWPT DEG K	SPCFC HMDTY	SPD MPS	DIR DEG	NS MPS	EW MPS
0.0	66	15.7	0.00000	30.1	.03	1005.2	299.8	299.4	303.55	92.2	298.5	.0202	1.0	320.0	-.8	.6
.2	111	15.4	.00006	29.6	.03	1000.0	299.6	299.5	303.15	90.1	297.8	.0190	1.4	325.1	-1.2	.8
1.0	272	14.3	.00028	27.6	.02	982.0	298.6	300.2	301.77	82.8	295.5	.0172	2.9	331.1	-2.6	1.4
2.0	490	21.0	.00062	40.8	.04	958.0	297.7	301.3	300.44	75.7	293.1	.0152	2.3	17.1	-2.2	-.7
3.0	731	18.8	.00105	36.8	.03	932.0	295.6	301.6	298.60	92.1	294.2	.0168	3.4	23.5	-3.2	-1.4
4.0	958	19.5	.00145	38.3	.04	908.0	294.0	302.2	296.84	93.5	292.9	.0159	4.0	25.0	-3.6	-1.7
4.4	1034	19.5	.00158	38.4	.04	900.0	293.5	302.5	296.30	93.5	292.4	.0154	3.9	27.1	-3.5	-1.8
5.0	1170	19.5	.00183	38.5	.04	886.0	292.7	303.0	295.34	93.5	291.6	.0150	3.7	31.1	-3.2	-1.9
6.0	1387	20.2	.00222	40.0	.04	864.0	291.6	304.0	294.08	91.2	290.1	.0140	2.6	38.4	-2.0	-1.6
6.7	1527	19.8	.00248	39.3	.04	850.0	291.2	305.0	293.52	87.1	289.0	.0130	2.1	42.1	-1.6	-1.4
7.0	1598	19.6	.00261	38.9	.04	843.0	290.9	305.5	293.23	85.0	288.4	.0128	1.9	44.6	-1.4	-1.4
8.0	1824	19.6	.00301	39.1	.04	821.0	289.5	306.3	291.79	92.2	288.2	.0130	3.0	35.9	-2.4	-1.7
9.0	2034	19.6	.00340	39.2	.04	801.0	288.5	307.3	290.52	85.9	286.1	.0117	4.3	75.1	-1.1	-4.2
9.0	2044	19.6	.00342	39.2	.04	800.0	288.4	307.4	290.45	85.6	286.0	.0115	4.4	76.3	-1.0	-4.3
10.0	2259	19.6	.00381	39.4	.04	780.0	287.3	308.4	289.06	79.9	283.8	.0103	6.1	93.5	.4	-6.1
11.0	2478	19.6	.00421	39.5	.04	760.0	286.9	310.3	288.40	68.3	281.1	.0088	6.7	87.6	-.3	-6.7
12.0	2736	19.0	.00468	38.5	.04	737.0	285.7	311.7	287.08	64.8	279.2	.0080	7.9	87.5	-.3	-7.9
13.0	2990	18.4	.00513	37.2	.04	715.0	285.3	314.0	286.49	55.2	276.6	.0068	8.5	84.6	-.8	-8.5
13.7	3167	23.4	.00549	47.7	.06	700.0	283.9	314.3	284.96	54.4	275.1	.0061	8.7	79.8	-1.5	-8.6
14.0	3227	25.1	.00561	51.2	.06	695.0	283.4	314.4	284.45	54.2	274.5	.0061	8.8	78.2	-1.8	-8.6
15.0	3457	27.1	.00618	55.4	.07	676.0	281.9	315.3	282.91	55.1	273.4	.0057	8.5	74.7	-2.2	-8.2
16.0	3705	30.3	.00686	62.4	.08	656.0	280.3	316.2	281.20	55.0	271.9	.0053	8.1	75.8	-2.0	-7.9
17.0	3946	27.6	.00754	57.3	.07	637.0	278.7	317.0	279.53	54.9	270.4	.0049	8.1	71.7	-2.5	-7.7
18.0	4193	28.3	.00820	58.9	.08	618.0	277.7	318.6	278.46	54.9	269.4	.0047	8.1	62.0	-3.8	-7.2
18.9	4433	30.1	.00889	63.0	.08	600.0	276.4	319.8	277.11	54.6	268.1	.0043	7.2	59.6	-3.6	-6.2
19.0	4447	30.2	.00893	63.2	.08	599.0	276.3	319.9	277.04	54.6	268.1	.0043	7.1	59.4	-3.6	-6.1
20.0	4679	30.0	.00961	63.0	.09	582.0	274.8	320.8	275.48	54.7	266.7	.0040	6.9	67.8	-2.6	-6.4
21.0	4874	29.3	.01018	62.1	.09	568.0	272.7	320.5	273.38	64.9	266.9	.0042	8.8	73.1	-2.6	-8.4
22.0	5116	28.1	.01087	59.9	.08	551.0	270.9	321.2	271.65	73.9	266.9	.0043	8.1	71.1	-2.6	-7.7
23.0	5439	26.8	.01175	57.3	.08	529.0	269.7	323.5	270.43	82.0	267.1	.0046	5.6	66.3	-2.2	-5.1
24.0	5774	24.7	.01261	53.4	.08	507.0	267.5	324.8	268.22	84.7	265.4	.0042	4.4	66.2	-1.8	-4.1
24.4	5882	24.1	.01287	52.1	.08	500.0	266.8	325.2	267.46	88.5	265.2	.0042	4.8	64.2	-2.1	-4.3
25.0	6072	22.9	.01333	49.8	.08	488.0	265.4	325.8	266.12	95.0	264.8	.0041	5.4	61.3	-2.6	-4.7
26.0	6396	22.8	.01408	50.0	.08	468.0	263.1	326.8	263.69	95.6	262.5	.0036	7.5	64.8	-3.2	-6.7
27.0	6714	22.1	.01482	48.9	.08	449.0	261.1	328.2	261.61	95.3	260.5	.0032	8.5	68.1	-3.2	-7.9
28.0	7026	21.4	.01552	47.6	.08	431.0	259.5	330.1	259.99	90.8	258.4	.0028	8.0	66.4	-3.2	-7.3
29.0	7294	20.7	.01611	46.4	.08	416.0	257.9	331.3	258.25	85.3	256.0	.0024	5.9	66.8	-2.3	-5.5
30.0	7589	21.4	.01676	48.2	.09	400.0	256.4	333.1	256.72	90.0	255.1	.0023	3.9	57.6	-2.1	-3.3
31.0	7894	19.9	.01743	45.2	.09	384.0	254.5	334.5	254.76	86.8	252.8	.0020	4.1	41.7	-3.1	-2.7
32.0	8170	18.3	.01799	41.8	.08	370.0	253.0	336.1	253.18	65.5	248.2	.0013	5.3	53.1	-3.2	-4.2
33.0	8455	19.6	.01856	45.1	.09	356.0	251.2	337.5	251.38	52.9	244.2	.0010	5.4	61.1	-2.6	-4.7
33.5	8579	19.0	.01882	43.7	.09	350.0	250.6	338.3	250.77	52.7	243.6	.0009	5.3	61.3	-2.6	-4.7
34.0	8728	18.2	.01912	42.1	.09	343.0	249.9	339.3	250.04	52.6	242.9	.0009	5.2	61.5	-2.5	-4.6
35.0	9009	18.9	.01969	44.0	.09	330.0	247.5	339.8	247.64	52.1	240.6	.0007	5.4	72.6	-1.6	-5.1
36.0	9299	18.8	.02028	44.1	.10	317.0	245.8	341.3	245.92	52.0	239.0	.0007	6.4	85.2	-.5	-6.4
37.0	9646	18.7	.02100	44.3	.10	302.0	243.6	342.9	243.67	51.8	236.9	.0006	5.1	96.1	.6	-5.1
37.2	9693	18.1	.02109	43.0	.10	300.0	243.2	343.0	243.26	51.8	236.5	.0005	4.7	100.2	.8	-4.6
38.0	9933	15.3	.02154	36.5	.09	290.0	241.1	343.4	241.16	51.7	234.5	.0005	2.9	139.9	2.2	-1.9
39.0	10255	18.4	.02215	44.5	.11	277.0	238.6	344.3	238.65	51.0	232.0	.0004	3.1	178.4	3.1	-.1
40.0	10615	15.6	.02285	38.2	.10	263.0	235.7	345.2	235.72	50.4	229.2	.0003	3.4	197.3	3.2	1.0
41.0	10935	16.3	.02343	40.3	.11	251.0	233.0	345.8	233.00	0.0	0.0	0.0000	3.2	200.2	3.0	1.1
41.1	10961	16.4	.02349	40.7	.11	250.0	232.7	345.9	232.74	0.0	0.0	0.0000	3.0	200.3	2.8	1.1
42.0	11238	17.6	.02403	44.1	.12	240.0	230.1	346.0	230.13	0.0	0.0	0.0000	1.5	202.5	1.4	.6
43.0	11552	14.1	.02462	35.9	.10	229.0	227.6	346.8	227.62	0.0	0.0	0.0000	1.4	277.4	-.2	1.4
44.0	11877	13.4	.02516	34.6	.10	218.0	224.3	346.7	224.33	0.0	0.0	0.0000	3.5	291.3	-1.3	3.3
45.0	12214	12.1	.02568	31.6	.10	207.0	221.2	346.9	221.20	0.0	0.0	0.0000	4.5	285.8	-1.2	4.3
45.7	12434	12.1	.02601	31.9	.10	200.0	218.9	346.7	218.93	0.0	0.0	0.0000	3.5	280.3	-.6	3.4
46.0	12532	12.1	.02615	32.0	.10	197.0	217.9	346.7	217.93	0.0	0.0	0.0000	3.0	276.7	-.4	3.0
47.0	12930	9.4	.02668	25.1	.08	185.0	215.2	348.4	215.16	0.0	0.0	0.0000	.6	290.7	-.2	.5
48.0	13277	13.3	.02718	36.2	.13	175.0	211.7	348.3	211.70	0.0	0.0	0.0000	.8	182.5	.8	0.0
49.0	13639	10.5	.02773	29.0	.11	165.0	208.6	349.0	208.57	0.0	0.0	0.0000	1.1	152.2	.9	-.5
50.0	13902	11.1	.02810	31.0	.12	158.0	206.4	349.7	206.42	0.0	0.0	0.0000	1.7	222.0	1.2	1.1
50.9	14215	11.2	.02855	31.3	.12	150.0	206.4	354.9	206.42	0.0	0.0	0.0000	4.2	214.2	3.5	2.4
51.0	14256	11.2	.02861	31.3	.12	149.0	206.4	355.6	206.42	0.0	0.0	0.0000	4.6	213.8	3.8	2.5
52.0	14589	11.1	.02910	31.1	.13	141.0	206.8	362.0	206.82	0.0	0.0	0.0000	8.4	189.2	8.3	1.4
53.0	14941	11.0	.02961	30.9	.14	133.0	205.6	365.9	205.61	0.0	0.0	0.0000	8.0	191.0	7.8	1.5
54.0	15313	11.7	.03016	33.1	.15	125.0	204.1	369.8	204.15	0.0	0.0	0.0000	5.1	215.2	4.2	2.9
55.0	15605	8.9	.03057	25.5	.12	119.0	202.2	371.4	202.19	0.0	0.0	0.0000	2.8	238.0	1.5	2.3
56.0	16014	10.1	.03109	29.1	.15	111.0	199.4	373.7	199.41	0.0	0.0	0.0000	3.1	24.7	-2.9	-1.3
57.0	16392	10.0	.03160	29.4	.16	104.0	196.9	375.9	196.92	0.0	0.0	0.0000	5.9	40.7	-4.5	-3.8
57.8	16616	8.4	.03188	24.8	.14	100.0	195.2	376.9	195.21	0.0	0.0	0.0000	8.8	61.0	-4.3	-7.7
58.0	16674	8.0	.03195	23.6	.13	99.0	194.8	377.1	194.77	0.0	0.0	0.0000	9.7	64.0	-4.2	-8.7
59.0	17059	9.4	.03242	28.1	.17	92.5	193.1	381.1	193.07	0.0	0.0	0.0000	14.6	63.8	-6.4	-13.1
60.0	17437	16.1	.03308	46.9	.31	86.6	198.7	399.7	198.68	0.0	0.0	0.0000	14.1	100.4	2.5	-13.8
61.0	17832	29.8	.03429	83.8	.61	81.0	205.6	421.6	205.61	0.0	0.0	0.0000	13.9	127.4	8.4	-11.0
61.2	17907	31.7	.03463	88.8	.66	80.0	206.0	423.9	206.00	0.0	0.0	0.0000	12.5	125.6	7.3	-10.1
62.0	18217	39.3	.03603	109.4	.86	76.0	207.6	433.5	207.60	0.0	0.0	0.0000	7.0	110.2	2.4	-6.5
63.0	18631	46.3	.03833	128.4	1.08	71.0	208.0	442.9	207.99	0.0	0.0	0.0000	5.6	114.5	2.3	-5.1
63.2	18717	47.6	.03889	132.1	1.13	70.0	208.2	445.0	208.15	0.0	0.0	0.0000	4.8	117.4	2.2	-4.3
64.0	19039	52.7	.04095	145.9	1.32	66.4	208.8	453.1	208.76	0.0	0.0	0.0000	2.4	143.0	1.9	-1.4
65.0	19379	56.3	.04335	156.1	1.49	62.8	208.4	459.5	208.38	0.0	0.0	0.0000	3.7	237.0	2.0	3.1
65.7	19655	57.0	.04539	159.0	1.58	60.0	207.1	462.7	207.09	0.0	0.0	0.0000	4.1	299.8	-2.0	3.5
66.0	19758	57.3	.04615	160.0	1.61	59.0	206.6	463.8	206.62	0.0	0.0	0.0000	5.1	313.7	-3.5	3.7

TIME MIN	ALT GPM	OZONE MICMB	TOTOZ ATMCM	OZDEN MG/M3	OZMXR MICGG	PRESS MB	TEMP DEG K	PTEMP DEG K	VTEMP DEG K	HMDTY PRCNT	DEWPT DEG K	SPCFC HMDTY	SPD MPS	DIR DEG	NS MPS	EW MPS
67.0	20172	60.6	.04933	169.0	1.82	55.1	207.2	474.3	207.21	0.0	0.0	0.0000	7.6	357.0	-7.6	.4
68.0	20527	73.6	.05239	200.7	2.34	52.0	211.7	492.7	211.70	0.0	0.0	0.0000	4.0	37.5	-3.2	-2.4
68.7	20769	77.8	.05477	211.8	2.58	50.0	211.9	498.8	211.94	0.0	0.0	0.0000	3.5	59.1	-1.8	-3.0
69.0	20895	79.9	.05599	217.6	2.70	49.0	212.1	502.0	212.06	0.0	0.0	0.0000	3.4	71.8	-1.1	-3.2
70.0	21287	84.9	.06010	231.5	3.06	46.0	211.7	510.3	211.70	0.0	0.0	0.0000	4.2	75.8	-1.0	-4.1
71.0	21720	94.8	.06505	257.5	3.66	42.9	212.6	522.7	212.59	0.0	0.0	0.0000	4.6	75.8	-1.1	-4.5
72.0	22141	103.3	.07032	278.8	4.27	40.1	214.0	536.4	213.97	0.0	0.0	0.0000	2.9	75.8	-.7	-2.9
72.0	22156	103.7	.07054	279.7	4.30	40.0	214.0	536.9	214.03	0.0	0.0	0.0000	2.8	75.8	-.7	-2.7
73.0	22545	112.7	.07581	302.0	4.97	37.6	215.5	550.2	215.49	0.0	0.0	0.0000	.3	255.8	.1	.3
74.0	22962	120.5	.08188	320.3	5.67	35.2	217.1	564.9	217.13	0.0	0.0	0.0000	.7	60.2	-.4	-.6
74.1	22998	120.7	.08242	320.9	5.72	35.0	217.2	565.9	217.16	0.0	0.0	0.0000	1.1	64.3	-.5	-.9
75.0	23315	122.8	.08720	326.0	6.11	33.3	217.5	574.8	217.45	0.0	0.0	0.0000	4.0	70.8	-1.3	-3.8
76.0	23690	127.7	.09301	337.3	6.74	31.4	218.6	587.5	218.57	0.0	0.0	0.0000	5.3	55.3	-3.0	-4.4
76.8	23982	133.5	.097[illegible]4	350.9	7.38	30.0	219.7	598.2	219.65	0.0	0.0	0.0000	5.5	49.9	-3.6	-4.2
77.0	24069	135.2	.099[illegible]	354.9	7.57	29.6	220.0	601.4	219.97	0.0	0.0	0.0000	5.6	48.4	-3.7	-4.2
78.0	24451	141.1	.10556	368.2	8.38	27.9	221.[illegible]	615.0	221.20	0.0	0.0	0.0000	7.1	67.2	-2.7	-6.5
79.0	24883	146.9	.11316	382.7	9.33	26.1	221.7	628.2	221.65	0.0	0.0	0.0000	10.2	93.2	.6	-10.2
79.6	25164	151.9	.11828	392.4	10.08	25.0	223.5	641.2	223.46	0.0	0.0	0.0000	10.0	111.8	3.7	-9.3
80.0	25323	154.7	.12117	397.9	10.51	24.4	224.5	648.5	224.47	0.0	0.0	0.0000	10.3	122.0	5.5	-8.7
81.0	25799	155.1	.13000	395.5	11.32	22.7	226.3	667.5	226.35	0.0	0.0	0.0000	7.3	129.6	4.6	-5.6
82.0	26220	154.8	.13778	395.6	12.04	21.3	225.9	678.5	225.92	0.0	0.0	0.0000	2.3	155.7	2.1	-.9
83.0	26636	151.7	.14540	388.2	12.57	20.0	225.6	689.9	225.63	0.0	0.0	0.0000	1.7	132.1	1.1	-1.3
84.0	27115	149.3	.15402	381.9	13.30	18.6	225.8	704.9	225.77	0.0	0.0	0.0000	8.8	86.5	-.5	-8.8
84.8	27518	145.5	.16108	370.8	13.78	17.5	226.6	719.8	226.55	0.0	0.0	0.0000	6.5	84.5	-.6	-6.4
85.0	27633	144.4	.16309	367.7	13.91	17.2	226.8	724.0	226.77	0.0	0.0	0.0000	5.8	83.7	-.6	-5.7
86.0	28115	141.5	.17124	357.9	14.66	16.0	228.3	744.2	228.33	0.0	0.0	0.0000	12.1	78.9	-2.3	-11.9
86.8	28544	135.2	.17826	343.9	14.94	15.0	227.0	753.8	227.04	0.0	0.0	0.0000	20.9	78.8	-4.1	-20.5
87.0	28634	133.9	.17972	341.0	14.99	14.8	226.8	755.7	226.77	0.0	0.0	0.0000	22.8	78.8	-4.4	-22.3
88.0	29051	127.8	.18620	323.6	15.24	13.9	228.0	773.7	228.05	0.0	0.0	0.0000	22.9	85.7	-1.7	-22.8
89.0	29497	122.1	.19280	309.6	15.57	13.0	227.8	787.7	227.76	0.0	0.0	0.0000	25.2	99.8	4.3	-24.8
89.5	29759	119.4	.19649	301.2	15.82	12.5	228.9	800.5	228.86	0.0	0.0	0.0000	24.8	105.0	6.4	-24.0
90.0	30033	116.5	.20033	292.4	16.08	12.0	230.0	813.8	229.99	0.0	0.0	0.0000	24.6	110.4	8.6	-23.0
91.0	30559	107.9	.20723	269.0	16.10	11.1	231.5	837.6	231.50	0.0	0.0	0.0000	24.5	109.4	8.1	-23.1
92.0	31131	100.3	.21418	250.7	16.30	10.2	231.1	856.6	231.09	0.0	0.0	0.0000	24.8	105.8	6.8	-23.9
92.2	31265	98.4	.21568	245.6	16.30	10.0	231.4	862.6	231.39	0.0	0.0	0.0000	24.3	105.2	6.4	-23.5
93.0	31685	92.4	.22039	229.5	16.28	9.4	232.3	881.4	232.32	0.0	0.0	0.0000	22.7	103.1	5.1	-22.1
94.0	32212	83.8	.22577	207.3	15.96	8.7	233.4	905.4	233.40	0.0	0.0	0.0000	19.7	96.9	2.4	-19.5
95.0	32701	78.7	.23035	194.1	16.10	8.1	234.1	926.7	234.08	0.0	0.0	0.0000	15.4	91.7	.5	-15.4
95.1	32786	77.9	.23109	192.2	16.14	8.0	234.1	930.[illegible]	234.13	0.0	0.0	0.0000	14.8	91.4	.4	-14.8
96.0	33321	73.2	.23577	180.3	16.40	7.4	234.5	952.[illegible]	234.48	0.0	0.0	0.0000	11.0	88.6	-.3	-10.9
96.7	33701	69.4	.23885	171.3	16.41	7.0	233.8	964.[illegible]	233.77	0.0	0.0	0.0000	11.8	85.8	-.9	-11.8
97.0	33900	67.4	.24046	166.7	16.42	6.8	233.4	971.4	233.40	0.0	0.0	0.0000	12.3	84.6	-1.2	-12.2
98.0	34534	60.1	.24510	147.6	16.07	6.2	235.3	1005.4	235.28	0.0	0.0	0.0000	20.8	74.1	-5.7	-20.0
98.5	34760	57.1	.24658	139.7	15.75	6.0	236.1	1018.6	236.13	0.0	0.0	0.0000	25.9	70.0	-8.9	-24.4
99.0	34995	54.0	.24811	131.5	15.42	5.8	237.0	1032.3	237.01	0.0	0.0	0.0000	31.3	67.2	-12.1	-28.8
100.0	35493	46.7	.25094	112.5	14.33	5.4	239.8	1065.9	239.78	0.0	0.0	0.0000	999.9	999.9	999.9	999.9

INTEGRAL .25094 RESIDUAL .03689 INTEGRATED TOTAL OZONE .28783

OZONAGRAM

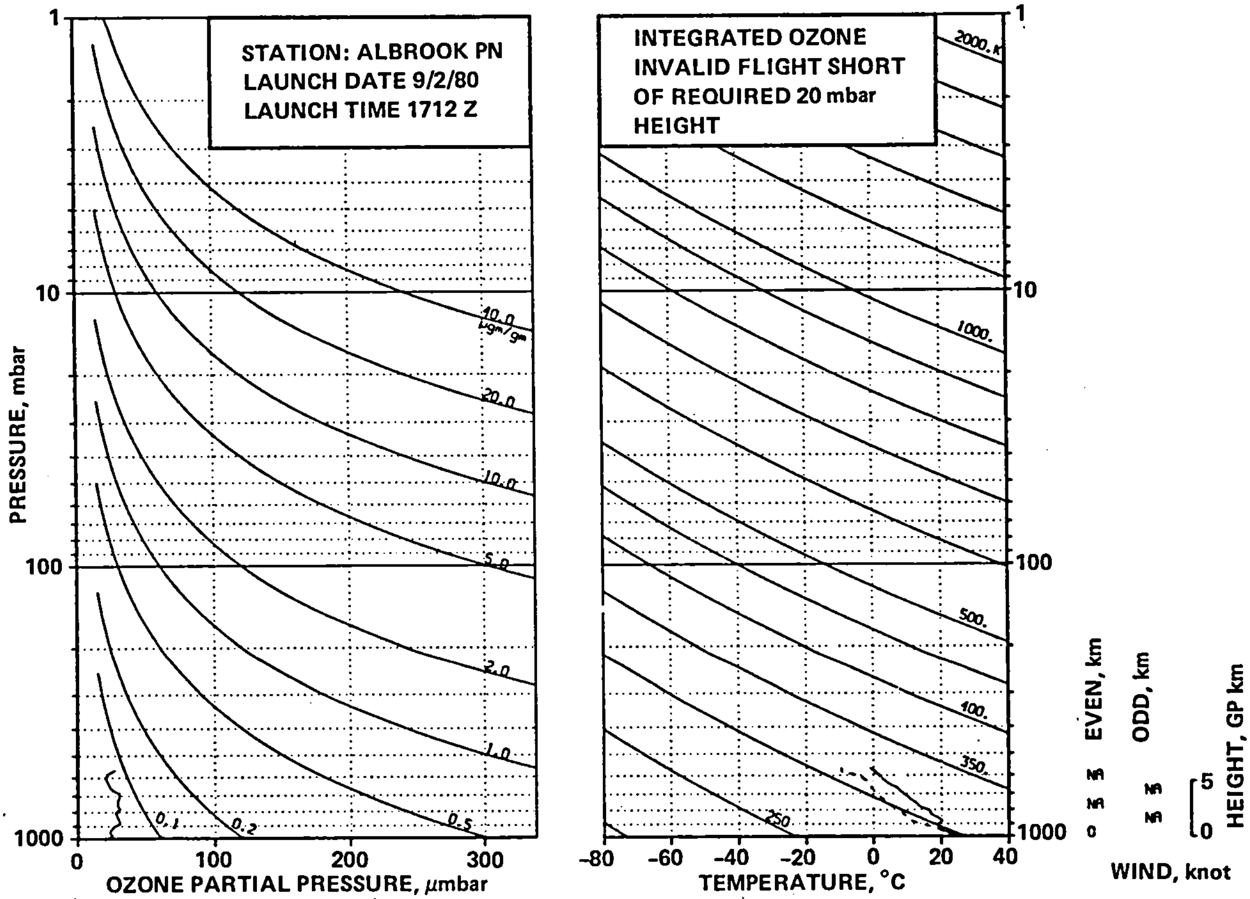

STATION: ALBROOK PN
LAUNCH DATE 9/2/80
LAUNCH TIME 1712 Z
INTEGRATED OZONE
INVALID FLIGHT SHORT
OF REQUIRED 20 mbar
HEIGHT
PRESSURE, mbar
1
10
100
1000
0
100
200
300
OZONE PARTIAL PRESSURE, μmbar
-80
-60
-40
-20
0
20
40
TEMPERATURE, °C
2000.
1000.
500.
400.
350.
250
40.0
20.0
10.0
5.0
2.0
1.0
0.5
0.2
0.1
EVEN, km
ODD, km
HEIGHT, GP km
WIND, knot

STATION ALBROOK PN   LAUNCH DATE 9/ 2/80   TIME 1712Z   ECC   SONDE 3A1317

SURFACE CONDITIONS   PRESS 1004.9MB   TEMP 298.5 DEG K   HUMIDITY   97.0 PRCNT

TIME MIN	ALT GPM	OZONE MICMB	TOTOZ ATMCM	OZDEN MG/M3	OZMXR MICGG	PRESS MB	TEMP DEG K	PTEMP DEG K	VTEMP DEG K	HMDTY PRCNT	DEWPT DEG K	SPCFC HMDTY	SPD MPS	DIR DEG	NS MPS	EW MPS
0.0	66	20.2	0.00000	39.1	.03	1004.9	298.7	298.3	302.12	91.8	297.3	.0187	0.0	0.0	0.0	0.0
.2	108	21.2	.00009	41.0	.04	1000.0	298.2	298.2	301.58	92.6	296.9	.0182	999.9	999.9	999.9	999.9
1.0	295	25.3	.00047	49.3	.04	979.0	296.1	297.9	299.25	96.0	295.5	.0172	999.9	999.9	999.9	999.9
2.0	529	23.4	.00099	46.0	.04	953.0	293.7	297.7	296.41	95.9	293.0	.0152	999.9	999.9	999.9	999.9
3.0	749	24.0	.00146	47.4	.04	929.0	292.4	298.6	294.93	95.1	291.6	.0143	999.9	999.9	999.9	999.9
4.0	984	26.5	.00201	52.4	.05	904.0	291.7	300.3	293.74	75.6	287.3	.0112	999.9	999.9	999.9	999.9
4.2	1022	27.2	.00211	53.7	.05	900.0	292.0	300.9	293.96	72.6	286.9	.0107	999.9	999.9	999.9	999.9
5.0	1235	31.0	.00267	60.9	.06	878.0	293.5	304.6	295.17	56.3	284.5	.0095	999.9	999.9	999.9	999.9
6.0	1484	29.9	.00336	59.1	.06	853.0	292.0	305.5	293.61	58.3	283.6	.0093	999.9	999.9	999.9	999.9
6.1	1514	29.7	.00344	58.8	.06	850.0	291.7	305.6	293.36	58.4	283.4	.0091	999.9	999.9	999.9	999.9
7.0	1728	28.7	.00402	57.1	.06	829.0	290.1	306.0	291.59	58.7	281.9	.0085	999.9	999.9	999.9	999.9
8.0	1989	27.6	.00470	54.9	.06	804.0	289.7	308.3	291.18	58.7	281.6	.0086	999.9	999.9	999.9	999.9
8.2	2031	28.1	.00481	56.1	.06	800.0	289.2	308.2	290.68	58.6	281.1	.0082	999.9	999.9	999.9	999.9
9.0	2246	30.8	.00540	61.9	.07	780.0	286.9	308.0	288.15	58.2	278.8	.0073	999.9	999.9	999.9	999.9
10.0	2498	29.0	.00610	58.5	.06	757.0	285.9	309.6	287.12	57.4	277.7	.0070	999.9	999.9	999.9	999.9
11.0	2768	29.0	.00684	59.0	.07	733.0	284.2	310.6	285.31	57.5	276.1	.0064	999.9	999.9	999.9	999.9
12.0	3033	30.4	.00759	62.0	.07	710.0	282.9	312.0	283.94	57.4	274.9	.0061	999.9	999.9	999.9	999.9
12.4	3150	30.4	.00793	62.1	.07	700.0	282.2	312.5	283.21	57.5	274.3	.0058	999.9	999.9	999.9	999.9
13.0	3306	30.4	.00838	62.4	.07	687.0	281.3	313.1	282.23	57.8	273.4	.0057	999.9	999.9	999.9	999.9
14.0	3562	25.1	.00906	51.7	.06	666.0	280.2	314.7	281.13	58.3	272.6	.0055	999.9	999.9	999.9	999.9
15.0	3824	23.2	.00967	48.2	.06	645.0	277.9	315.0	278.87	66.4	272.2	.0055	999.9	999.9	999.9	999.9
16.0	4093	21.9	.01026	45.8	.06	624.0	276.4	316.3	277.28	66.7	270.8	.0051	999.9	999.9	999.9	999.9
17.0	4370	20.5	.01083	43.0	.06	603.0	275.1	317.9	275.89	66.2	269.4	.0048	999.9	999.9	999.9	999.9
17.1	4410	20.7	.01091	43.5	.06	600.0	274.9	318.1	275.66	63.4	268.6	.0044	999.9	999.9	999.9	999.9
18.0	4641	21.9	.01139	46.1	.06	583.0	273.8	319.4	274.32	47.1	263.8	.0032	999.9	999.9	999.9	999.9
19.0	4920	27.6	.01207	58.6	.08	563.0	272.3	320.9	272.87	51.1	263.5	.0032	999.9	999.9	999.9	999.9

CALIBRATIONS APPLIED FOR PARTIAL PRESSURE OF OZONE
TOTAL INTEGRATED OZONE INVALID. BALLOON SHORT OF 20 MB HEIGHT

OZONAGRAM

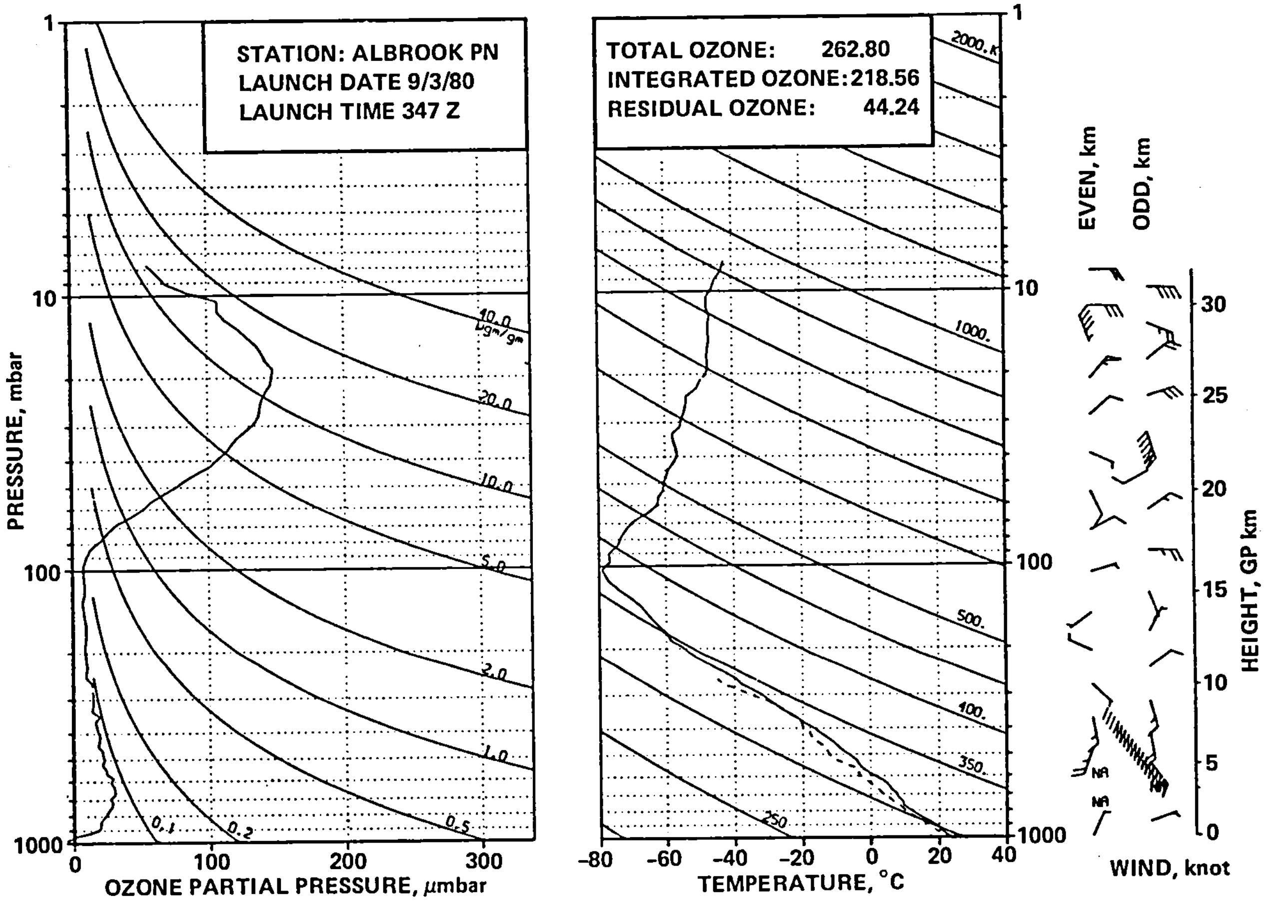

STATION: ALBROOK PN
LAUNCH DATE 9/3/80
LAUNCH TIME 347 Z
TOTAL OZONE: 262.80
INTEGRATED OZONE: 218.56
RESIDUAL OZONE: 44.24
PRESSURE, mbar
OZONE PARTIAL PRESSURE, μmbar
TEMPERATURE, °C
EVEN, km
ODD, km
HEIGHT, GP km
WIND, knot

STATION ALBROOK PN   LAUNCH DATE 9/ 3/80   TIME 347Z   ECC   SONDE 3A1318

SURFACE CONDITIONS   PRESS 1004.7MB   TEMP 297.2 DEG K   HUMIDITY 100.0 PRCNT

TIME MIN	ALT GPM	OZONE MICMB	TOTOZ ATMCM	OZDEN MG/M3	OZMXR MICGG	PRESS MB	TEMP DEG K	PTEMP DEG K	VTEMP DEG K	HMDTY PRCNT	DEWPT DEG K	SPCFC HMDTY	SPD MPS	DIR DEG	NS MPS	EW MPS
0.0	70	-4.8	0.00000	-9.3	-.01	1004.2	296.9	296.6	300.25	100.0	296.9	.0184	2.0	25.0	-1.8	-.8
.1	106	-4.8	-.00002	-9.4	-.01	1000.0	296.7	296.7	299.95	99.2	296.5	.0178	1.8	40.1	-1.4	-1.2
1.0	319	-4.8	-.00011	-9.4	-.01	976.0	295.3	297.3	298.20	94.2	294.3	.0161	3.3	106.7	.9	-3.2
2.0	581	1.1	-.00015	2.2	0.00	947.0	293.9	298.5	296.59	91.2	292.4	.0148	2.0	108.3	.6	-1.9
3.0	831	12.5	0.00000	24.7	.02	920.0	293.0	300.1	295.55	88.7	291.1	.0140	1.0	62.6	-.5	-.9
3.8	1020	17.7	.00028	35.0	.03	900.0	291.8	300.7	294.19	88.4	289.9	.0131	2.3	62.9	-1.0	-2.0
4.0	1068	19.0	.00035	37.6	.04	895.0	291.5	300.9	293.84	88.3	289.5	.0130	2.6	62.9	-1.2	-2.3
5.0	1311	19.9	.00078	39.6	.04	870.0	290.0	301.8	292.20	88.2	288.1	.0122	999.9	999.9	999.9	999.9
5.7	1508	20.0	.00115	40.0	.04	850.0	288.4	302.1	290.36	88.8	286.5	.0111	999.9	999.9	999.9	999.9
6.0	1579	20.0	.00128	40.1	.04	843.0	287.8	302.2	289.71	89.0	286.0	.0110	999.9	999.9	999.9	999.9
7.0	1833	21.7	.00177	43.8	.04	818.0	286.2	303.1	287.98	89.7	284.5	.0103	999.9	999.9	999.9	999.9
7.7	2019	23.3	.00217	47.3	.05	800.0	285.0	303.7	286.69	90.6	283.5	.0097	999.9	999.9	999.9	999.9
8.0	2104	24.1	.00235	48.9	.05	792.0	284.4	304.0	286.11	91.0	283.0	.0096	999.9	999.9	999.9	999.9
9.0	2372	25.8	.00299	52.6	.06	767.0	282.9	305.2	284.50	92.4	281.7	.0091	999.9	999.9	999.9	999.9
10.0	2647	27.9	.00369	57.0	.06	742.0	282.6	307.7	283.97	82.8	279.8	.0082	999.9	999.9	999.9	999.9
11.0	2919	28.7	.00442	58.9	.07	718.0	281.3	309.2	282.60	82.6	278.5	.0078	999.9	999.9	999.9	999.9
11.7	3128	27.7	.00498	56.9	.07	700.0	280.9	311.0	282.12	76.8	277.1	.0070	999.9	999.9	999.9	999.9
12.0	3211	27.3	.00521	56.1	.07	693.0	280.7	311.7	281.93	74.6	276.5	.0070	999.9	999.9	999.9	999.9
13.0	3476	30.3	.00594	62.6	.07	671.0	279.3	313.0	280.45	76.9	275.6	.0067	999.9	999.9	999.9	999.9
14.0	3736	30.3	.00670	62.8	.08	650.0	278.6	315.1	279.66	72.2	274.0	.0062	999.9	999.9	999.9	999.9
15.0	4017	29.7	.00751	61.8	.08	628.0	277.4	316.8	278.36	70.6	272.5	.0058	999.9	999.9	999.9	999.9
16.0	4306	27.3	.00832	57.4	.07	606.0	275.2	317.5	276.05	70.8	270.5	.0051	999.9	999.9	999.9	999.9
16.3	4385	27.9	.00854	58.6	.08	600.0	274.5	317.7	275.39	73.0	270.2	.0051	999.9	999.9	999.9	999.9
17.0	4589	29.2	.00910	61.8	.08	585.0	272.9	318.1	273.72	78.4	269.6	.0050	999.9	999.9	999.9	999.9
18.0	4881	24.5	.00988	52.2	.07	564.0	271.0	319.1	271.84	91.9	269.8	.0053	999.9	999.9	999.9	999.9
19.0	5182	23.8	.01060	51.0	.07	543.0	269.7	321.1	270.38	74.9	265.9	.0041	15.0	208.1	13.3	7.1
20.0	5493	21.3	.01130	45.7	.07	522.0	268.9	323.8	269.48	62.0	262.8	.0033	15.8	203.8	14.4	6.4
21.0	5831	23.0	.01205	49.8	.08	500.0	266.7	325.1	267.14	63.6	260.9	.0030	15.2	201.2	14.2	5.5
22.0	6100	21.6	.01266	47.1	.07	483.0	264.9	326.1	265.35	69.4	260.3	.0029	13.6	199.6	12.9	4.6
23.0	6394	21.6	.01331	47.4	.08	465.0	263.4	327.8	263.86	71.2	259.2	.0028	11.4	190.4	11.3	2.1
24.0	6698	18.3	.01393	40.2	.07	447.0	262.0	329.7	262.37	69.1	257.4	.0025	9.9	174.2	9.9	-1.0
25.0	6994	19.1	.01450	42.3	.07	430.0	260.1	331.1	260.48	69.9	255.8	.0023	10.2	169.9	10.0	-1.8
26.0	7355	19.8	.01523	44.3	.08	410.0	257.7	332.5	258.10	80.0	255.1	.0022	9.6	173.1	9.5	-1.2
26.6	7540	18.9	.01560	42.5	.08	400.0	256.5	333.2	256.79	81.3	254.0	.0020	8.3	172.1	8.3	-1.1
27.0	7692	18.2	.01590	41.0	.08	392.0	255.4	333.8	255.72	82.3	253.1	.0020	7.4	171.2	7.3	-1.1
28.0	7963	17.4	.01641	39.6	.08	378.0	253.1	334.2	253.42	96.8	252.7	.0020	7.1	170.1	7.0	-1.2
29.0	8282	16.5	.01699	38.1	.08	362.0	251.0	335.5	251.24	95.2	250.4	.0017	7.9	167.9	7.7	-1.7
29.8	8528	19.1	.01747	44.4	.09	350.0	248.9	335.9	249.10	99.0	248.8	.0015	7.6	165.3	7.4	-1.9
30.0	8591	19.8	.01760	46.0	.09	347.0	248.3	336.0	248.55	100.0	248.3	.0015	7.5	164.6	7.3	-2.0
31.0	8911	14.0	.01819	32.9	.07	332.0	246.0	337.1	246.15	100.0	246.0	.0012	7.1	164.6	6.8	-1.9
32.0	9265	14.9	.01875	35.3	.08	316.0	243.5	338.4	243.63	95.3	243.0	.0010	6.8	164.6	6.6	-1.8
33.0	9634	14.9	.01936	35.6	.08	300.0	241.3	340.3	241.35	72.1	237.9	.0006	4.6	151.8	4.1	-2.2
34.0	9920	14.9	.01984	36.0	.09	288.0	238.6	340.6	238.71	66.9	234.7	.0005	3.4	132.5	2.3	-2.5
35.0	10240	14.1	.02037	34.5	.08	275.0	235.3	340.3	235.38	57.2	230.0	.0003	3.2	133.6	2.2	-2.3
36.0	10572	14.0	.02091	34.6	.09	262.0	233.6	342.5	233.64	55.7	228.1	.0003	3.3	135.1	2.3	-2.3
37.0	10891	9.9	.02135	24.8	.07	250.0	231.0	343.3	231.03	0.0	0.0	0.0000	2.2	104.2	.5	-2.1
38.0	11165	9.9	.02167	25.1	.07	240.0	228.1	343.0	228.14	0.0	0.0	0.0000	5.2	22.8	-4.8	-2.0
39.0	11476	10.7	.02205	27.5	.08	229.0	225.3	343.3	225.31	0.0	0.0	0.0000	1.3	63.0	-.6	-1.2
40.0	11798	9.9	.02245	25.7	.08	218.0	222.5	343.9	222.54	0.0	0.0	0.0000	3.1	177.1	3.1	-.2
41.0	12133	9.8	.02285	25.8	.08	207.0	220.0	345.0	219.97	0.0	0.0	0.0000	1.4	320.4	-1.1	.9
41.6	12352	9.3	.02311	24.6	.08	200.0	218.5	346.1	218.49	0.0	0.0	0.0000	2.3	320.1	-1.8	1.5
42.0	12482	9.0	.02326	23.9	.08	196.0	217.6	346.7	217.63	0.0	0.0	0.0000	2.9	320.0	-2.2	1.9
43.0	12779	9.2	.02360	24.6	.08	187.0	214.5	346.4	214.52	0.0	0.0	0.0000	2.2	323.5	-1.8	1.3
44.0	13088	9.9	.02397	26.8	.09	178.0	213.7	349.9	213.68	0.0	0.0	0.0000	3.0	9.8	-3.0	-.5
45.0	13411	9.9	.02437	27.0	.10	169.0	211.8	351.9	211.77	0.0	0.0	0.0000	3.2	.1	-3.2	0.0
46.0	13787	9.9	.02485	27.2	.10	159.0	209.6	354.5	209.60	0.0	0.0	0.0000	2.7	307.5	-1.7	2.2
47.0	14143	9.1	.02529	25.3	.10	150.0	207.7	357.2	207.71	0.0	0.0	0.0000	1.3	215.1	1.0	.7
48.0	14560	8.2	.02576	23.1	.10	140.0	205.7	360.8	205.73	0.0	0.0	0.0000	4.2	177.4	4.2	-.2
49.0	14957	7.4	.02617	21.1	.09	131.0	202.8	362.5	202.80	0.0	0.0	0.0000	3.9	166.4	3.8	-.9
49.7	15232	8.4	.02647	24.3	.11	125.0	200.4	363.0	200.39	0.0	0.0	0.0000	2.4	147.4	2.1	-1.3
50.0	15375	8.9	.02663	25.9	.12	122.0	199.1	363.3	199.15	0.0	0.0	0.0000	1.9	127.4	1.2	-1.5
51.0	15818	9.0	.02717	26.5	.13	113.0	195.9	365.2	195.87	0.0	0.0	0.0000	.7	116.8	.3	-.6
52.0	16346	8.2	.02779	24.3	.13	103.0	194.0	371.3	193.96	0.0	0.0	0.0000	5.0	27.9	-4.4	-2.3
52.5	16514	8.2	.02798	24.2	.14	100.0	195.1	376.8	195.12	0.0	0.0	0.0000	7.0	46.1	-4.8	-5.0
53.0	16700	8.2	.02819	24.0	.14	96.8	196.4	382.7	196.40	0.0	0.0	0.0000	9.6	56.5	-5.3	-8.0
54.0	17112	10.5	.02872	30.9	.19	90.1	196.1	390.1	196.13	0.0	0.0	0.0000	12.2	94.6	1.0	-12.2
55.0	17545	13.7	.02944	39.7	.27	83.6	198.9	404.2	198.91	0.0	0.0	0.0000	9.1	91.8	.3	-9.1
55.6	17801	18.6	.03005	53.8	.39	80.0	199.5	410.6	199.51	0.0	0.0	0.0000	6.3	74.2	-1.7	-6.0
56.0	17949	21.4	.03040	61.9	.46	78.0	199.9	414.3	199.86	0.0	0.0	0.0000	5.1	56.4	-2.9	-4.3
57.0	18362	26.8	.03173	76.6	.61	72.7	201.7	426.6	201.70	0.0	0.0	0.0000	6.1	78.1	-1.3	-5.9
57.6	18586	30.5	.03263	86.6	.72	70.0	203.0	434.1	203.05	0.0	0.0	0.0000	7.2	72.7	-2.2	-6.9
58.0	18759	33.3	.03332	94.3	.81	68.0	204.1	439.9	204.09	0.0	0.0	0.0000	8.2	69.6	-2.8	-7.7
59.0	19134	43.6	.03521	120.9	1.13	63.9	208.1	456.6	208.09	0.0	0.0	0.0000	7.9	52.0	-4.9	-6.3
60.0	19520	52.2	.03758	143.0	1.44	60.0	210.7	470.7	210.69	0.0	0.0	0.0000	5.7	105.5	1.5	-5.5
61.0	19924	58.5	.04044	160.0	1.72	56.2	211.1	480.4	211.05	0.0	0.0	0.0000	5.7	151.1	5.0	-2.8
62.0	20311	67.8	.04355	184.1	2.13	52.8	212.6	492.7	212.64	0.0	0.0	0.0000	3.8	159.1	3.5	-1.3
63.0	20649	76.2	.04666	207.0	2.53	50.0	212.6	500.5	212.64	0.0	0.0	0.0000	5.4	210.6	4.6	2.7
63.0	20662	76.5	.04677	207.8	2.54	49.9	212.6	500.8	212.64	0.0	0.0	0.0000	5.5	211.7	4.7	2.9
64.0	20995	83.4	.05015	225.5	2.92	47.3	213.5	510.5	213.51	0.0	0.0	0.0000	7.4	239.8	3.7	6.4
65.0	21348	91.6	.05405	247.1	3.40	44.7	214.0	520.1	214.02	0.0	0.0	0.0000	2.8	247.6	1.1	2.6
66.0	21710	101.5	.05844	271.8	3.99	42.2	215.7	532.8	215.69	0.0	0.0	0.0000	1.4	123.5	.8	-1.2
66.9	22048	106.4	.06284	283.5	4.41	40.0	216.7	543.6	216.68	0.0	0.0	0.0000	2.0	115.0	.8	-1.8
67.0	22096	107.1	.06346	285.1	4.47	39.7	216.8	545.1	216.83	0.0	0.0	0.0000	2.0	114.1	.8	-1.9

TIME MIN	ALT GPM	OZONE MICMB	TOTOZ ATMCM	OZDEN MG/M3	OZMXR MICGG	PRESS MB	TEMP DEG K	PTEMP DEG K	VTEMP DEG K	HMDTY PRCNT	DEWPT DEG K	SPCFC HMDTY	SPD MPS	DIR DEG	NS MPS	EW MPS
68.0	22525	114.1	.06937	304.2	5.10	37.1	216.5	554.9	216.50	0.0	0.0	0.0000	2.9	75.2	-.7	-2.8
69.0	22875	117.5	.07443	314.6	5.55	35.1	215.7	561.6	215.69	0.0	0.0	0.0000	73.1	164.3	70.4	-19.8
69.0	22892	117.7	.07471	315.2	5.58	35.0	215.7	562.0	215.67	0.0	0.0	0.0000	73.0	164.1	70.2	-20.0
70.0	23264	122.5	.08028	328.3	6.15	33.0	215.4	570.7	215.36	0.0	0.0	0.0000	71.1	160.6	67.1	-23.6
71.0	23660	129.3	.08649	342.9	6.91	31.0	217.8	587.6	217.79	0.0	0.0	0.0000	11.3	42.9	-8.3	-7.7
71.5	23868	132.4	.08991	350.8	7.32	30.0	218.0	593.6	217.96	0.0	0.0	0.0000	7.5	42.0	-5.6	-5.0
72.0	24041	135.0	.09273	357.3	7.66	29.2	218.1	598.6	218.10	0.0	0.0	0.0000	4.3	40.2	-3.3	-2.8
73.0	24401	137.7	.09879	363.2	8.27	27.6	218.9	610.5	218.89	0.0	0.0	0.0000	2.7	146.4	2.2	-1.5
74.0	24809	138.5	.10571	364.2	8.86	25.9	219.5	623.4	219.51	0.0	0.0	0.0000	8.0	90.8	.1	-8.0
74.5	25036	139.2	.10960	366.1	9.24	25.0	219.6	630.0	219.58	0.0	0.0	0.0000	13.5	73.0	-3.9	-12.9
75.0	25272	140.0	.11363	368.0	9.63	24.1	219.7	636.9	219.66	0.0	0.0	0.0000	19.7	65.6	-8.1	-17.9
76.0	25717	143.0	.12130	370.7	10.53	22.5	222.7	658.4	222.68	0.0	0.0	0.0000	27.5	57.9	-14.6	-23.3
77.0	26106	146.5	.12809	378.0	11.45	21.2	223.7	672.8	223.71	0.0	0.0	0.0000	28.5	39.8	-21.9	-18.3
78.0	26489	147.3	.13485	377.1	12.21	20.0	225.6	689.8	225.59	0.0	0.0	0.0000	20.8	27.6	-18.5	-9.7
79.0	26933	148.5	.14269	379.3	13.16	18.7	226.0	704.5	226.02	0.0	0.0	0.0000	12.0	52.8	-7.2	-9.5
79.9	27371	143.4	.15032	366.6	13.57	17.5	225.8	717.2	225.76	0.0	0.0	0.0000	7.4	48.5	-4.9	-5.6
80.0	27409	142.9	.15097	365.5	13.61	17.4	225.7	718.3	225.74	0.0	0.0	0.0000	7.0	47.8	-4.7	-5.2
81.0	27922	139.4	.15962	356.1	14.35	16.1	226.0	735.3	226.02	0.0	0.0	0.0000	24.3	337.4	-22.4	9.3
82.0	28303	135.9	.16587	346.4	14.81	15.2	226.4	748.9	226.45	0.0	0.0	0.0000	22.0	340.7	-20.7	7.3
82.2	28390	134.5	.16725	343.1	14.86	15.0	226.4	751.6	226.39	0.0	0.0	0.0000	16.4	345.1	-15.8	4.2
83.0	28754	129.0	.17298	329.4	15.06	14.2	226.2	762.7	226.16	0.0	0.0	0.0000	9.5	117.6	4.4	-8.4
84.0	29187	122.7	.17949	313.3	15.29	13.3	226.2	777.1	226.16	0.0	0.0	0.0000	12.6	110.5	4.4	-11.8
84.8	29598	115.2	.18526	293.6	15.26	12.5	226.5	792.2	226.50	0.0	0.0	0.0000	11.0	89.0	-.2	-11.0
85.0	29705	113.2	.18676	288.5	15.25	12.3	226.6	796.1	226.59	0.0	0.0	0.0000	10.9	82.6	-1.4	-10.8
86.0	30150	107.8	.19263	275.7	15.53	11.5	225.7	808.5	225.74	0.0	0.0	0.0000	14.9	92.5	.6	-14.9
87.0	30751	107.7	.20036	275.5	17.00	10.5	225.7	829.8	225.74	0.0	0.0	0.0000	19.3	95.1	1.7	-19.2
87.7	31074	92.5	.20409	235.6	15.29	10.0	226.8	845.6	226.84	0.0	0.0	0.0000	21.6	90.9	.3	-21.6
88.0	31208	86.2	.20564	219.0	14.58	9.8	227.3	852.2	227.30	0.0	0.0	0.0000	22.7	89.4	-.2	-22.7
89.0	31702	70.3	.21022	177.9	12.80	9.1	228.1	873.6	228.14	0.0	0.0	0.0000	26.8	86.8	-1.5	-26.8
90.0	32239	63.7	.21445	159.8	12.56	8.4	230.1	901.4	230.07	0.0	0.0	0.0000	32.0	90.3	.2	-32.0
90.6	32568	59.4	.21675	148.7	12.28	8.0	230.5	916.0	230.53	0.0	0.0	0.0000	999.9	999.9	999.9	999.9
91.0	32826	56.0	.21856	140.1	12.06	7.7	230.9	927.4	230.89	0.0	0.0	0.0000	999.9	999.9	999.9	999.9

INTEGRAL .21856 RESIDUAL .04424 INTEGRATED TOTAL OZONE .26280

OZONAGRAM

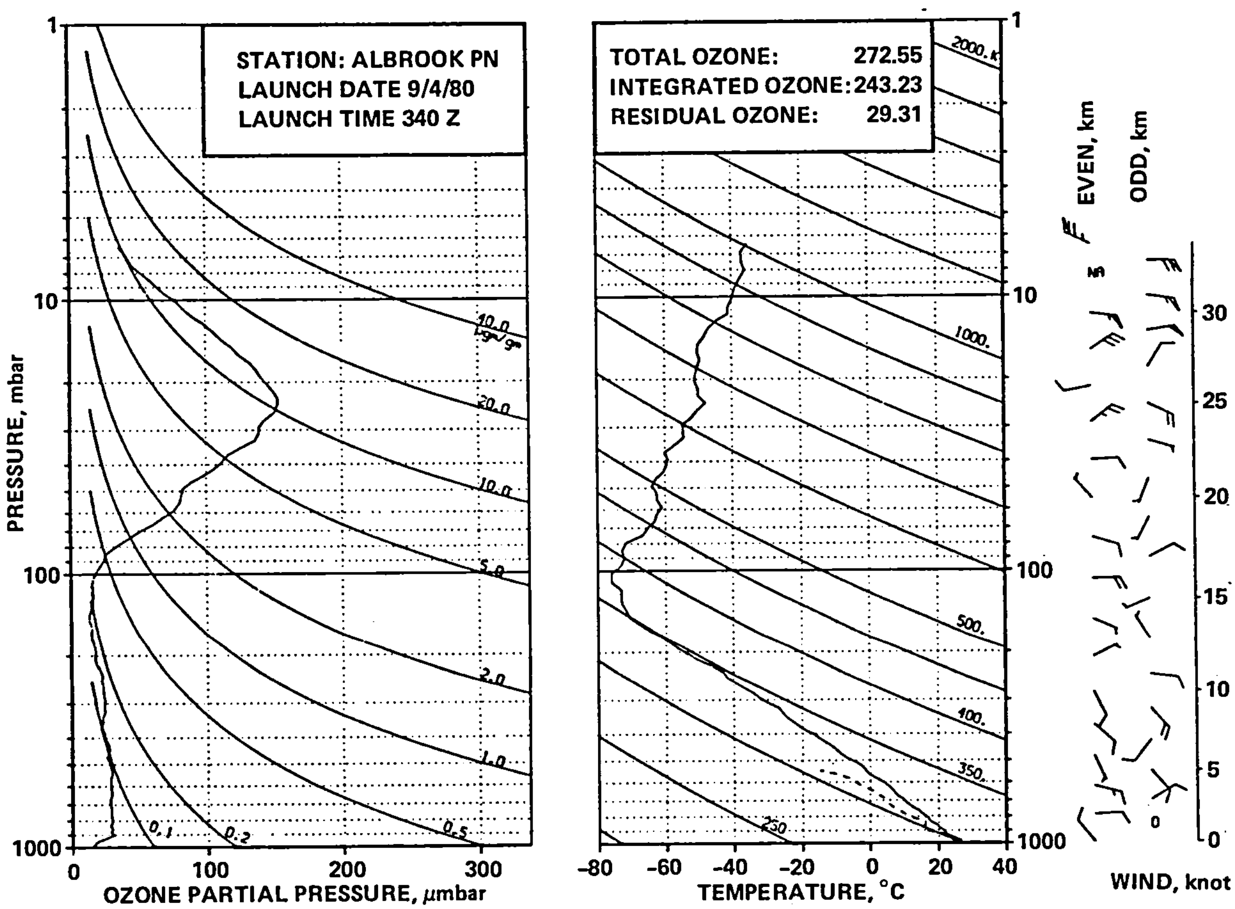
STATION: ALBROOK PN
LAUNCH DATE 9/4/80
LAUNCH TIME 340 Z
TOTAL OZONE: 272.55
INTEGRATED OZONE: 243.23
RESIDUAL OZONE: 29.31
PRESSURE, mbar
OZONE PARTIAL PRESSURE, μmbar
TEMPERATURE, °C
EVEN, km
ODD, km
HEIGHT, GP km
WIND, knot
1
10
100
1000
0
100
200
300
-80
-60
-40
-20
0
20
40
5
10
15
20
25
30

STATION ALBROOK PN   LAUNCH DATE 9/ 4/80   TIME 340Z   ECC   SONDE 3A1320

SURFACE CONDITIONS   PRESS 1003.8MB   TEMP 297.8 DEG K   HUMIDITY 100.0 PRCNT

TIME MIN	ALT GPM	OZONE MICMB	TOTOZ ATMCM	OZDEN MG/M3	OZMXR MICGG	PRESS MB	TEMP DEG K	PTEMP DEG K	VTEMP DEG K	HMDTY PRCNT	DEWPT DEG K	SPCFC HMDTY	SPD MPS	DIR DEG	NS MPS	EW MPS
0.0	66	14.8	0.00000	28.7	.02	1003.8	297.8	297.4	301.24	98.6	297.5	.0191	4.0	320.0	-3.1	2.6
.1	99	15.1	.00005	29.2	.02	1000.0	298.0	298.0	301.52	97.3	297.6	.0193	4.0	321.7	-3.1	2.5
1.0	314	17.0	.00035	32.7	.03	976.0	299.7	301.8	303.30	89.0	297.7	.0198	4.2	332.1	-3.7	2.0
2.0	552	19.7	.00074	38.3	.03	950.0	297.3	301.7	300.51	89.0	295.4	.0177	3.6	346.5	-3.5	.8
3.0	767	25.7	.00118	50.2	.05	927.0	295.5	301.9	298.71	93.1	295.2	.0179	3.2	333.9	-2.9	1.4
4.0	995	31.3	.00177	61.3	.06	903.0	294.8	303.5	297.17	73.2	289.8	.0131	1.2	327.9	-1.1	.7
4.1	1023	31.0	.00185	60.7	.06	900.0	294.6	303.6	296.96	73.1	289.6	.0129	1.0	329.6	-.9	.5
5.0	1199	28.9	.00233	56.9	.05	882.0	293.5	304.2	295.67	72.0	288.3	.0122	.3	95.0	0.0	-.3
6.0	1417	30.3	.00292	59.8	.06	860.0	292.8	305.7	295.23	80.2	289.3	.0134	1.4	63.9	-.6	-1.3
6.4	1517	29.7	.00319	58.7	.06	850.0	292.0	305.9	294.45	84.4	289.3	.0136	2.2	72.7	-.6	-2.1
7.0	1681	28.6	.00363	56.8	.06	834.0	290.7	306.2	293.17	91.3	289.3	.0138	3.4	78.9	-.6	-3.3
8.0	1931	30.2	.00431	60.1	.06	810.0	290.1	308.1	292.11	75.6	285.8	.0113	4.2	87.3	-.2	-4.2
8.4	2036	30.0	.00461	59.8	.06	800.0	289.5	308.6	291.39	73.7	284.8	.0104	4.4	87.0	-.2	-4.4
9.0	2176	29.7	.00499	59.5	.06	787.0	288.7	309.1	290.45	71.1	283.5	.0100	4.6	86.7	-.3	-4.6
10.0	2438	29.2	.00571	58.7	.06	763.0	287.5	310.6	289.11	68.8	281.8	.0092	4.6	85.9	-.3	-4.6
11.0	2696	29.4	.00642	59.4	.07	740.0	285.6	311.2	286.99	67.7	279.8	.0082	4.5	68.6	-1.6	-4.2
12.0	2949	29.4	.00712	59.7	.07	718.0	284.2	312.5	285.58	67.6	278.5	.0077	5.3	55.7	-3.0	-4.4
12.7	3160	28.9	.00770	59.0	.07	700.0	283.3	313.7	284.68	69.5	278.0	.0077	6.0	60.8	-2.9	-5.2
13.0	3256	28.7	.00797	58.6	.07	692.0	282.9	314.3	284.27	70.4	277.8	.0077	6.3	62.7	-2.9	-5.6
14.0	3524	28.6	.00870	58.8	.07	670.0	281.1	315.2	282.31	69.0	275.8	.0069	7.4	82.6	-1.0	-7.3
15.0	3799	29.9	.00947	61.7	.08	648.0	280.2	317.2	281.35	66.5	274.4	.0064	8.4	101.7	1.7	-8.3
16.0	4069	29.6	.01024	61.1	.08	627.0	279.2	319.0	280.12	58.0	271.6	.0054	7.5	104.5	1.9	-7.3
17.0	4374	28.9	.01111	60.1	.08	604.0	277.5	320.5	278.28	55.1	269.3	.0047	6.8	107.8	2.1	-6.5
17.2	4427	28.9	.01126	60.2	.08	600.0	277.1	320.6	277.86	55.4	268.9	.0046	6.7	110.1	2.3	-6.3
18.0	4661	29.0	.01191	60.7	.08	583.0	275.3	321.2	276.03	56.4	267.5	.0043	6.6	120.3	3.3	-5.7
19.0	4941	29.0	.01271	61.2	.09	563.0	273.0	321.7	273.58	49.4	263.7	.0033	5.8	134.8	4.1	-4.1
20.0	5215	30.2	.01351	64.0	.09	544.0	271.9	323.6	272.28	34.7	258.3	.0022	6.1	143.0	4.9	-3.7
21.0	5482	29.5	.01430	62.9	.09	526.0	271.1	325.8	271.27	0.0	0.0	0.0000	5.8	134.6	4.1	-4.1
22.0	5773	28.7	.01515	61.7	.09	507.0	269.0	326.6	269.42	50.0	260.1	.0027	4.5	127.5	2.7	-3.6
22.4	5881	28.4	.01546	61.2	.09	500.0	267.9	326.6	268.37	53.0	259.8	.0027	3.5	132.9	2.4	-2.6
23.0	6040	28.0	.01591	60.6	.09	490.0	266.4	326.6	266.84	57.3	259.4	.0027	2.2	148.8	1.9	-1.2
24.0	6331	26.1	.01671	56.9	.09	472.0	264.5	327.8	264.93	65.1	259.1	.0027	2.5	212.2	2.1	1.3
25.0	6631	28.1	.01754	61.6	.10	454.0	263.0	329.6	263.39	56.3	256.0	.0022	4.1	226.3	2.8	2.9
26.0	6924	28.1	.01839	62.0	.11	437.0	261.3	331.1	261.53	36.8	249.6	.0013	4.8	226.9	3.2	3.5
27.0	7226	27.4	.01925	61.1	.11	420.0	258.9	331.8	259.12	39.8	248.3	.0012	5.0	207.7	4.5	2.3
28.0	7575	24.1	.02020	54.2	.10	401.0	256.6	333.1	256.81	56.3	249.9	.0015	4.1	182.9	4.1	.2
28.1	7593	24.1	.02024	54.3	.10	400.0	256.4	333.1	256.63	57.3	249.9	.0015	4.1	180.1	4.1	0.0
29.0	7879	24.1	.02097	54.9	.10	385.0	253.6	333.1	253.83	72.5	249.9	.0015	4.7	137.8	3.5	-3.2
30.0	8213	22.2	.02179	50.9	.10	368.0	251.4	334.6	251.67	81.0	249.1	.0015	6.5	125.0	3.7	-5.3
31.0	8580	23.4	.02270	54.3	.11	350.0	249.0	336.2	249.26	91.5	248.1	.0014	7.6	128.9	4.8	-5.9
32.0	8855	23.2	.02339	54.1	.11	337.0	247.7	338.0	247.88	76.0	244.7	.0011	9.3	138.6	7.0	-6.2
33.0	9207	25.1	.02432	58.8	.13	321.0	246.4	340.9	246.46	34.8	235.5	.0005	9.3	139.5	7.1	-6.0
34.0	9480	24.3	.02506	57.7	.13	309.0	243.5	340.6	243.54	35.3	233.1	.0004	8.1	133.4	5.6	-5.9
34.6	9689	24.8	.02564	59.2	.14	300.0	241.7	341.0	241.76	31.0	230.2	.0003	6.5	133.7	4.5	-4.7
35.0	9808	25.0	.02597	60.0	.14	295.0	240.7	341.2	240.75	28.6	228.6	.0002	5.5	134.0	3.8	-4.0
36.0	10124	24.3	.02684	58.9	.14	282.0	238.7	342.7	238.75	24.9	225.6	.0002	3.9	157.6	3.7	-1.5
37.0	10400	23.8	.02760	58.1	.15	271.0	236.3	343.2	236.33	0.0	0.0	0.0000	5.2	162.1	4.9	-1.6
38.0	10685	23.8	.02838	58.7	.15	260.0	233.9	343.7	233.89	0.0	0.0	0.0000	4.6	134.5	3.2	-3.3
38.8	10951	22.8	.02909	56.7	.15	250.0	231.8	344.5	231.83	0.0	0.0	0.0000	4.2	102.5	.9	-4.1
39.0	11006	22.6	.02924	56.3	.15	248.0	231.4	344.7	231.40	0.0	0.0	0.0000	4.3	95.8	.4	-4.2
40.0	11312	23.3	.03006	58.4	.16	237.0	230.2	347.3	230.15	0.0	0.0	0.0000	3.8	104.2	.9	-3.7
41.0	11689	21.2	.03105	54.0	.16	224.0	226.6	347.4	226.59	0.0	0.0	0.0000	3.9	118.9	1.9	-3.4
42.0	11989	18.5	.03177	47.8	.14	214.0	222.9	346.3	222.89	0.0	0.0	0.0000	2.5	72.1	-.8	-2.4
43.0	12299	17.8	.03245	46.7	.14	204.0	220.0	346.4	219.96	0.0	0.0	0.0000	2.4	40.8	-1.8	-1.6
43.4	12425	18.0	.03273	47.6	.15	200.0	218.8	346.5	218.81	0.0	0.0	0.0000	1.9	46.4	-1.3	-1.4
44.0	12620	18.4	.03317	49.0	.16	194.0	217.0	346.8	217.05	0.0	0.0	0.0000	1.2	64.1	-.5	-1.1
45.0	12954	17.2	.03391	46.2	.15	184.0	214.3	347.7	214.34	0.0	0.0	0.0000	.9	324.4	-.8	.6
46.0	13302	15.8	.03464	43.1	.15	174.0	211.8	349.1	211.85	0.0	0.0	0.0000	2.4	329.9	-2.0	1.2
47.0	13591	15.1	.03521	41.8	.15	166.0	208.6	348.5	208.64	0.0	0.0	0.0000	1.0	344.4	-1.0	.3
48.0	13928	15.8	.03589	44.3	.17	157.0	205.4	348.6	205.39	0.0	0.0	0.0000	2.2	128.4	1.4	-1.7
48.9	14200	14.0	.03642	39.7	.15	150.0	202.9	348.9	202.91	0.0	0.0	0.0000	1.5	96.5	.2	-1.5
49.0	14240	13.7	.03650	39.1	.15	149.0	202.5	348.9	202.54	0.0	0.0	0.0000	1.4	89.7	0.0	-1.4
50.0	14566	13.7	.03710	39.2	.16	141.0	201.6	352.9	201.62	0.0	0.0	0.0000	2.5	353.5	-2.4	.3
51.0	14954	15.7	.03786	45.2	.20	132.0	200.2	357.0	200.20	0.0	0.0	0.0000	1.9	347.2	-1.8	.4
51.9	15272	16.3	.03855	47.1	.22	125.0	200.0	362.3	199.99	0.0	0.0	0.0000	3.5	62.4	-1.6	-3.1
52.0	15320	16.4	.03865	4'.3	.22	124.0	200.0	363.0	199.96	0.0	0.0	0.0000	4.0	66.2	-1.6	-3.7
53.0	15660	16.3	.03940	47.1	.23	117.0	200.0	369.1	199.96	0.0	0.0	0.0000	10.5	85.7	-.8	-10.5
54.0	16018	15.7	.04018	46.0	.24	110.0	197.2	370.4	197.16	0.0	0.0	0.0000	9.7	89.2	-.1	-9.7
55.0	16454	17.5	.04117	51.4	.28	102.0	197.2	378.5	197.16	0.0	0.0	0.0000	6.2	86.5	-.4	-6.1
55.3	16568	18.6	.04147	54.2	.31	100.0	198.1	382.5	198.07	0.0	0.0	0.0000	5.9	86.5	-.4	-5.9
56.0	16806	20.8	.04209	60.0	.36	96.0	200.0	390.6	199.96	0.0	0.0	0.0000	5.4	86.7	-.3	-5.3
57.0	17178	24.6	.04322	70.8	.45	90.1	200.9	399.6	200.92	0.0	0.0	0.0000	3.9	52.6	-2.4	-3.1
58.0	17534	26.4	.04445	76.2	.52	84.8	200.2	405.2	200.20	0.0	0.0	0.0000	4.7	51.4	-2.9	-3.7
58.9	17876	33.8	.04586	96.8	.70	80.0	201.4	414.5	201.41	0.0	0.0	0.0000	6.1	88.2	-.2	-6.1
59.0	17936	35.1	.04610	100.4	.73	79.2	201.6	416.1	201.62	0.0	0.0	0.0000	6.5	92.5	.3	-6.5
60.0	18293	43.5	.04796	121.7	.97	74.6	206.4	433.4	206.43	0.0	0.0	0.0000	5.1	130.0	3.3	-3.9
61.0	18670	51.7	.05030	143.8	1.22	70.1	207.9	444.2	207.85	0.0	0.0	0.0000	4.3	190.9	4.2	.8
61.0	18678	52.0	.05036	144.4	1.23	70.0	207.9	444.5	207.90	0.0	0.0	0.0000	4.3	191.0	4.2	.8
62.0	19020	61.2	.05285	168.3	1.53	66.2	210.0	456.1	209.99	0.0	0.0	0.0000	4.0	198.1	3.8	1.2
63.0	19374	68.2	.05578	187.0	1.81	62.5	210.6	464.9	210.55	0.0	0.0	0.0000	2.1	265.9	.1	2.1
63.7	19626	73.7	.05810	200.9	2.04	60.0	211.7	473.0	211.73	0.0	0.0	0.0000	2.2	309.5	-1.4	1.7
64.0	19730	75.9	.05906	206.6	2.13	59.0	212.2	476.4	212.21	0.0	0.0	0.0000	2.6	322.5	-2.1	1.6
65.0	20142	80.6	.06317	220.8	2.42	55.2	210.7	482.2	210.74	0.0	0.0	0.0000	1.5	317.7	-1.1	1.0

TIME MIN	ALT GPM	OZONE MICMB	TOTOZ ATMCM	OZDEN MG/M3	OZMXR MICGG	PRESS MB	TEMP DEG K	PTEMP DEG K	VTEMP DEG K	HMDTY PRCNT	DEWPT DEG K	SPCFC HMDTY	SPD MPS	DIR DEG	NS MPS	EW MPS
66.0	20498	81.6	.06687	223.8	2.60	52.1	210.6	489.8	210.55	0.0	0.0	0.0000	5.2	299.1	-2.5	4.5
66.7	20750	82.5	.06954	227.2	2.74	50.0	209.7	493.4	209.66	0.0	0.0	0.0000	4.3	305.2	-2.5	3.5
67.0	20875	82.9	.07085	228.9	2.80	49.0	209.2	495.3	209.22	0.0	0.0	0.0000	3.8	309.2	-2.4	3.0
68.0	21223	89.4	.07471	245.3	3.20	46.3	210.4	506.1	210.36	0.0	0.0	0.0000	2.8	113.5	1.1	-2.6
69.0	21580	98.9	.07900	268.7	3.75	43.7	212.6	519.9	212.57	0.0	0.0	0.0000	5.1	93.2	.3	-5.1
70.0	21902	106.0	.08318	286.6	4.23	41.5	213.5	529.9	213.46	0.0	0.0	0.0000	6.1	80.4	-1.0	-6.0
70.7	22131	109.9	.08634	296.7	4.56	40.0	213.8	536.4	213.82	0.0	0.0	0.0000	5.1	89.4	-.1	-5.1
71.0	22242	111.7	.08785	301.5	4.71	39.3	214.0	539.5	213.99	0.0	0.0	0.0000	4.7	94.9	.4	-4.7
72.0	22619	116.2	.09328	314.7	5.20	37.0	213.1	546.6	213.11	0.0	0.0	0.0000	4.4	127.3	2.6	-3.5
73.0	22968	124.9	.09857	333.9	5.91	35.0	215.9	562.7	215.90	0.0	0.0	0.0000	3.3	121.5	1.7	-2.8
73.0	22986	125.3	.09884	334.9	5.95	34.9	216.0	563.5	216.05	0.0	0.0	0.0000	3.2	121.1	1.7	-2.8
74.0	23381	136.4	.10525	359.8	6.89	32.8	218.8	581.0	218.84	0.0	0.0	0.0000	6.0	49.2	-3.9	-4.6
75.0	23742	139.1	.11139	367.2	7.43	31.0	218.7	590.0	218.68	0.0	0.0	0.0000	10.2	32.2	-8.6	-5.4
75.6	23951	139.3	.11499	368.0	7.69	30.0	218.5	595.0	218.48	0.0	0.0	0.0000	12.0	46.5	-8.3	-8.7
76.0	24081	139.4	.11721	368.5	7.85	29.4	218.4	598.1	218.36	0.0	0.0	0.0000	13.4	53.1	-8.0	-10.7
77.0	24441	142.8	.12344	372.9	8.51	27.8	221.1	615.3	221.05	0.0	0.0	0.0000	16.4	92.0	.6	-16.4
78.0	24876	150.5	.13118	389.8	9.59	26.0	222.9	632.4	222.89	0.0	0.0	0.0000	13.7	112.6	5.2	-12.6
78.6	25132	152.2	.13588	391.6	10.10	25.0	224.5	644.0	224.46	0.0	0.0	0.0000	10.6	117.0	4.8	-9.4
79.0	25292	153.3	.13879	392.6	10.41	24.4	225.4	651.3	225.43	0.0	0.0	0.0000	8.7	121.4	4.5	-7.4
80.0	25680	153.6	.14595	397.2	11.06	23.0	223.2	655.8	223.19	0.0	0.0	0.0000	5.2	207.7	4.6	2.4
81.0	26030	150.7	.15238	389.7	11.46	21.8	223.3	666.4	223.34	0.0	0.0	0.0000	5.2	254.8	1.4	5.1
82.0	26463	145.9	.16015	378.9	11.85	20.4	222.3	675.9	222.28	0.0	0.0	0.0000	.7	305.6	-.4	.6
82.4	26591	144.3	.16239	374.7	11.95	20.0	222.3	679.9	222.34	0.0	0.0	0.0000	1.2	355.5	-1.2	.1
83.0	26824	141.4	.16643	367.1	12.14	19.3	222.4	687.1	222.44	0.0	0.0	0.0000	2.7	17.3	-2.6	-.8
84.0	27278	137.4	.17410	355.7	12.65	18.0	223.0	702.9	223.04	0.0	0.0	0.0000	8.7	44.2	-6.3	-6.1
84.4	27462	135.2	.17710	349.4	12.80	17.5	223.4	709.7	223.38	0.0	0.0	0.0000	10.5	48.2	-7.0	-7.9
85.0	27690	132.4	.18081	341.5	12.98	16.9	223.8	718.1	223.80	0.0	0.0	0.0000	12.8	51.6	-8.0	-10.1
86.0	28089	124.7	.18700	322.9	13.00	15.9	223.0	728.2	223.04	0.0	0.0	0.0000	16.8	57.8	-8.9	-14.2
86.9	28469	120.0	.19261	310.2	13.25	15.0	223.3	741.4	223.31	0.0	0.0	0.0000	22.2	70.6	-7.4	-21.0
87.0	28513	119.4	.19326	308.8	13.28	14.9	223.3	742.9	223.34	0.0	0.0	0.0000	22.9	71.6	-7.2	-21.7
88.0	28922	112.0	.19894	287.1	13.25	14.0	225.1	762.3	225.13	0.0	0.0	0.0000	22.4	79.3	-4.1	-22.0
89.0	29361	105.8	.20465	270.2	13.39	13.1	226.2	780.4	226.16	0.0	0.0	0.0000	28.7	84.4	-2.8	-28.6
89.7	29673	101.0	.20843	255.9	13.38	12.5	228.0	797.3	227.95	0.0	0.0	0.0000	31.6	83.1	-1.0	-31.6
90.0	29835	98.5	.21039	248.5	13.38	12.2	228.9	806.1	228.88	0.0	0.0	0.0000	33.1	89.9	-.1	-33.1
91.0	30175	91.2	.21417	226.9	13.03	11.6	232.1	829.2	232.10	0.0	0.0	0.0000	27.9	100.3	5.0	-27.5
92.0	30598	84.7	.21849	210.7	12.88	10.9	232.2	844.6	232.23	0.0	0.0	0.0000	29.4	104.0	7.1	-28.6
93.0	31185	77.7	.22401	192.1	12.88	10.0	233.6	870.8	233.60	0.0	0.0	0.0000	999.9	999.9	999.9	999.9
94.0	31536	70.2	.22701	173.3	12.25	9.5	233.9	884.7	233.88	0.0	0.0	0.0000	28.6	113.5	11.4	-26.2
95.0	31907	65.0	.22989	159.8	11.96	9.0	234.8	902.1	234.83	0.0	0.0	0.0000	999.9	999.9	999.9	999.9
96.0	32301	59.7	.23270	146.0	11.63	8.5	235.9	921.2	235.91	0.0	0.0	0.0000	59.6	102.5	12.9	-58.2
97.0	32720	53.1	.23540	129.3	11.00	8.0	237.1	942.1	237.12	0.0	0.0	0.0000	40.9	83.1	-4.9	-40.6
98.0	33167	46.7	.23794	114.2	10.32	7.5	236.2	955.8	236.18	0.0	0.0	0.0000	33.7	92.8	1.7	-33.6
98.8	33643	43.1	.24037	105.5	10.21	7.0	236.1	974.4	236.07	0.0	0.0	0.0000	37.0	95.3	3.4	-36.9
99.0	33743	42.4	.24087	103.7	10.18	6.9	236.0	978.3	236.04	0.0	0.0	0.0000	37.7	95.7	3.8	-37.6
100.0	34265	37.1	.24323	90.1	9.61	6.4	237.9	1007.5	237.92	0.0	0.0	0.0000	999.9	999.9	999.9	999.9

INTEGRAL .24323 RESIDUAL .02931 INTEGRATED TOTAL OZONE .27255

OZONAGRAM

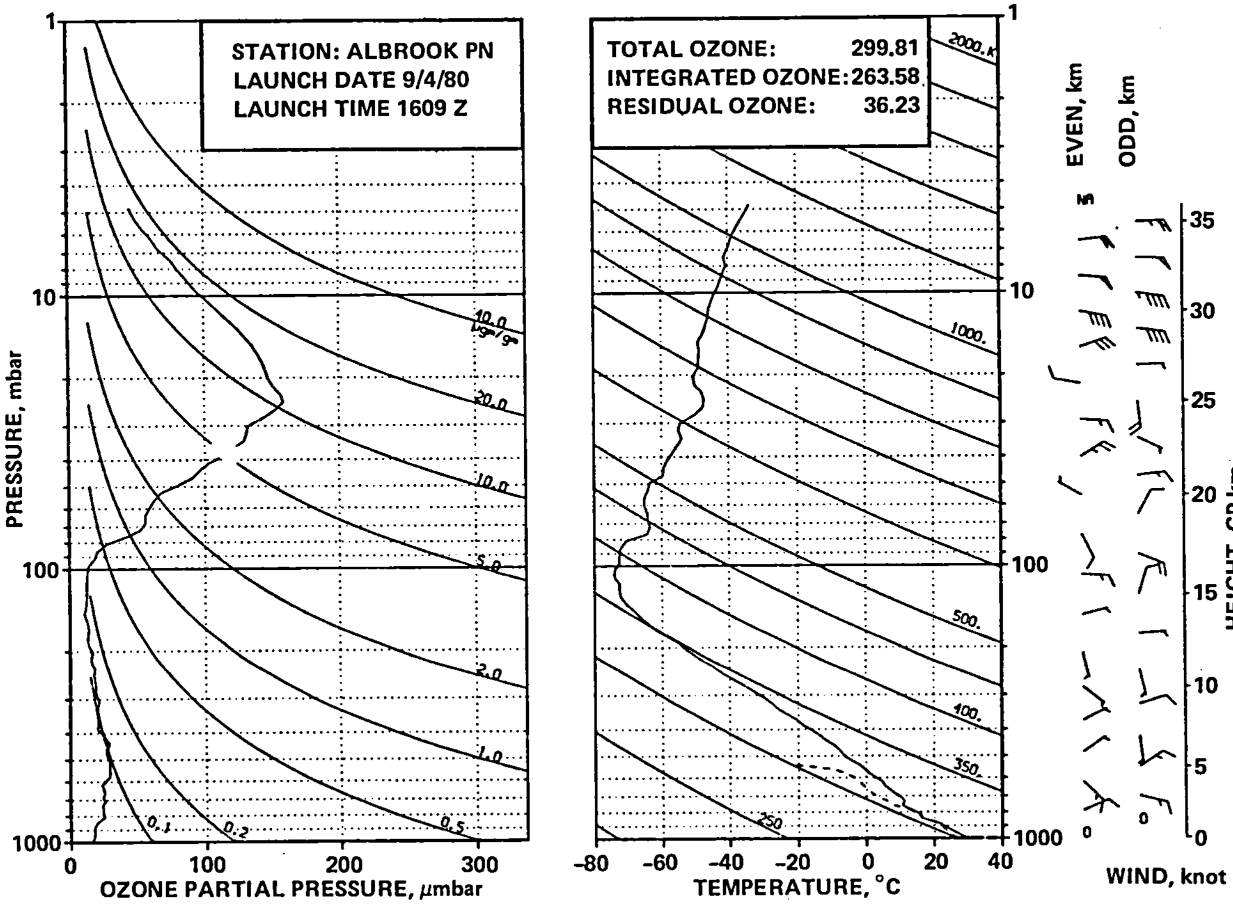
STATION: ALBROOK PN
LAUNCH DATE 9/4/80
LAUNCH TIME 1609 Z
TOTAL OZONE: 299.81
INTEGRATED OZONE: 263.58
RESIDUAL OZONE: 36.23
PRESSURE, mbar
OZONE PARTIAL PRESSURE, µmbar
TEMPERATURE, °C
EVEN, km
ODD, km
HEIGHT, GP km
WIND, knot
2000. K
1000.
500.
400.
350.
250
10.0
20.0
10.0
5.0
2.0
1.0
0.5
0.2
0.1

STATION ALBROOK PN   LAUNCH DATE 9/ 4/80   TIME 1609Z   ECC   SONDE 3A1321

SURFACE CONDITIONS   PRESS 1003.8MB   TEMP 303.0 DEG K   HUMIDITY 88.0 PRCNT

TIME MIN	ALT GPM	OZONE MICMB	TOTOZ ATMCM	OZDEN MG/M3	OZMXR MICGG	PRESS MB	TEMP DEG K	PTEMP DEG K	VTEMP DEG K	HMDTY PRCNT	DEWPT DEG K	SPCFC HMDTY	SPD MPS	DIR DEG	NS MPS	EW MPS
0.0	66	15.4	0.00000	29.4	.03	1003.8	303.2	302.8	307.26	83.3	300.0	.0221	1.0	310.0	-.6	.8
.1	99	15.6	.00005	29.8	.03	1000.0	302.9	302.9	306.96	83.6	299.8	.0218	1.1	314.3	-.7	.8
1.0	446	17.5	.00055	33.6	.03	962.0	300.2	303.5	303.91	87.4	297.9	.0204	1.9	338.4	-1.7	.7
2.0	841	17.8	.00117	34.6	.03	920.0	297.3	304.5	300.79	92.5	296.0	.0190	.9	6.2	-.9	-.1
2.5	1033	17.9	.00148	34.9	.03	900.0	296.0	305.0	299.36	95.8	295.3	.0183	1.0	357.8	-1.0	0.0
3.0	1230	17.9	.00180	35.1	.03	880.0	294.6	305.6	297.89	99.2	294.5	.0181	1.2	351.8	-1.2	.2
3.8	1529	19.8	.00233	39.4	.04	850.0	290.7	304.5	293.28	99.8	290.6	.0141	2.0	28.1	-1.7	-.9
4.0	1611	20.4	.00247	40.6	.04	842.0	289.6	304.2	292.02	100.0	289.6	.0139	2.2	33.2	-1.9	-1.2
5.0	1942	25.1	.00316	50.1	.05	810.0	289.0	306.9	291.41	100.0	289.0	.0139	4.8	65.7	-2.0	-4.4
5.4	2047	24.8	.00341	49.6	.05	800.0	287.9	306.9	290.24	100.0	287.9	.0127	5.3	67.4	-2.1	-4.9
6.0	2240	24.1	.00385	48.7	.05	782.0	286.0	306.8	288.10	100.0	286.0	.0119	6.3	69.8	-2.2	-5.9
7.0	2523	24.3	.00449	49.5	.05	756.0	283.8	307.4	285.29	83.1	281.0	.0088	7.3	80.0	-1.3	-7.2
8.0	2781	23.8	.00508	48.2	.05	733.0	284.5	310.9	285.93	71.6	279.6	.0082	7.9	91.8	.2	-7.9
9.0	3047	25.9	.00570	52.7	.06	710.0	283.6	312.7	284.80	63.5	277.0	.0070	7.7	103.2	1.7	-7.5
9.4	3164	25.1	.00598	51.3	.06	700.0	282.8	313.1	283.97	63.2	276.1	.0066	7.5	107.6	2.3	-7.2
10.0	3320	24.2	.00635	49.5	.06	687.0	281.8	313.7	282.86	62.8	275.1	.0064	7.4	113.6	3.0	-6.8
11.0	3601	25.5	.00702	52.5	.06	664.0	280.2	314.9	281.18	63.1	273.6	.0059	7.0	125.4	4.0	-5.7
12.0	3903	24.8	.00775	51.4	.06	640.0	278.6	316.5	279.55	63.1	272.2	.0055	7.1	133.3	4.8	-5.1
13.0	4188	23.5	.00842	48.8	.06	618.0	277.8	318.7	278.66	62.6	271.2	.0053	6.3	133.9	4.3	-4.5
13.9	4427	26.0	.00900	54.4	.07	600.0	276.0	319.4	276.83	63.0	269.7	.0049	8.7	159.9	8.2	-3.0
14.0	4441	26.1	.00903	54.7	.07	599.0	275.9	319.4	276.73	63.0	269.6	.0049	8.9	160.9	8.4	-2.9
15.0	4729	29.2	.00981	61.5	.08	578.0	274.1	320.6	274.80	59.1	267.0	.0042	5.0	113.0	2.0	-4.6
16.0	4997	29.6	.01059	62.7	.09	559.0	272.8	322.1	273.37	49.3	263.5	.0033	8.1	49.8	-5.2	-6.2
17.0	5287	29.2	.01143	62.2	.09	539.0	271.2	323.6	271.47	22.1	252.5	.0014	4.9	80.3	-.8	-4.8
18.0	5555	29.2	.01222	62.7	.09	521.0	269.1	324.2	269.23	0.0	0.0	0.0000	4.6	82.6	-.6	-4.6
19.0	5831	29.2	.01303	63.2	.10	503.0	267.0	324.9	267.36	51.2	258.6	.0024	4.7	69.5	-1.6	-4.4
19.1	5877	28.9	.01316	62.6	.10	500.0	266.8	325.2	267.16	48.1	257.4	.0021	4.4	67.8	-1.7	-4.1
20.0	6212	26.8	.01411	58.2	.09	479.0	265.5	327.6	265.67	25.6	249.2	.0011	2.7	46.8	-1.9	-2.0
21.0	6610	27.4	.01521	60.0	.10	455.0	263.7	330.3	263.74	0.0	0.0	0.0000	1.6	324.2	-1.3	.9
22.0	6920	29.4	.01611	64.9	.11	437.0	261.3	331.0	261.31	0.0	0.0	0.0000	2.6	331.7	-2.3	1.2
23.0	7222	26.8	.01699	59.6	.11	420.0	259.5	332.5	259.65	36.2	247.7	.0011	2.0	3.4	-2.0	-.1
24.0	7572	23.6	.01791	52.9	.10	401.0	257.0	333.6	257.19	51.7	249.4	.0014	1.9	62.9	-.8	-1.6
24.1	7590	23.3	.01795	52.5	.10	400.0	256.8	333.7	257.02	50.6	248.9	.0013	2.0	62.9	-.9	-1.8
25.0	7838	20.3	.01852	45.9	.09	387.0	254.7	334.0	254.78	36.4	243.4	.0008	3.5	62.9	-1.6	-3.1
26.0	8152	21.0	.01921	47.9	.09	371.0	253.0	335.9	253.16	41.7	243.4	.0009	3.9	63.7	-1.7	-3.5
27.0	8456	21.1	.01989	48.5	.10	356.0	250.5	336.5	250.58	37.3	239.9	.0006	4.1	64.7	-1.8	-3.7
27.4	8579	20.8	.02017	48.1	.10	350.0	249.5	336.8	249.57	29.8	236.2	.0004	4.5	63.0	-2.0	-4.0
28.0	8791	20.3	.02064	47.3	.10	340.0	247.8	337.3	247.86	0.0	0.0	0.0000	5.1	60.6	-2.5	-4.5
29.0	9161	20.4	.02147	47.9	.10	323.0	245.8	339.5	245.85	0.0	0.0	0.0000	4.1	78.4	-.8	-4.1
30.0	9455	21.7	.02215	51.4	.12	310.0	244.0	340.9	243.98	0.0	0.0	0.0000	4.4	107.4	1.3	-4.2
30.7	9687	20.7	.02269	49.3	.11	300.0	242.0	341.4	242.02	0.0	0.0	0.0000	4.4	113.6	1.8	-4.0
31.0	9783	20.2	.02292	48.4	.11	296.0	241.2	341.5	241.21	0.0	0.0	0.0000	4.4	116.1	2.0	-4.0
32.0	10123	19.0	.02366	45.9	.11	282.0	238.5	342.5	238.54	0.0	0.0	0.0000	3.6	128.1	2.2	-2.8
33.0	10425	19.1	.02432	46.6	.12	270.0	236.0	343.0	235.99	0.0	0.0	0.0000	2.7	137.0	2.0	-1.9
34.0	10763	18.4	.02505	45.6	.12	257.0	232.8	343.3	232.84	0.0	0.0	0.0000	2.4	160.1	2.2	-.8
34.6	10949	18.0	.02544	44.8	.12	250.0	231.3	343.8	231.35	0.0	0.0	0.0000	2.8	164.5	2.7	-.7
35.0	11059	17.7	.02567	44.4	.12	246.0	230.5	344.1	230.48	0.0	0.0	0.0000	3.0	166.5	2.9	-.7
36.0	11423	18.4	.02644	46.5	.13	233.0	227.9	345.6	227.92	0.0	0.0	0.0000	3.3	168.4	3.3	-.7
37.0	11743	16.3	.02710	41.9	.12	222.0	225.0	345.9	225.00	0.0	0.0	0.0000	2.6	185.4	2.6	.2
38.0	12045	15.6	.02768	40.4	.12	212.0	222.6	346.7	222.59	0.0	0.0	0.0000	1.6	168.7	1.6	-.3
39.0	12358	16.9	.02830	44.5	.14	202.0	219.9	347.4	219.94	0.0	0.0	0.0000	1.4	134.5	.9	-1.0
39.2	12421	16.4	.02842	43.0	.14	200.0	219.5	347.7	219.54	0.0	0.0	0.0000	1.4	132.6	.9	-1.0
40.0	12716	13.7	.02898	36.2	.12	191.0	217.7	349.3	217.68	0.0	0.0	0.0000	1.4	124.2	.8	-1.2
41.0	13021	13.1	.02949	35.2	.12	182.0	214.5	348.9	214.45	0.0	0.0	0.0000	1.6	90.4	0.0	-1.6
42.0	13337	13.6	.03002	37.1	.13	173.0	211.6	349.3	211.58	0.0	0.0	0.0000	2.3	60.7	-1.2	-2.0
43.0	13591	14.1	.03047	38.9	.14	166.0	209.7	350.3	209.69	0.0	0.0	0.0000	3.0	48.9	-2.0	-2.3
44.0	13970	12.9	.03114	35.8	.14	156.0	207.1	352.2	207.12	0.0	0.0	0.0000	2.7	75.6	-.7	-2.6
44.6	14206	11.7	.03150	32.7	.13	150.0	205.7	353.8	205.75	0.0	0.0	0.0000	2.4	76.8	-.6	-2.4
45.0	14369	10.8	.03175	30.5	.12	146.0	204.8	354.9	204.81	0.0	0.0	0.0000	2.3	77.8	-.5	-2.2
46.0	14662	12.0	.03220	34.3	.14	139.0	202.8	356.4	202.81	0.0	0.0	0.0000	5.3	9.2	-5.3	-.8
47.0	15057	12.6	.03285	36.3	.16	130.0	200.9	359.9	200.94	0.0	0.0	0.0000	6.0	16.9	-5.8	-1.8
47.6	15287	12.6	.03324	36.3	.17	125.0	200.6	363.5	200.64	0.0	0.0	0.0000	4.8	28.9	-4.2	-2.3
48.0	15430	12.6	.03348	36.3	.17	122.0	200.5	365.6	200.46	0.0	0.0	0.0000	4.1	39.7	-3.2	-2.6
49.0	15726	12.6	.03398	36.3	.18	116.0	200.5	371.0	200.46	0.0	0.0	0.0000	4.1	65.3	-1.7	-3.7
50.0	16036	12.8	.03451	37.0	.19	110.0	199.0	373.8	198.97	0.0	0.0	0.0000	6.9	92.0	.2	-6.9
51.0	16419	13.5	.03519	39.0	.22	103.0	199.2	381.4	199.22	0.0	0.0	0.0000	8.8	105.4	2.3	-8.5
51.6	16591	13.8	.03551	39.8	.23	100.0	200.0	386.1	199.96	0.0	0.0	0.0000	10.0	114.9	4.2	-9.1
52.0	16710	14.0	.03573	40.3	.24	98.0	200.5	389.3	200.46	0.0	0.0	0.0000	11.1	120.1	5.5	-9.6
53.0	17119	19.0	.03664	54.7	.34	91.4	200.5	397.1	200.46	0.0	0.0	0.0000	11.0	110.9	3.9	-10.3
54.0	17463	20.9	.03756	60.2	.40	86.2	200.9	404.8	200.94	0.0	0.0	0.0000	8.4	91.6	.2	-8.4
55.0	17837	27.9	.03879	79.6	.57	80.9	202.6	415.5	202.58	0.0	0.0	0.0000	5.6	114.2	2.3	-5.1
55.2	17904	30.6	.03909	86.6	.64	80.0	203.8	419.4	203.81	0.0	0.0	0.0000	5.2	124.7	3.0	-4.3
56.0	18173	41.4	.04032	114.4	.90	76.5	208.7	435.0	208.72	0.0	0.0	0.0000	5.7	171.4	5.6	-.9
57.0	18527	52.4	.04246	144.3	1.20	72.2	209.7	444.3	209.69	0.0	0.0	0.0000	2.6	120.1	1.3	-2.3
57.5	18716	54.6	.04379	150.6	1.29	70.0	209.4	447.7	209.39	0.0	0.0	0.0000	3.7	63.1	-1.7	-3.3
58.0	18894	56.6	.04504	156.4	1.38	68.0	209.1	450.8	209.11	0.0	0.0	0.0000	6.1	43.4	-4.4	-4.2
59.0	19265	56.4	.04774	155.8	1.46	64.0	208.9	458.2	208.92	0.0	0.0	0.0000	3.8	12.3	-3.7	-.8
60.0	19658	59.5	.05069	165.1	1.64	60.0	208.0	464.6	207.95	0.0	0.0	0.0000	2.3	326.7	-2.0	1.3
60.0	19669	59.5	.05077	165.3	1.65	59.9	207.9	464.7	207.93	0.0	0.0	0.0000	2.3	325.0	-1.9	1.3
61.0	20079	63.3	.05403	175.6	1.87	56.0	208.1	474.2	208.13	0.0	0.0	0.0000	2.7	298.6	-1.3	2.4
62.0	20426	67.5	.05697	186.3	2.11	52.9	209.1	484.3	209.11	0.0	0.0	0.0000	1.9	224.1	1.4	1.3
62.9	20771	78.2	.06023	215.7	2.59	50.0	209.5	493.0	209.48	0.0	0.0	0.0000	5.1	108.5	1.6	-4.8
63.0	20796	79.0	.06046	217.7	2.63	49.8	209.5	493.6	209.50	0.0	0.0	0.0000	5.5	107.2	1.6	-5.2

TIME MIN	ALT GPM	OZONE MICMB	TOTOZ ATMCM	OZDEN MG/M3	OZMXR MICGG	PRESS MB	TEMP DEG K	PTEMP DEG K	VTEMP DEG K	HMDTY PRCNT	DEWPT DEG K	SPCFC HMDTY	SPD MPS	DIR DEG	NS MPS	EW MPS
64.0	21194	90.4	.06475	244.3	3.21	46.7	213.6	512.6	213.57	0.0	0.0	0.0000	9.7	72.4	-2.9	-9.3
65.0	21595	96.3	.06947	260.1	3.64	43.8	213.8	522.5	213.75	0.0	0.0	0.0000	12.0	67.4	-4.6	-11.1
66.0	21963	102.4	.07408	275.4	4.11	41.3	214.8	533.9	214.80	0.0	0.0	0.0000	14.1	57.3	-7.6	-11.9
66.6	22164	108.2	.07680	289.5	4.49	40.0	215.7	541.0	215.66	0.0	0.0	0.0000	11.5	60.1	-5.7	-9.9
67.0	22324	112.7	.07895	300.8	4.79	39.0	216.3	546.6	216.34	0.0	0.0	0.0000	9.4	63.4	-4.2	-8.4
68.0	22710	119.6	.08451	317.1	5.40	36.7	217.7	559.6	217.68	0.0	0.0	0.0000	4.8	107.2	1.4	-4.6
68.7	23013	126.2	.08917	332.9	5.98	35.0	218.8	570.2	218.77	0.0	0.0	0.0000	2.5	113.0	1.0	-2.3
69.0	23161	129.4	.09144	340.6	6.27	34.2	219.3	575.3	219.30	0.0	0.0	0.0000	1.4	122.6	.8	-1.2
70.0	23586	131.2	.09828	347.2	6.79	32.0	218.2	583.3	218.17	0.0	0.0	0.0000	1.4	76.4	-.3	-1.3
71.0	23998	132.4	.10499	349.6	7.31	30.0	218.7	595.5	218.66	0.0	0.0	0.0000	7.2	90.2	0.0	-7.2
72.0	24421	143.9	.11212	372.5	8.49	28.1	223.0	618.9	223.05	0.0	0.0	0.0000	12.4	111.5	4.5	-11.5
73.0	24855	152.6	.11987	390.4	9.61	26.3	225.6	637.9	225.59	0.0	0.0	0.0000	10.9	141.5	8.5	-6.8
73.8	25189	157.4	.12610	402.2	10.44	25.0	225.9	648.2	225.93	0.0	0.0	0.0000	8.7	191.9	8.5	1.8
74.0	25296	158.9	.12808	406.0	10.71	24.6	226.0	651.5	226.03	0.0	0.0	0.0000	9.6	208.0	8.5	4.5
75.0	25711	157.1	.13592	402.6	11.27	23.1	225.3	661.1	225.30	0.0	0.0	0.0000	10.4	249.0	3.7	9.7
76.0	26121	151.8	.14354	392.7	11.59	21.7	223.2	666.8	223.20	0.0	0.0	0.0000	5.1	284.7	-1.3	5.0
77.0	26588	147.7	.15201	382.8	12.11	20.2	222.7	679.2	222.74	0.0	0.0	0.0000	1.1	326.5	-1.0	.6
77.2	26652	147.4	.15316	381.6	12.21	20.0	223.0	681.8	222.97	0.0	0.0	0.0000	.8	343.4	-.8	.2
78.0	26988	145.9	.15910	375.9	12.72	19.0	224.1	695.4	224.11	0.0	0.0	0.0000	1.9	95.9	.2	-1.8
79.0	27416	143.8	.16656	370.1	13.39	17.8	224.4	709.4	224.41	0.0	0.0	0.0000	9.2	56.2	-5.1	-7.7
79.2	27527	143.0	.16846	368.0	13.55	17.5	224.4	713.0	224.44	0.0	0.0	0.0000	10.4	59.2	-5.3	-8.9
80.0	27954	139.9	.17573	359.8	14.14	16.4	224.6	726.7	224.56	0.0	0.0	0.0000	14.9	66.4	-6.0	-13.6
81.0	28496	135.2	.18469	348.0	14.83	15.1	224.3	743.1	224.26	0.0	0.0	0.0000	15.6	88.5	-.4	-15.6
81.1	28539	134.6	.18539	346.4	14.87	15.0	224.4	745.0	224.40	0.0	0.0	0.0000	15.9	89.5	-.1	-15.9
82.0	28900	130.4	.19113	333.7	15.21	14.2	225.6	760.8	225.59	0.0	0.0	0.0000	18.3	96.7	2.1	-18.2
83.0	29333	125.4	.19774	319.7	15.62	13.3	226.5	778.1	226.47	0.0	0.0	0.0000	21.1	97.5	2.7	-20.9
83.8	29744	119.5	.20369	303.8	15.83	12.5	227.1	794.1	227.05	0.0	0.0	0.0000	20.7	99.5	3.4	-20.5
84.0	29852	117.9	.20524	299.6	15.88	12.3	227.2	798.3	227.20	0.0	0.0	0.0000	20.7	100.0	3.6	-20.3
85.0	30358	110.8	.21210	281.2	16.11	11.4	227.6	817.3	227.63	0.0	0.0	0.0000	21.6	101.1	4.1	-21.2
86.0	30971	102.3	.21982	258.2	16.30	10.4	228.8	843.3	228.78	0.0	0.0	0.0000	23.9	99.2	3.8	-23.6
86.5	31234	98.3	.22286	247.3	16.27	10.0	229.5	855.7	229.54	0.0	0.0	0.0000	23.4	96.3	2.6	-23.2
87.0	31509	94.1	.22603	235.9	16.24	9.6	230.3	868.7	230.34	0.0	0.0	0.0000	22.9	93.2	1.3	-22.9
88.0	32253	86.4	.23386	215.5	16.66	8.6	231.6	901.3	231.59	0.0	0.0	0.0000	25.0	94.7	2.0	-24.9
89.0	32744	80.8	.23863	200.5	16.74	8.0	232.7	924.5	232.70	0.0	0.0	0.0000	25.5	97.9	3.5	-25.3
90.0	33274	76.0	.24346	188.9	17.01	7.4	232.1	943.1	232.15	0.0	0.0	0.0000	24.2	87.6	-1.0	-24.1
90.7	33652	70.2	.24659	173.9	16.58	7.0	233.1	962.0	233.05	0.0	0.0	0.0000	27.6	84.2	-2.8	-27.5
91.0	33850	67.2	.24823	166.0	16.36	6.8	233.5	971.9	233.53	0.0	0.0	0.0000	29.5	82.7	-3.7	-29.3
92.0	34483	61.7	.25293	151.9	16.49	6.2	234.5	1002.0	234.48	0.0	0.0	0.0000	32.5	86.1	-2.2	-32.4
92.4	34708	59.1	.25444	145.1	16.29	6.0	235.2	1014.5	235.17	0.0	0.0	0.0000	33.0	86.5	-2.0	-32.9
93.0	35062	55.0	.25680	134.3	15.98	5.7	236.2	1034.1	236.25	0.0	0.0	0.0000	33.8	87.1	-1.7	-33.7
94.0	35567	50.4	.25982	122.4	15.75	5.3	237.7	1062.4	237.73	0.0	0.0	0.0000	38.6	88.9	-.8	-38.6
94.6	35973	47.7	.26203	115.4	15.80	5.0	238.9	1085.8	238.91	0.0	0.0	0.0000	999.9	999.9	999.9	999.9
95.0	36259	45.9	.26358	110.5	15.84	4.8	239.7	1102.1	239.73	0.0	0.0	0.0000	999.9	999.9	999.9	999.9

INTEGRAL .26358 RESIDUAL .03623 INTEGRATED TOTAL OZONE .29981

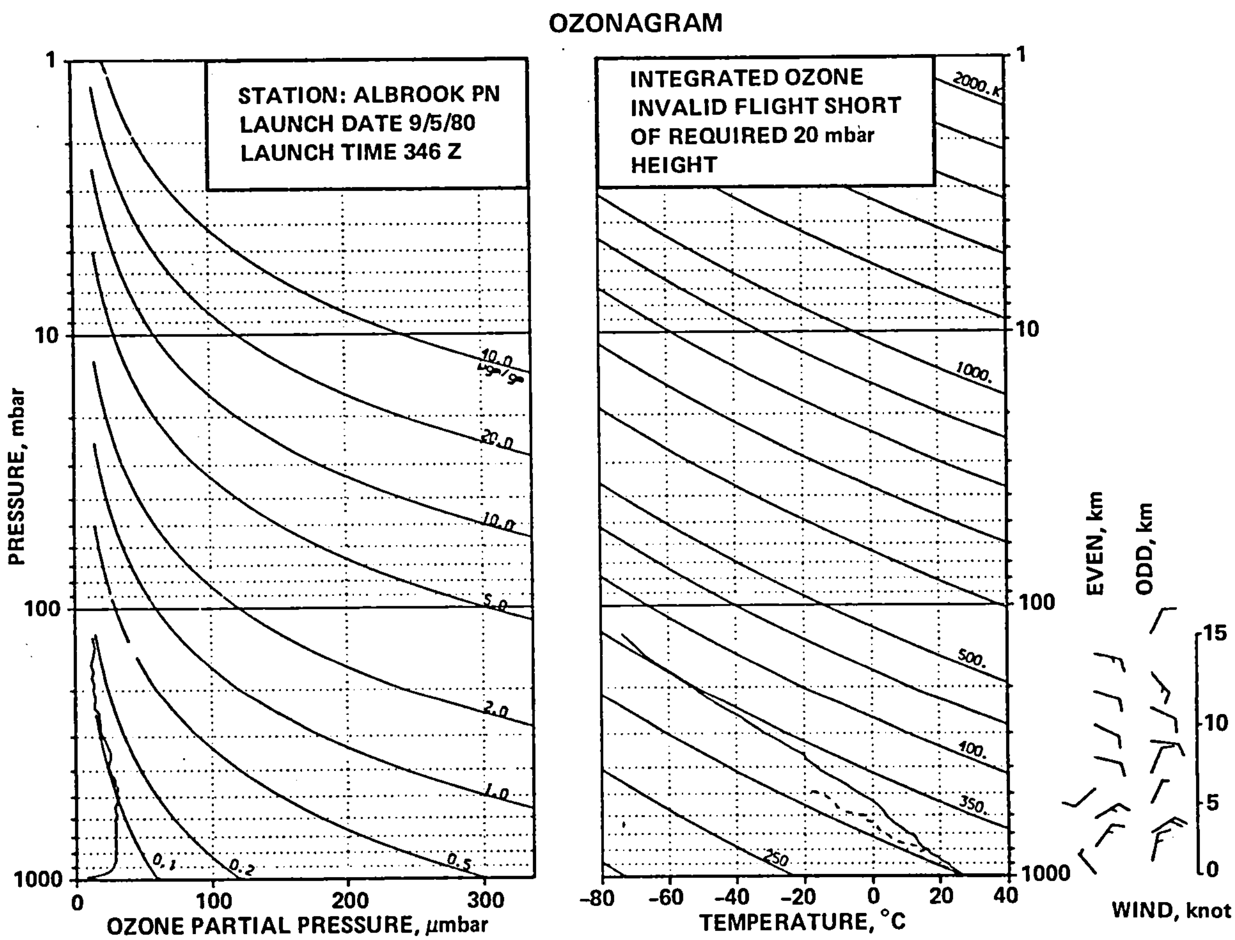

OZONAGRAM
STATION: ALBROOK PN
LAUNCH DATE 9/5/80
LAUNCH TIME 346 Z
INTEGRATED OZONE
INVALID FLIGHT SHORT
OF REQUIRED 20 mbar
HEIGHT
PRESSURE, mbar
OZONE PARTIAL PRESSURE, μmbar
TEMPERATURE, °C
EVEN, km
ODD, km
HEIGHT, GP km
WIND, knot

STATION ALBROOK PN LAUNCH DATE 9/ 5/80 TIME 346Z ECC SONDE 3A1322

SURFACE CONDITIONS PRESS 1003.8MB TEMP 299.7 DEG K HUMIDITY 95.0 PRCNT

TIME MIN	ALT GPM	OZONE MICMB	TOTOZ ATMCM	OZDEN MG/M3	OZMXR MICGG	PRESS MB	TEMP DEG K	PTEMP DEG K	VTEMP DEG K	HMDTY PRCNT	DEWPT DEG K	SPCFC HMDTY	SPD MPS	DIR DEG	NS MPS	EW MPS
0.0	66	20.2	0.00000	38.8	.03	1003.8	300.0	299.6	303.77	93.9	298.9	.0207	3.0	320.0	-2.3	1.9
.2	99	18.3	.00004	35.2	.03	1000.0	299.8	299.8	303.60	93.7	298.7	.0205	3.4	320.9	-2.7	2.2
1.0	288	7.8	.00028	15.1	.01	979.0	299.0	300.8	302.63	92.4	297.7	.0198	5.9	323.4	-4.7	3.5
2.0	525	20.2	.00057	39.1	.04	953.0	297.6	301.8	300.92	89.5	295.8	.0181	5.5	334.5	-5.0	2.4
3.0	739	24.4	.00100	47.6	.04	930.0	296.3	302.5	299.47	92.7	295.0	.0177	7.2	3.0	-7.2	-.4
4.0	958	26.7	.00151	52.2	.05	907.0	295.8	304.2	298.58	80.2	292.2	.0153	7.7	10.6	-7.6	-1.4
4.3	1025	27.0	.00168	52.8	.05	900.0	295.2	304.3	297.92	80.1	291.6	.0145	7.7	11.7	-7.5	-1.6
5.0	1211	27.6	.00213	54.3	.05	881.0	293.6	304.5	296.09	79.8	290.0	.0137	7.4	14.9	-7.2	-1.9
6.0	1470	29.0	.00280	57.3	.06	855.0	292.6	306.0	294.67	71.0	287.2	.0117	7.0	24.2	-6.4	-2.9
6.2	1520	29.0	.00294	57.4	.06	850.0	292.1	306.0	294.18	71.9	286.9	.0115	6.9	25.6	-6.2	-3.0
7.0	1714	29.0	.00346	57.7	.06	831.0	290.3	306.1	292.27	75.3	285.9	.0111	6.8	31.3	-5.8	-3.5
8.0	1954	28.7	.00409	57.2	.06	808.0	289.7	307.9	292.08	92.1	288.4	.0134	6.5	33.7	-5.4	-3.6
8.3	2038	28.9	.00432	57.8	.06	800.0	289.0	308.0	291.34	93.2	287.9	.0129	6.6	36.5	-5.3	-3.9
9.0	2200	29.3	.00476	58.8	.06	785.0	287.7	308.3	289.94	95.3	287.0	.0126	6.9	41.6	-5.1	-4.6
10.0	2462	29.3	.00547	59.0	.06	761.0	286.8	310.0	288.42	74.1	282.2	.0095	7.5	54.0	-4.4	-6.0
11.0	2709	29.4	.00615	59.3	.07	739.0	286.2	312.0	287.52	60.4	278.7	.0076	8.4	59.8	-4.2	-7.2
12.0	2963	28.9	.00685	58.4	.07	717.0	285.6	314.1	286.93	60.0	278.1	.0075	9.7	57.2	-5.2	-8.2
12.7	3163	29.1	.00740	59.2	.07	700.0	283.9	314.4	285.12	59.9	276.5	.0067	9.7	57.2	-5.3	-8.2
13.0	3247	29.2	.00763	59.5	.07	693.0	283.2	314.5	284.36	59.9	275.8	.0066	9.7	57.1	-5.3	-8.2
14.0	3527	29.2	.00841	59.8	.07	670.0	281.8	315.9	282.85	60.1	274.5	.0062	7.7	56.2	-4.3	-6.4
15.0	3802	29.2	.00918	60.2	.07	648.0	280.0	317.0	281.12	68.0	274.5	.0065	6.4	61.5	-3.1	-5.6
16.0	4072	29.2	.00993	60.4	.08	627.0	278.6	318.4	279.54	59.5	271.4	.0053	6.9	59.3	-3.5	-6.0
17.0	4377	28.7	.01079	59.7	.08	604.0	277.1	320.0	278.08	68.3	271.8	.0057	6.9	41.7	-5.1	-4.6
17.2	4430	28.9	.01094	60.3	.08	600.0	277.0	320.5	277.89	63.5	270.5	.0050	6.4	40.3	-4.9	-4.2
18.0	4678	30.3	.01165	63.2	.09	582.0	276.4	322.7	277.03	41.7	264.7	.0034	4.4	29.7	-3.8	-2.2
19.0	4961	29.1	.01247	61.0	.09	562.0	275.3	324.6	275.80	38.4	262.6	.0030	2.5	25.5	-2.2	-1.1
20.0	5267	28.7	.01334	60.6	.09	541.0	273.8	326.4	274.34	41.0	262.1	.0030	2.7	26.8	-2.4	-1.2
21.0	5477	30.0	.01394	63.6	.09	527.0	272.4	327.1	272.87	41.0	260.8	.0028	5.4	19.1	-5.1	-1.8
22.0	5863	31.2	.01512	66.9	.10	502.0	269.5	328.1	269.86	42.2	258.5	.0024	5.9	9.2	-5.8	-.9
22.1	5894	31.1	.01521	66.7	.10	500.0	269.2	328.2	269.63	41.2	258.0	.0023	5.7	8.2	-5.7	-.8
23.0	6166	30.0	.01605	64.8	.10	483.0	267.3	329.1	267.61	31.8	253.3	.0016	4.4	356.7	-4.4	.3
24.0	6496	31.0	.01707	67.4	.11	463.0	265.3	330.6	265.30	0.0	0.0	0.0000	4.5	2.3	-4.5	-.2
25.0	6785	28.6	.01795	62.9	.11	446.0	263.0	331.2	263.10	22.9	245.8	.0009	4.5	14.9	-4.3	-1.2
26.0	7100	28.6	.01888	63.5	.11	428.0	260.4	331.8	260.58	35.1	248.2	.0012	4.5	24.1	-4.1	-1.8
27.0	7426	25.6	.01980	57.3	.10	410.0	257.7	332.5	258.13	87.2	256.1	.0024	3.4	25.5	-3.1	-1.5
27.6	7611	24.8	.02028	55.8	.10	400.0	256.7	333.5	256.98	65.8	251.5	.0015	2.6	50.0	-1.7	-2.0
28.0	7744	24.3	.02063	54.8	.10	393.0	256.0	334.2	256.16	50.4	248.1	.0013	2.4	74.5	-.6	-2.3
29.0	8054	24.5	.02143	55.7	.11	377.0	253.9	335.5	254.12	57.7	247.7	.0013	4.6	103.0	1.0	-4.5
30.0	8376	25.7	.02229	58.7	.12	361.0	253.0	338.5	253.19	65.3	248.2	.0014	5.5	106.9	1.6	-5.3
30.7	8603	25.7	.02292	59.1	.12	350.0	251.0	338.7	251.14	65.0	246.2	.0011	5.2	107.4	1.6	-5.0
31.0	8710	25.7	.02321	59.4	.12	345.0	250.0	338.9	250.19	64.8	245.3	.0011	5.1	107.7	1.5	-4.8
32.0	9034	24.0	.02408	55.9	.12	330.0	247.5	339.7	247.62	65.4	242.9	.0009	4.8	96.6	.5	-4.8
33.0	9392	22.1	.02498	52.2	.12	314.0	244.8	340.9	244.95	71.0	241.2	.0008	3.9	93.7	.3	-3.9
34.0	9717	20.3	.02575	48.5	.11	300.0	241.8	341.0	241.88	89.5	240.6	.0008	4.5	110.0	1.5	-4.3
35.0	10029	18.3	.02642	44.2	.11	287.0	239.5	342.1	239.55	55.5	233.7	.0004	6.0	114.9	2.5	-5.5
36.0	10377	18.4	.02715	45.0	.11	273.0	236.5	342.7	236.56	50.4	230.0	.0003	5.7	111.9	2.1	-5.3
37.0	10713	17.7	.02784	43.6	.11	260.0	234.2	344.1	234.22	45.7	226.9	.0002	4.9	117.3	2.3	-4.4
37.8	10979	17.6	.02839	43.9	.12	250.0	231.6	344.2	231.64	0.0	0.0	0.0000	5.4	116.4	2.4	-4.9
38.0	11062	17.6	.02856	44.0	.12	247.0	230.8	344.2	230.84	0.0	0.0	0.0000	5.6	116.2	2.5	-5.0
39.0	11396	13.9	.02918	35.3	.10	235.0	227.8	344.6	227.83	0.0	0.0	0.0000	7.1	115.4	3.0	-6.4
40.0	11743	14.5	.02977	37.2	.11	223.0	225.2	345.7	225.18	0.0	0.0	0.0000	6.9	111.0	2.5	-6.4
41.0	12074	14.5	.03034	37.5	.11	212.0	222.9	347.2	222.90	0.0	0.0	0.0000	4.5	109.7	1.5	-4.2
42.0	12452	13.3	.03098	34.7	.11	200.0	220.4	349.0	220.38	0.0	0.0	0.0000	3.1	121.7	1.6	-2.7
43.0	12780	14.1	.03153	37.4	.12	190.0	217.3	349.2	217.26	0.0	0.0	0.0000	5.8	138.2	4.3	-3.9
44.0	13122	12.2	.03209	32.7	.11	180.0	214.7	350.4	214.68	0.0	0.0	0.0000	7.1	137.9	5.3	-4.8
45.0	13442	13.4	.03261	36.6	.13	171.0	211.6	350.4	211.58	0.0	0.0	0.0000	7.2	118.3	3.4	-6.3
46.0	13774	11.5	.03314	31.9	.12	162.0	208.7	351.0	208.68	0.0	0.0	0.0000	8.5	111.1	3.1	-8.0
47.0	14200	13.3	.03383	37.4	.15	151.0	205.6	352.8	205.56	0.0	0.0	0.0000	6.8	98.7	1.0	-6.7
47.1	14239	13.4	.03390	37.7	.15	150.0	205.3	353.0	205.32	0.0	0.0	0.0000	6.6	97.9	.9	-6.5
48.0	14652	14.5	.03466	41.2	.17	140.0	202.9	355.8	202.88	0.0	0.0	0.0000	4.9	85.4	-.4	-4.9
49.0	15225	12.6	.03570	36.5	.16	127.0	199.2	359.3	199.22	0.0	0.0	0.0000	999.9	999.9	999.9	999.9

CALIBRATIONS APPLIED FOR PARTIAL PRESSURE OF OZONE
TOTAL INTEGRATED OZONE INVALID. BALLOON SHORT OF 20 MB HEIGHT

OZONAGRAM

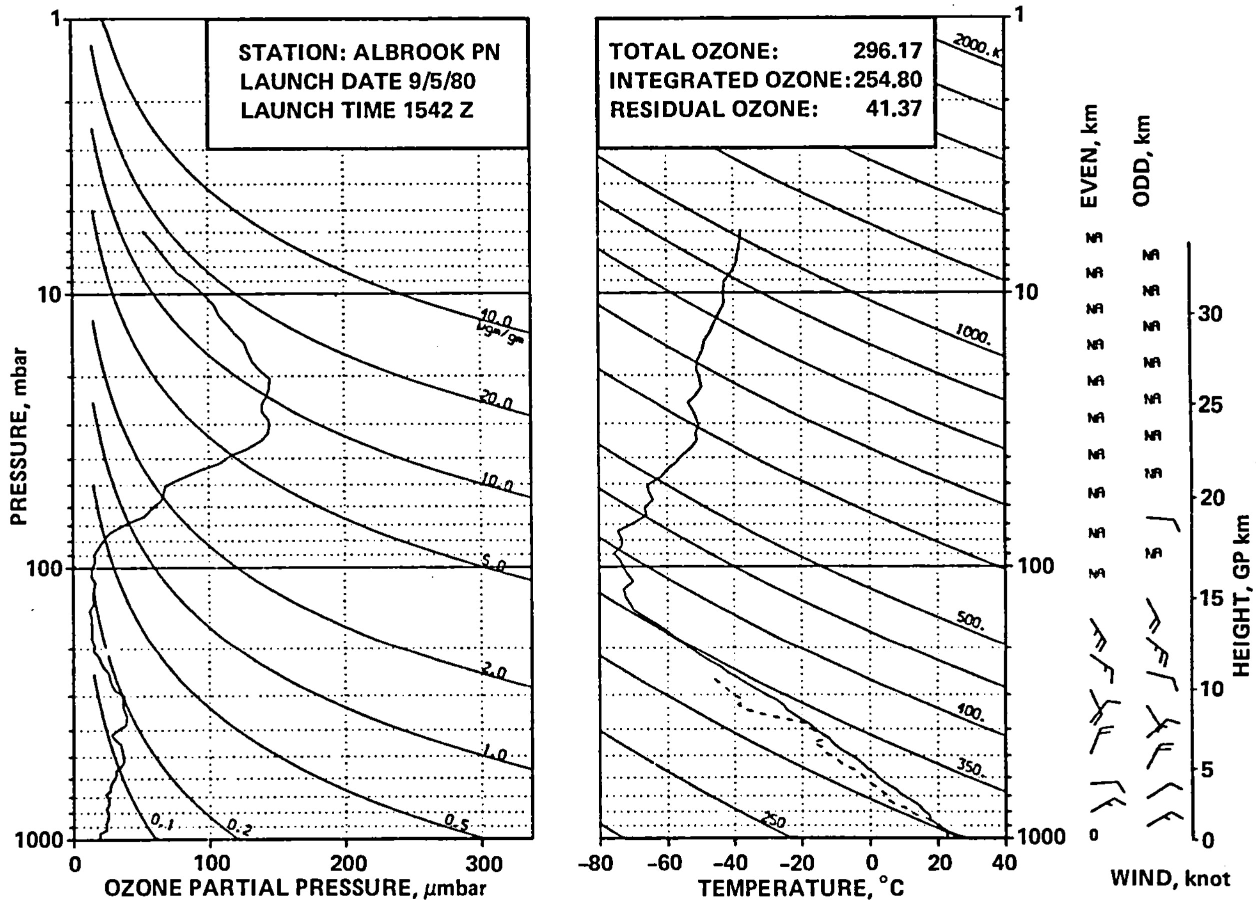

STATION: ALBROOK PN
LAUNCH DATE 9/5/80
LAUNCH TIME 1542 Z
TOTAL OZONE: 296.17
INTEGRATED OZONE: 254.80
RESIDUAL OZONE: 41.37
PRESSURE, mbar
OZONE PARTIAL PRESSURE, μmbar
TEMPERATURE, °C
WIND, knot
HEIGHT, GP km
EVEN, km
ODD, km

STATION ALBROOK PN LAUNCH DATE 9/ 5/80 TIME 1542Z ECC SONDE 3A1323

SURFACE CONDITIONS PRESS 1004.2MB TEMP 302.7 DEG K HUMIDITY 71.0 PRCNT

TIME MIN	ALT GPM	OZONE MICMB	TOTOZ ATMCM	OZDEN MG/M3	OZMXR MICGG	PRESS MB	TEMP DEG K	PTEMP DEG K	VTEMP DEG K	HMDTY PRCNT	DEWPT DEG K	SPCFC HMDTY	SPD MPS	DIR DEG	NS MPS	EW MPS
0.0	66	18.6	0.00000	35.4	.03	1004.2	302.6	302.3	305.74	64.9	295.3	.0167	1.0	360.0	-1.0	0.0
.2	103	18.7	.00006	35.7	.03	1000.0	302.1	302.1	305.24	67.7	295.5	.0171	1.0	18.3	-1.0	-.3
1.0	292	19.2	.00038	37.0	.03	979.0	299.4	301.3	302.71	81.7	296.1	.0179	2.2	65.1	-.9	-2.0
2.0	547	19.2	.00082	37.5	.03	951.0	296.4	300.7	299.54	92.1	295.0	.0173	3.1	73.1	-.9	-3.0
3.0	780	23.7	.00127	46.5	.04	926.0	294.8	301.4	297.77	93.2	293.7	.0163	5.5	66.7	-2.2	-5.0
4.0	1027	24.4	.00181	47.9	.04	900.0	293.5	302.5	296.42	97.4	293.1	.0162	8.4	60.6	-4.1	-7.3
5.0	1280	23.8	.00237	47.2	.05	874.0	291.8	303.3	294.44	96.0	291.2	.0148	9.3	54.6	-5.4	-7.6
6.0	1519	25.1	.00291	49.8	.05	850.0	290.8	304.0	293.27	95.3	290.0	.0141	9.0	49.6	-5.8	-6.8
7.0	1785	25.3	.00352	50.2	.05	824.0	290.6	307.1	292.66	78.6	286.8	.0119	8.5	53.8	-5.0	-6.9
8.0	2037	25.3	.00411	50.5	.05	800.0	289.2	308.2	291.07	75.1	284.8	.0106	7.6	59.6	-3.9	-6.6
8.0	2048	25.3	.00414	50.5	.05	799.0	289.1	308.3	291.01	75.0	284.7	.0106	7.6	59.9	-3.8	-6.6
9.0	2329	24.1	.00478	48.4	.05	773.0	288.1	310.1	289.89	72.8	283.3	.0100	6.3	58.4	-3.3	-5.4
10.0	2584	25.6	.00537	51.4	.06	750.0	287.0	311.5	288.42	63.9	280.2	.0084	5.4	57.8	-2.9	-4.6
11.0	2846	26.1	.00601	52.8	.06	727.0	285.2	312.4	285.57	63.8	278.6	.0077	4.4	58.5	-2.3	-3.7
12.0	3103	25.5	.00664	52.0	.06	705.0	283.4	313.1	284.76	73.7	278.9	.0081	4.1	57.4	-2.2	-3.4
12.2	3162	25.1	.00677	51.2	.06	700.0	283.0	313.4	284.37	73.4	278.5	.0078	4.2	63.6	-1.9	-3.8
13.0	3342	23.7	.00720	48.6	.06	685.0	281.9	314.1	283.18	72.5	277.2	.0074	4.9	79.5	-.9	-4.8
14.0	3612	27.0	.00785	55.4	.07	663.0	280.8	315.8	282.05	72.4	276.2	.0071	4.4	93.9	.3	-4.4
15.0	3889	26.9	.00856	55.6	.07	641.0	278.7	316.5	279.80	71.5	274.0	.0063	4.1	92.6	.2	-4.1
16.0	4161	28.1	.00929	58.6	.08	620.0	276.9	317.4	277.84	72.9	272.4	.0058	4.9	83.2	-.6	-4.8
17.0	4427	30.1	.01004	63.1	.08	600.0	275.5	318.8	276.46	74.2	271.4	.0056	6.2	63.0	-2.8	-5.6
18.0	4728	31.5	.01095	66.3	.09	578.0	274.5	321.1	275.41	71.7	270.0	.0052	8.4	44.1	-6.0	-5.8
19.0	4982	31.0	.01173	65.6	.09	560.0	272.6	321.7	273.39	71.8	268.2	.0047	10.3	29.4	-8.9	-5.0
20.0	5257	34.8	.01262	74.0	.11	541.0	271.3	323.4	271.98	62.7	265.2	.0039	12.1	27.2	-10.7	-5.5
21.0	5510	36.8	.01353	78.8	.12	524.0	269.9	324.7	270.54	62.9	263.9	.0036	13.2	26.7	-11.8	-5.9
22.0	5770	36.8	.01448	79.3	.12	507.0	268.4	325.9	268.96	62.7	262.4	.0033	12.1	29.3	-10.6	-5.9
22.4	5878	36.6	.01488	79.0	.12	500.0	267.5	326.1	268.00	62.5	261.5	.0030	11.5	27.0	-10.2	-5.2
23.0	6069	36.2	.01559	78.6	.12	488.0	265.9	326.4	266.32	62.0	259.8	.0028	10.4	22.2	-9.6	-3.9
24.0	6377	35.5	.01671	77.7	.13	469.0	263.8	327.5	264.27	70.0	259.4	.0028	8.7	12.9	-8.4	-1.9
25.0	6696	34.8	.01786	76.7	.13	450.0	262.2	329.4	262.60	61.9	256.4	.0023	6.6	28.8	-5.8	-3.2
26.0	7009	30.5	.01891	67.4	.12	432.0	261.0	331.7	261.51	100.0	261.0	.0034	6.5	44.4	-4.6	-4.5
27.0	7296	27.9	.01978	62.2	.11	416.0	258.9	332.6	259.30	94.3	258.1	.0028	7.4	58.5	-3.9	-6.3
27.9	7592	32.1	.02071	72.2	.13	400.0	256.9	333.8	257.29	92.1	255.9	.0024	8.3	57.9	-4.4	-7.0
28.0	7611	32.4	.02077	72.9	.13	399.0	256.8	333.9	257.16	91.9	255.8	.0024	8.4	57.9	-4.4	-7.1
29.0	7918	38.3	.02191	86.7	.17	383.0	255.4	336.0	255.79	97.8	255.1	.0024	7.1	42.4	-5.3	-4.8
30.0	8175	39.1	.02297	89.0	.17	370.0	253.2	336.4	253.47	70.4	249.3	.0015	4.2	36.5	-3.4	-2.5
31.0	8460	39.5	.02416	90.9	.18	356.0	251.1	337.3	251.22	45.4	242.5	.0008	2.9	65.9	-1.2	-2.7
31.4	8584	38.8	.02468	89.5	.18	350.0	250.2	337.7	250.31	40.1	240.3	.0006	2.4	85.6	-.2	-2.4
32.0	8775	37.7	.02547	87.4	.18	341.0	248.8	338.4	248.91	32.0	236.9	.0005	2.4	124.8	1.4	-2.0
33.0	9057	36.6	.02661	85.2	.18	328.0	247.9	340.9	247.96	26.9	234.4	.0004	3.3	147.2	2.8	-1.8
34.0	9395	36.6	.02796	85.9	.19	313.0	245.7	342.3	245.72	38.6	235.9	.0005	4.1	138.5	3.1	-2.7
35.0	9698	36.6	.02919	87.0	.20	300.0	242.7	342.4	242.80	35.3	232.4	.0004	4.7	149.1	4.0	-2.4
36.0	10035	31.0	.03046	74.6	.18	286.0	240.0	343.1	240.01	40.2	231.1	.0003	4.1	156.5	3.8	-1.6
37.0	10385	28.4	.03164	69.2	.17	272.0	237.0	343.8	237.06	42.1	228.8	.0003	2.5	147.4	2.1	-1.3
38.0	10696	27.1	.03263	66.6	.17	260.0	234.5	344.5	234.49	44.6	227.0	.0002	3.1	115.0	1.3	-2.8
38.8	10963	26.4	.03345	65.9	.18	250.0	231.8	344.5	231.83	0.0	0.0	0.0000	4.2	103.6	1.0	-4.1
39.0	11018	26.3	.03362	65.7	.18	248.0	231.3	344.5	231.29	0.0	0.0	0.0000	4.5	102.0	.9	-4.4
40.0	11360	22.5	.03466	56.8	.16	235.0	228.8	346.0	228.76	0.0	0.0	0.0000	6.1	111.3	2.2	-5.7
41.0	11640	20.6	.03532	52.6	.15	226.0	226.3	346.1	226.32	0.0	0.0	0.0000	7.6	126.7	4.5	-6.1
42.0	11968	18.8	.03610	48.5	.14	215.0	223.3	346.5	223.35	0.0	0.0	0.0000	7.7	126.3	4.5	-6.2
43.0	12309	14.8	.03679	38.7	.12	204.0	220.7	347.6	220.74	0.0	0.0	0.0000	8.5	119.5	4.2	-7.4
43.4	12436	15.0	.03703	39.4	.12	200.0	219.9	348.2	219.88	0.0	0.0	0.0000	9.0	121.2	4.7	-7.7
44.0	12665	15.4	.03745	40.7	.13	193.0	218.3	349.4	218.34	0.0	0.0	0.0000	9.8	124.0	5.5	-8.1
45.0	13037	13.5	.03812	36.1	.12	182.0	215.2	350.1	215.17	0.0	0.0	0.0000	11.8	131.5	7.8	-8.8
46.0	13391	13.5	.03872	36.6	.13	172.0	212.7	351.7	212.71	0.0	0.0	0.0000	13.1	139.1	9.9	-8.6
47.0	13761	13.5	.03936	37.2	.14	162.0	209.6	352.5	209.55	0.0	0.0	0.0000	12.7	150.0	11.0	-6.3
48.0	14108	13.5	.03997	37.8	.15	153.0	206.2	352.5	206.16	0.0	0.0	0.0000	11.8	145.9	9.8	-6.6
48.3	14226	13.0	.04017	36.6	.14	150.0	205.2	352.8	205.17	0.0	0.0	0.0000	11.5	146.0	9.6	-6.5
49.0	14471	12.0	.04058	34.2	.14	144.0	203.1	353.1	203.13	0.0	0.0	0.0000	10.9	146.2	9.1	-6.1
50.0	14766	14.7	.04110	41.8	.18	137.0	202.2	356.6	202.22	0.0	0.0	0.0000	10.9	178.3	10.9	-.3
51.0	15121	15.2	.04181	43.8	.20	129.0	200.8	360.5	200.81	0.0	0.0	0.0000	999.9	999.9	999.9	999.9
51.5	15305	15.1	.04219	43.6	.20	125.0	200.6	363.3	200.57	0.0	0.0	0.0000	999.9	999.9	999.9	999.9
52.0	15497	15.1	.04258	43.4	.21	121.0	200.3	366.3	200.33	0.0	0.0	0.0000	999.9	999.9	999.9	999.9
53.0	15901	16.3	.04342	46.2	.24	113.0	203.1	378.7	203.13	0.0	0.0	0.0000	999.9	999.9	999.9	999.9
54.0	16169	13.7	.04396	39.1	.21	108.0	201.8	381.1	201.76	0.0	0.0	0.0000	999.9	999.9	999.9	999.9
55.0	16563	13.7	.04468	39.4	.22	101.0	200.3	385.7	200.33	0.0	0.0	0.0000	999.9	999.9	999.9	999.9
55.2	16621	14.1	.04480	40.6	.23	100.0	200.2	386.5	200.17	0.0	0.0	0.0000	999.9	999.9	999.9	999.9
56.0	16927	16.2	.04541	47.0	.28	94.9	199.3	390.7	199.34	0.0	0.0	0.0000	999.9	999.9	999.9	999.9
57.0	17274	15.6	.04616	45.5	.29	89.4	197.6	393.8	197.55	0.0	0.0	0.0000	999.9	999.9	999.9	999.9
58.0	17629	19.1	.04700	55.1	.38	84.1	199.8	405.4	199.84	0.0	0.0	0.0000	999.9	999.9	999.9	999.9
58.8	17920	22.1	.04782	63.7	.46	80.0	199.8	411.2	199.84	0.0	0.0	0.0000	999.9	999.9	999.9	999.9
59.0	17987	22.7	.04801	65.7	.48	79.1	199.8	412.6	199.84	0.0	0.0	0.0000	999.9	999.9	999.9	999.9
60.0	18360	27.6	.04928	80.1	.62	74.2	198.6	417.5	198.59	0.0	0.0	0.0000	6.6	87.1	-.3	-6.6
60.8	18702	37.3	.05081	106.2	.89	70.0	202.6	433.1	202.57	0.0	0.0	0.0000	7.1	99.9	1.2	-7.0
61.0	18770	39.2	.05112	111.4	.94	69.2	203.4	436.2	203.35	0.0	0.0	0.0000	7.2	102.1	1.5	-7.1
62.0	19146	52.8	.05339	147.4	1.35	65.0	207.0	452.0	206.98	0.0	0.0	0.0000	6.0	92.8	.3	-6.0
63.0	19530	58.2	.05617	162.7	1.58	61.0	206.6	459.3	206.57	0.0	0.0	0.0000	4.9	77.8	-1.0	-4.8
63.2	19630	59.9	.05698	167.0	1.66	60.0	207.2	462.8	207.16	0.0	0.0	0.0000	999.9	999.9	999.9	999.9
64.0	19942	65.2	.05947	180.0	1.89	57.0	209.0	473.8	208.97	0.0	0.0	0.0000	999.9	999.9	999.9	999.9
65.0	20305	67.1	.06259	186.5	2.07	53.7	207.8	479.2	207.79	0.0	0.0	0.0000	999.9	999.9	999.9	999.9
66.0	20678	68.4	.06587	190.4	2.24	50.5	207.4	486.7	207.39	0.0	0.0	0.0000	999.9	999.9	999.9	999.9
66.1	20738	70.2	.06646	194.8	2.33	50.0	208.0	489.5	207.96	0.0	0.0	0.0000	999.9	999.9	999.9	999.9
67.0	21092	80.5	.06984	220.0	2.83	47.2	211.3	505.4	211.25	0.0	0.0	0.0000	999.9	999.9	999.9	999.9

TIME MIN	ALT GPM	OZONE MICMB	TOTOZ ATMCM	OZDEN MG/M3	OZMXR MICGG	PRESS MB	TEMP DEG K	PTEMP DEG K	VTEMP DEG K	HMDTY PRCNT	DEWPT DEG K	SPCFC HMDTY	SPD MPS	DIR DEG	NS MPS	EW MPS
68.0	21528	94.5	.07469	255.6	3.56	44.0	213.4	521.0	213.43	0.0	0.0	0.0000	999.9	999.9	999.9	999.9
69.0	21880	108.5	.07918	290.2	4.32	41.6	215.9	535.4	215.86	0.0	0.0	0.0000	999.9	999.9	999.9	999.9
69.6	22128	113.2	.08265	300.9	4.69	40.0	217.1	544.7	217.12	0.0	0.0	0.0000	999.9	999.9	999.9	999.9
70.0	22273	115.9	.08466	307.0	4.91	39.1	217.9	550.1	217.86	0.0	0.0	0.0000	999.9	999.9	999.9	999.9
71.0	22644	128.7	.09025	337.1	5.78	36.9	220.4	565.8	220.42	0.0	0.0	0.0000	999.9	999.9	999.9	999.9
71.8	22986	136.9	.09583	356.4	6.49	35.0	221.8	578.1	221.83	0.0	0.0	0.0000	999.9	999.9	999.9	999.9
72.0	23061	138.7	.09704	360.5	6.64	34.6	222.1	580.8	222.13	0.0	0.0	0.0000	999.9	999.9	999.9	999.9
73.0	23447	143.6	.10368	374.1	7.30	32.6	221.7	589.5	221.67	0.0	0.0	0.0000	999.9	999.9	999.9	999.9
74.0	23901	144.[illegible]	.11163	375.9	7.90	30.4	222.6	603.9	222.59	0.0	0.0	0.0000	999.9	999.9	999.9	999.9
74.2	23987	144.7	.11314	375.6	7.99	30.0	222.4	605.8	222.45	0.0	0.0	0.0000	999.9	999.9	999.9	999.9
75.0	24275	144.0	.11819	374.5	8.31	28.7	222.0	612.2	221.98	0.0	0.0	0.0000	999.9	999.9	999.9	999.9
76.0	24671	139.6	.12502	364.7	8.57	27.0	221.0	620.4	221.05	0.0	0.0	0.0000	999.9	999.9	999.9	999.9
77.0	25090	139.5	.13218	366.9	9.13	25.3	219.5	627.5	219.47	0.0	0.0	0.0000	999.9	999.9	999.9	999.9
77.2	25166	140.1	.13351	367.9	9.29	25.0	219.9	630.9	219.90	0.0	0.0	0.0000	999.9	999.9	999.9	999.9
78.0	25484	142.8	.13899	371.9	9.94	23.8	221.7	645.0	221.67	0.0	0.0	0.0000	999.9	999.9	999.9	999.9
79.0	25967	144.7	.14739	373.7	10.85	22.1	223.5	664.2	223.50	0.0	0.0	0.0000	999.9	999.9	999.9	999.9
80.0	26490	145.2	.15655	376.1	11.79	20.4	222.9	677.7	222.90	0.0	0.0	0.0000	999.9	999.9	999.9	999.9
80.3	26618	143.2	.15876	371.3	11.86	20.0	222.6	680.8	222.64	0.0	0.0	0.0000	999.9	999.9	999.9	999.9
81.0	26953	137.9	.16449	358.7	12.03	19.0	222.0	688.8	221.98	0.0	0.0	0.0000	999.9	999.9	999.9	999.9
82.0	27414	132.6	.17205	344.4	12.41	17.7	222.3	703.9	222.28	0.0	0.0	0.0000	999.9	999.9	999.9	999.9
82.1	27488	132.1	.17322	342.9	12.51	17.5	222.5	706.8	222.48	0.0	0.0	0.0000	999.9	999.9	999.9	999.9
83.0	27992	128.9	.18119	332.6	13.19	16.2	223.8	726.8	223.80	0.0	0.0	0.0000	999.9	999.9	999.9	999.9
84.0	28453	126.7	.18828	326.2	13.90	15.1	224.3	743.1	224.25	0.0	0.0	0.0000	999.9	999.9	999.9	999.9
84.1	28496	126.1	.1889[illegible]	324.5	13.93	15.0	224.4	745.0	224.41	0.0	0.0	0.0000	999.9	999.9	999.9	999.9
85.0	28951	119.9	.195[illegible]4	306.4	14.20	14.0	226.0	765.3	226.02	0.0	0.0	0.0000	999.9	999.9	999.9	999.9
86.0	29442	114.7	.20250	291.4	14.61	13.0	227.2	785.7	227.19	0.0	0.0	0.0000	999.9	999.9	999.9	999.9
86.5	29703	111.5	.20595	282.5	14.78	12.5	227.9	797.1	227.89	0.0	0.0	0.0000	999.9	999.9	999.9	999.9
87.0	29976	108.2	.20954	273.3	14.94	12.0	228.6	808.9	228.62	0.0	0.0	0.0000	999.9	999.9	999.9	999.9
88.0	30560	104.8	.21685	262.8	15.79	11.0	230.3	835.5	230.31	0.0	0.0	0.0000	999.9	999.9	999.9	999.9
89.0	31202	97.1	.22444	243.6	16.09	10.0	230.2	858.0	230.17	0.0	0.0	0.0000	999.9	999.9	999.9	999.9
90.0	31838	88.0	.23133	220.4	16.02	9.1	230.5	882.5	230.45	0.0	0.0	0.0000	999.9	999.9	999.9	999.9
91.0	32380	78.1	.23658	193.8	15.40	8.4	232.7	911.6	232.67	0.0	0.0	0.0000	999.9	999.9	999.9	999.9
91.7	32713	74.4	.23948	183.9	15.40	8.0	233.7	928.4	233.67	0.0	0.0	0.0000	999.9	999.9	999.9	999.9
92.0	32886	72.5	.24098	178.8	15.41	7.8	234.2	937.2	234.18	0.0	0.0	0.0000	999.9	999.9	999.9	999.9
93.0	33435	67.1	.24539	165.2	15.44	7.2	234.5	959.9	234.45	0.0	0.0	0.0000	999.9	999.9	999.9	999.9
93.3	33628	65.1	.24681	160.2	15.39	7.0	234.7	968.7	234.67	0.0	0.0	0.0000	999.9	999.9	999.9	999.9
94.0	34033	61.0	.24978	149.7	15.31	6.6	235.1	987.0	235.13	0.0	0.0	0.0000	999.9	999.9	999.9	999.9
94.9	34689	53.7	.25405	131.7	14.80	6.0	235.4	1015.3	235.36	0.0	0.0	0.0000	999.9	999.9	999.9	999.9
95.0	34805	52.4	.25480	128.5	14.71	5.9	235.4	1020.3	235.40	0.0	0.0	0.0000	999.9	999.9	999.9	999.9

INTEGRAL .25480 RESIDUAL .04137 INTEGRATED TOTAL OZONE .29617

OZONAGRAM

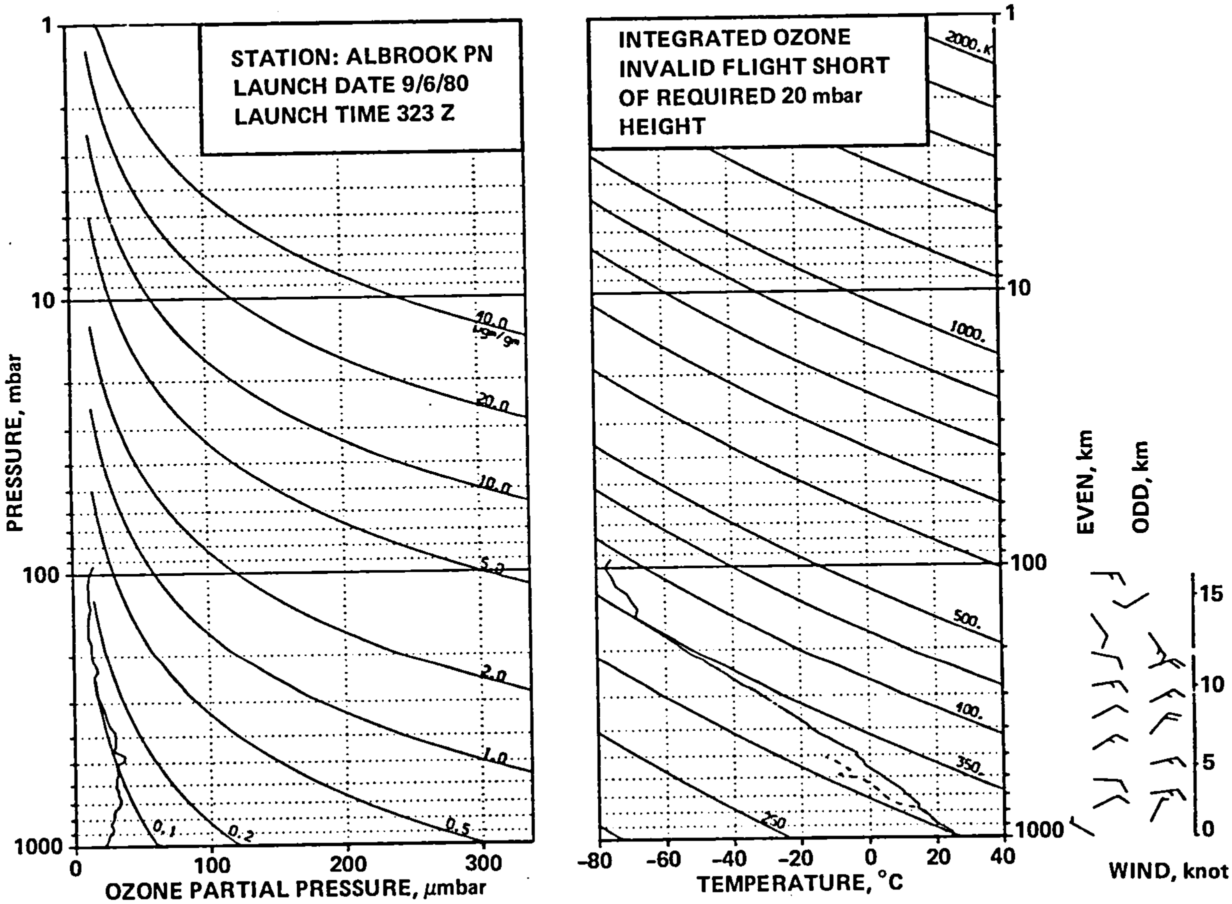

STATION: ALBROOK PN
LAUNCH DATE 9/6/80
LAUNCH TIME 323 Z
INTEGRATED OZONE
INVALID FLIGHT SHORT
OF REQUIRED 20 mbar
HEIGHT
PRESSURE, mbar
1
10
100
1000
0
100
200
300
OZONE PARTIAL PRESSURE, μmbar
10.0
20.0
10.0
5.0
2.0
1.0
0.1
0.2
0.5
-80
-60
-40
-20
0
20
40
TEMPERATURE, °C
2000. K
1000.
500.
400.
350.
250
EVEN, km
ODD, km
15
10
5
0
HEIGHT, GP km
WIND, knot

STATION ALBROOK PN LAUNCH DATE 9/ 6/80 TIME 323Z ECC SONDE 3A1324

SURFACE CONDITIONS PRESS 1003.8MB TEMP 299.4 DEG K HUMIDITY 100.0 PRCNT

TIME MIN	ALT GPM	OZONE MICMB	TOTOZ ATMCM	OZDEN MG/M3	OZMXR MICGG	PRESS MB	TEMP DEG K	PTEMP DEG K	VTEMP DEG K	HMDTY PRCNT	DEWPT DEG K	SPCFC HMDTY	SPD MPS	DIR DEG	NS MPS	EW MPS
0.0	66	21.8	0.00000	42.0	.04	1003.8	299.3	299.0	303.24	100.0	299.3	.0213	3.0	300.0	-1.5	2.6
.1	99	21.9	.00007	42.2	.04	1000.0	299.2	299.2	302.98	98.6	298.9	.0205	3.2	308.7	-2.0	2.5
1.0	296	22.4	.00045	43.4	.04	978.0	298.1	300.0	301.46	90.2	296.4	.0183	5.6	337.4	-5.1	2.1
2.0	533	23.7	.00094	46.0	.04	952.0	297.4	301.6	300.62	88.5	295.4	.0177	999.9	999.9	999.9	999.9
3.0	757	24.2	.00143	47.2	.04	928.0	295.8	302.2	298.81	90.7	294.2	.0168	5.0	28.9	-4.3	-2.4
4.0	1004	25.5	.00198	50.1	.05	902.0	294.0	302.8	296.90	95.8	293.3	.0164	3.8	27.0	-3.4	-1.7
4.1	1023	25.7	.00203	50.5	.05	900.0	293.8	302.8	296.77	96.2	293.2	.0163	3.8	27.1	-3.4	-1.7
5.0	1218	27.5	.00250	54.2	.05	880.0	292.6	303.5	295.52	100.0	292.6	.0161	3.3	28.0	-2.9	-1.6
6.0	1436	27.5	.00305	54.5	.05	858.0	291.6	304.6	294.31	100.0	291.6	.0154	3.1	39.5	-2.4	-2.0
6.3	1516	27.0	.00325	53.4	.05	850.0	291.3	305.1	294.02	100.0	291.3	.0153	3.2	43.8	-2.3	-2.2
7.0	1700	25.7	.00370	50.9	.05	832.0	290.7	306.4	293.38	100.0	290.7	.0151	3.4	52.9	-2.1	-2.7
8.0	1961	27.5	.00434	55.0	.06	807.0	289.0	307.3	291.51	100.0	289.0	.0140	4.2	56.8	-2.3	-3.5
8.3	2034	27.8	.00453	55.6	.06	800.0	288.6	307.6	290.97	99.6	288.5	.0134	4.6	62.3	-2.2	-4.1
9.0	2217	28.3	.00500	56.8	.06	783.0	287.4	308.2	289.66	98.5	287.2	.0128	5.7	72.3	-1.8	-5.5
10.0	2469	28.3	.00567	56.8	.06	760.0	287.6	311.1	289.28	70.0	282.2	.0095	7.5	82.4	-1.0	-7.5
11.0	2694	29.0	.00627	58.4	.06	740.0	286.4	312.2	287.82	61.9	279.3	.0080	8.1	82.2	-1.1	-8.0
12.0	2924	31.6	.00692	63.8	.07	720.0	285.4	313.5	286.78	61.7	278.3	.0076	8.1	80.8	-1.3	-8.0
12.9	3159	33.1	.00764	67.3	.08	700.0	284.1	314.5	285.30	61.7	277.0	.0071	8.2	84.3	-.8	-8.2
13.0	3183	33.2	.00772	67.6	.08	698.0	283.9	314.6	285.15	61.7	276.9	.0071	8.3	84.7	-.8	-8.2
14.0	3474	33.2	.00863	67.7	.08	674.0	282.8	316.5	283.97	61.3	275.7	.0068	8.0	92.3	.3	-8.0
15.0	3749	31.5	.00948	64.6	.08	652.0	281.3	317.9	282.41	61.1	274.3	.0063	7.2	96.2	.8	-7.1
16.0	4018	31.6	.01030	65.3	.08	631.0	279.5	318.8	280.52	61.4	272.6	.0058	6.4	93.9	.4	-6.4
17.0	4295	29.9	.01112	62.2	.08	610.0	277.8	319.9	278.68	60.9	270.9	.0053	5.6	88.1	-.2	-5.6
17.5	4428	30.1	.01151	62.8	.08	600.0	277.0	320.5	277.71	51.5	267.7	.0038	5.9	84.1	-.6	-5.8
18.0	4579	30.3	.01195	63.4	.09	589.0	276.1	321.2	276.63	41.0	264.1	.0033	6.2	80.0	-1.1	-6.1
19.0	4872	30.3	.01282	63.8	.09	568.0	273.9	322.0	274.65	61.5	267.4	.0043	7.8	76.5	-1.8	-7.6
20.0	5203	31.5	.01383	67.0	.10	545.0	271.7	323.1	272.29	60.4	265.0	.0038	8.2	76.7	-1.9	-8.0
21.0	5485	30.7	.01470	65.3	.10	526.0	271.3	326.0	271.90	53.2	263.1	.0034	9.3	77.1	-2.1	-9.0
22.0	5777	30.8	.01559	65.9	.10	507.0	269.6	327.4	270.08	47.8	260.2	.0028	9.6	73.0	-2.8	-9.2
22.4	5886	32.9	.01595	70.4	.11	500.0	269.5	328.5	269.76	0.0	0.0	0.0000	9.2	67.3	-3.6	-8.5
23.0	6046	35.9	.01649	77.0	.12	490.0	269.3	330.2	269.31	0.0	0.0	0.0000	8.9	58.5	-4.6	-7.6
24.0	6372	36.3	.01767	78.7	.13	470.0	266.4	330.6	266.44	0.0	0.0	0.0000	10.4	46.9	-7.1	-7.6
25.0	6709	28.4	.01878	62.3	.10	450.0	263.6	331.2	263.79	26.3	247.9	.0011	10.8	44.8	-7.7	-7.6
26.0	7023	29.7	.01972	65.7	.11	432.0	261.3	332.1	261.60	49.1	252.8	.0017	9.2	42.0	-6.8	-6.2
27.0	7310	29.7	.02060	66.3	.12	416.0	258.6	332.3	258.92	59.1	252.4	.0018	8.3	42.7	-6.1	-5.7
27.9	7606	29.6	.02152	66.7	.12	400.0	256.4	333.2	256.77	83.6	254.3	.0022	7.4	52.5	-4.5	-5.9
28.0	7625	29.6	.02158	66.8	.12	399.0	256.3	333.2	256.64	85.1	254.4	.0022	7.3	53.2	-4.4	-5.9
29.0	7931	29.1	.02253	65.9	.13	383.0	254.7	335.0	254.99	90.9	253.5	.0021	5.9	62.3	-2.7	-5.2
30.0	8248	25.7	.02345	58.9	.12	367.0	252.5	336.2	252.78	88.8	251.1	.0018	5.3	62.5	-2.5	-4.7
31.0	8597	24.0	.02438	55.5	.11	350.0	250.0	337.4	250.20	89.2	248.7	.0015	5.9	62.5	-2.7	-5.2
32.0	8959	22.7	.02530	53.1	.11	333.0	247.2	338.5	247.39	89.4	246.0	.0012	7.0	62.5	-3.2	-6.2
33.0	9313	21.5	.02616	50.7	.11	317.0	244.7	339.8	244.88	95.4	244.2	.0011	8.3	63.6	-3.7	-7.4
34.0	9706	19.5	.02705	46.4	.11	300.0	242.0	341.3	242.10	100.0	242.0	.0009	8.3	69.2	-2.9	-7.8
35.0	10043	17.4	.02775	42.0	.10	286.0	239.3	342.2	239.45	99.6	239.3	.0007	7.2	78.9	-1.4	-7.1
36.0	10316	16.3	.02827	39.9	.10	275.0	235.9	341.1	235.98	92.2	235.1	.0005	12.2	109.7	4.1	-11.5
37.0	10622	15.6	.02883	38.5	.10	263.0	233.6	342.2	233.69	78.9	231.4	.0004	13.6	100.5	2.5	-13.4
38.0	10940	15.5	.02940	38.7	.10	251.0	231.3	343.4	231.34	0.0	0.0	0.0000	10.7	69.0	-3.8	-10.0
38.1	10966	15.4	.02945	38.6	.10	250.0	231.1	343.4	231.12	0.0	0.0	0.0000	10.7	69.0	-3.8	-10.0
39.0	11242	14.7	.02994	37.2	.10	240.0	228.9	344.1	228.86	0.0	0.0	0.0000	10.7	69.2	-3.8	-10.0
40.0	11554	17.4	.03053	44.3	.13	229.0	22[illegible].9	344.2	225.90	0.0	0.0	0.0000	7.3	84.1	-.7	-7.2
41.0	11848	16.0	.03112	41.1	.12	219.0	224.2	346.0	224.17	0.0	0.0	0.0000	4.4	113.0	1.7	-4.1
42.0	12121	13.9	.03161	36.3	.11	210.0	221.3	345.7	221.35	0.0	0.0	0.0000	4.3	101.1	.8	-4.2
42.8	12434	13.2	.03213	34.9	.11	200.0	218.8	346.5	218.78	0.0	0.0	0.0000	5.2	106.2	1.4	-4.9
43.0	12499	13.1	.03224	34.6	.11	198.0	218.3	346.7	218.26	0.0	0.0	0.0000	5.3	107.1	1.6	-5.1
44.0	12828	12.8	.03277	34.3	.11	188.0	215.8	347.9	215.84	0.0	0.0	0.0000	5.9	138.2	4.4	-3.9
45.0	13136	12.8	.03327	34.6	.12	179.0	213.0	348.2	212.97	0.0	0.0	0.0000	7.4	145.2	6.1	-4.2
46.0	13455	10.7	.03374	29.4	.10	170.0	210.3	348.9	210.29	0.0	0.0	0.0000	7.6	139.3	5.8	-5.0
47.0	13787	10.7	.03420	29.7	.11	161.0	207.5	349.6	207.46	0.0	0.0	0.0000	6.3	155.5	5.8	-2.6
48.0	14133	10.6	.03469	29.9	.12	152.0	204.4	350.2	204.43	0.0	0.0	0.0000	5.2	142.0	4.1	-3.2
48.2	14212	10.7	.03480	30.2	.12	150.0	204.6	351.7	204.55	0.0	0.0	0.0000	4.5	153.4	4.0	-2.0
49.0	14541	11.2	.03527	31.6	.13	142.0	205.1	358.2	205.06	0.0	0.0	0.0000	4.6	220.6	3.5	3.0
50.0	14932	12.5	.03588	35.5	.16	133.0	203.4	361.9	203.37	0.0	0.0	0.0000	7.8	248.7	2.8	7.2
51.0	15300	11.2	.03646	31.9	.15	125.0	202.1	366.0	202.06	0.0	0.0	0.0000	2.3	223.1	1.7	1.6
52.0	15688	11.2	.037[illegible]	32.4	.16	117.0	198.8	367.0	198.80	0.0	0.0	0.0000	4.0	111.7	1.5	-3.7
53.0	16152	10.9	.037[illegible]4	31.9	.17	108.0	197.6	373.1	197.55	0.0	0.0	0.0000	7.2	85.6	-.6	-7.2
54.0	16595	12.2	.03845	36.0	.20	100.0	195.7	377.9	195.73	0.0	0.0	0.0000	7.2	88.4	-.2	-7.2
55.0	17012	15.3	.03923	44.7	.27	93.0	197.6	389.4	197.55	0.0	0.0	0.0000	999.9	999.9	999.9	999.9

CALIBRATIONS APPLIED FOR PARTIAL PRESSURE OF OZONE
TOTAL INTEGRATED OZONE INVALID. BALLOON SHORT OF 20 MB HEIGHT

OZONAGRAM

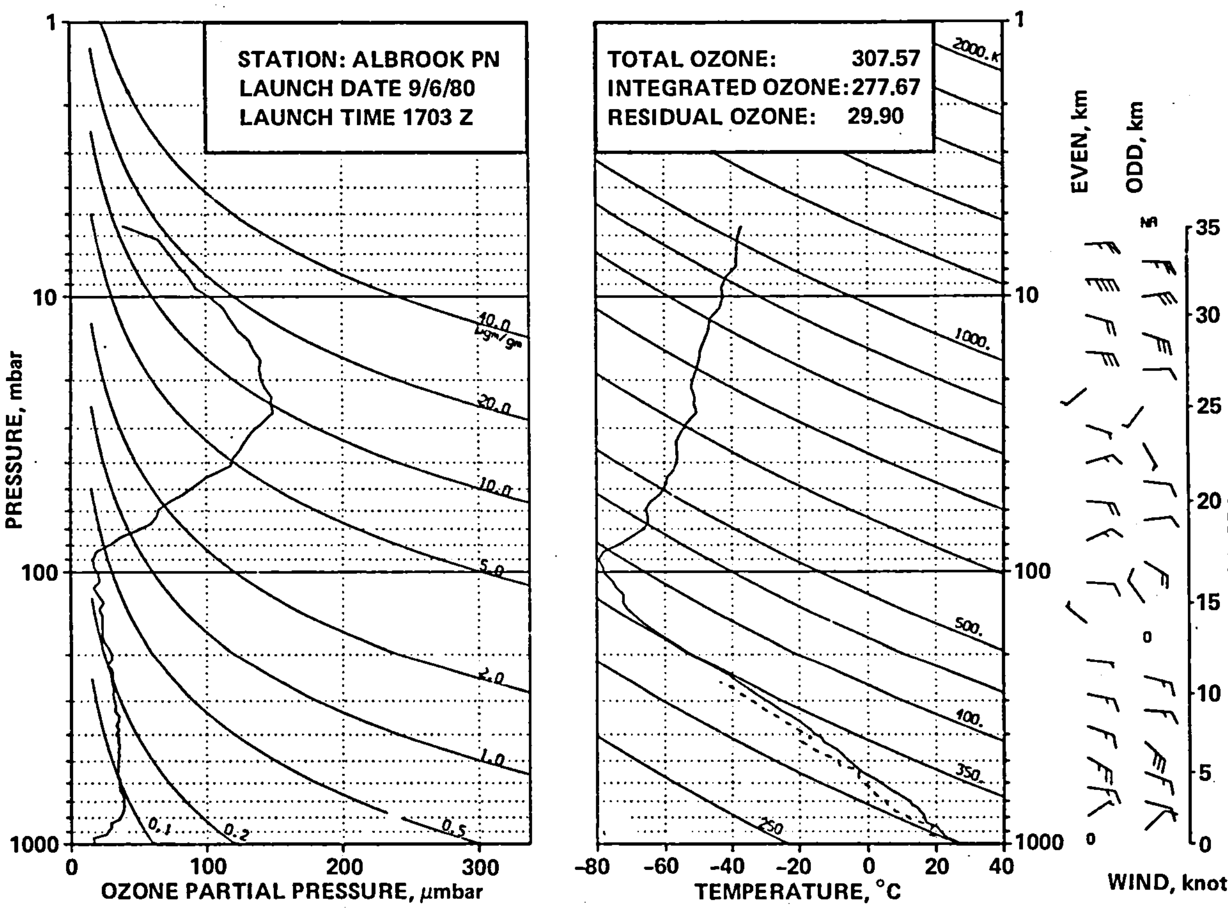

STATION: ALBROOK PN
LAUNCH DATE 9/6/80
LAUNCH TIME 1703 Z
TOTAL OZONE: 307.57
INTEGRATED OZONE: 277.67
RESIDUAL OZONE: 29.90
PRESSURE, mbar
OZONE PARTIAL PRESSURE, μmbar
TEMPERATURE, °C
EVEN, km
ODD, km
HEIGHT, GP km
WIND, knot
1
10
100
1000
0
100
200
300
-80
-60
-40
-20
0
20
40
35
30
25
20
15
10
5
0
40.0
20.0
10.0
5.0
2.0
1.0
0.5
0.2
0.1
2000. K
1000.
500.
400.
350.
250

STATION ALBROOK PN LAUNCH DATE 9/ 6/80 TIME 1703Z ECC SONDE 3A1325

SURFACE CONDITIONS PRESS 1003.2MB TEMP 300.5 DEG K HUMIDITY 100.0 PRCNT

TIME MIN	ALT GPM	OZONE MICMB	TOTOZ ATMCM	OZDEN MG/M3	OZMXR MICGG	PRESS MB	TEMP DEG K	PTEMP DEG K	VTEMP DEG K	HMDTY PRCNT	DEWPT DEG K	SPCFC HMDTY	SPD MPS	DIR DEG	NS MPS	EW MPS
0.0	66	16.6	0.00000	31.9	.03	1003.2	300.4	300.1	304.53	100.0	300.4	.0226	1.0	360.0	-1.0	0.0
.1	94	16.6	.00004	31.9	.03	1000.0	300.2	300.2	304.34	99.4	300.1	.0222	1.0	3.6	-1.0	-.1
1.0	310	16.6	.00036	32.0	.03	976.0	299.1	301.2	302.89	94.6	298.2	.0205	1.3	24.7	-1.2	-.5
2.0	566	15.9	.00073	31.0	.03	948.0	296.3	300.9	299.45	92.0	294.9	.0173	2.5	57.0	-1.3	-2.1
3.0	828	25.7	.00122	50.2	.05	920.0	295.2	302.3	297.62	75.0	290.5	.0135	4.6	53.0	-2.8	-3.7
3.7	1019	26.8	.00168	52.6	.05	900.0	294.4	303.4	296.97	82.1	291.2	.0146	5.1	47.7	-3.4	-3.8
4.0	1097	27.3	.00187	53.6	.05	892.0	294.1	303.8	296.71	84.9	291.4	.0147	5.3	45.9	-3.7	-3.8
5.0	1373	29.5	.00259	58.1	.06	864.0	293.4	305.9	296.28	93.1	292.2	.0160	4.6	40.4	-3.5	-3.0
5.5	1513	29.2	.00296	57.8	.06	850.0	291.8	305.7	294.44	92.9	290.6	.0142	4.2	43.8	-3.0	-2.9
6.0	1636	29.0	.00329	57.6	.06	838.0	290.4	305.5	292.84	92.6	289.2	.0136	3.9	47.4	-2.6	-2.8
7.0	1926	35.6	.00416	71.0	.07	810.0	289.8	307.8	291.75	75.4	285.4	.0110	3.4	57.7	-1.8	-2.9
7.4	2031	36.1	.00451	72.0	.07	800.0	289.7	308.8	291.63	73.3	284.9	.0106	3.2	57.0	-1.8	-2.7
8.0	2193	36.9	.00505	73.5	.08	785.0	289.6	310.3	291.44	70.1	284.1	.0104	3.0	55.7	-1.7	-2.5
9.0	2468	38.1	.00601	76.3	.08	760.0	288.4	311.9	289.90	61.1	280.9	.0087	2.7	51.7	-1.7	-2.2
10.0	2705	38.8	.00686	77.9	.09	739.0	287.8	313.8	289.29	61.2	280.4	.0086	3.4	78.7	-.7	-3.3
11.0	2936	38.9	.00770	78.5	.09	719.0	286.0	314.3	287.39	61.3	278.7	.0079	4.8	103.5	1.1	-4.6
12.0	3161	38.6	.00852	77.9	.09	700.0	285.6	316.3	287.00	61.1	278.3	.0079	4.9	106.1	1.4	-4.7
13.0	3403	38.6	.00940	78.5	.09	680.0	283.7	316.8	284.97	61.1	276.6	.0071	4.8	102.5	1.0	-4.7
14.0	3651	37.6	.01030	76.9	.09	660.0	282.1	317.6	283.21	61.8	275.1	.0067	5.4	101.8	1.1	-5.3
15.0	3905	35.9	.01119	74.0	.09	640.0	280.1	318.2	281.24	68.8	274.8	.0067	7.2	95.4	.7	-7.1
16.0	4179	35.5	.01213	73.5	.09	619.0	278.5	319.4	279.57	69.0	273.3	.0062	8.0	99.8	1.4	-7.8
16.9	4432	35.6	.01301	74.1	.10	600.0	277.0	320.5	277.94	68.7	271.8	.0057	8.0	105.1	2.1	-7.7
17.0	4460	35.6	.01310	74.2	.10	598.0	276.8	320.6	277.7	68.7	271.6	.0057	8.0	105.6	2.2	-7.7
18.0	4721	35.5	.01400	74.5	.10	579.0	275.1	321.6	276.04	70.6	270.4	.0053	7.9	104.7	2.0	-7.7
19.0	5003	33.8	.01497	71.6	.10	559.0	272.5	321.8	273.46	85.5	270.4	.0056	8.0	108.0	2.5	-7.6
20.0	5293	34.4	.01595	73.4	.11	539.0	270.6	322.9	271.60	98.4	270.4	.0058	9.0	116.9	4.1	-8.1
21.0	5592	34.6	.01698	74.2	.11	519.0	269.1	324.6	269.73	71.6	264.7	.0039	11.1	120.4	5.6	-9.6
21.9	5885	34.6	.01799	74.6	.11	500.0	267.6	326.2	268.23	78.6	264.4	.0039	12.6	118.9	6.1	-11.0
22.0	5917	34.6	.01810	74.7	.12	498.0	267.4	326.4	268.07	79.3	264.4	.0039	12.7	118.7	6.1	-11.2
23.0	6237	35.2	.01923	76.4	.12	478.0	265.9	328.4	266.44	68.0	261.0	.0031	13.9	123.3	7.6	-11.6
24.0	6569	34.7	.02041	75.9	.13	458.0	264.3	330.4	264.71	58.9	257.7	.0025	15.1	127.7	9.2	-11.9
25.0	6878	35.7	.02152	78.5	.13	440.0	262.1	331.4	262.49	59.0	255.7	.0022	14.9	131.4	9.8	-11.2
26.0	7125	34.6	.02242	76.8	.13	426.0	260.2	332.0	260.46	58.8	253.8	.0019	14.7	134.0	10.2	-10.6
27.0	7416	35.1	.02347	78.1	.14	410.0	259.5	334.7	259.86	79.6	256.7	.0026	11.8	129.6	7.5	-9.1
28.0	7603	32.9	.02414	73.6	.14	400.0	257.8	334.9	258.15	80.1	255.1	.0023	8.6	118.9	4.2	-7.5
29.0	7910	35.1	.02523	79.0	.15	384.0	256.3	336.9	256.57	73.1	252.6	.0019	7.6	111.3	2.7	-7.0
30.0	8188	33.3	.02623	75.4	.15	370.0	254.6	338.3	254.90	70.6	250.6	.0017	6.7	107.9	2.1	-6.4
31.0	8474	35.0	.02727	80.0	.16	356.0	252.9	339.7	253.10	67.1	248.4	.0014	7.2	106.4	2.0	-6.9
31.4	8599	35.1	.02774	80.3	.17	350.0	252.0	340.1	252.19	66.9	247.5	.0013	7.2	105.1	1.9	-7.0
32.0	8791	35.1	.02846	80.8	.17	341.0	250.6	340.8	250.79	66.7	246.1	.0012	7.2	103.1	1.6	-7.0
33.0	9074	32.2	.02949	74.9	.16	328.0	248.0	341.0	248.10	66.0	243.5	.0010	8.0	94.5	.6	-8.0
34.0	9458	32.6	.03085	76.8	.17	311.0	245.5	342.7	245.57	66.0	241.1	.0008	8.1	90.5	.1	-8.1
34.8	9715	31.7	.03176	75.0	.17	300.0	243.6	343.6	243.67	66.2	239.3	.0007	7.5	94.4	.6	-7.5
35.0	9763	31.5	.03193	74.7	.18	298.0	243.2	343.7	243.32	66.3	239.0	.0007	7.4	95.2	.7	-7.4
36.0	10128	30.8	.03320	74.0	.18	283.0	240.3	344.7	240.39	63.9	235.8	.0005	7.8	102.4	1.7	-7.6
37.0	10457	31.2	.03435	75.7	.19	270.0	237.8	345.7	237.86	63.4	233.3	.0004	7.6	103.8	1.8	-7.3
38.0	10798	29.8	.03554	73.3	.19	257.0	235.0	346.5	235.04	55.1	229.4	.0003	7.7	103.6	1.8	-7.5
38.5	10986	30.1	.03620	74.3	.20	250.0	233.7	347.3	233.75	0.0	0.0	0.0000	7.3	104.6	1.8	-7.1
39.0	11181	30.3	.03687	75.2	.21	243.0	232.4	348.2	232.42	0.0	0.0	0.0000	7.0	105.8	1.9	-6.7
40.0	11494	30.2	.03797	75.9	.22	232.0	229.5	348.4	229.52	0.0	0.0	0.0000	5.2	106.0	1.4	-5.0
41.0	11818	26.5	.03906	67.7	.20	221.0	226.5	348.7	226.54	0.0	0.0	0.0000	3.5	103.6	.8	-3.4
42.0	12154	29.8	.04020	77.1	.24	210.0	223.5	349.0	223.47	0.0	0.0	0.0000	1.2	95.6	.1	-1.2
43.0	12471	29.8	.04135	78.1	.25	200.0	220.6	349.4	220.59	0.0	0.0	0.0000	1.3	295.1	-.6	1.2
44.0	12800	27.6	.04251	73.1	.24	190.0	218.1	350.5	218.07	0.0	0.0	0.0000	1.0	316.7	-.7	.7
45.0	13142	24.1	.04361	64.7	.22	180.0	215.1	351.1	215.10	0.0	0.0	0.0000	.9	1.6	-.9	0.0
46.0	13462	22.9	.04456	62.3	.22	171.0	212.1	351.4	212.14	0.0	0.0	0.0000	2.2	324.4	-1.8	1.3
47.0	13795	22.9	.04554	63.0	.23	162.0	209.4	352.2	209.37	0.0	0.0	0.0000	2.6	317.1	-1.9	1.8
48.0	14143	22.8	.04657	63.8	.25	153.0	206.6	353.3	206.63	0.0	0.0	0.0000	2.4	308.0	-1.5	1.9
48.3	14261	22.8	.04693	64.0	.25	150.0	205.9	354.0	205.89	0.0	0.0	0.0000	3.2	298.7	-1.5	2.8
49.0	14507	22.8	.04766	64.4	.26	144.0	204.3	355.5	204.35	0.0	0.0	0.0000	5.0	289.5	-1.7	4.7
50.0	14847	20.5	.04864	58.5	.25	136.0	202.1	357.5	202.15	0.0	0.0	0.0000	6.4	299.2	-3.1	5.6
51.0	15158	23.9	.04956	68.8	.31	129.0	200.8	360.4	200.76	0.0	0.0	0.0000	4.5	334.3	-4.1	2.0
51.5	15342	21.9	.05011	63.0	.29	125.0	200.9	363.9	200.88	0.0	0.0	0.0000	3.4	354.2	-3.3	.3
52.0	15534	19.9	.05067	57.1	.27	121.0	201.0	367.5	200.99	0.0	0.0	0.0000	2.9	27.5	-2.6	-1.3
53.0	15882	16.4	.05152	47.6	.24	114.0	198.8	369.8	198.83	0.0	0.0	0.0000	3.3	82.8	-.4	-3.3
54.0	16196	21.1	.05232	61.4	.32	108.0	197.8	373.6	197.82	0.0	0.0	0.0000	6.3	101.0	1.2	-6.2
55.0	16581	19.7	.05340	58.3	.32	101.0	195.4	376.2	195.43	0.0	0.0	0.0000	9.7	102.6	2.1	-9.4
55.2	16637	19.2	.05354	56.7	.32	100.0	195.3	377.1	195.32	0.0	0.0	0.0000	9.9	106.3	2.8	-9.5
56.0	16865	16.9	.05412	50.2	.29	96.1	194.9	380.5	194.87	0.0	0.0	0.0000	11.1	119.4	5.5	-9.7
57.0	17231	16.3	.05496	48.6	.30	90.1	193.7	385.3	193.73	0.0	0.0	0.0000	9.3	123.7	5.2	-7.7
58.0	17609	18.5	.05588	54.6	.36	84.3	195.2	395.6	195.15	0.0	0.0	0.0000	6.5	79.2	-1.2	-6.3
58.9	17911	27.8	.05686	80.4	.58	80.0	199.3	410.2	199.34	0.0	0.0	0.0000	6.6	64.0	-2.9	-6.0
59.0	17962	29.4	.05703	84.8	.61	79.3	200.0	412.7	200.05	0.0	0.0	0.0000	6.7	61.5	-3.2	-5.9
60.0	18330	37.4	.05868	106.3	.83	74.5	203.5	427.3	203.48	0.0	0.0	0.0000	5.9	77.4	-1.3	-5.7
61.0	18669	50.0	.06063	139.7	1.18	70.4	206.6	441.0	206.63	0.0	0.0	0.0000	5.6	76.4	-1.3	-5.5
61.1	18703	51.0	.06088	142.4	1.21	70.0	206.8	442.1	206.80	0.0	0.0	0.0000	5.5	76.6	-1.3	-5.3
62.0	18987	59.3	.06289	164.4	1.47	66.8	208.2	451.1	208.22	0.0	0.0	0.0000	4.4	79.1	-.8	-4.4
63.0	19344	63.3	.06572	175.5	1.66	63.0	208.2	458.7	208.22	0.0	0.0	0.0000	4.5	96.6	.5	-4.5
63.8	19640	64.6	.06819	179.7	1.79	60.0	207.8	464.2	207.76	0.0	0.0	0.0000	7.5	92.4	.3	-7.5
64.0	19722	65.0	.06887	180.8	1.82	59.2	207.6	465.6	207.63	0.0	0.0	0.0000	8.3	91.8	.3	-8.3
65.0	20104	72.6	.07228	200.5	2.16	55.6	209.0	477.2	208.99	0.0	0.0	0.0000	11.3	95.8	1.1	-11.3
66.0	20516	83.6	.07641	227.8	2.66	52.0	212.0	493.3	211.96	0.0	0.0	0.0000	10.5	100.8	2.0	-10.3
66.5	20760	88.4	.07915	240.0	2.94	50.0	212.7	500.7	212.74	0.0	0.0	0.0000	8.3	99.8	1.4	-8.2

TIME MIN	ALT GPM	OZONE MICMB	TOTOZ ATMCM	OZDEN MG/M3	OZMXR MICGG	PRESS MB	TEMP DEG K	PTEMP DEG K	VTEMP DEG K	HMDTY PRCNT	DEWPT DEG K	SPCFC HMDTY	SPD MPS	DIR DEG	NS MPS	EW MPS
67.0	21014	93.5	.08200	252.7	3.23	48.0	213.6	508.5	213.55	0.0	0.0	0.0000	6.1	97.9	.8	-6.1
68.0	21376	100.0	.08642	269.8	3.66	45.3	213.9	517.8	213.90	0.0	0.0	0.0000	3.0	89.4	0.0	-3.0
69.0	21689	109.4	.09053	292.8	4.20	43.1	215.6	529.4	215.60	0.0	0.0	0.0000	4.9	59.3	-2.5	-4.2
70.0	22020	118.2	.09523	315.3	4.79	40.9	216.4	539.5	216.44	0.0	0.0	0.0000	7.0	70.4	-2.3	-6.6
70.4	22160	118.7	.09732	316.4	4.92	40.0	216.6	543.4	216.62	0.0	0.0	0.0000	7.0	80.2	-1.2	-6.9
71.0	22403	119.6	.10090	318.4	5.15	38.5	216.9	550.1	216.93	0.0	0.0	0.0000	7.5	95.9	.8	-7.5
72.0	22829	124.7	.10738	332.2	5.74	36.0	216.8	560.4	216.77	0.0	0.0	0.0000	3.9	113.3	1.6	-3.6
72.4	23007	126.2	.11019	336.2	5.98	35.0	216.7	564.7	216.70	0.0	0.0	0.0000	2.7	136.5	2.0	-1.9
73.0	23248	128.2	.11397	341.6	6.30	33.7	216.6	570.6	216.60	0.0	0.0	0.0000	2.6	190.1	2.6	.5
74.0	23779	133.4	.12258	353.3	7.13	31.0	218.1	588.3	218.07	0.0	0.0	0.0000	1.8	188.7	1.7	.3
74.4	23989	136.7	.12614	360.7	7.57	30.0	218.8	596.0	218.81	0.0	0.0	0.0000	1.9	117.9	.9	-1.7
75.0	24273	141.1	.13094	370.7	8.15	28.7	219.8	606.3	219.81	0.0	0.0	0.0000	4.3	86.1	-.3	-4.3
76.0	24838	149.1	.14094	386.6	9.40	26.3	222.7	629.8	222.73	0.0	0.0	0.0000	4.0	83.4	-.5	-3.9
76.8	25168	148.0	.14687	384.6	9.81	25.0	222.2	637.4	222.15	0.0	0.0	0.0000	1.8	277.5	-.2	1.8
77.0	25273	147.6	.14876	383.9	9.94	24.6	222.0	639.8	221.97	0.0	0.0	0.0000	3.6	272.6	-.2	3.6
78.0	25710	147.9	.15660	384.3	10.65	23.0	222.1	652.6	222.12	0.0	0.0	0.0000	4.1	269.2	.1	4.1
79.0	26238	142.8	.16595	373.1	11.17	21.2	221.1	664.8	221.05	0.0	0.0	0.0000	1.7	213.1	1.4	.9
79.9	26614	140.7	.17246	366.6	11.66	20.0	221.6	677.6	221.58	0.0	0.0	0.0000	1.0	112.4	.4	-.9
80.0	26680	140.3	.17358	365.4	11.74	19.8	221.7	679.8	221.67	0.0	0.0	0.0000	1.2	98.7	.2	-1.2
81.0	27228	139.1	.18287	360.5	12.66	18.2	222.7	699.7	222.73	0.0	0.0	0.0000	7.6	84.2	-.8	-7.5
81.5	27484	139.6	.18719	361.2	13.23	17.5	223.1	708.9	223.12	0.0	0.0	0.0000	10.9	90.0	0.0	-10.9
82.0	27712	140.0	.19103	361.8	13.73	16.9	223.5	717.0	223.47	0.0	0.0	0.0000	13.9	92.8	.7	-13.9
83.0	28194	135.3	.19903	349.2	14.28	15.7	223.8	733.3	223.77	0.0	0.0	0.0000	16.3	96.6	1.9	-16.2
83.5	28493	133.4	.20383	343.3	14.75	15.0	224.4	745.1	224.42	0.0	0.0	0.0000	16.6	101.4	3.3	-16.3
84.0	28807	131.4	.20886	337.1	15.23	14.3	225.1	757.6	225.10	0.0	0.0	0.0000	17.1	106.3	4.8	-16.4
85.0	29336	123.4	.21691	315.0	15.49	13.2	226.3	779.1	226.26	0.0	0.0	0.0000	14.5	110.7	5.1	-13.6
85.6	29697	120.1	.22209	306.1	15.92	12.5	226.5	792.2	226.50	0.0	0.0	0.0000	12.3	109.4	4.1	-11.6
86.0	29968	117.6	.22597	299.5	16.24	12.0	226.7	802.1	226.69	0.0	0.0	0.0000	10.6	108.2	3.3	-10.1
87.0	30549	112.9	.23388	283.7	17.00	11.0	229.7	833.1	229.66	0.0	0.0	0.0000	14.2	90.7	.2	-14.2
88.0	31191	102.6	.24198	256.9	17.00	10.0	230.6	859.7	230.63	0.0	0.0	0.0000	16.2	79.8	-2.9	-16.0
89.0	31680	92.5	.24757	231.9	16.48	9.3	230.2	876.1	230.22	0.0	0.0	0.0000	18.4	86.4	-1.1	-18.3
90.0	32288	87.6	.25396	218.6	17.08	8.5	231.5	903.8	231.46	0.0	0.0	0.0000	27.2	92.9	1.4	-27.1
90.7	32701	82.7	.25798	204.3	17.11	8.0	233.7	928.5	233.67	0.0	0.0	0.0000	30.9	93.0	1.6	-30.9
91.0	32874	80.6	.25966	198.4	17.12	7.8	234.6	938.8	234.59	0.0	0.0	0.0000	32.5	93.0	1.7	-32.5
92.0	33617	73.0	.26622	179.6	17.28	7.0	234.7	968.8	234.72	0.0	0.0	0.0000	33.2	87.6	-1.4	-33.1
93.0	34451	64.8	.27282	159.3	17.33	6.2	235.0	1004.2	234.99	0.0	0.0	0.0000	33.7	84.1	-3.5	-33.6
93.3	34677	57.4	.27415	141.0	15.71	6.0	235.4	1015.3	235.36	0.0	0.0	0.0000	999.9	999.9	999.9	999.9
94.0	35277	37.9	.27767	92.5	11.41	5.5	236.3	1045.1	236.33	0.0	0.0	0.0000	999.9	999.9	999.9	999.9

INTEGRAL .27767 RESIDUAL .02990 INTEGRATED TOTAL OZONE .30757

OZONAGRAM

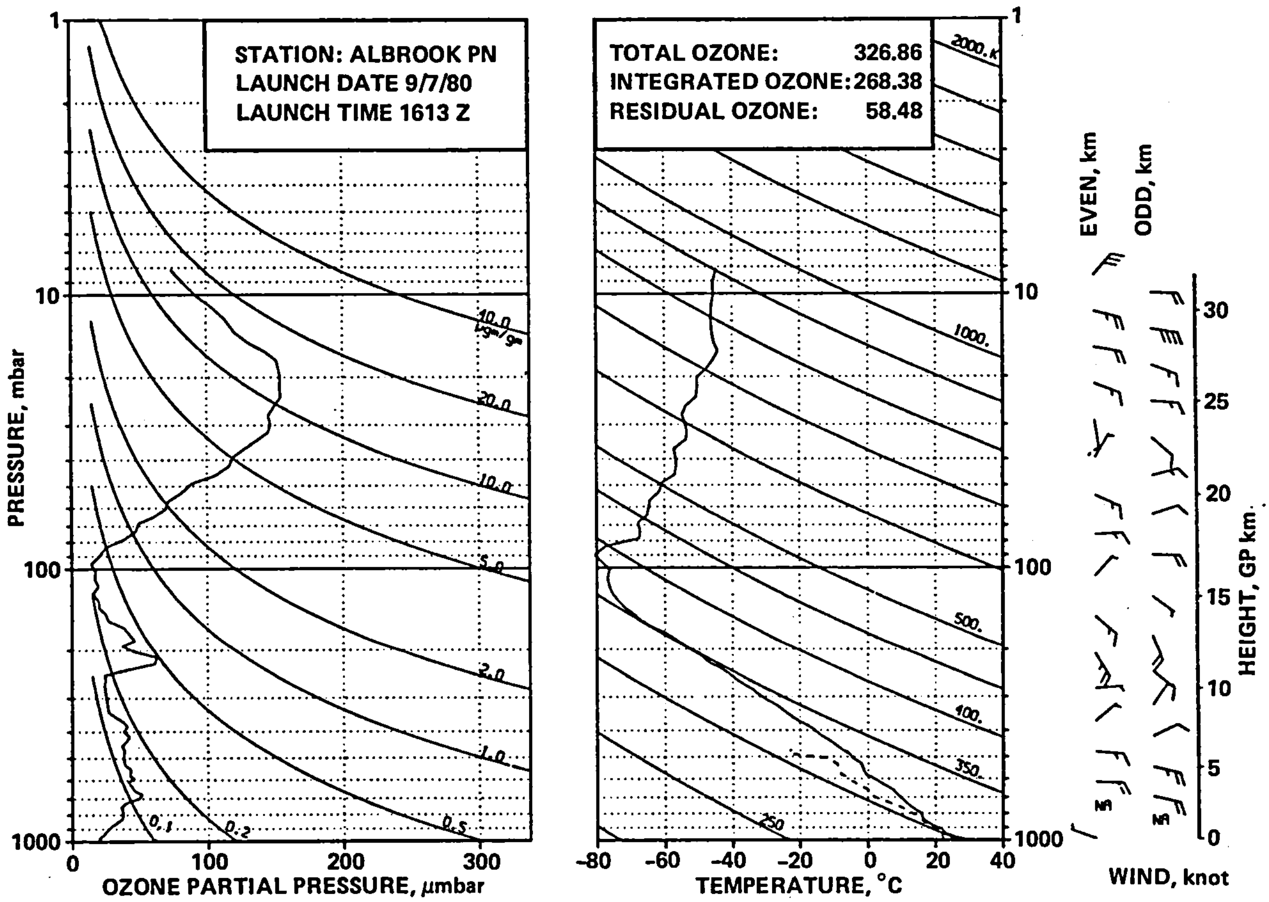
STATION: ALBROOK PN
LAUNCH DATE 9/7/80
LAUNCH TIME 1613 Z
TOTAL OZONE: 326.86
INTEGRATED OZONE: 268.38
RESIDUAL OZONE: 58.48
PRESSURE, mbar
OZONE PARTIAL PRESSURE, µmbar
TEMPERATURE, °C
EVEN, km
ODD, km
HEIGHT, GP km
WIND, knot
0
100
200
300
1
10
100
1000
-80
-60
-40
-20
0
20
40
0
5
10
15
20
25
30

STATION ALBROOK PN LAUNCH DATE 9/ 7/80 TIME 1613Z :CC SONDE 3A1326

SURFACE CONDITIONS PRESS 1002.8MB TEMP 304.2 DEG K HUMIDITY 68.0 PRCNT

TIME MIN	ALT GPM	OZONE MICMB	TOTOZ ATMCM	OZDEN MG/M3	OZMXR MICGG	PRESS MB	TEMP DEG K	PTEMP DEG K	VTEMP DEG K	HMDTY PRCNT	DEWPT DEG K	SPCFC HMDTY	SPD MPS	DIR DEG	NS MPS	EW MPS
0.0	66	20.0	0.00000	38.0	.03	1002.8	304.0	303.7	307.05	60.0	295.3	.0167	2.0	290.0	-.7	1.9
.1	90	20.0	.00004	38.0	.03	1000.0	303.5	303.5	306.62	61.8	295.3	.0168	999.9	999.9	999.9	999.9
1.0	326	19.9	.00046	38.3	.03	974.0	299.3	301.6	302.50	79.0	295.4	.0173	999.9	999.9	999.9	999.9
2.0	610	23.5	.00101	45.8	.04	943.0	296.0	301.0	299.07	91.4	294.5	.0169	999.9	999.9	999.9	999.9
3.0	892	25.6	.00164	50.1	.05	913.0	295.1	302.9	298.24	96.6	294.5	.0175	999.9	999.9	999.9	999.9
3.4	1016	26.9	.00194	52.8	.05	900.0	293.9	302.9	296.84	95.7	293.2	.0157	999.9	999.9	999.9	999.9
4.0	1172	28.4	.00233	56.0	.05	884.0	292.4	302.9	295.09	94.5	291.5	.0150	999.9	999.9	999.9	999.9
5.0	1459	32.8	.00313	65.3	.06	855.0	290.3	303.6	292.68	94.4	289.4	.0135	999.9	999.9	999.9	999.9
5.2	1509	33.6	.00329	66.8	.07	850.0	290.1	303.9	292.48	94.9	289.3	.0135	999.9	999.9	999.9	999.9
6.0	1733	36.9	.00401	73.6	.07	828.0	289.2	305.3	291.61	97.1	288.8	.0134	999.9	999.9	999.9	999.9
7.0	2015	37.4	.00499	74.7	.08	801.0	289.0	308.0	291.12	83.7	286.3	.0118	999.9	999.9	999.9	999.9
7.0	2025	37.4	.00502	74.7	.08	800.0	289.0	308.0	291.04	83.7	286.2	.0117	999.9	999.9	999.9	999.9
8.0	2284	37.0	.00592	74.4	.08	776.0	287.2	308.8	289.12	84.1	284.6	.0109	999.9	999.9	999.9	999.9
9.0	2571	36.2	.00690	73.3	.08	750.0	285.4	309.9	287.06	77.7	281.7	.0092	999.9	999.9	999.9	999.9
10.0	2866	39.9	.00796	81.0	.09	724.0	284.1	311.6	285.44	68.0	278.4	.00[illegible]7	8.6	103.6	2.0	-8.3
11.0	3147	48.9	.00914	99.9	.12	700.0	282.8	313.1	283.88	58.8	275.1	.0063	9.5	102.2	2.0	-9.3
12.0	3411	51.3	.01040	105.3	.13	678.0	281.5	314.6	282.53	59.3	274.0	.0060	9.8	98.5	1.4	-9.7
13.0	3696	45.6	.01172	93.9	.12	655.0	280.4	316.5	281.40	58.9	272.9	.0057	10.0	95.4	.9	-9.9
14.0	3963	44.0	.01288	91.3	.12	634.0	278.3	317.0	279.17	58.6	270.9	.0051	9.6	92.0	.3	-9.5
15.0	4250	41.0	.01406	85.6	.11	612.0	276.2	317.9	276.98	56.3	268.4	.0044	9.4	91.2	.2	-9.4
15.6	4409	43.6	.01474	91.6	.12	600.0	275.0	319.2	275.72	57.4	267.5	.0041	8.9	93.0	.5	-8.9
16.0	4532	45.6	.01525	96.1	.13	591.0	274.1	318.5	274.76	58.3	266.8	.0040	8.5	94.5	.7	-8.5
17.0	4682	42.7	.01591	90.4	.12	580.0	272.6	318.5	273.23	58.1	265.4	.0037	10.5	98.6	1.6	-10.4
18.0	5120	43.2	.01777	91.9	.13	549.0	271.7	322.4	272.26	58.0	264.5	.0036	12.7	103.9	3.0	-12.3
19.0	5415	38.8	.01897	82.7	.12	529.0	271.2	325.3	271.78	58.0	264.0	.0036	12.8	100.1	2.2	-12.6
20.0	5767	38.1	.02032	81.8	.12	506.0	268.7	326.4	269.18	54.7	261.0	.0029	11.7	93.3	.7	-11.7
20.3	5860	38.1	.02068	81.9	.13	500.0	268.4	327.1	268.76	44.9	257.5	.0020	10.8	93.6	.7	-10.8
21.0	6067	38.0	.02147	82.0	.13	487.0	267.6	328.7	267.82	23.1	249.9	.0012	8.9	94.6	.7	-8.9
22.0	6344	38.6	.02254	83.9	.14	470.0	265.4	329.3	265.59	29.2	250.6	.0013	8.2	95.1	.7	-8.2
23.0	6663	36.8	.02377	80.5	.14	451.0	263.6	331.0	263.65	0.0	0.0	0.0000	7.6	90.4	.1	-7.6
24.0	6976	40.2	.02501	88.6	.15	433.0	261.6	332.3	261.90	51.3	253.6	.0019	5.3	71.8	-1.6	-5.0
25.0	7263	42.1	.02623	93.8	.17	417.0	259.3	333.0	259.60	52.1	251.7	.0016	3.8	45.5	-2.7	-2.7
25.9	7578	38.1	.02754	85.3	.16	400.0	257.6	334.7	257.88	54.7	250.6	.0015	2.4	47.5	-1.6	-1.8
26.0	7597	37.8	.02762	84.8	.16	399.0	257.5	334.8	257.78	54.8	250.5	.0015	2.3	47.7	-1.6	-1.7
27.0	7904	40.6	.02889	91.8	.18	383.0	255.5	336.1	255.54	0.0	0.0	0.0000	2.4	51.8	-1.5	-1.9
28.0	8201	38.0	.03013	86.8	.17	368.0	252.8	336.3	252.84	21.0	236.2	.0004	2.5	48.8	-1.6	-1.8
29.0	8528	31.7	.03135	73.2	.15	352.0	250.4	337.4	250.46	32.0	238.3	.0006	1.4	3.4	-1.4	-.1
29.1	8569	31.0	.03148	71.6	.15	350.0	250.1	337.6	250.20	31.9	238.0	.0005	1.5	4.6	-1.5	-.1
30.0	8824	26.8	.03229	62.2	.13	338.0	248.5	338.8	248.59	31.0	236.3	.0005	1.9	10.3	-1.9	-.3
31.0	9175	26.1	.03330	61.2	.13	322.0	246.3	340.4	246.39	54.7	240.0	.0007	3.2	45.5	-2.2	-2.3
32.0	9517	25.5	.03427	60.5	.14	307.0	243.3	340.9	243.36	55.2	237.2	.0006	4.3	67.9	-1.6	-4.0
32.5	9680	25.2	.03473	60.2	.14	300.0	242.0	341.4	242.13	61.1	237.0	.0006	4.2	75.0	-1.1	-4.1
33.0	9847	25.0	.03520	59.8	.14	293.0	240.8	341.9	240.87	67.1	236.8	.0006	4.2	82.4	-.6	-4.2
34.0	10140	24.4	.03601	58.9	.14	281.0	239.1	343.6	239.15	62.0	234.4	.0005	3.3	86.0	-.2	-3.3
35.0	10418	24.0	.03677	58.5	.15	270.0	236.6	343.9	236.62	61.5	231.9	.0004	3.5	90.6	.2	-3.5
36.0	10758	24.6	.03772	60.7	.16	257.0	234.0	345.0	234.08	52.1	228.0	.0003	3.8	109.9	1.3	-3.5
36.7	10945	24.2	.03825	60.0	.16	250.0	232.7	345.8	232.74	0.0	0.0	0.0000	4.7	123.5	2.6	-3.9
37.0	11028	24.0	.03848	59.8	.16	247.0	232.2	346.2	232.15	0.0	0.0	0.0000	5.2	127.8	3.2	-4.1
38.0	11364	41.9	.03978	105.4	.30	235.0	229.6	347.2	229.55	0.0	0.0	0.0000	7.4	133.7	5.1	-5.3
39.0	11683	61.1	.04173	156.1	.45	224.0	226.2	346.8	226.18	0.0	0.0	0.0000	10.0	140.6	7.7	-6.3
40.0	12045	62.4	.04441	160.8	.49	212.0	223.9	348.7	223.87	0.0	0.0	0.0000	11.6	148.2	9.9	-6.1
41.0	12359	45.7	.04647	119.2	.37	202.0	221.2	349.3	221.19	0.0	0.0	0.0000	12.1	154.9	11.0	-5.1
41.2	12423	44.0	.04679	115.1	.36	200.0	220.7	349.6	220.71	0.0	0.0	0.0000	12.1	156.0	11.1	-4.9
42.0	12686	37.2	.04813	98.2	.32	192.0	218.7	350.5	218.73	0.0	0.0	0.0000	12.3	160.9	11.6	-4.0
43.0	12991	46.2	.04971	123.2	.42	183.0	216.3	351.4	216.33	0.0	0.0	0.0000	11.1	161.1	10.5	-3.6
44.0	13344	42.0	.05166	113.5	.40	173.0	213.3	352.1	213.31	0.0	0.0	0.0000	8.8	149.3	7.5	-4.5
45.0	13674	38.2	.05335	105.5	.39	164.0	208.8	350.3	208.81	0.0	0.0	0.0000	7.9	134.2	5.5	-5.7
46.0	14016	26.8	.05480	75.2	.29	155.0	205.9	350.7	205.87	0.0	0.0	0.0000	8.6	130.0	5.5	-6.6
46.5	14212	25.6	.05546	72.2	.28	150.0	204.6	351.8	204.62	0.0	0.0	0.0000	7.4	130.1	4.8	-5.7
47.0	14374	24.6	.05601	69.7	.28	146.0	203.6	352.8	203.59	0.0	0.0	0.0000	6.5	130.3	4.2	-4.9
48.0	14665	20.1	.05688	57.8	.24	139.0	201.2	353.5	201.15	0.0	0.0	0.0000	5.3	105.6	1.4	-5.1
49.0	15012	19.7	.05781	57.0	.25	131.0	199.3	356.2	199.28	0.0	0.0	0.0000	4.0	112.3	1.5	-3.7
49.7	15284	16.5	.05845	48.0	.22	125.0	198.0	358.7	198.00	0.0	0.0	0.0000	1.9	183.8	1.9	.1
50.0	15378	15.3	.05868	44.9	.21	123.0	197.6	359.5	197.55	0.0	0.0	0.0000	2.5	215.5	2.0	1.5
51.0	15716	19.5	.05948	57.2	.28	116.0	196.8	364.2	196.79	0.0	0.0	0.0000	3.9	271.2	-.1	3.9
52.0	16074	16.8	.06037	49.3	.25	109.0	196.3	369.7	196.26	0.0	0.0	0.0000	1.3	36.9	-1.1	-.8
53.0	16513	17.2	.06139	50.5	.28	101.0	197.0	379.4	197.04	0.0	0.0	0.0000	7.0	92.3	.3	-7.0
53.2	16570	16.6	.06152	48.7	.27	100.0	196.6	379.6	196.63	0.0	0.0	0.0000	7.3	93.0	.4	-7.3
54.0	16804	14.0	.06202	41.5	.24	96.0	194.9	380.7	194.92	0.0	0.0	0.0000	8.6	95.3	.8	-8.6
55.0	17182	20.3	.06292	60.8	.37	89.8	192.6	383.6	192.65	0.0	0.0	0.0000	11.3	89.6	-.1	-11.3
56.0	17588	24.8	.06420	73.3	.49	83.6	195.7	397.7	195.73	0.0	0.0	0.0000	10.1	93.2	.6	-10.0
56.7	17846	33.9	.06530	96.4	.71	80.0	202.3	416.4	202.28	0.0	0.0	0.0000	8.0	90.6	.1	-8.0
57.0	17980	38.6	.06587	108.3	.82	78.2	205.7	426.0	205.67	0.0	0.0	0.0000	7.0	88.6	-.2	-7.0
58.0	18378	47.0	.06810	131.8	1.06	73.2	205.9	434.5	205.87	0.0	0.0	0.0000	7.5	84.2	-.8	-7.4
58.7	18646	48.4	.06979	135.9	1.15	70.0	205.5	439.3	205.46	0.0	0.0	0.0000	5.9	81.3	-.9	-5.9
59.0	18777	49.0	.07061	137.9	1.19	68.5	205.3	441.5	205.26	0.0	0.0	0.0000	5.2	79.4	-1.0	-5.1
60.0	19131	60.5	.07315	168.0	1.55	64.6	207.9	454.7	207.85	0.0	0.0	0.0000	4.3	70.6	-1.4	-4.0
61.0	19520	69.2	.07642	191.7	1.89	60.6	208.4	464.3	208.43	0.0	0.0	0.0000	6.8	110.0	2.3	-6.4
61.2	19580	69.5	.07697	192.5	1.92	60.0	208.5	465.8	208.48	0.0	0.0	0.0000	7.0	111.9	2.6	-6.5
62.0	19915	71.2	.08001	197.0	2.08	56.8	208.8	473.9	208.81	0.0	0.0	0.0000	7.9	120.9	4.1	-6.8
63.0	20376	81.6	.08452	222.7	2.57	52.7	211.6	490.5	211.56	0.0	0.0	0.0000	6.9	99.8	1.2	-6.8
63.7	20702	86.7	.08806	235.9	2.88	50.0	212.2	499.4	212.20	0.0	0.0	0.0000	7.8	88.4	-.2	-7.8
64.0	20828	88.6	.08941	240.9	3.00	49.0	212.4	502.9	212.44	0.0	0.0	0.0000	8.2	84.7	-.8	-8.2

TIME MIN	ALT GPM	OZONE MICMB	TOTOZ ATMCM	OZDEN MG/M3	OZMXR MICGG	PRESS MB	TEMP DEG K	PTEMP DEG K	VTEMP DEG K	HMDTY PRCNT	DEWPT DEG K	SPCFC HMDTY	SPD MPS	DIR DEG	NS MPS	EW MPS
65.0	21265	106.2	.09477	283.6	3.85	45.7	216.2	522.0	216.16	0.0	0.0	0.0000	7.6	67.2	-2.9	-7.0
66.0	21770	116.3	.10177	309.9	4.57	42.2	216.7	535.2	216.65	0.0	0.0	0.0000	5.3	44.5	-3.8	-3.7
66.7	22109	118.5	.10675	316.0	4.91	40.0	216.4	542.9	216.43	0.0	0.0	0.0000	2.0	30.4	-1.7	-1.0
67.0	22270	119.5	.10910	318.9	5.08	39.0	216.3	546.6	216.33	0.0	0.0	0.0000	.8	338.9	-.7	.3
68.0	22654	126.8	.11501	339.0	5.73	36.7	216.0	555.3	216.00	0.0	0.0	0.0000	1.6	184.0	1.6	.1
68.6	22956	133.1	.11994	352.0	6.31	35.0	218.2	568.7	218.18	0.0	0.0	0.0000	3.2	135.1	2.2	-2.2
69.0	23141	136.9	.12296	360.0	6.67	34.0	219.5	576.8	219.51	0.0	0.0	0.0000	4.5	125.4	2.6	-3.7
70.0	23551	144.8	.13004	380.3	7.52	31.9	219.8	588.2	219.82	0.0	0.0	0.0000	5.8	141.8	4.6	-3.6
70.9	23945	146.6	.13711	385.7	8.10	30.0	219.4	597.5	219.40	0.0	0.0	0.0000	6.2	171.4	6.2	-.9
71.0	23988	146.8	.13786	386.3	8.16	29.8	219.4	598.5	219.35	0.0	0.0	0.0000	6.4	174.2	6.3	-.6
72.0	24479	145.0	.14670	383.5	8.70	27.6	218.3	608.7	218.26	0.0	0.0	0.0000	3.9	155.2	3.6	-1.7
73.0	24961	149.1	.15543	392.2	9.65	25.6	219.5	625.5	219.51	0.0	0.0	0.0000	6.9	93.0	.4	-6.9
73.3	25114	150.6	.15827	394.5	10.00	25.0	220.4	632.5	220.44	0.0	0.0	0.0000	7.4	94.4	.6	-7.3
74.0	25460	154.1	.16466	399.7	10.77	23.7	222.5	648.3	222.55	0.0	0.0	0.0000	8.5	97.0	1.0	-8.4
75.0	25945	153.6	.17369	397.9	11.57	22.0	222.8	663.1	222.84	0.0	0.0	0.0000	8.1	108.5	2.6	-7.7
76.0	26534	153.9	.18465	398.9	12.69	20.1	222.8	680.5	222.84	0.0	0.0	0.0000	9.3	119.1	4.5	-8.1
76.1	26566	153.9	.18525	398.3	12.75	20.0	223.0	682.0	223.02	0.0	0.0	0.0000	9.2	118.7	4.4	-8.1
77.0	27007	152.7	.19338	390.9	13.53	18.7	225.5	702.8	225.47	0.0	0.0	0.0000	8.7	112.8	3.4	-8.0
77.9	27446	151.3	.20133	384.2	14.33	17.5	227.3	722.1	227.29	0.0	0.0	0.0000	9.1	96.1	1.0	-9.1
78.0	27523	151.0	.20271	383.1	14.46	17.3	227.6	725.4	227.60	0.0	0.0	0.0000	9.3	93.5	.6	-9.3
79.0	28003	142.9	.21104	360.6	14.71	16.1	228.9	744.6	228.86	0.0	0.0	0.0000	9.5	100.1	1.7	-9.4
79.9	28475	131.5	.21868	333.3	14.52	15.0	227.8	756.4	227.84	0.0	0.0	0.0000	12.5	96.7	1.5	-12.4
80.0	28520	130.4	.21940	330.7	14.51	14.9	227.7	757.5	227.74	0.0	0.0	0.0000	12.7	96.5	1.4	-12.7
81.0	29079	120.8	.22772	306.9	14.60	13.7	227.2	774.0	227.18	0.0	0.0	0.0000	19.6	98.6	2.9	-19.3
81.9	29687	114.8	.23620	292.2	15.22	12.5	226.9	793.7	226.94	0.0	0.0	0.0000	16.9	103.1	3.8	-16.4
82.0	29795	113.8	.23770	289.6	15.33	12.3	226.9	797.2	226.89	0.0	0.0	0.0000	16.4	104.0	4.0	-15.9
83.0	30417	105.1	.24579	267.2	15.55	11.2	227.0	819.3	227.04	0.0	0.0	0.0000	10.9	103.8	2.6	-10.6
84.0	31105	92.9	.25386	235.8	15.25	10.1	227.6	846.0	227.60	0.0	0.0	0.0000	9.4	91.0	.2	-9.4
84.1	31171	92.1	.25456	233.6	15.25	10.0	227.6	848.4	227.59	0.0	0.0	0.0000	10.0	90.6	.1	-10.0
85.0	31799	83.7	.26113	212.5	15.25	9.1	227.5	871.0	227.46	0.0	0.0	0.0000	15.6	88.2	-.5	-15.6
86.0	32576	74.1	.26838	187.1	15.15	8.1	228.6	904.9	228.58	0.0	0.0	0.0000	999.9	999.9	999.9	999.9

INTEGRAL .26838 RESIDUAL .05848 INTEGRATED TOTAL OZONE .32686

OZONAGRAM

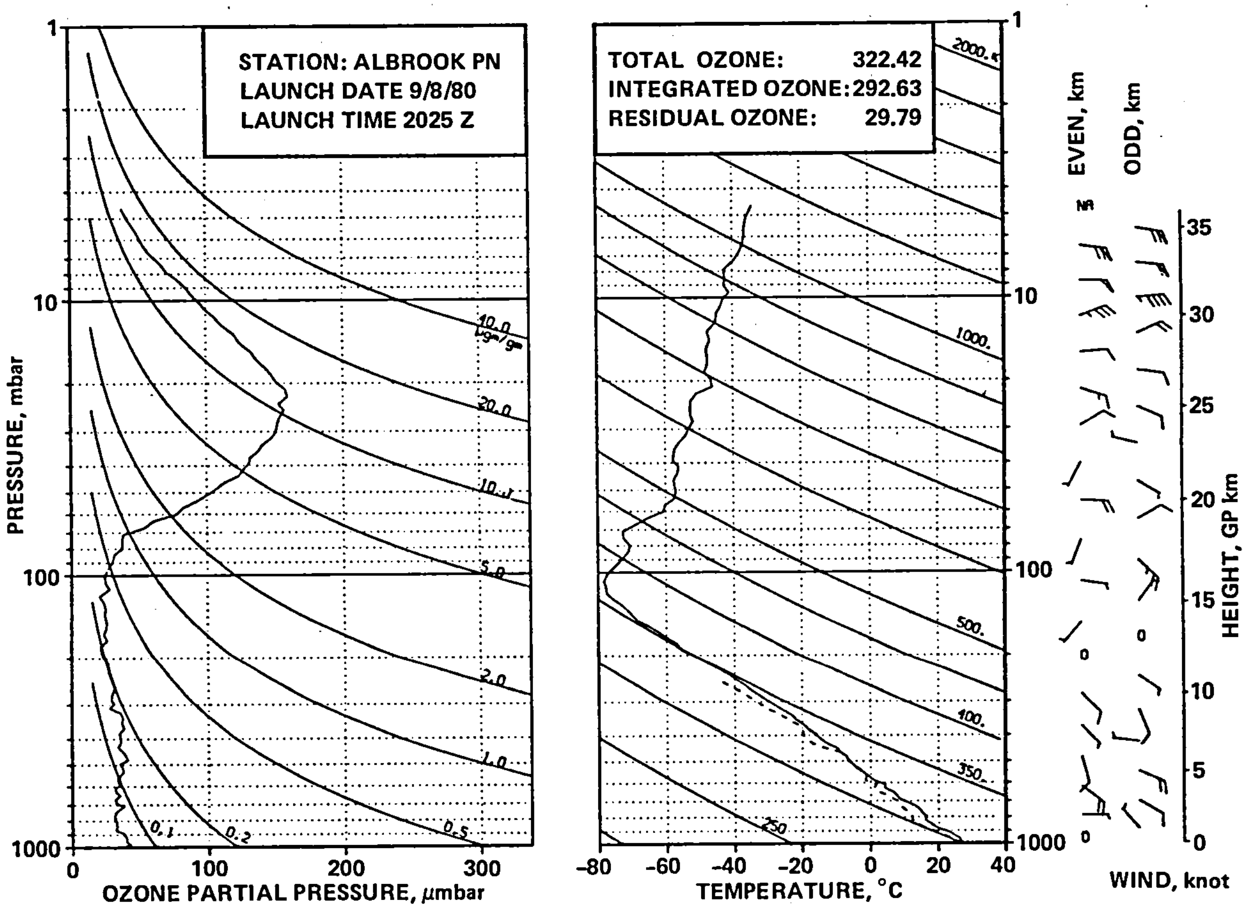

STATION: ALBROOK PN
LAUNCH DATE 9/8/80
LAUNCH TIME 2025 Z
TOTAL OZONE: 322.42
INTEGRATED OZONE: 292.63
RESIDUAL OZONE: 29.79
PRESSURE, mbar
OZONE PARTIAL PRESSURE, μmbar
TEMPERATURE, °C
EVEN, km
ODD, km
HEIGHT, GP km
WIND, knot

STATION ALBROOK PN   LAUNCH DATE 9/ 8/80   TIME 2025Z   ECC   SONDE 3A1329

SURFACE CONDITIONS   PRESS 1001.5MB   TEMP 300.4 DEG K   HUMIDITY 86.0 PRCNT

TIME MIN	ALT GPM	OZONE MICMB	TOTOZ ATMCM	OZDEN MG/M3	OZMXR MICGG	PRESS MB	TEMP DEG K	PTEMP DEG K	VTEMP DEG K	HMDTY PRCNT	DEWPT DEG K	SPCFC HMDTY	SPD MPS	DIR DEG	NS MPS	EW MPS
0.0	66	36.1	0.00000	69.4	.06	1001.5	300.4	300.3	303.79	81.8	297.0	.0185	1.0	300.0	-.5	.9
.1	79	36.5	.00005	70.2	.06	1000.0	300.3	300.3	303.77	82.6	297.1	.0188	1.2	304.2	-.7	1.0
1.0	258	42.4	.00067	81.7	.07	980.0	299.7	301.4	303.47	93.8	298.6	.0208	4.1	318.3	-3.1	2.7
2.0	468	39.0	.00144	75.2	.07	957.0	299.4	303.2	302.94	86.1	296.9	.0193	5.7	314.6	-4.0	4.1
3.0	673	39.3	.00215	76.3	.07	935.0	297.8	303.5	300.99	85.9	295.2	.0178	5.6	307.2	-3.4	4.4
4.0	901	38.6	.00295	75.1	.07	911.0	296.4	304.4	299.39	85.6	293.8	.0168	3.2	298.7	-1.5	2.8
4.5	1006	37.8	.00332	73.8	.07	900.0	295.2	304.2	297.95	82.5	292.1	.0146	2.7	310.1	-1.8	2.1
5.0	1104	37.0	.00365	72.6	.07	890.0	294.1	304.1	296.62	79.7	290.5	.0139	2.4	323.7	-2.0	1.4
6.0	1320	31.6	.00433	62.5	.06	868.0	292.0	304.0	294.12	77.6	288.0	.0121	3.1	347.1	-3.0	.7
6.8	1499	32.2	.00485	63.8	.06	850.0	291.1	305.0	293.25	78.6	287.4	.0119	2.3	9.0	-2.3	-.4
7.0	1550	32.3	.00500	64.1	.06	845.0	290.9	305.2	293.01	78.9	287.2	.0118	2.2	17.7	-2.0	-.7
8.0	1796	32.3	.00574	64.4	.07	821.0	289.3	306.0	291.18	77.9	285.4	.0108	2.2	62.7	-1.0	-2.0
8.9	2016	31.7	.00639	63.3	.07	800.0	289.6	308.7	291.61	76.6	285.5	.0112	3.2	87.3	-.2	-3.2
9.0	2038	31.7	.00646	63.2	.07	798.0	289.7	309.0	291.66	76.5	285.5	.0112	3.4	88.8	-.1	-3.4
10.0	2276	30.6	.00714	61.3	.07	776.0	288.5	310.1	290.34	76.5	284.4	.0107	4.6	98.6	.7	-4.5
11.0	2542	31.3	.00791	62.8	.07	752.0	287.7	312.1	289.46	74.9	283.3	.0103	5.9	104.1	1.4	-5.7
12.0	2781	33.7	.00864	67.8	.08	731.0	286.5	313.3	288.19	74.6	282.1	.0098	5.9	110.7	2.1	-5.5
13.0	3037	37.6	.00949	76.3	.09	709.0	284.2	313.5	285.91	85.5	281.8	.0099	6.2	118.7	3.0	-5.4
13.4	3143	34.9	.00984	71.2	.08	700.0	283.1	313.5	284.77	86.9	281.0	.0093	6.7	122.6	3.6	-5.7
14.0	3275	31.7	.01028	64.9	.08	689.0	281.8	313.4	283.35	88.7	280.0	.0090	7.4	126.6	4.4	-6.0
15.0	3519	31.4	.01101	64.6	.08	669.0	280.9	315.1	282.31	83.1	278.2	.0082	8.0	129.6	5.1	-6.2
16.0	3782	34.8	.01184	71.7	.09	648.0	279.8	316.8	281.05	75.1	275.7	.0071	8.7	127.4	5.3	-6.9
17.0	4025	31.8	.01262	66.1	.08	629.0	277.4	316.7	278.53	79.8	274.2	.0066	9.7	127.3	5.9	-7.7
18.0	4288	31.3	.01343	65.1	.09	609.0	277.4	319.7	278.63	83.8	274.9	.0071	10.4	129.1	6.6	-8.1
18.5	4408	32.8	.01382	68.6	.09	600.0	276.0	319.4	277.12	83.4	273.5	.0062	10.6	127.6	6.5	-8.4
19.0	4545	34.5	.01425	72.5	.10	590.0	274.4	319.1	275.41	82.9	271.8	.0059	10.9	126.0	6.4	-8.8
20.0	4822	32.9	.01517	69.6	.10	570.0	272.7	320.2	273.67	94.9	271.9	.0061	11.7	114.8	4.9	-10.7
21.0	5107	34.5	.01612	73.4	.10	550.0	271.1	321.6	272.05	99.5	271.0	.0059	10.8	112.1	4.0	-10.0
22.0	5371	37.1	.01706	79.4	.12	532.0	269.5	322.8	270.42	100.0	269.5	.0055	8.9	135.3	6.3	-6.2
23.0	5642	36.6	.01806	78.7	.12	514.0	268.1	324.3	268.98	100.0	268.1	.0051	8.1	157.7	7.5	-3.1
23.8	5858	35.0	.01883	75.7	.12	500.0	267.0	325.5	267.82	100.0	267.0	.0048	6.6	162.1	6.3	-2.0
24.0	5906	34.7	.01900	75.0	.12	497.0	266.8	325.8	267.57	100.0	266.8	.0047	6.3	163.4	6.0	-1.8
25.0	6178	40.5	.02003	87.8	.14	480.0	266.2	328.3	266.96	100.0	266.2	.0047	5.2	166.1	5.0	-1.2
26.0	6475	38.9	.02123	84.9	.14	462.0	264.4	329.7	265.11	99.7	264.4	.0042	3.9	168.7	3.8	-.8
27.0	6748	36.7	.02228	80.5	.14	446.0	263.4	331.8	263.90	74.7	259.8	.0030	2.0	190.5	2.0	.4
28.0	7028	33.4	.02329	74.0	.13	430.0	260.6	331.6	260.94	71.3	256.5	.0024	2.0	273.0	-.1	2.0
29.0	7353	35.7	.02446	79.8	.14	412.0	258.6	333.2	258.93	71.1	254.5	.0021	3.2	302.3	-1.7	2.7
29.9	7576	35.1	.02528	78.6	.15	400.0	257.6	334.8	257.97	71.5	253.7	.0020	1.0	322.2	-.8	.6
30.0	7614	35.0	.02542	78.4	.15	398.0	257.5	335.0	257.81	71.6	253.5	.0020	.7	337.6	-.6	.3
31.0	7922	34.5	.02655	78.0	.15	382.0	255.2	335.9	255.48	86.3	253.4	.0021	2.8	128.7	1.8	-2.2
32.0	8220	37.8	.02769	86.1	.17	367.0	253.7	337.8	253.97	86.9	252.0	.0019	4.0	142.8	3.2	-2.4
33.0	8550	36.1	.02899	83.0	.17	351.0	251.4	339.0	251.62	81.9	249.1	.0015	4.5	147.8	3.8	-2.4
33.1	8570	36.2	.02907	83.2	.17	350.0	251.3	339.2	251.53	81.4	249.0	.0015	4.5	148.6	3.8	-2.3
34.0	8827	36.9	.03008	85.3	.18	338.0	250.2	341.1	250.39	74.9	247.0	.0013	4.8	157.3	4.4	-1.9
35.0	9180	35.5	.03146	82.9	.18	322.0	247.3	341.8	247.42	70.7	243.5	.0010	5.0	158.3	4.6	-1.8
36.0	9477	27.5	.03249	64.9	.15	309.0	245.0	342.7	245.15	69.4	241.2	.0008	4.5	156.8	4.1	-1.8
36.7	9688	29.8	.03317	70.7	.16	300.0	243.5	343.4	243.56	68.9	239.6	.0007	3.8	153.8	3.4	-1.7
37.0	9760	30.6	.03340	72.7	.17	297.0	242.9	343.6	243.02	68.8	239.1	.0007	3.5	152.5	3.1	-1.6
38.0	10027	28.6	.03428	68.6	.17	286.0	240.9	344.5	241.02	68.4	237.1	.0006	3.8	136.1	2.8	-2.7
39.0	10327	29.3	.03526	71.0	.18	274.0	238.4	345.1	238.48	67.9	234.6	.0005	5.4	131.1	3.5	-4.0
40.0	10639	31.3	.03633	76.4	.20	262.0	236.3	346.4	236.33	59.5	231.3	.0004	4.5	137.0	3.3	-3.1
41.0	10933	30.1	.03737	74.3	.20	251.0	234.0	347.3	234.02	58.3	228.9	.0003	2.7	120.0	1.3	-2.3
41.1	10960	30.0	.03746	74.0	.20	250.0	233.8	347.4	233.84	0.0	0.0	0.0000	2.7	120.9	1.4	-2.3
42.0	11238	28.7	.03841	71.3	.20	240.0	231.9	348.7	231.93	0.0	0.0	0.0000	2.5	131.0	1.6	-1.9
43.0	11554	27.0	.03943	68.0	.20	229.0	228.9	348.7	228.86	0.0	0.0	0.0000	2.3	128.9	1.4	-1.8
44.0	11851	26.8	.04038	68.4	.20	219.0	226.1	349.0	226.14	0.0	0.0	0.0000	1.6	53.1	-1.0	-1.3
45.0	12127	26.5	.04126	68.4	.21	210.0	223.8	349.5	223.79	0.0	0.0	0.0000	.6	354.6	-.6	.1
46.0	12444	23.1	.04222	60.3	.19	200.0	221.1	350.1	221.05	0.0	0.0	0.0000	.3	142.9	.3	-.2
47.0	12739	21.7	.04303	57.5	.19	191.0	217.7	349.4	217.72	0.0	0.0	0.0000	.6	259.5	.1	.6
48.0	13080	21.3	.04395	56.9	.20	181.0	216.1	352.1	216.07	0.0	0.0	0.0000	.9	149.1	.8	-.5
49.0	13400	25.8	.04489	69.9	.25	172.0	213.1	352.4	213.14	0.0	0.0	0.0000	2.2	327.0	-1.9	1.2
50.0	13695	23.3	.04582	63.9	.24	164.0	210.6	353.0	210.60	0.0	0.0	0.0000	5.1	321.9	-4.0	3.1
51.0	13962	25.1	.04665	69.7	.27	157.0	208.1	353.2	208.11	0.0	0.0	0.0000	2.5	339.8	-2.3	.9
51.9	14237	25.6	.04756	72.0	.28	150.0	205.1	352.6	205.06	0.0	0.0	0.0000	1.4	24.1	-1.3	-.6
52.0	14[illegible]3	25.6	.04770	72.3	.28	149.0	204.6	352.5	204.62	0.0	0.0	0.0000	1.4	34.0	-1.1	-.8
53.0	14649	24.2	.04892	69.0	.29	140.0	202.6	355.4	202.64	0.0	0.0	0.0000	1.9	58.0	-1.0	-1.6
54.0	15040	24.7	.05020	71.4	.31	131.0	200.1	357.6	200.07	0.0	0.0	0.0000	3.6	3.0	-3.6	-.2
55.0	15313	23.3	.05109	68.2	.31	125.0	197.6	357.9	197.56	0.0	0.0	0.0000	5.5	357.4	-5.5	.3
56.0	15596	20.5	.05195	60.5	.29	119.0	195.7	359.5	195.68	0.0	0.0	0.0000	6.0	8.2	-5.9	-.8
57.0	15943	27.8	.05310	82.1	.41	112.0	195.4	365.2	195.41	0.0	0.0	0.0000	2.5	39.5	-1.9	-1.6
58.0	16150	25.2	.05386	74.7	.39	108.0	194.8	368.0	194.84	0.0	0.0	0.0000	3.5	138.0	2.6	-2.4
59.0	16533	23.9	.05516	70.5	.39	101.0	196.0	377.3	195.96	0.0	0.0	0.0000	8.6	136.1	6.2	-5.9
59.2	16590	24.4	.05536	71.6	.40	100.0	196.3	379.1	196.33	0.0	0.0	0.0000	9.5	135.3	6.7	-6.7
60.0	16856	26.3	.05627	76.8	.46	95.5	198.1	387.5	198.08	0.0	0.0	0.0000	13.8	133.0	9.4	-10.1
61.0	17260	30.0	.05781	86.3	.56	89.1	200.5	400.2	200.55	0.0	0.0	0.0000	11.9	132.7	8.1	-8.8
62.0	17593	31.2	.05918	89.1	.61	84.2	202.2	410.0	202.18	0.0	0.0	0.0000	6.4	129.9	4.1	-4.9
63.0	17896	36.8	.06056	105.0	.76	80.0	202.6	416.9	202.62	0.0	0.0	0.0000	2.3	116.3	1.0	-2.1
63.0	17911	37.1	.06062	105.8	.77	79.8	202.6	417.3	202.64	0.0	0.0	0.0000	2.2	114.3	.9	-2.0
64.0	18277	37.0	.06244	106.4	.82	75.0	200.8	420.9	200.79	0.0	0.0	0.0000	2.9	318.3	-2.2	1.9
65.0	18590	37.9	.06402	109.2	.88	71.1	200.5	426.8	200.55	0.0	0.0	0.0000	5.2	344.0	-5.0	1.4
65.3	18682	42.3	.06458	121.0	1.01	70.0	201.6	431.0	201.58	0.0	0.0	0.0000	4.6	355.9	-4.5	.3
66.0	18915	53.3	.06599	150.7	1.31	67.3	204.2	441.4	204.19	0.0	0.0	0.0000	4.3	34.6	-3.5	-2.4
67.0	19265	60.5	.06860	167.7	1.58	63.5	208.1	457.5	208.11	0.0	0.0	0.0000	7.6	94.8	.6	-7.6

TIME MIN	ALT GPM	OZONE MICMB	TOTOZ ATMCM	OZDEN MG/M3	OZMXR MICGG	PRESS MB	TEMP DEG K	PTEMP DEG K	VTEMP DEG K	HMDTY PRCNT	DEWPT DEG K	SPCFC HMDTY	SPD MPS	DIR DEG	NS MPS	EW MPS
68.0	19593	77.3	.07 50	210.1	2.13	60.2	212.4	474.1	212.43	0.0	0.0	0.0000	12.0	102.0	2.5	-11.8
68.1	19613	77.6	.07171	210.8	2.14	60.0	212.5	474.7	212.46	0.0	0.0	0.0000	12.0	101.1	2.3	-11.8
69.0	19922	81.9	.07482	222.0	2.38	57.1	213.0	482.6	212.96	0.0	0.0	0.0000	12.3	89.0	-.2	-12.3
70.0	20272	92.3	.07866	247.2	2.83	54.0	215.6	496.3	215.56	0.0	0.0	0.0000	10.0	98.0	1.4	-9.9
71.0	20621	100.2	.08285	267.6	3.25	51.1	216.2	505.8	216.23	0.0	0.0	0.0000	6.2	133.3	4.2	-4.5
71.5	20758	103.1	.08462	275.4	3.42	50.0	216.1	508.6	216.08	0.0	0.0	0.0000	4.7	129.1	2.9	-3.6
72.0	20912	106.2	.08660	284.1	3.61	48.8	215.9	511.7	215.90	0.0	0.0	0.0000	3.0	119.5	1.5	-2.5
73.0	21271	113.1	.09153	302.9	4.06	46.1	215.6	519.2	215.56	0.0	0.0	0.0000	3.9	120.0	2.0	-3.4
74.0	21609	123.5	.09652	328.9	4.68	43.7	216.7	530.1	216.73	0.0	0.0	0.0000	5.2	151.6	4.6	-2.5
75.0	21983	127.4	.10235	338.8	5.12	41.2	217.1	539.9	217.06	0.0	0.0	0.0000	3.9	201.5	3.7	1.4
75.6	22170	129.7	.10536	346.6	5.38	40.0	216.1	542.0	216.07	0.0	0.0	0.0000	3.8	215.3	3.1	2.2
76.0	22298	131.3	.10742	352.0	5.55	39.2	215.4	543.4	215.39	0.0	0.0	0.0000	3.9	224.9	2.8	2.7
77.0	22594	132.1	.11231	353.9	5.85	37.4	215.6	551.2	215.56	0.0	0.0	0.0000	3.2	224.6	2.3	2.2
78.0	22923	137.8	.11786	368.6	6.43	35.5	215.9	560.4	215.90	0.0	0.0	0.0000	3.5	269.0	.1	3.5
78.3	23012	138.6	.11942	370.1	6.57	35.0	216.3	563.6	216.26	0.0	0.0	0.0000	3.4	278.2	-.5	3.4
79.0	23253	140.8	.12358	374.1	6.92	33.7	217.2	572.3	217.23	0.0	0.0	0.0000	3.6	302.6	-1.9	3.0
80.0	23644	147.5	.13054	388.4	7.71	31.7	219.2	587.6	219.17	0.0	0.0	0.0000	3.6	2.0	-3.6	-.1
81.0	23998	150.9	.13703	396.2	8.34	30.0	220.0	599.0	219.96	0.0	0.0	0.0000	3.5	49.2	-2.3	-2.7
82.0	24420	151.9	.14485	396.1	8.95	28.1	221.4	614.2	221.36	0.0	0.0	0.0000	6.0	113.6	2.4	-5.5
83.0	24799	153.6	.15191	401.9	9.60	26.5	220.6	622.4	220.59	0.0	0.0	0.0000	8.9	110.6	3.1	-8.2
84.0	25175	156.9	.15905	410.7	10.40	25.0	220.6	632.9	220.59	0.0	0.0	0.0000	4.1	114.4	1.7	-3.7
85.0	25492	152.9	.16506	399.8	10.64	23.8	220.7	642.3	220.74	0.0	0.0	0.0000	2.8	108.8	.9	-2.7
86.0	25914	159.4	.17308	414.0	11.84	22.3	222.3	658.9	222.28	0.0	0.0	0.0000	6.7	111.8	2.5	-6.2
87.0	26309	157.7	.18059	400.8	12.44	21.0	227.2	685.0	227.15	0.0	0.0	0.0000	7.2	100.9	1.4	-7.1
87.8	26632	152.5	.18653	388.5	12.64	20.0	226.7	693.3	226.71	0.0	0.0	0.0000	6.9	88.4	-.2	-6.3
88.0	26733	151.0	.18837	384.7	12.70	19.7	226.6	695.8	226.58	0.0	0.0	0.0000	6.8	84.2	-.7	-6.8
89.0	27112	147.7	.19515	379.4	13.16	18.6	224.8	701.9	224.83	0.0	0.0	0.0000	5.0	99.6	.8	-4.9
90.0	27476	143.6	.20150	367.6	13.52	17.6	225.6	715.4	225.56	0.0	0.0	0.0000	4.7	89.0	-.1	-4.7
90.1	27513	143.1	.20213	366.2	13.54	17.5	225.6	716.6	225.57	0.0	0.0	0.0000	4.7	89.1	-.1	-4.7
91.0	27902	137.3	.20865	351.3	13.79	16.5	225.7	729.2	225.71	0.0	0.0	0.0000	4.7	89.5	0.0	-4.7
92.0	28357	133.2	.21602	341.4	14.33	15.4	225.3	742.2	225.27	0.0	0.0	0.0000	7.7	79.2	-1.5	-7.6
92.4	28531	130.2	.21870	333.2	14.38	15.0	225.7	749.3	225.66	0.0	0.0	0.0000	8.2	75.0	-2.1	-8.0
93.0	28847	124.9	.22356	318.4	14.47	14.3	226.4	762.1	226.43	0.0	0.0	0.0000	9.2	68.5	-3.4	-8.6
94.0	29327	120.6	.23058	308.5	15.03	13.3	225.7	775.5	225.71	0.0	0.0	0.0000	11.8	63.4	-5.3	-10.6
94.8	29738	113.5	.23627	288.0	15.04	12.5	227.6	796.2	227.65	0.0	0.0	0.0000	15.9	65.1	-6.7	-14.5
95.0	29846	111.7	.23775	282.7	15.05	12.3	228.2	801.6	228.15	0.0	0.0	0.0000	17.0	65.4	-7.1	-15.5
96.0	30354	105.5	.24426	266.7	15.33	11.4	228.4	820.2	228.44	0.0	0.0	0.0000	18.2	74.0	-5.0	-17.5
97.0	30716	99.9	.24864	251.3	15.33	10.8	229.6	837.1	229.57	0.0	0.0	0.0000	21.6	82.1	-3.0	-21.4
98.0	31167	94.8	.25379	237.6	15.56	10.1	230.4	856.4	230.41	0.0	0.0	0.0000	25.1	85.5	-2.0	-25.0
98.2	31234	93.9	.25452	234.9	15.55	10.0	230.8	860.2	230.76	0.0	0.0	0.0000	25.2	85.9	-1.8	-25.1
99.0	31510	89.9	.25749	223.5	15.51	9.6	232.2	875.7	232.20	0.0	0.0	0.0000	25.5	87.5	-1.1	-25.4
100.0	31947	85.4	.26195	213.7	15.72	9.0	230.7	886.2	230.68	0.0	0.0	0.0000	25.2	90.5	.2	-25.2
101.0	32413	79.1	.26643	197.7	15.60	8.4	231.0	904.9	230.96	0.0	0.0	0.0000	29.0	93.7	1.9	-28.9
101.8	32742	73.0	.26933	182.6	15.11	8.0	230.7	916.8	230.74	0.0	0.0	0.0000	30.7	95.6	3.0	-30.5
102.0	32827	71.4	.27007	178.8	14.98	7.9	230.7	919.8	230.68	0.0	0.0	0.0000	31.1	96.0	3.3	-31.0
103.0	33364	66.0	.27436	163.1	14.99	7.3	233.7	953.1	233.71	0.0	0.0	0.0000	32.9	96.0	3.4	-32.7
103.5	33652	62.1	.27641	152.7	14.66	7.0	234.6	968.6	234.64	0.0	0.0	0.0000	35.0	96.2	3.8	-34.8
104.0	33953	57.9	.27855	141.9	14.32	6.7	235.6	984.7	235.60	0.0	0.0	0.0000	37.1	96.4	4.1	-36.9
105.0	34489	53.0	.28195	129.4	14.17	6.2	236.5	1010.8	236.54	0.0	0.0	0.0000	36.4	98.4	5.3	-36.0
105.3	34716	51.4	.28325	125.5	14.19	6.0	236.6	1020.6	236.59	0.0	0.0	0.0000	36.7	98.7	5.6	-36.2
106.0	35194	48.1	.28601	117.4	14.23	5.6	236.7	1041.2	236.68	0.0	0.0	0.0000	37.2	99.3	6.0	-36.7
107.0	35843	42.7	.28936	103.9	13.88	5.1	237.3	1072.4	237.35	0.0	0.0	0.0000	37.7	97.5	4.9	-37.4
107.2	35980	41.8	.28999	101.4	13.82	5.0	237.7	1080.1	237.68	0.0	0.0	0.0000	999.9	999.9	999.9	999.9
108.0	36562	37.7	.29263	91.1	13.59	4.6	239.1	1112.6	239.08	0.0	0.0	0.0000	999.9	999.9	999.9	999.9

INTEGRAL .29263 RESIDUAL .02979 INTEGRATED TOTAL OZONE .32242

OZONAGRAM

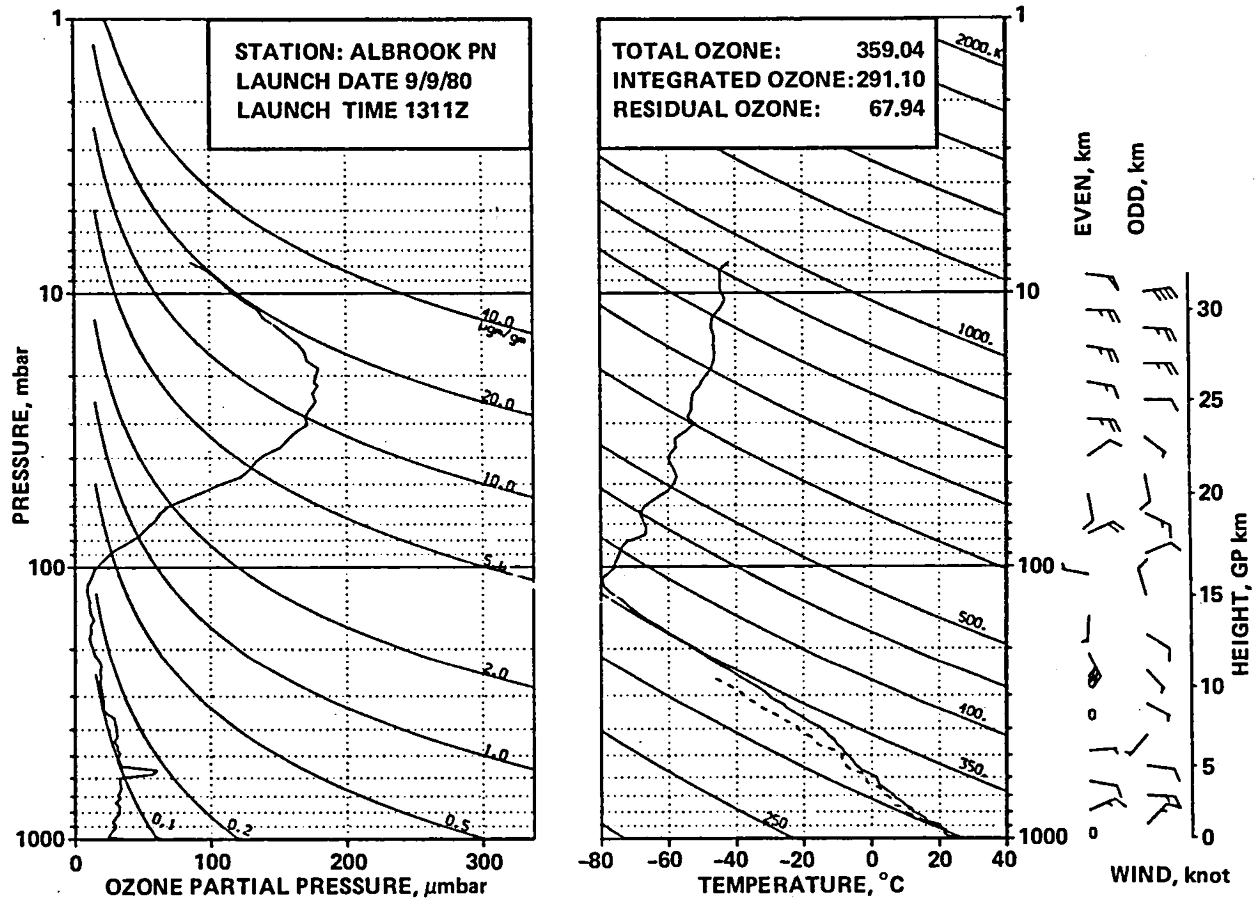
STATION: ALBROOK PN
LAUNCH DATE 9/9/80
LAUNCH TIME 1311Z
TOTAL OZONE: 359.04
INTEGRATED OZONE: 291.10
RESIDUAL OZONE: 67.94
PRESSURE, mbar
OZONE PARTIAL PRESSURE, μmbar
TEMPERATURE, °C
EVEN, km
ODD, km
HEIGHT, GP km
WIND, knot

STATION ALBROOK PN LAUNCH DATE 9/ 9/80 TIME 1311Z ECC SONDE 3A1330

SURFACC CONDITIONS PRESS 1003.8MB TEMP 299.6 DEG K HUMIDITY 94.0 PRCNT

TIME MIN	ALT GPM	OZONE MICMB	TOTOZ ATMCM	OZDEN MG/M3	OZMXR MICGG	PRESS MB	TEMP DEG K	PTEMP DEG K	VTEMP DEG K	HMDTY PRCNT	DEWPT DEG K	SPCFC HMDTY	SPD MPS	DIR DEG	NS MPS	EW MPS
0.0	66	39.3	0.00000	75.9	.06	1003.8	299.4	299.0	302.94	92.0	298.0	.0196	1.0	310.0	-.6	.8
.2	99	36.8	.00009	71.1	.06	1000.0	298.8	298.8	302.28	93.3	297.6	.0190	1.1	327.0	-1.0	.6
1.0	268	23.9	.00057	46.7	.04	981.0	295.8	297.4	298.97	100.0	295.8	.0176	2.5	2.7	-2.5	-.1
2.0	456	25.4	.00099	49.8	.04	960.0	294.4	297.9	297.40	100.0	294.4	.0165	3.5	26.2	-3.1	-1.5
3.0	676	27.0	.00152	52.9	.05	936.0	295.1	300.7	298.30	100.0	295.1	.0177	5.2	48.8	-3.4	-3.9
4.0	902	29.1	.00209	57.2	.05	912.0	293.5	301.4	296.39	96.4	292.9	.0159	6.5	3.7	-6.5	-.4
4.5	1016	29.4	.00240	57.9	.05	900.0	293.4	302.4	296.25	95.2	292.6	.0157	6.5	33.7	-5.4	-3.6
5.0	1113	29.7	.00266	58.5	.06	890.0	293.3	303.3	296.13	94.1	292.3	.0157	7.7	54.7	-4.4	-6.3
6.0	1328	27.2	.00322	54.1	.05	868.0	289.7	301.7	291.96	94.3	288.6	.0128	13.0	82.9	-1.6	-12.9
6.7	1506	28.6	.00369	57.0	.06	850.0	289.1	302.8	291.24	90.6	287.6	.0119	10.1	74.3	-2.7	-9.7
7.0	1577	29.1	.00387	58.2	.06	843.0	288.9	303.3	290.95	89.2	287.1	.0118	9.0	69.5	-3.2	-8.4
8.0	1801	30.7	.00449	61.8	.06	821.0	287.3	303.9	289.11	86.2	285.0	.0106	8.5	67.9	-3.2	-7.8
9.0	2019	32.6	.00514	66.0	.07	800.0	285.5	304.3	287.13	83.8	282.8	.0094	8.7	66.0	-3.5	-7.9
10.0	2231	31.9	.00579	64.6	.07	780.0	285.1	306.1	287.01	97.8	284.8	.0109	8.3	68.1	-3.1	-7.7
11.0	2459	32.6	.00648	66.4	.07	759.0	283.2	306.4	284.62	80.5	280.0	.0082	7.6	78.6	-1.5	-7.4
12.0	2715	29.4	.00723	60.2	.07	736.0	282.1	307.9	283.52	84.5	279.6	.0082	7.2	87.7	-.3	-7.2
13.0	2977	33.1	.00802	68.2	.08	713.0	280.1	308.5	281.46	90.0	278.6	.0079	6.8	91.6	.2	-6.8
13.6	3128	31.9	.00848	65.8	.08	700.0	279.8	309.8	281.07	87.3	277.8	.0075	6.5	94.5	.5	-6.5
14.0	3211	31.2	.00874	64.4	.07	693.0	279.6	310.5	280.85	85.8	277.4	.0074	6.4	96.3	.7	-6.3
15.0	3451	32.7	.00948	68.0	.08	673.0	277.8	311.1	279.05	90.3	276.4	.0071	5.7	89.3	-.1	-5.7
16.0	3697	33.6	.01027	70.0	.09	653.0	276.6	312.5	277.79	90.4	275.2	.0068	5.2	82.3	-.7	-5.1
17.0	3898	33.3	.01092	69.8	.09	637.0	275.3	313.2	276.26	81.9	272.5	.0057	5.4	94.5	.4	-5.3
18.0	4142	32.8	.01171	68.9	.09	618.0	275.0	315.5	275.88	77.8	271.5	.0055	6.0	103.2	1.4	-5.8
18.9	4380	32.6	.01247	68.5	.09	600.0	274.5	317.6	275.46	82.6	271.9	.0058	5.7	104.2	1.4	-5.6
19.0	4394	32.5	.01251	68.5	.09	599.0	274.5	317.8	275.44	82.8	271.9	.0058	5.7	104.3	1.4	-5.6
20.0	4652	57.6	.01366	122.2	.16	580.0	272.2	318.0	273.08	86.2	270.2	.0053	5.4	103.8	1.3	-5.2
21.0	4903	60.0	.01512	128.3	.18	562.0	270.1	318.5	270.85	78.5	266.9	.0043	5.2	99.0	.8	-5.1
22.0	5175	34.0	.01640	73.1	.10	543.0	268.6	319.8	269.26	79.5	265.6	.0040	5.0	96.2	.5	-5.0
23.0	5455	32.6	.01734	70.3	.10	524.0	267.7	322.0	268.30	77.2	264.3	.0037	5.2	99.0	.8	-5.1
24.0	5729	31.2	.01822	67.5	.10	506.0	266.6	323.9	267.28	85.5	264.6	.0039	4.9	103.9	1.2	-4.8
24.4	5821	31.8	.01852	69.0	.11	500.0	266.1	324.4	266.78	87.6	264.4	.0039	4.3	104.8	1.1	-4.1
25.0	5979	32.9	.01903	71.5	.11	490.0	265.3	325.3	265.93	91.1	264.1	.0039	3.2	107.2	.9	-3.0
26.0	6253	31.0	.01992	67.6	.11	473.0	264.6	327.7	265.07	75.5	261.0	.0032	1.3	39.6	-1.0	-.8
27.0	6502	31.0	.02071	67.9	.11	458.0	263.2	329.1	263.64	62.9	257.5	.0025	1.3	99.4	.2	-1.3
28.0	6793	28.5	.02159	62.6	.11	441.0	262.4	331.5	262.77	63.3	256.8	.0024	2.9	128.9	1.8	-2.3
29.0	7094	31.0	.02251	68.6	.12	424.0	260.7	333.1	261.01	61.1	254.8	.0021	2.3	230.0	1.5	1.8
30.0	7405	30.3	.02350	67.5	.12	407.0	259.3	335.2	259.54	53.5	251.9	.0017	.7	250.4	.2	.7
30.5	7536	30.3	.02392	67.6	.13	400.0	258.5	335.9	258.76	55.4	251.6	.0017	.6	61.6	-.3	-.5
31.0	7689	30.2	.02440	67.7	.13	392.0	257.6	336.6	257.86	57.7	251.2	.0017	2.2	65.0	-.9	-2.0
32.0	7962	29.1	.02525	66.0	.13	378.0	254.9	336.5	255.07	56.7	248.4	.0013	.8	281.0	-.2	.8
33.0	8263	28.6	.02617	65.3	.13	363.0	252.8	337.7	253.01	54.6	246.1	.0011	1.0	223.5	.7	.7
34.0	8532	23.7	.02693	54.6	.11	350.0	250.7	338.4	250.85	53.8	243.9	.0010	2.1	138.9	1.6	-1.4
35.0	8830	20.3	.02763	47.1	.10	336.0	248.4	339.3	248.56	49.6	241.0	.0008	2.2	135.2	1.6	-1.6
36.0	9138	21.1	.02833	49.3	.11	322.0	247.0	341.4	247.10	48.5	239.4	.0007	2.0	115.3	.8	-1.8
37.0	9457	20.5	.02906	48.5	.11	308.0	243.8	341.4	243.93	47.3	236.2	.0005	2.2	93.1	.1	-2.2
37.5	9644	20.1	.02948	47.9	.11	300.0	242.8	342.5	242.88	47.3	235.3	.0005	1.8	92.6	.1	-1.8
38.0	9812	19.8	.02985	47.3	.11	293.0	241.9	343.5	241.95	47.3	234.4	.0004	1.5	91.9	.1	-1.5
39.0	10132	19.1	.03055	46.1	.11	280.0	239.5	344.6	239.57	45.3	231.8	.0004	1.0	93.0	.1	-1.0
40.0	10437	18.1	.03119	44.1	.11	268.0	236.9	345.1	236.92	43.8	229.0	.0003	1.6	101.7	.3	-1.6
41.0	10752	18.8	.03186	46.3	.12	256.0	234.1	345.5	234.10	39.9	225.6	.0002	2.2	109.5	.7	-2.1
41.5	10913	18.5	.03221	46.0	.12	250.0	232.9	346.1	232.92	0.0	0.0	0.0000	2.1	123.3	1.1	-1.7
42.0	11107	18.3	.03262	45.6	.12	243.0	231.5	346.8	231.50	0.0	0.0	0.0000	2.0	141.5	1.6	-1.3
43.0	11419	19.0	.03330	47.9	.14	232.0	228.5	346.8	228.47	0.0	0.0	0.0000	52.2	334.1	-47.0	22.8
44.0	11742	17.6	.03400	44.9	.13	221.0	225.9	347.7	225.92	0.0	0.0	0.0000	3.1	166.8	3.1	-.7
45.0	12077	14.5	.03465	37.6	.11	210.0	223.3	348.8	223.30	0.0	0.0	0.0000	59.5	154.6	53.7	-25.6
46.0	12394	13.0	.03518	33.9	.11	200.0	220.7	349.6	220.74	0.0	0.0	0.0000	8.0	154.7	7.3	-3.4
47.0	12689	11.5	.03562	30.5	.10	191.0	217.9	349.7	217.93	0.0	0.0	0.0000	5.2	133.8	3.6	-3.8
48.0	12995	10.5	.03604	28.1	.10	182.0	215.2	350.1	215.16	0.0	0.0	0.0000	4.6	118.4	2.2	-4.1
49.0	13312	11.8	.03649	32.2	.11	173.0	212.6	350.9	212.59	0.0	0.0	0.0000	4.7	135.8	3.4	-3.3
50.0	13642	11.1	.03697	30.6	.11	164.0	209.9	351.8	209.88	0.0	0.0	0.0000	2.3	74.1	-.6	-2.2
51.0	13947	13.8	.03747	38.5	.15	156.0	206.8	351.7	206.82	0.0	0.0	0.0000	3.8	1.4	-3.8	-.1
51.7	14182	12.0	.03785	33.7	.13	150.0	204.9	352.3	204.92	0.0	0.0	0.0000	3.0	359.7	-3.0	0.0
52.0	14304	11.1	.03805	31.3	.12	147.0	203.9	352.7	203.94	0.0	0.0	0.0000	2.6	358.4	-2.6	.1
53.0	14636	10.4	.03852	29.8	.12	139.0	201.3	353.7	201.29	0.0	0.0	0.0000	2.7	11.5	-2.7	-.5
54.0	14939	10.4	.03894	30.1	.13	132.0	199.4	355.6	199.41	0.0	0.0	0.0000	5.0	347.6	-4.9	1.1
54.9	15253	9.1	.03936	26.9	.12	125.0	196.3	355.6	196.32	0.0	0.0	0.0000	4.9	338.8	-4.6	1.8
55.0	15300	9.0	.03942	26.4	.12	124.0	195.9	355.6	195.86	0.0	0.0	0.0000	4.9	337.4	-4.6	1.9
56.0	15631	8.9	.03983	26.5	.13	117.0	193.9	358.0	193.93	0.0	0.0	0.0000	4.9	332.7	-4.4	2.3
57.0	15981	11.8	.04033	35.2	.18	110.0	193.6	363.8	193.65	0.0	0.0	0.0000	3.6	345.8	-3.5	.9
58.0	16412	14.3	.04111	41.9	.23	102.0	196.9	378.0	196.92	0.0	0.0	0.0000	4.8	23.5	-4.4	-1.9
58.4	16526	16.0	.04137	46.9	.27	100.0	197.1	380.6	197.12	0.0	0.0	0.0000	5.0	31.0	-4.3	-2.6
59.0	16702	18.6	.04177	54.5	.32	97.0	197.4	384.5	197.43	0.0	0.0	0.0000	5.4	41.2	-4.1	-3.6
60.0	17034	23.5	.04272	68.3	.42	91.6	198.4	392.8	198.44	0.0	0.0	0.0000	4.5	70.4	-1.5	-4.2
61.0	17381	30.0	.04397	86.9	.58	86.3	199.2	401.1	199.17	0.0	0.0	0.0000	4.2	45.2	-2.9	-3.0
62.0	17723	39.4	.04557	113.1	.80	81.4	200.8	411.2	200.83	0.0	0.0	0.0000	7.3	48.8	-4.8	-5.5
62.3	17826	41.8	.04617	119.0	.87	80.0	202.5	416.7	202.46	0.0	0.0	0.0000	8.0	55.1	-4.6	-6.6
63.0	18077	47.7	.04761	133.3	1.03	76.7	206.4	429.9	206.42	0.0	0.0	0.0000	10.0	66.2	-4.0	-9.1
64.0	18442	52.8	.05001	147.5	1.21	72.2	206.8	438.2	206.82	0.0	0.0	0.0000	7.1	99.9	1.2	-7.0
64.5	18628	56.1	.05138	157.1	1.33	70.0	206.3	441.0	206.27	0.0	0.0	0.0000	7.3	113.9	2.9	-6.6
65.0	18786	58.9	.05252	165.2	1.43	68.2	205.8	443.3	205.81	0.0	0.0	0.0000	7.7	124.7	4.4	-6.3
66.0	19149	62.6	.05542	176.3	1.62	64.2	205.0	449.2	204.99	0.0	0.0	0.0000	8.8	113.3	3.5	-8.1
67.0	19526	68.5	.05866	191.9	1.88	60.3	206.2	460.0	206.22	0.0	0.0	0.0000	5.8	129.7	3.7	-4.5
67.1	19556	69.6	.05896	194.6	1.92	60.0	206.5	461.3	206.47	0.0	0.0	0.0000	5.6	132.0	3.7	-4.1

TIME MIN	ALT GPM	OZONE MICMB	TOTOZ ATMCM	OZDEN MG/M3	OZMXR MICGG	PRESS MB	TEMP DEG K	PTEMP DEG K	VTEMP DEG K	HMDTY PRCNT	DEWPT DEG K	SPCFC HMDTY	SPD MPS	DIR DEG	NS MPS	EW MPS
68.0	19889	81.3	.06220	224.3	2.37	56.8	209.3	475.0	209.33	0.0	0.0	0.0000	4.1	169.7	4.0	-.7
69.0	20270	94.9	.06649	257.4	2.94	53.4	212.8	491.4	212.76	0.0	0.0	0.0000	4.9	168.9	4.8	-1.0
70.0	20681	107.4	.07174	288.8	3.56	50.0	214.8	505.6	214.82	0.0	0.0	0.0000	4.5	165.3	4.4	-1.1
71.0	21071	123.2	.07737	329.9	4.34	47.0	215.7	516.6	215.66	0.0	0.0	0.0000	4.1	169.7	4.0	-.7
72.0	21486	130.0	.08396	349.3	4.89	44.0	214.8	524.4	214.82	0.0	0.0	0.0000	2.3	158.4	2.1	-.8
73.0	21883	134.0	.09055	362.5	5.38	41.3	213.5	530.6	213.46	0.0	0.0	0.0000	3.7	63.6	-1.7	-3.3
73.5	22082	137.6	.09402	371.8	5.71	40.0	213.6	535.9	213.64	0.0	0.0	0.0000	4.5	54.7	-2.6	-3.7
74.0	22257	140.7	.09704	380.0	5.99	38.9	213.8	540.6	213.80	0.0	0.0	0.0000	5.2	49.2	-3.4	-4.0
75.0	22640	151.9	.10408	407.0	6.88	36.6	215.5	554.4	215.49	0.0	0.0	0.0000	2.5	67.9	-.9	-2.3
75.7	22921	155.5	.10954	417.2	7.37	35.0	215.3	561.0	215.27	0.0	0.0	0.0000	1.8	104.0	.4	-1.8
76.0	23067	157.4	.11236	422.4	7.63	34.2	215.2	564.4	215.16	0.0	0.0	0.0000	1.9	127.2	1.1	-1.5
77.0	23469	163.4	.12038	431.9	8.43	32.1	218.4	583.4	218.41	0.0	0.0	0.0000	7.9	79.7	-1.4	-7.8
78.0	23882	172.1	.12889	449.7	9.47	30.1	220.9	601.0	220.89	0.0	0.0	0.0000	13.0	87.4	-.6	-13.0
78.1	23903	171.9	.12934	449.6	9.50	30.0	220.8	601.3	220.79	0.0	0.0	0.0000	12.8	88.0	-.4	-12.8
79.0	24256	169.8	.13673	447.5	9.91	28.4	219.0	605.9	219.04	0.0	0.0	0.0000	10.2	100.3	1.8	-10.1
80.0	24677	173.3	.14560	454.4	10.79	26.6	220.1	620.5	220.13	0.0	0.0	0.0000	6.1	97.9	.8	-6.1
80.9	25076	177.3	.15419	465.0	11.76	25.0	220.1	631.6	220.13	0.0	0.0	0.0000	5.7	89.6	0.0	-5.7
81.0	25128	177.8	.15530	466.4	11.88	24.8	220.1	633.0	220.13	0.0	0.0	0.0000	5.6	88.4	-.2	-5.6
82.0	25558	175.4	.16459	459.1	12.53	23.2	220.6	646.5	220.59	0.0	0.0	0.0000	7.8	81.3	-1.2	-7.7
83.0	25991	179.3	.17395	464.9	13.69	21.7	222.7	665.3	222.70	0.0	0.0	0.0000	6.1	99.0	1.0	-6.1
84.0	26174	176.5	.17789	457.0	13.86	21.1	223.0	671.6	223.00	0.0	0.0	0.0000	9.1	102.3	1.9	-8.9
84.5	26525	178.1	.18541	458.3	14.79	20.0	224.4	686.2	224.35	0.0	0.0	0.0000	10.5	94.9	.9	-10.5
85.0	26932	179.9	.19411	459.8	15.86	18.8	225.9	703.1	225.92	0.0	0.0	0.0000	12.2	88.4	-.3	-12.2
86.0	27369	171.4	.20326	436.3	16.13	17.6	226.8	719.2	226.77	0.0	0.0	0.0000	11.6	94.3	.9	-11.5
86.1	27406	171.2	.20402	436.0	16.22	17.5	226.8	720.5	226.79	0.0	0.0	0.0000	11.6	95.1	1.0	-11.6
87.0	27838	169.8	.21276	432.1	17.16	16.4	226.9	734.4	226.92	0.0	0.0	0.0000	12.7	103.1	2.9	-12.4
88.0	28299	165.3	.22194	421.0	17.90	15.3	226.6	748.1	226.63	0.0	0.0	0.0000	12.8	96.5	1.5	-12.7
88.3	28430	163.1	.22446	415.5	18.01	15.0	226.7	752.5	226.67	0.0	0.0	0.0000	12.4	95.0	1.1	-12.3
89.0	28794	157.2	.23143	400.1	18.34	14.2	226.8	764.7	226.77	0.0	0.0	0.0000	11.2	90.0	0.0	-11.2
90.0	29228	150.4	.23938	384.5	18.74	13.3	225.9	776.2	225.92	0.0	0.0	0.0000	14.4	96.9	1.7	-14.3
90.8	29638	142.2	.24649	363.0	18.85	12.5	226.3	791.3	226.26	0.0	0.0	0.0000	15.1	99.2	2.4	-14.9
91.0	29745	140.1	.24834	357.4	18.87	12.3	226.3	795.3	226.35	0.0	0.0	0.0000	15.3	99.7	2.6	-15.1
92.0	30251	135.3	.25659	341.6	19.66	11.4	228.6	820.8	228.61	0.0	0.0	0.0000	12.9	87.4	-.6	-12.9
93.0	30739	124.6	.26405	312.7	19.48	10.6	230.1	843.7	230.13	0.0	0.0	0.0000	19.3	80.5	-3.2	-19.1
93.7	31130	118.1	.26956	297.5	19.56	10.0	229.2	854.5	229.22	0.0	0.0	0.0000	22.3	82.8	-2.8	-22.1
94.0	31335	114.7	.27243	289.6	19.60	9.7	228.7	860.1	228.75	0.0	0.0	0.0000	23.9	83.8	-2.6	-23.7
95.0	31836	107.8	.27901	272.2	19.85	9.0	228.7	878.7	228.75	0.0	0.0	0.0000	26.4	95.8	2.7	-26.3
96.0	32378	99.0	.28562	250.2	19.77	8.3	228.6	898.7	228.61	0.0	0.0	0.0000	26.3	98.7	4.0	-26.0
96.5	32625	92.7	.28831	232.8	19.16	8.0	230.0	913.7	229.96	0.0	0.0	0.0000	999.9	999.9	999.9	999.9
97.0	32883	86.0	.29110	214.7	18.52	7.7	231.4	929.3	231.37	0.0	0.0	0.0000	999.9	999.9	999.9	999.9

INTEGRAL .29110 RESIDUAL .06794 INTEGRATED TOTAL OZONE .35904

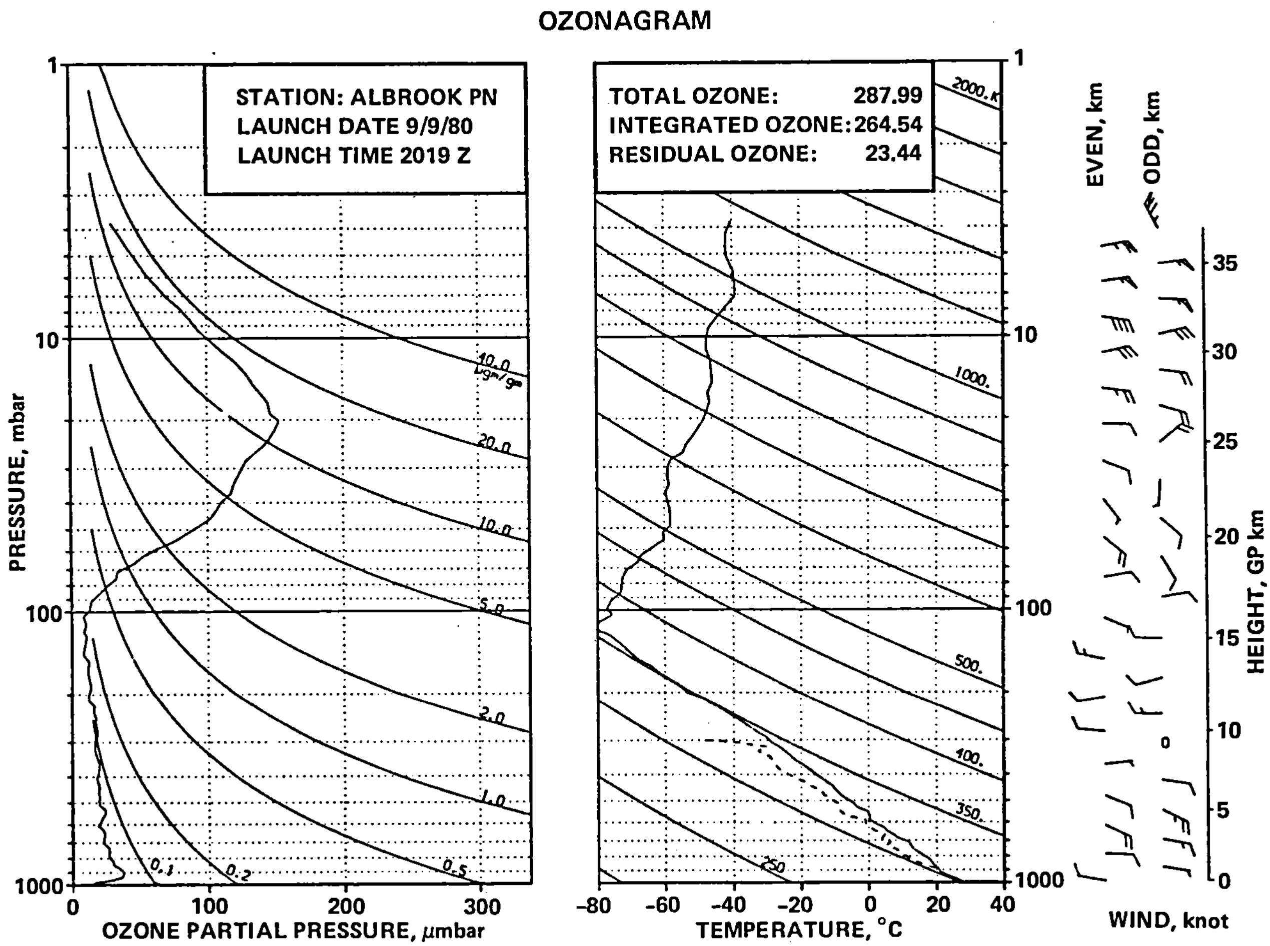

OZONAGRAM
STATION: ALBROOK PN
LAUNCH DATE 9/9/80
LAUNCH TIME 2019 Z
TOTAL OZONE: 287.99
INTEGRATED OZONE: 264.54
RESIDUAL OZONE: 23.44
PRESSURE, mbar
OZONE PARTIAL PRESSURE, μmbar
TEMPERATURE, °C
WIND, knot
HEIGHT, GP km
EVEN, km
ODD, km

STATION ‘_BROOK PN LAUNCH DATE 9/ 9/80 TIME 2019Z ECC SONDE 3A1331

SURFACE CONDITIONS PRESS 1000.4MB TEMP 301.2 DEG K HUMIDITY 87.0 PRCNT

TIME MIN	ALT GPM	OZONE MICMB	TOTOZ ATMCM	OZDEN MG/M3	OZMXR MICGG	PRESS MB	TEMP DEG K	PTEMP DEG K	VTEMP DEG K	HMDTY PRCNT	DEWPT DEG K	SPCFC HMDTY	SPD MPS	DIR DEG	NS MPS	EW MPS
0.0	66	14.2	0.00000	27.3	.02	1000.4	300.9	300.9	304.47	82.8	297.7	.0194	4.0	280.0	-.7	3.9
0.0	69	14.3	0.00000	27.4	.02	1000.0	300.9	300.9	304.46	83.0	297.7	.0194	4.0	280.6	-.7	4.0
1.0	240	16.8	.00024	32.4	.03	981.0	299.9	301.6	303.73	91.8	298.5	.0207	6.5	299.9	-3.2	5.6
2.0	422	29.4	.00062	56.9	.05	961.0	298.3	301.7	301.97	97.1	297.8	.0203	6.7	276.1	-.7	6.6
3.0	635	35.9	.00124	70.1	.06	938.0	296.0	301.5	299.24	96.8	295.5	.0180	4.5	240.1	2.2	3.9
4.0	870	37.0	.00202	72.6	.07	913.0	294.2	302.0	297.27	99.1	294.1	.0170	1.2	169.0	1.1	-.2
4.6	994	36.7	.00243	72.1	.07	900.0	293.9	302.8	296.83	97.7	293.5	.0164	1.1	119.1	.5	-1.0
5.0	1091	36.4	.00276	71.6	.07	890.0	293.6	303.5	296.49	96.6	293.0	.0163	1.5	92.1	.1	-1.5
6.0	1317	33.6	.00348	66.3	.06	867.0	292.5	304.7	294.97	85.5	290.0	.0138	1.8	90.5	0.0	-1.8
6.7	1487	30.7	.00397	60.7	.06	850.0	291.9	305.8	294.14	78.8	288.1	.0122	2.6	85.6	-.2	-2.6
7.0	1559	29.5	.03418	58.4	.06	843.0	291.7	306.2	293.80	76.1	287.4	.0120	2.9	84.3	-.3	-2.9
8.0	1796	29.5	.00482	58.6	.06	820.0	291.0	308.0	292.97	70.0	285.5	.0109	5.0	79.0	-1.0	-4.9
9.0	2006	27.4	.00538	54.7	.06	800.0	289.5	308.5	291.28	70.1	284.0	.0101	5.5	89.7	0.0	-5.5
9.0	2017	27.3	.00540	54.5	.06	799.0	289.4	308.6	291.19	70.1	283.9	.0101	5.5	90.2	0.0	-5.5
10.0	2254	26.2	.00599	52.5	.06	777.0	288.0	309.5	289.71	71.6	282.9	.0097	6.0	102.3	1.3	-5.8
11.0	2497	26.9	.00659	54.3	.06	755.0	286.4	310.4	287.99	69.7	281.0	.0088	7.0	110.7	2.5	-6.5
12.0	2780	26.3	.00730	53.1	.06	730.0	285.5	312.4	286.82	62.1	278.4	.0076	7.3	109.2	2.4	-6.9
13.0	3025	23.2	.00787	47.0	.05	709.0	284.9	314.3	286.41	70.0	279.6	.0085	7.4	100.2	1.3	-7.3
13.4	3131	22.9	.00810	46.6	.05	700.0	283.6	314.0	285.00	70.7	278.5	.0077	8.0	102.1	1.7	-7.8
14.0	3263	22.6	.00839	46.2	.05	689.0	282.0	313.7	283.26	71.5	277.1	.0073	8.8	104.0	2.1	-8.5
15.0	3531	23.2	.00897	47.9	.06	667.0	280.4	314.8	281.78	84.9	278.0	.0081	10.2	110.6	3.6	-9.6
16.0	3794	23.3	.00956	48.2	.06	646.0	278.5	315.5	279.63	78.3	275.0	.0067	10.7	115.5	4.6	-9.7
17.0	4051	21.9	.01012	45.6	.06	626.0	277.5	317.2	278.51	74.8	273.4	.0062	11.4	115.6	4.9	-10.3
18.0	4301	18.7	.01062	39.2	.05	607.0	275.1	317.3	276.12	81.1	272.2	.0059	12.0	119.9	6.0	-10.4
18.4	4394	19.4	.01080	40.8	.05	600.0	274.5	317.6	275.51	85.3	272.3	.0060	12.0	119.0	5.8	-10.5
19.0	4543	20.5	.01108	43.3	.06	589.0	273.5	318.2	274.54	92.0	272.4	.0061	12.1	117.5	5.6	-10.8
20.0	4820	21.9	.01166	46.2	.06	569.0	273.5	321.3	274.21	60.6	266.8	.0042	11.9	110.8	4.2	-11.2
21.0	5107	23.8	.01230	50.4	.07	549.0	273.0	324.1	273.66	54.2	264.9	.0037	11.9	117.0	5.4	-10.6
22.0	5387	23.7	.01297	50.8	.07	530.0	269.9	323.6	270.54	68.3	264.9	.0039	11.0	121.2	5.7	-9.4
23.0	5691	19.5	.01362	42.0	.06	510.0	268.7	325.7	269.29	69.5	264.0	.0037	8.2	117.7	3.8	-7.2
23.6	5846	19.5	.01393	42.2	.06	500.0	267.6	326.2	268.17	68.6	262.8	.0033	7.2	115.4	3.1	-6.5
24.0	5973	19.5	.01418	42.3	.07	492.0	266.7	326.5	267.26	67.9	261.8	.0032	6.4	113.0	2.5	-5.9
25.0	6230	19.8	.01469	43.1	.07	476.0	265.0	327.6	265.43	67.6	260.0	.0029	5.6	112.6	2.1	-5.1
26.0	6495	19.0	.01521	41.5	.07	460.0	263.8	329.3	264.25	70.0	259.3	.0028	5.1	108.8	1.6	-4.9
27.0	6820	19.7	.01586	43.4	.07	441.0	262.5	331.7	262.86	58.8	256.0	.0022	4.8	97.2	.6	-4.7
28.0	7103	19.1	.01642	42.2	.07	425.0	260.8	333.0	261.11	57.4	254.1	.0020	5.4	98.8	.8	-5.3
29.0	7432	17.9	.01705	39.9	.07	407.0	258.6	334.3	258.80	51.8	250.8	.0016	2.2	88.0	-.1	-2.2
29.4	7562	18.4	.01731	41.2	.08	400.0	257.7	334.8	257.93	48.9	249.4	.0013	1.7	79.3	-.3	-1.7
30.0	7773	19.2	.01771	43.3	.08	389.0	256.3	335.7	256.53	44.3	247.1	.0012	1.2	52.5	-.7	-.9
31.0	8107	19.6	.01840	44.5	.09	372.0	254.2	337.1	254.33	47.0	245.7	.0011	4.0	88.4	-.1	-4.0
32.0	8412	19.6	.01903	45.0	.09	357.0	251.7	337.9	251.89	52.8	244.7	.0010	4.9	61.5	-2.3	-4.3
32.5	8557	19.0	.01933	43.6	.09	350.0	250.9	338.7	251.09	53.9	244.2	.0010	4.5	63.1	-2.1	-4.1
33.0	8706	18.3	.01963	42.3	.09	343.0	250.1	339.6	250.28	55.1	243.6	.0010	4.2	65.1	-1.8	-3.8
34.0	8988	17.1	.02017	39.7	.09	330.0	248.4	341.0	248.51	46.9	240.4	.0007	.7	190.6	.6	.1
35.0	9256	16.5	.02066	38.6	.09	318.0	246.7	342.2	246.82	70.9	243.0	.0010	.7	190.1	.7	.1
36.0	9579	16.5	.02125	38.9	.09	304.0	244.2	343.1	244.21	32.6	232.9	.0004	1.0	252.5	.3	.9
36.3	9673	16.7	.02142	39.5	.09	300.0	243.7	343.8	243.76	22.2	223.0	.0002	2.4	258.8	.5	2.3
37.0	9866	17.1	.02178	40.8	.10	292.0	242.8	345.2	242.83	0.0	0.0	0.0000	5.3	261.2	.8	5.2
38.0	10162	18.6	.02237	44.7	.11	280.0	240.2	345.5	240.23	41.6	231.6	.0003	6.2	281.9	-1.3	6.0
39.0	10442	18.1	.02295	43.8	.11	269.0	238.0	346.4	238.07	39.6	229.2	.0003	5.8	290.6	-2.0	5.4
40.0	10758	17.3	.02359	42.4	.11	257.0	235.6	347.4	235.64	40.6	227.2	.0002	4.6	267.9	.2	4.6
40.5	10947	17.2	.02397	42.5	.11	250.0	234.1	347.8	234.09	0.0	0.0	0.0000	6.7	269.6	0.0	6.7
41.0	11114	17.2	.02430	42.6	.12	244.0	232.7	348.2	232.73	0.0	0.0	0.0000	8.5	270.4	-.1	8.5
42.0	11426	15.7	.02490	39.5	.11	233.0	230.1	348.8	230.08	0.0	0.0	0.0000	8.7	271.8	-.3	8.7
43.0	11749	16.4	.02551	41.6	.12	222.0	227.2	349.3	227.21	0.0	0.0	0.0000	5.0	265.7	.4	5.0
44.0	12085	12.3	.02608	31.5	.10	211.0	224.6	350.3	224.56	0.0	0.0	0.0000	5.1	259.0	1.0	5.0
45.0	12401	12.3	.02655	32.2	.10	201.0	219.9	347.8	219.93	0.0	0.0	0.0000	5.0	253.1	1.5	4.8
45.1	12432	12.4	.02660	32.6	.10	200.0	219.7	348.0	219.75	0.0	0.0	0.0000	5.0	252.6	1.5	4.8
46.0	12761	13.9	.02713	36.8	.12	190.0	217.8	350.1	217.82	0.0	0.0	0.0000	4.5	247.6	1.7	4.2
47.0	13103	13.1	.02771	35.3	.12	180.0	214.8	350.6	214.77	0.0	0.0	0.0000	4.7	255.9	1.1	4.5
48.0	13459	11.8	.02827	32.2	.11	170.0	211.5	351.0	211.54	0.0	0.0	0.0000	5.3	269.0	.1	5.3
49.0	13832	11.8	.02884	32.6	.12	160.0	209.1	352.9	209.06	0.0	0.0	0.0000	6.2	274.8	-.5	6.2
50.0	14143	12.5	.02933	35.0	.14	152.0	205.4	351.8	205.37	0.0	0.0	0.0000	6.6	283.4	-1.5	6.4
50.2	14221	11.6	.02944	32.6	.13	150.0	204.8	352.2	204.84	0.0	0.0	0.0000	6.4	284.3	-1.6	6.2
51.0	14507	8.3	.02983	23.7	.10	143.0	202.9	353.8	202.94	0.0	0.0	0.0000	6.1	287.9	-1.9	5.8
52.0	14934	9.5	.03034	27.5	.12	133.0	200.1	356.1	200.10	0.0	0.0	0.0000	5.8	276.5	-.7	5.7
52.8	15294	10.6	.03084	30.9	.14	125.0	197.4	357.6	197.43	0.0	0.0	0.0000	5.5	265.6	.4	5.5
53.0	15388	10.8	.03097	31.8	.15	123.0	196.7	358.0	196.73	0.0	0.0	0.0000	5.5	262.7	.7	5.5
54.0	15624	8.8	.03129	26.4	.12	118.0	193.0	355.4	192.98	0.0	0.0	0.0000	3.7	245.3	1.5	3.3
55.0	15969	10.4	.03175	31.1	.16	111.0	193.3	362.2	193.28	0.0	0.0	0.0000	2.3	122.8	1.2	-1.9
56.0	16341	8.5	.03224	24.7	.13	104.0	197.5	377.1	197.54	0.0	0.0	0.0000	7.1	82.2	-1.0	-7.0
56.8	16566	12.1	.03257	35.5	.20	100.0	196.2	378.9	196.24	0.0	0.0	0.0000	7.9	77.3	-1.7	-7.7
57.0	16624	13.0	.03266	38.3	.22	99.0	195.9	379.3	195.91	0.0	0.0	0.0000	8.1	76.2	-1.9	-7.9
58.0	17052	14.2	.03345	41.5	.26	91.9	197.3	390.2	197.27	0.0	0.0	0.0000	4.3	71.7	-1.3	-4.1
59.0	17438	20.2	.03435	58.3	.39	86.0	200.1	403.3	200.10	0.0	0.0	0.0000	2.7	327.7	-2.3	1.4
60.0	17847	26.2	.03563	75.6	.54	80.2	200.3	412.0	200.34	0.0	0.0	0.0000	2.5	41.7	-1.8	-1.6
60.0	17861	26.5	.03569	76.4	.55	80.0	200.4	412.3	200.35	0.0	0.0	0.0000	2.6	48.4	-1.7	-1.9
61.0	18178	32.5	.03694	93.6	.71	75.8	200.6	419.2	200.59	0.0	0.0	0.0000	8.1	98.3	1.2	-8.0
62.0	18546	33.6	.03858	96.1	.78	71.2	201.8	429.3	201.78	0.0	0.0	0.0000	5.6	132.8	3.8	-4.1
62.3	18647	36.7	.03911	104.5	.87	70.0	202.6	433.3	202.64	0.0	0.0	0.0000	5.3	139.2	4.0	-3.5
63.0	18944	45.9	.04067	129.1	1.14	66.6	205.2	444.9	205.16	0.0	0.0	0.0000	4.9	161.0	4.7	-1.6
64.0	19278	51.5	.04280	144.3	1.35	63.0	206.0	453.9	206.01	0.0	0.0	0.0000	5.9	127.4	3.6	-4.7
64.8	19574	59.4	.04499	164.2	1.64	60.0	208.6	466.1	208.63	0.0	0.0	0.0000	9.4	122.0	5.0	-8.0

TIME MIN	ALT GPM	OZONE MICMB	TOTOZ ATMCM	OZDEN MG/M3	OZMXR MICGG	PRESS MB	TEMP DEG K	PTEMP DEG K	VTEMP DEG K	HMDTY PRCNT	DEWPT DEG K	SPCFC HMDTY	SPD MPS	DIR DEG	NS MPS	EW MPS
65.0	19666	61.8	.04566	170.4	1.73	59.1	209.4	469.9	209.45	0.0	0.0	0.0000	10.5	121.0	5.4	-9.0
66.0	20077	75.3	.04926	204.0	2.26	55.3	213.0	487.1	213.00	0.0	0.0	0.0000	10.6	129.3	6.7	-8.2
67.0	20460	84.2	.05313	228.5	2.68	52.0	212.8	495.3	212.82	0.0	0.0	0.0000	6.4	130.8	4.2	-4.8
67.6	20705	89.8	.05587	242.0	2.98	50.0	214.2	504.1	214.18	0.0	0.0	0.0000	6.5	127.2	3.9	-5.2
68.0	20845	92.9	.05742	249.7	3.15	48.9	214.9	509.1	214.95	0.0	0.0	0.0000	6.5	125.2	3.8	-5.3
69.0	21257	101.6	.06245	272.8	3.67	45.8	214.9	518.7	214.95	0.0	0.0	0.0000	4.1	137.7	3.0	-2.8
70.0	21712	106.7	.06840	286.8	4.15	42.6	214.8	529.1	214.77	0.0	0.0	0.0000	2.3	150.7	2.0	-1.1
70.9	22106	109.9	.07379	296.5	4.56	40.0	214.1	537.1	214.12	0.0	0.0	0.0000	3.3	141.7	2.6	-2.0
71.0	22138	110.2	.07422	297.2	4.59	39.8	214.1	537.8	214.07	0.0	0.0	0.0000	3.4	141.2	2.6	-2.1
72.0	22577	117.4	.08053	317.4	5.24	37.1	213.5	547.3	213.54	0.0	0.0	0.0000	3.4	129.6	2.1	-2.6
72.9	22942	119.0	.08596	320.3	5.63	35.0	214.5	558.9	214.46	0.0	0.0	0.0000	3.4	175.6	3.4	-.3
73.0	22996	119.2	.08677	320.7	5.69	34.7	214.6	560.6	214.60	0.0	0.0	0.0000	3.5	181.4	3.5	.1
74.0	23426	122.2	.09330	329.6	6.25	32.4	214.1	570.3	214.07	0.0	0.0	0.0000	2.7	202.7	2.5	1.1
75.0	23887	125.8	.10050	339.0	6.93	30.1	214.2	582.9	214.22	0.0	0.0	0.0000	5.0	81.3	-.8	-4.9
75.1	23907	126.0	.10084	339.4	6.96	30.0	214.3	583.6	214.29	0.0	0.0	0.0000	4.9	85.6	-.4	-4.9
76.0	24296	128.9	.10706	346.0	7.58	28.2	215.1	596.3	215.12	0.0	0.0	0.0000	7.8	148.8	6.7	-4.1
77.0	24643	134.4	.11274	354.9	8.34	26.7	218.6	615.6	218.64	0.0	0.0	0.0000	5.8	112.3	2.2	-5.3
77.9	25064	141.3	.11990	371.7	9.37	25.0	219.6	629.9	219.56	0.0	0.0	0.0000	10.3	51.2	-6.4	-8.0
78.0	25090	141.8	.12034	372.7	9.43	24.9	219.6	630.8	219.61	0.0	0.0	0.0000	10.7	49.5	-7.0	-8.2
79.0	25518	146.5	.12789	382.0	10.42	23.3	221.4	648.0	221.35	0.0	0.0	0.0000	3.7	58.7	-1.9	-3.2
80.0	25921	150.2	.13515	389.1	11.37	21.9	222.9	664.1	222.90	0.0	0.0	0.0000	5.3	86.8	-.3	-5.3
81.0	26450	153.4	.14483	394.1	12.58	20.2	224.7	685.2	224.71	0.0	0.0	0.0000	8.3	103.7	2.0	-8.1
81.1	26515	152.4	.14600	391.4	12.63	20.0	224.8	687.5	224.82	0.0	0.0	0.0000	8.4	104.9	2.2	-8.1
82.0	26888	146.9	.15271	376.2	12.88	18.9	225.5	700.6	225.45	0.0	0.0	0.0000	9.0	111.5	3.3	-8.4
82.9	27396	145.6	.16158	371.4	13.79	17.5	226.4	719.1	226.35	0.0	0.0	0.0000	10.5	97.2	1.3	-10.4
83.0	27473	145.4	.16291	370.7	13.93	17.3	226.5	721.9	226.49	0.0	0.0	0.0000	10.8	95.5	1.0	-10.7
84.0	27949	140.6	.17102	359.4	14.47	16.1	225.9	734.9	225.90	0.0	0.0	0.0000	12.4	96.9	1.5	-12.3
84.8	28418	135.4	.17870	344.3	14.95	15.0	227.0	753.7	227.00	0.0	0.0	0.0000	12.2	99.2	1.9	-12.0
85.0	28507	134.4	.18015	341.5	15.04	14.8	227.2	757.2	227.21	0.0	0.0	0.0000	12.2	99.6	2.0	-12.0
86.0	29118	129.1	.18971	328.3	15.85	13.5	227.1	776.9	227.07	0.0	0.0	0.0000	10.0	97.3	1.3	-9.9
86.8	29628	123.0	.19731	313.0	16.30	12.5	226.8	793.4	226.85	0.0	0.0	0.0000	11.6	86.6	-.7	-11.5
87.0	29790	121.0	.19971	308.2	16.44	12.2	226.8	798.6	226.78	0.0	0.0	0.0000	12.1	83.9	-1.3	-12.0
88.0	30356	111.7	.20756	285.8	16.52	11.2	225.6	814.2	225.60	0.0	0.0	0.0000	17.7	71.3	-5.7	-16.8
89.0	31039	101.7	.21626	260.2	16.68	10.1	225.6	838.6	225.60	0.0	0.0	0.0000	15.1	76.1	-3.6	-14.6
89.1	31104	100.7	.21703	257.7	16.68	10.0	225.7	841.3	225.69	0.0	0.0	0.0000	15.1	78.7	-3.0	-14.8
90.0	31585	93.8	.22262	239.3	16.71	9.3	226.3	861.4	226.34	0.0	0.0	0.0000	16.4	96.3	1.8	-16.3
91.0	32184	87.6	.22906	221.2	17.08	8.5	228.7	892.8	228.65	0.0	0.0	0.0000	23.1	99.4	3.8	-22.8
91.6	32592	82.7	.23306	207.3	17.11	8.0	230.5	915.8	230.47	0.0	0.0	0.0000	25.2	96.5	2.8	-25.0
92.0	32850	79.6	.23558	198.5	17.13	7.7	231.6	930.3	231.62	0.0	0.0	0.0000	26.5	94.9	2.2	-26.4
93.0	33403	71.2	.24041	175.6	16.61	7.1	234.1	962.4	234.10	0.0	0.0	0.0000	28.8	89.1	-.5	-28.8
93.1	33500	70.0	.24116	172.7	16.56	7.0	234.1	966.2	234.09	0.0	0.0	0.0000	28.7	88.1	-1.0	-28.7
94.0	34114	62.7	.24589	154.7	16.23	6.4	234.0	990.7	233.97	0.0	0.0	0.0000	28.7	81.6	-4.2	-28.4
94.7	34555	57.6	.24888	142.2	15.87	6.0	233.7	1008.1	233.70	0.0	0.0	0.0000	28.7	82.1	-3.9	-28.4
95.0	34787	54.9	.25045	135.7	15.68	5.8	233.6	1017.2	233.56	0.0	0.0	0.0000	28.7	82.4	-3.8	-28.4
96.0	35663	47.3	.25564	117.8	15.35	5.1	231.6	1046.5	231.62	0.0	0.0	0.0000	30.2	82.8	-3.8	-29.9
96.2	35797	46.0	.25634	114.6	15.22	5.0	231.6	1052.2	231.55	0.0	0.0	0.0000	31.4	81.9	-4.4	-31.1
97.0	36216	42.0	.25851	104.7	14.80	4.7	231.3	1070.0	231.34	0.0	0.0	0.0000	35.4	79.4	-6.5	-34.8
98.0	36978	35.7	.26196	89.0	14.08	4.2	231.5	1105.6	231.48	0.0	0.0	0.0000	39.2	89.1	-.6	-39.2
98.5	37309	32.8	.26322	81.5	13.53	4.0	232.2	1124.9	232.22	0.0	0.0	0.0000	999.9	999.9	999.9	999.9
99.0	37658	29.7	.26454	73.6	12.95	3.8	233.0	1145.1	233.01	0.0	0.0	0.0000	999.9	999.9	999.9	999.9

INTEGRAL .26454 RESIDUAL .02344 INTEGRATED TOTAL OZONE .28799

OZONAGRAM

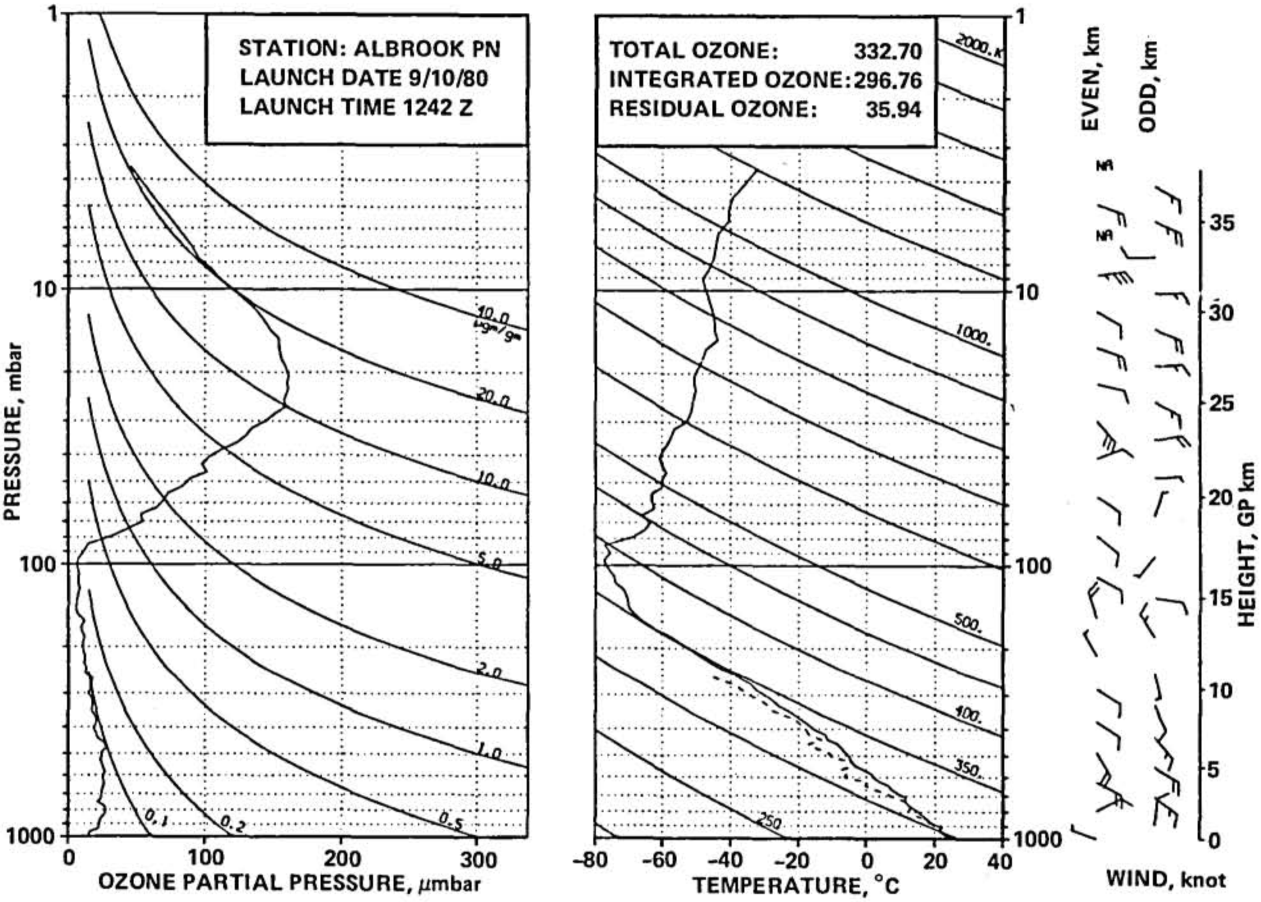
STATION: ALBROOK PN
LAUNCH DATE 9/10/80
LAUNCH TIME 1242 Z
TOTAL OZONE: 332.70
INTEGRATED OZONE: 296.76
RESIDUAL OZONE: 35.94
PRESSURE, mbar
OZONE PARTIAL PRESSURE, μmbar
TEMPERATURE, °C
WIND, knot
HEIGHT, GP km
EVEN, km
ODD, km

STATION ALBROOK PN   LAUNCH DATE 9/10/80   TIME 1242Z   ECC   SONDE 3A1333

SURFACE CONDITIONS   PRESS 1003.8MB   TEMP 297.8 DEG K   HUMIDITY 100.0 PRCNT

TIME MIN	ALT GPM	OZONE MICMB	TOTOZ ATMCM	OZDEN MG/M3	OZMXR MICGG	PRESS MB	TEMP DEG K	PTEMP DEG K	VTEMP DEG K	HMDTY PRCNT	DEWPT DEG K	SPCFC HMDTY	SPD MPS	DIR DEG	NS MPS	EW MPS
0.0	66	16.8	0.00000	32.5	.03	1003.8	298.0	297.7	301.59	100.0	298.0	.0197	3.0	290.0	-1.0	2.8
.2	99	16.5	.00005	32.0	.03	1000.0	297.8	297.8	301.36	100.0	297.8	.0194	2.9	291.2	-1.1	2.7
1.0	259	15.2	.00028	29.5	.03	982.0	296.9	298.4	300.25	100.0	296.9	.0187	2.5	297.7	-1.2	2.3
2.0	457	16.4	.00056	32.1	.03	960.0	295.3	298.7	298.41	100.0	295.3	.0174	1.5	339.4	-1.4	.5
3.0	678	22.4	.00095	43.9	.04	936.0	294.6	300.2	297.69	100.0	294.6	.0171	2.8	354.9	-2.8	.2
4.0	914	22.9	.00143	44.9	.04	911.0	295.3	303.2	298.58	100.0	295.3	.0183	3.8	2.0	-3.8	-.1
4.5	1019	23.2	.00165	45.6	.04	900.0	294.1	303.1	297.18	100.0	294.1	.0167	4.0	4.5	-4.0	-.3
5.0	1126	23.5	.00188	46.3	.04	889.0	292.9	302.9	295.76	100.0	292.9	.0162	4.3	6.7	-4.3	-.5
6.0	1362	23.7	.00239	46.9	.05	865.0	291.6	303.9	294.18	94.4	290.7	.0145	4.7	12.7	-4.6	-1.0
6.6	1511	25.2	.00273	50.0	.05	850.0	290.8	304.6	293.26	93.7	289.8	.0137	4.6	24.1	-4.2	-1.9
7.0	1593	26.0	.00292	51.6	.05	842.0	290.3	305.0	292.76	93.3	289.2	.0136	4.6	30.3	-4.0	-2.3
8.0	1819	26.8	.00347	53.5	.05	820.0	289.3	306.2	291.50	87.4	287.2	.0123	4.6	49.9	-3.0	-3.5
8.9	2029	27.4	.00400	54.8	.06	800.0	288.3	307.3	290.28	84.0	285.6	.0112	4.8	60.7	-2.3	-4.2
9.0	2061	27.4	.00408	55.0	.06	797.0	288.1	307.4	290.09	83.5	285.4	.0111	4.8	62.3	-2.3	-4.3
10.0	2320	26.1	.00472	52.6	.06	773.0	286.4	308.2	288.51	99.8	286.3	.0123	4.6	85.4	-.4	-4.6
11.0	2574	21.5	.00529	43.5	.05	750.0	285.2	309.7	287.27	100.0	285.2	.0117	4.9	121.0	2.5	-4.2
12.0	2801	23.9	.00577	48.5	.05	730.0	284.5	311.2	286.46	100.0	284.5	.0115	6.0	136.0	4.3	-4.2
13.0	3057	24.3	.00636	49.4	.06	708.0	284.7	314.2	286.29	78.7	281.1	.0094	6.4	127.3	3.9	-5.1
13.3	3151	24.4	.00657	49.7	.06	700.0	283.8	314.3	285.41	79.4	280.4	.0089	6.8	124.0	3.8	-5.7
14.0	3332	24.5	.00699	50.2	.06	685.0	282.3	314.5	283.72	80.7	279.1	.0085	7.8	118.8	3.7	-6.8
15.0	3602	25.6	.00764	52.7	.06	663.0	280.5	315.4	281.62	70.1	275.4	.0067	9.2	120.6	4.7	-7.9
16.0	3854	26.2	.00827	54.1	.07	643.0	279.6	317.2	280.59	62.3	272.9	.0058	9.3	119.6	4.6	-8.1
17.0	4125	25.6	.00894	53.4	.07	622.0	277.0	317.3	278.08	77.1	273.4	.0062	9.1	116.9	4.1	-8.1
18.0	4390	25.5	.00960	53.7	.07	602.0	275.5	318.5	276.19	53.1	266.9	.0040	9.8	121.9	5.2	-8.3
18.1	4416	25.8	.00967	54.0	.07	600.0	275.4	318.7	276.11	53.5	267.0	.0040	9.9	122.1	5.2	-8.4
19.0	4662	27.1	.01031	57.0	.08	582.0	274.7	320.6	275.41	57.8	267.3	.0042	10.3	123.3	5.7	-8.6
20.0	4914	25.7	.01096	54.4	.08	564.0	272.4	320.9	273.09	60.5	265.8	.0039	9.6	120.0	4.8	-8.4
21.0	5172	24.8	.01161	53.1	.08	546.0	270.1	321.1	271.02	100.0	270.1	.0056	9.1	121.0	4.7	-7.8
22.0	5452	23.7	.01229	50.9	.07	527.0	268.6	322.5	269.41	100.0	268.6	.0051	9.6	134.4	6.7	-6.9
23.0	5741	24.9	.01299	53.7	.08	508.0	268.3	325.5	268.83	67.0	263.1	.0035	10.4	146.7	8.7	-5.7
23.4	5865	25.0	.01330	53.8	.08	500.0	267.8	326.5	268.36	67.2	262.7	.0034	10.3	148.2	8.7	-5.4
24.0	6024	25.0	.01370	53.9	.08	490.0	267.2	327.6	267.76	67.5	262.2	.0034	10.1	150.2	8.8	-5.0
25.0	6300	28.8	.01445	62.5	.10	473.0	266.0	329.5	266.45	56.9	258.9	.0027	10.9	148.0	9.3	-5.8
26.0	6601	26.0	.01529	56.7	.09	455.0	264.7	331.5	265.05	49.8	256.1	.0022	9.4	143.3	7.6	-5.6
27.0	6895	21.9	.01601	48.3	.08	438.0	261.7	331.3	262.17	87.6	260.0	.0032	7.2	142.8	5.8	-4.4
28.0	7216	20.8	.01672	45.9	.08	420.0	261.1	334.5	261.48	67.0	256.2	.0024	5.9	136.6	4.3	-4.0
29.0	7530	18.9	.01736	42.4	.08	403.0	258.0	334.5	258.39	81.2	255.5	.0024	4.7	118.6	2.2	-4.1
29.2	7586	19.3	.01748	43.3	.08	400.0	257.7	334.8	258.06	81.5	255.2	.0023	4.7	118.3	2.2	-4.1
30.0	7816	20.7	.01796	46.7	.09	388.0	256.4	336.0	256.71	82.8	254.1	.0022	4.7	117.3	2.1	-4.1
31.0	8151	21.0	.01870	47.7	.09	371.0	254.3	337.6	254.63	85.9	252.6	.0020	4.5	127.0	2.7	-3.6
32.0	8457	19.2	.01935	44.0	.09	356.0	252.4	339.1	252.68	78.2	249.6	.0016	4.3	137.8	3.2	-2.9
32.4	8582	18.4	.01960	42.3	.09	350.0	251.5	339.4	251.70	73.2	248.0	.0013	4.4	144.5	3.6	-2.5
33.0	8774	17.2	.01997	39.8	.08	341.0	250.0	340.0	250.20	65.6	245.4	.0011	4.6	154.2	4.1	-2.0
34.0	9035	17.9	.02047	41.8	.09	329.0	247.4	339.9	247.53	75.3	244.3	.0011	5.1	156.2	4.6	-2.0
35.0	9372	17.9	.02113	42.1	.09	314.0	245.5	341.8	245.66	73.1	242.2	.0009	5.2	148.0	4.4	-2.7
36.0	9698	14.6	.02171	34.6	.08	300.0	243.3	343.2	243.37	64.3	238.7	.0007	4.6	139.8	3.5	-2.9
37.0	9987	16.6	.02221	39.8	.10	288.0	240.9	343.8	240.97	64.5	236.5	.0006	4.6	126.0	2.7	-3.7
38.0	10311	16.9	.02282	40.7	.10	275.0	239.3	346.0	239.36	61.2	234.4	.0005	5.5	113.7	2.2	-5.0
39.0	10622	17.9	.02344	43.7	.11	263.0	236.8	346.8	236.80	50.0	230.1	.0003	6.2	104.9	1.6	-6.0
40.0	10971	12.3	.02404	30.4	.08	250.0	234.5	348.4	234.49	44.0	226.8	.0002	2.6	68.8	-.9	-2.4
41.0	11249	13.7	.02446	34.1	.09	240.0	231.0	347.3	231.01	0.0	0.0	0.0000	3.0	359.0	-3.0	.1
42.0	11593	11.9	.02498	30.2	.09	228.0	227.9	347.7	227.90	0.0	0.0	0.0000	3.3	7.3	-3.3	-.4
43.0	11920	12.6	.02546	32.4	.10	217.0	225.0	348.1	224.99	0.0	0.0	0.0000	3.6	337.3	-3.3	1.4
44.0	12260	11.1	.02594	28.9	.09	206.0	222.3	349.1	222.28	0.0	0.0	0.0000	3.4	322.6	-2.7	2.0
44.5	12450	10.9	.02620	28.5	.09	200.0	220.7	349.6	220.74	0.0	0.0	0.0000	3.8	323.5	-3.0	2.2
45.0	12647	10.7	.02646	28.1	.09	194.0	219.2	350.1	219.15	0.0	0.0	0.0000	4.2	324.2	-3.4	2.4
46.0	13019	12.1	.02699	32.4	.11	183.0	216.2	351.2	216.19	0.0	0.0	0.0000	7.1	327.3	-6.0	3.8
47.0	13300	10.3	.02738	27.8	.10	175.0	213.3	350.9	213.25	0.0	0.0	0.0000	8.5	332.4	-7.6	4.0
48.0	13553	9.7	.02770	26.6	.10	168.0	210.1	349.8	210.13	0.0	0.0	0.0000	8.9	330.4	-7.7	4.4
49.0	13851	12.2	.02812	34.0	.13	160.0	207.4	350.1	207.39	0.0	0.0	0.0000	9.1	331.5	-8.0	4.4
50.0	14240	6.6	.02860	18.6	.07	150.0	204.9	352.3	204.89	0.0	0.0	0.0000	11.4	349.5	-11.2	2.1
51.0	14609	5.9	.02891	16.9	.07	141.0	202.9	355.1	202.90	0.0	0.0	0.0000	9.1	6.1	-9.0	-1.0
52.0	15000	6.5	.02923	18.6	.08	132.0	202.7	361.5	202.68	0.0	0.0	0.0000	3.8	85.9	-.3	-3.7
52.7	15322	7.8	.02955	22.4	.10	125.0	201.9	365.7	201.88	0.0	0.0	0.0000	4.2	144.6	3.4	-2.4
53.0	15466	8.4	.02970	24.0	.11	122.0	201.5	367.6	201.52	0.0	0.0	0.0000	5.4	160.1	5.0	-1.8
54.0	15761	7.1	.03000	20.5	.10	116.0	199.1	368.4	199.09	0.0	0.0	0.0000	4.8	166.6	4.7	-1.1
55.0	16123	7.9	.03037	23.1	.12	109.0	198.6	374.1	198.59	0.0	0.0	0.0000	4.6	109.2	1.5	-4.4
56.0	16564	6.7	.03081	19.7	.11	101.0	196.5	378.3	196.48	0.0	0.0	0.0000	3.3	94.7	.3	-3.3
56.2	16621	6.8	.03087	20.1	.11	100.0	196.3	379.0	196.33	0.0	0.0	0.0000	2.5	102.1	.5	-2.5
57.0	16867	7.3	.03111	21.6	.13	95.8	195.7	382.4	195.66	0.0	0.0	0.0000	2.0	217.2	1.6	1.2
58.0	17226	11.5	.03157	33.7	.21	90.0	197.6	393.1	197.55	0.0	0.0	0.0000	3.7	219.4	2.9	2.4
59.0	17596	14.9	.03224	43.9	.29	84.4	195.9	397.1	195.93	0.0	0.0	0.0000	4.8	171.0	4.7	-.7
59.8	17909	29.6	.03325	83.8	.62	80.0	202.8	417.5	202.83	0.0	0.0	0.0000	5.0	153.3	4.5	-2.3
60.0	17983	33.0	.03349	93.2	.69	79.0	204.5	422.2	204.46	0.0	0.0	0.0000	5.2	149.5	4.4	-2.6
61.0	18320	43.1	.03517	119.9	.96	74.7	207.8	436.0	207.79	0.0	0.0	0.0000	1.3	67.4	-.5	-1.2
62.0	18691	54.2	.03750	149.3	1.28	70.3	209.6	447.4	209.55	0.0	0.0	0.0000	3.2	23.1	-2.9	-1.3
62.1	18717	54.1	.03769	149.3	1.28	70.0	209.4	447.6	209.38	0.0	0.0	0.0000	3.1	22.7	-2.9	-1.2
63.0	19076	53.4	.04018	148.8	1.34	66.0	207.0	450.0	206.98	0.0	0.0	0.0000	2.3	15.9	-2.2	-.6
64.0	19438	64.7	.04294	177.1	1.72	62.2	210.9	466.3	210.88	0.0	0.0	0.0000	2.4	39.3	-1.9	-1.5
64.6	19659	67.5	.04484	185.2	1.87	60.0	210.3	469.8	210.28	0.0	0.0	0.0000	3.5	76.1	-.8	-3.4
65.0	19784	69.0	.04591	189.8	1.94	58.8	209.9	471.7	209.94	0.0	0.0	0.0000	4.4	86.7	-.3	-4.4
66.0	20183	72.6	.04954	199.6	2.18	55.1	209.9	480.6	209.94	0.0	0.0	0.0000	3.9	139.4	3.0	-2.5
67.0	20553	83.1	.05321	225.3	2.65	51.9	212.9	495.7	212.89	0.0	0.0	0.0000	3.4	142.8	2.7	-2.1

TIME MIN	ALT GPM	OZONE MICMB	TOTOZ ATMCM	OZDEN MG/M3	OZMXR MICGG	PRESS MB	TEMP DEG K	PTEMP DEG K	VTEMP DEG K	HMDTY PRCNT	DEWPT DEG K	SPCFC HMDTY	SPD MPS	DIR DEG	NS MPS	EW MPS
67.6	20785	86.6	.05575	234.7	2.87	50.0	213.0	501.3	213.00	0.0	0.0	0.0000	2.9	120.4	1.5	-2.5
68.0	20949	89.1	.05754	241.4	3.03	48.7	213.1	505.3	213.07	0.0	0.0	0.0000	2.9	102.4	.6	-2.9
69.0	21305	101.3	.06182	272.8	3.65	46.0	214.3	516.5	214.31	0.0	0.0	0.0000	1.7	52.0	-1.1	-1.4
70.0	21698	98.0	.06676	265.4	3.76	43.2	213.1	522.9	213.07	0.0	0.0	0.0000	2.5	40.0	-1.9	-1.6
71.0	22069	103.3	.07149	280.9	4.21	40.7	212.4	530.1	212.35	0.0	0.0	0.0000	3.9	69.3	-1.4	-3.6
71.3	22176	105.9	.07297	287.6	4.39	40.0	212.6	533.4	212.61	0.0	0.0	0.0000	4.4	67.8	-1.7	-4.0
72.0	22447	112.5	.07666	304.5	4.87	38.3	213.3	541.6	213.25	0.0	0.0	0.0000	5.7	65.2	-2.4	-5.1
73.0	22835	124.1	.08244	333.4	5.71	36.0	214.8	555.4	214.83	0.0	0.0	0.0000	9.5	67.0	-3.7	-8.8
73.4	23012	127.1	.08528	340.9	6.03	35.0	215.3	561.1	215.29	0.0	0.0	0.0000	11.0	78.0	-2.3	-10.8
74.0	23232	130.9	.08879	350.2	6.42	33.8	215.9	568.2	215.86	0.0	0.0	0.0000	13.3	87.7	-.5	-13.3
75.0	23638	135.4	.09553	360.5	7.08	31.7	216.9	581.4	216.86	0.0	0.0	0.0000	16.4	119.7	8.1	-14.2
76.0	23990	144.6	.10162	378.7	7.98	30.0	220.4	600.3	220.42	0.0	0.0	0.0000	15.8	136.7	11.5	-10.8
77.0	24390	151.9	.10885	395.9	8.92	28.2	221.5	614.0	221.51	0.0	0.0	0.0000	8.3	149.3	7.2	-4.3
78.0	24769	159.6	.11603	414.8	9.94	26.6	222.1	626.1	222.13	0.0	0.0	0.0000	4.6	140.8	3.6	-2.9
78.9	25171	158.6	.12382	412.1	10.52	25.0	222.3	637.7	222.28	0.0	0.0	0.0000	7.9	107.4	2.4	-7.6
79.0	25198	158.6	.12432	411.9	10.55	24.9	222.3	638.5	222.28	0.0	0.0	0.0000	8.2	106.2	2.3	-7.9
80.0	25687	161.2	.13379	417.3	11.56	23.1	223.0	654.5	223.05	0.0	0.0	0.0000	7.4	109.6	2.5	-7.0
81.0	26035	160.6	.14056	416.6	12.15	21.9	222.6	663.2	222.59	0.0	0.0	0.0000	4.6	105.1	1.2	-4.4
82.0	26465	161.5	.14896	418.8	13.05	20.5	222.6	675.9	222.59	0.0	0.0	0.0000	6.6	85.3	-.5	-6.6
82.3	26626	160.8	.15209	416.4	13.33	20.0	223.0	682.0	223.01	0.0	0.0	0.0000	7.2	84.5	-.7	-7.2
83.0	26927	159.6	.15792	411.9	13.85	19.1	223.8	693.4	223.80	0.0	0.0	0.0000	8.3	83.3	-1.0	-8.2
84.0	27390	156.5	.16671	401.6	14.57	17.8	225.0	711.3	224.99	0.0	0.0	0.0000	9.9	93.9	.7	-9.9
84.2	27502	156.2	.16880	400.4	14.79	17.5	225.2	715.5	225.21	0.0	0.0	0.0000	10.0	96.6	1.2	-10.0
85.0	27931	155.0	.17678	395.9	15.66	16.4	226.0	731.5	226.02	0.0	0.0	0.0000	10.7	106.0	3.0	-10.3
86.0	28481	154.9	.18687	389.6	16.99	15.1	229.5	760.4	229.47	0.0	0.0	0.0000	9.3	119.7	4.6	-8.1
86.1	28525	154.3	.18767	388.3	17.04	15.0	229.4	761.6	229.39	0.0	0.0	0.0000	9.4	119.1	4.6	-8.2
87.0	28908	148.5	.19593	375.0	17.57	14.0	228.6	774.1	228.62	0.0	0.0	0.0000	10.0	113.2	3.9	-9.2
88.0	29484	144.4	.20449	364.8	18.41	13.0	228.6	790.7	228.62	0.0	0.0	0.0000	10.0	103.5	2.3	-9.7
88.4	29746	141.8	.20887	358.5	18.80	12.5	228.4	798.7	228.37	0.0	0.0	0.0000	7.9	108.6	2.5	-7.4
89.0	30075	138.5	.21436	350.6	19.28	11.9	228.0	808.9	228.05	0.0	0.0	0.0000	5.4	120.5	2.7	-4.6
90.0	30721	128.6	.22458	327.2	19.74	10.8	227.0	827.9	227.04	0.0	0.0	0.0000	4.5	119.3	2.2	-4.0
91.0	31231	119.5	.23212	305.6	19.81	10.0	225.9	842.0	225.88	0.0	0.0	0.0000	9.8	73.2	-2.8	-9.3
92.0	31853	110.5	.24068	283.3	20.11	9.1	225.1	862.2	225.14	0.0	0.0	0.0000	17.5	66.2	-7.1	-16.0
93.0	32382	104.5	.24747	266.2	20.62	8.4	226.8	888.4	226.75	0.0	0.0	0.0000	999.9	999.9	999.9	999.9
93.6	32706	99.3	.25131	251.9	20.54	8.0	227.6	904.2	227.56	0.0	0.0	0.0000	999.9	999.9	999.9	999.9
94.0	32961	95.1	.25432	240.7	20.47	7.7	228.2	916.6	228.19	0.0	0.0	0.0000	4.9	124.8	2.8	-4.0
95.0	33598	90.3	.26129	228.0	21.38	7.0	228.8	944.2	228.76	0.0	0.0	0.0000	999.9	999.9	999.9	999.9
96.0	34412	82.1	.26955	206.5	21.95	6.2	229.6	981.2	229.61	0.0	0.0	0.0000	12.5	118.5	5.9	-11.0
96.3	34633	79.9	.27159	200.1	22.05	6.0	230.6	994.8	230.60	0.0	0.0	0.0000	12.5	116.7	5.6	-11.2
97.0	35101	75.2	.27587	196.7	22.26	5.6	232.7	1023.6	232.67	0.0	0.0	0.0000	12.7	112.9	4.9	-11.7
98.0	35738	68.7	.28118	170.4	22.32	5.1	232.7	1051.3	232.67	0.0	0.0	0.0000	12.1	103.3	2.8	-11.8
98.2	35873	67.3	.28220	166.9	22.28	5.0	232.9	1058.3	232.83	0.0	0.0	0.0000	11.0	105.2	2.9	-10.6
99.0	36442	61.4	.28648	151.7	22.13	4.6	233.8	1087.9	233.77	0.0	0.0	0.0000	6.5	120.5	3.3	-5.6
100.0	37235	53.4	.29169	129.9	21.57	4.1	237.3	1141.1	237.29	0.0	0.0	0.0000	7.1	116.8	3.2	-6.4
100.2	37407	51.9	.29265	125.9	21.45	4.0	238.0	1152.9	238.00	0.0	0.0	0.0000	999.9	999.9	999.9	999.9
101.0	38145	45.5	.29676	109.0	20.95	3.6	241.0	1203.0	241.02	0.0	0.0	0.0000	999.9	999.9	999.9	999.9

INTEGRAL .29676 RESIDUAL .03594 INTEGRATED TOTAL OZONE .33270

OZONAGRAM

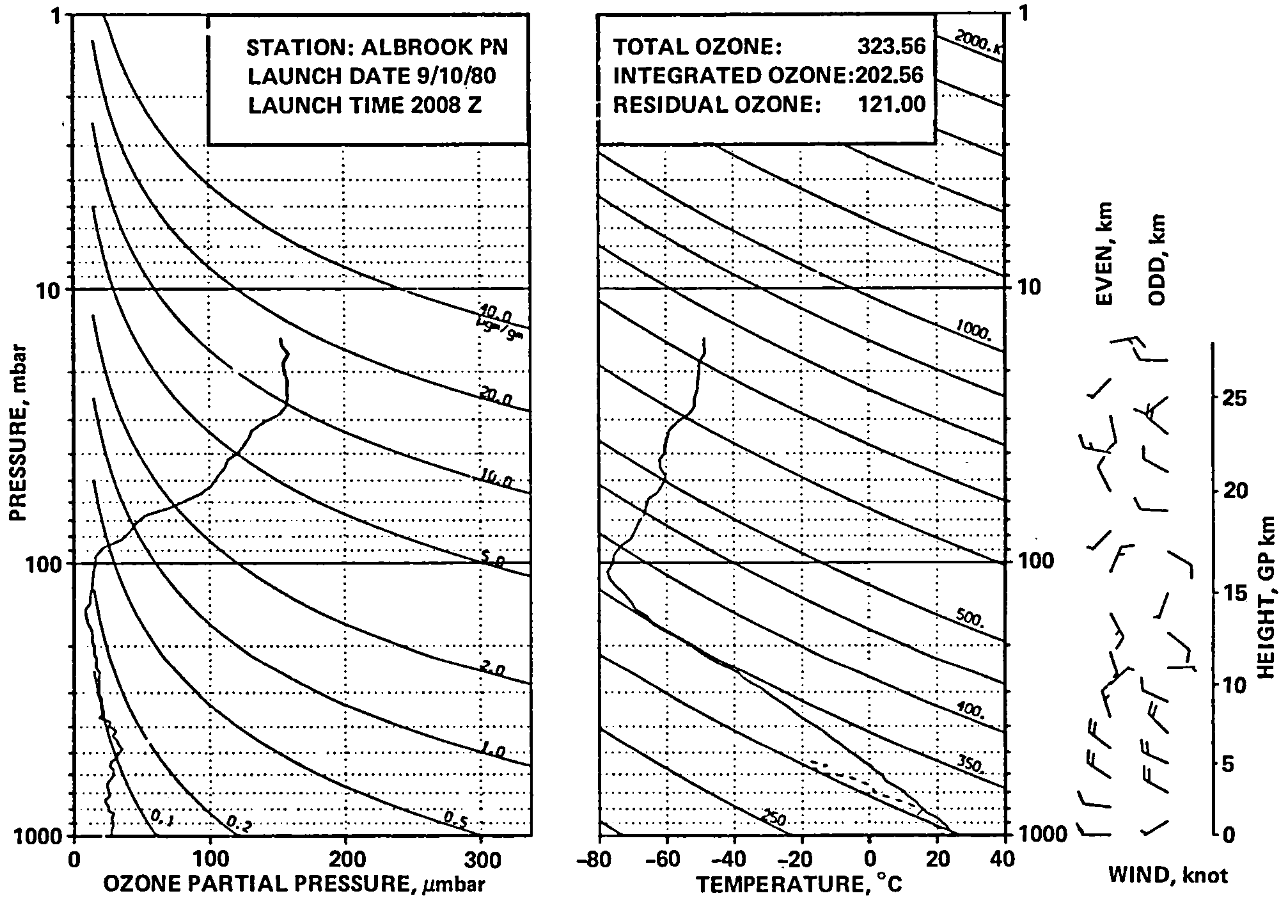
STATION: ALBROOK PN
LAUNCH DATE 9/10/80
LAUNCH TIME 2008 Z
TOTAL OZONE: 323.56
INTEGRATED OZONE:202.56
RESIDUAL OZONE: 121.00
PRESSURE, mbar
1
10
100
1000
0
100
200
300
OZONE PARTIAL PRESSURE, μmbar
40.0
20.0
10.0
5.0
2.0
1.0
0.5
0.2
0.1
-80
-60
-40
-20
0
20
40
TEMPERATURE, °C
2000.
1000.
500.
400.
350.
250.
EVEN, km
ODD, km
HEIGHT, GP km
25
20
15
10
5
0
WIND, knot

STATION ALBROOK PN LAUNCH DATE 9/10/80 TIME 2008Z ECC SONDE 3A1334

SURFACE CONDITIONS PRESS 1002.3MB TEMP 298.6 DEG K HUMIDITY 77.0 PRCNT

TIME MIN	ALT GPM	OZONE MICMB	TOTOZ ATMCM	OZDEN MG/M3	OZMXR MICGG	PRESS MB	TEMP DEG K	PTEMP DEG K	VTEMP DEG K	HMDTY PRCNT	DEWPT DEG K	SPCFC HMDTY	SPD MPS	DIR DEG	NS MPS	EW MPS
0.0	66	27.4	0.00000	53.1	.05	1002.3	298.5	298.3	301.22	72.4	293.2	.0147	4.0	270.0	0.0	4.0
.1	86	27.5	.00005	53.1	.05	1000.0	298.4	298.4	301.14	73.8	293.4	.0151	3.3	265.8	.2	3.3
1.0	282	27.7	.00053	53.7	.05	978.0	297.4	299.3	300.46	87.2	295.1	.0169	4.7	123.0	2.5	-3.9
2.0	527	27.7	.00114	53.9	.05	951.0	296.3	300.5	299.36	92.2	294.9	.0172	2.4	146.1	2.0	-1.4
3.0	769	28.7	.00176	55.9	.05	925.0	296.0	302.7	298.76	79.9	292.4	.0151	1.0	200.5	.9	.3
4.0	1008	29.3	.00239	57.5	.05	900.0	294.5	303.5	297.18	84.9	291.8	.0150	1.5	238.2	.8	1.2
5.0	1272	27.9	.00308	55.0	.05	873.0	293.6	305.2	295.89	73.5	288.7	.0127	2.3	240.7	1.1	2.0
5.9	1502	28.5	.00367	56.4	.06	850.0	292.1	305.9	294.21	74.9	287.5	.0120	2.8	244.4	1.2	2.6
6.0	1523	28.6	.00372	56.5	.06	848.0	291.9	306.0	294.06	75.0	287.4	.0120	2.9	244.6	1.2	2.6
7.0	1748	29.6	.00433	58.9	.06	826.0	289.9	306.1	292.14	88.9	288.0	.0128	3.1	265.7	.2	3.1
8.0	1883	25.8	.00467	51.5	.05	813.0	289.7	307.3	292.06	93.6	288.6	.0135	3.7	272.9	-.2	3.7
8.4	2020	25.8	.00500	51.6	.05	800.0	288.9	307.9	291.21	92.2	287.7	.0126	4.0	275.8	-.4	4.0
9.0	2214	25.8	.00547	51.8	.05	782.0	287.9	308.8	290.01	90.3	286.3	.0121	4.5	279.2	-.7	4.4
10.0	2456	23.4	.00602	47.0	.05	760.0	287.3	310.7	289.16	80.0	283.9	.0106	5.2	292.5	-2.0	4.8
11.0	2692	23.4	.00654	47.3	.05	739.0	286.0	311.8	287.46	68.8	280.4	.0086	6.7	297.0	-3.1	6.0
12.0	2957	26.6	.00716	54.0	.06	716.0	284.3	312.7	285.47	60.3	276.9	.0069	9.4	300.0	-4.7	8.1
12.8	3145	26.0	.00763	52.8	.06	700.0	283.8	314.3	284.90	54.4	275.0	.0061	10.4	299.2	-5.1	9.0
13.0	3193	25.8	.00775	52.5	.06	696.0	283.7	314.7	284.76	52.8	274.5	.0060	10.6	299.0	-5.2	9.3
14.0	3460	25.1	.00839	51.4	.06	674.0	281.9	315.5	282.98	59.8	274.5	.0062	10.5	299.7	-5.2	9.1
15.0	3721	24.5	.00901	50.5	.06	653.0	280.0	316.2	280.93	59.8	272.7	.0056	11.3	303.3	-6.2	9.4
16.0	3963	25.9	.00960	53.7	.07	634.0	278.1	316.7	278.88	56.0	270.0	.0048	11.7	304.0	-6.5	9.7
17.0	4237	28.5	.01032	59.4	.08	613.0	277.4	319.0	278.06	46.4	266.9	.0039	11.1	303.0	-6.0	9.3
17.7	4411	28.9	.01081	60.4	.08	600.0	276.4	319.9	276.87	31.7	260.8	.0022	10.9	301.6	-5.7	9.3
18.0	4479	29.1	.01100	60.8	.08	595.0	276.1	320.2	276.41	26.0	258.5	.0020	10.8	301.0	-5.6	9.2
19.0	4740	29.2	.01174	61.5	.08	576.0	274.4	321.3	274.73	25.0	256.6	.0018	10.7	296.7	-4.8	9.6
20.0	4995	26.7	.01245	56.5	.08	558.0	273.5	323.1	273.89	37.0	260.5	.0026	10.8	293.2	-4.3	10.0
21.0	5286	27.9	.01323	59.4	.09	538.0	271.3	323.8	271.54	28.0	255.2	.0017	10.9	296.4	-4.8	9.7
22.0	5586	31.9	.01413	68.3	.10	518.0	269.6	325.3	269.67	0.0	0.0	0.0000	10.3	301.5	-5.4	8.8
23.0	5864	33.7	.01504	72.6	.11	500.0	267.7	326.4	267.82	0.0	0.0	0.0000	10.0	304.8	-5.7	8.2
24.0	6134	35.8	.01599	77.7	.12	483.0	266.1	327.6	266.10	0.0	0.0	0.0000	10.4	309.5	-6.6	8.0
25.0	6429	33.1	.01702	72.3	.12	465.0	264.6	329.4	264.78	21.3	246.4	.0009	10.3	316.3	-7.5	7.1
26.0	6716	31.9	.01798	70.1	.12	448.0	262.6	330.3	262.86	40.9	251.9	.0016	10.9	320.7	-8.4	6.9
27.0	7012	28.8	.01890	63.8	.11	431.0	260.8	331.7	260.93	29.9	246.8	.0010	11.6	316.3	-8.4	8.0
28.0	7318	31.4	.01986	69.9	.13	414.0	259.1	333.3	259.15	0.0	0.0	0.0000	10.9	314.9	-7.7	7.7
28.8	7577	27.2	.02064	61.1	.11	400.0	257.3	334.3	257.46	0.0	0.0	0.0000	9.6	321.5	-7.5	6.0
29.0	7634	26.3	.02081	59.2	.11	397.0	256.9	334.5	257.08	51.8	249.3	.0014	9.3	323.2	-7.5	5.6
30.0	7903	27.0	.02157	61.2	.12	383.0	254.7	335.0	254.92	67.9	250.2	.0016	7.3	334.1	-6.6	3.2
31.0	8159	18.9	.02219	43.2	.08	370.0	252.8	335.8	253.08	93.9	252.1	.0019	6.2	347.8	-6.0	1.3
32.0	8443	22.2	.02282	51.0	.10	356.0	251.0	337.2	251.25	75.9	247.9	.0014	6.2	352.3	-6.1	.8
32.4	8567	21.9	.02311	50.4	.10	350.0	250.4	337.9	250.58	84.8	248.4	.0015	6.1	350.8	-6.0	1.0
33.0	8737	21.4	.02351	49.6	.10	342.0	249.4	338.9	249.68	96.9	249.1	.0016	6.0	348.6	-5.8	1.2
34.0	9019	20.8	.02416	48.5	.10	329.0	247.6	340.1	247.77	93.6	246.8	.0013	5.5	350.5	-5.4	.9
35.0	9310	20.8	.02482	48.9	.11	316.0	245.3	340.9	245.44	71.2	241.7	.0009	4.4	1.3	-4.4	-.1
36.0	9634	18.8	.02552	44.7	.10	302.0	242.9	342.0	243.00	56.2	237.0	.0006	2.9	20.5	-2.7	-1.0
36.2	9681	18.8	.02562	44.8	.10	300.0	242.6	342.3	242.72	55.9	236.7	.0005	2.8	23.7	-2.6	-1.1
37.0	9921	18.8	.02613	45.1	.11	290.0	241.2	343.5	241.26	54.7	235.1	.0005	2.4	43.8	-1.7	-1.6
38.0	10217	19.2	.02676	46.5	.11	278.0	238.5	343.8	238.57	54.6	232.6	.0004	2.1	49.7	-1.4	-1.6
39.0	10549	18.5	.02747	45.3	.12	265.0	235.8	344.6	235.85	51.4	229.5	.0003	2.2	38.6	-1.7	-1.4
40.0	10895	19.1	.02822	47.2	.13	252.0	234.2	347.2	234.20	47.6	227.3	.0002	2.6	68.5	-.9	-2.4
40.2	10949	18.6	.02833	46.0	.12	250.0	233.6	347.1	233.64	0.0	0.0	0.0000	2.5	73.8	-.7	-2.4
41.0	11171	16.5	.02879	41.2	.11	242.0	231.4	347.0	231.38	0.0	0.0	0.0000	2.3	99.2	.4	-2.3
42.0	11455	16.5	.02934	41.6	.12	232.0	228.5	346.9	228.54	0.0	0.0	0.0000	1.8	113.7	.7	-1.7
43.0	11748	17.1	.02992	43.7	.13	222.0	226.2	347.8	226.21	0.0	0.0	0.0000	2.0	123.3	1.1	-1.7
44.0	12051	15.1	.03051	39.1	.12	212.0	223.7	348.4	223.66	0.0	0.0	0.0000	2.9	163.1	2.8	-.8
45.0	12397	15.1	.03114	39.5	.12	201.0	220.7	349.1	220.71	0.0	0.0	0.0000	4.9	162.2	4.7	-1.5
45.1	12429	14.9	.03120	39.1	.12	200.0	220.4	349.1	220.43	0.0	0.0	0.0000	4.8	160.5	4.6	-1.6
46.0	12691	13.7	.03167	36.4	.12	192.0	218.1	349.5	218.12	0.0	0.0	0.0000	4.6	145.7	3.8	-2.6
47.0	12995	14.1	.03219	37.7	.13	183.0	215.1	349.4	215.06	0.0	0.0	0.0000	6.0	131.5	3.9	-4.5
48.0	13310	13.3	.03274	36.2	.13	174.0	211.6	348.8	211.63	0.0	0.0	0.0000	6.5	120.1	3.2	-5.6
49.0	13636	10.6	.03324	29.3	.11	165.0	208.7	349.3	208.74	0.0	0.0	0.0000	6.1	118.1	2.9	-5.4
50.0	13977	9.3	.03368	25.8	.10	156.0	207.5	352.9	207.53	0.0	0.0	0.0000	8.1	147.2	6.8	-4.4
50.7	14213	8.9	.03395	24.9	.10	150.0	205.1	352.7	205.12	0.0	0.0	0.0000	9.3	156.4	8.5	-3.7
51.0	14335	8.6	.03410	24.5	.10	147.0	203.9	352.6	203.88	0.0	0.0	0.0000	10.0	160.3	9.4	-3.4
52.0	14668	12.5	.03456	35.5	.15	139.0	202.7	356.3	202.74	0.0	0.0	0.0000	7.1	168.1	7.0	-1.5
53.0	15063	12.5	.03522	35.8	.16	130.0	200.8	359.8	200.85	0.0	0.0	0.0000	2.7	202.0	2.5	1.0
53.6	15292	13.2	.03562	38.2	.18	125.0	199.3	361.0	199.29	0.0	0.0	0.0000	.4	16.4	-.4	-.1
54.0	15434	13.6	.03587	39.7	.19	122.0	198.3	361.7	198.32	0.0	0.0	0.0000	2.3	20.5	-2.2	-.8
55.0	15775	14.2	.03652	41.7	.20	115.0	196.4	364.4	196.43	0.0	0.0	0.0000	6.6	35.9	-5.3	-3.9
56.0	16135	14.6	.03723	43.0	.22	108.0	195.6	369.4	195.59	0.0	0.0	0.0000	7.7	21.1	-7.2	-2.8
57.0	16577	16.3	.03817	47.8	.27	100.0	197.3	380.8	197.25	0.0	0.0	0.0000	9.0	26.4	-8.1	-4.0
58.0	16897	16.3	.03889	47.6	.29	94.6	197.5	387.5	197.52	0.0	0.0	0.0000	4.5	72.7	-1.3	-4.3
59.0	17323	21.8	.03999	63.1	.41	87.9	199.1	398.8	199.10	0.0	0.0	0.0000	6.5	194.2	6.3	1.6
60.0	17731	35.9	.04157	102.2	.72	82.0	202.7	414.3	202.74	0.0	0.0	0.0000	4.9	209.2	4.2	2.4
60.3	17877	38.0	.04233	108.0	.79	80.0	203.1	418.1	203.14	0.0	0.0	0.0000	3.7	212.4	3.1	2.0
61.0	18152	42.0	.04374	118.8	.91	76.4	203.9	425.1	203.88	0.0	0.0	0.0000	1.7	230.1	1.1	1.3
62.0	18565	46.3	.04615	130.5	1.08	71.3	205.0	435.9	204.99	0.0	0.0	0.0000	5.3	268.0	.2	5.3
62.3	18675	48.4	.04687	135.9	1.15	70.0	205.5	439.3	205.50	0.0	0.0	0.0000	5.8	271.8	-.2	5.8
63.0	18940	53.2	.04859	148.7	1.32	67.0	206.7	447.4	206.70	0.0	0.0	0.0000	7.0	278.7	-1.1	6.9
64.0	19313	70.7	.05160	197.1	1.86	63.0	207.1	456.3	207.11	0.0	0.0	0.0000	4.7	262.6	.6	4.7
64.7	19609	79.9	.05459	222.2	2.21	60.0	207.7	464.0	207.67	0.0	0.0	0.0000	3.8	275.3	-.4	3.8
65.0	19753	84.4	.05603	234.3	2.39	58.6	207.9	467.7	207.93	0.0	0.0	0.0000	3.4	283.6	-.8	3.4
66.0	20064	94.3	.05961	258.7	2.81	55.7	210.5	480.4	210.50	0.0	0.0	0.0000	5.5	332.4	-4.9	2.6
67.0	20477	101.6	.06477	276.6	3.23	52.1	212.0	493.1	212.00	0.0	0.0	0.0000	5.5	330.7	-4.8	2.7

TIME MIN	ALT GPM	OZONE MICMB	TOTOZ ATMCM	OZDEN MG/M3	OZMXR MICGG	PRESS MB	TEMP DEG K	PTEMP DEG K	VTEMP DEG K	HMDTY PRCNT	DEWPT DEG K	SPCFC HMDTY	SPD MPS	DIR DEG	NS MPS	EW MPS
67.6	20732	104.1	.06814	282.7	3.46	50.0	212.6	500.5	212.64	0.0	0.0	0.0000	5.8	312.0	-3.9	4.3
68.0	20922	106.0	.07064	287.3	3.62	48.5	213.1	505.9	213.10	0.0	0.0	0.0000	6.3	300.1	-3.2	5.5
69.0	21373	111.4	.07687	304.1	4.09	45.1	211.4	512.5	211.44	0.0	0.0	0.0000	6.3	296.4	-2.8	5.7
70.0	21799	113.8	.08299	311.1	4.48	42.1	211.3	522.2	211.26	0.0	0.0	0.0000	6.5	282.8	-1.4	6.3
70.9	22116	120.2	.08773	326.1	4.98	40.0	212.7	533.6	212.71	0.0	0.0	0.0000	8.5	282.0	-1.8	8.3
71.0	22163	121.1	.08843	328.4	5.05	39.7	212.9	535.3	212.92	0.0	0.0	0.0000	8.8	281.9	-1.8	8.6
72.0	22568	125.7	.09476	340.9	5.60	37.2	212.9	545.3	212.92	0.0	0.0	0.0000	8.9	301.6	-4.6	7.6
73.0	22948	129.2	.10090	349.1	6.12	35.0	213.6	556.7	213.61	0.0	0.0	0.0000	9.8	310.3	-6.3	7.4
73.0	22966	129.3	.10118	349.5	6.14	34.9	213.6	557.2	213.65	0.0	0.0	0.0000	9.8	310.7	-6.4	7.4
74.0	23354	131.8	.10758	355.4	6.66	32.8	214.2	568.6	214.18	0.0	0.0	0.0000	11.5	307.5	-7.0	9.1
75.0	23812	141.0	.11540	375.4	7.66	30.5	216.8	587.6	216.78	0.0	0.0	0.0000	8.7	322.8	-6.9	5.2
75.3	23917	143.9	.11732	381.7	7.96	30.0	217.6	592.7	217.63	0.0	0.0	0.0000	7.1	326.9	-6.0	3.9
76.0	24223	152.3	.12285	399.6	8.82	28.6	220.1	607.6	220.07	0.0	0.0	0.0000	3.2	.3	-3.2	0.0
77.0	24619	156.7	.13032	408.1	9.65	26.9	221.7	622.8	221.66	0.0	0.0	0.0000	2.9	204.3	2.7	1.2
78.0	25094	158.4	.13942	412.7	10.50	25.0	221.7	635.9	221.66	0.0	0.0	0.0000	5.8	233.6	3.4	4.6
79.0	25552	157.8	.14821	409.1	11.22	23.3	222.7	652.0	222.74	0.0	0.0	0.0000	4.4	241.5	2.1	3.9
80.0	26016	158.4	.15709	410.7	12.10	21.7	222.7	665.4	222.74	0.0	0.0	0.0000	2.9	220.7	2.2	1.9
81.0	26516	156.0	.16659	403.6	12.86	20.1	223.2	681.6	223.20	0.0	0.0	0.0000	3.8	255.4	1.0	3.7
81.1	26548	156.0	.16720	403.5	12.92	20.0	223.2	682.5	223.20	0.0	0.0	0.0000	3.9	256.8	.9	3.8
82.0	27022	155.2	.17611	401.6	13.82	18.6	223.1	696.4	223.05	0.0	0.0	0.0000	6.1	269.2	.1	6.1
82.8	27421	158.2	.18367	406.8	14.99	17.5	224.5	713.1	224.47	0.0	0.0	0.0000	7.2	285.5	-1.9	6.9
83.0	27535	159.0	.18581	408.2	15.32	17.2	224.9	717.9	224.87	0.0	0.0	0.0000	7.6	289.2	-2.5	7.2
84.0	27970	154.1	.19398	396.0	15.86	16.1	224.7	731.1	224.72	0.0	0.0	0.0000	7.0	293.6	-2.8	6.4
85.0	28435	153.2	.20256	393.7	16.93	15.0	224.7	746.0	224.72	0.0	0.0	0.0000	999.9	999.9	999.9	999.9

INTEGRAL .20256 RESIDUAL .12100 INTEGRATED TOTAL OZONE .32356

OZONAGRAM

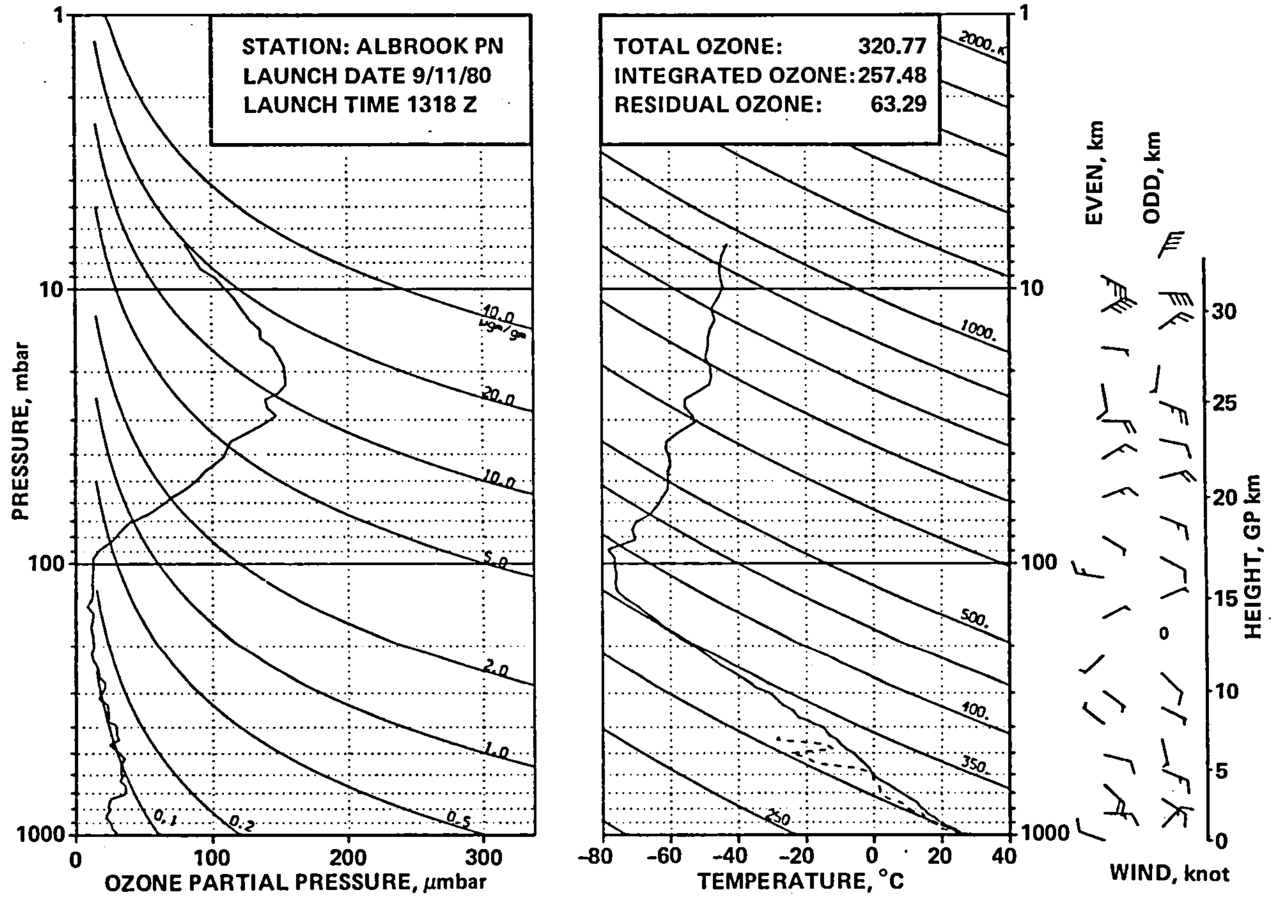
STATION: ALBROOK PN
LAUNCH DATE 9/11/80
LAUNCH TIME 1318 Z
TOTAL OZONE: 320.77
INTEGRATED OZONE: 257.48
RESIDUAL OZONE: 63.29
PRESSURE, mbar
OZONE PARTIAL PRESSURE, μmbar
TEMPERATURE, °C
EVEN, km
ODD, km
HEIGHT, GP km
WIND, knot

STATION ALBROOK PN LAUNCH DATE 9/11/80 TIME 1318Z ECC SONDE 3A1335

SURFACE CONDITIONS PRESS 1002.5MB TEMP 298.2 DEG K HUMIDITY 94.0 PRCNT

TIME MIN	ALT GPM	OZONE MICMB	TOTOZ ATMCM	OZDEN MG/M3	OZMXR MICGG	PRESS MB	TEMP DEG K	PTEMP DEG K	VTEMP DEG K	HMDTY PRCNT	DEWPT DEG K	SPCFC HMDTY	SPD MPS	DIR DEG	NS MPS	EW MPS
0.0	66	28.2	0.00000	54.7	.05	1002.5	298.1	297.9	301.40	92.9	296.8	.0183	5.0	290.0	-1.7	4.7
.1	87	28.3	.00006	54.9	.05	1000.0	298.1	298.1	301.42	93.2	296.9	.0185	4.8	293.8	-2.0	4.4
1.0	320	29.4	.00066	57.0	.05	974.0	298.1	300.3	301.65	97.0	297.5	.0197	4.8	339.7	-4.5	1.7
2.0	567	26.2	.00127	50.9	.05	947.0	296.6	301.3	299.25	75.9	292.1	.0145	4.3	22.0	-4.0	-1.6
3.0	819	25.7	.00186	50.4	.05	920.0	294.1	301.2	296.71	87.0	291.8	.0146	4.2	41.3	-3.2	-2.8
3.7	1008	24.8	.00230	48.9	.05	900.0	292.8	301.8	295.25	85.7	290.3	.0134	4.4	42.3	-3.2	-3.0
4.0	1086	24.5	.00248	48.3	.05	892.0	292.3	302.0	294.65	85.2	289.7	.0132	4.5	42.7	-3.3	-3.0
5.0	1360	21.6	.00306	42.8	.04	864.0	291.0	303.4	293.16	82.5	288.0	.0122	5.4	43.5	-3.9	-3.7
5.5	1499	22.0	.00334	43.8	.04	850.0	290.0	303.8	292.15	87.4	287.8	.0123	6.1	48.5	-4.1	-4.6
6.0	1621	22.4	.00359	44.7	.04	838.0	289.1	304.1	291.28	91.7	287.7	.0124	6.8	52.0	-4.2	-5.3
7.0	1910	24.5	.00422	49.1	.05	810.0	288.1	305.9	289.80	75.7	283.8	.0099	6.4	75.5	-1.6	-6.2
7.4	2015	24.1	.00445	48.3	.05	800.0	287.5	306.4	289.24	76.8	283.5	.0098	6.4	86.6	-.4	-6.4
8.0	2186	23.4	.00483	47.0	.05	784.0	286.6	307.3	288.34	78.7	283.0	.0097	6.8	103.9	1.6	-6.6
9.0	2470	24.2	.00546	48.8	.05	758.0	285.9	309.4	287.36	71.5	280.8	.0086	7.0	103.9	1.7	-6.8
10.0	2751	25.5	.00612	51.8	.06	733.0	283.9	310.3	285.12	63.3	277.2	.0070	7.8	115.0	3.3	-7.1
11.0	3039	35.1	.00695	71.8	.08	708.0	282.0	311.3	283.11	62.6	275.3	.0063	8.8	123.2	4.8	-7.4
11.3	3132	35.4	.00727	72.7	.08	700.0	281.4	311.6	282.48	65.0	275.2	.0063	8.7	123.5	4.8	-7.3
12.0	3360	36.3	.00804	74.9	.09	681.0	279.8	312.3	280.94	70.9	275.0	.0064	8.5	124.4	4.8	-7.0
13.0	3679	35.7	.00915	74.2	.09	655.0	277.7	313.4	278.83	80.6	274.7	.0065	9.4	129.3	6.0	-7.3
14.0	3969	32.0	.01011	67.2	.08	632.0	275.3	313.9	276.35	85.4	273.1	.0060	9.4	130.7	6.1	-7.1
15.0	4254	33.9	.01103	71.5	.09	610.0	273.5	315.0	274.55	96.5	273.0	.0062	8.3	138.3	6.2	-5.5
15.4	4386	33.2	.01146	70.3	.09	600.0	273.0	315.9	274.05	98.0	272.7	.0061	7.8	140.9	6.0	-4.9
16.0	4562	32.4	.01203	68.6	.09	587.0	272.4	317.2	273.40	100.0	272.4	.0061	7.2	145.0	5.9	-4.1
17.0	4853	33.0	.01297	70.1	.10	566.0	271.7	319.7	272.44	69.9	267.0	.0042	6.7	128.0	4.1	-5.3
18.0	5153	33.1	.01396	70.8	.10	545.0	270.3	321.5	270.60	31.6	255.8	.0018	7.1	108.0	2.2	-6.8
19.0	5478	35.6	.01508	76.5	.11	523.0	268.7	323.4	269.00	29.3	253.6	.0015	7.8	99.8	1.3	-7.7
20.0	5831	31.9	.01627	68.9	.11	500.0	267.2	325.7	267.39	21.0	248.5	.0010	7.0	97.8	.9	-7.0
21.0	6100	28.7	.01710	62.5	.10	483.0	265.0	326.2	265.47	72.5	260.9	.0031	4.0	105.2	1.0	-3.9
22.0	6411	24.4	.01794	53.4	.09	464.0	263.4	328.0	263.80	69.6	258.9	.0027	2.7	177.7	2.6	-.1
23.0	6715	31.2	.01881	68.8	.12	446.0	262.1	330.1	262.19	21.9	244.5	.0008	4.3	213.6	3.5	2.4
24.0	7012	29.7	.01974	66.0	.11	429.0	259.8	330.8	259.93	28.6	245.4	.0009	3.4	165.9	3.3	-.8
25.0	7543	29.4	.02137	65.7	.12	400.0	258.1	335.4	258.20	0.0	0.0	0.0000	2.0	184.0	2.0	.1
26.0	7733	28.6	.02195	64.6	.12	390.0	255.4	334.2	255.49	33.7	243.3	.0008	2.9	272.7	-.1	2.9
27.0	7946	23.0	.02254	52.3	.10	379.0	253.7	334.8	253.85	33.7	241.8	.0007	2.2	292.0	-.8	2.0
28.0	8163	23.8	.02308	54.7	.11	368.0	250.7	333.5	250.75	32.5	238.7	.0005	2.0	320.5	-1.6	1.3
28.9	8530	23.6	.02402	54.7	.11	350.0	249.3	336.5	249.35	28.2	236.1	.0004	.8	13.7	-.8	-.2
29.0	8551	23.6	.02407	54.7	.11	349.0	249.2	336.7	249.27	28.0	235.9	.0004	.8	20.6	-.7	-.3
30.0	8957	23.0	.02510	54.1	.12	330.0	245.9	337.6	245.99	33.6	234.8	.0004	1.8	120.4	.9	-1.6
31.0	9336	16.6	.02593	39.4	.09	313.0	244.0	340.0	244.02	32.2	232.6	.0003	2.6	107.6	.8	-2.5
31.9	9637	19.0	.02653	45.3	.11	300.0	242.4	341.9	242.43	22.6	227.9	.0002	2.2	107.5	.7	-2.1
32.0	9661	19.2	.02657	45.7	.11	299.0	242.3	342.1	242.31	21.8	227.6	.0002	2.1	107.5	.6	-2.0
33.0	9998	21.0	.02734	50.9	.12	285.0	238.2	341.0	238.27	36.7	228.7	.0002	1.9	124.6	1.1	-1.6
34.0	10297	21.3	.02805	52.1	.13	273.0	236.4	342.6	236.44	50.9	230.0	.0003	3.0	137.8	2.2	-2.0
35.0	10606	16.8	.02873	41.4	.11	261.0	233.7	343.1	233.78	47.2	226.8	.0002	3.5	127.4	2.1	-2.8
35.9	10898	16.7	.02930	41.6	.11	250.0	231.3	343.7	231.30	0.0	0.0	0.0000	3.7	136.3	2.7	-2.6
36.0	10926	16.6	.02935	41.6	.11	249.0	231.1	343.8	231.06	0.0	0.0	0.0000	3.8	137.1	2.8	-2.6
37.0	11258	15.3	.02997	38.7	.11	237.0	228.1	344.1	228.05	0.0	0.0	0.0000	8.2	128.6	5.1	-6.4
38.0	11603	12.3	.03054	31.4	.09	225.0	225.5	345.4	225.53	0.0	0.0	0.0000	3.8	158.9	3.5	-1.4
39.0	11962	11.5	.03105	29.3	.09	213.0	222.9	346.8	222.94	0.0	0.0	0.0000	3.9	241.6	1.8	3.4
40.0	12306	13.3	.03157	34.9	.11	202.0	220.7	348.6	220.72	0.0	0.0	0.0000	1.1	195.2	1.0	.3
40.2	12369	13.2	.03167	34.6	.11	200.0	220.1	348.6	220.11	0.0	0.0	0.0000	.8	211.8	.7	.4
41.0	12631	12.6	.03209	33.6	.11	192.0	217.6	348.7	217.64	0.0	0.0	0.0000	1.2	303.4	-.7	1.0
42.0	12969	12.3	.03262	33.1	.11	182.0	214.6	349.1	214.57	0.0	0.0	0.0000	.5	42.5	-.3	-.3
43.0	13321	11.0	.03314	30.2	.11	172.0	211.3	349.4	211.33	0.0	0.0	0.0000	1.4	80.4	-.2	-1.4
44.0	13689	12.2	.03369	33.8	.13	162.0	209.2	351.8	209.16	0.0	0.0	0.0000	2.4	68.9	-.9	-2.3
45.0	14076	12.8	.03432	35.9	.14	152.0	206.1	353.1	206.11	0.0	0.0	0.0000	3.1	61.4	-1.5	-2.7
45.2	14155	11.9	.03443	33.3	.13	150.0	205.5	353.4	205.54	0.0	0.0	0.0000	3.3	60.2	-1.7	-2.9
46.0	14442	8.4	.03483	23.9	.10	143.0	203.5	354.7	203.46	0.0	0.0	0.0000	4.1	56.9	-2.3	-3.5
47.0	14826	11.9	.03535	34.5	.15	134.0	199.9	355.0	199.93	0.0	0.0	0.0000	3.8	65.6	-1.6	-3.4
48.0	15184	12.6	.03595	36.9	.17	126.0	197.5	357.0	197.53	0.0	0.0	0.0000	2.0	67.2	-.8	-1.8
48.1	15230	12.5	.03602	36.6	.17	125.0	197.5	357.7	197.46	0.0	0.0	0.0000	1.2	51.1	-.7	-.9
49.0	15514	11.9	.03650	34.9	.17	119.0	197.0	362.0	197.03	0.0	0.0	0.0000	4.7	276.3	-.5	4.7
50.0	15968	12.2	.03725	35.8	.18	110.0	197.3	370.7	197.28	0.0	0.0	0.0000	8.3	274.6	-.7	8.3
51.0	16403	12.8	.03800	37.5	.21	102.0	196.8	377.8	196.78	0.0	0.0	0.0000	7.3	296.3	-3.3	6.6
51.3	16516	12.8	.03820	37.5	.21	100.0	196.8	379.9	196.78	0.0	0.0	0.0000	7.0	305.2	-4.1	5.7
52.0	16794	12.8	.03868	37.5	.22	95.3	196.8	385.2	196.78	0.0	0.0	0.0000	7.0	328.2	-6.0	3.7
53.0	17212	17.6	.03956	52.2	.33	88.6	194.9	389.6	194.95	0.0	0.0	0.0000	2.9	6.8	-2.9	-.3
54.0	17670	27.7	.04096	78.8	.56	81.9	202.8	414.6	202.82	0.0	0.0	0.0000	2.3	128.6	1.4	-1.8
54.3	17809	29.5	.04153	84.0	.61	80.0	202.6	416.9	202.58	0.0	0.0	0.0000	2.6	124.9	1.5	-2.1
55.0	18168	34.0	.04301	97.2	.75	75.3	202.0	422.8	201.95	0.0	0.0	0.0000	3.4	118.4	1.6	-3.0
56.0	18525	39.7	.04476	113.0	.93	70.9	203.0	432.5	203.04	0.0	0.0	0.0000	6.5	113.3	2.6	-5.9
56.2	18601	42.1	.04523	119.2	1.00	70.0	203.8	435.7	203.79	0.0	0.0	0.0000	6.7	113.2	2.6	-6.2
57.0	18955	53.1	.04738	147.9	1.33	66.0	207.3	450.6	207.28	0.0	0.0	0.0000	7.8	112.8	3.0	-7.2
58.0	19456	63.9	.05117	175.8	1.74	60.8	209.7	466.7	209.71	0.0	0.0	0.0000	6.6	109.0	2.1	-6.2
58.2	19537	65.3	.05187	179.6	1.81	60.0	210.0	469.1	209.96	0.0	0.0	0.0000	6.6	102.5	1.4	-6.4
59.0	19810	70.2	.0542[illegible]	192.2	2.03	57.4	210.8	476.9	210.79	0.0	0.0	0.0000	7.2	82.6	-.9	-7.2
60.0	20211	79.6	.05804	216.4	2.45	53.8	212.4	489.5	212.37	0.0	0.0	0.0000	9.0	61.5	-4.3	-7.9
61.0	20666	88.2	.06289	239.5	2.92	50.0	212.5	500.2	212.55	0.0	0.0	0.0000	9.9	72.5	-3.0	-9.4
62.0	21158	94.5	.06858	256.8	3.39	46.2	212.5	511.7	212.55	0.0	0.0	0.0000	9.9	76.3	-2.4	-9.7
63.0	21533	101.6	.07324	275.1	3.87	43.5	213.2	522.2	213.23	0.0	0.0	0.0000	9.1	68.3	-3.4	-8.4
64.0	21932	108.8	.07856	295.1	4.42	40.8	212.9	531.0	212.89	0.0	0.0	0.0000	6.9	60.2	-3.4	-6.0
64.3	22055	109.6	.08028	297.6	4.54	40.0	212.6	533.3	212.58	0.0	0.0	0.0000	6.6	59.0	-3.4	-5.7
65.0	22341	111.3	.08428	303.3	4.83	38.2	211.9	538.5	211.85	0.0	0.0	0.0000	5.8	55.9	-3.3	-4.8

TIME MIN	ALT GPM	OZONE MICMB	TOTOZ ATMCM	OZDEN MG/M3	OZMXR MICGG	PRESS MB	TEMP DEG K	PTEMP DEG K	VTEMP DEG K	HMDTY PRCNT	DEWPT DEG K	SPCFC HMDTY	SPD MPS	DIR DEG	NS MPS	EW MPS
66.0	22743	114.3	.09005	310.9	5.29	35.8	212.2	549.4	212.20	0.0	0.0	0.0000	4.5	74.5	-1.2	-4.3
66.3	22884	118.1	.09221	319.6	5.61	35.0	213.3	556.0	213.31	0.0	0.0	0.0000	4.1	85.5	-.3	-4.1
67.0	23234	127.7	.09754	341.2	6.39	33.1	216.0	572.1	216.04	0.0	0.0	0.0000	3.9	117.9	1.8	-3.5
68.0	23715	140.0	.10549	366.8	7.56	30.7	220.4	596.3	220.41	0.0	0.0	0.0000	4.5	116.3	2.0	-4.0
68.4	23863	143.0	.10811	375.0	7.91	30.0	220.2	599.7	220.18	0.0	0.0	0.0000	6.4	100.8	1.2	-6.3
69.0	24104	147.8	.11235	388.3	8.47	28.9	219.8	605.0	219.81	0.0	0.0	0.0000	9.9	89.4	-.1	-9.9
70.0	24539	141.2	.12011	374.7	8.67	27.0	217.6	610.8	217.64	0.0	0.0	0.0000	14.4	93.9	1.0	-14.4
71.0	24978	139.9	.12776	371.2	9.20	25.2	217.6	623.0	217.64	0.0	0.0	0.0000	12.9	109.5	4.3	-12.2
71.2	25029	141.4	.12867	374.1	9.38	25.0	218.1	625.8	218.12	0.0	0.0	0.0000	12.5	110.3	4.3	-11.7
72.0	25318	149.4	.13381	390.7	10.36	23.9	220.9	641.9	220.87	0.0	0.0	0.0000	10.2	116.2	4.5	-9.2
73.0	25770	154.8	.14212	397.6	11.50	22.3	224.8	666.4	224.82	0.0	0.0	0.0000	6.7	156.3	6.2	-2.7
74.0	26197	154.5	.15004	395.9	12.25	20.9	225.4	680.6	225.39	0.0	0.0	0.0000	6.2	176.0	6.2	-.4
74.5	26487	154.1	.15539	395.1	12.78	20.0	225.2	688.8	225.24	0.0	0.0	0.0000	4.8	175.6	4.7	-.4
75.0	26756	153.7	.16036	394.3	13.27	19.2	225.1	696.4	225.10	0.0	0.0	0.0000	3.4	174.8	3.4	-.3
76.0	27253	150.4	.16944	388.2	14.00	17.8	223.7	707.1	223.67	0.0	0.0	0.0000	2.3	196.0	2.2	.6
76.2	27364	149.5	.17143	385.7	14.16	17.5	223.8	711.0	223.81	0.0	0.0	0.0000	1.9	184.6	1.9	.2
77.0	27830	145.7	.17972	374.9	14.81	16.3	224.4	727.5	224.39	0.0	0.0	0.0000	2.0	108.9	.6	-1.9
78.0	28332	136.4	.18824	351.1	14.97	15.1	224.4	743.5	224.39	0.0	0.0	0.0000	5.9	82.9	-.7	-5.9
78.1	28375	136.4	.18895	350.9	15.07	15.0	224.5	745.2	224.45	0.0	0.0	0.0000	6.1	79.6	-1.1	-6.0
79.0	28829	136.1	.19637	349.0	16.11	14.0	225.1	762.2	225.10	0.0	0.0	0.0000	9.3	57.1	-5.0	-7.8
80.0	29319	128.9	.20412	328.4	16.42	13.0	226.5	783.4	226.52	0.0	0.0	0.0000	14.2	48.6	-9.4	-10.6
80.4	29578	126.3	.20801	322.4	16.74	12.5	226.1	790.9	226.12	0.0	0.0	0.0000	16.5	52.9	-10.0	-13.1
81.0	29960	122.5	.21372	313.6	17.20	11.8	225.5	801.9	225.53	0.0	0.0	0.0000	20.0	57.3	-10.8	-16.8
82.0	30609	116.4	.22295	295.3	18.03	10.7	227.6	832.3	227.64	0.0	0.0	0.0000	21.9	73.4	-6.3	-21.0
82.9	31060	110.6	.22898	279.3	18.33	10.0	228.7	852.6	228.72	0.0	0.0	0.0000	20.7	91.3	.5	-20.7
83.0	31128	109.8	.22988	276.9	18.37	9.9	228.9	855.6	228.88	0.0	0.0	0.0000	20.7	94.1	1.5	-20.6
84.0	31691	103.1	.23696	261.1	18.78	9.1	228.1	873.3	228.05	0.0	0.0	0.0000	18.5	112.7	7.2	-17.1
85.0	32225	92.0	.24312	233.0	18.14	8.4	227.9	893.0	227.92	0.0	0.0	0.0000	18.9	120.0	9.4	-16.3
85.5	32550	89.3	.24655	226.0	18.49	8.0	228.2	906.7	228.19	0.0	0.0	0.0000	19.5	113.5	7.8	-17.9
86.0	32893	86.5	.25017	218.7	18.87	7.6	228.5	921.1	228.47	0.0	0.0	0.0000	20.5	107.2	6.0	-19.6
86.7	33445	81.8	.25557	205.6	19.36	7.0	229.8	948.6	229.79	0.0	0.0	0.0000	999.9	999.9	999.9	999.9
87.0	33640	80.1	.25748	201.0	19.53	6.8	230.3	958.3	230.25	0.0	0.0	0.0000	999.9	999.9	999.9	999.9

INTEGRAL .25748 RESIDUAL .06329 INTEGRATED TOTAL OZONE .32077

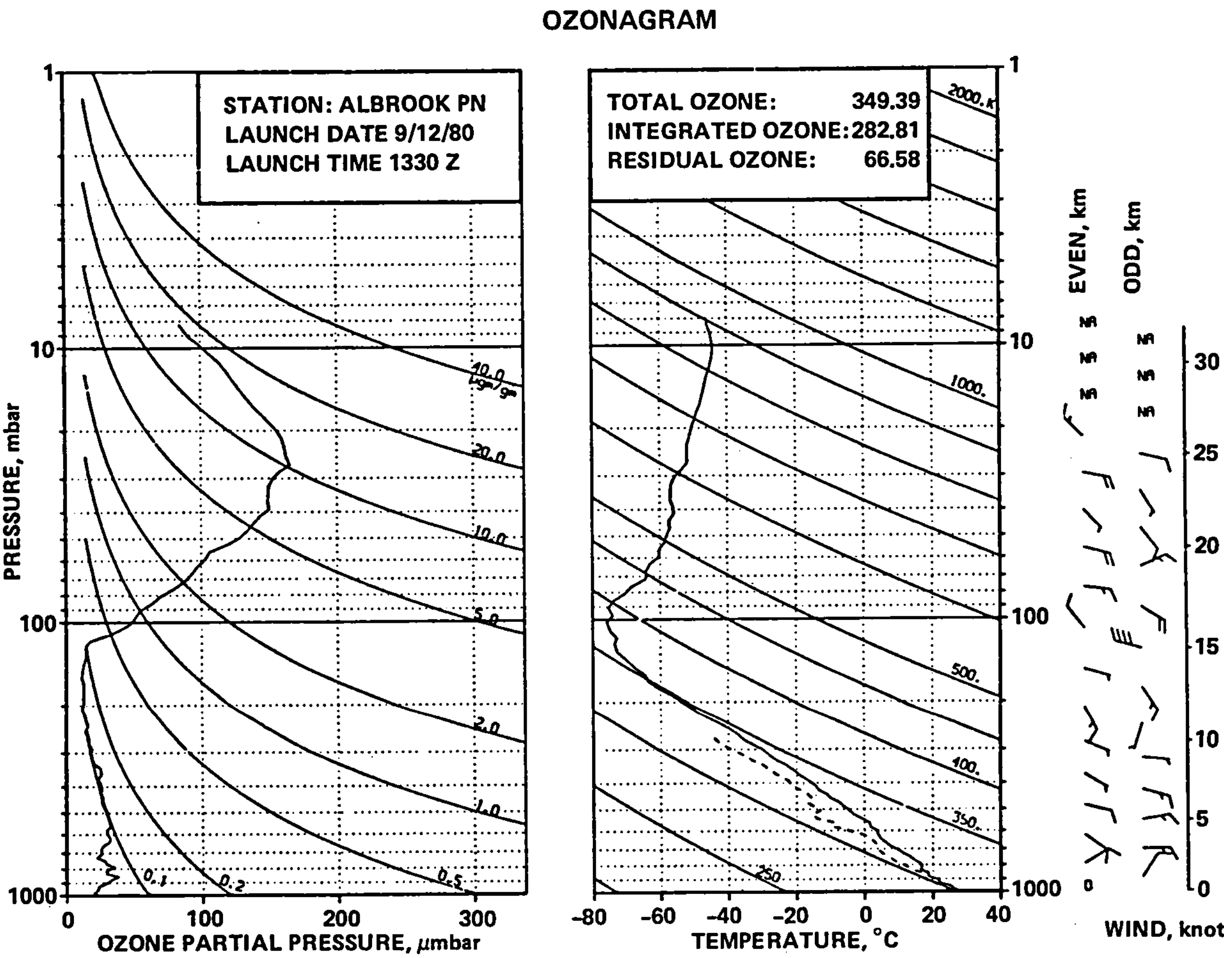
OZONAGRAM
STATION: ALBROOK PN
LAUNCH DATE 9/12/80
LAUNCH TIME 1330 Z
TOTAL OZONE: 349.39
INTEGRATED OZONE: 282.81
RESIDUAL OZONE: 66.58
PRESSURE, mbar
OZONE PARTIAL PRESSURE, μmbar
TEMPERATURE, °C
EVEN, km
ODD, km
HEIGHT, GP km
WIND, knot

STATION ALBROOK PN   LAUNCH DATE 9/12/80   TIME 1330Z   ECC   SONDE 3A1337

SURFACE CONDITIONS   PRESS 1002.5MB   TEMP 302.0 DEG K   HUMIDITY 0.0 PRCNT

TIME MIN	ALT GPM	OZONE MICMB	TOTOZ ATMCM	OZDEN MG/M3	OZMXR MICGG	PRESS MB	TEMP DEG K	PTEMP DEG K	VTEMP DEG K	HMDTY PRCNT	DEWPT DEG K	SPCFC HMDTY	SPD MPS	DIR DEG	NS MPS	EW MPS
0.0	66	22.6	0.00000	43.3	.04	1002.5	301.9	301.7	305.70	83.4	298.8	.0206	0.0	0.0	0.0	0.0
.1	88	22.5	.00004	43.0	.04	1000.0	301.6	301.6	305.41	83.5	298.6	.0202	.1	48.0	0.0	0.0
1.0	286	20.9	.00043	40.4	.04	978.0	299.4	301.3	302.81	84.2	296.5	.0185	.6	48.0	-.4	-.4
2.0	524	24.0	.00090	46.4	.04	952.0	298.3	302.5	301.63	83.2	296.2	.0185	1.9	17.6	-1.9	-.6
3.0	738	23.9	.00137	46.7	.04	929.0	295.3	301.6	298.06	86.1	292.8	.0155	3.3	15.9	-3.2	-.9
4.0	985	29.8	.00197	58.3	.05	903.0	294.6	303.3	297.18	80.7	291.1	.0143	3.7	29.1	-3.3	-1.8
4.1	1013	30.2	.00205	59.2	.06	900.0	294.2	303.2	296.79	81.3	290.9	.0140	4.0	30.7	-3.4	-2.0
5.0	1208	32.9	.00260	65.2	.06	880.0	291.8	302.7	294.14	85.8	289.4	.0131	5.4	38.5	-4.3	-3.4
6.0	1466	38.7	.00345	76.6	.08	854.0	291.8	305.3	294.27	87.9	289.8	.0138	6.8	43.4	-5.0	-4.7
6.2	1506	37.1	.00358	73.6	.07	850.0	291.4	305.2	293.80	87.5	289.3	.0132	6.8	44.5	-4.8	-4.7
7.0	1689	30.0	.00416	59.9	.06	832.0	289.5	305.2	291.65	85.6	287.1	.0120	6.5	49.5	-4.2	-4.9
8.0	1918	29.9	.00479	59.4	.06	810.0	290.1	308.1	292.12	74.6	285.6	.0111	6.3	51.2	-3.9	-4.9
8.5	2023	32.5	.00511	64.8	.07	800.0	289.9	308.9	291.71	70.6	284.5	.0101	5.7	56.9	-3.1	-4.7
9.0	2142	35.5	.00547	70.8	.07	789.0	289.5	309.8	291.25	66.0	283.2	.0097	5.1	64.7	-2.2	-4.6
10.0	2360	30.2	.00614	60.6	.07	769.0	287.9	310.4	289.52	66.1	281.7	.0090	5.0	88.1	-.2	-5.0
11.0	2605	28.4	.00681	57.1	.06	747.0	286.6	311.5	288.06	66.6	280.5	.0086	5.6	97.8	.8	-5.6
12.0	2833	22.9	.00736	46.4	.05	727.0	284.7	311.8	286.00	66.4	278.6	.0077	6.7	93.8	.4	-6.7
13.0	3077	26.1	.00792	53.1	.06	706.0	283.2	312.8	284.41	66.3	277.2	.0072	7.8	89.6	-.1	-7.8
13.3	3147	26.0	.00810	53.0	.06	700.0	282.5	312.8	283.78	69.0	277.1	.0072	7.8	92.4	.3	-7.8
14.0	3339	25.7	.00857	52.8	.06	684.0	280.8	313.0	282.08	76.6	277.0	.0073	8.0	99.8	1.4	-7.9
15.0	3608	27.3	.00925	56.3	.07	662.0	279.4	314.4	280.65	80.5	276.3	.0072	8.1	113.1	3.2	-7.5
16.0	3872	31.9	.01000	66.3	.08	641.0	277.9	315.5	279.02	81.2	274.9	.0067	6.9	126.0	4.1	-5.6
17.0	4143	32.7	.01085	68.2	.09	620.0	277.2	317.8	278.22	73.9	273.0	.0060	5.9	125.9	3.5	-4.8
18.0	4409	30.7	.01167	64.0	.08	600.0	276.9	320.4	277.62	55.0	268.7	.0045	4.8	105.0	1.2	-4.7
19.0	4683	30.1	.01249	63.2	.09	580.0	275.0	321.3	275.59	44.3	264.2	.0033	5.5	83.6	-.6	-5.5
20.0	4951	32.9	.01332	69.2	.10	561.0	274.7	324.0	275.31	47.8	264.8	.0036	6.5	80.7	-1.0	-6.4
21.0	5227	32.2	.01420	68.1	.10	542.0	272.6	324.7	273.01	35.7	259.3	.0024	6.6	79.7	-1.2	-6.5
22.0	5511	31.7	.01510	67.7	.10	523.0	270.1	325.0	270.46	37.7	257.7	.0022	6.5	92.4	.3	-6.5
23.0	5787	30.5	.01596	65.5	.10	505.0	268.7	326.6	269.17	51.3	260.2	.0028	6.4	108.8	2.1	-6.1
23.3	5865	30.2	.01619	65.0	.10	500.0	268.3	327.0	268.69	50.7	259.6	.0026	6.1	107.5	1.8	-5.8
24.0	6040	29.6	.01672	63.9	.10	489.0	267.2	327.8	267.61	49.4	258.3	.0025	5.5	104.3	1.4	-5.4
25.0	6333	27.3	.01756	59.4	.10	471.0	265.6	329.3	265.92	46.7	256.2	.0021	5.1	94.7	.4	-5.0
26.0	6618	26.5	.01834	58.1	.10	454.0	263.1	329.7	263.50	63.7	257.5	.0025	5.3	103.0	1.2	-5.2
27.0	6859	27.5	.01901	60.6	.10	440.0	262.0	331.2	262.33	64.0	256.5	.0023	6.3	109.1	2.1	-5.9
28.0	7142	25.8	.01979	57.5	.10	424.0	259.6	331.7	259.86	63.1	254.1	.0020	7.8	104.6	2.0	-7.5
29.0	7434	26.8	.02059	59.7	.11	408.0	258.7	334.2	258.98	55.5	251.8	.0017	7.6	104.5	1.9	-7.3
29.5	7583	26.3	.02100	58.9	.11	400.0	257.7	334.8	257.95	58.0	251.3	.0016	6.1	111.3	2.2	-5.7
30.0	7736	25.8	.02141	58.0	.11	392.0	256.6	335.4	256.89	60.5	250.8	.0016	4.8	122.2	2.5	-4.0
31.0	8048	23.9	.02223	54.2	.11	376.0	254.3	336.3	254.52	56.5	247.9	.0013	2.1	123.0	1.2	-1.8
32.0	8370	26.1	.02309	59.7	.12	360.0	252.4	338.0	252.60	53.7	245.5	.0011	2.7	80.3	-.5	-2.7
32.6	8577	25.7	.02366	59.0	.12	350.0	251.0	338.8	251.18	53.5	244.2	.0009	2.8	84.7	-.3	-2.7
33.0	8726	25.3	02407	58.5	.12	343.0	250.0	339.4	250.17	53.3	243.2	.0009	2.8	87.8	-.1	-2.8
34.0	9007	20.9	.02477	48.7	.10	330.0	247.4	339.6	247.48	50.7	240.2	.0007	2.6	94.9	.2	-2.6
35.0	9297	19.9	.02542	46.8	.10	317.0	245.4	340.7	245.48	49.6	238.1	.0006	3.0	98.2	.4	-3.0
36.0	9667	18.2	.02620	43.2	.10	301.0	243.4	343.0	243.47	40.5	234.3	.0004	2.0	99.2	.3	-1.9
36.1	9690	18.3	.02625	43.5	.10	300.0	243.2	343.0	243.23	40.4	234.1	.0004	2.0	99.8	.3	-2.0
37.0	9931	19.5	.02675	46.7	.11	290.0	240.8	342.9	240.81	39.7	231.7	.0003	2.1	105.1	.6	-2.0
38.0	10252	16.6	.02741	40.4	.10	277.0	237.8	343.2	237.87	42.4	229.6	.0003	3.3	122.4	1.8	-2.8
39.0	10611	16.6	.02809	40.6	.10	263.0	235.7	345.2	235.71	41.5	227.5	.0002	2.0	160.5	1.9	-.7
40.0	10931	14.3	.02865	35.3	.09	251.0	233.1	346.0	233.09	0.0	0.0	0.0000	2.0	209.9	1.7	1.0
40.1	10958	14.4	.02870	35.8	.10	250.0	232.8	346.0	232.84	0.0	0.0	0.0000	2.0	207.1	1.8	.9
41.0	11235	16.3	.02919	40.8	.11	240.0	230.3	346.3	230.31	0.0	0.0	0.0000	2.5	183.6	2.5	.2
42.0	11520	14.7	.02971	37.3	.11	230.0	227.3	346.0	227.33	0.0	0.0	0.0000	3.8	171.2	3.8	-.6
43.0	11844	13.9	.03027	35.9	.11	219.0	224.3	346.1	224.25	0.0	0.0	0.0000	5.7	159.3	5.4	-2.0
44.0	12211	11.7	.03084	30.4	.09	207.0	221.5	347.4	221.51	0.0	0.0	0.0000	7.3	149.4	6.3	-3.7
44.7	12432	12.7	.03117	33.3	.11	200.0	219.8	348.1	219.76	0.0	0.0	0.0000	7.8	149.1	6.7	-4.0
45.0	12530	13.1	.03132	34.6	.11	197.0	219.0	348.3	218.99	0.0	0.0	0.0000	8.0	149.0	6.9	-4.1
46.0	12861	13.0	.03186	34.8	.12	187.0	215.7	348.2	215.69	0.0	0.0	0.0000	7.9	147.8	6.7	-4.2
47.0	13170	13.3	.03237	36.1	.12	178.0	212.4	347.7	212.35	0.0	0.0	0.0000	7.0	144.5	5.7	-4.1
48.0	13490	13.2	.03291	36.3	.13	169.0	209.7	348.6	209.75	0.0	0.0	0.0000	6.1	138.9	4.6	-4.0
49.0	13863	11.6	.03351	32.1	.12	159.0	208.6	352.7	208.58	0.0	0.0	0.0000	3.3	136.6	2.4	-2.2
50.0	14216	12.3	.03406	34.5	.14	150.0	205.7	353.8	205.74	0.0	0.0	0.0000	.4	84.4	0.0	-.4
51.0	14629	13.7	.03476	38.9	.16	140.0	203.1	356.2	203.13	0.0	0.0	0.0000	2.0	291.3	-.7	1.9
52.0	15021	15.1	.03552	43.4	.19	131.0	200.3	358.1	200.33	0.0	0.0	0.0000	21.4	283.0	-4.8	20.8
52.7	15295	15.0	.03607	43.5	.20	125.0	199.8	362.0	199.84	0.0	0.0	0.0000	11.3	292.6	-4.3	10.4
53.0	15437	15.0	.03636	43.5	.20	122.0	199.6	364.1	199.59	0.0	0.0	0.0000	6.5	309.1	-4.1	5.0
54.0	15682	18.0	.03691	51.7	.25	117.0	200.3	369.8	200.33	0.0	0.0	0.0000	11.6	79.6	-2.1	-11.4
55.0	16042	34.6	.03819	100.7	.52	110.0	198.3	372.6	198.33	0.0	0.0	0.0000	4.3	319.5	-3.3	2.8
56.0	16479	47.4	.04063	138.7	.77	102.0	197.3	378.8	197.29	0.0	0.0	0.0000	1.2	335.1	-1.1	.5
56.4	16593	48.8	.04140	142.2	.81	100.0	198.0	382.2	197.97	0.0	0.0	0.0000	1.4	104.6	.3	-1.3
57.0	16782	51.1	.04266	148.0	.87	96.8	199.1	388.0	199.09	0.0	0.0	0.0000	5.1	122.0	2.7	-4.3
58.0	17141	54.6	.04524	159.2	.99	91.0	197.8	392.3	197.81	0.0	0.0	0.0000	10.2	121.3	5.3	-8.7
59.0	17469	63.2	.04786	183.4	1.22	86.0	199.1	401.3	199.09	0.0	0.0	0.0000	8.7	110.9	3.1	-8.1
60.0	17843	70.0	.05121	199.4	1.44	80.7	202.7	416.0	202.68	0.0	0.0	0.0000	8.9	94.7	.7	-8.8
60.1	17894	71.4	.05172	203.1	1.48	80.0	203.0	417.7	203.00	0.0	0.0	0.0000	8.3	95.1	.7	-8.3
61.0	18201	79.7	.05475	224.5	1.74	76.0	204.9	427.8	204.89	0.0	0.0	0.0000	5.2	98.6	.8	-5.2
62.0	18570	87.4	.05877	241.6	2.03	71.5	209.0	444.1	208.97	0.0	0.0	0.0000	.6	45.4	-.4	-.4
62.3	18699	89.3	.06028	246.6	2.12	70.0	209.0	446.8	208.97	0.0	0.0	0.0000	2.5	59.0	-1.3	-2.2
63.0	18967	93.0	.06340	256.9	2.30	67.0	209.0	452.4	208.97	0.0	0.0	0.0000	6.6	61.7	-3.1	-5.8
64.0	19344	97.3	.06802	267.0	2.56	63.0	210.3	463.4	210.32	0.0	0.0	0.0000	10.0	77.9	-2.1	-9.8
64.9	19646	102.1	.07188	277.4	2.82	60.0	212.5	474.8	212.52	0.0	0.0	0.0000	9.2	89.4	-.1	-9.2
65.0	19698	103.0	.07254	279.2	2.87	59.5	212.9	476.8	212.89	0.0	0.0	0.0000	9.1	91.5	.2	-9.1
66.0	20076	106.1	.07754	287.7	3.14	56.0	212.9	485.1	212.89	0.0	0.0	0.0000	9.7	104.1	2.4	-9.4

TIME MIN	ALT GPM	OZONE MICMB	TOTOZ ATMCM	OZDEN MG/M3	OZMXR MICGG	PRESS MB	TEMP DEG K	PTEMP DEG K	VTEMP DEG K	HMDTY PRCNT	DEWPT DEG K	SPCFC HMDTY	SPD MPS	DIR DEG	NS MPS	EW MPS
67.0	20480	119.8	.08329	322.2	3.78	52.5	214.7	498.2	214.66	0.0	0.0	0.0000	7.1	126.4	4.2	-5.7
68.0	20786	127.7	.08806	342.8	4.23	50.0	215.2	506.4	215.15	0.0	0.0	0.0000	5.5	148.1	4.7	-2.9
68.0	20799	128.1	.08826	343.7	4.25	49.9	215.2	506.7	215.17	0.0	0.0	0.0000	5.5	149.2	4.7	-2.8
69.0	21177	133.9	.09444	357.6	4.72	47.0	216.2	517.9	216.19	0.0	0.0	0.0000	4.8	138.4	3.6	-3.2
70.0	21594	138.7	.10154	370.6	5.22	44.0	216.0	527.3	216.03	0.0	0.0	0.0000	4.1	125.6	2.4	-3.3
71.0	22011	144.0	.10687	382.3	5.79	41.2	217.5	541.1	217.53	0.0	0.0	0.0000	3.4	136.1	2.4	-2.4
71.5	22198	147.4	.11230	391.6	6.11	40.0	217.3	545.2	217.35	0.0	0.0	0.0000	3.5	136.6	2.6	-2.4
72.0	22360	150.3	.11524	399.6	6.39	39.0	217.2	548.8	217.20	0.0	0.0	0.0000	3.6	137.0	2.6	-2.5
73.0	22728	149.3	.12211	398.3	6.72	36.8	216.4	555.8	216.36	0.0	0.0	0.0000	2.7	139.5	2.1	-1.8
73.7	23045	149.5	.12802	398.6	7.08	35.0	216.5	564.2	216.48	0.0	0.0	0.0000	1.6	147.1	1.3	-.8
74.0	23174	149.6	.13040	398.8	7.22	34.3	216.5	567.6	216.53	0.0	0.0	0.0000	1.1	154.6	1.0	-.5
75.0	23594	150.1	.13824	399.8	7.75	32.1	216.7	578.9	216.70	0.0	0.0	0.0000	4.5	91.8	.1	-4.5
76.0	24024	153.3	.14633	406.2	8.47	30.0	217.9	593.3	217.86	0.0	0.0	0.0000	9.5	99.4	1.5	-9.4
77.0	24375	157.9	.15306	414.8	9.21	28.4	219.8	608.0	219.79	0.0	0.0	0.0000	10.4	111.8	3.8	-9.6
78.0	24749	165.7	.16047	432.0	10.25	26.8	221.5	623.0	221.51	0.0	0.0	0.0000	6.7	112.8	2.6	-6.2
78.9	25199	163.1	.16948	425.4	10.81	25.0	221.4	635.1	221.37	0.0	0.0	0.0000	5.7	99.3	.9	-5.6
79.0	25225	163.0	.17000	425.1	10.84	24.9	221.4	635.8	221.36	0.0	0.0	0.0000	5.7	98.4	.8	-5.6
80.0	25711	161.9	.17962	422.2	11.61	23.1	221.4	649.6	221.36	0.0	0.0	0.0000	7.3	103.5	1.7	-7.1
81.0	26268	159.5	.19050	414.4	12.47	21.2	222.3	668.5	222.28	0.0	0.0	0.0000	999.9	999.9	999.9	999.9
81.8	26647	155.8	.19773	403.9	12.91	20.0	222.8	681.2	222.77	0.0	0.0	0.0000	999.9	999.9	999.9	999.9
82.0	26746	154.9	.19961	401.2	13.03	19.7	222.9	684.5	222.90	0.0	0.0	0.0000	999.9	999.9	999.9	999.9
83.0	27157	149.7	.20716	386.1	13.40	18.5	223.8	699.8	223.80	0.0	0.0	0.0000	999.9	999.9	999.9	999.9
83.9	27521	145.0	.21361	373.2	13.73	17.5	224.3	712.7	224.34	0.0	0.0	0.0000	999.9	999.9	999.9	999.9
84.0	27559	144.5	.21427	371.9	13.76	17.4	224.4	714.0	224.40	0.0	0.0	0.0000	999.9	999.9	999.9	999.9
85.0	27948	139.0	.22089	356.1	14.04	16.4	225.3	729.1	225.29	0.0	0.0	0.0000	999.9	999.9	999.9	999.9
86.0	28406	133.9	.22837	342.3	14.50	15.3	225.9	745.6	225.88	0.0	0.0	0.0000	999.9	999.9	999.9	999.9
86.3	28537	132.6	.23042	338.6	14.65	15.0	226.1	750.6	226.07	0.0	0.0	0.0000	999.9	999.9	999.9	999.9
87.0	28900	128.9	.23610	328.3	15.04	14.2	226.6	764.2	226.61	0.0	0.0	0.0000	999.9	999.9	999.9	999.9
88.0	29435	123.6	.24413	314.1	15.63	13.1	227.2	784.0	227.19	0.0	0.0	0.0000	999.9	999.9	999.9	999.9
88.5	29747	120.7	.24861	306.1	16.00	12.5	227.7	796.5	227.72	0.0	0.0	0.0000	999.9	999.9	999.9	999.9
89.0	30019	118.2	.25250	299.1	16.32	12.0	228.2	807.4	228.19	0.0	0.0	0.0000	999.9	999.9	999.9	999.9
90.0	30480	113.1	.25880	285.5	16.73	11.2	228.8	825.6	228.76	0.0	0.0	0.0000	999.9	999.9	999.9	999.9
91.0	30977	105.4	.26519	265.6	16.80	10.4	229.2	844.8	229.19	0.0	0.0	0.0000	999.9	999.9	999.9	999.9
91.6	31239	101.8	.26835	256.6	16.86	10.0	229.0	853.8	229.03	0.0	0.0	0.0000	999.9	999.9	999.9	999.9
92.0	31444	98.9	.27080	249.5	16.90	9.7	228.9	860.7	228.90	0.0	0.0	0.0000	999.9	999.9	999.9	999.9
93.0	31871	91.3	.27560	230.6	16.62	9.1	228.5	874.9	228.48	0.0	0.0	0.0000	999.9	999.9	999.9	999.9
94.0	32565	84.3	.28281	214.3	17.04	8.2	227.2	896.3	227.19	0.0	0.0	0.0000	999.9	999.9	999.9	999.9

INTEGRAL .28281 RESIDUAL .06658 INTEGRATED TOTAL OZONE .34939

OZONAGRAM

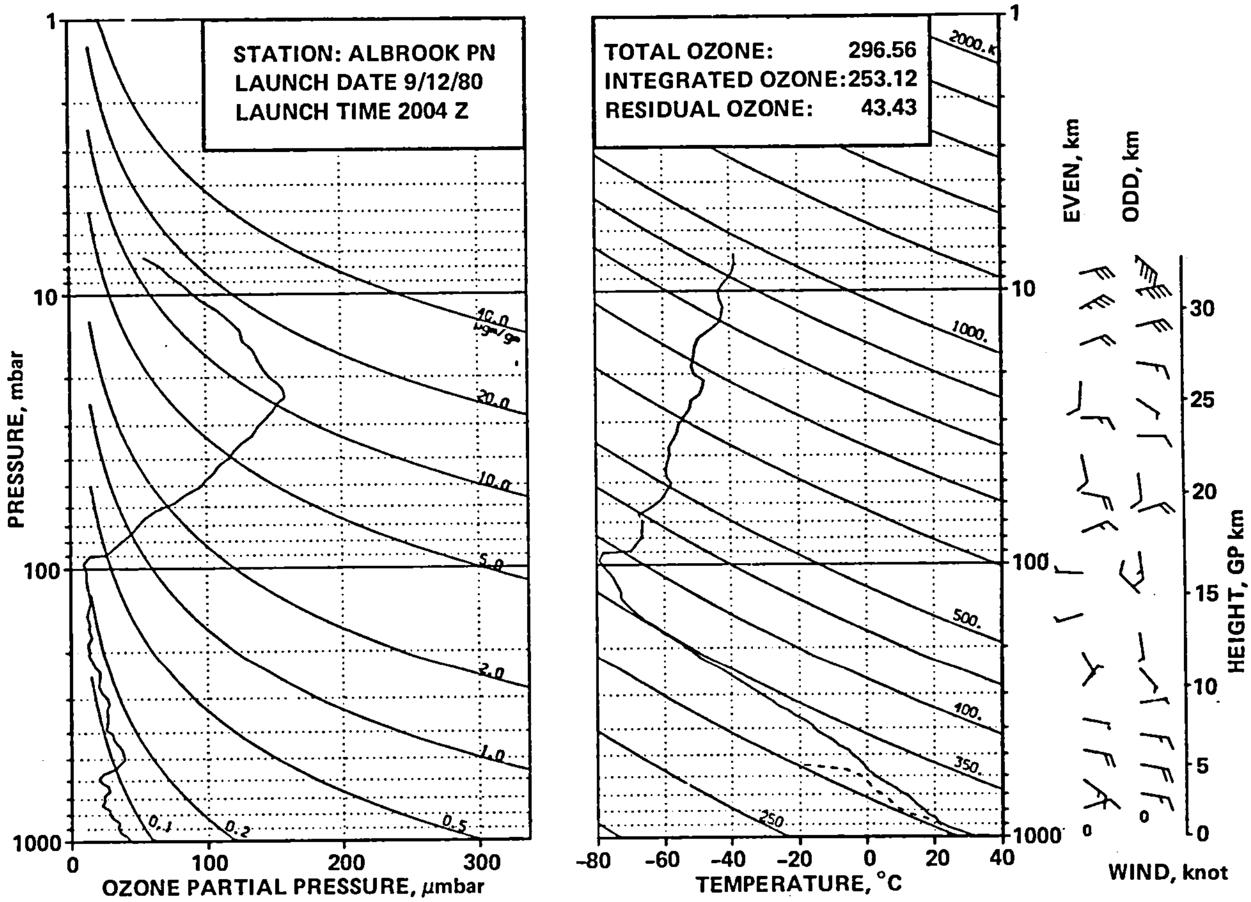

STATION: ALBROOK PN
LAUNCH DATE 9/12/80
LAUNCH TIME 2004 Z
TOTAL OZONE: 296.56
INTEGRATED OZONE: 253.12
RESIDUAL OZONE: 43.43
PRESSURE, mbar
OZONE PARTIAL PRESSURE, µmbar
TEMPERATURE, °C
EVEN, km
ODD, km
HEIGHT, GP km
WIND, knot

STATION ALBROOK PN   LAUNCH DATE 9/12/80   TIME 2004Z   ECC   SONDE 3A1338

SURFACE CONDITIONS   PRESS 1000.0MB   TEMP 304.8 DEG K   HUMIDITY 61.0 PRCNT

TIME MIN	ALT GPM	OZONE MICMB	TOTOZ ATMCM	OZDEN MG/M3	OZMXR MICGG	PRESS MB	TEMP DEG K	PTEMP DEG K	VTEMP DEG K	HMDTY PRCNT	DEWPT DEG K	SPCFC HMDTY	SPD MPS	DIR DEG	NS MPS	EW MPS
0.0	66	43.9	0.00000	83.1	.07	1000.0	305.0	305.0	308.51	63.9	297.3	.0189	1.0	140.0	.8	-.6
1.0	404	41.5	.00127	79.4	.07	963.0	301.6	304.9	305.16	75.4	296.9	.0191	1.6	181.9	1.6	.1
2.0	742	36.4	.00244	70.6	.07	927.0	297.5	304.1	300.90	89.2	295.6	.0184	1.5	198.4	1.4	.5
2.7	1001	35.2	.00327	68.9	.06	900.0	295.4	304.4	298.63	95.3	294.6	.0176	.2	303.6	-.1	.1
3.0	1099	34.8	.00358	68.2	.06	890.0	294.6	304.6	297.77	97.5	294.2	.0176	.6	359.2	-.6	0.0
4.0	1458	35.7	.00473	70.1	.07	854.0	293.5	307.1	296.10	82.3	290.4	.0144	2.3	12.1	-2.2	-.5
4.1	1498	35.0	.00486	69.0	.07	850.0	293.2	307.1	295.69	81.1	289.8	.0137	2.3	18.9	-2.2	-.7
5.0	1766	31.0	.00567	61.6	.06	824.0	291.0	307.5	292.98	73.0	286.1	.0113	3.2	53.3	-1.9	-2.5
5.8	2018	29.0	.00637	57.6	.06	800.0	290.3	309.4	292.05	65.2	283.7	.0097	3.8	69.8	-1.3	-3.6
6.0	2072	28.5	.00651	56.8	.06	795.0	290.1	309.8	291.86	63.6	283.2	.0097	4.0	72.5	-1.2	-3.8
7.0	2355	28.5	.00726	57.2	.06	769.0	288.3	310.8	289.88	62.9	281.3	.0088	4.7	86.1	-.3	-4.7
8.0	2680	22.9	.00804	46.1	.05	740.0	287.0	312.7	288.43	63.4	280.1	.0084	6.4	92.2	.2	-6.4
9.0	2993	24.9	.00874	50.2	.06	713.0	285.6	314.6	287.00	63.3	278.8	.0080	6.9	97.9	.9	-6.8
9.4	3146	24.7	.00910	50.2	.06	700.0	284.4	315.0	285.75	62.9	277.6	.0072	6.8	103.3	1.6	-6.6
10.0	3340	24.6	.00955	50.2	.06	684.0	283.0	315.4	284.18	62.5	276.2	.0069	6.9	110.2	2.4	-6.4
11.0	3661	28.5	.01037	58.6	.07	658.0	281.2	316.9	282.28	62.9	274.5	.0064	6.7	121.0	3.4	-5.7
12.0	4018	27.3	.01132	56.5	.07	630.0	278.4	317.7	279.43	70.6	273.5	.0062	7.0	127.6	4.3	-5.5
13.0	4307	22.1	.01202	46.2	.06	608.0	276.4	318.6	277.34	74.5	272.3	.0059	7.4	124.5	4.2	-6.1
13.4	4414	21.7	.01224	45.5	.06	600.0	275.7	319.1	276.67	72.8	271.3	.0054	7.6	120.4	3.8	-6.5
14.0	4591	21.0	.01261	44.2	.06	587.0	274.7	319.9	275.55	70.1	269.9	.0051	8.0	114.0	3.3	-7.3
15.0	4869	24.3	.01323	51.3	.07	567.0	273.1	321.1	273.77	61.3	266.5	.0041	9.9	104.7	2.5	-9.5
16.0	5185	33.1	.01413	70.3	.10	545.0	272.3	323.9	272.55	23.8	254.2	.0016	9.5	99.8	1.6	-9.4
17.0	5497	36.1	.01520	76.8	.11	524.0	271.0	326.0	271.04	0.0	0.0	0.0000	8.7	100.7	1.6	-8.6
18.0	5820	39.8	.01643	85.4	.13	503.0	269.0	327.4	269.02	0.0	0.0	0.0000	10.0	102.1	2.1	-9.8
18.1	5866	39.7	.01661	85.2	.13	500.0	268.8	327.7	268.83	0.0	0.0	0.0000	10.0	101.9	2.1	-9.7
19.0	6155	38.9	.01775	83.9	.13	482.0	267.7	329.7	267.66	0.0	0.0	0.0000	9.4	100.8	1.8	-9.2
20.0	6485	37.6	.01903	82.1	.13	462.0	264.7	330.0	264.69	0.0	0.0	0.0000	8.2	101.4	1.6	-8.1
21.0	6827	34.5	.02029	75.7	.13	442.0	263.2	332.4	263.36	0.0	0.0	0.0000	8.1	101.3	1.6	-7.9
22.0	7164	31.6	.02144	70.0	.12	423.0	260.4	333.0	260.51	21.0	242.7	.0007	7.8	96.3	.9	-7.7
23.0	7456	31.2	.02239	69.7	.13	407.0	258.2	333.8	258.31	33.4	245.6	.0010	6.6	92.6	.3	-6.6
23.4	7586	29.1	.02278	65.2	.12	400.0	257.7	334.8	257.83	39.0	246.7	.0012	5.5	94.7	.4	-5.5
24.0	7778	26.1	.02335	58.7	.11	390.0	256.9	336.2	257.12	47.2	248.3	.0013	4.1	99.5	.7	-4.0
25.0	8092	26.8	.02423	60.8	.12	374.0	254.9	337.6	255.00	36.3	243.6	.0009	1.9	101.0	.4	-1.9
26.0	8416	27.3	.02516	62.6	.13	358.0	251.8	337.6	251.86	33.3	239.9	.0006	3.3	87.7	-.1	-3.3
26.5	8581	27.2	.02565	62.6	.13	350.0	250.8	338.5	250.85	24.2	235.3	.0004	4.1	94.8	.3	-4.0
27.0	8730	27.1	.02608	62.7	.13	343.0	249.9	339.3	249.94	0.0	0.0	0.0000	4.8	99.2	.8	-4.7
28.0	9011	26.5	.02690	61.9	.13	330.0	247.1	339.2	247.15	0.0	0.0	0.0000	3.0	93.5	.2	-3.0
29.0	9346	28.5	.02791	67.1	.15	315.0	245.1	341.0	245.16	0.0	0.0	0.0000	2.0	21.3	-1.8	-.7
30.0	9694	27.3	.02898	65.1	.15	300.0	242.2	341.7	242.24	0.0	0.0	0.0000	1.9	10.8	-1.9	-.4
31.0	10031	23.0	.02993	55.3	.13	286.0	239.4	342.4	239.44	0.0	0.0	0.0000	2.1	6.1	-2.1	-.2
32.0	10432	20.4	.03091	49.8	.13	270.0	236.5	343.8	236.49	0.0	0.0	0.0000	2.9	359.5	-2.9	0.0
33.0	10851	21.6	.03193	53.6	.14	254.0	232.9	344.6	232.95	0.0	0.0	0.0000	3.1	7.5	-3.1	-.4
33.3	10958	21.6	.03220	53.7	.14	250.0	232.1	344.9	232.09	0.0	0.0	0.0000	2.9	3.8	-2.9	-.2
34.0	11235	21.5	.03289	54.1	.15	240.0	229.9	345.6	229.89	0.0	0.0	0.0000	2.5	352.1	-2.5	.3
35.0	11548	17.6	.03362	44.9	.13	229.0	227.0	345.9	227.04	0.0	0.0	0.0000	1.1	342.6	-1.0	.3
36.0	11873	16.3	.03428	41.9	.12	218.0	224.1	346.3	224.10	0.0	0.0	0.0000	1.8	145.8	1.5	-1.0
37.0	12211	13.6	.03489	35.5	.11	207.0	221.8	347.9	221.82	0.0	0.0	0.0000	3.4	157.7	3.1	-1.3
37.8	12433	13.6	.03526	35.8	.11	200.0	219.8	348.0	219.76	0.0	0.0	0.0000	3.0	163.5	2.9	-.9
38.0	12498	13.6	.03536	35.9	.11	198.0	219.2	348.1	219.15	0.0	0.0	0.0000	2.9	165.5	2.8	-.7
39.0	12862	13.1	.03597	35.1	.12	187.0	216.4	349.3	216.36	0.0	0.0	0.0000	3.6	171.0	3.5	-.6
40.0	13172	15.6	.03653	42.4	.15	178.0	213.1	348.9	213.07	0.0	0.0	0.0000	3.4	171.4	3.3	-.5
41.0	13567	13.6	.03726	37.3	.13	167.0	210.5	351.0	210.51	0.0	0.0	0.0000	2.6	184.6	2.6	.2
42.0	13867	14.2	.03780	39.5	.15	159.0	207.4	350.7	207.39	0.0	0.0	0.0000	1.8	211.5	1.5	.9
42.9	14217	12.4	.03841	34.9	.14	150.0	205.0	352.4	204.95	0.0	0.0	0.0000	3.9	286.0	-1.1	3.8
43.0	14258	12.2	.03848	34.3	.14	149.0	204.7	352.6	204.67	0.0	0.0	0.0000	4.3	288.6	-1.4	4.1
44.0	14629	13.4	.03911	38.3	.16	140.0	202.2	354.6	202.22	0.0	0.0	0.0000	7.2	297.5	-3.3	6.4
45.0	14975	14.6	.03976	42.2	.18	132.0	200.3	357.3	200.33	0.0	0.0	0.0000	5.3	309.6	-3.4	4.1
46.0	15247	14.0	.04028	40.3	.18	126.0	200.3	362.1	200.33	0.0	0.0	0.0000	4.6	326.7	-3.8	2.5
46.1	15293	13.8	.04037	39.9	.18	125.0	200.2	362.6	200.18	0.0	0.0	0.0000	4.3	329.0	-3.7	2.2
47.0	15630	12.7	.04097	37.0	.18	118.0	199.1	366.6	199.09	0.0	0.0	0.0000	3.0	355.2	-3.0	.3
48.0	16038	11.7	.04165	34.0	.18	110.0	197.8	371.7	197.81	0.0	0.0	0.0000	1.6	276.3	-.2	1.6
49.0	16472	11.6	.04234	34.4	.19	102.0	195.4	375.1	195.38	0.0	0.0	0.0000	4.7	218.4	3.7	2.9
49.3	16584	11.0	.04251	32.5	.18	100.0	194.9	376.3	194.89	0.0	0.0	0.0000	5.0	200.0	4.7	1.7
50.0	16805	9.6	.04284	28.7	.17	96.2	193.9	378.6	193.94	0.0	0.0	0.0000	6.7	173.9	6.6	-.7
51.0	17152	14.0	.04341	41.5	.26	90.5	195.1	387.6	195.09	0.0	0.0	0.0000	7.4	171.9	7.3	-1.0
52.0	17236	27.0	.04364	76.5	.50	89.2	203.4	405.6	203.35	0.0	0.0	0.0000	6.2	123.1	3.4	-5.2
52.9	17888	38.2	.04649	107.0	.79	80.0	206.3	424.6	206.30	0.0	0.0	0.0000	7.2	85.7	-.5	-7.2
53.0	17949	39.3	.04675	109.8	.82	79.2	206.6	426.3	206.57	0.0	0.0	0.0000	7.5	83.0	-.9	-7.4
54.0	18294	45.4	.04866	126.9	1.01	74.8	206.6	433.3	206.57	0.0	0.0	0.0000	5.8	40.9	-4.4	-3.8
55.0	18695	50.3	.05116	140.4	1.19	70.0	206.8	442.0	206.78	0.0	0.0	0.0000	8.2	35.7	-6.6	-4.8
56.0	19059	55.2	.05367	155.0	1.39	65.9	205.7	447.5	205.74	0.0	0.0	0.0000	10.4	72.1	-3.2	-9.9
57.0	19449	63.4	.05668	174.7	1.70	61.8	209.6	464.2	209.55	0.0	0.0	0.0000	12.7	91.6	.3	-12.7
57.5	19631	69.7	.05832	190.7	1.93	60.0	210.9	471.3	210.94	0.0	0.0	0.0000	12.3	94.3	.9	-12.2
58.0	19841	77.0	.06019	209.1	2.20	58.0	212.5	479.4	212.53	0.0	0.0	0.0000	11.7	97.7	1.6	-11.6
59.0	20264	84.6	.06451	228.3	2.59	54.2	214.0	492.1	213.96	0.0	0.0	0.0000	8.9	104.6	2.2	-8.6
60.0	20721	96.4	.06970	258.1	3.17	50.4	215.5	506.1	215.52	0.0	0.0	0.0000	4.5	133.1	3.1	-3.3
60.2	20771	96.9	.07032	259.8	3.21	50.0	215.3	506.7	215.31	0.0	0.0	0.0000	4.5	140.2	3.4	-2.9
61.0	21054	99.8	.07380	269.1	3.46	47.8	214.1	510.5	214.13	0.0	0.0	0.0000	5.7	173.6	5.7	-.6
62.0	21432	105.9	.07870	285.9	3.90	45.0	213.8	518.5	213.78	0.0	0.0	0.0000	6.7	181.1	6.7	.1
63.0	21819	109.7	.08396	295.4	4.30	42.3	214.3	529.1	214.31	0.0	0.0	0.0000	5.7	165.3	5.5	-1.4
63.9	22170	116.5	.08897	313.1	4.83	40.0	214.9	539.2	214.95	0.0	0.0	0.0000	6.2	168.8	6.0	-1.2
64.0	22202	117.2	.08941	314.6	4.88	39.8	215.0	540.1	215.00	0.0	0.0	0.0000	6.2	169.1	6.1	-1.2
65.0	22576	120.9	.09500	325.2	5.34	37.5	214.7	548.5	214.66	0.0	0.0	0.0000	4.8	173.2	4.8	-.6

TIME MIN	ALT GPM	OZONE MICMB	TOTOZ ATMCM	OZDEN MG/M3	OZMXR MICGG	PRESS MB	TEMP DEG K	PTEMP DEG K	VTEMP DEG K	HMDTY PRCNT	DEWPT DEG K	SPCFC HMDTY	SPD MPS	DIR DEG	NS MPS	EW MPS
66.0	22993	126.6	.10146	338.4	5.98	35.1	216.0	562.5	216.03	0.0	0.0	0.0000	3.3	96.1	.3	-3.2
66.0	23011	127.0	.10176	339.3	6.01	35.0	216.1	563.1	216.08	0.0	0.0	0.0000	3.4	93.9	.2	-3.4
67.0	23384	134.4	.10782	357.4	6.75	33.0	217.2	575.6	217.20	0.0	0.0	0.0000	6.8	71.6	-2.1	-6.4
68.0	23844	138.2	.11559	366.5	7.46	30.7	217.7	589.0	217.69	0.0	0.0	0.0000	8.5	84.0	-.9	-8.5
68.3	23991	140.1	.11816	370.6	7.75	30.0	218.3	594.5	218.27	0.0	0.0	0.0000	7.6	87.8	-.3	-7.6
69.0	24297	144.2	.12348	379.3	8.35	28.6	219.5	605.9	219.47	0.0	0.0	0.0000	5.7	99.5	.9	-5.7
70.0	24740	149.7	.13145	390.6	9.29	26.7	221.2	622.8	221.20	0.0	0.0	0.0000	2.1	116.0	.9	-1.9
71.0	25140	153.1	.13883	399.0	10.11	25.1	221.5	634.8	221.51	0.0	0.0	0.0000	2.3	126.7	1.4	-1.9
71.1	25166	153.5	.13932	399.7	10.18	25.0	221.7	636.1	221.71	0.0	0.0	0.0000	2.3	133.4	1.6	-1.7
72.0	25487	158.7	.14537	408.9	11.05	23.8	224.1	652.0	224.10	0.0	0.0	0.0000	3.8	194.2	3.7	.9
73.0	25944	157.2	.15405	403.0	11.73	22.2	225.1	668.2	225.14	0.0	0.0	0.0000	4.5	188.7	4.5	.7
74.0	26279	153.2	.16027	392.4	12.03	21.1	225.4	678.9	225.44	0.0	0.0	0.0000	5.0	173.7	5.0	-.5
75.0	26597	147.6	.16603	383.0	12.17	20.1	222.6	679.7	222.59	0.0	0.0	0.0000	3.4	142.9	2.7	-2.1
75.1	26629	147.3	.16660	382.1	12.20	20.0	222.5	680.4	222.52	0.0	0.0	0.0000	3.5	137.5	2.6	-2.4
76.0	27032	142.8	.17369	371.8	12.58	18.8	221.7	689.9	221.67	0.0	0.0	0.0000	6.5	99.0	1.0	-6.4
76.9	27497	139.1	.18165	361.4	13.17	17.5	222.2	706.0	222.24	0.0	0.0	0.0000	7.5	91.1	.1	-7.5
77.0	27535	138.8	.18229	360.6	13.22	17.4	222.3	707.3	222.28	0.0	0.0	0.0000	7.6	90.5	.1	-7.6
78.0	28081	135.3	.19136	350.6	14.01	16.0	222.7	726.0	222.74	0.0	0.0	0.0000	10.5	69.7	-3.6	-9.8
78.8	28503	128.9	.19805	332.7	14.24	15.0	223.7	742.8	223.74	0.0	0.0	0.0000	13.3	79.5	-2.4	-13.1
79.0	28591	127.6	.19945	328.9	14.28	14.8	224.0	746.3	223.95	0.0	0.0	0.0000	13.9	81.1	-2.2	-13.8
80.0	29150	125.9	.20790	318.5	15.34	13.6	228.2	779.1	228.19	0.0	0.0	0.0000	15.1	76.0	-3.7	-14.7
81.0	29504	121.4	.21306	304.4	15.60	12.9	230.3	798.3	230.31	0.0	0.0	0.0000	18.3	57.1	-9.9	-15.3
81.5	29716	118.3	.21600	296.2	15.68	12.5	230.6	806.5	230.59	0.0	0.0	0.0000	18.8	57.3	-10.2	-15.9
82.0	29936	115.1	.21903	287.8	15.76	12.1	230.9	815.0	230.87	0.0	0.0	0.0000	19.5	57.6	-10.4	-16.4
83.0	30339	108.7	.22429	271.6	15.80	11.4	231.2	830.0	231.15	0.0	0.0	0.0000	18.8	69.3	-6.6	-17.5
84.0	30767	99.2	.22949	248.8	15.36	10.7	230.2	841.6	230.17	0.0	0.0	0.0000	21.0	78.6	-4.2	-20.6
85.0	31222	91.2	.23457	229.1	15.11	10.0	229.8	856.4	229.75	0.0	0.0	0.0000	22.7	80.6	-3.7	-22.4
86.0	31712	84.5	.23960	210.5	15.05	9.3	231.7	881.8	231.71	0.0	0.0	0.0000	16.1	74.7	-4.2	-15.5
87.0	32245	75.3	.24453	185.8	14.50	8.6	233.9	910.3	233.91	0.0	0.0	0.0000	14.6	78.5	-2.9	-14.3
87.9	32740	68.5	.24860	168.6	14.18	8.0	234.6	932.1	234.60	0.0	0.0	0.0000	22.5	89.0	-.4	-22.5
88.0	32827	67.4	.24931	165.7	14.13	7.9	234.7	935.9	234.73	0.0	0.0	0.0000	23.9	90.2	.1	-23.9
89.0	33369	55.0	.25312	135.4	12.48	7.3	234.5	956.2	234.45	0.0	0.0	0.0000	999.9	999.9	999.9	999.9

INTEGRAL .25312 RESIDUAL .04343 INTEGRATED TOTAL OZONE .29656

OZONAGRAM

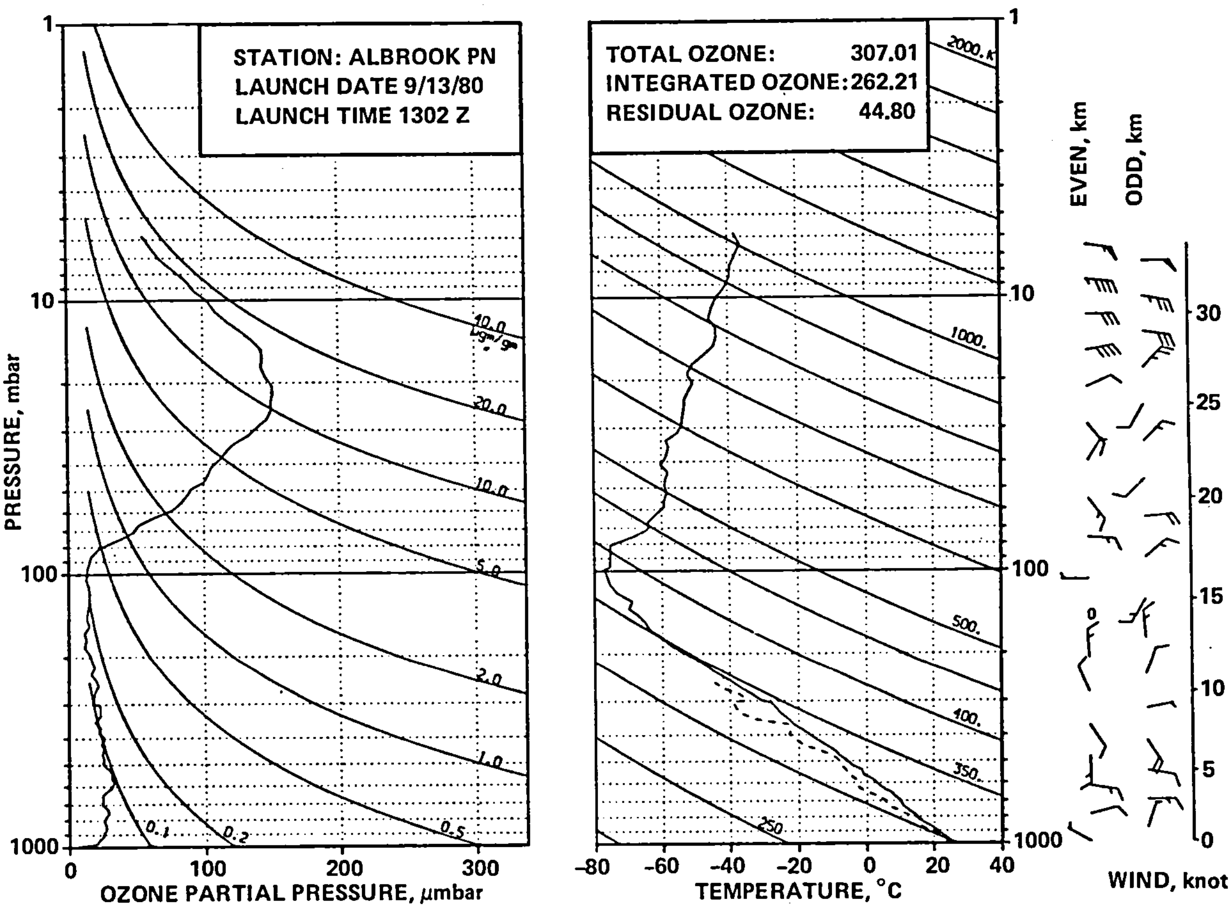
STATION: ALBROOK PN
LAUNCH DATE 9/13/80
LAUNCH TIME 1302 Z
TOTAL OZONE: 307.01
INTEGRATED OZONE: 262.21
RESIDUAL OZONE: 44.80
PRESSURE, mbar
OZONE PARTIAL PRESSURE, μmbar
TEMPERATURE, °C
EVEN, km
ODD, km
HEIGHT, GP km
WIND, knot
1
10
100
1000
0
100
200
300
-80
-60
-40
-20
0
20
40
0
5
10
15
20
25
30
10.0 μgm/gm
20.0
10.0
5.0
2.0
1.0
0.5
0.2
0.1
2000. K
1000.
500.
400.
350.
250.

STATION ALBROOK PN   LAUNCH DATE 9/13/80   TIME 1302Z   ECC   SONDE 3A1339

SURFACE CONDITIONS   PRESS 1004.2MB   TEMP 297.3 DEG K   HUMIDITY 99.0 PRCNT

TIME MIN	ALT GPM	OZONE MICMB	TOTOZ ATMCM	OZDEN MG/M3	OZMXR MICGG	PRESS MB	TEMP DEG K	PTEMP DEG K	VTEMP DEG K	HMDTY PRCNT	DEWPT DEG K	SPCFC HMDTY	SPD MPS	DIR DEG	NS MPS	EW MPS
0.0	66	.6	0.00000	1.1	0.00	1004.2	297.3	297.0	300.76	100.0	297.3	.0189	2.0	300.0	-1.0	1.7
.1	102	3.2	.00003	6.3	.01	1000.0	297.4	297.4	300.86	99.2	297.3	.0189	2.3	302.6	-1.2	1.9
1.0	335	20.2	.00025	39.1	.03	974.0	298.0	300.3	301.49	93.8	297.0	.0190	3.9	311.0	-2.6	3.0
2.0	610	21.8	.00077	42.5	.04	944.0	296.6	301.6	299.90	93.2	295.5	.0179	3.3	335.2	-3.0	1.4
3.0	864	24.8	.00130	48.5	.04	917.0	295.1	302.5	298.17	95.6	294.3	.0172	3.1	5.4	-3.1	-.3
3.6	1026	25.2	.00167	49.4	.05	900.0	294.3	303.3	297.09	89.3	292.4	.0150	3.1	15.8	-3.0	-.8
4.0	1134	25.4	.00192	50.0	.05	889.0	293.8	303.8	296.37	85.2	291.2	.0146	3.2	22.6	-2.9	-1.2
5.0	1410	27.1	.00258	53.6	.05	861.0	291.8	304.6	294.18	84.1	289.1	.0132	3.0	18.0	-2.9	-.9
5.4	1520	27.0	.00285	53.6	.05	850.0	291.0	304.8	293.38	90.7	289.4	.0138	2.8	25.4	-2.5	-1.2
6.0	1673	26.9	.00323	53.6	.05	835.0	289.8	305.1	292.28	100.0	289.8	.0142	2.6	37.3	-2.1	-1.6
7.0	1943	25.7	.00389	51.4	.05	809.0	288.6	306.6	290.88	97.2	288.1	.0131	4.5	71.3	-1.5	-4.3
7.3	2038	26.0	.00412	52.2	.05	800.0	288.1	307.1	290.33	93.1	287.0	.0119	4.9	74.9	-1.3	-4.8
8.0	2253	26.8	.00464	53.8	.06	780.0	287.2	308.3	289.08	84.1	284.5	.0108	5.9	81.1	-.9	-5.8
9.0	2505	29.2	.00530	59.1	.06	757.0	285.6	309.3	287.33	80.9	282.5	.0097	7.2	79.9	-1.3	-7.1
10.0	2855	28.0	.00625	57.0	.06	726.0	283.8	311.0	285.15	72.5	279.0	.0080	7.8	81.7	-1.1	-7.8
11.0	3159	24.4	.00700	49.7	.06	700.0	283.2	313.6	284.62	72.7	278.6	.0080	7.1	93.5	.4	-7.1
11.0	3171	24.3	.00703	49.4	.06	699.0	283.2	313.7	284.60	72.7	278.5	.0090	7.1	94.0	.5	-7.0
12.0	3473	25.0	.00774	51.4	.06	674.0	281.6	315.2	282.82	70.5	276.5	.0072	8.0	104.9	2.1	-7.7
13.0	3759	24.4	.00842	50.2	.06	651.0	280.5	317.1	281.56	61.6	273.6	.0060	8.7	110.4	3.0	-8.2
14.0	4015	26.9	.00905	55.9	.07	631.0	278.3	317.4	279.16	61.2	271.4	.0053	7.3	101.6	1.5	-7.2
15.0	4317	31.3	.00990	65.4	.09	608.0	276.6	318.8	277.40	61.1	269.8	.0049	6.9	85.1	-.6	-6.8
15.3	4424	31.8	.01024	66.6	.09	600.0	276.0	319.4	276.88	63.7	269.8	.0050	6.6	84.3	-.7	-6.6
16.0	4684	33.1	.01106	69.5	.09	581.0	274.8	320.9	275.62	70.0	269.9	.0051	6.0	82.2	-.8	-5.9
17.0	4979	31.3	.01199	66.5	.09	560.0	272.2	321.2	272.95	72.2	267.8	.0046	5.9	96.9	.7	-5.9
18.0	5313	31.4	.01303	66.7	.10	537.0	271.6	324.3	272.29	70.3	266.9	.0044	6.2	110.0	2.1	-5.8
19.0	5598	28.8	.01388	61.9	.09	518.0	268.9	324.5	269.61	77.8	265.6	.0042	20.1	93.5	1.2	-20.1
19.9	5875	25.6	.01464	55.2	.08	500.0	267.5	326.1	268.19	83.6	265.2	.0042	7.2	111.8	2.7	-6.6
20.0	5923	25.0	.01476	54.0	.08	497.0	267.3	326.4	267.95	84.5	265.1	.0042	5.2	123.6	2.9	-4.4
21.0	6244	25.6	.01558	55.8	.09	477.0	265.2	327.7	265.80	85.7	263.2	.0037	12.5	247.5	4.8	11.6
22.0	6593	24.4	.01647	53.5	.09	456.0	263.7	330.1	264.20	70.3	259.3	.0029	6.4	139.5	4.9	-4.2
23.0	6903	25.9	.01727	57.1	.10	438.0	261.4	331.0	261.77	57.9	254.9	.0020	8.5	144.3	6.9	-5.0
24.0	7223	24.1	.01810	53.8	.10	420.0	259.1	331.9	259.34	59.3	252.9	.0018	9.5	150.6	8.3	-4.7
25.0	7591	26.2	.01907	58.9	.11	400.0	256.6	333.3	256.80	58.5	250.4	.0015	9.0	153.9	8.0	-3.9
26.0	7955	22.2	.02000	50.5	.10	381.0	254.2	335.0	254.50	74.5	250.9	.0017	6.5	151.6	5.7	-3.1
27.0	8252	23.1	.02072	53.0	.10	366.0	251.7	335.4	251.94	89.4	250.4	.0017	4.6	136.8	3.4	-3.2
28.0	8580	19.3	.02146	44.5	.09	350.0	250.2	337.7	250.32	40.3	240.5	.0007	3.0	115.0	1.3	-2.7
29.0	8987	23.4	.02240	54.5	.12	331.0	247.8	339.9	247.89	31.3	235.8	.0005	3.1	85.8	-.2	-3.1
30.0	9625	22.9	.02402	53.9	.13	303.0	245.2	344.8	245.23	33.1	234.0	.0004	2.1	30.9	-1.8	-1.1
30.6	9695	20.2	.02418	47.8	.11	300.0	243.4	343.4	243.51	53.1	236.4	.0006	3.0	344.6	-2.9	.8
31.0	9743	18.3	.02429	43.7	.10	298.0	242.3	342.4	242.35	66.5	238.1	.0006	4.1	329.9	-3.5	2.1
32.0	10107	18.4	.02504	44.3	.11	283.0	239.6	343.7	239.68	69.1	235.9	.0005	3.9	337.0	-3.6	1.5
33.0	10435	19.3	.02573	47.1	.12	270.0	236.7	344.0	236.70	56.1	231.1	.0003	2.6	347.7	-2.5	.6
34.0	10775	21.9	.02654	54.0	.14	257.0	234.2	345.3	234.25	55.2	228.6	.0003	4.2	23.8	-3.8	-1.7
34.5	10962	20.8	.02699	51.6	.14	250.0	232.7	345.7	232.69	0.0	0.0	0.0000	5.1	20.9	-4.7	-1.8
35.0	11128	19.8	.02739	49.5	.13	244.0	231.3	346.1	231.32	0.0	0.0	0.0000	5.8	19.0	-5.5	-1.9
36.0	11438	16.5	.02805	41.6	.12	233.0	228.4	346.2	228.35	0.0	0.0	0.0000	4.4	3.8	-4.4	-.3
37.0	11819	19.0	.02886	48.6	.14	220.0	225.7	347.9	225.74	0.0	0.0	0.0000	5.7	357.2	-5.7	.3
38.0	12218	17.1	.02972	44.5	.14	207.0	222.3	348.6	222.29	0.0	0.0	0.0000	6.9	356.7	-6.9	.4
38.7	12439	16.2	.03017	42.6	.13	200.0	219.9	348.2	219.88	0.0	0.0	0.0000	7.2	357.8	-7.2	.3
39.0	12537	15.8	.03037	41.8	.13	197.0	218.8	348.1	218.82	0.0	0.0	0.0000	7.4	358.3	-7.4	.2
40.0	12936	11.8	.03105	31.7	.11	185.0	215.0	348.2	214.98	0.0	0.0	0.0000	9.0	358.0	-9.0	.3
41.0	13319	12.9	.03165	35.1	.12	174.0	212.7	350.5	212.68	0.0	0.0	0.0000	7.6	346.4	-7.4	1.8
42.0	13684	11.6	.03222	32.0	.12	164.0	209.5	351.2	209.50	0.0	0.0	0.0000	5.0	334.3	-4.5	2.2
43.0	14068	15.3	.03289	42.4	.16	154.0	208.1	355.2	208.13	0.0	0.0	0.0000	.7	252.5	.2	.7
43.4	14227	14.4	.03319	40.2	.16	150.0	207.2	356.3	207.23	0.0	0.0	0.0000	2.7	195.7	2.6	.7
44.0	14433	13.4	.03357	37.4	.15	145.0	206.1	357.8	206.08	0.0	0.0	0.0000	5.7	188.1	5.7	.8
45.0	14773	14.0	.03418	39.7	.17	137.0	203.3	358.7	203.26	0.0	0.0	0.0000	8.4	198.6	8.0	2.7
46.0	15131	15.1	.03487	42.6	.19	129.0	204.2	366.5	204.15	0.0	0.0	0.0000	7.4	214.3	6.1	4.2
46.4	15316	15.3	.03526	43.7	.20	125.0	202.2	366.3	202.22	0.0	0.0	0.0000	6.0	227.4	4.1	4.4
47.0	15558	15.6	.03575	45.0	.21	120.0	199.7	366.0	199.72	0.0	0.0	0.0000	4.9	253.8	1.4	4.7
48.0	15959	14.9	.03658	43.4	.22	112.0	197.7	369.5	197.68	0.0	0.0	0.0000	3.5	267.9	.1	3.5
49.0	16331	13.0	.03729	38.2	.21	105.0	196.9	374.9	196.88	0.0	0.0	0.0000	1.5	277.4	-.2	1.5
49.7	16611	13.5	.03780	39.7	.22	100.0	196.3	378.9	196.27	0.0	0.0	0.0000	1.5	344.9	-1.5	.4
50.0	16710	13.6	.03798	40.2	.23	98.3	196.1	380.4	196.06	0.0	0.0	0.0000	1.9	359.8	-1.9	0.0
51.0	16774	13.6	.03810	39.8	.23	97.2	197.7	384.8	197.68	0.0	0.0	0.0000	5.2	38.0	-4.1	-3.2
52.0	17449	16.7	.03950	48.7	.32	86.5	197.9	398.3	197.94	0.0	0.0	0.0000	9.8	66.3	-4.0	-9.0
53.0	17844	22.8	.04056	66.5	.47	80.8	197.9	406.2	197.94	0.0	0.0	0.0000	9.3	93.0	.5	-9.3
53.1	17902	24.9	.04080	72.0	.52	80.0	198.9	409.4	198.90	0.0	0.0	0.0000	8.9	93.2	.5	-8.9
54.0	18275	38.1	.04232	107.3	.84	75.1	205.0	429.6	205.02	0.0	0.0	0.0000	6.1	94.8	.5	-6.0
55.0	18615	48.5	.04424	133.9	1.13	71.0	208.9	444.8	208.92	0.0	0.0	0.0000	10.0	65.9	-4.1	-9.1
55.2	18701	49.4	.04480	136.5	1.17	70.0	209.0	446.7	208.96	0.0	0.0	0.0000	10.4	69.8	-3.6	-9.8
56.0	18988	52.5	.04666	144.8	1.30	66.8	209.1	453.1	209.11	0.0	0.0	0.0000	12.0	80.8	-1.9	-11.9
57.0	19378	64.3	.04958	175.7	1.70	62.7	211.4	466.4	211.39	0.0	0.0	0.0000	9.2	101.7	1.9	-9.0
57.7	19651	73.9	.05204	200.2	2.05	60.0	213.1	476.2	213.15	0.0	0.0	0.0000	7.6	112.0	2.8	-7.0
58.0	19746	77.2	.05288	208.6	2.16	59.1	213.8	479.6	213.75	0.0	0.0	0.0000	7.1	116.6	3.2	-6.3
59.0	20105	83.5	.05653	225.4	2.48	55.8	213.9	487.9	213.93	0.0	0.0	0.0000	7.2	144.6	5.9	-4.2
60.0	20523	88.2	.06105	237.1	2.80	52.2	214.8	499.4	214.80	0.0	0.0	0.0000	5.3	193.1	5.2	1.2
60.8	20793	90.6	.06410	244.2	3.01	50.0	214.3	504.3	214.28	0.0	0.0	0.0000	6.2	108.1	1.9	-5.9
61.0	20882	91.4	.06510	246.6	3.07	49.3	214.1	505.9	214.10	0.0	0.0	0.0000	8.2	96.0	.9	-8.2
62.0	21248	100.4	.06952	270.4	3.58	46.5	214.3	514.9	214.28	0.0	0.0	0.0000	1.2	354.0	-1.2	.1
63.0	21609	103.1	.07414	276.6	3.89	43.9	215.1	525.5	215.15	0.0	0.0	0.0000	9.6	279.4	-1.6	9.5
64.0	22037	105.9	.07978	287.1	4.28	41.0	213.0	530.6	213.04	0.0	0.0	0.0000	3.7	32.9	-3.1	-2.0
64.4	22191	108.3	08191	292.6	4.49	40.0	213.6	535.9	213.61	0.0	0.0	0.0000	4.5	29.9	-3.9	-2.2

TIME MIN	ALT GPM	OZONE MICMB	TOTOZ ATMCM	OZDEN MG/M3	OZMXR MICGG	PRESS MB	TEMP DEG K	PTEMP DEG K	VTEMP DEG K	HMDTY PRCNT	DEWPT DEG K	SPCFC HMDTY	SPD MPS	DIR DEG	NS MPS	EW MPS
65.0	22463	112.3	08565	302.2	4.86	38.3	214.6	545.1	214.63	0.0	0.0	0.0000	5.8	26.5	-5.2	-2.6
66.0	22958	117.9	.09280	316.1	5.52	35.4	215.3	559.3	215.32	0.0	0.0	0.0000	7.8	34.4	-6.5	-4.4
66.2	23029	118.9	.09388	319.1	5.63	35.0	215.2	560.8	215.18	0.0	0.0	0.0000	7.5	40.9	-5.7	-4.9
67.0	23305	123.0	.09804	330.8	6.08	33.5	214.6	566.4	214.63	0.0	0.0	0.0000	7.5	68.2	-2.8	-6.9
68.0	23735	133.4	.10491	353.4	7.06	31.3	218.0	586.6	218.00	0.0	0.0	0.0000	6.6	113.0	2.6	-6.1
68.6	24006	137.4	.10949	362.6	7.60	30.0	218.8	595.9	218.80	0.0	0.0	0.0000	5.0	133.4	3.5	-3.7
69.0	24179	140.0	.11240	368.5	7.94	29.2	219.3	601.9	219.30	0.0	0.0	0.0000	4.5	152.5	4.0	-2.1
70.0	24611	147.0	.12002	386.5	8.92	27.3	219.6	614.5	219.62	0.0	0.0	0.0000	5.4	205.3	4.9	2.3
71.0	25126	150.4	.12941	394.4	9.89	25.2	220.1	630.0	220.10	0.0	0.0	0.0000	4.9	211.1	4.2	2.5
71.1	25177	150.3	.13036	394.3	9.96	25.0	220.1	631.5	220.10	0.0	0.0	0.0000	4.3	207.9	3.8	2.0
72.0	25521	150.0	.13668	393.5	10.49	23.7	220.1	641.2	220.10	0.0	0.0	0.0000	2.0	142.7	1.6	-1.2
73.0	26002	151.4	.14553	394.9	11.40	22.0	221.4	658.7	221.36	0.0	0.0	0.0000	3.4	73.6	-1.0	-3.3
74.0	26461	151.1	.15396	391.7	12.22	20.5	222.7	676.3	222.74	0.0	0.0	0.0000	6.8	23.0	-6.2	-2.6
74.3	26621	149.5	.15686	388.3	12.38	20.0	222.2	679.4	222.19	0.0	0.0	0.0000	8.2	28.7	-7.2	-3.9
75.0	26954	146.0	.16287	381.3	12.73	19.0	221.0	685.9	221.04	0.0	0.0	0.0000	11.3	35.8	-9.1	-6.6
76.0	27488	143.0	.17225	370.7	13.54	17.5	222.7	707.6	222.74	0.0	0.0	0.0000	15.9	72.3	-4.8	-15.1
77.0	27954	144.0	.18029	368.1	14.64	16.3	225.9	732.3	225.89	0.0	0.0	0.0000	20.3	79.0	-3.9	-20.0
78.0	28463	143.0	.18895	360.7	15.69	15.1	228.9	758.5	228.92	0.0	0.0	0.0000	21.5	81.7	-3.1	-21.3
78.1	28507	142.5	.18968	359.2	15.74	15.0	229.0	760.3	229.00	0.0	0.0	0.0000	21.0	82.8	-2.6	-20.8
79.0	28971	136.6	.19730	343.3	16.17	14.0	229.8	778.0	229.77	0.0	0.0	0.0000	16.7	97.9	2.3	-16.5
80.0	29521	127.4	.20582	320.3	16.36	12.9	229.6	795.9	229.63	0.0	0.0	0.0000	15.6	96.6	1.8	-15.5
80.4	29731	123.4	.20887	311.4	16.35	12.5	228.8	800.1	228.76	0.0	0.0	0.0000	15.6	92.9	.8	-15.6
81.0	30005	118.3	.21283	300.0	16.33	12.0	227.6	805.5	227.63	0.0	0.0	0.0000	15.8	88.2	-.5	-15.7
82.0	30586	109.4	.22065	276.7	16.48	11.0	228.4	828.3	228.35	0.0	0.0	0.0000	15.3	98.9	2.4	-15.2
83.0	31225	103.4	.22865	259.6	17.13	10.0	229.9	857.0	229.91	0.0	0.0	0.0000	19.8	101.3	3.9	-19.4
84.0	31716	95.0	.23433	236.2	16.92	9.3	232.1	883.5	232.15	0.0	0.0	0.0000	24.0	99.4	3.9	-23.7
85.0	32410	87.6	.24166	216.3	17.28	8.4	233.8	916.0	233.80	0.0	0.0	0.0000	24.8	93.2	1.4	-24.7
85.6	32744	82.4	.24485	203.5	17.05	8.0	233.9	929.3	233.88	0.0	0.0	0.0000	25.5	90.2	.1	-25.5
86.0	33006	78.4	.24736	193.4	16.87	7.7	233.9	939.6	233.94	0.0	0.0	0.0000	26.1	87.9	-1.0	-26.0
87.0	33563	70.1	.25211	172.1	16.36	7.1	235.2	966.7	235.16	0.0	0.0	0.0000	28.5	98.4	4.2	-28.2
87.1	33660	69.1	.25285	169.6	16.35	7.0	235.4	971.7	235.41	0.0	0.0	0.0000	28.2	98.3	4.1	-27.9
88.0	34280	63.0	.25756	153.5	16.30	6.4	236.9	1003.3	236.92	0.0	0.0	0.0000	26.6	97.6	3.5	-26.4
88.7	34725	58.9	.26061	144.2	16.24	6.0	235.7	1016.6	235.68	0.0	0.0	0.0000	999.9	999.9	999.9	999.9
89.0	34960	56.7	.26221	139.4	16.21	5.8	235.0	1023.6	235.03	0.0	0.0	0.0000	999.9	999.9	999.9	999.9

INTEGRAL .26221 RESIDUAL .04480 INTEGRATED TOTAL OZONE .30701

OZONAGRAM

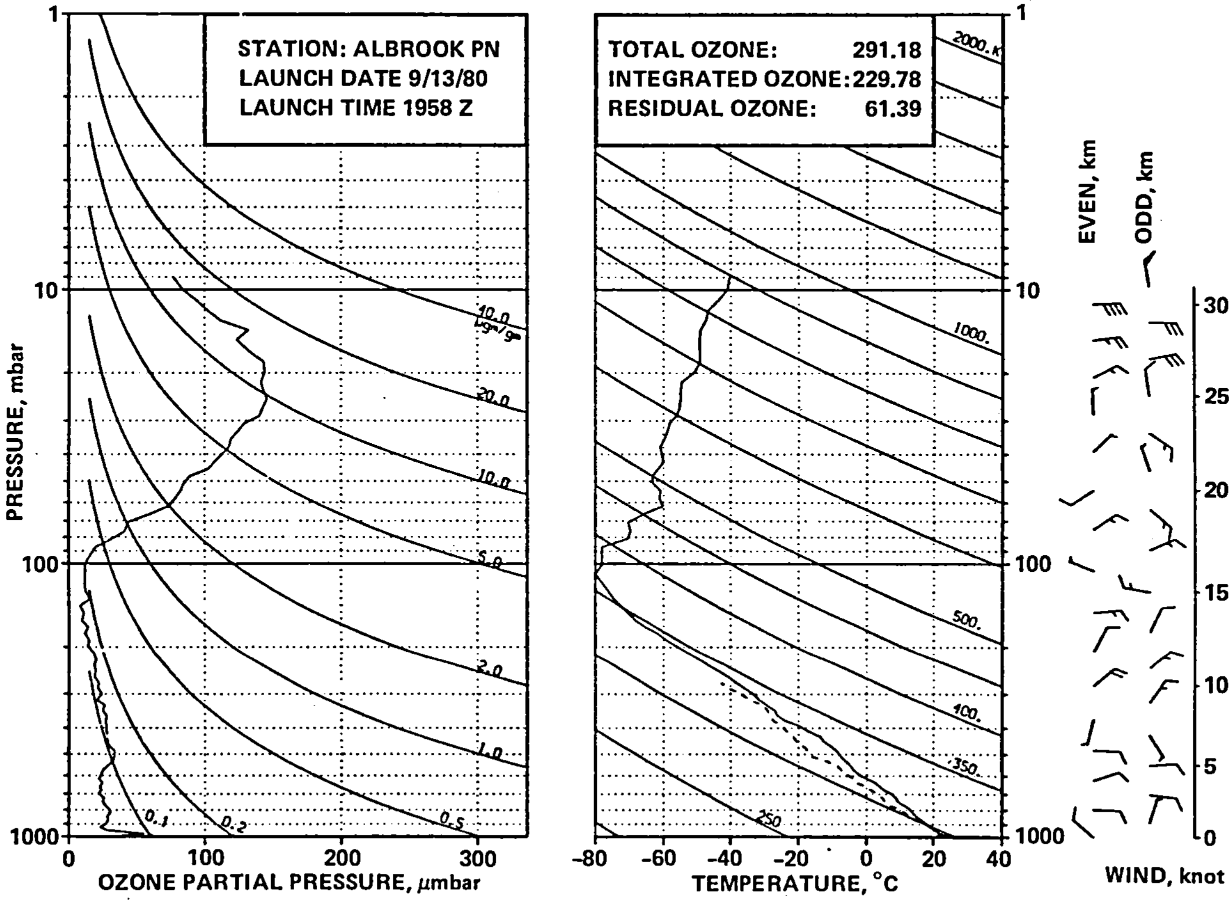
STATION: ALBROOK PN
LAUNCH DATE 9/13/80
LAUNCH TIME 1958 Z
TOTAL OZONE: 291.18
INTEGRATED OZONE: 229.78
RESIDUAL OZONE: 61.39
PRESSURE, mbar
OZONE PARTIAL PRESSURE, μmbar
TEMPERATURE, °C
EVEN, km
ODD, km
HEIGHT, GP km
WIND, knot
1
10
100
1000
0
100
200
300
-80
-60
-40
-20
0
20
40
30
25
20
15
10
5
0
2000. K
1000.
500.
400.
350.
250
10.0 μg/g
20.0
10.0
5.0
2.0
1.0
0.5
0.2
0.1

STATION ALBROOK PN   LAUNCH DATE 9/13/80   TIME 1958Z   ECC   SONDE 3A1340

SURFACE CONDITIONS   PRESS 1001.4MB   TEMP 298.2 DEG K   HUMIDITY 83.0 PRCNT

TIME MIN	ALT GPM	OZONE MICMB	TOTOZ ATMCM	OZDEN MG/M3	OZMXR MICGG	PRESS MB	TEMP DEG K	PTEMP DEG K	VTEMP DEG K	HMDTY PRCNT	DEWPT DEG K	SPCFC HMDTY	SPD MPS	DIR DEG	NS MPS	EW MPS
0.0	66	30.8	0.00000	59.6	.05	1001.4	298.2	298.1	301.13	80.6	294.6	.0160	6.0	310.0	-3.9	4.6
.1	78	32.1	.00005	62.3	.05	1000.0	298.1	298.1	301.00	81.3	294.6	.0161	6.0	310.7	-3.9	4.6
1.0	291	55.6	.00088	108.6	.09	976.0	295.8	297.8	298.79	94.7	294.9	.0167	6.6	321.2	-5.2	4.1
2.0	526	28.4	.00177	55.7	.05	950.0	293.9	298.2	296.80	100.0	293.9	.0162	6.5	328.0	-5.5	3.4
3.0	776	23.4	.00236	46.2	.04	923.0	292.5	299.3	295.27	100.0	292.5	.0153	4.2	339.4	-3.9	1.5
3.9	992	27.0	.00286	53.6	.05	900.0	291.1	300.0	293.66	100.0	291.1	.0142	2.2	5.4	-2.2	-.2
4.0	1012	27.3	.00291	54.2	.05	898.0	291.0	300.1	293.52	100.0	291.0	.0142	2.1	9.9	-2.0	-.4
5.0	1263	29.0	.00356	57.7	.06	872.0	289.9	301.5	292.03	87.5	287.8	.0120	2.9	45.3	-2.0	-2.0
5.8	1480	28.5	.00414	57.1	.06	850.0	288.5	302.2	290.46	87.6	286.4	.0111	4.0	64.5	-1.7	-3.6
6.0	1521	28.4	.00425	57.0	.06	846.0	288.2	302.3	290.17	87.6	286.2	.0111	4.2	66.9	-1.7	-3.9
7.0	1775	30.3	.00494	60.9	.06	821.0	287.2	303.8	289.04	86.7	285.0	.0106	5.2	86.3	-.3	-5.2
7.9	1993	30.2	.00556	60.9	.06	800.0	286.4	305.3	288.19	83.6	283.7	.0099	5.7	93.1	.3	-5.7
8.0	2015	30.2	.00562	60.9	.06	798.0	286.4	305.4	288.10	83.2	283.6	.0099	5.7	93.7	.4	-5.7
9.0	2293	27.2	.00637	55.1	.06	772.0	284.8	306.6	286.24	76.0	280.7	.0084	5.2	90.9	.1	-5.2
10.0	2567	25.1	.00705	51.2	.06	747.0	282.7	307.2	283.96	76.1	278.7	.0075	4.8	90.6	.1	-4.8
11.0	2849	25.9	.00773	53.0	.06	722.0	282.1	309.6	283.38	75.8	278.0	.0075	5.4	97.0	.7	-5.4
11.9	3104	22.5	.00832	46.2	.05	700.0	280.8	310.9	281.99	75.5	276.7	.0070	5.4	96.4	.6	-5.3
12.0	3140	22.0	.00840	45.3	.05	697.0	280.6	311.1	281.80	75.4	276.5	.0070	5.4	96.3	.6	-5.3
13.0	3367	24.2	.00890	50.1	.06	678.0	278.6	311.3	279.67	75.4	274.6	.0062	5.3	74.3	-1.4	-5.1
14.0	3611	22.8	.00946	47.5	.06	658.0	277.2	312.4	278.19	75.6	273.3	.0058	6.1	63.4	-2.7	-5.4
15.0	3874	25.0	.01007	52.3	.06	637.0	276.0	313.9	276.81	66.8	270.4	.0049	5.6	66.1	-2.2	-5.1
16.0	4144	22.2	.01069	46.8	.06	616.0	273.5	314.1	274.25	74.7	269.5	.0047	5.6	75.4	-1.4	-5.4
16.7	4353	23.4	.01117	49.7	.06	600.0	271.7	314.4	272.42	76.2	268.0	.0042	6.0	81.3	-.9	-5.9
17.0	4434	23.8	.01135	50.8	.07	594.0	271.0	314.5	271.72	76.7	267.5	.0042	6.2	83.3	-.7	-6.1
18.0	4733	25.2	.01208	53.9	.07	572.0	269.4	316.1	270.07	75.3	265.7	.0038	6.4	86.1	-.4	-6.4
19.0	5042	28.9	.01292	62.1	.09	550.0	268.4	318.3	268.94	74.1	264.5	.0036	6.4	86.0	-.4	-6.4
20.0	5333	32.4	.01382	70.1	.10	530.0	267.1	320.2	267.61	65.0	261.6	.0030	6.2	87.6	-.3	-6.2
21.0	5648	33.7	.01487	73.3	.11	509.0	265.6	322.1	265.96	50.2	257.1	.0021	5.8	92.4	.2	-5.8
21.4	5786	33.7	.01534	73.4	.11	500.0	265.1	323.2	265.47	50.4	256.7	.0021	5.8	92.8	.3	-5.8
22.0	5991	33.7	.01605	73.6	.11	487.0	264.4	324.8	264.75	50.6	256.0	.0020	5.9	93.5	.4	-5.9
23.0	6282	30.5	.01700	66.9	.11	469.0	262.8	326.3	263.11	51.9	254.8	.0019	6.1	90.9	.1	-6.1
24.0	6616	28.3	.01801	62.8	.10	449.0	260.7	327.7	260.92	51.7	252.8	.0017	5.5	97.8	.7	-5.5
25.0	6945	29.0	.01899	64.6	.11	430.0	259.5	[illegible]	259.77	51.4	251.7	.0016	2.3	97.5	.3	-2.3
26.0	7304	27.6	.02005	62.3	.11	410.0	255.9	330.2	256.13	58.3	249.7	.0014	.6	245.5	.2	.5
26.5	7488	27.6	.02059	62.6	.11	400.0	254.5	330.7	254.71	61.5	249.0	.0013	1.4	212.1	1.2	.8
27.0	7658	27.6	.02109	63.0	.12	391.0	253.2	331.1	253.40	64.6	248.3	.0013	2.3	205.1	2.1	1.0
28.0	7926	27.1	.02187	62.7	.12	377.0	249.6	329.8	249.78	72.5	246.1	.0011	3.1	208.9	2.7	1.5
29.0	8241	27.8	.02281	64.9	.13	361.0	247.1	330.6	247.28	81.5	244.9	.0010	1.0	175.2	1.0	-.1
29.8	8464	25.5	.02346	59.7	.12	350.0	246.6	332.9	246.77	81.5	244.4	.0010	3.8	42.4	-2.8	-2.6
30.0	8527	24.9	.02364	58.3	.12	347.0	246.5	333.5	246.62	81.5	244.3	.0010	5.0	40.2	-3.9	-3.3
31.0	8866	26.4	.02459	[illegible]	.13	331.0	244.1	334.8	244.28	90.4	243.1	.0009	8.6	34.6	-7.1	-4.9
32.0	9218	20.7	.02551	49.5	.11	315.0	241.8	336.4	241.90	75.0	238.9	.0007	9.2	35.4	-7.5	-5.3
33.0	9562	24.3	.02638	58.5	.13	300.0	240.1	338.7	240.21	69.6	236.5	.0005	9.3	47.1	-6.3	-6.8
34.0	9896	[illegible]	.02724	52.4	.12	286.0	237.5	339.7	237.59	61.2	232.8	.0004	9.4	52.1	-5.8	-7.4
35.0	10217	21.9	.02804	53.8	.13	273.0	234.9	340.4	234.98	60.6	230.2	.0003	9.0	50.4	-5.7	-6.9
36.0	10524	19.0	.02876	47.1	.12	261.0	232.6	341.4	232.56	0.0	0.0	0.0000	8.1	52.2	-5.0	-6.4
36.8	10814	19.6	.02942	49.3	.13	250.0	230.1	341.9	230.09	0.0	0.0	0.0000	7.3	51.6	-4.6	-5.7
37.0	10869	19.8	.02955	49.7	.13	248.0	229.6	342.0	229.63	0.0	0.0	0.0000	7.2	51.4	-4.5	-5.6
38.0	11200	18.8	.03030	47.9	.13	236.0	226.6	342.4	226.63	0.0	0.0	0.0000	6.9	46.8	-4.8	-5.1
39.0	11573	20.1	.03117	51.9	.15	223.0	223.7	343.4	223.69	0.0	0.0	0.0000	5.7	35.4	-4.6	-3.3
40.0	11932	18.5	.03201	48.4	.15	211.0	220.6	344.2	220.65	0.0	0.0	0.0000	4.8	27.3	-4.3	-2.2
40.9	12274	14.5	.03270	38.5	.12	200.0	217.5	344.4	217.47	0.0	0.0	0.0000	5.4	31.8	-4.6	-2.9
41.0	12307	14.1	.03277	37.6	.12	199.0	217.2	344.5	217.17	0.0	0.0	0.0000	5.5	32.2	-4.6	-2.9
42.0	12632	15.0	.03336	40.5	.13	189.0	214.1	344.7	214.15	0.0	0.0	0.0000	6.6	30.0	-5.7	-3.3
43.0	12970	12.0	.03394	32.8	.11	179.0	211.5	345.7	211.47	0.0	0.0	0.0000	6.7	25.3	-6.1	-2.9
44.0	13286	14.1	.03447	39.2	.14	170.0	207.9	345.0	207.92	0.0	0.0	0.0000	5.8	26.2	-5.2	-2.6
45.0	13614	9.8	.03498	27.6	.10	161.0	205.1	345.5	205.06	0.0	0.0	0.0000	6.3	45.5	-4.4	-4.5
46.0	14036	11.2	.03557	31.9	.12	150.0	202.6	348.4	202.62	0.0	0.0	0.0000	7.3	75.5	-1.8	-7.1
47.0	14359	8.4	.03599	24.2	.10	142.0	200.7	350.5	200.69	0.0	0.0	0.0000	1.5	170.3	1.5	-.3
48.0	14698	15.4	.03654	44.7	.19	134.0	198.6	352.8	198.65	0.0	0.0	0.0000	8.1	263.6	.9	8.0
49.0	15054	12.5	.03722	36.8	.17	126.0	197.0	356.0	196.98	0.0	0.0	0.0000	8.2	279.1	-1.3	8.1
49.1	15099	12.4	.03729	36.5	.16	125.0	196.8	356.4	196.77	0.0	0.0	0.0000	8.0	280.7	-1.5	7.9
50.0	15382	11.8	.03777	34.9	.16	119.0	195.5	359.1	195.47	0.0	0.0	0.0000	7.1	292.1	-2.7	6.6
51.0	15881	12.1	.03860	36.2	.18	109.0	193.1	363.7	193.08	0.0	0.0	0.0000	4.5	281.5	-.9	4.4
52.0	16314	12.2	.03933	36.0	.20	101.0	195.0	375.3	194.96	0.0	0.0	0.0000	1.1	304.0	-.6	1.0
52.2	16370	12.5	.03943	37.0	.21	100.0	195.0	376.4	194.96	0.0	0.0	0.0000	2.2	32.6	-1.9	-1.2
53.0	16544	13.6	.03974	40.2	.23	97.0	195.0	379.7	194.96	0.0	0.0	0.0000	9.6	54.1	-5.6	-7.7
54.0	17165	19.9	.04117	58.9	.38	87.0	195.0	391.7	194.96	0.0	0.0	0.0000	8.4	69.1	-3.0	-7.8
55.0	17581	32.2	.04264	91.9	.66	81.0	202.6	415.5	202.62	0.0	0.0	0.0000	2.2	72.8	-.7	-2.1
55.2	17654	34.1	.04301	96.9	.71	80.0	202.8	417.3	[illegible]2.78	0.0	0.0	0.0000	3.1	63.3	-1.4	-2.8
56.0	17959	41.6	.04450	118.0	.91	76.0	203.4	424.8	[illegible]03.45	0.0	0.0	0.0000	6.8	50.3	-4.4	-5.3
57.0	18380	43.6	.04688	124.0	1.02	70.8	202.8	432.2	202.83	0.0	0.0	0.0000	11.4	76.3	-2.7	-11.1
57.2	18448	46.3	.04735	131.2	1.10	70.0	203.6	435.3	203.59	0.0	0.0	0.0000	11.2	80.6	-1.8	-11.0
58.0	18801	60.5	.04976	168.2	1.52	66.0	207.5	451.2	207.55	0.0	0.0	0.0000	11.1	103.7	2.6	-10.8
59.0	19205	73.6	.05324	199.6	1.97	61.8	213.0	471.8	212.99	0.0	0.0	0.0000	7.2	142.9	5.8	-4.4
59.4	19388	76.0	.05502	206.4	2.10	60.0	212.5	474.9	212.55	0.0	0.0	0.0000	6.4	155.3	5.8	-2.7
60.0	19621	78.9	.05727	215.0	2.26	57.8	212.0	478.7	211.99	0.0	0.0	0.0000	5.8	175.0	5.8	-.5
61.0	20020	82.8	.06137	225.3	2.53	54.2	212.3	488.3	212.32	0.0	0.0	0.0000	5.6	232.3	3.4	4.4
62.0	20408	85.1	.06554	234.0	2.77	50.9	210.1	491.9	210.08	0.0	0.0	0.0000	6.6	277.0	-.8	6.6
62.3	20517	86.5	.06677	237.8	2.87	50.0	210.0	494.3	210.03	0.0	0.0	0.0000	5.5	285.7	-1.5	5.3
63.0	20768	89.7	.06958	246.6	3.09	48.0	209.9	499.8	209.91	0.0	0.0	0.0000	3.8	322.5	-3.0	2.3
64.0	21139	102.8	.07414	280.4	3.77	45.2	211.6	512.7	211.65	0.0	0.0	0.0000	3.6	345.6	-3.5	.9
65.0	21507	107.4	.07906	290.8	4.18	42.6	213.2	525.2	213.16	0.0	0.0	0.0000	3.0	335.0	-2.7	1.3

TIME MIN	ALT GPM	OZONE MICMB	TOTOZ ATMCM	OZDEN MG/M3	OZMXR MICGG	PRESS MB	TEMP DEG K	PTEMP DEG K	VTEMP DEG K	HMDTY PRCNT	DEWPT DEG K	SPCFC HMDTY	SPD MPS	DIR DEG	NS MPS	EW MPS
65.9	21898	112.8	.08454	306.2	4.67	40.0	212.7	533.6	212.70	0.0	0.0	0.0000	1.8	27.4	-1.6	-.8
66.0	21930	113.2	.08497	307.4	4.71	39.8	212.7	534.2	212.66	0.0	0.0	0.0000	1.8	33.4	-1.5	-1.0
67.0	22300	117.9	.09040	320.7	5.21	37.5	212.2	542.1	212.16	0.0	0.0	0.0000	4.5	68.1	-1.7	-4.1
68.0	22712	119.2	.09659	322.5	5.63	35.1	213.5	555.9	213.49	0.0	0.0	0.0000	6.4	112.4	2.4	-5.9
68.0	22729	119.4	.09686	323.0	5.66	35.0	213.5	556.5	213.53	0.0	0.0	0.0000	6.5	113.1	2.5	-5.9
69.0	23117	124.0	.10280	334.1	6.25	32.9	214.3	568.5	214.31	0.0	0.0	0.0000	7.6	126.0	4.5	-6.2
70.0	23572	129.3	.11004	347.4	7.00	30.6	215.0	582.1	214.96	0.0	0.0	0.0000	4.4	114.7	1.9	-4.0
70.3	23697	132.9	.11215	355.7	7.35	30.0	215.6	587.3	215.63	0.0	0.0	0.0000	2.7	98.7	.4	-2.7
71.0	23955	140.2	.11649	373.0	8.07	28.8	217.0	597.9	217.02	0.0	0.0	0.0000	2.6	359.3	-2.6	0.0
72.0	24366	142.4	.12368	377.2	8.74	27.0	217.9	611.7	217.94	0.0	0.0	0.0000	4.8	354.9	-4.8	.4
73.0	24857	145.6	.13243	385.3	9.65	25.0	218.2	626.2	218.25	0.0	0.0	0.0000	5.6	350.0	-5.5	1.0
74.0	25307	143.3	.14046	379.2	10.19	23.3	218.2	638.9	218.25	0.0	0.0	0.0000	7.3	352.4	-7.2	1.0
75.0	25791	141.2	.14896	372.9	10.83	21.6	218.6	653.8	218.55	0.0	0.0	0.0000	7.3	38.1	-5.7	-4.5
75.9	26287	143.7	.15762	373.9	11.91	20.0	222.0	678.8	221.96	0.0	0.0	0.0000	9.3	83.8	-1.0	-9.3
76.0	26352	144.1	.15875	374.0	12.06	19.8	222.4	682.0	222.40	0.0	0.0	0.0000	9.9	87.7	-.4	-9.9
77.0	26902	143.0	.16830	368.6	13.02	18.2	224.0	703.6	223.97	0.0	0.0	0.0000	14.2	85.5	-1.1	-14.2
77.5	27159	138.2	.17257	356.2	13.07	17.5	224.0	711.6	223.97	0.0	0.0	0.0000	16.7	76.1	-4.0	-16.3
78.0	27427	133.2	.17702	343.3	13.14	16.8	224.0	719.9	223.97	0.0	0.0	0.0000	19.7	69.1	-7.0	-18.4
79.0	28083	123.5	.18715	318.6	13.46	15.2	223.8	740.3	223.83	0.0	0.0	0.0000	12.5	82.5	-1.6	-12.4
79.2	28169	124.9	.18849	322.0	13.81	15.0	223.9	743.3	223.88	0.0	0.0	0.0000	12.2	85.5	-.9	-12.1
80.0	28622	131.9	.19544	339.7	15.61	14.0	224.1	758.8	224.12	0.0	0.0	0.0000	11.0	103.7	2.6	-10.7
81.0	29161	111.7	.20330	285.6	14.35	12.9	225.8	782.6	225.80	0.0	0.0	0.0000	15.4	88.2	-.5	-15.4
81.4	29369	108.1	.20597	276.3	14.32	12.5	226.0	790.5	226.02	0.0	0.0	0.0000	16.1	85.1	-1.4	-16.0
82.0	29695	102.6	.21012	261.6	14.28	11.9	226.4	802.8	226.35	0.0	0.0	0.0000	17.2	80.9	-2.7	-17.0
83.0	30280	94.4	.21694	237.4	14.35	10.9	229.5	834.7	229.49	0.0	0.0	0.0000	22.4	90.6	.2	-22.4
84.0	30862	84.6	.22303	210.5	14.02	10.0	232.2	865.4	232.17	0.0	0.0	0.0000	26.0	91.6	.7	-26.0
85.0	31579	77.7	.22978	192.8	14.31	9.0	232.8	894.4	232.83	0.0	0.0	0.0000	999.9	999.9	999.9	999.9

INTEGRAL .22978 RESIDUAL .06139 INTEGRATED TOTAL OZONE .29118

OZONAGRAM

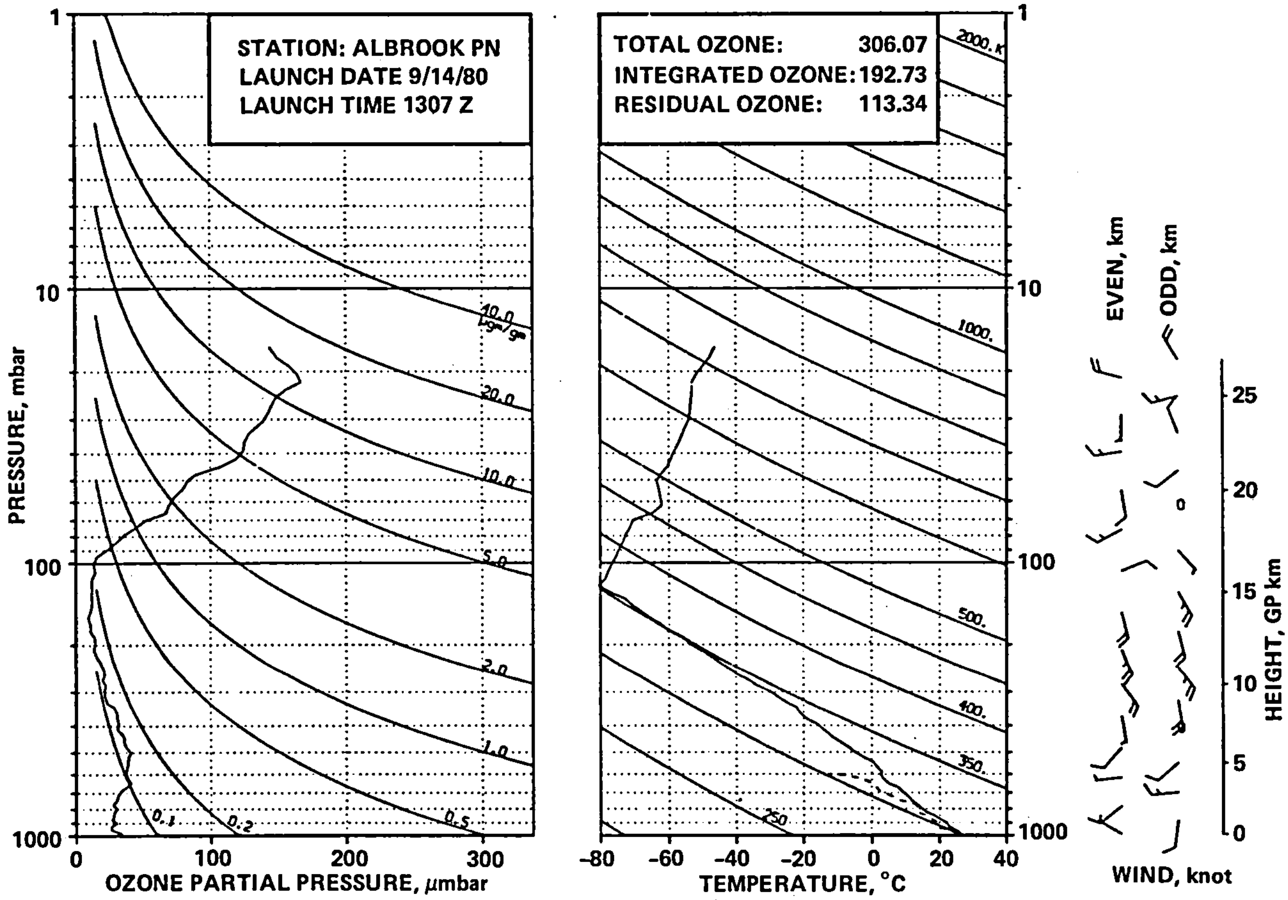

STATION: ALBROOK PN
LAUNCH DATE 9/14/80
LAUNCH TIME 1307 Z
TOTAL OZONE: 306.07
INTEGRATED OZONE: 192.73
RESIDUAL OZONE: 113.34
PRESSURE, mbar
OZONE PARTIAL PRESSURE, μmbar
TEMPERATURE, °C
WIND, knot
EVEN, km
ODD, km
HEIGHT, GP km

STATION ALBROOK PN   LAUNCH DATE 9/14/80   TIME 1307Z   ECC   SONDE 3A1341

SURFACE CONDITIONS   PRESS 1002.1MB   TEMP 297.8 DEG K   HUMIDITY 100.0 PRCNT

TIME MIN	ALT GPM	OZONE MICMB	TOTOZ ATMCM	OZDEN MG/M3	OZMXR MICGG	PRESS MB	TEMP DEG K	PTEMP DEG K	VTEMP DEG K	HMDTY PRCNT	DEWPT DEG K	SPCFC HMDTY	SPD MPS	DIR DEG	NS MPS	EW MPS
0.0	66	27.9	0.00000	54.1	.05	1002.1	297.8	297.6	301.31	100.0	297.8	.0194	3.0	300.0	-1.5	2.6
.1	84	28.4	.00005	55.0	.05	1000.0	297.9	297.9	301.46	99.4	297.8	.0196	2.4	294.2	-1.0	2.2
1.0	272	33.4	.00056	64.4	.06	979.0	299.2	301.0	302.90	93.6	298.1	.0202	4.7	154.6	4.3	-2.0
2.0	500	26.2	.00117	50.7	.05	954.0	297.8	301.8	300.96	85.9	295.2	.0175	5.3	171.6	5.2	-.8
3.0	742	25.9	.00174	50.5	.05	928.0	295.9	302.3	298.78	83.7	293.0	.0157	6.1	180.5	6.1	.1
4.0	1009	29.9	.00241	58.4	.06	900.0	295.3	304.3	298.17	86.7	292.9	.0161	5.6	184.5	5.6	.4
5.0	1264	26.6	.00307	52.3	.05	874.0	293.5	305.0	296.14	85.5	291.0	.0146	5.0	197.8	4.8	1.5
5.9	1504	27.8	.00366	54.9	.05	850.0	291.9	305.8	294.39	86.2	289.6	.0137	5.3	212.0	4.5	2.8
6.0	1525	27.9	.00372	55.1	.05	848.0	291.8	305.9	294.25	86.3	289.5	.0137	5.3	213.2	4.5	2.9
7.0	1792	28.0	.00440	55.9	.06	822.0	289.3	306.0	291.39	83.4	286.5	.0117	5.2	221.7	3.8	3.4
7.9	2022	30.0	.00502	60.2	.06	800.0	288.0	307.0	290.17	91.2	286.6	.0121	5.5	230.2	3.5	4.2
8.0	2044	30.2	.00508	60.6	.06	798.0	287.9	307.1	290.06	91.9	286.6	.0121	5.5	231.0	3.5	4.3
9.0	2346	27.4	.00589	55.3	.06	770.0	286.4	308.6	288.51	99.1	286.2	.0122	6.6	243.2	3.0	5.9
10.0	2646	30.2	.00671	61.2	.07	743.0	284.8	310.1	286.41	78.1	281.1	.0090	6.8	250.1	2.3	6.4
11.0	2944	30.8	.00756	62.6	.07	717.0	283.7	312.0	285.11	72.2	278.9	.0080	7.2	259.1	1.4	7.0
11.7	3143	32.2	.00817	65.7	.08	700.0	282.6	312.9	283.83	66.6	276.7	.0067	6.8	267.1	.3	6.8
12.0	3239	32.8	.00845	67.2	.08	692.0	282.1	313.4	283.21	64.0	275.6	.0066	6.6	271.3	-.1	6.6
13.0	3518	36.9	.00938	75.7	.09	669.0	281.0	315.2	282.09	64.1	274.6	.0063	4.8	276.2	-.5	4.8
14.0	3805	40.8	.01046	84.8	.10	646.0	278.0	315.0	279.05	71.6	273.3	.0060	4.3	268.9	.1	4.3
15.0	4087	38.5	.01154	80.3	.10	624.0	276.7	316.6	277.53	63.8	270.5	.0050	3.5	262.9	.4	3.4
16.0	4351	37.5	.01252	78.3	.10	604.0	276.0	318.8	276.59	43.5	264.9	.0034	2.4	253.6	.7	2.3
16.2	4404	37.4	.01271	78.2	.10	600.0	276.1	319.4	276.52	35.3	260.3	.0022	2.4	249.9	.8	2.3
17.0	4582	37.2	.01336	77.8	.10	587.0	276.2	321.6	276.29	0.0	0.0	0.0000	2.4	237.5	1.3	2.1
18.0	4862	37.8	.01438	79.4	.11	567.0	274.9	323.2	275.34	37.3	261.9	.0028	3.6	227.3	2.5	2.7
19.0	5224	38.5	.01574	81.4	.12	542.0	273.6	325.9	274.01	36.5	260.4	.0026	4.5	231.6	2.8	3.5
20.0	5554	38.9	.01701	83.0	.12	520.0	270.7	326.3	270.80	0.0	0.0	0.0000	4.1	232.3	2.5	3.2
21.0	5863	40.6	.01824	87.4	.13	500.0	268.3	327.0	268.34	0.0	0.0	0.0000	4.1	221.0	3.1	2.7
22.0	6199	37.4	.01956	81.1	.13	479.0	266.5	328.8	266.58	0.0	0.0	0.0000	4.6	221.8	3.4	3.0
23.0	6530	35.7	.02079	78.0	.13	459.0	264.1	329.9	264.26	22.3	246.5	.0009	3.2	229.8	2.1	2.5
24.0	6838	35.7	.02191	78.7	.13	441.0	261.8	330.8	261.97	27.2	246.7	.0010	2.0	229.4	1.3	1.5
25.0	7120	33.5	.02292	74.2	.13	425.0	260.3	332.3	260.44	35.5	248.2	.0012	.9	125.8	.6	-.8
26.0	7393	30.5	.02383	68.1	.12	410.0	258.7	333.8	258.93	45.4	249.5	.0014	2.2	88.3	-.1	-2.2
26.6	7579	31.1	.02443	69.6	.13	400.0	257.7	334.8	257.81	32.2	244.3	.0007	1.8	116.3	.8	-1.6
27.0	7712	31.4	.02487	70.7	.13	393.0	256.9	335.5	257.01	22.7	240.6	.0006	1.8	140.7	1.4	-1.1
28.0	8023	30.4	.02588	69.2	.13	377.0	254.1	335.7	254.18	36.2	242.8	.0008	3.4	169.0	3.4	-.7
29.0	8365	30.4	.02699	69.6	.14	360.0	252.4	338.0	252.51	24.1	237.3	.0005	5.1	179.2	5.1	-.1
29.5	8572	29.3	.02764	67.1	.14	350.0	251.7	339.8	251.77	0.0	0.0	0.0000	5.9	180.2	5.9	0.0
30.0	8786	28.1	.02871	64.5	.14	340.0	251.0	341.6	251.01	0.0	0.0	0.0000	6.8	180.9	6.8	.1
31.0	9004	23.1	.02891	53.6	.12	330.0	248.7	341.4	248.73	0.0	0.0	0.0000	8.8	173.9	8.8	-.9
32.0	9386	21.4	.02984	50.3	.11	313.0	245.7	342.3	245.67	0.0	0.0	0.0000	10.1	157.7	9.3	-3.8
32.9	9689	20.8	.03054	49.3	.11	300.0	243.7	343.8	243.73	0.0	0.0	0.0000	10.2	146.1	8.5	-5.7
33.0	9737	20.7	.03065	49.2	.12	298.0	243.4	344.0	243.42	0.0	0.0	0.0000	10.3	144.3	8.4	-6.0
34.0	10102	21.8	.03152	52.5	.13	283.0	239.4	343.4	239.44	0.0	0.0	0.0000	11.0	143.4	8.8	-6.6
35.0	10429	19.5	.03228	47.4	.12	270.0	236.8	344.2	236.77	0.0	0.0	0.0000	13.6	153.4	12.2	-6.1
36.0	10742	21.1	.03301	52.1	.14	258.0	233.6	344.1	233.66	30.8	223.0	.0001	12.6	149.6	10.9	-6.4
36.6	10955	20.4	.03352	50.7	.14	250.0	232.2	345.0	232.16	0.0	0.0	0.0000	12.0	145.2	9.9	-6.8
37.0	11121	19.9	.03391	49.7	.14	244.0	231.0	345.7	231.01	0.0	0.0	0.0000	11.6	141.6	9.1	-7.2
38.0	11460	18.2	.03467	46.1	.13	232.0	228.3	346.6	228.33	0.0	0.0	0.0000	12.9	151.9	11.3	-6.1
39.0	11813	15.3	.03537	39.0	.11	220.0	225.6	347.7	225.58	0.0	0.0	0.0000	12.2	157.2	11.2	-4.7
40.0	12149	13.4	.03595	34.7	.11	209.0	222.6	348.1	222.59	0.0	0.0	0.0000	12.2	156.5	11.2	-4.9
40.8	12433	13.8	.03643	36.4	.11	200.0	219.8	348.1	219.79	0.0	0.0	0.0000	11.7	157.8	10.8	-4.4
41.0	12498	14.0	.03654	36.8	.12	198.0	219.2	348.1	219.15	0.0	0.0	0.0000	11.6	158.2	10.7	-4.3
42.0	12829	14.0	.03711	37.2	.12	188.0	217.5	350.7	217.53	0.0	0.0	0.0000	11.1	158.2	10.3	-4.1
43.0	13173	10.9	.03765	29.6	.10	178.0	213.1	348.9	213.07	0.0	0.0	0.0000	11.1	168.8	10.9	-2.2
44.0	13531	10.9	.03815	29.9	.11	168.0	210.9	351.1	210.88	0.0	0.0	0.0000	11.2	167.6	11.0	-2.4
45.0	13868	9.1	.03858	25.2	.09	159.0	207.6	351.1	207.59	0.0	0.0	0.0000	10.5	161.8	10.0	-3.3
46.0	14219	10.8	.03904	30.3	.12	150.0	204.9	352.3	204.89	0.0	0.0	0.0000	10.7	169.5	10.5	-1.9
47.0	14545	11.9	.03952	33.9	.14	142.0	202.2	353.2	202.22	0.0	0.0	0.0000	12.5	165.6	12.1	-3.1
48.0	14843	11.8	.04000	34.2	.15	135.0	200.3	355.0	200.33	0.0	0.0	0.0000	8.7	144.0	7.0	-5.1
49.0	15107	11.8	.04042	34.8	.15	129.0	196.5	352.7	196.48	0.0	0.0	0.0000	13.0	150.6	11.3	-6.4
49.5	15286	11.8	.04072	35.1	.16	125.0	194.6	352.6	194.64	0.0	0.0	0.0000	12.5	149.8	10.8	-6.3
50.0	15471	11.8	.04102	35.4	.16	121.0	192.7	352.4	192.73	0.0	0.0	0.0000	12.1	148.9	10.3	-6.2
51.0	15759	11.8	.04149	34.9	.17	115.0	194.5	360.9	194.52	0.0	0.0	0.0000	7.3	80.9	-1.1	-7.2
52.0	16117	14.3	.04214	42.2	.22	108.0	195.4	369.0	195.38	0.0	0.0	0.0000	5.8	66.0	-2.4	-5.3
53.0	16501	13.1	.04286	38.5	.21	101.0	196.5	378.3	196.48	0.0	0.0	0.0000	4.4	26.5	-3.9	-1.9
53.2	16558	13.4	.04297	39.5	.22	100.0	196.7	379.8	196.69	0.0	0.0	0.0000	4.1	25.1	-3.7	-1.7
54.0	16872	15.4	.04359	44.9	.27	94.7	197.8	387.9	197.81	0.0	0.0	0.0000	2.6	12.8	-2.6	-.5
55.0	17219	23.3	.04450	67.9	.43	89.2	198.6	396.1	198.59	0.0	0.0	0.0000	3.9	236.0	2.2	3.2
56.0	17569	29.9	.04576	86.5	.59	84.0	199.8	405.5	199.84	0.0	0.0	0.0000	9.5	240.1	4.8	8.3
56.8	17854	34.7	.04703	99.9	.72	80.0	200.4	412.4	200.41	0.0	0.0	0.0000	9.7	240.4	4.8	8.4
57.0	17936	36.0	.04739	103.7	.76	78.9	200.6	414.4	200.57	0.0	0.0	0.0000	9.7	240.5	4.8	8.4
58.0	18258	44.0	.04912	126.0	.98	74.7	201.8	423.4	201.76	0.0	0.0	0.0000	6.4	244.5	2.8	5.8
59.0	18625	51.5	.05146	146.7	1.22	70.2	202.7	432.9	202.68	0.0	0.0	0.0000	3.0	297.9	-1.4	2.6
59.0	18642	52.2	.05160	148.6	1.24	70.0	202.9	433.9	202.95	0.0	0.0	0.0000	2.8	297.7	-1.3	2.5
60.0	18987	67.0	.05428	185.5	1.68	66.1	208.4	452.8	208.39	0.0	0.0	0.0000	.4	261.2	.1	.4
61.0	19380	69.2	.05772	189.4	1.85	62.0	211.1	467.1	211.07	0.0	0.0	0.0000	3.3	187.7	3.2	.4
61.5	19582	71.1	.05956	194.7	1.97	60.0	210.9	471.1	210.88	0.0	0.0	0.0000	3.5	178.6	3.5	-.1
62.0	19791	73.1	.06146	200.2	2.09	58.0	210.7	475.3	210.69	0.0	0.0	0.0000	3.8	170.4	3.7	-.6
63.0	20231	79.6	.06577	218.5	2.44	54.0	210.3	484.2	210.32	0.0	0.0	0.0000	4.7	171.0	4.6	-.7
64.0	20667	83.3	.07033	229.5	2.74	50.3	209.6	492.4	209.55	0.0	0.0	0.0000	6.2	205.5	5.6	2.7
64.1	20703	84.0	.07074	231.4	2.79	50.0	209.7	493.6	209.70	0.0	0.0	0.0000	6.1	208.2	5.4	2.9
65.0	20993	89.9	.07395	246.1	3.12	47.7	210.9	503.0	210.88	0.0	0.0	0.0000	5.9	230.7	3.8	4.6
66.0	21354	106.6	.07847	289.5	3.93	45.0	212.7	515.9	212.71	0.0	0.0	0.0000	6.3	243.9	2.8	5.6

TIME MIN	ALT GPM	OZONE MICMB	TOTOZ ATMCM	OZDEN MG/M3	OZMXR MICGG	PRESS MB	TEMP DEG K	PTEMP DEG K	VTEMP DEG K	HMDTY PRCNT	DEWPT DEG K	SPCFC HMDTY	SPD MPS	DIR DEG	NS MPS	EW MPS
67.0	21799	119.0	.08483	321.3	4.70	41.9	213.8	529.2	213.78	0.0	0.0	0.0000	8.1	255.5	2.0	7.9
67.6	22090	122.5	.08928	329.6	5.08	40.0	214.5	538.2	214.54	0.0	0.0	0.0000	6.9	261.8	1.0	6.9
68.0	22265	124.6	.09196	334.5	5.31	38.9	215.0	543.6	215.00	0.0	0.0	0.0000	6.2	266.6	.4	6.2
69.0	22684	125.1	.09851	334.2	5.70	36.4	216.2	557.1	216.19	0.0	0.0	0.0000	3.2	285.8	-.9	3.1
69.6	22932	126.9	.10243	337.9	6.01	35.0	216.8	565.0	216.77	0.0	0.0	0.0000	3.5	324.0	-2.8	2.0
70.0	23116	128.2	.10532	340.7	6.25	34.0	217.2	570.7	217.20	0.0	0.0	0.0000	4.4	343.6	-4.2	1.3
71.0	23423	133.0	.11029	352.5	6.80	32.4	217.9	580.4	217.86	0.0	0.0	0.0000	3.0	20.3	-2.8	-1.0
72.0	23830	139.3	.11714	367.2	7.59	30.4	219.0	594.1	218.99	0.0	0.0	0.0000	1.4	128.5	.9	-1.1
72.2	23914	139.9	.11861	368.8	7.73	30.0	219.1	596.7	219.08	0.0	0.0	0.0000	1.5	160.5	1.4	-.5
73.0	24266	142.7	.12471	375.3	8.32	28.4	219.5	607.1	219.47	0.0	0.0	0.0000	4.2	207.1	3.7	1.9
74.0	24662	145.2	.13172	381.6	9.01	26.7	219.6	618.4	219.63	0.0	0.0	0.0000	7.3	220.1	5.6	4.7
75.0	25085	148.3	.13933	389.2	9.83	25.0	219.9	631.0	219.95	0.0	0.0	0.0000	7.8	257.0	1.8	7.6
76.0	25538	155.9	.14778	409.0	11.09	23.3	220.1	644.3	220.11	0.0	0.0	0.0000	12.7	258.1	2.6	12.5
77.0	25937	166.8	.15567	437.4	12.62	21.9	220.1	655.8	220.11	0.0	0.0	0.0000	11.8	268.4	.3	11.8
78.0	26364	164.3	.16430	428.5	13.28	20.5	221.4	672.1	221.36	0.0	0.0	0.0000	7.7	321.5	-6.0	4.8
78.3	26524	162.1	.16744	421.6	13.43	20.0	222.1	679.1	222.05	0.0	0.0	0.0000	8.2	328.4	-7.0	4.3
79.0	26824	158.1	.17330	408.6	13.71	19.1	223.3	692.0	223.35	0.0	0.0	0.0000	9.3	339.0	-8.7	3.3
80.0	27287	149.4	.18185	382.9	13.91	17.8	225.3	712.2	225.29	0.0	0.0	0.0000	9.3	318.2	-6.9	6.2
80.2	27399	148.3	.18381	379.6	14.05	17.5	225.6	716.8	225.61	0.0	0.0	0.0000	999.9	999.9	999.9	999.9
81.0	27910	143.5	.19273	365.0	14.68	16.2	227.0	737.3	227.04	0.0	0.0	0.0000	999.9	999.9	999.9	999.9

INTEGRAL .19273 RESIDUAL .11334 INTEGRATED TOTAL OZONE .30607

OZONAGRAM

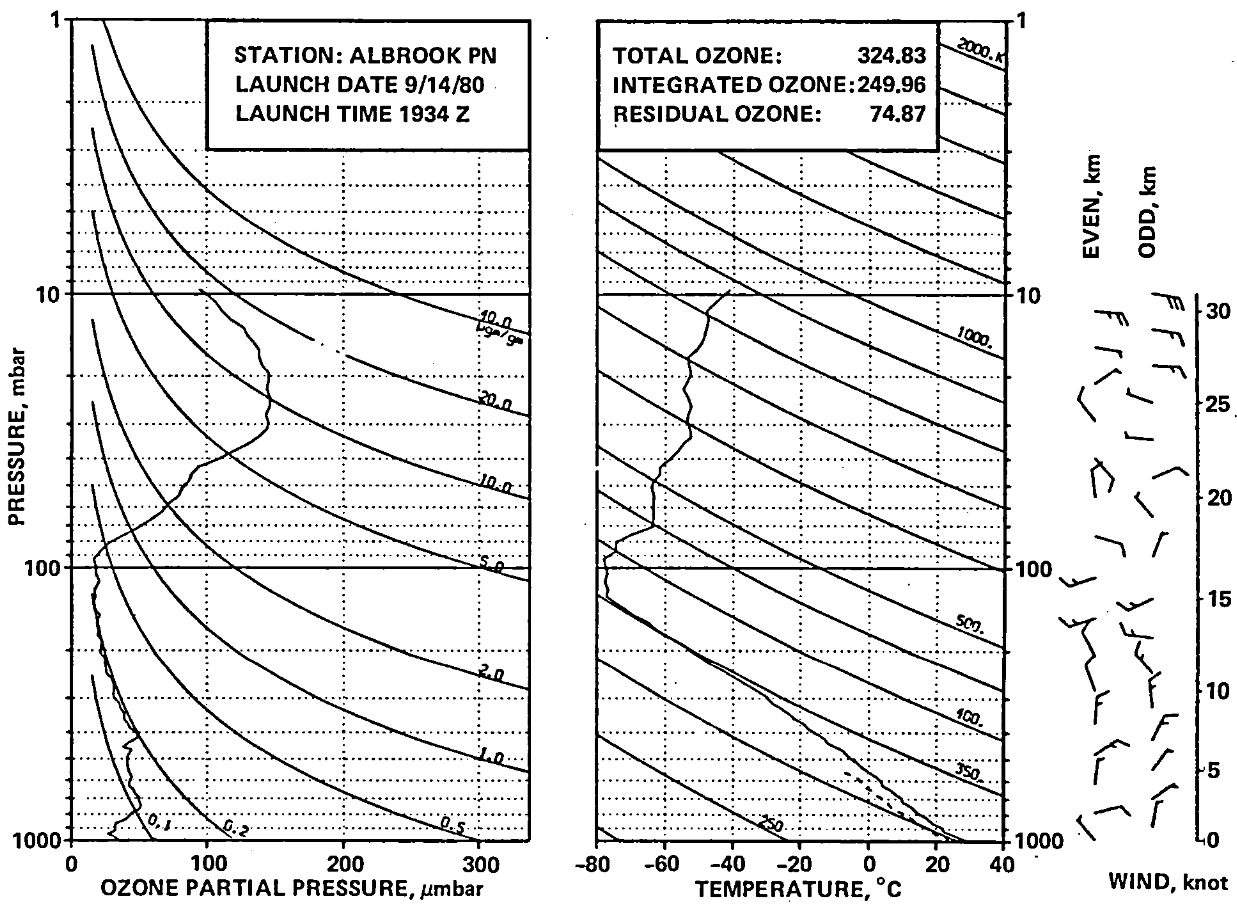
STATION: ALBROOK PN
LAUNCH DATE 9/14/80
LAUNCH TIME 1934 Z
TOTAL OZONE: 324.83
INTEGRATED OZONE: 249.96
RESIDUAL OZONE: 74.87
PRESSURE, mbar
OZONE PARTIAL PRESSURE, μmbar
TEMPERATURE, °C
WIND, knot
HEIGHT, GP km
EVEN, km
ODD, km
1
10
100
1000
0
100
200
300
-80
-60
-40
-20
0
20
40
30
25
20
15
10
5
0

STATION ALBROOK PN LAUNCH DATE 9/14/80 TIME 1934Z ECC SONDE 3A1342

SURFACE CONDITIONS PRESS 1000.0MB TEMP 302.9 DEG K HUMIDITY 67.0 PRCNT

TIME MIN	ALT GPM	OZONE MICMB	TOTOZ ATMCM	OZDEN MG/M3	OZMXR MICGG	PRESS MB	TEMP DEG K	PTEMP DEG K	VTEMP DEG K	HMDTY PRCNT	DEWPT DEG K	SPCFC HMDTY	SPD MPS	DIR DEG	NS MPS	EW MPS
0.0	66	34.4	0.00000	65.6	.06	1000.0	302.9	302.9	306.22	68.5	296.5	.0180	2.0	320.0	-1.5	1.3
1.0	328	32.5	.00078	62.6	.06	971.0	300.1	302.6	303.51	81.8	296.6	.0187	2.5	291.5	-.9	2.4
2.0	568	26.8	.00141	51.9	.05	945.0	297.9	302.7	300.80	77.5	293.7	.0160	2.9	304.3	-1.6	2.4
3.0	822	32.6	.00209	63.7	.06	918.0	295.3	302.6	297.88	78.1	291.3	.0142	3.6	345.5	-3.4	.9
3.7	994	32.2	.00259	62.9	.06	900.0	295.0	304.0	297.50	76.2	290.6	.0138	3.6	3.5	-3.6	-.2
4.0	1072	32.0	.00282	62.6	.06	892.0	294.9	304.6	297.33	75.3	290.3	.0137	3.8	11.1	-3.7	-.7
5.0	1338	32.8	.00361	64.7	.06	865.0	292.4	304.8	294.58	75.1	287.9	.0121	3.2	24.8	-2.9	-1.4
5.6	1488	36.7	.00411	72.6	.07	850.0	291.7	305.5	293.77	75.1	287.2	.0116	3.0	31.1	-2.6	-1.6
6.0	1600	39.6	.00448	78.5	.08	839.0	291.1	306.1	293.17	75.0	286.6	.0115	2.9	36.3	-2.4	-1.7
7.0	1859	42.5	.00546	84.7	.09	814.0	289.9	307.4	291.80	74.9	285.4	.0109	3.6	54.9	-2.1	-2.9
7.6	2006	43.6	.00605	87.3	.09	800.0	288.6	307.6	290.45	75.3	284.3	.0101	4.2	71.0	-1.4	-4.0
8.0	2103	44.4	.00644	89.0	.09	791.0	287.8	307.8	289.57	75.5	283.5	.0099	4.8	78.8	-.9	-4.7
9.0	2352	49.9	.00754	100.5	.11	768.0	286.8	309.3	288.31	66.8	280.8	.0085	5.3	83.8	-.6	-5.2
10.0	2641	51.2	.00891	103.7	.11	742.0	285.3	310.6	286.64	67.0	279.3	.0079	5.0	69.2	-1.8	-4.6
11.0	2892	49.8	.01011	101.6	.11	720.0	283.2	311.0	284.53	74.3	278.8	.0079	4.4	58.6	-2.3	-3.8
11.8	3126	49.7	.01122	101.4	.12	700.0	282.9	313.2	284.15	68.3	277.3	.0072	3.5	52.4	-2.1	-2.8
12.0	3198	49.6	.01156	101.3	.12	694.0	282.8	313.9	284.03	66.5	276.9	.0072	3.2	49.8	-2.1	-2.5
13.0	3465	46.8	.01278	96.1	.12	672.0	281.0	314.8	282.07	66.1	275.0	.0065	1.8	343.4	-1.7	.5
14.0	3739	45.6	.01400	94.1	.12	650.0	279.7	316.3	280.76	66.3	273.9	.0062	2.4	306.6	-1.4	1.9
15.0	4020	42.3	.01519	87.9	.11	628.0	277.4	316.9	278.36	65.8	271.6	.0054	1.8	3.9	-1.8	-.1
16.0	4337	42.9	.01650	89.5	.12	604.0	276.8	319.6	277.65	65.2	270.8	.0053	2.6	29.8	-2.2	-1.3
16.2	4390	43.2	.01673	90.1	.12	600.0	276.5	320.0	277.43	65.2	270.6	.0052	2.5	29.6	-2.2	-1.2
17.0	4638	44.3	.01777	92.8	.13	582.0	275.6	321.7	276.43	65.1	269.7	.0051	2.2	28.7	-1.9	-1.1
18.0	4962	42.4	.01915	89.6	.13	559.0	273.3	322.7	273.94	58.5	266.1	.0040	1.7	27.9	-1.5	-.8
19.0	5267	41.3	.02042	87.9	.13	538.0	271.3	323.9	271.55	0.0	0.0	0.0000	3.5	53.2	-2.1	-2.8
20.0	5644	41.2	.02197	88.2	.13	513.0	269.6	326.3	269.78	0.0	0.0	0.0000	6.9	59.1	-3.5	-5.9
20.6	5846	41.1	.02280	88.5	.14	500.0	268.3	327.1	268.49	0.0	0.0	0.0000	7.8	57.2	-4.2	-6.5
21.0	5957	41.1	.02326	88.7	.14	493.0	267.6	327.6	267.78	0.0	0.0	0.0000	8.3	56.3	-4.6	-6.9
22.0	6447	44.3	.02538	96.4	.16	463.0	265.4	330.7	265.51	0.0	0.0	0.0000	8.3	53.8	-4.9	-6.7
23.0	6616	38.3	.02609	83.9	.14	453.0	263.8	330.7	264.08	47.2	254.6	.0019	8.5	41.5	-6.4	-5.7
24.0	6910	42.1	.02730	93.2	.16	436.0	261.2	331.1	261.38	35.7	249.1	.0012	7.9	31.8	-6.7	-4.2
25.0	7232	48.6	.02881	107.8	.19	418.0	260.2	333.8	260.36	33.1	247.4	.0011	6.1	22.4	-5.6	-2.3
26.0	7528	47.9	.03030	107.4	.20	402.0	257.8	334.5	257.91	22.6	241.2	.0006	5.8	10.5	-5.7	-1.1
26.1	7565	47.3	.03048	106.1	.20	400.0	257.5	334.6	257.61	24.2	241.6	.0007	5.9	10.2	-5.8	-1.0
27.0	7813	43.3	.03167	97.8	.19	387.0	255.5	335.1	255.61	35.2	243.8	.0009	6.0	8.5	-5.9	-.9
28.0	8108	41.4	.03299	93.9	.18	372.0	254.3	337.3	254.37	32.7	242.0	.0007	6.6	4.5	-6.6	-.5
29.0	8392	38.8	.03420	89.0	.18	358.0	251.7	337.6	251.78	24.6	236.8	.0005	7.5	360.0	-7.5	0.0
29.5	8557	38.8	.03489	89.4	.18	350.0	250.8	338.5	250.85	21.9	234.8	.0004	7.8	356.9	-7.8	.4
30.0	8727	38.8	.03560	89.7	.19	342.0	249.8	339.5	249.89	0.0	0.0	0.0000	8.0	354.0	-8.0	.8
31.0	9053	36.3	.03693	84.8	.18	327.0	247.5	340.6	247.51	0.0	0.0	0.0000	8.6	353.5	-8.6	1.0
32.0	9414	34.9	.03834	82.3	.19	311.0	244.6	341.5	244.64	33.9	233.7	.0004	9.3	355.2	-9.2	.8
32.7	9671	31.9	.03927	75.7	.18	300.0	243.6	343.7	243.71	49.7	236.3	.0006	8.5	343.7	-8.1	2.4
33.0	9767	30.9	.03962	73.2	.17	296.0	243.3	344.5	243.36	55.5	237.3	.0006	8.3	338.9	-7.7	3.0
34.0	10060	31.4	.04064	75.3	.18	284.0	240.8	345.0	240.82	24.4	227.3	.0002	5.1	339.5	-4.8	1.8
35.0	10414	31.3	.04189	76.1	.19	270.0	237.6	345.4	237.65	24.2	224.5	.0002	6.0	324.9	-4.9	3.5
36.0	10755	29.9	.04308	73.6	.19	257.0	234.7	346.0	234.73	21.9	221.1	.0001	8.9	313.1	-6.1	6.5
36.6	10943	27.7	.04369	68.6	.18	250.0	233.0	346.2	233.00	0.0	0.0	0.0000	7.5	317.0	-5.5	5.1
37.0	11081	26.0	.04414	64.9	.18	245.0	231.7	346.4	231.74	0.0	0.0	0.0000	6.5	321.0	-5.1	4.1
38.0	11390	25.4	.04507	64.1	.18	234.0	228.9	346.6	228.86	0.0	0.0	0.0000	6.4	324.6	-5.2	3.7
39.0	11680	24.7	.04593	63.2	.18	224.0	226.0	346.6	226.04	0.0	0.0	0.0000	6.7	332.1	-5.9	3.1
40.0	11981	24.7	.04682	63.7	.19	214.0	224.0	348.0	224.02	0.0	0.0	0.0000	6.3	335.4	-5.8	2.6
41.0	12293	21.4	.04769	55.8	.17	204.0	221.5	348.8	221.50	0.0	0.0	0.0000	5.3	321.6	-4.2	3.3
41.4	12420	21.6	.04803	56.7	.18	200.0	220.6	349.4	220.59	0.0	0.0	0.0000	5.6	309.3	-3.5	4.3
42.0	12617	22.0	.04855	58.0	.19	194.0	219.2	350.2	219.20	0.0	0.0	0.0000	6.4	293.4	-2.5	5.9
43.0	12919	22.6	.04939	60.2	.20	185.0	216.3	350.3	216.33	0.0	0.0	0.0000	7.9	281.1	-1.5	7.8
44.0	13197	19.3	.05012	52.3	.18	177.0	213.3	349.8	213.31	0.0	0.0	0.0000	6.1	272.3	-.2	6.1
45.0	13484	19.8	.05083	54.3	.19	169.0	210.7	350.1	210.66	0.0	0.0	0.0000	7.5	285.7	-2.0	7.3
46.0	13896	18.4	.05185	51.1	.19	158.0	208.2	352.8	208.23	0.0	0.0	0.0000	9.1	260.3	1.5	9.0
46.9	14209	20.7	.05266	58.4	.23	150.0	204.5	351.6	204.49	0.0	0.0	0.0000	8.9	245.1	3.7	8.1
47.0	14250	21.0	.05276	59.4	.23	149.0	204.0	351.5	204.01	0.0	0.0	0.0000	8.9	243.2	4.0	7.9
48.0	14577	17.0	.05359	48.8	.20	141.0	201.4	352.5	201.38	0.0	0.0	0.0000	7.9	264.8	.7	7.9
49.0	14875	16.3	.05426	47.4	.20	134.0	198.6	352.6	198.55	0.0	0.0	0.0000	8.4	256.9	1.9	8.2
50.0	15185	17.6	.05498	51.8	.23	127.0	196.0	353.4	196.00	0.0	0.0	0.0000	8.8	236.3	4.9	7.3
50.3	15275	17.4	.05519	51.2	.23	125.0	196.1	355.3	196.15	0.0	0.0	0.0000	9.6	234.7	5.6	7.9
51.0	15510	16.9	.05575	49.5	.23	120.0	196.5	360.2	196.53	0.0	0.0	0.0000	11.9	231.8	7.4	9.4
52.0	15906	20.6	.05677	60.9	.31	112.0	195.5	365.4	195.47	0.0	0.0	0.0000	9.6	242.6	4.4	8.6
53.0	16276	18.0	.05775	52.9	.28	105.0	196.3	373.7	196.26	0.0	0.0	0.0000	4.7	261.6	.7	4.7
53.8	16555	17.9	.05844	52.7	.30	100.0	195.9	378.2	195.87	0.0	0.0	0.0000	3.8	292.0	-1.4	3.5
54.0	16648	17.9	.05867	52.7	.30	98.4	195.7	379.6	195.73	0.0	0.0	0.0000	3.8	304.2	-2.1	3.1
55.0	16983	16.5	.05946	48.9	.30	92.8	195.2	385.0	195.19	0.0	0.0	0.0000	3.5	12.6	-3.4	-.8
56.0	17368	21.5	.06047	62.5	.41	86.8	198.8	399.7	198.80	0.0	0.0	0.0000	4.7	53.4	-2.8	-3.7
57.0	17785	28.1	.06187	81.7	.58	80.8	198.8	407.9	198.80	0.0	0.0	0.0000	4.8	75.3	-1.2	-4.7
57.2	17843	29.8	.06213	86.2	.62	80.0	199.5	410.5	199.45	0.0	0.0	0.0000	4.8	82.1	-.7	-4.7
58.0	18153	38.7	.06352	110.0	.84	75.9	202.9	423.9	202.94	0.0	0.0	0.0000	5.5	115.6	2.4	-4.9
59.0	18590	50.8	.06607	139.9	1.19	70.6	209.6	446.9	209.56	0.0	0.0	0.0000	4.2	147.2	3.5	-2.3
59.1	18642	51.9	.06644	143.0	1.23	70.0	209.6	448.1	209.58	0.0	0.0	0.0000	3.3	148.2	2.8	-1.7
60.0	18985	59.5	.06887	163.8	1.49	66.2	209.7	455.6	209.74	0.0	0.0	0.0000	2.8	318.2	-2.1	1.9
61.0	19377	67.4	.07207	185.5	1.80	62.1	209.7	464.0	209.74	0.0	0.0	0.0000	2.8	321.4	-2.2	1.7
61.5	19587	69.6	.07396	191.7	1.93	60.0	209.7	468.6	209.74	0.0	0.0	0.0000	2.2	335.0	-2.0	.9
62.0	19764	71.5	.07553	196.9	2.03	58.3	209.7	472.4	209.74	0.0	0.0	0.0000	1.9	351.6	-1.9	.3
63.0	20166	79.4	.07944	218.3	2.41	54.6	209.9	481.8	209.93	0.0	0.0	0.0000	7.0	353.7	-7.0	.8
64.0	20584	82.0	.08378	226.4	2.67	51.0	209.2	489.5	209.18	0.0	0.0	0.0000	6.6	350.8	-6.5	1.1
64.3	20705	83.8	.08510	231.0	2.78	50.0	209.4	492.8	209.37	0.0	0.0	0.0000	5.5	2.0	-5.5	-.2

TIME MIN	ALT GPM	OZONE MICMB	TOTOZ ATMCM	OZDEN MG/M3	OZMXR MICGG	PRESS MB	TEMP DEG K	PTEMP DEG K	VTEMP DEG K	HMDTY PRCNT	DEWPT DEG K	SPCFC HMDTY	SPD MPS	DIR DEG	NS MPS	EW MPS
65.0	20943	87.2	.08769	240.1	3.00	48.1	209.7	499.1	209.74	0.0	0.0	0.0000	4.3	37.6	-3.4	-2.6
66.0	21272	89.0	.09140	243.0	3.23	45.6	211.6	511.2	211.56	0.0	0.0	0.0000	5.5	115.5	2.4	-5.0
67.0	21664	94.1	.09598	256.8	3.64	42.8	211.6	520.5	211.56	0.0	0.0	0.0000	5.8	139.8	4.4	-3.7
68.0	22070	108.9	.10119	293.0	4.50	40.1	214.5	537.7	214.50	0.0	0.0	0.0000	5.4	138.5	4.0	-3.6
68.0	22085	109.3	.10142	294.0	4.53	40.0	214.6	538.3	214.59	0.0	0.0	0.0000	5.4	138.8	4.0	-3.5
69.0	22493	120.4	.10726	320.7	5.32	37.5	216.8	554.0	216.82	0.0	0.0	0.0000	4.4	150.3	3.8	-2.2
70.0	22860	130.2	.11296	344.5	6.10	35.4	218.3	566.9	218.26	0.0	0.0	0.0000	2.5	219.8	1.9	1.6
70.2	22932	131.7	.11416	347.6	6.24	35.0	218.7	570.0	218.71	0.0	0.0	0.0000	2.1	242.1	1.0	1.9
71.0	23233	137.8	.11911	360.6	6.83	33.4	220.6	582.6	220.59	0.0	0.0	0.0000	4.1	314.9	-2.9	2.9
72.0	23673	144.0	.12668	377.3	7.65	31.2	220.4	593.6	220.43	0.0	0.0	0.0000	6.2	335.0	-5.6	2.6
72.7	23925	144.5	.13115	379.6	7.99	30.0	219.8	598.7	219.82	0.0	0.0	0.0000	5.0	332.4	-4.4	2.3
73.0	24055	144.8	.13345	380.8	8.16	29.4	219.5	601.3	219.51	0.0	0.0	0.0000	4.3	330.6	-3.8	2.1
74.0	24438	143.1	.14022	375.7	8.56	27.7	219.8	612.4	219.82	0.0	0.0	0.0000	2.7	37.5	-2.1	-1.6
75.0	24896	146.0	.14832	381.9	9.38	25.8	220.7	627.6	220.74	0.0	0.0	0.0000	1.3	19.0	-1.2	-.4
75.4	25098	146.0	.15195	382.6	9.68	25.0	220.3	632.2	220.34	0.0	0.0	0.0000	1.4	340.3	-1.3	.5
76.0	25362	146.0	.15665	383.6	10.08	24.0	219.8	638.1	219.82	0.0	0.0	0.0000	2.2	312.3	-1.5	1.6
77.0	25833	143.8	.16506	380.2	10.69	22.3	218.4	647.4	218.41	0.0	0.0	0.0000	1.9	35.5	-1.5	-1.1
78.0	26279	145.0	.17299	381.2	11.55	20.8	219.7	664.2	219.66	0.0	0.0	0.0000	4.7	72.1	-1.5	-4.5
78.6	26531	145.2	.17746	380.7	12.04	20.0	220.2	673.5	220.22	0.0	0.0	0.0000	7.6	82.9	-.9	-7.6
79.0	26695	145.4	.18038	380.4	12.35	19.5	220.6	679.4	220.59	0.0	0.0	0.0000	9.5	86.3	-.6	-9.5
80.0	27104	140.5	.18755	368.5	12.72	18.3	220.1	690.4	220.13	0.0	0.0	0.0000	8.3	92.8	.4	-8.3
80.6	27391	139.1	.19246	365.2	13.18	17.5	219.9	698.7	219.94	0.0	0.0	0.0000	5.3	89.7	0.0	-5.3
81.0	27578	138.2	.19565	363.1	13.47	17.0	219.8	704.1	219.82	0.0	0.0	0.0000	3.4	84.8	-.3	-3.4
82.0	27970	138.2	.20226	359.1	14.31	16.0	222.2	724.3	222.25	0.0	0.0	0.0000	2.9	103.3	.7	-2.8
83.0	28391	134.1	.20920	345.9	14.82	15.0	223.9	743.2	223.87	0.0	0.0	0.0000	4.2	86.8	-.2	-4.2
84.0	28750	129.9	.21491	334.0	15.16	14.2	224.6	757.4	224.60	0.0	0.0	0.0000	6.8	84.6	-.6	-6.8
85.0	29181	127.0	.22154	325.5	15.82	13.3	225.2	773.7	225.18	0.0	0.0	0.0000	7.1	104.6	1.8	-6.9
85.9	29590	118.6	.22753	303.5	15.72	12.5	225.7	789.3	225.69	0.0	0.0	0.0000	7.5	100.6	1.4	-7.3
86.0	29643	117.6	.22830	300.7	15.71	12.4	225.8	791.4	225.76	0.0	0.0	0.0000	7.5	100.1	1.3	-7.4
87.0	30140	111.2	.23510	285.2	16.03	11.5	225.2	806.5	225.18	0.0	0.0	0.0000	14.4	93.7	.9	-14.4
88.0	30618	106.7	.24130	270.3	16.52	10.7	227.9	833.2	227.88	0.0	0.0	0.0000	17.3	98.2	2.5	-17.1
89.0	31072	100.1	.24682	250.7	16.59	10.0	230.5	859.3	230.52	0.0	0.0	0.0000	15.3	99.3	2.5	-15.1
90.0	31348	94.8	.24996	235.8	16.36	9.6	232.2	875.5	232.15	0.0	0.0	0.0000	999.9	999.9	999.9	999.9

INTEGRAL .24996 RESIDUAL .07487 INTEGRATED TOTAL OZONE .32483

OZONAGRAM

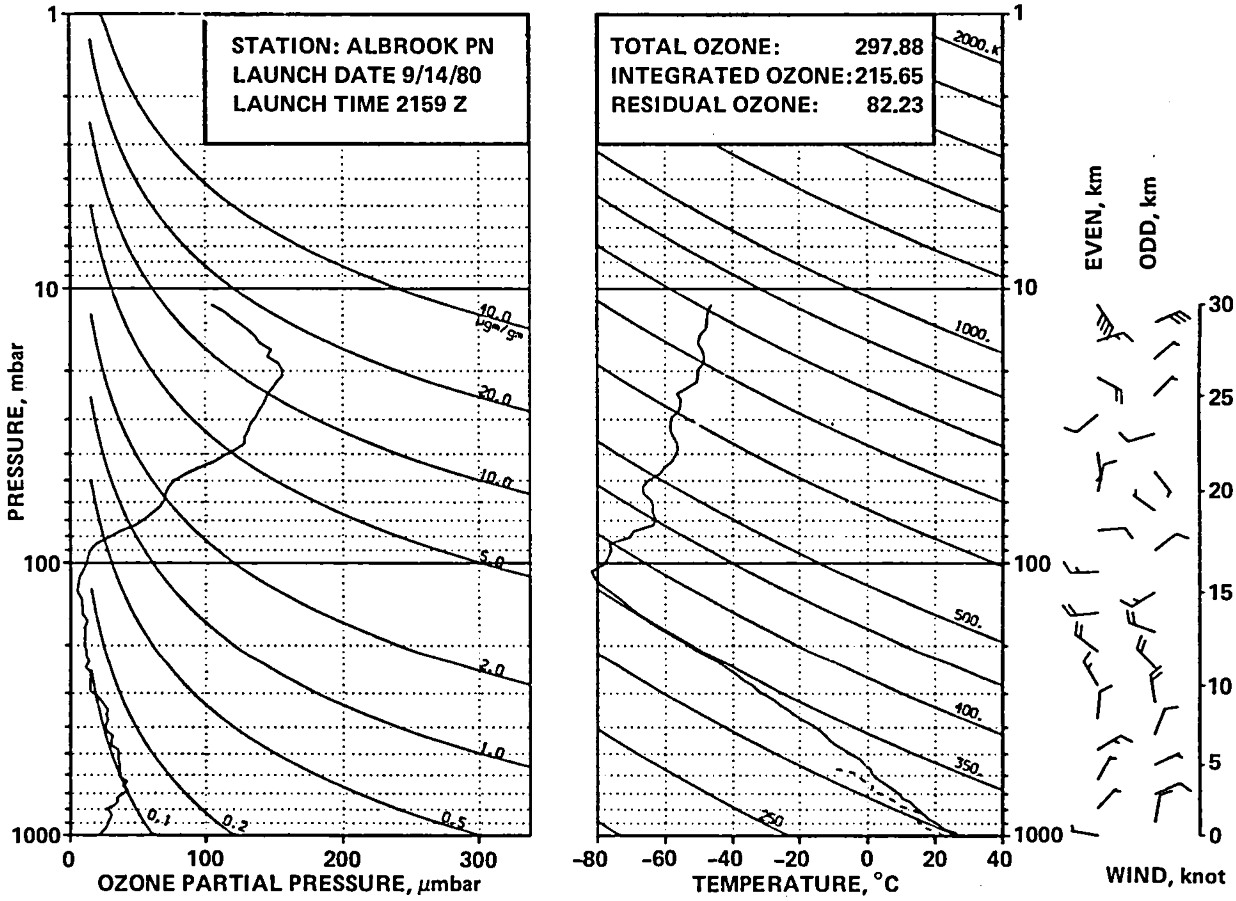
STATION: ALBROOK PN
LAUNCH DATE 9/14/80
LAUNCH TIME 2159 Z
TOTAL OZONE: 297.88
INTEGRATED OZONE: 215.65
RESIDUAL OZONE: 82.23
PRESSURE, mbar
OZONE PARTIAL PRESSURE, μmbar
TEMPERATURE, °C
EVEN, km
ODD, km
HEIGHT, GP km
WIND, knot

STATION ALBROOK PN   LAUNCH DATE 9/14/80   TIME 2159Z   ECC   SONDE 3A1343

SURFACE CONDITIONS   PRESS 998.4MB   TEMP 300.2 DEG K   HUMIDITY 82.0 PRCNT

TIME MIN	ALT GPM	OZONE MICMB	TOTOZ ATMCM	OZDEN MG/M3	OZMXR MICGG	PRESS MB	TEMP DEG K	PTEMP DEG K	VTEMP DEG K	HMDTY PRCNT	DEWPT DEG K	SPCFC HMDTY	SPD MPS	DIR DEG	NS MPS	EW MPS
0.0	66	21.2	0.00000	40.7	.04	998.4	299.8	300.0	302.94	77.1	295.5	.0169	2.0	280.0	-.3	2.0
1.0	303	22.7	.00046	43.8	.04	972.0	299.3	301.8	302.33	74.5	294.5	.0163	6.0	317.6	-4.5	4.1
2.0	550	25.3	.00100	49.3	.04	945.0	295.8	300.6	298.30	76.7	291.5	.0139	6.4	335.1	-5.8	2.7
3.0	802	26.8	.00159	52.6	.05	918.0	294.6	301.9	296.85	70.7	289.1	.0123	5.9	353.4	-5.9	.7
3.7	973	27.3	.00202	53.7	.05	900.0	293.7	302.7	295.87	71.7	288.4	.0120	5.3	4.0	-5.3	-.4
4.0	1051	27.5	.00221	54.2	.05	892.0	293.3	303.0	295.43	72.2	288.1	.0119	5.1	9.5	-5.0	-.8
5.0	1276	28.9	.00279	57.4	.06	869.0	291.3	303.3	293.50	80.7	288.0	.0121	5.5	17.2	-5.3	-1.6
5.8	1465	29.6	.00330	58.9	.06	850.0	290.5	304.3	292.86	89.6	288.8	.0133	6.1	14.7	-5.9	-1.6
6.0	1526	29.9	.00341	59.4	.06	844.0	290.3	304.7	292.66	92.5	289.0	.0134	6.3	14.0	-6.2	-1.5
7.0	1762	29.1	.00411	58.2	.06	821.0	289.0	305.8	291.35	95.2	288.3	.0131	5.7	18.0	-5.4	-1.8
7.9	1982	26.9	.00468	53.9	.06	800.0	288.3	307.3	290.35	86.7	286.1	.0115	3.7	31.9	-3.2	-2.0
8.0	2004	26.7	.00474	53.5	.06	798.0	288.2	307.4	290.25	85.9	285.9	.0115	3.6	34.0	-3.0	-2.0
9.0	2262	32.1	.00545	64.6	.07	774.0	286.8	308.6	288.50	76.2	282.7	.0096	2.7	71.1	-.9	-2.5
10.0	2527	34.6	.00628	69.9	.08	750.0	285.8	310.3	287.45	75.6	281.6	.0092	4.5	80.9	-.7	-4.5
11.0	2776	34.1	.00708	69.5	.08	728.0	283.5	310.5	284.98	77.2	279.7	.0083	5.0	79.3	-.9	-4.9
12.0	3055	38.3	.00804	78.2	.09	704.0	282.6	312.4	283.89	71.0	277.6	.0074	4.2	67.1	-1.7	-3.9
12.2	3102	38.9	.00822	79.5	.09	700.0	282.4	312.6	283.60	69.3	277.0	.0070	4.4	64.5	-1.9	-4.0
13.0	3330	41.8	.00909	85.9	.10	681.0	281.1	313.8	282.16	60.7	274.0	.0059	5.5	54.7	-3.2	-4.5
14.0	3600	38.4	.01013	79.4	.10	659.0	279.4	314.7	280.46	72.3	274.7	.0065	5.5	49.9	-3.5	-4.2
15.0	3916	41.8	.01135	87.1	.11	634.0	277.4	316.0	278.41	70.2	272.5	.0057	4.2	37.5	-3.3	-2.6
16.0	4202	36.5	.01245	76.5	.10	612.0	275.6	317.1	276.46	70.9	270.8	.0052	3.2	22.7	-2.9	-1.2
16.5	4361	36.5	.01302	76.6	.10	600.0	274.9	318.2	275.81	71.5	270.3	.0051	2.9	15.9	-2.8	-.8
17.0	4497	36.5	.01350	76.7	.10	590.0	274.4	319.1	275.26	72.0	269.9	.0051	2.7	9.1	-2.7	-.4
18.0	4817	35.9	.01463	75.6	.10	567.0	273.8	321.9	274.31	47.5	263.9	.0033	3.2	18.1	-3.0	-1.0
19.0	5133	35.9	.01575	76.1	.11	545.0	272.0	323.5	272.10	0.0	0.0	0.0000	2.8	76.5	-.6	-2.7
20.0	5460	35.1	.01691	74.9	.11	523.0	271.0	326.2	271.03	0.0	0.0	0.0000	4.8	91.3	.1	-4.8
21.0	5783	35.0	.01804	75.4	.12	502.0	268.4	326.8	268.39	0.0	0.0	0.0000	6.0	73.8	-1.7	-5.8
21.1	5814	35.0	.01815	75.4	.12	500.0	268.2	326.9	268.17	0.0	0.0	0.0000	6.2	71.7	-1.9	-5.9
22.0	6068	34.9	.01905	75.7	.12	484.0	266.4	327.8	266.42	0.0	0.0	0.0000	7.9	58.6	-4.1	-6.7
23.0	6362	29.9	.02002	65.5	.11	466.0	264.1	328.4	264.25	28.5	249.1	.0012	8.7	49.7	-5.6	-6.6
24.0	6665	29.8	.02095	65.6	.11	448.0	262.2	329.8	262.29	0.0	0.0	0.0000	6.1	37.4	-4.9	-3.7
25.0	6979	31.0	.02193	68.6	.12	430.0	261.0	332.2	261.22	32.7	248.0	.0011	4.8	21.1	-4.5	-1.7
26.0	7305	26.3	.02290	58.5	.11	412.0	259.3	334.1	259.63	56.4	252.6	.0018	4.0	21.9	-3.7	-1.5
26.6	7528	25.9	.02350	58.0	.11	400.0	257.9	335.0	258.08	45.7	248.7	.0012	3.8	16.0	-3.7	-1.1
27.0	7662	25.7	.02387	57.8	.11	393.0	257.0	335.6	257.15	39.3	246.4	.0011	3.8	12.4	-3.7	-.8
28.0	7992	27.4	.02479	62.2	.12	376.0	253.9	335.7	253.90	0.0	0.0	0.0000	5.7	2.6	-5.7	-.3
29.0	8313	26.1	.02571	60.0	.12	360.0	251.6	336.8	251.61	0.0	0.0	0.0000	5.9	11.2	-5.8	-1.1
29.7	8519	27.0	.02630	62.3	.13	350.0	250.3	337.9	250.36	0.0	0.0	0.0000	5.8	3.8	-5.8	-.4
30.0	8604	27.4	.02655	63.2	.13	346.0	249.8	338.3	249.85	0.0	0.0	0.0000	5.7	.8	-5.7	-.1
31.0	8882	24.9	.02734	58.2	.12	333.0	247.5	338.8	247.47	0.0	0.0	0.0000	8.9	353.9	-8.9	.9
32.0	9169	22.5	.02808	52.8	.12	320.0	245.9	340.5	245.91	0.0	0.0	0.0000	10.1	348.2	-9.9	2.1
33.0	9443	20.0	.02872	47.4	.11	308.0	243.8	341.3	243.83	22.0	229.0	.0002	9.4	338.9	-8.8	3.4
33.6	9629	16.7	.02908	39.7	.09	300.0	242.1	341.5	242.18	48.5	233.7	.0005	9.0	337.3	-8.3	3.5
34.0	9749	14.5	.02931	34.8	.08	295.0	241.0	341.7	241.13	65.4	236.8	.0006	8.7	336.1	-8.0	3.5
35.0	10090	14.4	.02987	34.9	.09	281.0	239.1	343.6	239.14	54.8	233.2	.0004	8.1	328.4	-6.9	4.3
36.0	10393	14.3	.03036	34.9	.09	269.0	236.3	343.9	236.33	25.6	223.8	.0002	10.2	318.8	-7.7	6.7
37.0	10788	14.9	.03102	36.7	.10	254.0	233.8	345.8	233.80	36.7	224.6	.0002	11.1	318.7	-8.4	7.4
37.3	10895	13.6	.03118	33.7	.09	250.0	232.9	346.1	232.90	0.0	0.0	0.0000	10.6	318.8	-8.0	7.0
38.0	11117	11.0	.03151	27.6	.08	242.0	231.1	346.6	231.06	0.0	0.0	0.0000	9.5	319.0	-7.2	6.2
39.0	11459	13.4	.03200	34.0	.10	230.0	228.4	347.6	228.44	0.0	0.0	0.0000	9.3	318.7	-7.0	6.1
40.0	11754	11.5	.03244	29.3	.09	220.0	225.6	347.7	225.61	0.0	0.0	0.0000	9.2	317.4	-6.8	6.3
41.0	12059	11.5	.03286	29.7	.09	210.0	222.8	348.1	222.84	0.0	0.0	0.0000	10.8	306.0	-6.3	8.7
42.0	12375	10.2	.03328	26.8	.08	200.0	220.1	348.6	220.13	0.0	0.0	0.0000	11.6	297.5	-5.3	10.3
43.0	12669	10.2	.03365	27.0	.09	191.0	217.3	348.7	217.30	0.0	0.0	0.0000	10.6	290.4	-3.7	9.9
44.0	12973	10.5	.03404	28.3	.10	182.0	214.2	348.5	214.17	0.0	0.0	0.0000	10.5	288.6	-3.3	10.0
45.0	13324	10.4	.03451	28.6	.10	172.0	210.8	348.6	210.84	0.0	0.0	0.0000	10.5	291.5	-3.8	9.8
46.0	13653	12.2	.03499	33.9	.12	163.0	208.2	349.7	208.23	0.0	0.0	0.0000	9.0	283.8	-2.2	8.8
47.0	14036	8.5	.03551	24.0	.09	153.0	205.1	350.6	205.06	0.0	0.0	0.0000	9.2	264.5	.9	9.2
47.4	14153	8.5	.03564	24.1	.09	150.0	204.2	351.1	204.20	0.0	0.0	0.0000	9.3	261.9	1.3	9.2
48.0	14356	8.5	.03587	24.3	.10	145.0	202.7	352.0	202.72	0.0	0.0	0.0000	9.5	257.7	2.0	9.3
49.0	14733	8.0	.03629	23.0	.10	136.0	200.0	353.7	199.99	0.0	0.0	0.0000	8.7	254.2	2.4	8.4
50.0	15130	4.9	.03663	14.3	.06	127.0	196.8	354.9	196.79	0.0	0.0	0.0000	8.2	236.1	4.6	6.8
50.3	15220	5.0	.03670	14.8	.07	125.0	196.0	355.1	196.03	0.0	0.0	0.0000	8.3	235.1	4.7	6.8
51.0	15454	5.4	.03686	16.2	.08	120.0	194.1	355.7	194.09	0.0	0.0	0.0000	8.6	232.7	5.2	6.8
52.0	15844	6.5	.03719	19.4	.10	112.0	192.1	359.0	192.05	0.0	0.0	0.0000	9.8	248.4	3.6	9.1
53.0	16100	8.8	.03746	26.6	.14	107.0	191.4	362.5	191.44	0.0	0.0	0.0000	7.6	270.5	-.1	7.6
54.0	16426	11.2	.03792	33.1	.18	101.0	195.2	375.8	195.19	0.0	0.0	0.0000	5.0	325.5	-4.1	2.9
54.2	16483	11.5	.03801	33.9	.19	100.0	195.4	377.3	195.40	0.0	0.0	0.0000	4.5	333.2	-4.0	2.0
55.0	16789	12.9	.03852	37.9	.23	94.8	196.5	385.3	196.53	0.0	0.0	0.0000	4.1	36.6	-3.3	-2.4
56.0	17095	14.1	.03909	41.1	.26	89.9	197.3	392.7	197.30	0.0	0.0	0.0000	5.3	53.5	-3.2	-4.3
57.0	17411	19.2	.03981	56.3	.37	85.1	196.8	397.9	196.79	0.0	0.0	0.0000	6.1	38.4	-4.8	-3.8
58.0	17721	28.2	.04080	80.3	.58	80.7	202.7	416.1	202.72	0.0	0.0	0.0000	6.9	51.1	-4.3	-5.4
58.2	17772	29.6	.04102	84.2	.61	80.0	202.9	417.6	202.93	0.0	0.0	0.0000	6.6	55.1	-3.8	-5.4
59.0	18047	37.0	.04221	104.6	.80	76.4	204.0	425.4	204.01	0.0	0.0	0.0000	5.7	81.2	-.9	-5.6
60.0	18347	48.2	.04387	132.7	1.10	72.7	209.7	443.6	209.74	0.0	0.0	0.0000	3.2	141.7	2.5	-2.0
60.7	18579	53.2	.04542	146.1	1.26	70.0	210.1	449.3	210.14	0.0	0.0	0.0000	2.4	220.2	1.9	1.6
61.0	18668	55.0	.04600	151.1	1.32	69.0	210.3	451.4	210.29	0.0	0.0	0.0000	3.3	241.3	1.6	2.9
62.0	19016	61.3	.04860	169.0	1.56	65.2	209.4	456.8	209.37	0.0	0.0	0.0000	3.3	295.8	-1.5	3.0
63.0	19324	66.3	.05113	182.6	1.77	62.0	209.6	463.8	209.56	0.0	0.0	0.0000	3.8	356.9	-3.8	.2
63.6	19524	68.1	.05289	188.1	1.88	60.0	209.2	467.4	209.20	0.0	0.0	0.0000	4.6	10.5	-4.5	-.8
64.0	19638	69.2	.05388	191.1	1.95	58.9	209.0	469.4	208.99	0.0	0.0	0.0000	5.1	15.1	-4.9	-1.4
65.0	19956	69.9	.05675	195.1	2.07	55.9	206.9	471.6	206.87	0.0	0.0	0.0000	5.7	14.0	-5.5	-1.4
66.0	20289	72.3	.05984	202.1	2.26	52.9	206.5	478.2	206.48	0.0	0.0	0.0000	3.7	10.4	-3.6	-.7

TIME MIN	ALT GPM	OZONE MICMB	TOTOZ ATMCM	OZDEN MG/M3	OZMXR MICGG	PRESS MB	TEMP DEG K	PTEMP DEG K	VTEMP DEG K	HMDTY PRCNT	DEWPT DEG K	SPCFC HMDTY	SPD MPS	DIR DEG	NS MPS	EW MPS
67.0	20630	76.8	.06316	213.0	2.55	50.0	208.2	490.0	208.17	0.0	0.0	0.0000	1.3	75.4	-.3	-1.3
67.0	20643	77.0	.06328	213.4	2.56	49.9	208.2	490.4	208.23	0.0	0.0	0.0000	1.3	80.4	-.2	-1.3
68.0	20998	85.6	.06693	233.5	3.01	47.1	211.6	506.5	211.56	0.0	0.0	0.0000	3.6	142.4	2.9	-2.2
69.0	21337	96.0	.07089	260.3	3.57	44.6	213.0	517.9	212.97	0.0	0.0	0.0000	2.8	140.4	2.2	-1.8
70.0	21609	105.8	.07435	284.1	4.11	42.7	215.0	529.4	215.01	0.0	0.0	0.0000	1.1	78.2	-.2	-1.1
71.0	21911	112.7	.07849	301.2	4.59	40.7	216.0	539.2	216.00	0.0	0.0	0.0000	2.5	145.3	2.0	-1.4
71.3	22020	115.7	.08009	308.8	4.80	40.0	216.3	542.6	216.28	0.0	0.0	0.0000	2.3	165.2	2.3	-.6
72.0	22230	121.4	.08314	323.4	5.20	38.7	216.8	549.0	216.82	0.0	0.0	0.0000	2.9	199.3	2.7	.9
73.0	22566	128.5	.08837	342.4	5.80	36.7	216.7	557.0	216.65	0.0	0.0	0.0000	4.7	244.5	2.0	4.2
73.9	22865	128.5	.09318	343.9	6.09	35.0	215.8	562.3	215.78	0.0	0.0	0.0000	6.1	233.5	3.6	4.9
74.0	22902	128.5	.09377	344.1	6.12	34.8	215.7	563.0	215.67	0.0	0.0	0.0000	6.2	232.5	3.8	4.9
75.0	23236	131.1	.09921	352.6	6.58	33.0	214.7	568.9	214.67	0.0	0.0	0.0000	5.1	275.5	-.5	5.1
76.0	23608	132.9	.10538	357.4	7.08	31.1	214.7	578.7	214.67	0.0	0.0	0.0000	7.0	332.4	-6.2	3.2
76.7	23834	135.4	.10921	363.8	7.48	30.0	214.9	585.3	214.90	0.0	0.0	0.0000	6.4	346.8	-6.2	1.5
77.0	23940	136.6	.11100	366.8	7.67	29.5	215.0	588.4	215.01	0.0	0.0	0.0000	6.3	354.1	-6.2	.6
78.0	24270	138.7	.11667	368.9	8.21	28.0	217.1	603.1	217.14	0.0	0.0	0.0000	6.5	30.6	-5.6	-3.3
79.0	24548	141.4	.12151	375.4	8.74	26.8	217.5	611.6	217.46	0.0	0.0	0.0000	6.5	41.3	-4.9	-4.3
80.0	24915	144.0	.12799	381.7	9.43	25.3	217.8	622.7	217.78	0.0	0.0	0.0000	3.3	13.8	-3.2	-.8
80.3	24990	144.3	.12935	383.2	9.57	25.0	217.5	623.9	217.48	0.0	0.0	0.0000	2.9	27.6	-2.6	-1.3
81.0	25197	145.3	.13307	387.3	9.95	24.2	216.7	627.4	216.65	0.0	0.0	0.0000	3.0	72.6	-.9	-2.9
82.0	25521	149.1	.13898	392.0	10.74	23.0	219.7	645.4	219.66	0.0	0.0	0.0000	7.4	98.6	1.1	-7.3
83.0	25838	152.0	.14480	394.7	11.50	21.9	222.4	662.7	222.40	0.0	0.0	0.0000	11.0	108.6	3.5	-10.4
84.0	26174	156.0	.15106	404.3	12.43	20.8	222.8	673.8	222.84	0.0	0.0	0.0000	10.3	123.1	5.6	-8.6
84.8	26429	155.9	.15589	403.9	12.92	20.0	222.8	681.4	222.84	0.0	0.0	0.0000	4.9	124.6	2.8	-4.1
85.0	26495	155.9	.15713	403.8	13.04	19.8	222.8	683.4	222.84	0.0	0.0	0.0000	3.6	125.7	2.1	-2.9
86.0	26869	153.0	.16409	393.6	13.56	18.7	224.5	699.7	224.46	0.0	0.0	0.0000	1.7	24.8	-1.5	-.7
87.0	27230	145.3	.17056	373.4	13.60	17.7	224.6	711.2	224.60	0.0	0.0	0.0000	1.1	68.9	-.4	-1.0
87.2	27304	145.8	.17187	374.9	13.81	17.5	224.5	713.2	224.49	0.0	0.0	0.0000	1.2	69.8	-.4	-1.2
88.0	27612	147.9	.17729	381.2	14.68	16.7	224.0	721.2	224.02	0.0	0.0	0.0000	1.7	72.3	-.5	-1.6
89.0	27974	139.9	.18358	362.5	14.67	15.8	222.8	728.9	222.84	0.0	0.0	0.0000	6.0	72.7	-1.8	-5.8
89.8	28313	136.6	.18923	353.3	15.09	15.0	223.3	741.4	223.31	0.0	0.0	0.0000	9.4	71.1	-3.0	-8.9
90.0	28401	135.8	.19069	350.9	15.20	14.8	223.4	744.6	223.43	0.0	0.0	0.0000	10.3	70.9	-3.4	-9.7
91.0	28813	129.7	.19726	332.2	15.46	13.9	225.3	764.5	225.32	0.0	0.0	0.0000	13.3	63.8	-5.9	-12.0
92.0	29254	121.3	.20389	310.7	15.47	13.0	225.5	779.8	225.47	0.0	0.0	0.0000	17.1	66.8	-6.8	-15.7
92.5	29513	117.1	.20752	299.5	15.51	12.5	225.6	789.1	225.63	0.0	0.0	0.0000	18.9	68.7	-6.9	-17.6
93.0	29728	113.5	.21054	290.3	15.54	12.1	225.8	796.9	225.76	0.0	0.0	0.0000	20.4	70.0	-7.0	-19.1
94.0	30123	104.1	.21565	265.0	15.14	11.4	226.9	814.7	226.89	0.0	0.0	0.0000	999.9	999.9	999.9	999.9

INTEGRAL .21565 RESIDUAL .08223 INTEGRATED TOTAL OZONE .29788

OZONAGRAM

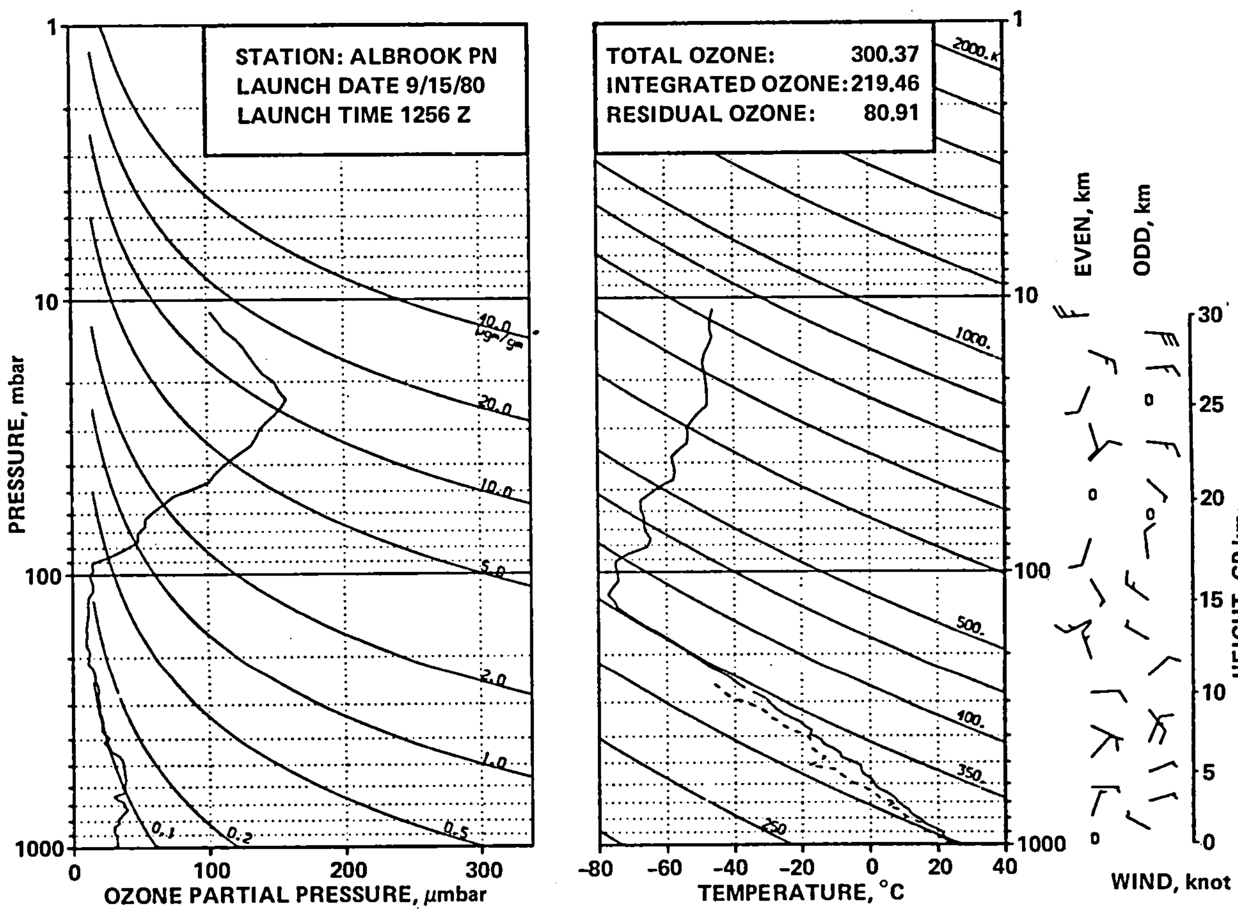

STATION: ALBROOK PN
LAUNCH DATE 9/15/80
LAUNCH TIME 1256 Z
TOTAL OZONE: 300.37
INTEGRATED OZONE: 219.46
RESIDUAL OZONE: 80.91
PRESSURE, mbar
OZONE PARTIAL PRESSURE, μmbar
TEMPERATURE, °C
EVEN, km
ODD, km
HEIGHT, GP km
WIND, knot

STATION ALBROOK PN LAUNCH DATE 9/15/80 TIME 1256Z ECC SONDE 3A1344

SURFACE CONDITIONS PRESS 1000.8MB TEMP 298.8 DEG K HUMIDITY 96.0 PRCNT

TIME MIN	ALT GPM	OZONE MICMB	TOTOZ ATMCM	OZDEN MG/M3	OZMXR MICGG	PRESS MB	TEMP DEG K	PTEMP DEG K	VTEMP DEG K	HMDTY PRCNT	DEWPT DEG K	SPCFC HMDTY	SPD MPS	DIR DEG	NS MPS	EW MPS
0.0	66	28.2	0.00000	54.5	.05	1000.8	298.6	298.5	302.16	95.8	297.9	.0195	0.0	0.0	0.0	0.0
0.0	73	28.3	.00002	54.8	.05	1000.0	298.5	298.5	302.05	95.9	297.8	.0194	.2	321.3	-.2	.1
1.0	259	32.0	.00052	62.4	.05	979.0	296.0	297.8	299.13	97.7	295.6	.0174	5.3	321.3	-4.2	3.3
2.0	485	31.5	.00117	61.6	.05	954.0	295.3	299.3	298.32	95.7	294.6	.0168	6.9	320.3	-5.3	4.4
3.0	707	31.1	.00180	61.0	.06	930.0	294.6	300.8	297.38	89.3	292.8	.0154	5.7	315.9	-4.1	4.0
4.0	925	31.4	.00242	61.4	.06	907.0	294.6	302.9	297.12	79.1	290.8	.0140	4.0	307.7	-2.4	3.2
4.3	992	30.8	.00260	60.5	.06	900.0	294.2	303.2	296.62	78.7	290.3	.0134	3.7	304.2	-2.1	3.0
5.0	1167	29.5	.00309	58.1	.06	882.0	293.0	303.7	295.33	77.5	289.0	.0128	3.0	292.2	-1.1	2.8
6.0	1394	29.5	.00370	58.5	.06	859.0	290.9	303.8	293.10	84.7	288.3	.0125	2.0	293.1	-.8	1.8
6.4	1484	29.6	.00395	58.9	.06	850.0	290.1	303.9	292.33	87.9	288.1	.0125	1.4	313.0	-1.0	1.0
7.0	1616	29.7	.00431	59.4	.06	837.0	289.0	304.1	291.20	92.7	287.8	.0125	1.3	3.8	-1.3	-.1
8.0	1863	33.2	.00503	66.6	.07	813.0	288.2	305.7	290.18	86.6	286.0	.0114	1.8	31.6	-1.6	-1.0
8.6	1999	32.5	.00545	65.3	.07	800.0	287.2	306.1	289.05	84.6	284.6	.0103	1.6	24.4	-1.4	-.7
9.0	2084	32.0	.00570	64.4	.07	792.0	286.6	306.3	288.35	83.4	283.8	.0101	1.4	18.5	-1.4	-.5
10.0	2321	34.6	.00645	70.2	.07	770.0	285.0	307.1	286.65	63.3	282.3	.0094	.2	297.3	-.1	.2
11.0	2564	36.2	.00726	73.5	.08	748.0	284.4	309.0	286.09	84.9	282.0	.0095	1.3	189.7	1.3	.2
12.0	2813	39.4	.00815	80.4	.09	726.0	282.7	309.8	284.02	72.3	278.0	.0074	1.4	111.6	.5	-1.3
13.0	3092	36.5	.00915	75.0	.09	702.0	281.3	311.2	282.90	98.4	281.0	.0095	3.4	70.8	-1.1	-3.2
13.1	3115	36.5	.00924	75.0	.09	700.0	281.2	311.4	282.79	95.7	280.5	.0089	3.5	70.3	-1.2	-3.3
14.0	3318	36.5	.00994	75.2	.09	683.0	280.7	313.0	281.91	72.3	276.1	.0069	4.2	66.6	-1.7	-3.9
15.0	3550	31.5	.01070	65.1	.08	664.0	279.5	314.2	280.63	75.1	275.4	.0067	1.6	90.4	0.0	-1.6
16.0	3762	29.7	.01133	61.7	.08	647.0	278.1	314.9	279.09	71.7	273.4	.0060	2.7	90.4	0.0	-2.7
17.0	4004	36.8	.01211	77.0	.10	628.0	275.9	315.1	276.82	77.8	272.4	.0057	3.2	68.3	-1.2	-3.0
18.0	4265	37.4	.01306	78.8	.10	608.0	274.4	316.3	275.21	74.6	270.3	.0051	.4	161.9	.4	-.1
18.4	4371	37.3	.01345	78.6	.10	600.0	274.3	317.4	275.07	68.1	269.0	.0044	.6	151.4	.6	-.3
19.0	4507	37.2	.01394	78.4	.10	590.0	274.2	318.8	274.89	59.9	267.3	.0042	1.0	146.3	.8	-.5
20.0	4783	38.0	.01497	80.5	.11	570.0	272.9	320.4	273.54	59.7	266.0	.0039	1.0	62.3	-.5	-.9
21.0	5068	37.5	.01603	80.0	.11	550.0	271.0	321.4	271.55	59.6	264.2	.0035	2.1	69.2	-.7	-2.0
22.0	5332	37.2	.01701	79.4	.12	532.0	270.5	323.9	271.06	58.6	263.5	.0034	3.5	96.0	.4	-3.5
23.0	5620	36.7	.01807	78.4	.12	513.0	270.3	327.1	270.64	30.2	255.3	.0018	4.4	90.8	.1	-4.4
23.7	5821	36.3	.01881	78.0	.12	500.0	268.5	327.2	268.83	43.3	257.7	.0024	4.1	69.1	-1.5	-3.8
24.0	5901	36.1	.01910	77.8	.12	495.0	267.7	327.3	268.12	48.4	258.6	.0025	4.2	60.4	-2.1	-3.6
25.0	6173	35.7	.02009	77.9	.12	478.0	264.7	326.9	265.19	68.5	260.0	.0029	5.5	29.4	-4.8	-2.7
26.0	6454	33.2	.02107	72.6	.12	461.0	264.3	329.7	264.69	59.4	257.8	.0025	8.3	20.8	-7.8	-3.0
27.0	6761	27.8	.02203	61.2	.10	443.0	262.3	330.9	262.62	60.8	256.2	.0023	9.5	21.4	-8.8	-3.4
28.0	7024	26.5	.02277	58.9	.10	428.0	259.7	331.0	260.06	71.8	255.7	.0023	8.6	23.3	-7.9	-3.4
29.0	7350	22.4	.02360	50.0	.09	410.0	258.6	333.6	258.95	77.8	255.6	.0023	6.9	30.4	-6.0	-3.5
29.7	7536	25.0	.02408	56.3	.10	400.0	256.6	333.4	256.92	85.0	254.6	.0022	5.2	40.8	-3.9	-3.4
30.0	7631	26.4	.02432	59.6	.11	395.0	255.6	333.2	255.89	88.7	254.1	.0021	4.4	49.0	-2.9	-3.3
31.0	7901	22.5	.02501	50.7	.10	381.0	256.1	337.4	256.34	58.5	249.9	.0015	5.0	101.1	1.0	-4.9
32.0	8140	20.7	.02556	47.1	.09	369.0	254.1	337.8	254.27	58.3	248.0	.0013	7.0	121.5	3.7	-6.0
33.0	8427	21.4	.02620	48.9	.10	355.0	252.6	339.6	252.77	57.9	246.5	.0012	6.8	124.7	3.9	-5.6
33.4	8531	21.4	.02644	49.1	.10	350.0	251.5	339.4	251.64	57.9	245.4	.0011	6.6	126.6	3.9	-5.3
34.0	8701	21.4	.02683	49.5	.10	342.0	249.7	339.2	249.80	57.7	243.7	.0010	6.3	129.9	4.0	-4.8
35.0	8961	20.8	.02743	48.6	.10	330.0	247.4	339.6	247.55	65.0	242.8	.0009	5.6	141.9	4.4	-3.4
36.0	9251	18.8	.02806	44.2	.10	317.0	245.4	340.8	245.56	65.2	240.9	.0008	4.5	145.8	3.7	-2.5
37.0	9598	19.5	.02879	46.1	.11	302.0	243.6	343.0	243.70	52.5	237.0	.0006	3.6	135.9	2.6	-2.5
37.2	9645	19.3	.02889	45.9	.11	300.0	243.4	343.3	243.46	49.6	236.2	.0005	3.6	127.9	2.2	-2.8
38.0	9862	18.8	.02935	44.7	.11	291.0	242.3	344.8	242.36	35.9	232.2	.0004	4.5	97.0	.5	-4.4
39.0	10158	18.0	.02996	43.4	.11	279.0	239.2	344.4	239.21	39.7	230.2	.0003	5.8	80.9	-.9	-5.7
40.0	10438	18.9	.03054	46.2	.12	268.0	236.4	344.4	236.43	44.9	228.8	.0003	6.2	73.8	-1.7	-5.9
41.0	10753	18.2	.03121	44.9	.12	256.0	233.7	345.0	233.76	46.2	226.6	.0002	5.8	63.0	-2.7	-5.2
41.5	10914	17.2	.03154	42.5	.11	250.0	232.7	345.7	232.68	0.0	0.0	0.0000	5.0	55.6	-2.9	-4.2
42.0	11080	16.1	.03186	40.2	.11	244.0	231.6	346.5	231.58	0.0	0.0	0.0000	4.3	45.3	-3.1	-3.1
43.0	11391	16.0	.03245	40.5	.11	233.0	228.8	347.0	228.83	0.0	0.0	0.0000	5.4	23.6	-5.0	-2.2
44.0	11742	14.7	.03309	37.5	.11	221.0	225.6	347.3	225.59	0.0	0.0	0.0000	7.1	10.8	-7.0	-1.3
45.0	12077	11.3	.03361	29.2	.09	210.0	223.3	348.7	223.27	0.0	0.0	0.0000	7.5	352.6	-7.4	1.0
46.0	12394	11.9	.03406	31.3	.10	200.0	220.4	349.1	220.43	0.0	0.0	0.0000	6.4	339.7	-6.0	2.2
47.0	12689	12.6	.03450	33.3	.11	191.0	218.1	350.0	218.10	0.0	0.0	0.0000	4.4	322.0	-3.5	2.7
48.0	12995	10.1	.03494	27.0	.09	182.0	215.4	350.4	215.36	0.0	0.0	0.0000	3.7	305.4	-2.1	3.0
49.0	13313	10.0	.03534	27.2	.10	173.0	212.8	351.3	212.82	0.0	0.0	0.0000	3.7	285.0	-1.0	3.6
50.0	13606	10.7	.03572	29.3	.11	165.0	210.1	351.6	210.15	0.0	0.0	0.0000	5.8	257.4	1.3	5.6
51.0	13870	10.0	.03608	28.0	.11	158.0	207.1	350.9	207.13	0.0	0.0	0.0000	7.4	246.8	2.9	6.8
51.8	14182	10.5	.03650	29.8	.12	150.0	204.2	351.1	204.20	0.0	0.0	0.0000	6.9	242.2	3.2	6.1
52.0	14263	10.7	.03661	30.3	.12	148.0	203.4	351.2	203.45	0.0	0.0	0.0000	6.8	240.9	3.3	6.0
53.0	14549	11.3	.03703	32.4	.13	141.0	201.0	351.8	201.02	0.0	0.0	0.0000	6.0	255.0	1.5	5.8
54.0	14803	11.6	.03743	33.7	.14	135.0	198.9	352.5	198.91	0.0	0.0	0.0000	6.1	285.6	-1.6	5.8
55.0	15112	11.2	.03790	32.6	.14	128.0	197.9	356.1	197.92	0.0	0.0	0.0000	9.2	309.8	-5.9	7.0
55.4	15246	11.4	.03812	33.5	.15	125.0	197.2	357.2	197.17	0.0	0.0	0.0000	9.3	320.4	-7.2	5.9
56.0	15436	11.8	.03841	34.7	.16	121.0	196.1	358.6	196.13	0.0	0.0	0.0000	9.9	334.0	-8.9	4.4
57.0	15779	15.1	.03905	44.1	.22	114.0	197.4	367.2	197.42	0.0	0.0	0.0000	3.7	3.9	-3.7	-.3
58.0	16093	14.6	.03968	42.4	.22	108.0	199.1	376.1	199.15	0.0	0.0	0.0000	1.3	162.6	1.3	-.4
59.0	16483	12.6	.04040	36.4	.21	101.0	198.9	382.9	198.91	0.0	0.0	0.0000	.8	236.7	.5	.7
59.2	16540	13.1	.04051	38.0	.22	100.0	198.8	383.8	198.81	0.0	0.0	0.0000	.9	275.8	-.1	.9
60.0	16766	15.2	.04093	44.1	.26	96.2	198.4	387.4	198.42	0.0	0.0	0.0000	2.8	322.8	-2.2	1.7
61.0	17076	13.9	.04154	40.3	.25	91.2	198.4	393.3	198.42	0.0	0.0	0.0000	3.9	354.4	-3.9	.4
62.0	17413	26.8	.04246	76.6	.52	86.1	201.9	406.9	201.92	0.0	0.0	0.0000	2.6	83.4	-.3	-2.5
63.0	17771	38.0	.04399	105.7	.78	81.1	207.7	425.8	207.71	0.0	0.0	0.0000	4.9	153.1	4.4	-2.2
63.2	17854	40.1	.04446	111.4	.83	80.0	207.9	427.9	207.91	0.0	0.0	0.0000	4.5	164.9	4.3	-1.2
64.0	18159	47.8	.04615	132.3	1.04	76.1	208.7	435.6	208.66	0.0	0.0	0.0000	5.0	212.3	4.2	2.7
65.0	18581	47.8	.04876	133.2	1.12	71.0	207.1	441.0	207.13	0.0	0.0	0.0000	5.0	248.0	1.9	4.7
65.2	18666	49.1	.04933	136.8	1.16	70.0	207.0	442.6	207.03	0.0	0.0	0.0000	4.0	250.4	1.4	3.8
66.0	18950	53.2	.05119	148.7	1.32	66.8	206.7	447.9	206.73	0.0	0.0	0.0000	1.0	294.0	-.4	.9

TIME MIN	ALT GPM	OZONE MICMB	TOTOZ ATMCM	OZDEN MG/M3	OZMXR MICGG	PRESS MB	TEMP DEG K	PTEMP DEG K	VTEMP DEG K	HMDTY PRCNT	DEWPT DEG K	SPCFC HMDTY	SPD MPS	DIR DEG	NS MPS	EW MPS
67.0	19314	53.3	.05372	148.9	1.40	62.9	206.7	455.7	206.73	0.0	0.0	0.0000	.8	343.4	-.8	.2
67.7	19598	58.0	.05583	162.5	1.60	60.0	206.0	460.2	206.00	0.0	0.0	0.0000	.8	275.1	-.1	.8
68.0	19700	59.6	.05658	167.3	1.67	59.0	205.7	461.8	205.73	0.0	0.0	0.0000	1.0	259.2	.2	1.0
69.0	20123	67.8	.06011	190.2	2.04	55.0	205.7	471.2	205.73	0.0	0.0	0.0000	1.2	312.6	-.8	.9
70.0	20474	74.5	.06336	206.3	2.38	51.9	208.5	485.5	208.47	0.0	0.0	0.0000	3.0	316.5	-2.2	2.1
70.6	20702	83.3	.06577	228.6	2.77	50.0	210.3	494.9	210.25	0.0	0.0	0.0000	3.3	315.1	-2.3	2.3
71.0	20852	89.0	.06733	243.1	3.02	48.8	211.4	501.0	211.41	0.0	0.0	0.0000	3.5	314.3	-2.4	2.5
72.0	21207	101.0	.07160	270.9	3.63	46.1	215.4	518.7	215.36	0.0	0.0	0.0000	1.9	13.5	-1.9	-.4
73.0	21588	105.1	.07651	281.1	4.01	43.4	215.8	529.0	215.85	0.0	0.0	0.0000	3.4	66.5	-1.4	-3.1
74.0	21962	110.4	.08156	295.8	4.47	40.9	215.5	537.2	215.52	0.0	0.0	0.0000	3.7	42.4	-2.7	-2.5
74.3	22102	112.9	.08356	302.7	4.68	40.0	215.3	540.1	215.30	0.0	0.0	0.0000	4.1	45.7	-2.8	-2.9
75.0	22392	118.0	.08771	317.0	5.12	38.2	214.9	546.1	214.86	0.0	0.0	0.0000	5.0	50.8	-3.1	-3.9
76.0	22767	125.4	.09341	333.7	5.77	36.0	217.0	560.9	216.99	0.0	0.0	0.0000	6.9	75.1	-1.8	-6.7
76.5	22946	128.8	.09627	340.8	6.10	35.0	218.2	568.6	218.15	0.0	0.0	0.0000	7.3	88.6	-.2	-7.3
77.0	23132	132.3	.09922	348.2	6.45	34.0	219.4	576.4	219.35	0.0	0.0	0.0000	8.2	100.3	1.5	-8.0
78.0	23521	135.6	.10562	356.5	7.02	32.0	219.7	587.3	219.66	0.0	0.0	0.0000	8.7	107.8	2.7	-8.3
78.9	23935	138.3	.11261	363.6	7.64	30.0	219.5	597.9	219.52	0.0	0.0	0.0000	4.6	139.8	3.5	-3.0
79.0	23979	138.5	.11333	364.4	7.70	29.8	219.5	598.9	219.51	0.0	0.0	0.0000	4.4	146.1	3.6	-2.4
80.0	24357	143.2	.11986	374.1	8.45	28.1	221.0	613.3	221.04	0.0	0.0	0.0000	5.6	220.3	4.2	3.6
81.0	24737	148.8	.12661	385.7	9.30	26.5	222.7	628.3	222.68	0.0	0.0	0.0000	1.9	274.6	-.2	1.9
81.9	25118	153.2	.13357	393.2	10.16	25.0	225.0	645.5	224.99	0.0	0.0	0.0000	.4	208.1	.4	.2
82.0	25171	153.9	.13453	394.3	10.28	24.8	225.3	647.9	225.31	0.0	0.0	0.0000	.5	175.9	.5	0.0
83.0	25611	157.8	.14273	404.1	11.27	23.2	225.4	660.8	225.45	0.0	0.0	0.0000	6.3	193.1	6.2	1.4
84.0	26082	152.6	.15148	391.0	11.70	21.6	225.3	674.0	225.31	0.0	0.0	0.0000	6.1	203.5	5.6	2.4
85.0	26589	148.9	.16063	382.1	12.34	20.0	225.0	688.1	225.02	0.0	0.0	0.0000	3.1	97.5	.4	-3.1
86.0	27031	141.0	.16832	362.4	12.49	18.7	224.6	700.1	224.59	0.0	0.0	0.0000	9.0	84.3	-.9	-9.0
86.9	27466	136.3	.17556	351.2	12.90	17.5	224.1	711.8	224.05	0.0	0.0	0.0000	8.3	95.1	.7	-8.2
87.0	27504	135.9	.17619	350.2	12.94	17.4	224.0	712.8	224.01	0.0	0.0	0.0000	8.2	96.2	.9	-8.2
88.0	28055	130.8	.18502	336.2	13.55	16.0	224.7	732.4	224.73	0.0	0.0	0.0000	8.3	112.5	3.2	-7.6
89.0	28480	127.0	.19158	324.5	14.02	15.0	225.9	749.9	225.88	0.0	0.0	0.0000	11.7	105.3	3.1	-11.3
90.0	28937	121.7	.19835	309.6	14.40	14.0	226.9	768.2	226.87	0.0	0.0	0.0000	14.6	92.8	.7	-14.6
91.0	29428	113.5	.20522	289.8	14.47	13.0	226.2	782.2	226.16	0.0	0.0	0.0000	13.1	99.1	2.1	-12.9
91.5	29687	110.9	.20865	282.9	14.70	12.5	226.3	791.5	226.30	0.0	0.0	0.0000	12.8	98.1	1.8	-12.7
92.0	29958	108.2	.21222	275.8	14.94	12.0	226.4	801.3	226.45	0.0	0.0	0.0000	12.5	97.1	1.5	-12.4
93.0	30536	102.5	.21946	260.4	15.43	11.0	227.2	824.0	227.15	0.0	0.0	0.0000	999.9	999.9	999.9	999.9

INTEGRAL .21946 RESIDUAL .08091 INTEGRATED TOTAL OZONE .30037

OZONAGRAM

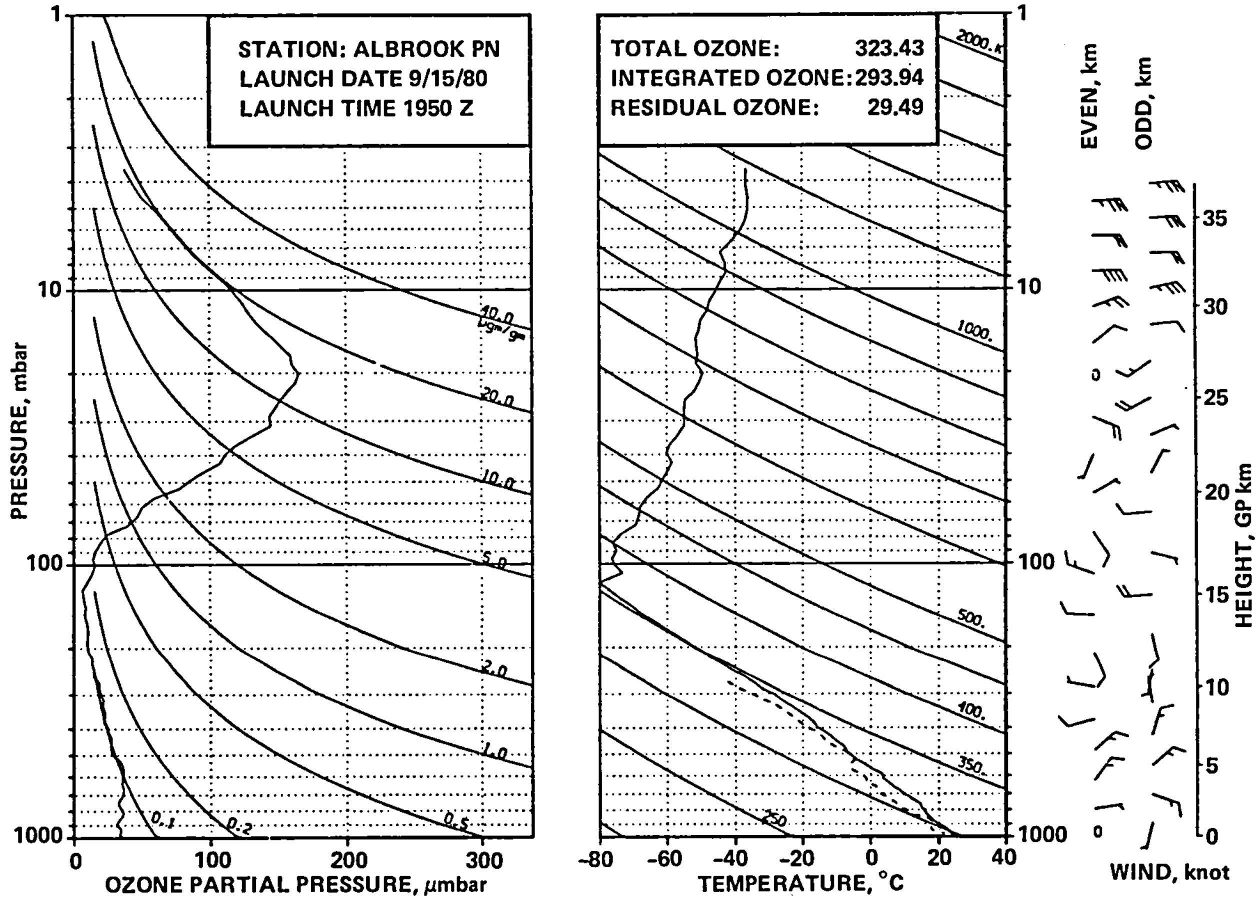

STATION: ALBROOK PN
LAUNCH DATE 9/15/80
LAUNCH TIME 1950 Z
TOTAL OZONE: 323.43
INTEGRATED OZONE: 293.94
RESIDUAL OZONE: 29.49
PRESSURE, mbar
OZONE PARTIAL PRESSURE, μmbar
TEMPERATURE, °C
EVEN, km
ODD, km
HEIGHT, GP km
WIND, knot

STATION ALBROOK PN   LAUNCH DATE 9/15/80   TIME 1950Z   ECC   SONDE 3A1447

SURFACE CONDITIONS   PRESS 1000.0MB   TEMP 298.7 DEG K   HUMIDITY 80.0 PRCNT

TIME MIN	ALT GPM	OZONE MICMB	TOTOZ ATMCM	OZDEN MG/M3	OZMXR MICGG	PRESS MB	TEMP DEG K	PTEMP DEG K	VTEMP DEG K	HMDTY PRCNT	DEWPT DEG K	SPCFC HMDTY	SPD MPS	DIR DEG	NS MPS	EW MPS
0.0	66	35.7	0.00000	69.0	.06	1000.0	298.8	298.8	301.61	75.9	294.2	.0156	0.0	0.0	0.0	0.0
1.0	325	33.3	.00080	64.8	.06	971.0	296.7	299.2	299.67	88.0	294.6	.0165	4.6	93.3	.3	-4.6
2.0	544	34.5	.00147	67.3	.06	947.0	296.0	300.6	298.47	74.0	291.1	.0136	3.8	91.6	.1	-3.8
3.0	767	33.8	.00216	66.3	.06	923.0	294.7	301.5	297.13	78.4	290.8	.0136	2.1	117.5	1.0	-1.8
4.0	986	31.2	.00281	61.5	.06	900.0	293.2	302.1	295.84	91.6	291.8	.0149	1.7	185.4	1.7	.2
5.0	1199	32.0	.00343	63.4	.06	878.0	291.7	302.7	294.28	95.7	291.0	.0146	2.0	207.6	1.8	.9
6.0	1447	34.0	.00418	67.4	.07	853.0	290.7	304.2	293.14	95.5	289.9	.0140	1.1	191.9	1.1	.2
6.1	1477	34.2	.00428	68.0	.07	850.0	290.5	304.3	292.93	92.8	289.3	.0132	.9	184.1	.9	.1
7.0	1681	35.9	.00493	71.5	.07	830.0	289.6	305.5	291.50	74.5	285.1	.0105	1.0	79.6	-.2	-1.0
8.0	1931	35.9	.00576	71.6	.07	806.0	289.0	307.4	290.84	73.0	284.2	.0102	2.2	70.4	-.7	-2.1
8.2	1994	35.5	.00597	70.9	.07	800.0	288.8	307.8	290.53	70.7	283.5	.0095	2.3	75.7	-.6	-2.3
9.0	2198	34.2	.00663	68.5	.07	781.0	288.0	309.1	289.55	63.3	281.1	.0086	2.8	89.3	0.0	-2.8
10.0	2429	32.8	.00735	65.8	.07	760.0	287.7	311.1	289.16	63.6	280.8	.0086	4.1	111.6	1.5	-3.8
11.0	2677	32.8	.00811	66.3	.07	738.0	286.1	312.1	287.51	63.6	279.4	.0080	6.1	114.6	2.5	-5.6
12.0	2931	34.8	.00892	70.6	.08	716.0	284.4	312.9	285.69	63.4	277.7	.0074	7.1	109.6	2.4	-6.7
12.8	3119	35.7	.00955	72.8	.08	700.0	282.9	313.2	284.03	62.8	276.1	.0066	6.5	108.8	2.1	-6.2
13.0	3155	35.8	.00967	73.2	.09	697.0	282.6	313.3	283.72	62.6	275.8	.0066	6.4	108.6	2.0	-6.1
14.0	3396	36.4	.01050	74.7	.09	677.0	281.5	314.7	282.60	63.1	274.9	.0064	4.9	97.5	.6	-4.9
15.0	3643	36.0	.01136	74.4	.09	657.0	279.7	315.4	280.86	70.8	274.8	.0065	5.4	63.2	-2.4	-4.8
16.0	3909	35.1	.01227	72.8	.09	636.0	278.5	317.0	279.47	62.5	271.9	.0055	6.7	43.7	-4.8	-4.6
17.0	4209	36.0	.01330	75.0	.10	613.0	276.8	318.4	277.81	70.7	272.0	.0057	6.3	29.5	-5.5	-3.1
17.6	4382	35.9	.01391	74.9	.10	600.0	276.7	320.1	277.57	66.2	270.9	.0052	6.0	29.0	-5.3	-2.9
18.0	4519	35.8	.01439	74.8	.10	590.0	276.5	321.5	277.38	62.6	270.1	.0051	5.8	28.6	-5.1	-2.8
19.0	4826	36.6	.01547	77.3	.11	568.0	273.7	321.7	274.46	62.6	267.4	.0044	7.2	46.0	-5.0	-5.2
20.0	5157	35.4	.01665	75.2	.11	545.0	271.7	323.1	272.41	71.9	267.3	.0045	8.8	51.6	-5.5	-6.9
21.0	5438	34.0	.01762	72.8	.11	526.0	269.3	323.6	270.19	93.7	268.5	.0051	7.7	43.4	-5.6	-5.3
22.0	5712	29.7	.01849	64.1	.10	508.0	267.8	325.0	268.65	99.0	267.7	.0050	6.9	41.6	-5.1	-4.6
22.4	5836	28.8	.01885	62.3	.10	500.0	267.1	325.7	267.93	98.6	266.9	.0047	6.9	45.2	-4.9	-4.9
23.0	6010	27.6	.01935	59.8	.09	489.0	266.2	326.6	266.93	98.0	265.9	.0045	7.1	50.3	-4.5	-5.5
24.0	6319	27.3	.02021	59.3	.10	470.0	265.5	329.4	266.05	81.0	262.8	.0037	6.0	38.4	-4.7	-3.7
25.0	6656	27.3	.02115	59.8	.10	450.0	263.4	330.9	263.92	78.0	260.3	.0031	5.6	20.0	-5.3	-1.9
26.0	7006	27.3	.02213	60.2	.11	430.0	261.6	332.9	262.03	80.7	258.9	.0029	6.5	20.6	-6.1	-2.3
27.0	7332	25.1	.02301	55.9	.10	412.0	259.6	334.4	260.01	82.5	257.2	.0027	7.0	2.1	-7.0	-.3
27.7	7555	25.0	.02359	56.1	.10	400.0	257.9	335.1	258.28	76.8	254.8	.0021	7.2	349.9	-7.1	1.3
28.0	7632	25.0	.02379	56.1	.10	396.0	257.4	335.3	257.69	74.8	253.9	.0021	7.4	346.1	-7.2	1.8
29.0	7962	22.1	.02461	49.7	.10	379.0	256.3	338.1	256.56	70.1	252.1	.0019	6.4	358.6	-6.4	.2
30.0	8305	22.6	.02542	51.2	.10	362.0	254.2	339.9	254.47	68.3	249.9	.0016	5.3	19.0	-5.1	-1.7
30.8	8554	22.6	.02602	51.6	.11	350.0	252.4	340.7	252.61	68.4	248.1	.0014	4.6	19.1	-4.3	-1.5
31.0	8618	22.6	.02617	51.7	.11	347.0	251.9	340.9	252.14	68.4	247.7	.0014	4.4	19.2	-4.2	-1.4
32.0	8964	21.0	.02698	48.7	.11	331.0	249.3	341.8	249.42	68.7	245.2	.0011	3.7	355.9	-3.7	.3
33.0	9301	21.8	.02776	50.9	.11	316.0	246.9	343.1	246.99	61.8	241.7	.0009	2.9	339.2	-2.7	1.0
34.0	9651	20.2	.02857	47.8	.11	301.0	244.7	344.9	244.83	54.4	238.4	.0007	1.7	330.1	-1.4	.8
34.1	9674	20.1	.02862	47.5	.11	300.0	244.5	344.8	244.57	54.2	238.2	.0006	1.6	328.1	-1.4	.8
35.0	9965	18.7	.02925	44.8	.11	288.0	241.3	344.3	241.35	51.9	234.7	.0005	1.2	293.4	-.5	1.1
36.0	10366	18.4	.03009	44.5	.11	272.0	238.5	345.9	238.52	45.7	230.9	.0003	1.8	237.9	1.0	1.5
37.0	10732	14.8	.03078	36.3	.10	258.0	235.6	347.0	235.68	53.3	229.7	.0003	2.9	200.8	2.8	1.0
37.6	10947	14.8	.03115	36.7	.10	250.0	233.5	346.9	233.48	0.0	0.0	0.0000	3.5	193.8	3.4	.8
38.0	11086	14.9	.03138	37.0	.10	245.0	232.1	346.8	232.06	0.0	0.0	0.0000	3.8	190.3	3.7	.7
39.0	11454	13.4	.03199	33.8	.10	232.0	229.1	347.8	229.10	0.0	0.0	0.0000	4.4	189.8	4.4	.8
40.0	11807	13.4	.03255	34.3	.10	220.0	225.9	348.2	225.91	0.0	0.0	0.0000	4.3	177.3	4.3	-.2
41.0	12239	10.5	.03317	27.3	.08	206.0	223.1	350.3	223.05	0.0	0.0	0.0000	4.3	144.3	3.5	-2.5
41.5	12430	10.2	.03341	26.7	.08	200.0	221.3	350.6	221.34	0.0	0.0	0.0000	4.4	144.0	3.6	-2.6
42.0	12661	9.8	.03370	25.9	.08	193.0	219.3	350.9	219.28	0.0	0.0	0.0000	4.6	143.6	3.7	-2.8
43.0	13035	10.3	.03417	27.7	.09	182.0	216.0	351.4	215.95	0.0	0.0	0.0000	4.3	166.3	4.2	-1.0
44.0	13389	10.3	.03463	28.0	.10	172.0	212.6	351.5	212.60	0.0	0.0	0.0000	2.7	175.7	2.7	-.2
45.0	13759	9.4	.03509	25.9	.10	162.0	209.4	352.2	209.39	0.0	0.0	0.0000	2.7	245.4	1.1	2.5
46.0	14146	7.9	.03553	22.3	.09	152.0	205.7	352.4	205.72	0.0	0.0	0.0000	5.2	279.8	-.9	5.2
46.2	14225	8.1	.03562	22.8	.09	150.0	205.1	352.7	205.14	0.0	0.0	0.0000	6.0	279.1	-.9	5.9
47.0	14511	8.7	.03593	24.6	.10	143.0	203.1	354.0	203.07	0.0	0.0	0.0000	8.6	277.5	-1.1	8.6
48.0	14938	7.2	.03638	20.8	.09	133.0	199.2	354.5	199.23	0.0	0.0	0.0000	10.9	265.3	.9	10.9
48.8	15295	6.6	.03671	19.3	.09	125.0	196.2	355.5	196.24	0.0	0.0	0.0000	10.9	265.8	.8	10.8
49.0	15389	6.4	.03680	18.9	.09	123.0	195.5	355.7	195.47	0.0	0.0	0.0000	10.9	265.9	.8	10.8
50.0	15673	9.3	.03711	27.7	.13	117.0	193.1	356.5	193.10	0.0	0.0	0.0000	10.1	283.6	-2.4	9.8
51.0	16133	13.3	.03782	38.5	.20	108.0	200.0	377.7	199.98	0.0	0.0	0.0000	6.1	291.0	-2.2	5.7
52.0	16523	15.4	.03858	45.1	.25	101.0	197.7	380.6	197.67	0.0	0.0	0.0000	4.7	247.1	1.8	4.3
52.2	16580	15.2	.03870	44.3	.25	100.0	197.5	381.3	197.52	0.0	0.0	0.0000	4.7	249.1	1.7	4.4
53.0	16834	13.9	.03921	40.7	.24	95.7	196.9	384.9	196.86	0.0	0.0	0.0000	4.8	257.7	1.0	4.7
54.0	17208	15.8	.03997	46.0	.29	89.7	198.2	394.7	198.19	0.0	0.0	0.0000	1.8	10.4	-1.8	-.2
55.0	17601	19.2	.04091	56.3	.38	83.8	197.1	400.3	197.13	0.0	0.0	0.0000	4.8	102.5	1.0	[illegible]
55.6	17870	22.2	.04170	64.5	.46	80.0	198.8	409.1	198.78	0.0	0.0	0.0000	5.0	127.1	3.0	-4.0
56.0	18025	23.9	.04215	69.2	.51	77.9	199.7	414.1	199.73	0.0	0.0	0.0000	5.5	139.1	4.1	-3.6
57.0	18457	39.1	.04397	110.7	.89	72.4	204.0	431.9	203.98	0.0	0.0	0.0000	3.8	215.5	3.1	2.2
57.4	18658	42.3	.04511	119.5	1.01	70.0	204.4	436.9	204.36	0.0	0.0	0.0000	4.2	235.5	2.4	3.5
58.0	18921	46.5	.04659	131.0	1.15	67.0	204.9	443.5	204.86	0.0	0.0	0.0000	5.4	253.7	1.5	5.2
59.0	19386	50.0	.04954	140.7	1.34	62.0	205.3	454.4	205.29	0.0	0.0	0.0000	2.3	289.8	-.8	2.1
59.4	19583	53.6	.05095	150.2	1.49	60.0	206.2	460.6	206.16	0.0	0.0	0.0000	1.2	305.5	-.7	.9
60.0	19862	58.7	.05292	163.4	1.70	57.3	207.4	469.5	207.39	0.0	0.0	0.0000	.9	52.9	-.5	-.7
61.0	20351	77.2	.05721	211.6	2.42	52.9	210.7	488.1	210.74	0.0	0.0	0.0000	3.3	70.4	-1.1	-3.1
62.0	20699	83.7	.06079	228.5	2.78	50.0	211.6	498.1	211.64	0.0	0.0	0.0000	3.6	55.2	-2.1	-3.0
62.0	20712	84.0	.06092	229.1	2.79	49.9	211.7	498.5	211.68	0.0	0.0	0.0000	3.6	54.7	-2.1	-3.0
63.0	21137	93.9	.06572	254.4	3.34	46.6	213.1	511.8	213.14	0.0	0.0	0.0000	1.5	23.3	-1.4	-.6
64.0	21684	107.9	.07268	290.0	4.19	42.7	214.7	528.7	214.74	0.0	0.0	0.0000	5.2	26.6	-4.7	-2.3
64.9	22093	111.4	.07835	301.6	4.62	40.0	213.4	535.2	213.36	0.0	0.0	0.0000	3.7	215.1	3.0	2.1

TIME MIN	ALT GPM	OZONE MICMB	TOTOZ ATMCM	OZDEN MG/M3	OZMXR MICGG	PRESS MB	TEMP DEG K	PTEMP DEG K	VTEMP DEG K	HMDTY PRCNT	DEWPT DEG K	SPCFC HMDTY	SPD MPS	DIR DEG	NS MPS	EW MPS
65.0	22156	112.0	.07922	303.3	4.69	39.6	213.1	536.2	213.14	0.0	0.0	0.0000	5.0	213.8	4.2	2.8
66.0	22580	118.9	.08541	320.9	5.32	37.0	213.9	548.5	213.86	0.0	0.0	0.0000	9.2	215.3	7.5	5.3
66.7	22929	127.2	.09089	340.6	6.04	35.0	215.5	561.7	215.52	0.0	0.0	0.0000	2.0	214.5	1.7	1.1
67.0	23094	131.1	.09345	349.8	6.37	34.1	216.3	567.9	216.30	0.0	0.0	0.0000	1.3	37.1	-1.1	-.8
68.0	23659	145.2	.10314	383.9	7.71	31.2	218.3	587.9	218.30	0.0	0.0	0.0000	3.4	165.6	3.3	-.9
68.5	23909	[illegible]	.10762	383.0	8.00	30.0	218.3	594.6	218.30	0.0	0.0	0.0000	6.5	120.8	3.3	-5.6
69.0	24170	144.4	.11228	382.0	8.31	28.8	218.3	601.5	218.30	0.0	0.0	0.0000	11.0	107.6	3.3	-10.5
70.0	24630	148.7	.12061	393.4	9.20	26.8	218.3	614.0	218.30	0.0	0.0	0.0000	6.0	149.9	5.2	-3.0
71.0	25023	152.2	.12792	402.0	10.01	25.2	218.6	625.8	218.63	0.0	0.0	0.0000	10.8	241.9	5.1	9.5
71.1	25074	152.8	.12889	402.9	10.13	25.0	218.9	628.1	218.92	0.0	0.0	0.0000	9.8	242.2	4.6	8.7
72.0	25472	157.1	.13644	410.2	11.08	23.5	221.2	645.9	221.19	0.0	0.0	0.0000	2.3	253.3	.7	2.2
73.0	25990	163.4	.14652	423.6	12.48	21.7	222.7	665.4	222.75	0.0	0.0	0.0000	1.0	111.3	.3	-.9
74.0	26490	165.7	.15647	427.4	13.66	20.1	223.8	683.4	223.81	0.0	0.0	0.0000	1.6	213.9	1.3	.9
74.1	26522	165.4	.15711	426.8	13.70	20.0	223.7	684.0	223.69	0.0	0.0	0.0000	2.0	218.3	1.5	1.2
75.0	27031	160.5	.16714	417.8	14.38	18.5	221.8	693.6	221.82	0.0	0.0	0.0000	7.5	233.6	4.4	6.0
75.8	27392	159.9	.17417	415.6	15.15	17.5	222.2	705.9	222.20	0.0	0.0	0.0000	6.8	258.4	1.4	6.7
76.0	27467	159.8	.17562	415.1	15.31	17.3	222.3	708.5	222.28	0.0	0.0	0.0000	6.8	263.9	.7	6.8
77.0	27854	154.1	.18299	401.0	15.67	16.3	222.0	719.6	221.97	0.0	0.0	0.0000	2.7	35.4	-2.2	-1.6
78.0	28393	147.2	.19288	383.5	16.26	15.0	221.7	735.9	221.66	0.0	0.0	0.0000	7.1	75.0	-1.8	-6.8
79.0	28842	140.4	.20071	363.8	16.61	14.0	222.7	754.2	222.75	0.0	0.0	0.0000	5.2	82.0	-.7	-5.2
80.0	29325	134.1	.20873	347.1	17.09	13.0	223.1	771.4	223.05	0.0	0.0	0.0000	6.1	88.7	-.1	-6.1
80.5	29582	131.5	.21280	339.0	17.43	12.5	223.9	783.3	223.94	0.0	0.0	0.0000	9.1	77.4	-2.0	-8.9
81.0	29850	128.7	.21703	330.5	17.77	12.0	224.9	795.7	224.87	0.0	0.0	0.0000	12.5	71.7	-3.9	-11.9
82.0	30424	123.8	.22570	316.5	18.64	11.0	225.8	818.9	225.76	0.0	0.0	0.0000	15.8	66.7	-6.3	-14.5
83.0	30925	118.1	.23290	299.8	19.19	10.2	227.5	843.3	227.52	0.0	0.0	0.0000	17.4	74.1	-4.8	-16.8
83.2	31057	116.6	.23470	295.5	19.32	10.0	227.8	849.3	227.83	0.0	0.0	0.0000	18.0	78.0	-3.8	-17.6
84.0	31470	111.8	.24032	282.2	19.72	9.4	228.8	868 1	228.81	0.0	0.0	0.0000	20.2	88.5	-.5	-20.2
85.0	31990	103.7	.24690	259.8	19.75	8.7	230.5	894.2	230.52	0.0	0.0	0.0000	19.8	89.1	-.3	-19.8
86.0	32556	95.4	.25349	239.2	19.77	8.0	230.4	915.3	230.38	0.0	0.0	0.0000	25.3	84.9	-2.2	-25.2
87.0	33171	87.1	.26008	219.7	19.78	7.3	229.0	933.8	228.96	0.0	0.0	0.0000	31.7	90.2	.1	-31.7
87.4	33454	84.1	.26285	210.8	19.89	7.0	230.4	951.3	230.42	0.0	0.0	0.0000	31.6	90.5	.3	-31.6
88.0	33852	79.9	.26673	198.3	20.05	6.6	232.5	975.8	232.48	0.0	0.0	0.0000	31.5	90.8	.5	-31.4
89.0	34391	73.7	.27150	181.3	20.03	6.1	234.8	1008.1	234.82	0.0	0.0	0.0000	32.9	88.4	-.9	-32.9
89.2	34505	72.6	.27242	178.3	20.03	6.0	235.1	1014.2	235.11	0.0	0.0	0.0000	33.6	88.1	-1.1	-33.5
90.0	34981	67.7	.27627	165.5	20.04	5.6	236.3	1039.6	236.32	0.0	0.0	0.0000	36.4	86.8	-2.0	-36.4
91.0	35629	60.3	.28100	146.9	19.60	5.1	237.1	1071.4	237.13	0.0	0.0	0.0000	37.2	86.4	-2.3	-37.1
91.2	35766	58.4	.28186	142.2	19.31	5.0	237.1	1077.6	237.13	0.0	0.0	0.0000	37.5	86.4	-2.3	-37.4
92.0	36345	50.3	.28550	122.4	18.10	4.6	237.1	1103.5	237.13	0.0	0.0	0.0000	38.6	86.6	-2.3	-38.6
93.0	37143	43.8	.28977	107.0	17.71	4.1	236.5	1137.1	236.45	0.0	0.0	0.0000	39.4	84.8	-3.6	-39.3
93.2	37313	42.6	.29056	104.0	17.61	4.0	236.5	1145.4	236.48	0.0	0.0	0.0000	999.9	999.9	999.9	999.9
94.0	38043	37.3	.29394	91.1	17.19	3.6	236.6	1180.8	236.59	0.0	0.0	0.0000	999.9	999.9	999.9	999.9

INTEGRAL .29394 RESIDUAL .02949 INTEGRATED TOTAL OZONE .32343

OZONAGRAM

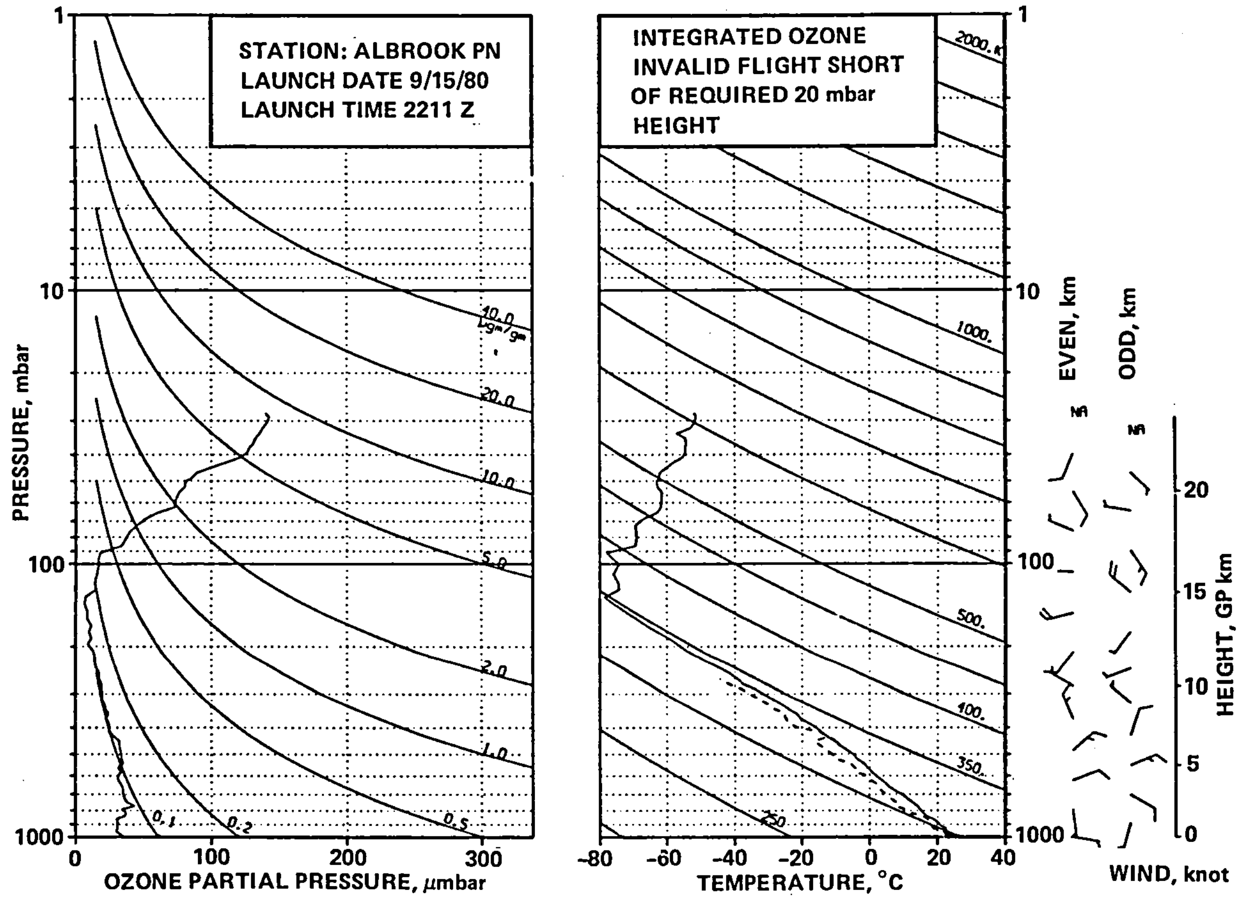

STATION: ALBROOK PN
LAUNCH DATE 9/15/80
LAUNCH TIME 2211 Z
INTEGRATED OZONE
INVALID FLIGHT SHORT
OF REQUIRED 20 mbar
HEIGHT
PRESSURE, mbar
OZONE PARTIAL PRESSURE, μmbar
TEMPERATURE, °C
EVEN, km
ODD, km
HEIGHT, GP km
WIND, knot
NA
1
10
100
1000
0
100
200
300
-80
-60
-40
-20
0
20
40
0.1
0.2
0.5
1.0
2.0
5.0
10.0
20.0
40.0
Lgm/gm
2000. K
1000.
500.
400.
350.
250
20
15
10
5
0

STATION ALBROOK PN LAUNCH DATE 9/15/80 TIME 2211Z ECC SONDE 3A1448

SURFACE CONDITIONS PRESS 1000.0MB TEMP 298.7 DEG K HUMIDITY 0.0 PRCNT

TIME MIN	ALT GPM	OZONE MICMB	TOTOZ ATMCM	OZDEN MG/M3	OZMXR MICGG	PRESS MB	TEMP DEG K	PTEMP DEG K	VTEMP DEG K	HMDTY PRCNT	DEWPT DEG K	SPCFC HMDTY	SPD MPS	DIR DEG	NS MPS	EW MPS
0.0	66	35.1	0.00000	68.0	.06	1000.0	298.4	298.4	301.59	86.4	296.0	.0174	2.0	100.0	.3	-2.0
1.0	270	32.7	.00062	63.6	.06	977.0	296.3	298.3	299.44	95.5	295.5	.0174	3.0	134.3	2.1	-2.1
2.0	469	29.6	.00118	57.9	.05	955.0	295.6	299.5	298.70	95.8	294.9	.0171	3.2	157.1	3.0	-1.3
3.0	700	30.4	.00181	59.4	.05	930.0	295.6	301.8	298.20	78.4	291.7	.0143	3.7	176.7	3.7	-.2
4.0	927	30.3	.00244	59.6	.06	906.0	294.0	302.5	296.67	85.7	291.5	.0146	3.8	189.8	3.7	.6
4.2	984	30.4	.00260	59.8	.06	900.0	293.8	302.8	296.44	86.1	291.4	.0146	3.6	192.0	3.6	.8
5.0	1159	30.7	.00308	60.5	.06	882.0	293.2	303.9	295.75	87.2	291.0	.0145	3.2	200.0	3.0	1.1
6.0	1377	29.9	.00369	59.2	.06	860.0	291.9	304.7	294.38	90.0	290.2	.0141	3.1	196.1	3.0	.9
6.4	1477	32.7	.00399	64.9	.06	850.0	291.0	304.8	293.40	91.3	289.5	.0135	3.2	196.6	3.1	.9
7.0	1609	36.3	.00440	72.3	.07	837.0	289.8	304.9	292.09	93.1	288.6	.0132	3.4	197.3	3.2	1.0
8.0	1857	36.6	.00523	73.2	.07	813.0	288.9	306.6	290.80	76.1	284.7	.0105	3.2	192.7	3.1	.7
8.6	1993	35.0	.00568	70.1	.07	800.0	288.4	307.3	290.15	75.6	284.1	.0101	2.9	179.9	2.9	0.0
9.0	2090	33.9	.00600	67.9	.07	791.0	287.9	307.9	289.69	75.2	283.6	.0100	2.9	170.0	2.8	-.5
10.0	2317	43.1	.00681	86.6	.09	770.0	287.3	309.6	288.81	63.0	280.6	.0084	3.5	139.7	2.7	-2.3
11.0	2572	37.5	.00778	75.8	.08	747.0	285.8	310.6	287.31	72.1	280.9	.0088	5.3	127.9	3.3	-4.2
12.0	2846	35.8	.00872	72.8	.08	723.0	284.2	311.8	285.67	72.0	279.4	.0082	5.6	126.6	3.3	-4.5
13.0	3103	35.0	.00959	71.4	.08	701.0	282.9	313.2	284.29	72.9	278.3	.0078	4.7	117.8	2.2	-4.1
13.0	3114	34.9	.00963	71.3	.08	700.0	282.8	313.2	284.19	73.0	278.2	.0078	4.6	117.2	2.1	-4.1
14.0	3343	34.5	.01038	71.0	.08	681.0	280.9	313.5	282.17	74.6	276.7	.0072	3.9	103.8	.9	-3.8
15.0	3588	34.5	.01119	71.4	.09	661.0	279.2	314.2	280.35	79.0	275.8	.0070	2.7	98.4	.4	-2.7
16.0	3839	32.9	.01201	68.3	.08	641.0	278.1	315.8	279.30	82.1	275.3	.0069	2.3	88.2	-.1	-2.3
17.0	4097	31.1	.01281	64.9	.08	621.0	276.8	317.1	277.82	79.2	273.5	.0063	4.1	66.7	-1.6	-3.7
18.0	4376	31.2	.01366	65.4	.09	600.0	275.1	318.3	276.09	82.4	272.4	.0060	5.9	65.9	-2.4	-5.4
19.0	4649	33.1	.01452	69.8	.09	580.0	273.8	319.9	274.58	71.1	269.1	.0049	6.8	71.0	-2.2	-6.4
20.0	4930	31.1	.01541	65.9	.09	560.0	272.6	321.8	273.47	76.0	268.9	.0050	6.8	73.6	-1.9	-6.5
21.0	5220	34.7	.01635	73.8	.11	540.0	271.5	323.8	272.29	73.8	267.5	.0046	7.2	59.6	-3.6	-6.2
22.0	5519	33.5	.01737	71.8	.11	520.0	269.5	324.9	270.07	62.7	263.4	.0035	8.3	52.0	-5.1	-6.5
23.0	5828	33.5	.01840	72.1	.11	500.0	268.4	327.2	268.96	61.0	262.1	.0033	8.5	52.5	-5.2	-6.7
24.0	6099	32.6	.01931	70.7	.11	483.0	266.6	328.2	267.10	62.4	260.6	.0030	8.2	47.6	-5.6	-6.1
25.0	6394	31.9	.02028	69.7	.11	465.0	264.5	329.2	264.96	61.8	258.6	.0026	7.4	40.9	-5.6	-4.9
26.0	6682	31.9	.02121	70.0	.12	448.0	263.2	331.1	263.62	60.2	257.0	.0024	5.9	36.1	-4.8	-3.5
27.0	6979	28.3	.02213	62.6	.11	431.0	260.8	331.7	261.34	100.0	260.8	.0034	5.2	23.4	-4.7	-2.1
28.0	7285	24.7	.02297	55.1	.10	414.0	258.7	332.8	259.17	100.0	258.7	.0030	7.3	6.6	-7.3	-.8
28.9	7545	24.6	.02364	55.2	.10	400.0	257.5	334.5	257.77	65.4	252.3	.0017	9.0	353.2	-8.9	1.1
29.0	7583	24.6	.02374	55.2	.10	398.0	257.3	334.8	257.57	60.4	251.4	.0017	9.3	351.7	-9.2	1.3
30.0	7871	24.1	.02448	54.6	.10	383.0	254.7	335.1	254.93	60.7	249.0	.0014	9.2	341.4	-8.7	2.9
31.0	8127	21.9	.02510	50.0	.10	370.0	252.6	335.5	252.76	68.7	248.3	.0014	7.1	336.1	-6.5	2.9
32.0	8412	24.3	.02581	55.9	.11	356.0	251.6	338.0	251.83	72.2	248.0	.0014	6.0	318.1	-4.5	4.0
32.4	8536	23.3	.02612	53.7	.11	350.0	250.5	338.2	250.74	71.1	246.8	.0012	5.6	315.7	-4.0	3.9
33.0	8706	21.9	.02654	50.8	.11	342.0	249.1	338.4	249.26	69.7	245.1	.0011	5.1	311.7	-3.4	3.8
34.0	8987	21.3	.02720	49.8	.11	329.0	247.2	339.7	247.38	68.5	243.2	.0009	4.0	310.7	-2.6	3.0
35.0	9300	19.6	.02790	46.2	.10	315.0	244.6	340.3	244.73	68.6	240.7	.0008	3.1	308.4	-1.9	2.4
36.0	9647	19.6	.02865	46.7	.11	300.0	241.6	340.8	241.68	67.8	237.6	.0006	1.3	314.8	-.9	.9
37.0	9934	18.9	.02927	45.7	.11	288.0	239.1	341.2	239.15	67.1	235.1	.0005	1.1	301.7	-.6	1.0
38.0	10204	19.1	.02986	46.7	.11	277.0	235.6	340.0	235.68	64.9	231.5	.0003	3.1	300.0	-1.5	2.7
39.0	10508	17.2	.03049	42.5	.11	265.0	234.0	342.0	234.05	56.9	228.7	.0003	3.8	301.5	-2.0	3.2
40.0	10850	17.2	.03117	42.9	.11	252.0	231.4	343.1	231.43	0.0	0.0	0.0000	2.5	278.7	-.4	2.5
40.2	10903	16.8	.03127	42.0	.11	250.0	230.9	343.1	230.91	0.0	0.0	0.0000	2.6	269.4	0.0	2.6
41.0	11178	14.7	.03179	37.1	.10	240.0	228.2	343.1	228.23	0.0	0.0	0.0000	3.8	236.5	2.1	3.2
42.0	11489	14.0	.03232	35.9	.10	229.0	225.1	343.0	225.08	0.0	0.0	0.0000	4.9	222.7	3.6	3.3
43.0	11811	14.0	.03286	36.2	.11	218.0	222.3	343.5	222.27	0.0	0.0	0.0000	3.9	211.8	3.3	2.1
44.0	12145	12.7	.03341	33.5	.10	207.0	219.0	343.5	219.03	0.0	0.0	0.0000	5.5	215.8	4.4	3.2
44.6	12364	10.3	.03370	27.5	.09	200.0	217.3	344.2	217.30	0.0	0.0	0.0000	4.9	218.9	3.8	3.1
45.0	12493	9.0	.03387	23.9	.08	196.0	216.3	344.5	216.29	0.0	0.0	0.0000	4.6	221.1	3.5	3.0
46.0	12789	11.6	.03426	31.3	.10	187.0	213.8	345.1	213.75	0.0	0.0	0.0000	2.5	225.9	1.7	1.8
47.0	13130	9.7	.03472	26.7	.09	177.0	210.2	344.7	210.17	0.0	0.0	0.0000	1.2	217.0	1.0	.7
48.0	13448	11.5	.03515	32.1	.11	168.0	207.1	344.8	207.10	0.0	0.0	0.0000	1.2	48.7	-.8	-.9
49.0	13817	8.4	.03564	23.8	.09	158.0	204.0	345.6	204.00	0.0	0.0	0.0000	9.1	254.3	2.5	8.7
49.8	14124	8.4	.03598	24.1	.09	150.0	201.1	345.8	201.13	0.0	0.0	0.0000	10.9	256.7	2.5	10.7
50.0	14204	8.4	.03607	24.2	.09	148.0	200.4	345.9	200.39	0.0	0.0	0.0000	11.4	257.2	2.5	11.1
51.0	14527	6.5	.03640	19.0	.08	140.0	197.4	346.2	197.43	0.0	0.0	0.0000	8.8	279.9	-1.5	8.7
52.0	14864	7.1	.03671	21.1	.09	132.0	194.5	346.8	194.47	0.0	0.0	0.0000	11.1	293.7	-4.4	10.1
52.9	15177	13.8	.03718	40.2	.18	125.0	198.4	359.4	198.37	0.0	0.0	0.0000	8.2	318.1	-6.1	5.5
53.0	15224	14.8	.03725	43.0	.20	124.0	198.9	361.2	198.94	0.0	0.0	0.0000	7.9	323.0	-6.3	4.8
54.0	15562	14.1	.03792	41.1	.20	117.0	198.7	366.8	198.70	0.0	0.0	0.0000	5.0	332.4	-4.4	2.3
55.0	15972	15.4	.03874	45.2	.23	109.0	197.2	371.4	197.17	0.0	0.0	0.0000	4.0	292.4	-1.5	3.7
56.0	16471	17.0	.03985	49.5	.28	100.0	198.9	384.1	198.94	0.0	0.0	0.0000	1.8	187.4	1.8	.2
57.0	16695	16.5	.04036	48.2	.28	96.2	197.2	384.9	197.17	0.0	0.0	0.0000	7.4	117.9	3.5	-6.6
58.0	17014	18.1	.04112	53.5	.33	91.0	195.3	387.4	195.30	0.0	0.0	0.0000	8.7	142.3	6.9	-5.3
59.0	17337	33.6	.04224	95.2	.65	86.1	203.8	410.6	203.78	0.0	0.0	0.0000	5.9	158.5	5.5	-2.2
60.0	17701	36.7	.04394	103.8	.75	81.0	204.2	418.7	204.21	0.0	0.0	0.0000	.3	96.8	0.0	-.3
60.2	17775	37.3	.04431	105.5	.77	80.0	204.2	420.1	204.16	0.0	0.0	0.0000	.1	298.3	-.1	.1
61.0	18019	39.3	.04554	111.2	.85	76.8	204.0	424.7	204.00	0.0	0.0	0.0000	1.6	285.0	-.4	1.5
62.0	18346	44.4	.04735	125.9	1.01	72.7	203.8	431.0	203.78	0.0	0.0	0.0000	2.1	343.1	-2.0	.6
62.7	18572	48.9	.04877	137.4	1.16	70.0	205.4	439.1	205.36	0.0	0.0	0.0000	2.3	6.8	-2.3	-.3
63.0	18676	50.9	.04942	142.6	1.23	68.8	206.1	442.8	206.09	0.0	0.0	0.0000	2.5	15.6	-2.4	-.7
64.0	18975	59.4	.05156	163.3	1.50	65.5	210.2	457.9	210.17	0.0	0.0	0.0000	1.8	355.5	-1.8	.1
65.0	19284	73.1	.05418	199.5	1.94	62.3	211.5	467.4	211.45	0.0	0.0	0.0000	1.1	97.1	.1	-1.1
65.8	19516	73.2	.05635	199.9	2.02	60.0	211.6	472.7	211.59	0.0	0.0	0.0000	5.0	107.3	1.5	-4.7
66.0	19589	73.3	.05703	200.0	2.05	59.3	211.6	474.4	211.64	0.0	0.0	0.0000	6.2	107.8	1.9	-5.9
67.0	20044	76.2	.06136	207.6	2.29	55.1	211.8	484.9	211.82	0.0	0.0	0.0000	4.9	145.2	4.0	-2.8
68.0	20331	80.6	.06423	220.9	2.54	52.6	210.5	488.4	210.54	0.0	0.0	0.0000	3.4	197.1	3.2	1.0
69.0	20618	81.1	.06721	222.7	2.68	50.2	210.2	494.1	210.17	0.0	0.0	0.0000	1.1	98.8	.2	-1.1

TIME MIN	ALT GPM	OZONE MICMB	TOTOZ ATMCM	OZDEN MG/M3	OZMXR MICGG	PRESS MB	TEMP DEG K	PTEMP DEG K	VTEMP DEG K	HMDTY PRCNT	DEWPT DEG K	SPCFC HMDTY	SPD MPS	DIR DEG	NS MPS	EW MPS
69.2	20642	81.7	.06747	224.3	2.71	50.0	210.3	494.9	210.29	0.0	0.0	0.0000	1.3	100.9	.3	-1.3
70.0	20767	85.0	.06880	232.7	2.87	49.0	210.9	499.3	210.91	0.0	0.0	0.0000	2.3	106.3	.6	-2.2
71.0	21077	89.5	.07225	244.8	3.18	46.6	211.1	506.9	211.09	0.0	0.0	0.0000	3.2	135.3	2.3	-2.3
72.0	21349	99.8	.07553	270.1	3.71	44.6	213.2	518.5	213.23	0.0	0.0	0.0000	2.9	120.3	1.5	-2.5
73.0	21622	111.3	.07915	298.8	4.32	42.7	215.1	529.6	215.12	0.0	0.0	0.0000	2.6	110.4	.9	-2.4
74.0	21879	121.6	.08289	322.5	4.92	41.0	217.8	542.4	217.75	0.0	0.0	0.0000	3.0	179.1	3.0	0.0
74.6	22036	124.9	.08531	330.3	5.18	40.0	218.3	547.7	218.31	0.0	0.0	0.0000	4.2	200.2	4.0	1.5
75.0	22149	127.2	.08705	335.9	5.36	39.3	218.7	551.4	218.71	0.0	0.0	0.0000	5.3	208.8	4.6	2.5
76.0	22415	128.9	.09125	340.4	5.66	37.7	218.6	557.6	218.56	0.0	0.0	0.0000	8.2	225.8	5.7	5.9
77.0	22604	131.5	.09429	346.8	5.95	36.6	218.9	563.2	218.87	0.0	0.0	0.0000	999.9	999.9	999.9	999.9
77.9	22889	133.2	.09896	351.7	6.31	35.0	218.7	570.0	218.72	0.0	0.0	0.0000	999.9	999.9	999.9	999.9
78.0	22908	133.3	.09926	352.0	6.33	34.9	218.7	570.4	218.71	0.0	0.0	0.0000	999.9	999.9	999.9	999.9
79.0	23187	136.3	.10393	364.0	6.76	33.4	216.1	570.8	216.12	0.0	0.0	0.0000	999.9	999.9	999.9	999.9
80.0	23460	138.5	.10857	363.2	7.17	32.0	220.1	588.5	220.13	0.0	0.0	0.0000	999.9	999.9	999.9	999.9
81.0	23770	141.8	.11388	369.8	7.70	30.5	221.4	600.0	221.36	0.0	0.0	0.0000	999.9	999.9	999.9	999.9
81.4	23876	142.3	.11574	371.0	7.87	30.0	221.5	603.3	221.52	0.0	0.0	0.0000	999.9	999.9	999.9	999.9
82.0	24074	143.4	.11917	373.2	8.16	29.1	221.8	609.4	221.82	0.0	0.0	0.0000	999.9	999.9	999.9	999.9
83.0	24324	140.8	.12349	367.6	8.33	28.0	221.2	614.4	221.21	0.0	0.0	0.0000	999.9	999.9	999.9	999.9

CALIBRATIONS APPLIED FOR PARTIAL PRESSURE OF OZONE
TOTAL INTEGRATED OZONE INVALID. BALLOON SHORT OF 20 MB HEIGHT

OZONAGRAM

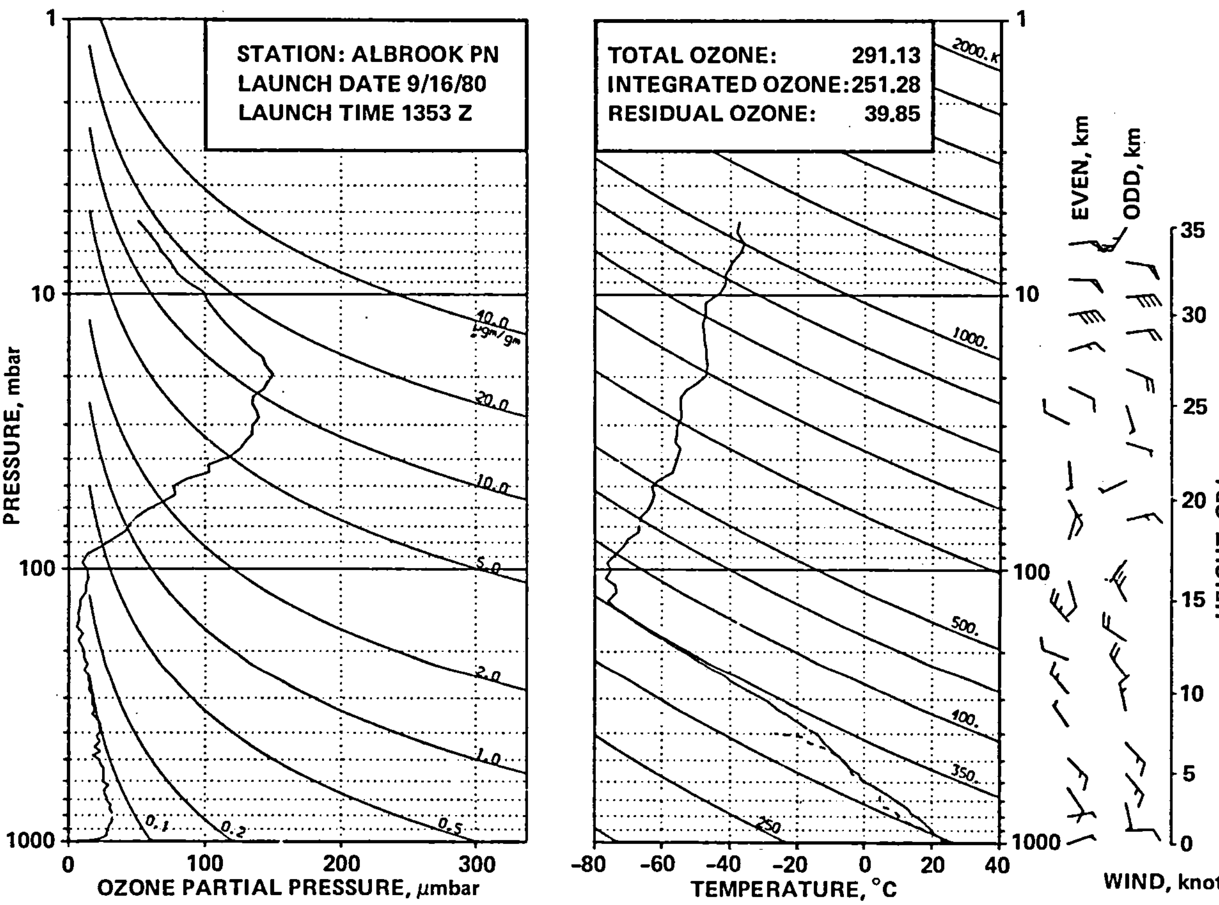

STATION: ALBROOK PN
LAUNCH DATE 9/16/80
LAUNCH TIME 1353 Z
TOTAL OZONE: 291.13
INTEGRATED OZONE: 251.28
RESIDUAL OZONE: 39.85
PRESSURE, mbar
OZONE PARTIAL PRESSURE, μmbar
TEMPERATURE, °C
WIND, knot
EVEN, km
ODD, km
HEIGHT, GP km
1
10
100
1000
0
100
200
300
-80
-60
-40
-20
0
20
40
35
30
25
20
15
10
5
0
2000. K
1000.
500.
400.
350.
250
40.0
20.0
10.0
5.0
2.0
1.0
0.5
0.2
0.1

STATION ALBROOK FN LAUNCH DATE 9/16/80 TIME 1353Z ECC SONDE 3A1449

SURFACE CONDITIONS PRESS 1002.5MB TEMP 273.2 DEG K HUMIDITY 0.0 PRCNT

TIME MIN	ALT GPM	OZONE MICMB	TOTOZ ATMCM	OZDEN MG/M3	OZMXR MICGG	PRESS MB	TEMP DEG K	PTEMP DEG K	VTEMP DEG K	HMDTY PRCNT	DEWPT DEG K	SPCFC HMDTY	SPD MPS	DIR DEG	NS MPS	EW MPS
0.0	66	7.1	0.00000	13.7	.01	1002.5	297.5	297.3	300.92	100.0	297.5	.0190	3.0	70.0	-1.0	-2.8
.1	87	8.6	.00003	16.8	.01	1000.0	297.3	297.3	300.79	100.0	297.3	.0189	3.2	72.1	-1.0	-3.0
1.0	283	22.6	.00029	44.1	.04	978.0	296.3	298.2	299.59	100.0	296.3	.0182	5.0	83.3	-.6	-5.0
2.0	509	28.0	.00081	54.7	.05	953.0	295.6	299.7	298.84	99.8	295.6	.0179	4.5	102.0	.9	-4.4
3.0	722	27.9	.00135	54.8	.05	930.0	294.0	300.2	297.03	100.0	294.0	.0166	4.2	110.4	1.5	-4.0
4.0	958	29.0	.00196	57.2	.05	905.0	293.4	301.9	296.08	91.9	292.0	.0151	4.3	93.0	.2	-4.3
4.2	1005	29.1	.00209	57.3	.05	900.0	293.2	302.2	295.85	90.7	291.6	.0146	4.3	90.5	0.0	-4.3
5.0	1190	29.4	.00258	58.0	.06	881.0	292.5	303.3	294.96	86.2	290.1	.0137	4.5	80.9	-.7	-4.4
6.0	1428	31.0	.00324	61.3	.06	857.0	291.4	304.6	293.56	77.9	287.5	.0119	4.2	78.2	-.9	-4.1
6.3	1498	31.2	.00344	61.9	.06	850.0	291.2	305.0	293.23	76.4	287.0	.0114	4.1	77.1	-.9	-4.0
7.0	1702	32.0	.00403	63.7	.06	830.0	290.4	306.3	292.28	72.2	285.3	.0107	3.9	73.5	-1.1	-3.8
8.0	1973	31.9	.00484	63.8	.07	804.0	288.9	307.5	290.74	73.1	284.1	.0102	3.7	74.4	-1.0	-3.5
8.2	2015	31.9	.00496	63.8	.07	800.0	288.6	307.7	290.43	73.5	283.9	.0100	3.7	76.9	-.8	-3.6
9.0	2230	31.6	.00559	63.5	.07	780.0	287.1	308.3	288.83	75.5	282.9	.0096	3.7	89.3	0.0	-3.7
10.0	2493	30.0	.00635	60.4	.07	756.0	286.4	310.2	287.97	73.7	281.8	.0092	3.1	110.9	1.1	-2.9
11.0	2741	30.6	.00706	62.0	.07	734.0	285.2	311.5	286.50	62.7	278.3	.0075	2.5	156.3	2.3	-1.0
12.0	3019	28.4	.00783	57.8	.07	710.0	283.3	312.4	284.65	71.2	278.3	.0078	2.8	170.5	2.7	-.5
12.5	3136	28.2	.00815	57.6	.07	700.0	282.6	313.0	283.98	73.0	278.0	.0077	2.9	162.0	2.7	-.9
13.0	3280	27.9	.00853	57.2	.07	688.0	281.8	313.6	283.15	75.1	277.7	.0076	3.1	152.7	2.8	-1.4
14.0	3548	26.2	.00923	54.0	.07	666.0	280.2	314.7	281.61	86.5	278.1	.0081	4.3	134.5	3.0	-3.1
15.0	3836	26.2	.00995	54.4	.07	643.0	278.1	315.5	279.52	97.4	277.7	.0082	4.5	133.1	3.1	-3.3
16.0	4106	29.2	.01068	61.0	.08	622.0	276.2	316.4	277.54	100.0	276.2	.0076	5.4	147.8	4.6	-2.9
17.0	4397	24.8	.01145	52.4	.07	600.0	273.6	316.6	274.70	100.0	273.6	.0066	6.8	158.8	6.3	-2.5
18.0	4668	25.7	.01212	54.4	.07	580.0	272.2	318.0	273.14	96.6	271.7	.0059	6.7	153.7	6.0	-3.0
19.0	4991	25.2	.01294	53.7	.08	557.0	271.5	320.9	272.39	85.8	269.5	.0052	7.3	141.9	5.7	-4.5
20.0	5311	25.5	.01374	54.7	.08	535.0	269.0	321.7	269.89	100.0	269.0	.0052	7.4	137.9	5.5	-5.0
21.0	5565	23.1	.01436	49.7	.07	518.0	268.1	323.6	268.94	100.0	268.1	.0050	7.3	130.5	4.7	-5.5
22.0	5842	22.5	.01500	48.6	.07	500.0	266.9	325.4	267.69	100.0	266.9	.0048	7.4	131.6	4.9	-5.5
23.0	6128	17.9	.01558	39.0	.06	482.0	265.6	327.1	266.29	100.0	265.6	.0045	8.2	135.2	5.8	-5.8
24.0	6373	23.4	.01610	51.1	.08	467.0	264.2	328.5	264.89	95.8	263.7	.0040	8.6	139.3	6.5	-5.6
25.0	6677	19.1	.01676	42.0	.07	449.0	262.8	330.4	263.34	88.1	261.2	.0034	8.0	138.6	6.0	-5.3
26.0	7009	23.0	.01747	50.8	.09	430.0	261.1	332.3	261.47	68.7	256.5	.0024	7.2	136.4	5.2	-5.0
27.0	7335	20.4	.01821	45.4	.08	412.0	260.0	334.9	260.33	71.7	255.9	.0024	3.9	137.9	2.9	-2.6
27.9	7559	22.8	.01871	50.7	.09	400.0	258.9	336.4	259.10	36.3	247.0	.0011	0.0	109.3	0.0	0.0
28.0	7578	23.0	.01875	51.2	.10	399.0	258.8	336.5	259.00	33.4	246.3	.0010	.3	322.2	-.2	.2
29.0	7847	23.0	.01940	51.7	.10	385.0	256.3	336.7	256.40	0.0	0.0	0.0000	2.4	315.3	-1.7	1.7
30.0	8144	22.9	.02012	52.1	.10	370.0	254.4	338.0	254.46	0.0	0.0	0.0000	2.0	329.2	-1.8	1.0
31.0	8451	20.4	.02083	46.8	.10	355.0	252.0	338.8	252.16	47.2	243.8	.0009	4.1	352.3	-4.0	.5
31.4	8554	19.3	.02104	44.4	.09	350.0	251.4	339.3	251.45	31.3	233.4	.0004	5.4	350.5	-5.3	.9
32.0	8746	17.3	.02143	39.9	.08	341.0	250.2	340.2	250.16	0.0	0.0	0.0000	7.8	348.7	-7.6	1.5
33.0	9007	19.2	.02194	44.7	.10	329.0	247.8	340.4	247.77	0.0	0.0	0.0000	7.7	347.1	-7.5	1.7
34.0	9321	17.2	.02257	40.4	.09	315.0	245.8	341.9	245.79	0.0	0.0	0.0000	7.6	346.7	-7.4	1.8
35.0	9623	17.3	.02314	40.9	.09	302.0	243.7	343.1	243.69	0.0	0.0	0.0000	7.8	348.3	-7.7	1.6
35.2	9670	17.3	.02323	41.0	.10	300.0	243.2	343.1	243.24	0.0	0.0	0.0000	8.0	347.8	-7.9	1.7
36.0	9910	17.3	.02369	41.4	.10	290.0	240.9	343.2	240.93	0.0	0.0	0.0000	9.1	345.6	-8.8	2.3
37.0	10181	14.7	.02418	35.6	.09	279.0	238.4	343.4	238.43	0.0	0.0	0.0000	4.8	300.9	-2.5	4.1
38.0	10460	15.3	.02466	37.3	.09	268.0	235.8	343.4	235.78	21.5	221.8	.0001	10.3	348.2	-10.1	2.1
39.0	10747	14.4	.02515	35.7	.09	257.0	233.2	343.8	233.23	43.1	225.5	.0002	17.4	351.9	-17.2	2.4
39.6	10934	14.4	.02546	35.9	.10	250.0	232.2	345.0	232.19	0.0	0.0	0.0000	12.8	340.0	-12.0	4.4
40.0	11072	14.4	.02569	36.0	.10	245.0	231.4	345.9	231.43	0.0	0.0	0.0000	10.1	325.0	-8.3	5.8
41.0	11381	11.3	.02616	28.4	.08	234.0	228.5	346.0	228.51	0.0	0.0	0.0000	7.9	313.9	-5.5	5.7
42.0	11731	13.9	.02668	35.5	.10	222.0	225.8	347.1	225.81	0.0	0.0	0.0000	6.2	295.0	-2.6	5.7
43.0	12033	11.4	.02714	29.6	.09	212.0	222.9	347.2	222.87	0.0	0.0	0.0000	5.4	289.4	-1.8	5.1
44.0	12346	11.4	.02757	29.9	.09	202.0	220.3	347.9	220.28	0.0	0.0	0.0000	5.3	296.6	-2.4	4.8
44.2	12409	11.1	.02766	29.2	.09	200.0	219.6	347.8	219.59	0.0	0.0	0.0000	5.8	299.3	-2.8	5.1
45.0	12637	10.0	.02796	26.7	.09	193.0	217.1	347.4	217.11	0.0	0.0	0.0000	7.5	305.9	-4.4	6.1
46.0	13007	7.3	.02836	19.8	.07	182.0	214.1	348.4	214.10	0.0	0.0	0.0000	9.5	303.8	-5.3	7.9
47.0	13358	10.5	.02876	28.8	.10	172.0	210.5	348.1	210.54	0.0	0.0	0.0000	9.9	305.5	-5.7	8.0
48.0	13724	6.0	.02915	16.6	.06	162.0	207.5	349.0	207.49	0.0	0.0	0.0000	10.4	312.2	-7.0	7.7
49.0	14068	7.8	.02946	21.9	.08	153.0	204.4	349.5	204.42	0.0	0.0	0.0000	11.8	317.5	-8.7	8.0
49.4	14185	7.5	.02958	21.3	.08	150.0	203.5	350.0	203.53	0.0	0.0	0.0000	13.5	318.2	-10.1	9.0
50.0	14387	7.1	.02977	20.2	.08	145.0	202.0	350.7	202.01	0.0	0.0	0.0000	16.5	319.0	-12.4	10.8
51.0	14677	8.3	.03007	23.9	.10	138.0	199.2	350.8	199.19	0.0	0.0	0.0000	20.0	317.7	-14.8	13.5
52.0	15023	8.4	.03047	24.5	.11	130.0	197.2	353.2	197.17	0.0	0.0	0.0000	16.4	329.3	-14.1	8.4
52.5	15250	10.8	.03079	31.3	.14	125.0	198.5	359.7	198.54	0.0	0.0	0.0000	11.6	342.8	-11.1	3.4
53.0	15439	12.8	.03106	36.9	.17	121.0	199.7	365.1	199.68	0.0	0.0	0.0000	8.6	4.5	-8.6	-.7
54.0	15787	12.8	.03166	37.0	.19	114.0	199.2	370.4	199.19	0.0	0.0	0.0000	4.4	106.3	1.2	-4.2
55.0	16100	14.4	.03224	42.5	.22	108.0	196.4	370.9	196.38	0.0	0.0	0.0000	6.1	170.6	6.0	-1.0
56.0	16486	13.7	.03299	40.1	.23	101.0	197.9	381.1	197.94	0.0	0.0	0.0000	5.3	211.0	4.6	2.7
56.2	16543	13.2	.03308	38.4	.22	100.0	197.8	381.9	197.78	0.0	0.0	0.0000	5.3	212.6	4.5	2.9
57.0	16852	10.1	.03358	29.5	.18	94.8	196.9	386.0	196.91	0.0	0.0	0.0000	5.4	221.4	4.1	3.6
58.0	17270	13.7	.03426	39.8	.26	88.2	199.2	398.6	199.19	0.0	0.0	0.0000	2.1	211.1	1.8	1.1
59.0	17626	23.8	.03516	68.1	.47	83.0	201.6	410.4	201.56	0.0	0.0	0.0000	1.6	15.1	-1.5	-.4
59.6	17844	28.8	.03597	82.0	.60	80.0	202.4	416.4	202.36	0.0	0.0	0.0000	2.3	14.4	-2.2	-.6
60.0	17994	32.2	.03653	91.6	.68	78.0	202.9	420.6	202.91	0.0	0.0	0.0000	2.8	14.1	-2.7	-.7
61.0	18391	41.2	.03845	115.3	.93	73.0	206.3	435.8	206.29	0.0	0.0	0.0000	4.2	31.4	-3.6	-2.2
61.7	18644	43.7	.03987	122.2	1.03	70.0	206.3	441.0	206.29	0.0	0.0	0.0000	4.9	46.9	-3.3	-3.6
62.0	18740	44.6	.04041	124.8	1.07	68.9	206.3	443.0	206.29	0.0	0.0	0.0000	5.2	51.5	-3.3	-4.1
63.0	19129	50.0	.04281	139.6	1.28	64.6	206.9	452.6	206.90	0.0	0.0	0.0000	6.8	81.2	-1.0	-6.7
64.0	19538	59.0	.04570	162.8	1.62	60.4	209.2	466.6	209.23	0.0	0.0	0.0000	8.2	106.6	2.3	-7.8
64.1	19578	60.2	.04604	166.0	1.66	60.0	209.3	467.7	209.34	0.0	0.0	0.0000	7.8	108.0	2.4	-7.5
65.0	19893	69.4	.04864	190.6	2.02	57.0	210.2	476.5	210.17	0.0	0.0	0.0000	5.6	124.3	3.2	-4.7
66.0	20260	78.2	.05211	214.1	2.41	53.7	210.9	486.4	210.91	0.0	0.0	0.0000	4.9	178.9	4.9	-.1

TIME MIN	ALT GPM	OZONE MICMB	TOTOZ ATMCM	OZDEN MG/M3	OZMXR MICGG	PRESS MB	TEMP DEG K	PTEMP DEG K	VTEMP DEG K	HMDTY PRCNT	DEWPT DEG K	SPCFC HMDTY	SPD MPS	DIR DEG	NS MPS	EW MPS
67.0	20700	76.9	.05648	211.1	2.55	50.0	210.2	494.6	210.17	0.0	0.0	0.0000	5.2	205.7	4.7	2.2
68.0	21069	87.1	.06034	236.6	3.06	47.1	212.5	508.8	212.53	0.0	0.0	0.0000	3.5	244.4	1.5	3.2
69.0	21411	103.3	.06444	275.7	3.84	44.6	216.3	525.9	216.29	0.0	0.0	0.0000	3.3	224.4	2.4	2.3
70.0	21792	102.7	.06932	273.2	4.05	42.0	217.1	537.1	217.11	0.0	0.0	0.0000	3.4	190.7	3.3	.6
70.7	22102	114.0	.07359	302.5	4.74	40.0	217.7	546.1	217.68	0.0	0.0	0.0000	2.6	171.8	2.6	-.4
71.0	22231	118.7	.07535	314.6	5.02	39.2	217.9	549.8	217.92	0.0	0.0	0.0000	2.5	161.4	2.3	-.8
72.0	22704	127.1	.08254	335.5	5.79	36.4	218.7	563.6	218.71	0.0	0.0	0.0000	3.7	108.9	1.2	-3.5
72.7	22954	129.3	.08652	343.2	6.13	35.0	217.5	566.9	217.54	0.0	0.0	0.0000	3.2	101.0	.6	-3.1
73.0	23046	130.1	.08798	346.1	6.25	34.5	217.1	568.1	217.11	0.0	0.0	0.0000	3.0	97.4	.4	-3.0
74.0	23426	135.2	.09423	358.7	6.89	32.5	217.6	579.2	217.59	0.0	0.0	0.0000	3.1	281.4	-.6	3.1
75.0	23872	135.4	.10171	359.0	7.40	30.3	217.8	591.3	217.75	0.0	0.0	0.0000	6.3	283.2	-1.4	6.1
75.1	23935	136.1	.10279	360.6	7.52	30.0	217.9	593.5	217.92	0.0	0.0	0.0000	5.9	286.1	-1.6	5.6
76.0	24308	140.1	.10914	369.7	8.21	28.3	218.9	606.1	218.87	0.0	0.0	0.0000	4.1	312.7	-2.8	3.0
77.0	24657	138.6	.11513	365.6	8.57	26.8	218.9	615.6	218.87	0.0	0.0	0.0000	3.5	8.3	-3.4	-.5
78.0	25102	135.2	.12264	357.0	8.96	25.0	218.7	627.5	218.71	0.0	0.0	0.0000	3.1	176.6	3.1	-.2
79.0	25471	136.1	.12881	359.1	9.56	23.6	218.9	638.4	218.87	0.0	0.0	0.0000	6.9	190.9	6.8	1.3
80.0	25864	143.7	.13556	376.2	10.73	22.2	220.6	654.7	220.59	0.0	0.0	0.0000	.9	160.7	.8	-.3
81.0	26225	146.5	.14192	378.2	11.56	21.0	223.6	674.3	223.61	0.0	0.0	0.0000	6.4	79.8	-1.1	-6.3
81.8	26545	149.6	.14764	382.9	12.40	20.0	225.6	690.0	225.62	0.0	0.0	0.0000	9.0	96.0	1.0	-9.0
82.0	26645	150.6	.14941	384.3	12.67	19.7	226.2	694.8	226.24	0.0	0.0	0.0000	9.9	99.2	1.6	-9.8
83.0	27170	145.2	.15865	370.0	13.22	18.2	226.5	711.6	226.53	0.0	0.0	0.0000	10.0	115.7	4.3	-9.0
83.6	27429	143.9	.16311	367.1	13.63	17.5	226.4	719.1	226.36	0.0	0.0	0.0000	8.6	112.0	3.2	-8.0
84.0	27622	143.0	.16641	364.9	13.94	17.0	226.2	724.7	226.24	0.0	0.0	0.0000	7.7	108.4	2.4	-7.3
85.0	28023	135.6	.17307	346.1	14.05	16.0	226.2	737.4	226.24	0.0	0.0	0.0000	6.7	72.2	-2.0	-6.3
85.8	28449	129.7	.17979	331.7	14.32	15.0	225.8	749.5	225.76	0.0	0.0	0.0000	6.0	69.7	-2.1	-5.6
86.0	28538	128.5	.18119	328.7	14.38	14.8	225.7	752.0	225.66	0.0	0.0	0.0000	5.8	69.1	-2.1	-5.4
87.0	29000	121.9	.18810	312.2	14.64	13.8	225.5	766.7	225.52	0.0	0.0	0.0000	8.6	83.0	-1.0	-8.5
88.0	29496	115.4	.19515	295.9	14.94	12.8	225.2	782.4	225.23	0.0	0.0	0.0000	16.9	79.7	-3.0	-16.6
88.3	29652	113.7	.19725	291.2	15.07	12.5	225.4	78[illegible].5	225.44	0.0	0.0	0.0000	18.1	79.8	-3.2	-17.8
89.0	30033	109.5	.20236	279.7	15.37	11.8	226.0	803.4	225.95	0.0	0.0	0.0000	21.1	80.0	-3.7	-20.8
90.0	30680	102.6	.21055	262.2	15.89	10.7	226.0	826.1	225.95	0.0	0.0	0.0000	20.4	86.1	-1.4	-20.4
90.8	31132	99.8	.21593	251.4	16.54	10.0	229.3	854.9	229.32	0.0	0.0	0.0000	21.2	84.4	-2.1	-21.1
91.0	31267	99.0	.21754	248.1	16.74	9.8	230.3	863.5	230.33	0.0	0.0	0.0000	21.4	83.9	-2.3	-21.3
92.0	31768	88.2	.22301	219.8	16.07	9.1	231.8	887.8	231.84	0.0	0.0	0.0000	25.6	86.9	-1.4	-25.6
93.0	32311	79.7	.22832	198.4	15.71	8.4	231.8	908.3	231.84	0.0	0.0	0.0000	28.0	95.6	2.7	-27.9
93.5	32643	77.1	.23128	191.2	15.95	8.0	232.8	924.9	232.77	0.0	0.0	0.0000	27.6	97.4	3.6	-27.4
94.0	32993	74.3	.23440	183.6	16.21	7.6	233.7	942.4	233.74	0.0	0.0	0.0000	27.2	99.4	4.4	-26.9
95.0	33558	68.0	.23901	166.2	16.09	7.0	236.2	974.8	236.16	0.0	0.0	0.0000	24.3	93.5	1.5	-24.3
96.0	34071	64.1	.24288	156.1	16.35	6.5	237.2	1000.1	237.23	0.0	0.0	0.0000	25.8	82.8	-3.2	-25.6
96.8	34623	58.5	.24671	143.3	16.13	6.0	235.5	1015.6	235.46	0.0	0.0	0.0000	32.3	80.6	-5.3	-31.9
97.0	34740	57.3	.24752	140.6	16.08	5.9	235.1	1018.9	235.09	0.0	0.0	0.0000	33.7	80.3	-5.7	-33.2
98.0	35350	50.5	.25128	123.5	15.49	5.4	235.9	1048.6	235.89	0.0	0.0	0.0000	999.9	999.9	999.9	999.9

INTEGRAL .25128 RESIDUAL .03985 INTEGRATED TOTAL OZONE .29113

STATION ALBROOK PN   LAUNCH DATE 9/17/80   TIME 1312Z   ECC   SONDE 3A1450

SURFACE CONDITIONS   PRESS 1004.0MB   TEMP 298.0 DEG K   HUMIDITY 94.0 PRCNT

TIME MIN	ALT GPM	OZONE MICMB	TOTOZ ATMCM	OZDEN MG/M3	OZMXR MICGG	PRESS MB	TEMP DEG K	PTEMP DEG K	VTEMP DEG K	HMDTY PRCNT	DEWPT DEG K	SPCFC HMDTY	SPD MPS	DIR DEG	NS MPS	EW MPS
0.0	66	13.9	0.00000	27.0	.02	1004.0	297.8	297.5	301.09	93.4	296.7	.0181	0.0	0.0	0.0	0.0
.2	101	13.9	.00004	27.0	.02	1000.0	297.8	297.8	301.06	92.3	296.4	.0178	.3	191.4	.3	.1
1.0	288	14.0	.00028	27.1	.02	979.0	297.8	299.6	300.92	86.3	295.4	.0171	1.8	191.4	1.7	.3
2.0	524	13.5	.00057	26.3	.02	953.0	296.9	301.0	299.90	86.5	294.5	.0167	1.7	129.6	1.1	-1.3
3.0	737	14.5	.00084	28.3	.03	930.0	295.1	301.3	297.61	79.4	291.3	.0141	2.4	93.6	.1	-2.4
4.0	983	15.2	.00117	29.8	.03	904.0	294.0	302.6	296.49	82.3	290.8	.0140	2.9	79.9	-.5	-2.9
4.2	1021	15.4	.00123	30.2	.03	900.0	293.6	302.6	296.12	84.1	290.8	.0140	3.0	80.6	-.5	-2.9
5.0	1225	16.2	.00152	32.1	.03	879.0	291.6	302.6	294.15	93.4	290.5	.0141	3.3	83.5	-.4	-3.3
6.0	1503	16.6	.00194	33.0	.03	851.0	290.4	304.1	292.54	88.2	288.4	.0127	3.8	91.3	.1	-3.8
6.0	1513	16.7	.00195	33.2	.03	850.0	290.3	304.1	292.58	88.3	288.4	.0127	3.8	91.1	.1	-3.8
7.0	1757	18.8	.00235	37.6	.04	826.0	289.0	305.2	291.17	92.0	297.7	.0125	3.6	86.6	-.2	-3.6
8.0	1902	23.0	.00264	46.1	.05	812.0	288.4	306.0	290.37	85.4	285.9	.0114	3.1	75.5	-.8	-3.0
8.4	2028	23.7	.00292	47.4	.05	800.0	288.4	307.4	290.35	83.3	285.5	.0112	2.7	74.2	-.7	-2.6
9.0	2243	24.8	.00339	49.6	.05	780.0	288.4	309.6	290.31	79.8	284.9	.0110	2.1	70.9	-.7	-2.0
10.0	2507	29.6	.00406	59.7	.06	756.0	286.4	310.2	288.10	76.9	282.4	.0097	1.5	78.0	-.3	-1.5
11.0	2778	26.8	.00478	54.4	.06	732.0	284.1	310.6	285.58	74.5	279.8	.0083	3.2	85.6	-.2	-3.2
12.0	3032	24.8	.00540	50.8	.06	710.0	282.3	311.3	283.77	83.3	279.6	.0085	5.2	92.1	.2	-5.2
12.5	3149	22.1	.00565	45.3	.05	700.0	281.8	312.1	283.38	90.8	280.3	.0094	6.3	93.8	.4	-6.3
13.0	3293	18.8	.00595	38.7	.05	688.0	281.2	312.9	282.91	100.0	281.2	.0098	7.6	95.2	.7	-7.6
14.0	3586	20.8	.00650	42.9	.05	664.0	279.6	314.3	281.06	91.5	278.4	.0083	8.3	94.9	.7	-8.3
15.0	3863	23.2	.00708	47.9	.06	642.0	279.3	317.0	280.58	82.3	276.5	.0075	6.6	93.4	.4	-6.6
16.0	4147	23.2	.00772	48.5	.06	620.0	276.1	316.5	277.22	89.8	274.6	.0068	4.9	93.2	.3	-4.9
17.0	4411	22.6	.00831	47.7	.06	600.0	273.7	316.8	274.84	99.5	273.7	.0066	3.4	113.3	1.3	-3.1
17.0	4425	22.6	.00834	47.7	.06	599.0	273.6	316.8	274.72	100.0	273.6	.0066	3.3	114.8	1.4	-3.0
18.0	4739	20.4	.00901	43.3	.06	576.0	272.3	318.8	273.38	100.0	272.3	.0062	3.5	133.2	2.4	-2.5
19.0	5035	21.1	.00962	44.9	.06	555.0	270.9	320.6	271.89	100.0	270.9	.0058	2.1	127.4	1.3	-1.7
20.0	5326	22.2	.01024	47.6	.07	535.0	269.2	321.9	270.11	100.0	269.2	.0053	1.2	46.3	-.8	-.8
21.0	5626	22.1	.01091	47.7	.07	515.0	267.6	323.4	268.36	100.0	267.6	.0049	1.0	57.1	-.6	-.9
21.7	5857	20.2	.01140	43.8	.07	500.0	266.2	324.5	266.97	100.0	266.2	.0044	.2	235.0	.1	.1
22.0	5936	19.6	.01156	42.5	.07	495.0	265.8	324.9	266.50	100.0	265.8	.0044	.6	236.3	.3	.5
23.0	6224	18.0	.01211	39.4	.06	477.0	264.2	326.4	264.82	100.0	264.2	.0040	1.2	253.6	.3	1.1
24.0	6521	17.4	.01265	38.3	.06	459.0	262.6	328.0	263.18	100.0	262.6	.0037	2.5	200.6	2.3	.9
25.0	6845	17.4	.01323	38.6	.07	440.0	260.9	329.8	261.37	92.4	259.9	.0031	2.8	177.6	2.8	-.1
26.0	7181	16.8	.01383	37.5	.07	421.0	258.9	331.5	259.25	72.3	255.0	.0022	1.3	209.2	1.2	.7
27.0	7530	17.4	.01445	39.2	.07	402.0	256.8	333.2	257.08	59.4	250.8	.0016	2.1	235.9	1.2	1.8
27.1	7567	17.4	.01452	39.0	.07	400.0	256.6	333.3	256.81	59.9	250.6	.0015	2.0	233.0	1.2	1.6
28.0	7795	16.8	.01493	38.1	.07	388.0	254.9	334.1	255.15	62.7	249.6	.0015	1.5	207.8	1.3	.7
29.0	8088	16.5	.01545	37.5	.07	373.0	253.3	335.7	253.48	57.0	247.0	.0012	.5	222.8	.4	.4
30.0	8349	20.7	.01597	47.7	.10	360.0	250.6	335.6	250.68	23.2	235.3	.0004	1.0	300.4	-.5	.9
30.7	8554	18.7	.01640	43.3	.09	350.0	249.6	336.8	249.60	0.0	0.0	0.0000	.5	299.1	-.3	.5
31.0	8660	17.7	.01661	41.1	.09	345.0	249.0	337.5	249.04	0.0	0.0	0.0000	.3	296.6	-.1	.2
32.0	8983	16.0	.01721	37.3	.08	330.0	247.6	339.8	247.66	51.1	240.4	.0007	.5	158.3	.5	-.2
33.0	9272	18.6	.01775	43.9	.10	317.0	244.9	340.1	244.94	0.0	0.0	0.0000	.7	296.2	-.3	.6
34.0	9641	14.3	.01843	34.0	.08	301.0	242.8	342.1	242.84	33.6	232.0	.0003	2.9	328.4	-2.5	1.5
34.1	9664	14.3	.01846	33.9	.08	300.0	242.6	342.1	242.61	35.6	232.2	.0004	3.1	330.2	-2.7	1.5
35.0	9953	13.6	.01891	32.9	.08	288.0	239.7	342.1	239.80	59.8	234.6	.0005	5.5	342.4	-5.2	1.7
36.0	10327	13.9	.01949	33.7	.08	273.0	237.7	344.5	237.79	58.5	232.5	.0004	7.9	354.1	-7.9	.8
37.0	10611	14.4	.01995	35.4	.09	262.0	235.2	344.8	235.20	46.3	228.0	.0002	10.3	350.9	-10.2	1.6
38.0	10877	13.1	.02038	32.4	.09	252.0	232.8	345.2	232.84	0.0	0.0	0.0000	11.0	343.0	-10.6	3.2
38.2	10930	13.4	.02046	33.2	.09	250.0	232.3	345.2	232.29	0.0	0.0	0.0000	11.0	342.7	-10.5	3.3
39.0	11179	14.8	.02087	37.2	.10	241.0	229.8	345.0	229.77	0.0	0.0	0.0000	11.1	341.4	-10.5	3.5
40.0	11491	13.4	.02138	34.0	.10	230.0	227.2	345.8	227.20	0.0	0.0	0.0000	10.8	341.3	-10.2	3.5
41.0	11815	14.0	.02191	36.0	.11	219.0	224.3	346.1	224.26	0.0	0.0	0.0000	10.9	341.2	-10.3	3.5
42.0	12151	12.0	.02244	31.4	.10	208.0	221.0	346.2	221.04	0.0	0.0	0.0000	12.9	346.8	-12.6	2.9
42.7	12402	11.6	.02281	30.5	.10	200.0	219.0	346.8	218.97	0.0	0.0	0.0000	13.8	349.9	-13.6	2.4
43.0	12500	11.4	.02294	30.2	.10	197.0	218.2	347.0	218.17	0.0	0.0	0.0000	14.2	351.0	-14.0	2.2
44.0	12796	10.6	.02335	28.5	.09	188.0	215.0	346.6	214.98	0.0	0.0	0.0000	12.9	346.6	-12.5	3.0
45.0	13138	10.1	.02380	27.5	.09	178.0	212.3	347.7	212.31	0.0	0.0	0.0000	11.8	345.5	-11.4	3.0
46.0	13494	10.1	.02426	27.8	.10	168.0	209.1	348.1	209.11	0.0	0.0	0.0000	11.6	341.5	-11.0	3.7
47.0	13868	9.5	.02473	26.3	.10	158.0	207.3	351.2	207.32	0.0	0.0	0.0000	11.5	337.7	-10.7	4.4
48.0	14181	9.3	.02512	26.4	.10	150.0	204.4	351.4	204.37	0.0	0.0	0.0000	12.6	344.6	-12.1	3.3
49.0	14507	8.7	.02551	24.8	.10	142.0	202.1	353.0	202.12	0.0	0.0	0.0000	12.3	345.8	-12.0	3.0
50.0	14848	11.6	.02597	33.6	.14	134.0	200.0	355.1	199.97	0.0	0.0	0.0000	10.6	347.1	-10.3	2.4
51.0	15115	9.8	.02636	28.6	.13	128.0	198.5	357.1	198.46	0.0	0.0	0.0000	8.3	353.1	-8.2	1.0
51.4	15252	10.6	.02656	30.8	.14	125.0	198.2	359.1	198.24	0.0	0.0	0.0000	6.3	351.2	-6.2	1.0
52.0	15441	11.6	.02683	33.9	.16	121.0	197.9	361.9	197.94	0.0	0.0	0.0000	3.6	345.4	-3.5	.9
53.0	15787	12.2	.02739	35.3	.18	114.0	198.7	369.6	198.72	0.0	0.0	0.0000	1.9	235.5	1.1	1.6
54.0	16103	11.8	.02790	34.0	.18	108.0	200.5	378.6	200.46	0.0	0.0	0.0000	3.0	149.5	2.6	-1.5
55.0	16495	11.8	.02853	34.1	.19	101.0	200.0	385.0	199.97	0.0	0.0	0.0000	6.6	122.9	3.6	-5.5
55.2	16552	11.5	.02861	33.3	.19	100.0	199.5	385.2	199.51	0.0	0.0	0.0000	6.8	123.6	3.8	-5.7
56.0	16851	10.0	.02906	29.2	.17	95.0	197.1	386.3	197.15	0.0	0.0	0.0000	7.9	126.5	4.7	-6.4
57.0	17280	12.2	.02971	35.8	.23	88.2	197.4	395.1	197.41	0.0	0.0	0.0000	6.8	113.3	2.7	-6.2
58.0	17635	25.1	.03060	71.8	.50	83.0	201.7	410.6	201.65	0.0	0.0	0.0000	5.7	90.8	.1	-5.7
58.6	17854	35.7	.03160	101.1	.75	80.0	203.7	419.2	203.69	0.0	0.0	0.0000	4.1	78.6	-.8	-4.1
59.0	18020	43.8	.03236	123.2	.93	77.8	205.2	425.7	205.24	0.0	0.0	0.0000	3.2	62.2	-1.5	-2.8
60.0	18429	55.8	.03502	155.6	1.27	72.7	207.1	438.0	207.12	0.0	0.0	0.0000	3.1	14.1	-3.0	-.7
60.6	18658	62.5	.03685	174.1	1.48	70.0	207.1	442.8	207.12	0.0	0.0	0.0000	3.7	1.7	-3.7	-.1
61.0	18807	66.8	.03804	186.2	1.62	68.3	207.1	445.9	207.12	0.0	0.0	0.0000	4.1	355.7	-4.1	.3
62.0	19201	74.1	.04166	206.6	1.92	64.0	207.1	454.3	207.12	0.0	0.0	0.0000	4.2	340.8	-4.0	1.4
63.0	19591	79.9	.04558	222.4	2.21	60.0	207.3	463.2	207.32	0.0	0.0	0.0000	4.1	347.9	-4.0	.9
63.0	19602	80.0	.04568	222.8	2.21	59.9	207.3	463.4	207.32	0.0	0.0	0.0000	4.0	348.0	-4.0	.8
64.0	19969	100.0	.04996	276.4	2.94	56.4	208.9	475.1	208.92	0.0	0.0	0.0000	5.1	5.3	-5.1	-.5
65.0	20351	109.8	.05511	300.9	3.43	53.0	210.6	487.6	210.65	0.0	0.0	0.0000	6.7	36.0	-5.5	-4.0

TIME MIN	ALT GPM	OZONE MICMB	TOTOZ ATMCM	OZDEN MG/M3	OZMXR MICGG	PRESS MB	TEMP DEG K	PTEMP DEG K	VTEMP DEG K	HMDTY PRCNT	DEWPT DEG K	SPCFC HMDTY	SPD MPS	DIR DEG	NS MPS	EW MPS
65.9	20711	118.2	.06038	321.5	3.92	50.0	212.2	499.5	212.22	0.0	0.0	0.0000	3.9	79.0	-.7	-3.8
66.0	20774	119.6	.06129	325.1	4.00	49.5	212.5	501.6	212.50	0.0	0.0	0.0000	3.8	91.0	.1	-3.8
67.0	21136	125.0	.06691	339.6	4.43	46.7	212.5	510.0	212.50	0.0	0.0	0.0000	5.9	187.9	5.8	.8
68.0	21508	133.3	.07298	359.2	5.02	44.0	214.3	523.1	214.28	0.0	0.0	0.0000	2.7	200.5	2.6	1.0
69.0	21890	142.1	.07960	382.2	5.69	41.4	214.6	533.1	214.63	0.0	0.0	0.0000	1.2	71.3	-.4	-1.1
69.6	22105	143.4	.08349	385.0	5.95	40.0	214.8	538.9	214.82	0.0	0.0	0.0000	.9	68.6	-.3	-.8
70.0	22281	144.5	.08664	388.2	6.16	38.9	215.0	543.6	214.98	0.0	0.0	0.0000	.6	64.6	-.3	-.6
71.0	22735	150.7	.09502	402.2	6.90	36.2	216.3	558.4	216.34	0.0	0.0	0.0000	1.3	9.3	-1.3	-.2
71.5	22947	151.2	.09904	404.0	7.16	35.0	216.2	563.3	216.16	0.0	0.0	0.0000	2.5	25.5	-2.2	-1.1
72.0	23131	151.7	.10250	405.5	7.39	34.0	216.0	567.5	216.00	0.0	0.0	0.0000	3.5	30.5	-3.0	-1.8
73.0	23514	153.2	.10979	409.4	7.93	32.0	216.0	577.5	216.00	0.0	0.0	0.0000	7.2	82.2	-1.0	-7.2
74.0	23924	157.4	.11770	416.3	8.70	30.0	218.3	594.6	218.33	0.0	0.0	0.0000	11.3	108.5	3.6	-10.7
75.0	24389	164.0	.12690	430.3	9.74	27.9	220.1	612.0	220.10	0.0	0.0	0.0000	7.1	117.9	3.3	-6.3
76.0	24819	164.2	.13554	429.5	10.43	26.1	220.7	625.5	220.73	0.0	0.0	0.0000	5.9	79.3	-1.1	-5.8
76.6	25096	162.4	.14107	425.5	10.77	25.0	220.4	632.5	220.45	0.0	0.0	0.0000	8.4	70.2	-2.8	-7.9
77.0	25280	161.3	.14472	422.8	11.00	24.3	220.3	637.1	220.26	0.0	0.0	0.0000	10.1	66.7	-4.0	-9.2
78.0	25720	161.0	.15338	419.4	11.75	22.7	221.7	653.7	221.67	0.0	0.0	0.0000	9.8	81.4	-1.5	-9.7
79.0	26167	169.8	.16230	435.0	13.27	21.2	225.3	677.6	225.30	0.0	0.0	0.0000	7.1	120.7	3.6	-6.1
79.9	26554	175.1	.17024	440.7	14.51	20.0	229.4	701.6	229.42	0.0	0.0	0.0000	4.7	151.5	4.2	-2.3
80.0	26588	175.6	.17092	441.2	14.62	19.9	229.8	703.6	229.77	0.0	0.0	0.0000	4.6	155.4	4.2	-1.9
81.0	26933	165.3	.17786	418.0	14.49	18.9	228.4	709.6	228.35	0.0	0.0	0.0000	1.2	111.9	.4	-1.1
82.0	27409	160.8	.18703	407.4	15.14	17.6	227.9	722.9	227.92	0.0	0.0	0.0000	2.4	137.3	1.8	-1.6
82.1	27446	160.0	.18772	405.5	15.15	17.5	227.8	723.7	227.79	0.0	0.0	0.0000	2.7	134.5	1.9	-1.9
83.0	27960	148.4	.19714	379.2	15.18	16.2	226.0	734.1	226.03	0.0	0.0	0.0000	6.9	121.4	3.6	-5.9
83.9	28470	147.4	.20612	374.6	16.29	15.0	227.2	754.4	227.24	0.0	0.0	0.0000	8.0	91.7	.2	-8.0
84.0	28515	147.4	.20690	374.2	16.39	14.9	227.3	756.2	227.34	0.0	0.0	0.0000	8.2	89.6	-.1	-8.2
85.0	29075	138.2	.21636	349.7	16.72	13.7	228.2	777.5	228.21	0.0	0.0	0.0000	9.1	62.0	-4.3	-8.0
85.9	29688	134.8	.22623	340.5	17.88	12.5	228.6	799.5	228.60	0.0	0.0	0.0000	14.9	68.9	-5.4	-13.9
86.0	29742	134.5	.22709	339.7	17.98	12.4	228.6	801.5	228.64	0.0	0.0	0.0000	15.5	69.3	-5.5	-14.5
87.0	30303	122.2	.23561	310.7	17.76	11.4	227.1	815.3	227.06	0.0	0.0	0.0000	23.1	65.4	-9.6	-21.0
88.0	30786	111.8	.24232	284.9	17.48	10.6	226.6	830.8	226.62	0.0	0.0	0.0000	20.5	75.0	-5.3	-19.8
88.7	31171	106.3	.24727	271.4	17.61	10.0	226.1	843.0	226.14	0.0	0.0	0.0000	19.5	84.8	-1.8	-19.4
89.0	31373	103.4	.24986	264.4	17.67	9.7	225.9	849.4	225.89	0.0	0.0	0.0000	19.2	90.3	.1	-19.2
90.0	31869	95.8	.25575	243.5	17.64	9.0	227.2	872.8	227.20	0.0	0.0	0.0000	22.0	81.2	-3.4	-21.7
91.0	32411	89.9	.26168	225.3	17.96	8.3	230.5	906.1	230.48	0.0	0.0	0.0000	22.8	83.4	-2.6	-22.7
91.4	32660	87.4	.26419	218.1	18.09	8.0	231.4	919.6	231.43	0.0	0.0	0.0000	23.3	85.1	-2.0	-23.2
92.0	33099	83.0	.26860	205.5	18.33	7.5	233.1	943.4	233.12	0.0	0.0	0.0000	24.1	88.0	-.9	-24.1
92.7	33572	79.2	.27297	194.3	18.75	7.0	235.5	972.2	235.51	0.0	0.0	0.0000	27.4	88.7	-.6	-27.4
93.0	33772	77.7	.27480	189.6	18.92	6.8	236.5	984.3	236.52	0.0	0.0	0.0000	28.8	89.0	-.5	-28.8
94.0	34411	68.0	.28011	166.4	18.18	6.2	236.0	1008.4	235.98	0.0	0.0	0.0000	33.2	87.6	-1.4	-33.2
94.3	34637	66.6	.28181	163.1	18.38	6.0	235.8	1017.0	235.76	0.0	0.0	0.0000	33.8	88.0	-1.2	-33.7
95.0	35237	62.8	.28630	154.2	18.92	5.5	235.2	1039.9	235.16	0.0	0.0	0.0000	35.3	89.0	-.6	-35.3
95.8	35896	56.6	.29074	138.0	18.73	5.0	236.8	1076.3	236.84	0.0	0.0	0.0000	999.9	999.9	999.9	999.9
96.0	36036	55.3	.29168	134.6	18.69	4.9	237.2	1084.0	237.19	0.0	0.0	0.0000	999.9	999.9	999.9	999.9

INTEGRAL .29168 RESIDUAL .04366 INTEGRATED TOTAL OZONE .33534

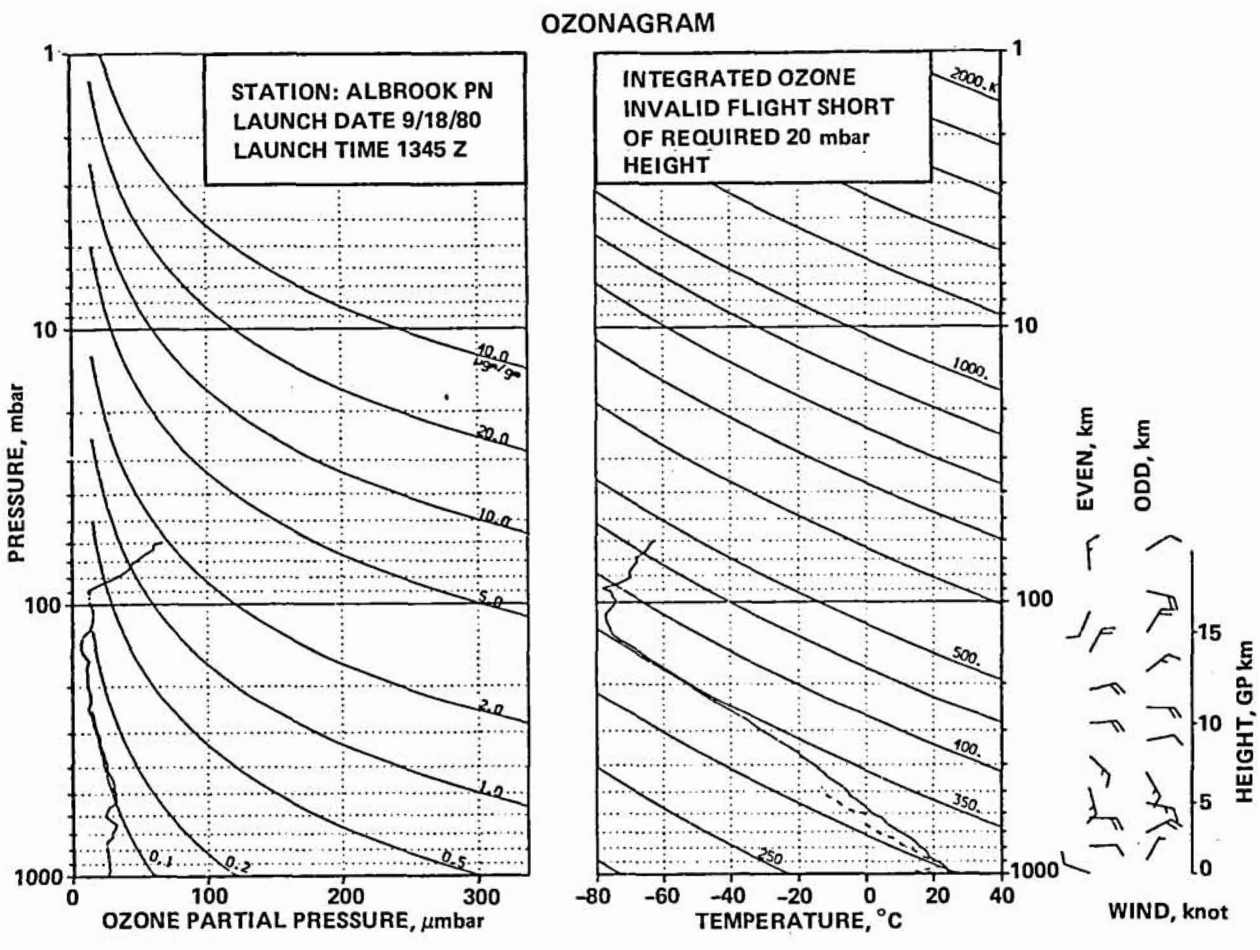

OZONAGRAM
STATION: ALBROOK PN
LAUNCH DATE 9/18/80
LAUNCH TIME 1345 Z
INTEGRATED OZONE
INVALID FLIGHT SHORT
OF REQUIRED 20 mbar
HEIGHT
PRESSURE, mbar
1
10
100
1000
OZONE PARTIAL PRESSURE, μmbar
0
100
200
300
TEMPERATURE, °C
-80
-60
-40
-20
0
20
40
EVEN, km
ODD, km
HEIGHT, GP km
WIND, knot

STATION ALBROOK PN   LAUNCH DATE 9/18/80   TIME 1345Z   ECC   SONDE 3A1451

SURFACE CONDITIONS   PRESS 1004.7MB   TEMP 297.6 DEG K   HUMIDITY 97.0 PRCNT

TIME MIN	ALT GPM	OZONE MICMB	TOTOZ ATMCM	OZDEN MG/M3	OZMXR MICGG	PRESS MB	TEMP DEG K	PTEMP DEG K	VTEMP DEG K	HMDTY PRCNT	DEWPT DEG K	SPCFC HMDTY	SPD MPS	DIR DEG	NS MPS	EW MPS
0.0	66	25.5	0.00000	49.5	.04	1004.7	297.5	297.2	300.96	98.2	297.2	.0187	4.0	290.0	-1.4	3.8
.2	107	25.8	.00010	50.0	.04	1000.0	297.5	297.5	300.66	90.8	295.6	.0162	4.3	291.2	-1.5	4.0
1.0	302	26.8	.00056	52.1	.05	978.0	297.3	299.2	299.26	55.4	287.8	.0107	5.6	295.4	-2.4	5.1
2.0	556	27.8	.00118	54.0	.05	950.0	296.9	301.2	299.90	86.8	294.5	.0168	3.8	288.6	-1.2	3.6
3.0	837	27.2	.00188	53.1	.05	920.0	295.5	302.6	298.40	87.5	293.3	.0161	1.5	298.2	-.7	1.3
3.7	1028	27.2	.00235	53.4	.05	900.0	294.0	303.0	296.89	92.6	292.8	.0159	1.1	17.5	-1.0	-.3
4.0	1096	27.2	.00252	53.6	.05	893.0	293.5	303.2	296.35	94.4	292.6	.0158	1.5	38.3	-1.1	-.9
5.0	1371	26.6	.00319	52.6	.05	865.0	291.8	304.2	294.32	90.7	290.2	.0141	3.5	65.8	-1.4	-3.2
5.6	1521	26.6	.00356	52.6	.05	850.0	291.6	305.4	293.96	86.8	289.3	.0133	4.3	69.2	-1.5	-4.0
6.0	1623	26.6	.00381	52.7	.05	840.0	291.4	306.3	293.72	84.1	288.7	.0131	4.9	70.9	-1.6	-4.6
7.0	1893	26.2	.00446	52.1	.05	814.0	290.6	308.2	292.73	80.1	287.1	.0122	5.5	77.6	-1.2	-5.3
7.6	2040	25.8	.00482	51.5	.05	800.0	289.6	308.7	291.61	77.1	285.6	.0109	6.2	85.4	-.5	-6.2
8.0	2148	25.6	.00508	51.1	.05	790.0	288.9	309.1	290.80	74.8	284.5	.0106	6.8	89.9	0.0	-6.8
9.0	2421	25.6	.00572	51.3	.06	765.0	287.9	310.8	289.65	71.4	282.8	.0098	6.9	94.3	.5	-6.8
10.0	2702	26.2	.00640	52.9	.06	740.0	286.6	312.3	288.17	70.9	281.4	.0092	6.4	56.6	-3.5	-5.3
11.0	2979	30.1	.00714	61.1	.07	716.0	284.7	313.2	285.94	62.7	277.8	.0074	8.8	56.6	-4.8	-7.3
11.7	3167	29.9	.00767	60.9	.07	700.0	283.4	313.8	284.64	62.7	276.6	.0068	9.6	69.6	-3.3	-9.0
12.0	3263	29.8	.00794	60.7	.07	692.0	282.8	314.2	283.97	62.6	276.0	.0068	10.2	75.2	-2.6	-9.8
13.0	3530	31.7	.00872	65.2	.08	670.0	280.6	314.7	281.67	62.1	273.9	.0060	11.3	73.5	-3.2	-10.8
14.0	3817	33.2	.00962	68.6	.09	647.0	279.2	316.2	280.21	62.5	272.6	.0057	11.2	78.3	-2.3	-11.0
15.0	4126	28.7	.01054	59.7	.08	623.0	277.9	318.1	278.89	70.6	273.0	.0060	10.5	93.6	.7	-10.4
16.0	4404	24.8	.01127	52.0	.07	602.0	275.0	317.9	276.05	84.2	272.6	.0061	11.4	99.8	1.9	-11.2
16.1	4430	24.9	.01133	52.3	.07	600.0	274.9	318.1	275.91	82.0	272.1	.0057	11.2	99.6	1.9	-11.1
17.0	4676	25.8	.01194	54.4	.07	582.0	273.9	319.7	274.60	[illegible]	267.4	.0043	9.9	97.0	1.2	-9.8
18.0	4984	27.4	.01275	58.0	.08	560.0	272.1	321.2	272.78	61.7	265.7	.0039	7.1	97.4	.9	-7.1
19.0	5273	32.0	.01360	68.3	.10	540.0	270.4	322.5	270.99	61.7	264.1	.0035	5.6	114.5	2.3	-5.1
20.0	5571	32.6	.01456	70.2	.10	520.0	268.4	323.6	268.91	58.3	261.5	.0030	6.1	158.7	5.7	-2.2
21.0	5879	32.7	.01557	70.4	.11	500.0	267.7	326.3	268.14	57.8	260.7	.0029	7.2	173.2	7.2	-.9
22.0	6166	31.0	.01649	67.2	.11	482.0	266.2	327.9	266.63	60.9	259.9	.0028	6.6	160.3	6.2	-2.2
23.0	6478	31.6	.01749	69.1	.11	463.0	264.0	328.9	264.10	0.0	0.0	0.0000	7.1	150.0	6.1	-3.5
24.0	6783	30.3	.01845	66.8	.11	445.0	261.8	330.0	262.23	72.9	257.9	.0026	7.8	145.0	6.4	-4.5
25.0	7117	28.3	.01946	62.8	.11	426.0	260.4	332.3	260.78	72.4	256.5	.0024	8.7	150.7	7.6	-4.2
26.0	7408	26.3	.02029	58.8	.11	410.0	258.6	333.6	258.94	76.6	255.4	.0023	7.3	150.6	6.4	-3.6
26.6	7594	26.4	.02080	59.2	.11	400.0	257.4	334.4	257.70	75.5	254.0	.0020	7.1	142.6	5.6	-4.3
27.0	7727	26.4	.02117	59.5	.11	393.0	256.5	335.0	256.81	74.8	253.1	.0020	6.9	136.6	5.0	-4.8
28.0	8038	24.7	.02201	56.1	.11	377.0	254.3	336.1	254.58	71.7	250.5	.0016	7.0	132.7	4.7	-5.1
29.0	8380	23.7	.02289	54.2	.11	360.0	252.7	338.4	252.93	71.4	248.9	.0015	6.1	116.5	2.7	-5.5
29.6	8587	22.7	.02340	52.1	.11	350.0	251.2	339.1	251.41	69.7	247.2	.0012	6.0	103.5	1.4	-5.8
30.0	8715	22.0	.02371	50.8	.11	344.0	250.3	339.5	250.48	68.7	246.1	.0012	6.0	95.5	.6	-6.0
31.0	9062	20.1	.02450	46.9	.10	328.0	247.4	340.2	247.52	68.1	243.2	.0010	6.3	79.4	-1.2	-6.2
32.0	9399	20.8	.02526	49.1	.11	313.0	245.0	341.4	245.11	68.1	241.0	.0008	6.3	67.6	-2.4	-5.9
33.0	9701	18.8	.02592	44.8	.10	300.0	242.2	341.7	242.31	68.2	238.3	.0006	8.4	72.4	-2.5	-8.0
34.0	10087	16.1	.02668	38.8	.09	284.0	239.7	343.4	239.77	65.9	235.5	.0005	10.3	84.5	-1.0	-10.3
35.0	10465	14.9	.02734	36.4	.09	269.0	237.0	344.9	237.08	64.3	232.7	.0004	11.3	91.5	.3	-11.3
36.0	10806	13.5	.02790	33.2	.09	256.0	234.0	345.4	234.08	55.8	228.6	.0003	12.3	93.5	.8	-12.3
36.5	10967	12.8	.02813	31.7	.08	250.0	232.8	345.9	232.81	0.0	0.0	0.0000	11.7	91.5	.3	-11.7
37.0	11161	12.0	.02842	30.0	.08	243.0	231.3	346.5	231.29	0.0	0.0	0.0000	10.9	88.8	-.2	-10.9
38.0	11444	13.4	.02884	33.8	.10	233.0	228.8	346.8	228.76	0.0	0.0	0.0000	10.9	79.2	-2.0	-10.7
39.0	11796	13.9	.02941	35.4	.10	221.0	226.0	347.9	226.02	0.0	0.0	0.0000	11.6	74.5	-3.1	-11.2
40.0	12131	13.1	.02995	33.9	.10	210.0	222.9	348.1	222.90	0.0	0.0	0.0000	9.4	75.0	-2.4	-9.1
41.0	12415	11.9	.03039	31.0	.10	201.0	220.9	349.4	220.69	0.0	0.0	0.0000	7.6	64.5	-3.3	-6.8
41.1	12446	11.8	.03043	31.0	.10	200.0	220.6	349.4	220.62	0.0	0.0	0.0000	7.5	63.4	-3.4	-6.7
42.0	12776	11.4	.03090	30.3	.10	190.0	217.9	350.1	217.86	0.0	0.0	0.0000	7.5	52.2	-4.6	-5.9
43.0	13118	11.4	.03139	30.7	.11	180.0	215.2	351.2	215.17	0.0	0.0	0.0000	6.5	51.0	-4.1	-5.0
44.0	13475	10.7	.03189	29.1	.10	170.0	212.2	352.0	212.17	0.0	0.0	0.0000	7.0	43.1	-5.1	-4.8
45.0	13810	12.6	.03239	34.9	.13	161.0	209.0	352.1	208.97	0.0	0.0	0.0000	9.0	37.1	-7.1	-5.4
46.0	14159	8.6	.03287	24.1	.09	152.0	206.2	353.1	206.16	0.0	0.0	0.0000	10.0	24.9	-9.1	-4.2
46.2	14238	8.1	.03295	22.7	.09	150.0	205.4	353.2	205.41	0.0	0.0	0.0000	10.2	22.0	-9.5	-3.8
47.0	14483	6.5	.03320	18.4	.07	144.0	203.1	353.4	203.13	0.0	0.0	0.0000	11.1	13.9	-10.8	-2.7
48.0	14734	6.5	.03341	18.7	.08	138.0	200.3	352.8	200.33	0.0	0.0	0.0000	12.0	17.2	-11.5	-3.6
49.0	15037	7.8	.03371	22.7	.10	131.0	197.8	353.6	197.81	0.0	0.0	0.0000	10.8	31.5	-9.2	-5.6
49.9	15307	12.3	.03409	35.9	.16	125.0	197.1	357.1	197.14	0.0	0.0	0.0000	6.6	38.9	-5.1	-4.1
50.0	15354	13.0	.03416	38.2	.17	124.0	197.0	357.7	197.02	0.0	0.0	0.0000	5.9	41.2	-4.4	-3.9
51.0	15639	14.9	.03470	43.9	.21	118.0	196.2	361.3	196.21	0.0	0.0	0.0000	3.3	281.0	-.6	3.2
52.0	15989	15.7	.03544	46.3	.23	111.0	195.7	366.7	195.66	0.0	0.0	0.0000	2.8	228.0	1.8	2.1
53.0	16364	15.6	.03625	45.5	.25	104.0	197.8	377.7	197.81	0.0	0.0	0.0000	10.8	108.9	3.5	-10.2
53.8	16591	13.6	.03669	39.4	.22	100.0	198.8	383.8	198.79	0.0	0.0	0.0000	15.6	104.2	3.8	-15.1
54.0	16662	13.0	.03683	37.6	.22	98.8	199.1	385.7	199.09	0.0	0.0	0.0000	17.1	103.2	3.9	-16.6
55.0	16865	12.9	.03718	37.8	.22	95.4	197.8	387.1	197.81	0.0	0.0	0.0000	13.7	104.5	3.4	-13.3
56.0	17056	12.9	.03752	37.7	.23	92.3	197.8	390.8	197.81	0.0	0.0	0.0000	10.1	103.8	2.4	-9.8
57.0	17278	12.4	.03791	36.6	.23	88.8	195.1	389.7	195.09	0.0	0.0	0.0000	9.1	95.1	.8	-9.1
58.0	17531	20.0	.03846	57.6	.39	85.0	200.3	405.2	200.33	0.0	0.0	0.0000	10.3	79.5	-1.9	-10.1
59.0	17794	29.9	.03934	84.9	.61	81.3	203.4	416.5	203.35	0.0	0.0	0.0000	8.5	53.2	-5.1	-6.8
59.4	17889	32.8	.03977	93.2	.68	80.0	203.3	418.3	203.27	0.0	0.0	0.0000	7.1	35.8	-5.8	-4.2
60.0	18055	37.8	.04052	107.5	.81	77.8	203.1	421.3	203.13	0.0	0.0	0.0000	7.0	356.5	-6.9	.4
61.0	18321	43.1	.04194	121.9	.96	74.4	204.2	429.1	204.24	0.0	0.0	0.0000	7.6	354.7	-7.5	.7
62.0	18542	44.8	.04323	126.1	1.04	71.7	205.3	435.9	205.31	0.0	0.0	0.0000	9.9	33.7	-8.3	-5.5
62.6	18685	47.7	.04412	134.3	1.13	70.0	205.2	438.6	205.18	0.0	0.0	0.0000	9.6	45.9	-6.7	-6.9
63.0	18772	49.4	.04465	139.2	1.19	69.0	205.1	440.3	205.10	0.0	0.0	0.0000	9.6	53.5	-5.7	-7.7
64.0	19022	54.6	.04635	152.1	1.37	66.2	207.4	450.5	207.39	0.0	0.0	0.0000	6.0	59.4	-3.1	-5.2
65.0	19285	61.0	.04833	168.7	1.59	63.4	208.8	459.1	208.78	0.0	0.0	0.0000	7.6	51.3	-4.8	-6.0
66.0	19521	61.0	.05018	168.1	1.66	61.0	209.6	466.0	209.55	0.0	0.0	0.0000	9.7	54.5	-5.6	-7.9

TIME MIN	ALT GPM	OZONE MICMB	TOTOZ ATMCM	OZDEN MG/M3	OZMXR MICGG	PRESS MB	TEMP DEG K	PTEMP DEG K	VTEMP DEG K	HMDTY PRCNT	DEWPT DEG K	SPCFC HMDTY	SPD MPS	DIR DEG	NS MPS	EW MPS
66.6	19622	65.3	.05102	179.1	1.80	60.0	210.4	470.0	210.38	0.0	0.0	0.0000	999.9	999.9	999.9	999.9
67.0	19684	67.8	.05153	185.8	1.89	59.4	210.9	472.5	210.88	0.0	0.0	0.0000	999.9	999.9	999.9	999.9

CALIBRATIONS APPLIED FOR PARTIAL PRESSURE OF OZONE
TOTAL INTEGRATED OZONE INVALID. BALLOON SHORT OF 20 MB HEIGHT

APPENDIX C

FLIGHT LOGS, PILOT COMMENTARIES, AND FLIGHT TAPE TRANSCRIPTS: FLIGHTS 1-11

William A. Page

This appendix contains the flight-track charts, flight logs, pilot debriefing comments, and, for most of the 11 flights, transcripts of the flight tapes. The flight-track charts show the routes flown and the times (GMT) at various points along the track. The flight logs are notes made by the pilots during the flights.

The debriefings were recorded within an hour of landing. Comments were solicited about the flight track flown; observations of cloud levels and structure; performance of the aircraft, such as roughness of the ride (turbulence); and any other observations or unusual events.

In the commentaries, magnetic headings and distances from the Howard AFB (in nautical miles) are shown as, for example, 058°/95. In the flight tape transcriptions, the times shown in brackets are universal times from the time code generator.

FLIGHT 1: 30 AUGUST 1980

(Pilot: Jerry Hoyt)

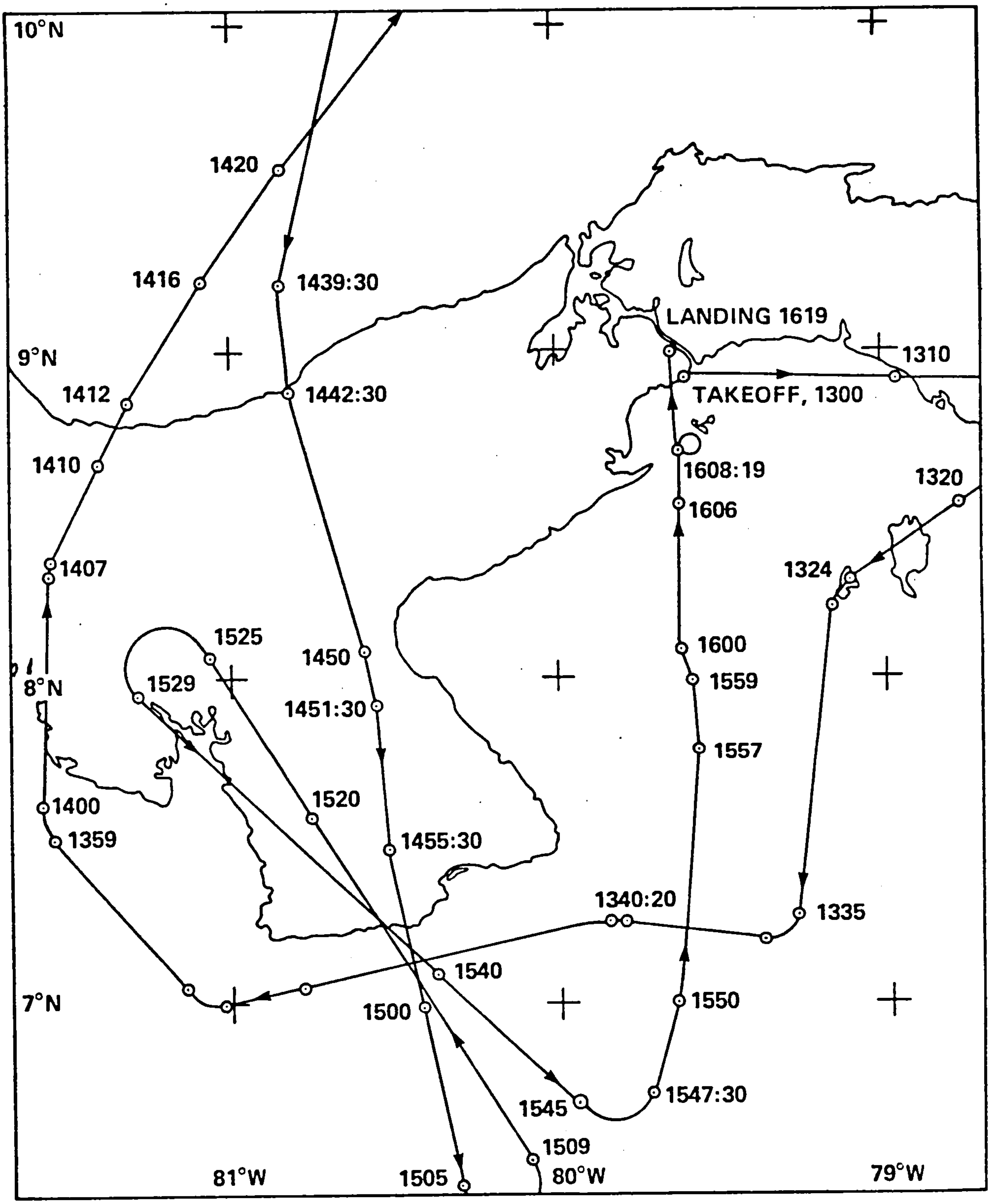

FLIGHT 1

[Pilot: Jerry Hoyt]

Flight Log: 30 August 1980

Altitude, 1000 ft	Universal time	Event
0	1300	Takeoff
46 (47.5)	1313	AGC sw to run
	1324	Turn to south
49	1330	
52	1350	360° heading
52	1401:30	APS No. 1 opened for 2 min, T = -63°C[a]
54.5	1406	030° heading
58	1424	190° heading
58	1431:45	APS No. 2 opened for 2 min, T = -60°C
61	1441	170° heading
64	1504	330° heading
64	1514:30	APS No. 3 opened for 2 min
67	1529	Level flight
	1550	Pitot heat on
	1551	Standby

Pilot Commentary

Takeoff normal at 1300 UT. Climed out on 090° heading. Top layer was about 46K ft, pretty complete coverage. Went to 9° N, 78.5° W, turned to SW. Saw line of thunderstorms at about 7° N, 80° W to 7° N, 81° W. Beyond, about 6°50' N it was like a cliff, could see all the way down to the low stratus, about 5K ft or so. North of 7°20' and 80°30', it was essentially clear, all the way to 8°30'. Flew over the clear area. Continued to 7°30', then turned westerly heading (270°), overflew one buildup, continued until parallel to another buildup, turned north at approximately 81° W, flew north. One buildup at 81° W, 9° N and another at 10° N, 80° W that Danielsen described. There were three buildups that dominated where I was flying. Most areas covered with cirrus at ~46K except over the land and south of a buildup at 7° N, 80° W. Flew a box pattern; at 9° N, came out of box pattern on 030° heading (at 1406 UT) and flew to 10° N, 80° W and overlfew buildup described by Danielsen. Changed altitude on each leg. Once beyond buildup, turned 180° to heading 190° to cross over it again. Flew back to buildup at 10° N, 80° W, but buildup looked discontinuous and the one at 7° N, 80° W looked better. So flew to south and overflew better-looking buildup (7° N, 80° W) at 61K, and 67K ft. It appeared that several small turrets would pop out at various times between 7° N, 80° W and 7° N, 81° W, tried to overfly biggest; keyed INS event marker when I crossed them. Set turning mirror down several times when passing over clusters, at least once for the north cluster and at least once or twice for the south clusters. I thought clusters to south were biggest. One to north appeared it had played itself out. When north and returning south saw lenticular cloud over one of the buildups. As I approached the cloud, it blended into background and was no longer discernible. At a distance of 150 miles, it was easy to see and appeared to be 500 to 1000 ft above the tower and not connected. Light turbulence was felt whenever I passed over or near cell. I felt

[a]Indicated ram temperature from cockpit indicator.

a lifting (vertical acceleration) (gained ~1000 ft in altitude) when passing over cell (to south). I estimate the cells' tops to be 52 to 54K ft high. Felt vertical acceleration when at 64K ft. Flew over cells to south three times. First two times felt light chop (turbulence). Last time at 67K (or possibly 64K ft, can't remember) got the vertical acceleration. After 67K pass returned to base. Saw thin layer (cirrus like) always above aircraft and in all directions. Standard cloud color; clearly distinguishable from horizon and above the horizon; not well defined, but top of layer has sharper edge than bottom. Lowest outside temperature on cockpit indicator occurred at 52K ft. Turned pitot heat off late, probably when at 49K ft. Turned pitot heat on again at about 1550 UT near end of flight.

FLIGHT 2: 31 AUGUST 1980

(Pilot: Ivor Webster)

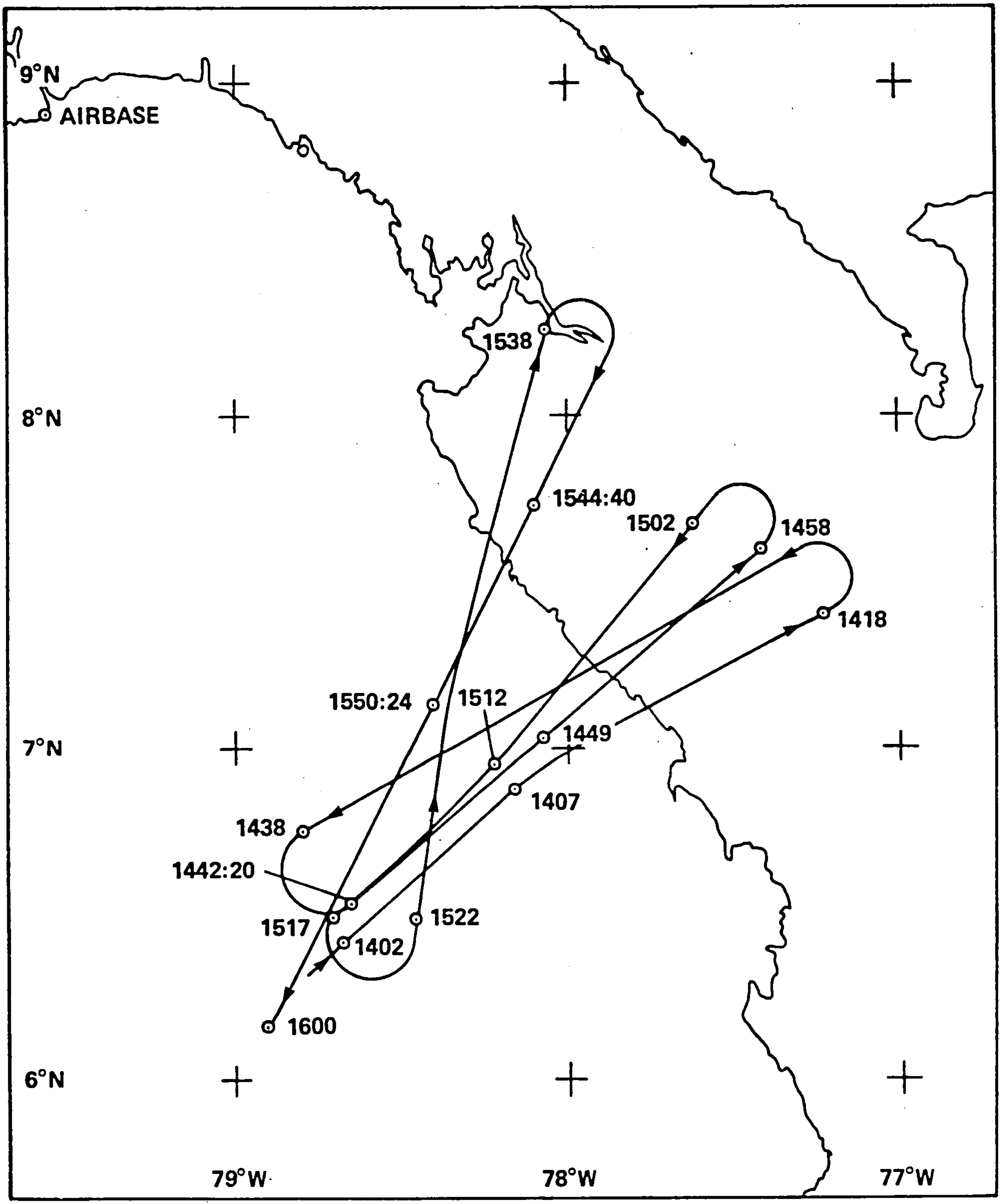

FLIGHT 2
[Pilot: Ivor Webster]

Flight Log: 31 August 1980

Altitude, 1000 ft	Universal time	Event
	1322:30	AGC off
	1324	AGC standby
	1324:14	Left tank on both standby
	1325:47	Right tank fwd sw on
	1341:20	AGC on
	1342:14	Pitot heat off
49.5	1354	Temp -50°C,[a] start climb from 49.5K ft
53	1402	-52°C, 160°/148 heading 060°
	1403	Turned mirror down
53.5	1407	(Small climb to clear cloud) 145°/149[b]
	1412:26	Retracted mirror
	1418	Turned left and climbed, 122°/168
56.5	1423	Level flight, -49°C
	1431	Mirror down
	1435:22	Mirror up
	1438	Turned left and climbed, 160°/138
59.5	1442:24	Leveled, 158°/153, 050° heading, -40°C
	1448:30	Mirror down
	1449	141°/145 (over cumulus tower), not well defined
	1452:40	Mirror up
	1458	Turned left and started climb, 121°/152
62.5	1502	Level, 122°/139, 220° heading, -40°C
	1510:30	Mirror down
	--	At 145°/143, over cumulus tower
	1513	Mirror up
	1517	Turned left, started climb, 160°/155
65	1522	Level, 155°/160, at 156°/165, 005° heading
	1524:42	Mirror down
	--	148°/137 over cumulus tower
	1538	Turned right, started climb, 113°/99
	1541:18	Mirror up
67	1544:40	128°/113, 205° heading
	1550:24	Mirror down, 146°/128, on this leg -32°C to -35°C
	1559:30	Mirror up
	1600	Started descent, 166°/170, AGC standby
	1600:52	Pitot heat on
	1641	Left and right tanks off

[a]Indicated ram temperature from cockpit indicator.
[b]Magnetic bearing and distance from Howard AFB.

Pilot Commentary

Takeoff at 1300 UT. Headed to general area agreed upon on heading of 160°. When I reached 50K ft could see buildup to the SE, looked farther away than they really were, only about 150 miles out. Cirrus deck seemed to increase in altitude as I flew along toward buildup. Perhaps at 41K when first went through it and I guess at 46K ft as I approached cells. Aircraft was at 49.5K ft. At 20-30 miles away cells appeared higher than aircraft so I climbed to 53.5K ft for first run. Turned a little bit south because I thought I identified line of at least two batches of cells lying in SW-NE direction. Finally identified three cells, two lay along a line of heading 060°; at about 6°40' N, 78°25' (best guess of location of first cell, other on heading of 060° farther along were batch of other cells). Southeast of the line there was another batch of cells (3). Throughout flight, these three batches of cells decayed to two batches of cells and, in a later run, into one batch of cells. Don't know whether they merged or some just dissipated because when you get far away and return you can't recognize previous pattern (it doesn't look the same). Near the end (the last three runs), there was just one batch of cells. Recorded most of the information on the tape. First run was 060° heading at 53.5K ft, started at 1402 UT. Shortly afterwards felt moderate to heavy turbulence (for about 20 sec or so). Thought I might have been a little too low. Cell tops were about 51K ft. Got very little turbulence after for the rest of the run. Believe turbulence occurred over cells. Turning mirror was operated. Fifteen-minute run. Last 10 min was smooth. When uplift or downdraft was felt, made remark in recorder. Also recorded on flight record the Tacan positions of aircraft at beginning and end of runs, and the times of various events. Generally turned mirror downward a minute or so before reaching cells. Recorded times. When looking at cluster from distance, could identify cirrus form cloud which seemed to be associated with the tops, sitting just above the tops (like Jerry mentioned yesterday), or sitting very close to, if not a part of (the tops). It appeared as a streamer to the SW, perhaps as far as 60 miles. Didn't appear as an anvil; the cells had a cumulo form top, but the cirrus form streamer was just above and appeared to possibly emanate at or above the cells. Streamer depth might have been about 500 ft thick, and tapered out to almost nothing at 40-50 miles away. Cloud streamer does appear transparent, easy to see against horizon. Another observation: cells which formed to SSW of aircraft, there appeared in middle of cluster a sort of burst, there was a faint type cirrus cloud coming out of cell top in very small area, not very large in size (hard to judge since it was about 75 miles away). General impression is that when approaching cell uplift occurred, when over the cells (on one or two or three occasions) dropping occurred; and when beyond cells, uplift occurred again. Comment from Jerry Hoyt: "When I flew yesterday, my uplift was well defined; felt like top of cell was only mile or so wide, and the lift was up one side and all the way over. Ivor seems to be describing cells that were larger. When asked, Ivor commented that he thought his cell area (cluster of cells) was at least 12 to 15 miles wide. On some passes, got slight uplift as I approached, no effect over the top, and slight uplift as I departed."

FLIGHT 3: 3 SEPTEMBER 1980

(Pilot: Ron Williams)

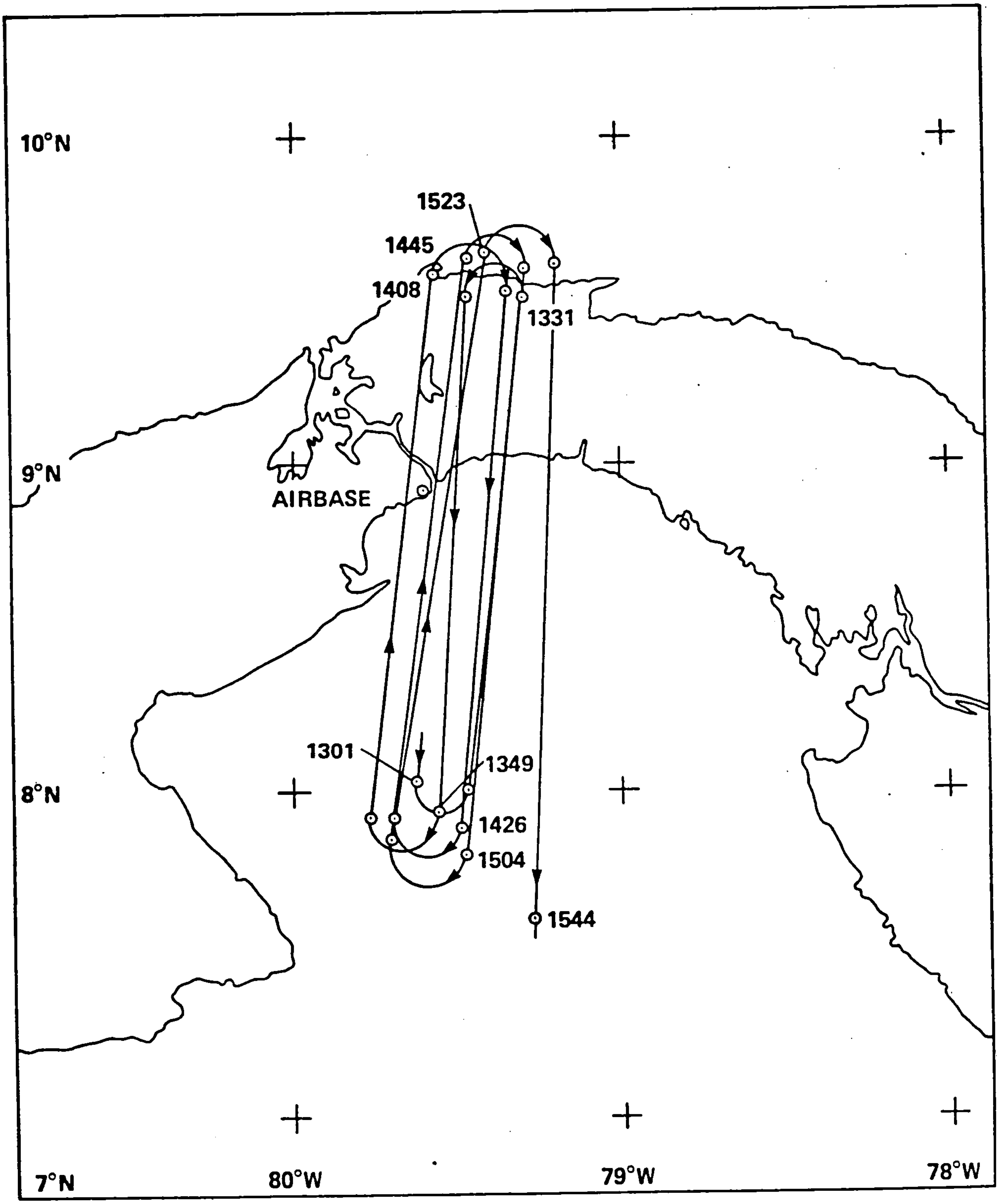

FLIGHT 3
[Pilot: Ron Williams]

Flight Log: 3 September 1980

Altitude, 1000 ft	Universal time	Event
0	1252:30	AGC off
	1253:30	AGC stdby
	1255	Left tank fwd sw stdby
	1255:05	Left tank aft sw stdby
	1255:30	Right tank fwd sw on; also aft on ~3 min turned right tank aft off
	1300	Takeoff
46	1310	Level S heading, 180°/53[a] start turn N heading, 170°/55 end turn
	1312:08	Pitot heat off
	1316:06	AGC to run
	1331	Start climb N heading, 025°/40
49	1333:10	End climb S heading, 010°/37
	1349	Start climb S heading, 176°/59 End climb N heading, 188°/61
52	1351:30	Level
	1355:15	Right aft sw on
	1401:09	Right aft sw off
	1408	Start climb, N heading, 360°/40 End climb, S heading, 020°/40
55.5	1409:50	Level
	1426	Start climb, S heading, 172°/62 End climb, N heading, 184°/60
58	1428:10	Level
	1431:35	Right aft sw on
	1437:10	Right aft sw off
	1445	Start climb, N heading, 008°/44 End climb, S heading, 022°/45
61	1448:20	Level
	1504	Start climb, S heading, 172°/67 End climb, N heading, 184°/64
64	1507:20	Level
	1523	Start climb, N heading, 012°/45 End climb, S heading, 028°/48
67	1528:45	Level
	1544	End run, S heading, 164°/81
	1544	AGC stdby
	1544:05	Pitot heat on
	~1613	Landing
	1621:04	Left tank fwd sw off
	1621:12	Left tank aft sw off
	1621:23	Right tank off

[a]Magnetic bearing and distance from Howard AFB.

Pilot Commentary

Flew a clear-sky reference run. Takeoff 1300 UT, reached 46K at 1310 UT, started first run, clear with scattered Q. Slight turbulence on one run which I mentioned on the tape. There was a middle deck, measured on letdown at 19,700 ft. Turbulence on two legs, one was close to moderate, 52K I think, close to trope, I guess. Ran back and forth right over Howard, 50 miles south and 50 miles north. Things didn't seem to change, no cells or towers within 100 miles. Some to south and east. Airplane was too heavy to go to 70K ft. Pretty warm out there. Took almost 6 min to climb from 64K to 67K ft. Smooth flying at higher altitudes. At or above 61K ft, however, on north part of leg, noticed slight disturbance, like airplane wanted to do wander, do a Dutch roll sort of, sort of unstable. A little pitch change too. It must have been atmospheric conditions because on southern part of leg autopilot held airplane stable. Think it was 52K but not sure. The other time was at 61K, I think. I was down south, I crossed over the base and then hit turbulence and that funny Dutch roll motion. Except over land, clouds went from scattered to broken during flight.

FLIGHT 4: 7 SEPTEMBER 1980

(Pilot: Jerry Hoyt)

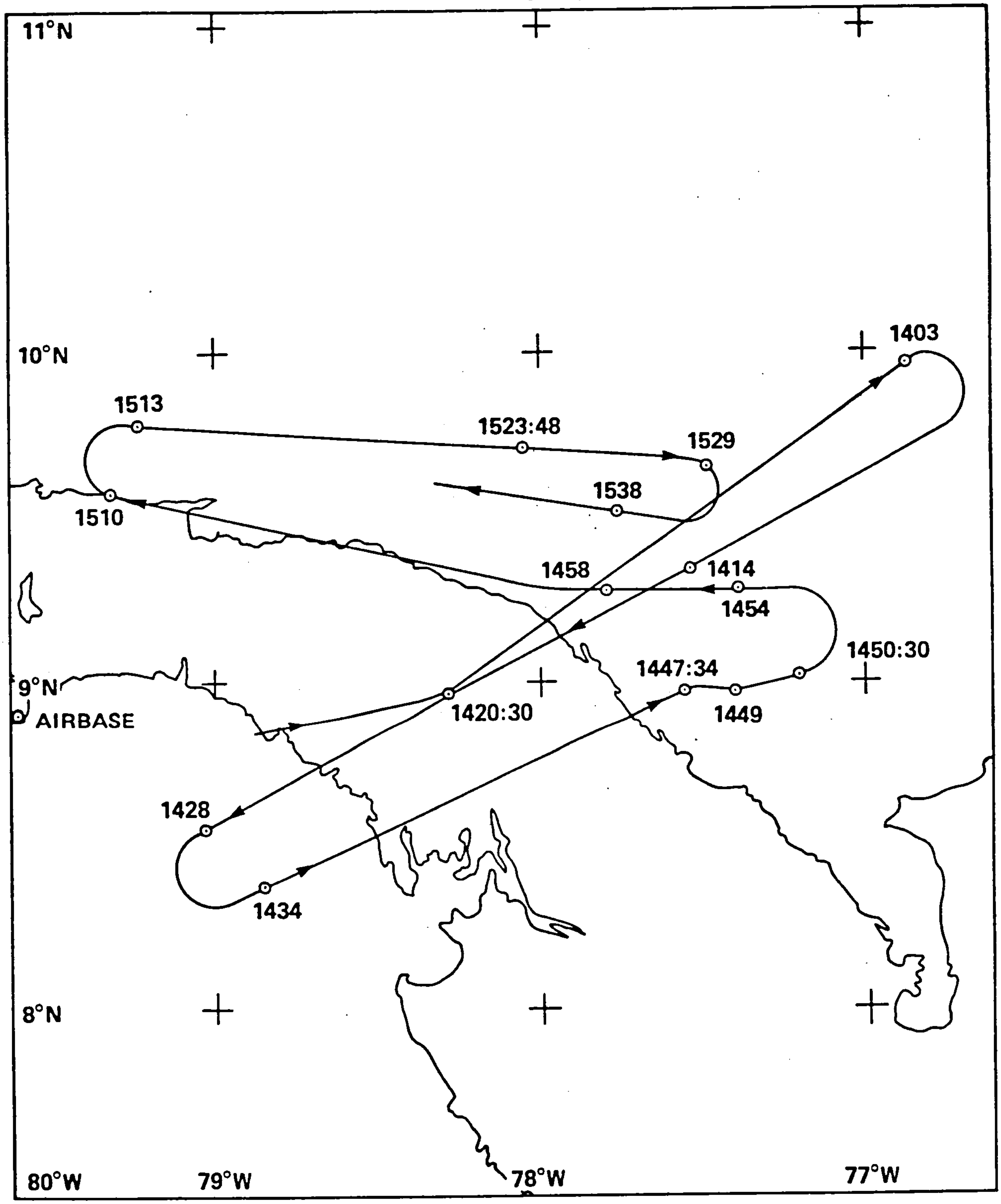

FLIGHT 4

[Pilot: Jerry Hoyt]

Flight Log: 7 September 1980

Altitude, 1000 ft	Universal time	Event
0	<1300	Verify: INS on, H_2O Rad on, AGC sw off
0	1324:19	Left tank rear sw on
	1324:33	Left tank fwd sw on
	1324:43	Right tank fwd sw on
	--	Right tank aft sw off
	1328:30	DASIBI to stdby
0	1330	Takeoff
56	1344	DASIBI to run, heading 060°, 063°/60[a]
	1354	Pitot heat off
	1403	Descending right turn, 066°/173, T_t = 060°C[b]
54	1408	Level, 240° heading
	1409	Mirror down
	1414	Mirror up
	1420:30	APS No. 1 open (for 1 min), 085°/78, -60°C, 54K ft
	1423	Mirror down (in streamer)
	1428	Mirror up (out of streamer)
	1428	Climbing left turn, 120°/40
59	1434	Level, 060° heading, 123°/55 T_t = -50°C
	1445:38	INS event key, reference
	1447:24	APS No. 2 open (for 1 min), 086°/121, -47°C, 59.6K ft
	1450:30	Climbing left turn, 085°/142
62	1454	Level, 270° heading, 078°/133, T_t = -43°C
	1458:08	APS No. 3 open (for 1 min), 076°/109, -42°C, 62K ft, 270 heading
	1510	Climbing right turn, 020°/44
64.5	1513	Level, 909° heading, 020°/57, T_t = -36°C
	1529	Climbing right turn, 068°/133
68	1533	Level, 280° heading, 069°/115, T_t = -33°C
	1552±	Start descent
60	1557	DASIBI to stdby
0	--	Landing
0	1626:48	Left tank aft sw off
	1626:49	Left tank fwd sw off
	1627:10	Right tank sw off

Pilot Commentary

Takeoff at 1330 UT, climb-out to the east to about 120 miles. Cirrus at 37K with tops at about 52K. Climbed to 56K, could see no cumulonimbus towers anywhere. Went to initial target area, flew 080° heading to a point 085°/78 miles from Howard.

---

[a]Magnetic bearing and distance from Howard AFB.
[b]Indicated ram temperature from cockpit indicator.

Turned to 060° heading and moved to 066°/173 miles before making a right turn as per flight log. Second run at 54K was close to cirrus tops, ran mirror down first time when in or close to tops. Went through more streamer-like clouds (a blow-off layer?) that seemed to be 1000 to 2000 ft above cirrus tops and turned mirror down a second time. Went to southeast of Howard at 123° — about 40 miles — and made a left climbing turn to 59K ft. Cloud tops looked stable and all the same. Turned back to NE and went due east of Howard and climbed to 62K ft. Flew 270°. Climbed to 64.5K ft for next run and at 68K (more or less the maximum altitude with the payload) for the final run. The area covered by the flight had a complete and uniform cirrus cover that didn't vary by more than 2000 to 4000 ft in altitude. However, near 10° N, 77° W, clouds dropped away and I could see deeper into atmosphere. Light turbulence was encountered on the 56K run and was mentioned on the flight tape. The only comment about the clouds was that you could see streamers that had blown off (from previous turrets). It was one of these that I flew through at 54K. During the second mirror turndown period I felt I was in streamers. Seemed to be 500 to 1000 ft thick and some 30 miles in length. Easy to see when at some distance but difficult to determine when you are in it. Other (two or three) streamers were seen off to the north. Not the same structure as seen on first flight [8/30/80]. The thin high haze layer (volcano?) was also observed again, more pronounced toward the south, always seems above the aircraft. I often observe similar layers over California but not always.

Flight Tape Transcript

I'm at 26K ft . . . Clouds are coming up now, some cirrus . . . Light to moderate turbulence here at 50K ft and -59°C . . . definitely out to 060 on the 250° radial . . . at 56K ft . . .. I can't see any bumpers coming up strong [1347:09] but it's . . . to the north of my position and . . . [1401:13] dropping off but I can't really tell for sure. . . . 2K ft and I'm turning to the south [1403:18] where the . . . the tops at 54K. I'm going to level at 54K [1406:14] and then drive at 54K ft for a while. . . . estimating the tops at about 52K and I'm level at 54K ft and I'm going to [1408:59] . . . come back down to 51.9K ft. Looks like the . . . clouds are . . . [1411:08] 53K ft now and I'm still not quite on the tops. . . . and I'll be going [1412:32] through some clouds here. [1413:43] 52K ft, my present position is on the 076° [1413:56] radial, 125 miles. It's gotten back up at 1450:00 (1415?) . . . maintain 54K now and . . . stuff is embedded, I'm remaining above it slightly [1415:11]. . . . relatively level at 54 to 54K ft [1418:10]. The tops are about 52K [1420:18], I'm at 54K ft so I'm going to take an APS sample. I'm level at 54K ft and about to go into some more light blow-off; it's a separate layer for sure, looks like about 500 to 1000 ft [1423:14] or so thick. I'm on . . . zero radial [1425:30] at 55 miles from Howard and this layer looks like it's probably 500 to 1000 ft thick and I'd say it's approximately at my level. It's probably about 4000 ft [1425:51] above the cloud tops; they look like they gradually slope off to around 50K ft. It looks like I'm in it [1427:06] but looking around, I can't distinguish whether I am in the cloud or not. Going [1428:26] back horizontal at 1428 [1428:45], I've flown completely through that thin layer now and am definitely on the western side. I couldn't tell really if I was in it or not, but I'm starting my climb now to a higher altitude [1428:59]. I'm at 59K ft [1434:38] heading 060°. I'm on the 086° radial at 130 miles [1448:58] and there're no buildups through the tops and it looks like there's been very little change since I was up here; it's just flat and every now and then you see some possible thin anvils that have been blown to the north. About two or three is about all I've seen on this 100 mile leg [1449:25] back to the east. . . . and a left climbing turn to 62K ft [1450:55], on the 085° radial [1451:02], 142 n. mi. . . . at 1458:08 [1459:31] for 1 min, 62K ft, -42°C, heading

270°. My position is 076° radial, 109 miles [1459:57]. I'll get slightly to the north of the others and still nowhere on the horizon can I see any big buildups breaking through the cirrus but I'll continue to work slightly to the north and see if I can't get out on the edge to see if there are any new ones starting, but basically it appears to be either dissipating or else there's none that are punching through that I can see. There is a definite thin layer that is above the main cirrus deck. I'm passing either close to right now or it's at my level, I can only see it to the north, I can't see it to the south. 1510:00, starting a right turn to 64.5K ft or so and still there's no change in the cloud tops [1511:20] except further to the west there might be some buildups; I'll come back to this particular point at 68K or so and take a look and possibly drop down at that point [1511:40]. The dust layer [1514:20] still appears to be at this altitude. It appears to be in all quadrants but I can't really tell what's happening here. No contrails at 64.5K ft [1519:20]; however, I did have slight contrails at 62K ft. Position is 060° radial [1523:48], 103 miles from Howard and due north of my position, probably 20 or 30 miles, the high clouds definitely drop off [1524:00] to where you can see the low Q. It's just a slight hole (a sucker hole), but to the south of my position it's still blanketed forever with clouds and it looks like the tops are pretty constant at about 52K ft or so [1524:18]. No new towers or anything building above the level tops.

FLIGHT 5: 9 SEPTEMBER 1980

(Pilot: Ivor Webster)

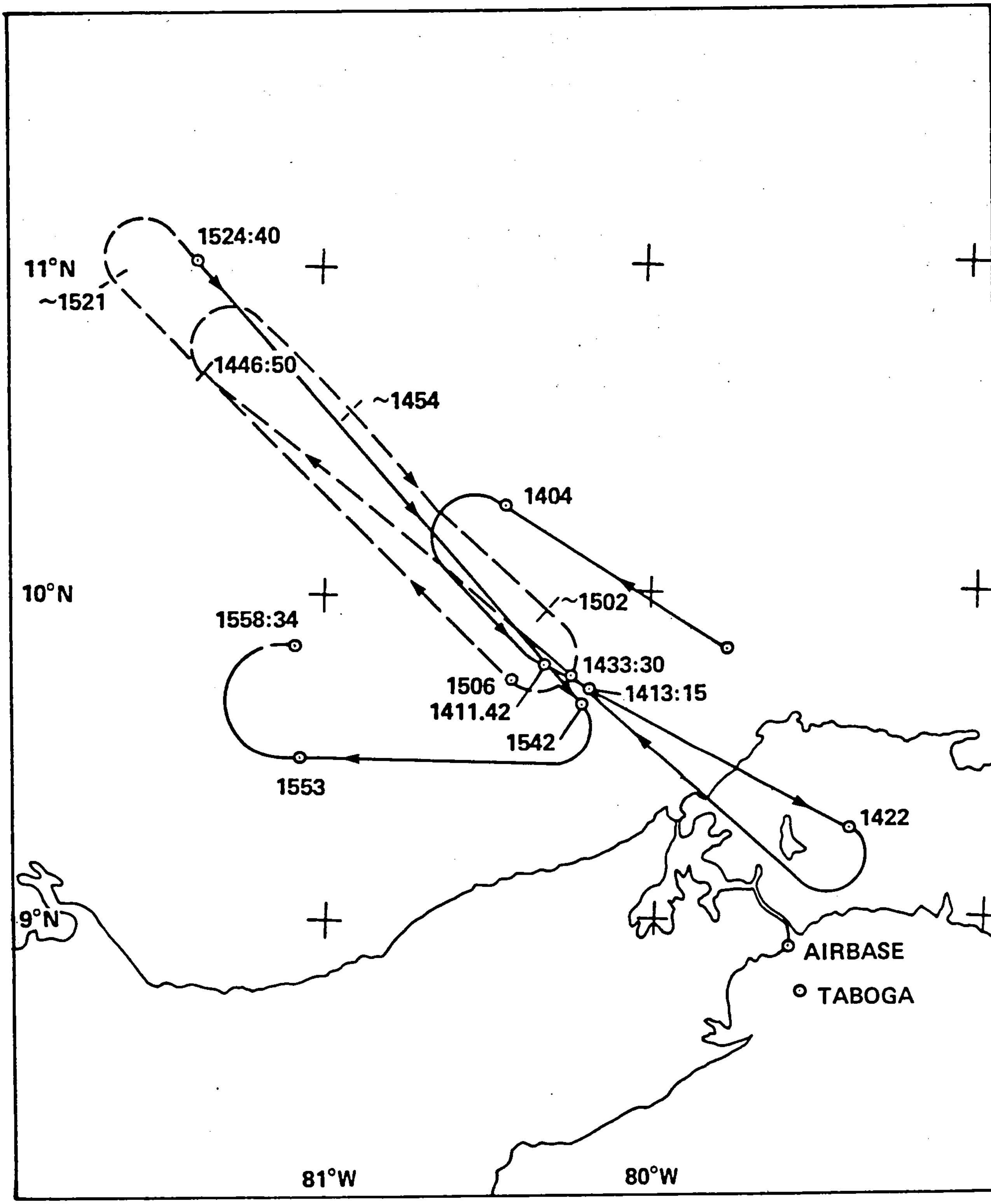

FLIGHT 5
[Pilot: Ivor Webster]

Flight Log: 9 September 1980

Altitude, 1000 ft	Universal time	Event
0	1322:44	AGC sw off
	1324:05	AGC stdby
	1324:23	Left tank aft sw stdby
	1324:36	Left tank fwd sw stdby
	1324:46	Right tank fwd sw on
	1330	Takeoff
54	1348:08	AGC sw on, T = -56°C
57.5	--	347°/56, heading 302°, T = -50°C
	1358	337°/55, minor turbulence over cell
55.5	1400:45	APS No. 1 open, T = 049°C
	1404	Climbing turn to left, 326°/096
59.5	1407	Level, heading 138°, T = -41°C
	1410	Left turn to heading 116°
	1413:15	Passed over cell at 321°/60
	1416:24	Pitot heat off
	1422	Climbing right turn at 026°/25
62	1425:30	Level, heading 310°, T = -41°C
	1433:30	Passed over cell at 320°/64
	1436:50	Left turn to heading 290°
	1440	Tacan station failure
	1440:25	Climb on heading 290°
64	1442:43	Level at 315° bearing from Taboga
		Note: Taboga is 170°/8 from Howard
	1446:50	Right turn, estimate 155 miles from Howard on 133° heading
	1454	Right turn to 138° heading
	--	Left turn to 128° heading
	1502	Estimate 75 miles from Howard
	1503	Climbing right turn
	1506	296° (316°)/77 from (Taboga), heading 325°
66	1508:30	Level, 325° heading, T = -38°C
	1516	APS No. 2 open, T = -38°C
	1521	Climbing right turn, 181 miles from Taboga
	1524:40	135° heading, 320°/174 from (Taboga) (at 67K, T = -038°C)
68.4	1531	Level, T = -33°C
	1542	Descending right turn, 318°/59, 280° heading
	1544	Pitot heat on
52	1553	290°/95, T = -56°C
		APS No. 3 open, T = -53°C
	1554	--/56
	1555	Right turn, 155° heading?
53.5	1557	Passed near cell
57-58	--	Climbed to check descent area
	1603-5	Started descent
	1611:33	AGC sw to stdby
	--	Landed

Altitude, 1000 ft	Universal time	Event
	1636:16	Left tank aft sw off
	1636:20	Left tank fwd sw off
	1636:39	Right tank fwd sw off

Pilot Commentary

Takeoff 1330 UT, climbed out to the SW, could see cluster at 8° N, 79° W. Could see it when underneath cirrus. Entered cirrus at 35K ft, top seemed to be at 48K ft. After breaking through top could see nothing in the direction of that thunderstorm. The cluster that was high early in the morning was not above 48K. Climbed some more, to about 54K and (8 min after takeoff), could see nothing to the east, turned to left, saw at ~100 mile range to NW cells coming. Headed to NW and saw single cell coming up through cirrus and starting to develop and ~5 miles to SW another cell emerging. There was nothing in NE quadrant. At about 3/4 of the flight I could see nothing to the NE. Then about the last quarter I could see what appeared to be a flattened top above the cirrus deck which could have been an anvil but quite a long way away and too far to investigate. First run to the NW on heading 347° was made at 57.5K ft, at about 56 miles from Howard. The cluster to NW was about at 10° N and a little over 81° W. Noted position on flight tape. As approached first cell it had developed to its maximum and already begun to collapse. The rapidity with which they built up and then spread out a little bit and then just collapsed over a period of about no more than 10 min was noticeable. "Extraordinary" was the speed with which they seemed to collapse. At 1358 UT, on bearing 337/055 miles and 57.5K ft, had minor turbulence, as noted on flight log. Hard to judge size of cells since when over them and looking down from above can't tell where the boundaries are. Estimated height of cells at about 54K ft by noting speed at which I was apparently passing overhead. Turned around and climbed to 59.5K ft and aimed for the same bunch of cells on heading 138°. There appeared to be about three, the one dying and . . . Turned left to 116°, at 1413:15 UT, believed I was over target I was aiming for at 321°/60. Continued for quite a long way past the cells to run a full 15 min. Turned right and climbed to 62K. Heading was 310° in level flight. At 1433:30 UT was at 320°/64 when over the buildup again, which had seemed to spread out more. Turned to left to 290° heading and started climbing, saw cell farther out. At 1440 UT started climbing, reached 64K ft at 1442 UT at 215° bearing from Taboga (which is located 10 miles to south of Howard and is a different navigational aid) guessed distance at 155 n. mi. when made turn to right at 1446:50 UT. Headed 133°. At 1454 changed to 138°. At 1502 UT, estimated position as 75 n. mi. from Howard, based on flight time from last known position. At 1503 UT level flight at 66K ft, heading 325°. At this time, all cell action seemed to have gone, no cells were appearing. At 1521 UT turned right around and climbed (was 181 n. mi. from Taboga). Was at 68.4K ft at 1531 UT in level flight. Except for earlier turbulence event noted, only very minor turbulence noted at other altitudes. May have mentioned on flight tape. At 1542 UT location was 318°/59 from Howard. Made turn to right and started descent to do another run at a lower level. At 1553 UT location 290°/95 from Howard, turned right. At 1557 UT climbed to 53.5K ft and headed for two buildups (cells) I could see. I was at 52K ft when I saw them but felt they were above me so climbed to 53.5K ft. Passed by the first one on right at distance of ~1/2 mile about or just below its top. Believe I indicated time on flight tape when I went by. Second cell was about (or 6 to 10 miles) 5 miles farther along to my left. I passed to the right of the second by about 1/2 mile at about level with its top. Cirrus deck was about 4000 ft below. Continued toward Howard, climbing above cirrus deck. Went to about 57-58K ft to get another look, until about 1603 UT to 1605 UT, before beginning descent. Can't remember when I went by cells,

could have been 1557 UT. Cirrus deck today was pretty complete, to the north solid, to the west at one time could see down (very hazy, but could see the sea). The different thing about today's flight was the speed of cell formation and decay; they would spread out, have sort of a flattish top; not much, still a few bumps in it. After that they would die and disappear into cirrus in 10 to 15 min.

Flight Tape Transcript

1335:22 [1335:24] I'm climbing out through 34K ft on a heading of 110° and I'm just entering some cirrus and I think a storm is developing to the southeast of me. [1336:49] In the cirrus; I'm climbing through 39K ft; just a little bit of turbulence, not much. The tops of that cirrus were 48K ft [1339:50], I'm now at 50K ft, I can't see anything to the southeast of me where that thunderstorm was that I could see below the cirrus when I was climbing. I don't see anything on top of the cirrus. . . . . to the northwest and I don't know how far away it is, I guess about 100 miles [1343:04], I'm heading in that direction. My present position; on the 90° radial [1343:13] at 49 miles from Howard, turning to the northwest to head for it. I guess it's about 100 miles away. I can see it punching up through the cirrus and not very high above it and what appeared to be a nice cell developing [1344:51]; it stopped to split up and flatten. Time 1347:05 [1347:09] and I'm heading on a course of 314°. I see a buildup to the northwest and there's now another cell that seems to be developing and I'll head towards that [1347:26]. It appears to be just a thin layer of cirrus, a very thin layer, higher than the main cirrus tops. I don't know how much distance there is between them, and I don't know whether it's associated with that bumper or not [1347:51]. The one I saw to the northwest of me subsided, but to the southwest of that one another is developing [1350:35]. It looks quite promising. They seem to be rising so rapidly. [1351:28] The one's completely collapsed now. Coming over the top of that one I spoke about which had topped that . . . It's just beginning to collapse. I guess those tops are not much more than [1358:27] 2000 ft below me at that. I'm 57.5K ft descending now to 57K ft [1358:34]. Not much turbulence [1358:52]. Second run now and I'm heading 138°, time is 1409:16 [1409:20] and I'm at 59.5K ft, temperature -41°C. The one I was hoping for not very far away now, about 10 miles, is collapsing a little bit, but there's one just off to my left now about 10° off to my left and really punching up and I'll go after that one [1409:46]. . . . [1411:25] right here appears to be the only ones which I can see in the whole sky. My present position is 318° radial [1411:42] from Howard, 68 n. mi. Very minor turbulence, not much. Just climbed up to 60K ft [1412:05], 59.5K ft [1412:19] and the tops are about 4000 ft below me [1413:04]. Looked down [1417:47] at the AGC panel and saw a light flash and it was the one which is labeled MECH. 1419:00 [1419:06] I'm continuing on a heading of 116° just to complete the 15 min. Since I left that thunderstorm area there's been no sign of any activity below me at all. I'm just completing the 15-min run [1419:27]. 62K ft on my third run and time is 1429:15 [1429:18] and I'm heading towards one other buildup, but it's collapsing right now, by the look of it. They just pop up and not many minutes later, collapse again. I don't know whether I'm going back over the same one I did on the second run [1429:46]. The fourth run I stayed on the same heading of 290° because there's one ahead of me, I don't know how far out it is, I'm guessing about 140 miles [1443:31] from base. My TACAN has just failed, so it's not giving me any information [1443:37]. Climbed to 64K ft and I'm just about over that one I saw, it doesn't look, well, I guess it's collapsing again [1443:51]. Shortly I'll turn around and try and come back along the most obvious thunderstorms. I'm still staying at the same altitude of 64K ft [1446:46]. Turned inbound, heading 132° [1450:32]; this is a continuance of my fourth run and I should pass over three of them eventually. The first one is dissipating [1450:54]; the

second one farther along the line; I don't know what that's doing and the far distant one is pumping up right now; I guess it'll collapse by the time I get to it [1451:08]. Time is 1515:30, I'm on the heading of 325° [1515:36] at 66K ft and all the action seems to have disappeared. No more thunder bumpers punching up through at all. Maybe a little one over to my right there, but just a perfectly even undercast. It looks pretty even from a distance [1515:59]. Got a lift there, put me up to little over 68K ft [1529:28]; I've been struggling to get above 67K ft. I'm at 68.4K ft [1545:00] and substantially nothing to report and I'm going to descend back down at this time and see if I can fly level at 52K ft. I'm on a heading of due west; I'm on the 300° radial at 51 miles out of Howard and to the west of me one has punched up but it doesn't look anything really spectacular [1546:03]. . . . 53K ft, I've just turned back to a heading of 090° [1558:34] about 105 miles out on about the 300° radial and this one that I passed over, I thought was building, it's up to my level right now, at 53K ft [1558:51], I'd say it was 53.5K ft [1559:21]. I'm at 53.5K ft and I'd say the one on my left is at 53.5K ft; just passing it now, no turbulence [1600:23] . . . I'm heading for home; I'll have to go a bit south to avoid these cumulus before I begin my descent.

FLIGHT 6: 11 SEPTEMBER 1980

(Pilot: Ron Williams)

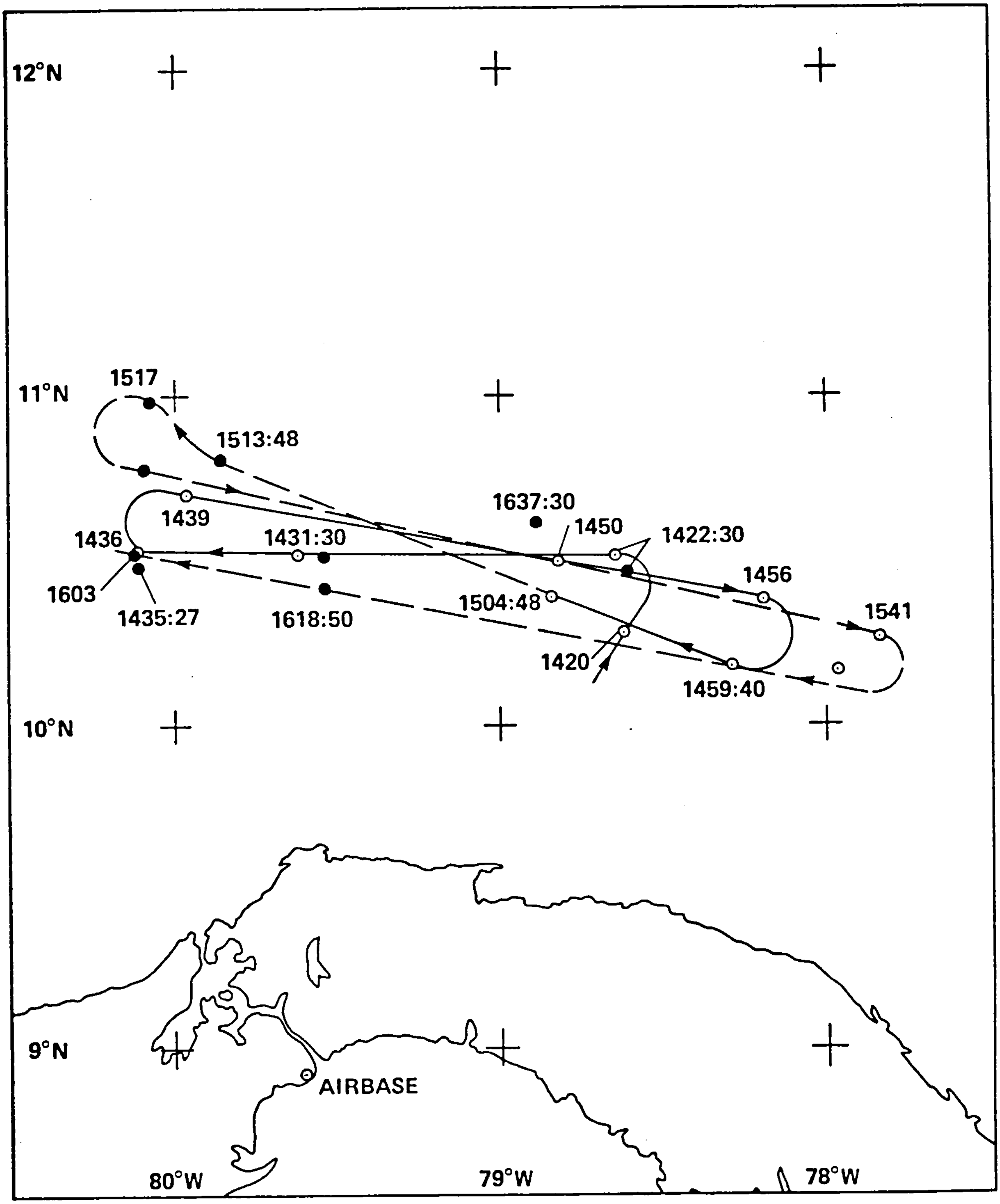

FLIGHT 6
[Pilot: Ron Williams]

Flight Log: 11 September 1980

Altitude, 1000 ft	Universal time	Event
0	--	Verify INS and H_2O Rad sw on
	1354	AGC sw off
	1355:15	AGC sw to stdby
	--	Verify INS and H_2O Rad sw on
	1356:15	Left tank fwd sw stdby
	1356:30	Left tank aft sw stdby
	1356:45	Right tank fwd sw on, verify aft sw off
0	1401	Takeoff
57	1415	Level
	1415:15	Pitot heat off
	1415:30	AGC sw to on
	--	Descend
55.5	--	Level
	--	Passed over cell
	1435	Started climbing turn
58	1439:20	Level
	1450:26	APS No. 1 opened for 1 min, T = -50°C
	1456	Started climbing turn
61	1501:30	Level
	1503	APS No. 2 opened for 1 min, T = -43°C
	1517	Started climbing turn, 345°/127
	--	End of turn, 343°/115, heading roughly E-W
64	1521:30	Level
	1535	Opened APS No. 3 for 1 min, T = -39°C
	1538	Pitot heat off?
	1541	Started climbing turn, 050°/132
	--	Ended turn, 050°/122
67	1547:36	Level
	1603	Started descent, 340°/101
	1609:03	Pitot heat on
	~1624	Level flight in cirrus
	1649:04	AGC on stdby
	--	Start descent
	~1725	Landing
	1728:43	Left tank fwd sw off
	1728:55	Left tank aft sw off
	1729:09	Right tank off

Pilot Commentary

Takeoff was at 1400 UT, climbed out to 59K so I could look around, could see thunderstorms to NE, as predicted. Approached the area and descended to 55.5K ft since I thought cell tops were at 52-54K ft. I probably passed about 1000 ft over the top. The cell had been there since I originally passed through 56K ft or so on the original climb. It was a little over 100-110 miles out (from Howard). When passing over the cell, I hit moderate to heavy turbulence. Passed over at less than

2000 ft clearance. Ran for a total of 15 min at 55.5K ft substantially past the cell and then turned back, climbing to 58K ft. Could see the cell still growing. Then saw a thin puff of cirrus emitted from the cell top (sort of a flowering), then the whole cell collapsed back into the cirrus deck, quite rapidly. Then it started to grow again as I approached it. It then completely collapsed again as I got there. I never saw it again. I ran the 58K ft and 61K ft run right over its location, back and forth. Second run over the cell was relatively smooth. At some altitudes light patches of turbulence occurred. Cirrus deck was somewhere near 54K (it was nearer 49K at end of flight); the high cirrus was thin. (Trope today was reported at 52K ft.) I swear cirrus was coming off the thunderhead, sort of blow-off. Continued surveying over general area in N-W direction all the way up to 67K ft. Afterwards I descended to cirrus deck . . . it fooled me; it looked like a heavy cirrus deck. I descended down into it, and all it was was thin layers of cirrus, just multiple layers of cirrus, so thin I could not tell when I was in it. I could not see it going by the canopy. I was in it but I wasn't. View forward and sideways is nothing but white, all around. Could not see horizon. In the layer about 1/2 hr. Could see blue sky above, some places could see ocean below. Went as low as 42 to 43K ft to try to get into heavy cirrus. Cirrus run was still in same area as high altitude runs. INS failed during latter part of flight and I wrote down Tacan positions on flight log. Failure noted on flight tape. After cirrus run, started descent to Howard. Interesting feature during mission was rapid collapse of thunderhead (cell). It was 3000 to 4000 ft above cirrus as I approached, and in ~3 min it was completely merged with the cirrus deck. The cirrus was higher at beginning of flight. I forgot to mention, as I turned around to approach the cell for the second pass, there was a "cirrus" cap over it [lenticular cloud], a thin curved layer over the top perhaps separated from the top of the cell by ~1000 ft (or less). Like a mountain wave. As soon as the cell starts building, the "cap" just disappears, just evaporates from sight. I've seen lenticular clouds before but they are not common. Seen before over tops of thunderheads. It's a short-lived thing. Also, when tower (cell) collapsed, I swear I saw blow-off from the top out to the south, but too thin to be sure.

Flight Tape Transcript

There are several buildups I can see, a buildup that's up around 50K-52K [1416:17] in my 11 o'clock position about, oh, 20 miles, and there's one out almost 12 o'clock, I can't tell the distance. It looks like it's coming up above the cirrus. [1416:35]. . . . 192 when I'll descend back down to that altitude it is just above. I'll stay up here awhile, look around and see which one's the best [1416:48]. It's looking like it's building here. . . . about 030° radial [1422:35], 110 miles from Howard and I'm descending but it's getting a little rough. See what the top looks like. It's about, oh, 54K ft. I'm at about 57K ft. It's getting kind of rough here. I'm descending on down to see what it looks like [1422:55]. There's a little cirrus in the area around 55K ft [1423:01] . . . up but I'm turning the pitot heat on at 1423:34 [1423:36]. About 55.5K ft [1424:15] at 1424:10. I'm kind of busy flying the airplane. I didn't have time to write anything down! . . . event marker [1424:42] just a little past the top of the thunderstorm. I didn't get it right over the top. I'm estimating about 2000 ft above the cloud top and I'm in moderate to heavy turbulence. Okay, it's starting to smooth out here [1425:00]. The top of the highest thunderstorm seems to be about 53K-54K ft. I'm at 55.5K ft [1425:22] and there's a cirrus . . . that I'm not quite in, so it's right at the top of the highest storm, must be down around 54K ft also. [1426:17] About 255° (265°). . . . down a ways and I'll just guess I can turn around that buildup about 15 min if I . . . down at 55K ft [1426:34]. Seems to be very good and I'm right over the thunderstorm . . . to pass it at about 5 or 10 miles. It seemed to smooth out a little [1428:16]. I'm quite a ways

past it now and I'm picking up turbulence again. All I can see underneath one now is just cirrus. . . . By the time I get down to 55K ft, I'll run out here till about 1440. I got to leave plenty of time to turn around, then go back to that thunderstorm; see if it's grown any [1429:05]. . . . to, oh, 58K ft [1429:13]. [1431:27] 360° radial from Howard, 95 miles. Still on the 275° (?) radial [1431:31] at 55.5K ft and I'm just on the edge of the heavy cirrus. To the west is scattered light cirrus and there are small buildups on a lot of them. I'm going to turn at 1435, climb to 58K ft and go back. On the 340° radial, approximately 98 miles from Howard [1435:26]. I can see the thunderstorm I just went over. It is above the trope. It looks like it's going to start dissipating though; it's got that thin cirrus coming out of the top now [1436:43]. . . . I'm heading back for that thunderstorm now. It's quite a ways away from me. Maybe I came out too far on the 55.5K ft pass [1438:47]. I'll be level here at 58.7K ft. But it's starting to grow again. The bubble's gone up. There's . . . it's got . . . I don't know how to describe it. It looks like thin cirrus layers right above it and off to the side of it but it's starting to grow up through that cirrus layer it's producing [1439:09]. . . . 1439:20. Okay, that thunderstorm ahead . . . was building up. All of a sudden that bubble that was building up collapsed again. Let's see what happens as I approach it [1440:40]. It left a small band of cirrus there. That's what it looks like. That's the best way I can describe it [1441:18]. All right, at the top it's building up [1441:39] and the only one I can see is the one I'm heading towards. I don't see any buildups above the cirrus except that one and right now it's collapsing [1441:51] right back down into the cirrus. Starting the other leg. I'm almost right over the top of the thunderstorm. I'll carry this one out for more than [1442:45] 15 min just to get a sample on the other side at 58K ft and I hope it's not as rough at 58K ft as it was at 55K ft. That thunderstorm that was way up above the cirrus — right now, I'd say it collapsed back down into the cirrus and I can't really even distinguish it now [1443:15]. The cirrus that it produced is blowing off to the south, southwest. I can see it right now but it's so thin [1444:00] that when I get up to it I probably won't be able to see it. I'm guessing the cirrus blow-off is at about 55K ft. . . . event marker [1449:47] on INS, the thunderstorm position. It's collapsed back into the cirrus and I really can't tell for sure. [1450:01] 10°29.7' N, 78°48.2' W. [1451:04] On this overpass there was no turbulence or very light if any. I'm going east of that thunderstorm. Heavy cirrus below me and I'm getting a little light [1453:07] turbulence, I can't see anything but this heavy cirrus in all directions right now. The plane is acting as though there must be a few buildups embedded in the cirrus below [1453:47] because the airplane is going up and down a little. I get touches of light turbulence here and there. I can't see any buildups below me [1454:01]. Can't see anything [1454:37]. I'll stop this leg in exactly 15 min and turn around, go back to the thunderstorm area. I could tell that the buildup is still there but it's now below the cirrus layer, or whether it may be just the flat top of the thunderstorm, I don't know. I'm at 61.5K ft but gradually going down. I'm getting a little uplift, very light though. This was about the position of the thunderstorm as best as I can tell. . . . is 101 on the INS with the warning light on; I'll turn it off. Ten degree [350°?] radial [1513:48], 114 n. mi. from Howard. I must be getting some temperature changes . . . autopilot engaged in Mach hold . . . airplane is going up and down about 500 ft. Not much below me right now. A little while back I left the edge of the cirrus and it's — scattered cirrus below me and a few down on the water [1514:37]. I'm level [1521:49] at 64K ft. Heading right towards last known position of that thunderstorm. At this distance I probably see where it's at but it's still embedded in the cirrus. Doesn't look like it's going to grow up again [1522:12]. . . . degree radial from Howard at about 115 miles [1522:30]. Keep running these altitudes up to 67K ft. I can't see any . . . storm . . . right underneath the edge here [1523:14]. I'm trying to hold altitude [1523:48] but it's kind

of hard. I see no buildups popping through the cirrus layer. Right on the edge here I can see a thunderstorm right underneath the cirrus at about my 11 o'clock position 50-75 miles away [1524:37] but it's way below the cirrus. I guess about 30K-35K ft. . . . this leg out a little more [1538:12] than 15 min. . . . cirrus deck and that thunderstorm never did pop up again. [1550:21], 150 miles south there's one that's going up to about 55K-57K ft, and that's about it. . . . cirrus layer [1618:44] at 16K to 18K ft. On [1618:50] 360° radial, 90 miles from Howard. Once you get down in the cirrus layer, it isn't one solid cirrus layer; it's several layers, the top one which I'm below, I couldn't even tell [1619:03] when I came through it. It's very, very thin. But now that I'm down below it, I can see it. And the second layer [1619:11] which I'm just skimming the top of, I'm not sure it's cirrus, it might be, well yes, I can see through it some places. I'm right down at 45.3K ft. I'll stay in here for a while [1619:37]. I'd like to get that higher layer but there's no way I can tell when I'm in it. Must be up around, oh, 53K, 52K ft, maybe 51K ft. I really can't tell exactly when I . . . Must be in it now. I'm getting some rough air here [1620:46]. I'm atop now [1621:18]. It's a little rough but not bad. I'm really not in any heavy stuff. It's even kind of hard to tell that I'm in it. There's some stuff way up there but it's so thin that there's no way I could tell when I'm in it. I probably passed through it coming down. [1621:43]. I'm at 43.5K ft [1621:50] . . . several [1623:59] thin layers at different altitudes, scattered layers. At each altitude, I go in and out of them and they're very thin. When you put them together, they're pretty thick. . . . 3000 now [1624:17], and 43.3K ft. At 43K ft [1635:09] I'm climbing up higher, see if I can get in this cirrus at a little higher altitude. I'm at 49K ft [1637:13], very thin layer of cirrus. It's going to be hard for me to stay in it. On the 020° [1637:30] radial at 110 n. mi. 49K ft deck [1644:18], low turbulence in it. Also can see a little thin layer of cirrus above this too.

FLIGHT 7: 12 SEPTEMBER 1980

(Pilot: Jerry Hoyt)

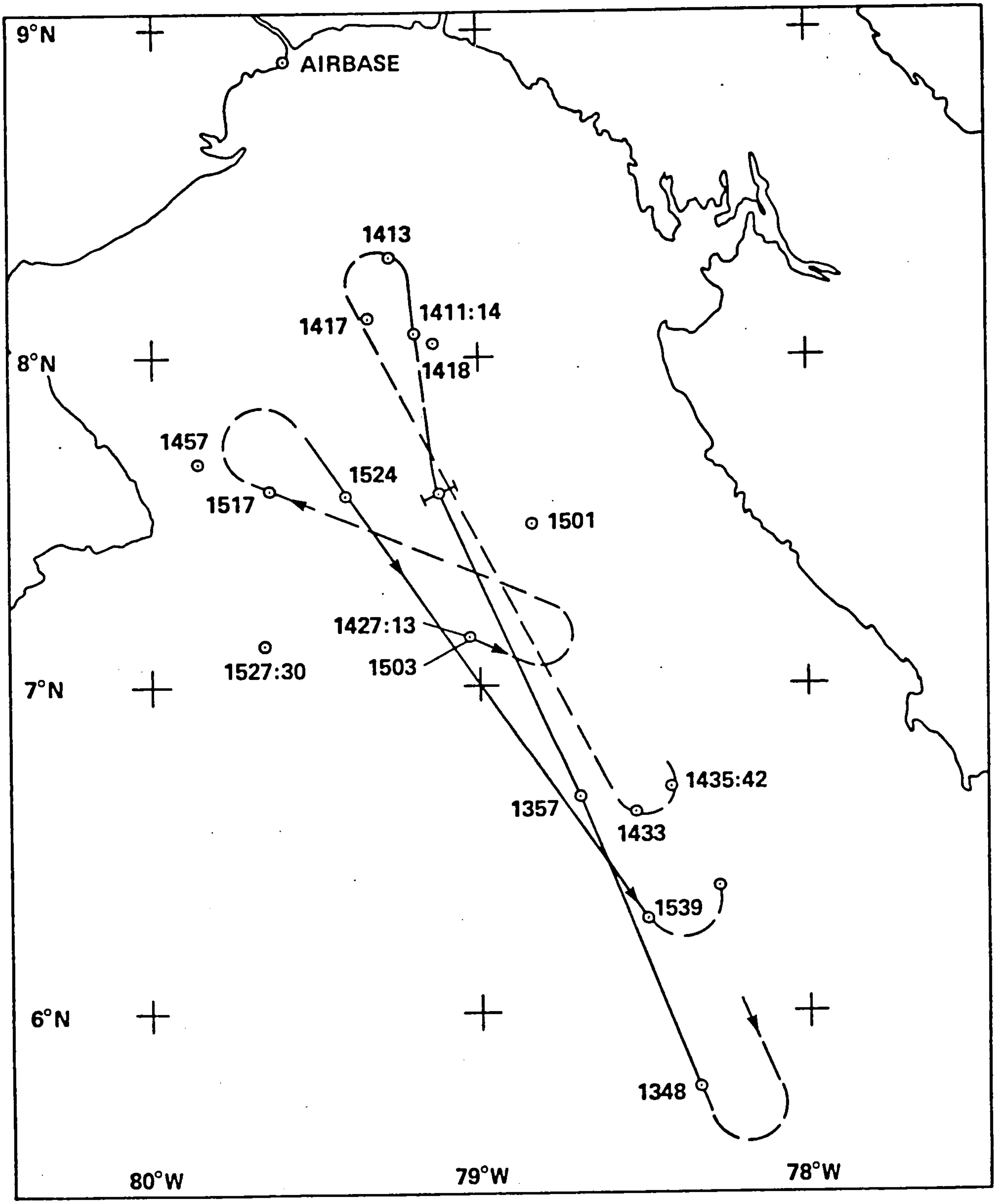

FLIGHT 7
[Pilot: Jerry Hoyt]

Flight Log: 12 September 1980

Altitude, 1000 ft	Universal time	Event
0	1256:25	AGC to stdby
	--	Verify INS and H_2O Rad sw on
	1256:53	Left tank aft sw stdby
	1257:08	Left tank fwd sw stdby
	1257:25	Right tank fwd sw on
	1257:25	Right tank aft sw off
0	1303	Takeoff
--	1313:39	AGC sw to run
49	1314	Pass through 49K ft, heading 120°-130°
51.5	--	T = -53°C
52.5	--	T = -53°C
53.5	--	T = -53°C
54.5	--	T = -57°C
55.5	--	T = -60°C Slow climb from 49K to 59.4K ft
55.8	--	T = -52°C
56.5	--	T = -52°C
57.6	--	T = -47°C
58.6	--	T = -43°C
59.4	--	T = -43°C
	1343	Begin descending right turn
54.5	1348	Level, 156°/203, heading 300°
	--	Passed by cumulonimbus tower to right, 156°-160°/84
	--	Passed by second tower to the right
55.5	1411:14	Opened APS No. 1, T = -60°C, 152°/55, in clear sky
	1413	Climbing left turn, 150°/40, heading 330°
58	1417	Level, 160°/49, heading 150°
	1423	Cell started to sink
	1427	Abeam cell, 160°/110
	1433	Climbing left turn, 153°/151
61	1436	Level, 150°/150, heading 300°
	--	Passed over old cell
	1454	Descending right turn
55	1457	Level, 190°/75
54	1503	160°/110, passed by tower, in anvil, heading 110°
	1514	Started climb, heading NW
59	1517:02	Opened APS No. 2, T = -43°C, 180°/78
62	1521	Opened APS No. 3, T = -40°C, during climb
64	1524	Level, 170°/080, heading 120°
	1539	Climbing left turn, 155°/170, T = -36°C
68	1543	Level
	1553	Started letdown, 180°/120
	1553:35	AGC to stdby
0	1620	Landing
	1625:07	Left tank aft sw off

Altitude, 1000 ft	Universal time	Event
	1625:08	Left tank fwd sw off
	1625:19	Right tank?

Pilot Commentary

Takeoff at 1303 UT. Climbed out to north, flew down to the SE over the Gulf to the area agreed upon. On the way I climbed slowly from about 48K ft to 59K ft as requested. Heading was about 120°-130°. Recorded indicated temperatures along the way. Finished climb at 1343 UT and began descending right (left) turn, position 156°/203. Arrived at 55.5K ft at 1348 UT. Things got very exciting. I saw a tower with a flower-like burst (like Chunky Webster described before). Tower seemed to be at 55-56K ft, whereas main cirrus deck was at 49-50K ft. Then tower (cell) sank back down to below 54K ft. The flower structure seemed to remain behind. Let me draw a picture. The cirrus deck is at 49-50K ft. A turret forms to 55-56K ft, round with structure. Looks turbulent. I was coming back from the south heading about 330°. As I watched the tower build, the flower formed and went puff. The flower formation was on the east (right) side of the top and went up above the top by perhaps 500 to 1000 ft. Took about 1 min. Time of event was recorded on flight tape. I passed to the right of the tower at 55K ft (54.5K ft) approximately 1/2 to 3/4 of a mile to the right. Slight turbulence was noted. Never felt moderate or severe turbulence during whole flight. Continued on till 1413 UT. Made climbing left turn to 58K ft and returned on heading of 150°. Estimated position of tower was 156°/84 to 160°/84. There was a group of about five cells in this area. The one I flew near appeared highest. Cells were distributed in a disorganized line and I was pretty much passing over center of cluster. The one I passed over was near SE edge of cluster. The line of cells was oriented SE-NW. The second pass lasted till 1433 UT. I did a climbing left turn and started another run at 1436 UT, at 61K ft, on heading of 300°. Descended to 55K ft reaching 55K ft at 1457 UT. I went back to 55K ft because I saw a tower starting to build that looked like it was going to be a pretty good one. I was at 190°/75. Heading is toward the south and more southerly than before. The new cell location was estimated at 160°/110. I flew directly toward cell. I was worried about passing through my wake but I lost track of previous route. The tower built from cirrus deck to maximum height in 10 to 15 min. When I was 3 to 10 miles away, the tower started to collapse. No flower structure. Sort of mushed down. When I was about 3 miles away (or 1 mile away) I saw 10 to 15 quick, vapor-like flashes (not lightning) close over the top, lasting perhaps for 1/2 sec each. The aircraft was at the same level of the cloud top at 55K ft. What I saw was hard to describe, like a flash of vapor over the wing of an aircraft passing through a humid area when at high angle of attack. I estimate the tower to be 1.5 miles in diameter and each vapor flash seemed to cover not more than a third of the top. The flashes were real close to the cloud top, maybe 100 to 200 ft, hard to judge. Whole process took about 1/2 to maybe 2 min. I passed the tower and couldn't see any more flashes. I was moving to the NW when all this was occurring. Passed by tower at about 1503 UT. Started climb at 1514 UT, still heading NW (SE)? Continued climbing to 62K where I took APS No. 3. Got to 64K ft at 1524 UT and after turn to heading of 120°. Headed back toward cluster. No, I'm confused about the sequence of events. I drove through the cloud earlier in the flight. The tower started to form a streamer or an anvil; after tower collapsed, it left behind a turret with a flat top, like an anvil. Cloud had smooth sides and no evidence of turbulence. Cloud seemed thinner. This change occurred while I was moving away and I couldn't describe details of changes. Seemed to be changing with wind effects, pushing anvil top to west, western

edge was longer side. Anvil top was about 55K-56K high, cirrus still at 49-50K, bottom of anvil about 53.5K-54K. I leveled at about 54.5K ft and flew right through anvil about 1 mile out from original turret. I didn't write anything down, but commented on flight tape. [Comment from Knollenberg: Evidence of cloud passage about 2 hr 5 min into flight, 1502 UT.] Felt light turbulence. Cloud was fairly thick, couldn't see horizon. Was in cloud maybe 1 min. I believe a sketch of the top view of the cloud would show a tower about 1-1/2 miles in diameter, an anvil about 2 miles by 10 miles, with long axis E-W, the west side longer. I flew through west side, turned around (to left) and about 8 min later flew through east side only about 1/2 mile from cloud stem. Now traveling to north. Couldn't see horizon during east pass either. Altitude varied a bit but about 54.5K ft. [Comment from Knollenberg: Particles as large as 1 mm observed during this period.] With the new time the flashes I saw must have occurred during an earlier pass. During later part of flight I passed over tower at 64K ft. Flight at 68K ft was not over cluster. Heading was toward north. Landed about 1620 UT. [Jerry listened to part of flight tape.] At 1426 UT, abeam of cell at 58K ft. Cirrus deck was 46K near Howard and 49K-50K out where cluster was located.

Flight Tape Transcript

1302:00. Altitude 35K ft, thunder showers to the southeast, several layers of cirrus blow-off ahead. At 36K ft, looks like I'm going to be above it pretty quick. The tops are right around 45-46K [1312:31]. Definitely [1314:44] on top about 49K ft and I'm starting my slow climb, 300 ft/min. The storm cells [1315:39] are building on top of the cirrus, I'm at 50K ft and it looks like it's probably down around 42K or 43K . . . sticking up more than 500 ft above the cirrus [1315:57]. At 51.5K ft, -53°C. About [1319:26] 6 to 10 miles out from the tower that's building, it's up to about 46K ft now [1319:50]. Light turbulence now and estimating about 2 to 3 miles out, and passing about a quarter of a mile to the right of it [1322:30]. Turbulence. . . . Builds up to about 51K ft or so [1322:46]. Back in this area there are several more cells that are sort of popping up but there doesn't seem to be any that are really punching up with a high amount of energy [1323:48]. -53°C at 53.5K ft [1324:21]. Turbulence only lasted on the north side of the buildup; on the south side, it's clear, although I felt like I was getting about 500 ft/min lift on the back side for a very brief moment [1324:36]. Farther to the south now, on the 156° radial [1325:09], 103 miles and for the next 20 or 30 miles will be some light cirrus, it's definitely higher than I am now; up to 55 to 57K ft. Present altitude 54K ft. Temperature -57°C [1326:21], at 54.5K ft. I'm in [1326:40] the cirrus now, but it's very thin and I can't really distinguish it for sure. Sometime within the next 4 min though [1326:49], I will have passed through it. More, choppier turbulence now, I'd say light. I'm at 55K ft [1328:42], -60°C. Some of the cirrus appears to be at [1329:27] my altitude but I'm not on top, definitely, but I'm not in anything either. It's difficult to tell where you are. In a couple of hundred feet I've had a temperature change of [1330:24] perhaps 6°, and I'm descending slightly now; we should be climbing here momentarily [1330:31]. Missed another little tower here [1330:44]. Passing a couple more towers [1332:19], I'm at 56K ft, 56.5K ft and I'd estimate it at about 54K or 53K ft. Going past the last of the bumpers to the south [1334:24]; however, I'm continuing on. Heading 120°. Temperature at 57.6K ft is -47°C [1335:29]. . . . turn at 1343 back around and descending to about 54K ft, one of the bumpers had a flower [1345:59] that came out and rose about 2000 ft above the cloud top and now is busting up and it's starting to spread out and the whole thing appears [1346:15] to be collapsing back into the cirrus. It was probably up about 5000 ft above the main cirrus deck which is around 49K or 50K ft. I'm passing through 56K ft [1346:31], and it's going down pretty rapidly; however, the flower remains, seems to

be up at the level that the cloud tops actually went to. I'll attempt to fly over the collapsing form at about 54.5K ft [1347:10]. Now, it's dissipating [1347:39] quite rapidly; it too appears to be sinking, the whole cloud is down below me, I'm at 54.8K ft [1347:48]. The flower [1348:24] is rapidly sinking back into the remains of the area. It has depressed almost to the cirrus level at this time. I would estimate that I was 45-50 miles from the cloud when it actually decayed [1349:01]. There is some cirrus or cloud structure above the deck, I don't know how to describe it. It's just some rough clouds now but the flower portion itself is indistinguishable [1349:27]. Heading towards the same cloud that I passed over approximately [1349:52] 15 min ago. I'm getting light to moderate [1350:07] turbulence, one or two little bumps, it's not severe [1350:22] . . . Passing approximately 1 to 2 miles [1350:52] to the east of the main central portion of where the flower was. Steady at 54.6K ft and the turbulence has subsided [1351:12]. I'm 15 miles from the cloud and there are cirrus-like clouds above the cirrus layer through which the bumper protruded. The latter cloud now is just thinning out [1351:40] to cirrus and it looks like it'll just mesh [1352:09] in with the rest of the cirrus clouds here in a few moments. I descended [1352:45] slightly, wanted to stay down around 54.5K ft or so. At 54.5K ft the flower was definitely above my position. I'm estimating about 7 to 8 miles from the cloud itself and displaced [1353:06] to the east about 2 miles. The actual tops of the bubble portion itself are located 254 miles [1353:14] from Howard. I'm in kind of a little valley between clouds and the flower is about 500 to 1000 [1353:28] ft above me. The remains of the flower are spread out as a little area of cirrus right over the top of the cloud itself [1353:40]. Encountering light [1353:47] turbulence. I'm about 3 miles from [1353:55] the cloud and 1 to 2 miles to the side [1353:59]. I'm about 2 miles [1354:33] out and 1 mile to the side of the flower now and it looks like the flower was about 100 yd across [1354:53], and the cirrus has spread out to an area [1355:02] about, oh, about 2 miles wide [1355:15]. I am getting some severe temperature [1355:43] changes, and I'm a mile to the side of the flower. The temperature changed [1356:14] about 10° or so and I'm about 1 mile past now and due to moderate turbulence [1356:22], I will climb to 57K ft. Temperature [1356:40] -58°C, 145 n. mi. from Howard [1356:49] on the 156° radial. I am well past the cloud [1357:40] that I passed over and I can't see it anymore. I'm getting light-to-moderate turbulence [1357:51]. I'm flying through some very thin cirrus [1358:55]. Another thin layer is 500 to 1000 ft above me. I'll try to climb up into it; it's not too high above me [1359:15]. The next cloud [1359:35] that I'm heading for is definitely blow-off from the top of another tower. The main cirrus layer is 49K or 50K ft [1359:45], I'm at 54.5K ft and climbing. Up ahead is another bumper coming up and it appears to have a small lenticular cloud above it and it looks like it's definitely rising. I'll try to fly over or next to it. Temperature variations in this area are too much for the Mach hold (autopilot control). I'll try to remain level at 55.3K ft as I drive past this one to the right. The lenticular cloud is breaking up now. It doesn't have the nice, neat form that it had when I first saw it. I would estimate the top at 52K or 53K ft, and I'm passing about 1 mile to the west. Seems to be sinking back into the main cirrus deck but I don't see a flower cloud associated with it. All I saw was the lenticular cloud which now has disappeared. I'm in the clear now. I can't determine any cirrus above me except maybe a very, very thin layer that is the background that we've talked about. Climbing from 55K to 58K ft [1413:50] and making a left turn. Heading 150° [1417:59]. I can see the clouds again but I think there's a new set of bumpers that have protruded through the cirrus layer. I'll be [1418:17] driving past one within a mile or so. I'll give the range and bearing in a couple of minutes when I get closer. I'm about 20 or 30 miles out from it now [1418:29]. I'm coming up [1422:50] on what appears to be the highest one so far. I'm at 58K ft now. I would estimate the tops of the tower at 56.5K ft which is about 1000 ft above a minor cirrus layer at 53K ft [1423:30]. I'm probably 20 miles out from it right now and it appears to be starting

Page 361 Missing
From Original

Page 362 Missing From Original

FLIGHT 8: 13 SEPTEMBER 1980

(Pilot: Ivor Webster)

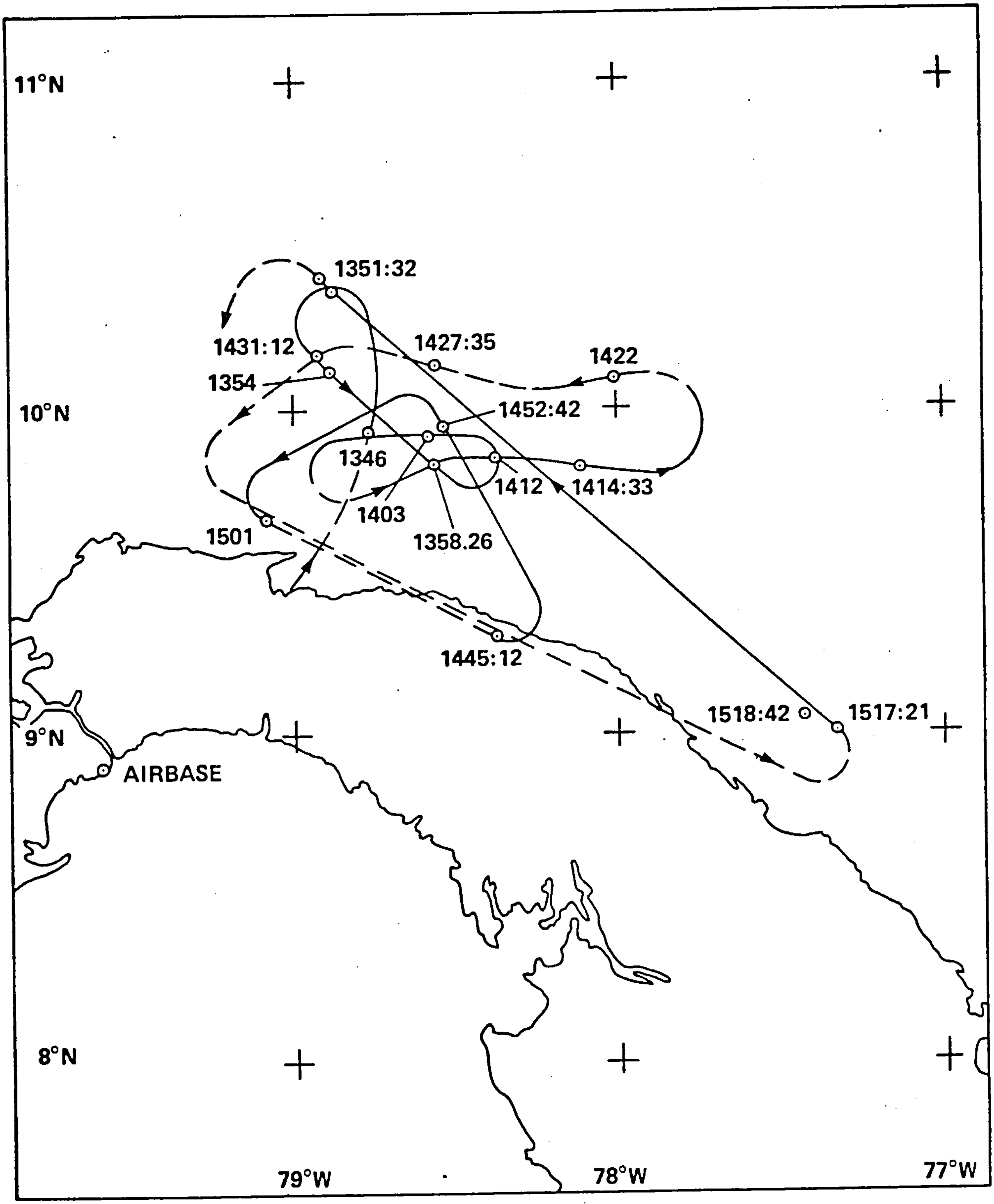

FLIGHT 8
[Pilot: Ivor Webster]

Flight Log: 13 September 1980

Altitude, 1000 ft	Universal time	Event
0	--	AGC to stdby
	1324:24	Left tank aft sw to stdby
	1324:36	Left tank fwd sw to stdby
	1324:49	Right tank fwd sw to on
	--	Right tank aft sw off
0	1330	Takeoff
49	1340:50	AGC to on, start 300 ft/min climb, heading NNE
~51	--	T = −55°C, bearing 042° from Howard
53	--	T = −51°C
55.8	1354	2 miles to right of mature cloud, 030°/83, 130° heading, T = −51°C
57.6	1358	Passing to right of 2-tier cloud, 048°/82, T = −50°C
58.8	1401:27	Circle to left around 2-tier cloud, on SE edge
57.5	1403	Pass over lower tier, heading 269°, estimate top of cloud 56K
	1405	Passed cloud, moderate turbulence
	1406	Left turn passed and around second tower, heading 270°
	1410	072° heading, moving away from second tower
55.5	1412:19	
54	1414	Pass to right of 55K high tower 2 miles, 058°/100, 072° heading
	1416:50	Turning to NE on E side
54	1419	Flower burst from old tower, 060°, T = −55°C
	1421:15	055°/120
52.5	1422	Heading 270°, T = −51°C, 053°/117
50.5	1424	Pass through cirrus layer above main deck, T = −55°C
	--	Turn to right?
50.7	1427	T = −56, −57°C
	1427:35	040°/95
52.5	1429:40	Pass through small cirrus, some turbulence, T = −55, −56°
	--	028°/85, heading 250°
54.5-55	1429-34	Passing through light anvil
	--	072°/76, turn to left, through 110° to north
54.5	1450:50	In light anvil, light to moderate turbulence
55.5	--	045°/88, passing over tower, 2000-3000 ft below
56.5	1455:40	Pass through light cirrus (streamer)
	1459:24	Climbing
	1501:02	034°/54, turning left through E
58.3	1503	Light turbulence, T = −41°C
52	1517:21	In streamer, 087°/135, T = −55°C

Altitude, 1000 ft	Universal time	Event
59.5	1533	T = -40°C
--	1536:26	Descending on NW heading, 97 miles Howard
54.5	1541	Pass through light vertical streamer (flower remnant?)
52	1546	APS No. 1, T = -55°C
56	1551	APS No. 3, T = -51°C
--	1553	Return to Base
	1559:37	AGC to stdby
	1630	Landing
	1631:20	Left tank fwd sw off
	1631:30	Right tank fwd sw off

Pilot Commentary

Takeoff at 1330 UT. Should have interesting data since I didn't do 15 min legs; I was in and around and about cloud structures. On climb-out after reaching 48K ft I held rate of climb at about 300 ft/min, till 58K ft. Coldest temperature seemed to be around 51K ft, about -55°C indicated on cockpit indicator. Later I hit -55°C at higher altitudes, as high as 54-55K ft. Saw buildups starting during climb-out to NNE, buildup ahead with thin cirrus coming off to WSW. Cirrus was also streaming off to NE or E. As I approached, cirrus layer could be seen above tower, well-defined layer, but extremely thin. On west side, multiple layers. To the right (east), another tower formed (punched up), saw small meniscus-shaped cloud, two small cirrus layers, well defined. Seemed to conform to top of cumulus. Not larger — maybe 1/2 miles across, few hundred feet above top. Things change quickly. Circled around tower (on east side) to left to north. Notes are not too complete. At 1358 UT to left and forward of me, heading 130°, 55K ft high, was interesting two-tiered cloud formation, lower tier with much broader base, definitely above cirrus deck, like a tiered wedding cake; the center higher portions had around its base a ring of cirrus like a band, very close about it. The structure seemed as if lower tier was shaped like doughnut, the center higher portion sticking upward through the center hole. Seemed to be a gap between them. On another occasion I saw a band of cirrus almost completely around the lower tier. Thin stratoform cloud, just like a band, or a ring. The lifetime of the two-tiered structure was only about 15 min. Changes were very rapid. Turbulence was mild during flight, sometimes moderate. Got light turbulence (30%-50% of time) when I flew through anvils or streamers. Didn't expect to get it. General cirrus deck was at 47K or so. During mission, seemed to get denser and I believe it increased in altitude too. On occasion saw thin cirrus-like streamers over locally curved portions of the deck. At 1403 UT, passed over lower tier and to right of upper tier of two-tiered cloud. Heading was 269°. Estimated top of center tier at 56K ft. Thought maybe structure was 2-3 miles in diameter, maybe a little smaller. At 1405 UT, on 265° heading, after passing cloud, saw new cell punching up just to SW of first two-tiered cloud. Got moderate turbulence between them. At 1406 UT, I turned to left around second tower. At 1410 UT, on easterly heading (072°), passed back by two-tiered structure. New tower was also beginning to show two-tier structure. It had very pronounced rings around base of upper tier. Didn't take very long for structure to form. At 1414 UT, 058°/100, to left, could see very, very thin sheets of cirrus forming over another buildup. Let's call this one No. 3 tower. Number 3 was to east of original tower (No. 1), thin sheets (two or three layers a few hundred feet apart) of cirrus that formed over top (very quickly); the lower sheet tended to follow the bumps of the top of the rising tower. Thereafter, I'm afraid I didn't keep good records. At 1419 UT, saw flower-like burst from tower top SW of aircraft about 25 miles away (I call it a

Prince of Wales feathers). Perhaps 700 ft tall, maybe more. Don't know what tower it came from, may have been No. 2. Think I was heading west at this time. Aircraft was at 54K ft. Since I was circling around, and didn't record positions very often, it is going to be hard to determine where I was. My prime objective was to try to get into interesting stuff, into anvils. Closest I came to center towers was about 1/2 to 3/4 mile. It's impressive to be up there when you are around them. You worry about what you might hit. Today I hit nothing more than moderate turbulence. Most of the time, hit turbulence in clear air. Highest I went was about 59K ft today. If you see an interesting feature at some distance and head for it, it may collapse and be gone by the time you get there. Also, as you approach, it blends into background of cirrus deck and you can't see it (unless you are below it); I flew through about three or four streamers or anvils today. Put info on flight tapes. Spent most of flight between 51K and 56K ft. At 1424 UT, passed through obvious cirrus layer above main cirrus deck. Got into other cirrus layers at higher altitudes, which were probably the result of cumuloform aftermath. At 1429-34 UT, I went through anvil. When I was almost through it, I looked at clock, I had 1434 UT. I guess 5 min — I maybe started to enter it. Altitude was 54.5K to 55K ft. Saw interesting formation, an ill-defined buildup, I didn't go through it. I thought the features were interesting. Couldn't see actual main core. Formation showed anvil to left (to WSW) out of side of tower (part way down the tower) to ENE wispier layers extended from near top, ill-defined, composed of cirrus, very fine streamers. Couldn't tell shape of tower-anvil structure whose anvil I went through between 1429-34 UT but it was the highest I went through. I could see it to SSW, increasing in altitude as it thinned out. I aimed for a point out along the anvil (streamer) which was about 30-40 miles long. Edge on it looks like a streamer, very thin; in it, the horizon was obscured. It's hard to establish its exact altitude as you approach. Sometimes you pop out the top, part way through. You try to get down in again. I stayed in one about 3 min or more; about 18 miles. Between 1429 UT and 1503 UT, I didn't keep a record. I was just turning round trying to find the most interesting features. Things started to disappear and action started to subside. At 1517 UT, went through streamer at 52K ft. Temperature was -55°C. At 1541 UT, aimed for (what seemed to be remains of a flower burst, vertical filaments) and passed through at about 54.5K ft. Things just calmed down after that, so I went home.

Flight Tape Transcript

Temperature -22°C [1339:32] came out on top at 43K ft, temperature -47°C [indicated ram temperature on cockpit dial]. Heading to the north-northeast, and 10° [1339:40] off to the left I see a big cluster of buildups. Above me stretching from the eastern edge of that buildup out to the east is another thin layer of cirrus about at 48K ft. Coming up to 49K ft [1340:09], and I don't know how high that thin cirrus band is. 0.42° radial out of [1344:09] Howard, climbing at about 300 ft/min through 51K ft, temperature -55°C. I can see them off the left of me now and they appear a little higher than me [1344:30]. There's an interesting cirrus form at the east end of the buildups, sort of lenticular [1344:42] pattern. On [1346:13] 039° radial, 78 n. mi. from Howard, just passing to the east of some little ragged tops [1346:20], not well-defined cumulus, a mile or so away. Through 52K ft [1346:34] and they're a little bit above me, I think about 53.5K ft and they're what appear to be just a little colder, it's about -53°C [1349:52]. 54.5K ft [1351:24], temperature -51°C. Turning to the left, on the 026° radial [1351:32] from Howard at 96 n. mi. There appears to the southeast (SW?) a new cell punching up about 20 miles away [1351:48]. The older bunch of cells are just about due south of me and they all seem to have dissipated except right in the middle. I was trying to keep 300 ft/min [1352:58] climb rate but it varies and I guess I went through (by?) the turret a

little bit too fast. It was right about 50-51K ft [1353:09]. Coming up here on my left is that new buildup [1357:09] that I saw and it seems like a two-tiered cake. The bottom layer is almost circular on the top, and it seems to be a partially cumulus and a partially cirrus cloud and it looks like the center portion is punching up through the lower tier and it's up to almost [1357:34] 57K ft. I'm at 57K ft [1357:38] at this time. Passing off to my left about 2 miles, and I just saw out of almost the center [1357:45] one of those wispy bursts of thin cloud and it must be going up about 500 ft, very thin, above the tops [1357:58]. On the 048° radial at [1358:29] 82 n. mi. I'm turning [1400:22] in a left-hand circle around this big one at this time, 58K ft, temperature -49°C. I'll quit [1400:33] my climb at this time; I'm on the southeast edge of it about 2 or 3 miles [1400:40] away and I can still see a ring of cirrus, quite smooth ring, around a good part of that bottom tier and that center tier is still punching up through it, I'm guessing to about 56K [1401:02]. . . . 57K ft, out to the northwest of that other turret but just to the southwest of me there's another one building up. I got quite a bit of turbulence there at 57K ft [1404:47] and I'm getting a lift, up about 1000 ft, temperature is -50°C. Time 1408:26, I'm heading east out to the south of those buildups, the one I told you was building up to the southeast of the other one is built considerably rapidly and the bottom [1408:46] cell had a sort of doughnut shape and the top cell is sitting in it. A very smooth ring of cirrus is around the base of the top cell [1408:53]. I should have said that new buildup was to the southwest of the original one I talked about [1409:28]. The old one, which seems to have disintegrated at the top, no cumula form shape now but it appears to have gone higher; I'm at [1410:00] 56K ft and it would appear to be a little bit above me. Present position is 052° radial [1411:56] at 91 miles, traveling in a generally easterly direction away from those original buildups. On my left and at my altitude of 55.5K ft [1412:10] are some scattered remains of previous buildups and dead ahead it looks like another one pumping up. Time is 1412:19, 55.5K ft, I'm going a little lower. I keep on getting a little lift here all the time. On 058° radial [1414:33], 103 n. mi. Interesting phenomenon to my left, the little buildup I was heading for off to my left, about 2 miles out at 54K or 55K ft, and over the cap — it's built a smooth dome of cirrus, with some type of curved thin layers of cirrus above it. That smooth dome appears to be behind the cumulus, so it might be on the level or a little lower to the north but I can see those thin strands of cirrus right above it still, and even in the center the thin storms form other contours of the little bumps of cumulus [1415:20]. Turning [1416:28] to the northeast on the east side of that buildup, and I'm heading toward what I thought was left over, little strands of that cirrus, but ahead of me I can't see them at this moment and I'm at 54K ft [1416.47] and a little bit of turbulence. Coming around [1418:49] to the north of that northeasterly buildup and I'll see if I can descend into a cirrus. I don't want to get too low or too close; there's evidence of some turbulence down there. We've had another [1419:08] flower burst from that one, I don't know whether it was the old original buildup I was over, or not. It looks like a Prince of Wales feathers [1419:15]. 52.5K ft, 1421:46. Turning to the west again, 117 miles [1422:07] out on the 053° radial and ahead I see what appears to be a fairly dense piece of cirrus. It appears to be a little bit below me. May be coming into that cirrus right now, at 50.5K ft [1424:37]. Temperature is -55°C, I'm in it now [1424:44], I can't see ahead very well, so it's moderately dense [1424:51] . . . climbing [1425:05] and coming out of the top. Through 51K ft again [1425:47], I think I'm getting into it again, yes, I'll try and hold it. -56°C, 50.5K ft [1426:39]; just off to my left there and I'm turning right [1426:59]. [1427:23], altitude 50.7K ft. Bearing 040° at 95 miles [1427:35] from Howard. This is thinning out now and over to my left there are two bumpers. The one to the west has those thin almost circular bands of cirrus all around it again. There appears [1428:27] to be very thin cirrus above; I'm climbing to get into it. Shot through it [1428:39]. 52.5K ft, 1429:40, I'm in a little bit of cirrus again and a bit of

turbulence too [1429:53]. Altitude 52.5K ft, temperature -55°C, -56°C . . . western edge of this bunch, on the 028° radial [1431:12] at 85 miles, on heading of 250° turning towards the south, I can see stretching to the west what appears to be a leftover anvil [1431:24] and I will see if I can go through it. I think [1434:25] I did go through it before, between about 54.5K and 55K ft; in fact, I might still be going through a little bit of it again. It doesn't [1435:06] look as thick as it did from a distance. There's cirrus out to [1436:32] the left, but it appears to be domed in the center and I was going to go through it but I've had second thoughts. Along the southern [1438:13] border of these storms and there's an extensive layer of undulating cirrus ahead of me to the east northeast; appears to be an anvil formed [1438:32] out of one of the old ones and I'll head generally in that direction. I'll try to get down into the cirrus, to see what altitude it's at. I'm at 50K ft and I've just passed in the descent a very, very thin [1439:51] cirrus layer. I'm just a bit below it now, but here and to the north of me, there's some above me, I'm just coming into it now. Brought it up to 52K [1440:41], temperature -54°C, I'm not going to head in this direction [1441:26] much more. 1443:01, -55°C, Just trying to get in and out of that cirrus, but sometimes there are just very thin layers [1444:48] of it, very well defined, but very thin. They're all around about 52K ft or thereabouts. On 072° radial at [1445:12] 76 n. mi., turning left through 110°, I'm turning back to the north again. See if I can get a little higher and find that anvil [1445:25] which I saw, not too well defined but fairly deep. Trying to find the anvil now, it's to the southwest of an old dissipated cloud, I'm at 54.5K ft [1449:24]. I see some of it coming up, I'm going to try and go through it. 1450:50 and I'm in it now. It's not as thick as I thought it was. I'm still at 54.5K ft and light-to-moderate turbulence. There's some [1451:47] stuff ahead of me; I'll go over the top of it. On the 045° radial at [1452:42] 88 n. mi. from Howard, passing over the top of something [1452:47] which is not very well defined; 55.5K ft and light turbulence, and I guess it's about 2000 to 3000 ft [1452:57] below me. I'm heading towards what appears [1455:13] to be an anvil streamer to the west of a cloud, cirrus which is at about 57K ft. Just went through it at about 56.5K ft at 1455.40, -52°C [1455:54]. Off to my left I can see some stuff which is about 56.5K ft; it's just stratoform cloud [1456:40] above cirraform cloud above a bumper, I think, underneath it. Another patch of cirrus. 1457:27, 56K ft, just to the west. 1459:24 climbing up again to have a look around. On the 034° [1501:02] radial from Howard at 54 n. mi. turning left to the east and not much activity right now except about 100 miles to the east. A small cumulus [1501:32] which was pumping up, but it's just disappearing completely. There's a lot of high cirrus just to the north of me that's pretty high, about 57K ft. Turbulence there for awhile at 58.3K ft, -41°C [1503:]. There's a tremendous [1504:13] amount of heavy cirrus below me, it's undulating, not uniform. I'm coming up to a streamer now; the thunder bumper is not too well defined, a bit fuzzy [1509:08], but the streamer is well defined. Might get into that, I suppose it might be what you call a bit of an anvil [1509:48]. 1517:21, I think I'm in one of those streamers [1517:26], it's not really an anvil at 53.2K ft, time 1517:33, temperature -55°C. On occasion [1518:27], you get a little light turbulence in it. 086° radial [1518:42] from Howard, 129 n. mi. Climbing a little to see if I can see any [1521:] further activity. Time is 1528:25, 59.5K ft, -41°C, light turbulence and I see some back to the northwest of me building up but they don't look all that interesting, the activity's really ceased. I'm getting light-to-moderate turbulence here. 1536:26, heading northwesterly at 97 miles from Howard and to my left are remains from a [1536:41] cluster, above and in the center is some very nice cirrus but I don't feel inclined to go right over the top of that, into the cirrus, doesn't look too healthy. The general cirrus deck seems to have risen [1537:03] and that's why it appears, I think, that there is less activity, the bumpers aren't coming up. I'm finding fewer of them and they don't seem to poke as high above the cirrus [1537:13]. 54.5K ft, went through what [1541:18] appeared to be the leftover tops just a little bit of

cirrus, it wasn't horizontal, it was formed vertically a bit, very little minor turbulence.

FLIGHT 9: 15 SEPTEMBER 1980

(Pilot: Ron Williams)

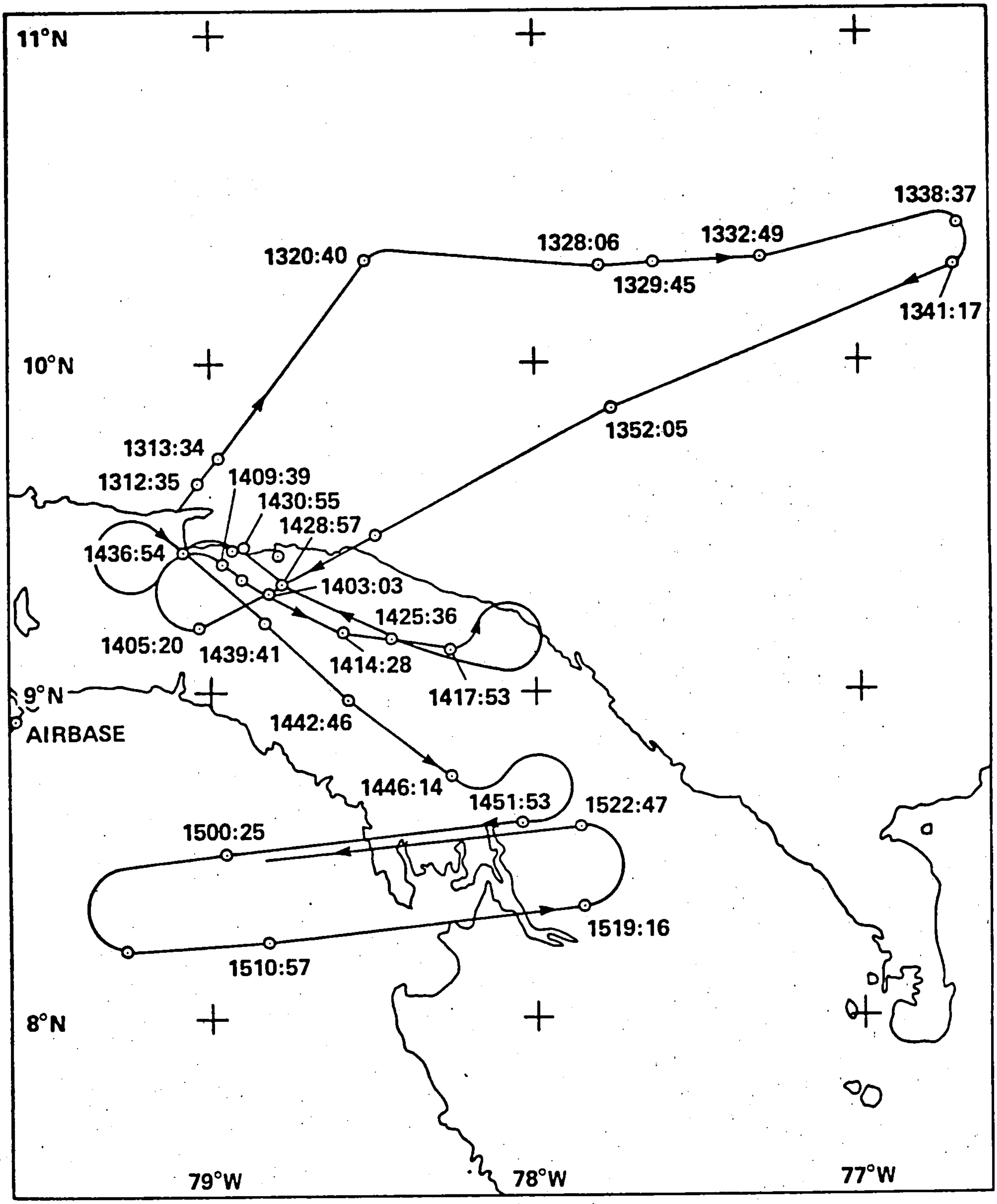

FLIGHT 9

[Pilot: Ron Williams]

Flight Log: 15 September 1980

Altitude, 1000 ft	Universal time	Event
0	--	Verify INS and H_2O Rad sw on
	1251:30	AGC sw off, then pwr transfer
	1252:30	AGC sw stdby
	1253	Left tank fwd sw stdby
	1253:10	Left tank aft sw stdby
	1253:25	Right tank fwd sw full on
	--	Verify right tank aft sw off
	1300	Takeoff
50	1310:14	AGC sw on, slow climb
	1312:35	30° heading 035°/55
58.5	--	Terminate climb
	--	Pass to right of tower, 052°/143
	1331	--
55.5	--	062°/190, heading 240°, start slow climb
65.5	1403:12	Over cell
	1409:47	Pitot heat on
56	--	Over small buildup, 055°/49
58	1501:20	APS No. 1, temp = -48°C
51	--	050°/48 close to cirrus, and passing over old buildup area
61	1519:15	106°/109, begin climbing left turn
64	1531	051°/?
67	1549	APS No. 3, temp = -49°C
50.5	--	Still above cirrus on descent
47	--	In heavy cirrus
	1558	AGC sw to stdby
0	1630	Landing
	1636:15	Left tank fwd sw off
	1636:22	Left tank aft sw off
	1636:30	Right tank fwd sw off

Pilot Commentary

Takeoff at 1300 UT. Debrief tape recorder malfunction. Ron had little to say; said important comments were on flight tape. Felt that flight was not too interesting because there wasn't much activity. He briefly described flight: Did slow climb from 49 to 59K ft. Went to area advised by Ed Danielsen and could not see any large towers. Buildups seem to reach only about 53K ft or so. Cirrus was at 50K or so. When buildup did occur, they came up fast and collapsed fast so they were never in sight for more than 5 or 10 min. Felt light turbulence on occasion, which he noted on tape. Made passes in area at 58.5K, 55.5K, and then climbed up to 65.5K. Returned to low altitudes at one time making run at 51K over area where there had been previous buildups. Made second series of runs increasing altitude in steps till he reached 67K. Returned to base.

Flight Tape Transcript

Above the heavy cirrus deck at about 47.5K ft, there's still some light cirrus above me. Little slow establishing my 300 ft/min climb, I'm about 50K ft and AGC turned on at 1310:13 [1310:16]. Cirrus is about [1310:49] 50.5K ft and I'm starting my slow climb to 59K ft. I came out on about 030° heading from Howard. My position is 035° radial at 55 n. mi. [1312:36]. . . . pretty high, I really don't see buildups, I can see some roll clouds in the cirrus at my 10 o'clock position about 30-40 miles, but they're not really out of the cirrus yet, they might be building through. My position is 035° at 61 n. mi. [1313:34] . . . here on the climb out [1315:13], not real bad and it's not continuous. On 035° radial from [1320:40] Howard, 105 n. mi., I'm going to make a right turn to 090° at this time [1320:45]. At 090°, I see another sort of low cloud in the cirrus; it isn't above the cirrus yet, about my 11 o'clock position about 50 miles [1321:50]. That's about the position that Ed was talking about this morning. At 9 o'clock position about 30 miles, there's a higher cirrus; it might be the remains of a buildup that has already collapsed [1322:32]. . . . 11 o'clock, about 30 miles now, looks like it might be building [1323:03]. The one buildup that I was talking about a little while ago, I'm on 0° (~47°?) radial [1326:28], 128 n. mi. from Howard, 57K ft, that one buildup still down in the cirrus is at my 11 o'clock position, about 20 miles now, but in my 11:30 position another just poked through. It's really building, it's about 50-60 miles away and that's the one I'm heading for. If it continues building, it will be a big one. On 50° radial [1328:06] at 135 n. mi. right now, I'm turning left about 10°, heading towards that big one that's really building, if it doesn't collapse on me. I'm going to stop this climb at 58.5K, just pass over [1328:32] the cloud at 58K ft. . . . If it keeps growing like it is now it will be higher than that when I get there. I'll pass it off to the side though. . . . Buildup, it's now in my 11:30 position, a close one, it's about 10 miles, 11 o'clock position and I'm on 052° radial from Howard [1329:45], 143 n. mi., I'll just pass about a mile to the right of it. I can tell it's a buildup, but it is still down in the cirrus; it hasn't poked up, and that one that's at 12 o'clock now; it was really building but I can tell that it's hit its peak [1330:03] and it's starting to spread out and collapse already. It's up at [1331:29] 56-57K ft, 12 o'clock position, has already collapsed back into the cirrus. That other buildup that's still — I can tell it's a buildup but it's still in the cirrus, it's . . . There's two buildups [1331:46], one at my 9 o'clock position, one in my 10 o'clock position; the one at 9 is about 3 miles away. The one at 10 o'clock is about a mile away. I'm still going to go over to this other one; it might start growing again, see what's over there anyway. I don't see anything else. That closest buildup, the tops are right into the top of the cirrus is now [1332:39] at my 9 o'clock position about a mile, I'm on the 056° radial [1332:49], 160 n. mi. from Howard. I'm at 58K ft, somewhere plus or minus a thousand [1333:18]. This thing that was up to 56, 57K ft, it's almost completely disappeared back in the cirrus [1335:18]. It did leave behind some residual cirrus, I guess you call it. I might drop down a thousand feet just to see if I can go through it; it's hard to tell where it is because it's all merged with a heavy deck of cirrus [1335:40] below. . . . the storm that was way up there — I'm in the area but I can't tell where it was anymore. On the 060° radial [1338:37], 194 n. mi. from Howard, turning back to the right. At 55.5K ft [1339:48]. Now on 062° radial, 190 n. mi. [1341:17], heading 240°. Starting a slow climb to 68K ft, I see no buildups, nothing but cirrus [1351:56]. At 61.5K ft, on 060° radial [1352:05], 123 n. mi. from Howard; you've probably heard all the conversation with Ed Danielsen. I'm going down to the southeast; I can see the buildups [1352:13] down there but they build up and collapse so fast that unless there are some new ones when I get down there, I won't arrive in time. On the 060° radial [1359:50], 74 n. mi. from Howard. I see a buildup and its about [1359:57] 200 miles away from me in about my 11 o'clock position

[1400:06]. . . . airplane is shaking here for some reason or other. At 65.5K ft, still in a slow climb. Shaking . . . I'm at 66K ft [1401:33] and I'm not pushing anymore, I'm just too heavy to keep on climbing. I'm getting into some kind of buffet. I'm pulling the power off and I'm going back down [1401:48]. I might be over a buildup here, I can't tell [1402:20]. I'm at 65.5K ft descending and I'll go out here about 5 min or so and turn around. I'm still in buffet here. On 60° radial at 52 n. mi. from Howard [1403:03] and I think one grew right underneath me that I didn't notice; in fact, I'm sure of it. It's 1403:12 [1403:15] now; I'll go till 1405:00, turn around and come back and see. I'm at 65.5K ft, gradually descending [1403:30]. I'm making a right turn, back to see if that is a real buildup, on 060° radial [1405:20], 38 n. mi. from Howard. At [1405:37] 63K ft. Now it's not very high, probably 51K ft or so, just judging it by the cirrus, just on the top of the [1406:16] cirrus layer. There are two of them in there; the tops are just at the cirrus layer which when I was climbing up I think was around 51K ft [1407:11]. I'll descend to about 53K ft and go across the tops of them. There are two of them right now; I'm still in a turn but they — I gave you the position [1407:30] when I ran over the top and I'll go over the top of both of them again. It's flat on top so I don't think they're building. Heading 110° (?), on 050° radial, 47 n. mi. [1409:39] from Howard, and I'm descending to 55.5K ft, to make my first run at 55.5K ft and the cirrus is getting back so the pitot heat is coming on at this time at 1409:47 [1409:51]. Hitting rough air [1409:55]. . . . Record all on the recorder and I'm right over the top of the first one now. I'm [1410:24] at 56K ft and going to stay here. That was hard getting down in time. I can't judge, it looks like they're about 53K ft. I'm right over the top. On the 055° radial from Howard at 40 n. mi. [1410;38]. Cloud is flat on top. It's embedded. It comes up about, maybe, 500 to 1000 ft above the cirrus [1411:05]. It's about 4 or 5 miles across. That's running from north to south. And it's very flat on top [1411:17]. I see no cirrus layers that it's pushed up or anything. It's just flat roll cloud on the top and that's about all I can describe [1411:26]. There's another one at 12 o'clock position and one about 10 [1411:30]. I'll make my run over both of them but it's collapsing fast. It's back down into the cirrus. I'm holding at [1411:37] 56K ft . . . here at 56K ft [1411:54] and descend down to 54K ft and then come back over them . . . down now. The one that's at 12 o'clock [1412:33] now is approximately the same size, about 4 miles across at the top. It's sort of flat on top although there are roll clouds and I can see the edges of the thunderstorm but the tops are right at the top of the cirrus now. It was a little higher a little while ago [1412:51]. You can tell now I'm right on the western edge of it here. The widest part runs from north to south. On the 072° radial [1414:23], 62 n. mi. from Howard. Right now, I'd estimate the top of this at about 51K ft. The other one is smoother across the top than this one [1414:45]. I'm getting some . . . I'm right in the middle of it now and it's a light turbulence but not as heavy as [1415:03] the other one . . . eastern edge of it now [1415:54] . . . 1417:00 [1417:00]. I'm going to make a 270° turn to the left and go back over it. 54K ft [1417:10]. On the 078° radial [1417:53], 80 n. mi. from Howard. . . . east [1420:52] of my position now. It goes up to about 55K ft. It looks like it's growing. I bet if I turn and go out there it'll be gone by the time I get there. It's about 100 miles away [1421:09]. Just went over [1421:30]. I'm turning back. I no longer can see it; I'll still make the run over their approximate position. 1422:30 [1422:35], I'm on the . . . radial 86 n. mi. from Howard . . . right in front of me about 12 o'clock, about 30 miles. I don't know whether they'll still be there when I get there or not [1423:21]. They're 53K ft right now but it's growing fast [1423:50]. I'm heading right towards it. I don't know if it's the same one that I just went over or not [1424:00]. Went up to about 53K ft and it's starting to collapse right now [1425:04]. It's just flattened out on top and it's going down almost as fast as it went up. . . . 075° radial, 70 n. mi. from Howard [1425:36] and I think I'm right over the ones I went over

before, in fact, it's a little rough right now [1425:41]. I'm coming up [1428:50] on this one that I can see. On the 060° radial. 55 n. mi. from Howard [1428:52] and this one that grew up to about 53K ft, it's now collapsed back down in. The tops are just even with the cirrus and I'm guessing they're at 51K ft, I'm at 54K ft. That one's a little bigger; it's about 5 or 6 miles across and no cirrus or anything associated with it on the top. I'm right on the edge of it now [1429:27] . . . just go past it. I made quite a long run here; I'm going to go past it and go out and do another 90-270° turn [1429:47] and descend down to 51K ft and come across at 51K and see what happens. I'm in the middle of it [1430:01] right now. It's about 6 or 7 miles across. The highest portion of it is just off to my left [1430:10] about one-half mile, not even that far, one-quarter mile. [1430:22] A little light turbulence. I'm getting on the other edge of it and I'm picking up a little turbulence but not much [1430:29] . . . doesn't completely disappear on me since it takes me quite a while to get around [1430:45] this 90-270° turn. I'm coming up on the edge now. My radial [1432:55] is 050°, 48 n. mi. from Howard and I'm making a 90-270 turn to the left. [1431:08] 51K ft. Bumps poking up all over in the cirrus but they last about 3 to 5 min and collapse right back down into it. If you're not right at that spot when it happens, you've just missed it [1431:54]. And they're different. No they're not pushing any cirrus cap on top of them or anything and I haven't seen any flowers or anything coming out of the top of them when they collapse. And they're only going up to about 53K ft. I saw one up to around 56, 57K ft earlier but that's the biggest one I've seen and right now most of them are going up around 53K before they collapse. And I'm down [1432:43] at 52K ft now. I'm starting to pick up a little turbulence [1432:48] . . . near one portion of that one I just passed over. It's starting to build but I've got about 3 or 4 more minutes before I roll out of my turn [1434:29]. I'll try to go over the top of it, if it's still there when I get around. It built up [1435:11] about 1000 ft and now it's collapsing. I can see a slight cirrus left over from it. Just a real small band of cirrus left; oh, there it was building up now. And I'm approaching it [1436:09]. I'm still in my turn. I'm going to go right over where that last buildup was. It looks like about 5 miles across. Where the buildup was is right on the right-hand edge of it. Heading about 120° when I roll out here [1436:33] . . . 042° radial at 44 miles [1436:54]. I'm heading 120°. I'm going to change this a little and go over the top of that last buildup. I'm at 51K ft . . . is up about 52K ft [1437:15]. I'm right over it [1437:45], as close as I can come. I'm just passing over the edge of it now. I can't tell anymore . . . kind of cirrus at the altitude it did build up to. I don't know if I'll go through it or not. I really can't tell whether I'm in it or not [1438:18] . . . uplift [1438:42]. I'm just passing over where the buildup was. I can see the cirrus out to the side of me so it's above me but I can't tell whether I'm going through it or not. I did get an uplift. My airspeed is changing quite a bit [1438:56] . . . heavy turbulence [1439:08]. I just call it moderate. Just going over the top of it. Now on the other side it's . . . me down here but I can't. On 066° radial [1439:41], 49 n. mi. from Howard. Over the [1439:54] — what I thought was the edge is where I'm picking up the heaviest turbulence. That light cirrus that it left over I can see on all sides of me but I can't really see it around the aircraft [1440:04]. My altitude is varying quite a bit here because of the turbulence. I'm going from 51K up to about 51.6K ft [1440:13] . . . this heading because those other two cells that I passed over earlier are on this heading [1440:25]. I really can't tell where they are any more. They're back down in the cirrus. At 1400 UT . . . tops, -76°C, located at 7.5 north, 78.4 west. [Radio message.] I'm right over the top of another one; I think the first one I went over. On the 084° radial [1442:46], 61 n. mi. from Howard, still heading 120° . . . due here. I'm on the 095° radial [1446:14], 80 miles . . . 90-270° turn to the left, go back, climb up to 58K ft, make a pass at 58K ft over the same area I went over. Then I'll go on down south where Ed Danielsen radioed is the heaviest area but I sure don't see

anything down there. . . . 270° to the left at this time [1446:39] . . . in my turn [1450:36] and I'm looking back and there's another cell building. I don't know whether it's the same one or not. It looks like it'll be on the same heading as before. . . . 30 miles out [1450:53]. I'm a little short here [1451:36] so it must be a new cell. But I'll head towards it; 099° radial [1451:53], 94 miles from Howard. I'm heading 255° at this new cell, at 58K ft. It's about 3 to 4 miles across and I'm heading for the highest part which is almost right in the middle [1452:55]. It's up to about 53K ft now. It's about 20 miles out . . . the others I've seen today, just rolling clouds building in altitude. It's not pushing any cirrus cap [1453:22] or anything above it . . . closer because I'm afraid it's still building. It must be up around 54K ft now [1453:36]. I'm at 58K ft [1453:46]. However, it petered out around 53, 54K ft. As soon as they hit that altitude they collapse [1454:06] just as fast as they built. It's collapsing fast, about 1000 ft every 30 sec. It's almost down in the cirrus layer again [1454:18]. Heading about 240°, 55K ft [1454:34]. Makes this run at 58K ft and see what happens. I guess I'll go down to about 53K [1455:05] and just drive along, hope I run into one . . . 30 miles out [1456:31]. It's still about 10 miles away. I½m on the edge of that thunderstorm now. On the 120° radial from Howard at 46 n. mi. [1500:25], just on the edge and going right over the center of it. As soon as I pass, I'll do a 90°-270° turn, climb to 61K ft and make a run [1501:01]. I'm just on the other edge of it now. There may be a buildup at my 10 o'clock position about 4 or 5 miles [1502:36] so I'll turn in that direction. 140° radial . . . 50° [150°?] radial of Howard at 35 n. mi. Starting a left turn and climbing to 61K ft. On 152° radial, 47 n. mi. from Howard. I'm at 51K ft [61K?] and I'm right over the edge of that buildup I passed over coming in this way. It's down in the cirrus now . . . and about my 10 o'clock position at 20 to 30 miles. I don't know if they're going to grow or not. I'm on the 129° radial [1510:57] at 61 n. mi. . . . as far as I can tell they poke up all over the place for a few minutes. What I'm going to do is run . . . back here [1511:59] at 61K ft and 64K ft and 67K and see what happens. 1519:15 [1519:15] On the 106° radial, 109 n. mi. Making a left turn. Climbing to 64K ft [1519:27]. On 278° (98°) radial [1522:47], 105 n. mi. from Howard. I'm heading 262°. There was a buildup there. It's already starting to collapse and it'll be gone by the time I get there. It's about 30 to 40 miles away. I'll make a run here for 10 to 15 min [1523:09] at 64K ft . . . radial, 51 n. mi. from Howard [1531:24]. And right off my right wing is — looks like a cell might be starting to grow. It's still in the cirrus deck but I can see the roll clouds down into the cirrus. I'm at 64K ft. I plan to turn around and go back the other direction shortly and climb to 67K ft [1531:39]. . . . off my right wing and it doesn't go above the cirrus. . . . just a little while ago in my 3 o'clock position, which is now back in my 4, isn't building so when I get down here, I'm going to make a left turn to keep in approximately the same area [1534:38] where I've been making these other runs. I'm going [1535:25] to start my climb to 67K ft . . . left, I'm on the 140° [1536:16] . . . Howard. At 67K ft [1542:13]. There seems to be a line here, I'm just over the edge of it now which is about 150° radial [1543:43], at 51 n. mi. and this line runs about north and south, and it seems that there's not much activity to the west. To the east there seems to be a lot of roll clouds in heavy cirrus. To the west I can almost see the ground. I'm right on the edge now . . . ° radial, 107 n. mi. and making a left turn back towards Howard and starting my descent . . . correction, 100 and 106. Heading back towards Howard in a descent. And here I'm going to have to penetrate the cirrus. I can see a buildup at my 1 o'clock position, a buildup at my 11 o'clock position. Straight ahead, all I can see is cirrus. I'm hoping there's not too much in there. I'm at 50.5K ft. I'm still not in the cirrus, although I can see cirrus above me in both directions but I can't see that I'm going through any of it. There is heavy cirrus at 47K ft.

FLIGHT 10: 16 SEPTEMBER 1980

(Pilot: Jerry Hoyt)

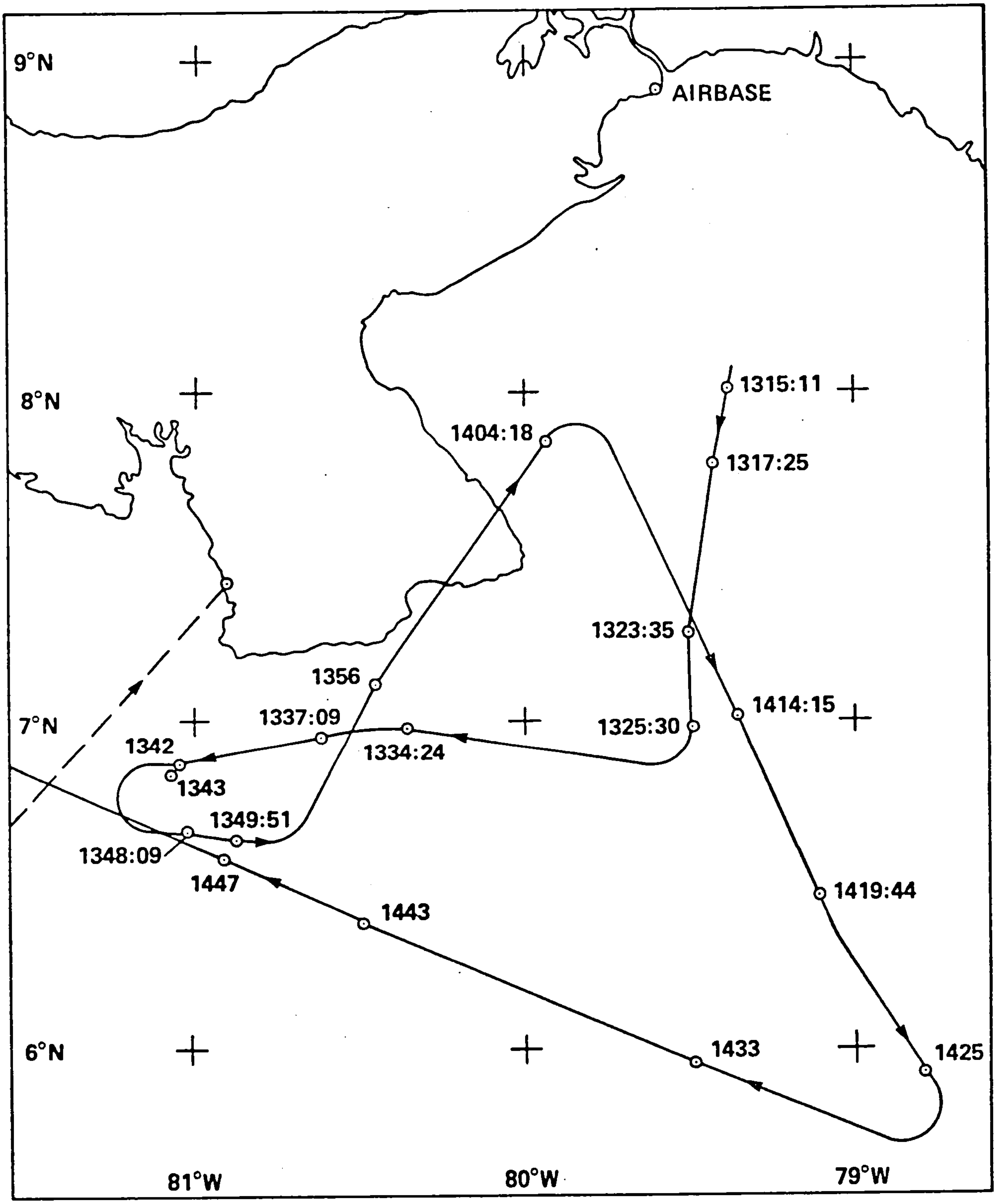

FLIGHT 10
[Pilot: Jerry Hoyt]

Flight Log: 16 September 1980

Altitude, 1000 ft	Universal time	Event
0	--	Verify INS and H_2O Rad sw on
	1253:29	AGC sw to stdby
	--	Verify INS and H_2O Rad sw on
	1253:53	Left tank fwd sw stdby
	1253:57	Left tank aft sw stdby
	1254:20	Right tank fwd sw full on
	--	Verify right tank aft sw off
0	1301	Takeoff
	1313:10	AGC sw to run
	1313:35	Pitot heat off
~45	--	Reach tops of cirrus deck
48	--	Start slow climb at 300 ft/min
49	1317:25	170°/68
51.5	1325	Start right turn, 175°/115, heading to 270°, T = -59°C
	1332	~15 miles from small cells ahead to left
53	1335	T = -58°C
	1337:09	207°/132, 260° heading, along edge of ~20 m diam low cluster, light turbulence
53.2	--	214°/150, T = -55°C, near end of small cluster
	1343	Start descending left turn, 214°/152, heading to 100°
50.8	--	211°/159, passing over low weak cluster at 47-48K ft
52.4	--	208°/156, turning to heading 025° toward Howard, T = -56°C
54	1356	T = -58°C, 204°/119, 025° heading
56	1404	Start right turn to heading 150°, 196°/66, T = -52°C
57	1410	1° (181°)/91, T = -47°C, heading 150°
58	1414	T = -43°C, 171°/114
59	1419:57	167°/149, T = -38-39°C, cirrus looks stable
60	1425	163°/185, T = -38°C, 150° heading, start right turn to 270°
	1428	290° heading
61.2	1432	T = -37 to -38°C, 176°/176, 290° heading
	--	Small cell ahead about 30 miles
	1437	Cell seems to stop rising, ~1000 ft above cirrus deck
	1443	198°/160, short distance (~7-10 miles) from cell
62	--	T = -37°C, ~5 miles from cell
	--	1/2 mile north of collapsed cell, 208°/160, no other buildups
63	--	T = -38°C

Altitude, 1000 ft	Universal time	Event
64	1456	T = -38°C, 226°/--, start left turn to 090°, start descent
63	~1500	Radio call to return to base, 170 miles to SW of Howard, 40 min to landing
	1513	Pitot heat on
	1513:15	AGC to stdby
	~1540	Landing
	1548:16	Left tank fwd sw to off
	1548:20	Left tank aft sw to stdby
	1548:27	Right tank fwd sw off

Pilot Commentary

Takeoff at 1301 UT. Climb-out at 180°, thence to 150° to SSE of Howard about 180 n. mi. No buildups were observed about the cirrus which was at 46-48K ft. Cirrus varied about 2000 ft. Turned to west and moved to area of possible activity SSW of Howard at 180 n. mi. Saw slight increase in cirrus (a sort of hump) about 30-40 miles in diameter. Flew over this area. One or two small cells appeared, very few. Probably saw only three. Cells only came up ~2000 ft or less above cirrus. Maybe they reached 48-49K ft. Overflew area, nothing much going on. Was in slow continuous climb. Turned to NE. Ed called and said the area I was in was best. Worried about crossing my own wake once, so noted it on the flight tape. Believe I was somewhat lower (but not sure) when I crossed prior track. Had reached 64K ft when I received call to return to base. May have reached 65K. No APS were taken. The activity today was very nondescript — buildups were fairly low, only light turbulence was encountered. No unusual cloud formations were seen as on prior flights. Buildups and collapse were happening very fast (perhaps 5 min total). In one case a buildup left a little valley in cirrus behind. No evidence that any cirrus was left behind after these small towers collapsed. Didn't write down much on flight card this trip; the voice tape is quite a convenience.

Flight Tape Transcript

[1304:20] stratos is a thin layer at 14K ft and we'll be going through another layer here momentarily at [1304:29] 16 K ft now. Stratos layers all over. There are well-defined layers here, I'm presently at 30.5K ft [1307:31], I'll be entering it shortly, can't tell how thick it's going to be [1310:31]. The tops are approximately 43 to 45K ft; I'm at 43K ft and not quite [1310:41] on top. I'm in the clear now [1313:56] and I can see at 47K ft that the tops are stubbly around 45K ft and it's absolutely super clear above and the level of the layers seems to be very stable [1314:12]. It's very difficult to tell the exact tops [1314:44] until I get a couple of thousand feet above them. I'm heading south; I'm presently on the [1315:11] 165° radial, 55 miles at 48.5K ft and I've begun my slow climb at 250-300 ft/min. Cruise on at 1313:10, pitot heat off at 1313:35 or 40 [1315:49]. [1316:03] I'm in an area that has no cirrus; the tops are some stratus clouds down there at about 25K ft [1317:06] light turbulence. Temperature -55°C, I'm coming up on 49K ft [1317:19], and I'm on the 170° radial at [1317:25] 68 miles. I have passed [1318:31] clear of the turbulence layer, temperature still seems to be -55°C and I've climbed [1318:38] 600 ft. I'm at 51K ft now; temperature is still -54°C, heading 180°, on the 175° radial [1323:35] 103 miles and there's a possibility of one or two bumpers that may come up a little bit later but right now I don't see any at all in my area and I'm

going to start a turnback to the north [1323:57] in just a couple of minutes. It looks [1325:13] like I'm getting a buildup to the west of my position and I'm going to start a right turn now at 1325:00 [1325:22]. Present position 175° radial [1325:31] for 115 miles. Turning right to 270°, temperature -59°C. I'm at 51.5K ft [1325:47]. A turret has poked through the cirrus a little bit, I would estimate no more than 1K ft [1326:11]; the cirrus looks like it's probably about 46K ft, in that neighborhood, and the turret couldn't have come up more than 1000 ft. 270° heading in about another [1326:30] 30 sec. . . . a fairly standard turret; I'd estimate 25 miles away, and it's pumped up through the cirrus about 1000 ft [1327:28], and another little cell is starting to grow now, it might be 1200 or 1500 ft above the cirrus. The other one has flattened out to the point where it might even be sinking [1327:41] back down. There doesn't appear to be much change except the one little cell that appeared to be building. Time 1328:00 [1328:47], and it's terminated its building stage and is approximately level with the rest of the cell; I would estimate I'm still 25 miles from it. On the southern end very light thin [1329:09] wispy clouds are starting to blow off to the north. The northwestern corner of the entire cell was the area that the newest turret had begun to climb out, but it's definitely sinking back down and the whole cell is [1329:32] level now. I would estimate from my position that it's probably about 3 miles in diameter [1329:38]. At this altitude they're fairly persistent, however; they are definitely not as thick [1330:30] as I have seen before. I'm presently 15 miles out, time 1332:00 [1332:10]. The cloud is pretty well settling down and I can't discern much of anything above the cirrus except for one area that's still probably 800 ft above the main cirrus deck. If the cirrus deck were very, very level, I wouldn't be able to tell it's there except for the fact that it's a kind of rolling type cloud. It's a cumulus, you can definitely tell that's it — a cumulus as compared to the cirrus as being a stratus type [1332:49] . . . left about 15°, present position 200° radial [1334:24] at 124 miles and I'm 10 to 15 miles out from the one little turret, that is hardly discernible with the surrounding cirrus; however, I'll fly [1334:43] to the right of it, by about a mile or so. Again I would estimate that it's at 46K to 47K ft, my present altitude is 53K ft, temperature -58°C, and time is 1335:00 [1335:06]. I'm coming up on the original turret's position. I originally estimated it had an area of [1336:38] 3 miles; however, I would say that now that I'm closer, it appears to be about 15 or 20 miles in area; however, it has a kind of ragged top, now, instead of having a nice cirrus top, it's all cumulus type, but it doesn't appear to be building [1337:01] now at all. On the 207° radial at [1337:09] 132 miles heading 260° and I'm just skirting the edge of this area by about 1 mile [1337:19] or so and I feel very, very light turbulence. I'm at 53K ft, time 1338:00 [1338:52], and temperature is -55°C, still heading 260°. Coming up on the end of this area now, and I would say it's about 20-25 miles in diameter and again it doesn't appear [1341:35] to have any turrets that are sticking up out of it. It's hard to describe, since I'm fairly close to it. I'm still just a [1341:44] mile or so, one-half mile off the edge, but it's more of a cumulus cloud than it is a cirrus cloud. Present position is [1342:02] 214° radial from Howard at 150 n. mi., flight level 53.2K ft, temperature -55°C, and I'm going to descend in another couple of minutes to just above the tops of this and see what the actual altitude of the tops are [1342:32]. I've turned to a heading of 100° [?] and I'm on the [1343:14] 214° radial at 152 miles or so. Lock on the TACAN, 1343:00 [1343:20] and I'm going to begin a descent at this point to the cloud tops. Cruising [1348:09] on 211° radial, 159 miles from Howard and I'm passing the 50.8K ft level [1348:20] descending, and I can't really decide how much higher I am than the clouds themselves. It looks like I'm probably another couple of thousand feet above them. I'm starting to get a little light turbulence, so I'll level here and start my climb back up [1348:37]. I would estimate that the cloud tops are at 47K to 48K ft and again it's just a sea of smooth stuff now; I can't discern [1348:59] any more turrets

at all. . . . Continuing the survey at about 53-52.5K ft and I'll be turning north. On the 208° radial at [1349:51] 156 miles, turning to a heading of 030° direct to Howard and passing 52.4K ft, temperature [1350:06] -56°C. I would estimate that I'll be passing fairly close to my wash from the last pass here [1353:07], since I'm headed 025°. I don't know exactly where [1353:22], i'm 136 n. mi. from Howard now. Passing level 54.0K ft, -58°C and on the 204° radial [1356:02] at 119 miles heading 025°, time now 1356:00 [1356:09]. [Radio message from Wallops: Ed Danielsen says the only active cell is at 6° N, 78.8° W. There are two turrets out there at 7° N, A1 and A2 are southwest. This is the only active region.] [1401:40] The area to the southwest, that is, 7.4° N, 82.5° W, was the area that I was driving over in the last 20 min or so. The tops were running about 48K ft and there were only one or two turrets that came up to maybe 49K ft. They just came up 1000 to 1500 ft above the cirrus. I could not see any over to the east, the 6° N, 78.8° W area, I'll go over that area in just a few minutes. Right now I'm heading northeast [1402:37], I'm 77 miles south. Turning right to 150° at 1404:00, I'm on the 196° radial at [1404:18] 66 miles from Howard, 56K ft, -52°C, and I'll drive down to the southeast and look at the 6° N, 78.8° W area. . . . 57K ft, temperature -47°C and I'm presently on the 1° (181°) radial at 91 n. mi. [1410:44] heading 150°. Time 1414:00, temperature -43°C, 58K ft, present position is 171° radial [1414:15] at 114 n. mi. from Howard and I don't see any buildups that are poking through the cirrus at all. Looks to me like there's some cumulus in the 30K ft range to the south [1414:38] of my position, but in that area there is no cirrus, so you can see down through it. The area that's ahead of me has got a couple of places where it looks like maybe one or two have buildup in the past but I don't see any now. On the 167° radial [1419:44], 149 n. mi. from Howard and I'm coming up on 58K ft. Temperature is -38°C or -39°C, and this area here is absolutely stable now. I don't see any cumulus at all, it's all stratus. I'll drive this way for another minute or two, and then I'll turn to the west and see what I can see out that [1420:31] way again. The tops of this I would reckon are still down around 46-47K ft. I'm at 60K ft, -38°C, heading 150° [1425:08], on the 163° radial, 185 n. mi. I'm starting a right turn to heading [1425:19] 270°. I'm going to continue on around a little bit further to about 280° or 290° [1427:09]. There are a couple of small turrets . . . well it's hard to describe, but they're sticking up such a small distance above the cirrus, that I call them small. They look like they're larger in diameter; a kind of mound-looking [1427:28] affair. Coming out on a heading of 290°, time 1428:00 [1428:22]. I wish I could describe the way that some of these look . . . kind of boiling mounds. The whole area that I'm looking at looks like it [1431:10] covers over 45° of the horizon. I would estimate 60 miles in front of me. It looks like it gradually increases to a mound and then decreases again and then the whole thing increases in altitude [1431:32] by 1500 ft. Then there's one little turret; it looks like it tries to bulge up, and then it'll just collapse, and again they're not going more than 1000-1500 ft above the cirrus area [1432:03]. I'm at 61.2K ft, time 1432:00 [1432:44], temperature -37°C or -38°C, on the 176° radial [1432:56], 176 n. mi. and still heading 290°. There's one that's starting to come up now; it's a little more discernible than some of the others; it's probably up [1435:05] 500 ft and it's definitely building. I'm heading toward it; it's about 40-50 miles out yet, and I'll just keep my eye on it, trying to describe it as it changes [1435:24]. I would estimate that it's about 800 ft or so above the rest of the cloud, it's rising fairly rapidly, there's no question that it's growing [1435:58]. About 1 mile or so in diameter. It's not going to get too much larger and I would estimate it at maybe 1K ft above the rest of the clouds. It's about 30 miles ahead [1436:32]. It doesn't seem to be growing as rapidly as it was [1437:01]. Time 1437:00. The turret itself has stabilized. It's definitely not growing any more, and it could be subsiding [1437:42]. I don't detect any of the type of clouds that we described in the past, no doughnuts, no flowers, no poof-poof; I'm a lot farther out than I was before and

there looks like there's a possible small lenticular pileus cloud, if that's what it was called, on one side of it, at another little bump [1438:34]. It's definitely reached its maximum height, and is now definitely lower. Again, it's difficult to tell because I'm getting fairly [1439:15] close, it's only 1000 ft above the main cirrus deck. Most of it has descended to approximate level; of course, I'm a lot closer now. I'm probably [1440:22] 15 miles out or so and it looks like it's in a little valley in the cirrus. In other words, there's a little valley of cirrus and it's down in the valley itself. It still remains as a little bumpiness; you can distinguish it from the cirrus [1442:11], but if I were out at 50 miles or so, it would be very difficult to discern that there is a cumulus cloud at that point because of the distance. Time is 1442:00 [1442:55], and we're on the 198° radial at 160 n. mi., and I'm still 7 to 10 miles from that glob [1443:05] I was describing. [1443:55] 62K ft, -37°C. Now about 5 miles out [1444:25], it's a nondescript cumulus cloud. It doesn't appear that any cloud remained at the higher altitude; in other words, if it went to 48K ft and the cirrus is at 46K, it did not leave any cloud at the 48K level [1444:57]. I'm at the [1446:51] position where the turret was; it's about one-half mile due south of me and I'm presently on the 208° radial [1446:59], 160 n. mi. A bumpy-type cloud with no violent movement in it is all I can see from the top [1447:33]. I have observed no other buildups since a [1447:54] half hour ago, since I made that turn to a heading of 290° [1449:42]. Light turbulence now, temperature is -38°C, and I'm at 63K ft [1450:03]. I've driven [1453:19] off the edge of the cirrus; it's broken cirrus below me with a few cumulus building up to maybe 35, 40K ft but that's about it. Flight level 64K ft, temperature -38°C, on the 226° radial [1456:00] and there's no DME, it's broken lock. Time 1556:00 [1456:06], and I'm going to start a turn now back to the east to the left [1456:16]. Farther to the west it's just absolute level layer cirrus; there are no turrets at all [1456:41]. I'm still continuing my left turn to 090° [1459:15] but I'm going to descend to just a couple of thousand feet over the tops of all this, just above the turbulence layer if I can get to that [1459:24] position and just drive across it at that altitude and see what we get. Looks like about 100° will be my heading, and still don't have any [1459:39] . . . I'm approximately on the 240° [1459:52] radial. I'll start my turn, I guess I'm about 170 miles to the southwest at this time; it'll be about 40 min or so before I can get on the ground. I'm at 62K ft, a heading of 040° . . . begin the slow descent from 63K ft on down. Presently on 220° radial, 119 n. mi. from Howard.

FLIGHT 11: 18 SEPTEMBER 1980

(Pilot: Ivor Webster)

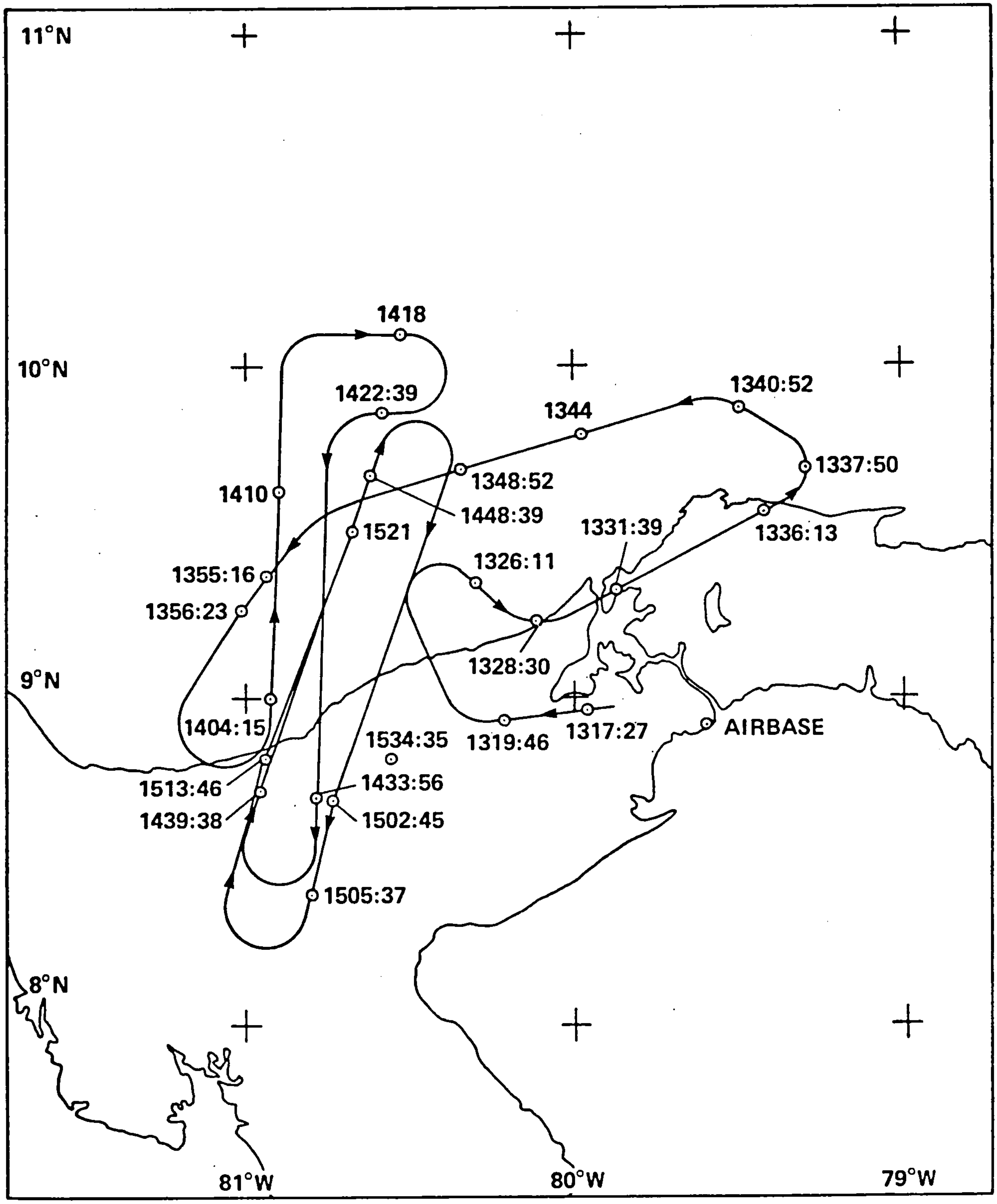

FLIGHT 11
[Pilot: Ivor Webster]

Flight Log: 18 September 1980

Altitude, 1000 ft	Universal time	Event
0	1254:15	AGC to stdby
	1255:06	Left tank aft sw stdby
	1255:18	Left tank fwd sw stdby
	1255:28	Right tank fwd sw on
0	1300	Takeoff
48	--	Break through cirrus deck, T = -55°C, start slow climb to 58K, heading to NNW
52.3	--	10 n. mi. SE of Howard, heading NW, T = -50°C
	1316	AGC, sw to run
	--	275°/22, 290° heading
55.2	--	Light turbulence, T = -51 - 52°C
	--	270°/37
56.3	--	T = -51°C, turning to E
	--	300°/50, heading 130°
56	--	300°/37, slow letdown, T = -48°C
	--	324°/30, heading 060°, tower 80 n. mi. ahead
59.8	1336:13	013°/40, heading 060°
	1337:50	Turning to N, 019°/50
60.3	1340:52	T = -47°C, turning to left to SW, 004°/58
	1344	345°/55, H = 253°, tower to left ~80 n. mi.
50.9	--	Skimming cirrus, light turbulence
51.5	1348:52	314°/65
55	1355:30	287°/85, T = -52°C, run at 55K
	--	282°/87, passing to right of collapsed cell
57	1404:12	272°/80, H = north, pass to left of collapsed cell
57	1409:52	H = 000°, 297°/89, T = -50°C
59	1413:36	H = 000°, turn to E
59	--	322°/90, T = -50°, turn to right to W
59.5	1422:47	Start slow climb, 312°/82, H = 225°, T = -48°C
63.8	1433:56	258°/73, T = -40°C, H = 160°, start right turn to N
65.7	1439:38	H = 015°, 260°/83, T = -38°C
68	--	Top altitude, evidence of lifting effect
65.6	--	Light to moderate turbulence
--	1448	305°/76
63.0	1454:23	Stay at 63K for awhile, no activity
	1502:45	257°/70, T = -40°C, start slow descent
61.9	1505:37	245°/79, T = -40°C
60	1513:46	264°/81, H = 020°, remains of cell to left about 1 mile
56.5	1521	297°/74, light turbulence, T = -50°C
53.1	1527:52	300°/86 from Taboga
52	--	Light cirrus, light to moderate turbulence, T = -51°C, 310°/70-80

Altitude, 1000 ft	Universal time	Event
50	1534:35	T = -55°C, 270°/60 from Taboga (trope?), thin cirrus?
49.3	1536:06	T = -54 -55°C
--	--	Passed through light cirrus above main deck
--	1557:30	AGC to stdby
	1610	Landing
0	1614:52	Left tank fwd sw off
	1615:02	Right tank fwd sw off

Pilot Commentary

Takeoff at 1300 UT. Climbed out to SSE, hit clouds at 19K ft, continuous to about 48K ft. Turned back north to the north side of Howard where radar suggested we should find active cumulus. There was very little activity, just a few small cells above the cirrus deck. I would see a small one, head for it, but before I got near it, it would collapse. They only reached 1000 to 2000 ft above the deck. Minimum temperature during climb was at about 50K ft — about -52°C indicated. Did slow climb to about 60K ft. Saw very few cells, about 5-min cycles. Saw them over all the area I operated in. Surveyed generally to the west of Howard, from about 10.3° N to 8.5° N at about 80.5° W longitude. Did slow climb to about 60K, then came down to 52K ft. Got into a little cirrus at 52K ft. Climbed to 55K ft, did a run, then did runs to 57K and 59K ft. Then started slow climb to maximum altitude. Reached about 68K. Got extraordinary lift at the highest altitude; I should not have been there. The airplane was flying too fast and the airspeed increasing at 67.5K ft when I was flying with Mach hold on the autopilot. Temperatures didn't seem abnormal; may have been due to some updraft. No real concentration of cells in area. When cells collapse, they look like a pot of bubbling stew, sitting level with the cirrus. The effect takes many minutes to die away, a long time. Went through cirrus, a separate layer above the cirrus deck, about 1000 ft. Could have been leftover from a collapsing cell, but I don't know. Hit light and light-to-moderate turbulence a few times, mostly light. Turbulence couldn't be related to any of the collapsed cells, since when you are directly above a disturbance, you can't really see it. You can only see things off to the side. I kept reversing course during the mission, generally stayed in the same area. May have passed through my old wake but I just don't know. Maybe the cirrus I went through just above the cirrus deck might have been my contrail, but we will be able to tell when the course is plotted out. Tacan went out for awhile during the flight. I was disappointed that the activity shown on radar this morning at 6 a.m. to almost 60K ft just didn't last. When I got there, there was absolutely nothing above the cirrus. It was lower than it was in the north, 48-49K ft in the south and 50-51K ft in the north. Saw some way out to west but I'm sure if I went they would have decayed when I got there. I could see about 200 miles. The flight was far less spectacular and less interesting than my last flight . . . it was just boring.

Flight Tape Transcript

Broke out on top at 48K ft, temperature -55°C [1310:35]. Starting [1311:35] a slow climb here 50.8K ft. I can't see [1312:59] any very definite formation above the cirrus to the south. If there is, it looks very small and it's spread out over quite a long distance. I see a couple of bumpers there above the cirrus, not terribly

well defined, and no towers poking up as yet [1313:32] . . . that [1313:57] climb about 10 miles to the southeast of Howard heading to the northwest through 52.3K ft [1314:08]; temperature is -50°C. Gas chromatograph on, at 1316 [1316:17] through 53.3K ft. 275° radial at 22 miles [1317:27] and heading 290° and just off 10-20° to my right, about 8 miles away [1317:42] I see some cumulus tops, but they're not poking above the cirrus very much. Dead ahead of me I can see a top about 50 miles away, it's punching [1318:03] through the cirrus, but nothing very much at this moment . . . 55.2K ft [1319:24], a little light turbulence, temperature -51, -52°C. [1319:16] I'm on the 270° radial from Howard at 37 n. mi. That line of cumulus should be off to my right; I'm just about running parallel to it, I would say, but there's not too much showing above the top of the cirrus [1320:36]. Through 56.3K ft [1325:32], temperature -51°C, turning around towards the east and I still don't see anything of any significance and at this point I should be traveling to the southeast almost directly above that line that was indicated [1325:53]. Nothing here though, a few small bumps down in amongst the cirrus. My position is 300° radial from Howard at 50 miles, heading 130° [1326:21]. [1328:30] On the 300° radial at 37 miles out of Howard and 56K ft, losing altitude here, going down about 800 ft [1328:44] a minute, it ceased, coming back up again. Temperature -48°C. [1331:29] I'm on the 324° radial at 30 miles heading 060° and directly ahead I see a turret which is building up, I don't know how far away it is, maybe about 80 miles [1331:50]. Looks promising, now it's starting to collapse [1331:55]. [1332:10] I'll make a slow descent through 57.6K ft, add a little more power here, temperature -48°C, a little bit of turbulence again [1332:23]. . . . Ahead of me [1334:42], it's just about collapsed completely, now heading back down into the cirrus, so it didn't develop into anything . . . about [1336:05] 59.8K ft on the 013° radial at 40 miles, still heading 060° and time is 1336:13 [1336:17]. That buildup ahead of me — and I don't know how far it is ahead — is just completely gone back down [1336:28], nothing to it now. At 1337:50 [1337:53] turning left to a heading of north. I'm on the 019° radial from Howard at 50 n. mi. and to the northwest I saw one building up but it collapsed in about 3 min [1338:13]; I guess it didn't reach much more than 1000 ft above the cirrus, going back down again. [1340:49] I'm at 60.3K ft; temperature is -47°C, time is 1340:52 [1340:56], and I'm turning left to the southwest. There appear to be some more building up ahead but I think I'm chasing ghosts [1341:05]; we'll see. I'm on the 004° [1341:08] radial from Howard at 58 n. mi. On the [1344:01] 345° radial from Howard at 55 n. mi.; the time is 1344, heading 253° [1344:08]. I saw what was a promising one about 10°-15° to my left about 80 miles away; it was the best one yet, but it's curled up some again [1344:23]. I'm down to 55.2K ft [1344:31], temperature is -49°C; I'm just in the top of the cirrus at 50.9K ft [1346:45]; I'll try and fly level here. Don't want to stay in it too long in case one of those ones punches up — getting a little bit of turbulence [1346:59]. Remains [1348:31] of one of those just off to my left. I'm heading 250° on the 314° radial [1348:52], 65 n. mi. from Howard, time 1348:52 [1348:58], 51.5K ft just getting a little lift there; [1349:05] minor turbulence and I see that one remains off to my left just about 2 miles away, nothing much left of it. Off to my right it just looks like a [1349:18] bubbling pan of soup in the cirrus. I might go [1349:32] through a little bit of stuff left over from an old one, a little bit of cirrus. I don't know if I'll actually go in it or not. Bit of turbulence [1350:22], and climbing up a little higher I can't see exactly what's ahead of me. I'm [1355:02] trying to maintain level flight at 55K ft. I'm on the 287° radial at 85 n. mi. [1355:16], temperature -52°C. I don't see much activity around me; I've just passed what little there was; I will stay on this heading for about 3 or 4 min, then climb to the next level. Time is 1355:30 [1355:34]. . . . At 200 the time is 1356 at 55K ft, on the 282° radial at 87 n. mi. [1356:23], and I'm just passing on my left the remains of what was one little bumper poking above the cirrus; it's collapsed now but the remains are there to be seen. Okay, I've finished [1359:16] the run at 55K ft, I'm trying to

level off at 57K ft. On the 272° radial from Howard at 80 miles [1404:15]; time is 1404:12, heading due north [1404:27] and just off to the right, about a mile away are the remains of a buildup which has collapsed; not much left of it [1404:40]. Time 1404:47, due north of me I saw what appeared to be the most promising buildup starting, but again, "kaput-ee" [1405:03]. Collapse once again. Even quicker than some of the others. 1409:52 [1409:56] Heading due north, 297° radial at 89 miles and level at 57K ft more or less, temperature -50°C and I'm climbing up another 2000 or 3000 ft [1410:16] to do another level. At [1413:30] 59K ft, TACAN has dropped out for the moment but heading still the same, due north, time 1413:36 [1413:40]. Time 1414:30, turning to the east, I'd like to get about 100 miles off the coast right now so I'll stay within it [1314:46]. The TACAN has come back in and the time is 1418:00 [1418:04], [1418:15] 322° radial at 90 miles, level at 59K ft, temperature -50°C . . . Turning back to my right [1418:31] to the west to see what's going on there. There is [1422:13] no activity at all right now, nothing. I'll start my slow climb from 59K ft [1422:18]. Heading 225°, on the 312° radial [1422:39] at 82 miles and climbing through 59.5K ft, temperature -48°C. Time is 1422:47 [1422:51] . . . At this time 1433:56 [1434:00], on the 258° radial at 73 n. mi., climbing through 63K ft, temperature -40°C, heading 160°. I'm going to make a right turn and go back in a northerly direction [1434:21]. I'm on a heading of 015°, on the 260° radial at 83 n. mi. [1439:38], the time is 1439:38 [1439:42] and I'm climbing slowly through 65.7K ft, temperature is -38°C and this Mach hold doesn't seem to be doing too well, up and down, up and down, and I'm on the very edge now [1442:44]. About 68K ft [1445:11] and speed dropping off so I've eased her over [1447:12]. Speed and altitude are all over the place; I'm getting a little bit of turbulence now at 65.6K ft [1447:18], light to moderate turbulence and I was all over the sky, Mach hold [autopilot control] was trying to chase it, and I guess it was due to some small lift . . . [1448:31] turbulence that I just experienced a few minutes ago. On the 305° radial [1448:39] at 75-76 n. mi., and I guess it took me up to 68K ft and down to about 65.5K ft and I was climbing there with speed actually increasing, so I was getting a bit of airplane buffet. The time is 1449:50 [1449:55] and there's just no activity from what I can see and just the remains of an occasional one that was up there or didn't quite make it through the cirrus. I'm back down to 63K ft, time is 1454:23 [1454:28] and I'm attempting a slow climb up to 68K ft, where I shouldn't have been, and I'll come down in levels this time, stay at 63K ft [1454:58] awhile, come down to 60K ft and so on, down until I get to the cirrus tops again [1502:00]. Not much going on, still at 63K at 257° radial at 70 miles; time is 1502:45 [1502:45], temperature is -40°C and I may as well start a very slow descent from this altitude. On the 245° radial from Howard at 79 miles; time is 1505:37 [1505:42] very slowly descending through 61.9K ft at the moment, temperature is -40°, -48°C and turning slowly right to a northerly heading again. On the 264° radial at 81 miles; heading 020°, time is 1513:46 [1513:50] just descending very slowly through 60K at this time. Off to my left, about a mile, I guess, the remains of one that punched up and collapsed or didn't quite make it at all. 1521:00 exactly; I'm on the 297° radial at 73 n. mi. from Howard and descending through 56.5K ft [1521:18]; just experienced a little bit of turbulence, and temperature is -50°C and nothing going on. I'm slowly descending through 53.1K ft, time is 1527:52 [1527:56], TACAN's gone out again, and I'm about on the 300° radial [1528:11] now to Taboga at about 86 n. mi. Still no activity; some remains of some, not much to the southwest of me [1528:25]. I'm into the top of that cirrus again, it's about 52K ft and a light to moderate turbulence at this time [1531:55], -51°C, at 310° radial, somewhere about 70 or 80 miles. Coming through 53K ft [1534:19], temperature -55°C, guess that's just about where the trope is and I guess I'm looking at some thin cirrus, I might be in it, actually I can't really tell [1534:36]. Time is 1534[35 [1534:40], somewhere on the 270° radial at about 60 miles out of Taboga. We're coming through [1536:03] 49.3K ft, temperature -54°, -55°C again. Time 1536:06 [1536:10] I think I came through a little bit of cirrus

which is about the basic level at the tops of the cirrus . . . a thin sheet sitting above the main cirrus [1536:32].

APPENDIX D

GEOPHYSICAL RESEARCH LETTERS

VOLUME 9, NUMBER 6, JUNE 1982

Geophysical Research Letters

Volume 9 Number 6 June 1982
GRLAJ 9(6) 599–730(1982)
ISSN 0094-8276

NASA Water Vapor Exchange Experiment

SPECIAL ISSUE ON

NASA EXPERIMENT ON TROPOSPHERIC-STRATOSPHERIC WATER VAPOR TRANSPORT IN THE INTERTROPICAL CONVERGENCE ZONE

GUEST EDITORIAL

The following six papers report preliminary results obtained from a field experiment designed to study the role of tropical cumulo-nimbus clouds in the transfer of water vapor from the troposphere to the stratosphere over the region of Panama. The measurements were made utilizing special NOAA enhanced IR satellite images, radiosonde-ozonesondes and a NASA U-2 aircraft carrying nine experiments. The experiments were provided by a group of NASA, NOAA, industry, and university scientists. Measurements included atmospheric humidity, air and cloud top temperatures, atmospheric tracer constituents, cloud particle characteristics and cloud morphology. The aircraft made a total of eleven flights from August 30 through September 18, 1980, from Howard Air Force Base, Panama; the pilots obtained horizontal and vertical profiles in and near convectively active regions and flew around and over cumulo-nimbus towers and through the extended anvils in the stratosphere.

Cumulo-nimbus clouds in the tropics appear to play an important role in upward water vapor transport and may represent the principal source influencing the stratospheric water vapor budget. The clouds provide strong vertical circulation in the troposphere, mixing surface air and its trace materials (water vapor, CFM's sulfur compounds, etc.) quickly up to the tropopause. It is usually assumed that large scale mean motions or eddy scale motions transport the trace materials through the tropopause and into the stratosphere where they are further dispersed and react with other stratospheric constituents. The important step between the troposphere and stratosphere for water vapor appears to depend upon processes occurring at or near the tropopause at the tops of the cumulo-nimbus towers. Several processes have been suggested:

(1) The highest towers penetrate the tropopause and carry water in the form of small ice particles directly into the stratosphere.

(2) Water vapor from the tops of the cumulonimbus clouds is transported somehow through the tropopause, the vapor pressure being controlled by the temperature at the tops of the clouds; the dryness of the stratosphere could be explained if most of the transport occurs in connection with very high clouds in regions with very high (and cold) tropopause.

(3) Cumulo-nimbus anvils act as terrestrial-radiation shields allowing the ice particle temperatures near cloud tops to cool radiatively below the supersaturation point; this cooling would cause a vapor deposition on the ice particles which will settle out and thus act as water scavengers.

The experiment was designed to collect information on these detailed physical processes near and above the tropopause in order to assess their importance and the role they play in controlling stratospheric water vapor humidity.

William A. Page
Space Science Division
NASA Ames Research Center
Moffett Field, CA 94035

(Received December 23, 1981;
accepted May 6, 1982.)

Paper number 2L0771.

GEOPHYSICAL RESEARCH LETTERS, VOL. 9, NO. 6, PAGES 601-604, JUNE 1982

STATISTICS OF COLD CUMULONIMBUS ANVILS BASED ON ENHANCED INFRARED PHOTOGRAPHS

Edwin F. Danielsen

NASA-Ames Research Center, Moffett Field, California 94035

Abstract. Infrared photographs from the Atlantic Geosynchronous Satellite, enhanced to resolve cold anvil temperatures of tropical clouds, are analyzed statistically to determine their spatial-temporal variability during the NASA-U2 Flight Experiment of 1980. Diurnal dependence varies regionally, indicating topographic control via low level convergence and release of convective instability. Anvil growth rates, area covered and duration are discussed for individual and merging anvil systems. Gradients of anvil temperatures implied by infrared photographs are shown to be caused, in part, by radial decrease in anvil depth, i.e., to emissivities less than 1. An error in cloud top temperature of 10C is caused by 10% reduction in emissivity. Errors are near zero in dense, actively growing portions of the anvil.

Introduction

A major objective of the 1980 Panama Experiment was to obtain in situ and remote measurements from the U2 aircraft before, during and after cumulonimbus turrets penetrated the lower stratosphere to assess their potentials for hydrating or dehydrating the stratosphere. Dehydration to the observed 3ppmv requires cloud top temperatures <-83C at pressures <100mb (see Danielsen, 1982 for a proposed mechanism). Infrared temperatures <-70C are considered statistically significant here on the basis of direct comparisons with in situ measurements.

To aid in forecasting the U2 operations and interpreting aircraft measurements, arrangements were made with Don Gaby of the National Environmental Satellite Service, Miami, FL, to have direct access to infrared cloud photographs. These photos, centered at 8N and 78W depicting the clouds in the operational area, were obtained every half-hour on a noninterference basis. The enhancement curve chosen from those available provides the best resolution of cold clouds. An example is shown in Fig 1 which includes for reference the coastal outline of lower Central America and northwestern South America.

Enhanced Infrared Photographs

Figure 1 contains three large anvils readily identified as a white area surrounded by a band of black, light, medium and dark grey. The corresponding equivalent black body temperatures (EBBT) at the transitions are -70, -64, -53 and -42C respectively (note scale at base of Table 1). Inside the white area the transition to light grey is -76C and that from light to dark grey is -82C. No colder EBBT's are resolved. These photos, providing approximately 8 km resolution, permit analyses of the area covered by anvils whose EBBT's are colder than a given threshold. Statistical analyses were made for thresholds of -70, -76 and -82C in each of 9 areas delineated and identified by two letters in Fig 1.

Anvil Statistics

Briefly, each region has its own diurnal dependence. The north continental (NC), including mountains and valleys of Columbia and part of Venezuela, has two distinct maximums. Following a minimum at local noon, the percentage area occupied by EBBT <-70C increases to a maximum of 6% just after sunset. Surprisingly, another maximum of 6%, but longer in duration, develops after 10 pm local time and maximizes at about 3 am local time. These storms, developing large, cold anvils, form in the river valleys, probably as a result of nocturnal cooling on the slopes. The drainage flows converge in the valleys where the forced ascent releases the ever present convective instability.

After sunrise, when drainage ceases, these clouds rapidly dissipate and new storms form over the adjacent oceans. Thus, the distribution over the Gulf of Panama is almost the inverse of that over the north continent, except that the maximum at 4% is of longer duration. The Isthmus of Panama follows the trend of the Gulf of Panama, delayed by 2 hrs, until noon. Then a sharp maximum develops in the late afternoon, reaching 14% at 4 pm local and decreasing to near 0 within 3 hrs.

Despite small changes in temperature and water vapor during the experiment, some days were very active and others were virtually cloud free. Notable examples in Fig 2 are Aug 30 and 31 and Sept 3-5. During these days the diurnal cycle was supressed. Since the lower atmosphere was always convectively unstable, supression of convective clouds implies low level convergence and subsidence. Local oscillations in low level divergence can be induced by easterly waves propagating along the Intertropical Convergence Zone (ITCZ), but no waves were detected during these days. Instead, tropical storms (two reached hurricane intensity), developing and moving northwestward in the eastern Atlantic, modified the flow, essentially eliminating the ITCZ over South America.

Anvil Evolution

The advantage of a weak ITCZ is a reduced tendency for cloud clustering and multi-anvil merging, permitting individual anvils to be studied for growth rates and duration. Despite weak initiating convergence, large storms do develop, as shown in Fig 1. The Lagrangian his-

Paper number 2L0463.

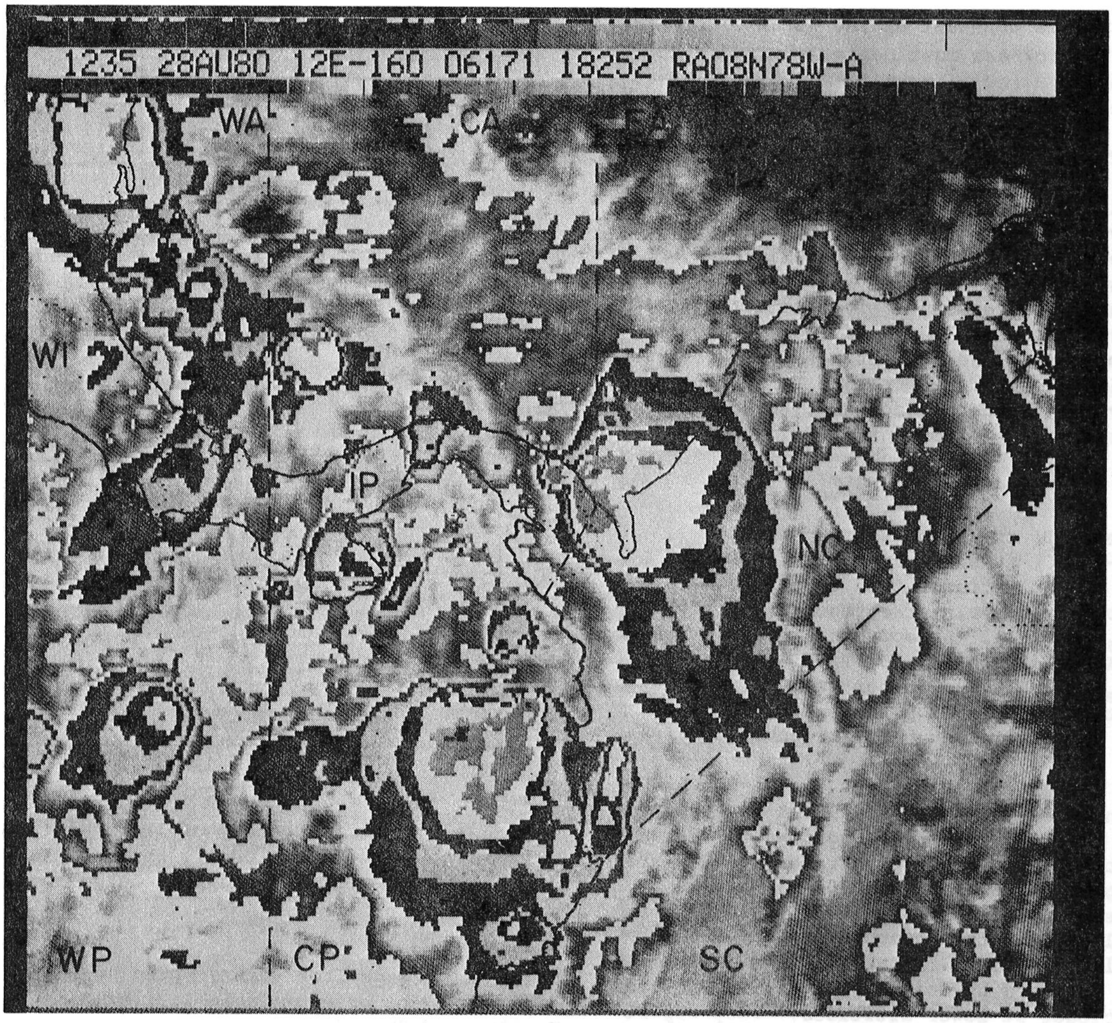

Fig. 1. Enhanced infrared photo of clouds over Isthmus of Panama and northwestern South America. Cold anvils evident by transition from black to white (T = -70C), white to light grey (T = -76C) and to dark grey (T = -82C). Dashed lines and continental boundaries define areas for cloud statistics.

tory of one (located at the eastern end of the Isthmus in Fig 1), is plotted in Fig 3. A total of more than 20 anvils, each having a duration of 3-5 hrs, merge successively, extending duration of the anvil system to >12 hrs. Comparisons of infrared and visible (1 km resolution) photographs indicate new anvils are generated from turrets sometimes contiguous, sometimes completely separated from the main cloud.

New turrets probably develop in convergent flow along the leading edge of a precipitation induced downdraft from the parent storm. By this process the storm becomes self sustaining, as do large cumulonimbus in the extratropics. An example is evident in Fig 1, where anvil 8 of Fig 3 appears as a small circle on the west flank of the large anvil. Note, this small anvil is light grey, i.e., <-76C. Note also, it is close to the coldest dark grey point <-82C in the large anvil.

The sequence of infrared photographs for this and all other days consistently indicates the coldest EBBTs where new anvils are forming and merging with the large anvil. As the anvil grows its edges develop a large apparent temperature gradient. An analysis of the growth of anvil 2 (Fig 3) yields a decreasing horizontal divergence from a maximum of $7.4 \times 10^{-4} s^{-1}$ at 0530 UT to $1.3 \times 10^{-4} s^{-1}$ at 0900 UT. This decrease, inversely proportional to anvil radius, implies a constant radial velocity of $6.6\ ms^{-1}$.

EMISSIVITY	1.0	0.98	0.96	0.92	0.84	0.68	0.36
APPROXIMATE ANVIL DEPTH	∞		1.5	1.1	.85	.6	.3 KM
225	190	190.9	191.8	193.6	197.0	203.2	214.3
250	190	191.9	193.7	197.2	203.6	215.1	233.4
275	190	193.1	196.1	201.7	211.7	233.1	253.5
300	190	194.8	199.2	207.3	221.1	239.8	272.2
T_o	D.GREY	L.GREY	WHITE	BLACK	L.G.	M.G.	D.G.
	-82	-76	-70	-64	-53	-42	-30 C

Table 1. Variation of infrared derived anvil temperature T_S with emissivity and temperature of lower level source T_0 for constant anvil top temperature of 190K. Grey scale and centigrade temperatures refer to transitions in Fig 1.

If the latter is constant as the radius increases, the anvil's thickness must decrease outward to assure a bounded radial mass flux. Indeed, such a decrease is implied by the name anvil.

Effects of Cloud Emissivities <1

As anvil thickness decreases radially the emissivity ϵ of the cirrus cloud must decrease also. The EBBT is obtained by assuming ϵ=1, but if ϵ<1 a systemmatic error is introduced. When ϵ<1 the satellite sensor receives some radiation emitted from the cloud and some from the lower, warmer atmosphere. We can estimate the error in the satellite derived temperature T_s by considering only two isothermal sources, the cloud at T_c and the warmer environment at T_0. Then

$$T_s^4 = \epsilon T_c^4 + (1-\epsilon)T_0^4 \tag{1}$$

Dependence of T_s on T_0 and ϵ for constant T_c=190K (-83.2C) is shown in Table 1. This temperature, slightly colder than the minimum in the enhancement curve, is representative of the coldest T_s in Fig 1. An appropriate value for T_0 is 275K, thus when ϵ=0.96, $T_s-T_c \simeq 6K$ and when ϵ=0.91, $T_s-T_c \simeq 13K$. The latter value of ϵ corresponds to the transition from white to black in Fig 1, the limit used here for anvil statistics.

During the flight of Sept 12 the U2 descended to skim an anvil top where T_c=190±2K were observed by the airborne sensor. According to the infrared photograph, the U2 penetrated a white area indicating T_s between 197 and 203K. The ice crystals encountered are reported by Knollenberg et al., (1982) and the water vapor equivalent by Kley et al., (1982). Similar ice crystal loadings were measured by Griffith et al., (1980) in tropical clouds at lower altitudes. They report ϵ increasing from 0 at cloud top to 0.5 at a depth of 400m, increasing more slowly to 0.9 at a depth of ~1km. Their values are used to approximate anvil depths in Table 1. With the aid of these values realistic anvil shapes are deduced from the infrared photographs encompassing

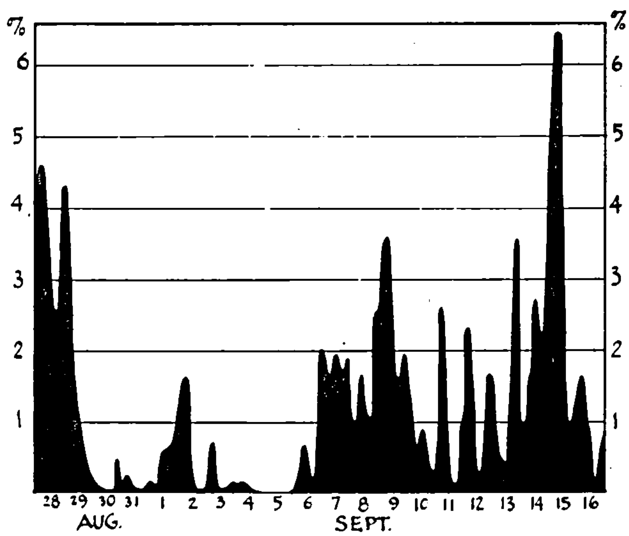

Fig. 2. Percentage of area of Fig 1 covered by clouds colder than -70C based on non-overlapping 4 hr averages.

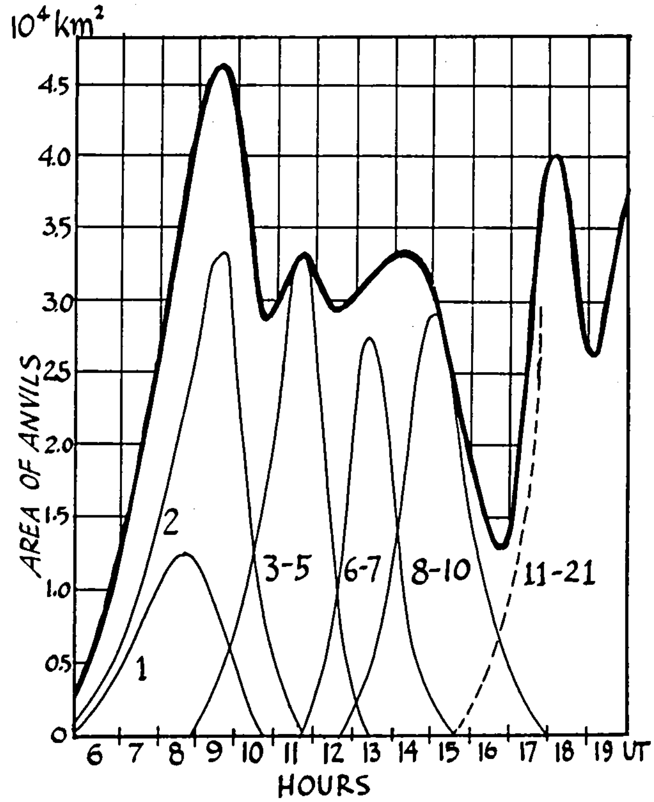

Fig. 3. Growth and decay of large anvil near Panama (see Fig 1 and text). Numbers refer to anvils which merge to maintain large anvil.

the entire range from dark grey to dark grey indicated at the base of Table 1, i.e., from T_s=190 to 250K. Conversely, if the EBBT's were converted to heights by assuming ϵ=1, the cloud top would be shaped like an umbrella, not an anvil.

Conclusions

The large, cold cirrus anvils (>200 km in diameter) observed in the tropics near Panama (by infrared photographs transmitted from the Atlantic Geosynchronous Satellite) are produced by the release of convective instability in the near surface air. Temperatures colder than -82C, determined occasionally and intermittently by satellite retrieval, are shown by direct in situ measurements made aboard the U2 to be representative of those at the anvil's upper surface. Warmer infrared temperatures and gradients in the anvil are due in part to emissivities <1, to gradients in anvil depth. The anvil's base tapers to zero thickness at its maximum radius, thus radiance received at the satellite includes an increasing component with increasing radius from lower, warmer clouds or the earth's surface. The anvils are maintained for several hours by the successive development of new storms whose anvils merge with the older anvil. Maximum percentage area of about 14% occurred over Panama. The secondary but more repeatable maximum developed during the late night over the river valleys of Columbia.

Acknowledgments. The author thanks the entire staff of the NOAA, National Environment Satellite Service, Miami, Florida, and especially Don Gaby, for their excellent cooperation.

References

Danielsen, E. F., A dehydration mechanism for the stratosphere, Geophys. Res. Lett., 1982, (same issue).

Griffith, K. T., S. Cox and R. Knollenberg, Infrared radiative properties of tropical cirrus clouds inferred from aircraft measurements, J. Atmos. Sci., 37, 1077-1087, 1980.

Kley, D., A. Schmeltekopf, K. Kelly, R. Winkler, T. Thompson and M. McFarland, Transport of water through the tropical tropopause, Geophys. Res. Lett., 1982, (same issue).

Knollenberg, R. G., A. Dascher and D. Huffman, Measurements of the aerosol and ice crystal populations in tropical stratospheric cumulonimbus anvils, Geophys. Res. Lett., 1982, (same issue).

(Received December 23, 1981; accepted March 15, 1982.)

GEOPHYSICAL RESEARCH LETTERS, VOL. 9, NO. 6, PAGES 605-608, JUNE 1982

A DEHYDRATION MECHANISM FOR THE STRATOSPHERE

Edwin F. Danielsen

NASA-Ames Research Center, Moffett Field, California 94035

Abstract. Although mean circulations are generally credited with dehydration of the earth's stratosphere, convective instability in the tropics converts mean circulations to small residuals of local convective circulations. The effects of large cumulonimbus which penetrate the stratosphere and form huge anvils in the lower stratosphere are discussed with respect to hydration and dehydration of the stratosphere. Radiative heating at anvil base combined with cooling at anvil top drives a dehydration engine considered essential to explain the dry stratosphere. Seasonal and longitudinal variations in dehydration potentials are examined with maximum potential attributed to Micronesian area during winter and early spring.

Introduction

Stratospheric air is characterized by extreme dryness, water vapor mixing ratios 3-6 ppmv, despite mounting evidence that a substantial fraction of its mass is exchanged each year with the moist troposphere. Intermittent outflows from the lower polar stratosphere at extratropical latitudes are thought to be compensated by quasi-steady inflows of ascending air in the tropics. Dehydration of the ascending air by ice crystal formation and precipitation is then invoked to explain the dryness. These concepts, requiring extremely cold temperatures are qualitatively consistent because the coldest tropospheric temperatures are observed in the tropics. The zonally symmetric Hadley circulation is a logical candidate for the inflow but it fails quantitatively because zonal mean temperatures are not cold enough. Recently Newell and Gould-Stewart (1981) proposed using monthly mean temperatures to identify the inflow area and compute the mean ascent rates. Their criterion satisfies the necessary condition of cold temperatures but does not assure a sufficient condition, that slow mean ascents are physically realizable. For example, if the mean circulations are but small mathematical residuals of much larger local convective circulations, the actual dehydration processes could be physically independent of the mean motions. Since large, tropical cumulonimbus clouds function like atmospheric elevators, rapidly transporting near surface air upward to the lower stratosphere, they are local centers of action for cloud microphysical processes, mass transfer, mixing and radiative processes in the tropics. For these reasons they were the object of this experiment and focus of this study.

Paper number 2L0212.

Effects of Convective Instability

Tropical tropospheric temperatures are characterized by small deviations from zonal or temporal means. Larger deviations are observed in water vapor mixing ratios X_v, but the lower troposphere is almost always convectively unstable. Its inevitable effect is to destroy homogeneous material circulations by amplifying small deviations, converting them to larger and larger cloud driven local circulations. Small, buoyant plumes coalesce to form cumulus updrafts; cumulonimbus clouds converge to form cloud clusters.

We can take advantage of small deviations and consider mean $\bar{T}$ profiles as representative of an undisturbed state. Then, disturbing effects of large cumulonimbus clouds can be analyzed by simulating the release of instability caused by low level convergence. Since maximum T and X_v occur close to the surface, maximum potential energy for cumulonimbus development is released by air ascending from the surface. We will consider first an isolated parcel to identify the energy source and its effects, then correct these for interactions imposed by mass continuity and friction.

As the parcel ascends it cools by expansion, causing water vapor to condense. The heat released reduces the rate of cooling with height such that the parcel's temperature is warmer and less dense than its environment throughout the troposphere (see Fig 1). Positive buoyancy forces accelerate the parcel to its maximum velocity at the equilibrium level. There the parcel overshoots until negative buoyancy decelerates it, first stopping, then reversing its direction of motion. If it were an isolated parcel it would oscillate about its equilibrium level. The stratospheric penetration would be transient and reversible. No mass transfer would occur.

Stratospheric Anvil Formation

When a parcel moves upward continuity requires that air above it be accelerated up and away from its path, while air beneath it converges and ascends to follow. Work done in generating these convective circulations reduces the mean kinetic energy of the resulting updraft but doesn't significantly alter the equilibrium level. The most important differences are caused above the equilibrium level by entrainment and mixing of environmental air, frictionally induced during rapid deceleration of cloud turrets. Entraining and mixing with warmer stratospheric air, the mean temperature in the turret increases, its maximum height decreases and its equilibrium level rises above that for an isolated parcel. As shown in Fig 2a, the collapsing turret and the still ascending air beneath it must diverge horizontally to form a large anvil cloud of ice crystals in

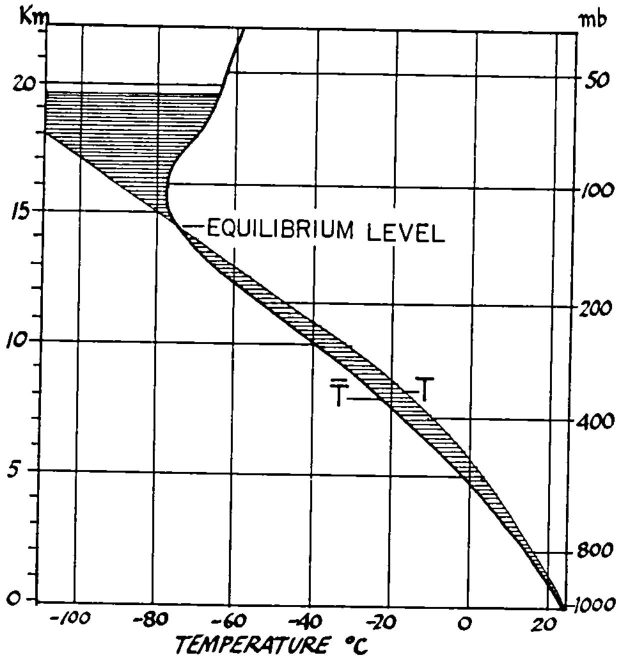

Fig. 1. September 1980 monthly mean temperature, $\bar{T}$, and temperature of ascending air parcel. Small positive deviations below equilibrium level are balanced by large negative deviations in the stratosphere.

the stratosphere. Assuming these two turbulent flows will mix, as well they must, the temperature profile in the anvil will approach an adiabatic gradient -10C km^{-1}. Correspondingly large positive gradients will then join the anvil temperatures to that of the less disturbed environment.

The predicted profile would include two minimums in T, one closely related to the mean tropopause, the other 1 to 2 km higher in the stratosphere. Plotted with the predicted profile in Fig 2b are observed temperatures from the U2 flight of Sept 12. The predicted profile is confirmed. Minimums in T and χ_v are at the anvil's top. See Knollenberg et al., (1982) and Kley et al., (1982) for ice crystal and water vapor measurements.

Potentials for Hydration or Dehydration

The mixture of tropospheric and stratospheric air in the anvil has potentials to hydrate or dehydrate the lower stratosphere. An immediate effect depends upon the difference between χ_v in the anvil and χ_{vs} in the stratospheric environment. If $\chi_v > \chi_{vs}$ some of the smallest ice crystals will evaporate, hydrating the entrained stratospheric air. Measurements by Kley et al., (1982) support this effect, indicating a relative maximum of χ_v at the heights of the penetration anvils. Thus the potentials for hydration are apparently realized.

However, we must consider also the potentials for dehydration, which are complicated by radiative effects of ice crystals in the anvil. Comparisons between observed and satellite infrared cloud temperatures indicate emissivities >0.9 for large portions of the anvil (Danielsen, 1982). These emissivities imply radiative cooling rates of 10-15C day^{-1} for the anvil top because the upward flux from the warmer lower troposphere is blocked. Similar rates are computed by Griffith, Cox and Knollenberg (1980) for comparable ice crystal concentrations.

Radiative cooling reduces the saturation χ_v, but induces subsidence and compressive warming. If the latter balances radiative cooling, the net effect would be to lower the elevation of the anvil and decrease the potential temperature of the mixture. This downward trend is opposite to that required to explain the dry air observed several kilometers higher in the stratosphere by Kley et al., (1979; 1980). An alternate balance is required.

A Dehydration Engine

A characteristic of tropical cumulonimbus (Danielsen, 1982) is their extremely large anvils, areas $\gtrsim(200\ \text{km})^2$, which persist for 5-10 hrs. most of the anvil extends well beyond the cumulus which feeds it, therefore, the anvil base is exposed to upward radiation emitted at warm temperatures. Radiative warming at the anvil base will accompany radiative cooling at the top. The combined effect is to maintain static instability and buoyancy generated turbulence in the extended anvil.

The associated turbulent heat flux carries energy absorbed near the base to the top where it is radiated to space. For an anvil ~1 km deep a cooling rate of 10C day^{-1} at the top can be maintained by $\overline{w'T'}$ = 5C cm s^{-1} at the center of the layer. If w', vertical velocity deviation, and T' were perfectly correlated, T' need not exceed ± 0.1C for w'≈ ± 50 cm s^{-1}. A correlation as small as 0.25 is compatible with w' = ± 2m s^{-1}, the value produced by 0.1C buoyancy acting over 0.5 km. As in a turbulent boundary layer, the temperature deviations need not be large.

In marked contrast, χ_v' and $\overline{w'\chi_v'}$ will be large because the anvil's base temperature is 10C warmer than its top. Assuming saturation with respect to ice and χ_v = 4 ppmv at the top, $\chi_v \simeq 12$ ppmv at the base. The resulting upward flux will produce supersaturation with respect to both water and ice near the top. New ice crystals will rapidly form there; any larger crystals carried upward will grow. The latter, accelerating down-

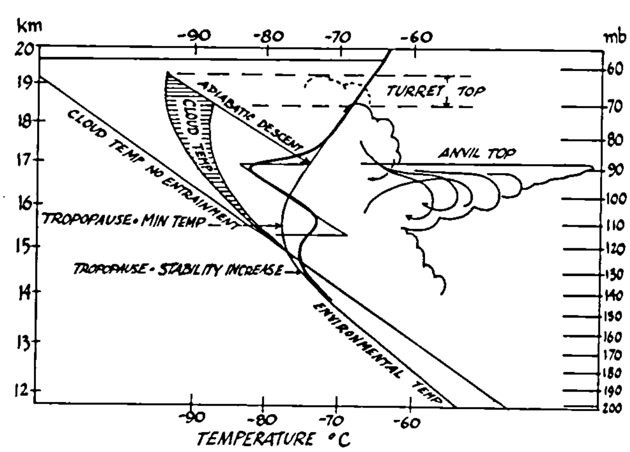

Fig. 2a. Anvil formation in stratosphere due to entrainment and mixing of stratospheric air in overshooting turret. Predicted temperature profile (heavy line) includes two minimums.

ward where w' <0 will be ejected from the cloud's base without a significant mass loss by evaporation. The circulating small crystals will have time to grow and sustain the ejection process.

Functioning as a thermally driven engine, the heat and vapor fluxes are upward, the ice crystal flux is downward. In principle, the process could continue until X_v approaches the minimum value, i.e., the value at the top. However, as the density of crystals decreases below some critical value, each of the crystals will warm by absorbing the radiation from below (Knollenberg, private communications), the stirring would cease and net heating would produce ascending motions. These trends are in the right direction to account for the dry air above the tropical tropopause.

Regional and Seasonal Dependence

The concepts proposed here of anvil formation and dehydration are based on the assumption that temporal mean soundings can be used to deduce heights and temperatures of large cumulonimbus clouds and their anvils. Using September mean soundings for Panama, anvil tops reaching ~17 km with T (min) ~83 to 84C and X_v (min) ~3 to 4 ppmv are deduced. If we apply the same concepts to other tropical regions or to the same Panama region at other seasons, higher, colder anvils and smaller X_v would be deduced. An examination of monthly mean soundings for 1973-1980, computed by objective error rejection methods at Ames Research Center, confirms colder, lower stratospheric temperatures during N.H. winter than summer, with coldest winter temperatures consistently centered over Micronesia (150E), in agreement with Newell and Gould-Stewart (1981).

Plots of several January mean soundings in Micronesia are almost identical, but consistently different than July-Sept means at Panama; tropospheric temperatures are ~3C warmer, lower stratospheric temperatures are 10C colder. The two mean profiles define the grey area in Fig 3. Perturbed profiles due to penetrating cumulonimbus and anvil formation oscillate about these mean profiles.

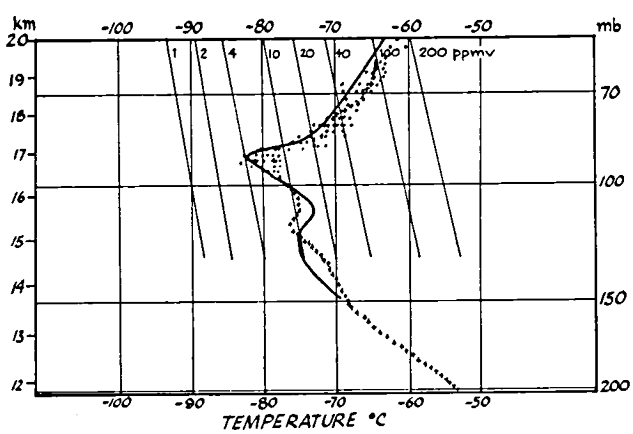

Fig. 2b. Observed temperatures from U2 flight of 12 Sept. 1980 superimposed on predicted profile of Fig 2a. Also included are ice saturation mixing ratio isolines.

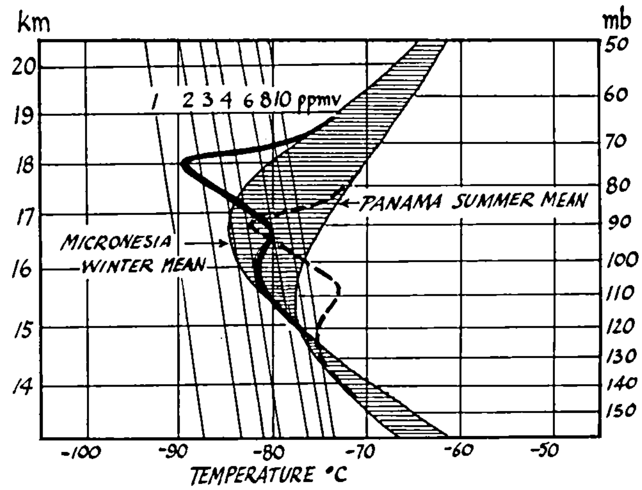

Fig. 3. Comparison of expected anvil temperature profiles based on summer means at Panama and winter means from Micronesia. Toned area represents differences between the two means.

Comparing the perturbed profiles with ice saturation isolines indicates X_v (min) of 3-4 ppmv for the Panama summer and 1-2 ppmv for the Micronesia winter anvils. Values of 2-3 ppmv are deduced for Panama winter soundings. These are compatible with those required to account for the dry stratosphere, providing that the ice crystals' precipitation can reduce the water vapor content of the anvils to these minimums. If they do not, the mean values will exceed those required as indicated by the U2 measurements at Panama. The turbulent heat and vapor flux produced by radiational cooling at cloud top and radiational heating at cloud base is proposed here as the dehydration mechanism.

Conclusions

The ever present convective instability of the tropical atmosphere precludes homogeneous mean circulations, concentrating upward transports into large cumulonimbus clouds, which penetrate the lower stratosphere, entrain warmer stratospheric air and produce large anvils above the mean tropopause. Turbulent mixing during anvil formation generates an adiabatic lapse rate in the anvil and a characteristic temperature profile with two minimums. U2 measurements confirm this profile and comparisons with infrared satellite photos indicate emissivities >0.9 for most anvils. Emissivities this large produce a gradient of radiative heating, heating at base, cooling at top, which keeps the anvil stirred. The resulting turbulent heat flux maintains steady state temperatures but dehydrates the layer. The large, positive vapor flux generates new ice crystals at cloud top and increases the size and mass of larger crystals which fall out. Assuming the dehydration mechanism operates, Panama summer mean profiles are marginally adequate to explain the dry stratosphere. Winter mean profiles are more favorable than summer with optimum profiles in the Micronesian area.

Acknowledgments. The author thanks Steve Gaines and Steve Hipskind for computing the

monthly mean soundings and standard deviations used in this paper.

References

Danielsen, E. F., Statistics of cold cumulonimbus anvils based on enhanced infrared photographs, Geophys. Res. Lett., 1982 (same issue).

Griffith, K. T., S. Cox and R. Knollenberg, Infrared radiative properties of tropical cirrus clouds inferred from aircraft measurements, J. Atmos. Sci., 37, 1077-1087, 1980.

Kley, D., E. Stone, W. Henderson, J. Drummond, W. Harrop, A. Schmeltekopf, T. Thompson and R. Winkler, In situ measurements of the mixing ratio of water vapor in the stratosphere, J. Atmos. Sci., 36, 2513-2524, 1979.

Kley, D., A. Schmeltekopf, K. Kelly, R. Winkler, T. Thompson and M. McFarland, Transport of water vapor through the tropical tropopause, Geophys. Res. Lett., 1982, (same issue).

Knollenberg, R. G., A. Dascher and D. Huffman, Measurements of the aerosol and ice crystal populations in tropical stratospheric cumulonimbus anvils, Geophys. Res. Lett., 1982, (same issue).

Newell, R. J. and S. Gould-Stewart, A stratospheric fountain?, J. Atmos. Sci., 38, 2789-2796, 1981.

(Received December 23, 1981;
accepted February 5, 1982.)

GEOPHYSICAL RESEARCH LETTERS, VOL. 9, NO. 6, PAGES 609-612, JUNE 1982

ALTITUDE VARIATIONS IN STRATOSPHERIC AEROSOLS OF A TROPICAL REGION

Jindra Goodman
San Jose State University, San Jose, CA 95192

K. G. Snetsinger, G. V. Ferry, and N. H. Farlow
NASA Ames Research Center, Moffett Field, CA 94035

H. Y. Lem and D. M. Hayes
EAL Corporation, Richmond, CA 94804

Abstract. To investigate the possibility that significant amounts of tropical tropospheric air may be convectively introduced into the stratosphere, aerosol samplings over Panama were made at various altitudes using a wire impactor collector.

Percentage of particle sizes less than the mean mode decreases with height above the tropopause, suggesting depletion of small particles, possibly due to coagulation. Larger aerosols (greater than 0.3 μm in diam.) are more abundant farther above the tropopause, indicating growth, mainly by condensation. The total particle concentration decreases with increasing height above the tropopause, and also with increasing temperature.

Aerosols containing smaller-size particles are thus found closer to the tropopause, and larger-size, more-evolved aerosols occur at higher altitudes. These data indicate that convective activity at the ITCZ may be a source mechanism for stratospheric aerosols.

Introduction

It has been pointed out that the upward-flowing branch of the Hadley cell moves significant amounts of tropical tropospheric air into the stratosphere [Reiter, 1975]. As argued by Riehl and Malkus [1958], this upward flux of mass does not occur as a continuous relatively slow motion. Instead, updrafts which penetrate through the tropopause into the stratosphere are concentrated in narrow "hot towers" of cumulus convection. If this is the case, and if stratospheric aerosols originate in the troposphere, then one should find a relatively high concentration of small particles in the tropical stratosphere. The Panama Water Vapor Exchange Experiment, 1980, provided an excellent opportunity to test this aerosol evolution theory.

Methods

Aerosol particles were collected in the lower stratosphere by a NASA Ames U-2 aircraft. The sampling device [Farlow et al., 1979] was exposed below the aircraft wing outside the boundary layer, and particles were collected by direct impaction on carbon-coated palladium wires 0.075 mm diameter. A sampling time of 1 min was sufficient to obtain adequate numbers of particles for size distribution analysis. After samples were returned to the laboratory, a scanning electron microscope was used to examine the wire surfaces, at 10,000X. Particle sizes and concentrations were manually determined by photographic methods. Details on efficiency of wire impactor are given by Lem and Farlow [1979]; data reduction methods are in Farlow et al. [1979], and Oberbeck et al. [1981]. Collections were made during the first two weeks of September, 1980, in a rectangular region bounded by 7.5 and 11°N latitude and 77 and 81.5°W longitude.

Paper number 2L0496.
0094-8276/82/002L-0496$3.00

Synoptic Situation

During the period of sampling, equatorial circulation within the Intertropical Convergence Zone (ITCZ), as typically positioned over Panama, was disturbed by several hurricanes in the upstream Atlantic region. The tropopause was typically located between 130 to 110 mb, and pronounced wave motions in the temperature field were observed in the lower stratosphere (Fig. 1). Wave periods averaged 3-3.5 days, with temperature variations of ±5°C. Wind speeds ranged from 3 to 12 m/s with a predominant easterly component in the lower stratosphere. The U-2 aircraft pilots often reported individual cloud turrets penetrating well into the stratosphere, and minimum temperatures were recorded near cells. Above these areas of penetration pilots typically experienced turbulence and/or wavelike motions.

Data Analysis and Results

The objective of this study was to analyze the character and dynamics of growth of stratospheric particles, and correlate the results with possible microphysical processes. Therefore, the data were compiled and presented in a format that helps reveal the effects of these processes. Specifically, plots of radius versus concentration were generated, these being the principal variables. Processes of interest are nucleation, coagulation, condensation, evaporation, and sedimentation, the most important of which in our sampling range ($r > 0.03$ μm) being thermal (Brownian) coagulation and condensation growth. Brownian coagulation, which affects the smallest particles most, causes the concentration of these particles to decrease with time. Condensation growth (or loss by evaporation) is dependent on the water vapor pressure and hence is temperature-dependent; concentration of sulfuric acid vapor is also important. Thus particles can grow or evaporate as conditions vary, and the largest particles can be affected by sedimentation.

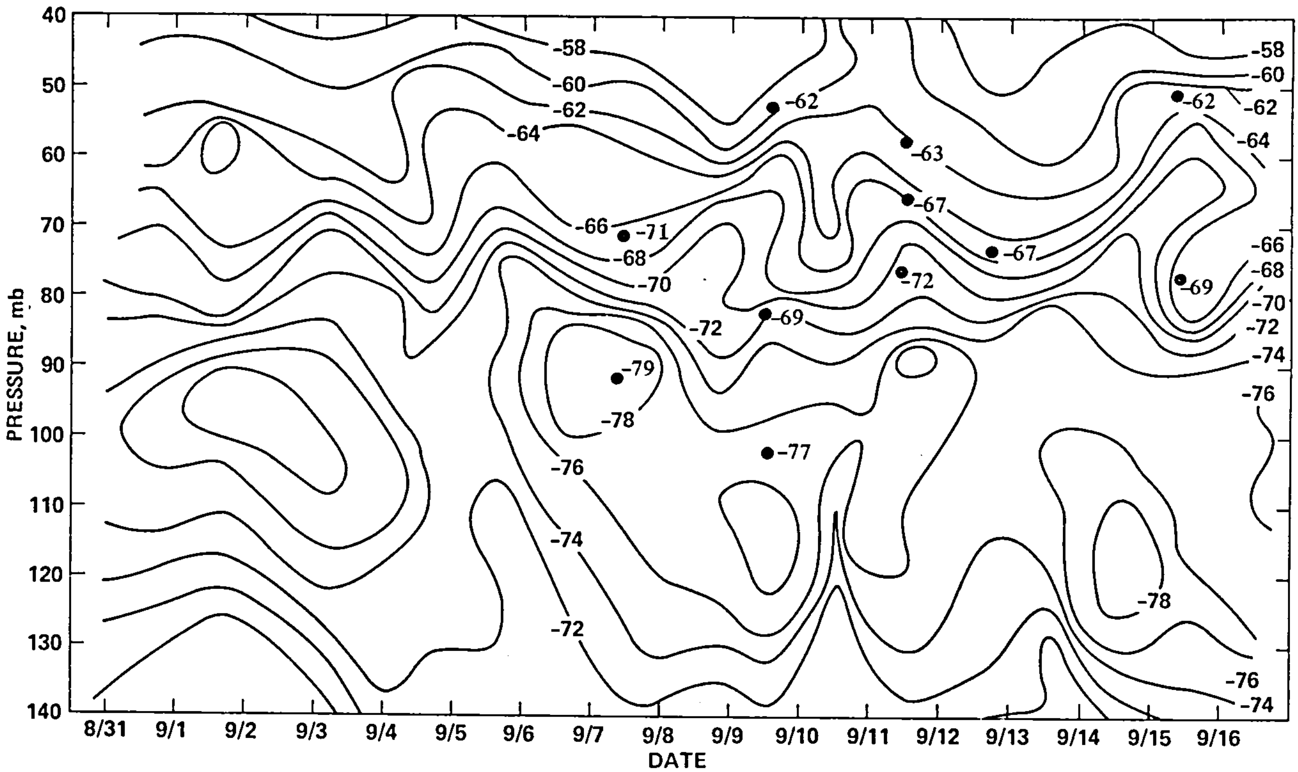

Fig. 1. Vertical cross section of thermal structure of upper troposphere and lower stratosphere at Panama from August 8 to September 16, 1980. Isotherms were constructed from radiosonde data taken 2 to 4 times a day. Dots represented the actual location of aerosol samples, and temperature during sampling is indicated next to the dot. Note wave structure above about 80 mb.

Because all these processes are dependent on environmental conditions and time, aerosol samples were analyzed with respect to temperature and distance from the tropopause. If it is accepted that the tropical troposphere is a source region for stratospheric aerosols, then particles in upper levels should represent more evolved aerosols.

The summer tropical tropopause is the level of the coldest temperature in the lower atmosphere. Temperature increases with height in the lower stratosphere, but also frequently fluctuates ±5°C due to wave motions (Fig. 1). For this reason it is more convenient to study size changes of aerosol particles as a function of temperature, and not use direct distance above the tropopause, as was done by Oberbeck et al. [1981] for polar areas. The samples discussed here were taken in the temperature range from -79.3°C to -61.7°C, and the distances above the tropopause varied between 400 m to 5550 m, respectively. Actual sampling altitude, and temperature at the time of collection are identified in Figure 1, and other pertinent data regarding the samples are shown in Table 1.

Theoretical models [Hamill et al., 1977; Turco et al., 1979; and Toon et al., 1979] assumed that coagulation and condensation are important processes that reduce the number of particles smaller than 0.05 μm radius. The 0.05 μm radius size range roughly corresponds to the statistical average mode of our aerosol distributions. Modes

Table 1. 1980 Panama Aerosol Data

Date	Sampling height (km)	Distance above trop. (km)	Temp. °C	Number >0.03 μm r per cm^3	Number >0.15 μm r per cm^3	Mixing ratio >0.03 μm/mg air	Mixing ratio >0.15 μm/mg air	Ratio >0.15/>0.25	Mass* μg/m^3
9/7/80	18.3	3.3	-79	19.9	3.7	172	32	2.9	0.52
9/7	19.0	4.0	-71	22.3	3.6	214	35	4.4	0.39
9/9	16.0	0.4	-77	18.1	0.9	108	5.0	--	0.10
9/9	17.6	2.0	-69	14.0	2.7	108	21	2.9	0.33
9/9	20.2	4.6	-62	10.0	2.4	116	28	5.2	0.23
9/11	17.8	3.0	-72	18.1	4.1	144	33	3.2	0.63
9/11	18.8	4.0	-67	13.7	2.1	128	20	4.3	0.25
9/11	19.6	4.8	-63	7.6	2.1	80	22	3.9	0.22
9/12	18.3	3.8	-67	15.8	3.5	136	30	2.6	0.52
9/15	17.9	2.8	-69	15.4	3.2	124	26	3.2	0.39
9/15	20.6	5.6	-62	7.2	1.6	91	21	7.3	0.14

*Assumes aerosol content of 75% H_2SO_4.

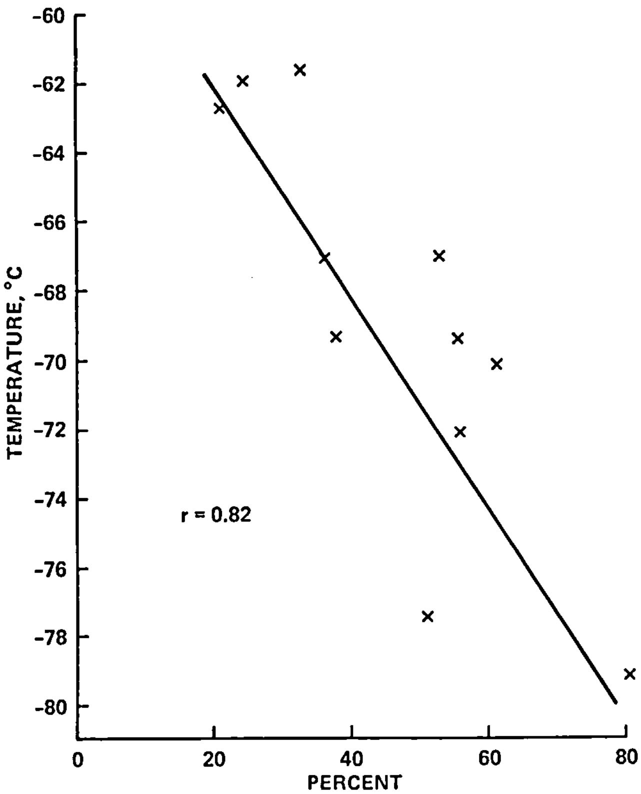

Fig. 2. Normalized distribution of particles with radius less than the mode, plotted against temperature. The coefficient of linear correlation is 0.82.

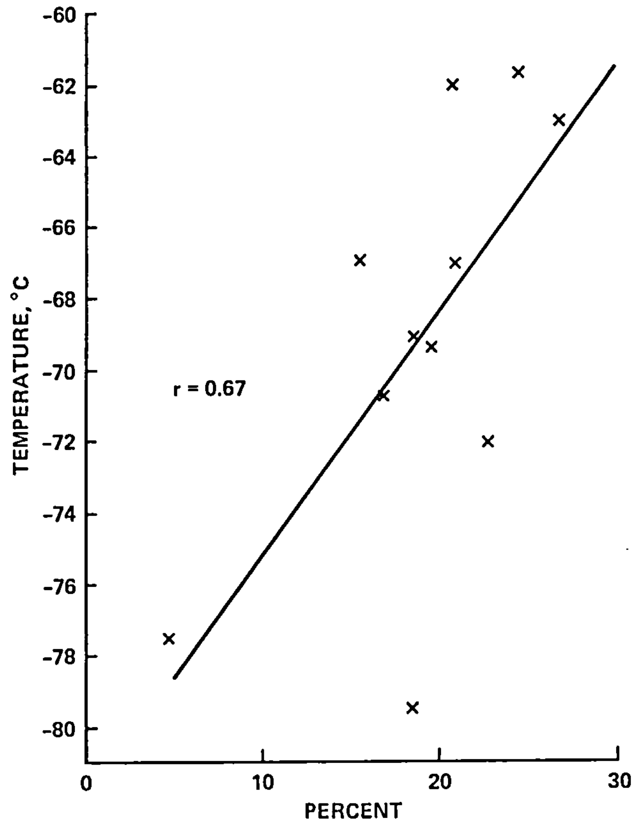

Fig. 4. Normalized distribution of particles with radius larger than 0.15 μm plotted against temperature. The coefficient of linear correlation is 0.67.

of the sampled aerosols ranged from 0.058 to 0.077 μm but did not shift noticeably with altitude. To simplify statistical analysis and avoid additional errors due to slight mode variations, the mean mode 0.069 μm was used. Percentage of particles in the size range less than or equal to the mean mode is plotted versus temperature in Figure 2. The plot shows a decrease in the number of small particles as temperature increases

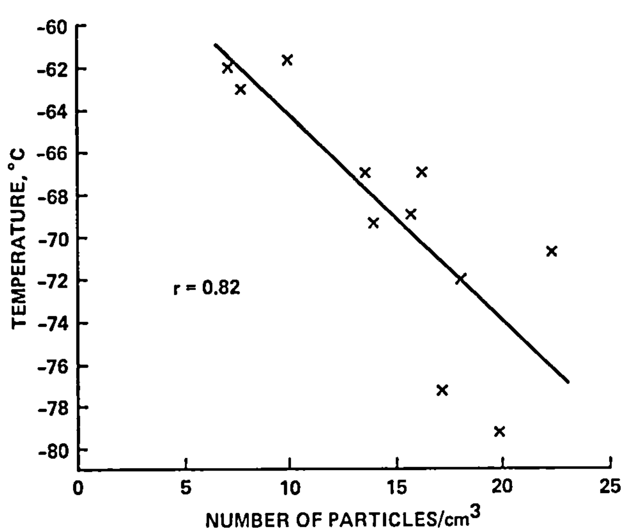

Fig. 3. Variation in total particle concentration plotted against temperature. The coefficient of linear correlation is 0.82.

or as distance from tropopause increases. The correlation coefficient (0.82) is statistically significant at the 1% significance level (analysis of variance test). The data show that there is a significant depletion of small particles. Since the total number of particles decreases (Fig. 3), together with the number of small particles below the mode (Fig. 2), coagulation is the most likely process responsible for this trend of decreasing particle concentration with increasing altitude and temperature.

Concentration variations with temperature of particles larger than 0.15 μm radius were examined; these are affected mostly by condensation growth. The percentage of these larger particles increases with increasing temperature (see Fig. 4), and the correlation coefficient of 0.67 is still statistically significant. The loss of particles due to sedimentation is not an important process here, because of small sedimentation velocities: at 20 km a particle of $r = 0.64$ μm has a sedimentation velocity of only 3.25×10^{-2} cm/s. Typical size distributions of the aerosols, one taken close (0.4 km above) to the tropopause and the other far (5.5 km) from the tropopause, are presented in Figure 5. These graphs also suggest that large particles are more abundant farther above the tropopause.

All the data strongly suggest that particle sizes of stratospheric aerosols increase with increasing temperature (or distance from the tropopause) and are controlled by the microphysical processes of coagulation and condensation.

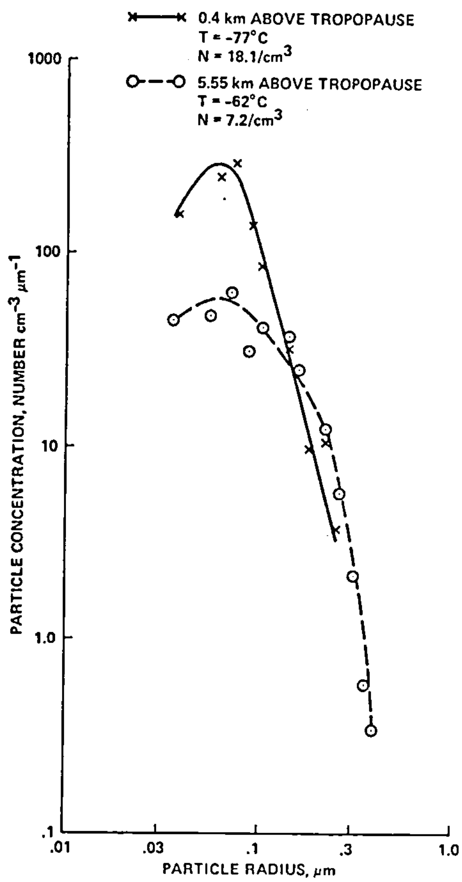

Fig. 5. Stratospheric aerosol size distributions for September 9 and September 15, 1980, over Panama. On September 9, the sampling temperature was -77°C and the distance from the tropopause was 0.4 km; on September 15 sampling temperature was -62°C and the distance from the tropopause was 5.5 km.

Data Comparisons

Because of the differences in aerosol sampling methods it is difficult to directly compare results obtained by different techniques. The results regarding concentration and particle size ratios (Table 1) are, however, consistent with the findings of Farlow et al. [1979] over Panama in 1976 and 1977. Further, concentrations of large particles agree quite well with the results obtained by Rosen et al. [1975], who used a photoelectric particle counter which detects particles having radius greater than 0.15 μm and those greater than 0.25 μm. Analysis of Aitken nuclei (AN) in tropical and subtropical regions by Podzimek et al. [1977] indicated that large fluctuations occurred in the concentration of AN. Sometimes these concentrations exceeded 150 cm^{-3} in the ITCZ region and above mountainous thunderheads, which is further evidence that the tropical troposphere is a source region of stratospheric particles. Our measurements suggest that background concentration of AN was relatively low, rarely exceeding 20 cm^{-3} at 18 km altitude. We were, however, unable to measure particles smaller than 0.03 μm radius.

Compared to other latitudes [Bigg, 1976; Gras and Michael, 1979; Farlow et al., 1979 and 1981; Ivlev and Ogorodnikov, 1975], aerosol size distributions for tropical aerosols show fewer numbers of large particles and higher concentrations of smaller particles.

Conclusion

The Panama aerosol results strongly indicate that convective activity in the ITCZ is a source region for stratospheric aerosols. Young aerosols with high concentrations of small particles are found close to the tropopause; larger, more mature aerosol particles are located at upper levels.

References

Bigg, K. E., Size distributions of stratospheric aerosols and their variations with altitude and times, J. Atmos. Sci., 33, 1080-1086, 1976.

Farlow, N. H., G. Ferry, H. Y. Lem, and D. M. Hayes, Latitudinal variations of stratospheric aerosols, J. Geo. Phys. Res., 84, 33-743, 1979.

Farlow, N. H., V. R. Oberbeck, D. S. Colburn, G. V. Ferry, H. Y. Lem, and D. M. Hayes, Comparison of stratospheric aerosol measurements over Poker Flat, Alaska, July 1979, Geophys. Res. Lett., 8, 15-17, 1981.

Gras, J. L., and C. G. Michael, Measurements of the stratospheric aerosol particles size distribution, J. Appl. Meteor., 18, 855-860, 1979.

Hamill, P., O. B. Toon, and C. S. Kiang, Microphysical processes affecting stratospheric aerosol particles, J. Atmos. Sci., 34, 1104-1119, 1977.

Ivlev, L. S., B. I. Ogorodnikov, Nature of aerosol in the upper atmospheric layers, Meteorologicheshiye Issledovaniya, 22, 26-33, 1975 (in Russian).

Lem, H. Y., N. H. Farlow, Efficiency of aerosol collection on wires exposed in the stratosphere, NASA TR-81147, 1979.

Oberbeck, V. R., N. H. Farlow, G. V. Ferry, H. Y. Lem, and D. M. Hayes, A study of stratospheric aerosol maturity, Geophys. Res. Lett., 8, 18-20, 1981.

Podzimek, J., W. A. Sedlacek, and J. Brookshaberl, Aitken nuclei measurements in the lower stratosphere, Tellus, 29, 116-127, 1977.

Reiter, E. R., Stratospheric-tropospheric exchange processes, Rev. Geoph. and Space Physics, 13, 459-474, 1975.

Riehl, H., and J. S. Malkus, On the heat balance of the equatorial trough zone, Geophysica, 6, 505-538, 1958.

Rosen, J. M., D. J. Hofmann, and J. Laby, Stratospheric aerosol measurements: II — The worldwide distribution, J. Atmos. Sci., 32, 1457-1462, 1975.

Toon, O. B., R. P. Turco, P. Hamill, C. S. Kiang, and R. C. Whitten, A one-dimensional model describing aerosol formation and evolution in the stratosphere: II — Sensitivity studies and comparison with observations, J. Atmos. Sci., 36, 718-736, 1979.

Turco, R. P., P. Hamill, O. B. Toon, R. C. Whitten, and C. S. Kiang, A one-dimensional model describing aerosol formation and evolution in the stratosphere: I — Physical processes and mathematical analogs, J. Atmos Sci., 36, 699-771, 1979.

(Received December 23, 1981; revised March 18, 1982.)

GEOPHYSICAL RESEARCH LETTERS, VOL. 9, NO. 6, PAGES 613-616, JUNE 1982

MEASUREMENTS OF THE AEROSOL AND ICE CRYSTAL POPULATIONS IN TROPICAL STRATOSPHERIC CUMULONIMBUS ANVILS

R. G. Knollenberg, A. J. Dascher, and D. Huffman

Particle Measuring Systems Inc., Boulder, CO 80301

Abstract. A pair of particle size spectrometers was flown aboard the NASA U-2 operating from the Canal Zone to make measurements of the aerosol and ice crystal budgets in cirrus produced by thunderstorms in the tropics. Measurements indicate that fairly large crystals up to 1 mm in size are injected into the stratosphere during cumulonimbus activity. Ice water contents range from a few thousandths to a few hundredths of a gram per cubic meter. Because the ambient temperature is typically around −80° C the mass of the larger crystals largely returns to lower altitudes before evaporating. Aerosol size distributions indicate a curious narrow growth mode between 0.15 and 0.2 μm in cirrus anvils which is absent outside these clouds. The presence of this narrow mode is attributed to near water saturation produced at cloud top. Nucleation of new ice crystals as well as aerosol is hypothesized.

Introduction

The discussion offered by Danielsen (1981, this issue) indicates that ice crystal microphysics plays an important role in water interchange between the troposphere and stratosphere. During thunderstorm activity much larger crystals are lofted to tropopause heights than would normally be expected to grow within the restricted water vapor available at these cold temperatures. Measurements by Heymsfield (1974) in cirrostratus over the Marshall Islands found particles of less than 20 μm diameter at tropopause levels, with ice water contents below 10^{-4} g m^{-3}. The fate of larger cumulonimbus generated crystals could strongly influence whether the net effect of thunderstorms is one of stratospheric hydration or dehydration. Prior to these NASA ARC water vapor exchange experiments (hereafter WVEE) we had little knowledge of the possible ice crystal numbers and sizes, and of the "free air" temperature within the cirrus anvil cloud tops.

That portion of a thunderstorm that actually penetrates the tropical tropopause is limited to the central turret and upper portions of the cirrus anvil. "In situ" measurements in these regions had not been made and their temperatures are available only from satellite remote measurements. However remote measurements are invariably probing below the cloud tops to lower cloud depths and are likely often indicating several degrees warmer than cloud top. As indicated by Danielsen (1972) the tops of active cumulonimbus clouds are several degrees colder than the surrounding air and although negatively buoyant, rise through excess kinetic energy. Radiational cooling is also a factor in further dropping temperatures at cloud top. The crystals at cloud top are effectively shielded from upwelling thermal radiation while receiving a low downward flux. The resulting net radiant losses at cloud top are small but the cooling rate can be appreciable because the volumetric heat capacity of the air is also low. How important such a mechanism is depends upon the particle cross section per unit volume of air and the length of time of particle residency.

The particle size spectrometer experiment flown during the WVEE on the NASA U-2 was primarily designed to provide information on the ice water mass budget at near tropopause levels. For this purpose an imaging instrument called a 2-D Grey Imaging Probe manufactured by Particle Measuring Systems Inc. of Boulder, Colorado was used (Knollenberg, 1976a). This device captures 2-dimensional shadow images of particles and either stores or processes these images as size distribution parameters. The 2-D Grey Imaging Probe covered sizes of 40–2500 μm and operated "in situ", sampling volumes of ~20 ℓ s^{-1}. A second objective of the particle size spectrometer experiment was to quantify the aerosol size distribution, and to define roles it may directly play in assisting the maintenance of a dry stratosphere or as a tracer of other processes operating. The instrument used for aerosol measurements was an "active cavity" aerosol spectrometer (Knollenberg and Luehr, 1974). This aerosol probe employs an active laser cavity and a parabolic collector of large solid angle operating on an aerodynamically focused aerosol sample stream to size particles in a 0.1–3.0 μm size range at sample flows of 2 cm^3 s^{-1}. Data from these measurements was logged on small magnetic tape cassettes, the recording rates programmed for periods up to 8 hours. The entire experiment package was located in the forward half of a wing-tank pod. The imaging probe was mounted in the forward most location in the wing-tank pod with its optical viewing volume ahead of flow disturbance. The aerosol spectrometer drew air samples through a Rosemount air sampling probe which was skin mounted below the wing tank.

Results

The Panama WVEE covered a time period of August 28 to September 22 during 1980. In addition to the eleven flights from Howard AFB, data were taken on the ferry flights to and from Panama. These flights had a number of goals and only a few of the flights were specified for cumulonimbus cirrus penetrations. However, nearly all flights provided cirrus deck penetrations as it is difficult to find days without at least thin cirrus shields. These were, however, typically at altitudes of 12-15 km and well below the tropopause. Flights 7 and 8 on September 12 and 13 both involved cirrus anvil penetrations above the tropopause and provided the bulk of ice crystal data at the higher altitudes (>15 km). We will emphasize the results of these two flights here. Flight 7 revealed 4 cirrus anvil penetrations with 2 of them in a satellite-selected primary cloud target. Flight 8 included 7 penetrations in cirrus anvils. Both flights were approximately 3½ hours in duration; however, data was lost for approximately 50 minutes during Flight 7 which included most of the second pass through the primary cirrus anvil target. The first pass was completely documented.

Since Flight 8 had continuous data and involved the largest number of cirrus anvil penetrations we have presented a selected data set for its full duration, in Figure 1. Figure 1 shows the altitude, temperature, and number and mass densities from the aerosol and imaging probes. Several features of these data are worth amplifying. Take off is obvious from the rapid rise in altitude and drop in aerosol number density from 10^4 down to 1–10 cm^{-3} at 15 km. Penetration through the cirrus deck is indicated by increases in aerosol and imaging probe mass. However

Paper number 2L0300.
0094-8276/82/002L-0300$3.00

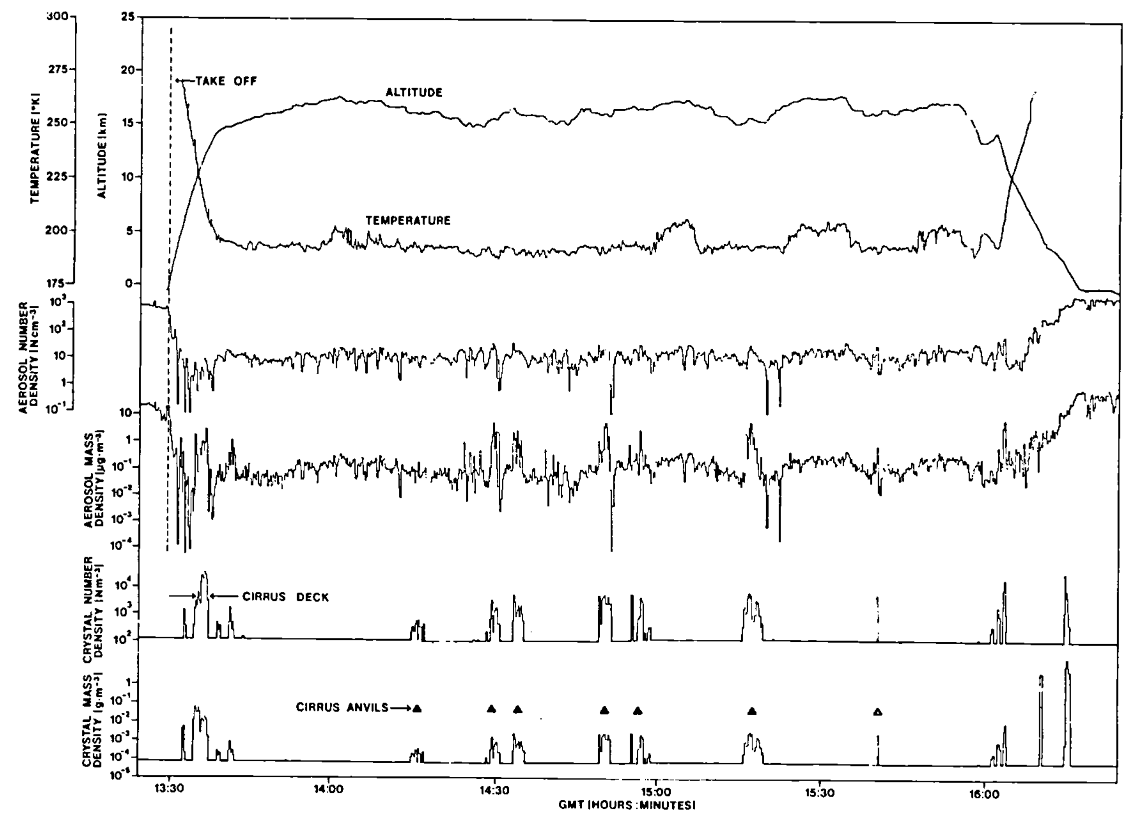

Figure 1. Complete data set for Flight 8. In processing the image data area-to-mass conversions were applied according to Knollenberg (1976). The aerosol mass computations assume spherical particles with $\rho = 2.0$ g cm^{-3}.

note that the aerosol number density is near the minimum values in this region. The slight positive correlation in aerosol and imaging probe number densities is attributed to small ice crystals. The cirrus anvil penetrations, at altitudes of 15–18 km and temperatures ranging from 195–205°K, show lower ice water contents (imaging probe mass density) than during the lower cirrus deck penetrations by approximately an order of magnitude. The values for cirrus anvil penetration are a few hundredths of a gram per cubic meter maximum. Most of the mass was concentrated at sizes less than 100 μm with the largest sizes approximately 150 μm. This contrasts with sizes of 1 mm in the cirrus deck just below. The aerosol populations show only small changes in number density during cirrus anvil penetrations but fairly large increases in mass. The latter is attributed to small ice crystals. Tests of possible fragmentation of ice crystals were conducted in the PMS wind tunnel during December 1981 using natural snow. No fragments smaller than 5 μm were observed using the Rosemount sampler. Thus it would appear that small intact crystals, and not fragments of larger crystals, are responsible for the large particles.

Flight 7 included two penetrations in a cirrus anvil selected as the best sample for extensive study by all experiments. As compared to the penetrations in Flight 8 which involved aged anvils this was a newly formed anvil still growing at penetration time. Only the first of the two penetrations was fully recovered by this experiment. Data for a 10 minute period associated with this cloud are shown in Figure 2. The first penetration was at 16.4 km along the side of the main rising core where the temperature was 194°K. Satellite temperature maps one-half hour before and after the penetrations revealed slow movement to the southwest but with minimum cloud top temperatures of only 197°K. The number density of both ice crystals and aerosol increase within this cirrus anvil; however, the increase in aerosol mass density is largely attributed to crystal contributions. A sample of observed crystal images is shown in Figure 3. Maximum crystal sizes of 1 mm were observed with ice water contents of several hundredths of a gram per cubic meter. [The ice water content here, expressed in ppm, ranges from 200–500 ppm in fairly good agreement with the total water measured by Kley (1981, this issue)]. The crystal mass distribution for the first penetration is presented in Figure 4. The distribution is bimodal with greater mass at sizes above 100 μm than below. The median mass size averages 400–500 μm. The crystal images produced by the imaging probe shown in Figure 3 are identified as column aggregates or rosettes. These are a very common cirrus crystal although active anvils at lower altitudes usually reveal a number of heavily rimmed structures and more frequent graupel.

We also observed several spectral changes in the aerosol population during the anvil penetrations. The increase in the number density of larger aerosol and associated mass is obvious in Figure 2. However, we must disregard aerosol particles larger than 1 μm since ice crystals could contribute to the distribution. At submicron sizes, spectral features are observed which cannot easily be attributed to crystals. The mass mode just prior to penetration is at 0.4 μm which is typical of background stratospheric air (see Figure 4). During the penetration this single mass mode is essentially replaced by a mode at 0.17 μm (excluding values above 1 μm) although remnants of the 0.4 μm mode are still evident. The other spectral features are statistically noisy. The behavior at 0.17 μm appears to be characteristic of the aerosol within anvil cirrus at these altitudes, but not of that in the lower cirrus deck. We were able to find the 0.17 μm mode present during anvil penetrations of Flight 8 as well, but conspicuously absent outside of cloud or in the lower cirrus deck. The overall aerosol population is reduced in the cirrus deck compared to out-of-cloud values. Otherwise there is little

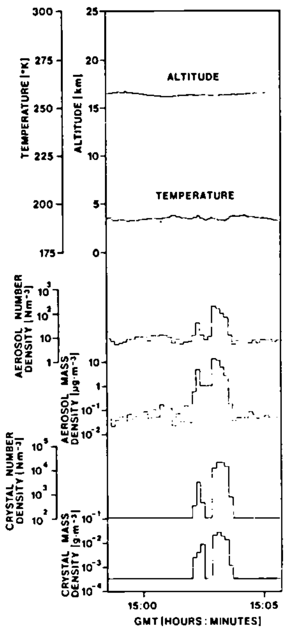

Figure 2. Partial data set for Flight 7. Samples of the ice crystals represented here are shown in Figure 3. In processing the image data area-to-mass conversions were applied according to Knollenberg (1976). The aerosol mass computations assume spherical particles with ρ = 2.0 g cm^{-3}.

difference between in-cloud and out-of-cloud aerosol spectral characteristics.

Discussion

It is important to examine the possible roles played by the ice crystals injected into the stratosphere. Do they evaporate and hydrate the lower stratosphere or do they largely fall out? What is the net flux of ice water mass through the troposphere? Is there sufficient infra-red cross section in the cirrus anvil crystals to provide a radiationally cooled top layer? What possible roles can the stratospheric aerosol play? Certainly with regard to the ice crystals samples we do not have sufficient cloud samples to offer statistical evidence of their behavior. This limited data set does however contain clues as to operative mechanisms and in this section we will discuss their relevance to the above posed questions.

A knowledge of crystal growth (evaporation) rates and terminal velocities is required to predict the ultimate fate of the observed ice crystals. Table 1 lists computed values for spheres,

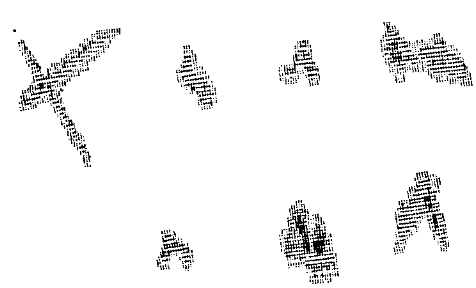

Figure 3. Image samples from Flights 7 and 8. The top four images are from Flight 7 while the lower three images are from Flight 8. Maximum crystal length is 1.3 mm and maximum equivalent circle diameter observed was 1.0 mm.

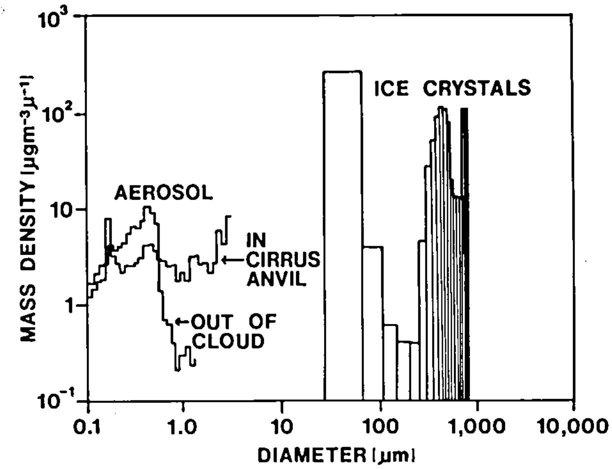

Figure 4. Ice crystal and aerosol mass distributions for Flight 7. The bimodal crystal mass distribution actually represents 2 separate regions of the cloud pass. However, the strong aerosol mode at 0.17 μm is characteristic for the entire pass length. The out-of-cloud sample was an average at the same altitude.

column aggregates, and thick plates. For computational purposes we have assumed a vapor density of ± 50% from saturation, at a temperature of 193°K (−80°C). Thus growth rates represent humidity values close to water saturation, while evaporation represents the approximate undersaturation values for ambient stratospheric air. An examination of Table 1 reveals that growth and evaporation processes are low while terminal velocities are significant. The majority of the mass of these crystals would be expected to return to lower altitudes. The core of the rising turret is above ice saturation until subsaturated stratospheric air is entrained. An approximate value of this entrainment has been determined by comparing the relative contribution of aerosol in the 0.4 μm mode inside and outside of cirrus anvil clouds. This estimated value is 40%. It would thus not be unreasonable for this mixed volume to be fairly close to ice saturation since at ice water contents of 10^{-2} g m^{-3} less than 5% of the mass would have to evaporate to saturate the air.

Perhaps of greater interest is what happens in the rising turret. Danielsen (1972) has shown that the tops of cumulonimbus may rise 1–2 km above their neutrally buoyant altitude due to the kinetic energy of the updraught. The growth rate limitations are of even greater significance here. In a parcel of air rising at 5 m

TABLE 1

Crystal Type	Size (μm)	Growth Rate (+) Evaporation Rate (−) (g s^{-1})	Time to Change Mass by 10% (seconds)	Terminal Velocity cm s^{-1}
Solid	D = 100	5.4×10^{-11}	720	40
Spheres	D = 200	1.4×10^{-10}	2,400	125
ρ = 0.9	D = 500	5.7×10^{-10}	10,800	410
Column	$\bar{D}$ = 100	4.96×10^{-11}	800	10
Aggregates	$\bar{D}$ = 200	1.1×10^{-10}	2,900	25
ρ = 0.4	$\bar{D}$ = 500	3.7×10^{-10}	14,000	67
Thick	L = 100	4.9×10^{-11}	270	9
Plates	L = 200	7.1×10^{-11}	1,440	40
ρ = 0.4	L = 500	2.5×10^{-10}	6,800	140

$\bar{D}$ denotes equivalent circle diameter of crystal and L denotes major axis of plate. Data from Heymsfield (1981).

sec^{-1} at 193° K excess water vapor is generated at the rate of 5×10^{-6} g m^{-3} sec^{-1}. If we compute the combined growth rate of all the crystals in Figure 4 at water saturation for one cubic meter of air a value of $\cong 2 \times 10^{-6}$ g m^{-3} sec^{-1} results, which is nearly independent of choice of crystalline habit. The exact value is unimportant. What is important is that these crystals would appear to grow too slowly to consume the water vapor generated, even though at water saturation. Water saturation is important because nucleation of the ice phase proceeds via freezing of water droplets much more rapidly than by a direct vapor-ice process. In fact, there is no direct observational evidence for ice formation without the transient liquid water phase; the required supersaturations are too high. The condensation process is followed by rapid ice nucleation. It is thus necessary to assume that water saturation can be exceeded even in the presence of abundant ice crystals resulting in new nucleation via condensation/freezing processes. We believe we have other evidence for near water saturation in the aerosol measurements. The aerosol distribution in Figure 4 within the cirrus anvil shows a new mode at 0.17 μm, the presence and narrowness of which are most easily explained as the result of new nucleation and diffusional growth of solution droplets. The 0.4 μm mode is still faintly evident and is attributed to entrained air. A slight increase in size is also evident in the 0.4 μm mode.

We also computed the cooling rate at cloud top assuming the crystals were radiating to space above and the cloud below was optically thick. The cooling rate of the layer depends upon the amount of cross section per unit volume. Using the measured size distributions in the first penetration of Flight 7 we computed cooling rates of 0.5–1.0° hr^{-1}. These compare favorably with Kuhn's (1981, this issue) measurements of 15° day^{-1}. It is noteworthy that an optical depth of unity requires about 1 km thickness. This easily accounts for the 3° K differential between satellite and U-2 measurements. Radiational cooling also aids in further lowering cloud top temperatures but is probably masked by much stronger dynamical effects.

Conclusions

The microphysical aerosol and ice crystal data are consistent with cirrus anvil humidity values between ice and water saturation albeit probable that transient periods of water saturation (and above) exist. Because of the very low temperatures and larger size of these clouds, the anvil cirrus ice crystals are not very effective in hydrating the stratosphere; they simply go along for the ride. However, it is also clear that hydration occurs anytime the humidity is less than that of entrained stratospheric air. It is necessary for the injected air to be colder than the surrounding stratospheric air by several degrees to effect dehydration. If one has to explain the dryness of the stratosphere by injections via such clouds as observed it is simply most likely that the world-wide average of the injected portions are colder than we currently realize from Panama measurements. The measurements by Heymsfield (1974) indicated cloud top temperatures closer to −85°C in the Marshall Islands. The satellite measurement problem was previously mentioned and nearly all of our cloud top temperature data is via satellite measurements.

The particle size spectrometer experiment has provided important microphysical measurements on this little known cloud region. These are among the highest altitude "in situ" measurements of ice crystals. The aerosol data is the most extensive set of such measurements yet available. The ability to measure aerosol while in cloud was found particularly useful.

Acknowledgment. This work was supported by NASA Ames Research Center under contract number NAS2-10576.

References

Danielsen, E., Bleck, R., and Morris, D., Hail growth by stochastic collection in a cumulus model, J. Atmos. Sci., 29, 135–155, 1972.

Danielsen, E., A dehydration mechanism for the stratosphere, this issue.

Heymsfield, A. J., Microstructure of tropopause cirrus layers, Proceedings from the 6th Conf. on Aerospace and Aeronautical Meteorology, sponsored by Ames at El Paso, Texas, 1974.

Heymsfield, A. J., personal communication, 1981.

Kley, D., Transport of water through the tropical tropopause, this issue.

Knollenberg, R. G. and Luehr, R., Open cavity laser 'active' scattering particle spectrometry from 0.05 to 5 microns, Fine Particles, Aerosol, Generation Msmt., Sampling and Analysis, Editor Benjamin Y. H. Lui, Academic Press, 669-696, May 1974.

Knollenberg, R. G., Three new instruments for cloud physics measurements: the 2-D spectrometer probe, and the active scattering aerosol spectrometer, American Met. Society, Int'l Conf. on Cloud Physics, 554–561, July 1976a.

Knollenberg, R. G., The response of optical array spectrometers to ice and snow: a study of 2-D probe area-to-mass relationships, Final Report, Air Force Geophysics Laboratory, AFGL-TR-76-9273, March 22-June 30, 1976b.

Kuhn, P., Broad band airborne water vapor radiometry, this issue.

(Received December 23, 1981;
accepted February 18, 1982.)

TRANSPORT OF WATER THROUGH THE TROPICAL TROPOPAUSE

D. Kley, A. L. Schmeltekopf, K. Kelly, R. H. Winkler, T. L. Thompson and M. McFarland

National Oceanic and Atmospheric Administration, Aeronomy Laboratory, Boulder, Colorado 80303

Abstract. Total water was measured in the high troposphere and low stratosphere over Panama during ten aircraft flights. The results show that convective storms provide the means of transporting water into the stratosphere. From a consideration of the anvil heights over different areas of the tropical zone, it follows that a negative gradient of water vapor mixing ratio with altitude must exist over most of the lower stratosphere.

Introduction

Brewer [1949] proposed a mechanism by which the tropical tropopause acts as a cold trap to freeze-dry air in its passage from the troposphere to the stratosphere. The 1980 NASA Tropospheric/Stratospheric Water Vapor Exchange Experiment (TSWVEE) was aimed at gaining information on the details of the drying process. Brewer assumed that "air circulates by a slow mean motion into the stratosphere at the equator...", providing the only source for stratospheric water. Later, an additional source for stratospheric water from CH_4 oxidation was identified [Weickmann et al., 1975]. Ellsaesser [1974], from an analysis of the water measurements made by a variety of authors, concluded that a poleward gradient of water vapor exists with the mixing ratio highest near the equator. Stanford [1973] and Ellsaesser [1974] pointed out that winter temperatures in the polar stratosphere often fall below tropical tropopause temperatures, making it possible for stratospheric water to condense and fall out as precipitation, thus providing a sink. Ellsaesser et al. [1980] reviewed the existing data base of stratospheric mixing ratios. They concluded that observed poleward-directed gradients needed to be confirmed by more homogeneous data sets before they could be considered as being established. Kley et al. [1979] observed an overall minimum of 2.6 ppmv (parts per million by volume) at 19 km in the tropical stratosphere. They concluded that this profile could not be explained by the original Brewer mechanism. Robinson [1980] has studied stratospheric water vapor distributions in search of a convective cloud version of the freeze-dry mechanism that assumes that the rising branch of the Hadley cell circulation is a residual caused by overshooting cumulonimbus (cb) clouds. He concluded that the available observations did not support the convective cloud version. Johnston and Solomon [1979] suggested that cumulonimbus clouds may even dehydrate stratospheric air.

Experimental Design

A Ly(α) photodissociation hygrometer [Kley et al., 1979] was used to measure the mixing ratio of total water. Total H_2O is the sum of the mixing ratios of water in the ice phase and water in the gaseous phase. The instrument was specifically designed for the TSWVEE. A full documentation will be given in a later publication. Only some of the more important instrumental details will be discussed here.

The instrument was located in the rear portion of the left wing tank of a NASA U2 aircraft. A modified, heated Rosemount inlet probe was used to direct the flow of air from outside the boundary layer through the instrument. The flow rate through the instrument was $\sim$ 10 ℓ/s at Mach 0.7. The connection from the inlet probe to the instrument was made by a length of heated stainless steel tubing. The applied heater power was such as to increase the temperature of the inflowing air from ambient to approximately 20 °C. This "flash-heating" achieved rapid evaporation of all incoming ice crystals, a necessary condition for the measurement of total H_2O. The instrument was temperature stabilized at +30 °C.

The principal data are count rates from a photomultiplier, detecting the OH($A^2\Sigma^+ \rightarrow X^2\Pi$) fluorescence. Integration times of 0.1 s were used to record count rates. A multitude of auxiliary and housekeeping data, including universal time, was also recorded.

The aircraft altitude, pressure and static temperature data, together with universal time, were provided on digital tape by Scott [priv. comm.] and merged with the hygrometer data during the final data analysis.

Results

The instrument was operated during ten U2 flights out of Howard AFB (Panama 9 °N, 81 °W) between August 30 and September 16, 1980. Table 1 lists relevant information.

In a typical clear air survey flight, the U2 climbs to its first pre-scheduled altitude, usually slightly above the tropopause, and then stays at that level for approximately 15 min before ascending to a different altitude. Toward the end of the survey mission, the aircraft was usually at or near its ceiling altitude. Since the time constant of the instrument and the gas flow through it is 0.1 s, it was always possible to get a sufficient number of data points during ascent and descent so that good quality altitude profiles of the H_2O mixing ratio were obtained. However, the data obtained within the first 1800 s of each flight need special consideration due to effects of outgassing and are not considered in this note.

Despite the proximity of the intertropical convergence zone, during flights 1 through 4 there was little Cb activity within the range of the aircraft. Flights 5 and 6 served as cloud survey flights without actual penetration or "skimming" of anvils. Penetration into anvils was achieved during flights 7 and 8 and flights 9 through 11 were again survey missions.

The instrument worked well on all flights. All data are presently stored and will be available to the community. An extensive coverage of results will be published elsewhere. For this work only some examples of the results will be presented.

Water mixing ratios from flight 8, one of the anvil flights, are

TABLE 1. U2 Flight Parameters

Flight	Synonym	Time +	Date	Note
1	U206	12:55:00	8/30	
2	U207	13:25:00	8/31	1
3	U208	12:56:00	9/03	1,2
4	U209	13:25:00	9/07	
5	U210	12:25:00	9/09	
6	U211	13:57:00	9/11	
7	U212	12:57:00	9/12	
8	U213	13:25:00	9/13	
9	U214	12:54:00	9/15	
10	U215	12:55:00	9/16	
11	—	—	9/18	3

+ Universal time at instrument turn on.
1 Not analyzed.
2 No altitude and temperature information available.
3 Not participated.

Paper number 2L0180.

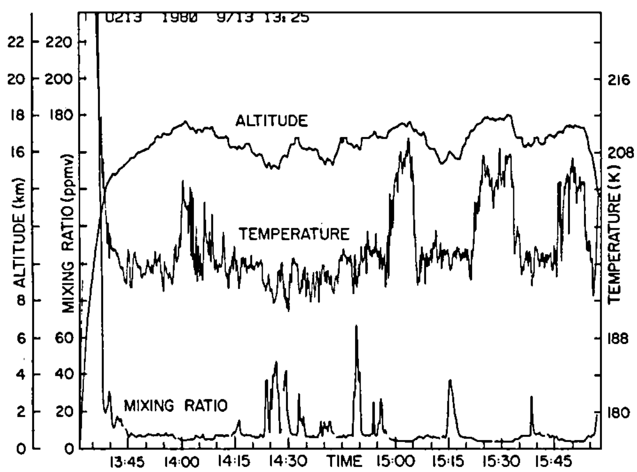

Fig. 1 Total H_2O mixing ratio, altitude and temperatures vs. time for flight 8. H_2O integration time 20 s.

plotted vs. time in Fig. 1, together with altitude and temperature. There are frequent bursts of large mixing ratios superimposed on a fairly uniform background. The meteorological tropopause was at 15.5 km. These bursts are by no means limited to altitudes very close to the tropopause. For example, one narrow spike was encountered at 17.4 km. The occurrences of the events were compared to the U2 flight log. In each case there was a coincidence between the events and the pilot's reporting of flying through a variety of cloud features. He used descriptions like cirrus layers, cirrus, light anvils, streamers, and vertical streamers.

The highest water mixing ratio of 120 ppmv was observed at t = 5100 s (14:50:00 UT) when the pilot reported flying in a light anvil. Note that 20 s integration time was used to generate Fig. 1. This resulted in approximately 40% reduction of peak mixing ratios. Some of the features of Fig. 1 have considerably more detailed structure when plotted with the shortest integration time.

Figure 2 shows a plot of saturation mixing ratios for flight 8 (dashed line) and observed water mixing ratios (solid line, 20 s integration time). Whenever the measured water mixing ratio exceeded the saturation mixing ratio, the area under the water trace was shaded. These occurrences of apparently supersaturated water vapor are produced by the flash heating; they actually represent vaporized ice. It can be safely concluded that the instrument had vaporized ice whenever supersaturation was indicated.

As a further example, a part of flight 7 is shown in Fig. 3. Two passes were made through the top of a mature storm, the first one at 15:03:00 UT through the downwind section and the second one through the upwind portion of the anvil, very close to the turret. On the first pass a peak mixing ratio of 760 ppmv was observed. As in Fig. 2, the saturation mixing ratios are plotted also. At 14:57:10 UT, some 5 min before the main part of the anvil (or turret?) was encountered, the results indicate ice.

Flights 7 and 8 had the largest number of stratospheric ice events indicated by apparent supersaturation. During the early part of the TSWVEE (flights 1, 4, 5, 6) and during the last two flights (9, 10), practically no ice was observed above the meteorological tropopause. However, the water mixing ratio from the tropopause up to about 17.5 km was close to saturation on all flights.

Overlayed descent profiles, together with temperature profiles, are shown for flights 1 and 4 through 10 in Fig. 4. For each flight on this plot, 2 s integrated values of the water mixing ratios were sorted in intervals of 100 m altitude range, averaged, and the standard deviation about the means calculated. The means and the $\pm 1\sigma$ deviations are given. It should be noted that points with large standard deviations are the result of flying through areas with large spatial water inhomogeneity. Most of those points come from flights 7 and 8. Temperatures were treated similarly. However, only their 100 m averaged means are shown.

As a first attempt toward a statistical analysis, water data and temperatures from all flights represented in Fig. 4 were averaged. Figure 5 shows the result. Rather than showing the means, only the lines representing $+1\sigma$ and -1σ deviations, respectively, are drawn. The areas in between are hatched.

The following significant observations are evident from Fig. 4 and 5:

1. Tropopause heights vary for individual flights. The mean tropopause height is at 15.0 km. Above the tropopause, up to 17 km altitude, temperature profiles are perturbed. Some flights and the mean even show a second temperature minimum at 17 km. Temperature fluctuations from the mean are small at 16 km and larger at the altitude of the second minimum.
2. The mean water profile has a first minimum at 15.75 km. Above, it increases to a maximum at 17 km, followed by a steep decline. An overall minimum is obtained between 18 and 19 km. Above 19 km, the mixing ratio increases slowly with altitude.
3. A tendency for the stratospheric mixing ratio to increase steadily with time of experiment was observed. Since identical symbols were used in Fig. 4, this effect is not obvious from looking at the figure.

Discussion

As Fig. 1, 2, and 3 show, many sudden bursts occurred during the "anvil" flights (7, 8). These were clearly related to encounteering ice. Some of those events were observed at the height of the second temperature minimum.

Two questions regarding the role of convective storms for the stratospheric water content will be posed. First, can the environment in which ice crystals and apparent supersaturation were observed be regarded as stratospheric?

The height range under consideration here extends from the meteorological tropopause up to 17.0 km. The question cannot be answered on the basis of the water measurements. The occurrence of the second temperature minimum shows that disturbed conditions prevailed during the TSWVEE. Danielsen [1981] suggests that these temperature perturbations are caused by overshooting cb turrets and subsequent anvil formation in which air from the cold dome is mixed with the warmer and drier surrounding stratospheric air. Danielsen favors the view that on a regional scale this air from overshooting cb has been converted by mixing to stratospheric air.

The second point concerns the hydration potential of the ice-

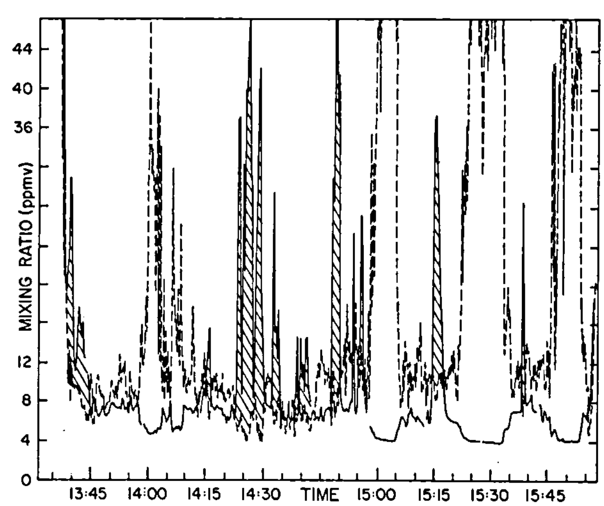

Fig. 2. Saturation mixing ratio over ice (dashed line) and total H_2O (solid line) vs. time for flight 8. Occurrence of ice is indicated by hatching. H_2O integration time 20 s.

carrying air parcels that have reached ~ 17 km by convective overshoot. All the evidence favors hydration of the stratosphere. Basically all the descent profiles collected in Fig. 4 are background profiles, since none of them invovled flying through anvils or cirrus. This can also be seen from the absence of apparent supersaturation during the descents. However, the effect of the overshooting cb's on the mixing ratio of this background air is believed to be shown by the positive "bulge" of the mixing ratio at 17 km (Fig. 4 and 5); i.e. they are adding water to the stratosphere.

An interestting relation, giving further proof for the hydration hypothesis, is evident from Fig. 5, in which the second temperature minimum of −79 °C, located at 17 km or 88 mb, corresponds to a water mixing ratio maximum of 7.2 ppmv. The equilibrium mixing ratio of vapor over ice is also 7.2 ppmv at this pressure and temperature. This seems to indicate that the processes causing the negative temperature perturbations have enhanced the background mixing ratio to the maximum possible level; i.e. saturation. Since this temperature is higher than that attained adiabatically by overshooting cb's, it also seems to indicate that the ice crystals of the cloud reached equilibrium by evaporating before falling back into the troposphere.

The approach taken in this note to discuss background profiles was chosen as a first and simple approach: What is observed are the results of complicated microphysical cloud processes. It seems that they act to hydrate the lower stratosphere. A necessary condition for this to happen would be that the penetrating and still-rising turret does not lose all of its excess ice by precipitation. When the cold dome decelerates and the anvil is formed by entrainment of warmer stratospheric air, some of the remaining ice crystals will sublime until saturation of the air mixture is reached. This process does not necessarily happen within the time frame of one single storm. The evaporation times of ice crystals brought up to these extreme heights are long and their terminal velocities are large [Knollenberg et al., 1981] and the bulk of crystals may indeed fall out. However, in the long term, acting over many storms, sublimation or partial evaporation of the crystals, even while they are falling out, apparently leads to saturation at the minimum temperature layer created by the mixing of adiabatically cooled cloud tops with ambient air.

The temperature lapse rate above 17 km altitude is clearly stratospheric. Although somewhat variable for individual flights, Fig. 5 shows a mean lapse rate of ~ −13 °C/km between 17 and 18 km. All flights revealed a strong negative gradient of the water mixing ratio between 17 km and ~ 18 km. The average gradient for the TSWVEE was −1.8 ppmv/km between 17 and

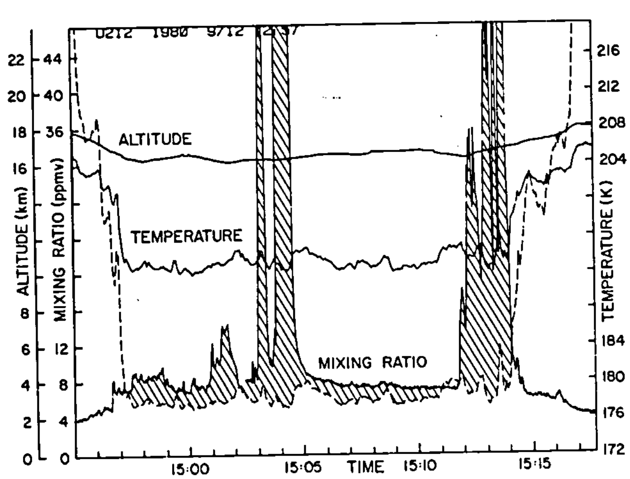

Fig. 3. Altitude, temperature, saturation mixing ratio and total H_2O mixing ratio vs. time for selected parts of flight 7. As in Fig. 2, apparent supersaturation is indicated by hatching. H_2O integration time 2 s.

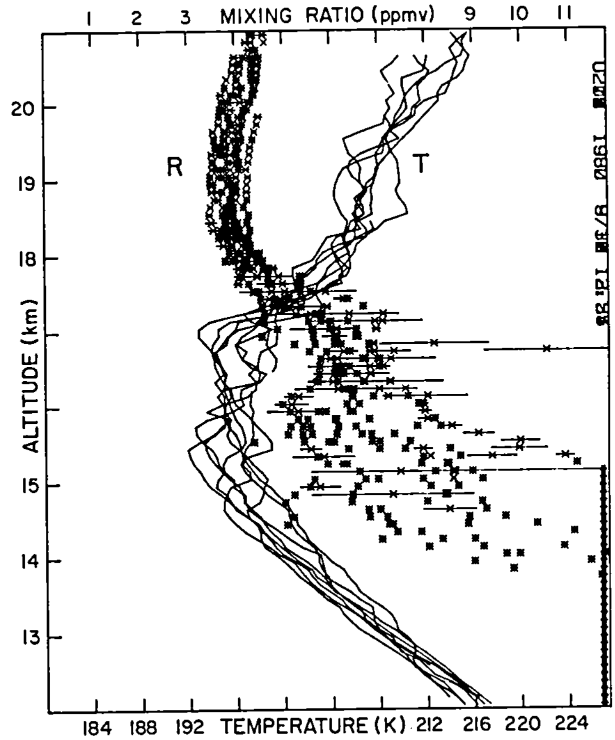

Fig. 4. Vertical descent profiles for flights 1, and 4 through 10. Data were averaged over 100 m height intervals. Means and standard deviations are drawn (symbol: —✱—). If the number of individual 100 m data points was less than two, only the mean is given (symbol: ✱). Mixing ratios > 12 ppmv are indicated by the ✱ symbol. R: mixing ratio; T: temperature.

18 km. A similar experimental result was observed over Brazil by Kley et al. [1979]. The negative gradient comes to a halt at about 19 km. This altitude was termed the tropical water vapor minimum by Kley et al. [1979]. It is now frequently being referred to as hygropause.

A mechanism that generates the hygropause and the negative water gradient will be proposed and discussed in the remainder of this section. This mechanism is based on the assumption that anvils reach different heights over different areas of the tropical zone. Different heights imply different perturbed temperatures at the heights of the anvil tops: the higher the anvils go, the lower will be the temperature of the air mixture, and, therefore, the saturation mixing ratios will be lower as well. The conjecture is that the negative water gradient and the hygropause observed over Brazil and Panama are the results of injections of air with very low water mixing ratios somewhere else. Since the lower stratospheric flow is mainly zonal, a water profile taken over Panama will show large mixing ratios from local and regional hydration above, but close to, 17 km. Higher up, the zonal flow will provide air with lower mixing ratios from injections at other longitudes and higher altitudes. A negative gradient will result. No active dehydration mechanism is required over Panama above 17 km.

The first assumption of anvils reaching different heights over different areas of the tropical zone is discussed in some detail by Danielsen [1981]. He points out that anvils over Micronesia (150 °E) during the northern hemisphere winter should be at 19 km with corresponding mixing ratios of 1.5 ppmv. Newell and Gould-Stewart [1981] made an analysis of radiosonde soundings and identified areas (centered over the western tropical Pacific) over which the monthly mean 100 mb temperatures were lower than −82.4 °C on a statistically significant basis. They proposed that all stratospheric air is injected over the area within the

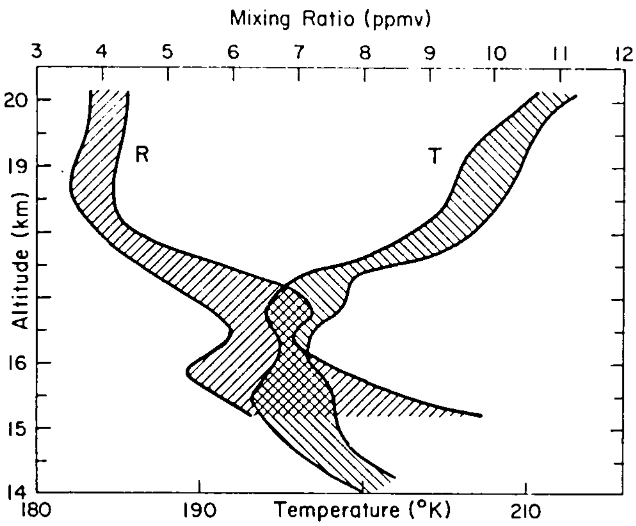

Fig. 5. Standard deviations from the mean (± 1σ) of the data from Fig. 4. Areas between the lines defining − 1σ and + 1σ are hatched. R: mixing ratio; T: temperature.

−82.4 °C isoline. Reid and Gage [1981] have analyzed the annual variation of the height of the tropical tropopause. Their curve for Ponape (7.0 °N, 158.2 °E) shows the meteorological tropopause to be at the 16 km (100 mb) only during the summer months. During winter, it has moved up to 17 km, implying substantially lower temperatures. The temperatures will be even lower above 17 km if the concept of cumulus convection is brought in.

Therefore, it seems that the water gradient and the hygropause over Panama and Brazil might be explained by mixing in air with the zonal flow from Micronesia.

Danielsen's estimate of the 19 km altitude and 1.5 ppmv mixing ratio will now be used in a simple two box model. Box one (fractional area F_M) is Micronesia. From Newell and Gould-Stewart, the yearly mean of its area showing 50% occurrence of $T < -82.4$ °C at 100 mb is 7% of the total tropical area. It is assumed that the same area will also have 50% occurrence of $T \leqslant -90$ °C at 60 mb (19 km), yielding a mixing ratio $\mu_M = 1.5$ ppmv. Box two is the area outside Micronesia. Panama is chosen as a representative location with a fractional area $F_P = 0.93$. From Fig. 5, the representative mixing ratio is $\mu_P = 7.2$ ppmv at 17 km. As the yearly mean over Panama, a value of $\bar{\mu} = 3.5$ ppmv is chosen at 19 km. If a tropical mean upwelling velocity of $\bar{w} = 0.03$ cm/s is adopted, from mass and flux balance equations, values for the vertical motions over Micronesia of $w_M = 0.28$ cm/s and over Panama of $w_P = 0.011$ cm/s are derived. The tropospheric to stratospheric flux over Micronesia comprises 28% of the total flux through the tropical tropopause. It is noted that the frational area having 50% occurrence of $T \leqslant -90$ °C may be significantly lower than the assumed 7%. If so, the values for w given above must be revised. Infrared satellite cloud photography may be of help for the derivation of more accurate numbers.

Conclusions

The results from the Ly(α) hygrometer obtained during the TSWVEE show that tropopause-penetrating convective storms apparently hydrate the lower stratosphere over Panama.

Negative gradients of the water vapor mixing ratios are observed above 17 km and tentatively explained as a consequence of anvils from deep convective storms reaching various altitudes above the tropopause over different areas of the tropical zone. Local dehydration mechanisms might act in addition; however, these do not seem to be necessary at this initial stage of the investigation.

More detailed work on the water profiles will be done. Correlative analyses of water, crystal and ozone data are especially needed. The results of such investigations will be published at a later time. More experimental work will also be required. Many of the still unresolved questions are likely to be answered from a field study over the central Pacific.

Acknowledgments. This work was supported, in part, by a grant from the NASA/Ames Research Center. We thank H. W. Ellsaesser, J. E. Harries, R. Penndorf and G. D. Robinson for helpful comments and J. D. Mahlman, S. C. Liu and S. Solomon for stimulating discussions.

References

Brewer, A. W., Evidence for a world circulation provided by the measurements of helium and water vapour distribution in the stratosphere, Quart. J. Roy. Meteorol. Soc., 75, 351-363 (1949).

Danielsen, E. F., A dehydration mechanism for the stratosphere, Geophys. Res. Lett. (this issue).

Ellsaesser, H. W., Water budget of the stratosphere, In: CIAP Monograph 3, DOT-TSC-OST-74-15 (NTIS, Springfield, VA), 273-283 (1974).

Ellsaesser, H. W., J. E. Harries, D. Kley and R. Penndorf, Stratospheric H_2O, Planet. Space Sci., 28, 827-835 (1980).

Johnston, H. S. and S. Solomon, Thunderstorms as possible micrometeorological sink for stratospheric water, J. Geophys. Res., 84, 3155-3158 (1979).

Kley, D., E. J. Stone, W. R. Henderson, J. W. Drummond, W. J. Harrop, A. L. Schmeltekopf and T. L. Thompson, In situ measurements of the mixing ratio of water vapor in the stratosphere, J. Atmos. Sci., 36, 2513-2524 (1979).

Knollenberg, R. G., A. J. Dasher and D. Huffman, Measurements of the aerosol and ice crystal population in tropical stratospheric cumulonimbus anvils, Geophys. Res. Lett. (this issue).

Newell, R. E. and S. Gould-Stewart, A stratospheric fountain?, J. Atmos. Sci. (December 1981, to be published).

Reid, G. C. and K. S. Gage, On the annual variation in height of the tropical tropopause, J. Atmos. Sci., 38, 1928-1938 (1981).

Robinson, G. D., The transport of minor atmospheric constituents between troposphere and stratosphere, Quart. J. Roy. Meteorol. Soc. 106, 227-253 (1980).

Stanford, J. L., Possible sink for stratospheric water vapor at the winter Antarctic pole, J. Atmos. Sci., 30, 1431-1436 (1973).

Weickmann, H., C. C. Van Valin and J. M. Anderson, Review of natural sources and sinks of stratospheric water vapor, In: CIAP Monograph 3, DOT-TST-75-53 (NTIS, Springfield, VA), 7-4 to 7-12 (1975).

(Received December 23, 1981;
accepted January 11, 1982.)

GEOPHYSICAL RESEARCH LETTERS, VOL. 9, NO. 6, PAGES 621-624, JUNE 1982

BROAD BAND AIRBORNE WATER VAPOR RADIOMETRY

Peter M. Kuhn
Northrop Services Inc.,
NASA Ames Research Center
Moffett Field, CA 94035

Abstract. An infrared radiometer with a pass band of 280 to 520 cm^{-1} (35.7 to 19.2 μm) is employed on the NASA Ames Research Center U-2 and C-141A aircraft in the measurement of water vapor burden in the upper troposphere and stratosphere. Coincidentally with altitude changes the water vapor mass mixing ratio is also inferred by observing the change in optical depth over a known vertical distance. Data from the December 1980 U-2 Water Vapor Exchange Experiment over the Panama Canal Zone adds to the concept that overshooting cumulonimbus towers "moisten" the lower stratosphere. The average mass mixing ratio in close proximity to or above such towers ranges from 3.5 to 5.0 parts per million above 18 km while the average background mass mixing ratio is only 2.9 parts per million. Generally the lowest background mixing ratios, averaging 2.6 parts per million occurred in the 18 to 21 km layer. For the same levels background Panama mass mixing ratios averaged from 1.0 to 3.0 parts per million higher than in middle latitudes.

Introduction

The Water Vapor Exchange Experiment was conducted out of Howard Air Force Base, Panama Canal Zone from 26 August to 22 September 1980. A NASA Ames Research Center U-2 aircraft carried the broad band water vapor radiometer and eight other related experiments on nine high altitude missions between 5° and 12° north latitude and 76° and 82° west longitude. The purpose of the experiment is to determine the mass exchange of water vapor between the upper troposphere and lower stratosphere and to examine the role "overshooting" cumulonimbus towers may play in the process.

Primarily the water vapor mass mixing ratio was measured at a series of levels from 15 to 22 km and in a variety of changing atmospheric conditions in the direct vicinity of the normal location of the ITCZ. Unfortunately during the experiment the normal equatorial circulation was so upset as to render the ITCZ virtually nonexistent. The time of the experiment, then, was one of general inactivity.

Past experiments [Kuhn, 1971] had produced some evidence, although somewhat controversial, that overshooting cumulonimbus towers might increase the water vapor burden of the stratosphere. The overburden of water had been observed as high as 6.0×10^{-4} g cm^{-2} (6.0 precipitable micrometers) at an altitude of 20 km. The Water Vapor Exchange Experiment may be able to determine via new data and analyses the validity of this conjecture. Ellsaesser et al [1980] discuss the discrepancies between observations and hypotheses and provide the historical developments prior to this experiment.

Paper number 2L0292.
0094-8276/82.002L-0292$3.00

Infrared Radiometer

The infrared radiometer [Kuhn, 1975] onboard the U-2 for the experiment measures the zenith radiance in a spectral band extending from 280 to 520 cm^{-1} (35.7 to 19.2 μm). The system response factor of the radiometer, R, is a calibration constant which is a function of the radiometer's field of view, optical collecting powers, the detector responsivity and the system electronic gain. The shape of the radiometer response function versus wave number (cm^{-1}) or wavelength (μm) is determined from the response curves of the separate components. The responsivity constant of the radiometer system ($v\ w^{-1} cm^2\ sr$) is calibrated under laboratory conditions employing a cooled and purged black body source under partial vacuum. It is given by,

$$R = GV/(N-N_r), \qquad (1)$$

where G is gain, V is voltage output of radiometer N is radiance in w cm^{-2} sr^{-1} and N_r is the radiometer source radiance.

Data Reduction Procedure

In flight, the radiometer "sees" the sky chopped against a 250K controlled black body reference. A separate radiometer operating in the Q branch of the 15 μm CO_2 band determines the air temperature at flight level. The precipitable water vapor overburden (g cm^{-2}) above the aircraft is then determined by adjusting the water vapor input iteratively in a multi-level, radiative transfer model so that predicted and observed radiance agree within experimental tolerance. Pressure, temperature and overburden of water vapor, as a set of observations, are inputs to the model to iteratively determine first U and then q. Air Force Geophysical Laboratory, formerly Air Force Cambridge Research Laboratories, compilation of line strength data [1973], with pressure broadening and temperature corrections to the absorption coefficients are adapted to the transfer model.

The mass mixing ratio is finally determined by the change in the burden of water vapor observed over a short period of time (approximately three to six minutes) at two different altitudes one to two kilometers apart. This produces the mean mixing ratio for the layer from the expression

$$\bar{q} = \Delta U / \rho \Delta z, \qquad (2)$$

where $\bar{q}$ is in units of grams of water vapor per gram of dry air; ΔU is the change in water vapor burden between the two levels; ρ is the mean

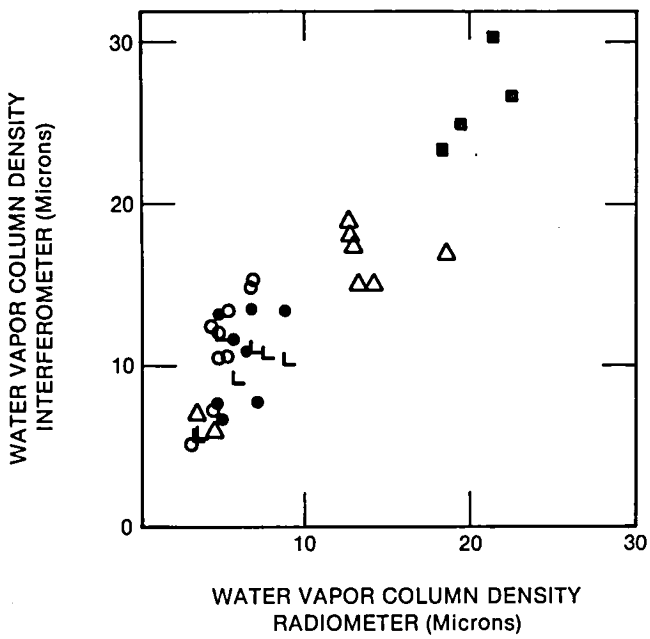

Fig. 1. Comparison of water vapor column overburden measured with Michelson interferometer and broad band radiometer for 17 Nov. 1977, O ; 21 Nov. 1977, Δ ; 21 April 1978 ■ ; 21 Jan. 1976 ● and 26 Jan. 1976 L . Erickson, et al,[1979].

atmospheric density and Δz is the change in altitude.

The accuracy of the radiometer system for the inference of water vapor burden and derived mixing ratio increases as the radiance observations increase. Calculating the mixing ratio from equation (2) for an average layer depth of 1 km and observing for three minutes (96 samples), the standard error of the mean layer mixing ratio inferred is $\pm$ 0.6 x 10^{-6} g g^{-1} (0.6 ppm). To illustrate the accuracy of the radiometer, Fig. 1 compares water vapor column density, U in equation (2), obtained simultaneously with the NASA - Ames Research Center Michelson interferometer and the broad band radiometer described. Comparisons were made during five NASA C-141A missions from 1976 through 1978 [Erickson, et al, 1979]. The correlation for all thirty-six points is 0.90. These totally independent instrument observations show a systematic difference. One explanation may be in the fact that the interferometer radiance observations reduced to water vapor overburden employed a single level model above flight level while the radiometer observations were input to a fourteen level radiative transfer model.

Results Summary

As stated, the purpose of the experiment is to determine tropospheric-stratospheric water vapor exchange in the tropics and to include the possible role overshooting cumulus towers may play in the process [Johnston and Solomon, 1979]. The tropical freeze-dry hypothesis by Brewer [1949], may also be examined relative to these late summer Panama observations.

In line with the goals of the experiment a discussion of four main observation results following includes: (1) The observed mean mixing ratio sounding related to the freeze-dry hypothesis; (2) Poleward gradient of mass mixing ratio from Panama maximum at constant altitudes; (3) Total water vapor burden above reference levels; (4) Classification of "wet" and "dry" atmosphere mission days.

Figure 2 summarizes in the mean the radiometric observations of water vapor mass mixing ratios as functions of height and mean temperature at that height. There are an average of 1207 observations per plotted point with each observation requiring some four seconds for the data acquisition process. This translates into approximately 90 minutes of radiometric data averaged into each point. The period of the observation was 30 August through 16 September 1980. Except within clouds, remote radiometric techniques are generally less sensitive to contamination than in situ measurements.

Assuming a temperature determined tropopause for the Panama vicinity of approximately 17 km the mixing ratios observed (Fig. 2) are below the saturation mixing ratio at 17 km for the average observed temperature of -76C. Saturation here would occur at this height and observed average temperature when the mixing ratio was 7.9 ppm. However freeze-out cannot take place for the observed mean 17 km mixing ratio of 3.0 ppm at temperatures above -82C. There does not appear to be sufficient evidence from this experiment, at least from the average sounding, that overshooting cumulonimbus towers can adiabatically cool and dry the lower stratosphere sufficiently to provide a satisfactory tropical cold trap.

The mean 18.2 and 20.0 km mass mixing ratios of 2.9 and 2.7 ppm (Fig. 2) are higher than similar altitude values from mid-latitudes even

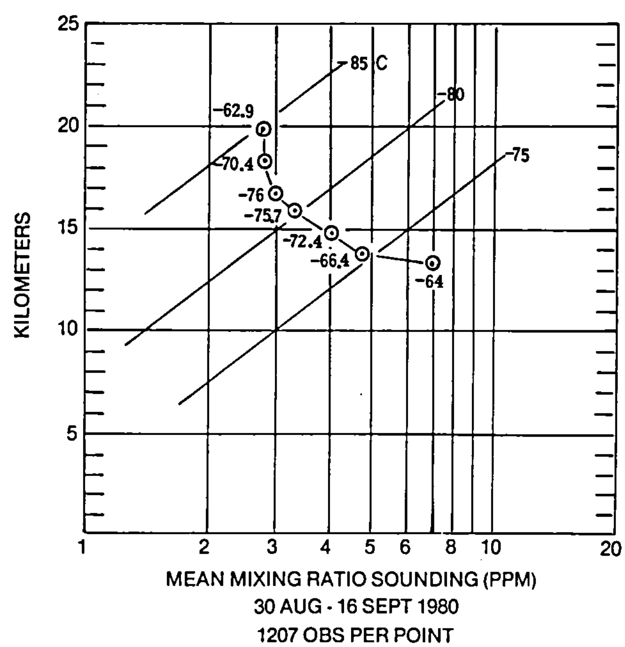

Fig. 2. Radiometer inferred mean water vapor mixing ratio sounding from data of 30 August to 16 September 1980 averaging 1207 observations per point. Mean temperatures for each plotted point are in degrees Celsius. Slanting straight lines are frost point temperatures in degrees Celsius.

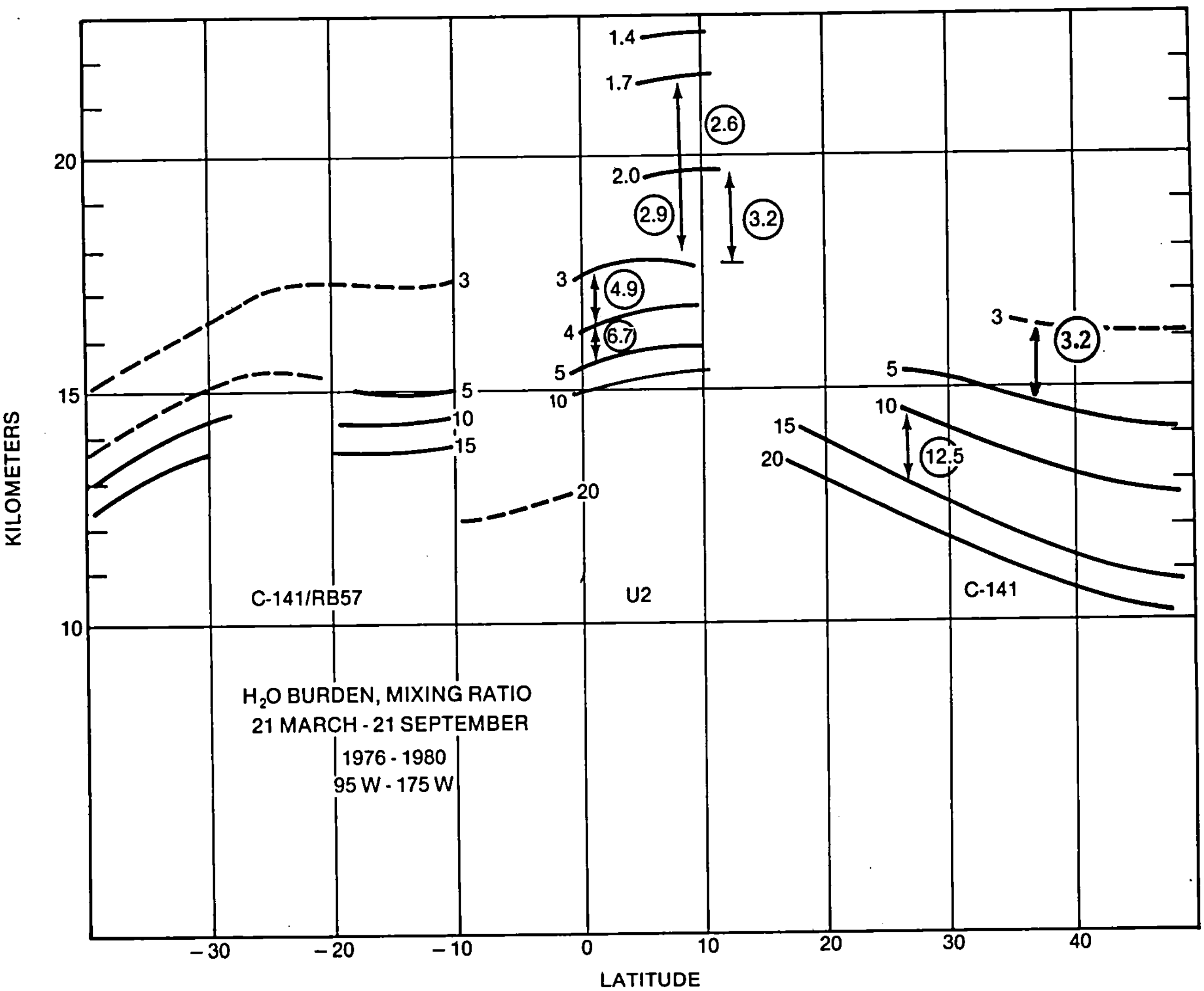

Fig. 3. Mean water vapor burdens in micrometers and mean mixing ratios in parts per million by mass as a function of latitude, longitude band and altitude. Mixing ratios are plotted within circles as mean for a layer and burdens are the plotted curves. Dashed curves indicate limited data availability from RB57 aircraft observations.

during this relatively quiescent period for the atmosphere over Panama. They do agree favorably with all but one set of experimental results of stratospheric water vapor observations for 5^{o} to 15^{o} north latitude summarized by Ellsaesser, et al, [1980].

In a broad, climate sense the observations appearing in Fig. 3, obtained from 1976 through 1980 aboard NASA's Ames Research Center C-141A, Convair 990 and U2 aircraft and a U.S. Air Force RB57, relate to the previous discussion in that they display mean column densities and mean mass mixing ratios for not only an equatorial region but also for mid-latitudes. The data analysis is more general than that of Fig. 2 in that it embraces data from five years and from three different aircraft platforms. However the same radiometric remote sensing technique was employed on each aircraft. Poleward as well as upward vertical gradients from an equatorial maximum are evident in the profiles. Again this is in agreement with comments by Ellsaesser, et al [1980]. Of interest is the mean equatorial mass mixing ratio of 6.7 ppm at 16 km compared with a 3.2 ppm mean at 40^{o} north latitude. While this comparison is below the Panama tropopause and generally below the mid-latitude tropopause it displays a pronounced poleward gradient.

Perhaps a better measure of increasing water vapor or changes in the water vapor is the over-vapor burden. This is displayed as a function of latitude and altitude in Fig. 3. This is so since the mixing ratios refer to measurements at a single level whereas changes in the burden of water vapor assess additions or subtractions of water vapor in an entire column above a reference level. It appears evident that the Panama region, in fact most of the equatorial region, is more moist during this experiment than mid-latitude observations from 95^{o} to 175^{o} west longitude.

During this experiment the water vapor radiometer soundings fall into two distributions classified by Kuhn [1979] as either "wet" or "dry" day soundings. However those of 1979 were more sharply divided into one or the other classification. Somewhat analogous profiles did occur

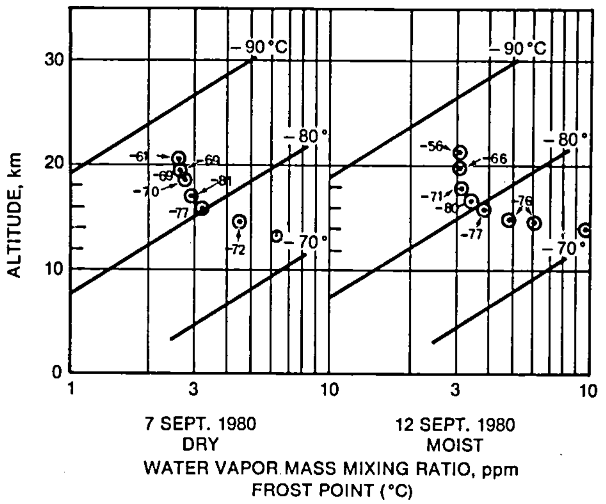

Fig. 4. Comparison of radiometer inferred water vapor mass mixing ratios for "dry" and "wet" days. Slanting straight lines are frost point temperatures in degrees Celsius. Atmospheric temperatures for each plotted point are indicated with arrows and are in degrees Celsius.

in 1980 but the differences are much less pronounced (Fig. 4). The "dry" sounding of 7 September reaches a minimum of 2.5 ppm at 20.5 km while the "wet" sounding of 12 September has a minimum mixing ratio of 3.1 ppm at 21.0 km. This is just barely significant in view of the limits of the instrumentation. However the atmospheric regime in 1980 was, as stated, not one of normal convective activity. In both cases the mixing ratios are below those corresponding to saturation at 20.5 km and an average temperature of -64C. In this instance saturation occurs with 63 ppm of water vapor.

The lowest temperature observed as a four minute average occurred at 16.7 km during the "wet" mission of 12 September, reaching -80.1C. The mixing ratio observed during this time is 3.4 ppm while the saturation mixing ratio for this temperature is 3.7 ppm. Freeze out of water vapor could not quite take place. On the "dry" mission of 7 September the lowest seven minute average temperature is -81.5C at 16.7 km. The observed mixing ratio during this period is 2.9 ppm and the saturation mixing ratio is approximately 2.9 ppm. Here freeze out of water vapor could possibly occur. But it is a singular case in one shallow layer centered on 16.7 km.

Below 16 km the differences in the mixing ratios between the observed soundings of the two days are more pronounced, reaching 2 ppm at 15 km. The analyses for the radiometer water vapor profiles on these two days is typical of such comparisons during the full period of the experiment. There were only two days during the 1980 experiment that could be classified as "wet." This is in contrast with 1979 when at least half of the days were noted as "wet." However on those occasions when convection was noted and when the U-2 flight track passed relatively close to a turret at or slightly above the top the mixing ratio did reach 5.5 to 6.5 ppm at 18 km. This occurred just above the tropopause and again indicates the inability of the lower Panama stratosphere to freeze out water vapor as a sink or cold trap. Temperatures averaging -76C at and just above the mean tropopause were simply not cold enough to provide a suitable cold trap. In fact the sporadic increases in the mixing ratio of the lower stratosphere above a background level of 2.6 to 2.9 ppm suggest that overshooting cumulonimbus turrets may in fact locally increase the water vapor. However residence times for the increases may be relatively short.

Acknowledgement

This research was supported by the Atmospheric Experiments Branch, Space Science Division, NASA Ames Research Center under Contract NAS2-10592.

References

Brewer, A.W., Evidence for a world circulation provided by measurements of helium and water vapor distribution in the stratosphere, Quart. J. Roy. Met. Soc., 75, 351, 1949.

Ellsaesser, E.F., J.E. Harries, D. Kley and R. Penndorf, Stratospheric Water Vapor, Space Sci., 28, 827-835, 1980.

Erickson, E.F., U.P. Simpson, P.M. Kuhn and L.P. Stearns, Determination of the telluric water absorption correction for astronomical data obtained from the Kuiper Airborne Observatory, NASA Tech. Memo. 75582, NASA Ames Research Center, Moffett Field, CA 94035, 1979.

Johnston, H.S. and S. Solomon, Thunderstorms as possible micrometeorological sink for stratospheric water, J. Geophys. Res., 84, 3155, 1979.

Kuhn, P.M., Water vapor: Stratospheric injection by thunderstorms, Science, 174, 1319-1321, 1971.

Kuhn, P.M. and L. P. Stearns, Latitudinal profiles of stratospheric water vapor, Geophys. Res. Lett., 227-230, 1975.

Kuhn, P.M., U-2 Water vapor burden observations through the tropopause, NASA Technical Memo. 78577, 1977 intertropical convergence zone experiment, Section XI, 145-152, NASA, Ames Res. Ctr., Moffett Field, CA 94035.

McClatchey, R.A., W.S. Benedict, S.A. Clough, D.E. Burch, R.F. Calfee, K. Fox, L.S. Rotman, and J.S. Garing, AFCRL atmospheric absorption line parameters compilation, AFCRL-TR-73-0096, 78 pp, Air Force Geophysical Laboratories, L.G. Hanscom Field, Bedford, MA 01730.

NASA, 1977 intertropical convergence zone experiment, NASA Tech Memo., 78577, NASA Ames Research Center, Moffett Field, CA 94035, 1979.

(Received December 23, 1981;
accepted February 25, 1982.)

1. Report No. NASA TM-84297	2. Government Accession No.	3. Recipient's Catalog No.
4. Title and Subtitle THE 1980 STRATOSPHERIC-TROPOSPHERIC EXCHANGE EXPERIMENT		5. Report Date June 1983
		6. Performing Organization Code
7. Author(s) Edited by A. P. Margozzi		8. Performing Organization Report No. A-9093
9. Performing Organization Name and Address NASA Ames Research Center Moffett Field, Calif. 94035		10. Work Unit No. T-4404
		11. Contract or Grant No.
12. Sponsoring Agency Name and Address National Aeronautics and Space Administration Washington, D.C. 20546		13. Type of Report and Period Covered Technical Memorandum
		14. Sponsoring Agency Code 147-10-03

15. Supplementary Notes
Point of contact: A. P. Margozzi, Ames Research Center, MS 245-5, Moffett Field, Mt. View, Calif. (415) 965-5517 or FTS 448-5517.

16. Abstract

Data are presented from the 1980 Stratospheric-Tropospheric Water Vapor Exchange Experiment conducted in the Republic of Panama in August and September of 1980. Measurements were made during 11 flights of the NASA U-2 aircraft which provided data from horizontal traverser and samplings in and about the tops of extensive cirrus-anvil clouds produced by overshooting cumulus turrets. Aircraft measurements were made of water vapor, ozone, ambient and cloud top temperature, fluorocarbons, nitrous oxide, nitric acid, aerosols, and ice crystal populations. Balloonsondes were flown about twice daily providing data on ozone, wind fields, pressure and temperature to altitudes near 30 km. Satellite photography provided detailed cloud and cloud top temperature information. Descriptions of individual experiments and detailed compilations of all results are provided in 10 chapters and 4 appendices.

17. Key Words (Suggested by Author(s)) Water vapor, Stratospheric-tropospheric exchange, stratosphere, ozone, aerosols, fluorocarbons, nitrous oxide, nitric acid	18. Distribution Statement Unlimited Subject Category: 47		
19. Security Classif. (of this report) Unclassified	20. Security Classif. (of this page) Unclassified	21. No. of Pages 424	22. Price* A-18

*For sale by the National Technical Information Service, Springfield, Virginia 22161